Chi-Sing Man

Crystallographic Texture and Group Representations

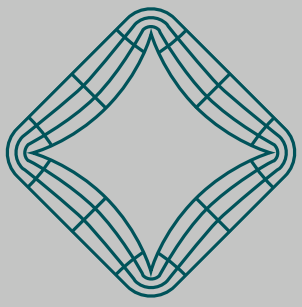

Springer

Crystallographic Texture and Group Representations

Chi-Sing Man

Crystallographic Texture and Group Representations

Previously published in *Journal of Elasticity*, Volume 149, Issues 1–2, April, 2022

Springer

Chi-Sing Man
Department of Mathematics
University of Kentucky
Lexington, KY, USA

ISBN 978-94-024-2157-6

Mathematics Subject Classification: 20C35, 74A99, 74E10, 74E15, 74E25, 60B05

This Springer imprint is published by the registered company Springer Nature B.V.
The registered company address is: Van Godewijckstraat 30, 3311 GX Dordrecht, The Netherlands

Journal of Elasticity (2022) 149:1
https://doi.org/10.1007/s10659-022-09880-w

Foreword

Roger Fosdick[1]

Accepted: 20 January 2022 / Published online: 5 July 2022

The *Journal of Elasticity: The Physical and Mathematical Science of Solids* is dedicated to the promotion of fundamental and physically based research which advances our understanding of various areas of solid mechanics and engages a breadth of disciplines including continuum mechanics, materials science, biology, chemistry, medicine, electromagnetics and rheology.

This volume contains an invited exposition, *Crystallographic Texture and Group Representations* by Chi-Sing Man, on the elements and foundational structure of the theory of crystallographic texture and its measurements. Polycrystalline materials are aggregates of crystallites separated by microscopic grain boundaries which contain defects, and natural formative processes as well as manufacturing usually introduce some ordering of this scattered arrangement. The resulting complex structure plays a significant role in characterizing the constitutive response and behavior of such materials in practice. Quantitative texture analysis offers a description of one aspect of this complex structure that is useful by itself or in tandem with descriptions of other aspects in building a constitutive model to describe the physical behavior of such materials. For example, the transmission of waves through a polycrystalline material is highly affected by the presence of crystallographic texture.

Professor Man has herein presented a masterful and complete research-level exposition of quantitative texture analysis that brings to light a novel approach where basic concepts are made precise through their mathematical definition, and the important role played by group representations is emphasized. A modern 'active', rather than a classical 'passive', view of rotations as linear transformations is introduced in order to enhance the conceptual understanding of the subject and to establish a workable setting for the basis of future advancements. This novel approach to the subject provides a natural link to known formulas and developments in mathematics and physics, and allows many aspects of the classical approach to be clarified, organized and developed further under one mathematical setting and common logical thread.

The work is completed in three parts, the first being an introduction to quantitative texture analysis. This contains a description of the classical approach and its reorganization into a systematic scheme. Parts two and three concentrate on the mathematical foundations of the subject which center around group representations and possible relations with crystallographic texture and material properties.

✉ R. Fosdick

[1] Minneapolis, USA

Journal of Elasticity (2022) 149:3–445
https://doi.org/10.1007/s10659-022-09882-8

Crystallographic Texture and Group Representations

Chi-Sing Man[1]

To May, with love and gratitude

Accepted: 20 January 2022 / Published online: 5 July 2022

Abstract
This exposition consists of three parts. Part I is an introduction to classical texture analysis. The harmonic method and the approach initiated by Roe, where the orientation distribution function (ODF) is always defined on the rotation group SO(3), is emphasized and given a systematic treatment. Basic concepts (e.g., the orientation density function) are made precise through their mathematical definition. The active view of rotations is implemented throughout. A conscientious effort is made to use machinery already available in mathematics and physics. The Wigner D-functions, whose properties are familiar in physics, are used instead of Bunge's and Roe's versions of generalized spherical harmonics. By including three mathematical appendices, it is hoped that engineering students would find Part I readable. The objectives of Parts II and III are threefold, namely: (i) To delve deeper into the mathematical foundations of the harmonic method. The Weyl method is used to prove that the Wigner D-functions are the matrix elements of a complete set of pairwise-inequivalent, continuous, irreducible unitary representation of SO(3). General formulas of the Wigner D-functions, valid for any parametrization of SO(3), are derived. An elementary proof (attributed to Wigner) of the Peter-Weyl theorem is presented. (ii) To provide mathematical prerequisites in group representations for research on representation theorems that delineate the effects of crystallographic texture on material properties defined by tensors or pseudotensors. (iii) To introduce tensorial Fourier expansion of the ODF and the tensorial texture coefficients. The classical ODF expansion in Wigner D-functions is recast as a special tensorial Fourier series. The relation between the tensorial and classical texture coefficients in this context is derived.

Keywords Quantitative texture analysis · Wigner D-function · Mathematical foundations of harmonic method · Group representations · Tensorial texture coefficients

Mathematics Subject Classification (2020) 20C35 · 74A99 · 74E10 · 74E15 · 74E25 · 60B05

✉ C.-S. Man
cman@uky.edu

[1] Department of Mathematics, University of Kentucky, Lexington, KY 40506-0027, USA

Contents

Preface

I first learned of crystallographic texture in the late 1980s when I began to work on acoustoelastic measurement of stress in structural metals. There the presence of crystallographic texture was the culprit for the difficulty in using ultrasonic waves for measurement of stress, and the central problem was deemed to be the separation of stress-induced and texture-induced shifts in wave velocities. From the mid-1990s till the untimely passing of my colleague James G. Morris in 2006, I collaborated with his research group at Materials Engineering, University of Kentucky. Jim's group was mainly interested in devising processing parameters to improve the mechanical properties of various continuous-cast aluminum alloys. My research efforts in the collaboration were focused on studying the effects of crystallographic texture on plastic anisotropy and formability parameters of sheet metals and on on-line measurement of texture coefficients and formability parameters of sheet metals by electromagnetic-acoustic transducers (EMATs) or laser ultrasonics. During that period the research of my own group remained to be centered around acoustoelastic measurement of stress in textured metals.

Since 1997, from time to time I offered graduate courses on the topics of this exposition, partly to teach myself the subject and partly to train graduate students for research in the area. Some of the classes were mainly targeted to students in Materials Engineering, some were meant exclusively for students in Mathematics, and some were attended by roughly equal mix from the two groups. In all the classes clarity of basic concepts was emphasized. No textbook was adopted in any of the classes. Instead, lecture notes that covered parts of each course were written and handed out in class. The present exposition is a revised, updated, and expanded version of those notes. The aforementioned research interests explain the bias in the selection of topics, particularly in the examples and applications, in the lecture notes and in this exposition. In particular, coverage on methods of inversion of pole figures and ghost correction is limited to those which my research group considered for implementation in our in-house computer programs.

When I first approached quantitative texture analysis, I was dismayed to find that both Bunge and Roe, pioneers of the subject, used passive rotations. From my background in mathematics, mechanics, and physics, using active rotations would be easier and more convenient. Moreover, both Bunge and Roe defined their own "generalized spherical harmonics", which are variants of the Wigner D-functions [340, 341]. The Wigner D-functions play a central role in the quantum theory of angular momentum. By the time when I lectured on the subject, they had long been thoroughly studied and formulas of their detailed properties were easily available in the physics literature [28, 39, 99, 238, 274, 313, 325]. Matthies [215, p. 432], for one, explains why he differs from Bunge in his choice of Euler angles and in his use of the Wigner D-function as follows:[1]

> The used mathematical apparatus differs somewhat from that of BUNGE .... It is commonly used in modern theoretical physics (EDMONDS), has from the view of the author definite comprehensible advantages in deriving geometric relations and is available in a manageable form since the publication of the extensive and detailed collection of formulas of WARSCHALOWITSCH et al. [i.e., the 1975 Russian edition of [325]]

Note also that any unwitting tinkering of the Wigner D-functions (e.g., their normalization) might destroy their most fundamental property, namely that they are matrix elements

[1] Matthies, however, uses passive rotations just as Edmonds [99].

of irreducible unitary representations of the rotation group. Hence, when I began to write lecture notes on the subject, I elected to rewrite the fundamentals with active rotations and Wigner D-functions. These conventions are kept in the present exposition. On the other hand, other conventions used most prominently in quantitative texture analysis that include those adopted by Bunge [60], Roe [270], Matthies et al. [224], and Gel'fand et al. [125] are also fully explained.

This exposition is meant for beginning learners of quantitative texture analysis, and its focus is on the fundamental concepts. It seeks conceptual clarity by using the appropriate mathematical language. Another distinguishing feature is that the approach initiated by Roe is emphasized. The exposition is divided into three parts. Part I is based on lecture notes originally written for classes on quantitative texture analysis that catered to graduate students in Materials Engineering and Engineering Mechanics. It presents the rudiments of classical texture analysis, where the orientation distribution function in the Roe approach is always defined on the rotation group. Mathematical prerequisites for much of this part are matrix algebra and advanced multivariate calculus. In refurbishing my lecture notes for this exposition, I have added in this part a number of new sections plus paragraphs and explanatory remarks that use some mathematical terms beyond the aforementioned prerequisites and refer to a few theorems in topology and measure theory, which I hope would make the mathematical foundations of the subject clearer. Three mathematical appendices have been added to Part I to aid reading. Moreover, suggestions are made either at the beginning of a chapter or in the Comments on Contents of the Introduction to specify which sections and remarks could be skipped on a first reading.

Parts II and III are largely based on lecture notes for classes taken by graduate students in Mathematics. The main objectives of those classes were twofold, namely: (i) to delve deeper into the mathematical foundations of the subject—in my view mathematics students should see how the Wigner D-functions could be derived and their fundamental attribute as matrix elements of irreducible unitary representations of the rotation group be proved; (ii) to prepare students for research on representation theorems that delineate the effects of crystallographic texture on material properties defined by tensors or pseudotensors. These objectives underlie the selection of topics in much of Parts II and III, which centers around group representations. Chapters 12 and 17 are newly written for this exposition.

I thank all my former students and associates who participated in work related to texture analysis. Among them I mention in particular: Roberto Paroni, Mojia Huang, and Scott Godefroy, whose keen observations and meticulous work helped deepen my understanding in several aspects of texture analysis; Wenwen Du, Leigh Noble, and Ding Zhao, who, like their three aforementioned peers, authored or coauthored writings cited in the present exposition. Huang, moreover, wrote in-house Maple and Fortran programs in texture analysis for use by the research group. Special contributions were made by Xingyan Fan, who was responsible for all X-ray measurements, and by Helen Xiang and Carl Gao, who at different times shouldered the work for EBSD measurements. I am deeply grateful to Roger Fosdick: as Editor-in-Chief he was the strongest advocate, whose unrelenting support was instrumental for this exposition to appear also as a hardbound spin-off; as the Handling Editor of the manuscript, he arranged its reviewing process, which he followed closely and nudged to a timely conclusion.

Lexington, Kentucky, 2021

Chi-Sing Man
Department of Mathematics
University of Kentucky

Introduction

Many materials are polycrystalline aggregates of tiny crystallites or grains of various sizes and shapes. Even for aggregates whose crystallites are chemically identical, the crystal lattices of the grains will still differ in their orientation in space. Since each crystallite is anisotropic in its physical properties, the macroscopic properties of a polycrystal will likewise be anisotropic unless the orientations of its constituent crystallites are completely random and the anisotropies of the crystallites even themselves out. Manufacturing processes (e.g., annealing and hot/cold rolling in the case of sheet metals) and natural processes (e.g., deformation of the earth's interior during the earth's long history), however, impart crystalline materials thus formed with crystallographic texture (i.e., the constituent crystallites have preferred orientations), which is found in metals, ceramics, polymers, rocks, and mineralized biological materials. While it does not need much imagination to speculate that crystallographic texture would play a major role in accounting for the anisotropy of physical properties of polycrystalline materials, to ascertain the quantitative relations between texture and anisotropy is an entirely different matter. In fact, it was not until the mid 1960's that quantitative texture analysis began to take shape as an exact science. Great advances in the subject have been made since then. Nowadays, "texture research is indeed a wide multidisciplinary field" that "connects many domains of science with metallurgy, ceramics, polymer science, geology, geophysics, and biology as just a few highlights", as Wenk and Van Houtte [338] assert in the conclusion of their 2004 review paper on texture and anisotropy. To their assertion, we may add that more recently crystallographic texture is a basic ingredient in some studies on microstructure-sensitive design to optimize engineering performance of polycrystalline materials (see, e.g., [3, 122, 189, 191]).

This exposition is an introduction to the basics of quantitative texture analysis (QTA), which has several special features as follows:

1. The approach to QTA as initiated by Roe [270, 271] is emphasized and given a systematic treatment. Its advantages are discussed. Roe no longer published papers in texture analysis after 1966. The presentation of the approach in his 1965–66 papers is incomplete. Here some aspects of the approach are clarified and developed further.
2. Basic concepts are made precise through their mathematical definition. Take the orientation (probability) density function and Roe's orientation distribution function (ODF) in classical texture analysis for instance. For simplicity, consider polycrystals without sample symmetry. Given the orientation space of a polycrystal with non-trivial crystallite symmetry, before an orientation density function can be defined on it, one has to specify an SO(3) left-invariant volume measure on the orientation space. Once the orientation density function is defined, Roe's ODF can be defined naturally. See Definition 6.5 in Chap. 6.
3. The active view of rotations is implemented throughout the exposition. Adopting the active viewpoint is the standard practice in mathematics and has become increasingly popular in physics since the 1980s. In contrast, the passive view of rotations is dominant in the literature of texture analysis. Changing to the active view has the clear advantage of smooth transition to the literature of mathematics and physics, where plenty of known theorems and formulas are already available.
4. A conscientious effort was made to make better use of the machinery already available in the literature of mathematics and physics.[2] For example, it has been a common misconception in the mainstream of QTA that the definition of the generalized spherical

[2]This is a lesson learned the hard way from the historical development of quantitative texture analysis. As Matthies [218, p. 119] remarked in 1988: "From our point of view it is a somewhat 'tragic' circumstance for

functions (or equivalently the Wigner D-functions) would be tied up with the use of Euler angles as parameters of the rotation group, while there are applications where the parametrization in the axis-angle parameters are much more preferable. In fact the general formulas for the D-functions, one of which already appears in Wigner's 1931 book [340, p. 176, equation (21)] and its 1959 expanded English edition [341, p. 164, equation (15.21)]), are valid for all parametrizations of the rotation group, with which the Wigner D-functions in axis-angle parameters can be written down easily. See Sect. 14.2.2.

Comments on Contents

This exposition is divided into three parts. Part I on the rudiments of classical texture analysis is the core of the exposition, and we consider only polycrystalline aggregates of crystallites of the same species. By classical texture analysis is meant the treatment where the orientation distribution function (ODF) is defined on the rotation group SO(3). Such a treatment of the ODF requires the point group $G_{\rm cr}$ of the crystallites in question to be proper, i.e., a subgroup of SO(3), and leads to the practice in texture analysis that an improper $G_{\rm cr}$ is replaced by $G_{\rm cr}^{+}$, the proper point group in the Laue class of $G_{\rm cr}$. Carrying this logical wart notwithstanding, classical texture analysis has dominated the literature of quantitative texture analysis from its inception in the mid-1960s to this day.

Part I is a rewritten and much expanded version of lecture notes for a course in quantitative texture analysis for graduate students in Materials Engineering, Engineering Mechanics, and Mathematics. The lecture notes were written with the mathematical preparations of the engineering students in mind, which were typically limited to linear or matrix algebra and advanced multivariate calculus. In the rewriting I have added sections, remarks, and paragraphs, some of which refer to mathematics beyond the limits set for the lecture notes to aid deeper understanding. By including three mathematical appendices, and by indicating (either at the beginning of a chapter or in comments below) which sections and remarks can be skipped on a first reading, I hope that engineering students would still find Part I readable as a first course in quantitative texture analysis.

The reader can glance over the table of contents to get an idea of topics covered in this exposition. In what follows I will give short comments on each chapter to draw attention to points I want to emphasize.

Section A.1 in Appendix A. We review the fundamental concepts of sets, relations, and functions, partly for the purpose of specifying mathematical terminology and notation for the entire exposition.

Chapter 1. The basic mathematical properties of rotations are described, and their parametrizations by Euler angles and axis-angle parameters are presented. We compare our parametrization of rotations by Euler angles with several other conventions in the literature of texture analysis. In Sect. 1.10 we define a distance function on the set of rotations SO(3) so that it becomes a metric space.

Chapter 2. Here is a comprehensive introduction to ideal crystals and their associated space groups, lattice groups, lattices, and crystallographic point groups. Full derivations of the 32 geometric crystal classes and the 14 Bravais lattice-types are presented. Appendix A provides the prerequisites in group theory for reading this chapter. The theory of classical

QTA that the 'theoretical texturists' in the sixties do not use the already existing modern apparatus what [*sic*] leads to a confusion in descriptions, inaccuracies, partly repeated 'inventions of the bicycle', loss of possible simplifications and other things."

texture analysis, however, concerns only macro-texture, i.e., it is a macroscopic theory. As a consequence, only crystallographic point groups would figure prominently in the theory (see Sect. 2.11). Moreover, as the ODF is defined on the rotation group, the point group of the crystallites G_{cr} is by default a finite rotation group—by Proposition 2.16 crystallographic point groups are finite. Thus on a first reading, one may just focus on Sects. 2.1, 2.2, 2.4, 2.5.1, 2.5.2, and 2.11, where every crystallographic point group $\mathcal{K}$, in the restricted context of classical texture analysis, is understood to be proper. What the other sections cover will become indispensable when one studies methods of texture measurement.

Chapter 3. The central formula is that of the left-invariant integral (3.36) on SO(3), our derivation of which follows largely the presentations by Gel'fand et al. [125] and Naimark [244]. In this chapter we put the invariant integral on SO(3) as one example, albeit the most important one for our present purpose, in the context of Haar integrals. Doing so not only will enhance understanding but will also facilitate extensions to other situations, e.g., when SO(3) is replaced by the orthogonal group O(3) in some sections of Parts II and III.

Chapter 4. The ODF is introduced for triclinic aggregates of triclinic crystallites, a case that occupies a central position in the Roe approach. Relations between ODFs defined on active and passive rotations are given. The Wigner D-functions are defined, but the derivation of the defining formulas is left to Chap. 14 in Part III. Likewise, the Peter-Weyl theorem, which leads to the conclusion that the normalized Wigner D-functions form a Hilbert basis in the space of square-integrable, complex-valued functions on SO(3), is proved in Chap. 15. Nevertheless, in Chap. 4, some properties of the Wigner D-functions are derived, and several alternate expressions for the Wigner D-functions and alternate formulations for the series expansions of the ODF are presented and discussed.

Many readers of Bunge's classic [60] would be puzzled by his definition of generalized spherical harmonics. He refers [60, p. 351] the reader to Gel'fand et al. [125], Vilenkin [327], and Wigner [340] "for detailed representations of these functions and their properties". The expression of Bunge's generalized spherical harmonics T_l^{mn}, however, is nowhere to be found in any of the three references. Moreover, there does not seem to be a natural way to convert any of its counterparts in the three references to T_l^{mn}. In fact Bunge's T_l^{mn} are the same as the generalized spherical functions $T_{l,m,n}$ of Viglin [326], who obtained his expression earlier by tragicomical happenstance. He started with an erroneous formula[3] from the 1952 paper of Gel'fand and Šapiro [124, §7] for their generalized spherical functions T_{mn}^l and arrived at his $T_{l,m,n}$ by making a second mistake when he converted Gel'fand and Šapiro's formula for T_{mn}^l from the active to the passive view of rotations. See Sects. 4.5.2 and 4.5.3 for more details.

To the uninitiated, the basic formulas that involve the D-functions in Matthies [215] and Matthies et al. [224] will provoke head-scratching, because the authors use the same symbol[4] $D_{m,n}^l(\cdot)$ for what we shall denote by $D_{mn}^l(\cdot)$ and $\mathfrak{D}_{mn}^l(\cdot)$, the Wigner D-functions under the active and passive view of rotations, respectively. As a result, the formulas will be valid only if the $D_{m,n}^l(\cdot)$ in question are correctly identified as $D_{mn}^l(\cdot)$ or $\mathfrak{D}_{mn}^l(\cdot)$ as appropriate. In Sect. 4.5.4 we shall undertake the identification of $D_{m,n}^l(\cdot)$ in some of the most basic formulas that include the defining equation of $D_{m,n}^l(\cdot)$, the addition theorem for $D_{m,n}^l(\cdot)$, and the series expansion of the ODF.

Chapter 5. This chapter is a presentation of the Roe approach to account for crystallite symmetries and/or sample symmetries of polycrystals.

[3] Later corrected in Gel'fand et al. [125].

[4] Note the comma between m and n in the suffix of the symbol.

Chapter 6. Suppose a single-orientation measurement is made at a point in a polycrystal, which delivers the crystallite orientation at the point in question. If the polycrystal consists of triclinic crystallites, after a reference single crystal is chosen, the space of all possible crystallite orientations (or orientation space, for short) is SO(3). If the polycrystal has non-trivial crystallite symmetry, what is the orientation space? Roe did not raise this question in his papers. Bunge, on the other hand, in effect tackled this problem directly in his work. In Sect. 6.8 we illustrate the Bunge approach by a simple example. In this exposition, however, we mainly follow the Roe approach, where the ODF is always defined on the entire rotation group (although it should satisfy all the constraints on texture coefficients imposed by the presence of crystallite and/or sample symmetry), and in the harmonic method the ODF is always expanded as an infinite series of the Wigner D-functions. For a polycrystal with non-trivial crystallite symmetry, SO(3) isn't the space of crystallite orientations, and Roe's ODF isn't an orientation probability density on SO(3). But Roe's ODF, when restricted to a fundamental domain in SO(3) that represents the space of orientations, can still be used to compute probabilities. Fundamental domains, which are not mentioned in Roe's papers, are presented in outline in this chapter, whereas proofs of mathematical assertions are provided in Appendices B and C. All the main ideas about fundamental domains, the difference between Roe's ODF (orientation distribution functions) and the orientation density functions, and the difference between the Roe approach and the Bunge approach are apparent in the special case where $G_{\text{cr}} \neq \{\boldsymbol{I}\}$ and $G_{\text{tex}} = \{\boldsymbol{I}\}$, on which we focus our discussions in Sects. 6.1–6.3 (see also the paragraphs on this case in Sect. 6.7).

Chapter 7. Sections 7.3–7.4 are indispensable for understanding of X-ray crystallography.

Chapter 8. The central topic of this chapter is the original and the modified Bunge–Haessner method for evaluation of texture coefficients from data obtained by single-orientation measurements (e.g., through electron backscatter diffraction). A mathematical basis for the original Bunge–Haessner method is presented in Sect. 8.5.1.

Chapter 9 and Appendix D. To understand what information on texture that X-ray pole figures do and do not contain, one needs to have a basic grasp of the physics of X-ray diffraction by crystals. It is hoped that Appendix D would serve that purpose. As far as our intended application is concerned, the central role is played by formula (D.96) for the integrated intensity, from which we obtain the physical meaning of normalized intensity in pole figures. Moreover, it is the basis by which we infer which (hkl) pole figure of what crystal structure will suffer from systematic extinction, and by which we derive the conditions for Friedel's rule to hold. As for the methods of inversion of pole figures and ghost correction, the coverage is limited to those which my research group considered for implementation in our in-house computer programs.

Most of the chapters in Parts II and III are based on my lecture notes for a course in group representations and crystallographic texture for graduate students in Mathematics.

Chapter 10. Here is another derivation of the Haar integral on SO(3) in Euler angles, which is more straightforward than that in Chap. 3. The extension to the Haar integral on O(3) is also straightforward.

Chapter 11. This chapter provides further properties of rotations, including their relations to quaternions with unit norm in particular, which pave the way for derivation of the Wigner D-functions by Weyl's method in Chap. 14.

Chapter 12. This chapter gives a brief summary of some basics that pertain to texture analysis based on O(3) as discussed in [95, 206].

Chapter 13. This chapter presents some rudiments in group representations, which serve as prerequisites for the discussions in Chaps. 14–17.

Chapter 14. In this chapter Weyl's method is applied to derive a complete set of finite-dimensional, continuous, irreducible unitary representations of SU(2) and obtain general formulas for the Wigner D-functions as matrix elements of these representations under some chosen orthonormal bases. A parallel complete set of irreducible representations of SO(3) and the corresponding general formulas for Wigner D-functions defined on SO(3) follow easily. The general formulas are valid for any parametrization of SU(2) and of SO(3), respectively. For example, for Wigner D-functions defined on SO(3), explicit formulas can be written down in Euler angles and in axis-angle parameters. A complete set of irreducible representations of O(3) is given together with what we call the Wigner D-functions of O(3).

Chapter 15. This chapter presents an elementary proof of the Peter-Weyl theorem under the assumption that the compact group in question has a faithful representation, a condition met by matrix groups such as SO(3) and O(3). The Peter-Weyl theorem is central to the mathematical foundation for the harmonic method in texture analysis based on SO(3) or O(3).

Chapter 16. This chapter is an extended version of the mathematical preliminaries for proving the representation theorems in [95, 203].

Chapter 17. The objective of this chapter is to give an introduction to harmonic tensors, the tensorial Fourier expansion of the ODF, and the tensorial texture coefficients. The classical ODF expansion in Wigner D-functions is recast as a tensorial Fourier series under a special orthonormal basis in each of the spaces of harmonic tensors $\mathscr{H}^l$ $(l = 0, 1, 2, \ldots)$. The relation between the tensorial and classical texture coefficients in this context is discussed, first for triclinic aggregates of triclinic crystallites and then for polycrystals with texture and/or crystallite symmetry.

PART I. RUDIMENTS OF CLASSICAL TEXTURE ANALYSIS

Chapter 1

1 Parametrization of Rotations

1.1 Preliminaries in Vector Algebra

We start by recapitulating some elementary facts in vector algebra, which, besides serving as a quick review, will introduce the notation adopted in this exposition.

Let E^3 be the physical space, which we assume to be Euclidean and three-dimensional. Let V be the translation space[5] of E^3, which is a three-dimensional vector space over the reals $\mathbb{R}$. After selecting one point O in E^3 and calling it the origin, each vector $\boldsymbol{a}$ in V can be identified with a unique directed line segment **OP**. We denote the magnitude or norm of a vector $\boldsymbol{a}$ by $\|\boldsymbol{a}\|$, the scalar or dot product of two vectors $\boldsymbol{a}$ and $\boldsymbol{b}$ by $\langle \boldsymbol{a}, \boldsymbol{b} \rangle$ or $\boldsymbol{a} \cdot \boldsymbol{b}$, and their cross product by $\boldsymbol{a} \times \boldsymbol{b}$.

Let $\{\boldsymbol{e}_i : i = 1, 2, 3\}$ be a right-handed, orthonormal triad in V, i.e., the unit vectors $\boldsymbol{e}_i$ satisfy $\boldsymbol{e}_i \times \boldsymbol{e}_j = \boldsymbol{e}_k$ if (i, j, k) is a cyclic permutation of $(1, 2, 3)$ and $\boldsymbol{e}_i \cdot \boldsymbol{e}_j = \delta_{ij}$, where δ_{ij} is the Kronecker delta satisfying $\delta_{ij} = 0$ for $i \neq j$ and $\delta_{ij} = 1$ for $i = j$. Each vector $\boldsymbol{a}$ in V can be expressed as a linear combination of $\boldsymbol{e}_1$, $\boldsymbol{e}_2$, and $\boldsymbol{e}_3$:

$$\boldsymbol{a} = a_1\boldsymbol{e}_1 + a_2\boldsymbol{e}_2 + a_3\boldsymbol{e}_3 = \sum_{i=1}^{3} (\boldsymbol{a} \cdot \boldsymbol{e}_i)\boldsymbol{e}_i . \tag{1.1}$$

Since the vectors $\boldsymbol{e}_i$ are also linearly independent (i.e., $\sum_i \alpha_i \boldsymbol{e}_i = \boldsymbol{0}$ implies $\alpha_i = 0$ for all i) they constitute a basis in V. The numbers a_i are called the components or coordinates of the vector $\boldsymbol{a}$ under the basis $\{\boldsymbol{e}_i\}$. When there is no confusion about the basis chosen, we often write $\boldsymbol{a}$ as the row vector (a_1, a_2, a_3) or the column vector

$$(a_1, a_2, a_3)^T \equiv \begin{pmatrix} a_1 \\ a_2 \\ a_3 \end{pmatrix} .$$

While the row vector and the column vector in question are representations of the vector $\boldsymbol{a}$ under the basis $\{\boldsymbol{e}_i\}$, for convenience we shall often abuse the language and confuse them with $\boldsymbol{a}$ when the chosen basis is understood. In terms of the coordinates of $\boldsymbol{a}$ and $\boldsymbol{b}$ under the basis $\{\boldsymbol{e}_i\}$, we have the formulae

$$\|\boldsymbol{a}\| = \sqrt{a_1^2 + a_2^2 + a_3^2}, \qquad \boldsymbol{a} \cdot \boldsymbol{b} = a_1b_1 + a_2b_2 + a_3b_3, \tag{1.2}$$

$$\boldsymbol{a} \times \boldsymbol{b} = (a_2b_3 - a_3b_2)\boldsymbol{e}_1 + (a_3b_1 - a_1b_3)\boldsymbol{e}_2 + (a_1b_2 - a_2b_1)\boldsymbol{e}_3. \tag{1.3}$$

With few exceptions, we shall use right-handed orthonormal bases throughout this exposition.

[5] For a formal definition see, e.g., [40, p. 297].

1.1.1 Linear Transformations

A mapping (or transformation) $\boldsymbol{L} : V \longrightarrow V$ is linear if

$$\boldsymbol{L}(\alpha_1 \boldsymbol{a}_1 + \alpha_2 \boldsymbol{a}_2) = \alpha_1 \boldsymbol{L}\boldsymbol{a}_1 + \alpha_2 \boldsymbol{L}\boldsymbol{a}_2 \tag{1.4}$$

for any vectors $\boldsymbol{a}_1, \boldsymbol{a}_2$ in V and for any numbers α_1 and α_2 in $\mathbb{R}$. Let $\{\boldsymbol{e}_i\}$ be a right-handed, orthonormal triad in V. Let $\boldsymbol{b} = \sum_i b_i \boldsymbol{e}_i$, $\boldsymbol{a} = \sum_j a_j \boldsymbol{e}_j$, and $\boldsymbol{b} = \boldsymbol{L}\boldsymbol{a}$. Then

$$b_i = \boldsymbol{e}_i \cdot \boldsymbol{b} = \boldsymbol{e}_i \cdot \boldsymbol{L}\boldsymbol{a} = \boldsymbol{e}_i \cdot \sum_j a_j \boldsymbol{L}\boldsymbol{e}_j = \sum_j L_{ij} a_j, \tag{1.5}$$

where $L_{ij} = \boldsymbol{e}_i \cdot \boldsymbol{L}\boldsymbol{e}_j$. Thus, under the basis $\{\boldsymbol{e}_i\}$, $\boldsymbol{L}$ is represented by the 3×3 matrix $(L_{ij})_{1 \le i,j \le 3}$, and the equation $\boldsymbol{b} = \boldsymbol{L}\boldsymbol{a}$ assumes the form

$$\begin{pmatrix} b_1 \\ b_2 \\ b_3 \end{pmatrix} = \begin{pmatrix} L_{11} & L_{12} & L_{13} \\ L_{21} & L_{22} & L_{23} \\ L_{31} & L_{32} & L_{33} \end{pmatrix} \begin{pmatrix} a_1 \\ a_2 \\ a_3 \end{pmatrix}$$

$$= \begin{pmatrix} \boldsymbol{e}_1 \cdot \boldsymbol{L}\boldsymbol{e}_1 & \boldsymbol{e}_1 \cdot \boldsymbol{L}\boldsymbol{e}_2 & \boldsymbol{e}_1 \cdot \boldsymbol{L}\boldsymbol{e}_3 \\ \boldsymbol{e}_2 \cdot \boldsymbol{L}\boldsymbol{e}_1 & \boldsymbol{e}_2 \cdot \boldsymbol{L}\boldsymbol{e}_2 & \boldsymbol{e}_2 \cdot \boldsymbol{L}\boldsymbol{e}_3 \\ \boldsymbol{e}_3 \cdot \boldsymbol{L}\boldsymbol{e}_1 & \boldsymbol{e}_3 \cdot \boldsymbol{L}\boldsymbol{e}_2 & \boldsymbol{e}_3 \cdot \boldsymbol{L}\boldsymbol{e}_3 \end{pmatrix} \begin{pmatrix} a_1 \\ a_2 \\ a_3 \end{pmatrix}. \tag{1.6}$$

From the preceding equation, we observe that the matrix representing $\boldsymbol{L}$ under basis $\{\boldsymbol{e}_i\}$ has its columns given by the column vectors representing $\boldsymbol{L}\boldsymbol{e}_1$, $\boldsymbol{L}\boldsymbol{e}_2$, and $\boldsymbol{L}\boldsymbol{e}_3$ under the same basis. Henceforth, for brevity, we shall often write this matrix as $[\boldsymbol{L}\boldsymbol{e}_1, \boldsymbol{L}\boldsymbol{e}_2, \boldsymbol{L}\boldsymbol{e}_3]$, which we may confuse with the linear transformation $\boldsymbol{L}$ itself when we fix and work only with one set of basis $\{\boldsymbol{e}_i\}$.

For a linear transformation $\boldsymbol{L}$ on V, we define the mapping $\boldsymbol{L}^T : V \longrightarrow V$ by

$$\langle \boldsymbol{L}^T \boldsymbol{a}, \boldsymbol{b} \rangle = \langle \boldsymbol{a}, \boldsymbol{L}\boldsymbol{b} \rangle \quad \text{or} \quad \boldsymbol{L}^T \boldsymbol{a} \cdot \boldsymbol{b} = \boldsymbol{a} \cdot \boldsymbol{L}\boldsymbol{b} \tag{1.7}$$

for any vectors $\boldsymbol{a}$ and $\boldsymbol{b}$ in V. It is straightforward to show that the mapping $\boldsymbol{L}^T$ thus defined is linear. Under an orthonormal basis $\{\boldsymbol{e}_i\}$, we have

$$(L^T)_{ij} = \boldsymbol{e}_i \cdot \boldsymbol{L}^T \boldsymbol{e}_j = \boldsymbol{e}_j \cdot \boldsymbol{L}\boldsymbol{e}_i = L_{ji}, \tag{1.8}$$

where $(L^T)_{ij}$ denotes the ij-th entry of the matrix $[\boldsymbol{L}^T\boldsymbol{e}_1, \boldsymbol{L}^T\boldsymbol{e}_2, \boldsymbol{L}^T\boldsymbol{e}_3]$ representing $\boldsymbol{L}^T$. Thus $\boldsymbol{L}^T$ is represented by the transpose of the matrix $(L_{ij})_{1 \le i,j \le 3}$ that represents $\boldsymbol{L}$. We call $\boldsymbol{L}^T$ the transpose of $\boldsymbol{L}$.

A linear transformation $\boldsymbol{L}$ on V is symmetric (resp. skew-symmetric) if it satisfies the condition $\boldsymbol{L} = \boldsymbol{L}^T$ (resp. $\boldsymbol{L} = -\boldsymbol{L}^T$). The entries of the matrix $[L_{ij}]$ that represents a symmetric (resp. skew-symmetric) linear transformation $\boldsymbol{L}$ under the orthonormal basis $\{\boldsymbol{e}_i : i = 1, 2, 3\}$ satisfies the condition $L_{ij} = L_{ji}$ (resp. $L_{ij} = -L_{ji}$).

For linear transformations $\boldsymbol{L}$, $\boldsymbol{L}_1$ and $\boldsymbol{L}_2$ on V and a real number α, we denote by $\boldsymbol{L}_1 + \boldsymbol{L}_2$ and $\alpha \boldsymbol{L}$ the linear transformations defined by

$$(\boldsymbol{L}_1 + \boldsymbol{L}_2)\boldsymbol{a} = \boldsymbol{L}_1 \boldsymbol{a} + \boldsymbol{L}_2 \boldsymbol{a}, \tag{1.9}$$

$$(\alpha \boldsymbol{L})\boldsymbol{a} = \alpha(\boldsymbol{L}\boldsymbol{a}) \tag{1.10}$$

for each vector $\boldsymbol{a}$ in V, respectively. With addition and scalar multiplication defined as in (1.9) and (1.10), we see that the set of linear transformations on V constitutes itself a vector space over $\mathbb{R}$. We denote this vector space by Lin.

Let Sym and Skw be the set of symmetric and skew-symmetric linear transformations on V, respectively. It is easy to verify that both Sym and Skw are linear subspaces of Lin.

For $\boldsymbol{L}_1$ and $\boldsymbol{L}_2$ in Lin, we denote by $\boldsymbol{L}_2\boldsymbol{L}_1$ the composition $\boldsymbol{L}_2 \circ \boldsymbol{L}_1$ defined by

$$(\boldsymbol{L}_2\boldsymbol{L}_1)\boldsymbol{a} = (\boldsymbol{L}_2 \circ \boldsymbol{L}_1)\boldsymbol{a} = \boldsymbol{L}_2(\boldsymbol{L}_1\boldsymbol{a}) \tag{1.11}$$

for each vector $\boldsymbol{a}$ in V. It is clear that the mapping $\boldsymbol{L}_2\boldsymbol{L}_1$ is linear.

1.1.2 Tensor Product of Two Vectors

For two vectors $\boldsymbol{a}$ and $\boldsymbol{b}$ in V, the tensor product $\boldsymbol{a} \otimes \boldsymbol{b}$ is the linear transformation defined by

$$(\boldsymbol{a} \otimes \boldsymbol{b})\boldsymbol{c} = (\boldsymbol{b} \cdot \boldsymbol{c})\boldsymbol{a} \tag{1.12}$$

for each vector $\boldsymbol{c}$ in V. Under the orthonormal basis $\{\boldsymbol{e}_i\}$, $\boldsymbol{a} \otimes \boldsymbol{b}$ is represented by the matrix whose ij-th entry is

$$\boldsymbol{e}_i \cdot (\boldsymbol{a} \otimes \boldsymbol{b})\boldsymbol{e}_j = \langle \boldsymbol{e}_i, (\boldsymbol{b} \cdot \boldsymbol{e}_j)\boldsymbol{a} \rangle = (\boldsymbol{b} \cdot \boldsymbol{e}_j)(\boldsymbol{e}_i \cdot \boldsymbol{a}) = a_i b_j. \tag{1.13}$$

In particular, we have $\boldsymbol{e}_i \otimes \boldsymbol{e}_j$ represented by the matrix with its ij-th entry equal to 1 and all other entries zero. Since $(\boldsymbol{a} \otimes \boldsymbol{b})(\boldsymbol{c} \otimes \boldsymbol{d})\boldsymbol{f} = (\boldsymbol{a} \otimes \boldsymbol{b})((\boldsymbol{d} \cdot \boldsymbol{f})\boldsymbol{c}) = (\boldsymbol{d} \cdot \boldsymbol{f})(\boldsymbol{b} \cdot \boldsymbol{c})\boldsymbol{a} = (\boldsymbol{b} \cdot \boldsymbol{c})((\boldsymbol{a} \otimes \boldsymbol{d})\boldsymbol{f})$ for each vector $\boldsymbol{f}$ in V, we have

$$(\boldsymbol{a} \otimes \boldsymbol{b})(\boldsymbol{c} \otimes \boldsymbol{d}) = (\boldsymbol{b} \cdot \boldsymbol{c})\boldsymbol{a} \otimes \boldsymbol{d}. \tag{1.14}$$

Another property of $\boldsymbol{a} \otimes \boldsymbol{b}$ that we shall sometimes use below is

$$(\boldsymbol{a} \otimes \boldsymbol{b})^T = \boldsymbol{b} \otimes \boldsymbol{a}, \tag{1.15}$$

the validity of which is obvious.

We call the linear space over $\mathbb{R}$ generated by the tensor products of two vectors in V the space of second-order tensors, which we denote by $V \otimes V$. By definition, every tensor product of two vectors $\boldsymbol{a} \otimes \boldsymbol{b} \in V \otimes V$ is in Lin. Clearly we have $V \otimes V \subset \text{Lin}$. On the other hand, let $\{\boldsymbol{e}_i\}$ be a right-handed, orthonormal basis in V. Each linear transformation on V may be written as

$$\boldsymbol{L} = \sum_{i,j} L_{ij}\boldsymbol{e}_i \otimes \boldsymbol{e}_j, \quad \text{where} \quad L_{ij} = \boldsymbol{e}_i \cdot \boldsymbol{L}\boldsymbol{e}_j, \tag{1.16}$$

as a glance at the matrix representing $\boldsymbol{L}$ under $\{\boldsymbol{e}_i\}$ reveals. Thus $\text{Lin} \subset V \otimes V$. It follows that $V \otimes V = \text{Lin}$.

For any two linear transformations $\boldsymbol{L}$ and $\boldsymbol{M}$ on V, we have

$$\begin{aligned} \boldsymbol{L}\boldsymbol{M} &= \left(\sum_{i,j} L_{ij}\boldsymbol{e}_i \otimes \boldsymbol{e}_j \right) \left(\sum_{k,l} M_{kl}\boldsymbol{e}_k \otimes \boldsymbol{e}_l \right) \\ &= \sum_{i,j} \sum_{k,l} L_{ij} M_{kl} \left(\boldsymbol{e}_i \otimes \boldsymbol{e}_j \right) (\boldsymbol{e}_k \otimes \boldsymbol{e}_l) \end{aligned}$$

$$= \sum_{i,j} \sum_{k,l} L_{ij} M_{kl} \delta_{jk} \boldsymbol{e}_i \otimes \boldsymbol{e}_l$$

$$= \sum_{i,l} \left(\sum_{k} L_{ik} M_{kl} \right) \boldsymbol{e}_i \otimes \boldsymbol{e}_l.$$

It follows that the ij-th entry of the matrix representing $\boldsymbol{L}\boldsymbol{M}$ under $\{\boldsymbol{e}_i\}$ is

$$(LM)_{ij} = \boldsymbol{e}_i \cdot \boldsymbol{L}\boldsymbol{M}\boldsymbol{e}_j = \sum_{k=1}^{3} L_{ik} M_{kj}, \tag{1.17}$$

which defines the rule of multiplication between the matrices $[\boldsymbol{L}\boldsymbol{e}_1, \boldsymbol{L}\boldsymbol{e}_2, \boldsymbol{L}\boldsymbol{e}_3]$ and $[\boldsymbol{M}\boldsymbol{e}_1, \boldsymbol{M}\boldsymbol{e}_2, \boldsymbol{M}\boldsymbol{e}_3]$.

Let $\boldsymbol{I} : V \longrightarrow V$ be the identity mapping, i.e., $\boldsymbol{I}\boldsymbol{a} = \boldsymbol{a}$ for each vector $\boldsymbol{a}$ in V. It is easy to verify that

$$\boldsymbol{I} = \sum_{i=1}^{3} \boldsymbol{e}_i \otimes \boldsymbol{e}_i. \tag{1.18}$$

1.1.3 Change of Orthonormal Basis

Let $\{\boldsymbol{e}'_i : i = 1, 2, 3\}$ be another right-handed orthonormal triad, and let $\boldsymbol{P}$ be the linear transformation on V that satisfies

$$\boldsymbol{P}\boldsymbol{e}_i = \boldsymbol{e}'_i \qquad \text{for} \quad i = 1, 2, 3. \tag{1.19}$$

Let $\boldsymbol{a} = \sum_i a_i \boldsymbol{e}_i$ and $\boldsymbol{b} = \sum_j b_j \boldsymbol{e}_j$ be vectors in V. Then $\boldsymbol{P}\boldsymbol{a} = \sum_i a_i \boldsymbol{e}'_i$ and $\boldsymbol{P}\boldsymbol{b} = \sum_j b_j \boldsymbol{e}'_j$. We observe that $\boldsymbol{P}$ satisfies

$$\boldsymbol{P}\boldsymbol{a} \cdot \boldsymbol{P}\boldsymbol{b} = \boldsymbol{a} \cdot \boldsymbol{b} \tag{1.20}$$

for any two vectors $\boldsymbol{a}$ and $\boldsymbol{b}$ in V.

A linear transformation $\boldsymbol{Q}$ on V which, like $\boldsymbol{P}$, satisfies (1.20) is said to be orthogonal. It follows from (1.7) and (1.20) that $\boldsymbol{Q}^T\boldsymbol{Q}\boldsymbol{a} \cdot \boldsymbol{b} = \boldsymbol{a} \cdot \boldsymbol{b}$ for all vectors $\boldsymbol{a}, \boldsymbol{b} \in V$, which implies

$$\boldsymbol{Q}^T\boldsymbol{Q} = \boldsymbol{I}. \tag{1.21}$$

Equation (1.21) shows that $\boldsymbol{Q}^T = \boldsymbol{Q}^{-1}$, the inverse of $\boldsymbol{Q}$. Thus we have also $\boldsymbol{Q}\boldsymbol{Q}^T = \boldsymbol{I}$. Let $\det \boldsymbol{Q}$ denote the determinant of $\boldsymbol{Q}$. Taking the determinant of both sides of (1.21), we obtain

$$(\det \boldsymbol{Q}^T)(\det \boldsymbol{Q}) = (\det \boldsymbol{Q})^2 = 1, \quad \text{or} \quad \det \boldsymbol{Q} = \pm 1. \tag{1.22}$$

By (1.20), we see that $\|\boldsymbol{Q}\boldsymbol{a}\| = \|\boldsymbol{a}\|$ for each vector $\boldsymbol{a}$ in V and

$$\frac{\boldsymbol{Q}\boldsymbol{a} \cdot \boldsymbol{Q}\boldsymbol{b}}{\|\boldsymbol{Q}\boldsymbol{a}\| \|\boldsymbol{Q}\boldsymbol{b}\|} = \frac{\boldsymbol{a} \cdot \boldsymbol{b}}{\|\boldsymbol{a}\| \|\boldsymbol{b}\|}$$

for $\boldsymbol{a} \neq \boldsymbol{0}$ and $\boldsymbol{b} \neq \boldsymbol{0}$. Thus $\boldsymbol{Q}$ preserves the lengths of vectors and the angles between them.

An orthogonal transformation $\boldsymbol{R}$ which satisfies $\det \boldsymbol{R} = 1$ is called a rotation. For the orthogonal transformation $\boldsymbol{P}$ defined by (1.19), which pertains to a change of right-handed orthonormal basis, we have $\det \boldsymbol{P} = \det \boldsymbol{P}^T = \boldsymbol{P}\boldsymbol{e}_1 \cdot (\boldsymbol{P}\boldsymbol{e}_2 \times \boldsymbol{P}\boldsymbol{e}_3) = \boldsymbol{e}'_1 \cdot (\boldsymbol{e}'_2 \times \boldsymbol{e}'_3) = 1$. Hence the orthogonal transformation $\boldsymbol{P}$ that defines a change of right-handed orthonormal basis in (1.19) is a rotation.

Expanding $\boldsymbol{P}\boldsymbol{e}_i$ as a linear combination of the basis $\boldsymbol{e}_1, \boldsymbol{e}_2$, and $\boldsymbol{e}_3$, we recast (1.19) as

$$\boldsymbol{e}'_j = \sum_{i=1}^{3} (\boldsymbol{e}_i \cdot \boldsymbol{P}\boldsymbol{e}_j)\boldsymbol{e}_i = \sum_{i=1}^{3} P_{ij}\boldsymbol{e}_i, \tag{1.23}$$

where $P_{ij} = \boldsymbol{e}_i \cdot \boldsymbol{P}\boldsymbol{e}_j$ and $[P] := [P_{ij}]$ is called the matrix of change of basis from $\{\boldsymbol{e}_i\}$ to $\{\boldsymbol{e}'_i\}$. For $\boldsymbol{a} \in V$, let $a_i = \boldsymbol{a} \cdot \boldsymbol{e}_i$ and $a'_i = \boldsymbol{a} \cdot \boldsymbol{e}'_i$ be the components of $\boldsymbol{a}$ with respect to the bases $\{\boldsymbol{e}_i\}$ and $\{\boldsymbol{e}'_i\}$, respectively. Writing $\boldsymbol{a}$ as linear combinations of the two bases, we obtain

$$\sum_i a_i \boldsymbol{e}_i = \sum_j a'_j \boldsymbol{e}'_j = \sum_j a'_j \left(\sum_i P_{ij} \boldsymbol{e}_i \right) = \sum_i \left(\sum_j P_{ij} a'_j \right) \boldsymbol{e}_i,$$

which implies

$$a_i = \sum_{j=1}^{3} P_{ij} a'_j, \qquad (i = 1, 2, 3) \tag{1.24}$$

or

$$\begin{pmatrix} a_1 \\ a_2 \\ a_3 \end{pmatrix} = \begin{pmatrix} \boldsymbol{e}_1 \cdot \boldsymbol{P}\boldsymbol{e}_1 & \boldsymbol{e}_1 \cdot \boldsymbol{P}\boldsymbol{e}_2 & \boldsymbol{e}_1 \cdot \boldsymbol{P}\boldsymbol{e}_3 \\ \boldsymbol{e}_2 \cdot \boldsymbol{P}\boldsymbol{e}_1 & \boldsymbol{e}_2 \cdot \boldsymbol{P}\boldsymbol{e}_2 & \boldsymbol{e}_2 \cdot \boldsymbol{P}\boldsymbol{e}_3 \\ \boldsymbol{e}_3 \cdot \boldsymbol{P}\boldsymbol{e}_1 & \boldsymbol{e}_3 \cdot \boldsymbol{P}\boldsymbol{e}_2 & \boldsymbol{e}_3 \cdot \boldsymbol{P}\boldsymbol{e}_3 \end{pmatrix} \begin{pmatrix} a'_1 \\ a'_2 \\ a'_3 \end{pmatrix}. \tag{1.25}$$

Note that

$$\boldsymbol{e}'_i \cdot \boldsymbol{P}\boldsymbol{e}'_j = \boldsymbol{P}\boldsymbol{e}_i \cdot \boldsymbol{P}\boldsymbol{P}\boldsymbol{e}_j = \boldsymbol{e}_i \cdot \boldsymbol{P}\boldsymbol{e}_j \qquad \text{for all } 1 \le i \le 3,\ 1 \le j \le 3. \tag{1.26}$$

Hence the matrix that represents $\boldsymbol{P}$ under the basis $\{\boldsymbol{e}'_i\}$ is the same as that under $\{\boldsymbol{e}_i\}$.

Under different bases, the same linear transformation $\boldsymbol{L}$ is represented by different matrices. The ij-th entry L'_{ij} of the matrix representing $\boldsymbol{L}$ under the basis $\{\boldsymbol{e}'_i\}$ is related to the elements L_{kl} of the matrix representing $\boldsymbol{L}$ under $\{\boldsymbol{e}_i\}$ by

$$\begin{aligned} L'_{ij} &= \boldsymbol{e}'_i \cdot \boldsymbol{L}\boldsymbol{e}'_j = \boldsymbol{P}\boldsymbol{e}_i \cdot \boldsymbol{L}\boldsymbol{P}\boldsymbol{e}_j \\ &= \boldsymbol{e}_i \cdot \boldsymbol{P}^T \boldsymbol{L}\boldsymbol{P}\boldsymbol{e}_j = \sum_{k,l} P_{ki} P_{lj} L_{kl} \qquad (1.27) \\ &= \boldsymbol{e}_i \cdot \boldsymbol{P}^{-1} \boldsymbol{L}\boldsymbol{P}\boldsymbol{e}_j = \sum_{k,l} P^{-1}_{ik} L_{kl} P_{lj}. \qquad (1.28) \end{aligned}$$

When there is no confusion about the specific basis chosen, we shall denote the matrix representing linear transformation $\boldsymbol{L}$ under the given basis by $(L_{ij})_{1 \le i,j \le 3}$ or simply by $[L]$ or $[L_{ij}]$. We shall write this matrix as $[\boldsymbol{L}\boldsymbol{e}_1, \boldsymbol{L}\boldsymbol{e}_2, \boldsymbol{L}\boldsymbol{e}_3]$ if we want to specify the orthonormal basis $\{\boldsymbol{e}_i\}$ in question.

Remark 1.1 In line with the convention commonly adopted in the literature of crystallography (see, e.g., [133, 241]), we shall, in some contexts where no confusion should arise, let $\boldsymbol{P}$ denote the matrix $P := [P_{ij}]$ and $\boldsymbol{a}'$, $\boldsymbol{a}$ stand for the column vectors $[a'_i]$, $[a_j]$, which represent the same vector under the bases $\{\boldsymbol{e}'_i\}$ and $\{\boldsymbol{e}_i\}$, respectively, and write (1.25) as

$$\boldsymbol{a} = \boldsymbol{P}\boldsymbol{a}'. \tag{1.29}$$

It follows from (1.29) that

$$\boldsymbol{a}' = \boldsymbol{P}^{-1}\boldsymbol{a} \qquad \text{or} \qquad \boldsymbol{a}' = \boldsymbol{P}^{T}\boldsymbol{a}, \tag{1.30}$$

because $\boldsymbol{P}$ is a rotation. In contrast to (1.19), where $\boldsymbol{P}$ is a linear transformation that maps each basis vector $\boldsymbol{e}_i$ $(i = 1, 2, 3)$ to a new basis vector $\boldsymbol{e}'_i$, in equations (1.29) and (1.30) $\boldsymbol{P}$ stands for the matrix $[P]$ or $[P_{ij}]$ of change of basis, which relates the coordinates of the same vector in V under the two orthonormal basis $\{\boldsymbol{e}'_i\}$ and $\{\boldsymbol{e}_i\}$. Under this convention, equation (1.28) is transcribed as

$$\boldsymbol{L}' = \boldsymbol{P}^{-1}\boldsymbol{L}\boldsymbol{P}, \tag{1.31}$$

which means the matrix equation

$$[\boldsymbol{L}\boldsymbol{e}'_1, \boldsymbol{L}\boldsymbol{e}'_2, \boldsymbol{L}\boldsymbol{e}'_3] = [P]^{-1}[\boldsymbol{L}\boldsymbol{e}_1, \boldsymbol{L}\boldsymbol{e}_2, \boldsymbol{L}\boldsymbol{e}_3][P] \tag{1.32}$$

when written in full. □

1.2 Affine Coordinate Systems

In crystallography it is essential to adopt a coordinate system adapted to the translational symmetries of the crystal in question. That means, in most cases, a suitable basis in V will not be orthonormal. Let $\boldsymbol{f}_j$ $(j = 1, 2, 3)$ be three vectors in V such that $J := \boldsymbol{f}_1 \cdot \boldsymbol{f}_2 \times \boldsymbol{f}_3 > 0$. They constitute a right-handed basis in V. The choice of an origin $\boldsymbol{O}$ and a right-handed basis $\{\boldsymbol{f}_i\}$ in V defines an (right-handed) affine coordinate system in E^3. Under this choice, each place in E^3 is specified by a position vector

$$\boldsymbol{x} = x^1\boldsymbol{f}_1 + x^2\boldsymbol{f}_2 + x^3\boldsymbol{f}_3, \tag{1.33}$$

and the map $\boldsymbol{x} \mapsto (x^1, x^2, x^3)$ sets up a one-to-one correspondence between E^3 and $\mathbb{R}^3$.

In this section we adopt the Einstein summation convention, namely: whenever an index appears twice in an expression, that index is to be summed over all its possible values. For example, $\delta^i{}_i = \delta^1{}_1 + \delta^2{}_2 + \delta^3{}_3 = 3$, and (1.33) appears as $\boldsymbol{x} = x^i\boldsymbol{f}_i$ under this convention.

1.2.1 Basis and Reciprocal Basis

Define three vectors $\boldsymbol{f}^i$ $(i = 1, 2, 3)$ in V by the equations

$$\boldsymbol{f}^1 = \frac{\boldsymbol{f}_2 \times \boldsymbol{f}_3}{J}, \qquad \boldsymbol{f}^2 = \frac{\boldsymbol{f}_3 \times \boldsymbol{f}_1}{J}, \qquad \boldsymbol{f}^3 = \frac{\boldsymbol{f}_1 \times \boldsymbol{f}_2}{J}. \tag{1.34}$$

By the vector identity $(\boldsymbol{u} \times \boldsymbol{v}) \times \boldsymbol{w} = (\boldsymbol{u} \cdot \boldsymbol{w})\boldsymbol{v} - (\boldsymbol{v} \cdot \boldsymbol{w})\boldsymbol{u}$, it is easy to verify that

$$\boldsymbol{f}^1 \cdot \boldsymbol{f}^2 \times \boldsymbol{f}^3 = \frac{1}{J}; \tag{1.35}$$

thus $\{\boldsymbol{f}^i : i = 1, 2, 3\}$ also constitutes a right-handed basis in V. Using again the aforementioned vector identity and (1.34), we easily obtain by direct computations that

$$\boldsymbol{f}_1 = J(\boldsymbol{f}^2 \times \boldsymbol{f}^3), \qquad \boldsymbol{f}_2 = J(\boldsymbol{f}^3 \times \boldsymbol{f}^1), \qquad \boldsymbol{f}_3 = J(\boldsymbol{f}^1 \times \boldsymbol{f}^2). \tag{1.36}$$

The bases $\{\boldsymbol{f}^i\}$ and $\{\boldsymbol{f}_j\}$ satisfy the equations

$$\boldsymbol{f}^i \cdot \boldsymbol{f}_j = \boldsymbol{f}_i \cdot \boldsymbol{f}^j = \delta^i{}_j = \delta_i{}^j = \begin{cases} 1 & \text{if } i = j, \\ 0 & \text{if } i \neq j, \end{cases} \quad \text{for all } i, j = 1, 2, 3 \tag{1.37}$$

and are said to be reciprocal to each other.

Any vector $\boldsymbol{u} \in V$ can be written as

$$\boldsymbol{u} = u^i \boldsymbol{f}_i \qquad \text{and} \qquad \boldsymbol{u} = u_i \boldsymbol{f}^i, \tag{1.38}$$

where u^i and u_i $(i = 1, 2, 3)$ are called the contravariant and covariant components of $\boldsymbol{u}$, respectively. It follows from (1.37) and (1.38) that

$$u^i = \boldsymbol{f}^i \cdot \boldsymbol{u}, \qquad u_i = \boldsymbol{f}_i \cdot \boldsymbol{u}, \qquad \text{for } i = 1, 2, 3 \tag{1.39}$$

and

$$\boldsymbol{u} = (\boldsymbol{u} \cdot \boldsymbol{f}^i)\boldsymbol{f}_i = (\boldsymbol{u} \cdot \boldsymbol{f}_i)\boldsymbol{f}^i. \tag{1.40}$$

From (1.40) we observe that

$$\boldsymbol{I} = \boldsymbol{f}_i \otimes \boldsymbol{f}^i = \boldsymbol{f}^i \otimes \boldsymbol{f}_i. \tag{1.41}$$

Let $\boldsymbol{L} : V \to V$ be a linear transformation on V. Let $\boldsymbol{v} = \boldsymbol{L}\boldsymbol{u}$. Then we have

$$v^k \boldsymbol{f}_k = \boldsymbol{L}(u^j \boldsymbol{f}_j).$$

Taking the dot product of both sides of the preceding equation with $\boldsymbol{f}^i$, we obtain

$$\boldsymbol{f}^i \cdot v^k \boldsymbol{f}_k = \boldsymbol{f}^i \cdot \boldsymbol{L}(u^j \boldsymbol{f}_j),$$

or

$$v^k \delta^i{}_k = (\boldsymbol{f}^i \cdot \boldsymbol{L}\boldsymbol{f}_j)u^j.$$

Thus follows the equation

$$v^i = L^i{}_j u^j = (\boldsymbol{f}^i \cdot \boldsymbol{L}\boldsymbol{f}_j)u^j, \tag{1.42}$$

where $L^i{}_j := \boldsymbol{f}^i \cdot \boldsymbol{L}\boldsymbol{f}_j$ is the ij-th entry of the matrix $[L^i{}_j]$ that represents the linear transformation $\boldsymbol{L}$ under the basis $\{\boldsymbol{f}_i \otimes \boldsymbol{f}^j\}$.

1.2.2 Change of Basis

Let $\{\boldsymbol{g}_i : i = 1, 2, 3\}$ be another right-handed basis in V and $\{\boldsymbol{g}^l\}$ the corresponding reciprocal basis. Let $\boldsymbol{A}, \boldsymbol{B} : V \to V$ be defined by

$$\boldsymbol{g}_i = \boldsymbol{A}\boldsymbol{f}_i = (\boldsymbol{f}^j \cdot \boldsymbol{A}\boldsymbol{f}_i)\boldsymbol{f}_j = A^j{}_i \boldsymbol{f}_j, \tag{1.43}$$

$$\boldsymbol{g}^l = \boldsymbol{B}\boldsymbol{f}^l = (\boldsymbol{f}_k \cdot \boldsymbol{B}\boldsymbol{f}^l)\boldsymbol{f}^k = B_k{}^l \boldsymbol{f}^k, \tag{1.44}$$

where $\boldsymbol{A} = A^j{}_i \boldsymbol{f}_j \otimes \boldsymbol{f}^i$, $\boldsymbol{B} = B_k{}^l \boldsymbol{f}^k \otimes \boldsymbol{f}_l$, $A^j{}_i = \boldsymbol{f}^j \cdot \boldsymbol{A}\boldsymbol{f}_i$, and $B_k{}^l = \boldsymbol{f}_k \cdot \boldsymbol{B}\boldsymbol{f}^l$. Note that

$$\begin{aligned} \delta^l{}_i = \boldsymbol{g}^l \cdot \boldsymbol{g}_i &= B_k{}^l \boldsymbol{f}^k \cdot A^j{}_i \boldsymbol{f}_j \\ &= B_k{}^l A^j{}_i \delta^k{}_j \\ &= A^k{}_i B_k{}^l = (A^T)_i{}^k B_k{}^l, \end{aligned} \tag{1.45}$$

where we have appealed to the fact that

$$A^k{}_i = \boldsymbol{f}^k \cdot \boldsymbol{A}\boldsymbol{f}_i = \boldsymbol{f}_i \cdot \boldsymbol{A}^T \boldsymbol{f}^k = (A^T)_i{}^k. \tag{1.46}$$

It follows from (1.45) that

$$\boldsymbol{A}^T \boldsymbol{B} = \boldsymbol{I} \qquad \text{or} \qquad \boldsymbol{A}^T = \boldsymbol{B}^{-1}. \tag{1.47}$$

Note that by (1.43), (1.44), and (1.47) there holds

$$\boldsymbol{f}^j \cdot \boldsymbol{A}\boldsymbol{f}_i = \boldsymbol{B}^{-1}\boldsymbol{g}^j \cdot \boldsymbol{g}_i = \boldsymbol{g}^j \cdot \boldsymbol{A}\boldsymbol{g}_i. \tag{1.48}$$

Hence the entries $A^i{}_j$ of $[A^i{}_j]$, which is called the matrix of the basis transformation from $\{\boldsymbol{f}_i\}$ to $\{\boldsymbol{g}_k\}$, are independent of whether the basis $\{\boldsymbol{f}_i\}$ or the basis $\{\boldsymbol{g}_i\}$ is used to define them.

We proceed to examine the transformations of components of a vector due to change of bases. Let

$$\boldsymbol{v} = v^i \boldsymbol{f}_i = \widetilde{v}^i \boldsymbol{g}_i \tag{1.49}$$

$$= v_i \boldsymbol{f}^i = \widetilde{v}_i \boldsymbol{g}^i. \tag{1.50}$$

By (1.43) and (1.49), we have

$$v^i \boldsymbol{f}_i = \widetilde{v}^j A^i{}_j \boldsymbol{f}_i, \tag{1.51}$$

which implies

$$v^i = A^i{}_j \widetilde{v}^j. \tag{1.52}$$

Similarly, by (1.44) and (1.50), we get

$$v_j \boldsymbol{f}^j = \widetilde{v}_i B_j{}^i \boldsymbol{f}^j, \tag{1.53}$$

which implies

$$v_j = B_j{}^i \widetilde{v}_i \qquad \text{or} \qquad \widetilde{v}_i = (A^T)_i{}^j v_j, \tag{1.54}$$

where have made use of the fact that $\boldsymbol{A}^T = \boldsymbol{B}^{-1}$. Note that (1.52) and (1.54) reduce to (1.29) and (1.30), respectively, when the basis $\{\boldsymbol{f}_i\}$ is orthonormal.

Let $\widetilde{L}^k_{\ l} := \boldsymbol{g}^k \cdot \boldsymbol{L}\boldsymbol{g}_l$. Using (1.40) and (1.42), we obtain

$$\begin{aligned}\widetilde{L}^k_{\ l} &= (\boldsymbol{g}^k \cdot \boldsymbol{f}_i)\boldsymbol{f}^i \cdot \boldsymbol{L}(\boldsymbol{g}_l \cdot \boldsymbol{f}^j)\boldsymbol{f}_j = (\boldsymbol{g}^k \cdot \boldsymbol{f}_i)(\boldsymbol{f}^i \cdot \boldsymbol{L}\boldsymbol{f}_j)(\boldsymbol{g}_l \cdot \boldsymbol{f}^j) \\ &= (\boldsymbol{g}^k \cdot \boldsymbol{f}_i)L^i_{\ j}(\boldsymbol{f}^j \cdot \boldsymbol{g}_l) = (A^{-1})^k_{\ i}L^i_{\ j}A^j_{\ l}, \end{aligned} \tag{1.55}$$

where we have made use of the identities

$$\begin{aligned}\boldsymbol{g}_l \cdot \boldsymbol{f}^j &= \boldsymbol{A}\boldsymbol{f}_l \cdot \boldsymbol{f}^j = \boldsymbol{f}^j \cdot \boldsymbol{A}\boldsymbol{f}_l = A^j_{\ l}, \\ \boldsymbol{g}^k \cdot \boldsymbol{f}_i &= \boldsymbol{B}\boldsymbol{f}^k \cdot \boldsymbol{f}_i = \boldsymbol{f}^k \cdot \boldsymbol{B}^T\boldsymbol{f}_i = \boldsymbol{f}^k \cdot \boldsymbol{A}^{-1}\boldsymbol{f}_i = (A^{-1})^k_{\ i}.\end{aligned}$$

Remark 1.2 In the literature of crystallography a commonly used convention is to use boldfaced letters to denote column vectors and matrices (cf. Remark 1.1). Under this convention, equations (1.52) and (1.55) appear as

$$\boldsymbol{v} = \boldsymbol{A}\widetilde{\boldsymbol{v}} \qquad \text{and} \qquad \widetilde{\boldsymbol{L}} = \boldsymbol{A}^{-1}\boldsymbol{L}\boldsymbol{A}, \tag{1.56}$$

respectively. □

1.3 Space of Linear Transformations

Let $\{\boldsymbol{e}_i\}$ be an orthonormal basis in V. We have already seen in Sect. 1.1.1 that the set of linear transformations on V is itself a vector space, which we call Lin. Because each $\boldsymbol{L}$ in Lin can be expressed (see (1.16)) as a linear combination of $\boldsymbol{e}_i \otimes \boldsymbol{e}_j$ $(i, j = 1, 2, 3)$, which are linearly independent in Lin, we conclude that Lin is a 9-dimensional vector space. Parallel to the definition of the dot product of vectors in V, we define the dot product of $\boldsymbol{L} = \sum_{i,j} L_{ij}\boldsymbol{e}_i \otimes \boldsymbol{e}_j$ and $\boldsymbol{M} = \sum_{k,l} L_{kl}\boldsymbol{e}_k \otimes \boldsymbol{e}_l$ by

$$\boldsymbol{L} \cdot \boldsymbol{M} = \sum_{i,j} L_{ij}M_{ij} = \mathrm{tr}(\boldsymbol{L}\boldsymbol{M}^T), \tag{1.57}$$

where $\mathrm{tr}(\cdot)$ denotes the trace of the linear transformation in question. By the intrinsic definition of the trace of a linear transformation, we see that definition (1.57) is independent of the basis we choose in Lin. It is straightforward to verify that this definition indeed satisfies all the properties we require of a dot product. Under this definition, a linear transformation $\boldsymbol{L}$ has its norm given by

$$\|\boldsymbol{L}\|_F = \sqrt{\mathrm{tr}(\boldsymbol{L}\boldsymbol{L}^T)}, \tag{1.58}$$

and the nine tensor products $\boldsymbol{e}_i \otimes \boldsymbol{e}_j$ $(i, j = 1, 2, 3)$ constitute an orthonormal basis in Lin. Equipped with this norm, called the Frobenius norm (or Euclidean norm), Lin becomes a metric space, where the distance between $\boldsymbol{L}, \boldsymbol{M} \in \mathrm{Lin}$ is $\|\boldsymbol{L} - \boldsymbol{M}\|_F$.

To prepare for defining the exponential function and logarithmic function of $\boldsymbol{L}$, we state some basic definitions and facts that concern infinite sequences and series of linear operators in Lin. A sequence $\{\boldsymbol{L}_k\}$ in Lin converges to $\boldsymbol{L}$ if and only if

$$\lim_{k\to\infty} \|\boldsymbol{L}_k - \boldsymbol{L}\|_F = 0. \tag{1.59}$$

A sequence $\{\boldsymbol{L}_k\}$ converges to a limit if and only if it satisfies the Cauchy criterion, i.e., for every $\varepsilon > 0$ there exists an integer $N > 0$ such that

$$\|\boldsymbol{L}_j - \boldsymbol{L}_k\|_F < \varepsilon \qquad \text{if } j \geq N \text{ and } k \geq N. \tag{1.60}$$

An infinite series $\sum_{k=0}^{\infty} \boldsymbol{L}_k$ of linear operators in Lin is said to converge to $\boldsymbol{S}$ in Lin if its sequence of partial sums $\{\boldsymbol{S}_n\}$, where $\boldsymbol{S}_n = \sum_{k=0}^{n} \boldsymbol{L}_k$, converges to $\boldsymbol{S}$, and we write

$$\sum_{k=0}^{\infty} \boldsymbol{L}_k = \boldsymbol{S}. \tag{1.61}$$

Applying the Cauchy criterion to the sequence of partial sums $\{\boldsymbol{S}_n\}$, we observe that the infinite series $\sum_{k=0}^{\infty} \boldsymbol{L}_k$ converges to a limit if and only if for every $\varepsilon > 0$ there is an integer $N > 0$ such that

$$\|\boldsymbol{L}_{m+1} + \boldsymbol{L}_{m+2} + \cdots + \boldsymbol{L}_n\|_F < \varepsilon \qquad \text{if } n > m > N. \tag{1.62}$$

A series $\sum_{k=0}^{\infty} \boldsymbol{L}_k$ is said to be absolutely convergent if the series of real numbers $\sum_{k=0}^{\infty} \|\boldsymbol{L}_k\|$ is convergent. It follows easily from the Cauchy criterion that a series is convergent if it is absolutely convergent.

As Lin is a finite-dimensional vector space, all norms on Lin are equivalent (see, e.g., [155, p. 78] in the following sense: Given two norms $\|\cdot\|_1$ and $\|\cdot\|_2$ on Lin, there exist two constants $\alpha > 0$, $\beta > 0$ such that

$$\alpha\|\boldsymbol{L}\|_1 \leq \|\boldsymbol{L}\|_2 \leq \beta\|\boldsymbol{L}\|_1, \qquad \text{for each } \boldsymbol{L} \in \text{Lin}. \tag{1.63}$$

It follows from (1.63) that all norms define the same topology on Lin. For instance, all the definitions and facts stated above remain valid if the Frobenius norm in the statements is replaced by any other norm on Lin; see [155, Chap. 5, Sect. 2]. Henceforth in Part I, where we will use only the Frobenius norm, except for some instances of emphasis we will suppress the subscript "F" and write $\|\cdot\|$ to mean the Frobenius norm $\|\cdot\|_F$.

1.4 Exponential and Logarithmic Function of a Matrix

1.4.1 Basic Definitions

In this section we choose and fix a right-handed orthonormal basis $\boldsymbol{e}_i$ $(i = 1, 2, 3)$ in V and identify each $\boldsymbol{A} \in \text{Lin}$ with the matrix $A := [A_{ij}]$ that represents $\boldsymbol{A}$ under the chosen basis. Then Lin is identical to $\text{M}_3(\mathbb{R})$, the space of 3×3 matrices with real entries. For later use, we will consider also matrices in $\text{M}_3(\mathbb{C})$, the space of 3×3 matrices with complex entries, where the Frobenius norm of $C \in \text{M}_3(\mathbb{C})$ is defined as

$$\|C\|_F := \sqrt{\sum_{i,j} C_{ij}\overline{C_{ij}}}; \tag{1.64}$$

here $\overline{C_{ij}}$ denotes the complex conjugate of C_{ij}. Note that $\text{M}_3(\mathbb{R}) \subset \text{M}_3(\mathbb{C})$ and (1.64) reduces to (1.58) for $C \in \text{M}_3(\mathbb{R})$. Henceforth in Part I, except for Sects. 1.9 and 1.10 we will suppress the subscript "F" and use $\|\cdot\|$ to denote the Frobenius norm $\|\cdot\|_F$ in $\text{M}_3(\mathbb{C})$.

The following lemma and theorem will be instrumental to our definition of the exponential and the logarithmic function of a matrix in $\text{M}_3(\mathbb{R})$ or in $\text{M}_3(\mathbb{C})$.

Lemma 1.3 *For any $A, B \in \mathrm{M}_3(\mathbb{K})$, where $\mathbb{K} = \mathbb{R}$, or $\mathbb{C}$, we have*

$$\|AB\| \le \|A\|\|B\|. \tag{1.65}$$

Proof For any $A, B \in \mathrm{M}_3(\mathbb{K})$, the ij-th entry of the product AB satisfies

$$|(AB)_{ij}|^2 = |\sum_k A_{ik}B_{kj}|^2 \le \left(\sum_k |A_{ik}|^2\right)\left(\sum_k |B_{kj}|^2\right),$$

where $|x|$ means the absolute value (resp. the modulus) of x (resp. z) for $x \in \mathbb{R}$ (resp. $z \in \mathbb{C}$), and we have appealed to the Cauchy-Schwarz inequality. Hence

$$\begin{aligned}\|AB\|^2 &= \sum_{i,j} |(AB)_{ij}|^2 \\ &\le \sum_{i,j}\left(\left(\sum_k |A_{ik}|^2\right)\left(\sum_k |B_{kj}|^2\right)\right) \\ &= \left(\sum_{i,k} |A_{ik}|^2\right)\left(\sum_{k,j} |B_{kj}|^2\right) = \|A\|^2\|B\|^2.\end{aligned}$$

Inequality (1.65) then follows easily. □

In what follows $A^0 = I$, the identity matrix. We phrase the next theorem so that it covers also the case where $A \in \mathrm{M}_3(\mathbb{C})$. An infinite series $\sum_{k=0}^{\infty} C_k$, where $C_k \in \mathrm{M}_3(\mathbb{C})$ for each k, is said to be absolutely convergent if the series of real numbers $\sum_{k=0}^{\infty} \|C_k\|$, where $\|C_k\|$ is defined by (1.64), is convergent.

Theorem 1.4 *Let $f(z) = \sum_{k=0}^{\infty} c_k z^k$ (resp. $f(x) = \sum_{k=0}^{\infty} c_k x^k$) be a complex (resp. real) power series with radius of convergence $R > 0$. Then*

$$f(A) = \sum_{k=0}^{\infty} c_k A^k \tag{1.66}$$

is absolutely convergent for any matrix $A \in \mathrm{M}_3(\mathbb{C})$ (resp. $A \in \mathrm{M}_3(\mathbb{R})$) with $\|A\| < R$.

Proof By the given assumption, the power series $f(\|A\|) = \sum_{k=0}^{\infty} c_k \|A\|^k$ is absolutely convergent for any $A \in \mathrm{M}_3(\mathbb{C})$ (resp. $A \in \mathrm{M}_3(\mathbb{R})$) with $\|A\| < R$. Let

$$S_n = \sum_{k=0}^{n} c_k A^k, \qquad s_n = \sum_{k=0}^{n} |c_k|\|A\|^k.$$

Let $\varepsilon > 0$ be given. Since $\{s_n\}$ is a Cauchy sequence, there exists an $N > 0$ such that if $m, n > N$ we have $|s_m - s_n| < \varepsilon$. Without loss of generality, consider $m > n > N$. We have

$$\begin{aligned}\|S_m - S_n\| = \|\sum_{k=n+1}^{m} c_k A^k\| &\le \sum_{k=n+1}^{m} |c_k|\|A^k\| \\ &\le \sum_{k=n+1}^{m} |c_k|\|A\|^k = |s_m - s_n| < \varepsilon,\end{aligned}$$

where we have appealed to (1.65). Therefore $\{S_n\}$ is a Cauchy sequence in $\mathrm{M}_3(\mathbb{C})$ (resp. $\mathrm{M}_3(\mathbb{R})$), and $\sum_{k=0}^{\infty} c_k A^k$ is absolutely convergent in $\mathrm{M}_3(\mathbb{C})$ (resp. $\mathrm{M}_3(\mathbb{R})$) for any A with $\|A\| < R$. □

Parallel to the power series

$$e^z = \sum_{k=0}^{\infty} \frac{1}{k!} z^k, \qquad \log(1+z) = \sum_{k=0}^{\infty} \frac{(-1)^{k-1}}{k} z^k, \qquad (z \in \mathbb{C})$$

which has radius of convergence $R = +\infty$ and $R = 1$, respectively, we define

$$\exp A := \sum_{k=0}^{\infty} \frac{1}{k!} A^k, \tag{1.67}$$

which by the preceding theorem converges absolutely for all $A \in \mathrm{M}_3(\mathbb{C})$, and

$$\log A := \sum_{k=0}^{\infty} \frac{(-1)^{k-1}}{k} (A - I)^k, \tag{1.68}$$

which converges absolutely for those $A \in \mathrm{M}_3(\mathbb{C})$ that satisfies $\|A - I\| < 1$.

Proposition 1.5 *For $A \in \mathrm{M}_3(\mathbb{C})$ the following identities are valid*:

$$\log(\exp A) = A \qquad \textit{for } \|A\| < \log 2, \tag{1.69}$$

$$\exp(\log A) = A \qquad \textit{for } \|A - I\| < 1. \tag{1.70}$$

Proof As a power series in $\exp A$, $\log(\exp A)$ converges absolutely for those A that satisfies $\|\exp A - I\| < 1$. A sufficient condition to this effect follows from the estimate

$$\|\exp A - I\| = \|\sum_{k=1}^{\infty} \frac{A^k}{k!}\| \le \sum_{k=1}^{\infty} \frac{\|A\|^k}{k!} = e^{\|A\|} - 1 < 1$$

if $\|A\| < \log 2$. As a double series in A that converges absolutely, the sum of $\log(\exp A)$ does not change under rearrangement. By collecting terms in like powers of A, we observe that

$$\begin{aligned}
\log(\exp A) &= \sum_{k=1}^{\infty} \frac{(-1)^{k-1}}{k} \left(\sum_{n=1}^{\infty} \frac{A^n}{n!} \right)^k \\
&= \left(A + \frac{A^2}{2!} + \frac{A^3}{3!} + \cdots \right) \\
&\quad - \frac{1}{2} \left(A + \frac{A^2}{2!} + \frac{A^3}{3!} + \cdots \right) \left(A + \frac{A^2}{2!} + \frac{A^3}{3!} + \cdots \right) \\
&\quad + \frac{1}{3} \left(A + \frac{A^2}{2!} + \cdots \right) \left(A + \frac{A^2}{2!} + \cdots \right) \left(A + \frac{A^2}{2!} + \cdots \right) + \cdots \\
&= A + \left(\frac{1}{2} - \frac{1}{2} \right) A^2 + \left(\frac{1}{6} - \frac{1}{2} + \frac{1}{3} \right) A^3 + \cdots \\
&= A + 0 + 0 + \cdots .
\end{aligned}$$

We know that the coefficient of each term in a higher power of A is zero because it is the same as that of the corresponding term in the expansion $\log(\exp x)$ for a real x. Hence we have proved (1.69).

Applying a similar argument to the double series

$$\exp(\log(I+B)) = \sum_{k=0}^{\infty} \frac{1}{k!} \left(\sum_{n=1}^{\infty} \frac{(-1)^{n-1}}{n} B^n \right)^k, \qquad (\|B\| < 1)$$

we obtain

$$\exp(\log(I+B)) = I + B.$$

Putting $B = A - I$ in the preceding identity leads to (1.70). □

Remark 1.6 The mapping $(A_{ij}) \mapsto (A_{11}, A_{12}, A_{13}, A_{21}, \ldots, A_{33})$ from $\mathrm{M}_3(\mathbb{R})$ to $\mathbb{R}^9$ defines a global chart on $\mathrm{M}_3(\mathbb{R})$ and makes it an analytic manifold. The exponential map $\exp : \mathrm{M}_3(\mathbb{R}) \to \mathrm{M}_3(\mathbb{R})$ is analytic. Likewise the map $\log : D \to \mathrm{M}_3(\mathbb{R})$, where $D = \{B \in \mathrm{M}_3(\mathbb{R}) : \|B - I\| < 1\}$, is also analytic. If we take the global chart as defining a C^∞ differentiable structure on $\mathrm{M}_3(\mathbb{R})$, the maps exp and log are of class C^∞. □

1.4.2 Properties of the Matrix Exponential

Recall that $\mathrm{M}_3(\mathbb{C})$ denotes the space of 3×3 matrices with complex entries. We say that a matrix $A \in \mathrm{M}_3(\mathbb{C})$ is diagonalizable if $A = P\mathrm{diag}(\lambda_1, \lambda_2, \lambda_3)P^{-1}$ for some $P \in \mathrm{M}_3(\mathbb{C})$ and some complex numbers λ_i $(i = 1, 2, 3)$.

Proposition 1.7 *The following three assertions are valid*:

(i) *Let $P \in \mathrm{M}_3(\mathbb{C})$ be invertible. Then*

$$\exp(PAP^{-1}) = P(\exp A)P^{-1} \qquad \textit{for each } A \in \mathrm{M}_3(\mathbb{C}). \tag{1.71}$$

(ii) *For any $A, B \in \mathrm{M}_3(\mathbb{C})$, if $AB = BA$, then*

$$\exp(A+B) = \exp A \exp B. \tag{1.72}$$

(iii) *Let $A \in \mathrm{M}_3(\mathbb{C})$ be diagonalizable.*[6] *There holds*

$$\det(\exp A) = \exp(\mathrm{tr}\, A). \tag{1.73}$$

Proof (i) Since $(PAP^{-1})^k = PA^kP^{-1}$ for each natural number k, we have

$$\sum_{k=1}^{\infty} \frac{(PAP^{-1})^k}{k!} = P \sum_{k=1}^{\infty} \left(\frac{A^k}{k!} \right) P^{-1}.$$

(ii) The scalar case, i.e., $e^{z_1}e^{z_2} = e^{z_1+z_2}$, where $z_i \in \mathbb{C}$ $(i = 1, 2)$, can be justified by the theorem that the product of two absolutely convergent series $\sum_{j=0}^{\infty} a_j = \mathtt{a}$ and $\sum_{k=0}^{\infty} b_k = \mathtt{b}$

[6] This condition can be relaxed. Formula (1.73) in fact holds for all $A \in \mathrm{M}_3(\mathbb{C})$; see, e.g., [138] for an algebraic proof, or [310, p. 88] for a proof that invokes matrix calculus. Since we shall use this formula for diagonalizable matrices only, we add this condition to get a simple proof.

can be written as an absolutely convergent series $\sum_{l=0}^{\infty} c_l = \mathtt{c}$ called their Cauchy product, where $c_l = \sum_{j=0}^{l} a_j b_{l-j}$ and $\mathtt{c} = \mathtt{ab}$. When $z_1, z_2 \in \mathbb{C}$ in the preceding assertion are replaced by $A, B \in \mathrm{M}_3(\mathbb{C})$, the resulting assertion remains valid and its proof is essentially the same as the scalar case.[7]

Here we have

$$\begin{aligned}\exp A \exp B &= \left(\sum_{r=0}^{\infty} \frac{A^r}{r!}\right)\left(\sum_{s=0}^{\infty} \frac{B^s}{s!}\right)\\ &= \sum_{n=0}^{\infty}\left(\sum_{r=0}^{n} \frac{A^r}{r!}\cdot\frac{B^{n-r}}{(n-r)!}\right),\end{aligned}$$

which is the Cauchy product of the two infinite series that define $\exp A$ and $\exp B$, respectively. On the other hand,

$$\begin{aligned}\exp(A+B) &= \sum_{n=0}^{\infty} \frac{(A+B)^n}{n!}\\ &= \sum_{n=0}^{\infty}\left(\sum_{r=0}^{n} \frac{A^r}{r!}\cdot\frac{B^{n-r}}{(n-r)!}\right),\end{aligned}$$

where we have used in the last step the hypothesis that $AB = BA$.

(iii) Since $A = P\,\mathrm{diag}(\lambda_1, \lambda_2, \lambda_3)P^{-1}$ for some $P \in \mathrm{M}_3(\mathbb{C})$ and some complex numbers λ_i $(i = 1, 2, 3)$, we obtain

$$\begin{aligned}\det(\exp A) &= \det\left(\exp(P\mathrm{diag}(\lambda_1, \lambda_2, \lambda_3)P^{-1})\right)\\ &= \det\left(P\exp(\mathrm{diag}(\lambda_1, \lambda_2, \lambda_3))P^{-1}\right)\\ &= \det(\mathrm{diag}(e^{\lambda_1}, e^{\lambda_2}, e^{\lambda_3})) = e^{\lambda_1}e^{\lambda_2}e^{\lambda_3}\\ &= e^{\lambda_1+\lambda_2+\lambda_3} = e^{\mathrm{tr}A},\end{aligned}$$

where we have appealed to (i) in the second step. □

1.5 Active Versus Passive View of Rotations

An orthogonal linear transformation $\boldsymbol{R}$ on the translation space V of physical space E^3 is a *rotation* if it further satisfies $\det \boldsymbol{R} = 1$. The set of all rotations is denoted by SO(3). Under a chosen orthonormal basis $\{\boldsymbol{e}_i : i = 1, 2, 3\}$ in V, each rotation $\boldsymbol{R}$ is represented by an orthogonal matrix $[R_{ij}]$ with unit determinant, the entries of which are given by the formula $R_{ij} = \boldsymbol{e}_i \cdot \boldsymbol{R}\boldsymbol{e}_j$. Before and after the rotation $\boldsymbol{R}$, a vector $\boldsymbol{a}$ has components $\boldsymbol{e}_i \cdot \boldsymbol{a}$ and $\boldsymbol{e}_i \cdot \boldsymbol{R}\boldsymbol{a}$ for $i = 1, 2, 3$, respectively. Note that the basis vectors $\boldsymbol{e}_i$ remain unchanged, whereas the vector $\boldsymbol{a}$ moves to $\boldsymbol{R}\boldsymbol{a}$ under the rotation. This treatment of rotations is called the active view.

[7] See, e.g., [121, Theorem 16.4a]. While the proof there is for the real scalar case, the same proof works if the absolute value $|\cdot|$ is interpreted as the modulus for the complex scalar case or is replaced by the appropriate norm $\|\cdot\|$ for $\mathrm{M}_3(\mathbb{R})$ and $\mathrm{M}_3(\mathbb{C})$, respectively.

But there is another characterization, called the passive view of rotations, which was adopted by Bunge and by Roe in their pioneering work on quantitative texture analysis and has remained predominant in the literature of this field. In the words of Morrison and Parker [238],

> a passive rotation is a rotation *of the coordinate system.* ... Under a passive rotation, the vector remains fixed, but the point it defines receives new labels. That is, the numbers that describe the location of the point change from those appropriate to the (initial) unrotated frame to the (final) rotated frame.

The passive rotation $\boldsymbol{R}^{(p)}$ that corresponds to the active rotation $\boldsymbol{R}$ is determined by the following requirement: For each vector $\boldsymbol{a} \in V$, the components of $\boldsymbol{a}$ under the basis $\boldsymbol{R}^{(p)}\boldsymbol{e}_1, \boldsymbol{R}^{(p)}\boldsymbol{e}_2, \boldsymbol{R}^{(p)}\boldsymbol{e}_3$ are exactly the same as the components of $\boldsymbol{Ra}$ under the original basis $\boldsymbol{e}_1, \boldsymbol{e}_2, \boldsymbol{e}_3$, i.e.,

$$\boldsymbol{R}^{(p)}\boldsymbol{e}_i \cdot \boldsymbol{a} = \boldsymbol{e}_i \cdot \boldsymbol{Ra} \qquad (i = 1, 2, 3). \tag{1.74}$$

It follows that we have

$$\boldsymbol{R}^{(p)} = \boldsymbol{R}^T = \boldsymbol{R}^{-1}. \tag{1.75}$$

Remark 1.8 The active view of rotations, which is consistent with all mathematical treatments of transformations on a space,[8] has long been the choice of the mathematics community. In physics both the active and the passive views have been widely used, with the active view gaining more practitioners in the last three or four decades.[9] There are instances where authors who adopt the passive viewpoint make major errors in their publications. The most notable of those are two classic books on angular momentum in quantum mechanics by Edmonds [98] and by Rose [274], respectively. As pointed out by Bouten [39] and by Wolf [343], there is a major inconsistency in Edmonds's treatment of passive rotations, which leads to errors. In response to the critiques, Edmonds makes corrections in the 1974 printing [99] of his book. Bouten also finds that Rose's treatment suffers from the same confusion as Edmonds's, which results in two errors that cancel and yields a correct formula for active rotations. In texture analysis Matthies and coworkers, while adopting the passive view of rotations, at places make use of formulas for active rotations, which lead to ambiguities for the reader; see Sect. 4.5.4 for more details. Nevertheless the active and passive viewpoints are equivalent, so long as the rules and procedures of each are followed consistently (cf. [207, 238]). In this exposition we adopt the active view of rotations for consistency with and smooth transition to the mathematical literature. □

1.5.1 Product of Rotations

Given two rotations $\boldsymbol{R}_1, \boldsymbol{R}_2$, their product $\boldsymbol{R} = \boldsymbol{R}_2\boldsymbol{R}_1 : V \to V$ is the linear transformation defined by

$$\boldsymbol{Ra} = \boldsymbol{R}_2(\boldsymbol{R}_1\boldsymbol{a}) \qquad \text{for each } \boldsymbol{a} \in V. \tag{1.76}$$

[8] Note that coordinate systems are out of the question for most spaces, abstract or otherwise.

[9] See, e.g., [28, 51, 238, 313, 352]. The long 2017 pedagogical article by P.P. Man [207], which discusses in detail the Wigner active and passive rotation matrices in quantum mechanics, lists at least 27 and 12 references that adopt the active and passive viewpoint, respectively.

It is easily checked that $\boldsymbol{R}$ is orthogonal and $\det \boldsymbol{R} = 1$. Hence $\boldsymbol{R}_2\boldsymbol{R}_1$ is a rotation, the effect of which on each vector $\boldsymbol{a}$ is the same as that of two successive rotations, $\boldsymbol{R}_1$ followed by $\boldsymbol{R}_2$.

Let $\boldsymbol{R}^{(p)}$, $\boldsymbol{R}_1^{(p)}$, and $\boldsymbol{R}_2^{(p)}$ be the passive rotation corresponding to $\boldsymbol{R}$, $\boldsymbol{R}_1$, and $\boldsymbol{R}_2$, respectively. Then we have

$$\boldsymbol{R}^{(p)} = (\boldsymbol{R}_2\boldsymbol{R}_1)^{-1} = \boldsymbol{R}_1^{-1}\boldsymbol{R}_2^{-1} = \boldsymbol{R}_1^{(p)}\boldsymbol{R}_2^{(p)}. \tag{1.77}$$

In this exposition we follow what has become the standard convention in mathematics and a common practice in physics and use active rotations. One advantage of doing so is that we can easily adopt, without modification, formulas available in the mathematics and physics literature or compare with them those we derive. On the other hand, we should also be acquainted with passive rotations, as they are predominantly used in the literature of texture analysis.

1.6 Euler's Theorem

A line ℓ in V is called an axis of the rotation $\boldsymbol{R}$ if every point in ℓ remains invariant under the action of $\boldsymbol{R}$, i.e., $\boldsymbol{R}\boldsymbol{a} = \boldsymbol{a}$ for each $\boldsymbol{a}$ in ℓ.

Lemma 1.9 *Every rotation $\boldsymbol{R}$ has an axis. If $\boldsymbol{R} \neq \boldsymbol{I}$, it has a unique axis.*

Proof It is easy to see that $\det(\boldsymbol{R} - \boldsymbol{I}) = 0$ from the following string of simple computations: $\det(\boldsymbol{R} - \boldsymbol{I}) = \det((\boldsymbol{R} - \boldsymbol{I})^T)) = \det(\boldsymbol{R}^T - \boldsymbol{I}) = \det(\boldsymbol{R}^T(\boldsymbol{I} - \boldsymbol{R})) = (\det \boldsymbol{R}^T)\det(\boldsymbol{I} - \boldsymbol{R}) = -\det(\boldsymbol{R} - \boldsymbol{I})$. Hence there exists a vector $\boldsymbol{a}$ such that $(\boldsymbol{R} - \boldsymbol{I})\boldsymbol{a} = \boldsymbol{0}$ or $\boldsymbol{R}\boldsymbol{a} = \boldsymbol{a}$, and the line $\ell = \{\alpha\boldsymbol{a} : \alpha \in \mathbb{R}\}$ is an axis of $\boldsymbol{R}$.

Now we proceed to prove the second part of the lemma. Suppose $\boldsymbol{R}$ has another axis $\{\beta\boldsymbol{b} : \beta \in \mathbb{R}\}$, where $\boldsymbol{b}$ is linearly independent of $\boldsymbol{a}$. Let Π be the plane subtended by $\boldsymbol{a}$ and $\boldsymbol{b}$. Let $\boldsymbol{c}$ be a vector orthogonal to Π such that $\boldsymbol{a}$, $\boldsymbol{b}$, and $\boldsymbol{c}$ constitute a right-handed triad. Since $\boldsymbol{R}$ is a rotation, $\boldsymbol{R}\boldsymbol{c}$ is perpendicular to both $\boldsymbol{R}\boldsymbol{a} = \boldsymbol{a}$ and $\boldsymbol{R}\boldsymbol{b} = \boldsymbol{b}$, $\|\boldsymbol{R}\boldsymbol{c}\| = \|\boldsymbol{c}\|$, and $\boldsymbol{a}$, $\boldsymbol{b}$, and $\boldsymbol{R}\boldsymbol{c}$ also form a right-handed triad. Therefore $\boldsymbol{R}\boldsymbol{c} = \boldsymbol{c}$, and we conclude that $\boldsymbol{R} = \boldsymbol{I}$. □

Let $\boldsymbol{n}$ be a unit vector on the axis of the rotation $\boldsymbol{R}$. We pick $\boldsymbol{e}_1 = \boldsymbol{n}$ and choose two unit vectors $\boldsymbol{e}_2$, $\boldsymbol{e}_3$ such that $\{\boldsymbol{e}_i : i = 1, 2, 3\}$ constitutes a right-handed orthonormal triad. Under the basis $\{\boldsymbol{e}_i\}$, $\boldsymbol{R}$ is represented by the matrix

$$\begin{pmatrix} 1 & 0 & 0 \\ 0 & a & b \\ 0 & c & d \end{pmatrix}, \tag{1.78}$$

where the real numbers a, b, c, and d satisfy

$$a^2 + c^2 = 1, \quad ab + cd = 0, \quad b^2 + d^2 = 1, \quad ad - bc = 1. \tag{1.79}$$

As $-1 \leq a \leq 1$, we may write $a = \cos\omega$ for some angle ω. By exploiting conditions (1.79), we observe that matrix (1.78) must be of either of the following two forms:

$$\text{(i)} \begin{pmatrix} 1 & 0 & 0 \\ 0 & \cos\omega & -\sin\omega \\ 0 & \sin\omega & \cos\omega \end{pmatrix}; \qquad \text{(ii)} \begin{pmatrix} 1 & 0 & 0 \\ 0 & \cos\omega & \sin\omega \\ 0 & -\sin\omega & \cos\omega \end{pmatrix}. \tag{1.80}$$

If we follow the convention that $\omega > 0$ means a counter-clockwise rotation about $\boldsymbol{n}$ according to the right-hand rule, a convention we shall henceforth adopt, it is easy to see that forms (i) and (ii) describe a rotation about $\boldsymbol{e}_1$ by an angle ω and by an angle $-\omega$, respectively. If we allow ω to run from $-\infty$ to ∞, it suffices to adopt form (i) to cover all the rotations about $\boldsymbol{e}_1$.

Let $\mathcal{S}^2$ be the unit sphere in V. Henceforth, unless explicitly stated otherwise, by $\boldsymbol{R}(\boldsymbol{n}, \omega)$ we mean the rotation with axis and sense specified by the unit vector $\boldsymbol{n} \in \mathcal{S}^2$ and rotation angle given by $\omega \in (-\infty, \infty)$ with sign convention specified just following (1.80). Note that

$$\boldsymbol{R}(\boldsymbol{n}, \omega) = \boldsymbol{R}(-\boldsymbol{n}, -\omega). \tag{1.81}$$

Hence it suffices to let $\boldsymbol{n}$ run over the unit sphere and restrict ω to the interval $[0, \pi]$ to cover all the rotations. For ω in $(0, \pi)$, the correspondence $(\boldsymbol{n}, \omega) \mapsto \boldsymbol{R}(\boldsymbol{n}, \omega)$ is one-to-one. For $\omega = 0$ and $\omega = \pi$, we have $\boldsymbol{R}(\boldsymbol{n}, 0) = \boldsymbol{I}$ and $\boldsymbol{R}(\boldsymbol{n}, \pi) = \boldsymbol{R}(-\boldsymbol{n}, \pi)$ for each unit vector $\boldsymbol{n}$, respectively.

The following theorem is instrumental for us to express the matrix representation of $\boldsymbol{R}(\boldsymbol{n}, \omega)$ in terms of Euler angles.

Theorem 1.10 (Euler's theorem) *For any rotation* $\boldsymbol{Q}$,

$$\boldsymbol{Q}\boldsymbol{R}(\boldsymbol{n}, \omega)\boldsymbol{Q}^{-1} = \boldsymbol{R}(\boldsymbol{Q}\boldsymbol{n}, \omega). \tag{1.82}$$

Proof It is easy to see that $\boldsymbol{Q}\boldsymbol{n}$ defines an axis for $\boldsymbol{Q}\boldsymbol{R}(\boldsymbol{n}, \omega)\boldsymbol{Q}^{-1}$. Take $\boldsymbol{e}_1 = \boldsymbol{n}$. Let $\boldsymbol{e}_2$ and $\boldsymbol{e}_3$ be a pair of unit vectors such that $\boldsymbol{e}_1 = \boldsymbol{n}$, $\boldsymbol{e}_2$, and $\boldsymbol{e}_3$ form a right-handed orthonormal basis in V. Under this basis, $\boldsymbol{R}(\boldsymbol{n}, \omega)$ is represented by the matrix

$$\begin{pmatrix} 1 & 0 & 0 \\ 0 & \cos\omega & -\sin\omega \\ 0 & \sin\omega & \cos\omega \end{pmatrix}.$$

The triad $\{\boldsymbol{Q}\boldsymbol{e}_i : i = 1, 2, 3\}$ also constitutes a right-handed orthonormal basis in V. Under this new basis, $\boldsymbol{Q}\boldsymbol{R}(\boldsymbol{n}, \omega)\boldsymbol{Q}^{-1}$ is represented by the same matrix above. Hence $\boldsymbol{Q}\boldsymbol{R}(\boldsymbol{n}, \omega)\boldsymbol{Q}^{-1}$ is the rotation with axis $\boldsymbol{Q}\boldsymbol{n}$ and angle ω, i.e., $\boldsymbol{R}(\boldsymbol{Q}\boldsymbol{n}, \omega)$. □

1.7 Parametrization of Rotations by Euler Angles

Let E^3 be the three-dimensional physical space and V be its translation space. Let $\{\boldsymbol{e}_i : i = 1, 2, 3\}$ be a chosen right-handed, orthonormal triad in V. All matrix representations of rotations below, unless explicitly specified otherwise, will refer to this triad as the chosen basis in V.

Each rotation g on V acts on the triad $\{\boldsymbol{e}_i\}$ to produce another orthonormal triad $\{g\boldsymbol{e}_i : i = 1, 2, 3\}$, which defines the rotation g itself. Indeed g is represented under the basis $\{\boldsymbol{e}_i\}$ by the matrix $[g\boldsymbol{e}_1, g\boldsymbol{e}_2, g\boldsymbol{e}_3]$ with $g\boldsymbol{e}_i$ as the ith column.

When $g\boldsymbol{e}_3 \neq \pm\boldsymbol{e}_3$, we may specify g by the Euler angles (ψ, θ, ϕ) as follows (see Fig. 1,[10] where the plane subtended by $\boldsymbol{e}_1$ and $\boldsymbol{e}_2$, by $\boldsymbol{e}_3$ and $g\boldsymbol{e}_3$, and by $g\boldsymbol{e}_1$ and $g\boldsymbol{e}_2$ is shaded with horizontal lines, shaded with vertical lines, and left without shading, respectively). Let O be

[10] This figure is adapted from Fig. 18 of [350], which is apparently an improved version of Figs. 9-1 and 9-2 of [209], for our present notation of Euler angles.

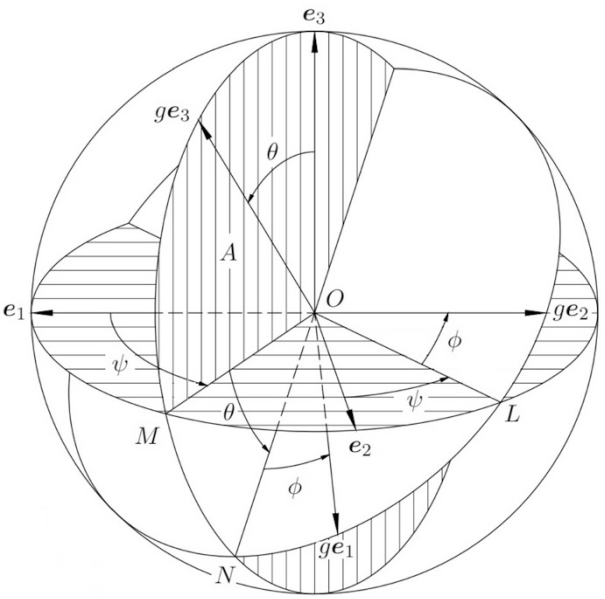

Fig. 1 Definition of the Euler angles ψ, θ, and ϕ

the origin of a coordinate system such that the tips of the vectors $\boldsymbol{e}_i$ and $g\boldsymbol{e}_i$ all lie on the unit sphere centered at O. The plane containing $g\boldsymbol{e}_1$ and $g\boldsymbol{e}_2$ meet the one containing $\boldsymbol{e}_1$ and $\boldsymbol{e}_2$ along a line called the line of nodes, which intersects the unit sphere at two points. One of these points will be called L, which is defined by certain conditions given below. We begin by picking arbitrarily one of the two points where the line of nodes meets the unit sphere and temporarily call it L. The Euler angles (ψ, θ, ϕ) are defined by the following sequence of rotations which brings the triad $\{\boldsymbol{e}_i\}$ to the triad $\{g\boldsymbol{e}_i\}$:

1. Rotate about $\boldsymbol{e}_3$ by an angle $0 \leq \psi < 2\pi$ so that $\boldsymbol{e}_2$ falls on **OL**. The new position of $\boldsymbol{e}_1$ is called **OM**. Since $\boldsymbol{e}_3$, $g\boldsymbol{e}_3$, and **OM** are perpendicular to **OL**, they lie in the plane A orthogonal to **OL**.
2. Rotate about **OL** by an angle θ so that $\boldsymbol{e}_3$ falls on $g\boldsymbol{e}_3$. There is only one choice of L so that $0 < \theta < \pi$. If the original choice doesn't lead to a θ in $(0, \pi)$, choose the other point where the line of nodes meets the unit sphere as L. Note that the definition of L determines ψ. If the original choice of L is incorrect, then the angle ψ must be revised so that it corresponds to the correct L.
3. After the rotation $\boldsymbol{R}(\mathbf{OL}, \theta)$, let M fall on N. The vector **ON** is perpendicular to **OL** and $g\boldsymbol{e}_3$; it lies in plane A and in the plane spanned by $g\boldsymbol{e}_1$ and $g\boldsymbol{e}_2$. Rotate about $g\boldsymbol{e}_3$ by an anlge ϕ $(0 \leq \phi < 2\pi)$ so that **ON** and **OL** fall on $g\boldsymbol{e}_1$ and $g\boldsymbol{e}_2$, respectively.

Obviously we have

$$g = \boldsymbol{R}(g\boldsymbol{e}_3, \phi)\boldsymbol{R}(\mathbf{OL}, \theta)\boldsymbol{R}(\boldsymbol{e}_3, \psi). \tag{1.83}$$

Note that

$$\mathbf{OL} = \boldsymbol{R}(\boldsymbol{e}_3, \psi)\boldsymbol{e}_2, \qquad g\boldsymbol{e}_3 = \boldsymbol{R}(\mathbf{OL}, \theta)\boldsymbol{R}(\boldsymbol{e}_3, \psi)\boldsymbol{e}_3. \tag{1.84}$$

Hence by Euler's theorem (see Theorem 1.10), we have

$$\boldsymbol{R}(g\boldsymbol{e}_3, \phi) = (\boldsymbol{R}(\mathbf{OL}, \theta)\boldsymbol{R}(\boldsymbol{e}_3, \psi))\, \boldsymbol{R}(\boldsymbol{e}_3, \phi)\, (\boldsymbol{R}(\mathbf{OL}, \theta)\boldsymbol{R}(\boldsymbol{e}_3, \psi))^{-1}, \tag{1.85}$$

and

$$\boldsymbol{R}(\mathbf{OL}, \theta) = \boldsymbol{R}(\boldsymbol{e}_3, \psi)\boldsymbol{R}(\boldsymbol{e}_2, \theta)\boldsymbol{R}(\boldsymbol{e}_3, \psi)^{-1}. \tag{1.86}$$

Substituting (1.85) and then (1.86) into (1.83), we obtain the formula

$$g = \boldsymbol{R}(\boldsymbol{e}_3, \psi)\boldsymbol{R}(\boldsymbol{e}_2, \theta)\boldsymbol{R}(\boldsymbol{e}_3, \phi). \tag{1.87}$$

Under the basis $\{\boldsymbol{e}_i\}$, the rotation g is represented by the matrix

$$\begin{pmatrix} \cos\psi & -\sin\psi & 0 \\ \sin\psi & \cos\psi & 0 \\ 0 & 0 & 1 \end{pmatrix} \begin{pmatrix} \cos\theta & 0 & \sin\theta \\ 0 & 1 & 0 \\ -\sin\theta & 0 & \cos\theta \end{pmatrix} \begin{pmatrix} \cos\phi & -\sin\phi & 0 \\ \sin\phi & \cos\phi & 0 \\ 0 & 0 & 1 \end{pmatrix} \tag{1.88}$$

or

$$\begin{aligned} &\boldsymbol{R}(\psi, \theta, \phi) \\ &= \begin{pmatrix} \cos\psi\cos\theta\cos\phi - \sin\psi\sin\phi & -\cos\psi\cos\theta\sin\phi - \sin\psi\cos\phi & \cos\psi\sin\theta \\ \sin\psi\cos\theta\cos\phi + \cos\psi\sin\phi & -\sin\psi\cos\theta\sin\phi + \cos\psi\cos\phi & \sin\psi\sin\theta \\ -\sin\theta\cos\phi & \sin\theta\sin\phi & \cos\theta \end{pmatrix}, \end{aligned} \tag{1.89}$$

which gives the parametrization of rotations by Euler angles (ψ, θ, ϕ).

Remark 1.11 Both the conventions adopted here (i) for using active rotations g in (1.87) and (ii) for definition of Euler angles (ψ, θ, ϕ) as above are common in the present-day physics literature (see, e.g., [28, 313], where the Euler angles are often written as (α, β, γ) instead. Hielscher and Schaeben [151] also use the same conventions as those of the physics literature in their paper on the MTEX algorithm. □

When $g\boldsymbol{e}_3 = \boldsymbol{e}_3$, the Euler angles ψ and ϕ are not uniquely defined. Indeed, in this case, we have $g = \boldsymbol{R}(\boldsymbol{e}_3, \beta)$ for some angle $0 \le \beta < 2\pi$. As $\theta \to 0$ in (1.89), we observe that the matrix representing g tends to

$$\begin{pmatrix} \cos(\psi+\phi) & -\sin(\psi+\phi) & 0 \\ \sin(\psi+\phi) & \cos(\psi+\phi) & 0 \\ 0 & 0 & 1 \end{pmatrix} \tag{1.90}$$

in the limit. Hence the only requirement on ψ and ϕ is $\psi + \phi = \beta$. Equation (1.87) remains valid if we take $\theta = 0$ and any ψ and ϕ that satisfy $\psi + \phi = \beta$. In fact, we have $g = \boldsymbol{R}(\boldsymbol{e}_3, \psi + \phi)$. This conclusion is also obvious from the geometrical meaning of the Euler angles.

When $g\boldsymbol{e}_3 = -\boldsymbol{e}_3$, we must take $\theta = \pi$. As $\theta \to \pi$ in (1.89), the matrix representing g approaches

$$\begin{pmatrix} -\cos(\psi-\phi) & -\sin(\psi-\phi) & 0 \\ -\sin(\psi-\phi) & \cos(\psi-\phi) & 0 \\ 0 & 0 & -1 \end{pmatrix}. \tag{1.91}$$

Equation (1.87) remains valid if we take $\theta = \pi$ and $\psi - \phi = \beta$, where $\boldsymbol{R}(\boldsymbol{e}_3, \beta)$ takes $\boldsymbol{e}_2$ to $g\boldsymbol{e}_2$.

Note that $(1, \theta, \psi)$ gives the spherical coordinates of $g\boldsymbol{e}_3$.

When the rotation matrix $[R_{ij}]$ is given, the corresponding Euler angles can be computed as follows: first θ is found from the equation $R_{33} = \cos\theta$; then ψ and ϕ are determined from

$$R_{13} = \sin\theta\cos\psi, \qquad R_{23} = \sin\theta\sin\psi,$$

and

$$R_{31} = -\sin\theta\cos\phi, \qquad R_{32} = \sin\theta\sin\phi,$$

respectively.

For a rotation g defined by the Euler angles (ψ, θ, ϕ), a glance at (1.87) reveals that

$$g^{-1} = \boldsymbol{R}(\boldsymbol{e}_3, -\phi)\boldsymbol{R}(\boldsymbol{e}_2, -\theta)\boldsymbol{R}(\boldsymbol{e}_3, -\psi). \tag{1.92}$$

Let us determine the Euler angles $(\psi^{\#}, \theta^{\#}, \phi^{\#})$ pertaining to g^{-1}, where $0 \le \psi^{\#} < 2\pi$, $0 \le \theta^{\#} \le \pi$, and $0 \le \phi^{\#} < 2\pi$.

Since $\boldsymbol{R}(\boldsymbol{e}_3, \pi)\boldsymbol{e}_2 = -\boldsymbol{e}_2$ and $\boldsymbol{R}(\boldsymbol{e}_3, \pi) = \boldsymbol{R}(\boldsymbol{e}_3, \pi)^{-1}$, we observe that

$$\begin{aligned}\boldsymbol{R}(\boldsymbol{e}_2, -\theta) &= \boldsymbol{R}(-\boldsymbol{e}_2, \theta)\\ &= \boldsymbol{R}(\boldsymbol{e}_3, \pi)\boldsymbol{R}(\boldsymbol{e}_2, \theta)\boldsymbol{R}(\boldsymbol{e}_3, \pi),\end{aligned} \tag{1.93}$$

where we have appealed to Euler's theorem in the last step. Therefore we have

$$\begin{aligned}g^{-1} &= \boldsymbol{R}(\boldsymbol{e}_3, -\phi)\boldsymbol{R}(\boldsymbol{e}_3, \pi)\boldsymbol{R}(\boldsymbol{e}_2, \theta)\boldsymbol{R}(\boldsymbol{e}_3, \pi)\boldsymbol{R}(\boldsymbol{e}_3, -\psi)\\ &= \boldsymbol{R}(\boldsymbol{e}_3, \pi - \phi)\boldsymbol{R}(\boldsymbol{e}_2, \theta)\boldsymbol{R}(\boldsymbol{e}_3, \pi - \psi).\end{aligned} \tag{1.94}$$

Taking into account the range of the Euler angles, we should take

$$\psi^{\#} = \begin{cases} \pi - \phi & \text{when } 0 \le \phi \le \pi \\ 3\pi - \phi & \text{when } \pi < \phi < 2\pi, \end{cases} \tag{1.95}$$

$$\theta^{\#} = \theta, \tag{1.96}$$

$$\phi^{\#} = \begin{cases} \pi - \psi & \text{when } 0 \le \psi \le \pi \\ 3\pi - \psi & \text{when } \pi < \psi < 2\pi. \end{cases} \tag{1.97}$$

For simplicity, however, it is usual to write

$$(\psi^{\#}, \theta^{\#}, \phi^{\#}) = (\pi - \phi, \theta, \pi - \psi), \tag{1.98}$$

as $\boldsymbol{R}(\boldsymbol{e}_3, 3\pi - \phi) = \boldsymbol{R}(\boldsymbol{e}_3, \pi - \phi)$ and $\boldsymbol{R}(\boldsymbol{e}_3, 3\pi - \psi) = \boldsymbol{R}(\boldsymbol{e}_3, \pi - \psi)$.

1.8 Comparison with Other Conventions

In the literature of quantitative texture analysis, the reader will usually encounter the passive view of rotations and see another convention adopted for the definition of Euler angles. In this section we present some other conventions, which are most commonly found in the literature of texture analysis, for comparison with ours.

1.8.1 Convention Adopted by Roe and by Matthies

Roe [270] defines the Euler's angles as we did in Sect. 1.7, but he adopts the passive view of rotations. A passive rotation $\boldsymbol{R}^{(p)}(\psi,\theta,\phi)$ and its active counterpart $\boldsymbol{R}(\psi,\theta,\phi)$ are related by (cf. (1.75))

$$\boldsymbol{R}^{(p)}(\psi,\theta,\psi)=\boldsymbol{R}(\psi,\theta,\phi)^T. \tag{1.99}$$

Under the chosen orthonormal basis $\{\boldsymbol{e}_i : i=1,2,3\}$, while $\boldsymbol{R}(\psi,\theta,\phi)$ is represented by the matrix (1.89), $\boldsymbol{R}^{(p)}(\psi,\theta,\phi)$—denoted by $\mathbf{T}$ in Roe's paper—is represented by the matrix

$$\begin{pmatrix} \cos\phi\cos\theta\cos\psi-\sin\phi\sin\psi & \cos\phi\cos\theta\sin\psi+\sin\phi\cos\psi & -\cos\phi\sin\theta \\ -\sin\phi\cos\theta\cos\psi-\cos\phi\sin\psi & -\sin\phi\cos\theta\sin\psi+\cos\phi\cos\psi & \sin\phi\sin\theta \\ \sin\theta\cos\psi & \sin\theta\sin\psi & \cos\theta \end{pmatrix}. \tag{1.100}$$

Matthies [215] and Matthies et al. [224, p. 7] use the same conventions on Euler angles and passive rotations as those of Roe [270], although the Euler angles are denoted by (α,β,γ). Roe [272, p. 131], however, changes his notation of the Euler angles to (α,β,γ) in his book published in 2000.

1.8.2 Conventions Adopted by Bunge and Gel'fand et al.

Bunge [60] adopts a different definition of the Euler angles than (ψ,θ,ϕ). For the non-degenerate cases the Euler angles $(\varphi_1,\Phi,\varphi_2)$ are specified by modifying the procedure that delivers (ψ,θ,ϕ) in Sect. 1.7, as follows (cf. Fig. 1):

1. Rotate about $\boldsymbol{e}_3$ by an angle $0\le\varphi_1<2\pi$ so that $\boldsymbol{e}_1$ falls on **OL**, the line of nodes.
2. Rotate about **OL** by an angle Φ so that $\boldsymbol{e}_3$ falls on $g\boldsymbol{e}_3$. There is only one choice of L so that $0<\Phi<\pi$.
3. Rotate about $g\boldsymbol{e}_3$ by an angle $0\le\varphi_2<2\pi$ so that

$$g=\boldsymbol{R}(g\boldsymbol{e}_3,\varphi_2)\boldsymbol{R}(\mathbf{OL},\Phi)\boldsymbol{R}(\boldsymbol{e}_3,\varphi_1). \tag{1.101}$$

It is easy to see that the angles $(\varphi_1,\Phi,\varphi_2)$ are related to (ψ,θ,ϕ) by the following formulas:

$$\varphi_1=\psi+\frac{\pi}{2},\qquad \Phi=\theta,\qquad \varphi_2=\phi-\frac{\pi}{2}. \tag{1.102}$$

For active rotations, by an argument similar to that which leads from (1.83) to (1.87), we derive from (1.101) the formula

$$g=\boldsymbol{R}(\boldsymbol{e}_3,\varphi_1)\boldsymbol{R}(\boldsymbol{e}_1,\Phi)\boldsymbol{R}(\boldsymbol{e}_3,\varphi_2). \tag{1.103}$$

Bunge, however, adopts the passive view of rotations. His rotation matrix [60, p. 21] is that of $g^{(p)}=g^T=g^{-1}$. Similar to the derivation of (1.94), we obtain from (1.103) that

$$\begin{aligned} g^{(p)}=g^{-1}&=\boldsymbol{R}(\boldsymbol{e}_3,-\varphi_2)\boldsymbol{R}(\boldsymbol{e}_1,-\Phi)\boldsymbol{R}(\boldsymbol{e}_3,-\varphi_1)\\ &=\boldsymbol{R}(\boldsymbol{e}_3,\pi-\varphi_2)\boldsymbol{R}(\boldsymbol{e}_1,\Phi)\boldsymbol{R}(\boldsymbol{e}_3,\pi-\varphi_1), \end{aligned} \tag{1.104}$$

and Bunge's rotation matrix $\boldsymbol{R}^{(p)}(\varphi_1, \Phi, \varphi_2)$ explicitly reads:

$$\begin{pmatrix} -\sin\varphi_1\cos\Phi\sin\varphi_2+\cos\varphi_1\cos\varphi_2 & \cos\varphi_1\cos\Phi\sin\varphi_2+\sin\varphi_1\cos\varphi_2 & \sin\varphi_2\sin\Phi \\ -\sin\varphi_1\cos\Phi\cos\varphi_2-\cos\varphi_1\sin\varphi_2 & \cos\varphi_1\cos\Phi\cos\varphi_2-\sin\varphi_1\sin\varphi_2 & \cos\varphi_2\sin\Phi \\ \sin\varphi_1\sin\Phi & -\cos\varphi_1\sin\Phi & \cos\Phi \end{pmatrix}. \tag{1.105}$$

It follows also from (1.104) that

$$\left(\boldsymbol{R}^{(p)}(\varphi_1, \Phi, \varphi_2)\right)^{-1} = \boldsymbol{R}^{(p)}(\pi-\varphi_2, \Phi, \pi-\varphi_1). \tag{1.106}$$

Before Bunge, Gel'fand et al. [125] use the convention described above for the definition of Euler angles, which they denote by $(\varphi_1, \theta, \varphi_2)$. On the other hand, they adopt the active view of rotations. Thus their rotation matrix [125, p. 6] is that of g in (1.103) and is the transpose of that given in (1.105).

1.9 Description of Rotations by Axis-Angle Parameters

Let $\{\boldsymbol{e}_i : i = 1, 2, 3\}$ be a right-handed orthonormal basis in V, and let $\mathcal{S}^2$ be the unit sphere. Let $\boldsymbol{n} \in \mathcal{S}^2$, and let n_1, n_2, n_3 be the components of $\boldsymbol{n}$ under the given basis, i.e., $\boldsymbol{n} = n_1\boldsymbol{e}_1 + n_2\boldsymbol{e}_2 + n_3\boldsymbol{e}_3$. Note that n_1, n_2, and n_3 are not independent; they must satisfy the relation $n_1^2 + n_2^2 + n_3^2 = 1$. In this section we find the matrix which represents $\boldsymbol{R}(\boldsymbol{n}, \omega)$ under the basis $\{\boldsymbol{e}_i : i = 1, 2, 3\}$ and has its entries parametrized by $\boldsymbol{n}$ and ω.

We begin with a simple lemma and its corollary.

Lemma 1.12 *Let $\boldsymbol{Q} = \boldsymbol{R}(\boldsymbol{e}_3, \omega)$, where $\omega \in (-\infty, \infty)$. Then*

$$\boldsymbol{Q}\boldsymbol{e}_1 = (\cos\omega)\boldsymbol{e}_1 + (\sin\omega)(\boldsymbol{e}_3 \times \boldsymbol{e}_1).$$

Proof We have $\boldsymbol{Q}\boldsymbol{e}_1 = \sum_i (\boldsymbol{e}_i \cdot \boldsymbol{Q}\boldsymbol{e}_1)\boldsymbol{e}_i = (\cos\omega)\boldsymbol{e}_1 + (\sin\omega)\boldsymbol{e}_2$. □

Corollary 1.13 *Let $\boldsymbol{n}$ and $\boldsymbol{m}$ be a pair of orthonormal vectors, and let $\boldsymbol{Q} = \boldsymbol{R}(\boldsymbol{n}, \omega)$. Then $\boldsymbol{Q}\boldsymbol{m} = (\cos\omega)\boldsymbol{m} + (\sin\omega)(\boldsymbol{n} \times \boldsymbol{m})$.* □

Each vector $\boldsymbol{x}$ in V can be written as $\boldsymbol{x} = (\boldsymbol{x}\cdot\boldsymbol{n})\boldsymbol{n} + (\boldsymbol{x} - (\boldsymbol{x}\cdot\boldsymbol{n})\boldsymbol{n})$. Let $\boldsymbol{a} = \boldsymbol{x} - (\boldsymbol{x}\cdot\boldsymbol{n})\boldsymbol{n}$ and $\boldsymbol{m} = \boldsymbol{a}/\|\boldsymbol{a}\|$. For each $\boldsymbol{n} \in \mathcal{S}^2$, $\omega \in (-\infty, \infty)$, and $\boldsymbol{x}$ in V, we have

$$\begin{aligned} \boldsymbol{R}(\boldsymbol{n}, \omega)\boldsymbol{x} &= \boldsymbol{R}(\boldsymbol{n}, \omega)((\boldsymbol{x}\cdot\boldsymbol{n})\boldsymbol{n} + \boldsymbol{a}) \\ &= (\boldsymbol{x}\cdot\boldsymbol{n})\boldsymbol{n} + \|\boldsymbol{a}\|\, \boldsymbol{R}(\boldsymbol{n}, \omega)\boldsymbol{m} \\ &= (\boldsymbol{x}\cdot\boldsymbol{n})\boldsymbol{n} + \|\boldsymbol{a}\|\, ((\cos\omega)\boldsymbol{m} + \sin\omega(\boldsymbol{n}\times\boldsymbol{m})) \\ &= (\boldsymbol{x}\cdot\boldsymbol{n})\boldsymbol{n} + (\cos\omega)\boldsymbol{a} + \sin\omega(\boldsymbol{n}\times\boldsymbol{a}) \\ &= (\boldsymbol{x}\cdot\boldsymbol{n})\boldsymbol{n} + (\cos\omega)(\boldsymbol{x} - (\boldsymbol{x}\cdot\boldsymbol{n})\boldsymbol{n}) + \sin\omega(\boldsymbol{n}\times\boldsymbol{x}) \\ &= (\cos\omega)\boldsymbol{x} + (1-\cos\omega)(\boldsymbol{n}\otimes\boldsymbol{n})\boldsymbol{x} + (\sin\omega)\boldsymbol{n}\times\boldsymbol{x}. \end{aligned} \tag{1.107}$$

Equation (1.107) is known as the Rodrigues rotation formula. It follows from (1.107) that we have two other versions of the Rodrigues formula as follows: For $\boldsymbol{n} \in \mathcal{S}^2$ and $\omega \in (-\infty, \infty)$,

$$\boldsymbol{R}(\boldsymbol{n}, \omega) = \cos\omega\boldsymbol{I} + (1-\cos\omega)\boldsymbol{n}\otimes\boldsymbol{n} + \sin\omega\boldsymbol{N} \tag{1.108}$$

$$= \boldsymbol{I} + \sin\omega\boldsymbol{N} + (1-\cos\omega)\boldsymbol{N}^2, \tag{1.109}$$

where the linear transformation $\boldsymbol{N}$ is given by the matrix

$$\begin{pmatrix} 0 & -n_3 & n_2 \\ n_3 & 0 & -n_1 \\ -n_2 & n_1 & 0 \end{pmatrix} \tag{1.110}$$

under the basis $\{\boldsymbol{e}_i\}$. In components, (1.108) reads

$$R_{ij} = \cos\omega\delta_{ij} + (1-\cos\omega)n_i n_j - (\sin\omega)\varepsilon_{ijk}n_k, \tag{1.111}$$

where the alternator

$$\varepsilon_{ijk} = \begin{cases} 1 & \text{if } (i,j,k) \text{ is a cyclic permutation of } (1,2,3) \\ -1 & \text{if } (i,j,k) \text{ is a non-cyclic permutation of } (1,2,3) \\ 0 & \text{if } i,j,k \text{ are not distinct.} \end{cases}$$

Under the basis $\{\boldsymbol{e}_i\}$, equation (1.108) is given by the matrix equation

$$\boldsymbol{R} = \cos\omega \begin{pmatrix} 1 & 0 & 0 \\ 0 & 1 & 0 \\ 0 & 0 & 1 \end{pmatrix} + (1-\cos\omega) \begin{pmatrix} n_1^2 & n_1n_2 & n_1n_3 \\ n_2n_1 & n_2^2 & n_2n_3 \\ n_3n_1 & n_3n_2 & n_3^2 \end{pmatrix} + \sin\omega \begin{pmatrix} 0 & -n_3 & n_2 \\ n_3 & 0 & -n_1 \\ -n_2 & n_1 & 0 \end{pmatrix}. \tag{1.112}$$

From (1.112) we observe that

$$\operatorname{tr}\boldsymbol{R} = 1 + 2\cos\omega, \qquad \text{or} \quad \cos\omega = \frac{1}{2}(\operatorname{tr}\boldsymbol{R} - 1), \tag{1.113}$$

from which we can determine ω if the matrix $[R_{ij}]$ is given. Similarly from (1.112) we obtain

$$n_1\sin\omega = \frac{1}{2}(R_{32}-R_{23}), \quad n_2\sin\omega = \frac{1}{2}(R_{13}-R_{31}), \quad n_3\sin\omega = \frac{1}{2}(R_{21}-R_{12}), \tag{1.114}$$

from which we can compute n_1, n_2, n_3 after we have determined ω. Also, it follows immediately from (1.108) that

$$\boldsymbol{R}(\boldsymbol{n},\pi) = \boldsymbol{R}(-\boldsymbol{n},\pi) = -\boldsymbol{I} + 2\boldsymbol{n}\otimes\boldsymbol{n}. \tag{1.115}$$

As mentioned in Sect. 1.6, the rotation $\boldsymbol{R}(\boldsymbol{n},\omega)$ with axis and sense specified by the unit vector $\boldsymbol{n}$ and rotation angle ω is well defined for any $\boldsymbol{n}\in\mathcal{S}^2$ and any $-\infty<\omega<\infty$. On the other hand, the set $\{\boldsymbol{R}(\boldsymbol{n},\omega) : \boldsymbol{n}\in\mathcal{S}^2, \omega\in[0,\pi]\}$ already covers all rotations, and the correspondence $(\boldsymbol{n},\omega)\mapsto\boldsymbol{R}(\boldsymbol{n},\omega)$ is one-to-one for $\omega\in(0,\pi)$. We may use spherical coordinates (Θ,Φ) on the unit sphere $\mathcal{S}^2$ to describe $\boldsymbol{n}$: thus, $n_1=\sin\Theta\cos\Phi$, $n_2=\sin\Theta\sin\Phi$, and $n_3=\cos\Theta$. Then the rotations are parametrized by the angles ω, Θ, and Φ.

Definition 1.14 Let $\boldsymbol{R}(\omega;\Theta,\Phi) := \boldsymbol{R}(\boldsymbol{n}(\Theta,\Phi),\omega)$, where $0\le\omega\le\pi$, $0\le\Theta\le\pi$, and $0\le\Phi<2\pi$. We call the map $(\omega;\Theta,\Phi)\mapsto\boldsymbol{R}(\omega;\Theta,\Phi)$ the parametrization of rotations by the axis-angle parameters $(\omega;\Theta,\Phi)$. □

By direct computations, we obtain from (1.110) that

$$\boldsymbol{N}^2 = \boldsymbol{n}\otimes\boldsymbol{n} - \boldsymbol{I}. \tag{1.116}$$

By (1.109), we have

$$\boldsymbol{R}(\boldsymbol{n},\omega)+\boldsymbol{R}(\boldsymbol{n},-\omega)=2\boldsymbol{I}+2(1-\cos\omega)\boldsymbol{N}^2. \tag{1.117}$$

For later use we introduce another second-order tensor

$$\boldsymbol{Z}^{\perp}(\boldsymbol{n},\omega):=2\boldsymbol{I}-\boldsymbol{R}(\boldsymbol{n},\omega)-\boldsymbol{R}(\boldsymbol{n},\omega)^{-1}. \tag{1.118}$$

By (1.116) and (1.117), we see that

$$\boldsymbol{Z}^{\perp}(\boldsymbol{n},\omega)=\lambda(\omega)(\boldsymbol{I}-\boldsymbol{n}\otimes\boldsymbol{n}),\qquad \text{where } \lambda(\omega)=2(1-\cos\omega). \tag{1.119}$$

Let

$$\boldsymbol{Z}^{\parallel}(\boldsymbol{n},\omega):=\lambda(\omega)\boldsymbol{I}-\boldsymbol{Z}^{\perp}(\boldsymbol{n},\omega)=\lambda(\omega)\boldsymbol{n}\otimes\boldsymbol{n}. \tag{1.120}$$

For each $\boldsymbol{x}\in V$, we have

$$\boldsymbol{Z}^{\perp}(\boldsymbol{n},\omega)\boldsymbol{x}=\lambda(\omega)\boldsymbol{x}^{\perp},\qquad \boldsymbol{Z}^{\parallel}(\boldsymbol{n},\omega)\boldsymbol{x}=\lambda(\omega)\boldsymbol{x}^{\parallel}, \tag{1.121}$$

where

$$\boldsymbol{x}^{\perp}=\boldsymbol{x}-(\boldsymbol{x}\cdot\boldsymbol{n})\boldsymbol{n},\qquad \text{and}\qquad \boldsymbol{x}^{\parallel}=(\boldsymbol{x}\cdot\boldsymbol{n})\boldsymbol{n}, \tag{1.122}$$

are the components of $\boldsymbol{x}$ perpendicular and parallel to $\boldsymbol{n}$, respectively.

Note that $\boldsymbol{N}$ is skew. It is often referred to as the skew tensor corresponding to the unit vector $\boldsymbol{n}$, which defines the axis of the rotation $\boldsymbol{R}(\boldsymbol{n},\omega)$, because

$$\boldsymbol{N}\boldsymbol{a}=\boldsymbol{n}\times\boldsymbol{a}\qquad \text{for any } \boldsymbol{a}\in V.$$

To emphasize the relationship between $\boldsymbol{N}$ and $\boldsymbol{n}$, in what follows we shall often simply put $\boldsymbol{n}\times$ for $\boldsymbol{N}$. Under a right-handed orthonormal basis $\{\boldsymbol{e}_i\}$ with $\boldsymbol{e}_1=\boldsymbol{n}$, the skew tensor $\boldsymbol{N}$ or $\boldsymbol{n}\times$ is represented by the matrix

$$\begin{pmatrix}0&0&0\\0&0&-1\\0&1&0\end{pmatrix}.$$

It is easily verified by direct computation that under the aforementioned basis

$$\exp(\omega\boldsymbol{N})=\sum_{n=0}^{\infty}\frac{\omega^n\boldsymbol{N}^n}{n!}=\begin{pmatrix}1&0&0\\0&\cos\omega&-\sin\omega\\0&\sin\omega&\cos\omega\end{pmatrix}=\boldsymbol{R}(\boldsymbol{n},\omega). \tag{1.123}$$

Since $\boldsymbol{R}$, $\boldsymbol{N}$, and $\exp(\omega\boldsymbol{N})$ are linear transformations, it is clear that the equality $\boldsymbol{R}(\boldsymbol{n},\omega)=\exp(\omega\boldsymbol{N})$ holds under all coordinate systems. As the sine and cosine functions are periodic with period 2π, the formula $\boldsymbol{R}(\boldsymbol{n},\omega)=\exp(\omega\boldsymbol{n}\times)$ makes sense for all $\omega\in(-\infty,\infty)$. On the other hand, $\boldsymbol{R}(\boldsymbol{n},\pi)=\boldsymbol{R}(-\boldsymbol{n},\pi)$, $\boldsymbol{R}(\boldsymbol{n},0)=\boldsymbol{I}$ for any unit vector $\boldsymbol{n}$, and all rotations are covered by $\{(\boldsymbol{n},\omega):\boldsymbol{n}\in\mathcal{S}^2,\omega\in[0,\pi]\}$. We record these findings as a theorem.

Theorem 1.15 *All rotations $\boldsymbol{R}(\boldsymbol{n},\omega)$ in SO(3) can be expressed in the form*

$$\boldsymbol{R}(\boldsymbol{n},\omega)=\exp(\omega\boldsymbol{n}\times),\qquad \text{where } 0\le\omega\le\pi \text{ and } \boldsymbol{n}\in\mathcal{S}^2. \tag{1.124}$$

For each unit vector $\boldsymbol{n}$, $\exp(\pi\boldsymbol{n}\times)=\exp(-\pi\boldsymbol{n}\times)$. □

By Theorem 1.15, SO(3) can be depicted as a closed ball $\overline{\mathrm{B}_\pi}$ of radius π: each point $\omega\boldsymbol{n}$ $(0\le\omega<\pi)$ in the open ball B_π stands for a rotation, namely $\boldsymbol{R}(\boldsymbol{n},\omega)$; each pair of antipodal points $\pi\boldsymbol{n}$ and $-\pi\boldsymbol{n}$ of $\overline{\mathrm{B}_\pi}$, as shown by (1.115), represent the same rotation $-\boldsymbol{I}+2\boldsymbol{n}\otimes\boldsymbol{n}$. As mentioned above, $\boldsymbol{R}(\boldsymbol{n},\omega)$ is a periodic function of ω with period 2π. Consider a steady rotation with axis and sense defined by $\boldsymbol{n}$ and with ω increasing with time t as $\omega=t$. At $t=0$, the point that represents $\boldsymbol{R}(\boldsymbol{n},0)=\boldsymbol{I}$ in $\overline{\mathrm{B}_\pi}$ is at the center O of $\overline{\mathrm{B}_\pi}$. Let the diameter specified by $\boldsymbol{n}$ meet the surface of $\overline{\mathrm{B}_\pi}$ at the antipodal points P and P', where $\mathbf{OP}=\boldsymbol{n}$. Note that the two antipodal points should be identified. As time progresses from $t=0$, the point that represents $\boldsymbol{R}(\boldsymbol{n},t)$ in $\overline{\mathrm{B}_\pi}$ moves towards P and reaches P at $t=\pi$. But point P is identified with P'. As time advances beyond $t=\pi$, the point that represents $\boldsymbol{R}(\boldsymbol{n},t)$ moves from P' towards O and it reaches O at $t=2\pi$, which completes one cycle. The cycle is then repeated without end with time.

Since $\omega\boldsymbol{n}\times$ is skew for any $0\le\omega\le\pi$ and any unit vector $\boldsymbol{n}$, the preceding theorem implies that $\mathrm{SO}(3)\subset\exp(\mathrm{Skw})$. In fact, we have:

Proposition 1.16 $\exp(\mathrm{Skw})=\mathrm{SO}(3)$.

Proof It suffices to prove that $\exp(\mathrm{Skw})\subset\mathrm{SO}(3)$. Let $\boldsymbol{A}\in\mathrm{Skw}$ be given. Under an orthonormal basis $\{\boldsymbol{e}_j\}$, $\boldsymbol{A}$ is represented by a matrix of the form

$$\begin{pmatrix} 0 & -a_3 & a_2\\ a_3 & 0 & -a_1\\ -a_2 & a_1 & 0\end{pmatrix}, \tag{1.125}$$

where $a_j\in\mathbb{R}$ for $j=1,2,3$. It is straightforward to show that $\boldsymbol{A}$ has three distinct eigenvalues: $0, i\alpha$, and $-i\alpha$, where $\alpha=\sqrt{a_1^2+a_2^2+a_3^2}$. Hence $\boldsymbol{A}$ is diagonalizable. By (1.72) we have

$$\exp(\boldsymbol{A})(\exp(\boldsymbol{A}))^T=\exp(\boldsymbol{A})\exp(\boldsymbol{A}^T)=\exp(\boldsymbol{A})\exp(-\boldsymbol{A})=\exp(\boldsymbol{0})=\boldsymbol{I}.$$

Moreover, it follows from (1.73) that $\det(\exp\boldsymbol{A})=e^{\mathrm{tr}\,\boldsymbol{A}}=e^0=1$. Hence $\exp(\boldsymbol{A})\in\mathrm{SO}(3)$. □

For later convenience we choose a norm $\|\cdot\|=\frac{1}{\sqrt{2}}\|\cdot\|_F$ in $\mathrm{M}_3(\mathbb{R})$ so that

$$\boldsymbol{E}_1=-\boldsymbol{e}_2\otimes\boldsymbol{e}_3+\boldsymbol{e}_3\otimes\boldsymbol{e}_2,\quad \boldsymbol{E}_2=-\boldsymbol{e}_3\otimes\boldsymbol{e}_1+\boldsymbol{e}_1\otimes\boldsymbol{e}_3,\quad \boldsymbol{E}_3=-\boldsymbol{e}_1\otimes\boldsymbol{e}_2+\boldsymbol{e}_2\otimes\boldsymbol{e}_1 \tag{1.126}$$

constitute an orthonormal basis in Skw. Using (1.110), we obtain by direct computations that

$$\|\boldsymbol{n}\times\|=\|\boldsymbol{N}\|=1. \tag{1.127}$$

Let $\boldsymbol{A} = a_1\boldsymbol{E}_1 + a_2\boldsymbol{E}_2 + a_3\boldsymbol{E}_3 \in \mathrm{Skw}$. Then $\|\boldsymbol{A}\| = \sqrt{a_1^2 + a_2^2 + a_3^2} := \alpha$, and $\boldsymbol{A} = \alpha\boldsymbol{N}$. Since the Rodrigues formula is valid for any rotation axis and angle, by (1.109) we have

$$\exp(\boldsymbol{A}) = \boldsymbol{R}(\boldsymbol{n}, \alpha) = \boldsymbol{I} + \frac{\sin\alpha}{\alpha}\boldsymbol{A} + \frac{2\sin^2(\alpha/2)}{\alpha^2}\boldsymbol{A}^2, \tag{1.128}$$

which is often called the Rodrigues formula in the literature. Note that formula (1.128) is valid for $\alpha \in (-\infty, \infty)$ as $\boldsymbol{A}/\alpha = \boldsymbol{N}$ and $\|\boldsymbol{N}\| = 1$.

While the map $\exp : \mathrm{Skw} \to \mathrm{SO}(3)$ is surjective, it is clearly not injective; see Theorem 1.15. The exponential function exp, however, is injective if we suitably restrict its domain.

Proposition 1.17 Let $\mathsf{B} = \{\omega\boldsymbol{n}\times \in \mathrm{Skw} : \boldsymbol{n} \in \mathcal{S}^2, 0 \le \omega < \pi\}$. The exponential function exp is injective on B.

Proof Suppose $\omega_i \in (0, \pi)$, $\boldsymbol{n}_i \in \mathcal{S}^2$ for $i = 1, 2$, and $\exp(\omega_1\boldsymbol{n}_1\times) = \exp(\omega_2\boldsymbol{n}_2\times)$. Then $\boldsymbol{R}(\boldsymbol{n}_1, \omega_1) = \boldsymbol{R}(\boldsymbol{n}_2, \omega_2)$, which implies either $\boldsymbol{n}_1 = \boldsymbol{n}_2$ or $\boldsymbol{n}_1 = -\boldsymbol{n}_2$. If $\boldsymbol{n}_1 = \boldsymbol{n}_2$, then we have $\boldsymbol{R}(\boldsymbol{n}_1, \omega_1) = \boldsymbol{R}(\boldsymbol{n}_1, \omega_2)$, which implies $\omega_1 = \omega_2$ because both $\omega_1, \omega_2 \in (0, \pi)$. If $\boldsymbol{n}_1 = -\boldsymbol{n}_2$, then by (1.81) we have $\boldsymbol{R}(\boldsymbol{n}_1, \omega_1) = \boldsymbol{R}(-\boldsymbol{n}_1, \omega_2) = \boldsymbol{R}(\boldsymbol{n}_1, -\omega_2)$, which is impossible because $\omega_1, \omega_2 \in (0, \pi)$. Hence under the asserted hypothesis, the relations $\boldsymbol{n}_1 = \boldsymbol{n}_2$ and $\omega_1 = \omega_2$ hold.

If one of the angles is zero, say $\omega_1 = 0$, then $\exp(\omega_1\boldsymbol{n}_1\times) = \exp(\boldsymbol{0}) = \boldsymbol{I}$ for any $\boldsymbol{n}_1$. Suppose $\exp(\omega_2\boldsymbol{n}_2\times) = \boldsymbol{I}$. Choose a Cartesian coordinate system such that $\boldsymbol{n}_2 = \boldsymbol{e}_1$ and the matrix $[P_{ij}]$ that represents $\exp(\omega_2\boldsymbol{n}_2\times)$ under the chosen Cartesian coordinate system has entries $P_{32} = -P_{23} = \sin\omega_2$; cf. (1.123). The hypothesis that $\exp(\omega_2\boldsymbol{n}_2\times) = \boldsymbol{I}$ implies that $\omega_2 = 0$ and thence $\omega_2\boldsymbol{n}_2\times = \boldsymbol{0}$ for any $\boldsymbol{n}_2$. □

Let $\mathrm{Log} : \exp(\mathsf{B}) \to \mathsf{B}$ be defined[11] by $\mathrm{Log} = \left(\exp\big|_{\mathsf{B}}\right)^{-1}$. Here we derive some explicit expressions for $\mathrm{Log}\,\boldsymbol{R}$.

Since $\mathrm{Log} = \left(\exp\big|_{\mathsf{B}}\right)^{-1}$ and $\boldsymbol{R}(\boldsymbol{n}, \omega) \in \exp(\mathsf{B})$ means that $\boldsymbol{R}(\boldsymbol{n}, \omega) = \exp(\omega\boldsymbol{n}\times)$, clearly we have

$$\mathrm{Log}\,\boldsymbol{R}(\boldsymbol{n}, \omega) = \omega\boldsymbol{n}\times = \omega\boldsymbol{N}, \qquad \text{for } \boldsymbol{R} \in \exp(\mathsf{B}). \tag{1.129}$$

Let $\boldsymbol{W} = \frac{1}{2}(\boldsymbol{R} - \boldsymbol{R}^T)$. From the Rodrigues formula (1.108) and from (1.127) we deduce that

$$\boldsymbol{W} = \sin\omega\boldsymbol{N}, \qquad \|\boldsymbol{W}\| = \sin\omega. \tag{1.130}$$

It follows that $\boldsymbol{W}/\|\boldsymbol{W}\| = \boldsymbol{N}$. By (1.129) and (1.130) we obtain the formula [162, eq. (B.14)]

$$\mathrm{Log}\,\boldsymbol{R}(\boldsymbol{n}, \omega) = \sin^{-1}(\|\boldsymbol{W}\|) \cdot \frac{\boldsymbol{W}}{\|\boldsymbol{W}\|}, \qquad \text{for } \boldsymbol{R} \in \exp(\mathsf{B}). \tag{1.131}$$

For yet another version of the same formula, we start with a slightly recast version of $(1.130)_1$:

$$\boldsymbol{R} - \boldsymbol{R}^T = 2\sin\omega\boldsymbol{N}. \tag{1.132}$$

[11] We use different notations for the Log function here and the log function defined by the convergent power series in (1.68), because Proposition 1.5 only guarantees $\log(\exp A) = A$ for $A \in \mathrm{M}_3(\mathbb{C})$ if $\|A\|_F < \log 2$. The two functions certainly agree where their domains of definition overlap.

For $\omega \neq 0, \pi$, we multiply both sides of (1.132) by $\omega/(2\sin\omega)$ to obtain from (1.129) the formula

$$\operatorname{Log} \boldsymbol{R}(\boldsymbol{n}, \omega) = \begin{cases} \dfrac{\omega}{2\sin\omega}\left(\boldsymbol{R} - \boldsymbol{R}^T\right) & \text{for } \boldsymbol{R} \neq \boldsymbol{I} \\ \boldsymbol{0} & \text{for } \boldsymbol{R} = \boldsymbol{I}, \end{cases} \qquad \text{for } \boldsymbol{R} \in \exp(\mathbb{B}). \tag{1.133}$$

Note that we have

$$\|\operatorname{Log} \boldsymbol{R}(\boldsymbol{n}, \omega)\| = \omega, \qquad \text{for } \boldsymbol{R} \in \exp(\mathbb{B}). \tag{1.134}$$

1.10 Misorientation and Distance Between Two Rotations

Given two rotations $\boldsymbol{P}$ and $\boldsymbol{Q}$, the rotation

$$\boldsymbol{M}(\widetilde{\boldsymbol{n}}, \widetilde{\omega}) := \boldsymbol{Q}\boldsymbol{P}^T, \tag{1.135}$$

which takes $\boldsymbol{P}$ to $\boldsymbol{Q}$, is called the misorientation of $\boldsymbol{Q}$ with respect to $\boldsymbol{P}$. The rotation axis (as specified by the unit vector $\widetilde{\boldsymbol{n}}$) and rotation angle $\widetilde{\omega}$ pertaining to $\boldsymbol{M}$ are called the misorientation axis and misorientation angle, respectively. By (1.113), the misorientation angle is given by the formula

$$\widetilde{\omega} = \cos^{-1}\left(\frac{1}{2}\left(\operatorname{tr}(\boldsymbol{Q}\boldsymbol{P}^T) - 1\right)\right). \tag{1.136}$$

It turns out that the misorientation angle is a distance function on the set of rotations SO(3). To proceed further, let us introduce the definition of distance function or metric on a set.

Definition 1.18 Let X be a set. A distance function or metric on X is a mapping $d : X \times X \to \mathbb{R}$, $(p, q) \mapsto d(p, q)$, such that the following conditions are satisfied:

(a) $d(p, q) > 0$ if $p \neq q$; $d(p, p) = 0$;
(b) $d(p, q) = d(q, p)$;
(c) $d(p, q) \leq d(p, r) + d(r, q)$, for any $r \in X$.

The number $d(p, q)$ is called the distance from p to q. □

Let $d_{\mathrm{SO}(3)} : \mathrm{SO}(3) \times \mathrm{SO}(3) \to \mathbb{R}$ be defined by

$$d_{\mathrm{SO}(3)}(\boldsymbol{P}, \boldsymbol{Q}) = \cos^{-1}\left(\frac{1}{2}\left(\operatorname{tr}(\boldsymbol{Q}\boldsymbol{P}^T) - 1\right)\right). \tag{1.137}$$

As a misorientation angle, we have $d_{\mathrm{SO}(3)}(\boldsymbol{P}, \boldsymbol{Q}) \in [0, \pi]$, and $d_{\mathrm{SO}(3)}(\boldsymbol{P}, \boldsymbol{Q}) = 0$ if and only if $\boldsymbol{P} = \boldsymbol{Q}$. Hence condition (a) of distance function is satisfied by $d_{\mathrm{SO}(3)}$. Condition (b) follows easily from the property of trace that $\operatorname{tr} \boldsymbol{R} = \operatorname{tr} \boldsymbol{R}^T$ for each rotation $\boldsymbol{R}$. Condition (c) for $d_{\mathrm{SO}(3)}(\cdot, \cdot)$ is an immediate consequence of the following lemma.

Lemma 1.19 *Let $\boldsymbol{P}$, $\boldsymbol{Q}$, and $\boldsymbol{R}$ be rotations, and let $\boldsymbol{Q}\boldsymbol{P}^T = \boldsymbol{M}_1(\widetilde{\boldsymbol{n}}_1, \widetilde{\omega}_1)$, $\boldsymbol{R}\boldsymbol{Q}^T = \boldsymbol{M}_2(\widetilde{\boldsymbol{n}}_2, \widetilde{\omega}_2)$, $\boldsymbol{P}\boldsymbol{R}^T = \boldsymbol{M}_3(\widetilde{\boldsymbol{n}}_3, \widetilde{\omega}_3)$. Then $\widetilde{\omega}_3 \leq \widetilde{\omega}_1 + \widetilde{\omega}_2$.*

Proof Note that $\boldsymbol{M}_3^T = \boldsymbol{M}_2\boldsymbol{M}_1$ and $\boldsymbol{M}_3^T$ has the same rotation angle $\widetilde{\omega}_3$ as $\boldsymbol{M}_3$. By formula (11.19), which we shall prove in Sect. 11.1.2, we have

$$\cos\frac{\widetilde{\omega}_3}{2} = \cos\frac{\widetilde{\omega}_2}{2}\cos\frac{\widetilde{\omega}_1}{2} - \sin\frac{\widetilde{\omega}_2}{2}\sin\frac{\widetilde{\omega}_1}{2}(\widetilde{\boldsymbol{n}}_2 \cdot \widetilde{\boldsymbol{n}}_1). \tag{1.138}$$

Since $\widetilde{\boldsymbol{n}}_2 \cdot \widetilde{\boldsymbol{n}}_1 \leq 1$, we observe from (1.138) that

$$\cos\frac{\widetilde{\omega}_3}{2} \geq \cos\frac{\widetilde{\omega}_2}{2}\cos\frac{\widetilde{\omega}_1}{2} - \sin\frac{\widetilde{\omega}_2}{2}\sin\frac{\widetilde{\omega}_1}{2} = \cos\frac{\widetilde{\omega}_1 + \widetilde{\omega}_2}{2}, \tag{1.139}$$

which implies $\widetilde{\omega}_3 \leq \widetilde{\omega}_1 + \widetilde{\omega}_2$, because the cosine function is strictly decreasing on $[0, \pi]$ and $\widetilde{\omega}_i \in [0, \pi]$ for $i = 1, 2, 3$. □

In Sect. 10.2 we shall show that $d_{\mathrm{SO}(3)}(\cdot, \cdot)$, as defined by (1.137), is the Riemannian distance on SO(3) as a Riemannian manifold.[12] Several distance functions on SO(3) have been proposed in the literature; cf. [161] for a comparison and analysis.

It follows easily from definition (1.137) and the properties of trace that

$$d_{\mathrm{SO}(3)}(\boldsymbol{P}^T, \boldsymbol{Q}^T) = d_{\mathrm{SO}(3)}(\boldsymbol{P}, \boldsymbol{Q}), \tag{1.140}$$

and that the distance function $d_{\mathrm{SO}(3)}(\cdot, \cdot)$ is bi-invariant, i.e.,

$$d_{\mathrm{SO}(3)}(\boldsymbol{R}\boldsymbol{P}, \boldsymbol{R}\boldsymbol{Q}) = d_{\mathrm{SO}(3)}(\boldsymbol{P}, \boldsymbol{Q}), \tag{1.141}$$

$$d_{\mathrm{SO}(3)}(\boldsymbol{P}\boldsymbol{R}, \boldsymbol{Q}\boldsymbol{R}) = d_{\mathrm{SO}(3)}(\boldsymbol{P}, \boldsymbol{Q}), \tag{1.142}$$

for all $\boldsymbol{P}$, $\boldsymbol{Q}$, and $\boldsymbol{R}$ in SO(3).

[12] This will also show that the metric topology defined by $d_{\mathrm{SO}(3)}$ is the same as the manifold topology of SO(3); see, e.g., [186, p. 278].

Chapter 2

2 Ideal Crystals and the Crystallographic Groups

In this chapter we cover, for later use, some basics on crystallography and crystallographic groups. Prerequisites in elementary group theory are presented in Appendix A. In particular, in Sect. A.1 we use a review of the fundamental concepts of sets, relations, and functions to specify terminology and notation.

2.1 Preliminaries

Mathematically the set of non-singular linear transformations on V constitutes a group (cf. Definition A.1 in Appendix A) under the binary operation of "composition of mappings", i.e.,

1. The composition of two non-singular linear transformations is still a non-singular linear transformation.
2. The composition of mappings is associative.
3. The identity map is a non-singular linear transformation.
4. Each non-singular linear transformation has an inverse, which is itself a non-singular linear transformation.

We denote by GL(3) the group of non-singular linear transformations on V.

Any subset of a group G, which itself constitutes a group under the same binary operation in G, is called a subgroup of G. A linear transformation $\boldsymbol{Q}$ on V is said to be orthogonal if it preserves the inner product, i.e.,

$$\boldsymbol{Q}\boldsymbol{u} \cdot \boldsymbol{Q}\boldsymbol{v} = \boldsymbol{u} \cdot \boldsymbol{v} \qquad \text{for any vectors } \boldsymbol{u}, \boldsymbol{v} \in V. \tag{2.1}$$

Let $\mathrm{O}(3) \subset \mathrm{GL}(3)$ be the set of orthogonal transformations on V. It follows immediately from (2.1) that every $\boldsymbol{Q} \in \mathrm{O}(3)$ satisfies

$$\boldsymbol{Q}\boldsymbol{Q}^T = \boldsymbol{Q}^T\boldsymbol{Q} = \boldsymbol{I}, \quad \boldsymbol{Q}^T = \boldsymbol{Q}^{-1}, \quad \text{and} \quad \det \boldsymbol{Q} = \det \boldsymbol{Q}^T = \pm 1. \tag{2.2}$$

By (2.1) and (2.2) it is easy to verify that O(3) is a subgroup of GL(3).

Recall that rotations are orthogonal transformations with determinant equal to 1. If $\boldsymbol{R}$, $\boldsymbol{R}_1$ and $\boldsymbol{R}_2$ are rotations, we have $\det(\boldsymbol{R}^{-1}) = \det(\boldsymbol{R}^T) = 1$, and $\det(\boldsymbol{R}_2\boldsymbol{R}_1) = \det(\boldsymbol{R}_2)\det(\boldsymbol{R}_1) = 1$. Hence the set of rotations

$$\mathrm{SO}(3) := \{\boldsymbol{R} \in \mathrm{O}(3) : \det \boldsymbol{R} = 1\} \tag{2.3}$$

is a subgroup of O(3) and of GL(3). Rotations are also called proper orthogonal transformations.

Let $\boldsymbol{Q} \in \mathrm{O}(3)$ and let $\boldsymbol{\mathcal{I}} := -\boldsymbol{I}$ be the inversion. Clearly $\boldsymbol{\mathcal{I}} \in \mathrm{O}(3)$. Moreover, we have

$$\boldsymbol{Q} = \begin{cases} \boldsymbol{R}, & \text{for some rotation } \boldsymbol{R} \text{ if } \det \boldsymbol{Q} = 1 \\ \boldsymbol{\mathcal{I}}\boldsymbol{R}, & \text{for some rotation } \boldsymbol{R} \text{ if } \det \boldsymbol{Q} = -1. \end{cases} \tag{2.4}$$

Indeed suppose $\det \boldsymbol{Q} = -1$. Then $\det(\boldsymbol{\mathcal{I}}\boldsymbol{Q}) = 1$ and $\boldsymbol{\mathcal{I}}\boldsymbol{Q} = \boldsymbol{R}$ for some rotation $\boldsymbol{R}$. Hence $\boldsymbol{Q} = \boldsymbol{\mathcal{I}}\boldsymbol{R}$, which is called a roto-inversion. Orthogonal transformations with determinant equal to -1 are said to be improper.

Table 1 Multiplication table of group D_3

	e	r	r^2	s	sr	sr^2
e	e	r	r^2	s	sr	sr^2
r	r	r^2	e	sr^2	s	sr
r^2	r^2	e	r	sr	sr^2	s
s	s	sr	sr^2	e	r	r^2
sr	sr	sr^2	s	r^2	e	r
sr^2	sr^2	s	sr	r	r^2	e

Subgroups of O(3) which are (resp. are not) subgroups of SO(3) are said to be proper (resp. improper).

In what follows we present the multiplication table of a finite subgroup of the rotation group, which we shall use later for illustrative purposes.

Example 2.1 Consider the set of rotations $D_3 = \{e, r, r^2, s, sr, sr^2\}$, where $e = \boldsymbol{I}$, $r = \boldsymbol{R}(\boldsymbol{n}, 2\pi/3)$, $s = \boldsymbol{R}(\boldsymbol{m}, \pi)$, and $\boldsymbol{m}$ and $\boldsymbol{n}$ are two given orthogonal unit vectors. Note that for each $k = 0, 1, 2$, we have

$$sr^k\boldsymbol{n} = -\boldsymbol{n}, \qquad (sr^k)^2\boldsymbol{n} = \boldsymbol{n}. \tag{2.5}$$

Let L be the axis of rotation of sr^k. Then it is also the axis of rotation of $(sr^k)^2$. Equations $(2.5)_1$ and $(2.5)_2$ say that $\boldsymbol{n}$ is perpendicular to L and that it defines an axis of rotation for $(sr^k)^2$, respectively. Hence $(sr^k)^2$ has two distinct axes of rotation, which implies $(sr^k)^2 = e$. It follows that for $k = 0, 1, 2$,

$$s^2 = e, \qquad sr = r^2 s, \qquad sr^2 = rs, \tag{2.6}$$

respectively. With the help of (2.6), we can easily construct the multiplication table for D_3; see Table 1. In the table the rows (resp. columns) are listed from top to bottom (resp. from left to right) under $g_1 = e$, $g_2 = r, \ldots, g_6 = sr^2$. The (i, j)-th entry of the table is the product $g_i g_j$. For example, the $(3, 4)$-th entry gives the product $r^2 s = sr$. Note that $\{r, s\}$ is a set of generators for D_3.

For $\boldsymbol{m} = \boldsymbol{e}_1$ and $\boldsymbol{n} = \boldsymbol{e}_3$, D_3 is the rotational symmetry group of the equilateral triangle in the 1-2 plane which has its centroid at the origin and one vertex at $(1, 0, 0)$. In other words, the equilateral triangle in question remains invariant under the rotations in D_3.

The symmetry of a physical object should not be affected by a rotation of the object. Suppose the equilateral triangle, which lies in the plane containing the origin and normal to $\boldsymbol{n}$ and has a vertex located at the point with position vector $\boldsymbol{m}$, undergoes a rotation $\boldsymbol{Q}$ about the origin. After the rotation, the rotational symmetry group G of the equilateral triangle is generated by $r' = \boldsymbol{R}(\boldsymbol{Q}\boldsymbol{n}, 2\pi/3)$ and $s' = \boldsymbol{R}(\boldsymbol{Q}\boldsymbol{m}, \pi)$. By Euler's theorem (1.82), we have

$$r' = \boldsymbol{Q}\boldsymbol{R}(\boldsymbol{n}, 2\pi/3)\,\boldsymbol{Q}^{-1} = \boldsymbol{Q}r\,\boldsymbol{Q}^{-1}, \qquad s' = \boldsymbol{Q}\boldsymbol{R}(\boldsymbol{m}, \pi)\,\boldsymbol{Q}^{-1} = \boldsymbol{Q}s\,\boldsymbol{Q}^{-1}. \tag{2.7}$$

The multiplication table of G is that which results after r and s in Table 1 are replaced by r' and s', respectively, and we have $G = \boldsymbol{Q}D_3\boldsymbol{Q}^{-1}$, i.e., G and D_3, as subgroups of SO(3), are conjugate[13] to each other. As G and D_3 describe the same symmetry, we will regard

[13] Cf. Sect. A.3.2 for definition of conjugacy relation and of conjugacy classes.

them as equivalent. Henceforth we will use the symbol D_3 to denote any subgroup of SO(3) generated by $r = \boldsymbol{R}(\boldsymbol{n}, 2\pi/3)$ and $s = \boldsymbol{R}(\boldsymbol{m}, \pi)$, where $\boldsymbol{m}$ and $\boldsymbol{n}$ are *any* two orthogonal unit vectors. In fact it is customary to use the symbol D_3 to denote also the conjugacy class of the aforementioned equivalent groups. Whether the symbol D_3 stands for the conjugacy class or a specific group in the class should be clear from the context where it appears. □

Remark 2.2 In general two conjugate subgroups G_1 and G_2 of SO(3) are regarded as equivalent, i.e., if there is a rotation $\boldsymbol{Q}$ such that $G_2 = \boldsymbol{Q} G_1 \boldsymbol{Q}^{-1}$. If we adopt the passive view of rotations, the preceding assertion will be reworded as follows: Two subgroups G_1 and G_2 of SO(3) are regarded as equivalent if there is a passive rotation $\boldsymbol{Q}^{(p)}$ (as defined by a rotation of the Cartesian coordinate system) such that $G_2 = (\boldsymbol{Q}^{(p)})^{-1} G_1 \boldsymbol{Q}^{(p)}$. In other words, the two groups G_1 and G_2 are equivalent if they can be taken as describing the symmetry of the same physical object under two Cartesian coordinate systems. □

2.2 The Euclidean Group

Consider a body C in a given placement[14] $\boldsymbol{\kappa}_0$, under which it occupies the entire Euclidean point space E^3, i.e., $\boldsymbol{\kappa}_0(\mathsf{C}) = E^3$. We shall refer to the body C in the placement $\boldsymbol{\kappa}_0$ as $(\mathsf{C}, \boldsymbol{\kappa}_0)$ but shall suppress $\boldsymbol{\kappa}_0$ when no confusion should arise. We label each point in C by the location $\boldsymbol{x} \in E^3$ that it occupies under $\boldsymbol{\kappa}_0$. A transplacement $\boldsymbol{h} : \boldsymbol{\kappa}_0(\mathsf{C}) \to E^3$ of C (i.e., $\boldsymbol{h} : E^3 \to E^3$, $\boldsymbol{x} \mapsto \boldsymbol{h}(\boldsymbol{x})$) is said to be rigid (or isometric) if it is distance-preserving,[15] i.e.,

$$\|\boldsymbol{h}(\boldsymbol{x}) - \boldsymbol{h}(\boldsymbol{y})\| = \|\boldsymbol{x} - \boldsymbol{y}\| \qquad \text{for each } \boldsymbol{x}, \boldsymbol{y} \in E^3. \tag{2.8}$$

We shall show presently that the isometries on E^3 under the operation of composition constitute a group, which we call the Euclidean group E(3).

For convenience of further discussions, we choose a Cartesian coordinate system in E^3 (with origin $\boldsymbol{O}$ and right-handed orthonormal basis $\boldsymbol{e}_1, \boldsymbol{e}_2, \boldsymbol{e}_3$) and henceforth identify each $\boldsymbol{x} \in E^3$ with its position vector $(x_1, x_2, x_3) \in \mathbb{R}^3$, where $x_i = \boldsymbol{x} \cdot \boldsymbol{e}_i$ $(i = 1, 2, 3)$.[16] Since position vectors are in the translation space[17] V of E^3, through the chosen Cartesian coordinate system we have established one-to-one correspondences among E^3, V, and $\mathbb{R}^3$. For simplicity we shall still denote by $\boldsymbol{x}$ the position vector that represents the location $\boldsymbol{x} \in E^3$ under the chosen coordinate system. Whether the symbol $\boldsymbol{x}$ stands for a location in E^3 or for the position vector of that location should be clear from the context where it appears. We shall write out $\boldsymbol{x} \in E^3$, $\boldsymbol{x} \in V$, $\boldsymbol{x} \in \mathbb{R}^3$, etc., explicitly whenever we want to emphasize the space in question for clarity.

Each rigid transplacement $\boldsymbol{h}$ of C can be taken as an isometric mapping on $\mathbb{R}^3$, for which the following representation theorem [322, pp. 45, 344–345]) is well known:

[14] Here we adopt the terminology in continuum mechanics as regards the terms body, placement, and transplacement; see Truesdell [322].

[15] What we call rigid transplacements here are given various other names in the literature, e.g., rigid motions ([66, p. 25], [232, p. 23]), rigid transformations [268, p. 16], Euclidean motions [304, p. 309], etc. As time is not involved, referring to a distance-preserving bijective mapping as "motion" is a misnomer.

[16] The Cartesian coordinate system here serves only as a means to establish one-to-one correspondences among the Euclidean point space E^3, its translation space V, and $\mathbb{R}^3$. As we shall use the direct notation in all our discussions and proofs, all the equations and assertions in the rest of this section remain valid under all affine coordinate systems.

[17] See, e.g., [40, p. 297] for definition.

Theorem 2.3 *Let $\boldsymbol{h} : \mathbb{R}^3 \to \mathbb{R}^3$ be an isometry, i.e., it satisfy (2.8). There is a unique orthogonal linear transformation $\boldsymbol{Q} : \mathbb{R}^3 \to \mathbb{R}^3$ such that for each $\boldsymbol{x} \in \mathbb{R}^3$*

$$\boldsymbol{h}(\boldsymbol{x}) = \boldsymbol{v} + \boldsymbol{Q}\boldsymbol{x}, \qquad \text{where} \qquad \boldsymbol{v} = \boldsymbol{h}(\boldsymbol{0}). \tag{2.9}$$

Proof Let $\boldsymbol{Q}(\boldsymbol{x}) = \boldsymbol{h}(\boldsymbol{x}) - \boldsymbol{h}(\boldsymbol{0})$. Then $\boldsymbol{Q}(\boldsymbol{0}) = \boldsymbol{0}$. By (2.8), we have (i) $\|\boldsymbol{Q}(\boldsymbol{x})\| = \|\boldsymbol{x}\|$ for each $\boldsymbol{x} \in \mathbb{R}^3$. By expanding both sides of the equation $\|\boldsymbol{Q}(\boldsymbol{x}) - \boldsymbol{Q}(\boldsymbol{y})\|^2 = \|\boldsymbol{x} - \boldsymbol{y}\|^2$ and appealing to (i), we obtain (ii) $\boldsymbol{Q}(\boldsymbol{x}) \cdot \boldsymbol{Q}(\boldsymbol{y}) = \boldsymbol{x} \cdot \boldsymbol{y}$ for all $\boldsymbol{x}, \boldsymbol{y} \in \mathbb{R}^3$. By (i) and (ii) it is straightforward to verify that $\|\boldsymbol{Q}(\boldsymbol{x} + \boldsymbol{y}) - [\boldsymbol{Q}(\boldsymbol{x}) + \boldsymbol{Q}(\boldsymbol{y})]\|^2 = 0$ for all $\boldsymbol{x}, \boldsymbol{y} \in \mathbb{R}^3$, and $\|\boldsymbol{Q}(\lambda\boldsymbol{x}) - \lambda\boldsymbol{Q}(\boldsymbol{x})\|^2 = 0$ for each $\lambda \in \mathbb{R}$ and $\boldsymbol{x} \in \mathbb{R}^3$. Hence $\boldsymbol{Q} : \mathbb{R}^3 \to \mathbb{R}^3$ is linear and, by (ii), is orthogonal. The uniqueness of $\boldsymbol{Q}$ that satisfies (2.9) is obvious. □

Remark 2.4 If we forgo the identifications of E^3 and V with $\mathbb{R}^3$, then we should write $\boldsymbol{h} : E^3 \to E^3$ and $\boldsymbol{Q} : V \to V$. While a coordinate system is no longer needed, we still have to specify a fixed point $\boldsymbol{O}$ in E^3 to relate V and E^3. Under this setting, formula (2.9) for the isometry $\boldsymbol{h}$ is replaced by

$$\boldsymbol{h}(\boldsymbol{x}) - \boldsymbol{h}(\boldsymbol{O}) = \boldsymbol{Q}(\boldsymbol{x} - \boldsymbol{O}) \qquad \text{for each } \boldsymbol{x} \in E^3. \tag{2.10}$$

Note that in (2.10), $\boldsymbol{x} - \boldsymbol{O} \in V$ and $\boldsymbol{h}(\boldsymbol{x}) - \boldsymbol{h}(\boldsymbol{O}) \in V$. After some slight and obvious modifications the preceding proof for (2.9) remains valid as one for (2.10). □

From (2.9) we observe that each rigid transplacement is bijective and $\boldsymbol{h}^{-1}$, the inverse of $\boldsymbol{h}$ given in (2.9), is defined by the formula

$$\boldsymbol{h}^{-1}(\boldsymbol{x}) = -\boldsymbol{Q}^T\boldsymbol{v} + \boldsymbol{Q}^T\boldsymbol{x} \qquad \text{for each } \boldsymbol{x} \in \mathbb{R}^3. \tag{2.11}$$

Through (2.9) each rigid transplacement $\boldsymbol{h}$ of C is defined by a pair $(\boldsymbol{v}, \boldsymbol{Q}) : \mathbb{R}^3 \to \mathbb{R}^3$, where $\boldsymbol{v} \in \mathbb{R}^3$ and $\boldsymbol{Q} \in \mathrm{O}(3)$, such that

$$(\boldsymbol{v}, \boldsymbol{Q})\boldsymbol{x} = \boldsymbol{v} + \boldsymbol{Q}\boldsymbol{x}. \tag{2.12}$$

In this notation we have

$$\boldsymbol{h} = (\boldsymbol{v}, \boldsymbol{Q}), \qquad \boldsymbol{h}^{-1} = (-\boldsymbol{Q}^T\boldsymbol{v}, \boldsymbol{Q}^T). \tag{2.13}$$

Moreover, let $\boldsymbol{h}_i = (\boldsymbol{v}_i, \boldsymbol{Q}_i)$ for $i = 1, 2$. From

$$\begin{aligned}(\boldsymbol{h}_2 \circ \boldsymbol{h}_1)\boldsymbol{x} &= (\boldsymbol{v}_2, \boldsymbol{Q}_2)(\boldsymbol{v}_1, \boldsymbol{Q}_1)\boldsymbol{x} \\ &= (\boldsymbol{v}_2, \boldsymbol{Q}_2)(\boldsymbol{v}_1 + \boldsymbol{Q}_1\boldsymbol{x}) \\ &= \boldsymbol{v}_2 + \boldsymbol{Q}_2\boldsymbol{v}_1 + \boldsymbol{Q}_2\boldsymbol{Q}_1\boldsymbol{x} \qquad \text{for each } \boldsymbol{x} \in \mathbb{R}^3,\end{aligned} \tag{2.14}$$

we get

$$(\boldsymbol{v}_2, \boldsymbol{Q}_2)(\boldsymbol{v}_1, \boldsymbol{Q}_1) = (\boldsymbol{v}_2 + \boldsymbol{Q}_2\boldsymbol{v}_1, \boldsymbol{Q}_2\boldsymbol{Q}_1), \tag{2.15}$$

which remains a rigid transplacement. Note that each rigid transplacement is a mapping and the composition of mappings is associative. Indeed we may verify by direct computation that

$$\begin{aligned}\big((\boldsymbol{v}_3, \boldsymbol{Q}_3)(\boldsymbol{v}_2, \boldsymbol{Q}_2)\big)(\boldsymbol{v}_1, \boldsymbol{Q}_1) &= (\boldsymbol{v}_3, \boldsymbol{Q}_3)\big((\boldsymbol{v}_2, \boldsymbol{Q}_2)(\boldsymbol{v}_1, \boldsymbol{Q}_1)\big) \\ &= (\boldsymbol{v}_3 + \boldsymbol{Q}_3\boldsymbol{v}_2 + \boldsymbol{Q}_3\boldsymbol{Q}_2\boldsymbol{v}_1, \boldsymbol{Q}_3\boldsymbol{Q}_2\boldsymbol{Q}_1).\end{aligned} \tag{2.16}$$

Also, as $(\mathbf{0}, \boldsymbol{I})\boldsymbol{x} = \mathbf{0} + \boldsymbol{I}\boldsymbol{x} = \boldsymbol{x}$ for each $\boldsymbol{x} \in \mathbb{R}^3$, $(\mathbf{0}, \boldsymbol{I})$ is clearly the identity rigid transplacement. Hence the rigid transplacements of C, with composition of mappings as the group operation, constitute a group, which we call the Euclidean group E(3).

Remark 2.5 The representation $\boldsymbol{h} = (\boldsymbol{v}, \boldsymbol{Q})$, where $\boldsymbol{v} \in V$ and $\boldsymbol{Q} \in \mathrm{O}(3)$, depends on the coordinate system chosen. Change of coordinate system will be discussed in Sect. 2.3.5. □

By (2.15) each rigid transplacement $(\boldsymbol{v}, \boldsymbol{Q})$ can be uniquely decomposed as a succession of two operations as follows:

$$(\boldsymbol{v}, \boldsymbol{Q}) = (\boldsymbol{v}, \boldsymbol{I})(\mathbf{0}, \boldsymbol{Q}), \tag{2.17}$$

where $(\mathbf{0}, \boldsymbol{Q})$ is a rotation, inversion, or roto-inversion with the origin $\boldsymbol{O}$ as a fixed point, and $(\boldsymbol{v}, \boldsymbol{I})$ is a translation. Note that the order of the two operations generally cannot be reversed, as $(\mathbf{0}, \boldsymbol{Q})(\boldsymbol{v}, \boldsymbol{I}) = (\boldsymbol{Q}\boldsymbol{v}, \boldsymbol{Q}) \neq (\boldsymbol{v}, \boldsymbol{Q})$ unless $\boldsymbol{Q}\boldsymbol{v} = \boldsymbol{v}$. Let

$$\mathrm{T}(3) := \{(\boldsymbol{v}, \boldsymbol{I}) \in \mathrm{E}(3) : \boldsymbol{v} \in V\} \tag{2.18}$$

be the subgroup of translations in E(3), and let[18]

$$\hat{\mathcal{O}} := \{(\mathbf{0}, \boldsymbol{Q}) \in \mathrm{E}(3) : \boldsymbol{Q} \in \mathrm{O}(3)\} \tag{2.19}$$

be the subgroup of rotations or roto-inversions in E(3) which have the origin $\boldsymbol{O}$ as fixed point. Then $\mathrm{T}(3)\hat{\mathcal{O}} = \mathrm{E}(3)$ and $\mathrm{T}(3) \cap \hat{\mathcal{O}} = \{(\mathbf{0}, \boldsymbol{I})\}$, where $(\mathbf{0}, \boldsymbol{I})$ is the identity in E(3). Moreover, we have

$$(\mathbf{0}, \boldsymbol{Q})(\boldsymbol{v}, \boldsymbol{I})(\mathbf{0}, \boldsymbol{Q})^{-1} = (\mathbf{0}, \boldsymbol{Q})(\boldsymbol{v}, \boldsymbol{I})(\mathbf{0}, \boldsymbol{Q}^{-1}) = (\boldsymbol{Q}\boldsymbol{v}, \boldsymbol{I}) \in \mathrm{T}(3) \tag{2.20}$$

for any $(\boldsymbol{v}, \boldsymbol{I}) \in \mathrm{T}(3)$ and $(\mathbf{0}, \boldsymbol{Q}) \in \hat{\mathcal{O}}$. Hence there holds

$$\mathrm{E}(3) = \mathrm{T}(3) \wedge \hat{\mathcal{O}}, \tag{2.21}$$

i.e., the Euclidean group is the semidirect product (cf. Definition A.28 in Appendix A) of T(3) and $\hat{\mathcal{O}}$, where $\hat{\mathcal{O}}$ acts on T(3) by conjugation (2.20).

Note that $\hat{G} := \{(0, \boldsymbol{Q}) : \boldsymbol{Q} \in G\}$, where G is a subgroup of O(3), has at least one point in E^3, namely the origin $\boldsymbol{O}$, as a fixed point. Hence every subgroup of O(3) is called a point group.

2.3 Ideal Crystals and Crystallographic Groups

2.3.1 Lattice Groups and Lattices

Our main reference for this section is Miller [232, pp. 23–24, 34–37].

Consider $(\mathsf{C}, \boldsymbol{\kappa}_0)$, i.e., the body C in the placement $\boldsymbol{\kappa}_0$, as discussed in Sect. 2.2. Henceforth in this chapter we restrict attention to a special class of systems $(\mathsf{C}, \boldsymbol{\kappa}_0)$ called ideal crystals, which will be characterized in Definition 2.10.

Let $(\mathsf{C}, \boldsymbol{\kappa}_0)$ be an ideal crystal, and let $\mathcal{G} \subset \mathrm{E}(3)$ be the set of all rigid transplacements that leave $(\mathsf{C}, \boldsymbol{\kappa}_0)$ invariant. In other words, there is no operational way of distinguishing $(\mathsf{C}, \boldsymbol{\kappa}_0)$

[18] Some authors (see, e.g., [232, p. 21]) do not distinguish $(\mathbf{0}, \boldsymbol{Q})$ from $\boldsymbol{Q}$. Then $\hat{\mathcal{O}}$ is the same as O(3).

before and after a rigid transplacement $\boldsymbol{h} \in \mathcal{G}$. The set $\mathcal{G}$ of such rigid transplacements clearly constitutes a subgroup of E(3), and it is called the complete symmetry group of $(\mathsf{C}, \boldsymbol{\kappa}_0)$ (with respect to rigid transplacements). As $\mathcal{G}$ has $(\boldsymbol{0}, \boldsymbol{I})$ as a member, it is non-empty. In what follows we assume that $\mathcal{G}$ is non-trivial, i.e., $\mathcal{G} \neq \{(\boldsymbol{0}, \boldsymbol{I})\}$.

Let $\mathcal{L} = \mathcal{G} \cap \mathrm{T}(3)$ be the subgroup of translations in $\mathcal{G}$. For any $(\boldsymbol{u}, \boldsymbol{I}), (\boldsymbol{v}, \boldsymbol{I}) \in \mathcal{L}$, we have $(\boldsymbol{u} - \boldsymbol{v}, \boldsymbol{I}) \in \mathcal{L}$ because $\mathcal{L}$ is a subgroup of T(3), and $\|\boldsymbol{u} - \boldsymbol{v}\|$ cannot be arbitrarily small because the crystal C comprises of atoms or molecules, which have finite sizes. Thus there is an $\epsilon > 0$ such that

$$\|\boldsymbol{u} - \boldsymbol{v}\| \geq \epsilon \qquad \text{for all translations } (\boldsymbol{u}, \boldsymbol{I}), (\boldsymbol{v}, \boldsymbol{I}) \in \mathcal{L}. \tag{2.22}$$

Next we define what we mean by saying that $\mathcal{L}$ is discrete, for which we use an assertion equivalent to (2.22), and that $\mathcal{L}$ is three-dimensional.

Definition 2.6 A subgroup $\mathcal{L}$ of T(3) is discrete if it satisfies the following condition: Let $r > 0$ and $\mathrm{B}_r := \{\boldsymbol{v} \in V : \|\boldsymbol{v}\| \leq r\}$; for any $r > 0$, the set $\{\boldsymbol{u} \in \mathrm{B}_r : (\boldsymbol{u}, \boldsymbol{I}) \in \mathcal{L}\}$ is finite. It is three-dimensional if there are three linearly independent vectors $\boldsymbol{f}_i$ $(i = 1, 2, 3)$ in V such that $(\boldsymbol{f}_i, \boldsymbol{I}) \in \mathcal{L}$ for each i. □

Definition 2.7 A subgroup $\mathcal{L}$ of T(3) is said to be a lattice group[19] if it is discrete and three-dimensional. □

Theorem 2.8 *Let $\mathcal{L}$ be a lattice group. Then there exists a right-handed triad of linearly independent vectors $\boldsymbol{b}_1, \boldsymbol{b}_2$, and $\boldsymbol{b}_3 \in V$ such that*

$$\mathcal{L} = \{(\boldsymbol{u}, \boldsymbol{I}) \in \mathcal{G} : \boldsymbol{u} = u_1\boldsymbol{b}_1 + u_2\boldsymbol{b}_2 + u_3\boldsymbol{b}_3, \ \ \textit{where } u_1, u_2, u_3 \in \mathbb{Z}\}, \tag{2.23}$$

where $\mathbb{Z}$ denotes the set of integers.

Proof By assumption there are three linearly independent vectors $\boldsymbol{f}_i \in V$ $(i = 1, 2, 3)$ such that $(\boldsymbol{f}_i, \boldsymbol{I}) \in \mathcal{L}$. Without loss of generality, we choose a labeling so that $\boldsymbol{f}_1$, $\boldsymbol{f}_2$, and $\boldsymbol{f}_3$ constitute a right-handed triad in V. Recall that we have chosen a Cartesian coordinate system in E^3 and identify V with $\mathbb{R}^3$ (see Sect. 2.2). Henceforth in this proof we will write $\mathbb{R}^3$ for V whenever no confusion should arise. Moreover, let $\mathsf{L} := \{\boldsymbol{u} \in \mathbb{R}^3 : (\boldsymbol{u}, \boldsymbol{I}) \in \mathcal{L}\}$.[20]

Let $\overline{\Pi}[\boldsymbol{f}_1, \boldsymbol{f}_2, \boldsymbol{f}_3]$ be the closed parallelepiped in $\mathbb{R}^3$ subtended by $\boldsymbol{f}_1$, $\boldsymbol{f}_2$, and $\boldsymbol{f}_3$. Since $\mathcal{L}$ is discrete, the number of vectors $\boldsymbol{u} \in \mathsf{L} \cap \overline{\Pi}[\boldsymbol{f}_1, \boldsymbol{f}_2, \boldsymbol{f}_3]$ is finite. Let $\boldsymbol{b}_1$ be the shortest vector in L that is parallel to $\boldsymbol{f}_1$; clearly $\boldsymbol{b}_1 \in \overline{\Pi}[\boldsymbol{f}_1, \boldsymbol{f}_2, \boldsymbol{f}_3]$. Let $\overline{P}[\boldsymbol{f}_1, \boldsymbol{f}_2]$ be the closed parallelogram subtended by $\boldsymbol{f}_1$ and $\boldsymbol{f}_2$. Let $A = \{\boldsymbol{u} \in \mathsf{L} \cap \overline{P}[\boldsymbol{f}_1, \boldsymbol{f}_2] : \boldsymbol{u}$ and $\boldsymbol{b}_1$ are linearly independent$\}$. The set A is non-empty because $\boldsymbol{f}_2 \in A$. Choose an element $\boldsymbol{b}_2 \in A$ such that among the parallelograms $\overline{P}[\boldsymbol{b}_1, \boldsymbol{u}]$ $(\boldsymbol{u} \in A)$, $\overline{P}[\boldsymbol{b}_1, \boldsymbol{b}_2]$ has the smallest non-zero area. Among the vectors in $\mathsf{L} \cap \overline{\Pi}[\boldsymbol{f}_1, \boldsymbol{f}_2, \boldsymbol{f}_3]$ choose one, which we call $\boldsymbol{b}_3$, such that the parallelepiped $\overline{\Pi}[\boldsymbol{b}_1, \boldsymbol{b}_2, \boldsymbol{b}_3]$ has the smallest non-zero volume. Clearly $\boldsymbol{b}_1$, $\boldsymbol{b}_2$, and $\boldsymbol{b}_3$ constitute a right-handed triad of linearly independent vectors in L, and $\overline{\Pi}[\boldsymbol{b}_1, \boldsymbol{b}_2, \boldsymbol{b}_3] \subset \overline{\Pi}[\boldsymbol{f}_1, \boldsymbol{f}_2, \boldsymbol{f}_3]$.

[19] Here we adopt the terminology of Yale [349, Sect. 3.3] and Miller [232, p. 34]. The term "lattice group", however, has been used by Ericksen [107], Pitteri and Zanzotto [260, p. 73], and others to mean what is called "Bravais group" in the sixth edition (2016) of the *ITA* [301, p. 29]).

[20] Later we shall identify L as the lattice that represents $\mathcal{L}$.

Let $\boldsymbol{u} \in \mathsf{L}$ and $\boldsymbol{u} = u_1\boldsymbol{b}_1 + u_2\boldsymbol{b}_2 + u_3\boldsymbol{b}_3$, where $u_i \in \mathbb{R}$ for $i = 1, 2, 3$. Let $[u_i]$ be the integral part of u_i, i.e., $[u_i]$ is the largest integer such that $[u_i] \le u_i < [u_i] + 1$. Let $\beta_i = u_i - [u_i]$ for each i. Then $0 \le \beta_i < 1$. Since $\mathcal{L}$ is a subgroup of T(3), we have

$$\boldsymbol{b} := \boldsymbol{u} - \sum_{i=1}^{3} [u_i]\boldsymbol{b}_i = \sum_{i=1}^{3} \beta_i \boldsymbol{b}_i \in \mathsf{L}. \tag{2.24}$$

Note that $\boldsymbol{b} \in \overline{\Pi}[\boldsymbol{b}_1, \boldsymbol{b}_2, \boldsymbol{b}_3] \subset \overline{\Pi}[\boldsymbol{f}_1, \boldsymbol{f}_2, \boldsymbol{f}_3]$. We claim that $\beta_i = 0$ for each i.

Suppose $0 < \beta_3 < 1$. Then the parallelepiped $\overline{\Pi}[\boldsymbol{b}_1, \boldsymbol{b}_2, \boldsymbol{b}]$ has volume

$$(\boldsymbol{b}_1 \times \boldsymbol{b}_2) \cdot \boldsymbol{b} = \beta_3 (\boldsymbol{b}_1 \times \boldsymbol{b}_2) \cdot \boldsymbol{b}_3,$$

which is smaller than that of $\overline{\Pi}[\boldsymbol{b}_1, \boldsymbol{b}_2, \boldsymbol{b}_3]$. This contradicts the fact that $\boldsymbol{b}_3 \in \mathsf{L}$ is chosen to make $\overline{\Pi}[\boldsymbol{b}_1, \boldsymbol{b}_2, \boldsymbol{b}_3]$ have the smallest volume among its peers. Hence we conclude that $\beta_3 = 0$.

Now suppose $0 < \beta_2 < 1$. Then $\overline{P}[\boldsymbol{b}_1, \beta_1\boldsymbol{b}_1 + \beta_2\boldsymbol{b}_2]$ has an area equal to $\beta_2 \|\boldsymbol{b}_1 \times \boldsymbol{b}_2\|$, which is smaller than that of $\overline{P}[\boldsymbol{b}_1, \boldsymbol{b}_2]$. This contradicts the fact that $\boldsymbol{b}_2 \in \mathsf{L}$ is chosen to make $\overline{P}[\boldsymbol{b}_1, \boldsymbol{b}_2]$ have the smallest area. Therefore there must hold $\beta_2 = 0$.

Finally, suppose $0 < \beta_1 < 1$. Then $\boldsymbol{b} = \beta_1\boldsymbol{b}_1$ is parallel to $\boldsymbol{f}_1$ and is shorter than $\boldsymbol{b}_1$, which is again a contradiction. Thus we have also $\beta_1 = 0$.

In conclusion $\boldsymbol{u} = u_1\boldsymbol{b}_1 + u_2\boldsymbol{b}_2 + u_3\boldsymbol{b}_3$, where $u_i = [u_i] \in \mathbb{Z}$ for each i. □

Clearly the conclusion of Theorem 2.8 is equivalent to the assumption that $\mathcal{L}$ is non-trivial, discrete, and three-dimensional. An alternate approach is to adopt assertion (2.23) directly as the starting point. In that approach assertion (2.23) is sometimes called the Lattice Postulate.

Definition 2.9 A subgroup $\mathcal{G}$ of the Euclidean group E(3) is said to be a space group if $\mathcal{L} := \mathcal{G} \cap \mathrm{T}(3)$ is a lattice group. □

Definition 2.10 A body C in a placement $\boldsymbol{\kappa}_0$ such that $\boldsymbol{\kappa}_0(\mathsf{C}) = E^3$ is said to be an ideal crystal if its complete symmetry group $\mathcal{G}$ under rigid transplacements is a space group. □

Let $\boldsymbol{x}$ be a point in $\boldsymbol{\kappa}_0(\mathsf{C})$. The orbit of $\boldsymbol{x}$ under the action of $\mathcal{L}$, namely

$$\begin{aligned} \mathcal{L}(\boldsymbol{x}) &= \{(\boldsymbol{u}, \boldsymbol{I})\boldsymbol{x} : (\boldsymbol{u}, \boldsymbol{I}) \in \mathcal{L}\} \\ &= \{\boldsymbol{x} + u_1\boldsymbol{b}_1 + u_2\boldsymbol{b}_2 + u_3\boldsymbol{b}_3 : u_1, u_2, u_3 \in \mathbb{Z}\} \end{aligned} \tag{2.25}$$

is called a lattice of the ideal crystal $(\mathsf{C}, \boldsymbol{\kappa}_0)$ in E^3. By definition of $\mathcal{L}$, every point in the $\mathcal{L}$-orbit of $\boldsymbol{x}$ is equivalent to $\boldsymbol{x}$. The lattice $\mathcal{L}(\boldsymbol{x})$ may be taken as a graphical representation of the lattice group $\mathcal{L}$. In this sense we may choose any specific $\boldsymbol{x}$ and take $\mathcal{L}(\boldsymbol{x})$ as the representative lattice, and the locations of the lattice points in E^3 has no particular meaning. On the other hand, for a given ideal crystal $(\mathsf{C}, \boldsymbol{\kappa}_0)$ with specific crystal structure (i.e., arrangement of atoms, ions, or molecules that comprise the crystal), there may be special locations in the crystal (see Sect. 2.10.2 for an example) which, for convenience of description and computations, are the best candidates to serve as both the origin $\boldsymbol{O}$ of the chosen Cartesian coordinate system (see Sect. 2.2) and the starting point $\boldsymbol{x}$ of a lattice. Under this choice, $\boldsymbol{x} = \boldsymbol{0} = (0, 0, 0)$ and the (representative) lattice of the ideal crystal is

$$\mathsf{L} := \mathcal{L}(\boldsymbol{0}) = \{\boldsymbol{s} \in \mathbb{R}^3 : \boldsymbol{s} = s_1\boldsymbol{b}_1 + s_2\boldsymbol{b}_2 + s_3\boldsymbol{b}_3, \text{ where } s_1, s_2, s_3 \in \mathbb{Z}\}. \tag{2.26}$$

Then the position vectors of lattice points in L are exactly the same vectors in $\mathbb{R}^3$ which define the translations in $\mathcal{L}$. The vector $\boldsymbol{s} = s_1\boldsymbol{b}_1 + s_2\boldsymbol{b}_2 + s_3\boldsymbol{b}_3$ for some specific $s_1, s_2, s_3 \in \mathbb{Z}$ is called a lattice vector. If $(\boldsymbol{u}, \boldsymbol{I}) \in \mathcal{L}$, then $(\boldsymbol{u}, \boldsymbol{I})\boldsymbol{s} = \boldsymbol{u} + \boldsymbol{s} \in \mathsf{L}$. Hence we have

$$(\boldsymbol{u}, \boldsymbol{I})\mathsf{L} = (\boldsymbol{u}, \boldsymbol{I})\mathcal{L}(\boldsymbol{0}) = \mathcal{L}(\boldsymbol{0}) = \mathsf{L}. \tag{2.27}$$

Thus the lattice L remains invariant under the translations $(\boldsymbol{u}, \boldsymbol{I}) \in \mathcal{L}$. By abuse of language we shall, for convenience, treat the assertions $(\boldsymbol{u}, \boldsymbol{I}) \in \mathcal{L}$ and $\boldsymbol{u} \in \mathsf{L}$ as synonymous and use them interchangeably.

Remark 2.11 The lattice group $\mathcal{L} = \mathrm{T}(3) \cap \mathcal{G}$ of an ideal crystal $(\mathsf{C}, \boldsymbol{\kappa}_0)$ describes the periodic translational symmetry of the crystal, whereas the space group $\mathcal{G}$ covers the full symmetry of the crystal structure (or crystal pattern) under rigid transplacements. The lattice $\mathsf{L} = \mathcal{L}(\boldsymbol{0})$ is a mathematical construct that serves as a graphical depiction of $\mathcal{L}$. In particular, the elements of L, i.e., the lattice points, should not be confused with the locations of the physical constituents (atoms, ions, etc.) of C. For instance, the lattice points of the hexagonal close-packed structure (see Sect. 2.10.2) are usually chosen such that they are all located within the interstitial voids. □

2.3.2 Primitive Unit Cells

Definition 2.12 The lattice vectors $\boldsymbol{b}_1$, $\boldsymbol{b}_2$, $\boldsymbol{b}_3$ in (2.23) and (2.26) are said to constitute a primitive lattice basis of L, and they are called primitive lattice vectors. The parallelepiped[21]

$$\Pi[\boldsymbol{b}_1, \boldsymbol{b}_2, \boldsymbol{b}_3] := \{u_1\boldsymbol{b}_1 + u_2\boldsymbol{b}_2 + u_3\boldsymbol{b}_3 : 0 \le u_i < 1 \text{ for } i = 1, 2, 3\} \tag{2.28}$$

is called a primitive unit cell of lattice L. □

Every translate of Π under $\mathcal{L}$, i.e., $h\Pi$, where $h \in \mathcal{L}$, is also called a primitive unit cell. Note that $h\Pi$ contains only one lattice point, namely $h\boldsymbol{0}$, and that $h_1\Pi \cap h_2\Pi = \emptyset$ if $h_1 \neq h_2$. Moreover, as $\mathbb{R}^3 = \bigcup_{h\in\mathcal{L}} h\Pi$, the entire space $\mathbb{R}^3$ can be covered by stacking translates of Π together. Given a translation subgroup $\mathcal{L}$ of $\mathcal{G}$, however, the linearly independent basis that generates $\mathcal{L}$ and its associated lattice L through (2.23) and (2.26), respectively, is not unique. For instance, we may replace the triad $\boldsymbol{b}_1, \boldsymbol{b}_2, \boldsymbol{b}_3$ by $\boldsymbol{b}_1', \boldsymbol{b}_2, \boldsymbol{b}_3$, where $\boldsymbol{b}_1' = \boldsymbol{b}_1 + \boldsymbol{b}_2$. In fact, the possible choices of basis are infinite. In general, a primary lattice basis $\boldsymbol{b}_1, \boldsymbol{b}_2, \boldsymbol{b}_3$ of L can be chosen as follows (cf. proof of Theorem 2.8): Pick any three linearly independent lattice vectors $\boldsymbol{f}_1, \boldsymbol{f}_2, \boldsymbol{f}_3$ such that $\boldsymbol{f}_1 \times \boldsymbol{f}_2 \cdot \boldsymbol{f}_3 > 0$. Let $\overline{\Pi}[\boldsymbol{f}_1, \boldsymbol{f}_2, \boldsymbol{f}_3]$ be the closed parallelepiped that they subtend. Choose the shortest non-zero lattice vector parallel to $\boldsymbol{f}_1$ as $\boldsymbol{b}_1$. In the closed parallelogram spanned by $\boldsymbol{f}_1$ and $\boldsymbol{f}_2$, choose a lattice vector $\boldsymbol{b}_2$ such that the parallelogram spanned by $\boldsymbol{b}_1$ and $\boldsymbol{b}_2$ has the smallest non-zero area. Finally pick a lattice vector $\boldsymbol{b}_3$ in $\overline{\Pi}[\boldsymbol{f}_1, \boldsymbol{f}_2, \boldsymbol{f}_3]$ such that the parallelepiped $\Pi[\boldsymbol{b}_1, \boldsymbol{b}_2, \boldsymbol{b}_3]$ has the smallest non-zero volume. Then $\boldsymbol{b}_1, \boldsymbol{b}_2, \boldsymbol{b}_3$ will serve as a primitive lattice basis of L.

Let $\boldsymbol{f}_1$, $\boldsymbol{f}_2$, and $\boldsymbol{f}_3$ be a right-handed triad of lattice vectors. Given a primitive lattice basis $\boldsymbol{b}_1, \boldsymbol{b}_2$, and $\boldsymbol{b}_3$ of L, we may express each $\boldsymbol{f}_i$ in terms of the primitive basis. By (1.43)

[21] Here we follow [344, p. 723]; see also [241, p. 14, Definition 2.8]. In the literature the unit cell is seldom explicitly defined but is often implicitly meant to be a translate under $\mathcal{L}$ of the closed parallelepiped $\overline{\Pi} = \{u_1\boldsymbol{b}_1 + u_2\boldsymbol{b}_2 + u_3\boldsymbol{b}_3 : 0 \le u_i \le 1 \text{ for } i = 1, 2, 3\}$. While each such unit cell $h\overline{\Pi}$ $(h \in \mathcal{L})$ contains eight lattice points located at its vertices, it is said that each lattice point at a vertex is shared by eight unit cells, which works out to one lattice point per unit cell.

$\boldsymbol{f}_i = P_i^j \boldsymbol{b}_j$, for some $P_i^j \in \mathbb{Z}$ $(1 \le i \le 3, 1 \le j \le 3)$, and the summation convention is in force. Let $\boldsymbol{P} = [(P^T)_i{}^j]$—cf. (1.46)—be the matrix of the change of basis from $\{\boldsymbol{b}_i\}$ to $\{\boldsymbol{f}_i\}$, and let $\mathrm{V}(\cdot)$ denote the volume of the parallelepiped in question. We have

$$\begin{aligned} \mathrm{V}(\Pi[\boldsymbol{f}_1, \boldsymbol{f}_2, \boldsymbol{f}_3]) &= (\boldsymbol{f}_1 \times \boldsymbol{f}_2) \cdot \boldsymbol{f}_3 \\ &= (\boldsymbol{P}\boldsymbol{f}_1 \times \boldsymbol{P}\boldsymbol{f}_2) \cdot \boldsymbol{P}\boldsymbol{f}_3 \\ &= (\det \boldsymbol{P}) \big((\boldsymbol{f}_1 \times \boldsymbol{f}_2) \cdot \boldsymbol{f}_3\big) \\ &= (\det \boldsymbol{P}) \mathrm{V}(\Pi[\boldsymbol{b}_1, \boldsymbol{b}_2, \boldsymbol{b}_3]). \end{aligned} \tag{2.29}$$

It follows that

$$\mathrm{V}(\Pi[\boldsymbol{b}_1, \boldsymbol{b}_2, \boldsymbol{b}_3]) \le \mathrm{V}(\Pi[\boldsymbol{f}_1, \boldsymbol{f}_2, \boldsymbol{f}_3]) \tag{2.30}$$

because $\det \boldsymbol{P}$ is a positive integer. If $\{\boldsymbol{f}_i\}$ is also a primitive lattice basis, reversing the roles of $\{\boldsymbol{b}_i\}$ and $\{\boldsymbol{f}_i\}$ in (2.30) yields $\mathrm{V}(\Pi[\boldsymbol{f}_1, \boldsymbol{f}_2, \boldsymbol{f}_3]) \le \mathrm{V}(\Pi[\boldsymbol{b}_1, \boldsymbol{b}_2, \boldsymbol{b}_3])$. Combining the preceding inequality with (2.30), we conclude that $\mathrm{V}(\Pi[\boldsymbol{f}_1, \boldsymbol{f}_2, \boldsymbol{f}_3]) = \mathrm{V}(\Pi[\boldsymbol{b}_1, \boldsymbol{b}_2, \boldsymbol{b}_3])$. Hence every primitive unit cell of lattice $\llcorner$ has the same volume.

Remark 2.13 In crystallography, besides primitive unit cells, it is standard practice to use also non-primitive lattice bases and centered unit cells to increase the symmetry of the cell and to get the simplest formulas for the calculation of distances and angles. In general, a set of symmetry-adapted conventional basis vectors $\boldsymbol{a}_1$, $\boldsymbol{a}_2$, and $\boldsymbol{a}_3$ is chosen, and the (conventional) unit cell is defined by

$$\Pi[\boldsymbol{a}_1, \boldsymbol{a}_2, \boldsymbol{a}_3] := \{u_1\boldsymbol{a}_1 + u_2\boldsymbol{a}_2 + u_3\boldsymbol{a}_3 : 0 \le u_i < 1 \text{ for } i = 1, 2, 3\}. \tag{2.31}$$

See Sect. 2.8. □

Remark 2.14 In physics texts the term "basis" is sometimes used (see, e.g., [37, p. 23], [128, p. 1-26]) in the description of crystal structure as follows [68, p. 19]: "The crystal structure can be described by associating with each lattice point a group of atoms. This group of atoms is called the basis of the structure. Thus, a crystal structure is made up of a lattice and a basis. Another way of putting this is to say that a crystal structure is obtained by repeating, throughout space, a unit cell and the atoms [i.e., the basis] within." We shall adopt this description of crystal structure at our convenience. □

2.3.3 Crystallographic Point Groups

Let $\pi : \mathrm{E}(3) \to \mathrm{O}(3)$ be the mapping $(\boldsymbol{v}, \boldsymbol{Q}) \mapsto \boldsymbol{Q}$. By (2.15) we have

$$\begin{aligned} \pi((\boldsymbol{v}_2, \boldsymbol{Q}_2)(\boldsymbol{v}_1, \boldsymbol{Q}_1)) &= \pi((\boldsymbol{v}_2 + \boldsymbol{Q}_2\boldsymbol{v}_1, \boldsymbol{Q}_2\boldsymbol{Q}_1)) \\ &= \boldsymbol{Q}_2\boldsymbol{Q}_1 = \pi((\boldsymbol{v}_2, \boldsymbol{Q}_2))\pi((\boldsymbol{v}_1, \boldsymbol{Q}_1)). \end{aligned} \tag{2.32}$$

Hence π is a homomorphism.[22] It follows that the kernel

$$\pi^{-1}(\boldsymbol{I}) = \{(\boldsymbol{v}, \boldsymbol{I}) \in \mathrm{E}(3) : \boldsymbol{v} \in V\} = \mathrm{T}(3), \tag{2.33}$$

the subgroup of translations in E(3).

[22] Cf. Sects. A.3 and A.4 in Appendix A for definitions of the terms homomorphism, isomorphism, kernel, normal subgroup, and quotient group.

Let $\mathcal{G}$ be a space group and $\mathcal{L} := \mathcal{G} \cap \mathrm{T}(3)$ the lattice group pertaining to $\mathcal{G}$. For any $g \in \mathcal{G}$ and $h \in \mathcal{L}$, since $\pi(h) = \boldsymbol{I}$ we have

$$\pi(ghg^{-1}) = \pi(g)\pi(h)\pi(g^{-1}) = \pi(g)\pi(g^{-1}) = \boldsymbol{I}, \tag{2.34}$$

which implies $ghg^{-1} \in \mathcal{L}$. Hence $g\mathcal{L}g^{-1} = \mathcal{L}$ for each $g \in \mathcal{G}$, i.e., $\mathcal{L}$ is a normal subgroup of $\mathcal{G}$. Consider the restriction of π to $\mathcal{G} \subset \mathrm{E}(3)$, which is still a homomorphism. The image

$$\mathcal{K} := \pi(\mathcal{G}) = \{\, \boldsymbol{Q} \in \mathrm{O}(3) : (\boldsymbol{v}, \boldsymbol{Q}) \in \mathcal{G} \ \text{ for some } \boldsymbol{v} \in V \,\} \tag{2.35}$$

is a subgroup of O(3), and $\mathcal{K} \cong \mathcal{G}/\mathcal{L}$, i.e., $\mathcal{K}$ is isomorphic to the quotient group $\mathcal{G}/\mathcal{L}$; cf. Appendix A.

Let $g = (\boldsymbol{v}, \boldsymbol{Q}) \in \mathcal{G}$ and $h = (\boldsymbol{u}, \boldsymbol{I}) \in \mathcal{L}$. By (2.34), we know that $ghg^{-1} \in \mathcal{L}$. Let us compute the explicit form of the element ghg^{-1}. Using (2.13), we have

$$\begin{aligned} ghg^{-1} &= (\boldsymbol{v}, \boldsymbol{Q})(\boldsymbol{u}, \boldsymbol{I})(-\boldsymbol{Q}^T\boldsymbol{v}, \boldsymbol{Q}^T) \\ &= (\boldsymbol{v}, \boldsymbol{Q})(\boldsymbol{u} - \boldsymbol{Q}^T\boldsymbol{v}, \boldsymbol{Q}^T) \\ &= (\boldsymbol{v} + \boldsymbol{Q}\boldsymbol{u} - \boldsymbol{v}, \boldsymbol{I}) = (\boldsymbol{Q}\boldsymbol{u}, \boldsymbol{I}). \end{aligned} \tag{2.36}$$

Hence $(\boldsymbol{u}, \boldsymbol{I}) \in \mathcal{L}$ implies that $(\boldsymbol{Q}\boldsymbol{u}, \boldsymbol{I}) \in \mathcal{L}$ for $\boldsymbol{Q} \in \mathcal{K} = \pi(\mathcal{G})$. Or, in terms of position vectors $\boldsymbol{s}$ of lattice points in $\mathsf{L} = \mathcal{L}(\boldsymbol{0})$, we have

$$\boldsymbol{s} \in \mathsf{L} \Longrightarrow \boldsymbol{Q}\boldsymbol{s} \in \mathsf{L} \quad \text{or} \quad \boldsymbol{Q}\mathsf{L} \subset \mathsf{L} \qquad \text{for each } \boldsymbol{Q} \in \mathcal{K}. \tag{2.37}$$

For $\boldsymbol{Q} \in \mathcal{K}$, we have $\boldsymbol{Q}^{-1} \in \mathcal{K}$. By (2.37), $\boldsymbol{Q}^{-1}\mathsf{L} \subset \mathsf{L}$, which implies $\boldsymbol{Q}(\boldsymbol{Q}^{-1}\mathsf{L}) \subset \boldsymbol{Q}\mathsf{L}$ or $\mathsf{L} \subset \boldsymbol{Q}\mathsf{L}$. Hence we conclude that

$$\boldsymbol{Q}\mathsf{L} = \mathsf{L} \qquad \text{for each } \boldsymbol{Q} \in \mathcal{K}, \tag{2.38}$$

i.e., the crystal lattice L is invariant under the action of the group $\mathcal{K}$. Note that by our choice of coordinate system, the lattice point $\boldsymbol{0}$ is a fixed point of $\mathcal{K}$.

Definition 2.15 Let $\mathcal{G}$ be the space group of an ideal crystal $(\mathsf{C}, \boldsymbol{\kappa}_0)$. The group $\mathcal{K} = \pi(\mathcal{G}) \subset \mathrm{O}(3)$ is called the crystallographic point group of $\mathcal{G}$ (or of the ideal crystal $(\mathsf{C}, \boldsymbol{\kappa}_0)$). □

We summarize (2.38) as the first part of the following proposition.

Proposition 2.16 *Let $\mathcal{K}$ and $\mathcal{L}$ be the crystallographic point group and lattice group, respectively, which pertain to the space group $\mathcal{G}$ of an ideal crystal $(\mathsf{C}, \boldsymbol{\kappa}_0)$. Let $\mathsf{L} = \mathcal{L}(\boldsymbol{0})$ be the lattice chosen to represent $\mathcal{L}$. Then $\boldsymbol{Q}\mathsf{L} = \mathsf{L}$ for each $\boldsymbol{Q} \in \mathcal{K}$, and $\mathcal{K}$ is finite.*

Proof We have already proved the first part of the proposition in (2.38). Let us proceed to prove that $\mathcal{K}$ is finite. Let $\{\boldsymbol{b}_i : i = 1, 2, 3\}$ be a primitive lattice basis of L. For each $\boldsymbol{Q} \in \mathcal{K} \subset \mathrm{O}(3)$, $\|\boldsymbol{Q}\boldsymbol{b}_i\| = \|\boldsymbol{b}_i\|$ and $\boldsymbol{Q}\boldsymbol{b}_i \in \mathsf{L}$. Conversely, the three position vectors $\boldsymbol{Q}\boldsymbol{b}_i$ determine $\boldsymbol{Q}$ as follows. Let $\boldsymbol{b}^1, \boldsymbol{b}^2$, and $\boldsymbol{b}^3$ be the basis reciprocal to $\boldsymbol{b}_1, \boldsymbol{b}_2$, and $\boldsymbol{b}_3$. By (1.42), the matrix $[Q^i{}_j]$ which represents $\boldsymbol{Q}$ under the basis $\boldsymbol{b}_i \otimes \boldsymbol{b}^j$ has entries $Q^i{}_j = \boldsymbol{b}^i \cdot \boldsymbol{Q}\boldsymbol{b}_j$. Since $\mathcal{L}$ is discrete, on the sphere $\mathcal{S}_{r_i}$ of radius $r_i = \|\boldsymbol{b}_i\|$ there is only a finite number of points $\boldsymbol{s} \in \mathsf{L}$. Thus the set $\{\boldsymbol{Q}\boldsymbol{b}_i \in \mathsf{L} : \boldsymbol{Q} \in \mathcal{K} \text{ and } i = 1, 2, 3\}$ is finite, which implies that there is only a finite number of rotations or roto-inversions $\boldsymbol{Q}$ which satisfy, for all $i = 1, 2, 3$, $\boldsymbol{Q}\boldsymbol{b}_i \in \mathsf{L} \cap \mathcal{S}_{r_i}$ for $r_i = \|\boldsymbol{b}_i\|$. Hence the crystallographic point group $\mathcal{K}$ has only a finite number of elements. □

Remark 2.17 As mentioned in Footnote 18, some authors identify O(3) with $\hat{\mathcal{O}} \subset \mathrm{E}(3)$, the subgroup of isometries on E^3 which are rotations or roto-inversions with the origin as fixed point. In the same vein, a crystallographic point group is defined as a group of isometries on E^3 which brings a translation lattice L into self-coincidence and leaves at least one point fixed (see, e.g., [101, p. 90]). By Proposition 2.16, $\hat{\mathcal{K}} := \{(\mathbf{0}, \boldsymbol{Q}) : \boldsymbol{Q} \in \mathcal{K}\}$ is a crystallographic point group in this sense if and only if $\mathcal{K}$ is one under Definition 2.15. □

2.3.4 Characterization of Elements of Space Group

Let $\mathcal{G} \subset \mathrm{E}(3)$ be the space group (i.e., the complete symmetry group) of an ideal crystal $(\mathsf{C}, \boldsymbol{\kappa}_0)$. As shown in Sect. 2.3.3, the translations $\mathcal{L} = \mathcal{G} \cap \mathrm{T}(3)$ in $\mathcal{G}$ constitute a normal subgroup of $\mathcal{G}$, which we call the lattice group of $\mathcal{G}$. Moreover the quotient group

$$\mathcal{G}/\mathcal{L} = \{(\boldsymbol{v}, \boldsymbol{Q})\mathcal{L} : (\boldsymbol{v}, \boldsymbol{Q}) \in \mathcal{G}\}, \tag{2.39}$$

under the map $(\boldsymbol{v}, \boldsymbol{Q})\mathcal{L} \mapsto \boldsymbol{Q}$, is isomorphic to the crystallographic point group $\mathcal{K}$ of $\mathcal{G}$. The space group $\mathcal{G}$ is partitioned into a disjoint union of left cosets:[23] The elements $(\boldsymbol{v}, \boldsymbol{Q})$ in the same coset have the same rotation or roto-inversion $\boldsymbol{Q} \in \mathcal{K}$, and they differ from each other by having different translations $\boldsymbol{v}$.

Let us examine more closely the elements in the left coset $(\boldsymbol{v}, \boldsymbol{Q})\mathcal{L} \in \mathcal{G}/\mathcal{L}$, where $(\boldsymbol{v}, \boldsymbol{Q}) \in \mathcal{G}$ and $\boldsymbol{Q} \in \mathcal{K}$. Let $(\boldsymbol{u}, \boldsymbol{I}) \in \mathcal{L}$. We have

$$(\boldsymbol{v}, \boldsymbol{Q})(\boldsymbol{u}, \boldsymbol{I}) = (\boldsymbol{v} + \boldsymbol{Q}\boldsymbol{u}, \boldsymbol{Q}). \tag{2.40}$$

Since $\boldsymbol{u} \in \mathsf{L}$ and $\boldsymbol{Q} \in \mathcal{K}$, by Proposition 2.16 we see that $\boldsymbol{Q}\boldsymbol{u} \in \mathsf{L}$. Moreover, as $\boldsymbol{u}$ runs over the lattice L, $\boldsymbol{Q}\boldsymbol{u}$ also runs over L. As $\mathbb{R}^3 = \bigcup_{h \in \mathcal{L}} h\Pi$ (cf. Sect. 2.3.2), there clearly exists a unique vector $\boldsymbol{\alpha}$ in the primitive unit cell Π (i.e., $\boldsymbol{\alpha} = \alpha_1\boldsymbol{b}_1 + \alpha_2\boldsymbol{b}_2 + \alpha_3\boldsymbol{b}_3$, where $0 \le \alpha_i < 1$ for $i = 1, 2, 3$) such that $\boldsymbol{v} = \boldsymbol{\alpha} + \boldsymbol{s}$ for some $\boldsymbol{s} \in \mathsf{L}$. Then

$$\boldsymbol{v} + \boldsymbol{Q}\boldsymbol{u} = \boldsymbol{\alpha} + \boldsymbol{s} + \boldsymbol{Q}\boldsymbol{u} = \boldsymbol{\alpha} + \boldsymbol{t} \qquad \text{for some } \boldsymbol{t} \in \mathsf{L}. \tag{2.41}$$

Since $(-\boldsymbol{Q}^{-1}\boldsymbol{t}, \boldsymbol{I}) \in \mathcal{L}$,

$$(\boldsymbol{v}, \boldsymbol{Q})(-\boldsymbol{Q}^{-1}\boldsymbol{t}, \boldsymbol{I}) = (\boldsymbol{\alpha}, \boldsymbol{Q}) \in (\boldsymbol{v}, \boldsymbol{Q})\mathcal{L}. \tag{2.42}$$

Hence each coset $(\boldsymbol{v}, \boldsymbol{Q})\mathcal{L}$ has a representative of the form $(\boldsymbol{\alpha}, \boldsymbol{Q})$, where $\boldsymbol{\alpha} \in \Pi$.

The discussion above indicates also that for each $\boldsymbol{Q} \in \mathcal{K}$ there is only one element $(\boldsymbol{\alpha}, \boldsymbol{Q}) \in \mathcal{G}$ with $\boldsymbol{\alpha} \in \Pi$. Let us prove the preceding assertion in another way. Let $\boldsymbol{\alpha}, \boldsymbol{\beta} \in \Pi$. Suppose that both $(\boldsymbol{\alpha}, \boldsymbol{Q})$ and $(\boldsymbol{\beta}, \boldsymbol{Q})$ are in $\mathcal{G}$. Then $(\boldsymbol{\alpha}, \boldsymbol{Q})(\boldsymbol{\beta}, \boldsymbol{Q})^{-1} \in \mathcal{G}$. But

$$(\boldsymbol{\alpha}, \boldsymbol{Q})(\boldsymbol{\beta}, \boldsymbol{Q})^{-1} = (\boldsymbol{\alpha}, \boldsymbol{Q})(-\boldsymbol{Q}^{-1}\boldsymbol{\beta}, \boldsymbol{Q}^{-1}) = (\boldsymbol{\alpha} - \boldsymbol{\beta}, \boldsymbol{I}) \in \mathcal{L}. \tag{2.43}$$

For each i, the components α_i and β_i of $\boldsymbol{\alpha}$ and $\boldsymbol{\beta}$ with respect to the basis $\boldsymbol{b}_1, \boldsymbol{b}_2$, and $\boldsymbol{b}_3$ satisfy $-1 < \alpha_i - \beta_i < 1$. Thus the only possibility for $\boldsymbol{\alpha} - \boldsymbol{\beta} \in \mathsf{L}$ is $\boldsymbol{\alpha} = \boldsymbol{\beta}$.

The findings in the present section can be summarized as follows. Let $\mathcal{G}$ be the space group of a given ideal crystal $(\mathsf{C}, \boldsymbol{\kappa}_0)$, and let $\mathcal{L}$ be the lattice group and $\mathcal{K}$ the crystallographic point group of $\mathcal{G}$. The space group $\mathcal{G}$ can be taken as a disjoint union of left cosets. Each coset consists of elements of the form $(\boldsymbol{\alpha} + \boldsymbol{t}, \boldsymbol{Q})$ with the following properties:

[23] Cf. Sect. A.3.1 in Appendix A on coset decomposition.

(i) $\boldsymbol{Q} \in \mathcal{K}$ is the same for all elements in the same coset and is different for elements belonging to different cosets. (ii) $\boldsymbol{\alpha} \in \Pi$, where the primitive unit cell Π is defined in Sect. 2.3.2, and it is the same for all elements of the same coset. (iii) $\boldsymbol{t} \in \mathcal{L}$, and it runs over the lattice group to cover all the elements of the same coset.

Note that $(\boldsymbol{0}, \boldsymbol{Q})$, where $\boldsymbol{Q} \in \mathcal{K}$, need not be an element of $\mathcal{G}$. Before we discuss further on space groups, we should add an interlude on change of coordinate system.

2.3.5 Change of Coordinate System

Suppose we start working with an affine coordinate system with origin $\boldsymbol{O}$ and right-handed basis $\boldsymbol{f}_1$, $\boldsymbol{f}_2$, and $\boldsymbol{f}_3$. Consider another affine coordinate system with origin at some $\boldsymbol{O}' \in \mathsf{L}$ and a right-handed triad $\boldsymbol{f}'_i$ $(i = 1, 2, 3)$ as basis. Let $\boldsymbol{f}'_i = \boldsymbol{P}\boldsymbol{f}_i$ $(i = 1, 2, 3)$, where $\boldsymbol{P}$ is the linear transformation that defines the change of basis (cf. (1.43) in Sect. 1.2). Let $\boldsymbol{p} = \overrightarrow{\boldsymbol{O}\boldsymbol{O}'}$. Since both $\boldsymbol{O}$ and $\boldsymbol{O}'$ are in L, $(\boldsymbol{p}, \boldsymbol{I}) \in \mathcal{L}$ and $\boldsymbol{p} \in \mathsf{L}$. Let $\boldsymbol{x}$ and $\boldsymbol{x}'$ be position vectors that describe the same place in E^3 under the original (unprimed) and new (primed) coordinate systems. Note that $\boldsymbol{x} \in T_{\boldsymbol{O}}E^3$ and $\boldsymbol{x}' \in T_{\boldsymbol{O}'}E^3$, where $T_{\boldsymbol{O}}E^3$ and $T_{\boldsymbol{O}'}E^3$ are the tangent spaces to E^3 at $\boldsymbol{O}$ and $\boldsymbol{O}'$, respectively. Henceforth in this section we shall identify $T_{\boldsymbol{O}}E^3$ and $T_{\boldsymbol{O}'}E^3$ with $\mathbb{R}^3$ and adopt the commonly used convention in the crystallography literature (see, e.g., [133, 241]) where $\boldsymbol{x}$, $\boldsymbol{p}$, and $\boldsymbol{x}'$ are treated as column vectors in $\mathbb{R}^3$ and $\boldsymbol{P}$ as the matrix of change of basis from $\{\boldsymbol{f}_i\}$ to $\{\boldsymbol{f}'_i\}$; cf. Remarks 1.1 and 1.2. Since the column vectors $\boldsymbol{x} - \boldsymbol{p}$ and $\boldsymbol{x}'$ represent the same vector in V under the basis $\{\boldsymbol{f}_i\}$ and $\{\boldsymbol{f}'_i\}$, respectively, we have (cf. $(1.56)_1$)

$$\boldsymbol{P}\boldsymbol{x}' = \boldsymbol{x} - \boldsymbol{p} \qquad \text{or} \qquad \boldsymbol{x} = \boldsymbol{P}\boldsymbol{x}' + \boldsymbol{p}, \tag{2.44}$$

and

$$\boldsymbol{x}' = \boldsymbol{P}^{-1}(\boldsymbol{x} - \boldsymbol{p}). \tag{2.45}$$

Formally the preceding equation has the same form as that of a rigid transplacement. Using the notation in Sect. 2.2, we have

$$\boldsymbol{x} = (\boldsymbol{p}, \boldsymbol{P})\boldsymbol{x}' = (\boldsymbol{p}, \boldsymbol{I})(\boldsymbol{0}, \boldsymbol{P})\boldsymbol{x}', \tag{2.46}$$

and

$$\boldsymbol{x}' = (\boldsymbol{p}, \boldsymbol{P})^{-1}\boldsymbol{x} = (-\boldsymbol{P}^{-1}\boldsymbol{p}, \boldsymbol{P}^{-1})\boldsymbol{x}. \tag{2.47}$$

In $(2.46)_2$ we have decomposed $(\boldsymbol{p}, \boldsymbol{P})$ as a succession of two operations: First, the column vector $\boldsymbol{x}' \in T_{\boldsymbol{O}'}E^3$ under the basis $\{\boldsymbol{f}'_i\}$ is transformed by $\boldsymbol{P}$ so that it has the correct components under the basis $\{\boldsymbol{f}_i\}$. Then the translation $\boldsymbol{p}$ is added to it so that the resulting vector is in $T_{\boldsymbol{O}}E^3$, the tangent space to E^3 at $\boldsymbol{O}$. Note that the order of the two operations cannot be reversed.

Let $\boldsymbol{h} : \boldsymbol{\kappa}_0(\mathsf{C}) \to E^3$ be a rigid transplacement of a perfect crystal $(\mathsf{C}, \boldsymbol{\kappa}_0(\mathsf{C}))$. Under the original (unprimed) and new (primed) affine coordinate system, the transplacement is given by

$$\boldsymbol{y} := \boldsymbol{h}(\boldsymbol{x}) = \boldsymbol{v} + \boldsymbol{Q}\boldsymbol{x} = (\boldsymbol{v}, \boldsymbol{Q})\boldsymbol{x}, \tag{2.48}$$

$$\boldsymbol{y}' := \boldsymbol{h}(\boldsymbol{x}') = \boldsymbol{v}' + \boldsymbol{Q}'\boldsymbol{x}' = (\boldsymbol{v}', \boldsymbol{Q}')\boldsymbol{x}', \tag{2.49}$$

respectively, where $\boldsymbol{Q}$ and $\boldsymbol{Q}'$ are a rotation or roto-inversion centered at $\boldsymbol{O}$ and $\boldsymbol{O}'$, respectively. From (2.48) and the rule (2.46) on change of coordinate system, we have

$$(\boldsymbol{p}, \boldsymbol{P})\boldsymbol{y}' = (\boldsymbol{v}, \boldsymbol{Q})(\boldsymbol{p}, \boldsymbol{P})\boldsymbol{x}'. \tag{2.50}$$

Substituting the right-hand side of (2.49) for $\boldsymbol{y}'$ in the preceding equation, we obtain

$$(\boldsymbol{p}, \boldsymbol{P})(\boldsymbol{v}', \boldsymbol{Q}')\boldsymbol{x}' = (\boldsymbol{v}, \boldsymbol{Q})(\boldsymbol{p}, \boldsymbol{P})\boldsymbol{x}' \tag{2.51}$$

for all $\boldsymbol{x}' \in \mathbb{R}^3$. Hence we conclude that

$$\begin{aligned}(\boldsymbol{v}', \boldsymbol{Q}') &= (\boldsymbol{p}, \boldsymbol{P})^{-1}(\boldsymbol{v}, \boldsymbol{Q})(\boldsymbol{p}, \boldsymbol{P}) \\ &= (-\boldsymbol{P}^{-1}\boldsymbol{p} + \boldsymbol{P}^{-1}(\boldsymbol{v} + \boldsymbol{Q}\boldsymbol{p}), \boldsymbol{P}^{-1}\boldsymbol{Q}\boldsymbol{P}),\end{aligned} \tag{2.52}$$

which implies

$$\boldsymbol{Q}' = \boldsymbol{P}^{-1}\boldsymbol{Q}\boldsymbol{P}, \tag{2.53}$$

$$\boldsymbol{v}' = -\boldsymbol{P}^{-1}\boldsymbol{p} + \boldsymbol{P}^{-1}(\boldsymbol{v} + \boldsymbol{Q}\boldsymbol{p}). \tag{2.54}$$

At the end of Sect. 2.3, we prove that if $(\boldsymbol{v}, \boldsymbol{Q}) \in \mathcal{G}$, the space group of ideal crystal $(\mathsf{C}, \boldsymbol{\kappa}_0(\mathsf{C}))$, and if $(\boldsymbol{u}, \boldsymbol{I}) \in \mathcal{L}$, the lattice group of $\mathcal{G}$, then $(\boldsymbol{Q}\boldsymbol{u}, \boldsymbol{I})\mathsf{L} = \mathsf{L}$. Under the new coordinate system, the space group $\mathcal{G}$ becomes $\mathcal{G}'$, the elements $(\boldsymbol{v}', \boldsymbol{Q}')$ of which are related to those $(\boldsymbol{v}, \boldsymbol{Q})$ of $\mathcal{G}$ by equations (2.53) and (2.54). Likewise, by (2.45) the position vector $\boldsymbol{s}$ of a lattice point in L becomes $\boldsymbol{s}' = \boldsymbol{P}^{-1}(\boldsymbol{s} - \boldsymbol{p})$, the position vector of the same lattice point under the new coordinate system.

Let $\mathcal{L}' = \{(\boldsymbol{u}', \boldsymbol{I}) : (\boldsymbol{u}, \boldsymbol{I}) \in \mathcal{L}\}$ and $\mathcal{K}' = \{\boldsymbol{Q}' : \boldsymbol{Q} \in \mathcal{K}\}$. Let $(\boldsymbol{u}', \boldsymbol{I}) \in \mathcal{L}'$ and $\boldsymbol{Q}' \in \mathcal{K}'$. Then we have

$$\begin{aligned}\boldsymbol{Q}'\boldsymbol{u}' &= \boldsymbol{P}^{-1}\boldsymbol{Q}\boldsymbol{P}(\boldsymbol{P}^{-1}(\boldsymbol{u} - \boldsymbol{p})) \\ &= \boldsymbol{P}^{-1}(\boldsymbol{Q}(\boldsymbol{u} - \boldsymbol{p})).\end{aligned} \tag{2.55}$$

Since $\boldsymbol{Q}\boldsymbol{u} \in \mathsf{L}$ and $\boldsymbol{Q}\boldsymbol{p} \in \mathsf{L}$ (because $\boldsymbol{p} \in \mathsf{L}$), $\boldsymbol{Q}(\boldsymbol{u} - \boldsymbol{p})$ is a lattice point in L and $\boldsymbol{Q}'\boldsymbol{u}'$ is simply the position vector of this lattice point in the new coordinate system. Thus $\boldsymbol{Q}'\boldsymbol{u}' \in \mathsf{L}$.

Hence it can be seen that our finding in Proposition 2.16 is independent of the affine coordinate system chosen.

2.3.6 Space-Group Types and International Tables A

Here we adopt the same convention as that of Sect. 2.3.5. In particular the pair $(\boldsymbol{p}, \boldsymbol{P})$, where $\boldsymbol{p}$ denotes the column vector specifying a shift of the origin and $\boldsymbol{P}$ (with $\det \boldsymbol{P} > 0$) is the matrix of change of basis in V, defines a change of the right-handed affine coordinate system.

Definition 2.18 Two space groups $\mathcal{G}$ and $\mathcal{G}'$ are said to be equivalent if there is a change $(\boldsymbol{p}, \boldsymbol{P})$ of right-handed affine coordinate system such that

$$\mathcal{G}' = (\boldsymbol{p}, \boldsymbol{P})^{-1}\mathcal{G}(\boldsymbol{p}, \boldsymbol{P}) = \{(\boldsymbol{p}, \boldsymbol{P})^{-1}(\boldsymbol{v}, \boldsymbol{Q})(\boldsymbol{p}, \boldsymbol{P}) : (\boldsymbol{v}, \boldsymbol{Q}) \in \mathcal{G}\}. \tag{2.56}$$

Each equivalence class of space groups defines a space-group type. Two equivalent space groups are of the same type. □

Building on the contributions by Camille Jordan, Leonhard Sohncke, and others, Ergraf Fedorov and Arthur Schöflies, who worked largely independently, successfully enumerated all 230 space-group types in 1891 [21, 67]. By now various methods for derivation of the 230 space-group types are available; see, e.g., [66, 101, 176, 177, 354] and the references therein. Derivation of the space-group types, however, is beyond the scope of this exposition.

The present exposition concerns texture analysis in the context of macroscopic physics. Space groups need not be mentioned and are mostly not mentioned in the theoretical development of macrotexture analysis (cf. Sect. 2.11 for further discussion), while point-group symmetries figure prominently in that development. On the other hand, measurements of macrotexture require knowledge on the structure of the crystallites that comprise the polycrystal in question. The space group $\mathcal{G}$ of an ideal crystal consists of symmetry operations $(\boldsymbol{v}, \boldsymbol{Q})$ of its crystal structure, which provide some essential and useful information about the structure. In fact the structure of a specific ideal crystal is often described succinctly by specifying its space-group type and appealing to the wealth of information related to each of the 230 space-group types given in *International Tables A* (*ITA*) [7, 133].

Take the mineral calcite ($CaCO_3$) for example [129, pp. 156–157]. The unit cell has 30 atoms: 6 Ca, 6 C, and 18 O. To specify the crystal structure, it suffices to name its space-group type ($R\bar{3}c$, No. 167),[24] provide the two metric parameters of the unit cell that are not determined by symmetry, and give the position of one Ca, one C, and one O atom, respectively. The positions of the other 27 atoms are determined by the space-group symmetry, all relevant information of which can be found in *ITA*.

With applications to common metals such as aluminum, copper, steels, and titanium in mind, we shall restrict attention to three simple crystal structures, namely: the face-centered cubic structure (fcc), the body-centered cubic structure (bcc), and the hexagonal close-packed structure (hcp). We shall study these three crystal structures at the end of this chapter. Until then we will shift our focus to crystallographic point groups and other topics.

2.3.7 Point-Group Types and Conjugacy Classes of Subgroups of O(3)

Let $\mathcal{K}_1$ and $\mathcal{K}_2$ be subgroups of O(3). The subgroup $\mathcal{K}_1$ is said to be conjugate to $\mathcal{K}_2$ if there is a rotation or roto-inversion $\boldsymbol{Q} \in \mathrm{O}(3)$ such that $\boldsymbol{Q}\mathcal{K}_1\boldsymbol{Q}^{-1} = \mathcal{K}_2$ as sets (cf. Definition A.9). Such two subgroups are said to be conjugate subgroups of O(3). For a subgroup $\mathcal{K}$ of O(3), the set $\{\boldsymbol{Q}\mathcal{K}\boldsymbol{Q}^{-1} : \boldsymbol{Q} \in \mathrm{O}(3)\}$ is called the conjugacy class of subgroups of O(3) represented by $\mathcal{K}$. It is easy to verify that two subgroups which belong to the same conjugacy class are conjugate to each other.

Let $\mathcal{K}$ be a subgroup of O(3), and let $\boldsymbol{Q} = \boldsymbol{\mathcal{I}}\boldsymbol{R}$ be a roto-inversion. Since

$$\boldsymbol{Q}\mathcal{K}\boldsymbol{Q}^{-1} = (\boldsymbol{\mathcal{I}}\boldsymbol{R})\mathcal{K}(\boldsymbol{\mathcal{I}}\boldsymbol{R})^{-1} = \boldsymbol{R}\mathcal{K}\boldsymbol{R}^{-1}, \tag{2.57}$$

it follows that

$$\{\boldsymbol{Q}\mathcal{K}\boldsymbol{Q}^{-1} : \boldsymbol{Q} \in \mathrm{O}(3)\} = \{\boldsymbol{R}\mathcal{K}\boldsymbol{R}^{-1} : \boldsymbol{R} \in \mathrm{SO}(3)\}. \tag{2.58}$$

Each element g of $\mathcal{K}$ is either of the form $\boldsymbol{P}(\boldsymbol{n}, \omega)$ or $\boldsymbol{\mathcal{I}}\boldsymbol{P}(\boldsymbol{n}, \omega)$, where $\boldsymbol{P}$ is a rotation. If the physical object of which $\mathcal{K}$ is its symmetry group undergoes a rotation $\boldsymbol{R}$, then the rotation $\boldsymbol{P}$ pertaining to the element g will become $\boldsymbol{P}(\boldsymbol{Rn}, \omega) = \boldsymbol{R}\boldsymbol{P}(\boldsymbol{n}, \omega)\boldsymbol{R}^{-1}$, where we have appealed to Euler's theorem (1.82) at the last step; cf. Example 2.1 in Sect. 2.1 for a

[24] In [129] the space-group type in question is mistyped as $R3c$, which is No. 161.

concrete illustration. Thus the symmetry group of the object after it undergoes a rotation $\boldsymbol{R}$ is $\boldsymbol{R}\mathcal{K}\boldsymbol{R}^{-1}$. Hence we can say that two subgroups of O(3) which belong to the same conjugacy class describe the same physical symmetry.

Alternatively, we may adopt the passive point of view: instead of rotating the object, we let it remain as it is and consider change of coordinate system. We write $\boldsymbol{R}\mathcal{K}\boldsymbol{R}^{-1} = (\boldsymbol{R}^{(p)})^{-1}\mathcal{K}\boldsymbol{R}^{(p)}$, where $\boldsymbol{R}^{(p)} = \boldsymbol{R}^{-1}$ is the passive rotation (cf. Sect. 1.5) pertaining to the active rotation $\boldsymbol{R}$. Under a given Cartesian coordinate system with origin at the common fixed point of elements in O(3), each rotation or roto-inversion $\boldsymbol{P} \in \mathcal{K}$ is given by a 3×3 orthogonal matrix $[P_{ij}]$. Hence two subgroups in the same conjugacy class of O(3) may be taken as representations of the symmetry group of the same physical object in two Cartesian coordinate systems.

The equivalence of two space groups naturally leads to the equivalence of their associated point groups.

Definition 2.19 Let $\mathcal{K}$ and $\mathcal{K}'$ be point groups pertaining to space groups $\mathcal{G}$ and $\mathcal{G}'$, respectively. The point groups $\mathcal{K}$ and $\mathcal{K}'$ are equivalent or are of the same point-group type if $\mathcal{G}$ and $\mathcal{G}'$ are of the same space-group type. □

Let $\mathcal{G}$ and $\mathcal{G}'$ be two equivalent space groups and $\mathcal{G}' = (\boldsymbol{p}, \boldsymbol{P})^{-1}\mathcal{G}\,(\boldsymbol{p}, \boldsymbol{P})$; see Definition 2.18. Let $\mathcal{K} = \{\boldsymbol{Q}_1, \ldots, \boldsymbol{Q}_n\}$ and $\mathcal{K}' = \{\boldsymbol{Q}'_1, \ldots, \boldsymbol{Q}'_n\}$ be crystallographic point groups that pertain to $\mathcal{G}$ and $\mathcal{G}'$, respectively. By (2.53), we may label the elements in $\mathcal{K}$ and $\mathcal{K}'$ so that

$$\boldsymbol{Q}'_k = \boldsymbol{P}^{-1}\boldsymbol{Q}_k\boldsymbol{P} \qquad \text{for } k = 1, \ldots, n. \tag{2.59}$$

The following proposition, however, shows that the criterion for equivalence of point groups can be sharpened.

Proposition 2.20 *Let I be an index set. Let $\mathcal{H} = \{\boldsymbol{Q}_\alpha : \alpha \in I\}$ and $\mathcal{H}' = \{\boldsymbol{Q}'_\alpha : \alpha \in I\}$ be subgroups of O(3) such that for some linear transformation $\boldsymbol{F}$ on V with* $\det \boldsymbol{F} > 0$ *there holds*

$$\boldsymbol{Q}'_\alpha = \boldsymbol{F}\,\boldsymbol{Q}_\alpha\boldsymbol{F}^{-1} \qquad \textit{for each } \alpha \in I. \tag{2.60}$$

Then there is a rotation $\boldsymbol{R}$ on V such that

$$\boldsymbol{Q}'_\alpha = \boldsymbol{R}\,\boldsymbol{Q}_\alpha\boldsymbol{R}^{-1} \qquad \textit{for each } \alpha \in I. \tag{2.61}$$

A version of this proposition for V being an n-dimensional space is the content of a 1947 paper by Bäbler [13]. However, as pointed out by C.C. MacDuffee in Mathematical Reviews (MR0020541), what Bäbler did was to give "[a]n elementary proof of [a] theorem of C. Jordan" ([168, p. 162] = p. 137 of *Œuvres*, Tome III). Here we give a proof that follows the broad outline of the proof presented in Burckhardt [66, §7 of both editions] but, as we are concerned only with the case $n = 3$, can be and is made considerably simpler. Before we proceed to the proof, we should go over some mathematical prerequisites.

A second-order tensor $\boldsymbol{S}$ is symmetric if $\boldsymbol{S}^T = \boldsymbol{S}$. It is positive definite if $\boldsymbol{u} \cdot \boldsymbol{S}\boldsymbol{u} > 0$ for all $\boldsymbol{u} \in V \setminus \{\boldsymbol{0}\}$. By the spectral theorem, each symmetric tensor $\boldsymbol{S}$ can be written as

$$\boldsymbol{S} = \lambda_1\boldsymbol{e}_1 \otimes \boldsymbol{e}_1 + \lambda_2\boldsymbol{e}_2 \otimes \boldsymbol{e}_2 + \lambda_3\boldsymbol{e}_3 \otimes \boldsymbol{e}_3, \tag{2.62}$$

where $\{\boldsymbol{e}_i : i = 1, 2, 3\}$ is a set of orthonormal eigenvectors of $\boldsymbol{S}$ and λ_i is the eigenvalue associated with the eigenvector $\boldsymbol{e}_i$. Let

$$I_1(\boldsymbol{S}) = \lambda_1 + \lambda_2 + \lambda_3, \quad I_2(\boldsymbol{S}) = \lambda_1\lambda_2 + \lambda_2\lambda_3 + \lambda_3\lambda_1, \quad I_3(\boldsymbol{S}) = \lambda_1\lambda_2\lambda_3, \tag{2.63}$$

which are called the principal invariants of the symmetric tensor $\boldsymbol{S}$. The polynomial

$$f(\lambda) := (\lambda - \lambda_1)(\lambda - \lambda_2)(\lambda - \lambda_3) = \lambda^3 - I_1(\boldsymbol{S})\lambda^2 + I_2(\boldsymbol{S})\lambda - I_3(\boldsymbol{S}) \tag{2.64}$$

is called the characteristic polynomial of $\boldsymbol{S}$, and the equation $f(\lambda) = 0$ its characteristic equation. Clearly the eigenvalues λ_1, λ_2, and λ_3 are roots of the characteristic equation of $\boldsymbol{S}$. Let $f(\boldsymbol{S}) = \boldsymbol{S}^3 - I_1(\boldsymbol{S})\boldsymbol{S}^2 + I_2(\boldsymbol{S})\boldsymbol{S} - I_3(\boldsymbol{S})\boldsymbol{I}$. For $i = 1, 2, 3$, it is easy to see that

$$f(\boldsymbol{S})\boldsymbol{e}_i = f(\lambda_i)\boldsymbol{e}_i = \boldsymbol{0}. \tag{2.65}$$

Since $\{\boldsymbol{e}_i : i = 1, 2, 3\}$ is a basis in V, we conclude that

$$\boldsymbol{S}^3 - I_1(\boldsymbol{S})\boldsymbol{S}^2 + I_2(\boldsymbol{S})\boldsymbol{S} - I_3(\boldsymbol{S})\boldsymbol{I} = \boldsymbol{0}, \tag{2.66}$$

i.e., a symmetric tensor satisfies its characteristic equation.[25]

If the symmetric tensor $\boldsymbol{S}$ is positive definite, all its eigenvalues $\lambda_i > 0$. Then the tensor

$$\boldsymbol{U} := \sqrt{\lambda_1}\,\boldsymbol{e}_1 \otimes \boldsymbol{e}_1 + \sqrt{\lambda_2}\,\boldsymbol{e}_2 \otimes \boldsymbol{e}_2 + \sqrt{\lambda_3}\,\boldsymbol{e}_3 \otimes \boldsymbol{e}_3, \tag{2.67}$$

is well defined, and it is symmetric and positive definite. Clearly we have $\boldsymbol{U}^2 = \boldsymbol{S}$, and it is easy to show[26] that $\boldsymbol{U}$, as defined in (2.67), is the only symmetric and positive definite tensor which satisfies the equation $\boldsymbol{U}^2 = \boldsymbol{S}$. We shall write $\boldsymbol{U} = \sqrt{\boldsymbol{S}}$ and call it the square root of $\boldsymbol{S}$.

The following lemma will be instrumental in our proof of Proposition 2.20. The short proof of this lemma presented here is taken from Ting [316].

Lemma 2.21 *Let $\boldsymbol{C}$ be a symmetric and positive definite second-order tensor, and let $\boldsymbol{U} = \sqrt{\boldsymbol{C}}$. Then $\boldsymbol{U}$ is given in terms of $\boldsymbol{C}$ by an explicit formula of the form*

$$\boldsymbol{U} = \beta_0(\lambda_1, \lambda_2, \lambda_3)\boldsymbol{I} + \beta_1(\lambda_1, \lambda_2, \lambda_3)\boldsymbol{C} + \beta_2(\lambda_1, \lambda_2, \lambda_3)\boldsymbol{C}^2, \tag{2.68}$$

where β_0, β_1, and β_2 are explicit, scalar symmetric functions of the eigenvalues λ_i ($i = 0, 1, 2$) of $\boldsymbol{U}$.

Proof Since $\boldsymbol{U}$ is symmetric, it satisfies its characteristic equation (cf. (2.66)):

$$\boldsymbol{U}^3 - I_1(\boldsymbol{U})\boldsymbol{U}^2 + I_2(\boldsymbol{U})\boldsymbol{U} - I_3(\boldsymbol{U})\boldsymbol{I} = \boldsymbol{0}. \tag{2.69}$$

[25] Of course, we may write down (2.66) immediately by appealing to the Cayley-Hamilton theorem (see, e.g., [33, p. 296], [40, p. 154]), which asserts that every real or complex square matrix satisfies its own characteristic equation. But, as we shall need the Cayley-Hamilton equation (2.66) only for symmetric second-order tensors and a proof for this special case is effortless, we include a proof here for completeness.

[26] The following short and elegant proof is due to Stephenson [303]. Let $\boldsymbol{e}_i$ be an eigenvector of $\boldsymbol{S}$ with positive eigenvalue λ_i. Then $(\boldsymbol{U}^2 - \lambda_i\boldsymbol{I})\boldsymbol{e}_i = (\boldsymbol{U} + \sqrt{\lambda_i}\boldsymbol{I})(\boldsymbol{U} - \sqrt{\lambda_i}\boldsymbol{I})\boldsymbol{e}_i = (\boldsymbol{U} + \sqrt{\lambda_i}\boldsymbol{I})\boldsymbol{v}_i = \boldsymbol{0}$, where $\boldsymbol{v}_i = (\boldsymbol{U} - \sqrt{\lambda_i}\boldsymbol{I})\boldsymbol{e}_i$. If $\boldsymbol{v}_i \neq \boldsymbol{0}$, then $\boldsymbol{U}\boldsymbol{v}_i = -\sqrt{\lambda_i}\boldsymbol{v}_i$, i.e., $\boldsymbol{U}$ has a negative eigenvalue $-\sqrt{\lambda_i}$, which is a contradiction. Hence it is necessary that $\boldsymbol{v}_i = \boldsymbol{0}$, i.e., $\boldsymbol{U}\boldsymbol{e}_i = \sqrt{\lambda_i}\boldsymbol{e}_i$.

Multiplying both sides of (2.69) by $\boldsymbol{U}$, we obtain

$$\boldsymbol{U}^4 - I_1(\boldsymbol{U})\boldsymbol{U}^3 + I_2(\boldsymbol{U})\boldsymbol{U}^2 - I_3(\boldsymbol{U})\boldsymbol{U} = \boldsymbol{0}. \tag{2.70}$$

Eliminating $\boldsymbol{U}^3$ from (2.69) and (2.70), and substituting $\boldsymbol{U}^2$ and $\boldsymbol{U}^4$ by $\boldsymbol{C}$ and $\boldsymbol{C}^2$, respectively, we arrive at an explicit formula of the form (2.68). □

Explicit formulas for the symmetric scalar functions β_i $(i = 1, 2, 3)$ are obtained at the last step of the proof of the lemma. We do not present them here because these explicit formulas are not needed for our proof of Proposition 2.20.

Proof of Proposition 2.20 Let $\boldsymbol{C} := \boldsymbol{F}^T\boldsymbol{F} = \boldsymbol{U}^2$. Fix an $\alpha \in I$. Substituting $\boldsymbol{Q}'_\alpha = \boldsymbol{F}\boldsymbol{Q}_\alpha\boldsymbol{F}^{-1}$ into the equation $(\boldsymbol{Q}'_\alpha)^T\boldsymbol{Q}'_\alpha = \boldsymbol{I}$, we observe after a simple computation that $\boldsymbol{C}\boldsymbol{Q}_\alpha = \boldsymbol{Q}_\alpha\boldsymbol{C}$, which together with (2.68) implies that $\boldsymbol{U}\boldsymbol{Q}_\alpha = \boldsymbol{Q}_\alpha\boldsymbol{U}$. Let $\boldsymbol{R} = \boldsymbol{F}\boldsymbol{U}^{-1}$. Then we have

$$\boldsymbol{R}^T\boldsymbol{R} = \boldsymbol{U}^{-T}\boldsymbol{F}^T\boldsymbol{F}\boldsymbol{U}^{-1} = \boldsymbol{U}^{-1}\boldsymbol{U}^2\boldsymbol{U}^{-1} = \boldsymbol{I},$$

where we have used the fact that $\boldsymbol{U}$ is symmetric, and $\det\boldsymbol{R} = \det\boldsymbol{F}\det(\boldsymbol{U}^{-1}) > 0$. Hence $\boldsymbol{R}$ is a rotation. Substituting $\boldsymbol{F} = \boldsymbol{R}\boldsymbol{U}$ into (2.60), we obtain

$$\boldsymbol{Q}'_\alpha = \boldsymbol{R}\boldsymbol{U}\boldsymbol{Q}_\alpha\boldsymbol{U}^{-1}\boldsymbol{R}^{-1} = \boldsymbol{R}\boldsymbol{Q}_\alpha\boldsymbol{U}\boldsymbol{U}^{-1}\boldsymbol{R}^{-1} = \boldsymbol{R}\boldsymbol{Q}_\alpha\boldsymbol{R}^{-1},$$

where $\boldsymbol{R}$ is a rotation on V. □

Note that we have put Proposition 2.20 in the context of active transformations, i.e., (2.60) is adopted in place of (2.59), where the transformation $\boldsymbol{P}$ arises from change of coordinate system. Under the passive view, (2.61) is replaced by

$$\boldsymbol{Q}'_\alpha = (\boldsymbol{R}^{(p)})^{-1}\boldsymbol{Q}_\alpha\boldsymbol{R}^{(p)} \qquad \text{for each } \alpha \in I, \tag{2.71}$$

where $\boldsymbol{R}^{(p)}$ defines a rotation of the coordinate system. Irrespective of whether one adopts the active or passive view of transformations, a criterion for the equivalence of two crystallographic point groups can be put as follows.

Corollary 2.22 *Two crystallographic point groups $\mathcal{K}$ and $\mathcal{K}'$ are equivalent or of the same point-group type if they belong to the same conjugacy class of $O(3)$, i.e., there exists a rotation $\boldsymbol{R}$ on V such that $\mathcal{K}' = \boldsymbol{R}\mathcal{K}\boldsymbol{R}^{-1}$.* □

In the literature it is usual to use the same name for a specific group in a conjugacy class of O(3) and for the conjugacy class (or point-group type) represented by this specific group. For instance, in Example 2.1 the group generated by the two rotations $\boldsymbol{R}(\boldsymbol{e}_3, 2\pi/3)$ and $\boldsymbol{R}(\boldsymbol{e}_1, \pi)$ is called D_3. So is each group generated by $\boldsymbol{R}(\boldsymbol{n}, 2\pi/3)$ and $\boldsymbol{R}(\boldsymbol{m}, \pi)$, where $\boldsymbol{n}$ and $\boldsymbol{m}$ are two orthogonal unit vectors. Moreover, the conjugacy class or point-group type that contains all the aforementioned groups as members is also called D_3. Whether the name D_3 refers to a point-group type or a specific group of that type should be clear from the context where the name appears.

2.4 Finite Subgroups of the Rotation Group

To prepare for our study of crystallographic point groups, in this section we enumerate the conjugacy classes of finite rotation groups.

2.4.1 Poles, Stabilizers, and Rotations About the Same Axis

Let G be a finite subgroup of SO(3). We denote by $|G|$ the number of elements in G. A point $\boldsymbol{b}$ on the unit sphere S^2 is a pole of G if $g\boldsymbol{b} = \boldsymbol{b}$ for some $g \neq \boldsymbol{I} \in G$. Each $g \neq \boldsymbol{I}$ in G has a rotation axis which meets S^2 at two diametrically opposite poles.

Let $\boldsymbol{a} \in S^2$ be a pole of G. It is easy to verify that

$$G_{\boldsymbol{a}} := \{g \in G : g\boldsymbol{a} = \boldsymbol{a}\}, \tag{2.72}$$

called the stabilizer of the pole $\boldsymbol{a}$, is a non-trivial subgroup of G. If $|G_{\boldsymbol{a}}| = r$, then $\boldsymbol{a} \in S^2$ is called a pole of multiplicity r [339, p. 149] or an r-tuple pole (or a double, triple, quadruple pole when $r = 2, 3, 4$, respectively) [353, second edition, p. 17], and the common axis L of rotations $g \in G_{\boldsymbol{a}}$ is called an axis of order r or an r-fold axis of G.

Proposition 2.23 *Let $G \neq \{\boldsymbol{I}\}$ be a finite group of rotations about the same axis, and let $|G| = n$. Then there is a rotation $\boldsymbol{P} \neq \boldsymbol{I}$ such that $G = \{\boldsymbol{I}, \boldsymbol{P}, \ldots, \boldsymbol{P}^{n-1}\}$.*

Proof Let $\boldsymbol{n}$ be a unit vector that defines the axis of rotations in G. Then we can write $G = \{\boldsymbol{R}(\boldsymbol{n}, \varphi_i) : i = 1, \ldots, n\}$, where $0 \leq \varphi_i < 2\pi$. Without loss of generality, let $\varphi_1 = 0$. Then $\varphi_i > 0$ for $i \neq 1$. Let $\theta \neq 0$ be the smallest of the non-zero rotation angles φ_i. Dividing φ_i by θ, we obtain for a given $2 \leq i \leq n$

$$\varphi_i = k\theta + \varphi_r, \qquad \text{where } k \geq 1 \text{ is a positive integer and } 0 \leq \varphi_r < \theta \text{ is the remainder.}$$

Thus we have

$$\boldsymbol{R}(\boldsymbol{n}, \varphi_i) = \boldsymbol{R}(\boldsymbol{n}, k\theta + \varphi_r) = \boldsymbol{R}(\boldsymbol{n}, \theta)^k \boldsymbol{R}(\boldsymbol{n}, \varphi_r),$$

which implies

$$\boldsymbol{R}(\boldsymbol{n}, \varphi_r) = \boldsymbol{R}(\boldsymbol{n}, \theta)^{-k} \boldsymbol{R}(\boldsymbol{n}, \varphi_i) \in G$$

as G is a group. Since θ is the smallest non-zero rotation angle among all φ_i and $0 \leq \varphi_r < \theta$, we conclude that $\varphi_r = 0$. Let $\boldsymbol{P} = \boldsymbol{R}(\boldsymbol{n}, \theta)$. Then $G = \{\boldsymbol{I}, \boldsymbol{P}, \ldots, \boldsymbol{P}^{n-1}\}$ and $\boldsymbol{P}^n = \boldsymbol{I}$. □

The following corollary is an immediate consequence of Proposition 2.23.

Corollary 2.24 *Let $\boldsymbol{a} \in S^2$ be a pole of the finite rotational group G. Then the stabilizer $G_{\boldsymbol{a}}$ of $\boldsymbol{a}$ is a cyclic subgroup of G, with the common rotational axis L of $\boldsymbol{R} \in G_{\boldsymbol{a}}$ defined by $\boldsymbol{a}$ and its diametrically opposite pole $\boldsymbol{a}'$. Moreover, we have $G_{\boldsymbol{a}} = G_{\boldsymbol{a}'}$.* □

By Proposition 2.23, $G_{\boldsymbol{a}}$ has a single generator $\boldsymbol{P}$, $G_{\boldsymbol{a}} = \{\boldsymbol{I}, \boldsymbol{P}, \ldots, \boldsymbol{P}^{n-1}\}$, and $\boldsymbol{P}^n = \boldsymbol{I}$. The element $\boldsymbol{P} \in G$ is said to be of order n.

From the discussions above, clearly each element $\boldsymbol{R} \neq \boldsymbol{I}$ of a non-trivial finite rotation group can be assigned a specific $r \geq 2$ so that it has an r-fold axis and two r-tuple poles.

2.4.2 Enumeration of Finite Rotational Groups

Let $G \neq \{\boldsymbol{I}\}$ be a finite rotation group and let X be the set of poles of G, i.e.,

$$X = \{\boldsymbol{x} \in S^2 : g\boldsymbol{x} = \boldsymbol{x} \text{ for some } g \neq e \in G\}, \tag{2.73}$$

and let

$$\Omega := \{(g, \boldsymbol{x}) : g \in G, g \neq \boldsymbol{I}, \boldsymbol{x} \in X, \text{and } g\boldsymbol{x} = \boldsymbol{x}\}. \tag{2.74}$$

We shall derive an equation, which will allow us to enumerate all conjugacy classes of finite rotation groups, by counting in two different ways the number of elements in Ω. Note that each element $(g, \boldsymbol{x}) \in \Omega$ consists of a pole $\boldsymbol{x} \in X$ and a non-trivial rotation $g \in G_{\boldsymbol{x}}$, the stabilizer of $\boldsymbol{x}$.

Before we proceed to do the counting, we have to go through some mathematical preliminaries.

Lemma 2.25 *Each g in G is a bijection on X.*

Proof Each $g \in G$ is a bijection on S^2 and, by restriction, is a bijection from X to its image $g(X)$. To show that g is a bijection on X, it suffices to show that $g(X) \subset X$. Let $\boldsymbol{x} \in X$ and $g \in G$. Since $\boldsymbol{x}$ is a pole of G, there is some $h \neq e \in G$ such that $h\boldsymbol{x} = \boldsymbol{x}$. Then $ghg^{-1}(g\boldsymbol{x}) = gh(\boldsymbol{x}) = g\boldsymbol{x}$. Since $ghg^{-1} \in G$, we conclude that $g\boldsymbol{x}$ is a pole of G. □

Let $\boldsymbol{a} \in X$ be a pole of G. The set

$$G(\boldsymbol{a}) := \{g\boldsymbol{a} \in X : g \in G\} \tag{2.75}$$

is called the G-orbit of $\boldsymbol{a}$ in X.

Lemma 2.26 *X is a disjoint union of G-orbits.*

Proof For each $\boldsymbol{a} \in X$, $G(\boldsymbol{a}) \subset X$; hence we have the union of G-orbits $\bigcup_{\boldsymbol{a} \in X} G(\boldsymbol{a}) \subset X$. Conversely, $\boldsymbol{a} \in G(\boldsymbol{a})$ for each $\boldsymbol{a} \in X$, which implies $X \subset \bigcup_{\boldsymbol{a} \in X} G(\boldsymbol{a})$. Hence $X = \bigcup_{\boldsymbol{a} \in X} G(\boldsymbol{a})$. We claim that distinct G-orbits of X are disjoint. Indeed, if $G(\boldsymbol{a}) \cap G(\boldsymbol{b}) \neq \emptyset$, then there is some $\boldsymbol{c} \in X$ and $g_1, g_2 \in G$ such that $g_1\boldsymbol{a} = g_2\boldsymbol{b} = \boldsymbol{c}$. Thus $\boldsymbol{a} = g_1^{-1}g_2\boldsymbol{b}$, $\boldsymbol{b} = g_2^{-1}g_1\boldsymbol{a}$, and $\boldsymbol{a} \in G(\boldsymbol{b})$, $\boldsymbol{b} \in G(\boldsymbol{a})$. It follows that $G(\boldsymbol{a}) = G(\boldsymbol{b})$. □

Lemma 2.27 *If $\boldsymbol{a}$ and $\boldsymbol{b}$ lie in the same G-orbit, then $|G_{\boldsymbol{a}}| = |G_{\boldsymbol{b}}|$. In other words, every pole in the same G-orbit has the same multiplicity.*

Proof Let $|G_{\boldsymbol{a}}| = r$, $|G_{\boldsymbol{b}}| = s$, and $G_{\boldsymbol{a}}$ and $G_{\boldsymbol{b}}$ have generators $\boldsymbol{R}(\boldsymbol{a}, 2\pi/r)$ and $\boldsymbol{R}(\boldsymbol{b}, 2\pi/s)$, respectively. Since $\boldsymbol{a}$ and $\boldsymbol{b}$ lie in the same G-orbit, there is a $\boldsymbol{Q} \in G$ such that $\boldsymbol{Q}\boldsymbol{a} = \boldsymbol{b}$. By Euler's theorem,

$$\boldsymbol{Q}\boldsymbol{R}(\boldsymbol{a}, 2\pi/r)\,\boldsymbol{Q}^{-1} = \boldsymbol{R}(\boldsymbol{Q}\boldsymbol{a}, 2\pi/r) = \boldsymbol{R}(\boldsymbol{b}, 2\pi/r) \in G_{\boldsymbol{b}}.$$

It follows that $r = s/m$ for some positive integer $m \geq 1$. On the other hand, since

$$\boldsymbol{Q}^{-1}\boldsymbol{R}(\boldsymbol{b}, 2\pi/s)\,\boldsymbol{Q} = \boldsymbol{R}(\boldsymbol{Q}^{-1}\boldsymbol{b}, 2\pi/s) = \boldsymbol{R}(\boldsymbol{a}, 2\pi/s) \in G_{\boldsymbol{a}},$$

there holds $s = r/n$ for some positive integer $n \geq 1$. Hence we have $m \geq 1$, $n \geq 1$, and $mn = 1$, which imply $m = n = 1$ and $r = s$. □

Proposition 2.28 *Let $|G(\boldsymbol{a})|$ be the number of elements in the G-orbit of pole $\boldsymbol{a}$ in X. There holds $|G(\boldsymbol{a})| = |G|/|G_{\boldsymbol{a}}|$.*

Proof Let $|G(\boldsymbol{a})| = p$ and $G(\boldsymbol{a}) = \{\boldsymbol{b}_0, \boldsymbol{b}_1, \ldots, \boldsymbol{b}_{p-1}\} \subset X$, where $\boldsymbol{b}_0 = \boldsymbol{a}$. Let $|G_{\boldsymbol{a}}| = r$. By Proposition 2.23, we have $G_{\boldsymbol{a}} = \{\boldsymbol{I}, \boldsymbol{P}, \ldots, \boldsymbol{P}^{r-1}\}$, where $\boldsymbol{P}$ is the generator of $G_{\boldsymbol{a}}$. For later notational convenience, we put $\boldsymbol{P}^0 := \boldsymbol{I}$. Since $G(\boldsymbol{a})$ is the G-orbit of $\boldsymbol{a}$, there exists $\boldsymbol{Q}_i \in G$ such that $\boldsymbol{Q}_i\boldsymbol{a} = \boldsymbol{b}_i$ for $i = 1, \ldots, p-1$. Let $\boldsymbol{Q}_0 := \boldsymbol{I}$ so that we have also $\boldsymbol{Q}_0\boldsymbol{a} = \boldsymbol{b}_0$. By the definition of $G(\boldsymbol{a})$, for each $g \in G$ we have $g\boldsymbol{a} = \boldsymbol{b}_i = \boldsymbol{Q}_i\boldsymbol{a}$ for some $i = 0, 1, \ldots, p-1$. Hence $\boldsymbol{Q}_i^{-1}g\boldsymbol{a} = \boldsymbol{a}$, i.e., $\boldsymbol{Q}_i^{-1}g \in G_{\boldsymbol{a}}$, which implies $g \in \boldsymbol{Q}_iG_{\boldsymbol{a}}$ for some i.

We claim that $\boldsymbol{Q}_iG_{\boldsymbol{a}} \cap \boldsymbol{Q}_jG_{\boldsymbol{a}} = \emptyset$ for $i \neq j$. Indeed, suppose $h \in \boldsymbol{Q}_iG_{\boldsymbol{a}} \cap \boldsymbol{Q}_jG_{\boldsymbol{a}}$, and $i \neq j$. Then $h = \boldsymbol{Q}_i\boldsymbol{P}^k = \boldsymbol{Q}_j\boldsymbol{P}^l$ for some $\boldsymbol{P}^k$ and $\boldsymbol{P}^l$ in $G_{\boldsymbol{a}}$. Since $\boldsymbol{Q}_i\boldsymbol{P}^k\boldsymbol{a} = \boldsymbol{b}_i$ and $\boldsymbol{Q}_j\boldsymbol{P}^l\boldsymbol{a} = \boldsymbol{b}_j$, it follows that $\boldsymbol{b}_i = \boldsymbol{b}_j$ and $i = j$, which contradicts the hypothesis.

By Lemma 2.27, each of the sets $\boldsymbol{Q}_iG_{\boldsymbol{a}}$ has r elements. Hence the disjoint union $\bigcup_{i=0}^{p-1}\boldsymbol{Q}_iG_{\boldsymbol{a}}$ has pr elements. We have already shown that for each $g \in G$, $g \in \boldsymbol{Q}_iG_{\boldsymbol{a}}$ for some i. Therefore $G \subset \bigcup_{i=0}^{p-1}\boldsymbol{Q}_iG_{\boldsymbol{a}}$, which implies $|G| \leq pr$. On the other hand, since $\boldsymbol{Q}_iG_{\boldsymbol{a}} \subset G$ for each i, we have $\bigcup_{i=0}^{p-1}\boldsymbol{Q}_iG_{\boldsymbol{a}} \subset G$. Hence we have $|G| \geq pr$. Thus we conclude that $|G| = pr = |G(\boldsymbol{a})|\,|G_{\boldsymbol{a}}|$. □

Remark 2.29 For each $0 \leq i \leq p-1$, $\boldsymbol{Q}_iG_{\boldsymbol{a}}$ is a left coset of $G_{\boldsymbol{a}}$ in G. Moreover, $\bigcup_{i=0}^{p-1}\boldsymbol{Q}_iG_{\boldsymbol{a}}$ is a decomposition of G into a disjoint union of left cosets, and $|G(\boldsymbol{a})|$ is the index of $G_{\boldsymbol{a}}$ in G. From the proof of Lemma 2.27 we see that $G_{\boldsymbol{b}_i} = \{\boldsymbol{I}, \boldsymbol{Q}_i\boldsymbol{P}\boldsymbol{Q}_i^{-1}, \ldots, \boldsymbol{Q}_i\boldsymbol{P}^{r-1}\boldsymbol{Q}_i^{-1}\}$ for $i = 0, 1, \ldots, p-1$. □

Remark 2.30 Lemma 2.26, Lemma 2.27, and Proposition 2.28 have their counterparts in abstract group theory; see Sect. A.5 in Appendix A. An alternative approach is to appeal to those theorems here. □

We are now ready to derive the required equation by counting the number of elements in Ω in two ways.

In the first method of counting, we let g in the pair $(g, \boldsymbol{x})$ runs over $G \setminus \{\boldsymbol{I}\}$. Let $n = |G|$, the order of G. Since there are $n-1$ non-trivial elements in G, each of which has two poles, there are a total of $2(n-1)$ pairs $(g, \boldsymbol{x})$ in Ω.

In the second method, we take X as a disjoint union of G-orbits (cf. Lemma 2.26) and count, orbit by orbit, the number of pairs $(g, \boldsymbol{x})$ with $\boldsymbol{x}$ running over each orbit. Suppose there are a total number K of G-orbits, say $P_1, \ldots, P_K$, in X. Then we have $X = \bigcup_{i=1}^{K} P_i$ and $P_i \cap P_j = \emptyset$ if $i \neq j$. For each $i = 1, \ldots, K$, we arbitrarily pick a pole $\boldsymbol{x}_i$ in the i-th G-orbit P_i. Let p_i be the number of poles in $P_i = G(\boldsymbol{x}_i)$, the orbit of $\boldsymbol{x}_i$ in X. Let $n_i = |G_{\boldsymbol{x}_i}|$, where $G_{\boldsymbol{x}_i}$ denotes the stabilizer of $\boldsymbol{x}_i$. By Lemma 2.27, the number n_i is independent of the choice of $\boldsymbol{x}_i$ in the orbit P_i. By Lemma 2.28, we have $p_i = |G(\boldsymbol{x}_i)| = |G|/|G_{\boldsymbol{x}_i}| = n/n_i$. For each $\boldsymbol{y} \in P_i$, there are $n_i - 1$ pairs of the form $(g, \boldsymbol{y})$ in Ω. Since there are a total of p_i poles in P_i, there are $p_i(n_i - 1)$ pairs of $(g, \boldsymbol{y}) \in \Omega$ such that $\boldsymbol{y}$ is a pole of g in the i-th G-orbit P_i. Since X is a disjoint union of the G-orbits, the sum $\sum_{i=1}^{K} p_i(n_i - 1)$ must be equal to the total number of pairs $(g, \boldsymbol{x})$ in Ω. Equating the results of the two methods of counting, we have

$$2(n-1) = \sum_{i=1}^{K} p_i(n_i - 1) = \sum_{i=1}^{K} \frac{n}{n_i}(n_i - 1) \tag{2.76}$$

or

$$2\left(1-\frac{1}{n}\right)=\sum_{i=1}^{K}\left(1-\frac{1}{n_i}\right). \tag{2.77}$$

Example 2.31 For illustration, let us consider again the group $G=D_3=\{e,r,r^2,s,sr,sr^2\}$, where $e=\boldsymbol{I}$, $r=\boldsymbol{R}(\boldsymbol{e}_3,2\pi/3)$, $r^2=\boldsymbol{R}(\boldsymbol{e}_3,4\pi/3)$, $s=\boldsymbol{R}(\boldsymbol{e}_1,\pi)$, $sr=\boldsymbol{R}(\boldsymbol{n},\pi)$, and $sr^2=\boldsymbol{R}(\boldsymbol{m},\pi)$; here $\boldsymbol{n}=\boldsymbol{R}(\boldsymbol{e}_3,2\pi/3)\boldsymbol{e}_1$, $\boldsymbol{m}=\boldsymbol{R}(\boldsymbol{e}_3,4\pi/3)\boldsymbol{e}_1$. The set X of poles of G has eight members, namely: $N=(0,0,1)$, $S=(0,0,-1)$, $A=(1,0,0)$ $A'=(-1,0,0)$, $B=(-1/2,\sqrt{3}/2,0)$, $B'=(1/2,-\sqrt{3}/2,0)$, $C=(-1/2,-\sqrt{3}/2,0)$, and $C'=(1/2,\sqrt{3}/2,0)$. There are three G-orbits, namely (i) $P_1:=G(N)=\{N,S\}$, (ii) $P_2:=G(A)=\{A,B,C\}$, and (iii) $P_3=G(A')=\{A',B',C'\}$. The stabilizers of poles in the first orbit are identical, with e,r, and r^2 as its elements. Each of the stabilizers of the poles in the second and the third orbit has two elements. Indeed we have $G_A=G_{A'}=\{e,s\}$, $G_B=G_{B'}=\{e,sr\}$, and $G_C=G_{C'}=\{e,sr^2\}$. Now, consider the number of elements in the set $\Omega=\{(g,\boldsymbol{x}):g\neq e\in G,\boldsymbol{x}\in X,\text{ and }g\boldsymbol{x}=\boldsymbol{x}\}$. If we gather the pairs under the elements in $G=D_3$, we easily see that there are $2\times(6-1)=10$ elements in the set Ω. In this way of counting, we obtain the number 10 through the formula given by the left-hand side of (2.77). Explicitly, the ten pairs in question are (r,N), (r,S), (r^2,N), (r^2,S), (s,A), (s,A'), (sr,B), (sr,B'), (sr^2,C) and (sr^2,C'). For orbit P_1, we have $p_1=2$ and $n_1=n/p_1=3$. Similarly, for orbits P_2 and P_3, we note that $p_2=p_3=3$ and $n_2=n_3=2$. Hence by the right-hand side of (2.76) we obtain $\sum_i p_i(n_i-1)=2\times2+3\times1+3\times1=10$. □

Let us now proceed to determine the possible sets of solutions to (2.77). Setting aside the trivial case where $n=1$, we have $n\geq2$ and thence

$$2>2\left(1-\frac{1}{n}\right)\geq1. \tag{2.78}$$

Also, because $n_i\geq2$, we observe that

$$1>1-\frac{1}{n_i}\geq\frac{1}{2},\quad\text{and}\quad K>\sum_{i=1}^{K}\left(1-\frac{1}{n_i}\right)\geq\frac{K}{2}. \tag{2.79}$$

Thus the left-hand-side of equation (2.77) is in $[1,2)$ and the right-hand side in $[K/2,K)$. These dictate that either $K=2$ or $K=3$.

Case I. $K=2$. Then

$$\frac{2}{n}=\frac{1}{n_1}+\frac{1}{n_2}. \tag{2.80}$$

Since $2\leq n_i\leq n$, we must have $n_1=n_2=n$. As we shall demonstrate below, the conjugacy classes under Case I are those of cyclic groups denoted by C_n in the Schönflies notation.[27]

Case II. $K=3$. Then

$$\frac{2}{n}=\frac{1}{n_1}+\frac{1}{n_2}+\frac{1}{n_3}-1. \tag{2.81}$$

[27] It is customary to denote a conjugacy class of point groups and its members by the same symbol.

Table 2 Conjugacy classes of finite rotation groups

K	n_1	n_2	n_3	n	Conjugacy class
2	n	n	–	n	C_n (cyclic)
3	2	2	m	$2m$	D_m (dihedral)
3	2	3	3	12	T (tetrahedral)
3	2	3	4	24	O (octahedral)
3	2	3	5	60	I (icosahedral)

Without loss of generality, let $n_1 \le n_2 \le n_3$. Then $1/n_1 \ge 1/n_2 \ge 1/n_3$. If $n_1 \ge 3$, then $1/n_1 \le 1/3$ and we conclude from (2.81) that $2/n \le 0$, which is impossible. Therefore we must have $n_1 = 2$.

For $n_1 = 2$, (2.81) becomes

$$\frac{2}{n} = \frac{1}{n_2} + \frac{1}{n_3} - \frac{1}{2}. \tag{2.82}$$

If $n_2 \ge 4$, (2.82) implies that $2/n \le 0$, which is again impossible. Therefore $n_2 \le 3$.

If $n_2 = 2$, then (2.82) reduces to $2/n = 1/n_3$ or $n = 2m$, where $m := n_3$.

If $n_2 = 3$, (2.82) reduces to

$$\frac{2}{n} = \frac{1}{n_3} - \frac{1}{6}, \tag{2.83}$$

which implies $n_3 \le 5$. There are three possibilities: $n_3 = 3, 4$, or 5, for which $n = 12, 24$, or 60, respectively.

The solutions of Diophantine equation (2.77) are displayed in Table 2, which specifies the attributes of possible finite rotation groups G. A finite rotation group that satisfies one set of conditions on K, n_i, and n given in Table 2 is the rotational symmetry group of a certain geometrical object (an n-pyramid, a dihedron,[28] a tetrahedron, a cube, an icosahedron, etc.) [6, 178, 232]. For example, as discussed in Examples 2.1 and 2.31, a rotation group that satisfies the conditions $K = 3$, $n_1 = n_2 = 2$, $n_3 = 3$, and $n = 6$ is the symmetry group of a plane equilateral triangle, but the conditions do not specify the orientation of the plane equilateral triangle with respect to a given Cartesian coordinate system. Thus those conditions do not specify one rotation group but a conjugacy class of subgroups of O(3). Indeed, for any orthonormal unit vectors $\boldsymbol{n}$ and $\boldsymbol{m}$ in $\mathbb{R}^3$, the rotations $\boldsymbol{R}(\boldsymbol{n}, 2\pi/3)$ and $\boldsymbol{R}(\boldsymbol{m}, \pi)$ generate a rotation group in the class D_3. Similarly all rotation groups which satisfy the same set of conditions on K, n_i, and n given in Table 2 constitute a conjugacy class of subgroups of O(3). The conjugacy classes are listed in the Schönflies notation in the table.

Remark 2.32 Table 2 provides a summary of the complete enumeration of finite rotation groups. In the last column, the adjective given for a row describes not only the conjugacy class defined by the parameters K, n_i, and n of that row but also the members of the class in question. Thus a rotation group that belongs to the tetrahedral class T is tetrahedral. Moreover, a generic member of class C_n, D_m, T, ... etc. is often referred to as "the cyclic

[28] In the words of Felix Klein [178, pp. 3–4], "... the *plane regular n-gon* [= n-sided polygon]. In fact, we can denote this latter by considering the portion of the plane limited by the sides of the n-gon to be doubled, as a regular solid—a dihedron, as we will say: only that this solid, contrary to the elementary notion of such, encloses no space."

group C_n", "the dihedral group D_m", "the tetrahedral group T", ...etc. In the same vein Table 1 of Sect. 2.1 is called "multiplication table of group D_3". □

Let us proceed to examine what further information on a finite rotation group G can be inferred from its values of K, n_i, and n. Recall that K denotes the number of G-orbits P_i in X, the set of poles of G; n_i, where $i = 1, 2$, or 3, is the multiplicity of any pole in orbit P_i; $n = |G|$, the number of elements in G. From this information, we obtain $p_i = n/n_i$, the number of poles of multiplicity n_i in orbit P_i. As it may occur that $n_i = n_j$ for $i \neq j$, for $r \geq 2$ the r-tuple poles should be grouped together. Let N_r be the total number of r-tuple poles. Since two diametrically opposite r-tuple poles determine one r-fold axis, we can infer that the number of r-fold axes in G is $N_r/2$. For illustration, consider the following two examples:

1. Let G be a group of class C_n ($n \geq 2$), for which $K = 2$ and $n_1 = n_2 = n$ (see Table 2). Hence G has two orbits, each of which has one n-tuple pole. As there are only two n-tuple poles, they must be diametrically opposite to each other. It follows that G has one n-fold axis.[29]
2. The tetrahedral group T has $K = 3$, $n_1 = 2$, $n_2 = n_3 = 3$, and $n = 12$, which give $p_1 = 6$, $p_2 = p_3 = 4$. There are a total of 6 double poles and 8 triple poles. Hence the tetrahedral group G has three 2-fold and four 3-fold rotational axes.

Note that a finite rotation group G, in general, may have an r-fold axis with two r-tuple poles that lie in two different orbits. This fact is clearly exemplified by the groups C_n. It is also illustrated by the tetrahedral group: each of its four 3-fold axes has one pole in orbit P_2 and one in P_3 (cf. Sect. 2.5.2).

Remark 2.33 The simple and elegant proof presented above to establish the enumeration of finite rotation groups as summarized in Table 2 is commonly attributed (see, e.g., [79, p. 275], [294], [295, p. 33] to Felix Klein [178, Part I, Chapter V, §2]. There Klein (p. 126) sets out to determine "all finite groups of linear substitutions of a variable" (i.e., all finite groups of linear fractional transformations of the Riemann sphere), a problem equivalent to the enumeration of finite rotation groups (cf. [117, pp. 129–136], [320, Sects. 1.1–1.3] for expositions of Klein's proof). While it may not be difficult for the initiated to extract from Klein's proof the simple argument to derive Diophantine equation (2.77) in an entirely elementary way, it won't be an easy feat for those who lack the relevant mathematical preparation to do the same. As for the elementary proof itself, it is difficult to pinpoint its first appearance. The earliest instance that I could trace is the 1908 book by Harold Hilton [154, Chapter VIII, §6–§7], where a proof written in a language that has become archaic[30] but follows essentially the same argument as the one above is presented. Hilton, however, does not cite any reference, perhaps because as he explains in the Preface "[i]n an elementary treatise references would be out of place" (p. iii). By the time when the elementary proof appears in the 1937 book of Zassenhaus [353, Chap. 1, §6] and the 1952 book of Weyl [339, Appendix A], it already assumes essentially the same form and content as that presented above. In the last few decades this elementary proof (or a minor variant of it) has been adopted in most books and texts on the subject; see, e.g., [6, 79, 232, 298]. Finally it

[29]The conclusion is valid for any group in the class C_n. It will save some writing if we start and end with "the cyclic group C_n", which means a generic member of class C_n.

[30]For instance, for what we call poles A, B, C or vectors **OA**, **OB**, **OC**, Hilton [154, p. 111] writes "lines OA, OB, OC, ... We suppose these lines only drawn in one direction from O."

should be pointed out that other elementary proofs of the enumeration are available in the literature; see, e.g., Engel [101, pp. 94–97], Hilton [153, Chapter V], and in particular Coxeter [79, §3.8], where the reader will find a proof which "is essentially that of Bravais [48]" plus an "amplification". □

2.5 The Crystallographic Point Groups

2.5.1 The Crystallographic Restriction

An orthogonal transformation $\boldsymbol{Q}$ is a symmetry operation on lattice L if it renders the crystal lattice invariant, i.e., $\boldsymbol{Q}\mathsf{L} = \mathsf{L}$. By (2.4), for the symmetry operation $\boldsymbol{Q}$, either $\boldsymbol{Q} = \boldsymbol{R}$ or $\boldsymbol{Q} = \boldsymbol{\mathcal{I}R}$ for some rotation $\boldsymbol{R}$. For both instances we call $\boldsymbol{R} = \boldsymbol{Q}$ and $\boldsymbol{R} = \boldsymbol{\mathcal{I}Q}$ the rotation associated with $\boldsymbol{Q}$, respectively. For either case we have $\boldsymbol{R}\mathsf{L} = \boldsymbol{Q}\mathsf{L} = \mathsf{L}$ or $\boldsymbol{R}\mathsf{L} = \boldsymbol{\mathcal{I}Q}\mathsf{L} = \boldsymbol{\mathcal{I}}\mathsf{L} = \mathsf{L}$. In what follows we show that the lattice structure of L imposes a severe restriction on the possible values of rotation angle ω of the rotation $\boldsymbol{R}(\boldsymbol{n}, \omega)$ associated with the symmetry operation $\boldsymbol{Q}$.

Let $\boldsymbol{f}_1 = \boldsymbol{a}$, $\boldsymbol{f}_2 = \boldsymbol{b}$, and $\boldsymbol{f}_3 = \boldsymbol{c}$ be the basis lattice vectors of L. The matrix $[\widetilde{\mathrm{R}}]$ representing $\boldsymbol{R}$ under the basis $\{\boldsymbol{f}_i\}$ has entries (cf. (1.42))

$$\widetilde{\mathrm{R}}_{ij} = \boldsymbol{f}^i \cdot \boldsymbol{R}\boldsymbol{f}_j, \tag{2.84}$$

which are integers because $\boldsymbol{R}(\boldsymbol{n}, \omega)$ renders the lattice L invariant. Let $\boldsymbol{e}_1$, $\boldsymbol{e}_2$, $\boldsymbol{e}_3$ be any chosen right-handed orthonormal triad. The matrix [R] representing $\boldsymbol{R}$ under the basis $\{\boldsymbol{e}_k\}$ has entries

$$\mathrm{R}_{kl} = \boldsymbol{e}^k \cdot \boldsymbol{R}\boldsymbol{e}_l = \boldsymbol{e}_k \cdot \boldsymbol{R}\boldsymbol{e}_l. \tag{2.85}$$

Let [A] be the matrix with entries $\mathrm{A}_{ij} = \boldsymbol{e}^i \cdot \boldsymbol{f}_j = \boldsymbol{e}_i \cdot \boldsymbol{f}_j$, which defines the change of basis from $\{\boldsymbol{e}_k\}$ to $\{\boldsymbol{f}_i\}$. There holds the relation (cf. (1.55))

$$[\widetilde{\mathrm{R}}] = [\mathrm{A}]^{-1}[\mathrm{R}][\mathrm{A}], \tag{2.86}$$

from which follows the equation

$$\mathrm{tr}[\widetilde{\mathrm{R}}] = \mathrm{tr}[\mathrm{R}] = 1 + 2\cos\omega \tag{2.87}$$

or

$$\cos\omega = \frac{\mathrm{tr}[\widetilde{\mathrm{R}}] - 1}{2}. \tag{2.88}$$

Since $\mathrm{tr}[\widetilde{\mathrm{R}}]$ is an integer, within the range $[0, \pi]$ the possible values of ω are:

$$0, \frac{\pi}{3}, \frac{\pi}{2}, \frac{2\pi}{3}, \pi. \tag{2.89}$$

This requirement on ω is called the crystallographic restriction on the rotation $\boldsymbol{R}(\boldsymbol{n}, \omega)$ associated with any orthogonal transformation $\boldsymbol{Q}$ that preserves a crystal lattice.

Recall that a rotation $\boldsymbol{R}(\boldsymbol{n}, \omega) \neq \boldsymbol{I}$ is said to be of order n if there is a positive integer n such that $\boldsymbol{R}^n = \boldsymbol{I}$ and $\boldsymbol{R}^k \neq \boldsymbol{I}$ for all $2 \leq k < n$. Let $\mathcal{K}$ be a crystallographic point group. The crystallographic restriction dictates that any rotation $\boldsymbol{R}$ which satisfies $\boldsymbol{R} \in \mathcal{K}$ or $\boldsymbol{\mathcal{I}R} \in \mathcal{K}$ is of order 2, 3, 4, or 6.

2.5.2 The Proper Crystallographic Point Groups

Subgroups of O(3) are called point groups (see the end of Sect. 2.2). Point groups which are and those which are not subgroups of SO(3) are called proper and improper point groups, respectively. Crystallographic point groups are point groups that satisfy the crystallographic restriction.

Let G be a proper crystallographic point group. The crystallographic restriction requires that the rotational axis of any $\boldsymbol{R} \neq \boldsymbol{I} \in G$ must be a 2-fold, 3-fold, 4-fold, or 6-fold axis. A glance at Table 2 reveals (cf. the paragraph which immediately follows Remark 2.32) that the icosahedral group I has six 5-fold axes, so it violates the crystallographic restriction. Also, the dihedral group D_m has two m-tuple poles, i.e., one m-fold axis. Thus D_m is a crystallographic point group if and only if $m = 2, 3, 4, 6$. From (2.80) we observe that C_n has an n-fold axis; see the paragraph on C_n below for a detailed discussion. It follows that for $n \geq 2$ only those C_n with $n = 2, 3, 4, 6$ are crystallographic. Hence the finite subgroups of SO(3) which satisfy the crystallographic restriction are:

$$C_1, C_2, C_3, C_4, C_6, D_2, D_3, D_4, D_6, T, O,$$

where $C_1 = \{\boldsymbol{I}\}$.

We are now ready to examine the structure of each proper crystallographic point group in turn. We shall largely follow the exposition [192] based on the outline in [353]; cf. also [6].

The Cyclic Groups C_n

Consider the proper crystallographic point group C_n with $n > 1$ elements, which has $K = 2, n_1 = n_2 = n$, and $p_1 = p_2 = 1$. There are two orbits, each of which has only 1 pole. As every non-trivial rotation has two poles, every non-trivial member of C_n has the same axis defined by the two poles of C_n. By Lemma 2.23, there is a rotation $\boldsymbol{P}$ such that $C_n = \{\boldsymbol{I}, \boldsymbol{P}, \ \ldots, \boldsymbol{P}^{n-1}\}$. Moreover, if we choose a coordinate system such that the poles of C_n are the points $(0, 0, 1)$ and $(0, 0, -1)$, then $\boldsymbol{P} = \boldsymbol{R}(\boldsymbol{e}_3, 2\pi/n)$. Since C_n is a crystallographic point group, the crystallographic restriction requires that $n = 2, 3, 4$, or 6.

It is easy to show that C_n ($n \geq 3$) is the rotational symmetry group of an n-pyramid, i.e., a right pyramid with a regular n-sided polygon as base and satisfying the condition $\ell \neq d$, where ℓ is the length of a side of the regular polygon and d the distance between the vertex of the pyramid and a vertex of the base polygon. When $n = 2$, the n-pyramid degenerates to an isosceles triangle and C_n is the rotational symmetry group of the isosceles triangle.

The Dihedral Groups D_m

Consider D_m, a group of $n = 2m \geq 4$ elements, which has $K = 3, n_1 = n_2 = 2, n_3 = m$, and $p_1 = p_2 = m$, $p_3 = 2$. The crystallographic restriction requires that $m = 2, 3, 4$, or 6. Let A and A' be the two poles in the orbit P_3. Let $G_A \subset G$ be the stabilizer of A, and let $\sigma \in G_A$. Then $\sigma A = A$. Since A and A' are the only two poles in the orbit P_3, we have either $\sigma A' = A'$ or $\sigma A' = A$. If $\sigma A' = A$, then $A' = \sigma^{-1} A = A$ because $\sigma^{-1} \in G_A$. Since $A \neq A'$, we conclude that $\sigma A' = A'$, $G_A = G_{A'}$, A and A' are diametrically opposite to each other, and AA' defines the m-fold axis of the rotations in G_A. By Lemma 2.23, $G_A = \{r^0, r^1, \ldots, r^{m-1}\}$, where r is a rotation with the line defined by A and A' as axis and rotation angle equal to $2\pi/m$, and $r^0 := \boldsymbol{I}$.

Let $s \in G$ and $s \notin G_A = G_{A'}$. Since $p_3 = 2$, we have $G = G_A \cup sG_A$, and $sA = A'$, $sA' = A$. It follows that $s^2 A = A$ and $s^2 A' = A'$, which imply that the line AA' is the axis of

rotation of s^2. Let L be the axis of rotation of s and thus also of s^2. Since s^2 has two distinct axes of rotation, we conclude that $s^2 = \boldsymbol{I}$ and L is a 2-fold axis. Note that $s\sigma \notin G_A$ for any $\sigma \in G_A$. Hence by the same argument as that for s, we see that $(s\sigma)^2 = \boldsymbol{I}$, which implies

$$s\sigma = (s\sigma)^{-1} = \sigma^{-1}s. \tag{2.90}$$

For $x, y \in \{0, 1, \ldots, m-1\}$, let the binary operation of addition modulo m be defined as follows:

$$x +_m y := \begin{cases} x + y & \text{if } x + y < m \\ x + y - m & \text{if } x + y \geq m. \end{cases} \tag{2.91}$$

The multiplication table for the group $G = \{r^0, r^1, \ldots, r^{m-1}, sr^0, sr^1, \ldots, sr^{m-1}\}$ can be readily written down with the help of the following formulas:

$$r^k r^l = r^{k+_m l}, \qquad (sr^k)r^l = sr^{k+_m l},$$
$$r^k(sr^l) = sr^{(m-k)+_m l}, \qquad (sr^k)(sr^l) = r^{(m-k)+_m l}.$$

Without loss of generality, let us choose a Cartesian coordinate system such that $A = (0, 0, 1)$ and $A' = (0, 0, -1)$. Since s interchanges A and A', the 2-fold rotation axis L of s lies in the equatorial plane. Let us pick one of the two points at which L meets the equator and call it $\boldsymbol{x}$. For $m \geq 3$, we have

$$\|\boldsymbol{x} - r(\boldsymbol{x})\| = \|r(\boldsymbol{x}) - r^2(\boldsymbol{x})\| = \cdots = \|r^{m-1}(\boldsymbol{x}) - \boldsymbol{x}\|.$$

Hence $\boldsymbol{x}, r(\boldsymbol{x}), \ldots, r^{m-1}(\boldsymbol{x})$ are the vertices of a regular m-sided polygon Π in the equatorial plane. Clearly Π is invariant under each rotation r^k $(0 \leq k \leq m-1)$. Moreover, since

$$sr^k(\boldsymbol{x}) = r^{m-k}s(\boldsymbol{x}) = r^{m-k}(\boldsymbol{x}),$$

the regular polygon Π remains invariant under each rotation sr^k $(0 \leq k \leq m-1)$. Thus D_m is the rotational symmetry group of the m-sided polygon Π.

For $m = 2$, the m-sided regular polygon Π degenerates to the diametric line-segment $[\boldsymbol{x}, r(\boldsymbol{x})]$, which connects the poles $\boldsymbol{x}$ and $r(\boldsymbol{x})$ of s. Let us choose the Cartesian coordinate system such that in addition to $A = (0, 0, 1)$ and $A' = (0, 0, -1)$ we have $\boldsymbol{x} = (1, 0, 0) = \boldsymbol{e}_1$ and $r(\boldsymbol{x}) = (-1, 0, 0)$. Then $r = \boldsymbol{R}(\boldsymbol{e}_3, \pi)$, $s = \boldsymbol{R}(\boldsymbol{e}_1, \pi)$, $sr = \boldsymbol{R}(\boldsymbol{e}_2, \pi)$, and $D_2 = \{\boldsymbol{I}, r, s, sr\}$ is the rotational symmetry group of the diametric line-segment $[\boldsymbol{x}, r(\boldsymbol{x})]$.

The Tetrahedral Group T

The group T, a group of 12 elements, has $K = 3$, $n_1 = 2$, $n_2 = n_3 = 3$, and $p_1 = 6$, $p_2 = p_3 = 4$. Let the poles in the orbit P_3 be labelled by the letters A, B, C, and D. To each rotation $\boldsymbol{R} \in T$ corresponds a permutation of the poles A, B, C, and D, and the correspondence is clearly one-to-one. Let us denote this correspondence by $f : T \to \mathcal{S}_4$, $\boldsymbol{R} \mapsto \sigma$, where $\mathcal{S}_4$ denotes the symmetric group of permutations of the four poles. If $\boldsymbol{R}_i \mapsto \sigma_i$ $(i = 1, 2)$, then $\boldsymbol{R}_2\boldsymbol{R}_1 \mapsto \sigma_2\sigma_1$. Hence f is a homomorphism. However, there does not exist a rotation $\boldsymbol{R} \in T$ which corresponds to a 4-cycle. Indeed suppose, for example, $\boldsymbol{Q} \in T \mapsto \tau := (ABCD) \in \mathcal{S}_4$, which satisfies $\tau A = B$, $\tau B = C$, $\tau C = D$, and $\tau D = A$. The 4-cycle permutation τ, just as all other 4-cycle permutations of $\{A, B, C, D\}$, satisfies $\tau^4 = e$, where e is the identity permutation. Then the rotation $\boldsymbol{Q}$ corresponding to τ, i.e.,

$\boldsymbol{Q} = f^{-1}(\tau)$, satisfies $\boldsymbol{Q}^4 = \boldsymbol{I}$, and its axis of rotation is a 4-fold axis. But there does not exist in T any rotation that has a 4-fold axis, so $\boldsymbol{Q} \notin T$. Also, there is no rotation $\boldsymbol{P} \in G$ which corresponds to a single transposition, e.g., $\eta = (AB)$, which observes $\eta A = B$, $\eta B = A$, $\eta C = C$, $\eta D = D$. For this η, we have $\eta^2 = e$, $\boldsymbol{P}^2 = \boldsymbol{I}$, and $|G_C| = |G_D| = 2$, which contradicts the fact that $|G_C| = |G_D| = 3$. The same argument applies to any rotation in T which purportedly corresponds to a single transposition of $\{A, B, C, D\}$.

After deleting the 4-cycles and single transpositions from the symmetric group $\mathcal{S}_4$ of the set $\{A, B, C, D\}$, we are left with the alternating group $\mathcal{A}_4$ of even permutations, which has 12 elements, namely:

$$\begin{array}{llll} e, & (AB)(CD), & (AC)(BD), & (AD)(BC), \\ (ABC), & (ABD), & (ACD), & (BCD), \\ (ACB), & (ADB) & (ADC), & (BDC). \end{array} \tag{2.92}$$

Since T also has 12 elements, the one-to-one correspondence between T and $\mathcal{A}_4$ must be bijective and the two groups are isomorphic.

From the list (2.92) of group elements in T, it is clear that the lengths of the line segments AB, AC, AD, BC, BD, and CD are equal. Hence the poles A, B. C, and D are the vertices of a regular tetrahedron, and T is its rotational symmetry group. The group has four 3-fold axes and three 2-fold ones. Each 3-fold axis passes through a vertex, the center of the unit sphere $\mathcal{S}^2$, and the center of the opposite face, which is an equilateral triangle; it is also perpendicular to the opposite face. Each 2-fold axis is determined by the mid-points of two opposite edges; i.e., the three 2-fold axes pass through the mid-points of AB and CD, AC and BD, AD and BC, respectively. The orbit P_1 has 6 poles, which are the points where the three 2-fold axes meet the unit sphere S^2. The orbit P_3 have 4 poles, which are the vertices A, B, C, and D of the regular tetrahedron. The orbit P_2 have 4 poles, namely A', B', C', and D', which are the points diametrically opposite to A, B, C, and D, respectively.

The Octahedral Group O

We begin our discussion with a simple lemma.

Lemma 2.34 *Let $\boldsymbol{a}, \boldsymbol{a}'$ and $\boldsymbol{b}, \boldsymbol{b}'$ be two pairs of diametrically opposite poles of the finite rotation group G. Suppose $\boldsymbol{Q}\boldsymbol{a} = \boldsymbol{b}$ for some $\boldsymbol{Q} \in G$. Then $\boldsymbol{Q}\boldsymbol{a}' = \boldsymbol{b}'$.*

Proof Given a pole $\boldsymbol{a} \in \mathcal{S}^2$, its diametrically opposite pole is $\boldsymbol{a}' = -\boldsymbol{a}$. Similarly we have $\boldsymbol{b}' = -\boldsymbol{b}$. Suppose $\boldsymbol{Q}\boldsymbol{a} = \boldsymbol{b}$ for some $\boldsymbol{Q} \in G$. Then $\boldsymbol{Q}\boldsymbol{a}' = \boldsymbol{Q}(-\boldsymbol{a}) = -\boldsymbol{Q}\boldsymbol{a} = -\boldsymbol{b} = \boldsymbol{b}'$. □

The group O, a group of $n = 24$ elements, has $K = 3$, $n_1 = 2$, $n_2 = 3$, $n_3 = 4$, and $p_1 = 12$, $p_2 = 8$, $p_3 = 6$. The orbit P_2 has 8 triple poles in 4 diametrically opposite pairs, which we call $\boldsymbol{b}_i$, $\boldsymbol{b}_i'$ $(i = 1, 2, 3, 4)$. The line segments $L_i := [\boldsymbol{b}_i, \boldsymbol{b}_i']$ are two-sided, i.e., $[\boldsymbol{b}_i, \boldsymbol{b}_i'] = [\boldsymbol{b}_i', \boldsymbol{b}_i]$ for each i. A rotation $\boldsymbol{R} \in O$ leads to a permutation of the aforementioned 8 poles. By Lemma 2.34, each rotation $\boldsymbol{R} \in O$ in fact corresponds to a permutation σ of the line segments L_1, L_2, L_3, and L_4. Let $\mathcal{S}_4$ be the symmetric group of permutations of the line segments L_i $(i = 1, 2, 3, 4)$. Let $f : O \to \mathcal{S}_4$, $\boldsymbol{R} \mapsto \sigma$, where $\sigma = f(\boldsymbol{R})$ is the permutation of the line segments L_i that results from the rotation $\boldsymbol{R} \in O$. It is easy to see that if $\boldsymbol{R}_j \mapsto \sigma_j$ $(j = 1, 2)$, then $\boldsymbol{R}_2\boldsymbol{R}_1 \mapsto \sigma_2\sigma_1$. Hence the mapping f is a homomorphism. Note that if $\boldsymbol{R} \in O \mapsto \sigma \in \mathcal{S}_4$ and $\sigma L_i = L_j$, either $\boldsymbol{R}\boldsymbol{b}_i = \boldsymbol{b}_j$, $\boldsymbol{R}\boldsymbol{b}_i' = \boldsymbol{b}_j'$ or $\boldsymbol{R}\boldsymbol{b}_i = \boldsymbol{b}_j'$, $\boldsymbol{R}\boldsymbol{b}_i' = \boldsymbol{b}_j$ may happen.

We claim that if $\boldsymbol{Q} \in O$ keeps all the line segments L_i invariant (i.e., $\boldsymbol{Q} \mapsto e$, the identity in $\mathcal{S}_4$), then $\boldsymbol{Q} = \boldsymbol{I}$. We prove the preceding claim by contradiction. Indeed, suppose $\boldsymbol{Q} \mapsto e$

and $\boldsymbol{Q} \neq \boldsymbol{I}$. Since $\boldsymbol{Q} \neq \boldsymbol{I}$ has only two poles, it can at most keep the poles of one line segment invariant. Hence, after renaming the 8 triple poles if necessary there are only two possibilities:

(i) $\boldsymbol{Q}\boldsymbol{b}_i = \boldsymbol{b}_i'$, $\boldsymbol{Q}\boldsymbol{b}_i' = \boldsymbol{b}_i$ for $i = 1, 2, 3$; $\boldsymbol{Q}\boldsymbol{b}_4 = \boldsymbol{b}_4$, $\boldsymbol{Q}\boldsymbol{b}_4' = \boldsymbol{b}_4'$.
(ii) $\boldsymbol{Q}\boldsymbol{b}_i = \boldsymbol{b}_i'$, $\boldsymbol{Q}\boldsymbol{b}_i' = \boldsymbol{b}_i$ for $i = 1, 2, 3, 4$.

Under Case (i), we have $\boldsymbol{Q}^2 = \boldsymbol{I}$. Hence $\boldsymbol{b}_4$ and $\boldsymbol{b}_4'$ are double poles, contradicting the fact that they are triple poles.

Under Case (ii), $\boldsymbol{Q}$ exchanges each pair of diametrically opposite poles. Let $\boldsymbol{P} \neq \boldsymbol{I}$ be an arbitrary non-trivial rotation in O. For each $i = 1, 2, 3, 4$, $\boldsymbol{P}\boldsymbol{b}_i$ and $\boldsymbol{P}\boldsymbol{b}_i'$ are a pair of diametrically opposite poles of the line segments L_i, and we have

$$(\boldsymbol{P}\,\boldsymbol{Q}\,\boldsymbol{P}^{-1})\boldsymbol{P}\boldsymbol{b}_i = \boldsymbol{P}\boldsymbol{b}_i', \qquad (\boldsymbol{P}\,\boldsymbol{Q}\,\boldsymbol{P}^{-1})\boldsymbol{P}\boldsymbol{b}_i' = \boldsymbol{P}\boldsymbol{b}_i. \tag{2.93}$$

Thus, like $\boldsymbol{Q}$, $\boldsymbol{P}\,\boldsymbol{Q}\,\boldsymbol{P}^{-1}$ also exchanges each pair of diametrically opposite poles of the line segments L_i. Then $\boldsymbol{Q}\,\boldsymbol{P}\,\boldsymbol{Q}\,\boldsymbol{P}^{-1}$ keeps all eight poles unchanged, which implies

$$\boldsymbol{Q}\,\boldsymbol{P}\,\boldsymbol{Q}\,\boldsymbol{P}^{-1} = \boldsymbol{I} \qquad \text{or} \qquad \boldsymbol{Q}\,\boldsymbol{P}\,\boldsymbol{Q} = \boldsymbol{P}. \tag{2.94}$$

Now pick a $\boldsymbol{P} \neq \boldsymbol{I} \in O$ such that $\boldsymbol{b}_1$ and $\boldsymbol{b}_1'$ are its triple poles. Then we have

$$\boldsymbol{Q}\boldsymbol{P}\boldsymbol{b}_1 = \boldsymbol{b}_1', \qquad \boldsymbol{Q}\boldsymbol{P}\boldsymbol{b}_1' = \boldsymbol{b}_1, \tag{2.95}$$

and

$$(\boldsymbol{Q}\boldsymbol{P})^2\boldsymbol{b}_1 = \boldsymbol{b}_1, \qquad (\boldsymbol{Q}\boldsymbol{P})^2\boldsymbol{b}_1' = \boldsymbol{b}_1'. \tag{2.96}$$

Equation (2.96) dictates that either $(\boldsymbol{Q}\boldsymbol{P})^2 = \boldsymbol{I}$ or $(\boldsymbol{Q}\boldsymbol{P})^2$ has the line containing L_1 as its axis of rotation. The latter contradicts (2.95) because $\boldsymbol{Q}\boldsymbol{P}$ has the same axis of rotation as $(\boldsymbol{Q}\boldsymbol{P})^2$. The former can be recast as $\boldsymbol{Q}\,\boldsymbol{P}\,\boldsymbol{Q}\,\boldsymbol{P} = \boldsymbol{I}$, which leads to the equation

$$\boldsymbol{Q}\,\boldsymbol{P}\,\boldsymbol{Q} = \boldsymbol{P}^{-1}. \tag{2.97}$$

Combining $(2.94)_2$ and (2.97), we conclude that $\boldsymbol{P}^2 = \boldsymbol{I}$ and that $\boldsymbol{b}_1, \boldsymbol{b}_1'$ are double poles, contradicting the fact that they are triple poles. Therefore, if $\boldsymbol{Q} \in O \mapsto e \in \mathcal{S}_4$, then $\boldsymbol{Q} = \boldsymbol{I}$.

Suppose under the homomorphism $f : O \to \mathcal{S}_4$, $\boldsymbol{R} \mapsto \sigma$, we have $f(\boldsymbol{R}_1) = f(\boldsymbol{R}_2) = \sigma$. Then $f(\boldsymbol{R}_2^{-1}) = \sigma^{-1}$. It follows that

$$f(\boldsymbol{R}_2^{-1}\boldsymbol{R}_1) = f(\boldsymbol{R}_2^{-1})f(\boldsymbol{R}_1) = \sigma^{-1}\sigma = e.$$

Hence $\boldsymbol{R}_2^{-1}\boldsymbol{R}_1 = \boldsymbol{I}$ or $\boldsymbol{R}_1 = \boldsymbol{R}_2$, and the homomorphism f is one-to-one. Since both O and $\mathcal{S}_4$ have 24 elements, the map $f : O \to \mathcal{S}_4$ is bijective and is an isomorphism.

Since the alternating group $\mathcal{A}_4$ is a subgroup of the symmetric group $\mathcal{S}_4$, let us start with the regular tetrahedron discussed in the paragraphs under the tetrahedral group. We rename the vertices A, B, C, and D of the regular tetrahedron by $\boldsymbol{b}_1$, $\boldsymbol{b}_2$, $\boldsymbol{b}_3$, and $\boldsymbol{b}_4$, respectively. The diametrically opposite points A', B', C', and D' are renamed as $\boldsymbol{b}_i'$ $(i = 1, 2, 3, 4)$ accordingly. For each $i = 1, 2, 3, 4$, join $\boldsymbol{b}_i'$ to $\boldsymbol{b}_j$ for all $j \neq i$ by straight line segments. The 8 poles $\boldsymbol{b}_i$, $\boldsymbol{b}_i'$ $(i = 1, 2, 3, 4)$ are the vertices of the cube that results. The line segments L_1, L_2, L_3, and L_4 are diagonals and O is the group of rotational symmetry of this cube about its center. The group O has three 4-fold axes, four 3-fold axes, and six two-fold axes. Each 4-fold axis passes through the centers of two opposite square faces. The 3-fold axes are the four

diagonals of the cube. Each 2-fold axis passes through the mid-points of two non-coplanar parallel edges that lie in two opposite faces. For example, one 2-fold axis passes through the mid-points of $[\boldsymbol{b}_1, \boldsymbol{b}_2']$ and $[\boldsymbol{b}_1', \boldsymbol{b}_2]$. The 12 poles in orbit P_1 are those of the six 2-fold axes. The 8 poles in orbit P_2 are the vertices of the cube. The 6 poles in orbit P_3 are those of the three 4-fold axes.

The centers of the six faces of the cube are the vertices of a regular octahedron. Any rotation which leaves the cube invariant also keeps the regular octahedron invariant. Hence O is also the rotational symmetry group of the regular octahedron, which explains the rationale behind the name "octahedral group" for O.

2.5.3 The Improper Crystallographic Point Groups

We now turn to obtain a complete enumeration of the conjugacy classes of improper crystallographic point groups. To this end, one way to proceed is to start from the following observation: "The rotations of G [i.e., any improper point group] form a normal subgroup H of index 2 ..., and G is completely given when we know H and a single rotatory-inversion of G." The preceding citation [154, p. 114] is taken from a 1908 "elementary treatise" (p. iii) on group theory by Harold Hilton. Hence the method in question, which is entirely elementary, has been around for a long time, and it has been widely adopted (see, e.g., [78, 229, 232, 277, 339]). The method is based on the following theorem, which provides a straightforward procedure to derive all the improper crystallographic point groups.

Recall that $\boldsymbol{\mathcal{I}} = -\boldsymbol{I}$, where $\boldsymbol{I}$ is the second-order identity tensor, and each $\boldsymbol{Q} \in \mathrm{O}(3)$ is either a rotation with $\det \boldsymbol{Q} = 1$ or a roto-inversion with $\det \boldsymbol{Q} = -1$.

Theorem 2.35 *Let G be a finite point group. Then $H := G \cap SO(3)$ is a normal subgroup of G, and there are three possibilities*:

- *Case* 1: $H = G$, *i.e.*, *G is a proper point group.*

If $H \neq G$, then $H \subset G$ is a normal subgroup of index 2 *in G. Moreover, we have*

- *Case* 2: $H \neq G$ *and* $\boldsymbol{\mathcal{I}} \in G$. *Then* $G = H \cup \boldsymbol{\mathcal{I}} H$.
- *Case* 3: $H \neq G$ *and* $\boldsymbol{\mathcal{I}} \notin G$. *Let* $H^+ = \{\boldsymbol{\mathcal{I}}\boldsymbol{Q} : \boldsymbol{Q} \in G \setminus H\}$. *Then* $G^+ = H \cup H^+$ *is a proper point group isomorphic to* G.

Proof Let Z be the group that consists of the integers 1 and -1 under multiplication. Let $h : G \to Z$ be the function defined by $h(\boldsymbol{Q}) = \det \boldsymbol{Q}$. Clearly h is a homomorphism, and $H := G \cap \mathrm{SO}(3) = \mathrm{Ker}\, h$. Hence H is a normal subgroup of G, and the quotient group G/H is isomorphic to $h(G)$. Note that either $h(G) = \{1\}$ or $h(G) = Z$, and we distinguish three possibilities.

Case 1. $h(G) = \{1\}$. Then $H = G$ and G is a proper point group.

Both the other two possibilities have $h(G) = Z$ and $|G/H| = |h(G)| = |Z| = 2$, which dictates that H is a normal subgroup of index 2 in G. See Proposition A.13 in Appendix A.

Case 2. $h(G) = Z$ and $\boldsymbol{\mathcal{I}} \in G \setminus H$. Then $G = H \cup \boldsymbol{\mathcal{I}} H$.

Case 3. $h(G) = Z$ and $\boldsymbol{\mathcal{I}} \notin G$. For each $\boldsymbol{Q} \in G \setminus H$, $\det \boldsymbol{Q} = -1$. Hence $\boldsymbol{\mathcal{I}}\boldsymbol{Q} \in \mathrm{SO}(3)$ and $G^+ = H \cup H^+ \subset \mathrm{SO}(3)$. In fact, G^+ is a subgroup of SO(3), as we shall now show. To this end, let

$$\eta(\boldsymbol{Q}) = \frac{1}{2}(1 - \det \boldsymbol{Q}) = \begin{cases} 0 & \text{for } \boldsymbol{Q} \in H \\ 1 & \text{for } \boldsymbol{Q} \in G \setminus H. \end{cases}$$

It is easily verified that

$$\eta(\boldsymbol{Q}_1\boldsymbol{Q}_2) = \eta(\boldsymbol{Q}_1) + \eta(\boldsymbol{Q}_2) \qquad \text{for all } \boldsymbol{Q}_1, \boldsymbol{Q}_2 \in G.$$

Let $\sigma : G \to G^+$ be defined by

$$\sigma(\boldsymbol{Q}) = \boldsymbol{\mathcal{I}}^{\eta(\boldsymbol{Q})}\boldsymbol{Q}.$$

It is clear that σ is bijective. Moreover for any $\boldsymbol{Q}_1, \boldsymbol{Q}_2 \in G$, we have

$$\begin{aligned}\sigma(\boldsymbol{Q}_1)\sigma(\boldsymbol{Q}_2) &= \boldsymbol{\mathcal{I}}^{\eta(\boldsymbol{Q}_1)}\boldsymbol{Q}_1\boldsymbol{\mathcal{I}}^{\eta(\boldsymbol{Q}_2)}\boldsymbol{Q}_2 \\ &= \boldsymbol{\mathcal{I}}^{\eta(\boldsymbol{Q}_1)+\eta(\boldsymbol{Q}_2)}\boldsymbol{Q}_1\boldsymbol{Q}_2 = \boldsymbol{\mathcal{I}}^{\eta(\boldsymbol{Q}_1\boldsymbol{Q}_2)}\boldsymbol{Q}_1\boldsymbol{Q}_2 \\ &= \sigma(\boldsymbol{Q}_1\boldsymbol{Q}_2).\end{aligned}$$

Hence G^+ is a proper point group isomorphic to G. □

Let us examine Case 3 in more detail. Let $H = \{\boldsymbol{R}_1, \ldots, \boldsymbol{R}_n\}$, where $\boldsymbol{R}_i \in \mathrm{SO}(3)$ for each i. Since $H = G \cap \mathrm{SO}(3)$ is a subgroup of index 2 in G, G is the union of H and a set of n roto-inversions, i.e.,

$$G = \{\boldsymbol{R}_1, \ldots, \boldsymbol{R}_n, \boldsymbol{\mathcal{I}}\boldsymbol{P}_1, \ldots, \boldsymbol{\mathcal{I}}\boldsymbol{P}_n\}, \qquad \text{where } \boldsymbol{P}_i \in \mathrm{SO}(3) \text{ for each } i.$$

We claim that $\boldsymbol{P}_i \notin H$ for all i. Indeed, if $\boldsymbol{P}_i \in H$, then $\boldsymbol{P}_i = \boldsymbol{R}_j$ for some j. Then $\boldsymbol{\mathcal{I}}\boldsymbol{R}_j = \boldsymbol{\mathcal{I}}\boldsymbol{P}_i \in G$, which implies $(\boldsymbol{\mathcal{I}}\boldsymbol{R}_j)\boldsymbol{R}_j^{-1} = \boldsymbol{\mathcal{I}} \in G$, which contradicts the hypothesis that $\boldsymbol{\mathcal{I}} \notin G$. Note that by definition $H^+ = \{\boldsymbol{P}_1, \ldots, \boldsymbol{P}_n\}$ and

$$G^+ = \{\boldsymbol{R}_1, \ldots, \boldsymbol{R}_n, \boldsymbol{P}_1, \ldots, \boldsymbol{P}_n\}$$

is a proper point group. Since H is also a normal subgroup of index 2 in G^+, we have

$$G^+ = H \cup \boldsymbol{P}H, \qquad \text{and} \qquad G = H \cup \boldsymbol{\mathcal{I}}\boldsymbol{P}H, \tag{2.98}$$

where $\boldsymbol{P}$ is an arbitrarily chosen element of H^+. To find all groups of Type III, we can examine each proper crystallographic point group to see if it can be decomposed as G^+ in (2.98), where H is a subgroup of index 2. Note that a subgroup of index 2 in a group is a normal subgroup of that group (see, e.g., [6, p. 82, Theorem 15.4]).

2.6 Geometric Crystal Classes and Laue Classes

2.6.1 The 32 Crystallographic Point-Group Types

Crystallographic point groups that pertain to Cases 1, 2, and 3 in Theorem 2.35 are said to be of Type I, Type II, and Type III, respectively. Every crystallographic point group belongs to one of these three types.

Those of Type I are proper. We have already determined all the proper crystallographic point groups in Sect. 2.5.2: there are 11 conjugacy classes of them.

Those of Type II are improper. They are of the form $G = H \cup \boldsymbol{\mathcal{I}}H$, where H is of Type I. Hence there are also 11 conjugacy classes of Type II crystallographic point groups.

By (2.98), each group of Type III, which is improper, has a subgroup H which is a normal subgroup of index 2 in some group G^+ of Type I. Following the discussion at the

Table 3 Representatives of the 32 crystallographic point-group types

Type I	Type II	Type III
C_1	$C_i = C_1 \cup \boldsymbol{\mathcal{I}} C_1$	
$C_2 = C_1 \cup \boldsymbol{R}(\boldsymbol{e}_3, \pi) C_1$	$C_{2h} = C_2 \cup \boldsymbol{\mathcal{I}} C_2$	$C_s = C_1 \cup \boldsymbol{\mathcal{I}} \boldsymbol{R}(\boldsymbol{e}_3, \pi) C_1$
C_3	$C_{3i} = C_3 \cup \boldsymbol{\mathcal{I}} C_3$	
$C_4 = C_2 \cup \boldsymbol{R}(\boldsymbol{e}_3, \frac{\pi}{2}) C_2$	$C_{4h} = C_4 \cup \boldsymbol{\mathcal{I}} C_4$	$S_4 = C_2 \cup \boldsymbol{\mathcal{I}} \boldsymbol{R}(\boldsymbol{e}_3, \frac{\pi}{2}) C_2$
$C_6 = C_3 \cup \boldsymbol{R}(\boldsymbol{e}_3, \pi) C_3$	$C_{6h} = C_6 \cup \boldsymbol{\mathcal{I}} C_6$	$C_{3h} = C_3 \cup \boldsymbol{\mathcal{I}} \boldsymbol{R}(\boldsymbol{e}_3, \pi) C_3$
$D_2 = C_2 \cup \boldsymbol{R}(\boldsymbol{e}_1, \pi) C_2$	$D_{2h} = D_2 \cup \boldsymbol{\mathcal{I}} D_2$	$C_{2v} = C_2 \cup \boldsymbol{\mathcal{I}} \boldsymbol{R}(\boldsymbol{e}_1, \pi) C_2$
$D_3 = C_3 \cup \boldsymbol{R}(\boldsymbol{e}_1, \pi) C_3$	$D_{3d} = D_3 \cup \boldsymbol{\mathcal{I}} D_3$	$C_{3v} = C_3 \cup \boldsymbol{\mathcal{I}} \boldsymbol{R}(\boldsymbol{e}_1, \pi) C_3$
$D_4 = C_4 \cup \boldsymbol{R}(\boldsymbol{e}_1, \pi) C_4$	$D_{4h} = D_4 \cup \boldsymbol{\mathcal{I}} D_4$	$C_{4v} = C_4 \cup \boldsymbol{\mathcal{I}} \boldsymbol{R}(\boldsymbol{e}_1, \pi) C_4$
$D_4 = D_2 \cup \boldsymbol{R}(\boldsymbol{e}_3, \frac{\pi}{2}) D_2$		$D_{2d} = D_2 \cup \boldsymbol{\mathcal{I}} \boldsymbol{R}(\boldsymbol{e}_3, \frac{\pi}{2}) D_2$
$D_6 = D_3 \cup \boldsymbol{R}(\boldsymbol{e}_3, \pi) D_3$	$D_{6h} = D_6 \cup \boldsymbol{\mathcal{I}} D_6$	$D_{3h} = D_3 \cup \boldsymbol{\mathcal{I}} \boldsymbol{R}(\boldsymbol{e}_3, \pi) D_3$
$D_6 = C_6 \cup \boldsymbol{R}(\boldsymbol{e}_1, \pi) C_6$		$C_{6v} = C_6 \cup \boldsymbol{\mathcal{I}} \boldsymbol{R}(\boldsymbol{e}_1, \pi) C_6$
T	$T_h = T \cup \boldsymbol{\mathcal{I}} T$	
$O = T \cup \boldsymbol{R}(\boldsymbol{e}_3, \frac{\pi}{2}) T$	$O_h = O \cup \boldsymbol{\mathcal{I}} O$	$T_d = T \cup \boldsymbol{\mathcal{I}} \boldsymbol{R}(\boldsymbol{e}_3, \frac{\pi}{2}) T$

All the matrix groups in this table refer to the same Cartesian coordinate system: $C_1 = \{\boldsymbol{I}\}$; C_n, where $n = 2, 3, 4, 6$, is the cyclic group generated by $\boldsymbol{R}(\boldsymbol{e}_3, 2\pi/n)$; T is the tetrahedral group generated by $\boldsymbol{R}(\boldsymbol{e}_3, \pi)$ and $\boldsymbol{R}(\boldsymbol{m}, 2\pi/3)$, where $\boldsymbol{m} = (\boldsymbol{e}_1 + \boldsymbol{e}_2 + \boldsymbol{e}_3)/\sqrt{3}$. With C_n and T specified, the other representative groups in the table are well defined by the formulas given in the table. See Remark 2.36 for further comments

end of Sect. 2.5.3, we determine the groups of Type III from those of Type I by inspection. It turns out that out of the 11 groups of Type I, C_1, C_3, and T do not have a normal subgroup of index 2 while D_4 and D_6 have two such decompositions and each of the rest has one. Hence there are $11 - 3 + 2 = 10$ conjugacy classes of Type III crystallographic point groups.

Thus there are 32 types of crystallographic point groups in total. In Table 3 a representative of each point-group type is given.

Remark 2.36 The representatives of point-group types in Table 3 are selected to facilitate the discussion of Bravais lattice types in Sect. 2.8. Because of our definition of Euler angles, later when we discuss crystallite and sample symmetries of orientation distribution functions with Euler angles as parameters, it will be more convenient to replace each representative group with explicit appearance of $\boldsymbol{R}(\boldsymbol{e}_1, \pi)$ in the table by its peer that has $\boldsymbol{R}(\boldsymbol{e}_2, \pi)$ serve the same role instead. Note also that in (2.98) $\boldsymbol{P}$ is an arbitrary element in H^+. When H^+ has more than one element, i.e., when $H \neq C_1$, the choice of $\boldsymbol{P}$ is not unique. □

Definition 2.37 Two ideal crystals (as characterized by their space groups) are said to belong to the same geometric crystal class if their point groups are of the same type. □

Since there are 32 point-group types, there are 32 geometric crystal classes, each of which is denoted by the same symbol as the corresponding point-group type.

All 32 (geometric)[31] crystal classes are exemplified in nature. According to Newnham [248], a survey of 127,000 inorganic and 156,000 organic compounds shows that about 82% among inorganic and about 75% among organic crystals are centrosymmetric, i.e., of Type II. Higher symmetry crystals are more abundant among metals, oxides and halides.

[31] We shall often suppress the adjective "geometric" in "geometric crystal class".

Table 4 The 11 Laue classes

1.	$C_1, \underline{C_i}$	7.	$D_3, C_{3v}, \underline{D_{3d}}$
2.	$C_2, C_s, \underline{C_{2h}}$	8.	$D_4, C_{4v}, D_{2d}, \underline{D_{4h}}$
3.	$C_3, \underline{C_{3i}}$	9.	$D_6, C_{6v}, D_{3h}, \underline{D_{6h}}$
4.	$C_4, S_4, \underline{C_{4h}}$	10.	$T, \underline{T_h}$
5.	$C_6, C_{3h}, \underline{C_{6h}}$	11.	$O, T_d, \underline{O_h}$
6.	$D_2, C_{2v}, \underline{D_{2h}}$		

Most metals have face centered-cubic (fcc), body-centered cubic (bcc), or hexagonal close-packed (hcp) structure, which are centrosymmetric and have O_h or D_{6h} as their point group. We shall study these crystal structures in Sect. 2.10.

2.6.2 The 11 Laue Classes

In X-ray crystallography, when Friedel's rule applies, the diffraction pattern from a crystal with space group $\mathcal{G}$ is the same as that which results if a center of inversion is added to the generators of $\mathcal{G}$.[32] Thus under Friedel's rule X-ray diffraction effects are inherently centrosymmetric. They belong to the class of tests which, in the words of Buerger [54], "inherently involve certain symmetry themselves and this prevents one from judging whether the symmetry resulting from such a test derives from the symmetry of the crystal or from the test."

If we add the inversion $\boldsymbol{\mathcal{I}}$ as a generator to each of the 21 non-centrosymmetric Type I or Type III point groups, then a Type II point group will result in each instance. This leads to another classification of crystallographic point groups, in which the 32 members are divided into 11 Laue classes. Each Laue class is named after the Type II group in that class. Each non-centrosymmetric member in a Laue class is either a Type I or a Type III group which becomes the Type II namesake of that class after the inversion $\boldsymbol{\mathcal{I}}$ is added as a generator to the group. See Table 4, where the members of each of the 11 Laue classes are listed. For each Laue class, the name of the class (i.e., the Type II point group in the class) is underlined.

Except for situations where Friedel's rule breaks down, X-ray diffraction effects can only reveal the Laue class to which the crystal belongs.

As we shall see in Chap. 9, Friedel's rule, which applies to the diffraction intensity measurements in the routine preparations of X-ray pole-figures, leads to a major problem in measurements of texture by inversion of X-ray pole-figures.

2.7 Holohedries

Let $\mathcal{G}$ be the space group (i.e., the complete symmetry group with respect to rigid transplacements) of an ideal crystal $(\mathsf{C}, \boldsymbol{\kappa}_0)$, $\mathcal{L}$ the lattice group of $\mathcal{G}$, $\mathcal{K}$ the crystallographic point group of $\mathcal{G}$, and $\mathsf{L} := \mathcal{L}(\mathbf{0})$ the lattice of the ideal crystal.[33] Let

$$\mathcal{H}_{\mathsf{L}} = \{\boldsymbol{Q} \in \mathrm{O}(3) : \boldsymbol{Q}\mathsf{L} = \mathsf{L}\}, \tag{2.99}$$

[32] See Sect. D.6 for more information on Friedel's rule and the assertion here.

[33] We assume that a Cartesian coordinate system has been chosen, under which each $\boldsymbol{Q} \in \mathcal{K}$ maps $\mathbb{R}^3$ onto $\mathbb{R}^3$. The $\mathcal{L}$-orbit of any $\boldsymbol{s} \in \boldsymbol{\kappa}_0(\mathsf{C})$ is a lattice of the ideal crystal $(\mathsf{C}, \boldsymbol{\kappa}_0)$. We restrict our choice of coordinate system such that the origin $\boldsymbol{O}$ is located at a lattice point $\boldsymbol{x}$, which is assigned the coordinates $(0, 0, 0) := \mathbf{0}$, and we take $\mathsf{L} := \mathcal{L}(\mathbf{0})$ as the lattice of the ideal crystal. See Sect. 2.3.1.

be the point group of the lattice L, which is the largest crystallographic point group that leaves L invariant. In Proposition 2.16 we prove that $\boldsymbol{Q}\mathsf{L} = \mathsf{L}$ for each $\boldsymbol{Q} \in \mathcal{K}$. Hence $\mathcal{K} \subset \mathcal{H}_{\mathsf{L}}$. On the other hand, since the crystallographic point group $\mathcal{K}$ of an ideal crystal is defined through the space group $\mathcal{G}$ that describes the symmetry of the crystal structure (or crystal pattern) and not that of the lattice L, $\mathcal{K}$ need not be equal to $\mathcal{H}_{\mathsf{L}}$, i.e., it need not contain all the $\boldsymbol{Q} \in \mathrm{O}(3)$ that preserves the lattice.[34]

Definition 2.38 The point group $\mathcal{K}$ of an ideal crystal with lattice L is said to be holohedral if it is the same as the point group of the lattice, $\mathcal{K} = \mathcal{H}_{\mathsf{L}}$.

A geometric crystal class is called a holohedry if its members (i.e., ideal crystals as characterized by their space groups) have point groups that are holohedral. A crystal class is merohedral if its members have point groups $\mathcal{K}$ and lattice point groups $\mathcal{H}_{\mathsf{L}}$ such that $\mathcal{K} \subsetneq \mathcal{H}_{\mathsf{L}}$. □

We begin with a simple lemma and a theorem, which together will cut down the number of holohedries to seven.

Lemma 2.39 *The inversion $\boldsymbol{\mathcal{I}}$ belongs to the lattice point group $\mathcal{H}_{\mathsf{L}}$ of any lattice L.*

Proof Let $\mathsf{L} = \mathcal{L}(\mathbf{0})$ be a lattice and $\{\boldsymbol{b}_i : i = 1, 2, 3\}$ be a set of basic lattice vectors of L. Then $\mathsf{L} = \{\boldsymbol{s} \in \mathbb{R}^3 : \boldsymbol{s} = s_1\boldsymbol{b}_1 + s_2\boldsymbol{b}_2 + s_3\boldsymbol{b}_3,\ \text{where } s_1, s_2, s_3 \in \mathbb{Z}\}$. Let $\mathcal{K}_{\mathsf{L}}$ be its lattice point group. For $\boldsymbol{s} \in \mathsf{L}$, we have $\boldsymbol{\mathcal{I}}\boldsymbol{s} = (-s_1)\boldsymbol{b}_1 + (-s_2)\boldsymbol{b}_2 + (-s_3)\boldsymbol{b}_3 \in \mathsf{L}$. Hence $\boldsymbol{\mathcal{I}} \in \mathcal{H}_{\mathsf{L}}$. □

Lemma 2.40 *Let L be a lattice, and let $\mathcal{K}$ be a crystallographic point group such that $\boldsymbol{Q}\mathsf{L} = \mathsf{L}$ for each $\boldsymbol{Q} \in \mathcal{K}$. If $\mathcal{K}$ has an axis ℓ of order $k = 2, 3, 4$ or 6, then L has a lattice vector normal to ℓ and a lattice vector parallel to ℓ. Moreover, the plane that is normal to ℓ and contains $\mathbf{0}$ is a lattice plane.*

Proof Let $\boldsymbol{n}$ be a unit vector parallel to ℓ, and Let $\boldsymbol{s} \neq \mathbf{0}$ be a lattice vector which is neither parallel nor perpendicular to ℓ. Then $\boldsymbol{R}(\boldsymbol{n}, 2\pi/k) \in \mathcal{K}$, $\boldsymbol{R}\boldsymbol{s} \in \mathsf{L}$, and $\boldsymbol{s} - \boldsymbol{R}\boldsymbol{s} \in \mathsf{L}$. Since

$$\boldsymbol{n} \cdot (\boldsymbol{s} - \boldsymbol{R}\boldsymbol{s}) = \boldsymbol{n} \cdot \boldsymbol{s} - \boldsymbol{n} \cdot \boldsymbol{R}\boldsymbol{s} = \boldsymbol{n} \cdot \boldsymbol{s} - \boldsymbol{R}(\boldsymbol{n}, -2\pi/k)\boldsymbol{n} \cdot \boldsymbol{s} = \mathbf{0},$$

$\boldsymbol{s} - \boldsymbol{R}\boldsymbol{s}$ is a non-zero lattice vector perpendicular to ℓ.

Let $\boldsymbol{P} := \boldsymbol{I} + \boldsymbol{R} + \cdots + \boldsymbol{R}^{k-1}$. Then $\boldsymbol{R}\boldsymbol{P} = \boldsymbol{P}$, and $\boldsymbol{R}(\boldsymbol{P}\boldsymbol{s}) = \boldsymbol{P}\boldsymbol{s}$. Hence $\boldsymbol{P}\boldsymbol{s}$ is a lattice vector parallel to ℓ. Moreover, let $\boldsymbol{s} = \boldsymbol{s}^{\parallel} + \boldsymbol{s}^{\perp}$, where $\boldsymbol{s}^{\parallel}$ and $\boldsymbol{s}^{\perp}$ stand for the component of $\boldsymbol{s}$ parallel and perpendicular to ℓ, respectively. Then $\boldsymbol{P}\boldsymbol{s} = k\boldsymbol{s}^{\parallel} \neq \mathbf{0}$.

Let $\boldsymbol{u}$ be a lattice vector parallel to ℓ, and let $\boldsymbol{s}$ and $\boldsymbol{t}$ be lattice vectors such that $\boldsymbol{s}, \boldsymbol{t}$, and $\boldsymbol{u}$ are linearly independent. Then $\boldsymbol{s} - \boldsymbol{R}\boldsymbol{s}$ and $\boldsymbol{t} - \boldsymbol{R}\boldsymbol{t}$ are two linearly independent lattice vectors that lie in the plane that is normal to $\boldsymbol{u}$ and contains $\mathbf{0}$. □

Lemma 2.39 dictates that only crystal classes defined by point groups of Type II could be holohedries. That leaves only eleven possibilities for holohedries. We proceed to show that four of the eleven crystal classes defined by Type II groups, namely C_{3i}, C_{4h}, C_{6h}, and T_h cannot be holohedries. Before we prove this fact, we go over some preliminaries.

[34] See [6, pp. 146–147] for a simple example where $\mathcal{K} \subsetneq \mathcal{H}_{\mathsf{L}}$ in the context of two-dimensional wallpaper groups. On the other hand, clearly $\mathcal{K} = \mathcal{H}_{\mathsf{L}}$ for an ideal crystal where identical atoms occupy one-to-one the nodes of the lattice.

For $k = 2, 3, 4$ or 6, let ℓ be a k-fold rotational axis of the lattice point group $\mathcal{H}_\mathsf{L}$ of lattice L, and let $\boldsymbol{n}$ be a unit vector parallel to ℓ. Then $\boldsymbol{R}(\boldsymbol{n}, 2\pi/k) \in \mathcal{H}_\mathsf{L}$. The following operators, which are special instances of $\boldsymbol{Z}^\perp(\boldsymbol{n}, \omega)$ and $\boldsymbol{Z}^\parallel(\boldsymbol{n}, \omega)$ in (1.118) and (1.120), will play a crucial role in our discussions of holohedries and Bravais lattice types. Let

$$\boldsymbol{Z}_k^\perp := \boldsymbol{Z}^\perp(\boldsymbol{n}, 2\pi/k) = 2\boldsymbol{I} - \boldsymbol{R}(\boldsymbol{n}, 2\pi/k) - \boldsymbol{R}^{-1}(\boldsymbol{n}, 2\pi/k), \tag{2.100}$$

$$\boldsymbol{Z}_k^\parallel := \boldsymbol{Z}^\parallel(\boldsymbol{n}, 2\pi/k) = \lambda_k \boldsymbol{I} - \boldsymbol{Z}_k^\perp, \qquad \text{where } \lambda_k := 2(1 - \cos(2\pi/k)). \tag{2.101}$$

Note that

$$\lambda_2 = 4, \quad \lambda_3 = 3, \quad \lambda_4 = 2, \quad \lambda_6 = 1. \tag{2.102}$$

For each $\boldsymbol{s} \in \mathsf{L}$, it follows from (1.121), (2.100) and (2.101) that

$$\boldsymbol{Z}_k^\perp \boldsymbol{s} = \lambda_k \boldsymbol{s}^\perp \in \mathsf{L}, \qquad \boldsymbol{Z}_k^\parallel \boldsymbol{s} = \lambda_k \boldsymbol{s}^\parallel \in \mathsf{L}. \tag{2.103}$$

In particular for $k = 2$, $\boldsymbol{R}(\boldsymbol{n}, \pi) = \boldsymbol{R}(\boldsymbol{n}, \pi)^{-1}$, so we have

$$\boldsymbol{Z}_2^\perp = 2\boldsymbol{I} - 2\boldsymbol{R}(\boldsymbol{n}, \pi), \qquad \boldsymbol{Z}_2^\parallel = 2\boldsymbol{I} + 2\boldsymbol{R}(\boldsymbol{n}, \pi). \tag{2.104}$$

It follows that

$$\frac{1}{2}\boldsymbol{Z}_2^\perp \boldsymbol{s} = (\boldsymbol{I} - \boldsymbol{R}(\boldsymbol{n}, \pi))\boldsymbol{s} \in \mathsf{L}, \qquad \frac{1}{2}\boldsymbol{Z}_2^\parallel \boldsymbol{s} = (\boldsymbol{I} + \boldsymbol{R}(\boldsymbol{n}, \pi))\boldsymbol{s} \in \mathsf{L}. \tag{2.105}$$

Theorem 2.41 *Let $\mathcal{H}_\mathsf{L}$ be the lattice point group of lattice L, which has a subgroup C_k with an axis ℓ of order $k = 3, 4$ or 6. Then $\mathcal{H}_\mathsf{L}$ has a subgroup $D_k \supset C_k$ with a two-fold axis that lies in the lattice plane normal to ℓ and is parallel to one of the shortest lattice vectors in that plane.*

Proof Let the subgroup C_k in question be generated by $\boldsymbol{R}(\boldsymbol{n}, 2\pi/k)$, where $\boldsymbol{n}$ is a unit vector parallel to ℓ. Henceforth in the proof we will simply write $\boldsymbol{R}$ for $\boldsymbol{R}(\boldsymbol{n}, 2\pi/k)$. Let Σ be the plane that passes through the origin and is normal to $\boldsymbol{n}$. By Lemma 2.40, Σ is a lattice plane, because it contains a lattice vector $\boldsymbol{b}$ and another lattice vector $\boldsymbol{Rb}$, which together span Σ. Pick one of the shortest lattice vectors in Σ and call it $\boldsymbol{b}_1$. Let $\boldsymbol{b}_2 = \boldsymbol{Rb}_1$. The closed parallelogram spaned by $\boldsymbol{b}_1$ and $\boldsymbol{b}_2$ contains no lattice points other than the vertices. Indeed if there is another lattice point $\boldsymbol{c}$ inside the parallelogram in question, then one of the following four lattice vectors in Σ, namely $\boldsymbol{c}$, $\boldsymbol{b}_1 - \boldsymbol{c}$, $\boldsymbol{b}_2 - \boldsymbol{c}$, and $\boldsymbol{b}_1 + \boldsymbol{b}_2 - \boldsymbol{c}$, will be shorter than $\boldsymbol{b}_1$. Let $\boldsymbol{b}_3$ be a lattice vector such that the parallelepiped $\Pi[\boldsymbol{b}_1, \boldsymbol{b}_2, \boldsymbol{b}_3]$ has the smallest volume. Then $\boldsymbol{b}_1, \boldsymbol{b}_2$, and $\boldsymbol{b}_3$ constitute a primitive lattice basis.

Let $\boldsymbol{\sigma}$ be the reflection with respect to the plane that contains ℓ and is normal to $\boldsymbol{b}_1$. We claim that $\boldsymbol{\sigma}\mathsf{L} = \mathsf{L}$, i.e., $\boldsymbol{\sigma} \in \mathcal{H}_\mathsf{L}$. To this end, it suffices to show that $\boldsymbol{\sigma}\boldsymbol{b}_i \in \mathsf{L}$ for $i = 1, 2, 3$. It is easy to see that

$$\boldsymbol{\sigma}\boldsymbol{b}_1 = -\boldsymbol{b}_1 \quad \text{for } k = 3, 4, 6, \qquad \boldsymbol{\sigma}\boldsymbol{b}_2 = \begin{cases} \boldsymbol{b}_1 + \boldsymbol{b}_2, & \text{for } k = 3 \\ \boldsymbol{b}_2, & \text{for } k = 4 \\ \boldsymbol{b}_2 - \boldsymbol{b}_1, & \text{for } k = 6. \end{cases} \tag{2.106}$$

Hence $\boldsymbol{\sigma}\boldsymbol{b}_1 \in \mathsf{L}$ and $\boldsymbol{\sigma}\boldsymbol{b}_2 \in \mathsf{L}$ for $k = 3, 4, 6$. Let us proceed to consider $\boldsymbol{\sigma}\boldsymbol{b}_3$. Let $\boldsymbol{b}_3 = \boldsymbol{u} + \boldsymbol{v}$, where $\boldsymbol{u} := \boldsymbol{b}_3^\parallel$ and $\boldsymbol{v} := \boldsymbol{b}_3^\perp$ are the component of $\boldsymbol{b}_3$ parallel to $\boldsymbol{n}$ and the projection of $\boldsymbol{b}_3$ onto the lattice plane Σ, respectively. If we can prove that $\boldsymbol{\sigma}\boldsymbol{b}_3 \in \mathsf{L}$, then the claim that $\boldsymbol{\sigma} \in \mathcal{H}_\mathsf{L}$ is valid. We break down our discussion into three cases:

For $k = 6$, by (2.102) $\lambda_6 = 1$, and by (2.103) and the fact that $\boldsymbol{v} \in \Sigma$ we have

$$\boldsymbol{Z}_6^{\perp} \boldsymbol{b}_3 = \boldsymbol{v} \in \mathsf{L} \cap \Sigma. \tag{2.107}$$

Hence $\boldsymbol{u} = \boldsymbol{b}_3 - \boldsymbol{v} \in \mathsf{L}$, and $\boldsymbol{v} = n_1 \boldsymbol{b}_1 + n_2 \boldsymbol{b}_2$ for some $n_1, n_2 \in \mathbb{Z}$. It follows then that $\boldsymbol{\sigma} \boldsymbol{b}_3 = \boldsymbol{\sigma} \boldsymbol{u} + \boldsymbol{\sigma} \boldsymbol{v} = \boldsymbol{u} + n_1 \boldsymbol{\sigma} \boldsymbol{b}_1 + n_2 \boldsymbol{\sigma} \boldsymbol{b}_2 \in \mathsf{L}$.

For $k = 4$, similarly we have $\lambda_4 = 2$ and

$$\boldsymbol{Z}_4^{\perp} \boldsymbol{b}_3 = 2\boldsymbol{v} \in \mathsf{L} \cap \Sigma. \tag{2.108}$$

Hence we have

$$\boldsymbol{v} = \frac{n_1}{2} \boldsymbol{b}_1 + \frac{n_2}{2} \boldsymbol{b}_2, \qquad \text{for some specific } n_1, n_2 \in \mathbb{Z}. \tag{2.109}$$

It follows from (2.106) and (2.109) that

$$\boldsymbol{\sigma} \boldsymbol{v} = -\frac{n_1}{2} \boldsymbol{b}_1 + \frac{n_2}{2} \boldsymbol{b}_2, \tag{2.110}$$

Subtracting (2.109) from (2.110), we obtain

$$\boldsymbol{\sigma} \boldsymbol{v} - \boldsymbol{v} = -n_1 \boldsymbol{b}_1. \tag{2.111}$$

Then we see that $\boldsymbol{\sigma} \boldsymbol{b}_3 = \boldsymbol{\sigma} \boldsymbol{u} + \boldsymbol{\sigma} \boldsymbol{v} = \boldsymbol{u} + \boldsymbol{v} - n_1 \boldsymbol{b}_1 = \boldsymbol{b}_3 - n_1 \boldsymbol{b}_1 \in \mathsf{L}$.

For $k = 3$, note that $\boldsymbol{R} \boldsymbol{b}_1 = \boldsymbol{b}_2$ and $\boldsymbol{R} \boldsymbol{b}_2 = -(\boldsymbol{b}_1 + \boldsymbol{b}_2)$. Let $\boldsymbol{v} = \alpha \boldsymbol{b}_1 + \beta \boldsymbol{b}_2$, where $\alpha, \beta \in \mathbb{R}$. Then $\boldsymbol{R} \boldsymbol{v} = -\beta \boldsymbol{b}_1 + (\alpha - \beta) \boldsymbol{b}_2$. Since $\boldsymbol{v} - \boldsymbol{R} \boldsymbol{v} = \boldsymbol{b}_3 - \boldsymbol{R} \boldsymbol{b}_3 \in \mathsf{L} \cap \Sigma$, we have

$$\begin{aligned} \boldsymbol{v} - \boldsymbol{R} \boldsymbol{v} &= (\alpha + \beta) \boldsymbol{b}_1 + (2\beta - \alpha) \boldsymbol{b}_2 \\ &= n_1 \boldsymbol{b}_1 + n_2 \boldsymbol{b}_2 \qquad \text{for some } n_1, n_2 \in \mathbb{Z}. \end{aligned} \tag{2.112}$$

Hence we have

$$\alpha + \beta = n_1, \qquad 2\beta - \alpha = n_2. \tag{2.113}$$

By (2.106), we obtain

$$\boldsymbol{\sigma} \boldsymbol{v} = \boldsymbol{\sigma} (\alpha \boldsymbol{b}_1 + \beta \boldsymbol{b}_2) = (\beta - \alpha) \boldsymbol{b}_1 + \beta \boldsymbol{b}_2. \tag{2.114}$$

It follows that

$$\boldsymbol{\sigma} \boldsymbol{v} - \boldsymbol{v} = (\beta - 2\alpha) \boldsymbol{b}_1 = (n_2 - n_1) \boldsymbol{b}_1, \tag{2.115}$$

where we have appealed to (2.113). Hence we conclude that $\boldsymbol{\sigma} \boldsymbol{b}_3 = \boldsymbol{\sigma} \boldsymbol{u} + \boldsymbol{\sigma} \boldsymbol{v} = \boldsymbol{u} + \boldsymbol{v} + (n_2 - n_1) \boldsymbol{b}_1 = \boldsymbol{b}_3 + (n_2 - n_1) \boldsymbol{b}_1 \in \mathsf{L}$.

In summary, we have proved that $\boldsymbol{\sigma} \in \mathcal{H}_{\mathsf{L}}$ as asserted for all cases in question.

Let $\boldsymbol{m} = \boldsymbol{b}_1 / \|\boldsymbol{b}_1\|$. By Lemma 2.39, $\boldsymbol{\mathcal{I}} \in \mathcal{H}_{\mathsf{L}}$. Then $\boldsymbol{R}(\boldsymbol{m}, \pi) = \boldsymbol{\mathcal{I}} \boldsymbol{\sigma} \in \mathcal{H}_{\mathsf{L}}$. The rotational group generated by $\boldsymbol{R}(\boldsymbol{n}, 2\pi/k)$ and $\boldsymbol{R}(\boldsymbol{m}, \pi)$ is the dihedral group D_k $(k = 3, 4, 6)$ described in the statement of the theorem. □

Remark 2.42 The proof of Theorem 2.41 further implies that $\boldsymbol{b}_2 = \boldsymbol{R}(\boldsymbol{n}, 2\pi/k)\boldsymbol{b}_1$ defines a rotational symmetry axis of order (at least) 2. Indeed, let $\boldsymbol{m}' := \boldsymbol{b}_2/\|\boldsymbol{b}_2\| = \boldsymbol{R}(\boldsymbol{n}, 2\pi/k)\boldsymbol{m}$. Then

$$\boldsymbol{R}(\boldsymbol{m}', \pi) = \boldsymbol{R}(\boldsymbol{R}(\boldsymbol{n}, 2\pi/k)\boldsymbol{m}, \pi) = \boldsymbol{R}(\boldsymbol{n}, 2\pi/k)\boldsymbol{R}(\boldsymbol{m}, \pi)\boldsymbol{R}(\boldsymbol{n}, 2\pi/k)^{-1},$$

which implies $\boldsymbol{R}(\boldsymbol{b}_2/\|\boldsymbol{b}_2\|, \pi) = \boldsymbol{R}(\boldsymbol{m}', \pi) \in \mathcal{H}_{\mathsf{L}}$. □

A glance at the structures of the Type II crystal classes given in Table 3 reveals that C_{3i}, C_{4h}, C_{6h}, and T_h cannot be holohedries, because their member groups contain as subgroup C_3, C_4, C_6, and C_3, respectively, but not D_3, D_4, D_6, and D_3, respectively. That leaves seven holohedries, namely: triclinic (C_i), monoclinic (C_{2h}), orthorhombic (D_{2h}), tetragonal (D_{4h}), trigonal (D_{3d}), hexagonal (D_{6h}), and cubic (O_h).

2.8 The Bravais Lattices

As shown in Sects. 2.5 and 2.6.1, the requirement that $\boldsymbol{Q}\mathsf{L} = \mathsf{L}$ for each $\boldsymbol{Q}$ in the crystallographic point group $\mathcal{K}$, i.e., each rotation or roto-inversion $\boldsymbol{Q}$ in $\mathcal{K}$ preserves the lattice L, delimits $\mathcal{K} \subset \mathrm{O}(3)$ to belong to one of 32 possible point-group types. Conversely, we know that there are seven holohedries. Can the point-group symmetry of a lattice L, as embodied in the holohedral group $\mathcal{K} = \mathcal{H}_{\mathsf{L}}$, be used to derive all possible lattice types? An affirmative answer to this question was first given by Auguste Bravais [49]. He classified all lattices into a total of 14 lattice types, which are now named after him. In this section we shall present a derivation of the 14 Bravais lattice types. Our main references for this section are: Kim [177, Sects. 13.3–13.4] and Miller [232, Sect. 2.8].

Note that we use the same Schönflies symbol to denote a geometric crystal class, the point-group type of that class, and specific groups of that point-group type. Whether a symbol, e.g., D_3, stands for the geometric crystal class, the point-group type, or a specific point group will be clear by the context where that symbol appears. Whenever confusion might arise, we will spell out explicitly what the symbol denotes.

2.8.1 Lattice Types

Let $\mathcal{G}$ and $\mathcal{G}'$ be two equivalent space groups, i.e., they are of the same space-group type; see Definition 2.18. Then their point groups $\mathcal{K}$ and $\mathcal{K}'$ are equivalent or are of the same point-group type; see Definition 2.19. Such equivalence should be extended to the lattice groups $\mathcal{L}$ and $\mathcal{L}'$ pertaining to $\mathcal{G}$ and $\mathcal{G}'$, respectively.

Definition 2.43 Let $\mathcal{L}$ and $\mathcal{L}'$ be the lattice groups associated with space group $\mathcal{G}$ and $\mathcal{G}'$, respectively. The groups $\mathcal{L}$ and $\mathcal{L}'$ (or the lattices $\mathsf{L} := \mathcal{L}(\mathbf{0})$ and $\mathsf{L}' := \mathcal{L}'(\mathbf{0})$) are of the same lattice type if $\mathcal{G}$ and $\mathcal{G}'$ are of the same space-group type. □

Consider an equivalence class of space groups. Within this equivalence class, all space groups have point groups of the same point-group type and lattices of the same lattice type. Let $\mathcal{G}$ be a space group of this class and $\mathcal{K}$ and L be its point group and lattice, respectively. To determine the possible lattice types, it suffices to restrict attention to the cases where $\mathcal{K}$ belongs to some holohedry and $\mathcal{K} = \mathcal{H}_{\mathsf{L}}$, the lattice point group of L. Any other space group $\mathcal{G}'$ in the same equivalence class has its point group, say $\mathcal{K}'$, being of the same point-group

type as that of $\mathcal{K}$. By Corollary 2.22, there is a rotation $\boldsymbol{R}$ such that $\mathcal{K}' = \boldsymbol{R}\mathcal{K}\boldsymbol{R}^{-1}$, i.e., each $\boldsymbol{Q}' \in \mathcal{K}'$ can be written as $\boldsymbol{Q}' = \boldsymbol{R}\boldsymbol{Q}\boldsymbol{R}^{-1}$ for some $\boldsymbol{Q} \in \mathcal{K}$. Then we have

$$\boldsymbol{Q}'(\boldsymbol{R}\mathsf{L}) = \boldsymbol{R}\boldsymbol{Q}\boldsymbol{R}^{-1}(\boldsymbol{R}\mathsf{L}) = \boldsymbol{R}\boldsymbol{Q}\mathsf{L} = \boldsymbol{R}\mathsf{L}, \qquad \text{for each } \boldsymbol{Q}' \in \mathcal{K}'. \tag{2.116}$$

Since $\mathcal{K}$ is the lattice point group of L, it follows easily from (2.116) that $\mathcal{K}'$ is the lattice point group of $\boldsymbol{R}\mathsf{L}$, the lattice that results after lattice L is rotated by $\boldsymbol{R}$. While $\boldsymbol{R}\mathsf{L}$ need not be equal to the lattice L' of space group $\mathcal{G}'$, it is the lattice of $(\boldsymbol{0}, \boldsymbol{R})\mathcal{G}(\boldsymbol{0}, \boldsymbol{R}^{-1})$. Hence by Definition 2.18 and 2.43, $\boldsymbol{R}\mathsf{L}$ and L are of the same lattice type.

For a point group $\mathcal{K}$ in a holohedry, suppose we can determine all types of lattices L such that $\mathcal{K} = \mathcal{H}_{\mathsf{L}}$. Let us call the set of all such lattices $\mathscr{A}$. If $\mathcal{K}$ is replaced by one of its peers $\mathcal{K}'$ in the same holohedry, then $\mathcal{K}' = \boldsymbol{R}\mathcal{K}\boldsymbol{R}^{-1}$ for some rotation $\boldsymbol{R}$, and the set of lattices L' that satisfy $\mathcal{K}' = \mathcal{H}_{\mathsf{L}'}$ is none other than $\{\boldsymbol{R}\mathsf{L} : \mathsf{L} \in \mathscr{A}\}$, which delivers the same lattice types. Hence, to determine all lattice types pertaining to a holohedry, it suffices to solve the following problem:

– For one specific group $\mathcal{K}$ in the holohedry, construct all lattices L such that $\mathcal{K} = \mathcal{H}_{\mathsf{L}}$.

In what follows we shall determine all Bravais lattice types by solving the preceding problem for the namesake point groups given in Table 3 for the seven holohedries C_i, C_{2h}, D_{2h}, D_{4h}, D_{3d}, D_{6h}, and O_h.

2.8.2 Conventional Lattice Basis and Unit Cell

In Sects. 2.3.1 and 2.3.2, we have learned that every lattice L has an abundance of primitive lattice bases, each of which can be used to define the lattice L. However, given a holohedral group $\mathcal{K}$, it is not obvious how one should proceed to determine primitive lattice bases for lattices L which have $\mathcal{K}$ as their lattice point group. On the other hand, there is a three-step procedure to construct such lattices, which circumvents the finding of primitive lattice bases.

Step 1 of this procedure is to use some of the rotational operations of $\mathcal{K}$ to determine what is called a conventional lattice basis $\boldsymbol{a}_1, \boldsymbol{a}_2, \boldsymbol{a}_3$ of L. Let us set aside $\mathcal{K} = C_i = \{\boldsymbol{I}, \mathcal{I}\}$, a trivial case that we will consider in Sect. 2.8.5. For the other holohedries, the point group $\mathcal{K}$ has at least one rotational axis of order 2, 3, 4, or 6. We construct a (symmetry-adapted) conventional lattice basis $\{\boldsymbol{a}_1, \boldsymbol{a}_2, \boldsymbol{a}_3\}$ for L as follows. Among the rotational axes of $\mathcal{K}$, pick one with the highest order, and call it ℓ. For example, if $\mathcal{K} = D_{3d}$, pick the 3-fold axis as ℓ; if $\mathcal{K} = O_h$, pick one of the 4-fold axes as ℓ. Let the order of ℓ be k. By Lemma 2.40 L has a lattice vector $\boldsymbol{u}$ parallel to ℓ and a lattice plane, say Σ, which contains $\boldsymbol{0}$ and is normal to $\boldsymbol{u}$. Let $\boldsymbol{a}_3$ be the shortest lattice vector in the direction of $\boldsymbol{u}$. Pick a planar primitive lattice basis $\boldsymbol{a}_1$ and $\boldsymbol{a}_2$ in Σ such that they are symmetry-adapted to $\mathcal{K}$ in the sense to be discussed under Case (i) and Case (ii) below, and that $\boldsymbol{a}_1$, $\boldsymbol{a}_2$, and $\boldsymbol{a}_3$ constitute a right-handed triad.

Case (i): The axis of highest rotational symmetry has its order $k = 3, 4$, or 6. For this case the conventional basis vectors $\boldsymbol{a}_1$, $\boldsymbol{a}_2$ are chosen to be symmetry-adapted to $\mathcal{K}$ in the following sense: Let $\boldsymbol{a}_1$ be one of the shortest lattice vector in the plane Σ, and let $\boldsymbol{a}_2 = \boldsymbol{R}(\boldsymbol{n}, 2\pi/k)\boldsymbol{a}_1$, where $\boldsymbol{n} = \boldsymbol{u}/\|\boldsymbol{u}\|$. Then $\boldsymbol{a}_1$ and $\boldsymbol{a}_2$ constitute a primitive lattice basis in Σ. Moreover, $\boldsymbol{a}_1$ and $\boldsymbol{a}_2$ define axes of rotational symmetry of $\mathcal{H}_{\mathsf{L}}$. In fact, we have already applied this construction in our proof of Theorem 2.41; cf. also Remark 2.42. The unit cell $\Pi[\boldsymbol{a}_1, \boldsymbol{a}_2, \boldsymbol{a}_3]$ is not primitive unless it happens that

$$\mathrm{V}(\Pi[\boldsymbol{a}_1, \boldsymbol{a}_2, \boldsymbol{a}_3]) \le \mathrm{V}(\Pi[\boldsymbol{a}_1, \boldsymbol{a}_2, \boldsymbol{f}]) \tag{2.117}$$

for any lattice vector $\boldsymbol{f}$ such that $\mathrm{V}(\Pi[\boldsymbol{a}_1, \boldsymbol{a}_2, \boldsymbol{f}]) > 0$, where $\mathrm{V}(\cdot)$ denotes the volume of the parallelepiped in question; see Sect. 2.3.2.

Consider the group of translations

$$\mathcal{L}^{(p)} = \{\boldsymbol{s} \in \mathbb{R}^3 : \boldsymbol{s} = s_1\boldsymbol{a}_1 + s_2\boldsymbol{a}_2 + s_3\boldsymbol{a}_3, \text{ where } s_1, s_2, s_3 \in \mathbb{Z}\}. \tag{2.118}$$

Unless the conventional basis $\{\boldsymbol{a}_1, \boldsymbol{a}_2, \boldsymbol{a}_3\}$ is primitive, the orbit $\mathcal{L}^{(p)}(\mathbf{0})$ is a proper sublattice of L. Hence, in general, the unit cell $\Pi[\boldsymbol{a}_1, \boldsymbol{a}_2, \boldsymbol{a}_3]$ may contain lattice points other than $\mathbf{0}$. Let

$$\boldsymbol{t} = t_1\boldsymbol{a}_1 + t_2\boldsymbol{a}_2 + t_3\boldsymbol{a}_3 \qquad (0 \le t_i < 1 \text{ for } i = 1, 2, 3). \tag{2.119}$$

Step 2 of the procedure concerns the problems to find the conditions on t_i $(i = 1, 2, 3)$ such that $\boldsymbol{t} \in \mathsf{L}$ and to determine the possible lattice vectors $\boldsymbol{t}$. We shall solve these problems for each holohedry in question. For brevity, we shall henceforth write $\boldsymbol{t} = (t_1, t_2, t_3)$ for the equation in (2.119) when no confusion should arise on the basis in question.

In Steps 1 and 2 we use the requirement $\boldsymbol{Q}\mathsf{L} = \mathsf{L}$ for $\boldsymbol{Q}$ in the holohedral group $\mathcal{K}$ to generate necessary conditions for the lattice L, which lead to one or more lattices of the form $\mathcal{L}^{(p)}(\mathbf{0})$, $\mathcal{L}^{(p)}(\mathbf{0}) \cup \mathcal{L}^{(p)}(\boldsymbol{t})$, etc. that satisfy those conditions. In Step 3 we check for each derived lattice L whether $\mathcal{H}_\mathsf{L} = \mathcal{K}$.

Remark 2.44 For Case (i) the conventional lattice basis $\boldsymbol{a}_1$, $\boldsymbol{a}_2$, and $\boldsymbol{a}_3$ delivered by the procedure outlined above for a lattice L such that $\mathcal{K} = \mathcal{H}_\mathsf{L}$ will enjoy the following properties:

1. The lattice vectors $\boldsymbol{a}_i$ $(i = 1, 2, 3)$ constitute a right-handed triad.
2. The lattice basis is symmetry-adapted to the lattice point group $\mathcal{H}_\mathsf{L}$ in the sense that $\boldsymbol{a}_3$ lies along an axis of highest rotational symmetry of $\mathcal{H}_\mathsf{L}$, whereas $\boldsymbol{a}_1$ and $\boldsymbol{a}_2$ are along axes of rotational symmetry of $\mathcal{H}_\mathsf{L}$, and $\boldsymbol{a}_2 = \boldsymbol{R}(\boldsymbol{a}_3/\|\boldsymbol{a}_3\|, 2\pi/k)\boldsymbol{a}_1$.
3. Among basis vectors that are symmetry-adapted to $\mathcal{H}_\mathsf{L}$ in the preceding sense, the unit cell $\Pi[\boldsymbol{a}_1, \boldsymbol{a}_2, \boldsymbol{a}_3]$ is one with the smallest volume. □

Case (ii): The axis of highest rotational symmetry has its order $k = 2$. There are only two holohedries which fit this description, namely D_{2h} and C_{2h}. If the lattice point group $\mathcal{H}_\mathsf{L}$ is of type D_{2h}, then it has three orthogonal 2-fold axes of rotational symmetry. Choose a right-handed triad, each of which is along one of the 2-fold axes and is the shortest lattice vector in its direction. The lattice vectors $\boldsymbol{a}_i$ $(i = 1, 2, 3)$ form a conventional lattice basis that satisfies all the properties listed in Remark 2.44.

If $\mathcal{H}_\mathsf{L}$ is of type C_{2h}, then it has only one 2-fold rotational axis. Choose one of the two shortest lattice vectors along the 2-fold axis as $\boldsymbol{a}_3$. Pick a primitive basis $\boldsymbol{a}_1$, $\boldsymbol{a}_2$ in the lattice plane Σ normal to $\boldsymbol{a}_3$ such that $\boldsymbol{a}_1$, $\boldsymbol{a}_2$, and $\boldsymbol{a}_3$ constitute a right-handed triad. We may still assert that the chosen basis is symmetry-adapted to $\mathcal{H}_\mathsf{L}$, the point group of lattice L, as it has only one axis of rotational symmetry.

The vectors of the conventional basis $\boldsymbol{a}_1$, $\boldsymbol{a}_2$, and $\boldsymbol{a}_3$ are commonly written as $\boldsymbol{a}, \boldsymbol{b}$, and $\boldsymbol{c}$, respectively. The lengths of these lattice vectors are: $a := \|\boldsymbol{a}\|$, $b := \|\boldsymbol{b}\|$, and $c := \|\boldsymbol{c}\|$. The angle between $\boldsymbol{b}$ and $\boldsymbol{c}$, $\boldsymbol{c}$ and $\boldsymbol{a}$, $\boldsymbol{a}$ and $\boldsymbol{b}$ are named α, β, γ, respectively. The variables a, b, c, α, β, and γ are called cell parameters.

We will now turn to work out for the seven holohedries what follows:[35]

[35]The lattice types derived for a holohedry are independent of the specific point group chosen to represent that holohedry. See Sect. 2.8.1.

– For each holohedral group $\mathcal{K}$ given in Table 3 (i.e., $\mathcal{K} = C_i$, C_{2h}, D_{2h}, D_{4h}, D_{3d}, D_{6h}, or O_h there), follow the procedure given earlier in the present section to determine all types of lattices L, called Bravais lattice types, for which $\mathcal{K} = \mathcal{H}_{\mathsf{L}}$, i.e., $\boldsymbol{Q}\mathsf{L} = \mathsf{L}$ for each $\boldsymbol{Q} \in \mathcal{K}$.

It turns out that the procedure described above delivers for each holohedry (except the trigonal[36]) a primitive lattice type $\mathcal{L}^{(p)}(\mathbf{0})$—see (2.118), where the conventional lattice basis is primitive. The primitive lattice types are: aP, mP, oP, tP, hP, and cP.[37] For the monoclinic, orthorhombic, tetragonal, and cubic holohedries, the primitive lattice $\mathcal{L}^{(p)}(\mathbf{0})$ serves also as a sublattice for centered lattice types (base-centered, body-centered, or face-centered) of the form $\mathcal{L}^{(p)}(\mathbf{0}) \cup \mathcal{L}^{(p)}(\boldsymbol{t})$, etc., where the centering vectors $\boldsymbol{t}$ satisfy (2.119). The centered lattice types for these holohedries are: mS, oS, oF, oI, tI, cF, and cI. The lattice types pertaining to the same holohedry together constitute a *lattice system*. Thus we have the triclinic, monoclinic, orthorhombic, tetragonal, hexagonal, and cubic lattice systems, which include lattice types that pertain to the C_i, C_{2h}, D_{2h}, D_{4h}, D_{6h}, and O_h holohedry, respectively. For the trigonal (D_{3d}) holohedry, Steps 1 and 2 lead to two lattice types, namely the primitive hexagonal (hP) of the hexagonal lattice system, and the rhombohedral hexagonal (hR),[38] which we assign to the rhombohedral lattice system.

2.8.3 The Hexagonal, Tetragonal, and Rhombohedral Lattice Systems

We discuss the hexagonal, tetragonal, and rhombohedral lattice systems together, because the mathematical derivations are similar. For each of these cases, let $\boldsymbol{a}_1$, $\boldsymbol{a}_2$, and $\boldsymbol{a}_3$ be constructed by following the recipe described in the preceding subsection.

In what follows, $k = 3, 4$, or 6; $\boldsymbol{n} := \boldsymbol{a}_3/\|\boldsymbol{a}_3\|$; when the arguments of $\boldsymbol{R}$ are not specified, $\boldsymbol{R} = \boldsymbol{R}(\boldsymbol{n}, 2\pi/k)$. Using the formulas $\boldsymbol{R}\boldsymbol{a}_1 = \boldsymbol{a}_2$, $\boldsymbol{R}\boldsymbol{a}_3 = \boldsymbol{a}_3$, and (see (2.100))

$$\boldsymbol{R}\boldsymbol{a}_2 = \left(2\boldsymbol{I} - \boldsymbol{R}^{-1} - \boldsymbol{Z}_k^{\perp}\right)\boldsymbol{a}_2 = 2\boldsymbol{a}_2 - \boldsymbol{a}_1 - \lambda_k \boldsymbol{a}_2, \tag{2.120}$$

we obtain the equation

$$\boldsymbol{t} - \boldsymbol{R}(\boldsymbol{n}, 2\pi/k)\boldsymbol{t} = (t_1 + t_2)\boldsymbol{a}_1 + (\lambda_k t_2 - (t_1 + t_2))\boldsymbol{a}_2, \tag{2.121}$$

where $\boldsymbol{t}$ is given in (2.119). Since $\boldsymbol{t} - \boldsymbol{R}(\boldsymbol{n}, 2\pi/k)\boldsymbol{t} \in \mathsf{L}$ and $\boldsymbol{a}_1$, $\boldsymbol{a}_2$ constitute a primitive basis in the lattice plane Σ, we have $t_1 + t_2 \in \mathbb{Z}$ and $\lambda_k t_2 - (t_1 + t_2) \in \mathbb{Z}$, where λ_k is given in (2.102). Hence $\lambda_k t_2 = m$ for some $m \in \mathbb{Z}$. Since $0 \le t_i < 1$ for $i = 1, 2$, we conclude that

$$t_1 = \begin{cases} 0 & \text{if } t_2 = 0 \\ 1 - t_2 & \text{if } t_2 \neq 0, \end{cases} \qquad t_2 = \frac{m}{\lambda_k}, \qquad \text{where } m \in \mathbb{Z} \text{ and } 0 \le m < \lambda_k. \tag{2.122}$$

Applying the operator $\boldsymbol{Z}_k^{\parallel}$ to both sides of (2.119), we get (cf. $(2.103)_2$)

$$\boldsymbol{Z}_k^{\parallel}\boldsymbol{t} = \lambda_k t_3 \boldsymbol{a}_3. \tag{2.123}$$

[36] The primitive lattice type $\mathcal{L}^{(p)}(\mathbf{0})$ obtained from Step 1 of the procedure for the holohedry D_{3d} consists of hexagonal lattices of type hP with holohedral groups of type D_{6h}. In Step 2, addition of two suitable centering lattice vectors in the unit cell leads to lattices of type hR with holohedral groups of type D_{3d}.

[37] Here we adopt the system of abbreviations given in *International Tables for Crystallography A* [133, p. 15].

[38] The hR lattice type is sometimes called double-centered hexagonal; see [177, p. 360]. See also Footnote 36.

Since $\boldsymbol{Z}_k^{\parallel}\boldsymbol{t} \in \mathsf{L}$ and $\boldsymbol{a}_3$ is the shortest lattice vector in the direction of $\boldsymbol{n}$, we see that $\lambda_k t_3 = m'$ for some $m' \in \mathbb{Z}$, which we rewrite as

$$t_3 = \frac{m'}{\lambda_k}, \qquad \text{where } m' \in \mathbb{Z} \text{ and } 0 \le m' < \lambda_k. \tag{2.124}$$

When $m > 0$, it is necessary that $m' \ge 1$, because $\{\boldsymbol{a}_1, \boldsymbol{a}_2\}$ is a primitive basis in the lattice plane Σ.

The Hexagonal System

For the hexagonal system, $k = 6$ and $\lambda_6 = 1$ in (2.122) and (2.124). Hence $m = m' = 0$, $t_1 = t_2 = t_3 = 0$, $\boldsymbol{t} = \boldsymbol{0}$, and $\mathsf{L} = \mathcal{L}^{(p)}(\boldsymbol{0})$. There is only one Bravais lattice type for the hexagonal system, which is named *primitive hexagonal* (hP).

Note that if we replace $\boldsymbol{a}_2$ by $\boldsymbol{a}_2' = \boldsymbol{a}_2 - \boldsymbol{a}_1$, the lattice L remains unchanged. In fact, the standard practice in crystallography is to take $\boldsymbol{a} = \boldsymbol{a}_1$, $\boldsymbol{b} = \boldsymbol{a}_2' = \boldsymbol{R}(\boldsymbol{n}, 2\pi/3)\boldsymbol{a}_1$, and $\boldsymbol{c} = \boldsymbol{a}_3$. The restrictions on cell parameters are then: $a = b$, $\alpha = \beta = \pi/2$, and $\gamma = 2\pi/3$. Two parameters, namely a and c, are required to specify a primitive hexagonal unit cell.

Let us prove that the holohedry of the hP lattice type is D_{6h}. Let $\boldsymbol{e}_i$ $(i = 1, 2, 3)$ be the right-handed orthonormal triad defined by $\boldsymbol{e}_3 := \boldsymbol{n} = \boldsymbol{a}_3/\|\boldsymbol{a}_3\|$, $\boldsymbol{e}_1 := \boldsymbol{a}_1/\|\boldsymbol{a}_1\|$. We take $\boldsymbol{R}(\boldsymbol{e}_3, \pi/3)$, $\boldsymbol{R}(\boldsymbol{e}_1, \pi)$, and $\mathcal{I}$ as the generators of the group D_{6h} given in Table 3. By Lemma 2.39, $\mathcal{I}\mathsf{L} = \mathsf{L}$. Hence it suffices to show that $\boldsymbol{R}(\boldsymbol{e}_3, \pi/3)\mathsf{L} = \mathsf{L}$ and $\boldsymbol{R}(\boldsymbol{e}_1, \pi)\mathsf{L} = \mathsf{L}$. Since

$$\begin{aligned} &\boldsymbol{R}(\boldsymbol{e}_3, \pi/3)\boldsymbol{a}_1 = \boldsymbol{a}_1 + \boldsymbol{a}_2', \qquad \boldsymbol{R}(\boldsymbol{e}_3, \pi/3)\boldsymbol{a}_2' = -\boldsymbol{a}_1, \qquad \boldsymbol{R}(\boldsymbol{e}_3, \pi/3)\boldsymbol{a}_3 = \boldsymbol{a}_3, \\ &\boldsymbol{R}(\boldsymbol{e}_1, \pi)\boldsymbol{a}_1 = \boldsymbol{a}_1, \qquad \boldsymbol{R}(\boldsymbol{e}_1, \pi)\boldsymbol{a}_2' = -\boldsymbol{a}_1 - \boldsymbol{a}_2', \qquad \boldsymbol{R}(\boldsymbol{e}_1, \pi)\boldsymbol{a}_3 = -\boldsymbol{a}_3, \end{aligned} \tag{2.125}$$

we conclude that $\boldsymbol{R}(\boldsymbol{e}_3, \pi/3)\mathsf{L} = \mathsf{L}$ and $\boldsymbol{R}(\boldsymbol{e}_1, \mathsf{L}) = \mathsf{L}$. Since there is no crystallographic point group that contains D_{6h} as a proper subgroup, we have $\mathcal{H}_{\mathsf{L}} = D_{6h}$.

The Tetragonal System

For the tetragonal system, $k = 4$ and $\lambda_4 = 2$ in (2.122) and (2.124). Hence $0 \le m < 2$ and $0 \le m' < 2$. As pointed out after equation (2.124), the case $(m, m') = (1, 0)$, which leads to $\boldsymbol{t} = (1/2, 1/2, 0) \in \Sigma$, is impossible, because $\boldsymbol{a}_1$ and $\boldsymbol{a}_2$ constitute a primitive basis in the lattice plane Σ. Similarly, the case $(m, m') = (0, 1)$ is impossible, because it leads to $\boldsymbol{t} = (0, 0, 1/2)$, which is parallel to and shorter than $\boldsymbol{a}_3$, the shortest lattice vector in its direction. That leaves only two possible cases:

(i) *Primitive tetragonal* (tP): $(m, m') = (0, 0)$, and $\boldsymbol{t} = \boldsymbol{0}$. Here $\mathsf{L} = \mathcal{L}^{(p)}(\boldsymbol{0})$. The restrictions on cell parameters are: $a = b$, $\alpha = \beta = \gamma = \pi/2$. Two undetermined parameters a and c specify a primitive tetragonal unit cell.

(ii) *Body-centered tetragonal* (tI): $(m, m') = (1, 1)$, and $\boldsymbol{t} = (1/2, 1/2, 1/2)$. The lattice is $\mathsf{L} = \mathcal{L}^{(p)}(\boldsymbol{t}) \cup \mathcal{L}^{(p)}(\boldsymbol{0})$. The restrictions on cell parameters and undetermined parameters are the same as those for the primitive tetragonal lattice.

We proceed to show that the holohedry of both the tP and tI lattice types is D_{4h}. Let $\boldsymbol{e}_i$ $(i = 1, 2, 3)$ be the right-handed orthonormal triad defined by $\boldsymbol{e}_3 := \boldsymbol{n} = \boldsymbol{a}_3/\|\boldsymbol{a}_3\|$, $\boldsymbol{e}_1 := \boldsymbol{a}_1/\|\boldsymbol{a}_1\|$. We take $\boldsymbol{R}(\boldsymbol{e}_3, \pi/2)$, $\boldsymbol{R}(\boldsymbol{e}_1, \pi)$, and $\mathcal{I}$ as the generators of the group D_{4h} given in Table 3. By Lemma 2.39, to prove that $\boldsymbol{Q}\mathsf{L} = \mathsf{L}$ for each $\boldsymbol{Q} \in D_{4h}$, it suffices to show that $\boldsymbol{R}(\boldsymbol{e}_3, \pi/2)\mathsf{L} = \mathsf{L}$ and $\boldsymbol{R}(\boldsymbol{e}_1, \pi)\mathsf{L} = \mathsf{L}$. For the conventional basis $\boldsymbol{a}_1, \boldsymbol{a}_2$, and $\boldsymbol{a}_3$ in question

we have

$$\boldsymbol{R}(\boldsymbol{e}_3,\pi/2)\boldsymbol{a}_1=\boldsymbol{a}_2,\qquad \boldsymbol{R}(\boldsymbol{e}_3,\pi/2)\boldsymbol{a}_2=-\boldsymbol{a}_1,\qquad \boldsymbol{R}(\boldsymbol{e}_3,\pi/2)\boldsymbol{a}_3=\boldsymbol{a}_3,$$
$$\boldsymbol{R}(\boldsymbol{e}_1,\pi)\boldsymbol{a}_1=\boldsymbol{a}_1,\qquad \boldsymbol{R}(\boldsymbol{e}_1,\pi)\boldsymbol{a}_2=-\boldsymbol{a}_2,\qquad \boldsymbol{R}(\boldsymbol{e}_1,\pi)\boldsymbol{a}_3=-\boldsymbol{a}_3. \tag{2.126}$$

For the tP lattice type, it follows immediately from (2.126) that $\boldsymbol{R}(\boldsymbol{e}_3,\pi/2)\mathcal{L}^{(p)}(\boldsymbol{0})=\mathcal{L}^{(p)}(\boldsymbol{0})$.

For the tI lattice type, (2.126) implies that

$$\boldsymbol{R}(\boldsymbol{e}_3,\pi/2)\boldsymbol{t}=\frac{1}{2}\boldsymbol{a}_2-\frac{1}{2}\boldsymbol{a}_1+\frac{1}{2}\boldsymbol{a}_3=\boldsymbol{t}-\boldsymbol{a}_1, \tag{2.127}$$

$$\boldsymbol{R}(\boldsymbol{e}_1,\pi)\boldsymbol{t}=\frac{1}{2}\boldsymbol{a}_1-\frac{1}{2}\boldsymbol{a}_2-\frac{1}{2}\boldsymbol{a}_3=\boldsymbol{t}-\boldsymbol{a}_2-\boldsymbol{a}_3. \tag{2.128}$$

Hence there holds also $\boldsymbol{R}(\boldsymbol{e}_3,\pi/2)\mathcal{L}^{(p)}(\boldsymbol{t})=\mathcal{L}^{(p)}(\boldsymbol{t})$ and $\boldsymbol{R}(\boldsymbol{e}_1,\pi)\mathcal{L}^{(p)}(\boldsymbol{t})=\mathcal{L}^{(p)}(\boldsymbol{t})$.

Thus $\boldsymbol{R}(\boldsymbol{e}_3,\pi/2)\mathsf{L}=\mathsf{L}$ and $\boldsymbol{R}(\boldsymbol{e}_1,\pi)\mathsf{L}=\mathsf{L}$ for both the tP and the tI lattice types. Moreover, since the holohedral group which contains the D_{4h} group in question as a proper subgroup is of type O_h and requires the metric restriction $a=b=c$, we conclude that the holohedry of both the tP and tI lattice types is D_{4h}.

The Rhombohedral System

Here we have $k=3$ and $\lambda_k=3$. By (2.122), (2.124), and the requirement that $m'\geq 1$ if $m>0$, there are the following possibilities for $\boldsymbol{t}$: (i) $(0,0,0)$, (ii) $(2/3,1/3,1/3)$, (iii) $(1/3,2/3,2/3)$, (iv) $(2/3,1/3,2/3)$, (v) $(1/3,2/3,1/3)$. Cases (ii) and (iii) correspond to $(m,m')=(1,1)$ and $(2,2)$, respectively, whereas cases (iv) and (v) to $(m,m')=(1,2)$ and $(2,1)$, respectively.

No new Bravais lattice type arises from the case $\boldsymbol{t}=\boldsymbol{0}$, because it leads to the same hP lattice type of the hexagonal system. This is an exceptional case: We follow our recipe and start from a lattice vector $\boldsymbol{a}_3$, which defines a 3-fold axis ℓ that is presumed to have the highest rotational symmetry in the holohedral group, but end up with a lattice where ℓ is an axis of 6-fold symmetry.

We now consider the other cases. Let $\boldsymbol{t}=\frac{2}{3}\boldsymbol{a}_1+\frac{1}{3}\boldsymbol{a}_2+\frac{1}{3}\boldsymbol{a}_3$ and $\boldsymbol{t}'=\frac{1}{3}\boldsymbol{a}_1+\frac{2}{3}\boldsymbol{a}_2+\frac{2}{3}\boldsymbol{a}_3$. Since $\boldsymbol{t}+\boldsymbol{t}'=\boldsymbol{a}_1+\boldsymbol{a}_2+\boldsymbol{a}_3$, we see that $\boldsymbol{t}'\in\mathcal{L}^{(p)}(\boldsymbol{t})$, $\boldsymbol{t}\in\mathcal{L}^{(p)}(\boldsymbol{t}')$, and $\mathcal{L}^{(p)}(\boldsymbol{t})=\mathcal{L}^{(p)}(\boldsymbol{t}')$. Hence cases (ii) and (iii) give rise to the same *rhombohedral* lattice (hR) with "hexagonal axes" and "triple obverse cell": $\mathsf{L}=\mathcal{L}^{(p)}(\boldsymbol{t})\cup\mathcal{L}^{(p)}(\boldsymbol{0})$. The restrictions on cell parameters for this description of the hR lattice are: $a=b$, $\alpha=\beta=\pi/2$, $\gamma=2\pi/3$. The undetermined cell parameters are a and c.

Consider now the following change of lattice basis: $\boldsymbol{a}'_1=-\boldsymbol{a}_1$, $\boldsymbol{a}'_2=-\boldsymbol{a}_2$, and $\boldsymbol{a}'_3=\boldsymbol{a}_3$. Let $\boldsymbol{t}=\frac{1}{3}\boldsymbol{a}'_1+\frac{2}{3}\boldsymbol{a}'_2+\frac{1}{3}\boldsymbol{a}'_3$ and $\boldsymbol{t}'=\frac{2}{3}\boldsymbol{a}'_1+\frac{1}{3}\boldsymbol{a}'_2+\frac{2}{3}\boldsymbol{a}'_3$, which under the primed basis correspond to Cases (iv) and (v), respectively. A moment of examination reveals that under the primed basis we have $\boldsymbol{t}'\in\mathcal{L}^{(p)}(\boldsymbol{t})$, $\boldsymbol{t}\in\mathcal{L}^{(p)}(\boldsymbol{t}')$, and $\mathcal{L}^{(p)}(\boldsymbol{t})=\mathcal{L}^{(p)}(\boldsymbol{t}')$; moreover, $\mathsf{L}:=\mathcal{L}^{(p)}(\boldsymbol{t})\cup\mathcal{L}^{(p)}(\boldsymbol{0})$ is the same hR lattice which still has "hexagonal axes" but a different unit cell called "triple reverse cell". While the "obverse" and "reverse" descriptions of the hR lattice are equivalent, it is customary in practice to keep to the obverse setting unless there are special reasons to do otherwise.

There is another description of the hR lattice where the unit cell is primitive and rhombohedral. Let $\boldsymbol{n} = \boldsymbol{a}_3/\|\boldsymbol{a}_3\|$, and let

$$\begin{aligned}\boldsymbol{b}_1 &= \frac{2}{3}\boldsymbol{a}_1 + \frac{1}{3}\boldsymbol{a}_2 + \frac{1}{3}\boldsymbol{a}_3,\\ \boldsymbol{b}_2 &= \boldsymbol{R}(\boldsymbol{n}, 2\pi/3)\,\boldsymbol{b}_1 = -\frac{1}{3}\boldsymbol{a}_1 + \frac{1}{3}\boldsymbol{a}_2 + \frac{1}{3}\boldsymbol{a}_3,\\ \boldsymbol{b}_3 &= (\boldsymbol{R}(\boldsymbol{n}, 2\pi/3))^2\,\boldsymbol{b}_1 = -\frac{1}{3}\boldsymbol{a}_1 - \frac{2}{3}\boldsymbol{a}_2 + \frac{1}{3}\boldsymbol{a}_3,\end{aligned} \tag{2.129}$$

where $\boldsymbol{a}_1$, $\boldsymbol{a}_2$, and $\boldsymbol{a}_3$ are the conventional basis vectors of the obverse-triple-cell description. Since $\boldsymbol{b}_1 = \boldsymbol{t}$ and $\boldsymbol{R}(\boldsymbol{n}, 2\pi/3)$ is a symmetry operation of the hR lattice, $\boldsymbol{b}_i$ $(i = 1, 2, 3)$ are lattice vectors. Note that $\det(\boldsymbol{b}_1, \boldsymbol{b}_2, \boldsymbol{b}_3) = \det(\boldsymbol{a}_1, \boldsymbol{a}_2, \boldsymbol{a}_3)/3 > 0$, and

$$\begin{aligned}\boldsymbol{a}_1 = \boldsymbol{b}_1 - \boldsymbol{b}_2, \qquad \boldsymbol{a}_2 = \boldsymbol{b}_2 - \boldsymbol{b}_3, \qquad \boldsymbol{a}_3 = \boldsymbol{b}_1 + \boldsymbol{b}_2 + \boldsymbol{b}_3,\\ \boldsymbol{t} = \boldsymbol{b}_1, \qquad \boldsymbol{t}' = \boldsymbol{b}_1 + \boldsymbol{b}_2.\end{aligned} \tag{2.130}$$

By (2.130) every lattice vector in the hR lattice can be expressed as a linear combination of the right-handed triad $\boldsymbol{b}_1$, $\boldsymbol{b}_2$, and $\boldsymbol{b}_3$ with coefficients being integers. Since

$$\|\boldsymbol{b}_1\| = \|\boldsymbol{R}(\boldsymbol{n}, 2\pi/3)\boldsymbol{b}_1\| = \|(\boldsymbol{R}(\boldsymbol{n}, 2\pi/3))^2\boldsymbol{b}_1\|, \tag{2.131}$$

$$\boldsymbol{b}_1 \cdot \boldsymbol{R}(\boldsymbol{n}, 2\pi/3)\boldsymbol{b}_1 = \boldsymbol{R}(\boldsymbol{n}, 2\pi/3)\boldsymbol{b}_1 \cdot (\boldsymbol{R}(\boldsymbol{n}, 2\pi/3))^2\boldsymbol{b}_1 = (\boldsymbol{R}(\boldsymbol{n}, 2\pi/3))^2 \cdot \boldsymbol{b}_1, \tag{2.132}$$

the restrictions on the rhombohedral cell parameters are: $a = b = c$, $\alpha = \beta = \gamma$. The undetermined cell parameters are a and α.

See [308, pp. 51–53] for some good depictions of the obverse, reverse, and rhombohedral unit cells of the rhombohedral lattice.

To prove that the holohedry of the hR lattice type is D_{3d}, it suffices to restrict attention to the obverse-triple-cell description. Let $\boldsymbol{e}_i$ $(i = 1, 2, 3)$ be the right-handed orthonormal triad defined by $\boldsymbol{e}_3 := \boldsymbol{n} = \boldsymbol{a}_3/\|\boldsymbol{a}_3\|$, $\boldsymbol{e}_1 := \boldsymbol{a}_1/\|\boldsymbol{a}_1\|$. We take $\boldsymbol{R}(\boldsymbol{e}_3, 2\pi/3)$, $\boldsymbol{R}(\boldsymbol{e}_1, \pi)$, and $\mathcal{I}$ as the generators of the group D_{3d} given in Table 3. By Lemma 2.39, to prove that $\boldsymbol{Q}\mathsf{L} = \mathsf{L}$ for each $\boldsymbol{Q} \in D_{3d}$, it suffices to show that for the hR lattice $\boldsymbol{R}(\boldsymbol{e}_3, 2\pi/3)\mathsf{L} = \mathsf{L}$ and $\boldsymbol{R}(\boldsymbol{e}_1, \pi)\mathsf{L} = \mathsf{L}$. For the conventional basis vectors $\boldsymbol{a}_1, \boldsymbol{a}_2, \boldsymbol{a}_3$ and for the lattice vector $\boldsymbol{t}$ in question we have

$$\begin{aligned}&\boldsymbol{R}(\boldsymbol{e}_3, 2\pi/3)\boldsymbol{a}_1 = \boldsymbol{a}_2, \qquad \boldsymbol{R}(\boldsymbol{e}_3, 2\pi/3)\boldsymbol{a}_2 = -\boldsymbol{a}_1 - \boldsymbol{a}_2, \qquad \boldsymbol{R}(\boldsymbol{e}_3, 2\pi/3)\boldsymbol{a}_3 = \boldsymbol{a}_3,\\ &\boldsymbol{R}(\boldsymbol{e}_1, \pi)\boldsymbol{a}_1 = \boldsymbol{a}_1, \qquad \boldsymbol{R}(\boldsymbol{e}_1, \pi)\boldsymbol{a}_2 = -\boldsymbol{a}_1 - \boldsymbol{a}_2, \qquad \boldsymbol{R}(\boldsymbol{e}_1, \pi)\boldsymbol{a}_3 = -\boldsymbol{a}_3,\end{aligned} \tag{2.133}$$

$$\boldsymbol{R}(\boldsymbol{e}_3, 2\pi/3)\boldsymbol{t} = \boldsymbol{t} - \boldsymbol{a}_1, \qquad \boldsymbol{R}(\boldsymbol{e}_1, \pi)\boldsymbol{t} = \boldsymbol{t}' - \boldsymbol{a}_2 - \boldsymbol{a}_3. \tag{2.134}$$

It follows from (2.133) and (2.134) that

$$\begin{aligned}&\boldsymbol{R}(\boldsymbol{e}_3, 2\pi/3)\mathcal{L}^{(p)}(\boldsymbol{0}) = \mathcal{L}^{(p)}(\boldsymbol{0}), \qquad \boldsymbol{R}(\boldsymbol{e}_1, \pi)\mathcal{L}^{(p)}(\boldsymbol{0}) = \mathcal{L}^{(p)}(\boldsymbol{0}),\\ &\boldsymbol{R}(\boldsymbol{e}_3, 2\pi/3)\mathcal{L}^{(p)}(\boldsymbol{t}) = \mathcal{L}^{(p)}(\boldsymbol{t}), \qquad \boldsymbol{R}(\boldsymbol{e}_1, \pi)\mathcal{L}^{(p)}(\boldsymbol{t}) = \mathcal{L}^{(p)}(\boldsymbol{t}') = \mathcal{L}^{(p)}(\boldsymbol{t}).\end{aligned}$$

Hence we conclude that for the hR Bravais lattice $\boldsymbol{Q}\mathsf{L} = \mathsf{L}$ for all $\boldsymbol{Q} \in D_{3d}$. The only crystallographic point groups that contain D_{3d} are of type D_{6h} or O_h. The axis defined by $\boldsymbol{a}_3$, which is a 6-fold axis of the hexagonal sub-lattice, becomes a 3-fold axis because of the presence of $\boldsymbol{t}$ and $\boldsymbol{t}'$ in the unit cell. There is no 4-fold axis of rotational symmetry. Hence there is no crystallographic point group larger than D_{3d} which keeps the hR lattice invariant.

2.8.4 The Orthorhombic and Cubic Lattice Systems

The Orthorhombic System

Let the three orthogonal 2-fold axes be ℓ_i $(i = 1, 2, 3)$. Pick one of the two shortest lattice vectors in ℓ_i as $\boldsymbol{a}_i$ and, if necessary, relabel i so that $\{\boldsymbol{a}_i\}$ constitutes a right-handed triad. Let $\boldsymbol{e}_i = \boldsymbol{a}_i/\|\boldsymbol{a}_i\|$. Apply the operator $\frac{1}{2}\boldsymbol{Z}_2^{\parallel}(\boldsymbol{e}_3, \pi)$ to both sides of (2.119), which yields (cf. equation $(2.105)_2$)

$$(\boldsymbol{I} + \boldsymbol{R}(\boldsymbol{e}_3, \pi))\,\boldsymbol{t} = 2t_3\boldsymbol{a}_3. \tag{2.135}$$

Since $(\boldsymbol{I} + \boldsymbol{R}(\boldsymbol{e}_3, \pi))\,\boldsymbol{t} \in \mathsf{L}$ and $\boldsymbol{a}_3$ is the shortest lattice vector in the direction of $\boldsymbol{a}_3$, we have $2t_3 = m_3$ or $t_3 = m_3/2$ for some $m_3 \in \mathbb{Z}$. It follows then from $0 \le t_3 < 1$ that $0 \le m_3 < 2$. Similarly, we can show for $i = 1, 2$ that $t_i = m_i/2$ for some integer m_i which satisfies $0 \le m_i < 2$. In summary, we have deduced that

$$\boldsymbol{t} = \frac{m_1}{2}\boldsymbol{a}_1 + \frac{m_2}{2}\boldsymbol{a}_2 + \frac{m_3}{2}\boldsymbol{a}_3, \qquad \text{where } m_i \in \mathbb{Z} \text{ and } 0 \le m_i < 2 \text{ for } i = 1, 2, 3. \tag{2.136}$$

There are four possible Bravais lattice types:[39]

(i) *Primitive orthorhombic* (oP): $(m_1, m_2, m_3) = (0, 0, 0)$, $\boldsymbol{t} = \boldsymbol{0}$, and $\mathsf{L} = \mathcal{L}^{(p)}(\boldsymbol{0})$.

(ii) *Based-centered orthorhombic* (oA, oB, oC; or oS): $(m_1, m_2, m_3) = (0, 1, 1)$, $(1, 0, 1)$, and $(1, 1, 0)$ for the oA, oB, oC lattice, respectively. There is one additional lattice point in the unit cell, which is placed at the center of the A face $(t_1 = 0)$ for oA, the B face $(t_2 = 0)$ for oB, and the C face $(t_3 = 0)$ for oC, respectively, for which $\boldsymbol{t} = (0, 1/2, 1/2)$, $(1/2, 0, 1/2)$, and $(1/2, 1/2, 0)$, respectively. For all three subcases, the lattice $\mathsf{L} = \mathcal{L}^{(p)}(\boldsymbol{0}) \cup \mathcal{L}^{(p)}(\boldsymbol{t})$.

The oA, oB, and oC lattices are equivalent because they can be taken as different names, which depend on how the three orthogonal 2-fold axes are labelled, given to the same lattice oS.

(iii) *Face-centered orthorhombic* (oF): If $\boldsymbol{t}_A := (0, 1/2, 1/2)$ and $\boldsymbol{t}_B := (1/2, 0, 1/2)$ are in lattice L, then $\boldsymbol{t}_C := (1/2, 1/2, 0) = (1, 0, 0) + \boldsymbol{t}_A - \boldsymbol{t}_B$ is in L. Thus it can be seen that if the unit cell $\Pi[\boldsymbol{a}_1, \boldsymbol{a}_2, \boldsymbol{a}_3]$ (see (2.31) for definition) has lattice points at the center of two of its faces, then it must also have a lattice point at the center of the remaining face. The face-centered orthorhombic (oF) lattice is given by

$$\mathsf{L} = \mathcal{L}^{(p)}(\boldsymbol{t}_A) \cup \mathcal{L}^{(p)}(\boldsymbol{t}_B) \cup \mathcal{L}^{(p)}(\boldsymbol{t}_C) \cup \mathcal{L}^{(p)}(\boldsymbol{0}).$$

(iv) *Body-centered orthorhombic* (oI): $(m_1, m_2, m_3) = (1, 1, 1)$, $\boldsymbol{t} = (1/2, 1/2, 1/2)$, and $\mathsf{L} = \mathcal{L}^{(p)}(\boldsymbol{t}) \cup \mathcal{L}^{(p)}(\boldsymbol{0})$.

The restrictions on cell parameters for all four lattice types of the orthorhombic system are: $\alpha = \beta = \gamma = \pi/2$. The undetermined cell parameters are a, b, and c.

Let us show that the holohedry of the oP, oS, oF, and oI lattice types is D_{2h}. We take $\boldsymbol{R}(\boldsymbol{e}_1, \pi)$, $\boldsymbol{R}(\boldsymbol{e}_3, \pi)$, and $\boldsymbol{\mathcal{I}}$ as the generators of group D_{2h} in Table 3. By Lemma 2.39, $\boldsymbol{\mathcal{I}}\mathsf{L} = \mathsf{L}$ for any lattice L. Hence it suffices to show that $\boldsymbol{R}(\boldsymbol{e}_1, \pi)\mathsf{L} = \mathsf{L}$ and $\boldsymbol{R}(\boldsymbol{e}_3, \pi)\mathsf{L} = \mathsf{L}$

[39] The cases where $(m_1, m_2, m_3) = (1, 0, 0)$, $(0, 1, 0)$, or $(0, 0, 1)$ are impossible, because $\pm\boldsymbol{a}_i$ are the shortest lattice vectors in ℓ_i for each i.

for lattice L of each type in the orthorhombic system. To this end, we shall use the following relations on the conventional basis vectors:

$$\begin{aligned} &\boldsymbol{R}(\boldsymbol{e}_1,\pi)\boldsymbol{a}_1=\boldsymbol{a}_1, \qquad \boldsymbol{R}(\boldsymbol{e}_1,\pi)\boldsymbol{a}_2=-\boldsymbol{a}_2, \qquad \boldsymbol{R}(\boldsymbol{e}_1,\pi)\boldsymbol{a}_3=-\boldsymbol{a}_3,\\ &\boldsymbol{R}(\boldsymbol{e}_3,\pi)\boldsymbol{a}_1=-\boldsymbol{a}_1, \qquad \boldsymbol{R}(\boldsymbol{e}_3,\pi)\boldsymbol{a}_2=-\boldsymbol{a}_2, \qquad \boldsymbol{R}(\boldsymbol{e}_1,\pi)\boldsymbol{a}_3=\boldsymbol{a}_3. \end{aligned} \tag{2.137}$$

For the oP lattice, by (2.137) we immediately see that

$$\boldsymbol{R}(\boldsymbol{e}_i,\pi)\mathsf{L}=\boldsymbol{R}(\boldsymbol{e}_i,\pi)\left(\mathcal{L}^{(p)}(\boldsymbol{0})\right)=\mathsf{L}, \qquad \text{for } i=1,3. \tag{2.138}$$

For the oS (or oA, oB, oC) and oF lattices, by (2.137) we obtain

$$\begin{aligned} &\boldsymbol{R}(\boldsymbol{e}_1,\pi)\boldsymbol{t}_A=\boldsymbol{t}_A-\boldsymbol{a}_2-\boldsymbol{a}_3, \quad \boldsymbol{R}(\boldsymbol{e}_1,\pi)\boldsymbol{t}_B=\boldsymbol{t}_B-\boldsymbol{a}_3, \quad \boldsymbol{R}(\boldsymbol{e}_1,\pi)\boldsymbol{t}_C=\boldsymbol{t}_C-\boldsymbol{a}_2,\\ &\boldsymbol{R}(\boldsymbol{e}_3,\pi)\boldsymbol{t}_A=\boldsymbol{t}_A-\boldsymbol{a}_2, \qquad \boldsymbol{R}(\boldsymbol{e}_3,\pi)\boldsymbol{t}_B=\boldsymbol{t}_B-\boldsymbol{a}_1, \qquad \boldsymbol{R}(\boldsymbol{e}_1,\pi)\boldsymbol{t}_3=\boldsymbol{t}_C-\boldsymbol{a}_1-\boldsymbol{a}_2. \end{aligned} \tag{2.139}$$

By (2.138) and (2.139), we have for the oC lattice

$$\boldsymbol{R}(\boldsymbol{e}_i,\pi)\mathsf{L}=\boldsymbol{R}(\boldsymbol{e}_i,\pi)\left(\mathcal{L}^{(p)}(\boldsymbol{t}_C)\cup\mathcal{L}^{(p)}(\boldsymbol{0})\right)=\mathsf{L}, \qquad \text{for } i=1,3.$$

Similarly, for the oA and oB lattices we conclude that $\boldsymbol{R}(\boldsymbol{e}_i,\pi)\mathsf{L}=\mathsf{L}$ for $i=1,3$. Likewise, for the oF lattice, by (2.138) and (2.139) we have

$$\boldsymbol{R}(\boldsymbol{e}_i,\pi)\mathsf{L}=\boldsymbol{R}(\boldsymbol{e}_i,\pi)\left(\mathcal{L}^{(p)}(\boldsymbol{t}_A)\cup\mathcal{L}^{(p)}(\boldsymbol{t}_B)\cup\mathcal{L}^{(p)}(\boldsymbol{t}_C)\cup\mathcal{L}^{(p)}(\boldsymbol{0})\right)=\mathsf{L}, \qquad \text{for } i=1,3.$$

For the oI lattice, by (2.137) we obtain the following relations:

$$\begin{aligned} \boldsymbol{R}(\boldsymbol{e}_1,\pi)\boldsymbol{t}&=\boldsymbol{R}(\boldsymbol{e}_1,\pi)\left(\frac{1}{2}\boldsymbol{a}_1+\frac{1}{2}\boldsymbol{a}_2+\frac{1}{2}\boldsymbol{a}_3\right)=\frac{1}{2}\boldsymbol{a}_1-\frac{1}{2}\boldsymbol{a}_2-\frac{1}{2}\boldsymbol{a}_3=\boldsymbol{t}-\boldsymbol{a}_2-\boldsymbol{a}_3,\\ \boldsymbol{R}(\boldsymbol{e}_3,\pi)\boldsymbol{t}&=-\frac{1}{2}\boldsymbol{a}_1-\frac{1}{2}\boldsymbol{a}_2+\frac{1}{2}\boldsymbol{a}_3=\boldsymbol{t}-\boldsymbol{a}_1-\boldsymbol{a}_2. \end{aligned} \tag{2.140}$$

By (2.138) and (2.140) we conclude that for the oI lattice

$$\boldsymbol{R}(\boldsymbol{e}_i,\pi)\mathsf{L}=\boldsymbol{R}(\boldsymbol{e}_i,\pi)\left(\mathcal{L}^{(p)}(\boldsymbol{t})\cup\mathcal{L}^{(p)}(\boldsymbol{0})\right)=\mathsf{L}, \qquad \text{for } i=1,3.$$

Since $\alpha=\beta=\gamma=\pi/2$ and there is no restriction on a, b, and c, there is no crystallographic point group larger than D_{2h} that preserves the lattice types in the orthorhombic system.

The Cubic System

The cubic system can be taken as a special case of the orthorhombic system where the cell parameters satisfy $a=b=c$. Except for this constraint, which can also be written as $\|\boldsymbol{a}_1\|=\|\boldsymbol{a}_2\|=\|\boldsymbol{a}_3\|$, and for one further exception, which we shall specify presently, much of what we assert about the orthorhombic system formally apply to the cubic system. The further exception is: the cubic system does not include the based-centered lattice type because the 3-fold rotation $\boldsymbol{R}((\boldsymbol{e}_1+\boldsymbol{e}_2+\boldsymbol{e}_3)/\sqrt{3},2\pi/3)\in O_h$, where $\boldsymbol{e}_i=\boldsymbol{a}_i/a$ $(i=1,2,3)$, leads to a cyclic permutation (ABC) of the three faces of the unit cell (see the proof below for details). Thus there are three Bravais lattice types in the cubic system, namely:

(i) *Primitive cubic* (cP), with lattice $\mathsf{L} = \mathcal{L}^{(p)}(\mathbf{0})$.
(ii) *Face-centered cubic* (cF), with lattice $\mathsf{L} = \mathcal{L}^{(p)}(\boldsymbol{t}_A) \cup \mathcal{L}^{(p)}(\boldsymbol{t}_B) \cup \mathcal{L}^{(p)}(\boldsymbol{t}_C) \cup \mathcal{L}^{(p)}(\mathbf{0})$, where $\boldsymbol{t}_A = \frac{1}{2}\boldsymbol{a}_2 + \frac{1}{2}\boldsymbol{a}_3$, $\boldsymbol{t}_B = \frac{1}{2}\boldsymbol{a}_3 + \frac{1}{2}\boldsymbol{a}_1$, and $\boldsymbol{t}_C = \frac{1}{2}\boldsymbol{a}_1 + \frac{1}{2}\boldsymbol{a}_2$.
(iii) *Body-centered cubic* (cI), with lattice $\mathsf{L} = \mathcal{L}^{(p)}(\boldsymbol{t}) \cup \mathcal{L}^{(p)}(\mathbf{0})$, where $\boldsymbol{t} = \frac{1}{2}\boldsymbol{a}_1 + \frac{1}{2}\boldsymbol{a}_2 + \frac{1}{2}\boldsymbol{a}_3$.

In the list above, the components of the lattice vectors $\boldsymbol{t}$, $\boldsymbol{t}_A$, $\boldsymbol{t}_B$, and $\boldsymbol{t}_C$ with respect to the basis $\boldsymbol{a}_1$, $\boldsymbol{a}_2$, and $\boldsymbol{a}_3$ are the same as their corresponding counterparts in the orthorhombic system.

The restrictions on cell parameters for all lattice types in the cubic system are: $a = b = c$, $\alpha = \beta = \gamma = \pi/2$. There is only one undetermined parameter a.

Let us prove that the holohedry of the cP, cF, and cI Bravais lattice types is O_h. In what follows all matrix representations of group elements in O_h of Table 3 refer to the right-handed orthonormal basis $\boldsymbol{e}_i = \boldsymbol{a}_i/a$ $(i = 1, 2, 3)$. Let $\boldsymbol{m} = (\boldsymbol{e}_1 + \boldsymbol{e}_2 + \boldsymbol{e}_3)/\sqrt{3}$. We take

$$\boldsymbol{R}(\boldsymbol{m}, 2\pi/3) = \begin{pmatrix} 0 & 0 & 1 \\ 1 & 0 & 0 \\ 0 & 1 & 0 \end{pmatrix}, \qquad \boldsymbol{R}(\boldsymbol{e}_3, \pi/2) = \begin{pmatrix} 0 & -1 & 0 \\ 1 & 0 & 0 \\ 0 & 0 & 1 \end{pmatrix}, \tag{2.141}$$

and the inversion $\mathcal{I}$ as the generators of O_h. By Lemma 2.39, every lattice remains invariant under the inversion $\mathcal{I}$. To establish what we want to prove, it suffices to show that $\boldsymbol{R}(\boldsymbol{m}, 2\pi/3)\mathsf{L} = \mathsf{L}$ and $\boldsymbol{R}(\boldsymbol{e}_3, \pi/2)\mathsf{L} = \mathsf{L}$ for the cP, cF, and cI Bravais lattice L, respectively. The following relations, which can be easily obtained by inspection or by direct computations, will be instrumental for our analysis:

$$\begin{aligned} &\boldsymbol{R}(\boldsymbol{m}, 2\pi/3)\boldsymbol{a}_1 = \boldsymbol{a}_2, \qquad \boldsymbol{R}(\boldsymbol{m}, 2\pi/3)\boldsymbol{a}_2 = \boldsymbol{a}_3, \qquad \boldsymbol{R}(\boldsymbol{m}, 2\pi/3)\boldsymbol{a}_3 = \boldsymbol{a}_1, \\ &\boldsymbol{R}(\boldsymbol{e}_3, \pi/2)\boldsymbol{a}_1 = \boldsymbol{a}_2, \qquad \boldsymbol{R}(\boldsymbol{e}_3, \pi/2)\boldsymbol{a}_2 = -\boldsymbol{a}_1, \qquad \boldsymbol{R}(\boldsymbol{e}_3, \pi/2)\boldsymbol{a}_3 = \boldsymbol{a}_3. \end{aligned} \tag{2.142}$$

For the primitive cubic (cP) lattice, it follows clearly from (2.142) that

$$\boldsymbol{R}(\boldsymbol{m}, 2\pi/3)\mathcal{L}^{(p)}(\mathbf{0}) = \mathcal{L}^{(p)}(\mathbf{0}), \qquad \boldsymbol{R}(\boldsymbol{e}_3, \pi/2)\mathcal{L}^{(p)}(\mathbf{0}) = \mathcal{L}^{(p)}(\mathbf{0}). \tag{2.143}$$

For the face-centered cubic (cF) lattice, by (2.142) we have

$$\boldsymbol{R}(\boldsymbol{m}, 2\pi/3)\boldsymbol{t}_A = \boldsymbol{t}_B, \qquad \boldsymbol{R}(\boldsymbol{m}, 2\pi/3)\boldsymbol{t}_B = \boldsymbol{t}_C, \qquad \boldsymbol{R}(\boldsymbol{m}, 2\pi/3)\boldsymbol{t}_C = \boldsymbol{t}_A, \tag{2.144}$$

and

$$\begin{aligned} \boldsymbol{R}(\boldsymbol{e}_3, \pi/2)\boldsymbol{t}_A &= -\frac{1}{2}\boldsymbol{a}_1 + \frac{1}{2}\boldsymbol{a}_3 = \boldsymbol{t}_B - \boldsymbol{a}_1, \\ \boldsymbol{R}(\boldsymbol{e}_3, \pi/2)\boldsymbol{t}_B &= \frac{1}{2}\boldsymbol{a}_3 + \frac{1}{2}\boldsymbol{a}_2 = \boldsymbol{t}_A, \\ \boldsymbol{R}(\boldsymbol{e}_3, \pi/2)\boldsymbol{t}_C &= \frac{1}{2}\boldsymbol{a}_2 - \frac{1}{2}\boldsymbol{a}_1 = \boldsymbol{t}_C - \boldsymbol{a}_1. \end{aligned} \tag{2.145}$$

It follows from (2.143), (2.144), and (2.145) that

$$\boldsymbol{R}(\boldsymbol{m}, 2\pi/3)\mathsf{L} = \boldsymbol{R}(\boldsymbol{m}, 2\pi/3)\left(\mathcal{L}^{(p)}(\boldsymbol{t}_A) \cup \mathcal{L}^{(p)}(\boldsymbol{t}_B) \cup \mathcal{L}^{(p)}(\boldsymbol{t}_C) \cup \mathcal{L}^{(p)}(\mathbf{0})\right) = \mathsf{L},$$

and $\boldsymbol{R}(\boldsymbol{e}_3, \pi/2)\mathsf{L} = \mathsf{L}$.

For the body-centered cubic (cI) lattice, by (2.142) we obtain

$$\boldsymbol{R}(\boldsymbol{m}, 2\pi/3)\boldsymbol{t} = \boldsymbol{R}(\boldsymbol{m}, 2\pi/3)\left(\frac{1}{2}\boldsymbol{a}_1 + \frac{1}{2}\boldsymbol{a}_2 + \frac{1}{2}\boldsymbol{a}_3\right) = \boldsymbol{t},$$
$$\boldsymbol{R}(\boldsymbol{e}_3, \pi/2)\boldsymbol{t} = \frac{1}{2}\boldsymbol{a}_2 - \frac{1}{2}\boldsymbol{a}_1 + \frac{1}{2}\boldsymbol{a}_3 = \boldsymbol{t} - \boldsymbol{a}_1. \tag{2.146}$$

By (2.143) and (2.146) we see that

$$\boldsymbol{R}(\boldsymbol{m}, 2\pi/3)\mathsf{L} = \boldsymbol{R}(\boldsymbol{m}, 2\pi/3)\left(\mathcal{L}^{(p)}(\boldsymbol{t}) \cup \mathcal{L}^{(p)}(\boldsymbol{0})\right) = \mathsf{L},$$

and $\boldsymbol{R}(\boldsymbol{e}_3, \pi/2)\mathsf{L} = \mathsf{L}$.

For later use, we write down a primitive lattice basis for the cF and cI lattice, respectively. For the face-centered cubic (cF) lattice, let

$$\boldsymbol{b}_1 = \boldsymbol{t}_A = \frac{1}{2}\boldsymbol{a}_2 + \frac{1}{2}\boldsymbol{a}_3, \quad \boldsymbol{b}_2 = \boldsymbol{t}_B = \frac{1}{2}\boldsymbol{a}_3 + \frac{1}{2}\boldsymbol{a}_1, \quad \boldsymbol{b}_3 = \boldsymbol{t}_C = \frac{1}{2}\boldsymbol{a}_1 + \frac{1}{2}\boldsymbol{a}_2. \tag{2.147}$$

We have

$$\boldsymbol{a}_1 = -\boldsymbol{b}_1 + \boldsymbol{b}_2 + \boldsymbol{b}_3, \quad \boldsymbol{a}_2 = \boldsymbol{b}_1 - \boldsymbol{b}_2 + \boldsymbol{b}_3, \quad \boldsymbol{a}_3 = \boldsymbol{b}_1 + \boldsymbol{b}_2 - \boldsymbol{b}_3. \tag{2.148}$$

Hence every lattice vector $\boldsymbol{s}$ of the cF lattice can be expressed as $\boldsymbol{s} = s_1\boldsymbol{b}_1 + s_2\boldsymbol{b}_2 + s_3\boldsymbol{b}_3$, where $s_i \in \mathbb{Z}$ $(i = 1, 2, 3)$. Thus $\boldsymbol{b}_1$, $\boldsymbol{b}_2$, and $\boldsymbol{b}_3$ constitute a primitive lattice basis of the cF lattice.

For the body-centered cubic (cI) lattice, let

$$\boldsymbol{b}_1 = -\frac{1}{2}\boldsymbol{a}_1 + \frac{1}{2}\boldsymbol{a}_2 + \frac{1}{2}\boldsymbol{a}_3 = \boldsymbol{t} - \boldsymbol{a}_1, \qquad \boldsymbol{b}_2 = \frac{1}{2}\boldsymbol{a}_1 - \frac{1}{2}\boldsymbol{a}_2 + \frac{1}{2}\boldsymbol{a}_3 = \boldsymbol{t} - \boldsymbol{a}_2,$$
$$\boldsymbol{b}_3 = \frac{1}{2}\boldsymbol{a}_1 + \frac{1}{2}\boldsymbol{a}_2 - \frac{1}{2}\boldsymbol{a}_3 = \boldsymbol{t} - \boldsymbol{a}_3. \tag{2.149}$$

Clearly $\boldsymbol{b}_i$ $(i = 1, 2, 3)$ are lattice vectors of the cI lattice. Moreover, we have

$$\boldsymbol{a}_1 = \boldsymbol{b}_2 + \boldsymbol{b}_3, \quad \boldsymbol{a}_2 = \boldsymbol{b}_3 + \boldsymbol{b}_1, \quad \boldsymbol{a}_3 = \boldsymbol{b}_1 + \boldsymbol{b}_2, \quad \boldsymbol{t} = \boldsymbol{b}_1 + \boldsymbol{b}_2 + \boldsymbol{b}_3. \tag{2.150}$$

Hence the lattice vectors $\boldsymbol{b}_i$ $(i = 1, 2, 3)$ constitute a primitive lattice basis of the cI lattice.

2.8.5 The Monoclinic and Triclinic Lattice Systems

The Monoclinic System

Let ℓ be the 2-fold rotational axis. By Lemma 2.40, there is a lattice vector parallel to ℓ and the plane, say Σ, which is normal to ℓ and contains the origin $\boldsymbol{0}$, is a lattice plane. Let $\boldsymbol{a}_3$ be one of the two shortest lattice vectors parallel to ℓ.[40] Pick two vectors $\boldsymbol{a}_1$ and $\boldsymbol{a}_2$ in Σ such that the parallelogram subtended by $\boldsymbol{a}_1$ and $\boldsymbol{a}_2$ is primitive in Σ, and that $\boldsymbol{a}_1, \boldsymbol{a}_2, \boldsymbol{a}_3$ constitute a right-handed triad. We want to investigate what additional lattice point(s) can be added to the unit cell $\Pi[\boldsymbol{a}_1, \boldsymbol{a}_2, \boldsymbol{a}_3]$; cf. Sect. 2.8.2.

[40] By convention $\boldsymbol{a}_2$ is usually taken, in crystallography, as the basis vector parallel to the 2-fold axis ℓ of the monoclinic lattice types. Here we elect to replace $\boldsymbol{a}_2$ by $\boldsymbol{a}_3$, which is taken to be parallel to a rotational axis of the highest order for the holohedry in question for the other crystal systems.

Let $\boldsymbol{t} = t_1\boldsymbol{a}_1 + t_2\boldsymbol{a}_2 + t_3\boldsymbol{a}_3$, where $0 \le t_i < 1$ $(i = 1, 2, 3)$ be a lattice vector. By $(2.102)_1$, (2.103), and (2.105), we obtain the equations

$$\frac{1}{2}\boldsymbol{Z}_2^{\perp}\boldsymbol{t} = 2(t_1\boldsymbol{a}_1 + t_2\boldsymbol{a}_2) \in \mathsf{L}, \qquad \frac{1}{2}\boldsymbol{Z}_2^{\parallel}\boldsymbol{t} = 2t_3\boldsymbol{a}_3 \in \mathsf{L}. \tag{2.151}$$

Because $\boldsymbol{a}_1$ and $\boldsymbol{a}_2$ are primitive basis vectors in the lattice plane Σ, and because $\boldsymbol{a}_3$ is a shortest lattice vector parallel to ℓ, we have $2t_1 = m_1$, $2t_2 = m_2$, and $2t_3 = m_3$, where $m_i \in \mathbb{Z}$ and $0 \le m_i < 2$ for $i = 1, 2, 3$. By our definition of $\boldsymbol{a}_i$ $(i = 1, 2, 3)$, the cases where $\boldsymbol{t}$ has one and only one non-zero component are impossible. The case $\boldsymbol{t} = (t_1, t_2, t_3) = (1/2, 1/2, 0)$ is also impossible, because it is at the center of the primitive parallelogram spanned by $\boldsymbol{a}_1$ and $\boldsymbol{a}_2$ in Σ. Thus there seem to be four possible cases: (i) $\boldsymbol{t} = \boldsymbol{0}$; (ii) $\boldsymbol{t} = (1/2, 0, 1/2)$; (iii) $\boldsymbol{t} = (0, 1/2, 1/2)$; (iv) $\boldsymbol{t} = (1/2, 1/2, 1/2)$. But, in fact there are only two, because case (ii), (iii), and (iv) are equivalent, as we shall explain.

The two cases are:

(i) *Primitive monoclinic* (mP), with $\mathsf{L} = \mathcal{L}^{(p)}(\boldsymbol{0})$.

(ii) *Base-centered monoclinic* (mA, mB, mI; or mS). Let $\boldsymbol{t}_A = \frac{1}{2}\boldsymbol{a}_2 + \frac{1}{2}\boldsymbol{a}_3$, $\boldsymbol{t}_B = \frac{1}{2}\boldsymbol{a}_1 + \frac{1}{2}\boldsymbol{a}_3$, and $\boldsymbol{t}_I = \frac{1}{2}\boldsymbol{a}_1 + \frac{1}{2}\boldsymbol{a}_2 + \frac{1}{2}\boldsymbol{a}_3$. The lattices in question are all given by the formula $\mathsf{L} = \mathcal{L}^{(p)}(\boldsymbol{t}) \cup \mathcal{L}^{(p)}(\boldsymbol{0})$, where $\boldsymbol{t} = \boldsymbol{t}_A, \boldsymbol{t}_B, \boldsymbol{t}_I$ for the mA, mB, and mI lattice, respectively. An mA and an mI lattice under the conventional basis $\{\boldsymbol{a}_i\}$ becomes an mB lattice under the basis $\boldsymbol{a}_1' = \boldsymbol{a}_2$, $\boldsymbol{a}_2' = -\boldsymbol{a}_1$, $\boldsymbol{a}_3' = \boldsymbol{a}_3$ and the basis $\boldsymbol{a}_1'' = \boldsymbol{a}_1$, $\boldsymbol{a}_2'' = \boldsymbol{a}_1 + \boldsymbol{a}_2$, $\boldsymbol{a}_3'' = \boldsymbol{a}_3$, respectively. Hence the mA, mB, and mI lattices can be taken as different descriptions of the same lattice, which is called mS.

The restrictions on cell parameters for the mP and mS (mA, mB, mI) lattices are: $\alpha = \beta = \pi/2$. The undetermined cell parameters are a, b, c, and γ.

Let us show that the holohedry of the mP and mS (mA, mB, mI) lattice types is C_{2h}: Let $\boldsymbol{n} = \boldsymbol{a}_3/\|\boldsymbol{a}_3\|$. Let $\boldsymbol{e}_i$ $(i = 1, 2, 3)$ be the right-handed orthonormal triad defined by $\boldsymbol{e}_3 := \boldsymbol{a}_3/\|\boldsymbol{a}_3\|$, $\boldsymbol{e}_1 := \boldsymbol{a}_1/\|\boldsymbol{a}_1\|$. We take $\boldsymbol{R}(\boldsymbol{e}_3, \pi)$ and $\mathcal{I}$ as the generators of the group C_{2h} given in Table 3. Since $\mathcal{I}\mathsf{L} = \mathsf{L}$ for any lattice L (see Lemma 2.39), it suffices to show that $\boldsymbol{R}(\boldsymbol{e}_3, \pi)$ preserves the mP and mB lattices. That $\boldsymbol{R}(\boldsymbol{e}_3, \pi)$ renders the mP lattice $\mathsf{L} = \mathcal{L}^{(p)}(\boldsymbol{0})$ invariant is clear from the following relations:

$$\boldsymbol{R}(\boldsymbol{e}_3, \pi)\boldsymbol{a}_1 = -\boldsymbol{a}_1, \qquad \boldsymbol{R}(\boldsymbol{e}_3, \pi)\boldsymbol{a}_2 = -\boldsymbol{a}_2, \qquad \boldsymbol{R}(\boldsymbol{e}_3, \pi)\boldsymbol{a}_3 = \boldsymbol{a}_3. \tag{2.152}$$

For the mB lattice, $\mathsf{L} = \mathcal{L}^{(p)}(\boldsymbol{t}_B) \cup \mathcal{L}^{(p)}(\boldsymbol{0})$. Since $\boldsymbol{R}(\boldsymbol{e}_3, \pi)\mathcal{L}^{(p)}(\boldsymbol{0}) = \mathcal{L}^{(p)}(\boldsymbol{0})$, to show that $\boldsymbol{R}(\boldsymbol{e}_3, \pi)\mathsf{L} = \mathsf{L}$ we just need to prove that $\boldsymbol{R}(\boldsymbol{e}_3, \pi)\mathcal{L}^{(p)}(\boldsymbol{t}_B) = \mathcal{L}^{(p)}(\boldsymbol{t}_B)$. But that follows immediately from the relation $\boldsymbol{R}(\boldsymbol{e}_3, \pi)(\boldsymbol{t}_B) = \boldsymbol{t}_B - \boldsymbol{a}_1$, which we can easily obtain from the definition of $\boldsymbol{t}_B$ and the formulas in (2.152).

Because a, b, c, and γ are undetermined, there is no crystallographic point group larger than C_{2h} which preserves the mP and the mS lattice.

The Triclinic System

All lattices L not belonging to any of the other six lattice systems are in the triclinic system. We choose a primitive lattice basis for L and call the lattice type *primitive triclinic* or primitive anorthic (aP). The aP lattice has no axis of rotational symmetry but is invariant under the inversion $\mathcal{I}$ (see Lemma 2.39). Hence its holohedry is C_i. There is no restriction on the parameters of the unit cell. All the cell parameters a, b, c, α, β, and γ are undetermined.

Table 5 The seven lattice systems

Lattice system	Cell parameters	Bravais lattice types	Holohedry
Triclinic	$a, b, c, \alpha, \beta, \gamma$	aP	C_i
Monoclinic	$a, b, c, \alpha = \beta = \frac{\pi}{2}, \gamma$	$mP, mS\,(mA, mB, mI)$	C_{2h}
Orthorhombic	$a, b, c, \alpha = \beta = \gamma = \frac{\pi}{2}$	$oP, oS\,(oA, oB, oC), oI, oF$	D_{2h}
Tetragonal	$a = b, c, \alpha = \beta = \gamma = \frac{\pi}{2}$	tP, tI	D_{4h}
Rhombohedral	$a = b, c, \alpha = \beta = \frac{\pi}{2}, \gamma = \frac{2\pi}{3}$ $a = b = c, \alpha = \beta = \gamma$	hR (hexagonal axes) (rhombohedral axes)	D_{3d}
Hexagonal	$a = b, c, \alpha = \beta = \frac{\pi}{2}, \gamma = \frac{2\pi}{3}$	hP	D_{6h}
Cubic	$a = b = c, \alpha = \beta = \gamma = \frac{\pi}{2}$	cP, cI, cF	O_h

Remark 2.45 In this section we have derived the 14 Bravais lattice types and presented a conventional lattice basis for each lattice. But every lattice L of each Bravais lattice type has a primitive basis, say $\boldsymbol{b}_1$, $\boldsymbol{b}_2$, and $\boldsymbol{b}_3$, such that $(\boldsymbol{b}_i, \boldsymbol{I})$ $(i = 1, 2, 3)$ span the lattice group $\mathcal{L}$ of the space group in question, and $\mathsf{L} = \mathcal{L}(\mathbf{0})$. We have not discussed primitive bases for the Bravais lattices except for three lattice types, namely: the rhombohedral (hR), the face-centered cubic (cF), and the body-centered cubic (cI). For further information on Bravais lattices and their primitive bases, see [177, pp. 295–313]. □

2.8.6 Summary. Metric Specialization

We summarize our findings on lattice systems in Table 5. Displayed there are the seven lattice systems, their associated Bravais lattice types and holohedries, and the restrictions imposed by symmetry on the metric parameters of the conventional unit cells. Some authors add further metric conditions on the unit cells to distinguish the lattice systems. For example, for the triclinic system, instead of the absence of any restriction on metric parameters, the conditions are written as $a \neq b \neq c$ and $\alpha \neq \beta \neq \gamma \neq \pi/2$. For the tetragonal system, the conditions on the lengths of the conventional basis vectors are put as $a = b \neq c$, instead of allowing c to be a free undetermined parameter. Such additional restrictions sometimes appear with the caution that the "$\neq$" sign or its equivalent should be interpreted as meaning "not necessarily equal to" [129, p. 43] or "not constrained by symmetry to equal" [183, p. xxii]. As such these additional conditions aren't restrictions. They are unnecessary and should simply be deleted.

As pointed out in Remark 2.11, the lattice $\mathsf{L} = \mathcal{L}(\mathbf{0})$ of an ideal crystal with space group $\mathcal{G}$ is a mathematical construct that serves as a graphical depiction of the lattice group $\mathcal{L} = \mathrm{T}(3) \cap \mathcal{G}$, which describes the translational symmetry of the crystal structure in question. The lattice L has no physical meaning independent of $\mathcal{G}$, the complete symmetry group of the crystal structure. Consider, for instance, a crystal C whose point group is of type D_{4h}. It is possible that when the metric parameters of the unit cell are determined in some ranges of temperature and pressure, the lengths a, b, and c are found to be equal within experimental precision. Such "accidental" increase in lattice symmetry is called metric specialization, "a phenomenon more frequent than is commonly thought" (see [246] and the references therein). On the other hand, under metric specialization the crystal structure of C has not changed, and the crystal still has the same space group, point group, and lattice group. The crystal has not undergone a tetragonal to cubic phase transition.

For each lattice system the restrictions on the cell parameters of a lattice L as given in Table 5 are imposed by the symmetry operations of the corresponding holohedral group $\mathcal{H}_{\mathsf{L}}$. Extraneous restrictions to disallow metric specialization are discarded.

2.9 The Seven Crystal Systems

In the preceding section we use holohedry, conventional lattice basis, and centering to classify lattices into 14 Bravais lattice types and 7 lattice systems. Here we classify the geometric crystal classes into seven crystal systems.

In this section, unless explicitly stated otherwise, all groups including generic ones such as $\mathcal{K}$ or those denoted by Schönflies symbols refer to the specific groups given in Table 3 that represent crystal classes. Let $\boldsymbol{e}_i$ $(i = 1, 2, 3)$ be the right-handed orthonormal basis under which the matrix groups in Table 3 are defined. We use the same generic or Schönflies symbol (e.g., $\mathcal{K}$, D_3) to denote a crystal class and the specific group which represents that class in Table 3. Whether the symbol refers to a crystal class or its representative given in Table 3 should be clear from the context. When confusion might arise, we will spell out what the symbol stands for.

Let A and B be subgroups of O(3). Then $A \subset B$, i.e., A is a subset of B, implies that A is a subgroup of B. Among the holohedral groups in Table 3 we have the following subset relations:

$$C_i \subset C_{2h} \subset D_{2h} \subset D_{4h} \subset O_h, \qquad C_i \subset C_{2h} \subset D_{3d} \subset O_h, \tag{2.153}$$

$$C_i \subset C_{2h} \subset D_{2h} \subset D_{6h}, \qquad C_i \subset C_{2h} \subset D_{3d} \subset D_{6h}. \tag{2.154}$$

Definition 2.46 A holohedry $\mathcal{H}$ is said to be subordinate to a holohedry $\mathcal{H}'$ (or $\mathcal{H}'$ dominates $\mathcal{H}$) if (i) $\mathcal{H} \subset \mathcal{H}'$, where the same symbols of the holohedries are used to denote the holohedral groups in Table 3 that represent them, respectively; (ii) a lattice type pertaining to holohedral group $\mathcal{H}'$ can be converted to one pertaining to $\mathcal{H}$ by an arbitrarily small continuous transformation of the basis vectors. □

It is easy to see that each subset relation of the holohedral groups in (2.153)–(2.154), with one exception, can be read also as a subordinate relation between the corresponding holohedries. The exception is $D_{3d} \subset D_{6h}$, for which condition (ii) in Definition 2.46 is not satisfied.

Let $\mathcal{K}$ be a crystallographic point group, $\mathcal{H}$ a holohedral group, and $\mathcal{K} \subset \mathcal{H}$. Clearly any lattice L invariant under the action of $\mathcal{H}$ are unchanged under $\mathcal{K}$. But there may exist lattices which remain unchanged under the action of $\mathcal{K}$ but are not invariant under $\mathcal{H}$. For instance, $D_2 \subset D_{4h}$; clearly any lattice that is invariant under the action of group D_{4h} remains so for group D_2. On the other hand, consider a lattice of type oP with conventional basis vectors $\boldsymbol{a}_1 = a\boldsymbol{e}_1$, $\boldsymbol{a}_2 = b\boldsymbol{e}_2$, $\boldsymbol{a}_3 = c\boldsymbol{e}_3$, and $a \neq b \neq c$. Such a lattice is invariant under the action of D_2 but not under D_{4h}.

Here we will present a classification of crystal classes into seven crystal systems, in which each holohedry defines a crystal system. The outstanding problem is how the merohedral crystal classes should be assigned to the seven crystal systems. To describe precisely what we are going to do, we introduce another definition.

Let a Cartesian coordinate system be chosen. In the definition below the matrix groups that represent the 32 crystal classes are those given in Table 3. All of them are defined with respect to the chosen Cartesian coordinate system. The 14 lattice types are those described

in Sect. 2.8. There, for each lattice type, the orthonormal basis vectors $\boldsymbol{e}_i$ $(i = 1, 2, 3)$ are expressed in terms of the conventional lattice basis vectors $\boldsymbol{a}_i$, from which the inverse relations follow immediately.

Definition 2.47 A crystal class represented by point group $\mathcal{K}$ is said to be compatible with a lattice type if there is a space group $\mathcal{G}$ with associated point group $\mathcal{K}$ and lattice L of the given type. □

We want to assign the merohedral crystal classes into the seven crystal systems such that the representative groups of crystal classes in the same crystal system are compatible with the same lattice types. A necessary condition for a merohedral crystal class to be compatible with a lattice type is clearly that the representative point group of the merohedral class be a subgroup of the representative holohedral group of the lattice type in question.

Let $\mathcal{K}$ be the representative point group of a merohedral class, $\mathcal{H}$ be the smallest holohedral group that contains $\mathcal{K}$ as a subgroup, and $\mathcal{H}'$ be another holohedral group that contains $\mathcal{K}$. Then we have $\mathcal{K} \subset \mathcal{H} \subset \mathcal{H}'$. Consider, for example, $D_2 \subset D_{2h} \subset D_{4h}$, where $\mathcal{H} = D_{2h}$ is the smallest holohedral group that contains $\mathcal{K} = D_2$ as a subgroup and $\mathcal{H}' = D_{4h}$. Note that D_{2h} is subordinate to the holohedry D_{4h}. Putting the D_2 class in the crystal system defined by the D_{4h} holohedry would result in an unstable arrangement because a lattice of type D_{4h} would be reduced to one of type D_{2h} by an arbitrarily small continuous transformation of the basis vectors $\boldsymbol{a}$ or $\boldsymbol{b}$ that yields $a \neq b$. A similar assertion applies to the cases where $\mathcal{H}' = D_{6h}$ or O_h, each of which dominates D_{2h}. Because of this, and because symmetry restrictions allow metric specialization, the lattice types compatible with the D_2 class should be those pertaining to the D_{2h} holohedry. In general, if $\mathcal{H}$ is the smallest holehedral group containing the merohedral class $\mathcal{K}$, and if $\mathcal{H}$ is subordinate to any holohedral group $\mathcal{H}'$ that contains it as a subgroup, then $\mathcal{K}$ is assigned to the crystal system defined by $\mathcal{H}$, and the lattice types compatible with the crystal class $\mathcal{K}$ are those pertaining to the holohedral class $\mathcal{H}$.

The only instance that requires separate consideration is $\mathcal{H} = D_{3d}$ and $\mathcal{H}' = D_{6h}$, where $D_{3d} \subset D_{6h}$ but D_{3d} is not subordinate to D_{6h}. In this case each merohedral class $\mathcal{K}$ which has D_{3d} as the smallest holehedral group containing it is still assigned to the crystal system defined by D_{3d}. The lattice types compatible with the crystal class $\mathcal{K}$, however, are hP and hR.

We formalize in Definition 2.48 the afore-described way of classifying crystal classes into crystal systems. Recall that for a finite group G, $|G|$ stands for the number of elements in G.

Definition 2.48 Each holohedry defines a crystal system. A crystal class specified by representative group $\mathcal{K}$ belongs to the crystal system defined by the holohedry with representative group $\mathcal{H}$ if

(i) $\mathcal{K}$ is a subgroup of $\mathcal{H}$;
(ii) the number $|\mathcal{H}|/|\mathcal{K}|$ is as small as possible. □

Table 6 displays the seven crystal systems and the crystal classes assigned to them according to conventions (i) and (ii) in Definition 2.48. In the table are also listed the lattice types which are compatible with the members of each crystal system.

Table 6 The seven crystal systems and their crystal classes

Crystal system	Crystal classes	Compatible lattice types
Triclinic	$C_1, \underline{C_i}$	aP
Monoclinic	$C_2, C_s, \underline{C_{2h}}$	$mP, mS\,(mA, mB, mI)$
Orthorhombic	$D_2, C_{2v}, \underline{D_{2h}}$	$oP, oS\,(oA, oB, oC), oI, oF$
Tetragonal	$C_4, S_4, C_{4h}, D_4, C_{4v}, D_{2d}, \underline{D_{4h}}$	tP, tI
Trigonal	$C_3, C_{3i}, D_3, C_{3v}, \underline{D_{3d}}$	hP, hR
Hexagonal	$C_6, C_{3h}, C_{6h}, D_6, C_{6v}, D_{3h}, \underline{D_{6h}}$	hP
Cubic	$T, T_h, T_d, O, \underline{O_h}$	cP, cI, cF

The holohedries are underlined

2.10 Some Crystal Structures and their Space Groups

In this exposition we shall restrict attention to three simple crystal structures, namely: the face-centered cubic structure (fcc), the body-centered cubic structure (bcc), and the hexagonal close-packed structure (hcp). About 50% of the elements crystallize in one of these structures under room temperature and normal pressure [308, Table 14, p. 88]. In particular, these three crystal structures are of prime importance in metallurgy. To wit, austenitic steels, aluminum, copper, nickel, silver, etc. have fcc structure. Ferritic steels, β titanium, chromium, molybdenum, tungsten, etc. have bcc structure. Magnesium, α titanium, zinc, cobalt, cadmium, etc. have hcp structure.

The bonding between metal atoms is typically metallic. "Because the valence electrons are in conduction bands and are free to migrate throughout the structure, the metal atoms tend to pack together in highly ordered arrangements that minimize void space." ([247, p. 57]; see also [198, pp. 178–180]). As far as crystal structure of a pure metal is concerned, a simple model which works quite well is to take the metal atoms as impenetrable hard spheres of a given radius. Under this hard-sphere model, the atoms in a metal crystal are congruent spheres, and the tightness of packing is described by a parameter called packing density. Let $\mathscr{S}$ be a packing of hard spheres, $\Pi[\boldsymbol{a}_1, \boldsymbol{a}_2, \boldsymbol{a}_3]$ the conventional unit cell, and $\mathrm{V}(\cdot)$ the Euclidean volume. The packing density is defined as[41]

$$D := \frac{\mathrm{V}(\Pi[\boldsymbol{a}_1, \boldsymbol{a}_2, \boldsymbol{a}_3] \cap \mathscr{S})}{\mathrm{V}(\Pi[\boldsymbol{a}_1, \boldsymbol{a}_2, \boldsymbol{a}_3])}. \tag{2.155}$$

Remark 2.49 Mathematical studies on the packing of congruent (or "equal") spheres have a long history [135]. Packings where the centers of the spheres form a three-dimensional lattice are called regular or lattice packings. Those aren't are called irregular or nonlattice packings. Definition 2.155 for the packing density clearly covers lattice packings and more (e.g., the hcp structure is a nonlattice packing, but its packing density is given by (2.155)). In 1831 Gauss [123] proved that among all lattice packings the face-centered cubic (fcc) structure is the densest with $D = \pi/\sqrt{18} \approx 0.74048\cdots$.[42]

[41] Here we use the conventional unit cell for convenience in computations. The value of D remains unchanged if we use any primitive unit cell instead.

[42] The original proof by Gauss is based on the theory of the arithmetic reduction of a ternary form. Dempster [87] provides an elementary proof, which John Todd describes in *Mathematical Reviews* (MR0085281) as

In 1611 Kepler [174] published a booklet in which he posed several deep scientific questions and offered some insightful speculations. Among the topics covered is the packing of equal spheres. Kepler examines sphere packings whose centers occupy lattices that are simple cubic, face-centered cubic (examined twice, in two perspectives), and hexagonal, where each sphere touches six, twelve, and eight neighboring spheres, respectively. He asserts [174, p. 57] that the fcc packing "is the tightest possible arrangement, and no other could fit more spheres in the same container." Mathematicians have rewritten this assertion in various mathematically precise ways to obtain different versions of Kepler's conjecture. One version, after the definition of packing density is extended to cover infinite nonlattice packings in E^3, is called "the Kepler conjecture" [134]: "No packing of congruent balls in Euclidean three-space has density greater than that of the face-centered cubic packing." Likewise, one may consider [156, Chap. 1] finite sphere packings without container. For our purposes, we need not go into the intricate mathematics of general sphere packings. It suffices to note what follows. Mathematical studies on infinite sphere packings and finite packings without container have all led to the inequality $D \leq \pi/\sqrt{18}$, where D is some suitably defined packing density for the setting in question. Moreover, the maximum value of $D = \pi/\sqrt{18}$ is attained by the close-packed structures, to which we now turn. □

2.10.1 Close-Packed Structures

The close-packed structures are what Barlow and Pope [20] call "the closest packed homogeneous assemblages of equal spheres" in their 1907 paper.

All three-dimensional close-packed structures are built up of planar layers of congruent hard spheres. In each layer the hard spheres are packed together in the densest way so that each sphere is surrounded by six of its peers.[43] Take one layer, and denote by Σ the plane that contains all the centers of spheres pertaining to the layer in question. We choose a unit normal $\boldsymbol{n}$ to Σ so that the top and bottom of the layer are well defined. Fix one sphere in the layer, and call its center O. Let the centers of the six spheres that surround the one with center O be $A_1, A_2, \ldots, A_6$ (going counter-clockwise about $\boldsymbol{n}$ at O), respectively. The line segments $A_1A_2, A_2A_3, \ldots, A_6A_1$ are the sides of a regular hexagon. This hexagon will be divided into six equilateral triangles if line segments OA_i $(i = 1, \ldots, 6)$ are added to join its vertices to O.

To understand how different three-dimensional close-packed structures can be constructed from the same building element, i.e., the planar layer described in the preceding

"very simple ..., using extremely elementary geometrical methods." Coxeter [78, pp. 335–337] adds three figures and a few more explanations to Dempster's proof, which further enhances its readability. Hales [136, pp. 13–14] presents "a short proof that does not require any calculations." That proof starts from the densest packing of equal spheres along an infinite linear string, then proceeds to the densest packing of such parallel strings to form a sheet, and finally advances to the densest stacking of such sheet layers to form the densest three-dimensional lattice packing of the spheres. The argument is similar to a discussion of Hilbert and Cohn-Vossen [152, pp. 45–46]. However Dempster, who was clearly aware of the discussion of Hilbert and Cohn-Vossen, seemed to have found the argument still wanting and proceeded to devise another proof.

[43] The packing of a planar layer of congruent hard spheres is densest if the packing of their circular cross-sections is closest in the plane that contains the centers of the spheres. For two-dimensional lattice packings it is easy to prove (see, e.g., [152, pp. 35–36]) that the packing is closest if and only if the lattice is built up of equilateral triangles, where each circle touches six neighbors, i.e., the packing is hexagonal. After the definition of packing density is extended to cover nonlattice packings, Thue's theorem asserts that a packing of congruent hard disks in the plane is densest among all possible packings if and only if the packing is hexagonal. For an elementary proof of Thue's theorem, see Hales [136, pp. 14–15] for a sketch and Casselman [72] for more details; information on Voronoi cell decomposition of the plane ($\mathbb{R}^2$) can be read off from [136, pp. 146–148], where parallel information for $\mathbb{R}^3$ is given.

paragraph, we have to examine the geometry of the planar layer more carefully. Let us go back to the layer discussed above, which we call the A-layer. The centers of all the hard spheres in the A-layer constitute a two-dimensional lattice in Σ, which we shall also call an A-plane. Let $\boldsymbol{a}_1 := \mathbf{OA}_1$ and $\boldsymbol{a}_2 := \mathbf{OA}_3$. Note that $\|\boldsymbol{a}_1\| = \|\boldsymbol{a}_2\| = a$ is the diameter of the spheres, and the angle between $\boldsymbol{a}_1$ and $\boldsymbol{a}_2$ is $2\pi/3$. The two-dimensional lattice of the A-centers in Σ is $\llcorner_A := \{s_1\boldsymbol{a}_1 + s_2\boldsymbol{a}_2 : s_1, s_2 \in \mathbb{Z}\}$. The two-dimensional primitive unit cell of the lattice $\llcorner_A$ is the parallelogram $P[\boldsymbol{a}_1, \boldsymbol{a}_2] = \{t_1\boldsymbol{a}_1 + t_2\boldsymbol{a}_2 : 0 \le t_i < 1\ (i = 1, 2)\}$, which consists of two equilateral triangles. In the unit cell $P[\boldsymbol{a}_1, \boldsymbol{a}_2]$ there are two hollow areas, with centers located at $\mathbf{OB} := \frac{2}{3}\boldsymbol{a}_1 + \frac{1}{3}\boldsymbol{a}_2$ and $\mathbf{OC} := \frac{1}{3}\boldsymbol{a}_1 + \frac{2}{3}\boldsymbol{a}_2$, which are the centers of the two equilateral triangles that make up P, respectively. We call $\mathbf{OB}$ and $\mathbf{OC}$ the B-center and C-center of the unit cell P, respectively. Let $\mathcal{L}_2 := \{s_1\boldsymbol{a}_1 + s_2\boldsymbol{a}_2 : s_1, s_2 \in \mathbb{Z}\}$ be the group of two-dimensional translations such that $\mathcal{L}_2(\mathbf{0}) = \llcorner_A$. The elements of $\mathcal{L}_2(\mathbf{OB})$ and $\mathcal{L}_2(\mathbf{OC})$ are the B-centers and C-centers of the translates of P, respectively.

There are two possible ways to add a second close-packed layer of spheres on top of the A-layer so that the distance between the two planes of centers is shortest, namely: the centers of all the spheres of the second layer are either (i) directly above the B-centers or (ii) above the C-centers of the A-plane (i.e., plane Σ). For case (i) and case (ii), we call the second layer a B-layer and a C-layer, respectively, and we denote the sequence of layers AB and AC, respectively. For definiteness, let us consider the AB (resp. AC) layer sequence and examine the B-plane (resp. C-plane) that contains the centers of spheres in the B (resp. C) layer. It is easily seen from the geometry that the hollow areas in the B-plane have their centers located directly above the A-centers and C-centers (resp. B-centers) of the plane Σ.

When a third close-packed layer is added on top of the B-layer (resp. C-layer) of the AB (resp. AC) layer sequence, there are again two possibilities: the centers of the spheres of the third layer can be placed either directly above the A-centers or above the C-centers (resp. B-centers) of the plane Σ, thus resulting in the ABA or ABC (resp. ACA or ACB) three-layer sequence.

It should now be clear that a great variety of three-dimensional close-packed structures is possible. In what follows we shall study in more detail the following close-packed structures and their space groups:

- the hexagonal close-packed (hcp) structure, with layer sequence $\cdots ABABAB\cdots$;
- the cubic close-packed (ccp) structure, with layer sequence $\cdots ABCABC\cdots$, which is better known as the face-centered cubic (fcc) structure.

Barlow and Pope [20] call the ccp and hcp structures cubic closest packing and hexagonal closest packing, respectively. Just like Kepler before and others (see, e.g., [37, pp. 248–249], [247, p. 57]) after them, they chose the superlative "closest" to describe the packing of spheres in the ccp and hcp structures. Their choice could only have been guided by a conviction based on observations and physical intuition. After the proof [134, 137] of the Kepler conjecture, however, this conviction has gained a mathematical justification.

2.10.2 Hexagonal Close-Packed Structure

The hexagonal close-packed (hcp) structure was first noticed by Barlow [19]. It has the layer sequence $\cdots ABABAB\cdots$. Clearly its Bravais lattice is of the primitive hexagonal type. In Sect. 2.10.1 we have defined the primitive basis vectors $\boldsymbol{a}_1$ and $\boldsymbol{a}_2$ in the A-plane Σ. The primitive basis vector $\boldsymbol{a}_3$ is parallel to the unit normal $\boldsymbol{n}$ to the plane Σ. Let us determine its length $\|\boldsymbol{a}_3\| = c$. In what follows a position vector $\boldsymbol{t} = t_1\boldsymbol{a}_1 + t_2\boldsymbol{a}_2 + t_3\boldsymbol{a}_3$ will be written as (t_1, t_2, t_3).

By symmetry the distance between the A- and B-plane of two contiguous layers is equal to $c/2$. Consider the sphere with center $\mathtt{A} := \mathtt{O} = (0, 0, 0)$ (which is an A-center) in the plane Σ and its contiguous peer with center $\mathtt{B} := (\frac{2}{3}, \frac{1}{3}, \frac{1}{2})$ in the neighboring B-layer, which is directly above a B-center in Σ. Let $\mathtt{P} := (\frac{2}{3}, \frac{1}{3}, 0)$ be the projection of $\mathtt{B}$ onto the plane Σ. Consider the right-angled triangle $\mathtt{BPO}$. The length of the hypotenuse $\mathtt{OB}$ is a, as it is the distance between the centers of two touching spheres. The length of $\mathtt{BP}$ is $c/2$, which is the perpendicular distance between the A- and B-plane in question. Since $\mathtt{P}$ is the center and $\mathtt{O}$ a vertex of an equilateral triangle (with the length of each side equal to a) in the plane Σ, the length of $\mathtt{OP}$ is $\frac{2}{3} \times \frac{\sqrt{3}}{2} \times a = a/\sqrt{3}$. By Pythagoras theorem, we get $c = \sqrt{8/3}\, a$.

The lattice group of the hcp structure is $\mathcal{L} = \{(\boldsymbol{u}, \boldsymbol{I}) : \boldsymbol{u} = u_1\boldsymbol{a}_1 + u_2\boldsymbol{a}_2, +u_3\boldsymbol{a}_3,\ u_i \in \mathbb{Z} \text{ for } i = 1, 2, 3\}$.

The family of lines $\{(\frac{1}{3}, \frac{2}{3}, t) + (u_1, u_2, u_3) : -\infty < t < \infty\}$, where $(u_1, u_2, u_3) \in \mathbb{Z}^3$, contains the C-centers of all the A- and B-planes. None of the lines in this family intersects any of the spheres in the hcp structure. Since

$$(\mathbf{0}, \boldsymbol{\mathcal{I}})\mathtt{B} = (\mathbf{0}, \boldsymbol{\mathcal{I}})(\tfrac{2}{3}, \tfrac{1}{3}, \tfrac{1}{2}) = (-\tfrac{2}{3}, -\tfrac{1}{3}, -\tfrac{1}{2}) = (\tfrac{1}{3}, \tfrac{2}{3}, -\tfrac{1}{2}) + (-1, -1, 0),$$

it is in one of the lines that does not intersect any of spheres in the hcp structure. Hence the origin $\mathtt{O}$ isn't a center of inversion of the structure. But, in fact, we can move the origin of the affine coordinate system to an inversion center of the structure.

Indeed, let $\boldsymbol{O} = (\frac{1}{3}, \frac{2}{3}, \frac{1}{4})$. When the origin of the affine coordinate system is moved to $\boldsymbol{O}$, the coordinates of the A-center and B-center in the original unit cell are:

$$\begin{aligned}
\boldsymbol{A} &:= (0, 0, 0) - (\tfrac{1}{3}, \tfrac{2}{3}, \tfrac{1}{4}) = (-\tfrac{1}{3}, -\tfrac{2}{3}, -\tfrac{1}{4}) \cong (\tfrac{2}{3}, \tfrac{1}{3}, \tfrac{3}{4}),\\
\boldsymbol{B} &:= (\tfrac{2}{3}, \tfrac{1}{3}, \tfrac{1}{2}) - (\tfrac{1}{3}, \tfrac{2}{3}, \tfrac{1}{4}) = (\tfrac{1}{3}, -\tfrac{1}{3}, \tfrac{1}{4}) \cong (\tfrac{1}{3}, \tfrac{2}{3}, \tfrac{1}{4}),
\end{aligned}$$

where the symbol "$\cong$" here signifies that $\mathcal{L}(\boldsymbol{A})$ (resp. $\mathcal{L}(\boldsymbol{B})$) remains the same irrespective of whether $(-\frac{1}{3}, -\frac{2}{3}, -\frac{1}{4})$ or $(\frac{2}{3}, \frac{1}{3}, \frac{3}{4})$ (resp. $(\frac{1}{3}, -\frac{1}{3}, \frac{1}{4})$ or $(\frac{1}{3}, \frac{2}{3}, \frac{1}{4})$) is used to represent $\boldsymbol{A}$ (resp. $\boldsymbol{B}$). After moving the origin to $\boldsymbol{O}$, all lattice points in $\mathtt{L} = \mathcal{L}(\boldsymbol{O})$ are located in the C-hollows. Under the new coordinate system, the unit cell $\Pi[\boldsymbol{a}_1, \boldsymbol{a}_2, \boldsymbol{a}_3]$ has the atoms (i.e., the spheres in the model) centered at $\boldsymbol{A} = (\frac{2}{3}, \frac{1}{3}, \frac{3}{4})$ and $\boldsymbol{B} = (\frac{1}{3}, \frac{2}{3}, \frac{1}{4})$ as "basis".[44] The entire hcp structure is: $\mathcal{L}(\boldsymbol{A}) \cup \mathcal{L}(\boldsymbol{B})$. For each $\boldsymbol{s} = (\frac{2}{3}, \frac{1}{3}, \frac{3}{4}) + (u_1, u_2, u_3) \in \mathcal{L}(\boldsymbol{A})$, where $(u_1, u_2, u_3) \in \mathbb{Z}^3$, we have

$$\begin{aligned}
(\mathbf{0}, \boldsymbol{\mathcal{I}})\boldsymbol{s} &= (-\tfrac{2}{3}, -\tfrac{1}{3}, -\tfrac{3}{4}) + (-u_1\boldsymbol{a}_1 - u_2\boldsymbol{a}_2 - u_3\boldsymbol{a}_3)\\
&= (\tfrac{1}{3}, \tfrac{2}{3}, \tfrac{1}{4}) + (-(u_1 + 1)\boldsymbol{a}_1 - (u_2 + 1)\boldsymbol{a}_2 - (u_3 + 1)\boldsymbol{a}_3) \in \mathcal{L}(\boldsymbol{B}) \qquad (2.156)
\end{aligned}$$

Similarly, we can easily show that if $\boldsymbol{s} \in \mathcal{L}(\boldsymbol{B})$, then $(\mathbf{0}, \boldsymbol{\mathcal{I}})\boldsymbol{s} \in \mathcal{L}(\boldsymbol{A})$. Hence

$$(\mathbf{0}, \boldsymbol{\mathcal{I}})\mathcal{L}(\boldsymbol{A}) = \mathcal{L}(\boldsymbol{B}) \qquad (\mathbf{0}, \boldsymbol{\mathcal{I}})\mathcal{L}(\boldsymbol{B}) = \mathcal{L}(\boldsymbol{A}),$$

which imply

$$(\mathbf{0}, \boldsymbol{\mathcal{I}})\,(\mathcal{L}(\boldsymbol{A}) \cup \mathcal{L}(\boldsymbol{B})) = \mathcal{L}(\boldsymbol{A}) \cup \mathcal{L}(\boldsymbol{B}).$$

Therefore $(\mathbf{0}, \boldsymbol{\mathcal{I}}) \in \mathcal{G}$, the space group of the ideal crystal with the hcp structure.

[44] Cf. Remark 2.14 for the meaning of the term "basis" here.

Next consider the rigid transplacements $(c\boldsymbol{n}/2, \boldsymbol{R}(\boldsymbol{n}, \pi/3))$, where $\boldsymbol{n} = \boldsymbol{a}_3/c$, and $(\boldsymbol{0}, \boldsymbol{R}(\boldsymbol{a}_1/a, \pi))$. The former isometry is called a screw rotation, because it is a rotation coupled with a translation along the rotation axis, and the latter is a rotation about $\boldsymbol{a}_1$ by angle π. Let us examine the effects of these isometries on an arbitrary vector $\boldsymbol{x} := x_1\boldsymbol{a}_1 + x_2\boldsymbol{a}_2 + x_3\boldsymbol{a}_3 \in E^3$. First recall that for the isometry $(\boldsymbol{v}, \boldsymbol{Q})$,

$$(\boldsymbol{v}, \boldsymbol{Q})\boldsymbol{x} = \boldsymbol{v} + \boldsymbol{Q}\boldsymbol{x} = \boldsymbol{v} + x_1\boldsymbol{Q}\boldsymbol{a}_1 + x_2\boldsymbol{Q}\boldsymbol{a}_2 + x_3\boldsymbol{Q}\boldsymbol{a}_3. \tag{2.157}$$

For the two rigid transplacements in question, we observe that

$$\boldsymbol{R}(\boldsymbol{n}, \pi/3)(\boldsymbol{a}_1, \boldsymbol{a}_2, \boldsymbol{a}_3) = (\boldsymbol{a}_1 + \boldsymbol{a}_2, -\boldsymbol{a}_1, \boldsymbol{a}_3), \tag{2.158}$$

$$\boldsymbol{R}(\boldsymbol{a}_1/a, \pi)(\boldsymbol{a}_1, \boldsymbol{a}_2, \boldsymbol{a}_3) = (\boldsymbol{a}_1, -\boldsymbol{a}_1 - \boldsymbol{a}_2, -\boldsymbol{a}_3). \tag{2.159}$$

For $\boldsymbol{s} = (\frac{2}{3}, \frac{1}{3}, \frac{3}{4}) + (u_1, u_2, u_3) \in \mathcal{L}(\boldsymbol{A})$, by (2.157)–(2.159) we have

$$\begin{aligned}(\boldsymbol{a}_3/2, \boldsymbol{R}(\boldsymbol{a}_3/c, \pi/3))\boldsymbol{s} &= (0, 0, \tfrac{1}{2}) + (\tfrac{2}{3} + u_1)(1, 1, 0) + (\tfrac{1}{3} + u_2)(-1, 0, 0) \\ &\quad + (\tfrac{3}{4} + u_3)(0, 0, 1) \\ &= (\tfrac{1}{3}, \tfrac{2}{3}, \tfrac{1}{4}) + (u_1 - u_2, u_1, u_3 + 1) \in \mathcal{L}(\boldsymbol{B}); \end{aligned} \tag{2.160}$$

$$\begin{aligned}(\boldsymbol{0}, \boldsymbol{R}(\boldsymbol{a}_1/a, \pi))\boldsymbol{s} &= (\tfrac{2}{3} + u_1)(1, 0, 0) + (\tfrac{1}{3} + u_2)(-1, -1, 0) + (\tfrac{3}{4} + u_3)(0, 0, -1) \\ &= (\tfrac{1}{3}, \tfrac{2}{3}, \tfrac{1}{4}) + (u_1 - u_2, -(u_2 + 1), -(u_3 + 1)) \in \mathcal{L}(\boldsymbol{B}). \end{aligned} \tag{2.161}$$

Similarly, for $\boldsymbol{s} = (\frac{1}{3}, \frac{2}{3}, \frac{1}{4}) + (u_1, u_2, u_3) \in \mathcal{L}(\boldsymbol{B})$, by (2.157)–(2.159) we obtain

$$(\boldsymbol{a}_3/2, \boldsymbol{R}(\boldsymbol{n}, \pi/3))\boldsymbol{s} = (\tfrac{2}{3}, \tfrac{1}{3}, \tfrac{3}{4}) + (u_1 - u_2 - 1, u_1, u_3) \in \mathcal{L}(\boldsymbol{A}); \tag{2.162}$$

$$(\boldsymbol{0}, \boldsymbol{R}(\boldsymbol{a}_1/a, \pi))\boldsymbol{s} = (\tfrac{2}{3}, \tfrac{1}{3}, \tfrac{3}{4}) + (u_1 - u_2 - 1, -(u_2 + 1), -(u_3 + 1)) \in \mathcal{L}(\boldsymbol{A}). \tag{2.163}$$

Hence the rigid transplacements $(\boldsymbol{a}_3/2, \boldsymbol{R}(\boldsymbol{a}_3/c, \pi/3))$ and $(\boldsymbol{0}, \boldsymbol{R}(\boldsymbol{a}_1/a, \pi))$ preserve the crystal pattern $\mathcal{L}(\boldsymbol{A}) \cup \mathcal{L}(\boldsymbol{B})$ of the hcp structure, and they are in the space group $\mathcal{G}$ of the ideal crystal in question. Also, it is obvious that the translations $(\boldsymbol{a}_1, \boldsymbol{I})$, $(\boldsymbol{a}_2, \boldsymbol{I})$, and $(\boldsymbol{a}_3, \boldsymbol{I})$ are in the same space group $\mathcal{G}$.

In fact the six rigid transplacements $(\boldsymbol{a}_3/2, \boldsymbol{R}(\boldsymbol{a}_3/c, \pi/3))$, $(\boldsymbol{0}, \boldsymbol{R}(\boldsymbol{a}_1/a, \pi))$, $(\boldsymbol{0}, \mathcal{I})$, $(\boldsymbol{a}_1, \boldsymbol{I})$, $(\boldsymbol{a}_2, \boldsymbol{I})$, and $(\boldsymbol{a}_3, \boldsymbol{I})$ generate the space group $P6_3/mmc$ (no. 194) [133, pp. 600–601].

2.10.3 Interlude: Symmorphic Types of Space Groups

Let L be a Bravais lattice which has its lattice point group $\mathcal{H}_\mathsf{L}$ given by a holohedral group in Table 3. Recall that each holohedral group in Table 3 is a matrix group defined with respect to a Cartesian coordinate system, which has its origin $\boldsymbol{O}$ located at a lattice point of the lattice L in question and has its orthonormal basis $\{\boldsymbol{e}_i\}$ defined by their relations with the conventional basis $\{\boldsymbol{a}_i\}$ of L; see Sect. 2.8. Let $\mathcal{L}$ be the lattice group corresponding to L and $\mathcal{L}(\boldsymbol{0}) = \mathsf{L}$. Let $\mathcal{K} \subset \mathcal{H}_\mathsf{L}$ be a crystallographic point group that leaves L invariant, and let

$$\hat{\mathcal{K}} := \{(\boldsymbol{0}, \boldsymbol{Q}) \in \mathrm{E}(3) : \boldsymbol{Q} \in \mathcal{K}\}. \tag{2.164}$$

Note that $\hat{\mathcal{K}}$ is the subgroup of isometries on E^3 which consists of rotations or roto-inversions with the origin $\boldsymbol{O}$ as a fixed point, is isomorphic to $\mathcal{K}$, and leaves the lattice L invariant. Instead of $\mathcal{K}$, some authors refer to $\hat{\mathcal{K}}$ as crystallographic point group; cf. Remark 2.17. We shall follow this convention at times when it is convenient to do so.

Both $\mathcal{L}$ and $\hat{\mathcal{K}}$ are subgroups of the Euclidean group E(3). Let

$$\mathcal{G} := \{(\boldsymbol{v}, \boldsymbol{I})(\boldsymbol{0}, \boldsymbol{Q}) : (\boldsymbol{v}, \boldsymbol{I}) \in \mathcal{L}, (\boldsymbol{0}, \boldsymbol{Q}) \in \hat{\mathcal{K}}\}. \tag{2.165}$$

Since $(\boldsymbol{v}, \boldsymbol{I})(\boldsymbol{0}, \boldsymbol{Q}) = (\boldsymbol{v}, \boldsymbol{Q}) \in \mathrm{E}(3)$, clearly $\mathcal{G} \subset \mathrm{E}(3)$. For $(\boldsymbol{v}_i, \boldsymbol{Q}_i) \in \mathcal{G}$ $(i = 1, 2)$, by (2.15) we have $(\boldsymbol{v}_2, \boldsymbol{Q}_2)(\boldsymbol{v}_1, \boldsymbol{Q}_1) = (\boldsymbol{v}_2 + \boldsymbol{Q}_2\boldsymbol{v}_1, \boldsymbol{Q}_2\boldsymbol{Q}_1) \in \mathcal{G}$, because $\boldsymbol{Q}\mathsf{L} = \mathsf{L}$ for each $\boldsymbol{Q} \in \mathcal{K}$. Also, for $(\boldsymbol{v}, \boldsymbol{Q}) \in \mathcal{G}$, by (2.13) we have $(\boldsymbol{v}, \boldsymbol{Q})^{-1} = (-\boldsymbol{Q}^{-1}\boldsymbol{v}, \boldsymbol{Q}^{-1}) \in \mathcal{G}$. Hence $\mathcal{G}$ is a subgroup of E(3).

For $(\boldsymbol{v}, \boldsymbol{Q}) \in \mathcal{G}$ and $(\boldsymbol{u}, \boldsymbol{I}) \in \mathcal{L}$, by the same calculations as those in (2.36) we obtain

$$(\boldsymbol{v}, \boldsymbol{Q})(\boldsymbol{u}, \boldsymbol{I})(\boldsymbol{v}, \boldsymbol{Q})^{-1} = (\boldsymbol{Q}\boldsymbol{u}, \boldsymbol{I}) \in \mathcal{L}. \tag{2.166}$$

Hence $\mathcal{L}$ is a normal subgroup of $\mathcal{G}$. It is easy to see that $\mathcal{L} = \mathcal{G} \cap \mathrm{T}(3)$ and the quotient group

$$\mathcal{G}/\mathcal{L} = \{(\boldsymbol{0}, \boldsymbol{Q})\mathcal{L} : \boldsymbol{Q} \in \mathcal{K}\} \tag{2.167}$$

is isomorphic to $\mathcal{K}$. Thus $\mathcal{G}$ is a space group with lattice group $\mathcal{L}$ and crystallographic point group $\mathcal{K}$.

In the discussion above, we have also shown that $\mathcal{G}$ is the semi-direct product (see [42, p. 14] and Definition A.28 in Appendix A) of $\mathcal{L}$ and $\hat{\mathcal{K}}$, i.e.,

$$\mathcal{G} = \mathcal{L} \wedge \hat{\mathcal{K}}. \tag{2.168}$$

A space group $\mathcal{G}$ which is the semi-direct product of its lattice group $\mathcal{L}$ and its crystallographic point group $\hat{\mathcal{K}}$ is said to be symmorphic. A space-group type is symmorphic if its members are equivalent symmorphic space groups. Clearly an ordered pair such as (aP, C_1) or (cF, O_h), where the second entry is a representative point group of a crystal class and the first entry is a lattice type compatible with the group in question, defines a symmorphic type of space groups. From Table 6 of Sect. 2.9, we see that there are 66 such pairs. If each pair gives rise to one symmorphic type of space groups, there will be 66 symmorphic types. A closer examination, however, reveals that there are seven pairs which correspond to two distinguished crystal patterns. Take the pairing of the group C_{2v} and the base-centered orthorhombic lattice type oS (oA, oB, oC) for example. If the directions specified by $\boldsymbol{e}_1$, $\boldsymbol{e}_2$, and $\boldsymbol{e}_3$ are equivalent, then the base-centered orthorhombic lattice types oA, oB, and oC are equivalent. They may all be called oS. The group C_{2v} given in Table 3, however, has only one 2-fold axis, which is parallel to $\boldsymbol{e}_3$. Then the pairs (oC, C_{2v}) and (oA, C_{2v}), which have the 2-fold axis perpendicular and parallel to the centered face, respectively, specify two different symmorphic types, namely $Cmm2$ (no. 35) and $Amm2$ (no. 38) in the *ITA* [133, pp. 238–239, 244–245], respectively. In what follows all page numbers refer to those in the fifth edition of *ITA* [133]. The other six pairings which yield two symmorphic types are as follows: (tP, D_{2d}): $P\bar{4}2m$ (no. 111) and $P\bar{4}m2$ (no. 115), pp. 406–407 and 414–415, respectively; (tI, D_{2d}): $I\bar{4}2m$ (no. 119) and $I\bar{4}m2$ (no. 121), pp. 422–423 and 426–427, respectively; (hP, D_3): $P312$ (no. 149) and $P321$ (no. 150), pp. 504–505 and 506–507, respectively; (hP, C_{3v}): $P3m1$ (no. 156) and $P31m$ (no. 157), pp. 520–521 and 522–523, respectively; (hP, D_{3d}): $P\bar{3}1m$ (no. 162) and $P\bar{3}m1$ (no. 164), pp. 530–537 and 540–541,

respectively; (hP, D_{3h}): $P\bar{6}m2$ (no. 187) and $P\bar{6}2m$ (no. 189), pp. 586–587 and 590–591, respectively.

There are thus a total of 73 symmorphic types of space groups. They are listed and their *ITA* numbers given, e.g., in Table 5.1 and Appendix 7 of [129, pp. 92, 337–345].

2.10.4 Face-Centered Cubic Structure

In the face-centered cubic (fcc) or cubic close-packed (ccp) structure, the centers of hard spheres, which model atoms, occupy the nodes of a face-centered cubic lattice (cF) so that each sphere touches 12 of its peers. For definiteness, consider a specific cF lattice and Cartesian coordinate system as described in Sect. 2.8.4. Then we have $\|\boldsymbol{a}_i\| = a$, $\boldsymbol{e}_i = \boldsymbol{a}_i/a$ $(i = 1, 2, 3)$. Let r be the radius of the spheres. The spheres with centers located at $(0, 0, 0)$ and $(a, a, 0)$ touch the one centered at $(a/2, a/2, 0)$, which implies $a = 4r\cos(\pi/4)$ or $a = 2\sqrt{2}r$. It follows that the packing density of the face-centered cubic structure is (cf. (2.155))

$$D = \frac{4 \cdot \frac{4}{3}\pi r^3}{(2\sqrt{2}r)^3} = \frac{\pi}{\sqrt{18}} = 0.74048\cdots, \tag{2.169}$$

the maximum density of all packings of equal spheres (cf. Remark 2.49).

Note that the lattice vectors (cf. (2.147))

$$\boldsymbol{b}_1 = (0, a/2, a/2), \qquad \boldsymbol{b}_2 = (a/2, 0, a/2), \qquad \boldsymbol{b}_3 = (a/2, a/2, 0) \tag{2.170}$$

constitute a primitive lattice basis that generate the cF lattice in question. These points are the vertices of an equilateral triangle of side $2r$ in the lattice plane $x + y + z = a$. Hence the spheres centered at $\boldsymbol{b}_i$ $(i = 1, 2, 3)$ define a planar close-packed layer of spheres. Consider the family of lattice planes Σ_m defined by the equations $x + y + z = ma$, where $m \in \mathbb{Z}$. The vector $\boldsymbol{n} = (1, 1, 1)/\sqrt{3}$ is a unit normal of all the lattice planes in the family. The distance between two consecutive planes Σ_m and Σ_{m+1} in the family is $a/\sqrt{3} = \sqrt{8/3}\,r$, which is exactly the distance between the planes of centers of two consecutive layers in a close-packed structure. Hence the face-centered cubic structure is a close-packed structure.

The sphere with center $(0, 0, 0)$ belongs to the Σ_0 layer, say, of type A. Let us call the Σ_1 layer, which contains the points $\boldsymbol{b}_i$ $(i = 1, 2, 3)$, of type B. None of the centers of spheres in the Σ_2 plane, which include the points $(a, a/2, a/2)$, $(a/2, a, a/2)$, and $(a/2, a/2, a)$, after perpendicular projection to the Σ_0 plane, falls on the origin $(0, 0, 0)$. Indeed the only point in the Σ_2 plane which falls onto $(0, 0, 0)$ under perpendicular projection is $(2a/3, 2a/3, 2a/3)$, which is not the center of any sphere in the Σ_2 layer. Hence the Σ_2 layer cannot be of type A. Then it must be of type C; cf. Sect. 2.10.1. On the other hand, the point (a, a, a) is the center of a sphere in the Σ_3 layer and its projection to the Σ_0 plane is the origin. Thus the Σ_3 layer is of type A. By symmetry of the crystal structure under the translation $\boldsymbol{b}_1 + \boldsymbol{b}_2 + \boldsymbol{b}_3 = (a, a, a)$, the face-centered cubic structure is close-packed with layer sequence $\cdots ABCABC\cdots$.

The space group of the fcc structure described above is the semi-direct product $\mathcal{G} = \mathcal{L}_F \wedge \hat{O}_h$, where $\mathcal{L}_F$ is the lattice group generated by $(\boldsymbol{b}_i, \boldsymbol{I})$ $(i = 1, 2, 3)$, $\hat{O}_h = \{(\boldsymbol{0}, \boldsymbol{Q}) \in \mathrm{E}(3) : \boldsymbol{Q} \in O_h\}$, and O_h has $\boldsymbol{R}((\boldsymbol{e}_1 + \boldsymbol{e}_2 + \boldsymbol{e}_3)/\sqrt{3}, 2\pi/3)$, $\boldsymbol{R}(\boldsymbol{e}_3, \pi/2)$, and $\boldsymbol{\mathcal{I}}$ as generators. The space-group type is $Fm\bar{3}m$ (no. 225) in the *ITA* [133, pp. 688–691].

2.10.5 Body-Centered Cubic Structure

In the body-centered cubic (bcc) structure, the centers of hard spheres, which model atoms, occupy the nodes of a body-centered cubic lattice (cI) such that each pair of diagonally opposite spheres in the unit cell touch the central one. For definiteness, consider a specific cI lattice and Cartesian coordinate system as described in Sect. 2.8.4. Then we have $\|\boldsymbol{a}_i\| = a$, $\boldsymbol{e}_i = \boldsymbol{a}_i/a$ $(i = 1, 2, 3)$. Let r be the radius of the spheres. The spheres with centers located at $(0, 0, 0)$ and (a, a, a) touch the one centered at $(a/2, a/2, a/2)$, which implies $3a^2 = (4r)^2$ or $a = 4r/\sqrt{3}$. It follows that the packing density of the body-centered cubic structure is (cf. (2.155))

$$D = \frac{2 \cdot \frac{4}{3}\pi r^3}{(4r/\sqrt{3})^3} = \frac{\sqrt{3}\pi}{8} = 0.68017\cdots . \tag{2.171}$$

Recall that the lattice vectors (cf. (2.8.4))

$$\boldsymbol{b}_1 = (-a/2, a/2, a/2), \qquad \boldsymbol{b}_2 = (a/2, -a/2, a/2), \qquad \boldsymbol{b}_3 = (a/2, a/2, -a/2) \tag{2.172}$$

constitute a primitive lattice basis that generate the cI lattice in question. The space group of the bcc structure described above is the semi-direct product $\mathcal{G} = \mathcal{L}_I \wedge \hat{O}_h$, where $\mathcal{L}_I$ is the lattice group generated by $(\boldsymbol{b}_i, \boldsymbol{I})$ $(i = 1, 2, 3)$, $\hat{O}_h = \{(\boldsymbol{0}, \boldsymbol{Q}) \in \mathrm{E}(3) : \boldsymbol{Q} \in O_h\}$, and O_h has $\boldsymbol{R}((\boldsymbol{e}_1 + \boldsymbol{e}_2 + \boldsymbol{e}_3)/\sqrt{3}, 2\pi/3)$, $\boldsymbol{R}(\boldsymbol{e}_3, \pi/2)$, and $\boldsymbol{\mathcal{I}}$ as generators. The space-group type is $Im\bar{3}m$ (no. 229) in the *ITA* [133, pp. 712–714].

2.11 Complete Symmetry Group of Single Crystal in Macroscopic Physics

In macroscopic physics, e.g., in continuum mechanics [322, pp. 264–270], an "undistorted" single crystal (i.e., what we call an ideal crystal modeled at the macro-scale) is taken as a homogeneous continuous medium, which is invariant under any translation $(\boldsymbol{v}, \boldsymbol{I}) \in \mathrm{T}(3)$ (where $\boldsymbol{v} \in V$) and has its complete symmetry group consist of elements of the form $(\boldsymbol{v}, \boldsymbol{I})(\boldsymbol{0}, \boldsymbol{Q}) = (\boldsymbol{v}, \boldsymbol{Q})$, where $\boldsymbol{Q} \in \mathcal{K}$, the crystallographic point group of the ideal crystal. Let us see how this practice can be reconciled with the analysis so far in this chapter.

Recall that the space group $\mathcal{G}$ of an ideal crystal $(\mathsf{C}, \boldsymbol{\kappa}_0)$ can be taken as a disjoint union of left cosets (see Sect. 2.3.4). Each coset consists of elements of the form $(\boldsymbol{\alpha} + \boldsymbol{t}, \boldsymbol{Q})$, where $(\boldsymbol{\alpha}, \boldsymbol{I})$, $(\boldsymbol{t}, \boldsymbol{I}) \in \mathrm{T}(3)$ and $\boldsymbol{Q} \in \mathrm{O}(3)$, with the following properties: (i) $\boldsymbol{Q} \in \mathcal{K}$, where $\mathcal{K}$ is the crystallographic point group of $\mathcal{G}$, is the same for all elements in the same coset and is different for elements belonging to different cosets. (ii) $\boldsymbol{\alpha} \in \Pi$, where the primitive unit cell Π is defined in Sect. 2.3.2, and it is the same for all elements of the same coset but may be different for different cosets. (iii) $\boldsymbol{t} \in \mathcal{L}$, the lattice group of $\mathcal{G}$, and it runs over $\mathcal{L}$ to cover all the elements of the same coset.

Let us examine the elements $(\boldsymbol{\alpha} + \boldsymbol{t}, \boldsymbol{Q})$ of the space group $\mathcal{G}$ more closely. For metallic elements that crystallize in the bcc, fcc, or hcp structure, at room temperature and normal pressure the lattice parameters $\|\boldsymbol{a}_i\|$ $(i = 1, 2, 3)$ are of the order of angstroms (Å; 1 Å $= 10^{-10}$ m); see, e.g., [308, Chapter III, Tables 9, 10, and 13]. Take, for example, an aluminum single crystal, which has face-centered cubic (fcc) structure (see Sect. 2.10.4). The conventional lattice vectors are usually taken to be $\boldsymbol{a}_i = a\boldsymbol{e}_i$ $(i = 1, 2, 3)$, where a is the lattice parameter and $\boldsymbol{e}_i$ are the orthonormal basis vectors of a Cartesian coordinate system. A commonly adopted set of primitive basis vectors $\boldsymbol{b}_i$ is given by (2.170). Accordingly we have $\|\boldsymbol{b}_1\| = \|\boldsymbol{b}_2\| = \|\boldsymbol{b}_3\| = a/\sqrt{2} \approx 2.86 \times 10^{-10}$ m, where the value of $a \approx 4.0496$ Å is taken from [308, p. 74, Table 10]. For the fcc structure, $\boldsymbol{\alpha} = \boldsymbol{0}$ for every coset. In general,

since $\boldsymbol{\alpha} \in \Pi$ (the primitive unit cell), the magnitude of the vector $\boldsymbol{\alpha}$ is either zero or of the same order of the lattice parameters $\|\boldsymbol{b}_i\|$. Hence, to the macroscopic observer, $\boldsymbol{\alpha}$ is in effect zero. For each translation $(\boldsymbol{v}, \boldsymbol{I}) \in \mathrm{T}(3)$, there are translations $(\boldsymbol{t}, \boldsymbol{I}) \in \mathcal{L}$ which cannot be distinguished from $(\boldsymbol{v}, \boldsymbol{I})$ by macroscopic observations. A single crystal behaves macroscopically as if it is homogeneous, and so is it modeled in macroscopic physics. The elements of the complete symmetry group of the single crystal $(\mathsf{C}, \boldsymbol{\kappa}_0)$ appears macroscopically to be $(\boldsymbol{v}, \boldsymbol{Q}) = (\boldsymbol{v}, \boldsymbol{I})(\boldsymbol{0}, \boldsymbol{Q})$, where $(\boldsymbol{v}, \boldsymbol{I})$ runs over T(3) and $\boldsymbol{Q}$ over the crystallographic point group $\mathcal{K}$ in question. In other words, in macroscopic physics the complete symmetry group of a single crystal is the semidirect product $\mathrm{T}(3) \wedge \hat{\mathcal{K}}$, where $\hat{\mathcal{K}} = \{(\boldsymbol{0}, \boldsymbol{Q}) \in \mathrm{E}(3) : \boldsymbol{Q} \in \mathcal{K}\}$ and $\mathcal{K}$ is one of the 32 crystallographic point groups.[45]

The present exposition concerns texture analysis as a branch of macroscopic physics, in which microscopic aspects of crystal structure (e.g., space groups, etc.) play a secondary role in the theoretical development. On the other hand, measurements of macro-texture, be it by X-ray diffraction (XRD) or by electron back-scatter diffraction (EBSD), rely on physics at the atomic scale. In this regard, knowledge about certain microscopic aspects of crystal structure becomes indispensable, and it will lead to deeper understanding of the subject.

Remark 2.50 An ideal crystal $(\mathsf{C}, \boldsymbol{\kappa}_0)$, at the macro-scale, becomes a homogenized version of itself, which we denote for clarity by $(\mathsf{C}, \boldsymbol{\kappa}_0)_{\mathrm{mac}}$; here the subscript "mac" means "the homogenized crystal at the macro-scale". While the complete symmetry group of the ideal crystal $(\mathsf{C}, \boldsymbol{\kappa}_0)$ is its space group $\mathcal{G}$, that of the undistorted single crystal $(\mathsf{C}, \boldsymbol{\kappa}_0)_{\mathrm{mac}}$ is the semidirect product $\mathrm{T}(3) \wedge \hat{\mathcal{K}}$, where $\mathcal{K}$ is the crystallographic point group of $\mathcal{G}$.[46] In this exposition we study texture analysis as a branch of macroscopic physics. Henceforth in the theoretic development of texture analysis, we shall mostly work with the macroscopic version $(\mathsf{C}, \boldsymbol{\kappa}_0)_{\mathrm{mac}}$ of the single crystal in question. But we shall have to refer also to the ideal crystal at the atomic scale when we discuss measurements of crystallographic texture that are made possible by microscopic observations. For simplicity we shall drop the subscript "mac" and denote the ideal crystal modeled at the macro-scale also by $(\mathsf{C}, \boldsymbol{\kappa}_0)$ when no confusion should arise. Whenever clarity is called for, we will either revert to using $(\mathsf{C}, \boldsymbol{\kappa}_0)_{\mathrm{mac}}$ or state explicitly what the symbol $(\mathsf{C}, \boldsymbol{\kappa}_0)$ denotes. □

[45] Cf. Miller [232, p. 55] for a similar discussion.

[46] For classical texture analysis, $\mathcal{K}$ is restricted to be one of the 11 finite rotation groups that satisfy the crystallographic restriction; thus $\boldsymbol{Q}$ is a rotation in that context.

Chapter 3

3 The Invariant Integral on SO(3)

For a first reading, the reader may glance over the introductory remarks in Sect. 3.1, stop after reading Sect. 3.1.2, skip the proofs, accept explicit formulas (3.36) and (3.49) for the invariant integral on SO(3), read Sect. 3.6 and accept the properties of the invariant integral summarized there, and move on to Chap. 4.

3.1 Introductory Remarks on Orientation Measures

Throughout this exposition we shall restrict our attention to polycrystals whose constituting crystallites are all of the same kind. For motivation of what we shall do in this chapter, it suffices to restrict attention to a substance S whose crystallites are triclinic.[47]

3.1.1 Crystallite Orientation at a Point in a Polycrystalline Sample

In first approximation, a polycrystalline sample $\mathcal{P}$ of substance S can be taken as an aggregate of single crystallites of S, which have different orientations in space and are separated by grain boundaries. The preceding assertion, however, will make sense only after the word "orientation" is defined.

Let $\mathtt{X}$ be a point in the polycrystalline sample $\mathcal{P}$, which does not fall on a grain boundary. To define crystallite orientation at the point $\mathtt{X}$, we start by choosing a reference ideal single crystal $(\mathsf{C}, \boldsymbol{\kappa}_0)$. As discussed in Remark 2.50, as far as macroscopic response of the ideal crystal is concerned, the fine details of crystal structure are blurred out; the ideal crystal behaves as if it is homogeneous (i.e., invariant under translations). In fact the symbol $(\mathsf{C}, \boldsymbol{\kappa}_0)_{\text{mac}}$ is introduced in Remark 2.50 to denote the ideal crystal $(\mathsf{C}, \boldsymbol{\kappa}_0)$ in macroscopic physics. In classical texture analysis, the complete symmetry group of $(\mathsf{C}, \boldsymbol{\kappa}_0)_{\text{mac}}$ consists elements of the form $(\boldsymbol{v}, \boldsymbol{I})(\boldsymbol{0}, \boldsymbol{R})$, where $(\boldsymbol{v}, \boldsymbol{I})$ is any translation in T(3) and $\boldsymbol{R}$ is a rotation in $\mathcal{K}$, the crystallographic point group of the ideal crystal (restricted to be one of the 11 finite rotation groups that satisfy the crystallographic restriction). Suppose we can identify a right-handed triad $\{\boldsymbol{f}_i : i = 1, 2, 3\}$ attached to any point in $(\boldsymbol{\kappa}_0(\mathsf{C}))_{\text{mac}}$—recall that at the macros-scale the reference single crystal is translation-invariant—and at the point $\mathtt{X}$ the corresponding triad becomes $\{\boldsymbol{R}\boldsymbol{f}_i : i = 1, 2, 3\}$ (we take $\mathtt{X}$ as the starting point of this triad), where $\boldsymbol{R}$ is a rotation. Then with respect to the reference single crystal the crystallite orientation at $\mathtt{X}$ is defined by the rotation $\boldsymbol{R}$. While following this outline to ascertain the crystallite orientation at $\mathtt{X}$ by macroscopic measurements is difficult, individual orientation measurements can be made with microscopic techniques, e.g., via orientation imaging microscopy (OIM; see Chap. 8). At the length scale of angstroms, we can choose a lattice in $\boldsymbol{\kappa}_0(\mathsf{C})$, say with conventional basis vectors $\{\boldsymbol{a}_i : i = 1, 2, 3\}$. Then the rotation $\boldsymbol{R}$ that takes the lattice basis vectors $\{\boldsymbol{a}_i\}$ in $\boldsymbol{\kappa}_0(\mathsf{C})$ to their counterparts $\{\boldsymbol{R}\boldsymbol{a}_i\}$ at $\mathtt{X}$ can be inferred from OIM measurements. The triad of lattice basis vectors $\{\boldsymbol{a}_i\}$ can be taken as one choice of $\{\boldsymbol{f}_i\}$ at the macro-scale, and the rotation $\boldsymbol{R}$, which takes $\{\boldsymbol{a}_i\}$ to $\{\boldsymbol{R}\boldsymbol{a}_i\}$, defines also the crystallite orientation at $\mathtt{X}$ with respect to the reference single crystal $(\boldsymbol{\kappa}_0(\mathsf{C}))_{\text{mac}}$.

From the preceding discussion, it is clear that there is a one-to-one correspondence between rotations and the orientations of the triclinic crystallite with respect to the chosen reference. Thus the rotation group SO(3) can be identified with the space of all possible orientations of the triclinic crystallite. We proceed next to have a first look at orientation measures defined on the orientation space SO(3) of the triclinic crystallite.

[47] As we shall see, the triclinic case occupies a central position in the Roe approach to texture analysis.

3.1.2 Orientation Measures

Consider a manufacturing process $\mathfrak{P}$ which produces polycrystalline samples of a substance S that can be taken as macroscopically identical. In texture analysis, we assume that each of the samples produced by process $\mathfrak{P}$ is a realization of what we call the (theoretical) polycrystal P specific to $\mathfrak{P}$, and P is a mathematical idealization. In what follows we shall use the term "polycrystal P" in two senses: (1) We take P geometrically as a set of points (similar to an abstract body in continuum mechanics), which is mapped bijectively onto each sample or realization, say $\mathcal{P}_\beta$, of it. Thus for a point $\mathtt{X}$ in P, we can identify the corresponding point in each $\mathcal{P}_\beta$, which we denote also by $\mathtt{X}$ for simplicity. (2) We take P as a probability space (see Definition C.7 in Appendix C), the sample space of which is the set of all its possible realizations. In general, in which sense we mean when we refer to polycrystal P should be clear from the context. To proceed further, one could (or should, if the preference is to go logically from the general to the particular) start with a mathematical model of a polycrystal P as a probability space (see e.g., Paroni [253, Sect. 2]). As our objective here, namely to present the rudiments of classical texture analysis, has a very limited scope, we take an easier route.

Take an ensemble $\mathcal{E} = \{\mathcal{P}_\alpha\}$ of samples produced by $\mathfrak{P}$ and measure the crystallite orientation $\boldsymbol{R}_\alpha$ at the same location $\mathtt{X}$ within each sample $\mathcal{P}_\alpha$ of the ensemble. By discarding a sample from the ensemble if the point $\mathtt{X}$ in that sample falls on a grain boundary,[48] we can say that a measurement at $\mathtt{X}$ on each $\mathcal{P}_\alpha$ delivers a well-defined crystallite orientation $\boldsymbol{R}_\alpha$. The resulting orientations $\boldsymbol{R}_\alpha$ will vary over the ensemble. In fact, if the ensemble does not show any preferred orientations at $\mathtt{X}$, the set of data points $\{\boldsymbol{R}_\alpha\}$ will largely distribute in SO(3) evenly. A fundamental assumption in classical texture analysis is that the set of data points $\{\boldsymbol{R}_\alpha\}$ is characterized by a probability measure $\wp(\cdot; \mathtt{X})$ on SO(3) that pertains to the polycrystal P specific to the process $\mathfrak{P}$. We call $\wp(\cdot; \mathtt{X})$ the orientation (probability) measure at $\mathtt{X}$, which defines the crystallographic texture at $\mathtt{X}$. Mathematically there is a large collection $\mathfrak{B}$ of subsets A of SO(3) called Borel sets[49] which are measurable, i.e., for which $\wp(A; \mathtt{X})$, the probability that the crystallite orientation $\boldsymbol{R}$ at $\mathtt{X}$ belongs to A, is defined. In particular, for any orientation measure $\wp(\cdot; \mathtt{X}) : \mathfrak{B} \to [0, 1]$, the empty set $\emptyset$ and the rotation group SO(3) itself are measurable, and

$$\wp(\emptyset; \mathtt{X}) = 0, \qquad \wp(\mathrm{SO}(3); \mathtt{X}) = 1, \tag{3.1}$$

which say that the probability of finding the crystallite orientation at $\mathtt{X}$ does not and does belong to SO(3) is 0 and 1, respectively. If the orientation measure $\wp(\cdot; \mathtt{X})$ remains the same

[48] Grain boundaries are not explicitly specified in the theoretical polycrystal P, but they may and generally will appear in realizations of P. We assume that in every realization the set of points in grain boundaries is of zero volume in three-dimensional space. They do not play any role in macro-texture analysis and will be ignored in this exposition.

[49] See Definition C.2 in Appendix C. In Appendices B and C the reader will find some basic definitions in topology and measure theory, respectively. The following brief description is meant for readers unfamiliar with measure theory, an intuitive grasp of which should suffice for reading the main contents of Part I (cf. also Footnote 50). The term "measure" is a technical description of "volume", and "measurable set" is a set which has a well-defined measure. Probability measures and volume measures cannot be assigned to all subsets of the rotation group SO(3) so that they enjoy properties necessary for the definition of the Lebesgue integral. Hence we restrict our discussion to a family $\mathfrak{B}$, albeit a large family, of "measurable" sets called the Borel sets of SO(3). Here we need not go into technical details about Borel sets. Suffice it to say that the empty set $\emptyset$, the entire space SO(3), all open subsets and all closed subsets of SO(3) belong to $\mathfrak{B}$; so are the union, intersection, and set difference of two Borel sets. Moreover, for every topological space its Borel sets are well defined.

for all $\mathtt{X}$ in a polycrystal P, we say that the polycrystal P has a statistically homogeneous crystallographic texture, in which case we will write $\wp(\cdot)$ for $\wp(\cdot;\mathtt{X})$. In what follows, for simplicity we shall suppress the general dependence of $\wp$ on the point $\mathtt{X}$ in question except for occasions that we want to emphasize that dependence. A formula where $\wp(\cdot)$ appears will be applicable to both the cases that the orientation measure pertains to a point $\mathtt{X} \in \mathsf{P}$ or to a statistically homogeneous P.

A simple example of orientation measure is that which pertains to a single triclinic crystal with orientation $\boldsymbol{R}_o$ with respect to the chosen reference $(\mathsf{C}, \boldsymbol{\kappa}_0)$, where we have suppressed the subscript "mac". Note that at the macro-scale $\boldsymbol{\kappa}_0(\mathsf{C})$ is homogeneous. For the ensemble in question, the orientation measure is given by the Dirac measure at $\boldsymbol{R}_o$, i.e.,

$$\wp(A) = \delta_{\boldsymbol{R}_o}(A) := \begin{cases} 1 & \text{if } \boldsymbol{R}_o \in A \\ 0 & \text{if } \boldsymbol{R}_o \notin A, \end{cases} \quad \text{for each measurable } A \subset \mathrm{SO}(3). \tag{3.2}$$

Consider another ensemble $\boldsymbol{Q}\mathcal{E}$ obtained by letting each sample in $\mathcal{E}$ undergo a rotation $\boldsymbol{Q}$. A sample $\mathcal{P}_\alpha$ in $\mathcal{E}$ with crystallite orientation $\boldsymbol{R}_\alpha$ at $\mathtt{X}$ has orientation $\boldsymbol{R} = \boldsymbol{Q}\boldsymbol{R}_\alpha$ at the same point in sample $\boldsymbol{Q}\mathcal{P}_\alpha$ of ensemble $\boldsymbol{Q}\mathcal{E}$. Let $\grave{\wp}$ and $\wp$ be the orientation measures which characterize crystallographic texture at $\mathtt{X}$ for the ensemble $\boldsymbol{Q}\mathcal{E}$ and $\mathcal{E}$, respectively. Let $A \subset \mathrm{SO}(3)$ be measurable and $\boldsymbol{Q}A := \{\boldsymbol{Q}\boldsymbol{R} : \boldsymbol{R} \in A\}$. Clearly, we have

$$\wp(A) = \grave{\wp}(\boldsymbol{Q}A) \qquad \text{for each } \boldsymbol{Q} \in \mathrm{SO}(3) \text{ and each measurable } A \subset \mathrm{SO}(3). \tag{3.3}$$

For the special case where all orientations are equally probable at $\mathtt{X}$, let $\wp_{\mathrm{iso}}$ be the orientation measure in question. From its physical meaning, we expect that $\wp_{\mathrm{iso}}$ should satisfy the requirement

$$\wp_{\mathrm{iso}}(A) = \wp_{\mathrm{iso}}(\boldsymbol{Q}A) \qquad \text{for each } \boldsymbol{Q} \in \mathrm{SO}(3) \text{ and each measurable } A \subset \mathrm{SO}(3). \tag{3.4}$$

In the ensemble $\mathcal{E} = \{\mathcal{P}_\alpha\}$, the rotation $\boldsymbol{R}_\alpha$ which describes the crystallite orientation at $\mathtt{X}$ of sample $\mathcal{P}_\alpha$ depends also on the choice of the reference configuration $\boldsymbol{\kappa}_0(\mathsf{C})$ for the single crystal. Suppose another configuration $\boldsymbol{Q} \circ \boldsymbol{\kappa}_0(\mathsf{C})$, which results after the homogeneous configuration $\boldsymbol{\kappa}_0(\mathsf{C})$ undergoes a rotation $\boldsymbol{Q}$, is chosen as reference. With respect to the new reference, the crystallite orientation at $\mathtt{X}$ of $\mathcal{P}_\alpha$ is described by the rotation $\boldsymbol{R} = \boldsymbol{R}_\alpha \boldsymbol{Q}^{-1}$, and the orientation measure at $\mathtt{X}$ of the polycrystal is also changed. It is $\check{\wp}$ defined by

$$\check{\wp}(A) = \wp(A\boldsymbol{Q}) \qquad \text{for each measurable } A \subset \mathrm{SO}(3), \tag{3.5}$$

where $A\boldsymbol{Q} = \{\boldsymbol{R}\boldsymbol{Q} : \boldsymbol{R} \in A\}$ and $\wp$ is the orientation measure of the polycrystal at $\mathtt{X}$ with respect to the original reference $\boldsymbol{\kappa}_0(\mathsf{C})$. For the special case where $\wp = \wp_{\mathrm{iso}}$, clearly there holds $\check{\wp} = \wp_{\mathrm{iso}}$. By (3.5), we have

$$\wp_{\mathrm{iso}}(A) = \wp_{\mathrm{iso}}(A\boldsymbol{Q}) \qquad \text{for each } \boldsymbol{Q} \in \mathrm{SO}(3) \text{ and each measurable } A \subset \mathrm{SO}(3). \tag{3.6}$$

A positive measure μ on the measurable space $(\mathrm{SO}(3), \mathfrak{B})$ is said to be left-invariant (resp. right-invariant) if it, like $\wp_{\mathrm{iso}}$, satisfies (3.4) (resp. (3.6)). The measure μ is bi-invariant (or invariant, for short) if it is both left- and right-invariant. The discussions above indicate that our physical formulation demands the existence of an invariant probability measure on the rotation group SO(3).[50]

[50]The main contents of Part I of this exposition have been written such that no prior preparations in general topology and measure theory would be necessary for reading. On the other hand, a number of sections and

Remark 3.1 As we shall explain in Chap. 10 of Part II, the rotation group is a compact topological group (cf. Definitions C.12 and C.13). It is well known (see Theorem C.14 and Corollary C.15 in Appendix C) that every compact topological group has a unique bi-invariant probability measure called the normalized Haar measure. In this exposition, however, we shall avoid dwelling into abstract mathematical theory as far as possible. In this chapter we will focus on the rotation group SO(3). □

3.1.3 Ensemble Average and Volume Average

In a thought experiment, the orientation measure $\wp(\cdot; \mathtt{X})$ at a point $\mathtt{X}$ of a polycrystal P can be determined on a countably infinite ensemble $\mathcal{E} = \{\mathcal{P}_\alpha\}$ of macroscopically identical samples of P. In practice, of course that can not be done. If the samples are statistically homogeneous, the question arises whether making orientation measurements at $\mathtt{X}$ of each $\mathcal{P}_\alpha$ of the ensemble could be replaced by making suitable measurements on one sample.

One possibility is suggested by a version of the ergodic theorem. Consider a polycrystal P of triclinic crystallites that pertains to a given manufacturing process $\mathfrak{P}$. We model the polycrystal as a probability space $(\Xi, \mathfrak{S}, \widetilde{P})$; see Definition C.7 in Appendix C. In our model each sample or realization of polycrystal P occupies the entire 3-dimensional space, which we denote by $\mathbb{R}^3$ after we have chosen a Cartesian coordinate system. For each realization of P, at each $\mathtt{X} \in \mathbb{R}^3$ is specified an orientation $\varpi(\mathtt{X}) \in \mathrm{SO}(3)$ with respect to the chosen reference. Hence the sample space Ξ, i.e., the set of all possible realizations of P, is the set of all mappings $\varpi : \mathbb{R}^3 \to \mathrm{SO}(3)$. We identify each map ϖ with a sample of the polycrystal P. The construction of the σ-algebra $\mathfrak{S}$ of measurable subsets of Ξ and the definition of the probability measure $\widetilde{P}$ are too technical to be presented here.[51] We are content just to give a prime example to illustrate their meaning. Let $\{\mathtt{X}_1, \ldots, \mathtt{X}_n\}$ be any finite set of points in $\mathbb{R}^3$. Given a sample ϖ of P, measurements at the points $\mathtt{X}_i$ $(i = 1, \ldots, n)$ yield orientations given by rotations $\varpi(\mathtt{X}_i)$ with respect to the reference. If we repeat the measurements on another sample ϖ', the resulting orientation $\varpi'(\mathtt{X}_i)$ at the point $\mathtt{X}_i$ will generally be different from $\varpi(\mathtt{X}_i)$. However, we assume what follows: Specific to the process $\mathfrak{P}$, the probability $\wp(A_1, \ldots, A_n; \mathtt{X}_1, \ldots, \mathtt{X}_n)$ of finding $\varpi(\mathtt{X}_i) \in A_i$ $(i = 1, \ldots, n)$ is well defined for each choice of Borel sets A_i. For a given set $\{\mathtt{X}_i\}$ of points in $\mathbb{R}^3$ and a given set $\{A_i\}$ of Borel sets in SO(3), the set $\{\varpi \in \Xi : \varpi(\mathtt{X}_1) \in A_1, \ldots, \varpi(\mathtt{X}_n) \in A_n\}$ is $\widetilde{P}$-measurable and

$$\widetilde{P}(\{\varpi \in \Xi : \varpi(\mathtt{X}_1) \in A_1, \ldots, \varpi(\mathtt{X}_n) \in A_n\}) = \wp(A_1, \ldots, A_n; \mathtt{X}_1, \ldots, \mathtt{X}_n). \tag{3.7}$$

In classical texture analysis we are interested only in the "one-point correlation" measure $\wp(\cdot; \mathtt{X})$. Under the mathematical model of P described above and under suitable mathematical assumptions, a version of the ergodic theorem suggests the possibility that $\wp$ could be determined by measurements on only one sample. The first assumption is the statistical homogeneity of P, the exact definition of which we need not go into here. But suffice it to say statistical homogeneity does imply that $\wp$ is independent of $\mathtt{X}$. The second assumption is that the polycrystal P is an ergodic system. Again we will skip the mathematical definition of the term "ergodic". Instead we will state a proposition that follows from these assumptions (see Paroni [253, Lemma 2.1]).

several paragraphs/remarks in Part I are written for readers who have had the equivalent of a first-year graduate course in analysis. Readers who find those sections, paragraphs, or remarks incomprehensible may just skip them.

[51] See Paroni [253, Sect. 2] for details.

Proposition 3.2 *Let $\varpi \in \Xi$ and let A be a Borel set in SO(3). For $\mathrm{x} \in \mathbb{R}^3$, let*

$$\chi_A(\varpi(\mathrm{x})) = \begin{cases} 1, & \text{if } \varpi(\mathrm{x}) \in A \\ 0, & \text{if } \varpi(\mathrm{x}) \notin A. \end{cases} \tag{3.8}$$

Then for almost every sample $\varpi \in \Xi$ (i.e., except for samples in a set of $\widetilde{P}$-measure zero in Ξ), we have

$$\wp(A) = \lim_{r\to\infty} \frac{1}{\mathrm{V}(\mathrm{B}_r)} \int_{\mathrm{B}_r} \chi_A(\varpi(\mathrm{x}))d\mathrm{V}(\mathrm{x}), \tag{3.9}$$

where V and B_r denote the three-dimensional Euclidean volume and the ball of radius r centered at the origin, respectively. □

In the literature assertions such as Proposition 3.2 are sometimes put forth as consequences of an "ergodic hypothesis" for statistically homogeneous media, namely that "the result of averaging over all realizations of the ensemble is equivalent to averaging over the volume for one realization in the infinite-volume limit." [319, p. 29] And systems which satisfy the ergodic hypothesis are called "ergodic media" [319, p. 30].

At any rate, should (3.9) be valid for a statistically homogeneous polycrystal P, then its orientation measure $\wp$ could be determined through volume averaging by measurements on one sufficiently large sample. In Chap. 9 we shall discuss measurement of $\wp$ of such polycrystal P by inversion of X-ray pole figures, where (3.9), if valid, would indeed serve as a theoretical basis (see Sect. 9.3). On the other hand, in Chap. 8 we shall present the Bunge–Haessner method that estimates $\wp$ of such P by individual orientation measurements, which has a different mathematical basis (see Sect. 8.5.1).

3.2 The Haar Integral on SO(3)

In Chap. 10, we shall construct a bi-invariant volume measure on the rotation group SO(3). In this chapter we will follow an alternate approach. Here we will outline the mathematical basis of this alternate approach.

Let $f : \mathrm{SO}(3) \to \mathbb{R}$. For each $\boldsymbol{Q} \in \mathrm{SO}(3)$, we define two new functions $\mathscr{L}_{\boldsymbol{Q}} f$ and $\mathscr{R}_{\boldsymbol{Q}} f$ on SO(3) as follows: For each $\boldsymbol{R}$ in SO(3),

$$(\mathscr{L}_{\boldsymbol{Q}} f)(\boldsymbol{R}) = f(\boldsymbol{Q}^{-1}\boldsymbol{R}), \qquad (\mathscr{R}_{\boldsymbol{Q}} f)(\boldsymbol{R}) = f(\boldsymbol{R}\boldsymbol{Q}). \tag{3.10}$$

Let $\mathscr{C}(\mathrm{SO}(3), \mathbb{R})$ be the space of real-valued continuous functions defined on the rotation group SO(3). Suppose a bi-invariant finite positive measure[52] μ on $(\mathrm{SO}(3), \mathfrak{B})$ is given. For each continuous function f in $\mathscr{C}(\mathrm{SO}(3), \mathbb{R})$, its (Lebesgue) integral on SO(3) with respect to the measure μ is defined. Let $I : \mathscr{C}(\mathrm{SO}(3), \mathbb{R}) \to \mathbb{R}$ be defined by

$$I(f) = \int_{\mathrm{SO}(3)} f(\boldsymbol{R})d\mu(\boldsymbol{R}) := \int_{\mathrm{SO}(3)} f d\mu. \tag{3.11}$$

[52] Some basic definitions in measure theory are given in Appendix C.

The functional $I(\cdot)$ is said to be left-invariant and right-invariant, respectively, if it satisfies for each $f \in \mathscr{C}(\mathrm{SO}(3), \mathbb{R})$ and each $\boldsymbol{Q} \in \mathrm{SO}(3)$,

$$I(\mathscr{L}_{\boldsymbol{Q}} f) = \int_{\mathrm{SO}(3)} f(\boldsymbol{Q}^{-1}\boldsymbol{R}) d\mu(\boldsymbol{R}) = \int_{\mathrm{SO}(3)} f(\boldsymbol{R}) d\mu(\boldsymbol{R}) = I(f) \tag{3.12}$$

and

$$I(\mathscr{R}_{\boldsymbol{Q}} f) = \int_{\mathrm{SO}(3)} f(\boldsymbol{R}\boldsymbol{Q}) d\mu(\boldsymbol{R}) = \int_{\mathrm{SO}(3)} f(\boldsymbol{R}) d\mu(\boldsymbol{R}) = I(f), \tag{3.13}$$

respectively; $I(\cdot)$ is said to be bi-invariant if it is both left-invariant and right-invariant. By the definition of the integral and the properties of the bi-invariant measure μ, it is easy to verify that the functional $I(\cdot)$ satisfies the following properties:

(i) $I(\cdot)$ is linear, i.e., it satisfies

$$I(c_1 f_1 + c_2 f_2) = c_1 f_1 + c_2 f_2, \qquad \text{for each } f_1, f_2 \in \mathscr{C}(\mathrm{SO}(3), \mathbb{R}) \text{ and each } c_1, c_2 \in \mathbb{R}; \tag{3.14}$$

(ii) $I(\cdot)$ is positive, i.e., $I(f) \geq 0$ for $f \geq 0$;
(iii) $I(\cdot)$ is bi-invariant,[53] i.e.,

$$I(\mathscr{L}_{\boldsymbol{Q}} f) = I(f) = I(\mathscr{R}_{\boldsymbol{Q}} f) \qquad \text{for each } f \in \mathscr{C}(\mathrm{SO}(3), \mathbb{R}) \text{ and each } \boldsymbol{Q} \in \mathrm{SO}(3). \tag{3.15}$$

If μ is a probability measure on SO(3), then $I(\cdot)$ satisfies the condition

(iv) $I(1) = 1$.

In general, we call any functional $I(\cdot)$ on $\mathscr{C}(\mathrm{SO}(3), \mathbb{R})$ that observes assertions (i)–(iii) a Haar functional on $\mathscr{C}(\mathrm{SO}(3), \mathbb{R})$. If $I(\cdot)$ also satisfies (iv), then we call it a normalized Haar functional. A Haar functional $I(\cdot)$ is said to be non-trivial if and only if there is an $f \in \mathscr{C}(\mathrm{SO}(3), \mathbb{R})$ such that $I(f) > 0$. A normalized Haar functional is clearly non-trivial.

Conversely, suppose a Haar functional $I(\cdot)$ is given on $\mathscr{C}(\mathrm{SO}(3), \mathbb{R})$. Since SO(3) is a compact metric space (see Sects. 1.10 and 10.1), by Theorem C.8 (i.e., Riesz representation theorem I; see Appendix C) there exists a unique finite positive measure μ on $(\mathrm{SO}(3), \mathfrak{B})$ such that $I(f)$ is given by

$$I(f) = \int_{\mathrm{SO}(3)} f d\mu \qquad \text{for each } f \text{ in } \mathscr{C}(\mathrm{SO}(3), \mathbb{R}). \tag{3.16}$$

Moreover, the left- and right-invariance of $I(\cdot)$—see (3.12) and (3.13)—dictate that the measure μ is bi-invariant. We call the integral in (3.16) that represents the Haar functional $I(\cdot)$ the invariant integral or the Haar integral, and the finite, bi-invariant positive Borel

[53] The weaker condition that $I(\cdot)$ is left-invariant (resp. right-invariant) suffices here. Left-invariance (resp. right-invariance) and the normalization $I(1) = 1$ lead to uniqueness of the Haar functional [185, pp. 353–354] and its right-invariance (resp. left-invariance) [305, p. 15], where the references cited cover the Haar integral on any compact topological group G. We shall prove the same assertion later in this chapter (see Sects. 3.2.1 and 3.5.1) for the special instance that $G = \mathrm{SO}(3)$. We write condition (iii) as it stands because we are following von Neumann [328], where a bi-invariant positive linear functional $I(\cdot)$ on $\mathscr{C}(G, \mathbb{R})$ is constructed such that (3.15) follows by definition.

measure μ the corresponding Haar measure. If the Haar functional $I(\cdot)$ is normalized (i.e., $I(1) = 1$), then the corresponding Haar measure μ is normalized, i.e., it satisfies $\mu(\mathrm{SO}(3)) = 1$. Also, by (3.16) we see that $I(\cdot)$ is non-trivial if and only if $I(1) > 0$.

Remark 3.3 Note that the invariant integral $I(f)$, as given by the right-hand side of (3.16), is nothing but the Lebesgue integral of f on SO(3) with respect to the Haar measure μ; it is defined if f is integrable. In particular, let A be a Borel set in (i.e., a measurable subset of) SO(3), and let

$$\chi_A(\boldsymbol{R}) = \begin{cases} 1 & \text{if } \boldsymbol{R} \in A \\ 0 & \text{otherwise} \end{cases} \tag{3.17}$$

be the characteristic function of A. Then χ_A is integrable, and $I(\chi_A) = \mu(A)$. Also, we have $I(1) = \mu(\mathrm{SO}(3))$. □

Remark 3.4 As mentioned at the end of Sect. 3.1, the rotation group is a compact topological group. In 1935 von Neumann [328] provided an elementary proof of the theorem (see Sect. C.3 in Appendix C for more details) that for each compact topological group G there is a unique normalized Haar functional $I(\cdot)$ on $\mathscr{C}(G, \mathbb{R})$ and thence a unique bi-invariant probability measure on G. Applying this theorem to $G = \mathrm{SO}(3)$, we see that there is a unique normalized Haar measure on SO(3). In this exposition we will not go into a proof of this general theorem. Instead, we will first prove a uniqueness theorem on Haar functionals and then construct an explicit Haar integral on SO(3) as parametrized by the Euler angles (ψ, θ, ϕ) and by the axis-angle parameters $(\boldsymbol{n}(\Theta, \Phi), \omega)$, which satisfies defining properties (i)–(iv). Note that even if we appeal to the general theorem, we still have to derive an explicit expression of the Haar functional for the rotation group SO(3), which we will need for computations in applications. □

3.2.1 Uniqueness

We will prove next that two Haar functionals $I(\cdot)$ and $J(\cdot)$ on $\mathscr{C}(\mathrm{SO}(3), \mathbb{R})$ necessarily observe the relation $I(\cdot) = cJ(\cdot)$, where $c = I(1)/J(1) > 0$. Thus there can only be one Haar functional $I(\cdot)$ with $I(1) = 1$. Or, in the language of Haar measures, there can only be one bi-invariant probability measure on the rotation group SO(3).

The following proof[54] on uniqueness is based on the bi-invariance of the Haar functional and Fubini's theorem on double and iterated integrals.

Proposition 3.5 *Let $I(\cdot)$ and $J(\cdot)$ be two Haar functionals on $\mathscr{C}(SO(3), \mathbb{R})$ with corresponding Haar measures μ and ν, respectively, i.e.,*

$$I(f) = \int_{SO(3)} f \, d\mu, \quad J(f) = \int_{SO(3)} f \, d\nu, \qquad \text{for each } f \in \mathscr{C}(SO(3), \mathbb{R}), \tag{3.18}$$

and let $J(\cdot)$ be normalized, i.e., $J(1) = 1$. Then $I(\cdot) = cJ(\cdot)$, where $c = \mu(SO(3))$.

In particular, if $I(\cdot)$ is also normalized, then $I(\cdot) = J(\cdot)$. Thus there can only be one bi-invariant probability measure on $SO(3)$.

[54] This simple proof of uniqueness appeals to both the left- and right-invariance of the normalized Haar functional. In Sect. 3.5.1 we shall prove that left-invariance implies right-invariance.

Proof For each $f \in \mathscr{C}(\mathrm{SO}(3), \mathbb{R})$, we observe that

$$\begin{aligned}\int_{\mathrm{SO}(3)} f(\boldsymbol{R}) d\mu(\boldsymbol{R}) &= \left(\int_{\mathrm{SO}(3)} d\nu(\boldsymbol{Q})\right)\left(\int_{\mathrm{SO}(3)} f(\boldsymbol{R}) d\mu(\boldsymbol{R})\right) \\ &= \left(\int_{\mathrm{SO}(3)} d\nu(\boldsymbol{Q})\right)\left(\int_{\mathrm{SO}(3)} f(\boldsymbol{R}\boldsymbol{Q}) d\mu(\boldsymbol{R})\right) \\ &= \int_{\mathrm{SO}(3)} \left(\int_{\mathrm{SO}(3)} f(\boldsymbol{R}\boldsymbol{Q}) d\nu(\boldsymbol{Q})\right) d\mu(\boldsymbol{R}), \\ &= \mu(\mathrm{SO}(3)) \int_{\mathrm{SO}(3)} f(\boldsymbol{Q}) d\nu(\boldsymbol{Q}), \end{aligned} \tag{3.19}$$

where we have appealed to the right-invariance of $I(\cdot)$ at the second step, Fubini's theorem at the third step, and the left invariance of $J(\cdot)$ at the final step. Hence we conclude that

$$I(\cdot) = cJ(\cdot), \qquad \text{where } c = \mu(\mathrm{SO}(3)). \tag{3.20}$$

If μ and ν are probability measures, i.e., $\mu(\mathrm{SO}(3)) = \nu(\mathrm{SO}(3)) = 1$, we get

$$\int_{\mathrm{SO}(3)} f(\boldsymbol{R}) d\mu(\boldsymbol{R}) = \int_{\mathrm{SO}(3)} f(\boldsymbol{R}) d\nu(\boldsymbol{R}) \qquad \text{for each } f \in \mathrm{SO}(3), \tag{3.21}$$

which implies $\mu = \nu$. Therefore there can only be one bi-invariant probability measure on the rotation group SO(3). □

Corollary 3.6 *Let $I(\cdot)$ and $J(\cdot)$ be two non-trivial Haar functionals on $\mathscr{C}(SO(3), \mathbb{R})$. Then $I(\cdot) = cJ(\cdot)$, where $c = I(1)/J(1) > 0$.*

Proof Since $I(\cdot)$ and $J(\cdot)$ are non-trivial Haar functionals, by (3.18) $I(1) = \mu(\mathrm{SO}(3)) > 0$ and $J(1) = \nu(\mathrm{SO}(3)) > 0$. Let $\widetilde{I}(\cdot) := I(\cdot)/I(1)$ and $\widetilde{J}(\cdot) := J(\cdot)/J(1)$. Both $\widetilde{I}$ and $\widetilde{J}$ are normalized Haar functionals on $\mathscr{C}(\mathrm{SO}(3), \mathbb{R})$. By Proposition 3.5, we have $\widetilde{I}(\cdot) = \widetilde{J}(\cdot)$, i.e., $I(\cdot) = cJ(\cdot)$, where $c = I(1)/J(1) > 0$. □

3.3 Left-Invariant Integral in Euler Angles

We now proceed to construct an explicit expression for a Haar functional $I(\cdot)$ on $\mathscr{C}(\mathrm{SO}(3), \mathbb{R})$. Then $I(\cdot)/I(1)$ will provide an explicit expression for the unique normalized Haar functional. To start with, we parametrize SO(3) with the Euler angles and seek, as an expression for a left-invariant positive linear functional, a left-invariant integral of a continuous function with respect to the Euler angles on SO(3).

In terms of Euler angles, the problem to find a left-invariant functional on SO(3) is tantamount to seeking a weight function $\rho(\psi, \theta, \phi)$ such that

$$\int_0^{2\pi}\int_0^{\pi}\int_0^{2\pi} f(\boldsymbol{Q}^T \boldsymbol{R}(\psi,\theta,\phi))\rho(\psi,\theta,\phi)d\psi d\theta d\phi$$
$$= \int_0^{2\pi}\int_0^{\pi}\int_0^{2\pi} f(\boldsymbol{R}(\psi,\theta,\phi))\rho(\psi,\theta,\phi)d\psi d\theta d\phi \tag{3.22}$$

for each rotation $\boldsymbol{Q}$ in SO(3). We proceed to construct a weight function ρ which satisfies (3.22).

Let $\mathcal{S}^2$ be the unit sphere. Let $(1, \theta, \psi)$ $(0 \le \theta \le \pi, 0 \le \psi < 2\pi)$ be spherical coordinates of points in $\mathcal{S}^2$ and $\boldsymbol{m}(\theta, \psi)$ be the position vector of the point $(1, \theta, \psi)$. Let $h : \mathcal{S}^2 \to \mathbb{R}$ be integrable and $\boldsymbol{Q}$ be a rotation. In our construction of a left-invariant integral on the rotation group SO(3), the formula below will be instrumental:

$$\int_0^{2\pi}\int_0^{\pi} h(\boldsymbol{Q}^T\boldsymbol{m}(\theta,\psi))\sin\theta d\theta d\psi = \int_0^{2\pi}\int_0^{\pi} h(\boldsymbol{m}(\theta,\psi))\sin\theta d\theta d\psi, \tag{3.23}$$

for each $\boldsymbol{Q} \in$ SO(3). This formula follows from the invariance of surface area of sets in $\mathcal{S}^2$ under rotation. Indeed let $\widetilde{\boldsymbol{m}} = \boldsymbol{Q}^T\boldsymbol{m}$. In Cartesian coordinates, $\boldsymbol{m} = (\sin\theta\cos\psi, \sin\theta\sin\psi, \cos\theta)$. Let

$$dA = \left\| \frac{\partial \boldsymbol{m}}{\partial\theta} \times \frac{\partial \boldsymbol{m}}{\partial\psi} \right\| d\theta d\psi = \sin\theta d\theta d\psi, \tag{3.24}$$

and

$$d\widetilde{A} = \left\| \frac{\partial \widetilde{\boldsymbol{m}}}{\partial\theta} \times \frac{\partial \widetilde{\boldsymbol{m}}}{\partial\psi} \right\| d\theta d\psi \tag{3.25}$$

be the element of surface area of $\mathcal{S}^2$ at $\boldsymbol{m}$ and $\widetilde{\boldsymbol{m}}$, respectively. Since

$$\left\| \frac{\partial \widetilde{\boldsymbol{m}}}{\partial\theta} \times \frac{\partial \widetilde{\boldsymbol{m}}}{\partial\psi} \right\| = \left\| \boldsymbol{Q}^T\frac{\partial \boldsymbol{m}}{\partial\theta} \times \boldsymbol{Q}^T\frac{\partial \boldsymbol{m}}{\partial\psi} \right\| = \left\| \boldsymbol{Q}^T\left(\frac{\partial \boldsymbol{m}}{\partial\theta} \times \frac{\partial \boldsymbol{m}}{\partial\psi}\right) \right\| = \left\| \frac{\partial \boldsymbol{m}}{\partial\theta} \times \frac{\partial \boldsymbol{m}}{\partial\psi} \right\|, \tag{3.26}$$

we have $d\widetilde{A} = dA$. It follows that

$$\int_{\mathcal{S}^2} h(\boldsymbol{Q}^T\boldsymbol{m})dA = \int_{\mathcal{S}^2} h(\widetilde{\boldsymbol{m}})d\widetilde{A} = \int_{\mathcal{S}^2} h(\boldsymbol{m})dA. \tag{3.27}$$

Each rotation $g \in$ SO(3) is characterized by the pair of unit vectors $g\boldsymbol{e}_3$ and $g\boldsymbol{e}_1$ (see Fig. 1). Consider those rotations g with $g\boldsymbol{e}_3 \ne \pm\boldsymbol{e}_3$ so that its Euler angles (ψ, θ, ϕ) are well defined. The angles (θ, ψ) specify the spherical coordinates $(1, \theta, \psi)$ of $\boldsymbol{m} := g\boldsymbol{e}_3$ on the unit sphere $\mathcal{S}^2$. The unit vector $g\boldsymbol{e}_1$ lies in the great circle $\mathcal{C}$ (specified by the points N and L in Fig. (1))—parametrized by ϕ—whose plane is perpendicular to $g\boldsymbol{e}_3$. Let $S(\theta, \psi) = \{g \in$

$\mathrm{SO}(3) : g\boldsymbol{e}_3 = (1, \theta, \psi)\}$; clearly the set of rotations $S(\theta, \psi)$ is parametrized by $\phi \in [0, 2\pi)$. Given $f : \mathrm{SO}(3) \to \mathbb{R}$, we define a new function f^* defined on $\mathcal{S}^2$ by

$$f^*(\boldsymbol{m}(\theta, \psi)) = \int_0^{2\pi} f(\boldsymbol{R}(\psi, \theta, \phi))d\phi, \tag{3.28}$$

where $\boldsymbol{R}(\psi, \theta, \phi)$ denotes the rotation with Euler angles (ψ, θ, ϕ). Thus $f^*(\boldsymbol{m}(\theta, \psi))$ is equal to 2π times the integral average of $f(\boldsymbol{R}(\psi, \theta, \phi))$ with respect to ϕ on the set $S(\theta, \psi)$. For a given rotation $\boldsymbol{Q}$, let $\widetilde{\boldsymbol{R}}(\widetilde{\psi}, \widetilde{\theta}, \widetilde{\phi}) := \boldsymbol{Q}^T \boldsymbol{R}(\psi, \theta, \phi)$, where $(\widetilde{\psi}, \widetilde{\theta}, \widetilde{\phi})$ are the Euler angles of $\widetilde{\boldsymbol{R}}$. The point

$$\widetilde{\boldsymbol{m}} := \widetilde{\boldsymbol{R}}\boldsymbol{e}_3 = \boldsymbol{Q}^T \boldsymbol{R}\boldsymbol{e}_3 = \boldsymbol{Q}^T \boldsymbol{m} \tag{3.29}$$

has spherical coordinates $(1, \widetilde{\theta}, \widetilde{\psi})$; it is the place which the point $(1, \theta, \psi)$ moves to after the unit sphere undergoes a rotation specified by $\boldsymbol{Q}^T$. Likewise, under the rotation $\boldsymbol{Q}^T$ the great circle $\mathcal{C}$ which contains $\boldsymbol{R}\boldsymbol{e}_1$ becomes the great circle $\widetilde{\mathcal{C}} = \boldsymbol{Q}^T\mathcal{C}$ which contains $\widetilde{\boldsymbol{R}}\boldsymbol{e}_1$. Let

$$\widetilde{f}^*(\widetilde{\boldsymbol{m}}(\widetilde{\theta}, \widetilde{\psi})) = \int_0^{2\pi} f(\widetilde{\boldsymbol{R}}(\widetilde{\psi}, \widetilde{\theta}, \widetilde{\phi}))d\widetilde{\phi}. \tag{3.30}$$

Clearly we have

$$\widetilde{f}^*(\widetilde{\boldsymbol{m}}) = f^*(\boldsymbol{Q}^T \boldsymbol{m}). \tag{3.31}$$

Since the elements of arc length $d\phi$ and $d\widetilde{\phi}$ for the great circles $\mathcal{C}$ and $\widetilde{\mathcal{C}}$, respectively, do not change under rotation, we have

$$d\phi = d\widetilde{\phi}. \tag{3.32}$$

Hence we may rewrite (3.30) as

$$f^*(\boldsymbol{Q}^T \boldsymbol{m}(\theta, \psi)) = \int_0^{2\pi} f(\boldsymbol{Q}^T \boldsymbol{R}(\psi, \theta, \phi))d\phi. \tag{3.33}$$

By (3.23), (3.28) and (3.33) we have

$$\int_0^{2\pi}\int_0^{\pi} f^*(\boldsymbol{Q}^T \boldsymbol{m}(\theta, \psi)) \sin\theta d\theta d\psi = \int_0^{2\pi}\int_0^{\pi} f^*(\boldsymbol{m}(\theta, \psi)) \sin\theta d\theta d\psi, \tag{3.34}$$

or

$$\int_0^{2\pi}\int_0^{\pi}\int_0^{2\pi} f(\boldsymbol{Q}^T \boldsymbol{R}(\psi, \theta, \phi)) \sin\theta d\psi d\theta d\phi = \int_0^{2\pi}\int_0^{\pi}\int_0^{2\pi} f(\boldsymbol{R}(\psi, \theta, \phi)) \sin\theta d\psi d\theta d\phi. \tag{3.35}$$

It follows that the weight function $\rho(\psi,\theta,\phi)=\sin\theta$ satisfies (3.22). Hence the functional $I(\cdot):\mathscr{C}(\mathrm{SO}(3),\mathbb{R})\to\mathbb{R}$ defined by

$$I(f)=\int_0^{2\pi}\int_0^{\pi}\int_0^{2\pi} f(\boldsymbol{R}(\psi,\theta,\phi))\sin\theta\,d\psi\,d\theta\,d\phi \tag{3.36}$$

is left-invariant. We shall prove in Sect. 3.5 that $I(\cdot)$ is also right-invariant. Moreover it clearly satisfies the linearity and positivity requirements (i) and (ii) on Haar functionals.

Remark 3.7 Our construction of the left-invariant integral (3.36) on SO(3) follows largely the presentations by Gel'fand et al. [125] and Naimark [244]. In fact this construction is an application of a method based on a theorem (see Knightly and Li [179, p. 78, Lemma 7.11], Rossmann [276, p. 176, Proposition 5]) on left-invariant integrals on locally compact groups, which when applied to the compact group SO(3), asserts that if there is a closed subgroup H of SO(3) such that left-invariant measures dh and $d(gH)$ exist on H and on the space of left cosets $\mathrm{SO}(3)/H=\{gH: g\in\mathrm{SO}(3)\}$, respectively, then there is a left SO(3)-invariant measure μ on SO(3) such that

$$\int_{\mathrm{SO}(3)} f(g)\,d\mu(g)=\int_{\mathrm{SO}(3)/H}\left(\int_H f(gh)\,dh\right)d(gH),\qquad \text{for each } f\in\mathscr{C}(\mathrm{SO}(3),\mathbb{R}). \tag{3.37}$$

Note that because of the left-invariance of the measure dh the expression in parentheses in (3.37) depends only on the cosets in $\mathrm{SO}(3)/H$. For the present application, $H=\mathrm{SO}(2)=\{h\in\mathrm{SO}(3): h\boldsymbol{e}_3=\boldsymbol{e}_3\}$, and SO(3)/SO(2) is identified with the unit sphere $\mathcal{S}^2$. Moreover, in (3.37)

$$\begin{aligned}\int_H f(gh)\,dh&=\int_0^{2\pi} f(\boldsymbol{R}(\psi,\theta,\phi)\boldsymbol{R}(\boldsymbol{e}_3,\phi_1))d\phi_1\\&=\int_0^{2\pi} f(\boldsymbol{R}(\boldsymbol{e}_3,\psi)\boldsymbol{R}(\boldsymbol{e}_2,\theta)\boldsymbol{R}(\boldsymbol{e}_3,\phi)\boldsymbol{R}(\boldsymbol{e}_3,\phi_1))d\phi_1\\&=\int_0^{2\pi} f(\boldsymbol{R}(\psi,\theta,\phi+\phi_1))d\phi_1\\&=\int_0^{2\pi} f(\boldsymbol{R}(\psi,\theta,\phi))d\phi,\end{aligned} \tag{3.38}$$

and

$$\int_{\mathrm{SO}(3)/H}\left(\int_H f(gh)\,dh\right)d(gH)=\int_0^{2\pi}\int_0^{\pi}\int_0^{2\pi} f(\boldsymbol{R}(\psi,\theta,\phi))\sin\theta\,d\phi\,d\theta\,d\psi. \tag{3.39}$$

□

For each positive constant c, the weight function $\rho = c \sin\theta$ obviously also satisfies (3.22) and $cI(\cdot)$ is also a Haar functional on $\mathscr{C}(\mathrm{SO}(3), \mathbb{R})$. By giving c a specific value, we assign a total group "volume" to SO(3). In classical texture analysis there are two commonly used conventions. One convention—initiated by Roe [270]—takes $c = 1$ and assigns to SO(3) the total volume

$$\mathcal{V}(\mathrm{SO}(3)) = \int_0^{2\pi}\int_0^{\pi}\int_0^{2\pi} \sin\theta \, d\psi \, d\theta \, d\phi = 8\pi^2. \tag{3.40}$$

Under this convention we write

$$d\mathcal{V} = \sin\theta \, d\psi \, d\theta \, d\phi. \tag{3.41}$$

Another convention—adopted by Bunge [60]—chooses $c = 1/(8\pi^2)$ so that the total group volume of SO(3) is 1. This convention is in line with the mathematical literature on the theory of group representations on compact topological groups. We will denote by $\mathfrak{g}$ the volume measure under this convention and write

$$d\mathfrak{g} = \frac{1}{8\pi^2} \sin\theta \, d\psi \, d\theta \, d\phi. \tag{3.42}$$

We have introduced in Sect. 3.1 the orientation measure $\wp_{\mathrm{iso}}$, which is a bi-invariant probability measure that pertains to the case where all crystallite orientations are equally probable. By its physical meaning, for a measurable $A \subset \mathrm{SO}(3)$, $\wp_{\mathrm{iso}}(A)$ should be proportional to the "size" or volume of A. The volume of A, however, is not a number until we specify a unit of volume by choosing a standard set and assign it a number for its volume. A convenient option is to choose SO(3) itself as the standard set. By the uniqueness of the bi-invariant probability measure on the rotation group SO(3), we have

$$\wp_{\mathrm{iso}} = \mathfrak{g}. \tag{3.43}$$

3.4 Invariant Integral in Axis-Angle Parameters

As preparation for a proof of right-invariance of the functional $I(\cdot)$ defined in (3.36), we derive an alternate expression of $I(f)$ in terms of axis-angle parameters, which is of interest in itself.

To rewrite the left-invariant integral in (3.36) in terms of the axis-angle parameters, we compute the absolute value of the Jacobian determinant $\partial(\psi, \theta, \phi)/\partial(\omega, \Theta, \Phi)$. To this end, first we seek three independent equations which relate the two sets of parameters.

By comparing the trace of the rotation matrix in the two sets of parameters (see (1.89) and (1.113)), we find

$$\cos\omega = \frac{1}{2}\left(\cos\theta + (1 + \cos\theta)\cos(\psi + \phi) - 1\right),$$

which can be recast as

$$\cos\frac{\omega}{2} = \left(\cos\frac{\theta}{2}\right)\left|\cos\frac{\psi + \phi}{2}\right|. \tag{3.44}$$

A comparison of the R_{33} term delivers the relation

$$\cos\theta = (1-\cos\omega)\cos^2\Theta + \cos\omega,$$

which can be simplified as

$$\sin\frac{\theta}{2} = \sin\Theta\sin\frac{\omega}{2}. \tag{3.45}$$

From (1.114) we observe that

$$\tan\Phi = \frac{R_{13}-R_{31}}{R_{32}-R_{23}} = \frac{\cos\psi+\cos\phi}{\sin\phi-\sin\psi} = \cot\frac{\phi-\psi}{2}.$$

Without loss of generality, we let Φ take value in $[-\pi/2, 3\pi/2)$ and simplify the preceding equation as

$$\Phi = \frac{\pi}{2} + \frac{\psi-\phi}{2}. \tag{3.46}$$

For later use, we deduce from (3.44) and (3.45) the relation

$$\left|\sin\frac{\psi+\phi}{2}\right| = \frac{|\cos\Theta|\sin(\omega/2)}{\cos(\theta/2)}. \tag{3.47}$$

Now let (see (3.44)–(3.46))

$$\begin{aligned}
F_1 &= \cos\frac{\omega}{2} - \left(\cos\frac{\theta}{2}\right)\left|\cos\frac{\psi+\phi}{2}\right|,\\
F_2 &= \sin\frac{\theta}{2} - \sin\Theta\sin\frac{\omega}{2},\\
F_3 &= \Phi - \frac{\pi}{2} - \frac{\psi-\phi}{2}.
\end{aligned}$$

After some easy computations we find

$$\begin{aligned}
\frac{\partial(F_1,F_2,F_3)}{\partial(\omega,\Theta,\Phi)} &= \frac{1}{2}\sin^2\frac{\omega}{2}\cos\Theta,\\
\frac{\partial(F_1,F_2,F_3)}{\partial(\psi,\theta,\phi)} &= \frac{1}{4}\cos^2\frac{\theta}{2}\sin\frac{\psi+\phi}{2}\operatorname{sgn}\left(\cos\frac{\psi+\phi}{2}\right).
\end{aligned}$$

Therefore we have

$$\begin{aligned}
\left|\frac{\partial(\psi,\theta,\phi)}{\partial(\omega,\Theta,\Phi)}\right| &= \left|-\frac{\partial(F_1,F_2,F_3)}{\partial(\omega,\Theta,\Phi)}\Big/\frac{\partial(F_1,F_2,F_3)}{\partial(\psi,\theta,\phi)}\right|\\
&= \frac{4\sin^2(\omega/2)|\cos\Theta|}{2\cos^2(\theta/2)|\sin((\psi+\phi)/2)|}\\
&= \frac{4\sin^2(\omega/2)\sin\Theta}{\sin\theta},
\end{aligned}$$

where we have used (3.45) and (3.47) in the last step. Hence we conclude that

$$d\psi d\theta d\phi = \frac{4\sin^2(\omega/2)\sin\Theta}{\sin\theta} d\omega d\Theta d\Phi,$$

or

$$d\mathcal{V} = \sin\theta d\psi d\theta d\phi = 4\sin^2\frac{\omega}{2}\sin\Theta d\omega d\Theta d\Phi. \tag{3.48}$$

Thus, in terms of the axis-angle parameters, the left-invariant integral $I(f)$ of a function f over the rotation group—see (3.36)—assumes the form

$$I(f) = 4\int_0^{2\pi}\int_0^{\pi}\int_0^{\pi} f(\boldsymbol{R}(\boldsymbol{n}(\Theta,\Phi),\omega))\sin^2\frac{\omega}{2}\sin\Theta d\omega d\Theta d\Phi, \tag{3.49}$$

which is the alternate expression for $I(f)$ that we seek.

3.5 Further Properties of the Invariant Integral

3.5.1 Right-Invariance

The functional given by (3.36) is right-invariant if it satisfies

$$I(\mathscr{R}_{\boldsymbol{Q}} f) = \int_{\mathrm{SO(3)}} f(\boldsymbol{R}\boldsymbol{Q})d\mathcal{V}(\boldsymbol{R}) = \int_{\mathrm{SO(3)}} f(\boldsymbol{R})d\mathcal{V}(\boldsymbol{R}) = I(f) \tag{3.50}$$

for each rotation $\boldsymbol{Q}$ in SO(3) and for each continuous function f on SO(3). Note that right-invariance of the Haar integral plays an essential role in our proof of its uniqueness in Sect. 3.2.1. Let us demonstrate (3.50) by using the alternate expression (3.49) for $I(f)$. Indeed we have for each $\boldsymbol{Q} \in \mathrm{SO(3)}$ and $f \in \mathscr{C}(\mathrm{SO(3)}, \mathbb{R})$,

$$\begin{aligned}
I(\mathscr{R}_{\boldsymbol{Q}} f) &= 4\int_0^{2\pi}\int_0^{\pi}\int_0^{\pi} f(\boldsymbol{R}(\boldsymbol{n}(\Theta,\Phi),\omega)\boldsymbol{Q})\sin^2\frac{\omega}{2}\sin\Theta d\omega d\Theta d\Phi \\
&= 4\int_0^{2\pi}\int_0^{\pi}\int_0^{\pi} f(\boldsymbol{Q}^T\boldsymbol{R}(\boldsymbol{n}(\Theta,\Phi),\omega)\boldsymbol{Q})\sin^2\frac{\omega}{2}\sin\Theta d\omega d\Theta d\Phi \\
&= 4\int_0^{2\pi}\int_0^{\pi}\int_0^{\pi} f(\boldsymbol{R}(\boldsymbol{Q}^T\boldsymbol{n}(\Theta,\Phi),\omega))\sin^2\frac{\omega}{2}\sin\Theta d\omega d\Theta d\Phi \\
&= 4\int_0^{\pi}\left(\int_0^{2\pi}\int_0^{\pi} f(\boldsymbol{R}(\boldsymbol{Q}^T\boldsymbol{n}(\Theta,\Phi),\omega))\sin\Theta d\Theta d\Phi\right)\sin^2\frac{\omega}{2}d\omega \\
&= 4\int_0^{\pi}\left(\int_0^{2\pi}\int_0^{\pi} f(\boldsymbol{R}(\boldsymbol{n}(\Theta,\Phi),\omega))\sin\Theta d\Theta d\Phi\right)\sin^2\frac{\omega}{2}d\omega
\end{aligned}$$

$$= 4 \int_0^{2\pi} \int_0^{\pi} \int_0^{\pi} f(\boldsymbol{R}(\boldsymbol{n}(\Theta, \Phi), \omega)) \sin^2 \frac{\omega}{2} \sin \Theta d\omega d\Theta d\Phi$$

$$= I(f), \tag{3.51}$$

where we have appealed to what follows: the left invariance of $I(f)$; Euler's theorem; formula (3.23) by taking $h = f \circ \boldsymbol{R}(\cdot, \omega) : \mathcal{S}^2 \to \mathbb{R}$.

As the functional $I(f)$ on $\mathscr{C}(\mathrm{SO}(3), \mathbb{R})$ defined by (3.36) or (3.49) linear, positive, and both left-invariant and right-invariant, it is a Haar functional. By the uniqueness property discussed in Sect. 3.2.1, Haar functionals on SO(3) are unique up to a positive multiplicative constant. The assignment of total group volume of SO(3) will define the Haar integral on SO(3) uniquely. The formulas (3.36) and (3.49) correspond to the choice of $I(1) = 8\pi^2$ and the volume measure $\mathcal{V}$. The choice of total group volume equal to 1 delivers the unique bi-invariant probability measure (or normalized Haar measure) $\mathfrak{g}$ on SO(3).

3.5.2 Inverse-Invariance

From the left- and right-invariance of the integral $I(f) = \int_{\mathrm{SO}(3)} f \, d\mathcal{V}$ follows its inverse-invariance, i.e., it enjoys the identity

$$\int_{\mathrm{SO}(3)} f(\boldsymbol{R}^{-1}) d\mathcal{V}(\boldsymbol{R}) = \int_{\mathrm{SO}(3)} f(\boldsymbol{R}) d\mathcal{V}(\boldsymbol{R}) \qquad \text{for each } f \in \mathscr{C}(\mathrm{SO}(3), \mathbb{R}). \tag{3.52}$$

Since we have already obtained explicit expressions (3.36) and (3.49) for $I(f)$, we can prove its inverse-invariance directly. We shall do this presently and add a remark at the end of the section to discuss the inverse-invariance of the normalized Haar integral on a general compact group.

We use expression (3.49) to prove its inverse-invariance. First note that

$$\boldsymbol{R}(\boldsymbol{n}(\Theta, \Phi), \omega)^{-1} = \boldsymbol{R}(\boldsymbol{n}(\pi - \Theta, \Phi + \pi), \omega). \tag{3.53}$$

Let $\widetilde{\Theta} = \pi - \Theta$, $\widetilde{\Phi} = \pi + \Phi$. Then $\sin \widetilde{\Theta} = \sin \Theta$, $d\widetilde{\Theta} = -d\Theta$, and $d\widetilde{\Phi} = d\Phi$. Hence we have

$$\begin{aligned}
\int_{\mathrm{SO}(3)} f(\boldsymbol{R}^{-1}) d\mathcal{V}(\boldsymbol{R}) &= 4 \int_0^{2\pi} \int_0^{\pi} \int_0^{\pi} f(\boldsymbol{R}(\boldsymbol{n}(\widetilde{\Theta}, \widetilde{\Phi}), \omega)) \sin^2 \frac{\omega}{2} \sin \Theta d\omega d\Theta d\Phi \\
&= 4 \int_{\pi}^{3\pi} \int_{\pi}^{0} \int_0^{\pi} f(\boldsymbol{R}(\boldsymbol{n}(\widetilde{\Theta}, \widetilde{\Phi}), \omega)) \sin^2 \frac{\omega}{2} \sin \widetilde{\Theta} d\omega (-d\widetilde{\Theta}) d\widetilde{\Phi} \\
&= 4 \int_0^{2\pi} \int_0^{\pi} \int_0^{\pi} f(\boldsymbol{R}(\boldsymbol{n}(\widetilde{\Theta}, \widetilde{\Phi}), \omega)) \sin^2 \frac{\omega}{2} \sin \widetilde{\Theta} d\omega d\widetilde{\Theta} d\widetilde{\Phi} \\
&= \int_{\mathrm{SO}(3)} f(\boldsymbol{R}) d\mathcal{V}(\boldsymbol{R}) \qquad \text{for each } f \in \mathscr{C}(\mathrm{SO}(3), \mathbb{R}).
\end{aligned} \tag{3.54}$$

Remark 3.8 Inverse-invariance of the invariant integral will play an important role in Chap. 4 when we compare various formulations of the orientation distribution function and its series expansion in Wigner D-functions or their variants. □

Remark 3.9 Here we show that left- and right-invariance imply inverse-invariance for a Haar functional $I(\cdot)$ defined on $\mathscr{C}(G,\mathbb{R})$, where G is any compact group G. For convenience, we shall use the same symbols as before, e.g., the elements of G are denoted by $\boldsymbol{R}$, $\boldsymbol{Q}$, etc., and the normalized Haar measure by $\mathfrak{g}$. Let $I(f)=\int_G f(\boldsymbol{R})d\mathfrak{g}(\boldsymbol{R})$ and $J(f)=\int_G f(\boldsymbol{R}^{-1})d\mathfrak{g}(\boldsymbol{R})$. We will show that the functional $J(\cdot)$ satisfies all the conditions for a Haar functional. Then we have $I(\cdot)=J(\cdot)$ by uniqueness of the normalized Haar functional, as the argument for uniqueness given in Sect. 3.2.1 goes through for any compact group G.

As it is obvious that $J(\cdot)$ satisfies conditions (i) and (ii) in Sect. 3.2, it suffices to prove that $J(\cdot)$ is both left- and right-invariant. Let $\mathscr{J}: G\to G$ be defined by $\mathscr{J}(\boldsymbol{R})=\boldsymbol{R}^{-1}$. Then $J(f)=\int_G(f\circ\mathscr{J})(\boldsymbol{R})d\mathfrak{g}(\boldsymbol{R})$. We have for each $\boldsymbol{Q}\in G$

$$\begin{aligned} J(\mathscr{L}_{\boldsymbol{Q}}f) &= \int_G f(\boldsymbol{Q}^{-1}\boldsymbol{R}^{-1})d\mathfrak{g}(\boldsymbol{R}) = \int_G f((\boldsymbol{R}\boldsymbol{Q})^{-1})d\mathfrak{g}(\boldsymbol{R}) \\ &= \int_G (f\circ\mathscr{J})(\boldsymbol{R}\boldsymbol{Q})d\mathfrak{g}(\boldsymbol{R}) = \int_G (f\circ\mathscr{J})(\boldsymbol{R})d\mathfrak{g}(\boldsymbol{R}) = J(f), \end{aligned} \tag{3.55}$$

where we have used the right-invariance of $I(\cdot)$. Similarly, we can use the left-invariance of $I(\cdot)$ to prove the right-invariance of $J(\cdot)$. □

3.6 Integrals with Complex-Valued Integrands

Later we shall have to consider functions which are complex-valued. Let $i:=\sqrt{-1}$ be the imaginary unit. Each function $f:\mathrm{SO}(3)\to\mathbb{C}$ gives rise to two real-valued functions $\mathfrak{Re}\,f:\mathrm{SO}(3)\to\mathbb{R}$ and $\mathfrak{Im}\,f:\mathrm{SO}(3)\to\mathbb{R}$ defined by

$$f(\boldsymbol{R})=\mathfrak{Re}\,f(\boldsymbol{R})+i\,\mathfrak{Im}\,f(\boldsymbol{R}), \qquad \text{for each } \boldsymbol{R}\in\mathrm{SO}(3) \tag{3.56}$$

and are called the real part and the imaginary part of f, respectively. A complex-valued function f is continuous on SO(3) if and only if its real part $\mathfrak{Re}\,f$ and imaginary part $\mathfrak{Im}\,f$ are continuous on SO(3). The integral of f with respect to the normalized Haar measure $\mathfrak{g}$ on a measurable set $E\subset\mathrm{SO}(3)$ is defined by

$$\int_E f(\boldsymbol{R})\,d\mathfrak{g}(\boldsymbol{R}) := \int_E \mathfrak{Re}\,f(\boldsymbol{R})\,d\mathfrak{g}(\boldsymbol{R}) + i\int_E \mathfrak{Im}\,f(\boldsymbol{R})\,d\mathfrak{g}(\boldsymbol{R}). \tag{3.57}$$

Let $\mathscr{C}(\mathrm{SO}(3),\mathbb{C})$ be the set of all continuous functions $f:\mathrm{SO}(3)\to\mathbb{C}$, and let

$$I(f)=\int_{\mathrm{SO}(3)} f(\boldsymbol{R})\,d\mathfrak{g}(\boldsymbol{R}) \qquad \text{for each } f\in\mathscr{C}(\mathrm{SO}(3),\mathbb{C}). \tag{3.58}$$

The complex-valued functional $I(\cdot)$ is linear in the sense that

$$I(c_1f_1+c_2f_2)=c_1f_1+c_2f_2, \qquad \text{for each } f_1,f_2\in\mathscr{C}(\mathrm{SO}(3),\mathbb{C}) \text{ and each } c_1,c_2\in\mathbb{C}. \tag{3.59}$$

Condition (ii) for real-valued Haar functionals no longer makes sense for complex-valued functionals, but it is valid for both the real part $\mathfrak{Re}\, f$ and imaginary part $\mathfrak{Im}\, f$ of f. Since $\mathfrak{Re}\, f$ and $\mathfrak{Im}\, f$ are bi-invariant and inverse-invariant, $I(\cdot)$ as a complex-valued functional remains bi-invariant and inverse-invariant, i.e., we have

$$\int_{\mathrm{SO}(3)} f(\boldsymbol{R})\, d\mathfrak{g}(\boldsymbol{R}) = \int_{\mathrm{SO}(3)} f(\boldsymbol{Q}^{-1}\boldsymbol{R})\, d\mathfrak{g}(\boldsymbol{R}) = \int_{\mathrm{SO}(3)} f(\boldsymbol{R}\boldsymbol{Q})\, d\mathfrak{g}(\boldsymbol{R}), \tag{3.60}$$

and

$$\int_{\mathrm{SO}(3)} f(\boldsymbol{R}^{-1})\, d\mathfrak{g}(\boldsymbol{R}) = \int_{\mathrm{SO}(3)} f(\boldsymbol{R})\, d\mathfrak{g}(\boldsymbol{R}), \tag{3.61}$$

for each $\boldsymbol{Q} \in \mathrm{SO}(3)$ and each $f \in \mathscr{C}(\mathrm{SO}(3), \mathbb{C})$. Moreover, clearly $I(1) = 1$.

Chapter 4

4 Orientation Distribution Function

Readers who have no prior exposure to quantitative texture analysis or have no strong urge to study at once various formulations and conventions (including those of Bunge and Roe) may skip Sects. 4.1.1, 4.4, and 4.5 on a first reading.

4.1 Definition of the ODF for Aggregates of Triclinic Crystallites

Mass density is a basic concept in continuum mechanics. It arises from a basic assumption on the mass and volume measures of a body.[55] Consider a body $\mathcal{B}$ that occupies a bounded region Ω in the physical space E^3. All the measurable subsets of Ω are bounded. Mass and volume are two positive finite measures defined on Ω. For a measurable subset E of $\mathcal{B}$, let $M(E)$ and $\mathrm{V}(E)$ be the mass and volume of E, respectively. A basic assumption in continuum mechanics is the absolute continuity of the mass measure with respect to the volume measure, i.e.,

$$M(E) = 0 \quad \text{for each measurable } E \text{ for which } \mathrm{V}(E) = 0. \tag{4.1}$$

Under this assumption, the Radon-Nikodym derivative $dM/d\mathrm{V}$ of the measure M with respect to the measure V is well defined at almost every $\boldsymbol{x} \in \mathcal{B}$ (i.e., except possibly for a set of zero volume) as follows. At almost every $\boldsymbol{x} \in \mathcal{B}$, for every sequence of Borel sets $\{E_n\}$ that "shrinks nicely" to $\boldsymbol{x}$,[56]

$$\lim_{n\to\infty} \frac{M(E_n)}{\mathrm{V}(E_n)} \quad \text{exists and is equal to the same number which we denote by } \rho(\boldsymbol{x}). \tag{4.2}$$

The function

$$\rho(\boldsymbol{x}) := \frac{dM}{d\mathrm{V}}(\boldsymbol{x}), \qquad (\boldsymbol{x} \in \mathcal{B}) \tag{4.3}$$

called the mass density, is integrable on Ω and satisfies

$$M(E) = \int_E \rho \, d\mathrm{V} \tag{4.4}$$

for each measurable subset E of Ω.

In texture analysis, for aggregates of triclinic crystallites the orientation distribution function (ODF) is a Radon-Nikodym derivative analogous to the mass density ρ. As a first step, we focus our attention in this chapter to aggregates of triclinic crystallites (whose group of crystallite symmetry $G_{\mathrm{cr}} = C_1 = \{\boldsymbol{I}\}$) for the following reasons:

1. Analysis of such aggregates is conceptually the simplest.
2. It can serve as the basis upon which analysis for aggregates with non-trivial crystallite symmetry is built.

[55] Cf. Footnote 49 of Chap. 3 for comments on the terms "measure", "measurable", and "Borel set".

[56] See Rudin [278, p. 140] for a precise definition of "shrinking nicely". What is important here is the general idea, not the mathematical details. An example of Borel sets that shrink nicely to $\boldsymbol{x}$ is a sequence of open balls $\mathrm{B}_n(\boldsymbol{x}; r_n)$ centered at $\boldsymbol{x}$ with radius r_n such that $r_n \to 0$ as $n \to \infty$.

3. In some problems of texture analysis the solution for aggregates of crystallites with any G_{cr} can be obtained by applying restrictions imposed by crystallite symmetry to the corresponding solution for aggregates of triclinic crystallites. In other words, we can largely solve each of such problems for all polycrystalline aggregates in one stroke by solving the corresponding problem for aggregates of triclinic crystallites.

For aggregates of triclinic crystallites, once a reference ideal crystal $(\mathsf{C}, \boldsymbol{\kappa}_0)$ has been chosen, the crystallographic orientation at a sampling point $\mathtt{x}$ in a polycrystalline sample is defined by a rotation $\boldsymbol{R}$ that takes the chosen lattice basis vectors of the reference ideal crystal to their counterparts at $\mathtt{x}$ (cf. Sect. 3.1.1 for a more detailed discussion). Hence the space of orientations in question is given by the rotation group SO(3).

In texture analysis of aggregates of triclinic crystallites, there are then two basic measures on the space of orientations SO(3), namely the orientation (probability) measure $\wp$ and the chosen bi-invariant volume measure, two common choices of which are $\mathcal{V}$ and $\mathfrak{g}$ with $\mathcal{V}(\mathrm{SO}(3)) = 8\pi^2$ and $\mathfrak{g}(\mathrm{SO}(3)) = 1$, respectively. Under situations where the probability measure $\wp$ is absolutely continuous with respect to the group volume $\mathcal{V}$ (resp. $\mathfrak{g}$),[57] i.e.,

$$\wp(A) = 0 \quad \text{for each Borel set } A \subset \mathrm{SO}(3) \text{ for which } \mathcal{V}(A) = 0, \tag{4.5}$$

the orientation distribution function $w^{(a)}$ (resp. $\mathtt{f}^{(a)}$) is defined as the Radon-Nikodym derivative of $\wp$ with respect to $\mathcal{V}$ (resp. $\mathfrak{g}$), i.e.,

$$w^{(a)}(\boldsymbol{R}) := \frac{d\wp}{d\mathcal{V}}(\boldsymbol{R}) \qquad \left(\text{resp. } \mathtt{f}^{(a)}(\boldsymbol{R}) := \frac{d\wp}{d\mathfrak{g}}(\boldsymbol{R})\right) \tag{4.6}$$

so that for a Borel subset A of SO(3)

$$\wp(A) = \int_A w^{(a)}\, d\mathcal{V} \qquad \left(\text{resp. } \wp(A) = \int_A \mathtt{f}^{(a)}\, d\mathfrak{g}\right) \tag{4.7}$$

gives the probability of finding the lattice orientation at the sampling point in question to be in A. Since $d\mathcal{V} = 8\pi^2 d\mathfrak{g}$, we have

$$w^{(a)} = \frac{1}{8\pi^2}\mathtt{f}^{(a)}. \tag{4.8}$$

In this exposition, we will take $w^{(a)}$ as the orientation distribution function, except when we discuss the formulations (e.g., Bunge's) that use $\mathtt{f}^{(p)} := \mathtt{f}^{(a)} \circ \mathscr{J}$, where $\mathscr{J} : \boldsymbol{R} \mapsto \boldsymbol{R}^{-1}$ is the inversion map on SO(3). We shall suppress the superscript "(a)" in $w^{(a)}$ and "(p)" in $\mathtt{f}^{(p)}$, respectively, i.e., writing w for $w^{(a)}$ and $\mathtt{f}$ for $\mathtt{f}^{(p)}$, after we explain in Sect. 4.1.1 the two conventions of using active and passive rotations, respectively, as arguments of the ODF.

Remark 4.1 Roe [270, 271] and Bunge [56, 60] call their w and $\mathtt{f}$ the "crystallite orientation distribution function" and "orientation distribution function", respectively, irrespective of the point group symmetry of the crystallites in question. Some authors elect to call these functions "orientation density function (ODF)". By (4.6) such renaming of these functions

[57] Note that a Dirac measure on SO(3) is not absolutely continuous with respect to $\mathcal{V}$.

is clearly apt for aggregates of triclinic crystallites. For aggregates of crystallites with non-trivial symmetry, however, SO(3) is not the space of crystallite orientations (see Chap. 6). In the Roe approach the orientation distribution function w is always defined on SO(3), and it is not an orientation probability density there unless the crystallites in question are triclinic. In the Bunge approach the preference is to take $\mathtt{f}$ as defined on the orientation space, which Bunge [60] identifies with a suitable "asymmetric unit" or fundamental domain (see Chap. 6) in SO(3). With a suitable volume measure defined on the orientation space, $\mathtt{f}$ can indeed be interpreted as an orientation (probability) density function. In this exposition we follow the Roe approach. Henceforth we will follow Roe and call w the orientation distribution function and reserve the initialism ODF to mean that. □

4.1.1 ODF Under the Active and Passive View of Rotations

Consider the orientation of a right-handed orthonormal triad $\{\boldsymbol{e}_i' : i = 1, 2, 3\}$ with respect to a fixed right-handed orthonormal triad $\{\boldsymbol{e}_i : i = 1, 2, 3\}$; see Fig. 1, where $\boldsymbol{e}_i' = g\boldsymbol{e}_i$ $(i = 1, 2, 3)$. The orientation can be described by various choices of Euler angles, and we have presented two main choices in the literature, namely (ψ, θ, ϕ) and $(\varphi_1, \Phi, \varphi_2)$. The set of all such orientations is the set of all rotations SO(3). There are, however, two conventions in assigning a rotation matrix to describe a given orientation $g \in \mathrm{SO}(3)$. As shown in Sect. 1.7, under the convention of active rotations, the orientation of the triad $\{g\boldsymbol{e}_i : 1, 2, 3\}$ with respect to the triad $\{\boldsymbol{e}_i : i = 1, 2, 3\}$ in Fig. 1 is described by the matrix $\boldsymbol{R}(\psi, \theta, \phi)$ given in (1.89). On the other hand, under the convention of passive rotations the same orientation g is described by the matrix $\boldsymbol{R}^{(p)} = \boldsymbol{R}^{-1}$. When SO(3) is parametrized by the Euler angles (ψ, θ, ϕ) (resp. $(\varphi_1, \Phi, \varphi_2)$), there holds $\boldsymbol{R}^{(p)}(\psi, \theta, \phi) = \boldsymbol{R}(\pi - \phi, \theta, \pi - \psi)$ (resp. $\boldsymbol{R}^{(p)}(\varphi_1, \Phi, \varphi_2) = (\pi - \varphi_2, \Phi, \pi - \varphi_1)$), which is given explicitly in (1.100) (resp. (1.105)).

We use active rotations in this exposition, under which $g(\psi, \theta, \phi) \in \mathrm{SO}(3)$ is represented by the active rotation matrix $\boldsymbol{R}(\psi, \theta, \phi)$. Under this convention the ODF $w^{(a)} : \boldsymbol{R}(\psi, \theta, \phi) \mapsto w^{(a)}(\boldsymbol{R}(\psi, \theta, \psi))$, where the superscript "(a)" indicates that the domain of the ODF $w^{(a)}$ consists of the active rotation matrices.

Under the convention of passive rotations, the orientation $g(\psi, \theta, \phi)$ is represented by the passive rotation matrix $\boldsymbol{R}^{(p)}(\psi, \theta, \phi) = \boldsymbol{R}^{-1}(\psi, \theta, \phi)$, and the ODF $w^{(p)} : \boldsymbol{R}^{(p)}(\psi, \theta, \phi) \mapsto w^{(p)}(\boldsymbol{R}^{(p)}(\psi, \theta, \phi))$. Since $w^{(a)}(\boldsymbol{R}(\psi, \theta, \phi))$ and $w^{(p)}(\boldsymbol{R}^{(p)}(\psi, \theta, \phi))$ give the same probability density of finding the orientation being $g(\psi, \theta, \phi)$ at the sampling point in question, they are equal, i.e.,

$$w^{(a)}(\boldsymbol{R}(\psi, \theta, \phi)) = w^{(p)}(\boldsymbol{R}^{-1}(\psi, \theta, \phi))) \qquad \text{for each } \boldsymbol{R} \in \mathrm{SO}(3). \tag{4.9}$$

Clearly we have

$$w^{(p)} = w^{(a)} \circ \mathscr{J}, \qquad w^{(a)} = w^{(p)} \circ \mathscr{J}, \qquad \text{where } \mathscr{J} : \boldsymbol{R} \mapsto \boldsymbol{R}^{-1}. \tag{4.10}$$

Mathematically $w^{(a)} : \mathrm{SO}(3) \to \mathbb{R}$ and $w^{(p)} : \mathrm{SO}(3) \to \mathbb{R}$ are two different functions but are related by (4.9) and (4.10).

In this exposition we will use $w^{(a)}$ as the primary ODF. For simplicity we will suppress the superscript and henceforth the ODF w will always mean $w^{(a)}$.

Similarly, let $\mathtt{f}^{(p)}$ be the ODF under the convention of passive rotations and the choice that the bi-invariant group volume $\mathtt{g}(\mathrm{SO}(3)) = 1$. Since $\mathtt{f} := \mathtt{f}^{(p)}$ is, after the works of Bunge and his coworkers (in particular, Bunge's influential treatise [60]), the most commonly used ODF in the literature of texture analysis, we will henceforth write $\mathtt{f}$ for $\mathtt{f}^{(p)}$.

Let $\mathtt{f}^{(a)}$ be the corresponding ODF under the convention of active rotations. Then we have

$$\mathtt{f}^{(a)} = \mathtt{f} \circ \mathscr{J}, \qquad \mathtt{f} = \mathtt{f}^{(a)} \circ \mathscr{J}, \qquad \text{where } \mathscr{J} : \boldsymbol{R} \mapsto \boldsymbol{R}^{-1}. \tag{4.11}$$

Moreover, if the generic orientation g is denoted by the Euler angles (ψ, θ, ϕ) (resp. $(\varphi_1, \Phi, \varphi_2)$) when w (resp. $\mathtt{f}$) is used as the ODF, there holds

$$w(\boldsymbol{R}(\psi, \theta, \phi)) = \frac{1}{8\pi^2}\mathtt{f}^{(a)}(\boldsymbol{R}(\psi, \theta, \phi)) = \frac{1}{8\pi^2}\mathtt{f}(\boldsymbol{R}^{-1}(\varphi_1, \Phi, \varphi_2)) = w^{(p)}(\boldsymbol{R}^{-1}(\varphi_1, \Phi, \varphi_2)). \tag{4.12}$$

Remark 4.2 The awareness that there are two types of ODF which have the active and the passive rotation matrices as arguments, respectively, will be the key to understanding of the interrelationships between various formulations of the ODF and texture coefficients in the literature. □

Remark 4.3 Every function $f : \mathrm{SO}(3) \to \mathbb{K}$, where $\mathbb{K} = \mathbb{R}$ or $\mathbb{C}$, can be taken as defined on the active rotation matrices $\boldsymbol{R}$ (i.e., $f = f^{(a)}$) or on the passive rotation matrices $\boldsymbol{R}^{(p)}$ (i.e., $f = f^{(p)}$). While $f^{(a)}(\boldsymbol{R}) = f^{(p)}(\boldsymbol{R}^{-1})$ for each rotation $\boldsymbol{R}$, $f^{(a)}$ and $f^{(p)}$ are different functions. Using the same symbol to denote these two functions will lead to ambiguity and confusion; cf. Sect. 4.5.4.

In this exposition we take the active view of rotations. Unless stated explicitly otherwise (e.g., the Bunge ODF $\mathtt{f}$ is a notable exception), by a real- or complex-valued function $f(\cdot)$ defined on SO(3) we will mean $f^{(a)}(\cdot)$ defined on the active rotation matrices with the superscript "(a)" suppressed. □

4.2 The Wigner D-Functions

The Wigner D-functions, which were introduced by Eugene P. Wigner in quantum theory of angular momentum, play a central role in classical texture analysis. We shall derive in Chap. 14 of this exposition all the formulas pertaining to the Wigner D-functions that we need. Here we will summarize some essential facts about them.

Let $\mathbb{C}$ be the set of complex numbers. For $\alpha \in \mathbb{C}$, we denote by $\overline{\alpha}$, $|\alpha|$, $\mathfrak{Re}\,\alpha$, and $\mathfrak{Im}\,\alpha$ the complex conjugate, the modulus, the real part, and the imaginary part of α, respectively.

Let $L^2(\mathrm{SO}(3), \mathbb{C})$ be the space of square-integrable complex-valued functions on SO(3), i.e., those $f : \mathrm{SO}(3) \to \mathbb{C}$ with

$$\int_{\mathrm{SO}(3)} |f(\boldsymbol{R})|^2 d\mathcal{V}(\boldsymbol{R}) < +\infty.$$

Addition and scalar multiplication in this space are defined by

$$(f_1 + f_2)(\boldsymbol{R}) = f_1(\boldsymbol{R}) + f_2(\boldsymbol{R}),$$
$$(\alpha f)(\boldsymbol{R}) = \alpha f(\boldsymbol{R})$$

for $\alpha \in \mathbb{C}$ and f, f_1, and $f_2 \in L^2(\mathrm{SO}(3), \mathbb{C})$. Under the (Hermitian) inner product[58]

$$\langle f_1, f_2 \rangle = \int_{\mathrm{SO}(3)} f_1(\boldsymbol{R}) \overline{f_2(\boldsymbol{R})}\, d\mathcal{V}(\boldsymbol{R}), \tag{4.13}$$

$L^2(\mathrm{SO}(3), \mathbb{C})$ becomes a Hilbert space. For $f \in L^2(\mathrm{SO}(3), \mathbb{C})$, henceforth we shall write $\|f\| = \sqrt{\langle f, f \rangle}$ and call it the norm of f.

The most essential attribute of the Wigner D-functions is captured by the following assertion:

(*) The Wigner D-functions $D^l_{mn} : \mathrm{SO}(3) \to \mathbb{C}$, $\boldsymbol{R} \mapsto D^l_{mn}(\boldsymbol{R})$ ($l = 0, 1, 2, \ldots; -l \leq m \leq l, -l \leq n \leq l$) are the matrix elements of a complete set of pairwise-inequivalent, continuous, irreducible unitary representations $\mathcal{D}^l$ of the rotation group SO(3).

A proof of this assertion will be given in Part III of this exposition. There all the technical terms of this assertion will be defined and its main consequences derived. Here we shall be content to explain about the unitary representations $\mathcal{D}^l$ and list some essential facts and formulas on the Wigner D-functions:[59]

1. For each l and each rotation $\boldsymbol{R}$, $D^l_{mn}(\boldsymbol{R})$ is the mn-th entry of a $(2l+1) \times (2l+1)$ matrix, which we denote by $[D^l(\boldsymbol{R})]$. In exhibiting these matrices, we let the indices m and n run from l to $-l$ when reading from top to bottom and when reading from left to right, respectively.[60] For instance, $[D^1(\boldsymbol{R})]$ is shown as

$$\begin{pmatrix} D^1_{11}(\boldsymbol{R}) & D^1_{10}(\boldsymbol{R}) & D^1_{1\bar{1}}(\boldsymbol{R}) \\ D^1_{01}(\boldsymbol{R}) & D^1_{00}(\boldsymbol{R}) & D^1_{0\bar{1}}(\boldsymbol{R}) \\ D^1_{\bar{1}1}(\boldsymbol{R}) & D^1_{\bar{1}0}(\boldsymbol{R}) & D^1_{\bar{1}\bar{1}}(\boldsymbol{R}) \end{pmatrix}.$$

   The matrices $[D^l(\boldsymbol{R})]$ are unitary, i.e.,

$$([D^l(\boldsymbol{R})]^{-1})_{mn} = \overline{D^l_{nm}(\boldsymbol{R})}, \tag{4.14}$$

   where $([D^l(\boldsymbol{R})]^{-1})_{mn}$ denotes the mn-th entry of the inverse matrix of $[D^l(\boldsymbol{R})]$.
2. As stated in assertion (*), the correspondence $\boldsymbol{R} \mapsto [D^l(\boldsymbol{R})]$ is a representation of the rotation group SO(3). It satisfies

$$\boldsymbol{R}_2 \boldsymbol{R}_1 \mapsto [D^l(\boldsymbol{R}_2 \boldsymbol{R}_1)] = [D^l(\boldsymbol{R}_2)][D^l(\boldsymbol{R}_1)] \tag{4.15}$$

[58] Here we follow Roe [270] and assign to SO(3) the bi-invariant volume measure $\mathcal{V}$ that satisfies $\mathcal{V}(\mathrm{SO}(3)) = 8\pi^2$. The number $8\pi^2$ arises in Roe's work because he uses Euler angles as parameters of SO(3). In Part III, where we shall present general theorems on group representations, the only reasonable volume measure that applies to all compact groups alike is their respective normalized Haar measure (see Sect. C.3 of Appendix C), which for SO(3) is $\mathcal{G} = \mathcal{V}/(8\pi^2)$.

[59] Following usual practice, when an integer m appears as an index such as in D^l_{mn}, we write $\bar{m}$ for $-m$. Thus $D^3_{1\bar{2}}$ denotes the Wigner D-function with $l = 3$, $m = -1$, and $n = -2$.

[60] Here we follow the standard convention in the physics literature; see, e.g., Biedenharn and Louck [28, p. 46].

for each $\boldsymbol{R}_1$ and $\boldsymbol{R}_2$ in SO(3). In terms of the entries of the matrices $[D^l(\boldsymbol{R})]$, we have[61]

$$D^l_{mn}(\boldsymbol{R}_2\boldsymbol{R}_1) = \sum_{k=-l}^{l} D^l_{mk}(\boldsymbol{R}_2) D^l_{kn}(\boldsymbol{R}_1). \tag{4.16}$$

By putting $\boldsymbol{R}_1 = \boldsymbol{I}$ and $\boldsymbol{R}_1 = \boldsymbol{R}_2^{-1}$ in (4.15), we obtain

$$D^l_{mn}(\boldsymbol{I}) = \delta_{mn}, \qquad \text{and} \quad [D^l(\boldsymbol{R}^{-1})] = [D^l(\boldsymbol{R})]^{-1}, \tag{4.17}$$

respectively. The representation $\boldsymbol{R} \mapsto [D^l(\boldsymbol{R})]$ is said to be unitary because the matrix $[D^l(\boldsymbol{R})]$ is unitary.

3. The property described by assertion (*), however, does not define the Wigner D-functions uniquely. For instance, if $\{D^l_{mn}\}$ is one valid set of Wigner D-functions, then the set $\{(-1)^{m+n} D^l_{mn}\}$ will work as well. In this exposition we will follow the convention most commonly adopted in the physics literature in the last three decades. Under this convention, when active rotations $\boldsymbol{R}$ are parametrized by the Euler angles (ψ, θ, ϕ), the Wigner D-functions are given by the explicit formula[62]

$$D^l_{mn}(\boldsymbol{R}(\psi, \theta, \phi)) = e^{-im\psi} d^l_{mn}(\theta) e^{-in\phi}, \tag{4.18}$$

where $\psi \in [0, 2\pi)$, $\theta \in [0, \pi]$, $\phi \in [0, 2\pi)$,

$$d^l_{mn}(\theta) = \sum_k (-1)^{m-n+k} \frac{\sqrt{(l+m)!(l-m)!(l+n)!(l-n)!}}{k!(l+n-k)!(l-m-k)!(m-n+k)!} \times \left(\cos\frac{\theta}{2}\right)^{2l+n-m-2k} \left(\sin\frac{\theta}{2}\right)^{2k+m-n}, \tag{4.19}$$

and the summation in (4.19) extends over integer values of k that satisfy

$$k \geq 0, \quad k \leq l+n, \quad k \leq l-m, \quad k \geq n-m. \tag{4.20}$$

Note that the function d^l_{mn} is real-valued and the inequalities (4.20) guarantee that the power of $\cos(\theta/2)$ and of $\sin(\theta/2)$ in (4.19) are non-negative. We will derive in Chap. 14 formulas (4.18) and (4.19) from the attribute of Wigner D-functions stated in assertion (*).

In quantum mechanics, the matrices $[D^l_{mn}(\psi, \theta, \phi)]$ are called Wigner (active) rotation matrices;[63] $D^l_{mn}(\psi, \theta, \phi)$ are the rotation matrix elements, and $d^l_{mn}(\theta)$ are called the reduced matrix elements.

[61] Equation (4.16) is often called the addition theorem in the literature.

[62] The formulas for D^l_{mn} and d^l_{mn} here are the same as those in Biedenharn and Louck [28, equations (3.59) and (3.65)], Rose [274, equations (4.12) and (4.13)], and Varshalovich et al. [325, pp. 76–77, equations (1) and (5)]. In [207], there are 27 references which adopt active rotations with (4.18) here for D^l_{mn} and (4.19) or (14.43) for d^l_{mn}. In comparison, there are 12 references which use the corresponding formulas for passive rotations, i.e., for $D^l_{mn} \circ \mathscr{J}$, etc., where $\mathscr{J} : \boldsymbol{R} \mapsto \boldsymbol{R}^{-1}$.

[63] As we take the active view of rotations, the adjective "active" will be suppressed except at places where we discuss it with its passive counterpart.

4. The Wigner D-functions $D^l_{mn} : \mathrm{SO}(3) \to \mathbb{C}$, where $l = 0, 1, 2, \ldots, -l \le m \le l$, and $-l \le n \le l$, constitute an orthogonal basis in $L^2(\mathrm{SO}(3), \mathbb{C})$. They satisfy the orthogonality relation

$$\begin{aligned}\langle D^l_{mn}, D^{l'}_{m'n'}\rangle &= \int_{\mathrm{SO}(3)} D^l_{mn}(\boldsymbol{R})\overline{D^{l'}_{m'n'}(\boldsymbol{R})}\, d\mathcal{V}(\boldsymbol{R}) \\ &= \int_0^{2\pi}\int_0^{\pi}\int_0^{2\pi} D^l_{mn}(\psi,\theta,\phi)\overline{D^{l'}_{m'n'}(\psi,\theta,\phi)}\sin\theta\, d\psi\, d\theta\, d\phi \\ &= \frac{8\pi^2}{2l+1}\delta_{ll'}\delta_{mm'}\delta_{nn'}, \end{aligned} \tag{4.21}$$

where we have appealed to assertion (*), (3.41), (3.42), and Theorem 13.20. Each function f in $L^2(\mathrm{SO}(3), \mathbb{C})$ can be expressed as an infinite series

$$f(\boldsymbol{R}) = \sum_{l=0}^{\infty}\sum_{m=-l}^{l}\sum_{n=-l}^{l} c^l_{mn} D^l_{mn}(\boldsymbol{R}), \tag{4.22}$$

where

$$c^l_{mn} = \frac{2l+1}{8\pi^2}\int_0^{2\pi}\int_0^{\pi}\int_0^{2\pi} f(\psi,\theta,\phi)\overline{D^l_{mn}(\psi,\theta,\phi)}\sin\theta\, d\psi\, d\theta\, d\phi; \tag{4.23}$$

see Corollary 15.8. The series on the right of (4.22) converges to f in the sense that

$$\lim_{N\to\infty}\|f - \sum_{l=0}^{N}\sum_{m=-l}^{l}\sum_{n=-l}^{l} c^l_{mn} D^l_{mn}\| = 0. \tag{4.24}$$

From (4.18) and (4.21) follows immediately the orthogonality relation for the functions d^l_{mn}:

$$\langle d^l_{mn}, d^{l'}_{mn}\rangle = \int_0^{\pi} d^l_{mn}(\theta) d^{l'}_{mn}(\theta)\sin\theta\, d\theta = \frac{2}{2l+1}\delta_{ll'}. \tag{4.25}$$

By (4.19) we have

$$d^0_{00}(\theta) \equiv 1. \tag{4.26}$$

From (4.25) and (4.26) we obtain for $l \neq 0$

$$\int_0^{\pi} d^l_{00}(\theta)\sin\theta\, d\theta = \int_0^{\pi} d^l_{00}(\theta) d^0_{00}(\theta)\sin\theta\, d\theta = \delta_{l0} = 0. \tag{4.27}$$

From (4.18) and (4.27) we observe that

$$\begin{aligned}\int_{\mathrm{SO}(3)} D^l_{mn}(\boldsymbol{R})d\mathcal{V}(\boldsymbol{R}) &= \int_0^{2\pi}\int_0^{\pi}\int_0^{2\pi} D^l_{mn}(\psi,\theta,\phi)\sin\theta d\psi d\theta d\phi \\ &= \left(\int_0^{2\pi} e^{-im\psi}d\psi\right)\left(\int_0^{\pi} d^l_{mn}(\theta)\sin\theta d\theta\right)\left(\int_0^{2\pi} e^{-in\phi}d\phi\right) \\ &= 0 \end{aligned} \tag{4.28}$$

unless $l=0$, $m=0$, and $n=0$.

Note that with the Euler angles as parameters, by $(4.17)_1$ we have

$$D^l_{mn}(0,0,0) = d^l_{mn}(0) = \delta_{mn}. \tag{4.29}$$

Also, it follows from (4.18) and (4.26) that

$$D^0_{00}(\psi,\theta,\phi) \equiv 1. \tag{4.30}$$

4.2.1 Symmetry Properties of d^l_{mn}

As formula (4.19) makes sense for all $\theta \in (-\infty,\infty)$, we extend the domain of $d^l_{mn}(\cdot)$ from $[0,\pi]$ to $(-\infty,\infty)$. For later use, we derive several symmetry properties observed by the functions $d^l_{mn}(\cdot)$:

$$d^l_{\bar{m}\bar{n}}(\theta) = d^l_{nm}(\theta), \qquad d^l_{mn}(-\theta) = (-1)^{m-n}d^l_{mn}(\theta), \tag{4.31}$$

$$d^l_{mn}(\theta) = (-1)^{m-n}d^l_{nm}(\theta), \qquad d^l_{mn}(-\theta) = d^l_{nm}(\theta), \tag{4.32}$$

$$d^l_{mn}(\pi-\theta) = (-1)^{l+m}d^l_{m\bar{n}}(\theta) = (-1)^{l+n}d^l_{\bar{m}n}(\theta). \tag{4.33}$$

The two equations in (4.31) can be read off from formula (4.19) by inspection. Equation $(4.32)_1$ follows from the fact that the matrix $[D^l_{mn}]$ is unitary and the function $d^l_{mn}(\cdot)$ is real-valued. Indeed, since $\boldsymbol{R}(\boldsymbol{e}_2,-\theta) = \boldsymbol{R}(\boldsymbol{e}_2,\theta)^{-1}$ and by (1.93) $\boldsymbol{R}(\boldsymbol{e}_2,-\theta) = \boldsymbol{R}(\boldsymbol{e}_3,\pi)\boldsymbol{R}(\boldsymbol{e}_2,\theta)\boldsymbol{R}(\boldsymbol{e}_3,\pi)$, we have

$$[D^l_{mn}(\boldsymbol{R}(\boldsymbol{e}_2,-\theta))] = [D^l_{mn}(\boldsymbol{R}(\boldsymbol{e}_2,\theta))]^{-1}, \tag{4.34}$$

or

$$e^{-im\pi}d^l_{mn}(\theta)e^{-in\pi} = \overline{d^l_{nm}(\theta)} = d^l_{nm}(\theta). \tag{4.35}$$

Equation $(4.32)_2$ is an immediate consequence of $(4.31)_2$ and $(4.32)_1$.

To prove (4.33), first note that by formula (4.19) we have

$$\begin{aligned} d^l_{mn}(\pi-\theta) = \sum_k (-1)^{m-n+k}\frac{\sqrt{(l+m)!(l-m)!(l+n)!(l-n)!}}{k!(l+n-k)!(l-m-k)!(m-n+k)!} \\ \times\left(\sin\frac{\theta}{2}\right)^{2l+n-m-2k}\left(\cos\frac{\theta}{2}\right)^{2k+m-n}. \end{aligned} \tag{4.36}$$

Changing the running parameter from k to $k' = l - m - k$, we get $l + n - k = m + n + k' = m - \bar{n} + k'$, $m - n + k = l + \bar{n} - k'$, $2l + n - m - 2k = m - \bar{n} + 2k'$, $2k + m - n = 2l + \bar{n} - m - 2k'$, and

$$d^l_{mn}(\pi - \theta) = \sum_{k'} (-1)^{l+\bar{n}-k'} \frac{\sqrt{(l+m)!(l-m)!(l+n)!(l-n)!}}{k'!(l+\bar{n}-k')!(l-m-k')!(m-\bar{n}+k')!} \times \left(\cos\frac{\theta}{2}\right)^{2l+\bar{n}-m-2k'} \left(\sin\frac{\theta}{2}\right)^{2k'+m-\bar{n}}$$
$$= (-1)^{l+\bar{n}}(-1)^{m+\bar{n}} d^l_{m\bar{n}}(\theta)$$
$$= (-1)^{l+m} d^l_{m\bar{n}}(\theta). \tag{4.37}$$

Substituting $(4.31)_1$ into $(4.32)_2$ and using $(4.31)_2$, we observe that

$$d^l_{mn}(\theta) = (-1)^{m-n} d^l_{\bar{m}\bar{n}}(\theta). \tag{4.38}$$

Substituting (4.38) into the right-hand side of (4.37) with $\bar{n}$ replacing n, we obtain

$$d^l_{mn}(\pi - \theta) = (-1)^{l+m}(-1)^{m+n} d^l_{\bar{m}n}(\theta) = (-1)^{l+n} d^l_{\bar{m}n}(\theta). \tag{4.39}$$

4.2.2 Symmetry Properties of D^l_{mn}

From the definition $D^l_{mn}(\psi, \theta, \phi) = e^{-im\psi} d^l_{mn}(\theta) e^{-in\phi}$ and the symmetry properties of the functions d^l_{mn}, we can easily derive symmetry properties of the Wigner D-functions. Here are some examples:

$$D^l_{\bar{m}\bar{n}}(\psi, \theta, \phi) = D^l_{mn}(-\psi, -\theta, -\phi) = (-1)^{m-n} \overline{D^l_{mn}(\psi, \theta, \phi)}, \tag{4.40}$$

$$D^l_{\bar{n}\bar{m}}(\psi, \theta, \phi) = (-1)^{m+n} D^l_{mn}(\pi - \phi, \theta, \pi - \psi), \tag{4.41}$$

$$D^l_{nm}(\psi, \theta, \phi) = (-1)^{n-m} D^l_{mn}(\phi, \theta, \psi), \tag{4.42}$$

$$D^l_{mn}(\psi, \pi - \theta, \phi) = (-1)^{l+m} D^l_{m\bar{n}}(\psi, \theta, -\phi) = (-1)^{l+n} D^l_{\bar{m}n}(-\psi, \theta, \phi). \tag{4.43}$$

Long lists of symmetry properties of d^l_{mn} and D^l_{mn} can be found in Sect. 4.4 of [325].

4.3 Series Expansion and Texture Coefficients

As pointed out in Sects. 3.1 and 4.1, once a reference placement of an ideal crystal has been chosen for the description of orientations by rotations, the texture of a material point in a polycrystalline aggregate of triclinic crystallites is described by an orientation probability measure $\wp$ defined on the rotation group SO(3). If $\wp$ is absolutely continuous with respect to the bi-invariant volume measure $\mathcal{V}$, the texture can be described by the orientation distribution function (ODF). The ODF w is a real-valued function defined on SO(3) and, as a probability density function, it satisfies the constraint

$$\int_{\mathrm{SO(3)}} w(\boldsymbol{R}) d\mathcal{V}(\boldsymbol{R}) = 1. \tag{4.44}$$

For $w \in L^2(\mathrm{SO}(3), \mathbb{C})$, we can expand the ODF as an infinite series in terms of the Wigner D-functions (see Remark 15.9 for justification):

$$w(\boldsymbol{R}(\psi,\theta,\phi)) = \sum_{l=0}^{\infty} \sum_{m=-l}^{l} \sum_{n=-l}^{l} c_{mn}^{l} D_{mn}^{l}(\boldsymbol{R}(\psi,\theta,\phi)), \tag{4.45}$$

where the expansion coefficients c_{mn}^{l} are called the texture coefficients of the ODF w. (Note that whenever the Euler angles are introduced, it is understood that a fixed spatial coordinate system has been chosen.)

As w is real-valued, we observe from formula (4.23) and symmetry condition (4.38) that the coefficients in the preceding expansion satisfy the condition

$$\begin{aligned}
\overline{c_{\bar{m}\bar{n}}^{l}} &= \overline{\frac{2l+1}{8\pi^2} \int_0^{2\pi}\int_0^{\pi}\int_0^{2\pi} w(\psi,\theta,\phi) \overline{e^{im\psi} d_{\bar{m}\bar{n}}^{l}(\theta) e^{in\psi}} \sin\theta \, d\psi \, d\theta \, d\phi} \\
&= \frac{2l+1}{8\pi^2} \int_0^{2\pi}\int_0^{\pi}\int_0^{2\pi} w(\psi,\theta,\phi) e^{im\psi} d_{\bar{m}\bar{n}}^{l}(\theta) e^{in\psi} \sin\theta \, d\psi \, d\theta \, d\phi \\
&= (-1)^{n-m} \frac{2l+1}{8\pi^2} \int_0^{2\pi}\int_0^{\pi}\int_0^{2\pi} w(\psi,\theta,\phi) \overline{e^{-im\psi} d_{mn}^{l}(\theta) e^{-in\psi}} \sin\theta \, d\psi \, d\theta \, d\phi \\
&= (-1)^{n-m} c_{mn}^{l}
\end{aligned}$$

or

$$c_{\bar{m}\bar{n}}^{l} = (-1)^{n-m} \overline{c_{mn}^{l}}. \tag{4.46}$$

Conversely, if condition (4.46) is satisfied by the coefficients c_{mn}^{l}, we have

$$\begin{aligned}
c_{\bar{m}\bar{n}}^{l} D_{\bar{m}\bar{n}}^{l}(\boldsymbol{R}(\psi,\theta,\phi)) &= (-1)^{n-m} \overline{c_{mn}^{l}} e^{im\psi} d_{\bar{m}\bar{n}}^{l}(\theta) e^{in\phi} \\
&= \overline{c_{mn}^{l}} e^{im\psi} d_{mn}^{l}(\theta) e^{in\phi} \\
&= \overline{c_{mn}^{l} D_{mn}^{l}(\boldsymbol{R}(\psi,\theta,\phi))},
\end{aligned}$$

so the function w in (4.45) is real.

Remark 4.4 By (4.46) the independent real parameters that define the ODF w can be taken as c_{00}^{l}, $\mathfrak{Re}\, c_{mn}^{l}$, $\mathfrak{Im}\, c_{mn}^{l}$ ($l \geq 1$, $-l \leq m \leq l$, $1 \leq n \leq l$; and for $n = 0$, $0 < m \leq l$). □

Let us now examine the integral condition (4.44). Equations (4.28) and (4.30) assert that

$$\int_{\mathrm{SO}(3)} D_{mn}^{l}(\boldsymbol{R}) d\mathcal{V}(\boldsymbol{R}) = 0 \quad \text{unless } l = m = n = 0 \tag{4.47}$$

and $D^0_{00} \equiv 1$, which imply

$$\int_{\mathrm{SO}(3)} w d\mathcal{V} = \int_{\mathrm{SO}(3)} \left(c^0_{00} + \sum_{l=1}^{\infty} \sum_{m=-l}^{l} \sum_{n=-l}^{l} c^l_{mn} D^l_{mn}(\boldsymbol{R}) \right) d\mathcal{V}(\boldsymbol{R}) = c^0_{00} \int_{\mathrm{SO}(3)} d\mathcal{V} = 8\pi^2 c^0_{00}. \tag{4.48}$$

Hence condition (4.44) dictates that the constant term in the expansion (4.45), which is none other than c^0_{00}, must be equal to $1/(8\pi^2)$. Thus we may recast (4.45) as

$$w(\boldsymbol{R}(\psi,\theta,\phi)) = \frac{1}{8\pi^2} + \sum_{l=1}^{\infty} \sum_{m=-l}^{l} \sum_{n=-l}^{l} c^l_{mn} D^l_{mn}(\boldsymbol{R}(\psi,\theta,\phi)). \tag{4.49}$$

From the preceding discussion (cf. (4.47) in particular) we observe also that the normalization condition (4.44) does not impose any restriction on the texture coefficients c^l_{mn} with $l \geq 1$.

When the crystallites in the polycrystal whose texture is described by the ODF w have no preferred orientations, we have $w = \text{constant} = 1/(8\pi^2)$, so all the coefficients c^l_{mn} with $l \geq 1$ vanish. We call c^l_{mn} ($l \geq 1$) the texture coefficients. By (4.23) and (4.45), the texture coefficients are given by the formula

$$c^l_{mn} = \frac{2l+1}{8\pi^2} \int_0^{2\pi} \int_0^{\pi} \int_0^{2\pi} w(\psi,\theta,\phi) \overline{D^l_{mn}(\psi,\theta,\phi)} \sin\theta \, d\psi \, d\theta \, d\phi. \tag{4.50}$$

4.4 Alternate Expressions for the Wigner D-functions

Bunge [60] and Roe [270] independently pioneered the development of quantitative texture analysis in the 1960s by proposing essentially the same experimental method to ascertain the ODF of a polycrystalline sample through inversion of measured X-ray pole figures. Their method starts by expanding the ODF in terms of some orthogonal basis T^{mn}_l [60] and $Z_{lmn}(\cos\theta)e^{-im\psi}e^{-in\phi}$ [270] in $L^2(\mathrm{SO}(3),\mathbb{C})$, which are different functions but are given the same name "generalized spherical harmonics" by Bunge and Roe, respectively. Both sets of generalized spherical harmonics are different from but are closely related to the Wigner D-functions D^l_{mn}, and the series expansions of the ODF by Bunge and by Roe are comparable to our (4.45). Before we can compare the series expansions, we should first look at some alternate expressions for the Wigner D-functions.

It has long been pointed out by Wigner ([340], p. 231; [341], p. 215) that the functions $\overline{D^l_{mn}(\psi,\theta,\phi)} = e^{im\psi} d^l_{mn}(\theta) e^{in\phi}$, which we have recast in our present notation, are energy eigenfunctions of the symmetric top in quantum mechanics.[64] The Schrödinger equation in question was first solved independently by Reiche and Rademacher [269] and by Kronig and Rabi [182]. The procedure of separation of variables leads to the following second-order differential equation that governs the reduced matrix elements d^l_{mn}:

$$\left(\frac{d^2}{d\theta^2} + \cot\theta \frac{d}{d\theta} + \left[l(l+1) - \frac{m^2 - 2mn\cos\theta + n^2}{\sin^2\theta} \right] \right) d^l_{mn} = 0. \tag{4.51}$$

[64] See Zare [352, pp. 104–105] for a proof in our present convention on active rotations and Euler angles, except that (ψ,θ,ϕ) is written as (ϕ,θ,χ).

For $\theta \in [0, \pi]$, let

$$x = \cos\theta, \qquad t = (1-x)/2; \tag{4.52}$$

Then $x \in [-1, 1]$ and $t = \sin^2 \frac{\theta}{2} \in [0, 1]$. By putting

$$d^l_{mn} = N(l, m, n) t^{|m-n|/2} (1-t)^{|m+n|/2} f(t), \tag{4.53}$$

in (4.51), where $N(l, m, n)$ is a constant, we observe [269] that the function f satisfies the hypergeometric equation

$$t(1-t)\frac{d^2 f}{dt^2} + [c - (1 + a + b)t]\frac{df}{dt} - abf = 0, \tag{4.54}$$

with the coefficients a, b, c given by the formulas

$$a = -l + \frac{1}{2}(|m-n| + |m+n|), \quad b = l + \frac{1}{2}(|m-n| + |m+n|) + 1, \quad c = |m-n| + 1. \tag{4.55}$$

Note that $c \geq 1$ is a positive integer, and $\frac{1}{2}(|m-n| + |m+n|)$ is equal to the larger of the two integers m and n (resp. $-m$ and $-n$) if $m + n \geq 0$ (resp. $m + n \leq 0$); thus $a \leq 0$ is a non-positive integer, and $b \geq 1$ is a positive integer. Henceforth we divide our discussion into four cases, namely: (i) $m + n \geq 0$ and $m - n \geq 0$; (ii) $m + n \geq 0$ and $m - n \leq 0$; (iii) $m + n \leq 0$ and $m - n \geq 0$; (iv) $m + n \leq 0$ and $m - n \leq 0$.

Roe [270, Appendix] defines his generalized spherical harmonics first for what we call case (i), where $m - n \geq 0$ and $m + n \geq 0$. Here for the purpose of comparison let us start our discussion also with this case. When $m - n \geq 0$ and $m + n \geq 0$,[65] the coefficients a, b, and c in (4.54) are given by

$$a = -l + m, \qquad b = l + m + 1, \qquad c = m - n + 1, \tag{4.56}$$

and the hypergeometric equation that governs the function f becomes[66]

$$t(1-t)\frac{d^2 f}{dt^2} + [(m-n+1) - 2(m+1)t]\frac{df}{dt} + [l(l+1) - m(m+1)]f = 0. \tag{4.57}$$

We are interested in solutions defined for $t \in [0, 1]$. By recasting the equation in question as

$$t^2\frac{d^2 f}{dt^2} + \frac{[(m-n+1) - 2(m+1)t]}{1-t} t\frac{df}{dt} + \frac{[l(l+1) - m(m+1)]t}{1-t} f = 0, \tag{4.58}$$

we see that it has a regular singular point at $t_0 = 0$. The indicial polynomial $r(r-1) + (m - n + 1)r$ has roots $r_1 = 0$ and $r_2 = n - m \leq 0$. By the Frobenius method, we know that there are (see, e.g., [73, p. 165]) two linearly independent solutions, one of which is in the form $f_1 = t^{r_1} \sum_{k=0}^{\infty} \beta_k t^k$, and the other of which depends on whether $r_1 - r_2$ is or is not zero or a positive integer. For the present case, $r_1 - r_2 = m - n$ is either zero or a positive integer. For both of these cases, the second solution f_2 has a singularity at $t = 0$ and is not defined there (see [73], [182]). Hence any physically acceptable solution to (4.57) is the first solution times some constant.

[65] Note that Roe mentions only the condition $m \geq n$ in his paper.

[66] This equation corresponds to equation (A4) of Roe's paper but has two typos there corrected.

To obtain the first solution, we substitute $f = \sum_{k=0}^{\infty} \beta_k t^k$ in (4.57), determine the constants β_k, and find that the solution is an arbitrary constant times the hypergeometric function [266, 300] ${}_2F(a, b; c; t)_1$—or $F(a, b; c; t)$ for simplicity—defined by

$$F(a, b; c; t) = 1 + \sum_{k=1}^{\infty} \frac{(a)_k (b)_k t^k}{(c)_k k!}, \tag{4.59}$$

where for $\gamma = a, b, c$ and for $k \geq 1$,

$$(\gamma)_k = \gamma(\gamma + 1)(\gamma + 2) \cdots (\gamma + k - 1). \tag{4.60}$$

Since $a = -l + m$ is a non-positive integer and $c \geq 1$ is a positive integer, the hypergeometric series $F(-l + m, l + m + 1; m - n + 1; (1 - x)/2)$ terminates and is a polynomial of degree $l - m$. In fact it is some constant times a Jacobi polynomial in x. The Jacobi polynomials can be defined (see, e.g., [80, pp. 373, 398], [266, pp. 253, 257]) by

$$P_s^{(\alpha,\beta)}(x) := \frac{(1 + \alpha)_s}{s!} F(-s, 1 + \alpha + \beta + s; 1 + \alpha; (1 - x)/2) \tag{4.61}$$

$$= \frac{(-1)^s (1 - x)^{-\alpha} (1 + x)^{-\beta}}{2^s s!} \frac{d^s}{dx^s} [(1 - x)^{s+\alpha} (1 + x)^{s+\beta}]. \tag{4.62}$$

For the present case (i.e., $m + n \geq 0$ and $m - n \geq 0$, which imply $m \geq 0$), we have

$$\alpha = m - n, \qquad \beta = m + n, \qquad s = l - m, \tag{4.63}$$

and

$$F(-l + m, l + m + 1; m - n + 1; (1 - x)/2) = \frac{(l - m)!(m - n)!}{(l - n)!} P_{l-m}^{(m-n,m+n)}(x). \tag{4.64}$$

Substitution of (4.64) into (4.53) yields the expression

$$d_{mn}^l(x) = N(l, m, n)(1 - x)^{(m-n)/2} (1 + x)^{(m+n)/2} \times F(-l + m, l + m + 1; m - n + 1; (1 - x)/2) \tag{4.65}$$

$$= \frac{N(l, m, n)(l - m)!(m - n)!}{2^m (l - n)!} (1 - x)^{(m-n)/2} (1 + x)^{(m+n)/2} P_{l-m}^{(m-n,m+n)}(x). \tag{4.66}$$

For $\alpha > -1$ and $\beta > -1$, the Jacobi polynomials satisfy the orthogonality relation (see, e.g., [80, pp. 397–401], [266, pp. 258–260])

$$\int_{-1}^{1} (1 - x)^{\alpha} (1 + x)^{\beta} P_r^{(\alpha,\beta)}(x) P_s^{(\alpha,\beta)}(x)\, dx = \frac{2^{1+\alpha+\beta} (\alpha + s)!(\beta + s)!}{(1 + \alpha + \beta + 2s) s!(\alpha + \beta + s)!} \delta_{rs}. \tag{4.67}$$

We proceed to use (4.25) and (4.67) to evaluate $N(l, m, n)$ in (4.66). On the one hand, by (4.25) we have

$$\int_{-1}^{1} [d_{mn}^l(x)]^2 dx = \frac{2}{2l + 1}. \tag{4.68}$$

On the other hand, we have

$$\left(\frac{N(l,m,n)(l-m)!(m-n)!}{2^m(l-n)!}\right)^2 \int_{-1}^{1}(1-x)^{m-n}(1+x)^{m+n}[P_{l-m}^{(m-n,m+n)}(x)]^2dx$$
$$=\left(\frac{N(l,m,n)(l-m)!(m-n)!}{2^m(l-n)!}\right)^2 \cdot \frac{2^{1+2m}(l-n)!(l+n)!}{(2l+1)(l-m)!(l+m)!}$$
$$=N(l,m,n)^2 \cdot \frac{2}{2l+1} \cdot \frac{(l-m)!(l+n)!}{(l+m)!(l-n)!} \cdot [(m-n)!]^2. \tag{4.69}$$

Equating the right-hand side of (4.68) and that of (4.69) yields

$$N(l,m,n) = \pm\sqrt{\frac{(l+m)!(l-n)!}{(l-m)!(l+n)!}} \cdot \frac{1}{(m-n)!} \tag{4.70}$$

for the case $m-n \geq 0$ and $m+n \geq 0$. Substituting (4.70) back into (4.66), we obtain

$$d_{mn}^l(\theta) = \pm\sqrt{\frac{(l+m)!(l-n)!}{(l-m)!(l+n)!}} \frac{1}{(m-n)!} \left(\frac{1-\cos\theta}{2}\right)^{(m-n)/2} \left(\frac{1+\cos\theta}{2}\right)^{(m+n)/2}$$
$$\times F(-l+m, l+m+1; m-n+1; \sin^2\frac{\theta}{2}) \tag{4.71}$$
$$= \pm\sqrt{\frac{(l-m)!(l+m)!}{(l-n)!(l+n)!}} \left(\sin\frac{\theta}{2}\right)^{m-n} \left(\cos\frac{\theta}{2}\right)^{m+n} P_{l-m}^{(m-n,m+n)}(\cos\theta) \tag{4.72}$$

for the case $m-n \geq 0$ and $m+n \geq 0$, where we have used the trigonometric identities

$$\frac{1-\cos\theta}{2} = \sin^2\frac{\theta}{2}, \qquad \frac{1+\cos\theta}{2} = \cos^2\frac{\theta}{2} \tag{4.73}$$

in the last step. For each (l,m,n), the d_{mn}^l function given in (4.72) is defined only up to an arbitrary sign. On the other hand, in formula (4.19) we have already adopted a convention on the choice of sign for d_{mn}^l. As we shall prove presently, we have to choose the sign in (4.72) as shown in the formula

$$d_{mn}^l(\theta) = (-1)^{m-n}\sqrt{\frac{(l-m)!(l+m)!}{(l-n)!(l+n)!}} \left(\sin\frac{\theta}{2}\right)^{m-n} \left(\cos\frac{\theta}{2}\right)^{m+n} P_{l-m}^{(m-n,m+n)}(\cos\theta), \tag{4.74}$$

for it to agree with (4.19) when $m-n \geq 0$ and $m+n \geq 0$. The proof will follow from an alternate expression that we now derive for d_{mn}^l, which agrees with (4.19) for all $-l \leq m \leq l$ and $-l \leq n \leq l$, irrespective of the sign of $m-n$ and $m+n$.

In this paragraph we let $\alpha = m - n$, $\beta = m + n$, $s = l - m$, $-l \le m \le l$, and $-l \le n \le l$, but we do not put any restriction on the sign of α and of β. Under the present assumptions, we have $s \ge 0$, $\alpha + s = l - n \ge 0$, and $\beta + s = l + n \ge 0$. By Leibniz's rule of differentiation, we observe that

$$\begin{aligned}
&\frac{d^s}{dx^s}\left[(1-x)^{\alpha+s}(1+x)^{\beta+s}\right] \\
&= \sum_{k=0}^{s} \frac{s!}{k!(s-k)!}\left[(1-x)^{\alpha+s}\right]^{(s-k)}\left[(1+x)^{\beta+s}\right]^{(k)} \\
&= \sum_{k} \frac{s!}{k!(s-k)!}\cdot(-1)^{s-k}\frac{(\alpha+s)!}{(\alpha+k)!}(1-x)^{\alpha+k}\cdot\frac{(\beta+s)!}{(\beta+s-k)!}(1+x)^{\beta+s-k} \\
&= (-1)^s(1-x)^{\alpha}(1+x)^{\beta}(\alpha+s)!(\beta+s)!s!\sum_{k}\frac{(x-1)^k(1+x)^{s-k}}{k!(s-k)!(\alpha+k)!(\beta+s-k)!}, \qquad (4.75)
\end{aligned}$$

where the unspecified summation on k is extended over all its integral values for which the arguments of the factorials in the denominator are non-negative, i.e. k satisfies the inequalities

$$k \ge 0, \quad k \le s, \quad k \ge -\alpha, \quad k \le \beta + s. \qquad (4.76)$$

Substituting $\alpha = m - n$, $\beta = m + n$, and $s = l - m$ into (4.75) yields

$$\begin{aligned}
\frac{d^{l-m}}{dx^{l-m}}\left[(1-x)^{l-n}(1+x)^{l+n}\right] = {} & (-1)^{l-m}(1-x)^{m-n}(1+x)^{m+n}(l-m)!(l-n)!(l+n)! \\
& \times \sum_{k}\frac{(x-1)^k(1+x)^{l-m-k}}{k!(l-m-k)!(m-n+k)!(l+n-k)!}, \qquad (4.77)
\end{aligned}$$

where the summation in (4.77) extends over the values of k that satisfies

$$k \ge 0, \quad k \le l - m, \quad k \ge n - m, \quad k \le l + n. \qquad (4.78)$$

Putting $x = \cos\theta$ in (4.77) and comparing the resulting equation with (4.19), we obtain the following alternate expression for d^l_{mn}:

$$\begin{aligned}
d^l_{mn}(\theta) = {} & \frac{(-1)^{l-n}}{2^l}(1-x)^{-(m-n)/2}(1+x)^{-(m+n)/2}\sqrt{\frac{(l+m)!}{(l-m)!(l+n)!(l-n)!}} \\
& \times \frac{d^{l-m}}{dx^{l-m}}\left[(1-x)^{l-n}(1+x)^{l+n}\right], \quad \text{where } x = \cos\theta \text{ and } \theta \in [0,\pi]. \qquad (4.79)
\end{aligned}$$

Using the identity $d^l_{mn} = (-1)^{m-n} d^l_{nm}$, we obtain from (4.79) yet another expression:

$$d^l_{mn}(\theta) = \frac{(-1)^{l-n}}{2^l}(1-x)^{-(n-m)/2}(1+x)^{-(n+m)/2}\sqrt{\frac{(l+n)!}{(l-n)!(l+m)!(l-m)!}} \times \frac{d^{l-n}}{dx^{l-n}}\left[(1-x)^{l-m}(1+x)^{l+m}\right], \quad \text{where } x = \cos\theta \text{ and } \theta \in [0,\pi]. \tag{4.80}$$

When $\alpha = m - n \geq 0$ and $\beta = m + n \geq 0$, k runs from 0 to $s = l - m$. For this case, substituting (4.75) into (4.62) yields

$$P^{(m-n,m+n)}_{l-m}(x) = (l-n)!(l+n)! \sum_{k=0}^{l-m} \frac{(\frac{x-1}{2})^k (\frac{1+x}{2})^{l-m-k}}{k!(l-m-k)!(m-n+k)!(l+n-k)!}. \tag{4.81}$$

Setting $x = \cos\theta$ in (4.81) and comparing the resulting equation with (4.19) confirms the correctness of the sign convention we have chosen for d^l_{mn} in (4.72) so that it agrees with (4.19).

For case (ii) $m - n \leq 0$ and $m + n \geq 0$, which imply $n \geq 0$, the differential equation (4.54) has the coefficients

$$a = -l + n, \qquad b = l + n + 1, \qquad c = n - m + 1 \tag{4.82}$$

so that it assumes the form

$$t(1-t)\frac{d^2 f}{dt^2} + [(n-m+1) - 2(n+1)t]\frac{df}{dt} + [l(l+1) - n(n+1)]f = 0, \tag{4.83}$$

which is none other than (4.57) with m and n exchanged. Following the same argument that leads to (4.72), we obtain the formula

$$d^l_{mn}(\theta) = \pm\sqrt{\frac{(l-n)!(l+n)!}{(l-m)!(l+m)!}}\left(\sin\frac{\theta}{2}\right)^{n-m}\left(\cos\frac{\theta}{2}\right)^{n+m} P^{(n-m,n+m)}_{l-n}(\cos\theta). \tag{4.84}$$

Applying Leibniz rule to the derivative $d^{l-n}[(1-x)^{l-m}(1+x)^{l+m}]/dx^{l-n}$ in $P^{(n-m,n+m)}_{l-n}$ just as what we did in (4.77), and comparing the resulting equation with (4.80), we obtain the formula

$$d^l_{mn}(\theta) = \sqrt{\frac{(l-n)!(l+n)!}{(l-m)!(l+m)!}}\left(\sin\frac{\theta}{2}\right)^{n-m}\left(\cos\frac{\theta}{2}\right)^{n+m} P^{(n-m,n+m)}_{l-n}(\cos\theta) \tag{4.85}$$

when $m - n \leq 0$ and $m + n \geq 0$.

In addition to the two combinations of signs of $m - n$ and $m + n$ that we have considered, there are two more combinations, namely cases (iii) and (iv), each of which results in one expression for $d^l_{mn}(\theta)$. These two formulas can be obtained from (4.74) and (4.85) through symmetry property $(4.31)_1$, i.e., $d^l_{mn}(\theta) = d^l_{\bar{n}\bar{m}}(\theta)$. For case (iii) $m + n \leq 0$ and $m - n \geq 0$, the defining inequalities can be recast as

$$\bar{n} + \bar{m} \geq 0, \quad \text{and} \quad \bar{n} - \bar{m} \geq 0, \qquad \text{which imply } \bar{n} \geq 0. \tag{4.86}$$

Under the condition given by (4.86), the expression for case (i) applies to $d^l_{\bar{n}\bar{m}}(\theta)$. Hence we have for case (iii):

$$\begin{aligned} d^l_{mn}(\theta) &= d^l_{\bar{n}\bar{m}}(\theta) \\ &= (-1)^{\bar{n}-\bar{m}} \sqrt{\frac{(l-\bar{n})!(l+\bar{n})!}{(l-\bar{m})!(l+\bar{m})!}} \left(\sin\frac{\theta}{2}\right)^{\bar{n}-\bar{m}} \left(\cos\frac{\theta}{2}\right)^{\bar{n}+\bar{m}} P_{l-\bar{n}}^{(\bar{n}-\bar{m},\bar{n}+\bar{m})}(\cos\theta) \\ &= (-1)^{m-n} \sqrt{\frac{(l+n)!(l-n)!}{(l+m)!(l-m)!}} \left(\sin\frac{\theta}{2}\right)^{m-n} \left(\cos\frac{\theta}{2}\right)^{\bar{n}+\bar{m}} P_{l-\bar{n}}^{(m-n,\bar{n}+\bar{m})}(\cos\theta). \end{aligned} \tag{4.87}$$

Similarly, we recast the defining inequalities $m+n \le 0$ and $m-n \le 0$ for case (iv) as

$$\bar{n}+\bar{m} \ge 0, \quad \text{and} \quad \bar{n}-\bar{m} \le 0, \qquad \text{which imply } \bar{m} \ge 0. \tag{4.88}$$

Under the condition given by (4.88), the expression for case (ii) applies to $d^l_{\bar{n}\bar{m}}(\theta)$. Hence it follows that for case (iv) we have

$$\begin{aligned} d^l_{mn}(\theta) &= d^l_{\bar{n}\bar{m}}(\theta) \\ &= \sqrt{\frac{(l-\bar{m})!(l+\bar{m})!}{(l-\bar{n})!(l+\bar{n})!}} \left(\sin\frac{\theta}{2}\right)^{\bar{m}-\bar{n}} \left(\cos\frac{\theta}{2}\right)^{\bar{m}+\bar{n}} P_{l-\bar{m}}^{(\bar{m}-\bar{n},\bar{m}+\bar{n})}(\cos\theta) \\ &= \sqrt{\frac{(l+m)!(l-m)!}{(l+n)!(l-n)!}} \left(\sin\frac{\theta}{2}\right)^{n-m} \left(\cos\frac{\theta}{2}\right)^{\bar{m}+\bar{n}} P_{l-\bar{m}}^{(n-m,\bar{m}+\bar{n})}(\cos\theta). \end{aligned} \tag{4.89}$$

The four expressions (4.74), (4.85), (4.87), and (4.89) can be combined into one general formula that covers all combinations of the signs of $m-n$ and $m+n$ as follows (cf. [325, p. 78, Eqs. (13)–(15)]):

$$d^l_{mn}(\theta) = \eta_{mn} \sqrt{\frac{s!(s+\alpha+\beta)!}{(s+\alpha)!(s+\beta)!}} \left(\sin\frac{\theta}{2}\right)^{\alpha} \left(\cos\frac{\theta}{2}\right)^{\beta} P_s^{(\alpha,\beta)}(\cos\theta), \tag{4.90}$$

where

$$\alpha = |m-n|, \quad \beta = |m+n|, \quad s = l - \frac{1}{2}(\alpha+\beta), \quad \eta_{mn} = \begin{cases} (-1)^{m-n} & \text{if } m \ge n \\ 1 & \text{if } n \ge m. \end{cases} \tag{4.91}$$

4.4.1 Generalized Spherical Functions of Gel'fand and Šapiro

For details about his generalized spherical harmonics, Bunge [57, p. 215] refers to the 1952 paper[67] of Gel'fand and Šapiro [124] and to the book by Gel'fand, Minlos, and Shapiro [125], Part 1 of which concerns the rotation group and is a slightly edited version of the 1952 paper. Gel'fand and Šapiro use the Euler angles (cf. Sect. 1.8.2)

$$\varphi_1 = \psi + \frac{\pi}{2}, \quad \theta = \theta, \quad \varphi_2 = \phi - \frac{\pi}{2}$$

[67] All references to [124] in this exposition refer to the 1956 English translation.

to define their "generalized spherical functions of order l" ([125, p. 85], [124, p. 278]) as follows:[68,69]

$$T^l_{mn}(\varphi_1, \theta, \varphi_2) = e^{-im\varphi_1} P^l_{mn}(\cos\theta) e^{-in\varphi_2}; \tag{4.92}$$

here we have followed the notation in Gel'fand et al. [125], and

$$P^l_{mn}(x) = \frac{(-1)^{l-m} i^{n-m}}{2^l} (1-x)^{-(n-m)/2} (1+x)^{-(n+m)/2} \sqrt{\frac{(l+n)!}{(l-n)!(l+m)!(l-m)!}} \times \frac{d^{l-n}}{dx^{l-n}} \left[(1-x)^{l-m} (1+x)^{l+m} \right], \qquad \text{where } x = \cos\theta \text{ and } \theta \in [0, \pi]. \tag{4.93}$$

Comparing (4.93) with (4.80), we observe that

$$P^l_{mn}(\cos\theta) = (-i)^{n-m} d^l_{mn}(\theta), \qquad \text{where } \theta \in [0, \pi]. \tag{4.94}$$

From (4.94) and the symmetry properties of d^l_{mn} (see Sect. 4.2.1) follow the symmetry properties of P^l_{mn}. For example, we have

$$P^l_{mn} = P^l_{nm}, \quad P^l_{\bar{m}\bar{n}} = P^l_{mn}, \quad \overline{P^l_{nm}} = (-1)^{m-n} P^l_{mn}. \tag{4.95}$$

It follows also from (4.94) that if $(\varphi_1, \Phi, \varphi_2) \equiv (\varphi_1, \theta, \varphi_2)$ and $(\psi.\theta, \phi)$ refer to the same rotation g, then

$$\begin{aligned} T^l_{mn}(\varphi_1, \Phi, \varphi_2) &= e^{-im(\psi+\frac{\pi}{2})} P^l_{mn}(\cos\theta) e^{-in(\phi-\frac{\pi}{2})} \\ &= \left(i^{-m} e^{-im\psi}\right) (-i)^{n-m} d^l_{mn}(\theta) \left(i^n e^{-in\phi}\right) \\ &= D^l_{mn}(\psi, \theta, \phi). \end{aligned} \tag{4.96}$$

Hence the generalized spherical functions of Gel'fand and Šapiro are none other than the Wigner D-functions with the rotations parameterized by the Euler angles $(\varphi_1, \Phi, \varphi_2)$.

[68] As pointed out in a "Translator's note" [124, p. 211], Gel'fand and Šapiro have inadvertently reversed the correct order of writing the product of matrices in our (1.103) as $g = \boldsymbol{R}(\boldsymbol{e}_3, \varphi_2)\boldsymbol{R}(\boldsymbol{e}_1, \theta)\boldsymbol{R}(\boldsymbol{e}_3, \varphi_1)$. As a result many formulas in their paper are incorrect but can be made correct by interchanging φ_1 and φ_2. When the contents of [124] are transferred to the book [125], many but not all of the incorrect formulas are corrected. Unfortunately the erroneous formula $T^l_{mn}(\varphi_1, \theta, \varphi_2) = e^{-im\varphi_2} P^l_{mn}(\cos\theta) e^{-in\varphi_1}$ that defines the generalized spherical functions in [124, p. 278], where the angles φ_1 and φ_2 should have been interchanged, gets through to the book [125, p. 85] without correction. In comparison, see, in particular, equation (15) on page 82 of [125], which reads

$$T_{mn}(\varphi_1, \theta, \varphi_2) = e^{-im\varphi_1} u_{mn}(\theta) e^{-in\varphi_2};$$

the function $u_{mn}(\theta)$ in the equation is determined on p. 84 to be $P^l_{mn}(\cos\theta)$. Note that on page 275 of Gel'fand and Šapiro [124] the same equation (15) for T_{mn} has φ_1 and φ_2 erroneously interchanged. This mistake is corrected in the book [125]. But the incorrect formula for T^l_{mn} in [124] remains unchanged in [125]. In what follows we will make silent corrections so that all the formulas of Gel'fand and Šapiro [124] and Gel'fand et al. [125] presented here are correct. At places where we want to display an erroneous formula, we will say so explicitly.

[69] Cf. also Lyubarsii [195, p. 204], where T^l_{mn} is written as $D^{(j)}_{km}$, P^l_{mn} as $P_{km,j}$, φ_1 as ψ, and φ_2 as φ; Vilenkin [327, p. 120, Eq. (6); p. 121, Eq. (3)], where T^l_{mn} is written as t^l_{mn}, φ_1 as φ, and φ_2 as ψ.

4.5 Alternate Formulations of the Series Expansion

From the beginning of quantitative texture analysis (i.e., the 1960s) up to the present, researchers in the field predominantly employ passive rotations (see Sect. 1.5). In this exposition we use active rotations to conform to the mathematics and physics literature of the last few decades. The series expansion (4.45) of the ODF, i.e.,

$$w(\boldsymbol{R}(\psi,\theta,\phi)) = \sum_{l=0}^{\infty}\sum_{m=-l}^{l}\sum_{n=-l}^{l} c_{mn}^{l} D_{mn}^{l}(\boldsymbol{R}(\psi,\theta,\phi)), \tag{4.97}$$

is valid for every rotation $\boldsymbol{R}$. It can certainly be rewritten as

$$w(\boldsymbol{R}^{-1}(\psi,\theta,\phi)) = \sum_{l=0}^{\infty}\sum_{m=-l}^{l}\sum_{n=-l}^{l} c_{mn}^{l} D_{mn}^{l}(\boldsymbol{R}^{-1}(\psi,\theta,\phi)). \tag{4.98}$$

Equation (4.98), however, should not be confused with the series expansion

$$w^{(p)}(\boldsymbol{R}^{-1}(\psi,\theta,\phi)) = \sum_{l=0}^{\infty}\sum_{m=-l}^{l}\sum_{n=-l}^{l} c_{mn}^{l,(p)} D_{mn}^{l}(\boldsymbol{R}^{-1}(\psi,\theta,\phi)), \tag{4.99}$$

because $w(\boldsymbol{R}^{-1}) \neq w^{(p)}(\boldsymbol{R}^{-1})$, as $w = w^{(p)} \circ \mathscr{J}$, where $\mathscr{J} : \boldsymbol{R} \mapsto \boldsymbol{R}^{-1}$ (see Sect. 4.1.1). On the other hand, from the fact (see (4.12) that $w(\boldsymbol{R}) = w^{(p)}(\boldsymbol{R}^{-1})$ we can easily determine how the two sets of texture coefficients c_{mn}^{l} and $c_{mn}^{l,(p)}$ are related.

First, note that

$$\begin{aligned} D_{mn}^{l}(\boldsymbol{R}^{-1}(\psi,\theta,\phi)) &= D_{mn}^{l}(\boldsymbol{R}(\pi-\phi,\theta,\pi-\psi)) \\ &= e^{-im(\pi-\phi)} d_{mn}^{l}(\theta) e^{-in(\pi-\psi)} \\ &= (-1)^{m+n} e^{im\phi} d_{mn}^{l}(\theta) e^{in\psi} \\ &= (-1)^{m+n} e^{-i\bar{n}\psi} d_{mn}^{l}(\theta) e^{-i\bar{m}\phi} \\ &= (-1)^{m+n} e^{-i\bar{n}\psi} d_{\bar{n}\bar{m}}^{l}(\theta) e^{-i\bar{m}\phi} \\ &= (-1)^{m+n} D_{\bar{n}\bar{m}}^{l}(\boldsymbol{R}(\psi,\theta,\phi)), \end{aligned} \tag{4.100}$$

where we have appealed to $(4.31)_1$ to get the identity $d_{mn}^{l}(\theta) = d_{\bar{n}\bar{m}}^{l}(\theta)$. Thus series expansion (4.99) may be recast as

$$w^{(p)}(\boldsymbol{R}^{-1}(\psi,\theta,\phi)) = \sum_{l=0}^{\infty}\sum_{m=-l}^{l}\sum_{n=-l}^{l} c_{mn}^{l,(p)} (-1)^{m+n} D_{\bar{n}\bar{m}}^{l}(\boldsymbol{R}(\psi,\theta,\phi)). \tag{4.101}$$

Replacing $w(\boldsymbol{R})$ in (4.50) by $w^{(p)}(\boldsymbol{R}^{-1})$ and using the series expansion (4.101), we obtain for $l \geq 1$

$$c_{mn}^{l} = \frac{2l+1}{8\pi^2} \int_{\mathrm{SO}(3)} w^{(p)}(\boldsymbol{R}^{-1})\, \overline{D_{mn}^{l}(\boldsymbol{R})}\, d\mathcal{V}(\boldsymbol{R}),$$

$$= \frac{2l+1}{8\pi^2} \int_{\mathrm{SO}(3)} \left(\sum_{l=1}^{\infty} \sum_{m=-l}^{l} \sum_{n=-l}^{l} c_{mn}^{l,(p)} (-1)^{m+n} D_{\bar{n}\bar{m}}^{l}(\boldsymbol{R}(\psi,\theta,\phi)) \right) \overline{D_{mn}^{l}(\boldsymbol{R})}\, d\mathcal{V}(\boldsymbol{R})$$

$$= (-1)^{m+n} c_{\bar{n}\bar{m}}^{l,(p)}, \tag{4.102}$$

or

$$c_{mn}^{l,(p)} = (-1)^{m+n} c_{\bar{n}\bar{m}}^{l}. \tag{4.103}$$

In the literature some authors, while using passive rotations, in effect write the series expansion of the ODF in (or in some variant of) the form[70]

$$w^{(p)}(\boldsymbol{R}^{-1}) = \sum_{l=0}^{\infty} \sum_{m=-l}^{l} \sum_{n=-l}^{l} c_{mn}^{l} D_{mn}^{l}(\boldsymbol{R}). \tag{4.104}$$

The right-hand side of (4.104) is the series expansion of $w(\boldsymbol{R})$. Hence, in writing down (4.104) the authors are in fact making use of equality (4.12), i.e., $w^{(p)}(\boldsymbol{R}^{-1}) = w(\boldsymbol{R})$.

After making the substitutions

$$w(\boldsymbol{R}) = \frac{1}{8\pi^2} \mathtt{f}^{(a)}(\boldsymbol{R}), \qquad w^{(p)}(\boldsymbol{R}^{-1}) = \frac{1}{8\pi^2} \mathtt{f}(\boldsymbol{R}^{-1}),$$

the discussion above applies verbatim to the pair $\mathtt{f}^{(a)}$ and $\mathtt{f}$.

4.5.1 Roe's Generalized Spherical Harmonics and Texture Coefficients

Roe [270] writes the ODF in an infinite series as follows:

$$w(\psi,\theta,\phi) = \sum_{l=0}^{\infty} \sum_{m=-l}^{l} \sum_{n=-l}^{l} W_{lmn} Z_{lmn}(\cos\theta) e^{-im\psi} e^{-in\phi} \tag{4.105}$$

$$= \frac{1}{8\pi^2} + \sum_{l=1}^{\infty} \sum_{m=-l}^{l} \sum_{n=-l}^{l} W_{lmn} Z_{lmn}(\cos\theta) e^{-im\psi} e^{-in\phi}, \tag{4.106}$$

where W_{lmn} are texture coefficients and $Z_{lmn}(\cos\theta)e^{-im\psi}e^{-in\phi}$ are his generalized spherical harmonics. While Roe works with passive rotations $\boldsymbol{R}^{(p)}$, the right-hand side is in fact an expansion in terms of the Wigner D-functions $D_{mn}^{l}(\boldsymbol{R}(\psi,\theta,\phi))$, as we shall explain in detail below. Hence Roe's series expansion (4.105) is an example of expansion of the type (4.104).

Roe [270, Appendix] defines his generalized spherical harmonics first for the case $m - n \geq 0$ and $m + n \geq 0$ (cf. Footnote 65 in Sect. 4.4). For that case, he has

$$Z_{lmn}(\cos\theta) := \widetilde{N}(l,m,n) \left(\frac{1-\cos\theta}{2}\right)^{(m-n)/2} \left(\frac{1+\cos\theta}{2}\right)^{(m+n)/2} \times F\left(-l+m, l+m+1; m-n+1; \frac{1-\cos\theta}{2}\right),$$

[70] Specific examples will be given in Sects. 4.5.1 and 4.5.4.

$$= \widetilde{N}(l,m,n)\left(\frac{1-\cos\theta}{2}\right)^{(m-n)/2}\left(\frac{1+\cos\theta}{2}\right)^{(m+n)/2} \times \frac{(l-m)!(m-n)!}{(l-n)!}\,P_{l-m}^{(m-n,m+n)}(x), \tag{4.107}$$

where we have appealed to (4.64) at the last step, and the constant $\widetilde{N}(l,m,n)$ is determined up to its sign from the normalization condition

$$\int_{-1}^{1} Z_{lmn}^2(x)dx = 1 \tag{4.108}$$

so that[71]

$$\widetilde{N}(l,m,n)^2 = \frac{2l+1}{2}\cdot\frac{(l+m)!(l-n)!}{(l-m)!(l+n)!}\cdot\frac{1}{[(m-n)!]^2}. \tag{4.109}$$

Noting that there is an ambiguity in sign for $\widetilde{N}(l,m,n)$ because the normalization condition (4.108) does not determine its sign, Roe [270, eq. (A11)] adopts the convention that

$$Z_{lmn} = (-1)^{m+n} Z_{lnm}, \tag{4.110}$$

which, as he seems to suggest, would clear up the ambiguity. Unfortunately the convention adopted by Roe does not really resolve the problem at issue, which may have led to some confusion in the literature (see Remark 4.6), as different choices for the sign convention of Roe's normalization constant $\widetilde{N}(l,m,n)$ satisfy (4.110). On the other hand, in a later paper Roe [271, Eq. (10)] does give an explicit expression for $Z_{lmn}(0)$, i.e., the value of $Z_{lmn}(\cos\theta)$ at $\theta = \pi/2$, namely:

$$Z_{lmn}(0) = \sqrt{\frac{2l+1}{2}}\cdot\frac{1}{2^l}\cdot\sum_k (-1)^k \frac{\sqrt{(l+m)!(l-m)!(l+n)!(l-n)!}}{k!(l+n-k)!(l-m-k)!(m-n+k)!}; \tag{4.111}$$

he cites as reference (Rose [274, Eq. (4.13)]) a formula of $d_{mn}^l(\theta)$ which is none other than our (4.19). A comparison of (4.111) with that which results after substitution of $\theta = \pi/2$ into (4.19) reveals that

$$d_{mn}^l(\pi/2) = (-1)^{m-n}\sqrt{\frac{2}{2l+1}}\,Z_{lmn}(0). \tag{4.112}$$

Substituting $\theta = \pi/2$ in (4.74) and (4.107), we obtain from (4.112) the formula

$$\widetilde{N}(l,m,n) = \sqrt{\frac{2l+1}{2}}\cdot\sqrt{\frac{(l+m)!(l-n)!}{(l-m)!(l+n)!}}\cdot\frac{1}{(m-n)!}. \tag{4.113}$$

Thus Roe's expression (4.111) for $Z_{lmn}(0)$ in [271] has revealed the sign convention he adopts for the normalization constant $\widetilde{N}(l,m,n)$.

[71] See Roe [270, eq. (A8)], where the constant $\widetilde{N}(l,m,n)$ is denoted as N_{lmn}.

Remark 4.5 Note that (4.113) simply gives $\widetilde{N}(l,m,n)$ as the positive square-root of the right-hand side of (4.109) for all (l,m,n). The method presented by Roe [270, Appendix] to derive the functions Z_{lmn}, as a factor in the energy eigenfunctions of the quantum symmetric top, can be traced back to the 1926 paper of Reiche and Rademacher [269]. There the normalization constant equivalent to $\widetilde{N}(l,m,n)$ is explicitly given—see their equations (33b) and (34), which is none other than that given by (4.113) here. At the end of the Appendix of Roe's paper [270], he writes: "[t]he function Z_{lmn} arises in the Schrödinger wave function of a symmetric rotator[16–18] ...". His reference 16 is the paper of Reiche and Rademacher [269]. His reference 18 is a paper by Nielsen [249], where the normalization constant in question is also explicitly given as that given by (4.113)—see Nielsen's equation (III.31). In fact, in presentations of the energy eigenfunctions of the quantum symmetric top which are derived by separation of variables, the normalization constant in question is often given as (4.113); see, e.g., Pauling and Wilson [256, equation (36–14)]. □

It follows from (4.71), (4.74), (4.107), and the choice (4.113) for $\widetilde{N}(l,m,n)$ that

$$d^l_{mn}(\theta) = (-1)^{m-n}\sqrt{\frac{2}{2l+1}}Z_{lmn}(\cos\theta) \qquad \text{for } m-n \geq 0 \text{ and } m+n \geq 0. \tag{4.114}$$

As mentioned in Sect. 4.2.1, the d^l_{mn} functions satisfy the relations

$$d^l_{mn}(\theta) = d^l_{\bar{n}\bar{m}}(\theta) = (-1)^{m-n}d^l_{nm}(\theta) = (-1)^{m-n}d^l_{\bar{m}\bar{n}}(\theta), \tag{4.115}$$

by which the values of d^l_{mn} for (i) $m-n \leq 0$ and $m+n \geq 0$, (ii) $m-n \leq 0$ and $m+n \leq 0$, (iii) $m-n \geq 0$ and $m+n \leq 0$ can be expressed in terms of those for the case $m-n \geq 0$ and $m+n \geq 0$. In fact, Roe also has his Z_{lmn} functions satisfy the same relations:

$$Z_{lmn}(\cos\theta) = Z_{l\bar{n}\bar{m}}(\cos\theta) = (-1)^{m-n}Z_{lnm}(\cos\theta) = (-1)^{m-n}Z_{l\bar{m}\bar{n}}(\cos\theta). \tag{4.116}$$

Hence, for all combinations of the signs of $m-n$ and $m+n$, we have

$$d^l_{mn}(\theta) = (-1)^{m-n}\sqrt{\frac{2}{2l+1}}Z_{lmn}(\cos\theta) \tag{4.117}$$

under the sign convention that the value of $\widetilde{N}(l.m,n)$ is given by (4.113). Substituting (4.117) into (4.45) and comparing the resulting equation with (4.99) leads to the formula (cf. [157, 199, 204])

$$W_{lmn} = (-1)^{m-n}\sqrt{\frac{2}{2l+1}}\,c^l_{mn}. \tag{4.118}$$

By $(4.32)_2$, $d^l_{mn} = (-1)^{m+n}d^l_{nm}$ for all $-l \leq m \leq l$ and $-l \leq n \leq l$. Hence formula (4.117) is consistent with the convention (4.110) adopted by Roe.

In this exposition we will take (4.117) to be the defining equation for Roe's "augmented Jacobi polynomials"[72] Z_{lmn}, which leads to (4.118) as the relation between the texture coefficients W_{lmn} and c^l_{mn}. By (4.118), the reality condition (4.46) on w, when expressed in

[72] A name that appears in Morris [236]. In the same paper Morris gives "$P_l^{mn}(\alpha) = \sqrt{(2/(2l+1)}Z_{lmn}(\alpha)$" as the equation that relates Z_{lmn} to the "generalized Legendre functions" P_l^{mn} of Bunge [56]. The equation given by Morris, however, is clearly erroneous, because Z_{lmn} is real-valued whereas the value of $P_l^{mn}(\alpha)$ is a multiple of the imaginary $\sqrt{-1}$ when $m-n$ is odd (see (4.93) and Sect. 4.5.3)).

terms of the coefficients W_{lmn}, reads

$$W_{lmn} = (-1)^{m-n}\overline{W_{l\bar{m}\bar{n}}}. \tag{4.119}$$

Remark 4.6 Bunge [60, p. 97] and Esling et al. [110, p. 99] assert without proof or reference[73] the relation

$$Z_{lmn}(\cos\theta) = i^{n-m}\sqrt{\frac{2l+1}{2}}\,P^l_{mn}(\cos\theta). \tag{A}$$

By (4.94), assertion (A) is equivalent to the expression

$$d^l_{mn}(\theta) = \sqrt{\frac{2}{2l+1}}\,Z_{lmn}(\cos\theta), \tag{B}$$

which corresponds to adoption of the value of $\widetilde{N}(l,m,n)$ as given by

$$\widetilde{N}(l,m,n) = (-1)^{m-n}\sqrt{\frac{2l+1}{2}}\cdot\sqrt{\frac{(l+m)!(l-n)!}{(l-m)!(l+n)!}}\cdot\frac{1}{(m-n)!}. \tag{C}$$

It can easily be checked that expression (B) is also consistent with the convention (4.110) adopted by Roe [270, eq. (A11)]. Under assertion (A), the relation between W_{lmn} and c^l_{mn} is:

$$W_{lmn} = \sqrt{\frac{2}{2l+1}}\,c^l_{mn}. \tag{D}$$

But assertion (A) is equivalent to equation (B), which contradicts the formula of $Z_{lmn}(0)$ given by Roe [271, Eq. (10)]. Since relation (D) is based on (B), the "W_{lmn}" of Bunge [60] and Esling et al. [110] in (D) aren't really Roe's W_{lmn} as claimed. □

4.5.2 Viglin's Generalized Spherical Functions and Texture Coefficients

The idea of describing crystallographic texture by a probability density function defined on the space of orientations was first expressed by Bitter [32, §64, pp. 214–215] in his 1937 book on ferromagnetism. By then the mathematical apparatus needed for development of this idea along the lines presented in the present chapter had already been created in quantum mechanics by Wigner and others. But, as is evident from §64 of his book, Bitter was unfamiliar with the mathematics required. Moreover, his idea pertaining to description of texture remained undeveloped as no one took it up. Many years later it was Viglin [326], another researcher in polycrystalline ferromagnetics, who independently came up with "the idea of describing texture by means of distribution functions" in 1959/60 and then found that the same idea "had been mentioned earlier" by Bitter.

Equipped with mathematical tools provided by the 1952 paper of Gel'fand and Šapiro [124, §7], Viglin [326] expanded the general "texture function" p, i.e., the ODF in his notation, which depends on the orientation g, in a series of generalized spherical functions $T_{l,m,n}$

[73] Bunge [60, p. 352] does cite Morris [236] for "the so-called augmented Jacobi polynomials" Z_{lmn}. But, as mentioned in Footnote 13, Morris's equation that relates Z_{lmn} to Bunge's P^{mn}_l is erroneous.

as follows (cf. his equations (2.2) and (A.13)):

$$p(g) = \sum_{l=0}^{\infty} \sum_{m=-l}^{l} \sum_{n=-l}^{l} C_{l,m,n} T_{l,m,n}(g), \tag{4.120}$$

where $C_{l,m,n}$ are the coefficients of the expansion. Besides making a few minor changes in notation, Viglin largely adopted the formulas given by Gel'fand and Šapiro, correct or otherwise, as they stand in [124], and he used the same convention on Euler angles, which are denoted by $(\varphi_1, \theta, \varphi_2)$. But he did make a doubly erroneous tweak, which through Bunge has left its mark on the texture literature to this day. In contrast to Gel'fand and Šapiro, who adopted the active view of rotations, Viglin elected to use passive rotations to represent orientations. He defined his generalized spherical functions as follows (see his equation (A.4)):

$$T_{l,m,n}(\varphi_1, \theta, \varphi_2) = e^{im\varphi_2} P_{l,m,n}(\cos\theta) e^{in\varphi_1}, \tag{4.121}$$

where $P_{l,m,n}$ is Viglin's notation for Gel'fand and Šapiro's P^l_{mn} (see (4.93)). He explained [326, p. 2204] that to obtain the version of (4.121) for active rotations,

> it is essential to make the replacement in the right hand side of (A.4) [= (4.121)]: $\varphi_1 \to -\varphi_1$, $\theta \to -\theta$ and $\varphi_2 \to -\varphi_2$.

The preceding assertion of Viglin on transformation from $\boldsymbol{R}^{-1}$ to $\boldsymbol{R}$ is incorrect; the rule of transformation should have been: $\varphi_1 \to \pi - \varphi_2$, $\theta \to \theta$ and $\varphi_2 \to \pi - \varphi_1$. Nevertheless, if we follow Viglin's assertion and use the notation of Gel'fand and Šapiro, then (4.121) becomes

$$T^l_{mn}(\varphi_1, \theta, \varphi_2) = e^{-im\varphi_2} P^l_{mn}(\cos\theta) e^{-in\varphi_1}, \tag{4.122}$$

which is exactly the original erroneous formula of Gel'fand and Šapiro with the angles φ_1 and φ_2 interchanged (cf. Footnote 68 for more details). Thus Viglin arrived at his formula (4.121) for the generalized spherical functions through two mistakes. First, he started with the incorrect formula (4.122). Then he followed an erroneous protocol for the transformation of Euler angles between active and passive rotations.

Following Gel'fand and Šapiro [124, p. 284], Viglin gave an incorrect formula (A.12) for the orthogonality relation of the generalized spherical functions: the right-hand side of his (A.12) is too large by a factor of 2. As a result, the right-hand side of his formula (A.14) for the texture coefficients $C_{l,m,n}$ should be multiplied by a factor of 2.

Viglin's formulation has been subsumed by that of Bunge and, by now, is seldom mentioned in the texture literature. On the other hand, understanding what Viglin did will shed light on a starting point of Bunge's formulation, which we shall discuss next.

4.5.3 Bunge's Generalized Spherical Harmonics and Texture Coefficients

Bunge ([60, p. 47]; see also [56], [57, p. 20]) cites Viglin's paper [326] when he asserts that "[a] function $f(g)$ ... can be developed in a series of generalized spherical harmonics". He adopts [56] (see also [57, p. 215], [60, p. 351]) Viglin's formula (4.121)—without mentioning Viglin—as definition for what he calls generalized spherical harmonics:[74]

$$T^{mn}_l(\boldsymbol{R}^{(p)}(\varphi_1, \Phi, \varphi_2)) = e^{im\varphi_2} P^{mn}_l(\cos\Phi) e^{in\varphi_1}, \tag{4.123}$$

[74] In his 1965 paper Bunge [56] refers the reader to the Russian original of Gelfand and Šapiro [124] for the definition of P^{mn}_l. In the 1982 English revised version of his treatise he cites [60, p. 47 and p. 351] the book

where the functions P_l^{mn} are the same as Viglin's $P_{l,m,n}$ or Gel'fand and Šapiro's P_{mn}^l defined in (4.93).

As mentioned in Sect. 4.5.2 Viglin arrived at his formula (4.121) for the generalized spherical functions $T_{l,m,n}$ by committing two errors. There arises the question whether Bunge's generalized spherical functions T_l^{mn}, which are none other than Viglin's $T_{l,m,n}$, would enjoy the mathematical properties expected of them, e.g., whether the mapping $\boldsymbol{Q} \mapsto [T_l^{mn}(\boldsymbol{Q})]$ for $\boldsymbol{Q} \in \mathrm{SO}(3)$ is an irreducible unitary representation of the rotation group. Fortunately the answer is affirmative.

To demonstrate this, we start by determining how the generalized spherical harmonics T_l^{mn} are related to Gel'fand and Šapiro's T_{mn}^l and to the Wigner D-functions D_{mn}^l. Indeed by (4.92) and (4.123) we have

$$\begin{aligned} T_{mn}^l(\boldsymbol{R}^{-1}(\varphi_1,\theta,\varphi_2)) &= e^{-im(\pi-\varphi_2)} P_{mn}^l(\cos\theta) e^{-in(\pi-\varphi_1)} \\ &= (-1)^{m+n} T_l^{mn}(\boldsymbol{R}^{-1}(\varphi_1,\Phi,\varphi_2)). \end{aligned} \tag{4.124}$$

Since the preceding equation holds for all $\boldsymbol{R}^{-1}$ in the rotation group SO(3) and by (4.96) $T_{mn}^l(\boldsymbol{R}) = D_{mn}^l(\boldsymbol{R})$, we may recast (4.124) as

$$T_l^{mn}(\boldsymbol{R}(\varphi_1,\Phi,\varphi_2)) = (-1)^{m+n} T_{mn}^l(\boldsymbol{R}(\varphi_1,\theta,\varphi_2)) \tag{4.125}$$

$$= (-1)^{m+n} D_{mn}^l(\boldsymbol{R}(\psi,\theta,\phi)) \qquad \text{for each } \boldsymbol{R} \in \mathrm{SO}(3). \tag{4.126}$$

It follows from (4.126), inverse-invariance of the Haar integral, and the orthogonality of the Wigner D-functions (4.21) that the functions T_l^{mn} obey the orthogonality relation

$$\int_{\mathrm{SO}(3)} T_l^{mn}(\boldsymbol{R}^{-1}) \overline{T_{l'}^{m'n'}(\boldsymbol{R}^{-1})}\, d\mathfrak{g}(\boldsymbol{R}) = \frac{1}{2l+1} \delta_{ll'} \delta_{mm'} \delta_{nn'}, \tag{4.127}$$

where $\mathfrak{g}$ is the normalized Haar measure on the rotation group SO(3).

Since the matrix $[D^l(\boldsymbol{R})]$ is unitary, it follows that $[T_l(\boldsymbol{R}^{(p)})]$ is unitary for each rotation $\boldsymbol{R}$. Moreover, let $\boldsymbol{Q}_1$ and $\boldsymbol{Q}_2$ be rotations. By (4.126) we obtain the addition theorem for $T_l^{mn}(\cdot)$:

$$\begin{aligned} T_l^{mn}(\boldsymbol{Q}_1\boldsymbol{Q}_2) &= (-1)^{m+n} D_{mn}^l(\boldsymbol{Q}_1\boldsymbol{Q}_2) \\ &= (-1)^{m+n} \sum_{s=-l}^{l} D_{ms}^l(\boldsymbol{Q}_1) D_{sn}^l(\boldsymbol{Q}_2) \\ &= (-1)^{m+n} \sum_{s=-l}^{l} (-1)^{m+s} T_l^{ms}(\boldsymbol{Q}_1)(-1)^{s+n} T_l^{sn}(\boldsymbol{Q}_2) \\ &= \sum_{s=-l}^{l} T_l^{ms}(\boldsymbol{Q}_1) T_l^{sn}(\boldsymbol{Q}_2). \end{aligned} \tag{4.128}$$

of Gel'fand et al. [125] for "the properties of the functions $P_l^{mn}(\Phi)$ as well as $T_l^{mn}(g)$" and for "detailed representations of these functions and their properties". In the corresponding section of the 1969 German edition of the book, he refers also to the 1952 paper of Gel'fand and Šapiro [124]. In fact, as explained in Footnote 68, the part of the book [125] on the rotation group is just a partially corrected version of the 1952 paper [124]. On p. 215 of [57] and p. 351 of [60] Bunge cites also the 1931 book of Wigner [340] and the 1965 Russian original of Vilenkin [327]. But his definition of the P_l^{mn} functions clearly indicates that Gel'fand and Šapiro [124] and Gel'fand et al. [125] were his main references.

Let $[T_l(\boldsymbol{Q})]$ be the $(2l+1)\times(2l+1)$ matrix with entries $T_l^{mn}(\boldsymbol{Q})$. By (4.128) and (4.126) the map $\boldsymbol{Q}\mapsto[T_l(\boldsymbol{Q})]$ is an irreducible representation of the rotation group.

Bunge [60] adopts the normalized Haar measure $\mathfrak{g}$ as the volume measure for the rotation group SO(3) and uses $\mathtt{f}=8\pi^2 w^{(p)}$ as the orientation distribution function. He expands the ODF $\mathtt{f}$ as an infinite series in terms of the T_l^{mn} functions:

$$\mathtt{f}(\boldsymbol{R}^{(p)}(\varphi_1,\Phi,\varphi_2))=1+\sum_{l=1}^{\infty}\sum_{m=-l}^{l}\sum_{n=-l}^{l}C_l^{mn}T_l^{mn}(\boldsymbol{R}^{(p)}(\varphi_1,\Phi,\varphi_2)),\tag{4.129}$$

where C_l^{mn} are the texture coefficients in Bunge's formulation. By (4.100) and (4.126), we observe that Bunge's series expansion (4.129) can be recast as

$$\begin{aligned}\mathtt{f}(\boldsymbol{R}^{(p)}(\varphi_1,\Phi,\varphi_2))&=1+\sum_{l=1}^{\infty}\sum_{m=-l}^{l}\sum_{n=-l}^{l}C_l^{mn}(-1)^{m+n}D^l_{mn}((\boldsymbol{R}(\psi,\theta,\phi))^{-1})\\&=1+\sum_{l=1}^{\infty}\sum_{m=-l}^{l}\sum_{n=-l}^{l}C_l^{mn}D^l_{\bar{n}\bar{m}}(\boldsymbol{R}(\psi,\theta,\phi)),\end{aligned}\tag{4.130}$$

where the Euler angles $(\varphi_1,\Phi,\varphi_2)$ and (ψ,θ,ϕ) pertain to the same orientation. On the other hand, we have

$$\mathtt{f}(\boldsymbol{R}^{(p)})=\mathtt{f}^{(a)}(\boldsymbol{R})=8\pi^2 w(\boldsymbol{R})=1+\sum_{l=1}^{\infty}\sum_{m=-l}^{l}\sum_{n=-l}^{l}8\pi^2 c_{mn}^l D_{mn}^l(\boldsymbol{R}(\psi,\theta,\phi)).\tag{4.131}$$

Following the same procedure as that in the derivation of (4.103), we deduce from (4.130) and (4.131) that the texture coefficients C_l^{mn} and c_{mn}^l are related by the formula

$$C_l^{mn}=8\pi^2 c^l_{\bar{n}\bar{m}}.\tag{4.132}$$

As it is pointed out in Sect. 4.5.1, Roe [270] does not unambiguously assign the sign of the normalization constant $\widetilde{N}(l,m,n)$ in formula (4.107) for his functions Z_{lmn}. The formula he obtained is that of $\widetilde{N}(l,m,n)^2$; see (4.109). Nevertheless, there is direct (see Roe [271, Eq. (10)] and discussions in Sect. 4.5.1) and indirect evidence (see Remark 4.5) which show clearly that for Roe $\widetilde{N}(l,m,n)$ is always the non-negative square root of the right-hand side of (4.109), i.e.,

$$\widetilde{N}(l,m,n)=\sqrt{\frac{2l+1}{2}}\cdot\sqrt{\frac{(l+m)!(l-n)!}{(l-m)!(l+n)!}}\cdot\frac{1}{(m-n)!},\tag{4.113}$$

which leads to (4.118). Inserting (4.132) into (4.118), we obtain

$$W_{lmn}=(-1)^{m-n}\cdot\frac{1}{8\pi^2}\sqrt{\frac{2}{2l+1}}\,C_l^{\bar{n}\bar{m}},\tag{4.133}$$

which is the relation between the texture coefficients of Roe and of Bunge. On the other hand, if we adopt assertion (A) of Bunge [60] and of Esling et al. [110] (see Remark 4.6 for more details), which the authors introduce without proof or reference, then

$$\widetilde{N}(l,m,n)=(-1)^{m-n}\sqrt{\frac{2l+1}{2}}\cdot\sqrt{\frac{(l+m)!(l-n)!}{(l-m)!(l+n)!}}\cdot\frac{1}{(m-n)!},\tag{C}$$

and we have (D), which leads to the formula

$$W_{lmn} = \frac{1}{8\pi^2}\sqrt{\frac{2}{2l+1}}\, C_l^{\bar{n}\bar{m}}, \tag{E}$$

as Bunge [60, p. 97] and Esling et al. [110] claimed. But the "W_{lmn}" of Bunge and of Esling et al. aren't Roe's W_{lmn}.

4.5.4 The D-Functions, ODF Expansion, and Texture Coefficients of Matthies

The reader will likely find the presentation of the D-functions in Matthies [215] and Matthies et al. [224] hard to follow, because the same symbol $D^l_{m,n}(\cdot)$ is used to denote two functions, which take arguments in active and passive rotations, respectively (cf. Sect. 4.1.1). In the physics literature (see P.P. Man [207] and the references therein) the two functions in question are entries of what are called the Wigner active and passive rotation matrices, respectively.

Citing the Russian original of the book by Varshalovich et al. [325], Matthies [215, see equations (1.26), (1.27), and (A1.5)] writes the D-functions as follows (see also Matthies et al. [224, equation (11.18)]):

$$D^l_{m,n}(g) = D^l_{m,n}(\psi,\theta,\phi) = e^{-im\psi} d^l_{m,n}(\theta) e^{-in\phi}, \tag{F}$$

where we have replaced Matthies's (α,β,γ) with our notation (ψ,θ,ϕ) for the Euler angles defined in the same way (cf. Sect. 1.8.1). A glance at (F) and the citation of Varshalovich et al. [325], where the formulas for the Wigner D-functions pertain to active rotations, suggest that (F) and (4.18) are the same equation. A check on the formulas[75] for $d^l_{m,n}(\theta)$ confirms this hunch. Hence the symbol "g" in (F) denotes an active rotation. There are other formulas in the two works cited (e.g., [215, equation (A.1.10)], which expresses the spherical harmonics in terms of $D^l_{m,0}$ (see (9.13)); [215, equation (A1.4)] and [224, equation (11.11)], which describe the transformation of spherical harmonics under rotation of coordinate system), where $D^l_{m,n}(\cdot)$ are clearly defined on active rotations.

In (F) we have kept the original notation of Matthies for the D-functions, where there is a comma between m and n in the suffix. If the domain of Matthies's $D^l_{m,n}$ is consistently the active rotations, by the defining formula (F) we have $D^l_{m,n}(\cdot) = D^l_{mn}(\cdot)$ and we should just drop the comma between m and n for notational consistency. There is, however, other evidence that leads to the opposite conclusion. Consider the formula

$$D^l_{m,n}(g_2 g_1) = \sum_{k=-l}^{l} D^l_{m,k}(g_1) D^l_{k,n}(g_2) \qquad \text{for each } g_1, g_2 \in \mathrm{SO}(3), \tag{4.134}$$

which appears in Matthies [215, equation (A1.12)] and Matthies et al. [224, equation (11.21)]. If the $D^l_{m,n}(\cdot)$ here are defined on active rotations, then (4.134) contradicts the important formula

$$D^l_{mn}(\boldsymbol{R}_2\boldsymbol{R}_1) = \sum_{k=-l}^{l} D^l_{mk}(\boldsymbol{R}_2) D^l_{kn}(\boldsymbol{R}_1), \tag{4.16}$$

[75] See Matthies et al. [224, equations (11.19) and (11.20)]. The same equations are given as (A1.6) and (A1.7) in [215], but equation (A1.7) has a typo. The analog of these equations for passive rotations can be found in Edmonds [98]; see his equations (4.5.2) and (4.5.3).

which follows from the fundamental attribute of the Wigner D-functions that for active rotations the correspondence $\boldsymbol{R} \mapsto [D^l(\boldsymbol{R})]$ is a representation of the rotation group SO(3). For (4.134) to be valid, the symbol "g" there must stand for a passive rotation. In Matthies et al. [224, Eq. (11.26)]) there is also the following formula which shows how $D^l_{m,n}$ is related to Bunge's T_l^{mn}:

$$T_l^{mn}(\boldsymbol{R}(\varphi_1, \Phi, \varphi_2)) = (-1)^{m+n} D^l_{m,n}(\boldsymbol{R}^{-1}(\psi, \theta, \phi)). \tag{4.135}$$

A comparison of (4.135) with (4.126) indicates that

$$D^l_{m,n}(\boldsymbol{R}^{-1}) = D^l_{mn}(\boldsymbol{R}) \qquad \text{for each } \boldsymbol{R} \in \mathrm{SO}(3); \tag{4.136}$$

in other words, $D^l_{m,n}(\cdot)$ in (4.135) is defined on passive rotations.[76] Given this confusing situation, for clarity we will henceforth do what follows: Wherever we are sure that Matthies's $D^l_{m,n}$ is meant to be defined on active rotations, we will write D^l_{mn} for $D^l_{m,n}$. If we are confident that $D^l_{m,n}$ is meant to be defined on passive rotations, we will denote it by a new symbol as follows:

$$\mathfrak{D}^l_{mn} := D^l_{m,n} = D^l_{mn} \circ \mathscr{J}, \qquad \text{where } \mathscr{J} : \boldsymbol{R} \mapsto \boldsymbol{R}^{-1}. \tag{4.137}$$

For an orientation g defined by the Euler angles (ψ, θ, ϕ), we have

$$\mathfrak{D}^l_{mn}(g(\psi, \theta, \phi)) = \mathfrak{D}^l_{mn}(\psi, \theta, \phi) = D^l_{mn}(\pi - \phi, \theta, \pi - \psi) = e^{im\phi} d^l_{mn}(-\theta) e^{in\psi}, \tag{4.138}$$

which are the Wigner D-functions for passive rotations.[77] We will keep using Matthies's notation $D^l_{m,n}$ for any D-function before its true specific meaning is identified.

Using our new notation regarding Wigner D-functions for passive rotations, we rewrite (4.135) as

$$T_l^{mn}(g(\varphi_1, \Phi, \varphi_2)) = (-1)^{m+n} \mathfrak{D}^l_{mn}(g^{-1}(\psi, \theta, \phi)). \tag{4.139}$$

Also if $D^l_{m,n}(\cdot) = \mathfrak{D}^l_{mn}(\cdot)$ in (4.134), then (4.134) follows immediately from (4.16) because $[\mathfrak{D}^l(g)] = [D^l(g^{-1})]$ for each $g \in \mathrm{SO}(3)$. Indeed we have

$$[\mathfrak{D}^l(g_2 g_1)] = [D^l((g_2 g_1)^{-1})] = [D^l(g_1^{-1} g_2^{-1})] = [D^l(g_1^{-1})][D^l(g_2^{-1})] = [\mathfrak{D}^l(g_1)][\mathfrak{D}^l(g_2)]. \tag{4.140}$$

Equation (4.140), which is equivalent to (4.134) after $D^l_{m,n}(\cdot)$ there is replaced by $\mathfrak{D}^l_{mn}(\cdot)$, can be called the addition theorem for $\mathfrak{D}^l_{mn}(\cdot)$. In quantum mechanics, the matrices $[\mathfrak{D}^l_{mn}(g(\psi, \theta, \phi))]$ are called the Wigner passive rotation matrices, where the matrix element $\mathfrak{D}^l_{mn}(g(\psi, \theta, \phi))$ is given by (4.138).[78]

[76] By substituting in (4.135) any specific $\boldsymbol{R}$ which observes $\boldsymbol{R} \neq \boldsymbol{R}^{-1}$, we can show directly that the interpretation $D^l_{m,n}(\cdot) = D^l_{mn}(\cdot)$ is untenable here.

[77] The Wigner D-functions for passive rotations, have been used for long in the physics literature. See [207] for references.

[78] See [207] for detailed discussions on Wigner active and passive rotation matrices.

Using passive rotations, Matthies et al. [224, equation (11.43)] (see also Matthies [214, 215]) expand the ODF as the series[79]

$$\begin{aligned}\mathtt{f}(\boldsymbol{R}^{(p)}) &= \sum_{l=0}^{\infty}\sum_{m=-l}^{l}\sum_{n=-l}^{l} C_l^{m,n} D_{m,n}^l((\boldsymbol{R}^{(p)})^{-1}) = \sum_{l=0}^{\infty}\sum_{m=-l}^{l}\sum_{n=-l}^{l} C_l^{m,n}\mathfrak{D}_{mn}^l((\boldsymbol{R}^{(p)})^{-1}) \\ &= \sum_{l=0}^{\infty}\sum_{m=-l}^{l}\sum_{n=-l}^{l} C_l^{m,n} D_{mn}^l(\boldsymbol{R}^{(p)}) \end{aligned} \tag{4.141}$$

for every passive rotation $\boldsymbol{R}^{(p)}$; here we are certain that $D_{m,n}^l$ in $(4.141)_1$ means $\mathfrak{D}_{mn}^l$ in $(4.141)_2$ because the authors invoke (4.135) as motivation to define the series expansion as given so that the texture coefficients $C_l^{m,n}$ differ from Bunge's C_l^{mn} only by a factor of $(-1)^{m+n}$. Using (4.126), (4.141), and the fact that Matthies takes the volume of SO(3) as 1, we recast (4.141) as

$$\mathtt{f}(\boldsymbol{R}^{(p)}) = 1 + \sum_{l=1}^{\infty}\sum_{m=-l}^{l}\sum_{n=-l}^{l} C_l^{m,n}(-1)^{m+n} T_l^{mn}(\boldsymbol{R}^{(p)}). \tag{4.142}$$

A comparison of (4.142) with (4.129) indicates that

$$C_l^{m,n} = (-1)^{m+n} C_l^{mn} = (-1)^{m+n}\cdot 8\pi^2 c_{\bar{n}\bar{m}}^l, \tag{4.143}$$

where we have appealed to (4.132) at the last step.

By the inverse invariance of the Haar integral and the orthogonality relation (4.21), we obtain from $(4.141)_3$ the formula

$$\begin{aligned} C_l^{m,n} &= \frac{2l+1}{8\pi^2}\int_{\mathrm{SO}(3)} \mathtt{f}(\boldsymbol{R}^{-1})\overline{D_{mn}^l(\boldsymbol{R}^{-1})}\, d\mathcal{V}(\boldsymbol{R}) \\ &= (2l+1)\int_{\mathrm{SO}(3)} \mathtt{f}(\boldsymbol{R})\overline{D_{mn}^l(\boldsymbol{R})}\, d\mathtt{g}(\boldsymbol{R}). \end{aligned} \tag{4.144}$$

[79] Note that Matthies's $C_l^{m,n}$ is distinguished from Bunge's C_l^{mn} by the comma between m and n in the superscript.

Chapter 5

5 Texture and Crystallite Symmetries

In Chaps. 3 and 4 we consider polycrystalline aggregates of triclinic crystallites (whose group of crystallite symmetry $G_{\text{cr}} = C_1 = \{\boldsymbol{I}\}$.[80] Most polycrystals in the physical world, however, consist of crystallites with non-trivial symmetry, i.e., $G_{\text{cr}} \neq \{\boldsymbol{I}\}$. Moreover, manufactural processes often impart macroscopic sample symmetry to their products. For instance, after passes of cold or hot rolling and subsequent annealing, samples of sheet metals often exhibit (imperfect) orthorhombic symmetry, with the rolling-, transverse-, and normal-direction of the sheet being axes of two-fold rotational symmetry.

In this chapter we study textures of polycrystals with non-trivial crystallite symmetry and/or sample symmetry. Working within the context of classical texture analysis, we shall restrict our discussion to the cases where G_{cr} is a proper crystallographic point group (see Sect. 2.5.2) and G_{tex},[81] the group of texture (or sample) symmetry, a subgroup of SO(3). Moreover, in this chapter we shall follow the approach initiated by Roe [270, 271], which works with ODFs introduced in the context of $G_{\text{cr}} = \{\boldsymbol{I}\}$ and $G_{\text{tex}} = \{\boldsymbol{I}\}$ and accounts for the effects of crystallite and sample symmetry by imposing suitable constraints on the texture coefficients of the ODF defined on the rotation group SO(3).[82] By the reference single crystal we mean the ideal crystal $(\mathsf{C}, \boldsymbol{\kappa}_0)$ at the macro-scale (cf. Remark 2.50), under which its configuration $\boldsymbol{\kappa}_0(\mathsf{C})$ is homogeneous and its complete symmetry group is given (see Sect. 2.11) by the semi-direct product

$$\mathrm{T}(3) \wedge \hat{G}_{\text{cr}} = \{(\boldsymbol{v}, \boldsymbol{I})(\boldsymbol{0}, \boldsymbol{R}) : (\boldsymbol{v}, \boldsymbol{I}) \in \mathrm{T}(3) \text{ and } \boldsymbol{R} \in G_{\text{cr}}\}, \tag{5.1}$$

where T(3) is the subgroup of translations in E(3) (the Euclidean group of rigid transplacements on the three-dimensional physical space E^3; see Sect. 2.2).

5.1 Transformation Formulas

5.1.1 Rotation of Polycrystal

Consider a polycrystal P and a sampling point $\mathtt{X}$ in P. Let a reference ideal crystal $(\mathsf{C}, \boldsymbol{\kappa}_0)$ be chosen (cf. Definition 2.10), and let $w : \mathrm{SO}(3) \to \mathbb{R}$ be the ODF[83] that specifies the texture of P at $\mathtt{X}$. After the polycrystal undergoes a rotation $\boldsymbol{Q}$ at $\mathtt{X}$, its texture at $\mathtt{X}$ is clearly described by a new ODF $\grave{w}$, which is related to the ODF w of the polycrystal before rotation by the equation

$$\grave{w}(\boldsymbol{Q}\boldsymbol{R}) = w(\boldsymbol{R}) \qquad \text{for each rotation } \boldsymbol{R}. \tag{5.2}$$

[80] See (5.18) for definition of G_{cr}.

[81] See (5.16) for definition of G_{tex}.

[82] In Chap. 6 we shall see that Roe's ODF w, which is defined on SO(3), isn't generally an orientation probability density. There we will detail how Roe's w is related to the orientation probability density $\hat{w}$ defined on the space of orientations for crystallites with non-trivial symmetry.

[83] By calling this w an ODF we follow Roe and customary usage in the texture literature. In Chap. 6, where we discuss the Roe approach thoroughly, we shall see that except for the case where the crystallites are triclinic Roe's ODF isn't an orientation probability density on SO(3).

After a change of variables, the preceding equation can be recast as

$$\grave{w}(\boldsymbol{R}) = w(\boldsymbol{Q}^{-1}\boldsymbol{R}) \qquad \text{for each rotation } \boldsymbol{R}. \tag{5.3}$$

Let $\grave{c}^l_{mn}$ and c^l_{mn} be the texture coefficients pertaining to $\grave{w}$ and w, respectively. We can easily derive from (5.3) the relationship between these two sets of texture coefficients.

Indeed, by (4.16), we have

$$\begin{aligned}
\grave{w}(\boldsymbol{R}) &= w(\boldsymbol{Q}^{-1}\boldsymbol{R}) \\
&= \sum_{l=0}^{\infty}\sum_{m=-l}^{l}\sum_{n=-l}^{l} c^l_{mn} D^l_{mn}(\boldsymbol{Q}^{-1}\boldsymbol{R}) \\
&= \sum_{l=0}^{\infty}\sum_{m=-l}^{l}\sum_{n=-l}^{l} c^l_{mn} \left(\sum_{s=-l}^{l} D^l_{ms}(\boldsymbol{Q}^{-1}) D^l_{sn}(\boldsymbol{R})\right) \\
&= \sum_{l=0}^{\infty}\sum_{s=-l}^{l}\sum_{n=-l}^{l} \left(\sum_{m=-l}^{l} c^l_{mn} D^l_{ms}(\boldsymbol{Q}^{-1})\right) D^l_{sn}(\boldsymbol{R}).
\end{aligned} \tag{5.4}$$

Hence we obtain the relation

$$\grave{c}^l_{sn} = \sum_{m=-l}^{l} c^l_{mn} D^l_{ms}(\boldsymbol{Q}^{-1}) \tag{5.5}$$

or, by renaming indices,

$$\grave{c}^l_{mn} = \sum_{p=-l}^{l} c^l_{pn} D^l_{pm}(\boldsymbol{Q}^{-1}). \tag{5.6}$$

From (4.18), (4.117) and (4.118), we obtain for Roe's coefficients the formula

$$\grave{W}_{lmn} = \sqrt{\frac{2}{2l+1}} \sum_{p=-l}^{l} W_{lpn} Z_{lpm}(\cos\beta) e^{-ip\alpha} e^{-im\gamma}, \tag{5.7}$$

where (α, β, γ) are the Euler angles pertaining to $\boldsymbol{Q}^{-1}$.

Remark 5.1 Note that $\boldsymbol{Q}$ is a rotation of the polycrystal at the sampling point X in question, and that Euler angles (e.g., in (5.7)) are defined with respect to some chosen right-handed orthonormal triad $\{\boldsymbol{e}_i : i = 1, 2, 3\}$ fixed to the tangent space of polycrystal P at X before rotation. In the presence of texture symmetry, the triad $\{\boldsymbol{e}_i\}$ should be chosen judiciously to simplify the texture coefficients as much as possible. For example, for sheet metals $\boldsymbol{e}_i$ $(i = 1, 2, 3)$ should be chosen to be parallel to the three axes of two-fold rotational symmetry, respectively. On the other hand, Roe's approach to texture analysis remains valid even if a suboptimal coordinate system is chosen and simplification by texture symmetry is not exploited to the fullest. □

5.1.2 Rotation of Reference Ideal Crystal

Similarly, when the reference ideal crystal $(\mathsf{C}, \boldsymbol{\kappa}_0)$ of the crystallites undergoes a rotation $\boldsymbol{P}$, the ODF of the polycrystal becomes $\check{w}$, which is related to the original ODF w by

$$\check{w}(\boldsymbol{R}\boldsymbol{P}^{-1}) = w(\boldsymbol{R}) \qquad \text{for each rotation } \boldsymbol{R}, \tag{5.8}$$

which is equivalent to the equation

$$\check{w}(\boldsymbol{R}) = w(\boldsymbol{R}\boldsymbol{P}) \qquad \text{for each rotation } \boldsymbol{R}. \tag{5.9}$$

The transformation formula for the texture coefficients can likewise be deduced from (5.9). Thus we have

$$\begin{aligned}
\check{w}(\boldsymbol{R}) &= w(\boldsymbol{R}\boldsymbol{P}) \\
&= \sum_{l=0}^{\infty} \sum_{m=-l}^{l} \sum_{n=-l}^{l} c_{mn}^{l} D_{mn}^{l}(\boldsymbol{R}\boldsymbol{P}) \\
&= \sum_{l=0}^{\infty} \sum_{m=-l}^{l} \sum_{n=-l}^{l} c_{mn}^{l} \left(\sum_{s=-l}^{l} D_{ms}^{l}(\boldsymbol{R}) D_{sn}^{l}(\boldsymbol{P}) \right) \\
&= \sum_{l=0}^{\infty} \sum_{m=-l}^{l} \sum_{s=-l}^{l} \left(\sum_{n=-l}^{l} c_{mn}^{l} D_{sn}^{l}(\boldsymbol{P}) \right) D_{ms}^{l}(\boldsymbol{R}).
\end{aligned} \tag{5.10}$$

Hence we obtain the relation

$$\check{c}_{ms}^{l} = \sum_{n=-l}^{l} c_{mn}^{l} D_{sn}^{l}(\boldsymbol{P}) \tag{5.11}$$

or, by renaming indices,

$$\check{c}_{mn}^{l} = \sum_{p=-l}^{l} c_{mp}^{l} D_{np}^{l}(\boldsymbol{P}). \tag{5.12}$$

Let $(\alpha^{\#}, \beta^{\#}, \gamma^{\#})$ and (α, β, γ) be the Euler angles pertaining to $\boldsymbol{P}$ and $\boldsymbol{P}^{-1}$, respectively. From the symmetry relation $(4.32)_1$ and the relationship between the two sets of Euler angles, we have

$$\begin{aligned}
D_{np}^{l}(\boldsymbol{P}) &= e^{-in\alpha^{\#}} d_{np}^{l}(\beta^{\#}) e^{-ip\gamma^{\#}} \\
&= (-1)^{n} e^{in\gamma} (-1)^{n-p} d_{pn}^{l}(\beta) (-1)^{p} e^{ip\alpha} \\
&= e^{in\gamma} d_{pn}^{l}(\beta) e^{ip\alpha}.
\end{aligned} \tag{5.13}$$

For the Roe coefficients we obtain from (4.18), (4.117), (4.118), and (5.12) the transformation formula

$$\check{W}_{lmn} = \sqrt{\frac{2}{2l+1}} \sum_{p=-l}^{l} W_{lmp} Z_{lpn}(\cos\beta) e^{ip\alpha} e^{in\gamma}. \tag{5.14}$$

Remark 5.2 As the Euler angles of $\boldsymbol{P}$ are defined with respect to some right-handed orthonormal triad $\{\check{\boldsymbol{e}}_i : i = 1, 2, 3\}$ fixed to the reference ideal crystal $(\mathsf{C}, \boldsymbol{\kappa}_0)$, the triad $\check{\boldsymbol{e}}_i$ should be chosen so that crystallite symmetry could be exploited most efficiently. For example, for cubic crystallites $\check{\boldsymbol{e}}_i$ $(i = 1, 2, 3)$ should be chosen to be parallel to the three axes of four-fold rotational symmetry, respectively. When non-trivial crystallite and sample symmetries are present, we should choose both orthonormal triads $\{\boldsymbol{e}_i\}$ and $\{\check{\boldsymbol{e}}_i\}$ judiciously to take advantage of both symmetries to simplify the ODF (see Remark 5.4). Nevertheless Roe's approach to texture analysis is valid irrespective of the coordinate systems chosen for the polycrystal and for the ideal reference crystal. □

5.2 Restrictions on Texture Coefficients Imposed by Sample and Crystallite Symmetries

Let w be the ODF characterizing the texture of a polycrystal P at sampling point $\mathtt{x}$. A rotation $\boldsymbol{Q}$ at $\mathtt{x}$ is a symmetry operation for this texture if w remains unchanged when the polycrystal P undergoes the rotation $\boldsymbol{Q}$, i.e., (cf. (5.3))

$$\grave{w}(\boldsymbol{R}) = w(\boldsymbol{Q}^T\boldsymbol{R}) = w(\boldsymbol{R}) \tag{5.15}$$

for each $\boldsymbol{R}$ in SO(3). The collection of such texture-preserving rotations $\boldsymbol{Q}$ clearly forms a subgroup of rotations

$$G_{\text{tex}} = \{\boldsymbol{Q} \in \text{SO}(3) : w(\boldsymbol{Q}^T\boldsymbol{R}) = w(\boldsymbol{R}) \text{ for each } \boldsymbol{R} \in \text{SO}(3)\}, \tag{5.16}$$

which we call the group of texture (or sample) symmetry of P.

Similarly, when the crystallites constituting P possess symmetry operations described by a subgroup of rotations G_{cr}, a rotation of the reference orientation by $\boldsymbol{P} \in G_{\text{cr}}$ will not affect w, i.e., (cf. (5.9))

$$\check{w}(\boldsymbol{R}) = w(\boldsymbol{R}\boldsymbol{P}) = w(\boldsymbol{R}) \tag{5.17}$$

for each $\boldsymbol{R}$ in SO(3). Thus the group of crystallite symmetry of P is defined by

$$G_{\text{cr}} = \{\boldsymbol{P} \in \text{SO}(3) : w(\boldsymbol{R}\boldsymbol{P}) = w(\boldsymbol{R}) \text{ for each } \boldsymbol{R} \in \text{SO}(3)\}. \tag{5.18}$$

Remark 5.3 The symmetry operations in G_{tex} and G_{cr} are restricted to be rotations because in classical texture analysis the ODF w is defined on the rotation group SO(3). In particular we assume henceforth that G_{cr} is the Type I point group in the Laue class that contains the crystallographic point group $\mathcal{K}$ of the crystallites which constitute the polycrystal P in question. □

Equations (5.15) and (5.17) impose restrictions that the ODF w must satisfy in the presence of texture and crystal symmetries. These restrictions translate into requirements on the texture coefficients c^l_{mn} and W_{lmn}. Indeed by (5.6), (5.15), (5.12), and (5.17) we observe that the texture coefficients satisfy the restrictions

$$c^l_{mn} = \sum_{p=-l}^{l} c^l_{pn} D^l_{pm}(\boldsymbol{Q}^{-1}) \qquad \text{for each } \boldsymbol{Q} \in G_{\text{tex}} \tag{5.19}$$

and

$$c^l_{mn} = \sum_{p=-l}^{l} c^l_{mp} D^l_{np}(\boldsymbol{P}) \qquad \text{for each } \boldsymbol{P} \in G_{\text{cr}}. \tag{5.20}$$

In computations to determine explicit restrictions for specific instances, suitable coordinate systems and the reference ideal crystal $(\mathsf{C}, \boldsymbol{\kappa}_0)$ (see Remarks 5.1 and 5.2) should be chosen so that G_{cr} and G_{tex} have as many common elements as possible.

Remark 5.4 It can be seen from (5.19) and (5.20) that texture and crystallite symmetry imposes restrictions on the index m and index n in the texture coefficients c^l_{mn}, respectively. When non-trivial crystallite and sample symmetries are present, we should take advantage of both (5.19) and (5.20) to simplify the ODF. To this end, after we have chosen an "optimal" orthonormal triad $\{\boldsymbol{e}_i\}$ and $\{\check{\boldsymbol{e}}_i\}$, which are attached to the sample and to the reference ideal crystal, respectively, we can always choose a configuration (or orientation) of the ideal reference crystal so that $\check{\boldsymbol{e}}_i$ agrees with $\boldsymbol{e}_i$ for each i. Then the Euler angles of $\boldsymbol{Q}$ in (5.19) and of $\boldsymbol{P}$ in (5.20) are referred to the same coordinate system. □

Remark 5.5 Restrictions on the texture coefficients C^{mn}_l imposed by texture and crystallite symmetry can be inferred from those on c^l_{mn} through formula (4.132), i.e., $C^{mn}_l = 8\pi^2 c^l_{\bar{n}\bar{m}}$. By Remark 5.4, texture and crystallite symmetry imposes restrictions on the index n and index m in the texture coefficients C^{mn}_l, respectively.

If one elects to work with $\mathtt{f}(\boldsymbol{R}^{(p)})$ as the primary ODF, formulas that deliver the restrictions on C^{mn}_l can be derived directly. Let us illustrate with crystallite symmetry. There the basic restriction is:

$$\mathtt{f}(\boldsymbol{R}^{-1}) = \mathtt{f}^{(a)}(\boldsymbol{R}) = \mathtt{f}^{(a)}(\boldsymbol{RP}) = \mathtt{f}((\boldsymbol{RP})^{-1}) \qquad \text{for each } \boldsymbol{P} \in G_{\text{cr}}. \tag{5.21}$$

Comparing the equations

$$\mathtt{f}(\boldsymbol{R}^{-1}) = \sum_{l=0}^{\infty} \sum_{m=-l}^{l} \sum_{n=-l}^{l} C^{mn}_l T^{mn}_l(\boldsymbol{R}^{-1}), \tag{5.22}$$

$$\begin{aligned} \mathtt{f}((\boldsymbol{RP})^{-1}) &= \sum_{l=0}^{\infty} \sum_{m=-l}^{l} \sum_{n=-l}^{l} C^{mn}_l T^{mn}_l(\boldsymbol{P}^{-1}\boldsymbol{R}^{-1}) \\ &= \sum_{l=0}^{\infty} \sum_{m=-l}^{l} \sum_{n=-l}^{l} C^{mn}_l \left(\sum_{s=-l}^{l} T^{ms}_l(\boldsymbol{P}^{-1}) T^{sn}_l(\boldsymbol{R}^{-1}) \right) \\ &= \sum_{l=0}^{\infty} \sum_{m=-l}^{l} \sum_{n=-l}^{l} \left(\sum_{p=-l}^{l} C^{pn}_l T^{pm}_l(\boldsymbol{P}^{-1}) \right) T^{mn}_l(\boldsymbol{R}^{-1}), \end{aligned} \tag{5.23}$$

after renaming some repeated indices we obtain the restriction

$$C^{mn}_l = \sum_{p=-l}^{l} C^{pn}_l T^{pm}_l(\boldsymbol{P}^{-1}) \qquad \text{for each } \boldsymbol{P} \in G_{\text{cr}}. \tag{5.24}$$

It is easy to show that restrictions on C_l^{mn} imposed by (5.24) is equivalent to those on c_{mn}^l imposed by (5.20). Indeed by (4.100) and (4.126), we have

$$T_l^{pm}(\boldsymbol{P}^{-1}) = (-1)^{p+m} D_{pm}^l(\boldsymbol{P}^{-1}) = D_{\bar{m}\bar{p}}^l(\boldsymbol{P}). \tag{5.25}$$

Substituting (4.132) and (5.25) into (5.24), we obtain

$$8\pi^2 c_{\bar{n}\bar{m}}^l = \sum_{p=-l}^{l} 8\pi^2 c_{\bar{n}\bar{p}}^l D_{\bar{m}\bar{p}}^l(\boldsymbol{P}) \qquad \text{for each } \boldsymbol{P} \in G_{\text{cr}}, \tag{5.26}$$

which reduces to (5.20) after simplification and renaming of some repeated indices. □

5.3 Examples of Low Symmetry

Derivations of the restrictions imposed by texture and crystal symmetries are simple for the cases of low symmetry, i.e., when the symmetry groups involved are C_2, C_3, C_4, C_6, D_2, D_3, D_4, or D_6. In this section we shall restrict our attention to these cases of low symmetry. A few examples will suffice to illustrate the method to derive the restrictions for all these cases.

5.3.1 Orthorhombic Texture Symmetry

Here $G_{\text{tex}} = D_2$. Let the spatial coordinate system be chosen so that the elements of G_{tex} are: $\boldsymbol{I}$, $\boldsymbol{Q}(\boldsymbol{e}_1, \pi)$, $\boldsymbol{Q}(\boldsymbol{e}_2, \pi)$, and $\boldsymbol{Q}(\boldsymbol{e}_3, \pi)$. Orthorhombic texture symmetry dictates that $\grave{c}_{mn}^l = c_{mn}^l$ for $\boldsymbol{Q}^{-1}$ given by the Euler angles $(0, \pi, \pi)$, $(0, \pi, 0)$, and $(0, 0, \pi)$, respectively.

For convenience of the reader, we begin by recapitulating a few formulas (see (4.29), $(4.33)_1$, (4.118) and (5.6)), which we shall use in the derivations below:

$$d_{mn}^l(0) = \delta_{mn}, \qquad d_{mn}^l(\pi - \theta) = (-1)^{l+m} d_{m\bar{n}}^l(\theta),$$

$$c_{mn}^l = (-1)^{m-n} \sqrt{\frac{2l+1}{2}} W_{lmn}, \qquad \grave{c}_{mn}^l = \sum_{p=-l}^{l} c_{pn}^l D_{pm}^l(\boldsymbol{Q}^{-1}),$$

where $\grave{c}_{mn}^l$ are the texture coefficients pertaining to the rotated orientation distribution function $\grave{w}$ defined by

$$\grave{w}(\boldsymbol{R}) = w(\boldsymbol{Q}^{-1}\boldsymbol{R}) \qquad \text{for each rotation } \boldsymbol{R}.$$

For $\boldsymbol{Q}^{-1}$ given by $(0, \pi, 0)$, we have

$$\begin{aligned} c_{mn}^l &= \sum_p c_{pn}^l D_{pm}^l(0, \pi, 0) = \sum_p c_{pn}^l d_{pm}^l(\pi) \\ &= \sum_p c_{pn}^l (-1)^{l+p} d_{p\bar{m}}^l(0) = (-1)^{l-m} c_{\bar{m}n}^l. \end{aligned} \tag{5.27}$$

In terms of the Roe coefficients, (5.27) reads:

$$W_{lmn} = (-1)^{l-m} W_{l\bar{m}n}. \tag{5.28}$$

For $\boldsymbol{Q}^{-1}$ given by $(0, 0, \pi)$, we have

$$c^l_{mn} = \sum_p c^l_{pn} D^l_{pm}(0, 0, \pi) = \sum_p c^l_{pn} d^l_{pm}(0) e^{-im\pi} = c^l_{mn} \cos(m\pi). \tag{5.29}$$

Equation (5.29) dictates that

$$c^l_{mn} = 0 \quad (\text{or equivalently, } W_{lmn} = 0) \qquad \text{if } m \text{ is odd.} \tag{5.30}$$

For $\boldsymbol{Q}^{-1}$ given by $(0, \pi, \pi)$, we have

$$\begin{aligned} c^l_{mn} &= \sum_p c^l_{pn} D^l_{pm}(0, \pi, \pi) = \sum_p c^l_{pn} d^l_{pm}(\pi) e^{-im\pi} \\ &= \sum_p c^l_{pn} (-1)^{l+p} d^l_{p\bar{m}}(0) e^{-im\pi} \\ &= (-1)^{l-m} c^l_{\bar{m}n} \cos(m\pi) = (-1)^l c^l_{\bar{m}n}, \end{aligned} \tag{5.31}$$

which translates to

$$W_{lmn} = (-1)^l W_{l\bar{m}n} \tag{5.32}$$

for the Roe coefficients.

When all three symmetries are present, we have

$$c^l_{mn} = \begin{cases} (-1)^l c^l_{\bar{m}n} & \text{for even } m \\ 0 & \text{for odd } m \end{cases} \quad \text{or} \quad W_{lmn} = \begin{cases} (-1)^l W_{l\bar{m}n} & \text{for even } m \\ 0 & \text{for odd } m. \end{cases} \tag{5.33}$$

Note that the computations involving the Euler angles $(0, \pi, \pi)$ for $\boldsymbol{Q}^{-1}$ are in fact redundant, for this symmetry operation is generated by those with Euler angles $(0, \pi, 0)$ and $(0, 0, \pi)$. Also, (5.33) is valid only for the particular spatial coordinate systems where the coordinate axes are the axes of orthorhombic texture symmetry.

5.3.2 Orthorhombic Crystallite Symmetry

To derive implications of crystal symmetry, (5.12), namely

$$\check{c}^l_{mn} = \sum_{p=-l}^{l} c^l_{mp} D^l_{np}(\boldsymbol{P})$$

is crucial. As the reader will see, the derivation of restrictions imposed by D_2 crystal symmetry is completely parallel to that for D_2 texture symmetry above.

Let the reference ideal crystal $(\mathsf{C}, \boldsymbol{\kappa}_0)$ of the crystallites and the coordinate system for the definition of Euler angles be chosen so that

$$G_{\text{cr}} = \{\boldsymbol{I}, \boldsymbol{R}(\check{\boldsymbol{e}}_1, \pi), \boldsymbol{R}(\check{\boldsymbol{e}}_2, \pi), \boldsymbol{R}(\check{\boldsymbol{e}}_3, \pi)\}. \tag{5.34}$$

Orthorhombic crystal symmetry dictates that $\check{c}^l_{mn} = c^l_{mn}$ for $\boldsymbol{R}$ given by the Euler angles $(0, \pi, 0)$, $(0, 0, \pi)$, and $(0, \pi, \pi)$, respectively.

For $\boldsymbol{R}$ given by $(0, \pi, 0)$, we have

$$c^l_{mn} = \sum_p c^l_{mp} D^l_{np}(0, \pi, 0) = \sum_p c^l_{mp} d^l_{np}(\pi)$$
$$= \sum_p c^l_{mp} (-1)^{l+n} d^l_{n\bar{p}}(0) = (-1)^{l+n} c^l_{m\bar{n}}, \tag{5.35}$$

which, in terms of the Roe coefficients, reads

$$W_{lmn} = (-1)^{l+n} W_{lm\bar{n}}. \tag{5.36}$$

For $\boldsymbol{R}$ given by $(0, 0, \pi)$, we have

$$c^l_{mn} = \sum_p c^l_{mp} D^l_{np}(0, 0, \pi) = \sum_p c^l_{mp} d^l_{np}(0) e^{-ip\pi} = c^l_{mn} \cos(n\pi). \tag{5.37}$$

Therefore

$$c^l_{mn} = 0 \quad \text{(or equivalently, } W_{lmn} = 0) \qquad \text{if } n \text{ is odd.} \tag{5.38}$$

Combining the preceding two requirements, we obtain the constraint

$$c^l_{mn} = \begin{cases} (-1)^l c^l_{m\bar{n}} & \text{for even } n \\ 0 & \text{for odd } n \end{cases} \quad \text{or} \quad W_{lmn} = \begin{cases} (-1)^l W_{lm\bar{n}} & \text{for even } n \\ 0 & \text{for odd } n. \end{cases} \tag{5.39}$$

Note also that by (5.39) we have

$$c^l_{m0} = 0 \qquad \text{for odd } l \text{ and for each } m. \tag{5.40}$$

Again the validity of the preceding formulas are predicated upon the choice of the reference ideal crystal $(\mathsf{C}, \boldsymbol{\kappa}_0)$ and of the coordinate system for the definition of Euler angles so that G_{cr} is given by (5.34) above. A similar caveat will apply, even if there is no explicit warning, to all our further discussions on restrictions on texture coefficients imposed by texture and/or crystallite symmetry.

5.3.3 Orthorhombic Aggregates of Orthorhombic Crystallites

When both D_2 texture symmetry and D_2 crystal symmetry are present, we choose the reference ideal crystal $(\mathsf{C}, \boldsymbol{\kappa}_0)$ and the basis vectors $\{\boldsymbol{e}_i\}$ and $\{\check{\boldsymbol{e}}_i\}$, which pertain to the sample and to the reference ideal crystal, respectively, so that

$$\boldsymbol{e}_i = \check{\boldsymbol{e}}_i \qquad \text{for } i = 1, 2, 3, \tag{5.41}$$

$$G_{\text{tex}} = G_{\text{cr}} = \{\boldsymbol{I}, \boldsymbol{R}(\boldsymbol{e}_1, \pi), \boldsymbol{R}(\boldsymbol{e}_2, \pi), \boldsymbol{R}(\boldsymbol{e}_3, \pi)\}. \tag{5.42}$$

Then both the constraints (5.33) and (5.39) are valid. Moreover, we can combine them with the reality condition (4.119) to show that all the texture coefficients c^l_{mn} are real. Indeed, from the requirements (5.33) and (5.39) imposed by texture and crystal symmetry, we observe that

$$c^l_{\bar{m}\bar{n}} = (-1)^l c^l_{m\bar{n}} = (-1)^{2l} c^l_{mn} = c^l_{mn}. \tag{5.43}$$

On the other hand, combining (5.43) with the reality condition (4.119), we have

$$c^l_{mn} = (-1)^{m-n}\overline{c^l_{\bar{m}\bar{n}}} = \overline{c^l_{mn}}, \tag{5.44}$$

because the constraints (5.33) and (5.39) imposed by the orthorhombic symmetries dictate that $c^l_{mn} = 0$ unless both m and n are even.

In summary, for orthorhombic aggregates of orthorhombic crystallites, the independent texture coefficients (with $l \geq 1$) are:

$$c^l_{mn} \in \mathbb{R} \qquad \text{where } m \geq 0 \text{ and } n \geq 0 \text{ are even, and } l = 2, 3, 4, \ldots, \tag{5.45}$$

excluding all c^l_{m0} and c^l_{0n} with odd l, which are equal to zero. The non-trivial dependent texture coefficients are:

$$c^l_{\bar{m}n} = (-1)^l c^l_{mn}, \qquad c^l_{m\bar{n}} = (-1)^l c^l_{mn}, \qquad c^l_{\bar{m}\bar{n}} = c^l_{mn}, \tag{5.46}$$

where $m \geq 0$ and $n \geq 0$ are even, and $l = 2, 3, 4, \ldots$. Parallel statements in terms of the Roe coefficients can be easily obtained by changing each c^l_{mn} in assertions (5.45) and (5.46) to W_{lmn}.

5.3.4 Trigonal, Tetragonal, and Hexagonal Crystallite Symmetries

For trigonal, tetragonal, and hexagonal crystallite symmetries, here we restrict attention to the cases where $G_{\text{cr}} = D_3$, D_4, or D_6. We discuss these three cases together because we can write our derivation of restrictions imposed by G_{cr} on c^l_{mn} in terms of a parameter $\alpha = 3, 4, 6$, which will cover the case of $G_{\text{cr}} = D_\alpha$, respectively.

Let the reference ideal crystal $(\mathsf{C}, \boldsymbol{\kappa}_0)$ and the orthonormal basis $\{\check{\boldsymbol{e}}_i : i = 1, 2, 3\}$ attached to it be chosen such that $\boldsymbol{R}(\check{\boldsymbol{e}}_2, \pi)$ and $\boldsymbol{R}(\check{\boldsymbol{e}}_3, 2\pi/\alpha)$ are the generators of the $G_{\text{cr}} = D_\alpha$ group, where $\alpha = 3, 4, 6$, which covers the case of trigonal, tetragonal and hexagonal crystallite symmetry, respectively.[84]

The restriction imposed by $\boldsymbol{R}(\check{\boldsymbol{e}}_2, \pi)$ is given by (5.35) above. Now, for the restrictions imposed by $\boldsymbol{R}(\check{\boldsymbol{e}}_3, 2\pi/\alpha)$, where $\alpha = 3, 4, 6$, by (5.20) we obtain for $G_{\text{cr}} = D_\alpha$ what follows:

$$c^l_{mn} = \sum_p c^l_{mp} D^l_{np}(0, 0, 2\pi/\alpha) = \sum_p c^l_{mp} d^l_{np}(0) e^{-i2p\pi/\alpha} = c^l_{mn} e^{-in2\pi/\alpha}. \tag{5.47}$$

Hence for trigonal, tetragonal, and hexgonal crystallite symmetry, $c^l_{mn} = 0$ unless $n = \alpha k$ for some $k \in \mathbb{Z}$, where $\mathbb{Z}$ denotes the set of integers.

In conclusion, we deduce the following restriction imposed by trigonal, tetragonal, and hexagonal crystallite symmetry for the case of $\alpha = 3, 4, 6$, respectively:

$$c^l_{mn} = \begin{cases} (-1)^{l+n} c^l_{m\bar{n}} & \text{for } n = \alpha k, k \in \mathbb{Z} \\ 0 & \text{for } n \neq \alpha k, k \in \mathbb{Z}, \end{cases} \tag{5.48}$$

or

$$W_{lmn} = \begin{cases} (-1)^{l+n} W_{lm\bar{n}} & \text{for } n = \alpha k, k \in \mathbb{Z} \\ 0 & \text{for } n \neq \alpha k, k \in \mathbb{Z}. \end{cases} \tag{5.49}$$

[84] Here we use $\boldsymbol{R}(\check{\boldsymbol{e}}_2, \pi)$ instead of $\boldsymbol{R}(\check{\boldsymbol{e}}_1, \pi)$, which we employ in Chap. 2, as a generator of D_α ($\alpha = 3, 4, 6$), because our definition of Euler angles renders this choice more convenient. In what follows we will keep this choice in all discussions that involve the ODF with Euler angles as parameters.

The restrictions (5.48) are valid for the choice of reference ideal crystal $(\mathsf{C}, \boldsymbol{\kappa}_0)$ and of the orthonormal basis given at the beginning of this subsection. One consequence of (5.48) that we shall use later is:

$$c^l_{m0} = 0 \qquad \text{for odd } l \text{ and for each } m, \tag{5.50}$$

which holds for $G_{cr} = D_3$, D_4, or D_6. Earlier we have seen in (5.40) that the same relation is valid for $G_{\mathrm{cr}} = D_2$.

5.4 Some Cases Frequently Encountered in Applications

5.4.1 Fiber Textures

A material point $\mathtt{x}$ in a polycrystal is said to have fiber texture (or has transversely-isotropic texture symmetry) if the ODF $w(\cdot; \mathtt{x})$ remains invariant under all rotations about some axis through $\mathtt{x}$. As G_{tex} in classical texture analysis is restricted to be a subgroup of SO(3), there are only two types of fiber textures. The first, which is said to be of type C_∞, has

$$G_{\mathrm{tex}} = \{\boldsymbol{R}(\boldsymbol{n}, \vartheta) : \boldsymbol{n} \text{ is a unit vector}, \vartheta \in \mathbb{R}\}, \tag{5.51}$$

where $\boldsymbol{n}$ specifies the distinguished axis of rotation. The second, which is of type D_∞, has G_{tex} being the group that results by adding the generator $\boldsymbol{R}(\boldsymbol{m}, \pi)$ to the group defined by the right-hand-side of (5.51), where $\boldsymbol{m}$ is a unit vector orthogonal to $\boldsymbol{n}$. For brevity, in what follows we shall simply write $G_{\mathrm{tex}} = C_\infty$ and $G_{\mathrm{tex}} = D_\infty$ to mean that G_{tex} is of type C_∞ and of type D_∞, respectively.

Let us now proceed to derive the restrictions that the two types of fiber texture impose on texture coefficients, respectively.

$\underline{G_{\mathrm{tex}} = C_\infty}$

We choose a sample orthonormal triad $\boldsymbol{e}_i$ $(i = 1, 2, 3)$ such that $\boldsymbol{e}_3 = \boldsymbol{n}$. Then

$$G_{\mathrm{tex}} = \{\boldsymbol{R}(\boldsymbol{e}_3, \vartheta) : \vartheta \in \mathbb{R}\}. \tag{5.52}$$

For $\boldsymbol{R}^{-1} = (0, 0, \vartheta)$, by (5.19) we have

$$c^l_{mn} = \sum_{p=-l}^{l} c^l_{pn} D^l_{pm}(0, 0, \vartheta) = \sum_{p=-l}^{l} c^l_{pn} d^l_{pm}(0) e^{-im\vartheta} = c^l_{mn} e^{-im\vartheta} \qquad \text{for each } \vartheta \in \mathbb{R}. \tag{5.53}$$

Hence we conclude that $m = 0$ for each c^l_{mn}.

$\underline{G_{\mathrm{tex}} = D_\infty}$

We choose the sample orthonormal triad such that $\boldsymbol{e}_2 = \boldsymbol{m}$ and $\boldsymbol{e}_3 = \boldsymbol{n}$. Since $\boldsymbol{R}(\boldsymbol{e}_3, \vartheta) \in G_{\mathrm{tex}}$ for each ϑ, we know from the derivation above that $m = 0$ for each c^l_{mn}. We just need to determine the restriction imposed by the generator $\boldsymbol{R}(\boldsymbol{e}_2, \pi)$ in G_{tex}. In fact we have already obtained the required restriction in (5.27), i.e.,

$$c^l_{mn} = (-1)^{l-m} c^l_{\bar{m}n}. \tag{5.54}$$

Since $m = 0$ for each c^l_{mn}, we conclude from (5.54) that

$$c^l_{0n} = 0 \qquad \text{for odd } l \text{ and for each } n. \tag{5.55}$$

5.4.2 Orthorhombic Aggregates of Hexagonal Crystallites

The sampling point x of the given polycrystal has orthorhombic sample symmetry. We choose a right-handed orthonormal basis $\{\boldsymbol{e}_i : i = 1, 2, 3\}$ for the tangent space of the sample at x so that $G_{\text{tex}} = D_2 = \{\boldsymbol{I}, \boldsymbol{R}(\boldsymbol{e}_1, \pi), \boldsymbol{R}(\boldsymbol{e}_2, \pi), \boldsymbol{R}(\boldsymbol{e}_3, \pi)\}$. We select a reference ideal crystal $(\mathsf{C}, \boldsymbol{\kappa}_0)$ and a right-handed orthonormal triad $\{\check{\boldsymbol{e}}_i : i = 1, 2, 3\}$ for the definition of Euler angles for rotations of $(\mathsf{C}, \boldsymbol{\kappa}_0)$ such that $\check{\boldsymbol{e}}_i = \boldsymbol{e}_i$ for each i, and $G_{\text{cr}} = D_6$ is generated by $\boldsymbol{R}(\boldsymbol{e}_2, \pi)$ and $\boldsymbol{R}(\boldsymbol{e}_3, \pi/3)$. Then G_{tex} is clearly a subgroup of G_{cr}.

Since G_{tex} in Sect. 5.3.3 is the same as the G_{tex} here and $G_{\text{cr}} = D_2$ there is a subgroup of the $G_{\text{cr}} = D_6$ here, all the restrictions on texture coefficients that we derive for orthorhombic aggregates of orthorhombic crystallites remain valid here. We just need to add the restrictions imposed by $\boldsymbol{R}(\boldsymbol{e}_3, \pi/3) \in G_{\text{cr}}$, which are given by (5.48).

In summary, for orthorhombic aggregates of hexagonal crystallites, the independent texture coefficients (with $l \geq 1$) are:

$$c^l_{mn} \in \mathbb{R} \qquad \text{where } m \geq 0 \text{ are even and } n = 6k \text{ for some integer } k \geq 0, \text{ and } l \neq 1, 3, 5, \tag{5.56}$$

excluding all c^l_{m0} and c^l_{0n} with odd l, which are equal to zero. The non-trivial dependent texture coefficients are:

$$c^l_{\bar{m}n} = (-1)^l c^l_{mn}, \qquad c^l_{m\bar{n}} = (-1)^l c^l_{mn}, \qquad c^l_{\bar{m}\bar{n}} = c^l_{mn}, \tag{5.57}$$

where $m \geq 0$ are even and $n = 6k$ for some integer $k \geq 0$, and $l \neq 1, 3, 5$. Parallel statements in terms of the Roe coefficients can be easily obtained by changing each c^l_{mn} in assertions (5.56) and (5.57) to W_{lmn}.

5.4.3 Cubic Crystallite Symmetry

We choose an orthonormal basis $\{\check{\boldsymbol{e}}_i : i = 1, 2, 3\}$ attached to the reference ideal crystal $(\mathsf{C}, \boldsymbol{\kappa}_0)$ such that they agree with the three four-fold axes of cubic symmetry of $(\mathsf{C}, \boldsymbol{\kappa}_0)$. Under this choice, the group $G_{\text{cr}} = O$ of octahedral crystallite symmetry is generated by $\boldsymbol{R}(\check{\boldsymbol{e}}_2, \pi/2)$ and $\boldsymbol{R}(\check{\boldsymbol{e}}_3, \pi/2)$, and it contains as a subgroup the group $G_{\text{cr}} = D_4$ of tetragonal crystallite symmetry studied in Sect. 5.3.4. Hence the restriction

$$c^l_{mn} = \begin{cases} (-1)^l c^l_{m\bar{n}} & \text{for } n = 4k, k \in \mathbb{Z} \\ 0 & \text{for } n \neq 4k, k \in \mathbb{Z} \end{cases} \tag{5.58}$$

imposed by tetragonal crystallite symmetry remains valid in the present context. We just need to add new restrictions imposed by the generator $\boldsymbol{R}(\check{\boldsymbol{e}}_2, \pi/2)$, which are embodied in the equation

$$c^l_{mn} = \sum_{p=-l}^{l} c^l_{mp} D^l_{np}(0, \pi/2, 0) = \sum_{p=-l}^{l} c^l_{mp} d^l_{np}(\pi/2). \tag{5.59}$$

Note that in (5.59) both n and p are even. By (4.33) we have

$$d^l_{np}(\pi/2) = (-1)^l d^l_{n\bar{p}}(\pi/2) = (-1)^l d^l_{\bar{n}p}(\pi/2) \tag{5.60}$$

for even n and p. Combining (5.58) with $(5.60)_1$, we recast (5.59) as follows:[85]

$$\begin{pmatrix} d^l_{00}(\pi/2)-1 & 2d^l_{04}(\pi/2) & \dots & 2d^l_{0N}(\pi/2) \\ d^l_{40}(\pi/2) & 2d^l_{44}(\pi/2)-1 & \dots & 2d^l_{4N}(\pi/2) \\ & \dots & \dots & \\ & \dots & \dots & \\ d^l_{N0}(\pi/2) & 2d^l_{N4}(\pi/2) & \dots & 2d^l_{NN}(\pi/2)-1 \end{pmatrix} \begin{pmatrix} c^l_{m0} \\ c^l_{m4} \\ c^l_{m8} \\ \dots \\ c^l_{mN} \end{pmatrix} = \mathbf{0}; \tag{5.61}$$

here N is the largest positive integer that satisfies $N \le l$ and $N = 4k$ for some positive integer k. Equation (5.61) is valid for both even and odd l. For odd l, however, (5.60) dictates that

$$d^l_{np}(\pi/2) = -d^l_{n\bar{p}}(\pi/2), \qquad d^l_{np}(\pi/2) = -d^l_{\bar{n}p}(\pi/2), \tag{5.62}$$

which implies that

$$d^l_{n0}(\pi/2) = 0, \quad d^l_{0p}(\pi/2) = 0 \qquad \text{for odd } l \text{ and even } n, \text{ even } p. \tag{5.63}$$

Hence for odd l, the matrix in (5.61) reduces to the form

$$\begin{pmatrix} -1 & 0 & \dots & 0 \\ 0 & 2d^l_{44}(\pi/2)-1 & \dots & 2d^l_{4N}(\pi/2) \\ & \dots & \dots & \\ & \dots & \dots & \\ 0 & 2d^l_{N4}(\pi/2) & \dots & 2d^l_{NN}(\pi/2)-1 \end{pmatrix}, \tag{5.64}$$

and since $c^l_{0n} = 0$ for odd l by (5.58), it suffices to consider those texture coefficients c^l_{mn} in (5.61) with $m > 0$. Equation (5.61), of course, may be expressed in terms of Roe's Z_{lmn}'s and W_{lmn}'s. In that context, (5.61) was solved numerically by Roe [271] for even l up to $l = 22$ and by P.R. Morris [237] for odd l up to $l = 23$. Their findings are tabulated in their papers. Equation (5.61) can also be solved exactly by symbolic computation.

In Table 7, we list the *exact* relations imposed by (5.61) on c^l_{mn} for $1 \le l \le 15$, $-l \le m \le l$, and $n \ge 0$. The non-trivial c^l_{mn} with $n < 0$ can be determined from those in Table 7 through formula (5.58). The relations given in the table are obtained through a Maple program,[86] which delivers also the relations for higher l. With increasing l, however, the exact relations soon become too complicated and unwieldy for practical use.

5.4.4 Orthorhombic Aggregates of Cubic Crystallites

We choose an orthonormal basis $\{\boldsymbol{e}_i : i = 1, 2, 3\}$ at the sampling point X of the polycrystal such that they agree with the axes of orthorhombic texture symmetry, i.e., $G_{\text{tex}} = \{\boldsymbol{I}, \boldsymbol{R}(\boldsymbol{e}_1, \pi), \boldsymbol{R}(\boldsymbol{e}_2, \pi), \boldsymbol{R}(\boldsymbol{e}_3, \pi)\}$, and choose a reference ideal crystal $(\subset, \boldsymbol{\kappa}_0)$ for the cubic crystallites such that the three four-fold axes of cubic symmetry of G_{cr} are parallel to the unit vectors $\boldsymbol{e}_i$ $(i = 1, 2, 3)$. Under the given G_{tex} and G_{cr}, which includes $\boldsymbol{R}(\boldsymbol{e}_2, \pi)$ and

[85] Cf. Roe [271, Eq. (7)].

[86] Written by Mojia Huang.

Table 7 Relations imposed by (5.61) on the texture coefficients c^l_{mn} of aggregates of cubic crystallites with arbitrary sample anisotropy for $1 \le l \le 15$, $-l \le m \le l$, and $n \ge 0$. The linearly independent coefficients are selected so that they have the smallest possible n's. For those $1 \le l \le 15$ not given in the table, all c^l_{mn} are zero. Also, $c^l_{m0} = 0$ for odd l. The corresponding table for the Roe coefficients can be obtained by replacing each c^l_{mn} with W_{lmn}

l	Linearly indep. coeff.	Linearly depend. coeff.
4	c^4_{m0}	$c^4_{m4} = \frac{\sqrt{70}}{14} c^4_{m0}$
6	c^6_{m0}	$c^6_{m4} = \frac{-\sqrt{14}}{2} c^6_{m0}$
8	c^8_{m0}	$c^8_{m4} = \frac{\sqrt{154}}{33} c^8_{m0}$
		$c^8_{m8} = \frac{\sqrt{1430}}{66} c^8_{m0}$
9	c^9_{m4}	$c^9_{m8} = \frac{-\sqrt{119}}{17} c^9_{m4}$
10	c^{10}_{m0}	$c^{10}_{m4} = \frac{-\sqrt{4290}}{65} c^{10}_{m0}$
		$c^{10}_{m8} = \frac{-\sqrt{1430}\sqrt{17}}{130} c^{10}_{m0}$
12	c^{12}_{m0}	$c^{12}_{m8} = \frac{\sqrt{1938}}{646} (\sqrt{143}\, c^{12}_{m0} - 8\sqrt{7}\, c^{12}_{m4})$
	c^{12}_{m4}	$c^{12}_{m12} = \frac{\sqrt{323}\sqrt{23}}{7429} (4\sqrt{91}\, c^{12}_{m0} + 9\sqrt{11}\, c^{12}_{m4})$
13	c^{13}_{m4}	$c^{13}_{m8} = \frac{2\sqrt{190}}{95} c^{13}_{m4}$
		$c^{13}_{m12} = -\frac{\sqrt{253}\sqrt{19}}{95} c^{13}_{m4}$
14	c^{14}_{m0}	$c^{14}_{m4} = -\frac{3\sqrt{1309}\sqrt{65}}{1190} c^{14}_{m0}$
		$c^{14}_{m8} = -\frac{\sqrt{19}\sqrt{39}\sqrt{1190}}{1190} c^{14}_{m0}$
		$c^{14}_{m12} = -\frac{\sqrt{19}\sqrt{2737}}{238} c^{14}_{m0}$
15	c^{15}_{m4}	$c^{15}_{m8} = -\frac{2\sqrt{966}}{23} c^{15}_{m4}$
		$c^{15}_{m12} = \frac{\sqrt{1495}}{23} c^{15}_{m4}$

$\boldsymbol{R}(\boldsymbol{e}_3, \pi/2)$ as members, the combination of all restrictions on texture coefficients which we derive earlier for orthorhombic aggregates and for tetragonal crystallites remains in force here, i.e.,

(i) all c^l_{mn} are real;
(ii) $c^l_{mn} = 0$ unless m is even and $n = 4k$ for some integer k;
(iii) $c^l_{mn} = (-1)^l c^l_{\bar{m}n} = (-1)^l c^l_{m\bar{n}} = c^l_{\bar{m}\bar{n}}$.

In addition there are:

(iv) the restrictions imposed by (5.61).

The non-trivial texture coefficients ($l \ge 1$; $-l \le m \le l$, $-l \le n \le l$) are:

– $c^l_{mn} \in \mathbb{R}$ where m is even and $n = 4k$ for some $k \in \mathbb{Z}$, and $l \ne 1, 2, 3, 5, 7, 11$,

excluding all c^l_{m0} and c^l_{0n} with odd l, which are equal to zero. Among the non-trivial texture coefficients, we may select the independent ones as follows: For each l, $m \geq 0$, and $n \geq 0$ where there are non-trivial c^l_{mn}'s, determine from (5.61) linear relations between the non-trivial c^l_{mn}'s. Select the smallest subset of texture coefficients with the smallest n's in terms of which the linear relations from (5.61) will deliver the other non-trivial c^l_{mn}'s. Take the members of this smallest subset as the independent coefficients for the given l and $m \geq 0$, $n \geq 0$.

Once the independent coefficients with a given l, $m \geq 0$, and $n \geq 0$ are determined, the dependent coefficients with the same l and $m \geq 0$ are given by the linear relations from (5.61). The non-trivial $c^l_{\bar{m}n}$, $c^l_{m\bar{n}}$, and $c^l_{\bar{m}\bar{n}}$ are determined from c^l_{mn} through the equations given in requirement (iii).

Chapter 6

6 Orientation Space for Polycrystals with Crystallite Symmetry

6.1 Introduction

In Chap. 4 we have introduced an ODF $w : \mathrm{SO}(3) \to \mathbb{R}$ to describe the crystallographic texture at a sampling point $\mathtt{X}$ for a triclinic aggregate of triclinic crystallites, i.e., where $G_{\mathrm{cr}} = \{\boldsymbol{I}\}$ and $G_{\mathrm{tex}} = \{\boldsymbol{I}\}$.[87] In Chap. 5 we follow Roe, who in his two seminal papers [270, 271] shows that the presence of non-trivial sample and/or crystallite symmetries leads to restrictions that the texture coefficients must satisfy. There the main problem that Roe in effect studied is: inversion of X-ray pole figures to estimate the texture coefficients of even $l = 0, 2, 4, \ldots$ up to a certain $l_{\max}$ (say $l_{\max} = 22$). In Roe's treatment of the inverse problem, the ODF of a polycrystal is, irrespective of the absence or presence of any crystallite and/or sample symmetry, always defined on the rotation group. The effects of a non-trivial G_{cr} or G_{tex} are accounted for by the restrictions that the symmetries impose on the texture coefficients. For problems where such a treatment works, the Roe approach indicates a possible way to solve the problem for all crystallite and sample symmetries in one stroke.[88]

While the mathematical treatments of crystallite and sample symmetry in Chap. 5 are entirely analogous, these two types of symmetry arise for different reasons and play different roles in the physical theory. As pointed out by Roe [270, p. 2028], members of G_{tex} are "symmetry elements in the statistical distribution of crystallites" that "are introduced into the sample in its fabrication process regardless of the nature of crystallites. For example, in a uniaxially stretched sample there is cylindrical symmetry around the axis." Thus G_{tex} is the symmetry group of the macro-texture. In contrast, G_{cr} is none other than the crystallographic point group of the crystallites. Its elements are symmetry elements of crystal structure as manifested at the macro-scale. In fact, G_{cr} affects the definition of crystallite orientation for the polycrystal in question.

6.1.1 Introductory Remarks on Orientation Space

For a triclinic crystal, once a reference single crystal is chosen, the (relative) crystallite orientation at a sampling point $\mathtt{X}$ in a polycrystal is defined by a rotation $\boldsymbol{R}$ (see Sect. 3.1.1). For a Type I crystal with symmetry group

$$G_{\mathrm{cr}} = \{\boldsymbol{P}_1, \ldots, \boldsymbol{P}_{N_{\mathrm{cr}}}\} \subset \mathrm{SO}(3), \quad \text{where } \boldsymbol{P}_1 = \boldsymbol{I} \text{ and } N_{\mathrm{cr}} = |G_{\mathrm{cr}}|, \tag{6.1}$$

the reference single crystal remains unchanged under any rotation $\boldsymbol{P}_i \in G_{\mathrm{cr}}$. Hence, if $\boldsymbol{R}$ specifies the crystallite orientation at $\mathtt{X}$ with respect to the reference, so does $\boldsymbol{R}\boldsymbol{P}_i$ for all $\boldsymbol{P}_i \in G_{\mathrm{cr}}$. Thus the crystallite orientation at $\mathtt{X}$ is in fact defined by the set

$$\boldsymbol{R}G_{\mathrm{cr}} := \{\boldsymbol{R}\boldsymbol{P}_i : \boldsymbol{P}_i \in G_{\mathrm{cr}}\} \tag{6.2}$$

of equivalent rotations. In the mathematics literature, $\boldsymbol{R}G_{\mathrm{cr}}$ is called the left coset of $\boldsymbol{R}$ modulo G_{cr} (or the orbit of $\boldsymbol{R}$ in SO(3) under the right-action of G_{cr}). Note that no two

[87] Hencefoth we shall suppress the dependence on the sampling point $\mathtt{X}$ in $w(\cdot; \mathtt{X})$ except at places where we want to emphasize the dependence.

[88] Roe's papers [270, 271] on inversion of X-ray pole figures provide one example. See [202] for another.

left cosets intersect, and every rotation belongs to one of the cosets (see Sect. A.3.1 in Appendix A). The collection of all possible crystallite orientations is given by the set of left cosets, i.e., the quotient set

$$\mathrm{SO}(3)/G_{\mathrm{cr}} := \{\boldsymbol{R}G_{\mathrm{cr}} : \boldsymbol{R} \in \mathrm{SO}(3)\}. \tag{6.3}$$

As we shall see, $\mathrm{SO}(3)/G_{\mathrm{cr}}$ inherits natural mathematical structures from SO(3), with which it is called a quotient space. For us the elements of $\mathrm{SO}(3)/G_{\mathrm{cr}}$ are crystallite orientations; thus we will refer to it as the orientation space.

Let P be a polycrystal with $G_{\mathrm{cr}} \neq \{\boldsymbol{I}\}$. Clearly the orientation (probability) measure $\hat{\wp}$ of P and its corresponding orientation density function $\hat{w}$ should be defined on the orientation space. In Roe's papers, however, the quotient space $\mathrm{SO}(3)/G_{\mathrm{cr}}$ is never mentioned. Under the situation at hand, in the Roe approach the polycrystal P will have its orientation distribution function $w : \mathrm{SO}(3) \to \mathbb{R}$, but w satisfies the restriction

$$w(\boldsymbol{R}) = w(\boldsymbol{R}\boldsymbol{P}) \qquad \text{for each } \boldsymbol{R} \in \mathrm{SO}(3) \text{ and } \boldsymbol{P} \in G_{\mathrm{cr}}. \tag{6.4}$$

In this chapter we shall develop a formulation of texture analysis for polycrystals with non-trivial G_{cr} and/or G_{tex} by defining crystallite orientations as equivalence classes of rotations. We shall gain, through the perspective of this formulation, a deeper understanding of the Roe approach, i.e., the approach in which the ODF (albeit with texture coefficients observing restrictions imposed by crystallite and sample symmetries) is always defined on SO(3).

6.2 Polycrystals with Non-trivial Crystallite Symmetry

We start by giving an overview of the basic concepts and main findings, which serves as a reader's guide to the rest of this chapter and Appendices B and C, where most of the proofs are given. We restrict the overview to the case $G_{\mathrm{cr}} \neq \{\boldsymbol{I}\}$ without considering the effects of sample symmetry for simplicity, conceptual clarity, and the importance of this case (see Remark 6.1). On one hand doing so can be taken as restricting the discussion to the special case $G_{\mathrm{cr}} \neq \{\boldsymbol{I}\}$ and $G_{\mathrm{tex}} = \{\boldsymbol{I}\}$, in the context of which we shall discuss the Roe approach in Sect. 6.3. On the other hand, even if $G_{\mathrm{tex}} \neq \{\boldsymbol{I}\}$, the orientation space is still $\mathrm{SO}(3)/G_{\mathrm{cr}}$ and what we shall present in this section remains valid, although a treatment that includes the effects of sample symmetry (see Sect. 6.5) would usually be more preferable.

Remark 6.1 An important method for determination of texture in samples is by single-orientation measurements (see Chap. 8). Each measurement at a sampling point delivers a crystallite orientation in the orientation space $\mathrm{SO}(3)/G_{\mathrm{cr}}$. The measurements altogether result in a set of data points in $\mathrm{SO}(3)/G_{\mathrm{cr}}$, which correspond to the case $G_{\mathrm{tex}} = \{\boldsymbol{I}\}$ as they stand. The data points may be used as they are or be symmetrized with respect to a suitable G_{tex} if they suggest its presence or if there are other reasons for doing so (e.g., as suggested by the processing history of the sample, for modeling, etc.). □

Remark 6.2 Sample symmetry is a statistical symmetry, while crystallite symmetry is a manifestation at the macro scale of an intrinsic material symmetry at the micro scale. In practice the assumption that a sample has a $G_{\mathrm{tex}} \neq \{\boldsymbol{I}\}$ is an idealization, which helps simplify the problem in question when it is a good approximation. The group G_{tex} has no bearing on the definition of crystallite orientation. Ignoring the possibility that the sample may be taken as having a non-trivial texture symmetry and working solely with the orientation space

$\mathrm{SO}(3)/G_{\mathrm{cr}}$ (and not with $(\mathrm{SO}(3)/G_{\mathrm{cr}})/G_{\mathrm{tex}}$ as in Sect. 6.5) could complicate problems unnecessarily but does not abuse any logical or physical principle. If one adopts this standpoint, then $G_{\mathrm{tex}} = \{\boldsymbol{I}\}$ and $G_{\mathrm{cr}} \neq \{\boldsymbol{I}\}$ covers all cases other than $G_{\mathrm{cr}} = \{\boldsymbol{I}\}$. □

6.2.1 Fundamental Domains

As pointed out in Sect. 6.1.1, for a polycrystal $\mathcal{P}$ with $G_{\mathrm{cr}} \neq \{\boldsymbol{I}\}$, the quotient set $\mathrm{SO}(3)/G_{\mathrm{cr}}$ should be taken as the space of crystallite orientations.

Let $\pi : \mathrm{SO}(3) \to \mathrm{SO}(3)/G_{\mathrm{cr}}$ be the projection defined by

$$\pi(\boldsymbol{R}) = \boldsymbol{R}G_{\mathrm{cr}} \qquad \text{for each } \boldsymbol{R} \in \mathrm{SO}(3); \tag{6.5}$$

cf. (6.1)–(6.3). The function π is clearly surjective, and it is often called the natural surjection. We make $\mathrm{SO}(3)/G_{\mathrm{cr}}$ a topological space by giving it the quotient topology: i.e., $U \subset \mathrm{SO}(3)/G_{\mathrm{cr}}$ is said to be open if and only if $\pi^{-1}(U)$ is open in SO(3). With the quotient topology defined on $\mathrm{SO}(3)/G_{\mathrm{cr}}$, the projection π is continuous. Moreover, as $\mathrm{SO}(3)/G_{\mathrm{cr}}$ is a topological space, the family $\hat{\mathfrak{B}}$ of Borel sets in $\mathrm{SO}(3)/G_{\mathrm{cr}}$ is well defined.

Definition 6.3 A subset $\mathcal{F} \subset \mathrm{SO}(3)$ is said to be a strict fundamental domain[89] in SO(3) for $\mathrm{SO}(3)/G_{\mathrm{cr}}$ if

(i) the restriction $\pi|_{\mathcal{F}} : \mathcal{F} \to \mathrm{SO}(3)/G_{\mathrm{cr}}$ is bijective;
(ii) $\mathcal{F}$ is a Borel set in SO(3). □

The existence of strict fundamental domain for the orientation space $\mathrm{SO}(3)/G_{\mathrm{cr}}$ is proved in Appendix B. If $\mathcal{F}$ is a strict fundamental domain for $\mathrm{SO}(3)/G_{\mathrm{cr}}$, clearly so are its right translates $\mathcal{F}\boldsymbol{P}_j$ for $j = 2, \ldots, N_{\mathrm{cr}}$. Moreover, $\mathcal{F}\boldsymbol{P}_i$ and $\mathcal{F}\boldsymbol{P}_j$ are disjoint if $\boldsymbol{P}_i \neq \boldsymbol{P}_j$, and the rotation group is a disjoint union of the fundamental domains $\mathcal{F}\boldsymbol{P}_j$, i.e.,

$$\mathrm{SO}(3) = \bigcup_{j=1}^{N_{\mathrm{cr}}} \mathcal{F}\boldsymbol{P}_j. \tag{6.6}$$

For a subset $\hat{A} \subset \mathrm{SO}(3)/G_{\mathrm{cr}}$, by (6.6) we have

$$\pi^{-1}(\hat{A}) = \pi^{-1}(\hat{A}) \cap \bigcup_{j=1}^{N_{\mathrm{cr}}} \mathcal{F}\boldsymbol{P}_j = \bigcup_{j=1}^{N_{\mathrm{cr}}} \left(\pi^{-1}(\hat{A}) \cap \mathcal{F}\boldsymbol{P}_j\right), \tag{6.7}$$

i.e., $\pi^{-1}(\hat{A})$ is a disjoint union of N_{cr} subsets of SO(3), namely $A_j := \pi^{-1}(\hat{A}) \cap \mathcal{F}\boldsymbol{P}_j \subset \mathcal{F}\boldsymbol{P}_j$ for $j = 1, \ldots, N_{\mathrm{cr}}$. Note that for each $j = 1, \ldots, N_{\mathrm{cr}}$,

$$(\pi^{-1}(\hat{A}))\boldsymbol{P}_j = \pi^{-1}(\hat{A}) \qquad \text{and} \qquad (\pi^{-1}(\hat{A}) \cap \mathcal{F})\boldsymbol{P}_j = A_j. \tag{6.8}$$

Let $f \in L^2(\mathrm{SO}(3), \mathbb{C})$. By (6.6), we have

$$\int_{\mathrm{SO}(3)} f(\boldsymbol{R})d\mathcal{V}(\boldsymbol{R}) = \sum_{j=1}^{N_{\mathrm{cr}}} \int_{\mathcal{F}\boldsymbol{P}_j} f(\boldsymbol{R})d\mathcal{V}(\boldsymbol{R}). \tag{6.9}$$

[89] Here and in Definition 6.4 we specialize to SO(3) the definitions in [179, p. 96]; cf. [50, p. 101] for another definition. In texture analysis, instead of fundamental domain, many names have been used, some of which are: asymmetric domain [235], asymmetric unit of ODF [337, p. 601], elementary region [224], fundamental unit [324, p. 250], fundamental zone [3], etc.

Integral formula (6.9) remains valid if the strict fundamental domain $\mathcal{F}$ in these formulas is replaced by another measurable subset of SO(3) which differs from it by a set of measure zero in the bi-invariant volume $\mathcal{V}$. We call such sets fundamental domains for $\mathrm{SO}(3)/G_{\mathrm{cr}}$, for which we introduce the following definition.

Definition 6.4 A subset $\Omega \subset \mathrm{SO}(3)$ is a fundamental domain in SO(3) for $\mathrm{SO}(3)/G_{\mathrm{cr}}$ if Ω differs from a strict fundamental domain $\mathcal{F}$ in SO(3) for $\mathrm{SO}(3)/G_{\mathrm{cr}}$ by a set of measure zero in the measure space $(\mathrm{SO}(3), \mathfrak{B}, \mathcal{V})$. □

In practice it will be much easier to determine a fundamental domain than a strict fundamental domain for $\mathrm{SO}(3)/G_{\mathrm{cr}}$. See Sects. 6.6.1 and 6.6.2 for examples of fundamental domains.

6.2.2 Quotient Measure, Orientation Density Function, and Roe's ODF

Let P be a polycrystal of crystallites with $G_{\mathrm{cr}} \neq \{\boldsymbol{I}\}$ (cf. the first paragraph of Sect. 6.2 as regards G_{tex}), and let a reference single crystal be chosen. As pointed out in Sect. 6.1.1, the orientation space of the crystallites of the polycrystal should be $\mathrm{SO}(3)/G_{\mathrm{cr}}$. In parallel to what we did in Sect. 3.1.2 for the case $G_{\mathrm{cr}} = \{\boldsymbol{I}\}$, we assume that the crystallographic texture of P at a point x in P is defined by an orientation (probability) measure $\hat{\wp}(\cdot; \mathrm{x})$ on $\mathrm{SO}(3)/G_{\mathrm{cr}}$: For each Borel set $\hat{A} \subset \mathrm{SO}(3)/G_{\mathrm{cr}}$, $\hat{\wp}(\hat{A}; \mathrm{x})$ gives the probability of finding the crystallite orientation at x in $\hat{A}$. A polycrystal P is said to have a homogenous texture if its orientation measure $\hat{\wp}$ is independent of the sampling point x. For simplicity, even if the polycrystal P in question has an inhomogeneous texture, we shall suppress the dependence of $\hat{\wp}$ on x except at places where confusion might arise or we want to emphasize the dependence.

Before we can define an orientation probability density $\hat{w} : \mathrm{SO}(3)/G_{\mathrm{cr}} \to \mathbb{R}$ pertaining to $\hat{\wp}$, we have to settle on a volume measure $\hat{\mathcal{V}}$ on the orientation space $\mathrm{SO}(3)/G_{\mathrm{cr}}$. Let $\hat{\mathfrak{B}}$ be the family of Borel sets in $\mathrm{SO}(3)/G_{\mathrm{cr}}$. Consider a Borel set $\hat{A} \in \hat{\mathfrak{B}}$. After the polycrystal undergoes a rotation $\boldsymbol{Q}$, $\hat{A}$ becomes $\boldsymbol{Q}\hat{A}$. Any acceptable volume measure $\hat{\mathrm{v}}$ on $\mathrm{SO}(3)/G_{\mathrm{cr}}$ should satisfy the requirement

$$\hat{\mathrm{v}}(\boldsymbol{Q}\hat{A}) = \hat{\mathrm{v}}(\hat{A}) \qquad \text{for each } \boldsymbol{Q} \in \mathrm{SO}(3) \text{ and } \hat{A} \in \hat{\mathfrak{B}}. \tag{6.10}$$

A finite positive measure $\hat{\mathrm{v}}$ on $\mathrm{SO}(3)/G_{\mathrm{cr}}$ is said to be left SO(3)-invariant if it satisfies (6.10). It turns out that the left SO(3)-invariant measure on $\mathrm{SO}(3)/G_{\mathrm{cr}}$ is unique up to a multiplicative positive constant (see Proposition C.19 in Appendix C for a proof), and that the quotient measure $\hat{\mathcal{V}}$ on $\mathrm{SO}(3)/G_{\mathrm{cr}}$ defined by

$$\hat{\mathcal{V}}(\hat{A}) = \mathcal{V}\left(\pi^{-1}(\hat{A})\right) \qquad \text{for each Borel set } \hat{A} \in \hat{\mathfrak{B}} \tag{6.11}$$

is left SO(3)-invariant (see Sect. C.4 and Proposition C.18). Hence we may choose the quotient measure $\hat{\mathcal{V}}$ as the volume measure on the orientation space $\mathrm{SO}(3)/G_{\mathrm{cr}}$, which we will do.[90] We are now ready to define what we mean by the orientation density function and Roe's ODF on the orientation space and on SO(3), respectively.

[90] A left SO(3)-invariant volume measure $\hat{\mathrm{v}}$ can be distinguished from its peers by the value $\hat{\mathrm{v}}(\mathrm{SO}(3))/G_{\mathrm{cr}})$. By (6.11) we see that $\hat{\mathcal{V}}(\mathrm{SO}(3))/G_{\mathrm{cr}}) = \mathcal{V}(\mathrm{SO}(3)) = 8\pi^2$.

Definition 6.5 Let P be a polycrystal with orientation space $\mathrm{SO}(3)/G_{\mathrm{cr}}$ and texture defined by orientation measure $\hat{\wp}$. If $\hat{\wp}$ is absolutely continuous with respect to the quotient measure $\hat{\mathcal{V}}$ on $\mathrm{SO}(3)/G_{\mathrm{cr}}$, the Radon-Nikodym derivative of $\hat{\wp}$ with respect to $\hat{\mathcal{V}}$, namely

$$\hat{w}(\boldsymbol{R}G_{\mathrm{cr}}) := \frac{d\hat{\wp}}{d\hat{\mathcal{V}}}(\boldsymbol{R}G_{\mathrm{cr}}), \tag{6.12}$$

is called the orientation (probability) density function pertaining to $\hat{\wp}$. Roe's orientation distribution function (ODF) for polycrystal P is defined by

$$w := \hat{w} \circ \pi, \tag{6.13}$$

where $\pi : \mathrm{SO}(3) \to \mathrm{SO}(3)/G_{\mathrm{cr}}$ is the natural surjection. □

Let $G_{\mathrm{cr}} = \{\boldsymbol{P}_1, \ldots, \boldsymbol{P}_{N_{\mathrm{cr}}}\}$ (cf. (6.1)), where $\boldsymbol{P}_1 = \boldsymbol{I}$. It follows immediately from (6.13) that

$$w(\boldsymbol{R}) = (\hat{w} \circ \pi)(\boldsymbol{R}) = \hat{w}(\boldsymbol{R}G_{\mathrm{cr}}) \qquad \text{for each } \boldsymbol{R} \in \mathrm{SO}(3), \tag{6.14}$$

and that

$$w(\boldsymbol{R}\boldsymbol{P}_j) = \hat{w}(\boldsymbol{R}\boldsymbol{P}_j G_{\mathrm{cr}}) = \hat{w}(\boldsymbol{R}G_{\mathrm{cr}}) = w(\boldsymbol{R}) \qquad \text{for each } \boldsymbol{P}_j \in G_{\mathrm{cr}}, \tag{6.15}$$

which is none other than (6.4), the restriction that Roe put on the ODF w because of crystallite symmetry.

Since $\hat{\wp}$ is a probability density, definition (6.12) implies that the orientation density function $\hat{w} \geq 0$ and satisfies the normalization condition

$$\int_{\mathrm{SO}(3)/G_{\mathrm{cr}}} \hat{w}\, d\hat{\mathcal{V}} = 1. \tag{6.16}$$

Similarly, by (6.11) and (6.14) we observe that the orientation distribution function $w \geq 0$ and the normalization condition

$$\int_{\mathrm{SO}(3)} w\, d\mathcal{V} = 1. \tag{6.17}$$

Remark 6.6 We have shown that each orientation density function $\hat{w} : \mathrm{SO}(3)/G_{\mathrm{cr}} \to \mathbb{R}$ determines through (6.13) a unique ODF $w : \mathrm{SO}(3) \to \mathbb{R}$ that is non-negative and satisfies the restriction (6.15) and the normalization condition (6.17). Conversely, it is easy to verify that each given ODF w which is non-negative and satisfies (6.15) and the normalization condition (6.17) determines through (6.13) a unique orientation density function $\hat{w}$ defined on the quotient space $\mathrm{SO}(3)/G_{\mathrm{cr}}$ which is non-negative and satisfies (6.14) and the normalization condition (6.16). □

For each Borel set $\hat{A} \in \hat{\mathfrak{B}}$, $\pi^{-1}(\hat{A})$ is a Borel set in SO(3). Let $\mathcal{F} \subset \mathrm{SO}(3)$ be a chosen strict fundamental domain for $\mathrm{SO}(3)/G_{\mathrm{cr}}$. For a Borel set $\hat{A} \subset \mathrm{SO}(3)/G_{\mathrm{cr}}$, by (6.7), (6.8), and (6.11) we have

$$\hat{\mathcal{V}}(\hat{A}) = \mathcal{V}\left(\bigcup_{j=1}^{N_{\mathrm{cr}}} \left(\pi^{-1}(\hat{A}) \cap \mathcal{F}\boldsymbol{P}_j\right)\right) = N_{\mathrm{cr}}\mathcal{V}(A_1), \qquad \text{where } A_1 = \pi^{-1}(\hat{A}) \cap \mathcal{F}. \tag{6.18}$$

Given an orientation density function $\hat{w}$, the orientation measure $\hat{\wp}$ on $\mathrm{SO}(3)/G_{\mathrm{cr}}$ defined by $\hat{w}$ is given by

$$\begin{aligned}\hat{\wp}(\hat{A}) &= \int_{\hat{A}} \hat{w}(\boldsymbol{R}G_{\mathrm{cr}})\, d\hat{\mathcal{V}}(\boldsymbol{R}G_{\mathrm{cr}}) \\ &= \int_{\pi^{-1}(\hat{A})} w(\boldsymbol{R})\, d\mathcal{V}(\boldsymbol{R}), \qquad \text{for each Borel set } \hat{A} \subset \mathrm{SO}(3)/G_{\mathrm{cr}}, \end{aligned} \tag{6.19}$$

where $(6.19)_2$ follows from (6.14) and from the defining equation (6.11) of the quotient measure.

Also, by (6.4), (6.7), (6.8), $(6.19)_2$, and the right-invariance of the volume measure $\mathcal{V}$, we observe that

$$\hat{\wp}(\hat{A}) = \sum_{j=1}^{N_{\mathrm{cr}}} \int_{A_1 \boldsymbol{P}_j} w(\boldsymbol{R}) d\mathcal{V}(\boldsymbol{R}) = \sum_{j=1}^{N_{\mathrm{cr}}} \int_{A_1} w(\boldsymbol{R}\boldsymbol{P}_j) d\mathcal{V}(\boldsymbol{R}\boldsymbol{P}_j) = N_{\mathrm{cr}} \int_{A_1} w(\boldsymbol{R}) d\mathcal{V}(\boldsymbol{R}), \tag{6.20}$$

where $A_1 = \pi^{-1}(\hat{A}) \cap \mathcal{F}$.

6.2.3 Orientation Averaging and Texture Coefficients

The orientation average of a function $\hat{F} : \mathrm{SO}(3)/G_{\mathrm{cr}} \to \mathbb{R}$ with respect to the orientation measure $\hat{\wp}$ in (6.19) is given by

$$\int_{\mathrm{SO}(3)/G_{\mathrm{cr}}} \hat{F}(\boldsymbol{R}G_{\mathrm{cr}}) \hat{w}(\boldsymbol{R}G_{\mathrm{cr}})\, d\hat{\mathcal{V}}(\boldsymbol{R}G_{\mathrm{cr}}) = \int_{\mathrm{SO}(3)} F(\boldsymbol{R}) w(\boldsymbol{R}) d\mathcal{V}(\boldsymbol{R}), \tag{6.21}$$

where $F = \hat{F} \circ \pi$ satisfies restriction (6.4).

Conversely, let N_{cr} be the order of G_{cr} and $G_{\mathrm{cr}} = \{\boldsymbol{P}_1, \ldots, \boldsymbol{P}_{N_{\mathrm{cr}}}\}$. Given a function $F : \mathrm{SO}(3) \to \mathbb{R}$, by the right-invariance of the volume measure $\mathcal{V}$ and restriction (6.4), we obtain

$$\begin{aligned}\int_{\mathrm{SO}(3)} F(\boldsymbol{R}) w(\boldsymbol{R}) d\mathcal{V}(\boldsymbol{R}) &= \int_{\mathrm{SO}(3)} \frac{1}{N_{\mathrm{cr}}} \left(\sum_j F(\boldsymbol{R}\boldsymbol{P}_j) w(\boldsymbol{R}\boldsymbol{P}_j) \right) d\mathcal{V}(\boldsymbol{R}) \\ &= \int_{\mathrm{SO}(3)} \frac{1}{N_{\mathrm{cr}}} \left(\sum_j F(\boldsymbol{R}\boldsymbol{P}_j) \right) w(\boldsymbol{R}) d\mathcal{V}(\boldsymbol{R}) \\ &= \int_{\mathrm{SO}(3)} \mathfrak{F}(\boldsymbol{R}) w(\boldsymbol{R}) d\mathcal{V}(\boldsymbol{R}), \end{aligned} \tag{6.22}$$

where $\mathfrak{F}(\boldsymbol{R}) := (\sum_j F(\boldsymbol{R}\boldsymbol{P}_j))/N_{\mathrm{cr}}$, a function which obviously satisfies restriction (6.4). It follows from (6.21) that

$$\int_{\mathrm{SO}(3)} \mathfrak{F}(\boldsymbol{R}) w(\boldsymbol{R}) d\mathcal{V}(\boldsymbol{R}) = \int_{\mathrm{SO}(3)/G_{\mathrm{cr}}} \hat{\mathfrak{F}}(\boldsymbol{R}G_{\mathrm{cr}}) \hat{w}(\boldsymbol{R}G_{\mathrm{cr}})\, d\hat{\mathcal{V}}(\boldsymbol{R}G_{\mathrm{cr}}), \tag{6.23}$$

where $\mathfrak{F} = \hat{\mathfrak{F}} \circ \pi$. On the other hand, by (6.9) we have

$$\begin{aligned}\int_{\mathrm{SO}(3)} \mathfrak{F}(\boldsymbol{R}) w(\boldsymbol{R}) d\mathcal{V}(\boldsymbol{R}) &= \sum_{j=1}^{N_{\mathrm{cr}}} \int_{\mathcal{F}\boldsymbol{P}_j} \mathfrak{F}(\boldsymbol{R}) w(\boldsymbol{R}) d\mathcal{V}(\boldsymbol{R}) \\ &= \sum_{j=1}^{N_{\mathrm{cr}}} \int_{\mathcal{F}} \mathfrak{F}(\boldsymbol{R}\boldsymbol{P}_j) w(\boldsymbol{R}\boldsymbol{P}_j) d\mathcal{V}(\boldsymbol{R}\boldsymbol{P}_j) \\ &= N_{\mathrm{cr}} \int_{\mathcal{F}} \mathfrak{F}(\boldsymbol{R}) w(\boldsymbol{R}) d\mathcal{V}(\boldsymbol{R}), \end{aligned} \tag{6.24}$$

where we have appealed to the fact that $w(\boldsymbol{R}\boldsymbol{P}) = w(\boldsymbol{R})$ and $\mathfrak{F}(\boldsymbol{R}\boldsymbol{P}) = \mathfrak{F}(\boldsymbol{R})$ for each $\boldsymbol{P} \in G_{\mathrm{cr}}$ as well as the right-invariance of the volume measure $\mathcal{V}$. By combining (6.23) and (6.24) we obtain the formula

$$\int_{\mathrm{SO}(3)/G_{\mathrm{cr}}} \hat{\mathfrak{F}}(\boldsymbol{R}G_{\mathrm{cr}}) \hat{w}(\boldsymbol{R}G_{\mathrm{cr}})\, d\hat{\mathcal{V}}(\boldsymbol{R}G_{\mathrm{cr}}) = N_{\mathrm{cr}} \int_{\mathcal{F}} \mathfrak{F}(\boldsymbol{R}) w(\boldsymbol{R}) d\mathcal{V}(\boldsymbol{R}). \tag{6.25}$$

Consider the case where the function F is complex-valued. Then we have $F = \mathfrak{Re}F + i\,\mathfrak{Im}F : \mathrm{SO}(3) \to \mathbb{C}$ (see Sect. 3.6), where $\mathfrak{Re}F$ and $\mathfrak{Im}F$ are the real and imaginary parts of F, respectively. Note that $\mathfrak{F}$ is linear in F, and that each integral in (6.21)–(6.25) is linear in F, $\hat{F}$, $\mathfrak{F}$, or $\hat{\mathfrak{F}}$. Since each equation in (6.21)–(6.25) is valid for the real and imaginary parts of F, $\hat{F}$, $\mathfrak{F}$, and $\hat{\mathfrak{F}}$, respectively, they remain valid for complex-valued F, $\hat{F}$, $\mathfrak{F}$, and $\hat{\mathfrak{F}}$ by linearity.

In his treatment of polycrystals with non-trivial crystallite symmetry, Roe [270, 271] never mentions the orientation density function $\hat{w}$ and, in effect, makes use of the function $w = \hat{w} \circ \pi : \mathrm{SO}(3) \to \mathbb{R}$ as the ODF instead. All functions $w \in L^2(\mathrm{SO}(3), \mathbb{C})$ can be expanded as an infinite series of the form (see (4.45))

$$w(\boldsymbol{R}(\psi, \theta, \phi)) = \sum_{l=0}^{\infty} \sum_{m=-l}^{l} \sum_{n=-l}^{l} c^l_{mn} D^l_{mn}(\boldsymbol{R}(\psi, \theta, \phi)). \tag{6.26}$$

By the orthogonality relation (4.21) of the Wigner D-functions, the expansion coefficients are given by

$$c^l_{mn} = \frac{2l+1}{8\pi^2} \int_{\mathrm{SO}(3)} \overline{D^l_{mn}(\boldsymbol{R})} w(\boldsymbol{R})\, d\mathcal{V}(\boldsymbol{R}), \tag{6.27}$$

which correspond through (4.118) to the texture coefficients W_{lmn} that Roe assigns to all polycrystals irrespective of the presence or absence of texture and/or crystallite symmetry.

Let $\mathfrak{F}^l_{mn}(\boldsymbol{R}) := (\sum_j D^l_{mn}(\boldsymbol{R}\boldsymbol{P}_j))/N_{\mathrm{cr}}$. In the presence of crystallite symmetry, since Roe's ODF w satisfies restriction (6.4), by (6.21)–(6.24) we obtain from (6.27)

$$\begin{aligned} c^l_{mn} &= \frac{2l+1}{8\pi^2} \int_{\mathrm{SO}(3)} \overline{\mathfrak{F}^l_{mn}(\boldsymbol{R})} w(\boldsymbol{R})\, d\mathcal{V}(\boldsymbol{R}) \\ &= \frac{2l+1}{8\pi^2} \int_{\mathrm{SO}(3)/G_{\mathrm{cr}}} \overline{\hat{\mathfrak{F}}^l_{mn}(\boldsymbol{R}G_{\mathrm{cr}})} \hat{w}(\boldsymbol{R}G_{\mathrm{cr}})\, d\hat{\mathcal{V}}(\boldsymbol{R}G_{\mathrm{cr}}) \end{aligned}$$

$$= \frac{2l+1}{8\pi^2} \cdot N_{\mathrm{cr}} \int_{\mathcal{F}} \overline{\mathfrak{F}^l_{mn}(\boldsymbol{R})} w(\boldsymbol{R})\, d\mathcal{V}(\boldsymbol{R}), \tag{6.28}$$

where $\mathfrak{F}^l_{mn} = \hat{\mathfrak{F}}^l_{mn} \circ \pi$. Equation $(6.28)_2$ shows that formula (6.27), where $\hat{w}$ does not appear explicitly, delivers in the presence of crystallite symmetry texture coefficients c^l_{mn} which depend only on quantities defined on $\mathrm{SO}(3)/G_{\mathrm{cr}}$. By $(6.28)_3$, to evaluate the texture coefficients c^l_{mn}, it suffices to compute the appropriate integral over the chosen strict fundamental domain $\mathcal{F}$. In fact, as mentioned in the paragraph that immediately follows (6.9), we may replace the strict fundamental domain $\mathcal{F}$ in $(6.28)_3$ by a fundamental domain Ω that differs from $\mathcal{F}$ by a set of measure zero in the bi-invariant volume $\mathcal{V}$.

6.3 The Roe Approach

For a polycrystal P of crystallites with $G_{\mathrm{cr}} \neq \{\boldsymbol{I}\}$ and $G_{\mathrm{tex}} = \{\boldsymbol{I}\}$, it is natural to characterize its crystallographic texture by an orientation density function $\hat{w} : \mathrm{SO}(3)/G_{\mathrm{cr}} \to \mathbb{R}$, where $\mathrm{SO}(3)/G_{\mathrm{cr}}$ is the space of crystallite orientations, and $\hat{w}$ as a probability density is non-negative and satisfies the normalization condition

$$\int_{\mathrm{SO}(3)/G_{\mathrm{cr}}} \hat{w}(\boldsymbol{R}G_{\mathrm{cr}}) d\hat{\mathcal{V}}(\boldsymbol{R}G_{\mathrm{cr}}) = 1. \tag{6.29}$$

In the Roe approach, however, we work instead with

$$w := \hat{w} \circ \pi : \mathrm{SO}(3) \to \mathbb{R}, \qquad \text{where } \pi : \mathrm{SO}(3) \to \mathrm{SO}(3)/G_{\mathrm{cr}} \text{ is the natural surjection.} \tag{6.30}$$

It follows immediately from the definition of w in (6.30) that w is non-negative, satisfies the constraint (6.4), and observes the normalization condition $\int_{\mathrm{SO}(3)} w(\boldsymbol{R}) d\mathcal{V}(\boldsymbol{R}) = 1$. In fact, through (6.30) the two functions $\hat{w}$ and w determine each other uniquely.

In what sense can $\hat{w}$ be replaced by w as a descriptor of crystallographic texture that pertains to polycrystal P with $G_{\mathrm{cr}} \neq \{\boldsymbol{I}\}$? To start with, there exists in $\mathrm{SO}(3)$ a strict fundamental domain $\mathcal{F}$ such that $\pi|_{\mathcal{F}} : \mathcal{F} \to \mathrm{SO}(3)/G_{\mathrm{cr}}$ is a bijection. Thus each crystallite orientation of P is represented by a rotation in $\mathcal{F}$. Let $\hat{\wp}$ be an orientation measure on the space of crystallite orientations $\mathrm{SO}(3)/G_{\mathrm{cr}}$ defined by $\hat{\wp}(\hat{A}) = \int_{\hat{A}} \hat{w} d\hat{V}$ for each Borel set $\hat{A} \subset \mathrm{SO}(3)/G_{\mathrm{cr}}$. In terms of w, by (6.19) and (6.20) we have

$$\int_{\hat{A}} \hat{w}\, d\hat{V} = N_{\mathrm{cr}} \int_{(\pi|_{\mathcal{F}})^{-1}(\hat{A})} w\, d\mathcal{V} \qquad \text{for each Borel set } \hat{A} \subset \mathrm{SO}(3)/G_{\mathrm{cr}}. \tag{6.31}$$

For a function $\hat{F} : \mathrm{SO}(3)/G_{\mathrm{cr}} \to \mathbb{C}$, $F := \hat{F} \circ \pi$ satisfies restriction (6.4). By (6.21) and (6.24), the orientation average with respect to the orientation measure $\hat{\wp}$ in (6.31) is given by

$$\int_{\mathrm{SO}(3)/G_{\mathrm{cr}}} \hat{F}(\boldsymbol{R}G_{\mathrm{cr}}) \hat{w}(\boldsymbol{R}G_{\mathrm{cr}})\, d\hat{\mathcal{V}}(\boldsymbol{R}G_{\mathrm{cr}}) = N_{\mathrm{cr}} \int_{\mathcal{F}} F(\boldsymbol{R}) w(\boldsymbol{R}) d\mathcal{V}(\boldsymbol{R})$$

$$= \int_{\mathrm{SO}(3)} F(\boldsymbol{R}) w(\boldsymbol{R}) d\mathcal{V}(\boldsymbol{R}), \tag{6.32}$$

where we have appealed to the fact that F can be taken as $\mathfrak{F}$ in (6.24) because F satisfies restriction (6.4). Hence in texture analysis of polycrystals with non-trivial crystallite symmetry, we can choose a strict fundamental domain $\mathcal{F}$ in SO(3), use $\mathcal{F}$ and w in place of $\mathrm{SO}(3)/G_{\mathrm{cr}}$ and $\hat{w}$, respectively, and work with the right-hand side of (6.31) and $(6.32)_1$ instead of their counterparts on the left-hand side, respectively.

The crux of the Roe approach, however, is to use, as far as possible, w defined on the entire rotation group SO(3), series expansion (6.26), and formula (6.27) for texture coefficients, i.e., the same formulas that apply to all cases of crystallite and sample symmetries. For instance, in orientation averaging use $(6.32)_2$ instead of $(6.32)_1$. In using $(6.32)_2$ the domain of integration is fixed; if a computer program has been written for triclinic aggregates of triclinic crystallites, for other crystallite or sample symmetries, we just need to include the appropriate restrictions on texture coefficients. In contrast, every pair of $(G_{\mathrm{cr}}, G_{\mathrm{tex}})$ has its own fundamental domain $\mathcal{F}$ in the appropriate form of $(6.32)_1$.

On the other hand, while $\hat{w}$ is a genuine orientation density function on the orientation space $\mathrm{SO}(3)/G_{\mathrm{cr}}$, Roe's ODF $w := \hat{w} \circ \pi$ isn't an orientation probability density defined on SO(3). For instance, let P be a polycrystal with non-trivial crystallite symmetry, and let E be a Borel set in SO(3) such that $E \neq \pi^{-1}(\hat{A})$ for any Borel set $\hat{A}$ in $\mathrm{SO}(3)/G_{\mathrm{cr}}$. Then the integral $\int_E w(\boldsymbol{R})\, d\mathcal{V}(\boldsymbol{R})$ makes no physical sense. Roe's ODF w can be used to compute probabilities as follows. Let $\mathcal{F}$ be a strict fundamental domain in SO(3) for $\mathrm{SO}(3)/G_{\mathrm{cr}}$. Then each rotation in $\mathcal{F}$ represents a crystallite orientation. If E is a Borel set in $\mathcal{F}$, the probability of finding the crystallite orientation in E at a sampling point of a sample of P is $N_{\mathrm{cr}} \int_E w(\boldsymbol{R})\, d\mathcal{V}(\boldsymbol{R})$.

Remark 6.7 In the 1960s Bunge [56, 57] and Roe [270] independently proposed what is now commonly called the harmonic method for determination of crystallographic texture by inversion of X-ray pole figures. In what follows we describe the different approaches in effect adopted by Roe and by Bunge, respectively, albeit the descriptions are restricted to the present context (i.e., $G_{\mathrm{tex}} = \{\boldsymbol{I}\}$, $G_{\mathrm{cr}} \neq \{\boldsymbol{I}\}$) and are reworded in the convention and notation of this exposition. In the Roe approach, texture analysis is based on the ODF $w = \hat{w} \circ \pi$ defined on SO(3), which satisfies the constraints (6.4) imposed by crystallite symmetry. Under the harmonic method, the ODF w is expanded in the infinite series displayed in (6.26). In practice, the infinite series (6.26) is truncated after some selected suitable $l = l_{\max}$. The texture coefficients c^l_{mn} of w from $l = 1$ to $l = l_{\max}$ are to be estimated from measurement data (e.g., X-ray pole figures). In the Bunge approach, texture analysis is in effect based on the ODF $\hat{w}$ defined on $\mathrm{SO}(3)/G_{\mathrm{cr}}$. The ODF $\hat{w}$ is expanded in an orthogonal series of functions defined on $\mathrm{SO}(3)/G_{\mathrm{cr}}$ (see Sect. 6.8). Again, the texture coefficients $c^{\mu\nu}$ of the truncated expansion of $\hat{w}$ from $l = 1$ to $l = l_{\max}$ are to be estimated from measurement data.

In principle the Roe approach and the Bunge approach are equivalent. In execution, however, there is one big difference. In the Roe approach the ODFs for all crystallite symmetries are in the same space $L^2(\mathrm{SO}(3), \mathbb{C})$, and the basis functions D^l_{mn} work for all crystallite symmetries. Moreover, as far as the texture coefficients are concerned, for instance those of an ODF that pertains to a polycrystal with $G_{\mathrm{cr}} = O$ can be looked upon as a special case of their counterparts that pertain to one with $G_{\mathrm{cr}} = \{\boldsymbol{I}\}$ which happen to observe the required restrictions (6.4). In some problems, it may be possible to obtain solutions for all crystallite symmetries by solving the triclinic case and getting solutions for each case of non-trivial crystallite symmetry by imposing appropriate restrictions on the texture coefficients. In the Bunge approach the spaces $L^2(\mathrm{SO}(3)/G_{\mathrm{cr}}, \mathbb{C})$ that contain the ODF $\hat{w}$ are different for different G_{cr}. The possible convenience described above for the Roe approach will be impossible for the Bunge approach.

In this exposition we follow the Roe approach but will illustrate the Bunge approach by one concrete example in Sect. 6.8. □

6.4 Disorientation Angle as Distance Function on Orientations

In Sect. 1.10, the misorientation angle of two rotations defines a distance function $d_{\mathrm{SO}(3)}$ on SO(3). In this section we show that the angle of disorientation[91] of two orientations defines a distance function on the orientation space $\mathrm{SO}(3)/G_{\mathrm{cr}}$.

Let $G_{\mathrm{cr}} = \{\boldsymbol{P}_1, \ldots, \boldsymbol{P}_{N_{\mathrm{cr}}}\}$. For brevity, in what follows we shall sometimes write M for $\mathrm{SO}(3)/G_{\mathrm{cr}}$, particularly when it is used as a subscript. Given two orientations $\boldsymbol{R}_1 G_{\mathrm{cr}}$ and $\boldsymbol{R}_2 G_{\mathrm{cr}}$ in $\mathrm{SO}(3)/G_{\mathrm{cr}}$, their disorientation angle is given by[92]

$$\widetilde{\omega}_d := \min\{d_{\mathrm{SO}(3)}(\boldsymbol{R}_1 \boldsymbol{P}_i, \boldsymbol{R}_2 \boldsymbol{P}_j) : \boldsymbol{P}_i, \boldsymbol{P}_j \in G_{\mathrm{cr}}\}. \tag{6.33}$$

By (1.142), we can simplify (6.33) a little as follows:

$$\begin{aligned} \widetilde{\omega}_d &= \min\{d_{\mathrm{SO}(3)}(\boldsymbol{R}_1, \boldsymbol{R}_2 \boldsymbol{P}_j \boldsymbol{P}_i^T) : \boldsymbol{P}_i, \boldsymbol{P}_j \in G_{\mathrm{cr}}\} \\ &= \min_{\boldsymbol{P} \in G_{\mathrm{cr}}} d_{\mathrm{SO}(3)}(\boldsymbol{R}_1, \boldsymbol{R}_2 \boldsymbol{P}). \end{aligned} \tag{6.34}$$

Let $d_M : \mathrm{SO}(3)/G_{\mathrm{cr}} \times \mathrm{SO}(3)/G_{\mathrm{cr}} \to \mathbb{R}$ be defined by

$$d_M(\boldsymbol{R}_1 G_{\mathrm{cr}}, \boldsymbol{R}_2 G_{\mathrm{cr}}) = \min_{\boldsymbol{P} \in G_{\mathrm{cr}}} d_{\mathrm{SO}(3)}(\boldsymbol{R}_1, \boldsymbol{R}_2 \boldsymbol{P}), \tag{6.35}$$

where the right-hand side is none other than the disorientation angle of the two orientations in question.

We claim that d_M is a distance function on the orientation space $\mathrm{SO}(3)/G_{\mathrm{cr}}$. By definition of the disorientation angle 6.33 and the properties of $d_{\mathrm{SO}(3)}$, d_M clearly satisfies conditions (a) and (b) of Definition 1.18 for a distance function. It remains to show that d_M observes the triangle inequality, i.e., for any $\boldsymbol{R}_1$, $\boldsymbol{R}_2$ and $\boldsymbol{R}_3$ in SO(3),

$$d_M(\boldsymbol{R}_1 G_{\mathrm{cr}}, \boldsymbol{R}_2 G_{\mathrm{cr}}) + d_M(\boldsymbol{R}_2 G_{\mathrm{cr}}, \boldsymbol{R}_3 G_{\mathrm{cr}}) \geq d_M(\boldsymbol{R}_1 G_{\mathrm{cr}}, \boldsymbol{R}_3 G_{\mathrm{cr}}). \tag{6.36}$$

To prove (6.36), note that by (6.34) we have

$$d_M(\boldsymbol{R}_1 G_{\mathrm{cr}}, \boldsymbol{R}_2 G_{\mathrm{cr}}) = d_{\mathrm{SO}(3)}(\boldsymbol{R}_1, \boldsymbol{R}_2 \boldsymbol{P}_a) \qquad \text{for some } \boldsymbol{P}_a \in G_{\mathrm{cr}}. \tag{6.37}$$

Similarly, by (6.34) and (1.142) we obtain

$$\begin{aligned} d_M(\boldsymbol{R}_2 G_{\mathrm{cr}}, \boldsymbol{R}_3 G_{\mathrm{cr}}) &= d_{\mathrm{SO}(3)}(\boldsymbol{R}_2, \boldsymbol{R}_3 \boldsymbol{P}_b) \qquad \text{for some } \boldsymbol{P}_b \in G_{\mathrm{cr}} \\ &= d_{\mathrm{SO}(3)}(\boldsymbol{R}_2 \boldsymbol{P}_a, \boldsymbol{R}_3 \boldsymbol{P}_b \boldsymbol{P}_a) \\ &= d_{\mathrm{SO}(3)}(\boldsymbol{R}_2 \boldsymbol{P}_a, \boldsymbol{R}_3 \boldsymbol{P}_c), \qquad \text{where } \boldsymbol{P}_c = \boldsymbol{P}_b \boldsymbol{P}_a \in \mathrm{SO}(3). \end{aligned} \tag{6.38}$$

[91] The term "angle of disorientation" was introduced by MacKenzie and Thomson [197] in a paper on geometrical probability to mean "the least angle of rotation required to rotate a crystal into the same orientation as a neighboring crystal" (see also [196]). By now it has been used widely in the literature of texture analysis (see, e.g., [86, 104, 333]). Some authors (see, e.g., [235]), however, elect to use the word "misorientation" in the sense of disorientation here.

[92] Recall that $d_{\mathrm{SO}(3)}(\boldsymbol{R}_1 \boldsymbol{P}_i, \boldsymbol{R}_2 \boldsymbol{P}_j)$ is the misorientation angle of the two rotations $\boldsymbol{R}_1 \boldsymbol{P}_i$ and $\boldsymbol{R}_2 \boldsymbol{P}_j$.

Combining (6.37) and $(6.38)_3$, we conclude that

$$\begin{aligned} d_M(\boldsymbol{R}_1 G_{\text{cr}}, \boldsymbol{R}_2 G_{\text{cr}}) + d_M(\boldsymbol{R}_2 G_{\text{cr}}, \boldsymbol{R}_3 G_{\text{cr}}) &= d_{\text{SO(3)}}(\boldsymbol{R}_1, \boldsymbol{R}_2 \boldsymbol{P}_a) + d_{\text{SO(3)}}(\boldsymbol{R}_2 \boldsymbol{P}_a, \boldsymbol{R}_3 \boldsymbol{P}_c), \\ &\geq d_{\text{SO(3)}}(\boldsymbol{R}_1, \boldsymbol{R}_3 \boldsymbol{P}_c) \\ &\geq \min_{\boldsymbol{P} \in G_{\text{cr}}} d_{\text{SO(3)}}(\boldsymbol{R}_1, \boldsymbol{R}_3 \boldsymbol{P}) \\ &= d_M(\boldsymbol{R}_1 G_{\text{cr}}, \boldsymbol{R}_3 G_{\text{cr}}). \end{aligned} \tag{6.39}$$

In Sect. 10.4 we shall see that the orientation space $\text{SO(3)}/G_{\text{cr}}$ is a Riemannian manifold with d_M as its Riemannian distance function.

6.5 Polycrystals with Non-trivial Sample Symmetry

6.5.1 Sample Symmetry Revisited

For a polycrystal P with non-trivial crystallite symmetry, we see in Sect. 6.1.1 that the crystallite orientation at a point $\mathtt{x}$ in P is characterized by a set of equivalent rotations $\boldsymbol{R}\boldsymbol{P}_i$ ($\boldsymbol{P}_i \in G_{\text{cr}}$), each of which brings the reference single crystal to the crystallite orientation at $\mathtt{x}$. The crystallite orientation at $\mathtt{x}$ is then denoted by $\boldsymbol{R}G_{\text{cr}}$, and the set of all possible orientations as $\boldsymbol{R}$ runs over SO(3) is the orientation space $\text{SO(3)}/G_{\text{cr}}$.

Suppose the polycrystal P also has non-trivial sample symmetry defined by G_{tex}. Henceforth in this chapter we assume that $G_{\text{tex}} = \{\boldsymbol{Q}_1, \ldots, \boldsymbol{Q}_{N_{\text{tex}}}\}$ is a finite rotation group, except when we introduce the term "isotropic texture" or "random texture". Since $w(\boldsymbol{R}) = \hat{w}(\boldsymbol{R}G_{\text{cr}})$ for each $\boldsymbol{R} \in \text{SO(3)}$, the definition of G_{tex} in (5.16) can be recast as

$$G_{\text{tex}} = \{\boldsymbol{Q} \in \text{SO(3)} : \hat{w}(\boldsymbol{Q}^T \boldsymbol{R} G_{\text{cr}}) = \hat{w}(\boldsymbol{R}G_{\text{cr}}) \text{ for each } \boldsymbol{R}G_{\text{cr}} \in \text{SO(3)}/G_{\text{cr}}\}, \tag{6.40}$$

For brevity in further discussions, let $M := \text{SO(3)}/G_{\text{cr}}$ be the orientation space with the quotient topology (see Sect. 6.2.1). Equation (6.40) indicates that the orientations $\boldsymbol{Q}^T \boldsymbol{R} G_{\text{cr}}$ ($\boldsymbol{Q} \in G_{\text{tex}}$) are equivalent as far as the orientation density function $\hat{w}$ is concerned. In analogy to the definition of the orientation space M, we introduce the G_{tex} equivalence classes of orientations

$$[\boldsymbol{R}G_{\text{cr}}] = \{\boldsymbol{Q}^T \boldsymbol{R} G_{\text{cr}} : \boldsymbol{Q} \in G_{\text{tex}}\} = \{\boldsymbol{Q}_1^T \boldsymbol{R} G_{\text{cr}}, \ldots, \boldsymbol{Q}_{N_{\text{tex}}}^T \boldsymbol{R} G_{\text{cr}}\} \tag{6.41}$$

and the space of such equivalence classes

$$M/G_{\text{tex}} = \{[\boldsymbol{R}G_{\text{cr}}] : \boldsymbol{R}G_{\text{cr}} \in M\} \tag{6.42}$$

with the quotient topology.

Remark 6.8 An alternate view of M/G_{tex} is as follows. Let $\mathcal{T} : G_{\text{tex}} \times M \to M$ be the mapping defined by

$$\mathcal{T}(\boldsymbol{Q}, \boldsymbol{R}G_{\text{cr}}) = \boldsymbol{Q}\boldsymbol{R}G_{\text{cr}}. \tag{6.43}$$

In Sect. B.2 of Appendix B, it is shown that $\mathcal{T}$ is a continuous left action of the group G_{tex} on the orientation space M and that for each $\boldsymbol{Q} \in G_{\text{tex}}$ the map $\mathcal{T}_{\boldsymbol{Q}} : M \to M$ defined by $\mathcal{T}_{\boldsymbol{Q}}(\boldsymbol{R}G_{\text{cr}}) := \boldsymbol{Q}\boldsymbol{R}G_{\text{cr}}$ is a homeomorphism on M. The G_{tex}-orbit of orientation $\boldsymbol{R}G_{\text{cr}} \in M$, namely $\{\boldsymbol{Q}\boldsymbol{R}G_{\text{cr}} : \boldsymbol{Q} \in G_{\text{tex}}\}$ is none other than $[\boldsymbol{R}G_{\text{cr}}]$ and the space of G_{tex}-orbits in the orientation space M is the quotient space M/G_{tex}. □

Definition 6.9 Let P be a polycrystal with its $G_{\text{tex}} \neq \{\boldsymbol{I}\}$ being a finite rotation group. Let $M := \text{SO}(3)/G_{\text{cr}}$ be its orientation space. For each $\boldsymbol{R} \in \text{SO}(3)$, the equivalence class $[\boldsymbol{R}G_{\text{cr}}]$ as defined by (6.41) is called the G_{tex}-orbit of $\boldsymbol{R}$ in M. The quotient space M/G_{tex} as defined by (6.42) is called the space of G_{tex}-orbits in M. □

Remark 6.10 The mathematics behind the equivalence classes $\boldsymbol{R}G_{\text{cr}}$ and the space $\text{SO}(3)/G_{\text{cr}}$ on one hand and that of $[\boldsymbol{R}G_{\text{cr}}]$ and M/G_{tex} on the other are similar (cf. Sect. B.2). But there is a basic difference in the physics. The concepts of crystallite orientation and orientation space are central to quantitative texture analysis, while those of G_{tex}-orbits in M and the space of such orbits are important and useful but less fundamental. Cf. Remarks 6.1 and 6.2. □

Let $\hat{\pi} : M \to M/G_{\text{tex}}$, $\boldsymbol{R}G_{\text{cr}} \mapsto [\boldsymbol{R}G_{\text{cr}}]$ be the natural surjection, and let $\widetilde{w} : M/G_{\text{tex}} \to \mathbb{R}$ be the unique function defined by $\hat{w} = \widetilde{w} \circ \hat{\pi}$. The three ODFs w, $\hat{w}$, and $\tilde{w}$ are related as follows:

$$w = \hat{w} \circ \pi, \qquad \hat{w} = \widetilde{w} \circ \hat{\pi}, \qquad w = \widetilde{w} \circ \widetilde{\pi}, \tag{6.44}$$

where $\widetilde{\pi} = \hat{\pi} \circ \pi : \text{SO}(3) \to (\text{SO}(3)/G_{\text{cr}})/G_{\text{tex}}$, and

$$w(\boldsymbol{R}) = \hat{w}(\boldsymbol{R}G_{\text{cr}}) = \widetilde{w}([\boldsymbol{R}G_{\text{cr}}]), \qquad \text{for each } \boldsymbol{R} \in \text{SO}(3). \tag{6.45}$$

Note that for each $\boldsymbol{Q} \in G_{\text{tex}}$, $\boldsymbol{P} \in G_{\text{cr}}$, and $\boldsymbol{R} \in \text{SO}(3)$, we have

$$w(\boldsymbol{Q}^T\boldsymbol{R}\boldsymbol{P}) = \hat{w}(\boldsymbol{Q}^T\boldsymbol{R}\boldsymbol{P}G_{\text{cr}}) = \hat{w}(\boldsymbol{Q}^T\boldsymbol{R}G_{\text{cr}}) = \hat{w}(\boldsymbol{R}G_{\text{cr}}) = w(\boldsymbol{R}), \tag{6.46}$$

where we have appealed to (6.40) at the third step.

Example 6.11 Let $\boldsymbol{e}_i$ $(i = 1, 2, 3)$ be a right-handed orthonormal triad. Consider a monoclinic aggregate P of orthorhombic crystallites with

$$G_{\text{tex}} = C_2 = \{\boldsymbol{I}, \boldsymbol{R}(\boldsymbol{e}_3, \pi)\}, \qquad G_{\text{cr}} = D_2 = \{\boldsymbol{I}, \boldsymbol{R}(\boldsymbol{e}_1, \pi), \boldsymbol{R}(\boldsymbol{e}_2, \pi), \boldsymbol{R}(\boldsymbol{e}_3, \pi)\}.$$

Suppose P has a homogeneous texture $\widetilde{p} = \delta_{[\boldsymbol{R}_o D_2]}$ on M/G_{tex}, where $\boldsymbol{R}_o$ is a rotation with respect to the triad $\{\boldsymbol{e}_i\}$ and $M = \text{SO}(3)/G_{\text{cr}}$. Note that

$$[\boldsymbol{R}_o D_2] = \{\boldsymbol{R}_o D_2, \boldsymbol{R}(\boldsymbol{e}_3, \pi)\boldsymbol{R}_o D_2\}.$$

In single-orientation measurements, each measurement at a sampling point $\mathtt{x}$ of P will deliver one orientation, which is either $\boldsymbol{R}_o D_2$ or $\boldsymbol{R}(\boldsymbol{e}_3, \pi)\boldsymbol{R}_o D_2$, and the probability of getting either one is $1/2$. For the elements of G_{tex}, let

$$\boldsymbol{Q}_1 = \boldsymbol{I}, \qquad \boldsymbol{Q}_2 = \boldsymbol{R}(\boldsymbol{e}_3, \pi).$$

For the elements of G_{cr}, let

$$\boldsymbol{P}_1 = \boldsymbol{I}, \qquad \boldsymbol{P}_j = \boldsymbol{R}(\boldsymbol{e}_{j-1}, \pi), \quad (j = 2, 3, 4).$$

On the orientation space M, the orientation (probability) measure of the crystallographic texture in question is:

$$\hat{\wp} = \frac{1}{2}\left(\delta_{\boldsymbol{R}_o D_2} + \delta_{\boldsymbol{Q}_2\boldsymbol{R}_o D_2}\right).$$

As represented on SO(3), the orientation measure in question is given by

$$\wp = \frac{1}{8}\sum_{i=1}^{2}\sum_{j=1}^{4}\delta_{\boldsymbol{Q}_i \boldsymbol{R}_o \boldsymbol{P}_j}.$$

Note that crystallite symmetry is intrinsic. Every single orientation measurement gives one orientation, e.g., $\boldsymbol{R}_o D_2$, not one of the equivalent rotations in the equivalence class $\boldsymbol{R}_o D_2 = \{\boldsymbol{R}_o, \boldsymbol{R}_o \boldsymbol{P}_2, \boldsymbol{R}_o \boldsymbol{P}_3, \boldsymbol{R}_o \boldsymbol{P}_4\}$. In contrast, texture symmetry is statistical and is often imperfect in practice. The ODF with the requisite sample symmetry is usually obtained either by symmetrization of raw data before inversion to get the ODF or by symmetrization of the raw ODF after inversion. □

Before we close this section, we define what we mean by the term "isotropic texture" or "random texture".

Definition 6.12 A polycrystal P is said to have an isotropic texture at a sampling point $\mathtt{X}$ if its $G_{\mathrm{tex}} = \mathrm{SO}(3)$ at $\mathtt{X}$. □

For a polycrystal with its $G_{\mathrm{tex}} = \mathrm{SO}(3)$, we write its orientation density function $\hat{w}$ as $\hat{w}_{\mathrm{iso}}$. Let $\boldsymbol{R}G_{\mathrm{cr}}$ and $\boldsymbol{P}G_{\mathrm{cr}}$ be two arbitrary crystallite orientations in $\mathrm{SO}(3)/G_{\mathrm{cr}}$. By definition of w_{iso} and (6.40), we have

$$\hat{w}_{\mathrm{iso}}(\boldsymbol{P}G_{\mathrm{cr}}) = \hat{w}_{\mathrm{iso}}((\boldsymbol{P}\boldsymbol{R}^T)^T \boldsymbol{P}G_{\mathrm{cr}}) = \hat{w}_{\mathrm{iso}}(\boldsymbol{R}G_{\mathrm{cr}}). \tag{6.47}$$

Hence $\hat{w}_{\mathrm{iso}}$ is a constant function on the orientation space $\mathrm{SO}(3)/G_{\mathrm{cr}}$. By the normalization condition $\int_{\mathrm{SO}(3)/G_{\mathrm{cr}}} \hat{w}\, d\hat{\mathcal{V}} = 1$, we see that

$$\hat{w}_{\mathrm{iso}} = \frac{1}{\hat{\mathcal{V}}(\mathrm{SO}(3)/G_{\mathrm{cr}})} = \frac{1}{\mathcal{V}(\mathrm{SO}(3))} = \frac{1}{8\pi^2}. \tag{6.48}$$

In the Roe approach, since $w_{\mathrm{iso}} = \hat{w}_{\mathrm{iso}} \circ \pi$, it follows from (6.48) that $w_{\mathrm{iso}} = 1/(8\pi^2)$.

6.5.2 Fundamental Domains

To examine fundamental domains for polycrystals with $G_{\mathrm{tex}} \neq \{\boldsymbol{I}\}$, we start by extending our discussions in Sect. 6.2.1. Henceforth until the end of this chapter, we assume that G_{tex} is a finite rotation group and G_{cr} a Type I crystallographic point group.

Let $\pi : \mathrm{SO}(3) \to \mathrm{SO}(3)/G_{\mathrm{cr}}$, $\boldsymbol{R} \mapsto \boldsymbol{R}G_{\mathrm{cr}}$. For brevity let $M := \mathrm{SO}(3)/G_{\mathrm{cr}}$ be the orientation space and M/G_{tex} the space of G_{tex}-orbits in M; see Sect. 6.5.1. Let $\hat{\pi} : M \to M/G_{\mathrm{tex}}$, $\boldsymbol{R}G_{\mathrm{cr}} \mapsto [\boldsymbol{R}G_{\mathrm{cr}}]$, where $[\boldsymbol{R}G_{\mathrm{cr}}]$ denotes the G_{tex}-orbit of $\boldsymbol{R}G_{\mathrm{cr}}$ (see (6.41)). In Sect. B.3 of Appendix B, it is shown that there exist strict fundamental domains $\mathcal{F} \subset \mathrm{SO}(3)$ for M and $\hat{\mathcal{F}} \subset M$ for M/G_{tex} such that $\mathcal{F}$ and $\hat{\mathcal{F}}$ are Borel sets in SO(3) and in M, respectively, and the maps $\pi|_{\mathcal{F}} : \mathcal{F} \to M$ and $\hat{\pi}|_{\hat{\mathcal{F}}} : \hat{\mathcal{F}} \to M/G_{\mathrm{tex}}$ are bijective.

Let $\widetilde{\mathcal{F}} = (\pi|_{\mathcal{F}})^{-1}(\hat{\mathcal{F}})$. As $\pi|_{\mathcal{F}} : \mathcal{F} \to M$ is a bijection and $\hat{\mathcal{F}} \subset M$, we see that $\widetilde{\mathcal{F}} = \pi^{-1}(\hat{\mathcal{F}}) \cap \mathcal{F}$, where $\mathcal{F}$ is a Borel set in SO(3). Since $\hat{\mathcal{F}}$ is a Borel set in M and π is a continuous surjection, it follows from Proposition C.16 (i) of Appendix C that $\pi^{-1}(\hat{\mathcal{F}})$ is a Borel set in SO(3). Hence $\widetilde{\mathcal{F}}$ is a Borel set in SO(3).

Let $\widetilde{\pi} = \hat{\pi} \circ \pi$. As the maps $\pi : \mathrm{SO}(3) \to M$ and $\hat{\pi} : M \to M/G_{\mathrm{tex}}$ are continuous, open, and surjective, so is the mapping $\widetilde{\pi} : \mathrm{SO}(3) \to M/G_{\mathrm{tex}}$, $\boldsymbol{R} \mapsto [\boldsymbol{R}G_{\mathrm{cr}}]$. Moreover, since

$\widetilde{\mathcal{F}} \subset \mathcal{F}$, $\pi|_{\widetilde{\mathcal{F}}}$ is injective, and $\pi|_{\widetilde{\mathcal{F}}}(\widetilde{\mathcal{F}}) = \hat{\mathcal{F}}$, the mapping $\widetilde{\pi}|_{\widetilde{\mathcal{F}}} = \hat{\pi} \circ \pi|_{\widetilde{\mathcal{F}}} : \widetilde{\mathcal{F}} \to M/G_{\text{tex}}$ is bijective.

Comparing the properties of $\widetilde{\mathcal{F}}$ and those of $\mathcal{F}$ in Definition 6.3, we introduce the following definition.

Definition 6.13 A subset $\widetilde{\mathcal{F}} \subset \mathrm{SO}(3)$ is said to be a strict fundamental domain in SO(3) for M/G_{tex} if

(i) the restriction $\pi|_{\widetilde{\mathcal{F}}} : \widetilde{\mathcal{F}} \to M/G_{\text{tex}}$ is bijective;
(ii) $\widetilde{\mathcal{F}}$ is a Borel set in SO(3). □

Since $\mathcal{F}$ is a strict fundamental domain in SO(3) for the orientation space M and $\hat{\mathcal{F}}$ is a strict fundamental domain in M for the space of G_{tex}-orbits, we observe (cf. (6.6)) that SO(3) and M can be expressed as the following disjoint unions, respectively:

$$\mathrm{SO}(3) = \bigcup_{j=1}^{N_{\text{cr}}} \mathcal{F}\boldsymbol{P}_j, \qquad M = \bigcup_{i=1}^{N_{\text{tex}}} \boldsymbol{Q}_i^T \hat{\mathcal{F}}, \tag{6.49}$$

where we have put[93] $\boldsymbol{Q}_i^T = \boldsymbol{Q}_i^{-1}$ for $\boldsymbol{Q}_i$ in $(6.49)_2$ for later convenience. On the other hand, we have

$$\mathcal{F} = (\pi|_{\mathcal{F}})^{-1}(M) = \bigcup_{i=1}^{N_{\text{tex}}} \boldsymbol{Q}_i^T (\pi|_{\mathcal{F}})^{-1}(\hat{\mathcal{F}}) = \bigcup_{i=1}^{N_{\text{tex}}} \boldsymbol{Q}_i^T \widetilde{\mathcal{F}}. \tag{6.50}$$

Substituting $(6.50)_3$ into $(6.49)_1$, we obtain the following decomposition of SO(3) as a disjoint union of translates of a chosen strict fundamental domain $\widetilde{\mathcal{F}}$:

$$\mathrm{SO}(3) = \bigcup_{i=1}^{N_{\text{tex}}} \bigcup_{j=1}^{N_{\text{cr}}} \boldsymbol{Q}_i^T \widetilde{\mathcal{F}} \boldsymbol{P}_j. \tag{6.51}$$

Definition 6.14 A subset $\Omega \subset \mathrm{SO}(3)$ is a fundamental domain in SO(3) for M/G_{tex} if Ω differs from a strict fundamental domain $\widetilde{\mathcal{F}}$ in SO(3) for M/G_{tex} by a set of measure zero in the measure space $(\mathrm{SO}(3), \mathfrak{B}, \mathcal{V})$. □

Remark 6.15 As mentioned earlier, in applications it will often suffice to use a fundamental domain in place of a strict fundamental domain (cf. Definitions 6.13 and 6.14). To determine a fundamental domain in practice, we may seek a measurable $\Omega \subset \mathrm{SO}(3)$ such that

(a) for each $(\boldsymbol{Q}_i, \boldsymbol{P}_j) \neq (\boldsymbol{I}, \boldsymbol{I})$, where $\boldsymbol{Q}_i \in G_{\text{tex}}$ and $\boldsymbol{P}_j \in G_{\text{cr}}$, $\Omega \cap \boldsymbol{Q}_i \Omega \boldsymbol{P}_j$ is a set of $\mathcal{V}$-measure zero in SO(3);[94]
(b) there holds

$$\bigcup_{i=1}^{N_{\text{tex}}} \bigcup_{j=1}^{N_{\text{cr}}} \boldsymbol{Q}_i^T \Omega \boldsymbol{P}_j = \mathrm{SO}(3) \setminus Z, \tag{6.52}$$

where Z is a set of $\mathcal{V}$-measure zero in SO(3).

[93] Doing so does not change the disjoint union in $(6.49)_2$. As the rotations $\boldsymbol{Q}_i$ run over G_{tex} there, so do $\boldsymbol{Q}_i^{-1}$.

[94] Note that the empty set $\emptyset$ is a set of $\mathcal{V}$-measure zero in SO(3).

It is straightforward to show that such a set Ω can differ from a strict fundamental domain only by a set of $\mathcal{V}$-measure zero. Indeed, since $\boldsymbol{R} \in \boldsymbol{Q}_{i_1}^T \Omega \boldsymbol{P}_{j_1} \cap \boldsymbol{Q}_{i_2}^T \Omega \boldsymbol{P}_{j_2}$ if and only if $\boldsymbol{Q}_{i_1} \boldsymbol{R} \boldsymbol{P}_{j_1}^T \in \Omega \cap \boldsymbol{Q}_{i_1} \boldsymbol{Q}_{i_2}^T \Omega \boldsymbol{P}_{j_2} \boldsymbol{P}_{j_1}^T$, condition (a) implies that after a suitable set of $\mathcal{V}$-measure zero, say E, is deleted from Ω, the sets $\boldsymbol{Q}_i^T (\Omega \setminus E) \boldsymbol{P}_j$ $(i = 1, \ldots, N_{\text{tex}}; j = 1, \ldots, N_{\text{cr}})$ are disjoint. Condition (b) guarantees that the disjoint union $\bigcup_{i=1}^{N_{\text{tex}}} \bigcup_{j=1}^{N_{\text{cr}}} \boldsymbol{Q}_i^T (\Omega \setminus E) \boldsymbol{P}_j$ can differ from SO(3) only by a set of $\mathcal{V}$-measure zero. Thus Ω can differ from a strict fundamental domain only by a set of $\mathcal{V}$-measure zero. □

6.5.3 Quotient Measure and Texture Coefficients

Physically crystallite symmetry is intrinsic and texture symmetry is statistical. Mathematically, however, their effects on the ODF mirror each other (cf. Chap. 5). Moreover, we can often account for their effects together.

In the presence of non-trivial texture symmetry, we may still work with the orientation space $M := \text{SO}(3)/G_{\text{cr}}$ and use orientation density functions $\hat{w}$ that satisfy $\hat{w}(\boldsymbol{Q}^T \boldsymbol{R} G_{\text{cr}}) = \hat{w}(\boldsymbol{R} G_{\text{cr}})$ for $\boldsymbol{Q} \in G_{\text{tex}}$ (see (6.40)). Alternatively, we may work with the quotient space M/G_{tex}, which we call the space of G_{tex}-orbits of orientations. As shown in Appendix C, the quotient measure on M/G_{tex} can be similarly defined in parallel to its counterpart on $\text{SO}(3)/G_{\text{cr}}$, i.e.,

$$\widetilde{\mathcal{V}}(\widetilde{A}) = \hat{\mathcal{V}}(\hat{\pi}^{-1}(\widetilde{A})) \qquad \text{for each Borel set } \widetilde{A} \subset M/G_{\text{tex}}, \tag{6.53}$$

where $\hat{\pi} : M \to M/G_{\text{tex}}$ is the natural surjection. Because of this, and because of (6.51) and the existence of a strict fundamental domain for M/G_{tex} in SO(3), all formulas derived in Sects. 6.2.2 and 6.2.3 where the quotient space in question is $\text{SO}(3)/G_{\text{cr}}$, after obvious modifications, will be valid for the present context. Likewise, after replacing $\text{SO}(3)/G_{\text{cr}}$ by M/G_{tex} in Section (6.3), everything said about the Roe approach there after obvious modifications applies to the case where $G_{\text{tex}} \neq \{\boldsymbol{I}\}$.

Remark 6.16 Each single-orientation measurement at a point x of a sample of polycrystal P yields an orientation, say, $\boldsymbol{R} G_{\text{cr}}$. However, if P has non-trivial sample symmetry, the measurement result can be interpreted as the equivalence class or G_{tex}-orbit $[\boldsymbol{R} G_{\text{cr}}]$. Let $\widetilde{A}$ be a Borel set in M/G_{tex}. The probability of finding $[\boldsymbol{R} G_{\text{cr}}]$ in $\widetilde{A}$ is

$$\widetilde{\wp}(\widetilde{A}) = \int\limits_{\hat{\pi}^{-1}(\widetilde{A})} \hat{w}\, d\hat{\mathcal{V}} = \int\limits_{\widetilde{A}} \widetilde{w}\, d\widetilde{\mathcal{V}}. \tag{6.54}$$

It can be seen that $\widetilde{w}$ is a probability density function on M/G_{tex}. As we follow the Roe approach, we will not pursue the properties of $\widetilde{w}$ further. □

As illustration, let us give a couple of examples. For a function $\widetilde{F} : M/G_{\text{tex}} \to \mathbb{C}$ and $F := \hat{F} \circ \pi$, which satisfies restriction (6.46), in parallel to (6.32) we have

$$\int\limits_{M/G_{\text{tex}}} \widetilde{F}([\boldsymbol{R} G_{\text{cr}}]) \widetilde{w}([\boldsymbol{R} G_{\text{cr}}])\, d\widetilde{\mathcal{V}}([\boldsymbol{R} G_{\text{cr}}]) = N_{\text{tex}} \cdot N_{\text{cr}} \int\limits_{\widetilde{\mathcal{F}}} F(\boldsymbol{R}) w(\boldsymbol{R}) d\mathcal{V}(\boldsymbol{R}), \tag{6.55}$$

where $[\boldsymbol{R} G_{\text{cr}}]$ is a generic element in the space M/G_{tex} of G_{tex}-orbits of orientations and $\widetilde{\mathcal{F}}$ is a chosen strict fundamental domain for M/G_{tex} in SO(3).

For $F : \mathrm{SO}(3) \to \mathbb{C}$, its symmetrized version

$$\mathfrak{F}(\boldsymbol{R}) = \frac{1}{N_{\mathrm{tex}} N_{\mathrm{cr}}} \left(\sum_{i=1}^{N_{\mathrm{tex}}} \sum_{j=1}^{N_{\mathrm{cr}}} F(\boldsymbol{Q}_i^T \boldsymbol{R} \boldsymbol{P}_j) \right),$$

and an ODF $w(\cdot)$ that satisfies the constraint $w(\boldsymbol{Q}^T \boldsymbol{R} \boldsymbol{P}) = w(\boldsymbol{R})$ for each $\boldsymbol{Q} \in G_{\mathrm{tex}}$ and $\boldsymbol{P} \in G_{\mathrm{cr}}$, we have

$$\begin{aligned}
&\int_{\mathrm{SO}(3)} F(\boldsymbol{R}) w(\boldsymbol{R}) d\mathcal{V}(\boldsymbol{R}) \\
&= \int_{\mathrm{SO}(3)} \mathfrak{F}(\boldsymbol{R}) w(\boldsymbol{R}) d\mathcal{V}(\boldsymbol{R}) = \sum_{i=1}^{N_{\mathrm{tex}}} \sum_{j=1}^{N_{\mathrm{cr}}} \int_{\boldsymbol{Q}_i^T \widetilde{\mathcal{F}} \boldsymbol{P}_j} \mathfrak{F}(\boldsymbol{R}) w(\boldsymbol{R}) d\mathcal{V}(\boldsymbol{R}) \\
&= \sum_{i=1}^{N_{\mathrm{tex}}} \sum_{j=1}^{N_{\mathrm{cr}}} \int_{\widetilde{\mathcal{F}}} \mathfrak{F}(\boldsymbol{Q}_i^T \widetilde{\boldsymbol{R}} \boldsymbol{P}_j) w(\boldsymbol{Q}_i^T \widetilde{\boldsymbol{R}} \boldsymbol{P}_j) d\mathcal{V}(\boldsymbol{Q}_i^T \widetilde{\boldsymbol{R}} \boldsymbol{P}_j), \qquad \text{where } \widetilde{\boldsymbol{R}} = \boldsymbol{Q}_i \boldsymbol{R} \boldsymbol{P}_j^T \in \widetilde{\mathcal{F}} \\
&= N_{\mathrm{tex}} \cdot N_{\mathrm{cr}} \int_{\widetilde{\mathcal{F}}} \mathfrak{F}(\boldsymbol{R}) w(\boldsymbol{R}) d\mathcal{V}(\boldsymbol{R}),
\end{aligned} \tag{6.56}$$

where $\widetilde{\mathcal{F}}$ is the chosen strict fundamental domain, and we have appealed to the bi-invariance of the volume measure $\mathcal{V}$, the fact that $\mathfrak{F}(\boldsymbol{Q}^T \boldsymbol{R} \boldsymbol{P}) = \mathfrak{F}(\boldsymbol{R})$ for each $\boldsymbol{Q} \in G_{\mathrm{tex}}$ and $\boldsymbol{P} \in G_{\mathrm{cr}}$, and a change of dummy variable from $\widetilde{\boldsymbol{R}}$ to $\boldsymbol{R}$ at the last step.

Appying (6.56) to formulas (6.27) for c_{mn}^l, where $F(\boldsymbol{R})$ is $\overline{D_{mn}^l(\boldsymbol{R})}$, we have

$$c_{mn}^l = \frac{2l+1}{8\pi^2} \cdot N_{\mathrm{tex}} \cdot N_{\mathrm{cr}} \int_{\widetilde{\mathcal{F}}} \overline{\mathfrak{F}_{mn}^l(\boldsymbol{R})} w(\boldsymbol{R}) \, d\mathcal{V}(\boldsymbol{R}), \tag{6.57}$$

where $\mathfrak{F}_{mn}^l(\boldsymbol{R}) = \left(\sum_{i=1}^{N_{\mathrm{tex}}} \sum_{j=1}^{N_{\mathrm{cr}}} D_{mn}^l(\boldsymbol{Q}_i^T \boldsymbol{R} \boldsymbol{P}_j) \right) / (N_{\mathrm{tex}} N_{\mathrm{cr}})$. Hence, to evaluate the texture coefficients c_{mn}^l, it suffices to compute the appropriate integral over the chosen strict fundamental domain $\widetilde{\mathcal{F}}$. In fact, it is obvious that the strict fundamental domain $\widetilde{\mathcal{F}}$ in formula (6.57) can be replaced by any fundamental domain $\Omega \subset G$ (cf. Definition 6.4) which differs from $\widetilde{\mathcal{F}}$ by a set of zero bi-invariant volume $\mathcal{V}$.

6.6 Examples of Explicit Fundamental Domains

In this section we will follow the guidelines given in Remark 6.52 to construct, for various G_{cr} and G_{tex}, explicit fundamental domains for $\mathrm{SO}(3)/G_{\mathrm{cr}}$ or $(\mathrm{SO}(3)/G_{\mathrm{cr}})/G_{\mathrm{tex}}$ in SO(3). Henceforth we will say that two subsets A_1 and A_2 of SO(3) are essentially disjoint if $A \cap B$ is a set of $\mathcal{V}$-measure zero in SO(3). Condition (a) in Remark 6.52 can then be paraphrased as the requirement that the sets $\boldsymbol{Q}_i^T \Omega \boldsymbol{P}_j$ $(i = 1, \ldots, N_{\mathrm{tex}}; j = 1, \ldots, N_{\mathrm{cr}})$ are pairwise essentially disjoint.

6.6.1 Triclinic Aggregates of Crystallites with a Dihedral-Group Symmetry

Consider the cases where G_{cr} is the dihedral group D_k ($k = 2, 3, 4$ or 6), which has $\boldsymbol{R}(\boldsymbol{e}_3, 2\pi/k)$ and $\boldsymbol{R}(\boldsymbol{e}_2, \pi)$ as generators. Since $D_k = \{\boldsymbol{P}_1, \ldots, \boldsymbol{P}_{2k}\}$ has order $2k$, once a

fundamental domain Ω for $\mathrm{SO}(3)/G_{\mathrm{cr}}$ is chosen, the set of rotations SO(3) is, up to a set of $\mathcal{V}$-measure zero, the union of $2k$ regions $\Omega \boldsymbol{P}_j$ ($j = 1, \ldots, 2k$), which are pairwise essentially disjoint (see Remark 6.15).

The following lemma will be instrumental to our discussion below.

Lemma 6.17 $\boldsymbol{R}(\boldsymbol{e}_3, \psi)\boldsymbol{R}(\boldsymbol{e}_2, \theta)\boldsymbol{R}(\boldsymbol{e}_3, \phi)\boldsymbol{R}(\boldsymbol{e}_2, \pi) = \boldsymbol{R}(\pi + \psi, \pi - \theta, \pi - \phi)$.

Proof The proof below appeals to (1.81), (1.93), and the identity $\boldsymbol{R}(\boldsymbol{e}_3, \phi)\boldsymbol{R}(\boldsymbol{e}_2, \pi) = \boldsymbol{R}(\boldsymbol{e}_2, \pi)\boldsymbol{R}(\boldsymbol{e}_3, -\phi)$, which follows easily from (1.81) and Euler's theorem (1.82). Indeed we have

$$\begin{aligned}
\boldsymbol{R}(\boldsymbol{e}_3, \psi)\boldsymbol{R}(\boldsymbol{e}_2, \theta)\boldsymbol{R}(\boldsymbol{e}_3, \phi)\boldsymbol{R}(\boldsymbol{e}_2, \pi) &= \boldsymbol{R}(\boldsymbol{e}_3, \psi)\boldsymbol{R}(\boldsymbol{e}_2, \theta)\boldsymbol{R}(\boldsymbol{e}_2, \pi)\boldsymbol{R}(\boldsymbol{e}_3, -\phi) \\
&= \boldsymbol{R}(\boldsymbol{e}_3, \psi)\boldsymbol{R}(\boldsymbol{e}_2, \theta - \pi)\boldsymbol{R}(\boldsymbol{e}_3, -\phi) \\
&= \boldsymbol{R}(\boldsymbol{e}_3, \psi)\boldsymbol{R}(-\boldsymbol{e}_2, \pi - \theta)\boldsymbol{R}(\boldsymbol{e}_3, -\phi) \\
&= \boldsymbol{R}(\boldsymbol{e}_3, \psi)\boldsymbol{R}(\boldsymbol{e}_3, \pi)\boldsymbol{R}(\boldsymbol{e}_2, \pi - \theta)\boldsymbol{R}(\boldsymbol{e}_3, \pi)\boldsymbol{R}(\boldsymbol{e}_3, -\phi) \\
&= \boldsymbol{R}(\pi + \psi, \pi - \theta, \pi - \phi), \qquad (6.58)
\end{aligned}$$

where we have also used the fact that $\boldsymbol{R}(\boldsymbol{e}_2, \pi) = \boldsymbol{R}(\boldsymbol{e}_2, -\pi) = (\boldsymbol{R}(\boldsymbol{e}_2, \pi))^{-1}$. □

The procedure to arrive at a fundamental domain for $\mathrm{SO}(3)/G_{\mathrm{cr}}$ is essentially the same for all cases of $G_{\mathrm{cr}} = D_k$ ($k = 2, 3, 4$ or 6). For a generic rotation $\boldsymbol{R}(\psi_0, \theta_0, \phi_0)$ in an as yet undetermined fundamental domain Ω, determine the location of $\boldsymbol{R}(\psi_0, \theta_0, \phi_0)\boldsymbol{P}$ for each $\boldsymbol{P} \in G_{\mathrm{cr}}$. From the locations of the $2k$ rotations in Euler space, make a guess on a possible fundamental domain. Use the criteria given in Remark 6.15 to check whether the guess is acceptable. If it isn't, make adjustments and check again.

Remark 6.18 Here we want to write SO(3) as an essentially-disjoint union of sets of the form $\Omega \boldsymbol{P}_j$, where $\boldsymbol{P}_j \in G_{\mathrm{cr}}$. Hence we examine

$$\boldsymbol{R}(\psi_0, \theta_0, \phi_0)\boldsymbol{P} = \boldsymbol{R}(\boldsymbol{e}_3, \psi_0)\boldsymbol{R}(\boldsymbol{e}_2, \theta_0)\boldsymbol{R}(\boldsymbol{e}_3, \phi_0)\boldsymbol{P} \qquad \text{for } \boldsymbol{P} \in G_{\mathrm{cr}}. \qquad (6.59)$$

When we consider the effects of texture symmetry, we shall consider $\boldsymbol{Q}^T\boldsymbol{R}(\psi_0, \theta_0, \phi_0)$ (or equivalently $\boldsymbol{Q}\boldsymbol{R}(\psi_0, \theta_0, \phi_0)$) for $\boldsymbol{Q} \in G_{\mathrm{tex}}$. □

To illustrate the procedure, let us examine in detail the simplest case, i.e., triclinic aggregates of orthorhombic crystallites, where

$$G_{\mathrm{cr}} = D_2 = \{\boldsymbol{I}, \boldsymbol{R}(\boldsymbol{e}_1, \pi), \boldsymbol{R}(\boldsymbol{e}_2, \pi), \boldsymbol{R}(\boldsymbol{e}_3, \pi)\}.$$

Let $\boldsymbol{R}(\psi_0, \theta_0, \phi_0)$ be a generic point in the as yet undetermined fundamental domain Ω. By using Lemma 6.17 and the fact that $\boldsymbol{R}(\boldsymbol{e}_1, \pi) = \boldsymbol{R}(\boldsymbol{e}_2, \pi)\boldsymbol{R}(\boldsymbol{e}_3, \pi)$, we have

$$\begin{aligned}
&\boldsymbol{R}(\psi_0, \theta_0, \phi_0)\boldsymbol{R}(\boldsymbol{e}_3, \pi) = \boldsymbol{R}(\psi_0, \theta_0, \pi + \phi_0), \\
&\boldsymbol{R}(\psi_0, \theta_0, \phi_0)\boldsymbol{R}(\boldsymbol{e}_2, \pi) = \boldsymbol{R}(\pi + \psi_0, \pi - \theta_0, \pi - \phi_0), \\
&\boldsymbol{R}(\psi_0, \theta_0, \phi_0)\boldsymbol{R}(\boldsymbol{e}_1, \pi) = \boldsymbol{R}(\pi + \psi_0, \pi - \theta_0, 2\pi - \phi_0). \qquad (6.60)
\end{aligned}$$

Note that $(6.60)_1$ and $(6.60)_{2-3}$ suggest that we may restrict Ω to the ranges $0 \le \phi < \pi$ and $0 \le \theta \le \pi/2$, respectively. Thus we let $\Omega \subset \mathrm{SO}(3)$ be defined by

$$\Omega = \{\boldsymbol{R}(\psi, \theta, \phi) : 0 \le \psi < 2\pi, 0 \le \theta \le \pi/2, 0 \le \phi < \pi\}. \tag{6.61}$$

By (6.60) and the definition of Ω we obtain

$$\begin{aligned}
\Omega \boldsymbol{R}(\boldsymbol{e}_3, \pi) &= \{\boldsymbol{R}(\psi, \theta, \phi) : 0 \le \psi < 2\pi, 0 \le \theta \le \pi/2, \pi \le \phi < 2\pi\},\\
\Omega \boldsymbol{R}(\boldsymbol{e}_2, \pi) &= \{\boldsymbol{R}(\psi, \theta, \phi) : 0 \le \psi < 2\pi, \pi/2 \le \theta \le \pi, 0 < \phi \le \pi\},\\
\Omega \boldsymbol{R}(\boldsymbol{e}_1, \pi) &= \{\boldsymbol{R}(\psi, \theta, \phi) : 0 \le \psi < 2\pi, \pi/2 \le \theta \le \pi, \pi < \phi \le 2\pi\}.
\end{aligned} \tag{6.62}$$

It follows that

$$\begin{aligned}
\Omega \cap \Omega \boldsymbol{R}(\boldsymbol{e}_3, \pi) &= \emptyset,\\
\Omega \cap \Omega \boldsymbol{R}(\boldsymbol{e}_2, \pi) &= \{\boldsymbol{R}(\psi, \theta, \phi) : 0 \le \psi < 2\pi, \theta = \pi/2, 0 < \phi < \pi\},\\
\Omega \cap \Omega \boldsymbol{R}(\boldsymbol{e}_1, \pi) &= \{\boldsymbol{R}(\psi, \theta, \phi) : 0 \le \psi < 2\pi, \theta = \pi/2, \phi = 0\},
\end{aligned} \tag{6.63}$$

which are all of $\mathcal{V}$-measure zero in SO(3). Moreover, there holds

$$\Omega \cup \left(\bigcup_{i=1}^{3} \Omega \boldsymbol{R}(\boldsymbol{e}_i, \pi) \right) = \mathrm{SO}(3). \tag{6.64}$$

Hence by Remark 6.15, Ω as given by (6.61) is a fundamental domain for $\mathrm{SO}(3)/G_{\mathrm{cr}}$ in SO(3) for triclinic aggregates of orthorhombic crystallites.

For triclinic aggregates of crystallites with $G_{\mathrm{cr}} = D_k$ for $k = 3, 4, 6$, let $r = \boldsymbol{R}(\boldsymbol{e}_3, 2\pi/k)$, $s = \boldsymbol{R}(\boldsymbol{e}_2, \pi)$. Then the elements of G_{cr} are:

$$\begin{aligned}
&\boldsymbol{P}_1 = e, \qquad \boldsymbol{P}_2 = r, \qquad \cdots \qquad \boldsymbol{P}_k = r^{k-1},\\
&\boldsymbol{P}_{k+1} = s, \qquad \boldsymbol{P}_{k+2} = sr, \qquad \cdots \qquad \boldsymbol{P}_{2k} = sr^{k-1}.
\end{aligned}$$

After considerations parallel to those taken in the case of $G_{\mathrm{cr}} = D_2$, we let[95]

$$\Omega = \{\boldsymbol{R}(\psi, \theta, \phi) : 0 \le \psi < 2\pi, 0 \le \theta \le \pi/2, 0 \le \phi < 2\pi/k\}. \tag{6.65}$$

In what follows we will put $e = r^0$ when it is more convenient to do so. For $\boldsymbol{R}(\psi_0, \theta_0, \phi_0) \in \Omega$ and $\alpha = 0, 1, \ldots, k-1$, we have

$$\boldsymbol{R}(\psi_0, \theta_0, \phi_0) r^\alpha = \boldsymbol{R}(\psi_0, \theta_0, \phi_0 + \alpha \cdot 2\pi/k) \in \Omega r^\alpha, \tag{6.66}$$

$$\boldsymbol{R}(\psi_0, \theta_0, \phi_0) s r^\alpha = \boldsymbol{R}(\pi + \psi_0, \pi - \theta_0, \pi - \phi_0 + \alpha \cdot 2\pi/k) \in \Omega s r^\alpha \tag{6.67}$$

describe the same orientation as that of $\boldsymbol{R}(\psi_0, \theta_0, \phi_0)$. Moreover, it is easily checked that the sets Ωr^α, $\Omega s r^\alpha$, where α runs from 0 to $k-1$, i.e., the sets $\Omega \boldsymbol{P}_j$ $(j = 1, \ldots, 2k)$, are pairwise essentially disjoint, and $\bigcup_j \Omega \boldsymbol{P}_j = \mathrm{SO}(3)$. Hence Ω, as given by (6.65), is a fundamental domain for $\mathrm{SO}(3)/G_{\mathrm{cr}}$ in SO(3) for triclinic aggregates of crystallites with $G_{\mathrm{cr}} = D_k$ $(k = 2, 3, 4, 6)$.

[95] Note that (6.65) reduces to (6.61) when $k = 2$.

6.6.2 Triclinic Aggregates of Cubic Crystallites

Let $G_{\rm cr} = O$ be the group that contains D_4 (generated by $\boldsymbol{R}(\boldsymbol{e}_3, \pi/2)$ and $\boldsymbol{R}(\boldsymbol{e}_2, \pi)$) as a subgroup and $\boldsymbol{R}(\boldsymbol{m}, 2\pi/3)$, where $\boldsymbol{m} = (-\boldsymbol{e}_1 + \boldsymbol{e}_2 + \boldsymbol{e}_3)/\sqrt{3}$, as a generator. The subgroup D_4 has the region B defined by $(\psi, \theta, \phi) \in [0, 2\pi) \times [0, \pi/2] \times [0, \pi/2]$ as a fundamental domain, which is divided under O into three equivalent regions. Since we are examining the effects of crystallite symmetry, we may restrict attention (cf. Remark 6.18) to the cross-section $\mathscr{S} := \{(\theta, \phi) : 0 \le \theta \le \pi/2, 0 \le \phi \le \pi/2\}$ of B for each ψ. Note that $\mathscr{S}$ can be represented as the spherical triangle in the unit sphere S^2 that lies in the first octant and has vertices $(1, 0, 0)$, $(0, 1, 0)$, $(0, 0, 1)$ and sides being parts of great circles. Let $\boldsymbol{P} \in G_{\rm cr}$ be $\boldsymbol{P} = \boldsymbol{R}(\boldsymbol{m}, 2\pi/3)$, where $\boldsymbol{m} = (-1, 1, 1)/\sqrt{3}$. Under the basis $\{\boldsymbol{e}_i : i = 1, 2, 3\}$, $\boldsymbol{P}$ is represented by the matrix

$$[P_{ij}] = \begin{pmatrix} 0 & -1 & 0 \\ 0 & 0 & 1 \\ -1 & 0 & 0 \end{pmatrix}. \tag{6.68}$$

The rotation $\boldsymbol{P}$ generates a right translation in SO(3). Let $\boldsymbol{R}(\alpha, \beta, \gamma)$ be a generic rotation with Euler angles (α, β, γ) before the right translation, and let

$$\boldsymbol{R}(\psi, \theta, \phi) = \boldsymbol{R}(\alpha, \beta, \gamma)\boldsymbol{P}. \tag{6.69}$$

By (1.89) and (6.68), we obtain the equations

$$\sin\theta\cos\phi = \cos\beta, \quad \sin\theta\sin\phi = \sin\beta\cos\gamma, \quad \cos\theta = \sin\beta\sin\gamma, \tag{6.70}$$

which can be given as

$$\begin{pmatrix} \sin\theta\cos\phi \\ \sin\theta\sin\phi \\ \cos\theta \end{pmatrix} = \begin{pmatrix} 0 & 0 & 1 \\ 1 & 0 & 0 \\ 0 & 1 & 0 \end{pmatrix} \begin{pmatrix} \sin\beta\cos\gamma \\ \sin\beta\sin\gamma \\ \cos\beta \end{pmatrix} = \boldsymbol{R}(\boldsymbol{n}, \omega) \begin{pmatrix} \sin\beta\cos\gamma \\ \sin\beta\sin\gamma \\ \cos\beta \end{pmatrix}, \tag{6.71}$$

where $\boldsymbol{n} = (1, 1, 1)/\sqrt{3}$ and $\omega = 2\pi/3$. Hence $\boldsymbol{P}$ induces a transformation $(\beta, \gamma) \mapsto (\theta, \phi)$ on $\mathscr{S}$ defined by the rotation $\boldsymbol{R}((1, 1, 1)/\sqrt{3}, 2\pi/3)$. For $i = 1, 2, 3$, let $\mathscr{C}_i$ be the part of the great circle that lies in the spherical triangle $\mathscr{S}$ and passes through $\boldsymbol{e}_i$ and $\boldsymbol{n} = (\boldsymbol{e}_1 + \boldsymbol{e}_2 + \boldsymbol{e}_3)/\sqrt{3}$. Clearly $\mathscr{C}_3 = \{(\theta, \phi) \in S^2 : \phi = \pi/4, 0 \le \theta \le \pi/2\}$. The equations that specify $\mathscr{C}_1$ and $\mathscr{C}_2$ in the coordinates (θ, ϕ), respectively, can be obtained as follows.

Let $\boldsymbol{e}'_1 = \boldsymbol{e}_2$, $\boldsymbol{e}'_2 = \boldsymbol{e}_3$, and $\boldsymbol{e}'_3 = \boldsymbol{e}_1$. Under the primed coordinate system defined by $\boldsymbol{e}'_i$ $(i = 1, 2, 3)$, a generic point $\boldsymbol{a} \in \mathscr{C}_1$ has spherical coordinates $(r', \theta', \phi') = (1, \theta', \pi/4)$, where $0 \le \theta' \le \pi/2$. We have

$$\begin{aligned} \boldsymbol{a} &= \frac{1}{\sqrt{2}}\sin\theta'\boldsymbol{e}'_1 + \frac{1}{\sqrt{2}}\sin\theta'\boldsymbol{e}'_2 + \cos\theta'\boldsymbol{e}'_3 \\ &= \frac{1}{\sqrt{2}}\sin\theta'\boldsymbol{e}_2 + \frac{1}{\sqrt{2}}\sin\theta'\boldsymbol{e}_3 + \cos\theta'\boldsymbol{e}_1 \\ &= \sin\theta\cos\phi\,\boldsymbol{e}_1 + \sin\theta\sin\phi\,\boldsymbol{e}_2 + \cos\theta\,\boldsymbol{e}_3. \end{aligned} \tag{6.72}$$

Hence $\mathscr{C}_1$ is given by the equation $\sin\theta\sin\phi = \cos\theta$, i.e.

$$\tan\theta = \frac{1}{\sin\phi} \qquad \text{or} \qquad \cos\theta = \frac{\sin\phi}{\sqrt{1 + \sin^2\phi}}. \tag{6.73}$$

Similarly, we can show that $\mathscr{C}_2$ is given by the equation

$$\tan\theta = \frac{1}{\cos\phi} \qquad \text{or} \qquad \cos\theta = \frac{\cos\phi}{\sqrt{1+\cos^2\phi}}. \tag{6.74}$$

Hence we have

$$\mathscr{C}_1 = \left\{ (\theta,\phi) \in S^2 : \cos\theta = \frac{\sin\phi}{\sqrt{1+\sin^2\phi}}, 0 \le \phi \le \frac{\pi}{2} \right\}, \tag{6.75}$$

$$\mathscr{C}_2 = \left\{ (\theta,\phi) \in S^2 : \cos\theta = \frac{\cos\phi}{\sqrt{1+\cos^2\phi}}, 0 \le \phi \le \frac{\pi}{2} \right\}. \tag{6.76}$$

There are many possible choices of fundamental domains, two of which are:

$$\Omega_1 = \left\{ \boldsymbol{R}(\psi,\theta,\phi) : 0 \le \psi < 2\pi, \cos^{-1}\left(\frac{\cos\phi}{\sqrt{1+\cos^2\phi}}\right) \le \theta \le \frac{\pi}{2}, 0 \le \phi \le \frac{\pi}{4} \right\}, \tag{6.77}$$

$$\Omega_2 = \left\{ \boldsymbol{R}(\psi,\theta,\phi) : 0 \le \psi < 2\pi, \cos^{-1}\left(\frac{\sin\phi}{\sqrt{1+\sin^2\phi}}\right) \le \theta \le \frac{\pi}{2} \text{ for } 0 \le \phi \le \frac{\pi}{4}, \right.$$
$$\left. \cos^{-1}\left(\frac{\cos\phi}{\sqrt{1+\cos^2\phi}}\right) \le \theta \le \frac{\pi}{2} \text{ for } \frac{\pi}{4} \le \phi \le \frac{\pi}{2} \right\}. \tag{6.78}$$

Note that the two-fold domain Ω_2 is often preferred in practice for "simplifying calculations in a grid with equidistant steps for the Euler angles" [224, p. 25].

6.6.3 Orthorhombic Aggregates

We consider aggregates with $G_{\text{tex}} = D_2 = \{\boldsymbol{I}, \boldsymbol{R}(\boldsymbol{e}_1,\pi), \boldsymbol{R}(\boldsymbol{e}_2,\pi), \boldsymbol{R}(\boldsymbol{e}_3,\pi)\}$. Our discussions below (cf. Remark 6.18) are based on a lemma parallel to Lemma 6.17, which can be proved similarly.

Lemma 6.19 $\boldsymbol{R}(\boldsymbol{e}_2,\pi)\boldsymbol{R}(\boldsymbol{e}_3,\psi)\boldsymbol{R}(\boldsymbol{e}_2,\theta)\boldsymbol{R}(\boldsymbol{e}_3,\phi) = \boldsymbol{R}(\pi-\psi,\pi-\theta,\pi+\phi)$. □

Orthorhombic Aggregates of Triclinic Crystallites

Let us start with orthorhombic aggregates of triclinic crystallites.

For a generic rotation $\boldsymbol{R}(\psi_0,\theta_0,\phi_0)$ in an as yet undetermined fundamental domain Ω, we appeal to Lemma 6.19 and obtain the following relations:

$$\begin{aligned}
\boldsymbol{R}(\boldsymbol{e}_3,\pi)\boldsymbol{R}(\psi_0,\theta_0,\phi_0) &= \boldsymbol{R}(\pi+\psi_0,\theta_0,\phi_0),\\
\boldsymbol{R}(\boldsymbol{e}_2,\pi)\boldsymbol{R}(\psi_0,\theta_0,\phi_0) &= \boldsymbol{R}(\pi-\psi_0,\pi-\theta_0,\pi+\phi_0)\\
\boldsymbol{R}(\boldsymbol{e}_1,\pi)\boldsymbol{R}(\psi_0,\theta_0,\phi_0) &= \boldsymbol{R}(\boldsymbol{e}_3,\pi)\boldsymbol{R}(\boldsymbol{e}_2,\pi)\boldsymbol{R}(\psi_0,\theta_0,\phi_0)\\
&= \boldsymbol{R}(2\pi-\psi_0,\pi-\theta_0,\pi+\phi_0).
\end{aligned} \tag{6.79}$$

Thus, if $\boldsymbol{R}_0 := \boldsymbol{R}(\psi_0, \theta_0, \phi_0)$ has its Euler angle $\psi = \psi_0$ in the interior of the first quadrant (i.e., $0 < \psi_0 < \pi/2$), then $\boldsymbol{R}(\boldsymbol{e}_2, \pi)\boldsymbol{R}_0$, $\boldsymbol{R}(\boldsymbol{e}_3, \pi)\boldsymbol{R}_0$, and $\boldsymbol{R}(\boldsymbol{e}_1, \pi)\boldsymbol{R}_0$ have their respective Euler angle ψ in the interior of the second, third, and fourth quadrant, respectively. This observation suggests that a possible fundamental domain for $(\mathrm{SO}(3)/G_{\mathrm{cr}})/G_{\mathrm{tex}}$, where $G_{\mathrm{cr}} = \{\boldsymbol{I}\}$ and $G_{\mathrm{tex}} = D_2$, is:

$$\Omega = \{\boldsymbol{R}(\psi, \theta, \phi) : 0 \le \psi < \pi/2, 0 \le \theta \le \pi, 0 \le \phi < 2\pi\}. \tag{6.80}$$

Noting that $(\boldsymbol{R}(\boldsymbol{e}_i, \pi))^T = \boldsymbol{R}(\boldsymbol{e}_i, \pi)$ for $i = 1, 2, 3$, we use (6.79) and (6.80) to obtain the formulas

$$\begin{aligned} &\Omega \cap (\boldsymbol{R}(\boldsymbol{e}_3, \pi))^T \Omega = \emptyset, \qquad \Omega \cap (\boldsymbol{R}(\boldsymbol{e}_2, \pi))^T \Omega = \emptyset, \\ &\Omega \cap (\boldsymbol{R}(\boldsymbol{e}_1, \pi))^T \Omega = \{\boldsymbol{R}(\psi, \theta, \phi) : \psi = 0, 0 \le \theta \le \pi, 0 \le \phi < 2\pi\}, \end{aligned} \tag{6.81}$$

which are all of $\mathcal{V}$-measure zero in SO(3). Moreover, there holds

$$\Omega \cup \left(\bigcup_{i=1}^{3} (\boldsymbol{R}(\boldsymbol{e}_i, \pi))^T \Omega \right) = \mathrm{SO}(3) \setminus Z, \tag{6.82}$$

where $Z = \{\boldsymbol{R}(\psi, \theta, \phi) : \psi = \pi/2 \text{ or } 3\pi/2, 0 \le \theta \le \pi, 0 \le \phi < 2\pi\}$ is of $\mathcal{V}$-measure zero in SO(3). Hence by Remark 6.15, Ω as defined by (6.80) is a fundamental domain for $(\mathrm{SO}(3)/G_{\mathrm{cr}})/G_{\mathrm{tex}}$ in SO(3) for orthorhombic aggregates of triclinic crystallites ($G_{\mathrm{tex}} = D_2$, $G_{\mathrm{cr}} = \{\boldsymbol{I}\}$).

There are, of course, numerous choices of fundamental domain. For instance, we may replace (6.80) by

$$\Omega = \{\boldsymbol{R}(\psi, \theta, \phi) : 0 \le \psi \le \pi, 0 \le \theta \le \pi/2, 0 \le \phi < 2\pi\}, \tag{6.83}$$

the analogs of which often appear under other conventions (in the choice of Euler angles, etc.) in the literature of texture analysis.

Orthorhombic Aggregates of Hexagonal Crystallites

We may combine (6.65) for the case $k = 6$ and (6.80) to get

$$\Omega = \{\boldsymbol{R}(\psi, \theta, \phi) : 0 \le \psi < \pi/2, 0 \le \theta \le \pi/2, 0 \le \phi < \pi/3\} \tag{6.84}$$

as a fundamental domain for $(\mathrm{SO}(3)/G_{\mathrm{cr}})/G_{\mathrm{tex}}$ in SO(3) for orthorhombic aggregates of hexagonal crystallites ($G_{\mathrm{tex}} = D_2$, $G_{\mathrm{cr}} = D_6$).

Orthorhombic Aggregates of Cubic Crystallites

We may combine (6.78) and (6.80) to obtain

$$\begin{aligned} \Omega = \Bigg\{ \boldsymbol{R}(\psi, \theta, \phi) : 0 \le \psi < \pi/2, \cos^{-1}\left(\frac{\sin\phi}{\sqrt{1+\sin^2\phi}}\right) \le \theta \le \frac{\pi}{2} \text{ for } 0 \le \phi \le \frac{\pi}{4}, \\ \cos^{-1}\left(\frac{\cos\phi}{\sqrt{1+\cos^2\phi}}\right) \le \theta \le \frac{\pi}{2} \text{ for } \frac{\pi}{4} \le \phi \le \frac{\pi}{2} \Bigg\} \end{aligned} \tag{6.85}$$

as a fundamental domain for $(\mathrm{SO}(3)/(G_{\mathrm{cr}})/G_{\mathrm{tex}}$ in SO(3) for orthorhombic aggregates of cubic crystallites ($G_{\mathrm{tex}} = D_2$, $G_{\mathrm{cr}} = O$).

6.7 Spaces of Symmetrized Functions

Functions which satisfy restriction (6.4) and lie in the $(2l+1)^2$-dimensional subspace $\mathfrak{D}_l$ of $L^2(\mathrm{SO}(3),\mathbb{C})$ generated by D^l_{mn} $(-l \le m \le l,\ -l \le n \le l)$ constitute a linear subspace $\mathfrak{S}_l$ of $\mathfrak{D}_l$, and because of the restriction(s) imposed by (6.4) $\dim \mathfrak{S}_l < \dim \mathfrak{D}_l$ if $G_{\mathrm{cr}} \neq \{\boldsymbol{I}\}$. By (6.4), we observe that

$$w(\boldsymbol{R}) = w(\boldsymbol{R}\boldsymbol{P}_j) = \sum_{l=0}^{\infty}\sum_{m=-l}^{l}\sum_{n=-l}^{l} c^l_{mn} D^l_{mn}(\boldsymbol{R}\boldsymbol{P}_j), \quad \text{for each } \boldsymbol{P}_j \in G_{\mathrm{cr}} \text{ and } \boldsymbol{R} \in \mathrm{SO}(3). \tag{6.86}$$

It follows that

$$\begin{aligned} w(\boldsymbol{R}) &= \sum_{l=0}^{\infty}\sum_{m=-l}^{l}\sum_{n=-l}^{l} c^l_{mn}\left(\frac{1}{N_{\mathrm{cr}}}\sum_{j=1}^{N_{\mathrm{cr}}} D^l_{mn}(\boldsymbol{R}\boldsymbol{P}_j)\right) \\ &= \sum_{l=0}^{\infty}\sum_{m=-l}^{l}\sum_{n=-l}^{l} c^l_{mn}\mathfrak{F}^l_{mn}(\boldsymbol{R}), \end{aligned} \tag{6.87}$$

where

$$\mathfrak{F}^l_{mn}(\boldsymbol{R}) = \frac{1}{N_{\mathrm{cr}}}\sum_{j=1}^{N_{\mathrm{cr}}} D^l_{mn}(\boldsymbol{R}\boldsymbol{P}_j) \tag{6.88}$$

is the symmetrization of the corresponding D^l_{mn} with respect to the group G_{cr}. Equation (6.87) shows that the ODF w can be written as an infinite series of the symmetrized Wigner D-functions $\mathfrak{F}^l_{mn}$ $(l = 0, 1, 2, \ldots;\ -l \le m \le l,\ -l \le n \le l)$. On the other hand, because $\mathfrak{F}^l_{mn} \in \mathfrak{S}_l$ for all m and n, and because $\dim \mathfrak{S}_l < \dim \mathfrak{D}_l$ unless $G_{\mathrm{cr}} = \{\boldsymbol{I}\}$, the functions $\mathfrak{F}^l_{mn}$ are not linearly independent.

When there is also non-trivial sample symmetry, i.e., $G_{\mathrm{tex}} \neq \{\boldsymbol{I}\}$ and is of order $N_{\mathrm{tex}} < \infty$, the ODF w satisfies in addition the restriction (5.19). Then we have

$$w(\boldsymbol{R}) = w(\boldsymbol{Q}_i^T\boldsymbol{R}\boldsymbol{P}_j) = \sum_{l=0}^{\infty}\sum_{m=-l}^{l}\sum_{n=-l}^{l} c^l_{mn} D^l_{mn}(\boldsymbol{Q}_i^T\boldsymbol{R}\boldsymbol{P}_j),$$
$$\text{for each } \boldsymbol{Q}_i \in G_{\mathrm{tex}},\ \boldsymbol{P}_j \in G_{\mathrm{cr}} \text{ and } \boldsymbol{R} \in \mathrm{SO}(3). \tag{6.89}$$

It follows that

$$\begin{aligned} w(\boldsymbol{R}) &= \sum_{l=0}^{\infty}\sum_{m=-l}^{l}\sum_{n=-l}^{l} c^l_{mn}\left(\frac{1}{N_{\mathrm{tex}}}\cdot\frac{1}{N_{\mathrm{cr}}}\sum_{i=1}^{N_{\mathrm{tex}}}\sum_{j=1}^{N_{\mathrm{cr}}} D^l_{mn}(\boldsymbol{Q}^T\boldsymbol{R}\boldsymbol{P}_j)\right) \\ &= \sum_{l=0}^{\infty}\sum_{m=-l}^{l}\sum_{n=-l}^{l} c^l_{mn}\mathfrak{F}^l_{mn}(\boldsymbol{R}), \end{aligned} \tag{6.90}$$

and

$$\mathfrak{F}^l_{mn}(\boldsymbol{R}) = \frac{1}{N_{\mathrm{tex}}}\cdot\frac{1}{N_{\mathrm{cr}}}\sum_{i=1}^{N_{\mathrm{tex}}}\sum_{j=1}^{N_{\mathrm{cr}}} D^l_{mn}(\boldsymbol{Q}_i^T\boldsymbol{R}\boldsymbol{P}_j) \tag{6.91}$$

is the symmetrization of the corresponding D^l_{mn} with respect to the groups G_{tex} and G_{cr}. Let $\mathfrak{S}_l$ be the linear subspace of $\mathfrak{D}_l$ which consists of functions that satisfy $(6.46)_4$. By (6.90) the ODF w can be expanded as an infinite series of the symmetrized Wigner D-functions $\mathfrak{F}^l_{mn}$ for all m and n. However, when $G_{\text{tex}} \neq \{\boldsymbol{I}\}$ or $G_{\text{cr}} \neq \{\boldsymbol{I}\}$, since $\dim \mathfrak{S}_l < \dim \mathfrak{D}_l$, the functions $\mathfrak{S}_l$ are not linearly independent. In Sect. 6.8 we shall illustrate by an example how a basis in $\mathfrak{S}_l$ can be constructed from the D^l_{mn}'s after the restrictions imposed by sample and crystallite symmetry on the texture coefficients c^l_{mn} have already been ascertained.

Remark 6.20 Note that the symmetrized functions $\mathfrak{F}^l_{mn}$ in (6.88) and in (6.91) satisfy the restrictions (6.4) and (6.46), respectively. Hence they are in effect defined on the orientation space $\mathrm{SO}(3)/G_{\text{cr}}$ and the space $(\mathrm{SO}(3)/(G_{\text{cr}})/G_{\text{tex}}$ of G_{tex}-orbits of orientations, respectively. Indeed by the formula $\mathfrak{F}^l_{mn} = \hat{\mathfrak{F}}^l_{mn} \circ \pi$ (resp. $\mathfrak{F}^l_{mn} = \widetilde{\mathfrak{F}}^l_{mn} \circ \widetilde{\pi}$), where π (resp. $\widetilde{\pi}$) maps $\mathrm{SO}(3)$ onto $\mathrm{SO}(3)/G_{\text{cr}}$ (resp. $(\mathrm{SO}(3)/G_{\text{cr}})/G_{\text{tex}}$), $\mathfrak{F}^l_{mn}$ in (6.88) (resp. (6.91)) specifies a complex-valued function $\hat{\mathfrak{F}}^l_{mn}$ (resp. $\widetilde{\mathfrak{F}}^l_{mn}$) defined on $\mathrm{SO}(3)/G_{\text{cr}}$ (resp. $(\mathrm{SO}(3)/G_{\text{cr}})/G_{\text{tex}}$). The expansion (6.90) can be interpreted as one concerning functions defined on $(\mathrm{SO}(3)/(G_{\text{cr}})/G_{\text{tex}}$, namely

$$\widetilde{w}([\boldsymbol{R}G_{\text{cr}}]) = \sum_{l=0}^{\infty} \sum_{m=-l}^{l} \sum_{n=-l}^{l} c^l_{mn} \widetilde{\mathfrak{F}}^l_{mn}([\boldsymbol{R}G_{\text{cr}}]), \tag{6.92}$$

where $[\boldsymbol{R}G_{\text{cr}}]$ is the G_{tex}-orbit of the orientation $\boldsymbol{R}G_{\text{cr}}$ in $(\mathrm{SO}(3)/G_{\text{cr}})/G_{\text{tex}}$. Likewise, the expansion (6.87) can be interpreted similarly. In a theory that works only with functions defined on the orientations or the G_{tex}-orbits of orientations, one should proceed further to construct a set of basis functions in each $\mathfrak{S}_l$ and study their properties. This is in line with the Bunge approach to texture analysis, to which we now turn. □

6.8 The Bunge Approach: Symmetric Generalized Spherical Functions

In this exposition we mainly follow the approach initiated by Roe [270, 271], where the ODF w is always defined on $\mathrm{SO}(3)$ and the effects of sample and crystallite symmetry are accounted for through the restrictions that the symmetries impose on texture coefficients. Bunge [56, 57, 60], on the other hand, elects to work with functions symmetrized with respect to G_{tex} and G_{cr} that include bases in the spaces $\mathfrak{S}_l$, which he calls "symmetric generalized spherical functions". Since we are not going to follow Bunge's approach in this exposition, we shall be content to illustrate by one concrete example how a basis in $\mathfrak{S}_l$ can be constructed from the D^l_{mn}'s after the restrictions imposed by sample and crystallite symmetry on the texture coefficients c^l_{mn} have already been ascertained.

Passive rotations are used in Bunge's original formulation. In this exposition, however, we have followed the recent trend in mathematics, physics, and chemistry and use active rotations. We will keep using active rotations in our illustration on construction of symmetric generalized spherical functions. While reading the rest of this section, the reader should keep in mind that what is presented is a rewrite of Bunge's formulation in terms of active rotations and the conventions (i.e., the ODF w, Wigner D-functions D^l_{mn}, bi-invariant volume measure $\mathcal{V}$ on $\mathrm{SO}(3)$, etc.) adopted in this exposition.

Consider an orthorhombic aggregate of cubic crystallites. Let us focus our attention on the terms with $l = 4$ and $m = 0$ in the following expansion of the ODF:

$$\begin{aligned} w(\boldsymbol{R}) &= \sum_{l=0}^{\infty} \sum_{m=-l}^{l} \sum_{n=-l}^{l} c_{mn}^{l} D_{mn}^{l}(\boldsymbol{R}) \\ &= \cdots + c_{00}^{4} D_{00}^{4}(\boldsymbol{R}) + c_{04}^{4} D_{04}^{4}(\boldsymbol{R}) + c_{0\bar{4}}^{4} D_{0\bar{4}}^{4}(\boldsymbol{R}) + \cdots \\ &= \cdots + c_{00}^{4} \left(D_{00}^{4}(\boldsymbol{R}) + \frac{\sqrt{70}}{14} D_{04}^{4}(\boldsymbol{R}) + \frac{\sqrt{70}}{14} D_{0\bar{4}}^{4}(\boldsymbol{R}) \right) + \cdots \end{aligned} \tag{6.93}$$

where we have appealed to the fact that $c_{04}^{4} = c_{0\bar{4}}^{4} = \frac{\sqrt{70}}{14} c_{00}^{4}$. Note that the first step of the procedure is to write down all terms with non-trivial c_{mn}^{l}. For the case $(l = 4, m = 0)$ in question, the non-trivial texture coefficients c_{mn}^{l} are c_{00}^{4}, c_{04}^{4}, and $c_{0\bar{4}}^{4}$; see Sect. 5.4.4. The second step is to express the dependent texture coefficients in terms of the independent ones. For orthorhombic aggregates of cubic crystallites, the number of linear independent coefficients for $1 \leq l \leq 15$ and for a fixed m are given in Table 7 of Sect. 5.4.3. By convention, for a fixed l and m the non-trivial texture coefficient with the lowest (resp. second, third, ...) $n \geq 0$ is taken as the first (resp. second, third, ...) independent coefficient, etc., and the assignment of independent coefficients is stopped when the number of independent coefficients is met. For the present case, the independent non-trivial coefficient is c_{00}^{4}, whereas c_{04}^{4} and $c_{0\bar{4}}^{4}$ are the dependent ones. In Table 7 is also listed the relations that express the dependent non-trivial texture coefficients with $n \geq 0$ in terms of the independent ones. The linear relations between c_{04}^{4} and between $c_{0\bar{4}}^{4}$ and c_{00}^{4} are exploited in (6.93). Let

$$\overset{\cdot\cdot}{D}{}_{4}^{11}(\boldsymbol{R}) = N_{4}^{11} \left(D_{00}^{4}(\boldsymbol{R}) + \frac{\sqrt{70}}{14} D_{04}^{4}(\boldsymbol{R}) + \frac{\sqrt{70}}{14} D_{0\bar{4}}^{4}(\boldsymbol{R}) \right), \tag{6.94}$$

where N_{4}^{11} is a normalization constant that renders

$$\langle \overset{\cdot\cdot}{D}{}_{4}^{11}, \overset{\cdot\cdot}{D}{}_{4}^{11} \rangle = \int_{\mathrm{SO}(3)} \overset{\cdot\cdot}{D}{}_{4}^{11}(\boldsymbol{R}) \overline{\overset{\cdot\cdot}{D}{}_{4}^{11}(\boldsymbol{R})}\, d\mathcal{V}(\boldsymbol{R}) = \frac{8\pi^2}{2 \times 4 + 1}.$$

Thus we have

$$|N_{4}^{11}|^2 = (1 + 2 \times \frac{70}{14^2})^{-1} = \frac{7}{12}.$$

Since D_{00}^{4} is real and $D_{04}^{4}(\boldsymbol{R}) = \overline{D_{0\bar{4}}^{4}(\boldsymbol{R})}$, $\overset{\cdot\cdot}{D}{}_{4}^{11}$ is a real-valued function if we choose N_{4}^{11} to be real, which we will do. Then N_{4}^{11} is specified to within a sign. By convention we choose $N_{4}^{11} = \sqrt{7/12}$. Note that because of the texture and crystallite symmetry the ODF satisfies

$$w(\boldsymbol{Q}_i^T \boldsymbol{R} \boldsymbol{P}_j) = w(\boldsymbol{R}) \tag{6.95}$$

for each $\boldsymbol{Q}_i \in G_{\mathrm{tex}}$, $\boldsymbol{P}_j \in G_{\mathrm{cr}}$, and $\boldsymbol{R} \in \mathrm{SO}(3)$. Since c_{00}^{4} is an independent coefficient, it follows that the function $\overset{\cdot\cdot}{D}{}_{4}^{11}$ also enjoys the texture and crystal symmetries in question, i.e.,

$$\overset{\cdot\cdot}{D}{}_{4}^{11}(\boldsymbol{Q}_i^T \boldsymbol{R} \boldsymbol{P}_j) = \overset{\cdot\cdot}{D}{}_{4}^{11}(\boldsymbol{R}) \tag{6.96}$$

for each $\boldsymbol{Q}_i \in G_{\mathrm{tex}}$, $\boldsymbol{P}_j \in G_{\mathrm{cr}}$, and $\boldsymbol{R} \in \mathrm{SO}(3)$.

Now we consider the terms in the expansion of the ODF with $l = 4$ and $m = 2$ or -2:

$$c_{20}^4 D_{20}^4(\boldsymbol{R}) + c_{2\bar{4}}^4 D_{2\bar{4}}^4(\boldsymbol{R}) + c_{\bar{2}4}^4 D_{\bar{2}4}^4(\boldsymbol{R}) + c_{\bar{2}0}^4 D_{\bar{2}0}^4(\boldsymbol{R}) + c_{\bar{2}\bar{4}}^4 D_{\bar{2}\bar{4}}^4(\boldsymbol{R}) + c_{\bar{2}\bar{4}}^4 D_{\bar{2}\bar{4}}^4(\boldsymbol{R})$$
$$= c_{20}^4 \left(D_{20}^4(\boldsymbol{R}) + D_{\bar{2}0}^4(\boldsymbol{R}) + \frac{\sqrt{70}}{14} \left(D_{24}^4(\boldsymbol{R}) + D_{2\bar{4}}^4(\boldsymbol{R}) + D_{\bar{2}4}^4(\boldsymbol{R}) + D_{\bar{2}\bar{4}}^4(\boldsymbol{R}) \right) \right).$$

Let

$$\dddot{D}_4^{12}(\boldsymbol{R}) = N_4^{12} \left(D_{20}^4(\boldsymbol{R}) + D_{\bar{2}0}^4(\boldsymbol{R}) + \frac{\sqrt{70}}{14} \left(D_{24}^4(\boldsymbol{R}) + D_{2\bar{4}}^4(\boldsymbol{R}) + D_{\bar{2}4}^4(\boldsymbol{R}) + D_{\bar{2}\bar{4}}^4(\boldsymbol{R}) \right) \right), \tag{6.97}$$

where N_4^{12} is a normalization constant. Again, we choose a real N_4^{12} so that

$$\langle \dddot{D}_4^{12}, \dddot{D}_4^{12} \rangle = \frac{8\pi^2}{2 \times 4 + 1}$$

or

$$|N_4^{12}|^2 = (2 + 4 \times \frac{70}{14^2})^{-1} = \frac{7}{24}.$$

By convention we take $N_4^{12} = \sqrt{7/24}$ here. Similar to $\dddot{D}_4^{11}$, as c_{20}^4 is an independent coefficient, the function $\dddot{D}_4^{12}$ observes the same texture and crystallite symmetries (cf. (6.96)).

Likewise, we consider the remaining terms in the expansion of the ODF with $l = 4$, i.e., those with $m = 4$ or -4, and we define the function

$$\dddot{D}_4^{13}(\boldsymbol{R}) = \sqrt{\frac{7}{24}} \left(D_{40}^4(\boldsymbol{R}) + D_{\bar{4}0}^4(\boldsymbol{R}) + \frac{\sqrt{70}}{14} \left(D_{44}^4(\boldsymbol{R}) + D_{4\bar{4}}^4(\boldsymbol{R}) + D_{\bar{4}4}^4(\boldsymbol{R}) + D_{\bar{4}\bar{4}}^4(\boldsymbol{R}) \right) \right), \tag{6.98}$$

which satisfies

$$\langle \dddot{D}_4^{13}, \dddot{D}_4^{13} \rangle = \frac{8\pi^2}{2 \times 4 + 1}$$

and enjoys the texture and crystallite symmetries. Note that the functions $\dddot{D}_4^{11}$, $\dddot{D}_4^{12}$ and $\dddot{D}_4^{11}$ are orthogonal in the space $L^2(\mathrm{SO}(3), \mathbb{C})$.

For orthorhombic aggregates of cubic crystallites, it should now be clear how to proceed to choose a sequence of real-valued basis functions $\dddot{D}_l^{\mu\nu}$ ($l = 0, 1, 2, 3, 4, \ldots$) which enjoy the texture and crystal symmetries and satisfy the orthogonality relation

$$\langle \dddot{D}_l^{\mu\nu}, \dddot{D}_l^{\mu'\nu'} \rangle = \frac{8\pi^2}{2l + 1} \delta_{ll'} \delta_{\mu\mu'} \delta_{\nu\nu'}. \tag{6.99}$$

In terms of the basis $\dddot{D}_l^{\mu\nu}$, the expansion of the ODF now reads:

$$w(\boldsymbol{R}) = \sum_{l=0}^{\infty} \sum_{\mu=1}^{M(l)} \sum_{\nu=1}^{N(l)} \mathrm{c}_l^{\mu\nu} \dddot{D}_l^{\mu\nu}(\boldsymbol{R}). \tag{6.100}$$

Table 8 Values of $M(l)$ and $N(l)$ for $1 \le l \le 15$ for orthorhombic aggregates of cubic crystallites

l	4	6	8	9	10	12	13	14	15
$M(l)$	1	1	1	1	1	2	1	1	1
$N(l)$	3	4	5	5	6	7	7	8	8

Here for $l = 0$, there is only one term $\mathsf{c}_0^{11}\dddot{D}_0^{11} = 1/(8\pi^2)$. In general, for each l, $M(l)$ is the number of linearly independent coefficient c_{mn}^l for a fixed m, and $N(l)$ is the number of non-negative integers k for which $2k \le l$. For $1 \le l \le 15$, the values of $M(l)$ can be read off from Table 7. These values and those of the corresponding $N(l)$'s are displayed in Table 8. For those $1 \le l \le 15$ that are not included in this table, no term of such l's appears in the series expansion (6.100) of the ODF.

For each l and m, we take the non-trivial coefficient(s) c_{mn}^l with the lowest n('s) as the linearly independent coefficient(s). For instance, for $l = 4$, we take c_{m0}^4; for $l = 12$, we take c_{m0}^{12} and c_{m4}^{12}. We assign the indices ν and μ in the order of increasing m and of increasing n in the linearly independent coefficients, respectively. For instance, c_8^{12}, c_9^{15} and c_{12}^{24} in the $\mathsf{c}_l^{\mu\nu}$ series correspond to c_{20}^8, c_{84}^9, and c_{64}^{12} in the c_{mn}^l series, respectively. In general, by convention of how the normalization constants $N_l^{\mu\nu}$ are defined, we have

$$\mathsf{c}_l^{\mu\nu} = \frac{\text{the corresponding } c_{mn}^l}{N_l^{\mu\nu}}, \tag{6.101}$$

where $N_l^{\mu\nu}$ is the normalization constant in the definition of $\dddot{D}_l^{\mu\nu}$. For instance, we have

$$\mathsf{c}_4^{11} = \sqrt{\frac{12}{7}}c_{00}^4, \qquad \mathsf{c}_4^{12} = \sqrt{\frac{24}{7}}c_{20}^4, \qquad \mathsf{c}_4^{13} = \sqrt{\frac{24}{7}}c_{40}^4.$$

In summary, by (4.118) and (6.101) the chosen independent c_{mn}^l and W_{lmn} are related to the corresponding $\mathsf{c}_l^{\mu\nu}$ as follows:

$$c_{mn}^l = N_l^{\mu\nu}\mathsf{c}_l^{\mu\nu}, \tag{6.102}$$

$$W_{lmn} = (-1)^{m-n}\sqrt{\frac{2}{2l+1}}N_l^{\mu\nu}\mathsf{c}_l^{\mu\nu}. \tag{6.103}$$

Chapter 7

7 Reciprocal Space and Reciprocal Lattice

7.1 Dual Space

Let V be the translation space of E^3. Let V^* be the set of linear mappings from V to the reals $\mathbb{R}$. We define addition and scalar multiplication in V^* by

$$(F_1 + F_2)(\boldsymbol{u}) = F_1(\boldsymbol{u}) + F_2(\boldsymbol{u}) \qquad \text{for any } F_1, F_2 \in V^*, \text{ and } \boldsymbol{u} \in V, \tag{7.1}$$

$$(cF)(\boldsymbol{u}) = c\,F(\boldsymbol{u}) \qquad \text{for any } c \in \mathbb{R},\ F \in V^*, \text{ and } \boldsymbol{u} \in V, \tag{7.2}$$

and define the zero vector $O \in V^*$ as the zero mapping

$$O(\boldsymbol{u}) = 0 \qquad \text{for any } \boldsymbol{u} \in V \tag{7.3}$$

so that V^* is a vector space. Each $F \in V^*$ is a vector, the magnitude or norm of which is defined by

$$\|F\| = \max\{|F(\boldsymbol{u})| : \boldsymbol{u} \in V \text{ and } \|\boldsymbol{u}\| = 1\}. \tag{7.4}$$

After a right-handed basis, say $\{\boldsymbol{f}_j : j = 1, 2, 3\}$, is chosen for V, each $F \in V^*$ is represented by a 1×3 matrix. The linear maps $H^i : V \to \mathbb{R}$ $(i = 1, 2, 3)$ defined by

$$H^i(\boldsymbol{f}_j) = \delta^i{}_j \qquad \text{for } i, j = 1, 2, 3 \tag{7.5}$$

clearly constitute a basis in V^*. Hence $\dim V^* = 3$. In mathematics, V^* is called the dual space of V and $\{H^i\}$, as defined by (7.5), the dual basis with respect to $\{\boldsymbol{f}_j\}$.

Let $\langle \cdot, \cdot \rangle : V^* \times V \to \mathbb{R}$ be defined by

$$\langle F, \boldsymbol{u} \rangle = F(\boldsymbol{u}) \qquad \text{for each } F \in V^* \text{ and each } \boldsymbol{u} \in V. \tag{7.6}$$

The notation given in (7.6) emphasizes the symmetry between V^* and V: while each $F \in V^*$ is a real-valued linear mapping on V, each $\boldsymbol{u} \in V$ can likewise be taken as a real-valued linear mapping on V^*. In fact, it can be shown that $V^{**} := (V^*)^* = V$. Under the notation defined in (7.6), (7.5) reads:

$$\langle H^i, \boldsymbol{f}_j \rangle = \delta^i{}_j \qquad \text{for } i, j = 1, 2, 3, \tag{7.7}$$

which asserts that $\{H^i\}$ and $\{\boldsymbol{f}_j\}$ are dual bases of each other.

For $F \in V^*$ and $c \in \mathbb{R}$, the set $\Pi_{(F,c)} = \{\boldsymbol{u} \in V : \langle F, \boldsymbol{u} \rangle = c\}$ is a continuous family of parallel planes in V. In particular, $\Pi_{(F,0)}$ is the plane in the family that passes through $\mathbf{0}$, the zero vector of V.

Note that each $\boldsymbol{u} \in V$ denotes a translation. Hence the magnitude $\|\boldsymbol{u}\|$ has the physical dimension of length L and the direction of $\boldsymbol{u}$ is dimensionless. Since the real number c in the expression $\langle F, \boldsymbol{u} \rangle = c$ is dimensionless, the magnitude $\|F\|$ of the vector F in V^* carries the dimension of L^{-1}.

7.2 Reciprocal Space

In crystallography, V is called the direct space. The dual space V^* of V, however, is given an alternate description, which is based on the following mathematical observation.

Proposition 7.1 *For each $F \in V^*$, there is a unique $\boldsymbol{v}_F \in V$ such that*

$$F(\boldsymbol{w}) = \boldsymbol{v}_F \cdot \boldsymbol{w} \qquad \text{for each } \boldsymbol{w} \in V, \tag{7.8}$$

and $\|\boldsymbol{v}_F\| = \|F\|$.

Proof Existence of $\boldsymbol{v}_F$. If $F = O$, then $\boldsymbol{v}_F = \boldsymbol{0}$ satisfies (7.8). Suppose $F \neq O$. Then the equation $F(\boldsymbol{u}) = \langle F, \boldsymbol{u}\rangle = 0$ defines a plane $\Pi_{(F,0)}$ through the origin in V. For simplicity, we will write Π for $\Pi_{(F,0)}$ for the rest of this proof. Let $\boldsymbol{w} \in V$ be given. Pick one of the two unit normals of Π and call it $\boldsymbol{n}$. Then we have

$$\boldsymbol{w} = \boldsymbol{w}^{\parallel} + \boldsymbol{w}^{\perp} = (\boldsymbol{w} \cdot \boldsymbol{n})\boldsymbol{n} + (\boldsymbol{w} - (\boldsymbol{w} \cdot \boldsymbol{n})\boldsymbol{n}), \tag{7.9}$$

where $\boldsymbol{w}^{\parallel} = (\boldsymbol{w} \cdot \boldsymbol{n})\boldsymbol{n}$ is the component of $\boldsymbol{w}$ normal to Π and $\boldsymbol{w}^{\perp}$ is the projection of $\boldsymbol{w}$ onto Π. Since $\boldsymbol{w}^{\perp} \in \Pi$ and $F(\boldsymbol{u}) = 0$ if $\boldsymbol{u} \in \Pi$, we obtain

$$F(\boldsymbol{w}) = F(\boldsymbol{w}^{\parallel}) = (\boldsymbol{w} \cdot \boldsymbol{n})F(\boldsymbol{n}) = F(\boldsymbol{n})\boldsymbol{n} \cdot \boldsymbol{w}. \tag{7.10}$$

As $\boldsymbol{w}$ in (7.10) is an arbitrary vector in V, (7.8) holds with $\boldsymbol{v}_F = F(\boldsymbol{n})\boldsymbol{n}$.

Uniqueness of $\boldsymbol{v}_F$. Let $F(\boldsymbol{w}) = \boldsymbol{v}_F \cdot \boldsymbol{w} = \boldsymbol{v}'_F \cdot \boldsymbol{w}$ for each $\boldsymbol{w} \in V$. Then $(\boldsymbol{v}_F - \boldsymbol{v}'_F) \cdot \boldsymbol{w} = 0$ for each $\boldsymbol{w} \in V$, which implies $\boldsymbol{v}_F = \boldsymbol{v}'_F$.

As for the equality of the norms, we have $\|\boldsymbol{v}_F\| = \sqrt{F(\boldsymbol{n})\boldsymbol{n} \cdot F(\boldsymbol{n})\boldsymbol{n}} = |F(\boldsymbol{n})|$. On the other hand, let $\boldsymbol{m} \in V$ such that $\|\boldsymbol{m}\| = 1$. Then by (7.10), $|F(\boldsymbol{m})| = |F(\boldsymbol{n})\boldsymbol{n} \cdot \boldsymbol{m}| \leq |F(\boldsymbol{n})|$, which by (7.4) implies $\|F\| = |F(\boldsymbol{n})|$. □

The preceding proposition is the finite-dimensional version of the Riesz representation theorem for Hilbert spaces (see, e.g., [273, p. 351]). Let $\tau : V^* \to V$ be defined by

$$\tau(F) = \boldsymbol{v}_F, \qquad \text{for each } F \in V^*. \tag{7.11}$$

Clearly the mapping τ is linear. By (7.7) and (7.11),

$$\langle H^i, \boldsymbol{f}_j\rangle = \tau(H^i) \cdot \boldsymbol{f}_j = \delta^i{}_j \qquad \text{for } i, j = 1, 2, 3. \tag{7.12}$$

It follows that $\tau(H^i) = \boldsymbol{f}^i$ $(i = 1, 2, 3)$, the basis reciprocal to $\boldsymbol{f}_j$ $(j = 1, 2, 3)$ in V (see Sect. 1.2.1), as the reciprocal basis is uniquely defined by the orthonormality relations $(7.12)_2$. Hence τ is an isomorphism. Let us define an inner product $\langle \cdot, \cdot \rangle$ on V^* by $\langle F_1, F_2\rangle = \tau(F_1) \cdot \tau(F_2)$. Since $\|F\| = \|\tau(F)\|$ for each $F \in V^*$, we obtain [273, p. 211] the following corollary.

Corollary 7.2 *The linear mapping $\tau : V^* \to V$ defined by (7.11) is an isometric isomorphism.* □

The representation $\tau(V^*)$ of the dual space V^* is called the reciprocal space of the direct space V.

Remark 7.3 Proposition 7.8 and Corollary 7.2 assert that the dual space V^* can be represented by V as the reciprocal space $\tau(V^*)$. However, it should be emphasized that physically the reciprocal space $\tau(V^*)$ and the direct space V are completely different spaces. A vector $\boldsymbol{v} \in V$ denotes a translation with its magnitude $\|\boldsymbol{v}\|$ carrying the physical dimension of length L. The same vector $\boldsymbol{v} \in \tau(V^*)$ is a representation of the linear mapping $\tau^{-1}(\boldsymbol{v}) \in V^*$; its magnitude $\|\boldsymbol{v}\| = \|\tau^{-1}(\boldsymbol{v})\|$ has the physical dimension of L^{-1}. This fact can also be easily read off from (1.34), the equation that defines the reciprocal basis vectors in terms of the direct basis vectors. On the other hand, mathematically the direct and reciprocal basis vectors are elements of the same vector space V which are related through (1.34) and (1.36). In Sect. 7.5 we will exploit the intimate relationship between the two sets of basis vectors to derive useful mathematical formulas. □

7.3 Reciprocal Lattice

Our discussions henceforth in this chapter refer equally well to crystal lattices L as described in Sect. 2.3.1 and to the primitive sublattices $\mathsf{L}^{(p)} := \mathcal{L}^{(p)}(\mathbf{0})$ of Bravais lattices (see Sect. 2.8.2). For simplicity we will refer to them all as lattices L.

Let $\mathbb{Z}$ be the set of integers, L a lattice or primitive sublattice, and $\boldsymbol{a}, \boldsymbol{b}, \boldsymbol{c} \in V$ a right-handed triad of lattice basis vectors for L. The lattice L is then given by the collection of points in V located at

$$\boldsymbol{u} = u\boldsymbol{a} + v\boldsymbol{b} + w\boldsymbol{c}, \tag{7.13}$$

where u, v, and w run over $\mathbb{Z}$. Each vector of the form (7.13) is called a lattice vector.

The right-handed basis in V reciprocal to the triad $\boldsymbol{a}, \boldsymbol{b}$, and $\boldsymbol{c}$ is given (see Sect. 1.2.1) by the vectors

$$\boldsymbol{a}^* = \frac{\boldsymbol{b} \times \boldsymbol{c}}{\boldsymbol{a} \cdot (\boldsymbol{b} \times \boldsymbol{c})}, \qquad \boldsymbol{b}^* = \frac{\boldsymbol{c} \times \boldsymbol{a}}{\boldsymbol{b} \cdot (\boldsymbol{c} \times \boldsymbol{a})}, \qquad \boldsymbol{c}^* = \frac{\boldsymbol{a} \times \boldsymbol{b}}{\boldsymbol{c} \cdot (\boldsymbol{a} \times \boldsymbol{b})}, \tag{7.14}$$

which satisfy the following conditions:

$$\begin{array}{lll} \boldsymbol{a}^* \cdot \boldsymbol{a} = 1, & \boldsymbol{a}^* \cdot \boldsymbol{b} = 0, & \boldsymbol{a}^* \cdot \boldsymbol{c} = 0, \\ \boldsymbol{b}^* \cdot \boldsymbol{a} = 0, & \boldsymbol{b}^* \cdot \boldsymbol{b} = 1, & \boldsymbol{b}^* \cdot \boldsymbol{c} = 0, \\ \boldsymbol{c}^* \cdot \boldsymbol{a} = 0, & \boldsymbol{c}^* \cdot \boldsymbol{b} = 0, & \boldsymbol{c}^* \cdot \boldsymbol{c} = 1. \end{array} \tag{7.15}$$

The reciprocal lattice L^* corresponding to L is defined by

$$\mathsf{L}^* = \{\mathbf{H} \in \tau(V^*) : \mathbf{H} = h\boldsymbol{a}^* + k\boldsymbol{b}^* + l\boldsymbol{c}^*, \text{where } h, k, l \in \mathbb{Z}\}. \tag{7.16}$$

Any vector $\mathbf{H}$ in L^* is called a reciprocal lattice vector. In mathematics, L^* is called the dual lattice (see, e.g., [295, p. 53]).

Remark 7.4 Here we have adopted a system of notations common in crystallography. At times we will use the index notation instead (see Sect. 1.34) when it is particularly convenient to do so. Then, for instance, for the primitive sublattice of a Bravais lattice, we shall write $\boldsymbol{a}_1$, $\boldsymbol{a}_2$, and $\boldsymbol{a}_3$ for $\boldsymbol{a}$, $\boldsymbol{b}$, and $\boldsymbol{c}$, respectively, and $\boldsymbol{a}^1$, $\boldsymbol{a}^2$, and $\boldsymbol{a}^3$ for $\boldsymbol{a}^*$, $\boldsymbol{b}^*$, and $\boldsymbol{c}^*$, respectively. □

7.4 Families of Parallel Lattice Planes

We shall phrase our discussion below in the context of a lattice L with a primitive lattice basis $\boldsymbol{b}_i$ $(i = 1, 2, 3)$. The discussion, however, applies equally well for the primitive sublattice $\mathsf{L}^{(p)}$ of a Bravais lattice with a conventional lattice basis $\boldsymbol{a}_i$ $(i = 1, 2, 3)$.

Let $\mathsf{L} = \{\boldsymbol{u} \in V : \boldsymbol{u} = u\boldsymbol{b}_1 + v\boldsymbol{b}_2 + w\boldsymbol{b}_3, \text{where } u, v, w \in \mathbb{Z}\}$ be a lattice. Let h, k, and l be three coprime integers, i.e., they have their greatest common divisor $\gcd(h, k, l) = 1$. Consider the family $\mathcal{F}_{hkl}$ of planes Π_m $(m \in \mathbb{Z})$ in V defined by

$$\Pi_m = \{\boldsymbol{u} \in V : \boldsymbol{u} = u\boldsymbol{b}_1 + v\boldsymbol{b}_2 + w\boldsymbol{b}_3, (u, v, w) \in \mathbb{R}^3, \text{and } hu + kv + lw = m\}. \tag{7.17}$$

The family of planes $\mathcal{F}_{hkl}$ enjoys the following properties:

(i) The planes in $\mathcal{F}_{hkl}$ are parallel, with the same distance between any two adjacent planes.

(ii) Every lattice point is contained in one of the planes in the family. Thus the union of planes in $\mathcal{F}_{hkl}$ covers the lattice L.

(iii) Since $\gcd(h, k, l) = 1$, for each $m \in \mathbb{Z}$ the linear diophantine equation

$$hu + kv + lw = m \tag{7.18}$$

is solvable and has an infinite number of solutions $(u, v, w) \in \mathbb{Z}^3$ (see, e.g., [5, p. 70]). Hence each member of $\mathcal{F}_{hkl}$ is a lattice plane[96] that contains an infinite number of lattice points.

In what follows we shall call the members of $\mathcal{F}_{hkl}$ the (hkl) planes.[97]

7.4.1 Distance Between Two Adjacent Lattice Planes

Let $\Pi_0 \in \mathcal{F}_{hkl}$ be the plane defined by the equation $hu + kv + lw = 0$; see (7.17). Let $\mathbf{H}_{hkl}$ be the reciprocal lattice vector defined by $\mathbf{H}_{hkl} = h\boldsymbol{b}_1^* + k\boldsymbol{b}_2^* + l\boldsymbol{b}_3^*$. For each $\boldsymbol{u} \in \Pi_0$, we have $\mathbf{H}_{hkl} \cdot \boldsymbol{u} = hu + kv + lw = 0$. Hence the reciprocal lattice vector $\mathbf{H}_{hkl}$ is normal to the (hkl) lattice planes.

To determine the distance between two adjacent (hkl) planes, it suffices to find the distance of the origin $O \in \Pi_0$ from Π_1. Let $P \in \Pi_1$. The required distance is

$$d_{hkl} = \left| \frac{\mathbf{H}_{hkl}}{\|\mathbf{H}_{hkl}\|} \cdot \mathbf{OP} \right| = \frac{1}{\|\mathbf{H}_{hkl}\|}. \tag{7.19}$$

We summarize these findings as a proposition.

Proposition 7.5 *(a) The reciprocal lattice vector* $\mathbf{H}_{hkl} = h\boldsymbol{b}_1^* + k\boldsymbol{b}_2^* + l\boldsymbol{b}_3^*$ *is normal to the* (hkl) *planes. (b) The distance between two adjacent* (hkl) *planes is* $d_{hkl} = 1/\|\mathbf{H}_{hkl}\|$. □

[96] Any plane in V which contains a lattice point is called a lattice plane.

[97] For a given $m \in \mathbb{Z}$, if $\gcd(h, k, l) = n > 1$ and m is not divisible by n, the linear diophantine equation (7.18) does not have a solution. Hence the coprime condition on the integers h, k, l here is essential in defining the (hkl) lattice planes.

7.4.2 Fictitious Lattice Planes and Higher-Order Bragg Reflections

In 1912 W.L. Bragg [43] pointed out that when an X-ray beam falls on a crystal, if the wavelength λ and the angle of incidence $\pi/2 - \theta$ of the incident beam satisfy the equation (now called the Bragg equation)

$$2d_{hkl} \sin\theta = n\lambda, \qquad (n = 1, 2, 3, \ldots) \tag{7.20}$$

then constructive interference of secondary radiations from the atoms of the crystal will result in a "reflected" beam that obeys Snell's law as if the parallel (hkl) planes of the crystal serve as atomic mirrors. The natural number n in (7.20) specifies the order of the Bragg reflection in question. See Sect. D.4.2 for more details.

In (7.20), d_{hkl} satisfies (7.19) and the integers h, k, and l are coprime, i.e., their greatest common divisor satisfies $\gcd(h, k, l) = 1$. Consider $(h', k', l') \in \mathbb{Z}^3$ such that

$$(h', k', l') = (nh, nk, nl) = n(h, k, l), \qquad \text{where } n \geq 2. \tag{7.21}$$

Since $\|\mathbf{H}_{h'k'l'}\| = n\|\mathbf{H}_{hkl}\|$, equation (7.19) formally gives $d_{h'k'l'} = d_{hkl}/n$. By rewriting (h', k', l') as (h, k, l) and by relaxing the condition that $\gcd(h, k, l) = 1$, we recast the Bragg equation as

$$2d_{hkl} \sin\theta = \lambda, \tag{7.22}$$

and we define $n := \gcd(h, k, l)$ as the order of the Bragg reflection. For a monochromatic incident beam, different orders of Bragg reflection correspond to different Bragg angles θ and thence different spots or locations in the diffraction pattern. By rewriting the Bragg equation as (7.22) and relaxing the coprime requirement on the indices h, k, l so that different reciprocal lattice vectors $\mathbf{H}_{hkl}$ are assigned to different orders of Bragg reflection, we open up the entire reciprocal lattice and reciprocal space for the description of X-ray diffraction. On the other hand, it should be noted that an (hkl) plane with $\gcd(h, k, l) \geq 2$ need not contain a lattice point and hence need not be a real lattice plane.

Remark 7.6 Let $(H, K, L) = (h, k, l)/\gcd(h, k, l)$. Henceforth we will denote by $\mathcal{F}_{HKL}$ the family of real lattice planes to which the reciprocal lattice vector $\mathbf{H}_{hkl}$ is normal. Cf. Footnote 97. □

7.5 Metric Tensors

In this section (except for Examples 7.7 and 7.8) we shall use the index notation (i.e., $\boldsymbol{a}_1$ for $\boldsymbol{a}$, $\boldsymbol{a}^1$ for $\boldsymbol{a}^*$, $\boldsymbol{a}_2$ for $\boldsymbol{b}$, etc.) and the Einstein summation convention for vectors and tensors (see Sect. 1.2).

Let $\{\boldsymbol{a}_i\}$ be the chosen lattice basis of the primitive sublattice $\mathsf{L}^{(p)}$ of a Bravais lattice, and let $\{\boldsymbol{a}^i\}$ be the corresponding reciprocal basis. Let

$$g_{ij} := \boldsymbol{a}_i \cdot \boldsymbol{a}_j, \qquad g^{ij} := \boldsymbol{a}^i \cdot \boldsymbol{a}^j. \tag{7.23}$$

Note that the expressions g_{ij} and g^{ij} are symmetric, i.e., $g_{ij} = g_{ji}$ and $g^{ij} = g^{ji}$ for all i and j. For $\boldsymbol{u} = u^i \boldsymbol{a}_i$ and $\boldsymbol{v} = v^j \boldsymbol{a}_j$ in the direct space V, we have

$$\boldsymbol{u} \cdot \boldsymbol{v} = u^i \boldsymbol{a}_i \cdot v^j \boldsymbol{a}_j = u^i v^j (\boldsymbol{a}_i \cdot \boldsymbol{a}_j) = g_{ij} u^i v^j. \tag{7.24}$$

Similarly, for $\boldsymbol{u} = u_i \boldsymbol{a}^i$ and $\boldsymbol{v} = v_j \boldsymbol{a}^j$ in the reciprocal space $\tau(V^*)$, we obtain

$$\boldsymbol{u} \cdot \boldsymbol{v} = u_i \boldsymbol{a}^i \cdot v_j \boldsymbol{a}^j = u_i v_j (\boldsymbol{a}^i \cdot \boldsymbol{a}^j) = g^{ij} u_i v_j. \tag{7.25}$$

The second-order symmetric tensors

$$\boldsymbol{G} := g_{ij} \boldsymbol{a}^i \otimes \boldsymbol{a}^j, \qquad \boldsymbol{G}^* := g^{ij} \boldsymbol{a}_i \otimes \boldsymbol{a}_j \tag{7.26}$$

are called the metric tensors in the direct space V and reciprocal space $\tau(V^*)$, respectively. The dot products in (7.24)–(7.25) can be written in terms of the metric tensors as follows:

$$\boldsymbol{u} \cdot \boldsymbol{v} = \boldsymbol{u} \cdot \boldsymbol{G} \boldsymbol{v} = u^i \boldsymbol{a}_i \cdot \left(g_{kl} \boldsymbol{a}^k \otimes \boldsymbol{a}^l \right) v^j \boldsymbol{a}_j = g_{ij} u^i v^j \qquad \text{in } V; \tag{7.27}$$

$$\boldsymbol{u} \cdot \boldsymbol{v} = \boldsymbol{u} \cdot \boldsymbol{G}^* \boldsymbol{v} = u_i \boldsymbol{a}^i \cdot \left(g^{kl} \boldsymbol{a}_k \otimes \boldsymbol{a}_l \right) v_j \boldsymbol{a}^j = g^{ij} u_i v_j \qquad \text{in } \tau(V^*). \tag{7.28}$$

Since $\tau(V^*) = V$, mathematically a vector $\boldsymbol{u} \in V$ is also an element of $\tau(V^*)$ and vice versa. As a vector in V, $\boldsymbol{u} = u^i \boldsymbol{a}_i$; as a member of $\tau(V^*)$, $\boldsymbol{u} = u_i \boldsymbol{a}^i$. By (1.39), (1.40), and (7.23), we have

$$g_{ij} u^j = (\boldsymbol{a}_i \cdot \boldsymbol{a}_j) u^j = \boldsymbol{a}_i \cdot \boldsymbol{u} = u_i, \tag{7.29}$$

$$g^{ij} u_j = (\boldsymbol{a}^i \cdot \boldsymbol{a}^j) u_j = \boldsymbol{a}^i \cdot \boldsymbol{u} = u^i. \tag{7.30}$$

Thus g_{ij} and g^{ij} can be used to lower and raise the component index of a vector, respectively. Similarly for any $\boldsymbol{u} \in V$,

$$. \left(g_{ij} \boldsymbol{a}^j \right) \cdot \boldsymbol{u} = g_{ij} u^j = u_i = \boldsymbol{a}_i \cdot \boldsymbol{u}, \tag{7.31}$$

$$\left(g^{ij} \boldsymbol{a}_j \right) \cdot \boldsymbol{u} = g^{ij} u_j = u^i = \boldsymbol{a}^i \cdot \boldsymbol{u}. \tag{7.32}$$

As the vector $\boldsymbol{u}$ is arbitrary in (7.31) and (7.32), we obtain

$$g_{ij} \boldsymbol{a}^j = \boldsymbol{a}_i, \qquad g^{ij} \boldsymbol{a}_j = \boldsymbol{a}^i. \tag{7.33}$$

Moreover, we have

$$\boldsymbol{G}(u^k \boldsymbol{a}_k) = (g_{ij} \boldsymbol{a}^i \otimes \boldsymbol{a}^j) u^k \boldsymbol{a}_k = g_{ij} \delta^j{}_k u^k \boldsymbol{a}^i = g_{ij} u^j \boldsymbol{a}_i = u_i \boldsymbol{a}^i, \tag{7.34}$$

where we have used (7.29) at the last step. Similarly, there holds

$$\boldsymbol{G}^*(u_k \boldsymbol{a}^k) = u^i \boldsymbol{a}_i. \tag{7.35}$$

For each $\boldsymbol{v} \in V$, since

$$g^{ij} g_{jk} v^k = g^{ij} v_j = v^i \qquad \text{and} \qquad \delta^i{}_k v^k = v^i, \tag{7.36}$$

we have

$$g^{ij} g_{jk} = \delta^i{}_k. \tag{7.37}$$

Thus we arrive at the matrix equation

$$[g^{ij}][g_{jk}] = [\delta^i{}_j], \qquad \text{or} \qquad [g^{ij}] = [g_{ij}]^{-1}. \tag{7.38}$$

Example 7.7 Consider a lattice L that belongs to a Bravais lattice type in the cubic system. Its sublattice $\mathsf{L}^{(p)}$ has only one undetermined cell parameter, namely a. We choose a Cartesian coordinate system with orthonormal basis $\boldsymbol{e}_i$ $(i = 1, 2, 3)$ such that the lattice basis vectors of $\mathsf{L}^{(p)}$ are as follows:

$$\boldsymbol{a} = a\,\boldsymbol{e}_1, \qquad \boldsymbol{b} = a\,\boldsymbol{e}_2, \qquad \boldsymbol{c} = a\,\boldsymbol{e}_3. \tag{7.39}$$

It follows immediately that the corresponding reciprocal basis is given by the vectors

$$\boldsymbol{a}^* = \frac{1}{a}\,\boldsymbol{e}_1, \qquad \boldsymbol{b}^* = \frac{1}{a}\,\boldsymbol{e}_2, \qquad \boldsymbol{c}^* = \frac{1}{a}\,\boldsymbol{e}_3. \tag{7.40}$$

Following common practice in crystallography, we use the symbols $\boldsymbol{G}$, $\boldsymbol{G}^*$ for the metric tensors to denote also the matrices $[g_{ij}]$ and $[g^{ij}]$ that represent them under the direct and reciprocal basis, respectively. Thus by (7.23), (7.39), and (7.40), we obtain

$$\boldsymbol{G} = [g_{ij}] = \operatorname{diag}[a^2, a^2, a^2], \qquad \boldsymbol{G}^* = [g^{ij}] = \operatorname{diag}[1/a^2, 1/a^2, 1/a^2]. \tag{7.41}$$

For reciprocal lattice vector $\mathbf{H}_{hkl} = h\boldsymbol{a}^* + k\boldsymbol{b}^* + l\boldsymbol{c}^*$, we have

$$\|\mathbf{H}_{hkl}\|^2 = \mathbf{H}_{hkl} \cdot \boldsymbol{G}^*\mathbf{H}_{hkl} = \frac{1}{a^2}\left(h^2 + k^2 + l^2\right), \tag{7.42}$$

which by (7.19) delivers the formula

$$d_{hkl} = \frac{a}{\sqrt{h^2 + k^2 + l^2}} \tag{7.43}$$

for the distance between two adjacent (hkl) planes. □

Example 7.8 The hexagonal crystal system has only one Bravais lattice type, namely primitive hexagonal (hp). An hp lattice L has two undetermined cell parameters, namely a and c. We choose a Cartesian coordinate system with orthonormal basis $\boldsymbol{e}_i$ $(i = 1, 2, 3)$ such that the lattice basis vectors of L are as follows:

$$\boldsymbol{a} = a\,\boldsymbol{e}_1, \qquad \boldsymbol{b} = a\left(-\frac{1}{2}\boldsymbol{e}_1 + \frac{\sqrt{3}}{2}\boldsymbol{e}_2\right), \qquad \boldsymbol{c} = c\,\boldsymbol{e}_3. \tag{7.44}$$

Substituting (7.44) into (7.14), we obtain

$$\boldsymbol{a}^* = \frac{1}{a}\left(\boldsymbol{e}_1 + \frac{1}{\sqrt{3}}\boldsymbol{e}_2\right), \qquad \boldsymbol{b}^* = \frac{2}{a\sqrt{3}}\,\boldsymbol{e}_2, \qquad \boldsymbol{c}^* = \frac{1}{c}\,\boldsymbol{e}_3. \tag{7.45}$$

Using (7.23), (7.44), and (7.45), we obtain the matrices $[g_{ij}]$ and $[g^{ij}]$ as follows:

$$\boldsymbol{G} = \begin{pmatrix} a^2 & -\frac{a^2}{2} & 0 \\ -\frac{a^2}{2} & a^2 & 0 \\ 0 & 0 & c \end{pmatrix}, \qquad \boldsymbol{G}^* = \begin{pmatrix} \frac{4}{3a^2} & \frac{2}{3a^2} & 0 \\ \frac{2}{3a^2} & \frac{4}{3a^2} & 0 \\ 0 & 0 & \frac{1}{c^2} \end{pmatrix}. \tag{7.46}$$

For reciprocal lattice vector $\mathbf{H}_{hkl} = h\boldsymbol{a}^* + k\boldsymbol{b}^* + l\boldsymbol{c}^*$, we have

$$\|\mathbf{H}_{hkl}\| = \sqrt{\mathbf{H}_{hkl} \cdot \boldsymbol{G}^*\mathbf{H}_{hkl}} = \sqrt{\frac{4(h^2 + hk + k^2)}{3a^2} + \frac{l^2}{c^2}}, \tag{7.47}$$

from which we obtain an explicit formula for $d_{hkl} = 1/\|\mathbf{H}_{hkl}\|$. □

7.6 Description of Orientations of Lattice Basis by Miller Indices

Let L be the chosen lattice of an ideal crystal with basis $\boldsymbol{a}$, $\boldsymbol{b}$, and $\boldsymbol{c}$, and let a spatial Cartesian coordinate system be given. The Miller indices $(HKL)[UVW]$ provide a simple way to describe the orientation of the basis $\boldsymbol{a}$, $\boldsymbol{b}$, and $\boldsymbol{c}$ of L with respect to the given Cartesian coordinate system.

In the Miller indices $(HKL)[UVW]$ the symbol (HKL), where H, K, and L are meant to be coprime integers (i.e., their greatest common divisor $\gcd(H, K, L) = 1$), refers to the family of (HKL) lattice planes, to which the non-trivial reciprocal lattice vector $\mathbf{H} = H\boldsymbol{a}^* + K\boldsymbol{b}^* + L\boldsymbol{c}^*$ is normal.[98] Let $\Pi_0 = \{\boldsymbol{u} \in V : \mathbf{H} \cdot \boldsymbol{u} = 0\}$ the lattice plane that is orthogonal to $\mathbf{H}$ and passes through the origin. The lattice plane Π_0 contains an infinite number of lattice points (cf. assertion (iii) in Sect. 7.4). The symbol $[UVW]$, where U, V, and W are also coprime integers, denotes the lattice direction in L specified by a lattice vector $U\boldsymbol{a} + V\boldsymbol{b} + W\boldsymbol{c} \in \Pi_0$. Thus the two 3-tuples (H, K, L) and $(U, V, W) \in \mathbb{Z}^3$ satisfy the condition that $HU + KV + LW = 0$.

The ordered sextet $(HKL)[UVW]$ gives the Miller indices of the orientation of L such that the reciprocal lattice vector $H\boldsymbol{a}^* + K\boldsymbol{b}^* + L\boldsymbol{c}^*$ and the lattice vector $U\boldsymbol{a} + V\boldsymbol{b} + W\boldsymbol{c}$ point in the 3- and 1-direction of the given Cartesian coordinate system, respectively. In the symbol $(HKL)[UVW]$, the negative sign of a negative integer is shown as an overhead bar; e.g., $\bar{1}$ stands for -1.

As the numbers in $(HKL)[UVW]$ are integers, it is clear that not all orientations can be described exactly by this notation. But, under some precise sense (cf. Sect. 1.10), any orientation of a crystal can be approximated as closely as we please by some orientation defined by the Miller indices.

7.6.1 Cubic Crystallites in a Sheet Metal

Let C be an ideal crystal,[99] the Bravais lattice of which can be of type cP (primitive), cF (face-centered), or cI (body-centered). We shall be concerned only with the primitive sublattice $\mathsf{L}^{(p)}$. The basis lattice vectors $\boldsymbol{a}$, $\boldsymbol{b}$, $\boldsymbol{c}$ of $\mathsf{L}^{(p)}$ are orthogonal and of the same length. By changing the unit of length, we may treat the basis vectors as a right-handed orthonormal triad, which we will do. Under this choice of unit of length, the reciprocal lattice is identical to the crystal lattice. In fact, we have $\boldsymbol{a}^* = \boldsymbol{a}$, $\boldsymbol{b}^* = \boldsymbol{b}$, and $\boldsymbol{c}^* = \boldsymbol{c}$, so we need not distinguish reciprocal lattice vectors from direct lattice vectors.

Sheet metals have three distinct directions: the rolling (RD), transverse (TD), and normal direction (ND). Whenever we talk about sheet metals, unless stated otherwise we shall use a spatial coordinate system whose 1-, 2-, and 3-axis coincides with RD, TD, and ND, respectively. Let $\boldsymbol{e}_1$, $\boldsymbol{e}_2$, and $\boldsymbol{e}_3$ be orthonormal basis vectors associated with the chosen spatial coordinate system.

Consider a sheet metal, which is a polycrystalline aggregate of cubic crystallites of the same kind as C. To describe the orientation of a crystallite $\mathcal{B}_\alpha$ in the polycrystalline metal sheet, we choose a reference placement $\boldsymbol{\kappa}_0$ of C such that the basis lattice vectors $\boldsymbol{a}$, $\boldsymbol{b}$, and $\boldsymbol{c}$ agree with the spatial basis $\boldsymbol{e}_1$, $\boldsymbol{e}_2$, and $\boldsymbol{e}_3$, respectively. We imagine that the crystallite $\mathcal{B}_\alpha$ in question be extended by periodicity so that it occupies all space and can be taken as a rotated copy of C. The orientation of $\mathcal{B}_\alpha$ in the metal sheet is then characterized by the rotation $\boldsymbol{R}$ which takes the basis vectors $\boldsymbol{a}$, $\boldsymbol{b}$, and $\boldsymbol{c}$ of C to their rotated counterparts, respectively. The

[98] See Sect. 7.4 and, in particular, Remark 7.6.

[99] The reference placement $\boldsymbol{\kappa}_0$ of C will be chosen later.

rotation $\boldsymbol{R}$ can be described by Euler angles or by the axis-angle parameters $(\boldsymbol{n}, \omega)$ as discussed in Sects. 1.7 and 1.9, respectively. Here we determine the rotation matrix pertaining to the orientation defined by the Miller indices $(HKL)[UVW]$.

Under the present circumstances, the notation $(HKL)[UVW]$ describes the orientation which has the following properties: the (HKL) planes of the crystallite are parallel to the sheet plane, and the $[UVW]$ crystal direction agrees with the rolling direction. Note that the first condition is equivalent to the requirement that the (H, K, L) vector points in the normal direction. Since RD $\perp$ ND, the requirement that

$$(H, K, L) \cdot (U, V, W) = 0 \tag{7.48}$$

is verified.

Let $\widetilde{\boldsymbol{e}}_3 = (H/M, K/M, L/M)$, $\widetilde{\boldsymbol{e}}_1 = (U/N, V/N, W/N)$, and $\widetilde{\boldsymbol{e}}_2 = \widetilde{\boldsymbol{e}}_3 \times \widetilde{\boldsymbol{e}}_1$, where $M = \sqrt{H^2 + K^2 + L^2}$ and $N = \sqrt{U^2 + V^2 + W^2}$. Then $\boldsymbol{R}$ is defined by $\boldsymbol{R}\widetilde{\boldsymbol{e}}_i = \boldsymbol{e}_i$ for $i = 1, 2, 3$. Under the basis $\{\boldsymbol{e}_i\}$, the rotation $\boldsymbol{R}$ is represented by the matrix $[\boldsymbol{e}_i \cdot \boldsymbol{R}\boldsymbol{e}_j] = [(\boldsymbol{R}^T \boldsymbol{e}_i) \cdot \boldsymbol{e}_j] = [\widetilde{\boldsymbol{e}}_i \cdot \boldsymbol{e}_j]$ or

$$\begin{pmatrix} \frac{U}{N} & \frac{V}{N} & \frac{W}{N} \\ \frac{KW-LV}{MN} & \frac{LU-HW}{MN} & \frac{HV-KU}{MN} \\ \frac{H}{M} & \frac{K}{M} & \frac{L}{M} \end{pmatrix}. \tag{7.49}$$

In materials science, particular orientations $(HKL)[UVW]$ of cubic crystallites are given proper names. For example, Cube = (100)[001]; R-Cube = (100)[011]; Goss = (110)[001]; Copper = (112)[11$\bar{1}$]; S = (123)[63$\bar{4}$]; Brass = (110)[$\bar{1}$12].

Example 7.9 Let us determine the Euler angles (ψ, θ, ϕ) and axis-angle parameters $(\boldsymbol{n}, \omega)$ pertaining to the Goss orientation (110)[001].

By expression (7.49), the rotation matrix defining the (110)[001] orientation is

$$\begin{pmatrix} 0 & 0 & 1 \\ \frac{1}{\sqrt{2}} & -\frac{1}{\sqrt{2}} & 0 \\ \frac{1}{\sqrt{2}} & \frac{1}{\sqrt{2}} & 0 \end{pmatrix}.$$

Comparing the third row of this matrix with that of expression (1.89), we have

$$R_{31} = -\sin\theta\cos\phi = \frac{1}{\sqrt{2}}, \quad R_{32} = \sin\theta\sin\phi = \frac{1}{\sqrt{2}}, \quad R_{33} = \cos\theta = 0,$$

from which we conclude that $\theta = \pi/2$ and $\phi = 3\pi/4$. Similarly, by comparing the third column of the two matrices we obtain

$$R_{13} = \sin\theta\cos\psi = 1, \qquad R_{23} = \sin\theta\sin\psi = 0.$$

Since $\theta = \pi/2$, we must have $\psi = 0$.

From (1.113), we observe that

$$\cos\omega = \frac{1}{2}(-\frac{1}{\sqrt{2}} - 1).$$

Therefore $\omega \approx 148.6^\circ$. From (1.114), we obtain

$$(n_1, n_2, n_3) = \left(\frac{1}{\sqrt{5-2\sqrt{2}}}, \frac{\sqrt{2}-1}{\sqrt{5-2\sqrt{2}}}, \frac{1}{\sqrt{5-2\sqrt{2}}}\right)$$
$$\approx (0.6786, 0.2811, 0.6786),$$

and $\Theta \approx 47.27^\circ$, $\Phi = 22.5^\circ$.

While the algebraic method used above for finding the Euler angles corresponding to a given rotation matrix is generally preferable, it is instructive to repeat this simple example by determining (ψ, θ, ϕ) geometrically. Let $\widetilde{\boldsymbol{e}}_1 = (0, 0, 1)$, $\widetilde{\boldsymbol{e}}_3 = (1, 1, 0)/\sqrt{2}$, and $\widetilde{\boldsymbol{e}}_2 = \widetilde{\boldsymbol{e}}_3 \times \widetilde{\boldsymbol{e}}_1 = (1, -1, 0)/\sqrt{2}$. The rotation $\boldsymbol{R}$ we seek satisfies $\boldsymbol{R}\widetilde{\boldsymbol{e}}_i = \boldsymbol{e}_i$ for each i. It is easier to determine first the Euler angles $(\psi^\#, \theta^\#, \phi^\#)$ pertaining to $\boldsymbol{R}^{-1}$ and then use formulae (1.95)–(1.97) to find those pertaining to $\boldsymbol{R}$. For the present example, clearly the line of nodes lies in the X_1-X_2 plane and is given by the equation $x_2 = -x_1$. Hence either $\psi^\# = \pi/4$ or $\psi^\# = 3\pi/4$. A simple trial and error shows that the correct $\mathbf{OL} = (-1, -1, 0)/\sqrt{2}$, $\psi^\# = \pi/4$, $\boldsymbol{R}(\mathbf{OL}, \pi/2)\boldsymbol{e}_3 = \widetilde{\boldsymbol{e}}_3$, and $\boldsymbol{R}(\mathbf{OL}, \pi/2)\boldsymbol{R}(\boldsymbol{e}_3, \pi/4)\boldsymbol{e}_1 = -\boldsymbol{e}_3$. Finally it is easy to see that $\boldsymbol{R}(\widetilde{\boldsymbol{e}}_3, \pi)\mathbf{OL} = \widetilde{\boldsymbol{e}}_2$, and $\boldsymbol{R}(\widetilde{\boldsymbol{e}}_3, \pi)(-\boldsymbol{e}_3) = \boldsymbol{e}_3 = \widetilde{\boldsymbol{e}}_1$. Therefore $(\psi^\#, \theta^\#, \phi^\#) = (\pi/4, \pi/2, \pi)$ and $(\psi, \theta, \phi) = (0, \pi/2, 3\pi/4)$. □

Chapter 8

8 Texture Approximation by Individual Orientation Measurements

8.1 Introduction

So far we have been talking about orientation measures defined by square-integrable orientation distribution functions w, each of which can be taken as being specified by its texture coefficients c^l_{mn}. An example discussed in Sect. 3.1, however, concerns an ensemble of a single triclinic crystal C at orientation $\boldsymbol{R}_o$ with respect to the chosen reference configuration $\boldsymbol{\kappa}_0(\mathrm{C})$. There it is pointed out that the orientation measure in question should be the Dirac measure $\delta_{\boldsymbol{R}_o}$ as given by (3.2), which cannot be expressed in terms of a continuously distributed density function. How can we resolve this conceptual gap?

As we shall see in Sect. 8.2, a so-called "vague topology" can be defined on the space of orientation measures under which both the ODFs and the discrete orientation measures $\wp = \sum_i a_i \delta_{x_i}$ (where x_i denote orientations; $\sum_i a_i = 1, a_i > 0$ for each i) constitute "dense" subsets. Some consequences are:

1. Each Dirac measure can be unambiguously assigned its texture coefficients as the limits of corresponding c^l_{mn} of orientation measures defined by ODFs.
2. Every orientation measure, including those defined by ODFs, in principle can be approximated by individual orientation measurements.

Assertion 2 above serves as the theoretical basis for texture evaluation by individual orientation measurements, including the EBSD (electron backscatter diffraction) or OIM (orientation imaging microscopy) technique, which, as compared with inversion of X-ray pole figures, enjoys the advantage that no "ghost correction" is necessary.

8.1.1 EBSD and "Ghost Correction"

The introduction of the orientation distribution function (ODF) and of the harmonic method for evaluation of texture coefficients through inversion of X-ray pole figures marked the birth of quantitative texture analysis (QTA) in the 1960s. For an ODF w, let $w^{(\mathrm{e})}$ be the corresponding "reduced" ODF which results when the terms with odd l in the series expansion $\sum_l \sum_{m,n} c^l_{mn} D^l_{mn}$ of w are deleted, i.e., $w^{(\mathrm{e})}$ is the l-even part of the "true" ODF w. In routine preparations of X-ray pole figures in the laboratory, Friedel's rule (see Sect. D.6 in Appendix D) is in force. The physics of X-ray diffraction (XRD) then dictates the mathematical consequence (see Sect. 9.3) that pole figures depend only on texture coefficients c^l_{mn} with even l, and that they do not carry any information on texture coefficients with odd l. Unfortunately, while Bunge [57] and Roe [270]—pioneers of the harmonic method—were aware of Friedel's rule and its effects on pole figures, both initially imposed the l-even property of pole figures as an intrinsic restriction to the series expansion of the ODF. As a result, in the 1960s and much of the 1970s, although the ODFs reproduced from pole figures were the "reduced" ODFs $w^{(\mathrm{e})}$, they were commonly regarded as the "true" ODFs w. In practice anomalies sometimes arose (see, e.g., [193] and the references therein): Such ODFs, in addition to the true maxima (but with heights reduced), included false maxima (called "ghosts"), "strong fluctuations at low intensities and even rather strong negative values of the ODF", which were sometimes attributed to truncation error of the ODF series expansion [59, 63]. After Matthies [214] and others (see, e.g., [193]) showed definitively that the ghost phenomena were caused by the unwitting replacement of the ODF w by its l-even part $w^{(\mathrm{e})}$, various

"ghost-correction" methods and algorithms[100] for inversion of pole figures were proposed in the 1980s and 1990s. Meanwhile, single-orientation measurements by electron backscatter diffraction (EBSD) in the scanning electron microscope (SEM), which enjoy the major advantage over inversion of pole figures in that they deliver direct approximations to the "true" ODF w (i.e., no ghost-correction is necessary), has gradually emerged as the preferable method for determination of texture of materials that the technique is applicable (cf. [291], [293, Sect. 1.6]).

It has long been demonstrated that the ODF can be determined experimentally by single-orientation measurements. For instance Bunge and Haessner [63], in a 1968 paper, compare the ODFs of a cold-rolled copper as determined by single-orientation measurements through selected-area electron diffraction and by inversion of X-ray pole figures. But up until the end of the 1980s, as remarked by Wright and Adams [346], "the number of single orientation measurements required to calculate a statistically reliable ODF has generally been considered too large to practically obtain." The situation began to change in the 1990s when EBSD in the SEM became a fully automated technique. Subsequent technological and software advances have made EBSD a common laboratory-based tool for orientation microscopy today. By means of EBSD, large quantity of individual orientation data of a sample can now be collected and analyzed online so rapidly [52, 251, 292, 293] that the speed of measurement has become a distinct advantage of EBSD over the route through preparation of X-ray pole figures.

In this chapter we shall examine the mathematical basis behind and several issues around determination of an approximate ODF from single-orientation measurements in general and such measurements by EBSD in particular. Before we do that in Sect. 8.5, we derive some formulas that we shall use there. In particular, in Sect. 8.4 we introduce the notions of model functions and texture components, which we shall also need when we discuss inversion of X-ray pole figures in the next chapter.

8.2 Mathematical Preliminaries

In this section we introduce some mathematical terms so that our discussion can be put in a precise language. Readers who elect not to go into mathematical details may skip this section, go directly to Sect. 8.3, and return to read this section as necessary.

The rotation group SO(3) is a compact[101] metric space. The distance function $d_{\mathrm{SO}(3)}(\cdot,\cdot)$ is the misorientation angle between two rotations (see Sect. 1.10). It is also the Riemannian distance when SO(3) is taken as an embedded submanifold of M(3), the linear space of 3×3 real matrices with inner product defined by $\boldsymbol{A}\cdot\boldsymbol{B}=\frac{1}{2}\mathrm{tr}(\boldsymbol{A}\boldsymbol{B}^T)$; see Sects. 10.1 and 10.2. The orientation space $M:=\mathrm{SO}(3)/G_{\mathrm{cr}}$ is compact because the projection $\pi:\mathrm{SO}(3)\to M$ is a continuous open surjection. It is also a metric space. The distance function $d_M(\cdot,\cdot)$ on M is the disorientation angle between two orientations (see Sect. 6.4), which is also the Riemannian distance when M is given the Riemannian metric such that the natural surjection $\pi:\mathrm{SO}(3)\to M$ is a local isometry (see Sect. 10.4). Since the projection $\hat{\pi}:M\to M/G_{\mathrm{tex}}$ is also a continuous open surjection, M/G_{tex} (i.e., the space of G_{tex}-orbits of orientations in M) is compact and has a countable base [97, p. 174]. Moreover, by Proposition B.19

[100] We shall discuss a couple of these methods in Chap. 9.

[101] There are two different definitions of "compact topological space" in the references cited in the bibliography of this exposition. Here we adopt the one given in Definition B.6, which seems to have increasingly gained wider acceptance. Some authors who use the other definition call a space that satisfies Definition B.6 "quasi-compact". To these authors "compact" means "quasi-compact and Hausdorff". See Remark B.7 for more details.

in Appendix B, M/G_{tex} is a Hausdorff space. Hence M/G_{tex} is metrizable (see Theorem B.10).

Let X be a compact metric or metrizable space, and let $\mathscr{C}(X)$ be the space of real-valued continuous functions defined on X. A (positive) Radon measure[102] on X is a positive linear functional $\mu : \mathscr{C}(X) \to \mathbb{R}$, $f \mapsto \langle \mu, f \rangle$, such that $\langle \mu, f \rangle \geq 0$ whenever $f \geq 0$. Let $\mathscr{M}_+(X)$ be the set of positive Radon measures on X. By the Riesz representation theorem (see Theorem C.8 in Appendix C), each Radon measure μ on $\mathscr{C}(X)$ determines a unique finite, positive Borel measure (cf. Definition C.4) on X, which we denote also by μ (cf. Remark C.10), such that for each $f \in \mathscr{C}(X)$ the value of the Radon measure μ at f is given by the Lebesgue integral with respect to the corresponding Borel measure:

$$\langle \mu, f \rangle = \int_X f \, d\mu. \tag{8.1}$$

In the context of general probability theory, a probability space is a triple $(\Omega, \mathfrak{M}, P)$, where Ω is a set called the sample space, $\mathfrak{M}$ a σ-algebra of subsets of Ω, and P a positive measure on Ω that satisfies $P(\Omega) = 1$. In our present context where the sample space X is a compact metric space, we may say that a probability space is an ordered pair (X, μ), where $\mu \in \mathscr{M}_+(X)$ is a positive Radon measure that satisfies $\langle \mu, 1 \rangle = 1$. Alternatively, the probability space can be described as $(X, \mathfrak{B}, \mu)$, where $\mathfrak{B}$ is the Borel σ-algebra in X and μ (with $\mu(X) = 1$) is the Borel measure on $\mathfrak{B}$ corresponding to its Radon-measure namesake. In either representation we call μ a probability measure on X and denote by $\mathscr{P}(X)$ the set of probability measures on X.

The Dirac measure at $x \in X$, namely δ_x, is the probability measure defined as follows:

$$\delta_x(A) := \begin{cases} 1 & \text{if } x \in A \\ 0 & \text{if } x \notin A, \end{cases} \quad \text{for each Borel set } A \subset X. \tag{8.2}$$

It follows immediately from (8.1) and (8.2) that

$$\langle \delta_x, f \rangle = f(x) \tag{8.3}$$

A probability measure μ of the form

$$\mu = \sum_{i=1}^{K} a_i \delta_{x_i}, \qquad \left(x_1, \ldots, x_K \in X; \ \sum_{i=1}^{K} a_i = 1, \ \ a_i > 0 \text{ for each } i \right), \tag{8.4}$$

i.e., a convex combination of Dirac measures, is said to be discrete. Let $\mathscr{P}_d(X) \subset \mathscr{P}(X)$ denote the set of discrete probability measures. We endow $\mathscr{P}(X)$ with a topology, called the vague topology,[103] under which $\mathscr{P}(X)$ is compact and metrizable [25, p. 208]. Moreover, $\mathscr{P}_d(X)$ is dense in $\mathscr{P}(X)$ in the following sense: For any given probability measure $\mu \in$

[102] The term "Radon measure" has been used in different senses. Our usage here follows that of the French school (cf. the remarks and references at the end of each chapter in Part 1 of [318]). Another common usage takes a Radon measure as a Borel measure that satisfies certain regularity conditions; see, e.g., [25, p. 155]. When X is a compact metrizable space, the Borel measure on the right-hand side of (8.1) is a Radon measure in this sense [25, p. 185]. See Remarks C.9, C.10, and the paragraph that contains equation (C.4) in Appendix C for more detailed discussions.

[103] Cf. [206] and the references therein for details and proofs. Note that in [206] a compact space is a Hausdorff space that satisfies Definition B.6.

$\mathscr{P}(X)$, there is a sequence of discrete probability measures μ_n $(n = 1, 2, \ldots)$ in $\mathscr{P}_d(X)$ such that $\mu_n \to \mu$ vaguely, i.e.,

$$\lim_{n\to\infty} \int_X f \, d\mu_n = \int_X f \, d\mu, \qquad \text{for each } f \in \mathscr{C}(X). \tag{8.5}$$

Let $\mathscr{C}(X, \mathbb{C})$ be the set of complex-valued continuous functions on X (cf. Sect. 3.6). It follows from (8.5) that if the sequence of discrete probability measures $\{\mu_n\}$ converges vaguely to $\mu \in \mathscr{P}(X)$, then

$$\begin{aligned} \lim_{n\to\infty} \int_X f \, d\mu_n &= \lim_{n\to\infty} \int_X (\mathfrak{Re} f + i\,\mathfrak{Im} f)\, d\mu_n \\ &= \int_X \mathfrak{Re} f \, d\mu + i \int_X \mathfrak{Im} f \, d\mu \\ &= \int_X f \, d\mu, \qquad \text{for each } f \in \mathscr{C}(X, \mathbb{C}). \end{aligned} \tag{8.6}$$

8.3 Texture Coefficients of Discrete Orientations

8.3.1 Texture Coefficients of a Single Crystal

Consider a single triclinic crystal C, a reference configuration $\boldsymbol{\kappa}_0(\mathsf{C})$ of which has been chosen. The orientation space of the single crystal is then the rotation group SO(3). Suppose the single crystal in question has orientation defined by a rotation $\boldsymbol{R}_0$ with respect to the chosen reference configuation $\boldsymbol{\kappa}_0(\mathsf{C})$. As described in Sect. 3.1, the orientation measure of the single triclinic crystal is $\delta_{\boldsymbol{R}_0}$, the Dirac measure at $\boldsymbol{R}_0$. For an orientation measure $\wp$ defined by a square-integrable ODF w, the texture-coefficients pertaining to $\wp$ are given by the formula (cf. (4.50) and (6.27))

$$c^l_{mn} = \frac{2l+1}{8\pi^2} \int_{\mathrm{SO(3)}} \overline{D^l_{mn}(\boldsymbol{R})}\, w(\boldsymbol{R})\, d\mathcal{V}(\boldsymbol{R}) = \frac{2l+1}{8\pi^2} \int_{\mathrm{SO(3)}} \overline{D^l_{mn}(\boldsymbol{R})}\, d\wp(\boldsymbol{R}), \tag{8.7}$$

because $w = d\wp/d\mathcal{V}$. Can texture coefficients be assigned naturally and unambiguously to the Dirac measure $\delta_{\boldsymbol{R}_0}$?

The answer is affirmative. Indeed, the set of orientation measures defined by square-integrable ODFs is dense in $\mathscr{P}(\mathrm{SO(3)})$ with respect to the vague topology (see [254] and Proposition 2.2 of [206]). Hence for any probability measure μ, there exists a sequence of probability measures μ_n, which are defined by square-integrable probability densities and converge vaguely to μ. In particular, there exists a sequence of orientation measures $\wp_n$ defined by ODFs w_n such that $\wp_n \to \delta_{\boldsymbol{R}_0}$ vaguely as $n \to \infty$. The texture coefficients that pertain to the Dirac measure $\delta_{\boldsymbol{R}_0}$ are then given by

$$c^l_{mn} = \lim_{n\to\infty} \frac{2l+1}{8\pi^2} \int_{\mathrm{SO(3)}} \overline{D^l_{mn}(\boldsymbol{R})}\, d\wp_n(\boldsymbol{R}) = \frac{2l+1}{8\pi^2} \langle \delta_{\boldsymbol{R}_0}, \overline{D^l_{mn}(\boldsymbol{R})} \rangle = \frac{2l+1}{8\pi^2} \overline{D^l_{mn}(\boldsymbol{R}_0)}. \tag{8.8}$$

For a single crystal C with chosen reference configuation $\boldsymbol{\kappa}_0(\mathsf{C})$ and $G_{\mathrm{cr}} = \{\boldsymbol{P}_1, \ldots, \boldsymbol{P}_{N_{\mathrm{cr}}}\} \subset \mathrm{SO}(3)$, where $\boldsymbol{P}_1 = \boldsymbol{I}$ and N_{cr} denotes the order of G_{cr}, the orientation space is $\mathrm{SO}(3)/G_{\mathrm{cr}} = \{\boldsymbol{R}G_{\mathrm{cr}} : \boldsymbol{R} \in \mathrm{SO}(3)\}$, where

$$\boldsymbol{R}G_{\mathrm{cr}} = \{\boldsymbol{R}\boldsymbol{P}_1, \ldots, \boldsymbol{R}\boldsymbol{P}_{N_{\mathrm{cr}}}\} \tag{8.9}$$

is the orientation specified by the rotation $\boldsymbol{R}$ with respect to the reference configuration. The orientation measure of a single crystal with orientation $\boldsymbol{R}_0 G_{\mathrm{cr}}$ is the Dirac measure $\delta_{\boldsymbol{R}_0 G_{\mathrm{cr}}}$ at $\boldsymbol{R}_0 G_{\mathrm{cr}}$ in the orientation space $\mathrm{SO}(3)/G_{\mathrm{cr}}$. If we follow Roe's approach and use $\mathrm{SO}(3)$ as the underlying space, by (6.28) the texture coefficients of a square-integrable ODF w are given the formula

$$c^l_{mn} = \frac{2l+1}{8\pi^2} \int\limits_{\mathcal{F}} \left(\sum_{j=1}^{N_{\mathrm{cr}}} \overline{D^l_{mn}(\boldsymbol{R}\boldsymbol{P}_j)} \right) w(\boldsymbol{R})\, d\mathcal{V}(\boldsymbol{R}) \tag{8.10}$$

where $\mathcal{F}$ is a chosen strict fundamental domain for $\mathrm{SO}(3)/G_{\mathrm{cr}}$ in $\mathrm{SO}(3)$. Because the map $\pi|_{\mathcal{F}} : \mathcal{F} \to \mathrm{SO}(3)/G_{\mathrm{cr}}$ is a bijection, one of the equivalent rotations in $\boldsymbol{R}_0 G_{\mathrm{cr}}$ falls in the strict fundamental domain $\mathcal{F}$. As we are free to rename the elements of $\boldsymbol{R}_0 G_{\mathrm{cr}}$, there is no loss in generality to let $\boldsymbol{R}_0 \in \mathcal{F}$. Then, following an argument similar to that used in the derivation of (8.8), by (8.10) we see that the texture coefficients pertaining to the single crystal with orientation $\boldsymbol{R}_0 G_{\mathrm{cr}}$ are given by

$$c^l_{mn} = \frac{2l+1}{8\pi^2} \langle \frac{1}{N_{\mathrm{cr}}} \delta_{\boldsymbol{R}_0}, \sum_{j=1}^{N_{\mathrm{cr}}} \overline{D^l_{mn}(\boldsymbol{R}\boldsymbol{P}_j)} \rangle = \frac{2l+1}{8\pi^2} \cdot \frac{1}{N_{\mathrm{cr}}} \sum_{j=1}^{N_{\mathrm{cr}}} \overline{D^l_{mn}(\boldsymbol{R}_0\boldsymbol{P}_j)}. \tag{8.11}$$

Alternatively, formula (8.11) can be obtained by writing down the orientation measure pertaining to the single crystal in question directly, which by symmetry is clearly the discrete measure on $\mathrm{SO}(3)$ given by

$$\wp = \frac{1}{N_{\mathrm{cr}}} \sum_{j=1}^{N_{\mathrm{cr}}} \delta_{\boldsymbol{R}_0\boldsymbol{P}_j}. \tag{8.12}$$

Using (8.8) and (8.12), we obtain

$$c^l_{mn} = \frac{2l+1}{8\pi^2} \langle \wp, \overline{D^l_{mn}(\boldsymbol{R})} \rangle, \tag{8.13}$$

which is the same as (8.11)

Formulas (8.11) and (8.12) reduce to the corresponding formulas for a triclinic crystal when $G_{\mathrm{cr}} = \{\boldsymbol{I}\}$.

8.3.2 Texture Coefficients of Ideal Orientations

In texture analysis, a polycrystal with sample and crystallite symmetry groups G_{tex} and G_{cr}, respectively, is said to have an ideal orientation if its orientation measure is the Dirac measure $\delta_{[\boldsymbol{R}_0 G_{\mathrm{cr}}]}$ for some $[\boldsymbol{R}_0 G_{\mathrm{cr}}] \in M/G_{\mathrm{tex}}$ (see Sect. 6.5.1), where $M := \mathrm{SO}(3)/G_{\mathrm{cr}}$ is the space of crystallite orientations. If we follow Roe's approach and take $\mathrm{SO}(3)$ as the underlying space, similar to the derivation of their counterparts in Sect. 8.3.1, we obtain what

follows. The orientation measure in $\mathscr{P}(\mathrm{SO}(3))$ that corresponds to $\delta_{[\boldsymbol{R}_0 G_{\mathrm{cr}}]}$ in $\mathscr{P}(M/G_{\mathrm{tex}})$ is:

$$\wp = \frac{1}{N_{\mathrm{tex}} N_{\mathrm{cr}}} \sum_{i=1}^{N_{\mathrm{tex}}} \sum_{j=1}^{N_{\mathrm{cr}}} \delta_{\boldsymbol{Q}_i^T \boldsymbol{R}_0 \boldsymbol{P}_j}. \tag{8.14}$$

The texture coefficients pertaining to the orientation measure (8.14) are:

$$c_{mn}^l = \frac{2l+1}{8\pi^2} \cdot \frac{1}{N_{\mathrm{tex}} N_{\mathrm{cr}}} \sum_{i=1}^{N_{\mathrm{tex}}} \sum_{j=1}^{N_{\mathrm{cr}}} \overline{D_{mn}^l(\boldsymbol{Q}_i^T \boldsymbol{R}_0 \boldsymbol{P}_j)}. \tag{8.15}$$

When $G_{\mathrm{tex}} = \{\boldsymbol{I}\}$, equations (8.14) and (8.15) reduce to (8.12) and (8.11), respectively. Hence, orientations of single crystals are, according to the present terminology, also ideal orientations.

Remark 8.1 The formula for texture coefficients of ideal orientations that corresponds to (8.15) in Bunge's approach already appears in his works [56, 57] in the 1960s (cf. also [60, p. 50]). Here we present a derivation in Roe's approach made precise through the mathematical notions of probability measures, Dirac measures, and vague convergence. □

As we shall discuss in more details in the next section, the ODFs of sheet metals often have peaks at some specific ideal orientations, which are given common names and are specified by the Miller indices of a rotation in the class of equivalent rotations pertaining to the ideal orientation in question. For example, for orthorhombic aggregates of cubic crystallites, Cube = (100)[001], Goss = (110)[001], Copper = (112)[11$\bar{1}$], etc., are ideal orientations. The ideal orientation "Cube" specifies one point in $(\mathrm{SO}(3)/O)/D_2$, 4 equivalent single-crystal orientations in $\mathrm{SO}(3)/O$, and $4 \times 24 = 96$ equivalent rotations in SO(3), one of which is the rotation (100)[001]. As an illustration, we list in Table 9 the values of (Roe's) texture coefficients W_{4m0} $(m = 0, 2, 4)$ and W_{6m0} $(m = 0, 2, 4, 6)$ for several ideal orientations in orthorhombic sheets of cubic metals.[104] Our usual choice of reference orientation and spatial coordinate system for such sheet metals (cf. Sect. 7.6.1) is in force here. Note that for orthorhombic aggregates of cubic crystallites each W_{lmn} is real and, by (8.15), is a continuous function defined on SO(3). Hence it attains its maximum and minimum values on SO(3). Let W_{lmn} (max) and W_{lmn} (min) denote the maximum and minimum value of W_{lmn}, respectively. A comparison with the analysis of Paroni [254] reveals what follows. The Cube orientation gives W_{400} (max), W_{440} (max), W_{640} (min); R-Cube: W_{400} (max), W_{440} (min), W_{640} (max); Goss: W_{420} (min), W_{600} (min); Brass: W_{600} (min).

8.4 Model Functions and Texture Components

The ODF w is specified, through its series expansion in terms of the Wigner D-functions, by an infinite number of texture coefficients c_{mn}^l. Even if it would be adequate in applications to truncate the series at $l = 34$, $l = 22$, or in some cases even at $l = 16$, a large number of texture coefficients with no direct physical meaning are still involved. Tracking texture evolution through these changing numbers is uninspiring.

Textures of materials that have undergone specific processing treatments often exhibit definite patterns. In some cases (e.g., in fully annealed aluminum alloy sheets), the texture

[104] We use Roe's coefficients here to facilitate comparison with papers in the literature.

Table 9 Texture coefficients of several ideal orientations for orthorhombic aggregates of cubic crystallites. Cube = (100)[001]; R-Cube = (100)[011]; Goss = (110)[001]; Copper = (112)[11$\bar{1}$]; S = (123)[63$\bar{4}$]; Brass = (110)[$\bar{1}$12]

	Cube	R-Cube	Goss	Copper	S	Brass
W_{400}	.0313	.0313	-.0078	-.0078	-.0078	-.0078
W_{420}	0	0	-.0248	.0083	.0003	-.0083
W_{440}	.0187	-.0187	.0140	-.0109	-.0090	-.0109
W_{600}	.0081	.0081	-.0131	.0041	-.0009	-.0131
W_{620}	0	0	.0052	.0109	.0075	.0017
W_{640}	-.0151	.0151	.0094	-.0027	-.0047	-.0073
W_{660}	0	0	.0077	.0071	-.0029	-.0065

can be qualitatively described as a superposition of several ideal orientations with some spread about them, which before the advent of quantitative texture analysis were called "texture components". The following remarks on texture components are taken from Bunge [62, p. 99]:

> "It may be assumed that the crystallites of a component have been brought into their orientations by the same physical process. This process is further understood as leading to an ideal orientation g_o which is, however, not reached completely (due to some disturbing effects) so that some spread about it occurs.
> "The spread function can be described by a simple mathematical function. This facilitates the mathematical description of a component. It is also assumed that the form of the spread function follows from the physical process which formed the component."

Bunge [57] was the first to introduce a model ODF as mathematical description of such texture components. Bunge's model ODF is within the class of central functions, which we shall examine in detail next. Other central functions, which use a spread function different than Bunge's, have been proposed [216, 224, 225] for the same purpose. Other classes of model ODFs, commonly simply called model functions, have been introduced as mathematical descriptions of texture patterns other than ideal orientations with spread. As we shall see, model functions provide a possible means not only for "data compression" [224, p. 13] but also for the reproduction of the true ODF from pole figures [193, 194].

8.4.1 Texture Components Defined by Central Functions

Here we study central functions, which are mathematical models for texture components that can be roughly described as ideal orientations with spread. To start with, we consider triclinic aggregates of triclinic crystallites. It will be straightforward to rewrite the resulting formulas for the case where $G_{\text{tex}} \neq \{\boldsymbol{I}\}$ and/or $G_{\text{cr}} \neq \{\boldsymbol{I}\}$.

Let $\boldsymbol{R}_0 \in \text{SO}(3)$, and let $\boldsymbol{M}(\widetilde{\boldsymbol{n}}, \widetilde{\omega}) = \boldsymbol{R}\boldsymbol{R}_0^T$ be the misorientation (see Sect. 1.10) that takes $\boldsymbol{R}_0$ to the rotation $\boldsymbol{R}$. A model ODF or model function is called a central function if it assumes the form

$$w(\boldsymbol{R}; \kappa) = w(\boldsymbol{M}(\widetilde{\boldsymbol{n}}, \widetilde{\omega})\boldsymbol{R}_0) = \mathfrak{z}(\widetilde{\omega}; \kappa); \tag{8.16}$$

here $\boldsymbol{R}_0$ is the ideal orientation in question; κ is a parameter; $\mathfrak{z}$, the "spread function", is a non-negative function chosen so that the model function $w(\cdot; \kappa)$ satisfies the normalization condition (cf. (4.44))

$$\int_{\text{SO}(3)} w(\boldsymbol{R}; \kappa) d\mathcal{V}(\boldsymbol{R}) = 1 \qquad \text{for each } \kappa \tag{8.17}$$

and the following

– Convergence condition: Let $\wp_\kappa$ be the orientation measure defined by $w(\cdot;\kappa)$; see (4.7). There exists an extended real number $a \in \mathbb{R} \cup \{-\infty, \infty\}$ such that $\wp_\kappa \to \delta_{\boldsymbol{R}_0}$ vaguely in the space $\mathscr{P}(\mathrm{SO}(3))$ of probability measures as $\kappa \to a$.

In (8.16), each orientation $\boldsymbol{R}$ is taken as a deviation from the ideal orientation $\boldsymbol{R}_0$ by a rotation $\boldsymbol{M}(\widetilde{\boldsymbol{n}}, \widetilde{\omega})$ acting on the left. The value of w depends on the "spread angle" $\widetilde{\omega}$ and is independent of the unit vector $\widetilde{\boldsymbol{n}}$ that defines the axis of the rotation $\boldsymbol{M}$. Thus (8.16) describes isotropic spreading of the orientation density around $\boldsymbol{R}_0$.

Remark 8.2 As the model function (8.16) is meant to be a description of an "ideal orientation with spread", for each κ the spread function $\mathfrak{z}(\cdot;\kappa)$ should assume its maximum at $\widetilde{\omega} = 0$ and decrease rather rapidly to zero (or some negligible value) as $\widetilde{\omega}$ increases. Moreover, the parameter κ, which controls the sharpness of the texture or the extent of the spread, should be close to the extended real number a given in the convergence condition. □

We now proceed to evaluate the texture coefficients pertaining to the ODF w given by (8.16). For the expansion $w(\boldsymbol{R}) = \sum_{l,m,n} c^l_{mn} D^l_{mn}(\boldsymbol{R})$, we have (cf. (4.23))

$$c^l_{mn} = \frac{2l+1}{8\pi^2} \int_{\mathrm{SO}(3)} w(\boldsymbol{R}) \overline{D^l_{mn}(\boldsymbol{R})} d\mathcal{V}(\boldsymbol{R}), \tag{8.18}$$

where $\int_{\mathrm{SO}(3)} \cdots d\mathcal{V}(\boldsymbol{R})$ is given by

$$4 \int_0^{2\pi} \int_0^{\pi} \int_0^{\pi} \cdots \sin^2 \frac{\omega}{2} \sin\Theta \, d\omega d\Theta d\Phi$$

if SO(3) is parametrized by the axis-angle parameters $(\boldsymbol{n}(\Theta, \Phi), \omega)$. Using the fact that

$$D^l_{mn}(\boldsymbol{R}) = D^l_{mn}(\boldsymbol{M}\boldsymbol{R}_0) = \sum_{p=-l}^{l} D^l_{mp}(\boldsymbol{M}) D^l_{pn}(\boldsymbol{R}_0),$$

we may recast (8.18) as

$$\begin{aligned} c^l_{mn} &= \frac{2l+1}{8\pi^2} \sum_{p=-l}^{l} \overline{D^l_{pn}(\boldsymbol{R}_0)} \int_{\mathrm{SO}(3)} w(\boldsymbol{M}(\widetilde{\boldsymbol{n}}, \widetilde{\omega})\boldsymbol{R}_0) \overline{D^l_{mp}(\boldsymbol{M})} d\mathcal{V}(\boldsymbol{M}\boldsymbol{R}_0) \\ &= \frac{2l+1}{8\pi^2} \sum_{p=-l}^{l} \overline{D^l_{pn}(\boldsymbol{R}_0)} \int_{\mathrm{SO}(3)} w(\boldsymbol{M}(\widetilde{\boldsymbol{n}}, \widetilde{\omega})\boldsymbol{R}_0) \overline{D^l_{mp}(\boldsymbol{M})} d\mathcal{V}(\boldsymbol{M}), \end{aligned} \tag{8.19}$$

where we have used the right invariance of the measure $\mathcal{V}$ at the last step. Let $\boldsymbol{R}(\Phi, \Theta, 0)$ be the rotation defined by the Euler angles $(\psi, \theta, \phi) = (\Phi, \Theta, 0)$. Clearly we have

$$\boldsymbol{R}(\Phi, \Theta, 0)\boldsymbol{e}_3 = \widetilde{\boldsymbol{n}}(\Theta, \Phi). \tag{8.20}$$

By Euler's theorem,

$$\boldsymbol{M}(\widetilde{\boldsymbol{n}}(\Theta, \Phi), \widetilde{\omega}) = \boldsymbol{R}(\Phi, \Theta, 0)\boldsymbol{M}(\boldsymbol{e}_3, \widetilde{\omega})\boldsymbol{R}(\Phi, \Theta, 0)^{-1}.$$

Moreover, there holds

$$\begin{aligned}\overline{D^l_{mp}(\boldsymbol{M}(\widetilde{\boldsymbol{n}}(\Theta,\Phi),\widetilde{\omega}))} &= \sum_{r=-l}^{l}\sum_{s=-l}^{l}\overline{D^l_{mr}(\boldsymbol{R}(\Phi,\Theta,0))D^l_{rs}(\boldsymbol{M}(0,0,\widetilde{\omega}))D^l_{sp}(\boldsymbol{R}(\Phi,\Theta,0)^{-1})}\\ &= \sum_{r=-l}^{l}\sum_{s=-l}^{l}\overline{D^l_{mr}(\boldsymbol{R}(\Phi,\Theta,0))}\delta_{rs}e^{is\widetilde{\omega}}D^l_{ps}(\boldsymbol{R}(\Phi,\Theta,0))\\ &= \sum_{r=-l}^{l}\overline{D^l_{mr}(\boldsymbol{R}(\Phi,\Theta,0))}D^l_{pr}(\boldsymbol{R}(\Phi,\Theta,0))e^{ir\widetilde{\omega}}, \end{aligned} \tag{8.21}$$

where we have appealed to (4.14), (4.18), and $(4.29)_2$. Substituting (8.16) and (8.21) into the integrand of (8.19), we obtain

$$\begin{aligned}&\int_{\mathrm{SO}(3)} w(\boldsymbol{M}(\widetilde{\boldsymbol{n}},\widetilde{\omega})\boldsymbol{R}_0)\overline{D^l_{mp}(\boldsymbol{M})}d\mathcal{V}(\boldsymbol{M})\\ &= 4\int_0^{\pi}\left(\mathfrak{z}(\widetilde{\omega};\kappa)\left(\sum_{r=-l}^{l}e^{ir\widetilde{\omega}}\int_0^{2\pi}\int_0^{\pi}e^{i(m-p)\Phi}d^l_{mr}(\Theta)d^l_{pr}(\Theta)\sin\Theta d\Theta d\Phi\right)\right)\sin^2\frac{\widetilde{\omega}}{2}d\widetilde{\omega}\\ &= 4\int_0^{\pi}\mathfrak{z}(\widetilde{\omega};\kappa)\left(\sum_{r=-l}^{l}e^{ir\widetilde{\omega}}\delta_{mp}\cdot 2\pi\cdot\frac{2}{2l+1}\right)\sin^2\frac{\widetilde{\omega}}{2}d\widetilde{\omega}, \end{aligned} \tag{8.22}$$

where we have used the orthogonality relation (4.25). It follows then from (8.19) that

$$\begin{aligned}c^l_{mn} &= \frac{2}{\pi}\left(\int_0^{\pi}\mathfrak{z}(\widetilde{\omega};\kappa)\sin\left(\frac{2l+1}{2}\widetilde{\omega}\right)\sin\frac{\widetilde{\omega}}{2}d\widetilde{\omega}\right)\overline{D^l_{mn}(\boldsymbol{R}_0)}\\ &= \mathcal{Z}_l(\kappa)\overline{D^l_{mn}(\boldsymbol{R}_0)} \end{aligned} \tag{8.23}$$

where we have made use of the trigonometric identity

$$\sum_{r=-l}^{l}e^{ir\widetilde{\omega}} = \frac{\sin(\frac{2l+1}{2}\widetilde{\omega})}{\sin\frac{\widetilde{\omega}}{2}}$$

and put

$$\mathcal{Z}_l(\kappa) = \frac{2}{\pi}\left(\int_0^{\pi}\mathfrak{z}(\widetilde{\omega};\kappa)\sin\left(\frac{2l+1}{2}\widetilde{\omega}\right)\sin\frac{\widetilde{\omega}}{2}d\widetilde{\omega}\right). \tag{8.24}$$

Note that the function $\mathcal{Z}_l$ depends only on the spread function $\mathfrak{z}$ and is independent of the ideal orientation $\boldsymbol{R}_0$. A comparison of (8.23) with (8.8) reveals that the convergence condition on the model function $w(\cdot;\kappa)$ requires that the spread function $\mathfrak{z}(\widetilde{\omega};\kappa)$ satisfies

the condition

$$\lim_{\kappa\to a}\mathcal{Z}_l(\kappa)=\lim_{\kappa\to a}\frac{2}{\pi}\left(\int_0^{\pi}\mathfrak{z}(\widetilde{\omega};\kappa)\sin\left(\frac{2l+1}{2}\widetilde{\omega}\right)\sin\frac{\widetilde{\omega}}{2}\,d\widetilde{\omega}\right)=\frac{2l+1}{8\pi^2}. \tag{8.25}$$

For polycrystals with both G_{tex} and G_{cr} being finite groups, it suffices to consider only rotations $\boldsymbol{R}_0$ in the chosen strict fundamental domain. Let $G_{\text{tex}}=\{\boldsymbol{Q}_i : i=1,\dots,N_{\text{tex}}\}$ and $G_{\text{cr}}=\{\boldsymbol{P}_j : j=1,\dots,N_{\text{cr}}\}$, where N_{tex} and N_{cr} denote the order of G_{tex} and of G_{cr}, respectively. It is obvious that the texture coefficients of the central function which models an "ideal orientation with spread" are:

$$c^l_{mn}=\mathcal{Z}_l(\kappa)\cdot\frac{1}{N_{\text{tex}}N_{\text{cr}}}\sum_{i=1}^{N_{\text{tex}}}\sum_{j=1}^{N_{\text{cr}}}\overline{D^l_{mn}(\boldsymbol{Q}_i^T\boldsymbol{R}_0\boldsymbol{P}_j)}. \tag{8.26}$$

8.4.2 Bunge's "Gaussian" Components

We begin again our discussion with triclinic aggregates of triclinic crystallites.

As a model ODF for texture components that pertain to ideal orientations with spread, Bunge [57, 60] proposed (8.16) with the spread function given by

$$\mathfrak{z}(\widetilde{\omega};\kappa)=S(\kappa)e^{-\widetilde{\omega}^2/\kappa^2},\qquad(\kappa>0) \tag{8.27}$$

which he called "Gaussian distribution". The function $S(\kappa)$ in (8.27) is to be determined by the normalization condition (4.44) on the model ODF $w(\cdot;\kappa)$. Accordingly, we have

$$\int_{\text{SO(3)}}w(\boldsymbol{R};\kappa)d\mathcal{V}(\boldsymbol{R})=4\left(\int_0^{\pi}S(\kappa)e^{-\widetilde{\omega}^2/\kappa^2}\sin^2\frac{\widetilde{\omega}}{2}d\widetilde{\omega}\right)\left(\int_0^{2\pi}\int_0^{\pi}\sin\Theta d\Theta d\Phi\right)=1, \tag{8.28}$$

which gives

$$S(\kappa)=\frac{1}{8\pi}\left(\int_0^{\pi}e^{-\widetilde{\omega}^2/\kappa^2}(1-\cos\widetilde{\omega})d\widetilde{\omega}\right)^{-1}. \tag{8.29}$$

We are primarily interested in the case that $\kappa\ll\pi$ (say, $\kappa<\pi/12$). Hence we may obtain a good approximation of the integral in (8.29) by extending its upper limit to ∞. It follows that

$$\begin{aligned}S(\kappa)&\approx\frac{1}{8\pi}\left(\int_0^{\infty}e^{-\widetilde{\omega}^2/\kappa^2}(1-\cos\widetilde{\omega})d\widetilde{\omega}\right)^{-1}\\&=\frac{1}{4\pi\sqrt{\pi}\kappa}\left(1-e^{-\kappa^2/4}\right)^{-1},\end{aligned} \tag{8.30}$$

where we have appealed to the integral formulas

$$\int_0^{\infty}e^{-ax^2}dx=\frac{1}{2}\sqrt{\frac{\pi}{a}},\qquad\int_0^{\infty}e^{-ax^2}\cos bx\,dx=\frac{1}{2}\sqrt{\frac{\pi}{a}}e^{-b^2/4a}.$$

Let us proceed to evaluate the function $\mathcal{Z}_l(\kappa)$. Using the trigonometric identity

$$\sin A \sin B = \frac{1}{2}(\cos(A-B) - \cos(A+B)),$$

we recast (8.24) and obtain

$$\begin{aligned}\mathcal{Z}_l(\kappa) &= \frac{2}{\pi}\left(\int_0^{\pi} \mathfrak{z}(\widetilde{\omega};\kappa)\cdot\frac{1}{2}\big(\cos l\widetilde{\omega} - \cos(l+1)\widetilde{\omega}\big)\,d\widetilde{\omega}\right)\\ &\approx \frac{2S(\kappa)}{\pi}\left(\int_0^{\infty} e^{-\widetilde{\omega}^2/\kappa^2}\cdot\frac{1}{2}\big(\cos l\widetilde{\omega} - \cos(l+1)\widetilde{\omega}\big)\,d\widetilde{\omega}\right)\\ &= \frac{S(\kappa)\kappa}{2\sqrt{\pi}}\left(e^{-l^2\kappa^2/4} - e^{-(l+1)^2\kappa^2/4}\right). \end{aligned} \tag{8.31}$$

Substituting formula (8.30) for $S(\kappa)$ into the preceding equation, we arrive at the formula

$$\mathcal{Z}_l(\kappa) \approx \frac{1}{8\pi^2}\frac{e^{-l^2\kappa^2/4} - e^{-(l+1)^2\kappa^2/4}}{1-e^{-\kappa^2/4}}. \tag{8.32}$$

Substituting (8.32) into (8.23), we obtain

$$c^l_{mn}(\boldsymbol{R}_0;\kappa) \approx \frac{1}{8\pi^2}\frac{e^{-l^2\kappa^2/4} - e^{-(l+1)^2\kappa^2/4}}{1-e^{-\kappa^2/4}}\cdot\overline{D^l_{mn}(\boldsymbol{R}_0)}, \tag{8.33}$$

which delivers the texture coefficients of the Gaussian texture component centered at $\boldsymbol{R}_0$ and with spread parameter κ. Taking the limit as $\kappa \to 0$ on both sides of formula (8.33), we observe that

$$c^l_{mn}(\boldsymbol{R}_0, 0) = \frac{2l+1}{8\pi^2}\overline{D^l_{mn}(\boldsymbol{R}_0)}, \tag{8.34}$$

where we have replaced the "$\approx$" sign with the "$=$" sign, because the approximation (8.31) becomes exact as $\kappa \to 0$. Note that (8.34) delivers the texture coefficients for the orientation measure pertaining to the ideal orientation at $\boldsymbol{R}_0$ for triclinic crystallites, which agree with (8.8) as expected. By (4.118), we can easily recast (8.33) and (8.34) in Roe's notation. Thus we have

$$W_{lmn}(\boldsymbol{R}_0;\kappa) \approx \frac{1}{2l+1}\frac{e^{-l^2\kappa^2/4} - e^{-(l+1)^2\kappa^2/4}}{1-e^{-\kappa^2/4}}\cdot W_{lmn}(\boldsymbol{R}_0;0), \tag{8.35}$$

$$\begin{aligned} W_{lmn}(\boldsymbol{R}_0;0) &= \frac{1}{4\pi^2}Z_{lmn}(\cos\theta_0)e^{im\psi_0}e^{in\phi_0},\\ &= \frac{(-1)^{n-m}}{4\pi^2}\sqrt{\frac{2l+1}{2}}d^l_{mn}(\theta_0)e^{im\psi_0}e^{in\phi_0}, \end{aligned} \tag{8.36}$$

where $(\psi_0, \theta_0, \phi_0)$ are the Euler angles pertaining to $\boldsymbol{R}_0$.

Consider now the case that both G_{tex} and G_{cr} are finite groups. Let $G_{\text{tex}} = \{\boldsymbol{Q}_i : i = 1, 2, \ldots, N_{\text{tex}}\}$ and $G_{\text{cr}} = \{\boldsymbol{P}_j : j = 1, 2, \ldots, N_{\text{cr}}\}$, where N_{tex} and N_{cr} are the order of G_{tex} and G_{cr}, respectively. We may restrict our attention to rotations $\boldsymbol{R}_0$ in the chosen strict

fundamental domain. The texture coefficients of the ideal orientation at $\boldsymbol{R}_0$ and the Gaussian texture component $(\boldsymbol{R}_0, \kappa)$ are clearly given by the formulas

$$c^l_{mn}(\boldsymbol{R}_0; 0) = \frac{2l+1}{8\pi^2} \cdot \frac{1}{N_{\text{tex}}} \frac{1}{N_{\text{cr}}} \sum_{i=1}^{N_{\text{tex}}} \sum_{j=1}^{N_{\text{cr}}} \overline{D^l_{mn}(\boldsymbol{Q}_i^T \boldsymbol{R}_0 \boldsymbol{P}_j)}, \tag{8.37}$$

$$c^l_{mn}(\boldsymbol{R}_0; \kappa) \approx \frac{1}{2l+1} \cdot \frac{e^{-l^2\kappa^2/4} - e^{-(l+1)^2\kappa^2/4}}{1 - e^{-\kappa^2/4}} \cdot c^l_{mn}(\boldsymbol{R}_0; 0), \tag{8.38}$$

respectively.

8.5 The Bunge–Haessner Method and Its Modification

A commonly-adopted protocol (see, e.g., [104, p. 268]) to infer an approximate ODF from individual orientation data obtained by ESBD measurements still follows in broad outline what Bunge and Haessner [63] did in their 1968 paper. In short, Bunge and Haessner's indirect method is to get (in the convention and notation adopted in this exposition) estimates of all non-trivial texture coefficients c^l_{mn} that appear in the series expansion (4.49) of the ODF truncated at a selected $l = L$ (e.g., $L = 22$, $L = 34$, etc.), i.e., put $w = \sum_{l=0}^{L} \sum_{m,n} c^l_{mn} D^l_{mn}$, which is presumed to give a good representation of the texture in question.

In their paper Bunge and Haessner [63] did not explain why the method and formula they used to estimate the texture coefficients c^l_{mn} $(1 \le l \le L)$ would work, except for the following remark in the introduction where they listed and briefly described the two indirect methods available then for inferring the ODF from results of single-orientation measurements:

> ... one may measure the orientation parameters for as large a number of crystallites as is practicable and then determine the relative frequency of specific orientations.

Bunge and Haessner's assertion cited above is unclear on how they would treat the single-orientation data, but what they do in practice is apparent from their paper.

We will now present the method of Bunge and Haessner, with an emphasis on its mathematical foundations.

8.5.1 Mathematical Basis

Consider a sequence $\{\mathcal{P}_n\}$ of single-phase polycrystalline samples of the same chemical composition (e.g., aluminum plates), which are produced by the same manufacturing process and are geometrically congruent to each other. We take the samples $\mathcal{P}_n$ as macroscopically equivalent representatives of one polycrystal P. Let $\mathtt{X}_0$ be a point in P, and we call the corresponding point in each $\mathcal{P}_n$ the same name $\mathtt{X}_0$. Suppose the texture at $\mathtt{X}_0$ is given by orientation measure $\hat{\wp}$, which is defined on orientation space $\mathrm{SO}(3)/G_{\text{cr}}$, where $G_{\text{cr}} = \{\boldsymbol{P}_1, \ldots, \boldsymbol{P}_{N_{\text{cr}}}\}$. In a thought experiment $\mathscr{E}$, we conduct single-orientation measurement $\mathscr{E}_n$ at point $\mathtt{X}_0$ of each $\mathcal{P}_n$ $(n = 1, 2, 3, \ldots)$, which is similar to tossing identical dices in a sequence. Each individual orientation measurement delivers an orientation $\boldsymbol{R}G_{\text{cr}}$ or, equivalently, a Dirac measure $\delta_{\boldsymbol{R}G_{\text{cr}}}$, where $\boldsymbol{R} \in \mathrm{SO}(3)$. Thus we obtain a sequence of Dirac measures $\delta_{\boldsymbol{R}_1 G_{\text{cr}}}$, $\delta_{\boldsymbol{R}_2 G_{\text{cr}}}$, $\delta_{\boldsymbol{R}_3 G_{\text{cr}}}, \ldots$ on $\mathrm{SO}(3)/G_{\text{cr}}$, where $\boldsymbol{R}_1 G_{\text{cr}}$, $\boldsymbol{R}_2 G_{\text{cr}}$, $\cdots$ are independent random variables. For $k = 1, 2, \ldots$, the empirical measures $\hat{\mu}_k$ are defined by

$$\hat{\mu}_k := \frac{1}{k} \left(\delta_{\boldsymbol{R}_1 G_{\text{cr}}} + \delta_{\boldsymbol{R}_2 G_{\text{cr}}} + \cdots + \delta_{\boldsymbol{R}_k G_{\text{cr}}} \right). \tag{8.39}$$

Under a natural mathematical setting (see Remark 8.3), there is probability 1 that the sequence of empirical measures $\hat{\mu}_k$ converges vaguely to $\hat{\wp}$ as $k \to \infty$ in $\mathscr{P}(\mathrm{SO}(3)/G_{\mathrm{cr}})$.

Remark 8.3 For each single-orientation measurement $\mathscr{E}_n$, the probability space is $(M, \hat{\mathfrak{B}}, \hat{\wp})$, where we have put $M := \mathrm{SO}(3)/G_{\mathrm{cr}}$ for brevity, $\hat{\mathfrak{B}}$ is the Borel σ-algebra in M, and $\hat{\wp}$ the orientation measure. Alternatively, we can put the probability space as $(M, \hat{\wp})$, where the probability measure $\hat{\wp}$ is treated as a Radon measure on M (cf. Sect. 8.2). In what follows we start by taking this alternate representation. Let $x \in M$ denote the elementary events (i.e., the crystallite orientations). We write the probability space for measurement $\mathscr{E}_n$ as $(M_n, \hat{\wp}_n)$, where $M_n = M$ and $\hat{\wp}_n = \hat{\wp}$ for each $n = 1, 2, 3, \ldots$. For the experiment $\mathscr{E}$, there is a natural probability space (Ω, P) as follows. Each elementary event $\omega \in \Omega$ is a sequence $(x_1, x_2, x_3, \ldots)$, where $x_n \in M_n$ for each $n \in \mathbb{N}$. Hence $\Omega = \prod_{n=1}^{\infty} M_n$, where $M_n = M$ for each n, is the countably-infinite Cartesian product. Since M is a compact metric space, so is Ω (see, e.g., [102, pp. 112, 178]). There is a unique probability (Radon) measure $P = \bigotimes_{n=1}^{\infty} \hat{\wp}_n$ on Ω, called the product measure of $\hat{\wp}_1, \hat{\wp}_2, \ldots$, such that for $(x_1, x_2, \ldots) \in \Omega$ the random variables $x_1, x_2, \ldots$ are independent with probability measures $\hat{\wp}_1, \hat{\wp}_2, \ldots$, respectively. At this point it is easier to explain the assertion that follows (8.39) if we revert to writing the probability space (Ω, P) as $(\Omega, \mathfrak{B}_\Omega, P)$, where $\mathfrak{B}_\Omega$ is the Borel σ-algebra in Ω and $P : \mathfrak{B}_\Omega \to [0, 1]$ the Borel measure pertaining to the Radon measure P (cf. Sect. 8.2). Under this setting, it can be proved (see [96, p. 399]; [318, pp. 130–131]) that $P(\{\omega \in \Omega : \hat{\mu}_k(\omega) \to \hat{\wp}\}) = 1$. The main tool in the proof is the strong law of large numbers. □

Let $\wp$ and μ_k be the orientation measures on SO(3) that pertain to $\hat{\wp}$ and $\hat{\mu}_k$ on $\mathrm{SO}(3)/G_{\mathrm{cr}}$, respectively. Note that $\delta_{\boldsymbol{R}G_{\mathrm{cr}}}$ and $\hat{\mu}_k$ on $\mathrm{SO}(3)/G_{\mathrm{cr}}$ correspond to

$$\frac{1}{N_{\mathrm{cr}}} \sum_{j=1}^{N_{\mathrm{cr}}} \delta_{\boldsymbol{R}\boldsymbol{P}_j} \qquad \text{and} \qquad \mu_k = \frac{1}{k} \sum_{s=1}^{k} \left(\frac{1}{N_{\mathrm{cr}}} \sum_{j=1}^{N_{\mathrm{cr}}} \delta_{\boldsymbol{R}_s \boldsymbol{P}_j} \right) \tag{8.40}$$

on SO(3), respectively. If $\hat{\mu}_k \to \hat{\wp}$ vaguely as $k \to \infty$, then $\mu_k \to \wp$ vaguely as $k \to \infty$. Thus we have

$$c_{mn}^{l} = \frac{2l+1}{8\pi^2} \int_{\mathrm{SO}(3)} \overline{D_{mn}^{l}(\boldsymbol{R})}\, d\wp(\boldsymbol{R}) = \frac{2l+1}{8\pi^2} \langle \wp, \overline{D_{mn}^{l}} \rangle = \lim_{k \to \infty} \frac{2l+1}{8\pi^2} \langle \mu_k, \overline{D_{mn}^{l}} \rangle. \tag{8.41}$$

Let $\varepsilon > 0$ and a natural number $L := l_{\max} > 1$, which is the maximum value of l above which we shall truncate the ODF series expansion (4.49), be given. For a complex number z, let $|z| = \sqrt{(\Re\mathfrak{e}\, z)^2 + (\Im\mathfrak{m}\, z)^2}$ be its modulus. By (8.41) for each (l, m, n), where $1 < l \leq L$, $-l \leq m \leq l$, and $-l \leq n \leq l$, there is a number $K_{mn}^{l} > 0$ such that

$$\left| c_{mn}^{l} - \frac{2l+1}{8\pi^2} \langle \mu_k, \overline{D_{mn}^{l}} \rangle \right| < \varepsilon \qquad \text{for all } k > K_{mn}^{l}. \tag{8.42}$$

Let $K = \max\{K_{mn}^{l} : 1 < l \leq L, -l \leq m \leq l, -l \leq n \leq l\}$. Then for $k > K$, we have

$$\left| c_{mn}^{l} - \frac{2l+1}{8\pi^2} \langle \mu_k, \overline{D_{mn}^{l}} \rangle \right| < \varepsilon \qquad \text{for all } c_{mn}^{l} \text{ with } 1 < l \leq L. \tag{8.43}$$

Hence a procedure to obtain from single-orientation measurements an approximate ODF for a polycrystalline sample with a homogeneous texture is as follows. Choose a natural

number L (e.g., $L = 22$, or $L = 34$, etc.) such that truncation of the series expansion (4.49) at $l = L$ will give a good enough approximation of the ODF w. Make a sufficient large number N of individual orientation measurements that deliver independent orientations specified by the rotations $\boldsymbol{R}_s$ $(s = 1, 2, \ldots, N)$ in the chosen strict fundamental domain, and put for $1 < l \leq L$

$$c^l_{mn} \approx \frac{2l+1}{8\pi^2}\langle \mu_N, \overline{D^l_{mn}}\rangle = \frac{2l+1}{8\pi^2} \cdot \frac{1}{N}\sum_{s=1}^{N}\left(\frac{1}{N_{\mathrm{cr}}}\sum_{j=1}^{N_{\mathrm{cr}}}\overline{D^l_{mn}(\boldsymbol{R}_s\boldsymbol{P}_j)}\right). \tag{8.44}$$

Remark 8.4 Note that formula (8.44) remains unchanged if $\boldsymbol{R}_s$ is replaced by $\boldsymbol{R}_s\boldsymbol{P}_k$ for any $\boldsymbol{P}_k \in G_{\mathrm{cr}}$. Hence $\boldsymbol{R}_s$ in (8.44) should read any rotation in $\boldsymbol{R}_s G_{\mathrm{cr}}$. Specification of a chosen strict fundamental domain is unnecessary. □

If it is desirable that sample symmetry be imposed on the single-orientation data, then (8.44) should be replaced by the formula

$$c^l_{mn} \approx \frac{2l+1}{8\pi^2}\langle \mu_N, \overline{D^l_{mn}}\rangle = \frac{2l+1}{8\pi^2} \cdot \frac{1}{N}\sum_{s=1}^{N}\left(\frac{1}{N_{\mathrm{tex}}N_{\mathrm{cr}}}\sum_{i=1}^{N_{\mathrm{tex}}}\sum_{j=1}^{N_{\mathrm{cr}}}\overline{D^l_{mn}(\boldsymbol{Q}_i^T\boldsymbol{R}_s\boldsymbol{P}_j)}\right), \tag{8.45}$$

where $\boldsymbol{Q}_i$ $(i = 1, \ldots, N_{\mathrm{tex}})$ are elements of G_{tex}. Similar to the observation in Remark 8.4, the rotation $\boldsymbol{R}_s$ in (8.45) should read any rotation in $G_{\mathrm{tex}}\boldsymbol{R}_s G_{\mathrm{cr}}$.

Note that the choice of L and of ε defines through (8.43) the desired resolution of our single-orientation measurements of the ODF w. For $N \in \mathbb{N}$, let

$$w_N(\boldsymbol{R}) = \frac{1}{8\pi^2} + \sum_{l=1}^{L}\sum_{m=-l}^{l}\sum_{n=-l}^{l}\widetilde{c}^l_{mn}(N)D^l_{mn}(\boldsymbol{R}), \tag{8.46}$$

where the texture coefficients

$$\widetilde{c}^l_{mn}(N) = \frac{2l+1}{8\pi^2}\langle \mu_N, \overline{D^l_{mn}}\rangle \tag{8.47}$$

are given by the right-hand side of either (8.44) or of (8.45) as appropriate. For the polycrystalline sample in question, the function w_N given by (8.46) is a good approximation of the ODF w, i.e., it satisfies the resolution defined by (8.43), if N is sufficiently large. Given a (finite but sufficiently long) sequence of independent single-orientation measurements, in Sect. 8.6.2 we shall discuss the problem how to determine the critical number N_C such that all $N \geq N_C$ are sufficiently large for w_N to be a good approximation to the true ODF w.

Bunge and Haessner [63] used, in essence, the parallels of (8.45) and (8.46) in Bunge's formulation (cf. [60, pp. 50–51]) to treat their single-orientation data ($k = 512$, $L = 22$), with one difference: They erroneously put all texture coefficients with odd l equal to zero, which until the late 1970s was a common mistake in the literature of quantitative texture analysis. While they noticed that their calculated ODF "contained negative values of about 20% of the maximum value", they attributed the unphysical negative values to experimental error and truncation error.

Henceforth by "the method of Bunge and Haessner" or "the Bunge–Haessner method" we mean treatment of single-orientation data that is based on either (8.44) or (8.45) and (8.46).

Remark 8.5 We have presented above a possible mathematical basis of the Bunge–Haessner method for inference of an approximate ODF from single-orientation data. One of our basic assumptions is that the measured orientations constitute a sequence of independent random variables, which is certainly valid for the setting of our thought experiment. In reality, however, single-orientation measurements are performed on one sample and results of measurements made at points within the same grain are not independent. We shall return to discuss this and some other issues in EBSD measurements in Sect. 8.6. □

8.5.2 Modification of the Bunge–Haessner Method

In the method of Bunge and Haessner, each single-orientation measurement delivers a Dirac measure with texture coefficients that pertain to an ideal orientation. When Pospiech and Lücke [263] applied the Bunge–Haessner method to treat the single-orientation data of Perlwitz et al. [257] from selected-area electron diffraction, they modified the method by replacing each measured ideal orientation by the corresponding Gaussian component centered at that ideal orientation. Hence in our notation and convention, while formula (8.46) is kept, (8.45) and (8.47) on $\widetilde{c}^{\,l}_{mn}(N)$ is replaced by[105]

$$\widetilde{c}^{\,l}_{mn}(N) = \frac{1}{8\pi^2} \cdot \frac{e^{-l^2\kappa^2/4} - e^{-(l+1)^2\kappa^2/4}}{1 - e^{-\kappa^2/4}} \cdot \frac{1}{N} \sum_{s=1}^{N} \left(\frac{1}{N_{\text{tex}} N_{\text{cr}}} \sum_{i=1}^{N_{\text{tex}}} \sum_{j=1}^{N_{\text{cr}}} \overline{D^l_{mn}(\boldsymbol{Q}_i^T \boldsymbol{R}_s \boldsymbol{P}_j)} \right); \tag{8.48}$$

cf. (8.38). They took the spread parameter $\kappa = 5°$, and they did not explain why they made such a modification.

A plausible explanation for the modification was provided by Wagner et al. [330, p. 273]. They write:

> This [i.e., the analog of (8.45) in Bunge's formulation] can be understood as the expansion of an ODF which consists of N Dirac functions situated in N points g_i in Euler space. Unfortunately a truncation error arises because the $C_l^{\mu n}$ coefficients are necessarily calculated up to a finite order $l_{\max}$ for l. This error is important because the convergence of the series is very poor when representing Dirac functions. An illustration of this fact can be seen in Fig. 3a. It represents the section $\varphi_1 = 60°$ of a theoretical ODF which is composed of three ideal orientations g_1, g_2, g_3, calculated using formula (4) [i.e., the analog of (8.45)] up to $l_{\max} = 22$. Although up to $l_{\max} = 22$ ... truncation errors exist and negative values appear for the ODF which is meaningless.
>
> To overcome such difficulties it is advantages to use Gauss functions, instead of Dirac functions, to represent the measurements (mathematicians call this regularizing the function).

They proceed to show that when the aforementioned three ideal orientations g_1, g_2, g_3 are replaced by their corresponding Gaussian components with spread parameter equal to 10°, "the negative values have disappeared" from the modified theoretical ODF truncated at $l_{\max} = 22$.[106]

[105] Note that if sample symmetry is not imposed on the orientation data, the modified formula is that which results by putting $G_{\text{tex}} = \{\boldsymbol{I}\}$, $N_{\text{tex}} = 1$, and $\boldsymbol{Q}_1 = \boldsymbol{I}$ in (8.48).

[106] The counter-example of three ideal orientations given by Wagner et al. is unconvincing. If one substitutes formally into the series expansion (4.49) of the ODF the texture coefficients that pertain to a Dirac measure,

For the value of κ to be used in the modified recipe of the Bunge–Haessner method, Wagner et al. [330] proposed a heuristic formula, which in its corrected form [329, p. 120] reads:[107]

$$\kappa = \left(\frac{6\pi p}{\mathtt{M} N} \right)^{1/3}, \tag{8.49}$$

where $\mathtt{M} := N_{\text{tex}} N_{\text{cr}}$ is "the multiplicity of an orientation in the Euler space",[108] N is the number of "individual orientation measurements" (called "individual crystal measurements" in Wagner et al. [330, p. 274]), and p is "an empirical parameter between 0 and 1 which takes into account the 'sharpness' of the texture". Typical values of p are: "$p = 1$ for weak textures", $p = 0.5$ for what Wagner et al. [330] call "intermediate textures", and "$p = 0.2$ for sharp textures." Formula (8.49), in its original erroneous form (see Footnote 107), was adopted in a number of studies on texture determination by EBSD in the 1990s and beyond (cf. e.g., [22, 23, 346–348]). However, it is problematic to use formula (8.49) as a guide to determine the spread angle κ in (8.48) for the texture coefficients c_{mn}^{l}; see Remark 8.6 for further discussions in this regard.

8.5.3 Ideal Orientations Versus Gaussian Components

As pointed out by Hutchinson et al. [160] in 1999, the argument of Wagner et al. in support of replacing the ideal orientations by Gaussian components is fundamentally flawed. Let us recast the counter-argument of Hutchinson et al. in our present language, which slightly sharpens their counter-argument and renders it mathematically rigorous, but keep their crucial starting point, namely: "consider a material having a texture of typical severity which can properly be described by a limited number of terms (e.g. $\mathrm{L}_{\max} = 22$) in the standard manner." In other words, suppose for some $l_{\max}$ an ODF of the form $w(\boldsymbol{R}) = \frac{1}{8\pi^2} + \sum_{l=1}^{l_{\max}} \sum_{m=-l}^{l} \sum_{n=-l}^{l} c_{mn}^{l} D_{mn}^{l}(\boldsymbol{R})$ gives a good description of the texture of the material. Note that this ODF w is completely specified by the texture coefficients c_{mn}^{l} for $1 \le l \le l_{\max}$. In Sect. 8.5.1 we have learned that by making a sufficiently large number of independent single-orientation measurements the relevant texture coefficients (i.e., those with $1 \le l \le l_{\max}$) can be approximated arbitrarily closely by their namesakes which pertain to suitable empirical discrete orientation measures μ_N (cf. $(8.40)_2$ for the case $G_{\text{tex}} = \{\boldsymbol{I}\}$) obtained from such measurements. The texture coefficients with $l > l_{\max}$ of such μ_N are irrelevant. Whether the formal expansion of μ_N in terms of Wigner D-functions is convergent or divergent is also irrelevant. As far as the single-orientation measurements are concerned,

the series becomes *divergent*. We do not expect that any truncated version of the formal series which includes terms up to some $l_{\max}$, no matter how large, could serve as an acceptable approximation to the density of the Dirac measure. Hence the "theoretical ODF" in question isn't an ODF in the usual sense of the term, i.e., a square-integrable probability density which can be expanded as a convergent series in terms of the Wigner D-functions (or in other conventions, the generalized spherical harmonics, etc.). See the first paragraph of Sect. 8.5.3 for further discussions.

[107] There is an error in [330] on the computation of the volume of a ball of radius R_0 in SO(3) so that the resulting formula for κ is too large by a factor of $2^{1/3} \approx 1.26$. While Wagner silently presented the corrected form of the formula in 1986, unfortunately it was the erroneous form, particularly that which pertains to aggregates of cubic crystallites without enforcement of sample symmetry, namely $\kappa = (\pi p/2N)^{1/3}$, that propagated in the texture literature up to at least 2007 [348].

[108] This quotation and, unless stated explicitly otherwise, all the quotations in the rest of this paragraph are from Wagner [329].

the important points are: (i) the measurements are independent; (ii) the number of Dirac measures involved in the composition of μ_N is sufficiently large.

After presenting their counter-argument to refute the claim of Wagner et al., Hutchinson et al. [160, p. 36] conclude as follows:

> ... nothing is achieved by describing the individual gaussians with a longer series expansion than that necessary for the texture of the material as a whole. The angle of spread may therefore be reduced, even to zero, without introducing any error ...
>
> If oscillations or negative density values result from the calculations, these must imply that the number of measurements is too small.

Remark 8.6 Suppose a number of independent single-orientation measurements have been made on a statistically homogeneous sample. There are two possibilities. (1) The number of measurements made is sufficiently large to deliver an empirical orientation measure μ_N which gives a good description of the texture of the material in question. If we replace each ideal orientation in μ_N by a Gaussian component with a spread angle κ given by (8.49), the resulting ODF will be flatter than it should be. (2) If the number of measurements is insufficient, it is extremely unlikely that the practice of changing κ in (8.48) from zero to the value given by (8.49) will make the resulting ODF a good description of the texture of the material. In case (1), following the scheme suggested by Wagner et al. [330] will degrade the outcome; in case (2), the practice will not miraculously deliver the texture sought. □

There is one issue that remains to be clarified. In the 1990s and 2000s when XRD and EBSD were the established and the emergent technique for texture determination, respectively, there were several comparative studies of the two techniques with the XRD results serving as the standard against which the quality of the EBSD findings was assessed. In most of those studies, the modified Bunge–Haessner method was used for treatment of the EBSD data with κ "ranging in values from 3 to 10 deg" [348, p. 1845]. In some cases where the number of measurements seemed to be sufficient, it was found that assigning κ in (8.48) a suitable value $\geq 3°$ gave a better fit to the XRD results than putting $\kappa = 0°$ there. How could such findings be explained?

This query has been answered by Hutchinson et al. [160, p. 35]:

> ... x-ray textures also suffer from instrument broadening which causes the measurements to be less sharp than the true texture. ... conventional goniometers typically have a full-width-half maximum (FWHM) breadth of about 3°. ... The intrinsic resolution of the method is considerably less (by a factor of about six) than that of an EBSP measurement.

The authors proceed to present an example of a recrystallized IF steel containing a sharp ⟨111⟩/ND fiber texture (γ-fiber). The texture of the material was determined by XRD and EBSD measurements. In a figure the authors show plots of orientation density with varying Euler angle[109] Φ ($\varphi_1 = 0°$, $\varphi_2 = 45°$) as determined by the XRD and EBSD measurements, where the plots of the EBSD data pertain to results delivered by the modified Bunge–Haessner method with Gaussian spreads of 0°, 3°, 5°, 10°, and 20°, respectively. It turns out [160, p. 39] that

> the curve for the x-ray diffraction measurements coincides quite closely with the EBSP results for a gaussian spread of about 4°.

[109] Here the Euler angles are expressed in the convention adopted by Bunge and Gel'fand et al. (see Sect. 1.8.2).

But, as noted by the authors, "it is ... logical that the [XRD] results should correspond to those of EBSP measurements when the same degree of instrumental broadening (gaussian spread) is applied to these data."

The conclusions of Hutchinson et al. were confirmed by an experimental study by Schwarzer [291].

In summary, as we have shown in Sect. 8.5.1, in theory each single-orientation measurement delivers an ideal orientation; by making a sufficiently large number of independent measurements, for any chosen $l_{\max}$ we can obtain estimates of texture coefficients c^l_{mn} for $1 \le l \le l_{\max}$ to any degree of accuracy and arrive at an approximate ODF (8.46) for the polycrystalline material in question. This is none other than the Bunge–Haessner method. There is no place for Bunge's Gaussian components in this theoretical scheme.

EBSD measurements, of course, also carry uncertainty or "instrument broadening". The angular resolution for orientation measurement by EBSD has been found to be approximately 0.5°–1.0° (see, e.g., Brough et al., [53], Demirel et al. [86, p. 68], Engler and Randle [104, p. 224], Humphreys [159, pp. 172, 179], Hutchinson et al. [160, p. 35], Schwarzer [291, p. 1387], Wright et al. [348, p. 1845]). This suggests the question whether, for each individual measurement, it would be beneficial to replace the ideal orientation in question by its corresponding Gaussian component with a small spread angle κ. In Remark 8.7 we shall discuss this question further in a broader perspective.

8.6 Further Issues Concerning the Bunge–Haessner Method in Practice

The method of Bunge and Haessner for determination of the ODF from single-orientation measurements is based on three premises:

1. The ODF is a square-integrable function defined on SO(3). Its series expansion (4.49) converges in the sense of (4.24). Truncation of the series at some finite $L := l_{\max}$ gives a good approximation of the ODF.
2. The individual orientation measurements deliver orientations that are independent random variables.
3. Data for a sufficiently large number of measured orientations are available.

In a thought experiment, we can easily imagine that we are provided with an unlimited supply of nominally identical samples (i.e., all produced by the same manufacturing process, with the same chemical composition, the same physical dimensions, etc.), and that we make single-orientation measurement at the same location in each sample. Similar to the tossing of identical dices, measurements on different but nominally identical samples $\mathcal{P}_\alpha$ of a polycrystal P are clearly independent. In applications, however, we are often provided with one sample or a small number of nominally identical samples. Even if the polycrystal P in question can be taken as statistically homogeneous, orientation measurements at two points within the same grain of a sample are not independent. Hence premise 2 is a concern that should be addressed when we consider applications.

Premise 3 begs the following question: Given a sample of a polycrystal which can be taken as statistically homogeneous, how many single-orientation measurements will be sufficiently large for determination of its ODF? This question drew the attention of researchers when automation of the EBSD technique in the 1990s showed promise that it might someday become a common tool and, as compared with X-ray diffraction, a more preferable means for determination of texture at least in some types of polycrystalline samples. This promise has been borne out by the rapid advancement of the EBSD technique in the last two decades.

We shall discuss these two issues in this section. In what follows whenever we talk about single-orientation measurements in practice we mean EBSD measurements made on a sample $\mathcal{P}$ of a statistical homogeneous polycrystal P.

8.6.1 "Grains" and Independence in Orientation Measurements by EBSD

As our objective is just to give an introduction of the subject, we shall consider only the simplest case and restrict attention to EBSD orientation measurements made on fully recrystallized polycrystalline materials. For such measurements, EBSD indexing rate is high, orientation maps of good quality are routinely obtained, and an ASTM standard protocol for determination of average grain size is available [8].

EBSD orientation measurements[110] are made at a regular grid of scan points in a planar surface of a specimen after suitable preparation. The scan points are typically centers of a repeating pattern of regular hexagons or squares which, if continued indefinitely, would fill out the entire plane. In the literature each regular hexagon or square that contains a sampling point is sometimes called a "pixel". At each sampling point an EBSD pattern is obtained, from which the lattice orientation at that point could be inferred if the crystal structure of the specimen is known.[111] A disorientation tolerance[112] (angle) is set by the operator. Two neighboring sampling points (and the two pixels to which they pertain) are taken as belonging to the same "grain" if their disorientation angle is not bigger than the preset tolerance. It is also common to refrain from calling a group of pixels a "grain" unless the number of scan points contained in the group exceeds a certain prescribed minimum. To complete the orientation map, scan points which are non-indexed, mis-indexed, or otherwise left unclassified, are assigned to existing grains by some cleanup routine (e.g., grain dilation [345], where the unclassified pixels are iteratively assigned to neighboring grains via some chosen scheme). The distance between two neighboring sampling points is called the step size. Clearly for a fixed disorientation tolerance, reducing the step size will, in general, increase the average number of sampling points contained in a grain. With the present-day EBSD technology, more than a million of orientations can be ascertained within a score of minutes. Hence it is typical, for construction of orientation maps with sufficient accuracy, to select a step size substantially smaller than the average grain size. Thus a grain will contain tens or hundreds of scan points.[113] On the other hand, for the determination of ODF a primary requirement for the single-orientation measurements which define the sequence of empirical measures (8.39) is that they be independent. As measurements at scan points within the same grain cannot be expected to be independent, it raises the questions whether and how data from EBSD measurements made for construction of orientation maps, microstructural studies, or

[110] For more information on EBSD orientation measurements, see Engler and Randle [104] and the references therein.

[111] For our present purpose we need not go into details on indexing, treatment of non-indexed or mis-indexed points, and cleanup to arrive at an orientation map, where the sampling area is partitioned into a union of individual grains.

[112] By "disorientation tolerance" is meant the largest distance (cf. Sect. 6.4) between the orientations at two adjacent sampling points above which the two pixels containing the points are assigned to different "grains". It is often called "misorientation tolerance" in the literature; see, e.g., the assertion quoted from [8] in Footnote 113. Since the distance between two orientations is at issue, "misorientation tolerance" is a misnomer.

[113] For instance, in ASTM Standard E2627-13 [8], which pertains to determination of average grain size in fully recrystallized polycrystalline materials by EBSD, "[a] misorientation tolerance value of 5° is recommended"; moreover, an EBSD scan be set up "so that the average grain contains about 500 [scan] points" and "[e]xclude grains with point counts less than 100."

evaluation of average grain size could and should be treated for ODF determination. In this regard an experimental study by Engler [103] provides an illustrative example.

Engler compared ODFs (truncated at $L := l_{\max} = 22$) obtained by EBSD and by X-ray diffraction (XRD) for an Al–1%Mg alloy (AA 5005) sheet in various back-annealed states from the as-rolled material (temper H18) to the fully annealed, recrystallized material (O temper). Here we restrict attention to Engler's work on the fully recrystallized O-temper material. The AA 5005-O material had an average grain size of about 20 μm and "a quite strong cube recrystallization texture". The EBSD scan was performed with a step size of 2 μm, and it included in excess of 3×10^5 sampling points. By his "highly simplified" estimate, "the number of actual *grains*" covered by the scan "was only about 3000." As for ghost-correction (see Chap. 9) in the X-ray texture analysis, Engler used the positivity method of Dahms and Bunge [84] (cf. Sect. 9.6) to estimate the texture coefficients with odd $l < 22$.

To investigate the number of EBSD single-orientation measurements necessary for adequate description of a texture represented by an XRD-determined ODF (with $L = 22$), Engler examined the evolution of the parameter[114]

$$\begin{aligned}\rho(N) &:= \int\limits_{\mathrm{SO(3)}} (\mathtt{f}_N(\boldsymbol{R}^{(p)}) - \mathtt{f}_{\mathrm{XRD}}(\boldsymbol{R}^{(p)}))^2 d\mathtt{g}(\boldsymbol{R}^{(p)}) \Big/ \int\limits_{\mathrm{SO(3)}} (\mathtt{f}_{\mathrm{XRD}}(\boldsymbol{R}^{(p)}))^2 d\mathtt{g}(\boldsymbol{R}^{(p)}) \\ &= \int\limits_{\mathrm{SO(3)}} (w_N(\boldsymbol{R}) - w_{\mathrm{XRD}}(\boldsymbol{R}))^2 d\mathcal{V}(\boldsymbol{R}) \Big/ \int\limits_{\mathrm{SO(3)}} (w_{\mathrm{XRD}}(\boldsymbol{R}))^2 d\mathcal{V}(\boldsymbol{R}) \end{aligned} \tag{8.50}$$

as the number N of EBSD single-orientation measurements used increases. In (8.50), w_N is the approximate ODF from EBSD with $L = 22$ and texture coefficients c_{mn}^l given by (8.48), where the spread parameter κ is taken as 2.5°;[115] w_{XRD} is the ODF (truncated at $L = l_{\max} = 22$) from X-ray measurements. Clearly

$$\rho(N) = \left(\frac{\| w_N - w_{\mathrm{XRD}} \|_{L^2}}{\| w_{\mathrm{XRD}} \|_{L^2}} \right)^2 \tag{8.51}$$

is the square of the relative error in L^2-norm of w_N with respect to w_{XRD}. Citing supporting references, Engler [103, p. 1149] asserts what follows: "According to former experience, ρ values of 0.1–0.2 ... provide a good accuracy for subsequent texture and/or property simulation".

Engler found [103, pp. 1151–1152]:

> The ODF computed from all EBSD-derived single orientations ($N \approx 300\,000$ orientations; ...) is very similar to the corresponding macrotexture of the recrystallized sample AA 5005-O ... [and] the resulting ρ value of 0.096 – *i.e.* a deviation below 10% – substantiates the high accuracy of EBSD measurements for macrotexture analysis.

On the other hand, the parameter ρ was found to decrease rather slowly with N:

[114] Here we rewrite Engler's expression $(8.50)_1$, which is in Bunge's convention and notation for the ODF, in our present convention and notation. Note that Engler's $\rho(N)$ is a slightly modified version of the parameter $\rho_{0,N}$ introduced by Pospiech et al. [264] in 1994, where $\mathtt{f}_{\mathrm{XRD}}$ is written as $\mathtt{f}_0$ and the integrand of the denominator is $(\mathtt{f}_N)^2$ instead of $(\mathtt{f}_0)^2$.

[115] In view of our discussions in Sect. 8.5.3, the value of κ chosen by Engler is reasonable.

> At 10 000 orientations ... the texture peaks appear to be displaced and their relative intensities are wrong ... This is reflected in a very high ρ value of 0.50. ... [A]t $N = 50\,000$ the ODF is much closer to the X-ray macrotexture ... and ρ has dropped to 0.2. ... [I]t is only at N values in excess of 150 000 that the ρ value levels at about 0.1 ...

As pointed out by Engler, "[i]t appears that the above numbers of N necessary to provide a reasonable macrotexture description are larger by several orders of magnitude than the values of the order of 1000 grains reported earlier".[116] He attributed "the (on first sight) surprising slow convergence of the ρ parameter" to the fact that "although [the] scan gives a very satisfactory detailed orientation map ..., the statistical relevance of the data is not that good," because "each grain is on average measured 100 times, producing a very large number of redundant data." In comparison, he explored treating the EBSD data in two other ways:

- First, a second "scan" with a step size of 10 μm "was performed by picking the corresponding orientations from the data set of the first, fine, EBSD map." For this second "scan", "the ρ parameter drops much faster, reaching values of 0.1 after only 5000 measurement points".
- Second, "the fine EBSD data set (2 μm step width) was re-shuffled with a random generator, and the evolution of ρ with N was again computed for these randomized data. Here, ρ converges much faster, and only ~ 1000 orientations are required to get a sound description of the corresponding macrotexture".

The first procedure, where a coarser measuring grid with respect to average grain size is chosen so that each grain would be hit at most a few times, has long been established (see, e.g., [106, 222, 291]) as one way to enhance statistical relevance of the EBSD single-orientation measurements. The second procedure is based on the simple idea of artificial randomization of data. It is in the same spirit as but easier to implement than the suggestion of "a stochastic scanning of the same area" [222]. As shown by Engler, it produces independent single-orientation data out of detailed EBSD scans meant for high-quality orientation maps. For texture determination this procedure will be applicable to any data file "as long as enough *grains* (*i.e.* not measured points) have been record in the EBSD scan" [103].

8.6.2 Minimum Number of Independent Single-Orientation Measurements Required

Soon after the indexing of EBSD patterns became automated in the early 1990s [2], there began the appearance of papers[117] which address questions concerning the "critical" or minimum number N_C of independent[118] single-orientation measurements required for determination of the texture of a sample. For definiteness, let us consider a polycrystal P, which is statistically homogeneous and has orientation measure $\hat{\wp}$ on $\mathrm{SO}(3)/G_{\mathrm{cr}}$, where G_{cr} is its

[116] Earlier in the same paper Engler [103, p. 1147] asserted that "for cubic materials with reasonably sharp textures ... a statistically sound representation of the textures required 500–1000 orientations. He cited several earlier studies [22, 23, 105, 346] to support his assertion.

[117] As early examples, see [23, 105, 169, 188, 221, 264, 347], which were published in 1994–96.

[118] As discussed in Sect. 8.5.1 on the mathematical basis of the Bunge-Haessner method, independence of the single-orientation measurements is a pre-requisite for the method to work. Without the adjective "independent", N_C need not exist. For example, making every measurement on the same grain in a sample of a polycrystal, irrespective of the number of measurements, will not deliver the ODF of the polycrystal. As shown by Engler [103], independence in single-orientation measurements can be simulated by artificial randomization of the order of the measurements.

group of crystallite symmetry. In the context of our discussion on the mathematical basis of the Bunge–Haessner method (see Sect. 8.5.1), an experiment $\mathscr{E}$ to determine an approximate ODF for the orientation measure $\hat{\wp}$ of P by single-orientation measurements will result in a sequence of Dirac measures $\{\delta_{\boldsymbol{R}_i G_{\mathrm{cr}}} : i = 1, 2, 3, \ldots\}$ so that the sequence of empirical measures $\hat{\mu}_N := \frac{1}{N}(\delta_{\boldsymbol{R}_1 G_{\mathrm{cr}}} + \cdots + \delta_{\boldsymbol{R}_N G_{\mathrm{cr}}})$ converges vaguely to $\hat{\wp}$ as $N \to \infty$.[119] Before N_C can be defined, the resolution required of the experiment has to be prescribed. Under the setting of Sect. 8.5.1, the resolution of the single-orientation measurements is specified by the pair of numbers (L, ε), where $L := l_{\max}$ is the highest value of l that the texture coefficients $\widetilde{c}(N)^l_{mn}$ of the approximate ODF w_N in (8.46) are allowed to be non-zero, and $\varepsilon > 0$ as shown in (8.43), which can be rewritten as $|c^l_{mn} - \widetilde{c}^l_{mn}(N)| < \varepsilon$, gives the tolerated uncertainly in each of the texture coefficient in the approximate ODF. With the resolution defined by (L, ε) chosen, N_C is the smallest positive integer K that (8.43) is valid for all $N > K$, $1 \le l \le L$, $-l \le m \le l$, and $-l \le n \le l$. Clearly N_C depends on the resolution defined by (L, ε). But it depends also on crystallite and/or sample symmetry (the presence of which reduces the number of independent texture coefficients and makes the requirement that inequalities (8.43) be observed less stringent), on the sequence of measured individual orientations $\{\delta_{\boldsymbol{R}_i G_{\mathrm{cr}}}\}$ (cf. [332, p. 93]), and most significantly on the orientation measure $\wp$ of P (e.g., if P is a single crystal, then $N_C = 1$).

As noted by Matthies and Wagner [221] in 1996, a problem of "practical importance" in single-orientation measurements was "to stop at $[N \ge N_C]$ the expensive determination of grain orientations in a sample with an unknown texture". In the 1990s and 2000s several studies [23, 103, 105, 106, 346–348] were set out to estimate N_C of a sample by using w_{XRD} or w_{nd}, the ODF as obtained by XRD or neutron diffraction measurements with series expansion (4.49) truncated at a selected $l = l_{\max}$, as the standard for comparison. In what follows we briefly summarize the main assumptions and some findings of these papers.

1. All the cited studies refer to N_C as the minimum number of *grains* included in the scan.
2. To evaluate the approximate w_N from the EBSD measurements, all those studies used the modified Bunge–Haessner method with various values of the spread parameter κ.
3. The samples used in the studies were those of cubic or hexagonal metals, and most of them had (approximate) orthorhombic sample symmetry.
4. As for the truncation parameter for the series expansion of w, most papers used $L = l_{\max} = 22$.
5. Most of the cited studies obtained N_C by following the evolution of some scalar parameter of N as N increases. For definiteness, let us use $\rho(N)$ as defined in (8.50) as example for illustration. If we follow the evolution of $\rho(N)$ as N increases to a sufficiently large number, and if we ignore minor local fluctuations, typically we shall see that $\rho(N)$ largely decreases as N increases and comes to a constant value, say ρ_∞, after N crosses a critical number $\mathtt{N}_c$, which is taken as an estimate of N_C. Moreover, if $\rho_\infty \le 0.2$, w_N for $N \ge \mathtt{N}_c$ would usually give a good representation of w_{XRD}. This number $\mathtt{N}_c$ is taken as N_C. The following description remains valid if $\rho(N)$ is replaced by any other scalar parameter used in the studies.[120]

[119] In practice the experiment will be discontinued at some $N > N_C$.

[120] As mentioned in Footnote 114, the original version of $\rho(N)$ in (8.50) was introduced by Pospiech et al. [264], which they denote by $\rho_{0,N}$, and w_0 is their notation for w_{XRD} in our present context. The parameter $\rho_{0,N}$ was used in [23, 105]. Other scalar parameters used included those relating to the texture symmetry of the sample [348]. Wright and Kocks [347, p. 60], however, warned about "the danger of using a single scalar parameter to describe the difference between two ODs [i.e., w_N and w_{XRD}]".

6. The number N_C obtained, with other factors that affect it kept the same, depends significantly on the orientation measure $\wp$ in question. In general, the sharper (resp. weaker) the texture, the smaller (resp. larger) is N_C. For instance, for cubic metals with approximate orthorhombic sample symmetry, N_C was found to run from about 1,000 grain orientations for samples with "reasonably sharp textures" (see [103] and the references therein) to 10,000 grain orientations for a rolled stainless steel of "moderate texture strength" [348].

Many papers that addressed the comparison of EBSD and XRD measurements were published in the 1990s and 2000s.[121] Those papers show general agreement between the EBSD and XRD results, provided that a sufficiently large number of grains are sampled in the EBSD scan and allowance is made on texture difference between the surface and the bulk. Hence single-orientation measurements by EBSD has already passed the test as a technique for texture determination. Further justification by comparison with XRD results is unnecessary. Moreover, as pointed out in Sect. 8.5.3, texture determination by EBSD is intrinsically more accurate than determination by XRD because the former has significantly smaller "instrument broadening". In fact in the 1990s and 2000s, there were already papers [41, 221, 222, 332] exploring methods for the determination of N_C from EBSD data.

On the other hand, while it was of practical importance in 1996 to stop the "the expensive determination of grain orientations in a sample with an unknown texture" when $N \geq N_C$ [221], the situation has completely changed. Today a large amount of EBSD single-orientation data can be obtained quickly and inexpensively. In practice one may just made grain-orientation measurements at so huge a number N that leaves little doubt for $N \geq N_C$. In fact EBSD data now usually contain such a large number of data points that they must be significantly reduced to be used for micromechanical computation of polycrystalline material response. As a result research efforts have recently been made [31, 100, 167] to investigate various methods that reduce EBSD data but preserve their important characteristics and enhance computational efficiency.

Remark 8.7 In this chapter we have covered only the original and the modified Bunge–Haessner method for treatment of single-orientation data, which played a dominant role in the area until serious attempts were made to develop better methods in the 2010s. The original Bunge-Haessner method makes no provisions for "instrument broadening" and other errors/uncertainties in the single-orientation measurements. In the modified method, each ideal orientation in the original method is replaced by a corresponding Gaussian component of Bunge with a spread angle. While it remains unclear why Pospiech and Lücke [263] first made this change, its subsequent widespread and sustained acceptance by texture researchers could be understood as the result of two possible reasons: (i) The change provides one way to account for the effects of instrument broadening. (ii) Making the modification could, in comparative studies, give better fits of EBSD results with textures determined by XRD, which has significant instrument-broadening issues itself. The change is, however, entirely ad hoc. There is no theoretical basis that the modified Bunge-Haessner method is the optimal way to treat orientation data from EBSD measurements. Several other methods, which could possibly improve on the original and the modified Bunge-Haessner method, have been proposed recently (see, e.g., [150, 250, 333]). Another recent paper of related interest is one [267] on error analysis of the crystal orientations and disorientations obtained by the classical EBSD technique. □

[121] Cf. Wright et al. [348, Introduction], where the authors assert that they perused over 50 papers.

Chapter 9

9 Determination of Texture Coefficients via X-Ray Diffraction

The harmonic or series expansion method, which was independently introduced by Bunge [56] and by Roe [270] for inference of texture coefficients from X-ray pole figures, marks the birth of quantitative texture analysis in 1965. Since then, various other methods have been proposed and developed, including the WIMV (Williams–Imhof–Matthies–Vinel) method ([219, 223, 226]; cf. also [170] for an exposition and comments), which is implemented in the Los Alamos texture software package popLA [171, 172].[122] In this exposition we will restrict our attention to the harmonic method. Some basic information on X-ray diffraction (XRD) by crystals is given in Appendix D.

In this chapter we will follow the Roe approach. Unless stated explicitly otherwise, all theoretical discussions and derivations will pertain to triclinic aggregates of triclinic crystallites (i.e., with $G_{\text{tex}} = \{\boldsymbol{I}\}$ and $G_{\text{cr}} = \{\boldsymbol{I}\}$). The general formulas derived will be applicable to polycrystals with non-trivial texture and/or crystallite symmetry after the requisite restrictions on texture coefficients imposed by G_{tex} and/or G_{cr} are implemented in the formulas.

9.1 Representation of Orientations in Pole Figures

9.1.1 Stereographic Projection and Pole Figures

Let $(\mathsf{C}, \boldsymbol{\kappa}_0)$ be the reference configuration of an ideal triclinic crystal, and let L be its chosen lattice. Let $\boldsymbol{h}$ be the unit normal to the family of (hkl) planes of the ideal crystal. Consider a transplacement (see Sect. 2.2) $\boldsymbol{g} : \boldsymbol{\kappa}_0(\mathsf{C}) \to E^3$ and a Cartesian coordinate system in the codomain E^3 of $\boldsymbol{g}$ such that $\boldsymbol{g}$ maps the origin of L to the origin of the Cartesian coordinate system and $\boldsymbol{g} = (\boldsymbol{0}, \boldsymbol{R})$, where $\boldsymbol{R} : \mathbb{R}^3 \to \mathbb{R}^3$ is a rotation such that $\boldsymbol{R}\boldsymbol{h} = \boldsymbol{n} = (n_1, n_2, n_3)$ with $n_3 \geq 0$.

Let $\mathcal{S}^2$ be the unit sphere. The stereographic projection of $\boldsymbol{n}$ to the equatorial plane is defined as follows. Let $N = (0, 0, 1)$ and $S = (0, 0, -1)$ be the north and south pole of the unit sphere, respectively. Let $(1, \alpha, \beta)$, where α is the polar angle and β the azimuthal angle, be the spherical coordinates of $P := (n_1, n_2, n_3) \in \mathcal{S}^2$ with $n_3 \geq 0$. The two sets of coordinates are related by the equations

$$n_1 = \sin\alpha \cos\beta, \qquad n_2 = \sin\alpha \sin\beta, \qquad n_3 = \cos\alpha. \tag{9.1}$$

Consider the cross-section of the unit ball that includes the origin O and the great circle of $\mathcal{S}^2$ defined by the azimuthal angle β, which contains the points N, S, and P. Let the line segment SP meet the equatorial plane at the point with polar coordinates $(\hat{r}, \hat{\theta})$. Since $\triangle SOP$ is isosceles with $OS = OP$ and $\alpha = \angle NOP$ is the exterior angle adjacent to $\angle O$ of the triangle, we have $\angle OSP = \alpha/2$. It follows that

$$\hat{r} = \tan\frac{\alpha}{2} = \frac{\sin\alpha}{1 + \cos\alpha}, \qquad \hat{\theta} = \beta. \tag{9.2}$$

[122] During 1997–2007 when the research group of the author undertook also experimental work in texture analysis, we used popLA and in-house Fortran and Maple programs (written by Mojia Huang) based on the harmonic method for inversion of X-ray pole figures. We checked the results from the two methods against each other on a few cases. The findings from the two were found to be consistent.

For the triclinic ideal crystal, what we shall obtain in X-ray measurements of (hkl) pole figures will be a picture of the unit disc in the equatorial plane with the intensity at the location $(\hat{r}, \hat{\theta})$ (or equivalently (α, β)) ascertained empirically.

9.1.2 Pole Figure of a Cubic Crystallite in a Sheet Metal

Suppose a cubic crystallite in a sheet metal has the orientation $\boldsymbol{R} = (HKL)[UVW]$. Where will this orientation show up in an (hkl) pole figure of the crystallite?

Let $\boldsymbol{h}$ be the unit vector normal to the (hkl) crystal planes which has a non-negative spatial 3-component n_3 in the $(HKL)[UVW]$ orientation. Without loss of generality, say $\boldsymbol{h} = (h, k, l)/\sqrt{h^2 + k^2 + l^2}$ in the crystal frame. In the $(HKL)[UVW]$ orientation, $\boldsymbol{h}$ has spatial components given by the column vector

$$\begin{pmatrix} n_1 \\ n_2 \\ n_3 \end{pmatrix} = \frac{1}{\sqrt{h^2 + k^2 + l^2}} \begin{pmatrix} \frac{U}{N} & \frac{V}{N} & \frac{W}{N} \\ \frac{KW - LV}{MN} & \frac{LU - HW}{MN} & \frac{HV - KU}{MN} \\ \frac{H}{M} & \frac{K}{M} & \frac{L}{M} \end{pmatrix} \begin{pmatrix} h \\ k \\ l \end{pmatrix}. \tag{9.3}$$

Here we assume that $n_3 \geq 0$; otherwise we just replace $\boldsymbol{h}$ by $-\boldsymbol{h}$.

The location of $(HKL)[UVW]$ in the (hkl) pole figure is given by the stereographic projection of (n_1, n_2, n_3) in the spatial equatorial plane. Under a polar coordinate system where the polar axis runs in the rolling direction, the $(HKL)[UVW]$ orientation is represented by the point with polar coordinates $(\hat{r}, \hat{\theta})$ given by (9.2). Note that all orientations obtained by rotating the orientation $(HKL)[UVW]$ about the axis defined by the spatial vector $\boldsymbol{n} = (n_1, n_2, n_3)$ are represented by the same point in the (hkl) pole figure. Thus there is some loss of information when we depict the three-dimensional manifold of orientations by a two-dimensional pole figure.

Example 9.1 In this example we treat the cubic crystallite as if it were triclinic. We will consider the effects of crystal symmetry in the next subsection. In the (111) pole figure the orientation (110)[001] of a triclinic crystallite is given by the stereographic projection of the spatial vector

$$\frac{1}{\sqrt{3}} \begin{pmatrix} 0 & 0 & 1 \\ \frac{1}{\sqrt{2}} & -\frac{1}{\sqrt{2}} & 0 \\ \frac{1}{\sqrt{2}} & \frac{1}{\sqrt{2}} & 0 \end{pmatrix} \begin{pmatrix} 1 \\ 1 \\ 1 \end{pmatrix} = \begin{pmatrix} \sqrt{\frac{1}{3}} \\ 0 \\ \sqrt{\frac{2}{3}} \end{pmatrix}.$$

Thus $\cos\alpha = \sqrt{2/3}$ and $\beta = 0$. In the (111) pole figure the orientation (110)[001] is located at the point with polar coordinates $(1/(\sqrt{3} + \sqrt{2}), 0) \approx (0.3178, 0)$. □

9.1.3 Effects of Crystal Symmetry

Because of crystal symmetry, the orientation of a cubic crystallite is not described by one rotation $\boldsymbol{R}$ but by 24 equivalent rotations $\boldsymbol{R}\boldsymbol{Q}_\alpha$ $(\alpha = 1, \ldots, 24)$, where $\boldsymbol{Q}_\alpha \in O$. Hence, in a pole figure, a cubic crystallite shows up as spots of equal intensity at a number of locations. The number of spots depends on the orientation of the crystallite and on the (hkl) pole figure in question.

Example 9.2 Consider a cubic crystallite in the Cube or (001)[100] orientation. By formula (7.49), the rotation $\boldsymbol{R}$ corresponding to the orientation (001)[100] is simply the identity $\boldsymbol{I}$. For the (111) pole figure, $\boldsymbol{h} = (1, 1, 1)/\sqrt{3}$. To find the locations in the (111) pole figure where this cubic crystallite will contribute to the X-ray intensity, we compute $\boldsymbol{R}\boldsymbol{Q}_\alpha\boldsymbol{h}$ for $\boldsymbol{Q}_\alpha \in O$. While the group O has 24 elements $\boldsymbol{Q}_\alpha$, we find that in the present case there are only 4 distinct vectors $\boldsymbol{R}\boldsymbol{Q}_\alpha\boldsymbol{h}$ with a non-negative 3-component. They are:

$$\frac{1}{\sqrt{3}}(1, 1, 1), \quad \frac{1}{\sqrt{3}}(1, -1, 1), \quad \frac{1}{\sqrt{3}}(-1, 1, 1), \quad \text{and} \quad \frac{1}{\sqrt{3}}(-1, -1, 1).$$

Hence the (111) pole figure of this cubic crystallite consists of 4 spots located at

$$(\frac{\sqrt{2}}{\sqrt{3}+\sqrt{2}}, \frac{\pi}{4}), \quad (\frac{\sqrt{2}}{\sqrt{3}+\sqrt{2}}, \frac{3\pi}{4}), \quad (\frac{\sqrt{2}}{\sqrt{3}+\sqrt{2}}, \frac{5\pi}{4}), \quad \text{and} \quad (\frac{\sqrt{2}}{\sqrt{3}+\sqrt{2}}, \frac{7\pi}{4}). \quad \square$$

9.1.4 Effects of Texture Symmetry

An X-ray pole figure in fact shows the responses of all the crystallites within a sampling volume. These crystallites, as a whole, may exhibit texture symmetry. By means of the orientation distribution function (ODF) we have already defined precisely in Chap. 5 what we mean by texture symmetry. Here we give a heuristic discussion in the context of pole-figure measurements.

Let Ω be the sampling volume of a measurement, which we simply call the sample in question. Consider triclinic crystallites $\mathcal{B}_k$ $(k = 1, 2, \ldots, n)$ contained in Ω. Suppose the sample Ω undergoes a rotation $\boldsymbol{Q}$. We denote by $\mathcal{T}_{\boldsymbol{Q}}\Omega$ the new configuration of the sample after the rotation. A crystallite $\mathcal{B}_k$ whose orientation is specified by $\boldsymbol{R}_k$ in the original configuration has orientation $\boldsymbol{Q}\boldsymbol{R}_k$ in the rotated configuration. The (hkl) pole figure of Ω and of $\mathcal{T}_{\boldsymbol{Q}}\Omega$ shows X-ray intensities at the spots corresponding to the orientations $\{\boldsymbol{R}_1, \boldsymbol{R}_2, \ldots, \boldsymbol{R}_n\}$ and $\{\boldsymbol{Q}\boldsymbol{R}_1, \boldsymbol{Q}\boldsymbol{R}_2, \ldots, \boldsymbol{Q}\boldsymbol{R}_n\}$, respectively. Suppose $\boldsymbol{Q} \in G_{\text{tex}}$. Strict texture symmetry will require that the (hkl) pole figure for $\mathcal{T}_{\boldsymbol{Q}}\Omega$ be the same as its counterpart for Ω, i.e., for each spot P with non-zero intensity in the pole figure for Ω, a corresponding spot shows up at the same location as P in the pole figure for $\mathcal{T}_{\boldsymbol{Q}}\Omega$, and the two spots have the same intensity. Clearly, this will not occur in practice exactly. Hence texture symmetry should be understood only in a probabilistic sense.

Example 9.3 Suppose $G_{\text{tex}} = \{\boldsymbol{I}, \boldsymbol{R}(\boldsymbol{e}_1, \pi)\}$ for a sample that consists of triclinic crystallites as discussed in Example 9.1. In Example 7.9, we have already shown that in Euler angles (ψ, θ, ϕ) the orientation (110)[001] is given by $\boldsymbol{R}(0, \pi/2, 3\pi/4)$. By texture symmetry, measurement at a sampling point has the same chance of yielding orientation $\boldsymbol{R}(0, \pi/2, 3\pi/4)$ or orientation $\boldsymbol{R}(0, \pi, \pi)\boldsymbol{R}(0, \pi/2, 3\pi/4)$, because $\boldsymbol{R}(\boldsymbol{e}_1, \pi)$ has Euler angles $(0, \pi, \pi)$. A straightforward computation indicates that in the (111) pole figure orientation $\boldsymbol{R}(0, \pi, \pi)\boldsymbol{R}(0, \pi/2, 3\pi/4)$ is located at the spot $(\hat{r}, \hat{\theta}) = (-1/(\sqrt{3}+\sqrt{2}), 0)$. Thus by texture symmetry the (111) pole figure of the given sample should have the same intensity at two spots, namely $(\hat{r}, \hat{\theta}) = (1/(\sqrt{3}+\sqrt{2}), 0)$ and $(\hat{r}, \hat{\theta}) = (-1/(\sqrt{3}+\sqrt{2}), 0)$. $\square$

For more information on representing ideal orientations of an orthorhombic aggregate of cubic crystallites in pole figures and in Euler space (i.e., the (ψ, θ, ϕ) space), see Hansen et al. [140].

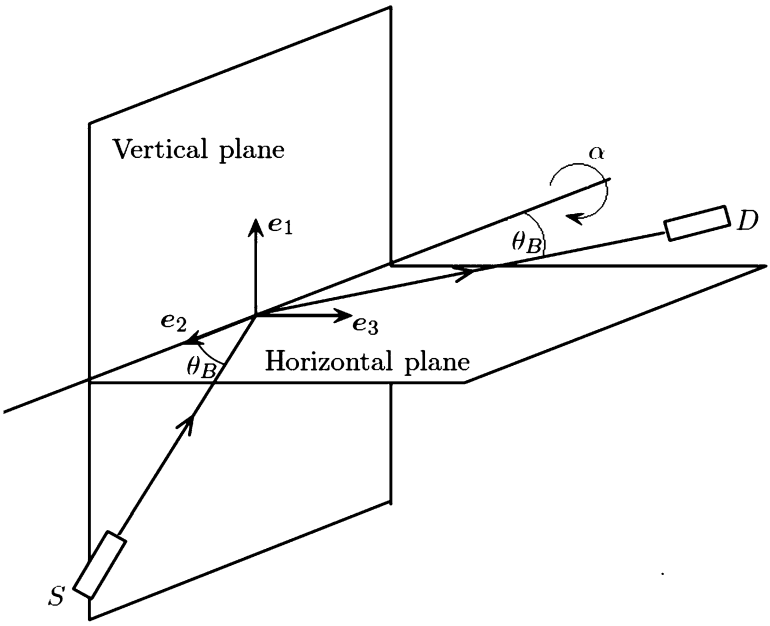

Fig. 2 Setup for measurement of X-ray pole figures by the reflection method

9.2 Rotation of Sample in Pole-Figure Measurements

In what follows we are concerned only with obtaining information about the crystallographic texture of a sheet metal by X-ray diffraction (XRD). Moreover, we restrict our attention to the reflection method. Pole figures of the given sheet sample are measured under the reflection geometry. These pole figures are the experimental data from which the texture of the sample is to be inferred. When the orientations of the crystallites in a polycrystalline sample are ascertained, all the pole figures of the sample are determined, and it is then straightforward to carry out the easy computations to obtain a specific pole figure. The inverse problem of inferring texture from pole figures is much more difficult and was for almost three decades one of the central problems in quantitative texture analysis.

We will follow the Roe approach in the theoretical development in this chapter. As the first step, all the general formulas will be derived for triclinic aggregates of triclinic crystallites. Corresponding formulas for polycrystals with non-trivial G_{tex} and/or G_{cr} will be obtained simply from the general formulas by applying appropriate restrictions imposed by symmetry to the texture coefficients in the general formulas.

In the reflection method, the diffractometer is set up such that the incident X-ray beam from the source S and the reflected beam towards the detector D lie in the horizontal plane. Let θ_B be the Bragg angle pertaining to the (hkl) pole figure. We select a spatial coordinate system with orthonormal basis $\{\boldsymbol{e}_i\}$ which satisfies the following conditions (see Fig. 2):

1. The basis vector $\boldsymbol{e}_1$ points vertically up.
2. Should we put a mirror in the 1-2 plane, $\boldsymbol{e}_3$ would bisect the angle between the incident and the reflected beam.
3. The incident beam and the reflected beam propagate in the directions $(0, -\cos\theta_B, -\sin\theta_B)$ and $(0, \cos(\pi - \theta_B), \sin(\pi - \theta_B))$, respectively.

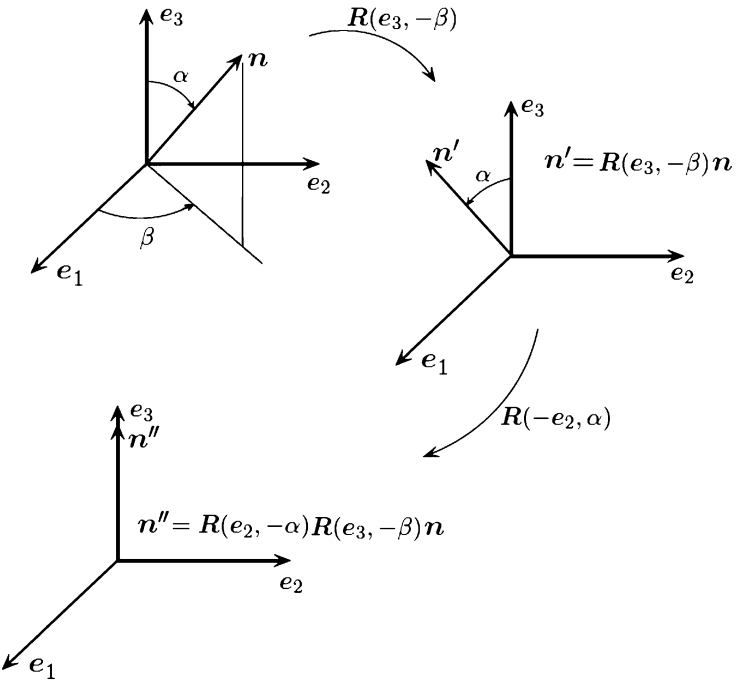

Fig. 3 Sequence of rotations that brings $\boldsymbol{n}$ to $\boldsymbol{e}_3$

The sample sheet—a triclinic aggregate of triclinic crystallites—is initially mounted so that it lies in the 1-2 plane with the rolling direction parallel to $\boldsymbol{e}_1$. In this setting a crystallite whose (hkl) planes are normal to $\boldsymbol{e}_3$ will contribute to the intensity of the signal picked up by the detector.

Let L be the lattice of the reference ideal triclinic crystal, and let L^* be the reciprocal lattice of L with basis vectors $\boldsymbol{a}^*$, $\boldsymbol{b}^*$, and $\boldsymbol{c}^*$. Let $\mathbf{H} = h\boldsymbol{a}^* + k\boldsymbol{b}^* + l\boldsymbol{c}^*$. Then the unit vector $\boldsymbol{h} := \mathbf{H}/\|\mathbf{H}\|$ is normal to the (hkl) planes in the configuration of the reference crystal. Consider a crystallite $\mathcal{B}_o$ whose orientation in the sample sheet is defined by the rotation $\boldsymbol{R}_o$ with respect to the reference crystal. The vectors $\boldsymbol{R}_o\boldsymbol{h}$ and $-\boldsymbol{R}_o\boldsymbol{h}$ are the two unit normals to the (hkl) planes in $\mathcal{B}_o$. Let $\boldsymbol{n} = \boldsymbol{R}_o\boldsymbol{h}$. Without loss of generality, suppose $n_3 \geq 0$ (otherwise we just define[123] $\boldsymbol{n} = -\boldsymbol{R}_o\boldsymbol{h}$). Let $(1, \alpha, \beta)$, where $0 \leq \alpha \leq \pi/2$ and $0 \leq \beta < 2\pi$, be the spherical coordinates of $\boldsymbol{n}$ in the upper hemisphere. When the sample undergoes a rotation defined by $\boldsymbol{R}(\boldsymbol{e}_2, -\alpha)\boldsymbol{R}(\boldsymbol{e}_3, -\beta)$, the unit vector $\boldsymbol{e}_3$ becomes normal to the (hkl) planes of $\mathcal{B}_o$ (see Fig. 3). This rotation can be accomplished by first rotating the sample an angle α about $-\boldsymbol{e}_2$, and then rotating it by an angle $-\beta$ about its new normal $\boldsymbol{R}(-\boldsymbol{e}_2, \alpha)\boldsymbol{e}_3$ (see Fig. 4), because by Euler's theorem (1.82) we have

$$\begin{aligned}\boldsymbol{R}(\boldsymbol{R}(-\boldsymbol{e}_2, \alpha)\boldsymbol{e}_3, -\beta)\boldsymbol{R}(-\boldsymbol{e}_2, \alpha) &= \boldsymbol{R}(-\boldsymbol{e}_2, \alpha)\boldsymbol{R}(\boldsymbol{e}_3, -\beta)\boldsymbol{R}(-\boldsymbol{e}_2, \alpha)^{-1}\boldsymbol{R}(-\boldsymbol{e}_2, \alpha) \\ &= \boldsymbol{R}(\boldsymbol{e}_2, -\alpha)\boldsymbol{R}(\boldsymbol{e}_3, -\beta). \end{aligned} \tag{9.4}$$

[123] This will be justified by Friedel's rule in Sect. 9.3.

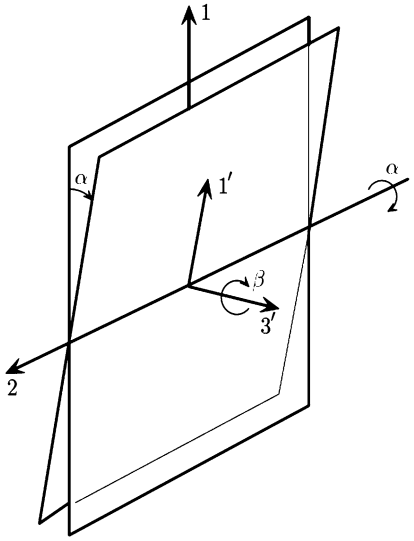

Fig. 4 Rotations of sample in measurement of pole figures

Remark 9.4 Unless $\boldsymbol{R}_o\boldsymbol{h}$ or $-\boldsymbol{R}_o\boldsymbol{h}$ is sufficiently close[124] to $\boldsymbol{e}_3$, the (hkl) planes of $\mathcal{B}_o$ will not act as Bragg mirrors to reflect the incident X-ray beam. The rotation $\boldsymbol{R}(\boldsymbol{e}_2, -\alpha)\boldsymbol{R}(\boldsymbol{e}_3, -\beta)$ of the sample renders either $\boldsymbol{R}_o\boldsymbol{h}$ or $-\boldsymbol{R}_o\boldsymbol{h}$, one of the unit normals of the (hkl) planes in $\mathcal{B}_o$, parallel to $\boldsymbol{e}_3$, and thus make those planes Bragg mirrors. In fact the (hkl) planes of any crystallite in the sampling volume, which after the rotation $\boldsymbol{R}(\boldsymbol{e}_2, -\alpha)\boldsymbol{R}(\boldsymbol{e}_3, -\beta)$ of the sample have one of its unit normals sufficiently close to $\boldsymbol{e}_3$, will become Bragg mirrors in the pole-figure measurement. By (D.96), the integrated intensity[125] of the reflected beam in question would be proportional to the total volume of such crystallites in the sampling volume. □

Remark 9.5 The integrated intensity of the X-ray radiation that reaches the detector D in Fig. 2, however, requires corrections before it can be used in theoretical analysis. The theory of X-ray diffraction by crystals, as outlined in Appendix D, is based on elastic scattering of X-ray by the target atoms. However, even if the detector is at a position for which according to the theory it should not receive any elastically scattered X-ray, the intensity of radiation received by the detector is non-zero. That is called the background intensity, one source of which is inelastic scattering. In general, when X-rays fall on a substance, they are partly scattered inelastically. Besides the background error, correction has to be made to mitigate the defocusing error, namely that the measured intensity as recorded by the detector is strongly dependent on the tilt angle α and the Bragg angle θ_B. This error arises because the shape of the irradiated spot depends on α and θ_B, whereas the detector, equipped with a system of receiving slits sees only a small, constant area of the sample surface. For further discussions on the background error, the defocusing error, and their corrections, see Humbert [158] and Engler and Randle [104, Sect. 4.3.6]. Henceforth when we refer to the intensity $I(\alpha, \beta; \Theta, \Phi)$ of the reflected beam, we mean the intensity after correction. □

[124] See Sect. D.4 and particularly (D.67) in Appendix D for a quantitative description. Henceforth we will write $\boldsymbol{R}_o\boldsymbol{h} \approx \boldsymbol{e}_3$ if $\boldsymbol{R}_o\boldsymbol{h}$ is "sufficiently close" to $\boldsymbol{e}_3$.

[125] See Footnote 194 in Appendix D for definition.

9.3 Pole Figures and the Orientation Distribution Function

Following the Roe approach, we restrict attention to a polycrystal P of substance S which is a triclinic aggregate of triclinic crystallites (i.e., with $G_{\text{tex}} = \{\boldsymbol{I}\}$ and $G_{\text{cr}} = \{\boldsymbol{I}\}$). Let the texture of P, with respect to a chosen reference[126] perfect crystal C, be described by an orientation distribution function w. The orientation space for the polycrystal is SO(3), and each orientation is defined by one rotation $\boldsymbol{R}$. We assume the polycrystal P is statistically homogeneous so that w is independent of the sampling point and is a function of the orientation $\boldsymbol{R}$ only.

To motivate what we shall do, let us re-examine (3.9) in Proposition 3.2. The ball B_r in (3.9) can be interpreted as the sampling volume. Let A be a Borel set in SO(3). If the sampling volume B_r is large enough, (3.9) can be interpreted as

$$\int_A w(\boldsymbol{R}) d\mathcal{V}(\boldsymbol{R}) \approx \frac{\mathrm{V}(\{\mathtt{X} \in B_r : \boldsymbol{R}(\mathtt{X}) \in A\})}{\mathrm{V}(B_r)}, \tag{9.5}$$

where V is the three-dimensional Euclidean volume. In words, on the left-hand side is the probability of finding $\boldsymbol{R}(\mathtt{X}) \in A$ for any $\mathtt{X} \in B_r$; on the right-hand side is the volume fraction of B_r where $\boldsymbol{R}(\mathtt{X}) \in A$. Formula (9.5) follows from the ergodic hypothesis or the assumption that the polycrystal P is an ergodic system. Nevertheless it does suggest that the ODF is related to some appropriate volume fraction. As each X-ray (hkl) pole figure can be taken as a catalogue of normalized intensities $p(\alpha_i, \beta_i)$ on an (almost) equal-area grid $\{(\alpha_i, \beta_i) : i = 1, \ldots, n\}$ [104, Sect. 4.3.3], which give the volume fraction (with respect to the sampling volume) of crystallites with either of the two unit normals of their (hkl) planes sufficiently close to the unit vector $\boldsymbol{n}(\alpha_i, \beta_i)$ (see Remarks 9.4 and D.8), the possible relation between p and w should be investigated thoroughly, which is what we shall do next.

Henceforth we adopt a spatial Cartesian coordinate system (with basis vectors $\boldsymbol{e}_1$, $\boldsymbol{e}_2$ and $\boldsymbol{e}_3$) as defined by the geometry of the X-ray diffractometer (cf. Fig. 2).

Let L be the chosen lattice for C and $\{\boldsymbol{b}_i : i = 1, 2, 3\}$ be a right-handed triad of primitive basis vectors of L. The corresponding reciprocal lattice and reciprocal basis vectors are denoted by L^* and $\{\boldsymbol{b}_i^* : i = 1, 2, 3\}$, respectively. We choose a Cartesian coordinate system in C such that it has the same orthonormal basis $\boldsymbol{e}_i$ $(i = 1, 2, 3))$ as that of the spatial coordinate system. Let $\boldsymbol{h}$ and $-\boldsymbol{h}$ be the unit normals to the family of (hkl) planes[127] of C, i.e., $\boldsymbol{h} = \mathbf{H}_{hkl}/\|\mathbf{H}_{hkl}\|$, where $\mathbf{H}_{hkl} = h\boldsymbol{b}_1^* + k\boldsymbol{b}_2^* + l\boldsymbol{b}_3^*$ is a reciprocal lattice vector. Let $(1, \Theta, \Phi)$ be the spherical coordinates of $\boldsymbol{h}$. Let $(1, \alpha, \beta)$ be the spherical coordinates of a spatial unit vector $\boldsymbol{n}$. Let us begin by asking the following question:

– Given that the ODF is given by w, what is the probability density $q(\boldsymbol{n}; \boldsymbol{h})$ or $q(\alpha, \beta; \Theta, \Phi)$ that at a sampling point the unit plane-normal $\boldsymbol{h} := \mathbf{H}_{hkl}/\|\mathbf{H}_{hkl}\|$ is pointing in the $\boldsymbol{n}$ direction in space?

In the preceding question, we let $\boldsymbol{n}$ range over the entire unit sphere without restriction. The function $q(\boldsymbol{n}; \boldsymbol{h})$ is called the plane-normal distribution by Roe [270].

Let $\mathcal{P}$ be a polycrystalline sample of P. Given a reciprocal lattice vector $\mathbf{H}_{hkl}$, we consider an XRD experiment on $\mathcal{P}$ to produce an (hkl) pole figure by Bragg reflection. In

[126] For simplicity we will write C both for $(\mathsf{C}, \boldsymbol{\kappa}_0)$ and for $(\mathsf{C}, \boldsymbol{\kappa}_0)_{\text{mac}}$ in this chapter. Whether C stands for $(\mathsf{C}, \boldsymbol{\kappa}_0)$ or for $(\mathsf{C}, \boldsymbol{\kappa}_0)_{\text{mac}}$ should be clear from the context.

[127] An (hkl) plane is a lattice plane if the integers h, k, and l are coprime. It is a fictitious lattice plane for a higher-order Bragg reflection if h, k, and l are not coprime. Cf. Sect. 7.4.

Remark D.8 in Appendix D we observe that in an (hkl) pole figure the normalized intensity

$$p(\alpha_i, \beta_i; \Theta, \Phi) = I(\alpha_i, \beta_i; \Theta, \Phi) / \sum_i I(\alpha_i, \beta_i; \Theta, \Phi) \tag{9.6}$$

gives the volume fraction on an equal-area grid $\{(\alpha_i, \beta_i) : i = 1, \ldots, n\}$, with respect to the sampling volume, of $\mathfrak{C}(\alpha_i, \beta_i)$—the set of crystallites which contribute to the integrated intensity of the reflected beam when the sample is at the configuration specified by the angles (α_i, β_i). Let $\boldsymbol{n}_i$ be the unit vector with spherical coordinates $(1, \alpha_i, \beta_i)$, where $0 \le \alpha_i \le \pi/2$ and $0 \le \beta_i < 2\pi$. By the discussion in the preceding section, it is clear that $\mathfrak{C}(\alpha_i, \beta_i)$ includes crystallites whose orientation in the initial configuration of the sample is given by any $\boldsymbol{R}_o$ such that $\boldsymbol{n}_i \approx \boldsymbol{R}_o \boldsymbol{h}$ (cf. Footnote 9.4 for the meaning of "$\approx$" here). For routine XRD measurements, however, Friedel's rule is valid, which implies that XRD does not distinguish any reciprocal vector $\mathbf{H}$ from $-\mathbf{H}$. Then $\mathfrak{C}(\alpha_i, \beta_i)$ consists of crystallites in the sampling volume whose orientation in the sampling volume is given by any $\boldsymbol{R}_o$ such that $\boldsymbol{n}_i \approx \pm \boldsymbol{R}_o \boldsymbol{h}$.

Let us recast (9.6) into its continuous form for further theoretical discussion. We write

$$p(\alpha, \beta; \Theta, \Phi) = \frac{I(\alpha, \beta; \Theta, \Phi)}{\int_0^{2\pi} \int_0^{\pi/2} I(\alpha, \beta; \Theta, \Phi) \sin\alpha \, d\alpha d\beta}, \quad \text{where } 0 \le \alpha \le \tfrac{\pi}{2}, 0 \le \beta < 2\pi, \tag{9.7}$$

which we call the density of normalized intensity. Let $\mathcal{A} \subset \mathcal{S}^2_+ := \{\boldsymbol{n} \in \mathcal{S}^2 : n_3 \ge 0\}$. The quantity

$$\iint_{\mathcal{A}} p(\alpha, \beta; \Theta, \Phi) \sin\alpha \, d\alpha d\beta \tag{9.8}$$

gives the volume fraction of crystallites in the sampling volume whose initial orientation $\boldsymbol{R}_o$ in SO(3) satisfies $\boldsymbol{n} \approx \pm \boldsymbol{R}_o \boldsymbol{h}$ for $\boldsymbol{n} \in \mathcal{A}$. Noting our discussion on (9.5), the physical meaning of $q(\boldsymbol{n}; \boldsymbol{h})$, and the effect of Friedel's rule, we assume that

$$p(\boldsymbol{n}; \boldsymbol{h}) = q(\boldsymbol{n}; \boldsymbol{h}) + q(\boldsymbol{n}; -\boldsymbol{h}) \tag{9.9}$$

for $\boldsymbol{n} \in \mathcal{S}^2_+$.

We proceed to find a formula for $p(\boldsymbol{n}; \boldsymbol{h})$ by deriving one for $\boldsymbol{q}(\boldsymbol{n}; \boldsymbol{h})$. For the special case where $\boldsymbol{h} = \boldsymbol{n} = \boldsymbol{e}_3$ (cf. Schaeben and Boogaart [284, p. 257]), it is clear that

$$\begin{aligned} q(\boldsymbol{e}_3; \boldsymbol{e}_3) &= \int_0^{2\pi} w(0, 0, \phi) d\phi \\ &= \frac{1}{4\pi} + \sum_{l=1}^{\infty} \sum_{m=-l}^{l} \sum_{n=-l}^{l} c^l_{mn} \int_0^{2\pi} D^l_{mn}(0, 0, \phi) d\phi \\ &= \frac{1}{4\pi} + \sum_{l=1}^{\infty} \sum_{m=-l}^{l} \sum_{n=-l}^{l} c^l_{mn} \delta_{mn} \int_0^{2\pi} e^{-in\phi} d\phi \\ &= \frac{1}{4\pi} + 2\pi \sum_{l=1}^{\infty} c^l_{00}. \end{aligned} \tag{9.10}$$

The general $q(\boldsymbol{n}; \boldsymbol{h})$ can be obtained from (9.10) by a simple trick.

Let $\boldsymbol{Q}$ be a rotation of the sample which brings the spatial unit vector $\boldsymbol{n}$ to $\boldsymbol{e}_3$, and let $\boldsymbol{Q}_r$ be a rotation of C which brings the reciprocal lattice vector $\boldsymbol{h}$ to $\boldsymbol{e}_3$. We may take $\boldsymbol{Q}$ and $\boldsymbol{Q}_r$ to be the rotation whose transpose $\boldsymbol{Q}^T$ and $\boldsymbol{Q}_r^T$ has Euler angles $(\beta, \alpha, 0)$ and $(\Phi, \Theta, 0)$, respectively. Let $\mathring{w}$ be the ODF of the $\boldsymbol{Q}$-rotated sample with respect to the $\boldsymbol{Q}_r$-rotated reference, and let $\mathring{c}^l_{mn}$ be the corresponding texture coefficients. Then

$$\begin{aligned} q(\alpha, \beta; \Theta, \Phi) &= \frac{1}{4\pi} + 2\pi \sum_{l=1}^{\infty} \mathring{c}^l_{00} \\ &= \frac{1}{4\pi} + 2\pi \sum_{l=1}^{\infty} \sum_{m=-l}^{l} \mathring{c}^l_{m0} d^l_{m0}(\alpha) e^{-im\beta} \\ &= \frac{1}{4\pi} + 2\pi \sum_{l=1}^{\infty} \sum_{m=-l}^{l} \sum_{n=-l}^{l} c^l_{mn} d^l_{m0}(\alpha) d^l_{n0}(\Theta) e^{-im\beta} e^{in\Phi}, \end{aligned} \tag{9.11}$$

where we have appealed to transformation formulas for texture coefficients (5.6), (5.12), and the symmetry property $(4.32)_1$ of d^l_{mn}. By (4.27), we observe that the function q satisfies the normalization condition

$$\int_0^{2\pi} \int_0^{\pi} q(\alpha, \beta; \Theta, \Phi) \sin\alpha d\alpha d\beta = 1. \tag{9.12}$$

In terms of the spherical harmonics

$$Y_{lm}(\alpha, \beta) := \sqrt{\frac{2l+1}{4\pi}} d^l_{m0}(\alpha) e^{im\beta}, \tag{9.13}$$

which satisfy the orthonormality condition

$$\int_0^{2\pi} \int_0^{\pi} \overline{Y_{lm}(\alpha, \beta)} Y_{l'm'}(\alpha, \beta) \sin\alpha d\alpha d\beta = \delta_{ll'}\delta_{mm'}, \tag{9.14}$$

we may recast (9.11) as

$$q(\alpha, \beta; \Theta, \Phi) = \frac{1}{4\pi} + \sum_{l=1}^{\infty} \sum_{m=-l}^{l} \sum_{n=-l}^{l} \frac{8\pi^2}{2l+1} c^l_{mn} \overline{Y_{lm}(\alpha, \beta)} Y_{ln}(\Theta, \Phi). \tag{9.15}$$

By (9.9), (9.11) and the identities[128]

$$d^l_{n0}(\pi - \Theta) = (-1)^{l+n} d^l_{n0}(\Theta) \quad \text{and} \quad e^{in\pi} = (-1)^n, \tag{9.16}$$

[128] Identity $(9.16)_1$ is a special case of $(4.33)_1$.

we have

$$p(\alpha,\beta;\Theta,\Phi)=\frac{1}{2\pi}+2\pi\sum_{l=1}^{\infty}(1+(-1)^l)\left(\sum_{m=-l}^{l}\sum_{n=-l}^{l}c_{mn}^{l}d_{m0}^{l}(\alpha)d_{n0}^{l}(\Theta)e^{-im\beta}e^{in\Phi}\right)$$
$$=\frac{1}{2\pi}+4\pi\sum_{\text{even } l\geq 2}^{\infty}\sum_{m=-l}^{l}\sum_{n=-l}^{l}c_{mn}^{l}d_{m0}^{l}(\alpha)d_{n0}^{l}(\Theta)e^{-im\beta}e^{in\Phi},\tag{9.17}$$

where $0\leq\alpha\leq\pi/2$ and $0\leq\beta<2\pi$. Equation (9.17) shows how the density of normalized intensity of the (hkl) pole figure is related to the ODF. By $(4.33)_2$, we have for even l

$$d_{\bar{m}0}^{l}(\theta)=(-1)^m d_{m0}^{l}(\theta).\tag{9.18}$$

By (4.46) and (9.18), we obtain

$$\overline{c_{\bar{m}\bar{n}}^{l}d_{\bar{m}0}^{l}(\alpha)d_{\bar{n}0}^{l}(\Theta)e^{-i\bar{m}\beta}e^{i\bar{n}\Phi}}=c_{mn}^{l}\cdot((-1)^m d_{m0}^{l}(\alpha))\cdot((-1)^n d_{n0}^{l}(\Theta))\cdot e^{-im\beta}e^{in\Phi}$$
$$=c_{mn}^{l}d_{m0}^{l}(\alpha)d_{n0}^{l}(\Theta)e^{-im\beta}e^{in\Phi}.\tag{9.19}$$

Thus we have verified that $p(\alpha,\beta;\Theta,\Phi)$ is real-valued.

Remark 9.6 Using (9.19), we can easily show by direct computations that the sum

$$c_{mn}^{l}d_{m0}^{l}(\alpha)d_{n0}^{l}(\Theta)e^{-im\beta}e^{in\Phi}+c_{\bar{m}\bar{n}}^{l}d_{\bar{m}0}^{l}(\alpha)d_{\bar{n}0}^{l}(\Theta)e^{-i\bar{m}\beta}e^{i\bar{n}\Phi}$$
$$=2d_{m0}^{l}(\alpha)d_{n0}^{l}(\Theta)\left(\cos(n\Phi-m\beta)\mathfrak{Re}\,c_{mn}^{l}-\sin(n\Phi-m\beta)\mathfrak{Im}\,c_{mn}^{l}\right).$$

Hence for a given $(\alpha,\beta;\Theta,\Phi)$, the independent real parameters for $p(\alpha,\beta;\Theta,\Phi)$ in the case where $G_{\text{tex}}=\{\boldsymbol{I}\}$ and $G_{\text{cr}}=\{\boldsymbol{I}\}$ can be taken as c_{00}^{l}, $\mathfrak{Re}\,c_{mn}^{l}$, $\mathfrak{Im}\,c_{mn}^{l}$ for even $l\geq 2$ and either $-l\leq m\leq l$, $0<n\leq l$ or $0<m\leq l$, $n=0$. □

Note that the function q satisfies the relation

$$q(\boldsymbol{n};-\boldsymbol{h})=q(-\boldsymbol{n};\boldsymbol{h}).\tag{9.20}$$

As a result, the function p satisfies the normalization condition

$$\int_0^{2\pi}\int_0^{\pi/2}p(\alpha,\beta;\Theta,\Phi)\sin\alpha d\alpha d\beta$$
$$=\int_0^{2\pi}\int_0^{\pi/2}q(\alpha,\beta;\Theta,\Phi)\sin\alpha d\alpha d\beta+\int_0^{2\pi}\int_0^{\pi/2}q(\pi-\alpha,\pi+\beta;\Theta,\Phi)\sin\alpha d\alpha d\beta$$
$$=\int_0^{2\pi}\int_0^{\pi/2}q(\alpha,\beta;\Theta,\Phi)\sin\alpha d\alpha d\beta+\int_0^{2\pi}\int_{\pi/2}^{\pi}q(\alpha,\beta;\Theta,\Phi)\sin\alpha d\alpha d\beta$$
$$=\int_0^{2\pi}\int_0^{\pi}q(\alpha,\beta;\Theta,\Phi)\sin\alpha d\alpha d\beta=1,\tag{9.21}$$

where we have appealed to (9.12) at the last step. Alternatively, (9.17) may be rewritten in terms of the spherical harmonics as

$$p(\alpha,\beta;\Theta,\Phi)=\frac{1}{2\pi}+\sum_{\text{even } l\geq 2}^{\infty}\sum_{m=-l}^{l}\sum_{n=-l}^{l}\frac{16\pi^2}{2l+1}c_{mn}^{l}\overline{Y_{lm}(\alpha,\beta)}Y_{ln}(\Theta,\Phi), \tag{9.22}$$

or in Roe's notation as (see (4.117) and (4.118))

$$p(\alpha,\beta;\Theta,\Phi)=\frac{1}{2\pi}+4\pi\sum_{\text{even } l\geq 2}^{\infty}\sum_{m=-l}^{l}\sum_{n=-l}^{l}\sqrt{\frac{2}{2l+1}}W_{lmn}Z_{lm0}(\cos\alpha)Z_{ln0}(\cos\Theta)e^{-im\beta}e^{in\Phi}. \tag{9.23}$$

Remark 9.7 Since q is a probability density, we have $q\geq 0$, which implies that $p\geq 0$. When $w=w_{\text{iso}}$, all texture coefficients are zero. Hence all pole figures $p(\alpha,\beta;\Theta,\Phi)=p_{\text{iso}}=\frac{1}{2\pi}$. When the texture of a sample is the mixture of a random part with volume fraction $0<r<1$ and a non-random part with volume fraction $1-r$, the ODF of the sample is

$$w=rw_{\text{iso}}+(1-r)\widetilde{w}, \tag{9.24}$$

where $\widetilde{w}$ is the ODF of the non-random part with the usual normalization; see Sect. 9.6.2 for further discussion. Then the pole figures of the sample are given by

$$p(\alpha,\beta;\Theta,\Phi)=rp_{\text{iso}}+(1-r)\widetilde{p}(\alpha,\beta;\Theta,\Phi), \tag{9.25}$$

where $\widetilde{p}(\alpha,\beta;\Theta,\Phi)$ denote the pole figures pertaining to $\widetilde{w}$. As $\widetilde{p}\geq 0$, we observe that $p\geq r/(2\pi)$ for the mixture that contains a random part. □

9.4 Pole Figures of Sheet Metals

Sheet metals often inherit orthorhombic texture symmetry from their thermomechanical processing histories. As a result, pole figures of sheet metals usually enjoy the following symmetry relations:

$$p(\alpha,\beta;\Theta,\Phi)=p(\alpha,-\beta;\Theta,\Phi)=p(\alpha,\pi-\beta;\Theta,\Phi)=p(\alpha,\pi+\beta;\Theta,\Phi), \tag{9.26}$$

i.e., such pole figures are symmetric under reflection about the two axes defined by the rolling (RD) and the transverse direction (TD), respectively.

To prove the preceding relations, we appeal to the equality

$$c_{mn}^{l}=\begin{cases}c_{\bar{m}n}^{l} & \text{for even } l \text{ and } m\\ 0 & \text{for odd } m,\end{cases} \tag{9.27}$$

which follows from the orthorhombic texture symmetry (cf. $(5.33)_1$), as well as the property

$$d_{m0}^{l}(\alpha)=d_{\bar{m}0}^{l}(\alpha)\qquad \text{for even } m \tag{9.28}$$

observed by the $d_{mn}^{l}(\cdot)$ functions (cf. $(4.33)_2$), and recast formula (9.17) for p as follows:

$$\begin{aligned}p(\alpha,\beta;\Theta,\Phi)&=\frac{1}{2\pi}+4\pi\sum_{\text{even } l\geq 2}\sum_{n}d_{n0}^{l}(\Theta)e^{in\Phi}\left(\sum_{\text{even m}}c_{mn}^{l}d_{m0}^{l}(\alpha)e^{-im\beta}\right)\\&=\frac{1}{2\pi}+4\pi\sum_{\text{even } l\geq 2}\sum_{n}d_{n0}^{l}(\Theta)e^{in\Phi}\left(c_{0n}^{l}d_{00}^{l}(\alpha)+\left(c_{2n}^{l}d_{20}^{l}(\alpha)e^{-i2\beta}\right.\right.\end{aligned}$$

$$+ c^l_{2n} d^l_{\bar{2}0}(\alpha) e^{i2\beta}\Big) + \cdots + \Big(c^l_{kn} d^l_{k0}(\alpha) e^{-ik\beta} + c^l_{\bar{k}n} d^l_{\bar{k}0}(\alpha) e^{ik\beta}\Big)\Big)$$

$$= \frac{1}{2\pi} + 4\pi \sum_{\text{even } l\geq 2} \sum_{n} d^l_{n0}(\Theta) e^{in\Phi} \Big(c^l_{0n} d^l_{00}(\alpha) + 2c^l_{2n} d^l_{20}(\alpha)\cos 2\beta$$

$$+ \cdots + 2c^l_{kn} d^l_{k0}(\alpha)\cos k\beta\Big), \tag{9.29}$$

where $k = 2s$ is the largest even integer $\leq l$. The symmetry relations (9.26) follow immediately from (9.29) because the cosine function is even and is periodic with period 2π.

If we obtain from experimental measurement a pole figure which does not obey (9.26), i.e., if it is not symmetrical under reflections about the axes defined by RD and TD, then either the sample does not enjoy orthorhombic texture symmetry or something is wrong with the measurement.

9.5 Inversion of Pole Figures for l-Even Part of ODF

We write a given ODF as

$$w(\boldsymbol{R}) = w^{(\mathrm{e})}(\boldsymbol{R}) + w^{(\mathrm{o})}(\boldsymbol{R}) \geq 0, \qquad \text{where } \boldsymbol{R} \in \mathrm{SO}(3); \tag{9.30}$$

$$w^{(\mathrm{e})}(\boldsymbol{R}) = \sum_{\text{even } l\geq 0}^{\infty} \sum_{m=-l}^{l} \sum_{n=-l}^{l} c^l_{mn} D^l_{mn}(\boldsymbol{R}), \qquad w^{(\mathrm{o})}(\boldsymbol{R}) = \sum_{\text{odd } l\geq 1}^{\infty} \sum_{m=-l}^{l} \sum_{n=-l}^{l} c^l_{mn} D^l_{mn}(\boldsymbol{R}), \tag{9.31}$$

where $w^{(\mathrm{e})}$ and $w^{(\mathrm{o})}$ are called the l-even and l-odd part of w, respectively.

Formula (9.17) clearly shows that pole figures do not carry any information on texture coefficients c^l_{mn} with odd l. Inferring l-even texture coefficients from measured pole figures, however, has remained an important topic in quantitative texture analysis for the following reasons:

- Some applications require only knowledge of texture coefficients of even orders. For example, in the theory of acoustoelasticity proposed by Man and Paroni [200, 205, 255] for weakly-textured materials, only texture coefficients of order $l = 4, 6$ and $l = 2, 4, 6$ bear on the acoustoelastic effect in aggregates of cubic and hexagonal crystallites, respectively.[129]
- Determination of the even-l coefficients up to a certain $L := l_{\max}$ serves as a starting point or a basis for some "ghost-correcting" methods which provide estimates for the missing odd-l coefficients. See Sect. 9.6.
- Texture coefficients obtained from X-ray measurements can be used for checking the validity of the results of other techniques, particularly those still in development.

[129] This assertion follows from what follows. Man [199] showed that the sixth-order acoustoelastic tensor for weakly-textured materials depends on texture coefficients c^l_{mn} only in those with $l \leq 6$. For aggregates of cubic crystallites, $c^l_{mn} = 0$ for $l = 1, 2, 3, 5$; see Table 7. For aggregates of hexagonal crystallites, $c^l_{mn} = 0$ for $l = 1, 3, 5$; see (5.48) and (5.50). For the same reason, this assertion is also valid for weakly-textured materials in the context of the classical acoustoelastic theory (see [321] and the references therein). In fact, with the help of an analysis [203] more refined than that of [199], one can read off from the decomposition formula (16.51) that, as far as the effect of texture coefficients on the acoustoelastic tensor in classical acoustoelastic theory is concerned, only those with $l = 2, 4, 6$ are relevant for weakly-textured aggregates of tetragonal crystallites.

9.5.1 Inversion of Complete Pole Figures

For a given (Θ, Φ), we say that we have a complete pole figure if we know the values of the function $p(\alpha, \beta; \Theta, \Phi)$ for $0 \le \alpha \le \pi/2$ and $0 \le \beta < 2\pi$. In this section we discuss how we could recover the texture coefficients c^l_{mn} for even $l \ge 2$ if we have complete pole figures at our disposal.

For a given even $l \ge 2$ and a given m, we obtain an equation in the unknowns c^l_{mn} by multiplying both sides of (9.17) with $d^l_{m0}(\alpha)e^{im\beta}$ and integrating the products over the upper hemisphere:

$$\begin{aligned}
&\int_0^{2\pi}\int_0^{\pi/2} p(\alpha,\beta;\Theta,\Phi)d^l_{m0}(\alpha)e^{im\beta}\sin\alpha d\alpha d\beta \\
&= 4\pi \sum_{\text{even } l'\ge 2}^{\infty}\sum_{s=-l'}^{l'}\sum_{n=-l'}^{l'} c^{l'}_{sn}d^{l'}_{n0}(\Theta)e^{in\Phi}\int_0^{\pi/2} d^l_{m0}(\alpha)d^{l'}_{s0}(\alpha)\sin\alpha\left(\int_0^{2\pi} e^{i(m-s)\beta}d\beta\right)d\alpha \\
&= 8\pi^2 \sum_{\text{even } l'\ge 2}^{\infty}\sum_{n=-l'}^{l'} c^{l'}_{mn}d^{l'}_{n0}(\Theta)e^{in\Phi}\int_0^{\pi/2} d^l_{m0}(\alpha)d^{l'}_{m0}(\alpha)\sin\alpha d\alpha \\
&= \frac{8\pi^2}{2l+1}\sum_{n=-l}^{l} c^l_{mn}d^l_{n0}(\Theta)e^{in\Phi},
\end{aligned} \tag{9.32}$$

where we have appealed to (4.25), (4.27), and the fact that

$$\int_0^{\pi/2} d^l_{m0}(\alpha)d^{l'}_{m0}(\alpha)\sin\alpha d\alpha = \frac{1}{2}\int_0^{\pi} d^l_{m0}(\alpha)d^{l'}_{m0}(\alpha)\sin\alpha d\alpha = \frac{1}{2l+1}\delta_{ll'} \tag{9.33}$$

for even l and l', because

$$\begin{aligned}
\int_{\pi/2}^{\pi} d^l_{m0}(\alpha)d^{l'}_{m0}(\alpha)\sin\alpha d\alpha &= \int_0^{\pi/2} d^l_{m0}(\pi-\alpha)d^{l'}_{m0}(\pi-\alpha)\sin\alpha d\alpha \\
&= (-1)^{l+l'}\int_0^{\pi/2} d^l_{m0}(\alpha)d^{l'}_{m0}(\alpha)\sin\alpha d\alpha \\
&= \int_0^{\pi/2} d^l_{m0}(\alpha)d^{l'}_{m0}(\alpha)\sin\alpha d\alpha.
\end{aligned} \tag{9.34}$$

In terms of the spherical harmonics, we may rewrite (9.32) as

$$\frac{8\pi^2}{2l+1}\sum_{n=-l}^{l} c^l_{mn}Y_{ln}(\Theta,\Phi) = \int_0^{2\pi}\int_0^{\pi/2} p(\alpha,\beta;\Theta,\Phi)Y_{lm}(\alpha,\beta)\sin\alpha d\alpha d\beta. \tag{9.35}$$

Thus in the absence of crystallite symmetry (i.e., $G_{\rm cr} = C_1$), each complete pole figure delivers through (9.32) or (9.35) one linear equation, which for each given even-l and $-l \le m \le l$ relates a linear combination of $2l+1$ undetermined texture coefficients c_{mn}^l $(-l \le n \le l)$ to a given complex number. Hence we shall need $2l+1$ pole figures to determine the $2l+1$ coefficients c_{mn}^l $(-l \le n \le l)$.

The inversion of complete pole figures simplifies considerably when the crystallites possess high crystal symmetry, which significantly reduces the number of independent texture coefficients c_{mn}^l for a given even-l and m. Consider, for instance, aggregates of cubic crystallites and $l = 4$, $m = 2$. From Table 7 of Sect. 5.4.3, we observe that only one of the c_{2n}^4 coefficients, for which we may pick c_{20}^4, is independent. Hence all the c_{2n}^4 coefficients can be determined from one pole figure. Indeed, a glance at Table 7 reveals that we may use the same complete pole figure to recover, for orthorhomic aggregates of cubic crystallites, all the c_{mn}^l or W_{lmn} coefficients for $l = 4, 6, 8, 10, 14$. On the other hand, for $l = 12$, since there are two independent coefficients c_{12m0} and c_{12m4} for each m, two complete pole figures will be required for the determination of the c_{12mn} coefficients.

For any given even-l and m, the number of independent c_{mn}^l has been worked out for any $G_{\rm cr}$. The results are summarized in Table 11.1 in [224, p. 50].[130] The recursion formula for cubic crystallites is $N(l+12) = N(l) + 1$, where N is the number of independent c_{mn}^l. From Table 7 of Sect. 5.4.3, we observe that $N(l) \le 1$ for $l < 12$ and $N(12) = N(0+12) = N(0) + 1 = 2$. Hence by the recursion formula $N(l) \le 2$ for $l < 24$ and $N(l) \le 3$ for $l < 36$. Thus two and three complete pole figures will suffice to determine all c_{mn}^l up to $L = l_{\max} = 22$ and $L = 34$, respectively.

Example 9.8 Let us write down, for orthorhombic aggregates of cubic crystallites, an explicit formula for the recovery of the coefficient W_{420}. Substituting $l = 4$ and $m = 2$ into (9.32), we have

$$\begin{aligned}
&\int_0^{2\pi}\int_0^{\pi/2} p(\alpha,\beta;\Theta,\Phi) d_{20}^4(\alpha) e^{i2\beta} \sin\alpha d\alpha d\beta \\
&= \frac{8\pi^2}{9}\left(c_{20}^4 d_{00}^4(\Theta) + c_{24}^4 d_{40}^4(\Theta) e^{i4\Phi} + c_{2\bar{4}}^4 d_{40}^4(\Theta) e^{-i4\Phi}\right) \\
&= \frac{8\pi^2}{9} c_{20}^4 \left(d_{00}^4(\Theta) + 2\cdot\frac{\sqrt{70}}{14}\cdot d_{40}^4(\Theta)\cos 4\Phi\right),
\end{aligned} \tag{9.36}$$

which implies

$$c_{420} = \frac{9}{8\pi^2}\cdot\frac{\int_0^{2\pi}\int_0^{\pi/2} p(\alpha,\beta;\Theta,\Phi) d_{20}^4(\alpha) e^{i2\beta}\sin\alpha d\alpha d\beta}{d_{00}^4(\Theta) + \frac{\sqrt{70}}{7} d_{40}^4(\Theta)\cos 4\Phi}. \tag{9.37}$$

Note that c_{420}, as delivered by (9.37), is in general complex. However, it is real if $p(\alpha,\beta;\Theta,\Phi)$ happens to be an even function of β for each α and (Θ,Φ), a property enjoyed by p, e.g., if the sample in question is a sheet metal whose rolling direction is a 2-fold axis of rotational symmetry. □

[130] But remember that in classical texture analysis a crystal with Type II or III point-group symmetry is treated as if it were its Type I peer in the same Laue class.

X-ray pole-figure measurements are made at isolated (α_i, β_j) 's. Hence integrals such as that in (9.37) will have to be computed numerically. In the next section we shall present a numerical method for the inversion of incomplete pole figures. The same numerical method, which is none other than an application of the method of least squares, can be used also for inversion of complete pole figures. However, when the numerical method in Sect. 9.5.2 is used, it is customary to use more pole figures than the minimum required number as indicated in the paragraph preceding Example 9.8. For example, for aggregates of cubic crystallites, three (resp. four) pole figures are commonly used to determine texture coefficients c_{mn}^l up to $L = 22$ (resp. $L = 34$).

9.5.2 Inversion of Incomplete Pole Figures

When an X-ray pole figure is obtained by the reflection method, the geometry of the experimental setup dictates that reliable measurement data cannot be obtained for the full range of $0 \le \alpha \le 90°$. Usually, only the data for $0 \le \beta < 360°$ and $0 \le \alpha \le \alpha_{\max}$ (where $\alpha_{\max} = 70°$ for example) are taken, which constitute an incomplete pole figure. A number of methods have been proposed in the literature to recover information on the ODF from incomplete pole figures. Here we will rewrite only one version of the harmonic method [57, 58, 60, 262] in the context of the Roe approach.

Following the general procedure of the Roe approach, we start by considering the case where $G_{\text{tex}} = \{\boldsymbol{I}\}$ and $G_{\text{cr}} = \{\boldsymbol{I}\}$. Suppose we obtain from X-ray measurements, one function for each incomplete pole figure, a total of K intensity functions $I_k(\alpha, \beta; \Theta_k, \Phi_k)$ $(k = 1, 2, \ldots, K)$, where $0 \le \alpha \le \alpha_{\max}$, $0 \le \beta < 2\pi$, and $(1, \Theta_k, \Phi_k)$ specifies the spherical coordinates of the unit normal $\boldsymbol{h}_k$ to the (hkl) planes pertaining to the k-th pole figure. We seek texture coefficients c_{mn}^l in the theoretical formula (9.22) for pole figures such that the objective function

$$F = \int_0^{2\pi} \int_0^{\alpha_{\max}} \sum_k \left(N_k I_k(\alpha, \beta; \Theta_k, \Phi_k) - p_{\text{th}}(\alpha, \beta; \Theta_k, \Phi_k)\right)^2 \sin\alpha \, d\alpha \, d\beta, \tag{9.38}$$

assumes a minimum; here N_k denotes the undetermined normalization constant for the k-th measured pole figure, and we have written p_{th} for p in (9.22) to underscore that it denotes the theoretical formula. For our present purpose it will be most convenient to rewrite (9.17) explicitly in terms of the set of independent real texture coefficients given in Remark 9.6, namely $\mathfrak{Re}\, c_{mn}^l$ and $\mathfrak{Im}\, c_{mn}^l$ $(2 \le l \le L$; (i) $-l \le m \le l$, $1 \le n \le l$ or (ii) $n = 0$, $0 \le m \le l$ for $\mathfrak{Re}\, c_{mn}^l$, $1 \le m \le l$ for $\mathfrak{Im}\, c_{mn}^l)$:

$$p_{\text{th}}(\alpha, \beta; \Theta, \Phi) = \frac{1}{2\pi} + 8\pi \sum_{\text{even } l \ge 2}^{L} \sum_{m=-l}^{l} \sum_{n=0}^{l} d_{m0}^l(\alpha) d_{n0}^l(\Theta) \Big(\cos(n\Phi - m\beta) \mathfrak{Re}\, c_{mn}^l - \sin(n\Phi - m\beta) \mathfrak{Im}\, c_{mn}^l \Big), \tag{9.39}$$

where L is the highest order of l after which the series is truncated. Note that in (9.39) all terms of the form $\mathfrak{Im}\, c_{00}^l$ drop out, because each is multiplied to a factor which is zero when $m = 0$ and $n = 0$; in fact those terms by themselves will not appear, as $\mathfrak{Im}\, c_{00}^l = 0$ for all l. It is readily seen that the total number of real independent texture coefficients is $\sum_{\text{even } l \ge 2}^{L} (2l + 1)^2$.

In practice, measurements are usually made at isolated points of (α_i, β_j), say with α_i and β_j starting from $\alpha_0 = 0$ and $\beta_0 = 0$ and, in 5° increments, running to $\alpha_{\max}$ and $\beta_{72} = 355°$, respectively. For definiteness, say $\alpha_{\max} = \alpha_{15} = 70°$. Then we replace the objective function (9.38) by its discrete form

$$F = \sum_{k=1}^{K} \sum_{i=0}^{15} \sum_{j=0}^{32} \big(N_k I_k(\alpha_i, \beta_j; \Theta_k, \Phi_k) - p_{\text{th}}(\alpha_i, \beta_j; \Theta_k, \Phi_k)\big)^2 (\cos\alpha_i - \cos\alpha_{i+1})\Delta\beta, \tag{9.40}$$

where $\Delta\beta = \beta_{j+1} - \beta_j$ for all j is the uniform step length for β. In (9.40) we have replaced $\sin\alpha_i \Delta\alpha$ by $\cos\alpha_i - \cos\alpha_{i+1}$ so that the experimental data for $\alpha = 0$ (i.e., no tilting of sample) are not inadvertently set aside unused. This step is equivalent to using $x = \cos\alpha$ instead of α as independent variable of the associated Legendre polynomials in the spherical harmonics Y_{lm}.

The best estimates of the normalization constants N_k and the independent texture coefficients $\mathfrak{Re}\, c^l_{mn}$ and $\mathfrak{Im}\, c^l_{mn}$ in formula (9.39) for p_{th} are those which render the objective function F in (9.40) a minimum. They satisfy the equations

$$\frac{\partial F}{\partial N_k} = 0, \qquad \frac{\partial F}{\partial(\mathfrak{Re}\, c^l_{mn})} = 0, \qquad \frac{\partial F}{\partial(\mathfrak{Im}\, c^l_{mn})} = 0, \tag{9.41}$$

where each independent variable leads to one equation. Equation $(9.41)_1$ leads to the formula

$$N_k = \frac{\sum_{i,j} p_{\text{th}}(\alpha_i, \beta_j; \Theta_k, \Phi_k) I_k(\alpha_i, \beta_j; \Theta_k, \Phi_k)(\cos\alpha_{i+1} - \cos\alpha_i)}{\sum_{i,j} I_k^2(\alpha_i, \beta_j; \Theta_k, \Phi_k)(\cos\alpha_{i+1} - \cos\alpha_i)}. \qquad (k = 1, 2, \ldots K) \tag{9.42}$$

Note that p_{th} and thence each N_k is an affine function of the independent texture coefficients. From $(9.41)_2$ and $(9.41)_3$ we obtain the equations

$$\sum_{i,j,k} \big(N_k I_k(\alpha_i, \beta_j; \Theta_k, \Phi_k) - p_{\text{th}}(\alpha_i, \beta_j; \Theta_k, \Phi_k)\big) d^l_{m0}(\alpha_i) d^l_{n0}(\Theta_k) \times \cos(n\Phi_k - m\beta_j)(\cos\alpha_{i+1} - \cos\alpha_i) = 0, \tag{9.43}$$

$$\sum_{i,j,k} \big(N_k I_k(\alpha_i, \beta_j; \Theta_k, \Phi_k) - p_{\text{th}}(\alpha_i, \beta_j; \Theta_k, \Phi_k)\big) d^l_{m0}(\alpha_i) d^l_{n0}(\Theta_k) \times -\sin(n\Phi_k - m\beta_j)(\cos\alpha_{i+1} - \cos\alpha_i) = 0. \tag{9.44}$$

Substituting (9.42) for N_k $(k = 1, 2, \ldots, K)$ in (9.43) and (9.44) leads to a system of $\sum^{L}_{\text{even } l \geq 2}(2l+1)^2$ inhomogeneous linear equations for the determination of the same number of independent real texture coefficients.

When $G_{\text{tex}} \neq \{\boldsymbol{I}\}$ and/or $G_{\text{cr}} \neq \{\boldsymbol{I}\}$, we should add the restrictions imposed by texture and crystallite symmetry to the procedure described above, which for high symmetries will significantly reduce the number of independent texture coefficients. For instance, for orthorhombic aggregates of cubic crystallites the number of independent texture coefficients is reduced to 124 for $L = 22$ after the imposition of symmetry restrictions (cf. Sect. 5.4.4 and [271, Table I] for the symmetry restrictions). For orthorhombic aggregates of hexagonal crystallites, the number of independent texture coefficients is 239 for $L = 22$ (cf. (5.56) for the symmetry restrictions).

For sheet metals that we want to model as having orthorhombic texture symmetry, imposing the $G_{\text{tex}} = D_2$ restrictions on the undetermined texture coefficients in the procedure

above will lead to a truncated $w^{(e)}$ from which any calculated pole figure will show orthorhombic symmetry as described in Sect. 9.4. Alternatively, we may start by symmetrizing each pole figure p obtained from X-ray measurements by defining

$$p^{(s)}(\alpha,\beta;\Theta,\Phi) = \frac{1}{4}\Big(p(\alpha,\beta;\Theta,\Phi)+p(\alpha,-\beta;\Theta,\Phi)+p(\alpha,\pi-\beta;\Theta,\Phi)+p(\alpha,\pi+\beta;\Theta,\Phi)\Big). \tag{9.45}$$

Then we follow the procedure above with appropriate symmetry restrictions on independent texture coefficients but, instead of the pole figures p in the range $0 \le \beta < 360°$, use the symmetrized pole figures $p^{(s)}$ only in the range $0 \le \beta < 90°$.

9.6 Ghost Correction (I): Generalized Positivity Method

If Friedel's rule is observed, X-ray pole figures will not carry any information on texture coefficients c^l_{mn} with odd l. As pointed out at the beginning of Chap. 8, in the early days of quantitative texture analysis $w^{(e)}$, the l-even part of the ODF (i.e., that which results when all terms with odd l in the series expansion $\sum_l \sum_{m,n} c^l_{mn} D^l_{mn}$ of w are deleted), was commonly misconstrued as the "true" ODF w. The substitution of $w^{(e)}$ for w sometimes led to anomalous experimental findings such as false maxima (called "ghosts"), strong fluctuations at low intensities, and rather strong negative values of the ODF. After the culprit behind such ghost phenomena was determined [193, 214], various "ghost-correction" methods and algorithms for inversion of pole figures were proposed in the 1980s and 1990s. In this section we will outline one of those methods.

In this section we outline, in the context of the Roe approach, the general idea and procedure of the generalized positivity method[131] proposed by Dahms and Bunge [83, 84] for ghost correction. Again we focus on the general case where $G_{\text{tex}} = \{\boldsymbol{I}\}$ and $G_{\text{cr}} = \{\boldsymbol{I}\}$. The cases where $G_{\text{tex}} \neq \{\boldsymbol{I}\}$ and/or $G_{\text{cr}} \neq \{\boldsymbol{I}\}$ will be covered by enforcing the restrictions on texture coefficients imposed by the non-trivial G_{tex} and/or G_{cr} in question.

9.6.1 The Positivity Method

As an introduction to the generalized positivity method, let us consider the positivity method first.

Suppose by inversion of X-ray pole figures we have already determined a truncated series of $w^{(e)}$ up to $l = L$, for some desirable even L. While w as a probability density should be non-negative, it may happen that $w^{(e)}(\boldsymbol{R}) < 0$ in some region of SO(3). In the positivity method, an iterative procedure is designed to compute from the truncated l-even part[132]

$$w^{(e)}(\boldsymbol{R}) = \sum_{\text{even } l\ge 0}^{L} \sum_{m=-l}^{l} \sum_{n=-l}^{l} c^l_{mn} D^l_{mn}(\boldsymbol{R}) \tag{9.46}$$

[131] This term, introduced by Dahms and Bunge [84] to name what they mentioned in passing as a "slight modification" of the positivity method in [83], is rarely used in the literature, where the term "positivity method" usually encompasses both. We distinguish the two here, because the modification in the generalized method, while mathematically trivial, immensely broadens the scope of the method in applications. Dahms in his later papers [81, 82], in effect, refers to the generalized positivity method as the "iterative series-expansion method", a term used more broadly in [84] to mean a family of methods.

[132] Note that we have kept the same symbols $w^{(e)}$ and $w^{(o)}$ for the truncated series.

a truncated series of the odd-part up to $l = L + 1$,[133] namely

$$w^{(\mathrm{o})}(\boldsymbol{R}) = \sum_{\text{odd } l \geq 1}^{L+1} \sum_{m=-l}^{l} \sum_{n=-l}^{l} c_{mn}^{l} D_{mn}^{l}(\boldsymbol{R}) \tag{9.47}$$

until a parameter S^-, which describes the size of w^- (the negative part of $w = w^{(\mathrm{e})} + w^{(\mathrm{o})}$), e.g.,

$$S^- := \|w^-\|^2 = \int_{\mathrm{SO}(3)} (w^-)^2(\boldsymbol{R}) d\mathcal{V}(\boldsymbol{R}), \qquad \text{where} \quad w^- = \frac{1}{2}(|w| - w) = \begin{cases} w & \text{if } w < 0 \\ 0 & \text{if } w \geq 0, \end{cases} \tag{9.48}$$

is less than some selected tolerance value.[134]

The mathematics of the positivity method is based on the following proposition.

Proposition 9.9 *Let $u \in L^2(\mathrm{SO}(3), \mathbb{C})$, and let*

$$S^{(\mathrm{o})} = \Big\{ s \in L^2(\mathrm{SO}(3), \mathbb{C}) : s = \sum_{\text{odd } l \geq 1}^{L+1} \sum_{m=-l}^{l} \sum_{n=-l}^{l} c_{mn}^{l} D_{mn}^{l}(\boldsymbol{R}), \\ \text{where } c_{\bar{m}\bar{n}}^{l} = (-1)^{n-m} \overline{c_{mn}^{l}}, \text{for some } c_{mn}^{l} \in \mathbb{C} \Big\}, \tag{9.49}$$

where $L \geq 2$ is the (even) order of l after which the series of $w^{(\mathrm{e})}$ is truncated. Then

$$\hat{u} := \sum_{\text{odd } l \geq 1}^{L+1} \sum_{m=-l}^{l} \sum_{n=-l}^{l} \hat{c}_{mn}^{l} D_{mn}^{l}(\boldsymbol{R}), \tag{9.50}$$

where

$$\hat{c}_{mn}^{l} = \frac{2l+1}{8\pi^2} \langle u, D_{mn}^{l} \rangle = \frac{2l+1}{8\pi^2} \int_{SO(3)} u(\boldsymbol{R}) \overline{D_{mn}^{l}(\boldsymbol{R})} d\mathcal{V}(\boldsymbol{R}) \tag{9.51}$$

is the element in $S^{(\mathrm{o})}$ that best approximates u in the sense that

$$\|u - \hat{u}\| < \|u - s\| \qquad \text{for all } s \neq \hat{u} \in S^{(\mathrm{o})}. \tag{9.52}$$

Proof This proposition is a direct application of the best-approximation theorem in inner product spaces (see, e.g., [273, p. 219], [278, p. 83]). Note that by (4.21) $\{\sqrt{\frac{2l+1}{8\pi^2}} D_{mn}^{l}\}$ is an orthonormal set of vectors in $L^2(\mathrm{SO}(3), \mathbb{C})$. Given $u \in L^2(\mathrm{SO}(3), \mathbb{C})$, the best approximation to u in $S^{(\mathrm{o})}$ is given by

$$\hat{u} = \sum_{\text{odd } l \geq 1}^{L+1} \sum_{m=-l}^{l} \sum_{n=-l}^{l} \langle u, \sqrt{\frac{2l+1}{8\pi^2}} D_{mn}^{l} \rangle \sqrt{\frac{2l+1}{8\pi^2}} D_{mn}^{l} = \sum_{\text{odd } l \geq 1}^{L+1} \sum_{m=-l}^{l} \sum_{n=-l}^{l} \hat{c}_{mn}^{l} D_{mn}^{l}(\boldsymbol{R}), \tag{9.53}$$

where $\hat{c}_{mn}^{l}$ is given by (9.51). □

[133] The choice of $l = L + 1$ here will yield an S^- that could be smaller and is definitely not larger than its counterpart delivered by taking $l = L - 1$.

[134] Our reason for this choice of definition of S^- will be clear in Sect. 9.6.3. As far as serving as a stopping criterion is concerned, we may define S^- as the norm $\|w^-\|$ or any other strictly increasing function of $\|w^-\|$. All these definitions with compatible tolerance values are clearly equivalent. Dahms and Bunge [83], however, defines S^- as $\int_{\mathrm{SO}(3)} w^-(\boldsymbol{R}) d\mathcal{V}(\boldsymbol{R})$.

The procedure in the positivity method is as follows. In Step 1, let $w_0 = w^{(e)}$ and let

$$u_1(\boldsymbol{R}) = \begin{cases} -w_0(\boldsymbol{R}) & \text{if } w_0(\boldsymbol{R}) < 0 \\ 0 & \text{if } w_0(\boldsymbol{R}) \geq 0. \end{cases} \tag{9.54}$$

By Proposition 9.9, the best approximation to u_1 in $S^{(o)}$ is

$$w_1^{(o)} = \sum_{\text{odd } l \geq 1}^{L+1} \sum_{m=-l}^{l} \sum_{n=-l}^{l} {}^{(1)}c_{mn}^{l} D_{mn}^{l}, \tag{9.55}$$

where the texture coefficients ${}^{(1)}c_{mn}^{l}$, with odd l, are given by

$${}^{(1)}c_{mn}^{l} = \frac{2l+1}{8\pi^2} \int_{\mathrm{SO}(3)} u_1(\boldsymbol{R}) \overline{D_{mn}^{l}(\boldsymbol{R})} d\mathcal{V}(\boldsymbol{R}). \tag{9.56}$$

After $w_1^{(o)}$ is determined, write $w_1 = w_0 + w_1^{(o)}$ and proceed to Step 2. Note that $\int_{\mathrm{SO}(3)} w_1(\boldsymbol{R})\, d\mathcal{V}(\boldsymbol{R}) = 1$.

In general at the beginning of Step k, where $k \geq 2$, we have determined $w_{k-1} = w_{k-2} + w_{k-1}^{(o)}$. Let

$$u_k(\boldsymbol{R}) = \begin{cases} -w_{k-1}(\boldsymbol{R}) & \text{if } w_{k-1}(\boldsymbol{R}) < 0 \\ 0 & \text{if } w_{k-1}(\boldsymbol{R}) \geq 0. \end{cases} \tag{9.57}$$

By Proposition 9.9, the best approximation to u_k in $S^{(o)}$ is

$$w_k^{(o)} = \sum_{\text{odd } l \geq 1}^{L+1} \sum_{m=-l}^{l} \sum_{n=-l}^{l} {}^{(k)}c_{mn}^{l} D_{mn}^{l}, \tag{9.58}$$

where the texture coefficients ${}^{(k)}c_{mn}^{l}$, with odd l, are given by

$${}^{(k)}c_{mn}^{l} = \frac{2l+1}{8\pi^2} \int_{\mathrm{SO}(3)} u_k(\boldsymbol{R}) \overline{D_{mn}^{l}(\boldsymbol{R})} d\mathcal{V}(\boldsymbol{R}). \tag{9.59}$$

After $w_k^{(o)}$ is determined, write $w_k = w_{k-1} + w_k^{(o)}$. Note that $\int_{\mathrm{SO}(3)} w_k(\boldsymbol{R})\, d\mathcal{V}(\boldsymbol{R}) = 1$ for each k.

We use a discrete analog of (9.48) as the stopping criterion for the iteration procedure; cf. [83, 331]. Let $\{\boldsymbol{R}_i : 1 \leq i \leq N\}$ be a fixed regular grid of rotations (e.g., the nearly equal distant grid proposed by Helming [144] with resolution $\Delta = 5^\circ = \pi/36$ radians) which satisfies the following criterion: for any $\boldsymbol{R} \in \mathrm{SO}(3)$, there is an $\boldsymbol{R}_i$ in the grid such that $d_{\mathrm{SO}(3)}(\boldsymbol{R}, \boldsymbol{R}_i)$, the misorientation between $\boldsymbol{R}$ and $\boldsymbol{R}_i$ (see Sect. 1.10), is at most $\pi/36$. We stop the procedure at the p-th step as soon as we obtain a w_p such that

$$S^{-}(w_p) := \sum_{i=1}^{N} \left(w_p^{-}(\boldsymbol{R}_i)\right)^2 \tag{9.60}$$

is less than some selected tolerance value. Then we take the "ghost-corrected" $w = w_p$, i.e.,

$$\begin{aligned} w &= w_0 + w_1^{(\mathrm{o})} + \cdots + w_p^{(\mathrm{o})} \\ &= w^{(\mathrm{e})} + \sum_{\text{odd } l \geq 1}^{L+1} \sum_{m=-l}^{l} \sum_{n=-l}^{l} \left(\sum_{k=1}^{p} {}^{(k)}c_{mn}^{l} \right) D_{mn}^{l}, \end{aligned} \tag{9.61}$$

where $w^{(\mathrm{e})}$ is obtained by inversion of X-ray pole figures and is given by (9.46).

Remark 9.10 The positivity method is basically a procedure to eliminate or substantially mitigate the ghost phenomena that arise if there is a region in the orientation space where $w^{(\mathrm{e})} < 0$. If $w^{(\mathrm{e})} \geq 0$ everywhere, then Step 1 of the positivity method will not even start. Given a $w^{(\mathrm{e})}$, the condition on $w^{(\mathrm{o})}$ that $w = w^{(\mathrm{e})} + w^{(\mathrm{o})} \geq 0$ will generally allow more than one solution. Moreover, if $v_1, v_2 \in S^{(\mathrm{o})}$ are two solutions, i.e., $w^{(\mathrm{e})} + v_1 \geq 0$ and $w^{(\mathrm{e})} + v_2 \geq 0$, then their convex combination $c_1 v_1 + c_2 v_2$, where $c_1 \geq 0, c_2 \geq 0$ and $c_1 + c_2 = 1$ is also a solution, because $w^{(\mathrm{e})} + c_1 v_1 + c_2 v_2 = c_1(w^{(\mathrm{e})} + v_1) + c_2(w^{(\mathrm{e})} + v_2) \geq 0$. Thus if there are two solutions, then there will be an infinite number of solutions. Indeed Matthies and Wagner [220] presents an explicit counter-example with an infinite number of solutions, and $w^{(\mathrm{e})} \geq 0$ in their counter-example. □

Further restrictions on $w^{(\mathrm{o})}$ will have to come from additional conditions, to which we now turn.

9.6.2 Inclusion of an Isotropic Component

Let $0 \leq r < 1$. Here we are primarily interested in the cases that $r \neq 0$. The discussion below reduces to the special case covered by the positivity method when $r = 0$.

Consider a sample, the texture of which is the mixture of a random part with volume fraction $r \neq 0$ and a non-random part with volume fraction $1 - r$.[135] Let the ODF of the random and of the non-random part be w_{iso} and $\widetilde{w}$, respectively, with the usual normalization. The ODF of the sample in question is then given by

$$w = r w_{\mathrm{iso}} + (1 - r)\widetilde{w}. \tag{9.62}$$

Substituting w_{iso} and $\widetilde{w}$ in (9.62) by their series expansions, respectively, we obtain

$$\begin{aligned} w &= \frac{r}{8\pi^2} + (1 - r)\left(\frac{1}{8\pi^2} + \sum_{l=1}^{\infty} \sum_{m=-l}^{l} \sum_{n=-l}^{l} \widetilde{c}_{mn}^{l} D_{mn}^{l} \right) \\ &= \frac{1}{8\pi^2} + \sum_{l=1}^{\infty} \sum_{m=-l}^{l} \sum_{n=-l}^{l} c_{mn}^{l} D_{mn}^{l}, \qquad \text{where } c_{mn}^{l} = (1 - r)\widetilde{c}_{mn}^{l}. \end{aligned} \tag{9.63}$$

Hence we may still write w as a sum of its l-even part $w^{(\mathrm{e})}$ and l-odd part $w^{(\mathrm{o})}$, as defined by (9.31). But, as $\widetilde{w} \geq 0$ in (9.62), we have

$$w(\boldsymbol{R}) = w^{(\mathrm{e})}(\boldsymbol{R}) + w^{(\mathrm{o})}(\boldsymbol{R}) \geq \frac{r}{8\pi^2}, \qquad \text{for each } \boldsymbol{R} \in \mathrm{SO}(3). \tag{9.64}$$

[135] The importance of including a random part is emphasized in Dahms [82].

Suppose by inversion of X-ray pole figures we have already determined a truncated series of $w^{(\mathrm{e})}$ up to $l = L$, for some desirable even L; cf. (9.46). We follow an iterative procedure parallel to that of the positivity method to obtain truncated series for $w^{(\mathrm{o})}(\boldsymbol{R})$ (cf. (9.47)) so that $w^{(\mathrm{e})} + w^{(\mathrm{o})}$ satisfies inequality $(9.64)_2$.

As the iteration procedure is entirely parallel to that of the positivity method, a brief description will suffice. Let $w_0 = w^{(\mathrm{e})}$. For Step $k \geq 1$, let

$$u_k(\boldsymbol{R}) = \begin{cases} -(w_0(\boldsymbol{R}) - \frac{r}{8\pi^2}) & \text{if } w_{k-1}(\boldsymbol{R}) < \frac{r}{8\pi^2} \\ 0 & \text{if } w_{k-1}(\boldsymbol{R}) \geq \frac{r}{8\pi^2}. \end{cases} \tag{9.65}$$

By Proposition 9.9, the best approximation to u_k in $S^{(\mathrm{o})}$ (see (9.49)) is

$$w_k^{(\mathrm{o})} = \sum_{\text{odd } l \geq 1}^{L+1} \sum_{m=-l}^{l} \sum_{n=-l}^{l} {}^{(k)}c_{mn}^l D_{mn}^l, \tag{9.66}$$

where the texture coefficients ${}^{(k)}c_{mn}^l$, with odd l, are given by

$${}^{(k)}c_{mn}^l = \frac{2l+1}{8\pi^2} \int_{\mathrm{SO}(3)} u_k(\boldsymbol{R}) \overline{D_{mn}^l(\boldsymbol{R})} d\mathcal{V}(\boldsymbol{R}). \tag{9.67}$$

After $w_k^{(\mathrm{o})}$ is determined, write $w_k = w_{k-1} + w_k^{(\mathrm{o})}$ and proceed to Step $k+1$. Note that $\int_{\mathrm{SO}(3)} w_k(\boldsymbol{R})\, d\mathcal{V}(\boldsymbol{R}) = 1$ for each k.

The stopping criterion is also similar to that of the positivity method: Let $\{\boldsymbol{R}_i : 1 \leq N\}$ be the nearly equal distant grid in SO(3) mentioned just before (9.60). We stop the iteration process at Step p as soon as we obtain a w_p such that

$$S^-(w_p) := \sum_{i=1}^{N} \left(\left(w_p(\boldsymbol{R}_i) - \frac{r}{8\pi^2} \right)^- \right)^2 \tag{9.68}$$

is less than some selected tolerance value.

When $G_{\mathrm{tex}} \neq \{\boldsymbol{I}\}$ and/or $G_{\mathrm{cr}} \neq \{\boldsymbol{I}\}$, appropriate symmetry restrictions should be imposed on $w^{(\mathrm{e})}$ and all the elements of the subspace $S^{(\mathrm{o})}$. Following the same procedure as before, we obtain at Step k the functions $w_k^{(\mathrm{o})}$ and $w_k = w_{k-1} + w_k^{(\mathrm{o})}$ $(k = 1, 2, 3, \ldots)$, both of which satisfy all the required symmetry restrictions.

Dahms and Bunge [84] call the procedure described in this subsection the generalized positivity method. They further write:

> By the choice of different r values, the 'width' of the solution range may thus be estimated.

In the WIMV method [219] for reproduction of the ODF from pole figures, "ghost correction is based on the assumption that within the range of variation of ODFs that are compatible with pole figures, that one displaying the fewest peaks that concentrate a maximum of intensity and possessing the maximum possible background is the correct one." [223, p. 146] Likewise, we may adopt the same assumption in selecting one solution from those delivered by the generalized positivity method for various r values. Note that "possessing the maximum background" means the solution with the highest r value in the present context.

9.6.3 An Improved Algorithm

Wagner et al. [331] propose an improved algorithm for the generalized positivity method. What follows is a brief description of their algorithm.

Let $0 < r < 1$ be given. We take $w_0 = w^{(e)}$. Suppose w_0 does not satisfy the stopping criterion (9.68). We then start the following iteration procedure with $k = 1$. At Step k, instead of following the original algorithm of the generalized positivity method by putting $w_k = w_{k-1} + w_k^{(o)}$, where $w_k^{(o)} \in S^{(o)}$ is given by (9.66), we seek a $\lambda \in \mathbb{R}$ such that

$$\begin{aligned} S_k^-(\lambda) &= \int_{\mathrm{SO}(3)} \left(\left(w_{k-1}(\boldsymbol{R}) + \lambda w_k^{(o)}(\boldsymbol{R}) - \frac{r}{8\pi^2} \right)^- \right)^2 d\mathcal{V}(\boldsymbol{R}) \\ &= \int_{Z_k(\lambda)} \left(w_{k-1}(\boldsymbol{R}) + \lambda w_k^{(o)}(\boldsymbol{R}) - \frac{r}{8\pi^2} \right)^2 d\mathcal{V}(\boldsymbol{R}) \end{aligned} \tag{9.69}$$

assumes a minimum as a function of λ; here

$$Z_k(\lambda) := \{ \boldsymbol{R} \in \mathrm{SO}(3) : w_{k-1}(\boldsymbol{R}) + \lambda w_k^{(o)}(\boldsymbol{R}) - \frac{r}{8\pi^2} \le 0 \}; \tag{9.70}$$

cf. (9.48) and (9.68). Note that $w_k^{(o)}$ is the element in $S^{(o)}$ that best approximates u_k as given by (9.65). When $\lambda = 1$, $w_k = w_{k-1} + w_k^{(o)}$ is the candidate function chosen by the original algorithm of the generalized positivity method. But $S_k^-(1)$ need not be the minimum value of $S_k^-(\lambda)$.

Since $S_k^-(\cdot)$ is a function of a real variable, to locate its minima we compute its first and second derivatives. They are:

$$\frac{dS_k^-}{d\lambda} = 2 \int_{Z_k(\lambda)} \left(w_{k-1}(\boldsymbol{R}) + \lambda w_k^{(o)}(\boldsymbol{R}) - \frac{r}{8\pi^2} \right) w_k^{(o)}(\boldsymbol{R})\, d\mathcal{V}(\boldsymbol{R}), \tag{9.71}$$

$$\frac{d^2 S_k^-}{d\lambda^2} = 2 \int_{Z_k(\lambda)} \left(w_k^{(o)}(\boldsymbol{R}) \right)^2 d\mathcal{V}(\boldsymbol{R}). \tag{9.72}$$

The boundary terms in (9.71) and (9.72) do not appear because the integrand of (9.69) and of (9.71) are zero at the boundary of $Z_k(\lambda)$.

Let $F_k(\lambda) = dS_k^-/d\lambda$. We follow Newton's method to find a $\lambda^{(k)}$ that satisfies the equation $F_k(\lambda) = 0$. Since we do not stop the iteration procedure at Step $k-1$, w_{k-1} does not satisfy the stopping criterion. Take $\lambda_1^{(k)} = 1$. If $w_{k-1)} + \lambda_1^{(k)} w_k^{(o)}$ satisfies the stopping criterion, then we are done. If it doesn't, then $Z_k(\lambda_1^{(k)})$ has a positive volume. By (9.72), we have $F_k'(\lambda_1^{(k)}) > 0$. We define $\lambda_2^{(k)}$ be the following formula:

$$\lambda_2^{(k)} = \lambda_1^{(k)} - \frac{F_k(\lambda_1^{(k)})}{F_k'(\lambda_1^{(k)})}. \tag{9.73}$$

In general, if we have already computed $\lambda_p^{(k)}$ and $w_{k-1} + \lambda_p^{(k)} w_k^{(o)}$ does not satisfy the stopping criterion, we proceed to determine $\lambda_{p+1}^{(k)}$ by the recurrence relation

$$\lambda_{p+1}^{(k)} = \lambda_p^{(k)} - \frac{F_k(\lambda_p^{(k)})}{F_k'(\lambda_p^{(k)})}. \tag{9.74}$$

We continue the computations to find a root for the equation $F_k(\lambda) = 0$ until we obtain a λ_q^k which either $w_{k-1} + \lambda_q^{(k)} w_k^{(o)}$ satisfies the stopping criterion or $\lambda_q^{(k)}$ is an acceptable solution of $F_k(\lambda) = 0$. In either case we put $\lambda_q^k = \lambda^{(k)}$ and $w_k = w_{k-1} + \lambda^{(k)} w_k^{(o)}$. If w_k does not satisfy the stopping criterion, then we proceed to Step $k + 1$ to compute w_{k+1}.

The paper of Wagner et al. includes a couple of examples which suggest that the improved algorithm delivers in fewer steps a lower S^- (see (9.68)) than the original algorithm.

9.7 Ghost Correction (II): Method of Texture Components

The main assumption of this method is that we may adequately represent the unknown ODF w as that of a mixture, by volume fractions, of the randomly oriented background and a relatively small number (typically from 5 to 20 for a one-phase material) of suitable texture components as described by model functions [145, 146, 148, 193, 194]:

$$w \approx \nu_0 w_{\text{iso}} + \sum_{k=1}^{K} \nu_k w_k^{(m)}; \tag{9.75}$$

here K is the number of texture components (excluding the random background); $w_k^{(m)}$ and ν_k are the model function and the volume fraction, respectively, that pertain to the i-th texture component; ν_0 is the volume fraction of the random background; the volume fractions satisfy the equation

$$\nu_0 + \sum_k \nu_k = 1. \tag{9.76}$$

Many model functions have been proposed in the literature, e.g., Bunge's "Gaussian distributions" (see Sect. 8.4.2), Matthies's "Gaussian standard function" (including a modification for description of fiber textures) and "Lorentzian standard function" ([216, 217], [224, pp. 87–106]), Helming's "generalized Gauss components" [142, 143], and others [108, 143]. Since we have not covered any model function except those proposed by Bunge, we shall be content, in our outline below to illustrate how the method could be used for ghost correction, to take every model function in (9.75) as some Bunge Gaussian component.

Following the Roe approach, we will examine the case $G_{\text{tex}} = \{\boldsymbol{I}\}$ and $G_{\text{cr}} = \{\boldsymbol{I}\}$. The cases $G_{\text{tex}} \neq \{\boldsymbol{I}\}$ and/or $G_{\text{cr}} \neq \{\boldsymbol{I}\}$ will be covered by enforcing the appropriate restrictions on the texture coefficients of all components used. Suppose the crystallographic texture of the given sample can be taken as a mixture of the "random" background and Bunge Gaussian components $(\boldsymbol{R}_0^{(k)}; \kappa_k)$ $(k = 1, \ldots, K)$, the ODF $w_k^{(m)}$ of which has texture coefficients $c_{mn}^l(\boldsymbol{R}_0^{(k)}; \kappa_k)$ given by (8.33). Let

$$p[\boldsymbol{R}_0^{(k)}; \kappa_k](\alpha, \beta; \Theta, \Phi) = \frac{1}{2\pi} + 4\pi \sum_{\text{even } l \geq 2}^{\infty} \sum_{m=-l}^{l} \sum_{n=-l}^{l} c_{mn}^l(\boldsymbol{R}_0^{(k)}; \kappa_k) d_{m0}^l(\alpha) d_{n0}^l(\Theta) e^{-im\beta} e^{in\Phi} \tag{9.77}$$

be the (Θ, Φ) pole figure pertaining to the Gaussian component $(\boldsymbol{R}_0^{(k)}; \kappa_k)$. The pole figure of the mixture is given by

$$\sum_{k=0}^{K} \nu_k p[\boldsymbol{R}_0^{(k)}; \kappa_k] = \nu_0 \cdot \frac{1}{2\pi} + \sum_{k=1}^{K} \nu_k p[\boldsymbol{R}_0^{(k)}; \kappa_k] = \frac{1}{2\pi} + \sum_{k=1}^{K} \nu_k \left(p[\boldsymbol{R}_0^{(k)}; \kappa_k] - \frac{1}{2\pi} \right). \tag{9.78}$$

Suppose we are given a total of M measured incomplete pole figures p_m $(m = 1, \ldots, M)$ as follows. Let $p_m(\alpha, \beta; \Theta_m, \Phi_m) = N_m I_m(\alpha, \beta; \Theta_m, \Phi_m)$, where I_m is the measured X-ray intensity of the (Θ_m, Φ_m) incomplete pole figure, N_m is an undetermined normalization constant, and $0 \le \alpha \le \alpha_{\max}$ and $0 \le \beta < 2\pi$. We seek normalization constants N_m $(m = 1, \ldots, M)$, volume fractions ν_k, ideal orientations $\boldsymbol{R}_0^{(k)}$, and spread parameters κ_k $(k = 1, \ldots, K)$ which minimize the objective function (cf. (9.38))

$$F = \int_0^{2\pi} \int_0^{\alpha_{\max}} \left(\sum_{m=1}^{M} N_m I_m - \frac{1}{2\pi} - \sum_{k=1}^{K} \nu_j \left(p[\boldsymbol{R}_0^{(k)}; \kappa_k] - \frac{1}{2\pi} \right) \right)^2 \sin\alpha d\alpha d\beta. \tag{9.79}$$

Since X-ray intensity measurements are made at isolated grid points, we work with a discrete form of (9.79) instead. Parallel to (9.40) that pertains to a grid with uniform steps in α and β,[136] here we have

$$F = \sum_{m=1}^{M} \sum_{i,j} \left(N_m I_m(\alpha_i, \beta_j; \Theta_m, \Phi_m) - \frac{1}{2\pi} - \sum_{k=1}^{K} \nu_k \left(p[\boldsymbol{R}_0^{(k)}; \kappa_k](\alpha_i, \beta_j; \Theta_m, \Phi_m) - \frac{1}{2\pi} \right) \right)^2 \times (\cos\alpha_i - \cos\alpha_{i+1}) \Delta\beta. \tag{9.80}$$

As $(\cos\alpha_i - \cos\alpha_{i+1}) > 0$ and $\Delta\beta > 0$, F is the sum of squares of functions, which are linear in the parameters N_m, ν_k, and nonlinear in κ_k and the parameters that specify $\boldsymbol{R}_0^{(k)}$.

According to a general summary by Helming [145], one systematic way to solve the present minimization problem in question will go through an iteration procedure as follows:

1. Estimate the number K, the centers $\boldsymbol{R}_0^{(k)}$, and the spreads κ_k of the Gaussian components by inspection of the available incomplete pole figures.
2. Substitute these estimates into (9.80) and determine the parameters N_m, ν_k by linear least squares.
3. Keep the values of N_m, ν_k found, use those obtained in Step 1 for K, $\boldsymbol{R}_0^{(k)}$, and κ_k as first estimates and determine the refinements of $\boldsymbol{R}_0^{(k)}$ and κ_k by some nonlinear optimization procedure (e.g., the Levenberg-Marquardt method as reported in [143] and [147]).

The values of all parameters obtained after one iteration are used to compute the recalculated pole figures, which are compared with the measured (but normalized) $N_m I_m$. Some criterion (see, e.g., [224, pp. 76–77], [226, Sect. 4] for acceptable fit of pole figures is adopted. The iteration procedure is stopped if the fit is satisfactory. Otherwise another iteration will begin with Step 1, where suitable adjustments on K, $\boldsymbol{R}_0^{(k)}$, and κ_k are attempted.

The method outlined above, of course, can be used for any mixture of all types of texture components. The procedure generally remains the same. In Step 1 we try to get an estimate of the number and specifications of the required texture components. With these estimates, Step 2 will definitely provide the corresponding values of the linear parameters. On the other hand, whether Step 3 will deliver something meaningful depends on the quality of the estimates in Step 1. Moreover, while Steps 2 and 3 will be done by the computer, Step 1 will require manual operations and subjective judgement. More details on how Step 1 could be executed are discussed in [143, 146].

[136] See the description before (9.40) for details of the grid used.

Once we have found the best v_j's from minimization of F in (9.80), we can write down the texture coefficients of the predicted ODF w, namely:

$$c^l_{mn} = \sum_{k=1}^{K} v_k c^l_{mn}(\boldsymbol{R}_0^{(k)}; \kappa_k), \tag{9.81}$$

where the $c^l_{mn}(\boldsymbol{R}_0^{(k)}; \kappa)$'s are given by (8.33).

Note that the present method determines all the texture coefficients c^l_{mn} of the unknown ODF, including those with odd l, which represents a distinct advantage of this method. On the other hand, the method at hand will work only for situations where the main assumption given at the beginning of this subsection is valid and we know which particular Gaussian components we should use as constituents of the mixture.

Remark 9.11 See Schaeben [283] for valuable comments on the method of components in general. □

PART II. MATHEMATICAL FOUNDATIONS AND EXTENSIONS

Chapter 10

10 SO(3) and O(3) as Riemannian Manifolds

10.1 SO(3) and O(3) as Riemannian Submanifolds of M(3)

Let V be the translation space of the three-dimensional physical Euclidean space, and let Lin be the space of linear transformations on V. We adopt and fix a right-handed orthonormal basis $\{\boldsymbol{e}_i\}$ $(i = 1, 2, 3)$ in V, under which each linear transformation in Lin is represented by a matrix in $\mathrm{M}_3(\mathbb{R})$, which we will henceforth write as M(3) for short. In what follows we shall identify each linear transformation $\boldsymbol{A}$ in Lin with its representative in M(3), which we denote by the same symbol $\boldsymbol{A}$.

We equip M(3) with the inner product defined by[137]

$$\boldsymbol{A} \cdot \boldsymbol{B} = \frac{1}{2}\mathrm{tr}(\boldsymbol{A}\boldsymbol{B}^T) \qquad \text{for } \boldsymbol{A}, \boldsymbol{B} \in \mathrm{M}(3). \tag{10.1}$$

We choose and fix an orthonormal basis $\boldsymbol{E}_i$ $(i = 1, 2, \ldots, 9)$ in M(3) as follows. Let

$$\boldsymbol{E}_1 = -\boldsymbol{e}_2 \otimes \boldsymbol{e}_3 + \boldsymbol{e}_3 \otimes \boldsymbol{e}_2, \quad \boldsymbol{E}_2 = -\boldsymbol{e}_3 \otimes \boldsymbol{e}_1 + \boldsymbol{e}_1 \otimes \boldsymbol{e}_3, \quad \boldsymbol{E}_3 = -\boldsymbol{e}_1 \otimes \boldsymbol{e}_2 + \boldsymbol{e}_2 \otimes \boldsymbol{e}_1,$$

$$\boldsymbol{E}_4 = \sqrt{2}(\boldsymbol{e}_1 \otimes \boldsymbol{e}_1), \quad \boldsymbol{E}_5 = \sqrt{2}(\boldsymbol{e}_2 \otimes \boldsymbol{e}_2), \quad \boldsymbol{E}_6 = \sqrt{2}(\boldsymbol{e}_3 \otimes \boldsymbol{e}_3),$$

$$\boldsymbol{E}_7 = \boldsymbol{e}_2 \otimes \boldsymbol{e}_3 + \boldsymbol{e}_3 \otimes \boldsymbol{e}_2, \quad \boldsymbol{E}_8 = \boldsymbol{e}_3 \otimes \boldsymbol{e}_1 + \boldsymbol{e}_1 \otimes \boldsymbol{e}_3, \quad \boldsymbol{E}_9 = \boldsymbol{e}_1 \otimes \boldsymbol{e}_2 + \boldsymbol{e}_2 \otimes \boldsymbol{e}_1.$$

It is easy to verify that under the inner product (10.1) the matrices $\boldsymbol{E}_i$ $(i = 1, 2, \ldots, 9)$ constitute an orthonormal basis in M(3). Every $\boldsymbol{X} \in \mathrm{M}(3)$ can be written uniquely as a linear combination $\boldsymbol{X} = \sum_i X_i \boldsymbol{E}_i$, where $X_i \in \mathbb{R}$ for each i. Let $\varphi : \mathrm{M}(3) \to \mathbb{R}^9$ be defined by

$$\varphi(\sum_i X_i \boldsymbol{E}_i) = (X_1, X_2, \ldots, X_9). \tag{10.2}$$

The function φ, which is clearly a homeomorphism between M(3) and $\mathbb{R}^9$, defines a global chart on M(3) and a C^∞ differentiable structure there. It is easy to show that this differentiable structure is independent of the basis chosen in M(3). A function $f : \mathrm{M}(3) \to \mathbb{R}$ is of class C^∞ if $f \circ \varphi^{-1} : \mathbb{R}^9 \to \mathbb{R}$ is of class C^∞. A function $F : \mathrm{M}(3) \to \mathrm{M}(3)$ is of class C^∞ if $\varphi \circ F \circ \varphi^{-1} : \mathbb{R}^9 \to \mathbb{R}^9$ is of class C^∞. We take GL(3), the set of non-singular 3×3 matrices, as an open submanifold of M(3), and endow the subspaces Sym and Skw each with the differentiable structure that make them embedded submanifolds of M(3). Henceforth we use the adjective "smooth" to mean "of class C^∞". The subsets GL(3), Sym, and Skw are smooth submanifolds of M(3).

Let $\Psi : \mathrm{M}(3) \to \mathrm{Sym}$ be the function defined by

$$\Psi(\boldsymbol{A}) = \boldsymbol{A}\boldsymbol{A}^T. \tag{10.3}$$

[137] We follow common practice and introduce the factor 1/2 here to simplify formulas. The Haar measure on a compact group is unique up to a positive multiplicative constant. In this chapter we shall define the Haar measure on SO(3) through the bi-invariant Riemannian metric of the group. Introducing the factor 1/2 in (10.1) is equivalent to adopting another choice of the positive multiplicative constant in defining the Haar measure.

It is clear that Ψ is of class C^∞ and that $\Psi^{-1}(\boldsymbol{I}) = \mathrm{O}(3)$. The differential of Ψ at $\boldsymbol{A} \in \mathrm{M}(3)$,[138] $D\Psi(\boldsymbol{A}) : \mathrm{M}(3) \to \mathrm{Sym}$, where we have identified the tangent spaces $T_{\boldsymbol{A}}\mathrm{M}(3)$ and $T_{\Psi(\boldsymbol{A})}\mathrm{Sym}$ with M(3) and Sym, respectively, is given by the formula

$$D\Psi(\boldsymbol{A})[\boldsymbol{H}] = \boldsymbol{A}\boldsymbol{H}^T + \boldsymbol{H}\boldsymbol{A}^T \qquad \text{for any } \boldsymbol{H} \in \mathrm{M}(3). \tag{10.4}$$

Let $\boldsymbol{Q} \in \mathrm{O}(3)$ be arbitrarily given. For any $\boldsymbol{C} \in \mathrm{Sym}$, we have

$$D\Psi(\boldsymbol{Q})[\frac{1}{2}\boldsymbol{C}\boldsymbol{Q}] = \frac{1}{2}\boldsymbol{Q}(\boldsymbol{C}\boldsymbol{Q})^T + \frac{1}{2}\boldsymbol{C}\boldsymbol{Q}\boldsymbol{Q}^T = \boldsymbol{C}, \tag{10.5}$$

which shows that $D\Psi(\boldsymbol{A})$ is surjective for each $\boldsymbol{Q} \in \mathrm{O}(3)$. Hence $\boldsymbol{I}$ is a regular value of Ψ and O(3) is an embedded smooth submanifold of M(3); cf. [186, p. 182, Corollary 8.9].

Since O(3) is a level set of the continuous function Ψ, it is a closed subset of M(3). Moreover, O(3) is bounded in M(3) because $\|\boldsymbol{Q}\| = \sqrt{3/2}$ for each $\boldsymbol{Q} \in \mathrm{O}(3)$. Hence O(3) is compact. As a closed and open subset of O(3), SO(3) is compact and is an embedded smooth submanifold of M(3).

A smooth manifold M is said to be Riemannian if for each $\mathbf{x} \in \mathsf{M}$ the tangent space $T_{\mathbf{x}}\mathsf{M}$ is equipped with an inner product $\langle\cdot,\cdot\rangle_{\mathbf{x}}$ which varies smoothly in the following sense: For each coordinate chart $(U, \boldsymbol{\xi})$ of M such that $\xi : U \to \boldsymbol{\xi}(U) \subset \mathbb{R}^n$, $\mathbf{x} \mapsto (\xi_1, \ldots, \xi_n)$, the components of the metric tensor

$$g_{ij} := \langle \frac{\partial \mathbf{x}}{\partial \xi_i}, \frac{\partial \mathbf{x}}{\partial \xi_j} \rangle \tag{10.6}$$

are smooth functions on $\boldsymbol{\xi}(U)$. For each $\boldsymbol{A} \in \mathrm{M}(3)$, $T_{\boldsymbol{A}}\mathrm{M}(3)$—the tangent space to M(3) at $\boldsymbol{A}$—can be identified with M(3), which carries the inner product (10.1). Hence M(3) is a Riemannian manifold. As embedded submanifolds of M(3), both O(3) and SO(3) are Riemannian. Indeed for each $\boldsymbol{Q} \in \mathrm{O}(3)$, $T_{\boldsymbol{Q}}\mathrm{O}(3)$ is a linear subspace of $T_{\boldsymbol{Q}}\mathrm{M}(3)$ and carries the inner product induced by that of M(3), namely (10.1). A similar statement holds for the tangent spaces to SO(3). Section 10.3 provides an example where SO(3) is the Riemannian manifold and the components of the metric tensor g_{ij} are computed with the Euler angles (ψ, θ, ϕ) serving as local coordinates.

10.1.1 Smooth Structure on SO(3) and on O(3)

For completeness we outline in this section the smooth structure on SO(3) and O(3). See, e.g., [130, 276] for details.

There exists a neighborhood U of $\mathbf{0} \in M(3)$ such that the exponential map $\exp : U \to \exp(U)$ and its inverse $\log : \exp(U) \to U$ are diffeomorphisms. In fact we may take

$$U = \{\boldsymbol{A} \in \mathrm{M}(3) : 0 \le \|\boldsymbol{A}\| < \sqrt{2}\log 2\},$$

which we will do below. Note that

$$U \cap \mathrm{Skw} = \{\boldsymbol{W} \in \mathrm{Skw} : 0 \le \|\boldsymbol{W}\| < \sqrt{2}\log 2\}$$

is a neighborhood of $\mathbf{0} \in \mathrm{Skw}$, and $\exp(U)$ is a neighborhood of $\boldsymbol{I}$ in GL(3). Since the map $\exp : U \to \exp(U)$ is bijective, we have

$$\exp(U \cap \mathrm{Skw}) = \exp(U) \cap \exp(\mathrm{Skw}) = \exp(U) \cap \mathrm{SO}(3), \tag{10.7}$$

and $\exp(U \cap \mathrm{Skw})$ is a neighborhood of $\boldsymbol{I}$ in SO(3).

[138] Other common notations of the differential of Ψ are $d\Psi$, Ψ_*, etc.

The pair $(\exp(U), \varphi \circ \log)$, where φ is defined in (10.2), defines a chart on GL(3) that is compatible with its smooth structure as an open submanifold of M(3). Indeed, let $\boldsymbol{Y} = \sum_i Y_i \boldsymbol{E}_i \in \exp(U)$. Under $\varphi \circ \log$, $(Y_1, \ldots, Y_9)$ is mapped to $(X_1, \ldots, X_9)$, which are the coordinates of $\boldsymbol{X} = \log \boldsymbol{Y}$. Both this coordinate transformation and its inverse, which corresponds to the coordinate form of $\boldsymbol{Y} = \exp \boldsymbol{X}$, are of class C^∞. In what follows we use the chart $(\exp(U), \varphi \circ \log)$ and the left translations to construct a smooth atlas on GL(3), with which we can obtain a smooth atlas for O(3) and one for SO(3).

For $\boldsymbol{A} \in \mathrm{GL}(3)$, let $U_{\boldsymbol{A}} := \boldsymbol{A} \exp(U)$, and let $L_{\boldsymbol{A}} : \mathrm{GL}(3) \to \mathrm{GL}(3)$, $\boldsymbol{H} \mapsto \boldsymbol{A}\boldsymbol{H}$, be the left translations on GL(3). Let $\varphi_{\boldsymbol{A}} : U_{\boldsymbol{A}} \to \mathbb{R}^9$ be defined by

$$\varphi_{\boldsymbol{A}} = \varphi \circ \log \circ L_{\boldsymbol{A}}^{-1}. \tag{10.8}$$

For $\boldsymbol{Y} = \sum_i Y_i \boldsymbol{E}_i \in \boldsymbol{A} \exp(U)$, $\varphi_{\boldsymbol{A}} \circ (\varphi\big|_{U_{\boldsymbol{A}}})^{-1}$ maps $(Y_1, \ldots, Y_9)$ to $(X_1, \ldots, X_9)$, which are the coordinates of $\boldsymbol{X} = \log(\boldsymbol{A}^{-1}\boldsymbol{Y}) \in \exp(U)$. This coordinate transformation and its inverse, which pertains to the correspondence $\boldsymbol{Y} \mapsto \boldsymbol{A} \exp \boldsymbol{X}$, are of class C^∞. Hence for each $\boldsymbol{A} \in \mathrm{GL}(3)$, $(U_{\boldsymbol{A}}, \varphi_{\boldsymbol{A}})$ defines a smooth chart on the manifold GL(3). The union of the domains of the charts $\Pi := \{(U_{\boldsymbol{A}}, \varphi_{\boldsymbol{A}}) : \boldsymbol{A} \in \mathrm{GL}(3)\}$ clearly covers GL(3). We further claim that these charts are smoothly compatible. Indeed, suppose $U_{\boldsymbol{A}} \cap U_{\boldsymbol{B}} \neq \emptyset$ for some $\boldsymbol{A}$ and $\boldsymbol{B}$ in GL(3). Since $U_{\boldsymbol{A}} \cap U_{\boldsymbol{B}}$ is open, $\log \circ L_{\boldsymbol{A}}^{-1}(U_{\boldsymbol{A}} \cap U_{\boldsymbol{B}}) \subset U$ and $\log \circ L_{\boldsymbol{B}}^{-1}(U_{\boldsymbol{A}} \cap U_{\boldsymbol{B}}) \subset U$ are open. For each $\boldsymbol{Y} \in U_{\boldsymbol{A}} \cap U_{\boldsymbol{B}}$, there is a unique $\boldsymbol{X} \in \log \circ L_{\boldsymbol{A}}^{-1}(U_{\boldsymbol{A}} \cap U_{\boldsymbol{B}})$ and a unique $\widetilde{\boldsymbol{X}} \in \log \circ L_{\boldsymbol{B}}^{-1}(U_{\boldsymbol{A}} \cap U_{\boldsymbol{B}})$ such that

$$\boldsymbol{Y} = \boldsymbol{A} \exp \boldsymbol{X} = \boldsymbol{B} \exp \widetilde{\boldsymbol{X}},$$

which shows that $\boldsymbol{X}$ and $\widetilde{\boldsymbol{X}}$ are related by the formulas

$$\boldsymbol{X} = \log(\boldsymbol{A}^{-1}\boldsymbol{B} \exp \widetilde{\boldsymbol{X}}), \qquad \widetilde{\boldsymbol{X}} = \log(\boldsymbol{B}^{-1}\boldsymbol{A} \exp \boldsymbol{X}).$$

Hence the coordinate transformations in question are of class C^∞, and the collection of charts Π defines an atlas on the manifold GL(3), which defines a smooth structure on GL(3).

For each $\boldsymbol{Q} \in \mathrm{O}(3)$, let $W_{\boldsymbol{Q}} = \boldsymbol{Q}(\exp(U) \cap \mathrm{SO}(3))$ and $\psi_{\boldsymbol{Q}} = \varphi_{\boldsymbol{Q}}\,|_{W_{\boldsymbol{Q}}}$. Then for each $\boldsymbol{Q} \in \mathrm{O}(3)$, $\boldsymbol{Q} \in W_{\boldsymbol{Q}}$ and

$$\psi_{\boldsymbol{Q}}(W_{\boldsymbol{Q}}) \subset \varphi(\mathrm{Skw}) \subset \{(X_1, \ldots, X_9) \in \mathbb{R}^9 : X_4 = \cdots = X_9 = 0\}. \tag{10.9}$$

Thus $\{(W_{\boldsymbol{Q}}, \psi_{\boldsymbol{Q}}) : \boldsymbol{Q} \in \mathrm{O}(3)\}$ (resp. $\{(W_{\boldsymbol{R}}, \psi_{\boldsymbol{R}}) : \boldsymbol{R} \in \mathrm{SO}(3)\}$) serves as an atlas on O(3) (resp. SO(3)) which defines the unique smooth structure that makes the inclusion of O(3) (resp. SO(3)) in GL(3) a smooth embedding.

10.1.2 Bi-invariant Metric on O(3) and SO(3)

A smooth manifold G is a Lie group if the following two assertions hold:

1. G is a group.
2. The group operations $G \times G \to G$, $(x, y) \mapsto xy$ and $G \to G$, $x \mapsto x^{-1}$ are smooth functions.

For each $a \in G$, we define the left translation $L_a : G \to G$ and right translation $R_a : G \to G$ by

$$L_a(x) = ax \qquad \text{for each } x \in G, \tag{10.10}$$

and

$$R_a(x) = xa \qquad \text{for each } x \in G, \tag{10.11}$$

respectively. It is clear that both L_a and R_a are smooth functions. The groups GL(3), O(3), and SO(3) are examples of Lie groups.

Let G be a Lie group and a Riemannian manifold. Let $\langle u, v\rangle_x$ denote the inner product of tangent vectors u, v in T_xG. The Riemannian metric on G is said to be left-invariant if each left-translation on G is an isometry, i.e.,

$$\langle u, v\rangle_x = \langle DL_a(x)[u], DL_a(x)[v]\rangle_{L_a(x)} \qquad \text{for all } a, x \in G \text{ and } u, v \in T_xG, \tag{10.12}$$

and right-invariant if each right-translation is an isometry. A Riemannian metric is bi-invariant if it is both left-invariant and right-invariant.

In what follows we show that the Riemannian metric on O(3) is bi-invariant. To start with, let us characterize the structure of the tangent spaces $T_{\boldsymbol{Q}}\mathrm{O}(3)$, where $\boldsymbol{Q} \in \mathrm{O}(3)$.

Consider a smooth curve $\boldsymbol{B}(t)$ in O(3) that passes through the element $\boldsymbol{Q}$ at $t = 0$, i.e., $\boldsymbol{B}(0) = \boldsymbol{Q}$. Then $\boldsymbol{A}(t) := \boldsymbol{Q}^T\boldsymbol{B}(t)$ defines a smooth curve in O(3) that satisfies $\boldsymbol{A}(0) = \boldsymbol{I}$. Differentiating both sides of the equation $\boldsymbol{A}(t)\boldsymbol{A}(t)^T = \boldsymbol{I}$ with respect to t and then setting $t = 0$, we obtain

$$\dot{\boldsymbol{A}}(0)\boldsymbol{A}(0)^T + \boldsymbol{A}(0)\dot{\boldsymbol{A}}(0)^T = \boldsymbol{0},$$

which implies $\dot{\boldsymbol{A}}(0) = -\dot{\boldsymbol{A}}(0)^T$ or $\boldsymbol{Q}^T\dot{\boldsymbol{B}}(0)$ is skew. Thus there exists a skew matrix $\boldsymbol{W}$ such that the tangent vector $\dot{\boldsymbol{B}}(0) \in T_{\boldsymbol{Q}}\mathrm{O}(3)$ is given by $\dot{\boldsymbol{B}}(0) = \boldsymbol{Q}\boldsymbol{W}$. Conversely, for each $\boldsymbol{W} \in \mathrm{Skw}$, $\boldsymbol{C}(t) := \boldsymbol{Q}\exp(t\boldsymbol{W})$ defines a smooth curve in O(3) that satisfies $\boldsymbol{C}(0) = \boldsymbol{Q}$ and $\dot{\boldsymbol{C}}(0) = \boldsymbol{Q}\boldsymbol{W}$ is a tangent vector in $T_{\boldsymbol{Q}}\mathrm{O}(3)$. We conclude that

$$T_{\boldsymbol{Q}}\mathrm{O}(3) = \{\boldsymbol{Q}\boldsymbol{W} : \boldsymbol{W} \in \mathrm{Skw}\}. \tag{10.13}$$

In particular, $T_{\boldsymbol{I}}\mathrm{O}(3)$ is none other than the space of skew tensors Skw.

We proceed to show that the Riemannian metric on O(3) is left-invariant. For a given $\boldsymbol{A} \in \mathrm{O}(3)$, we have by definition (10.10)

$$L_{\boldsymbol{A}}(\boldsymbol{Q}) = \boldsymbol{A}\boldsymbol{Q} \qquad \text{for each } \boldsymbol{Q} \in \mathrm{O}(3). \tag{10.14}$$

Let $\boldsymbol{W}$ be skew and let $\boldsymbol{Q}\boldsymbol{W}$ be a tangent vector in $T_{\boldsymbol{Q}}\mathrm{O}(3)$. It is easy to verify that

$$DL_{\boldsymbol{A}}(\boldsymbol{Q})[\boldsymbol{Q}\boldsymbol{W}] = \boldsymbol{A}\boldsymbol{Q}\boldsymbol{W}. \tag{10.15}$$

To verify that the Riemannian metric on O(3) is left-invariant, we have to check that requirement (10.12) is observed. Let $\boldsymbol{A}$, $\boldsymbol{Q}$ be in O(3), and let $\boldsymbol{X}$ and $\boldsymbol{Y}$ be skew. On the left-hand side of requirement (10.12), we have

$$\langle \boldsymbol{Q}\boldsymbol{X}, \boldsymbol{Q}\boldsymbol{Y}\rangle_{\boldsymbol{Q}} = \frac{1}{2}\mathrm{tr}\left(\boldsymbol{Q}\boldsymbol{X}(\boldsymbol{Q}\boldsymbol{Y})^T\right) = \frac{1}{2}\mathrm{tr}\left(\boldsymbol{X}\boldsymbol{Y}^T\right).$$

On the right-hand side, there holds

$$\begin{aligned}\langle DL_{\boldsymbol{A}}(\boldsymbol{Q})[\boldsymbol{Q}\boldsymbol{X}], DL_{\boldsymbol{A}}(\boldsymbol{Q})[\boldsymbol{Q}\boldsymbol{Y}]\rangle_{L_{\boldsymbol{A}}(\boldsymbol{Q})} &= \frac{1}{2}\mathrm{tr}\left(\boldsymbol{A}\boldsymbol{Q}\boldsymbol{X}(\boldsymbol{A}\boldsymbol{Q}\boldsymbol{Y})^T\right)\\ &= \frac{1}{2}\mathrm{tr}\left(\boldsymbol{X}\boldsymbol{Y}^T\right).\end{aligned}$$

Hence the Riemannian metric on O(3) is left-invariant. That it is also right-invariant can be proved in a similar way. In conclusion, the Riemannian metric on O(3) is bi-invariant.

Similarly the Riemannian metric on SO(3) is also bi-invariant.

10.2 SO(3) as Metric Space

The rotation group SO(3), as a connected Riemannian manifold, is a metric space with the metric $d_{\mathrm{SO}(3)}(\boldsymbol{P}, \boldsymbol{Q})$ given by the infimum of the lengths of piecewise C^1 curves from $\boldsymbol{P}$ to $\boldsymbol{Q}$. Moreover, the metric space topology agrees with its manifold topology. See, e.g., Boothby [36, pp. 189–191].

Let $\boldsymbol{P}, \boldsymbol{Q} \in \mathrm{SO}(3)$, and let $\boldsymbol{Q}\boldsymbol{P}^T = \boldsymbol{M}(\widetilde{\boldsymbol{n}}, \widetilde{\omega}) \in \mathrm{SO}(3)$ be the misorientation of $\boldsymbol{Q}$ with respect to $\boldsymbol{P}$ (see Sect. 1.10). Since the right translation $R_{\boldsymbol{P}^T} : \boldsymbol{R} \mapsto \boldsymbol{R}\boldsymbol{P}^T$ on SO(3) is an isometry, we have

$$d_{\mathrm{SO}(3)}(\boldsymbol{P}, \boldsymbol{Q}) = d_{\mathrm{SO}(3)}(\boldsymbol{I}, \boldsymbol{Q}\boldsymbol{P}^T) = d_{\mathrm{SO}(3)}(\boldsymbol{I}, \boldsymbol{M}(\widetilde{\boldsymbol{n}}, \widetilde{\omega})). \tag{10.16}$$

Note that $\boldsymbol{M} = \exp(\widetilde{\omega}\widetilde{\boldsymbol{n}}\times)$. Let $\boldsymbol{\alpha} : [0, 1] \to \mathrm{SO}(3)$ be defined by

$$\boldsymbol{\alpha}(t) = \exp(t\,\widetilde{\omega}\widetilde{\boldsymbol{n}}\times). \tag{10.17}$$

We distinguish two cases: (i) $0 \le \widetilde{\omega} < \pi$; (ii) $\widetilde{\omega} = \pi$

Case (i): $0 \le \widetilde{\omega} < \pi$. Let $\mathsf{B} = \{\boldsymbol{R}(\boldsymbol{n}, \omega) \in \mathrm{SO}(3) : \boldsymbol{n} \in \mathcal{S}^2, 0 \le \omega < 2\pi\}$. The curve $\boldsymbol{\alpha}$ is the only geodesic in B from $\boldsymbol{I}$ to $\boldsymbol{M}$; cf. [36, p. 356]. Hence we have

$$\begin{aligned} d_{\mathrm{SO}(3)}(\boldsymbol{I}, \boldsymbol{M}) &= \int_0^1 \langle \boldsymbol{\alpha}'(t), \boldsymbol{\alpha}'(t) \rangle^{1/2}\, dt \\ &= \int_0^1 \langle (\widetilde{\omega}\widetilde{\boldsymbol{n}}\times) \exp(t\,\widetilde{\omega}\widetilde{\boldsymbol{n}}\times), (\widetilde{\omega}\widetilde{\boldsymbol{n}}\times) \exp(t\,\widetilde{\omega}\widetilde{\boldsymbol{n}}\times) \rangle^{1/2}\, dt \\ &= \int_0^1 \langle \widetilde{\omega}\widetilde{\boldsymbol{n}}\times, \widetilde{\omega}\widetilde{\boldsymbol{n}}\times \rangle^{1/2}\, dt = \| \widetilde{\omega}\widetilde{\boldsymbol{n}}\times \| = \widetilde{\omega}, \end{aligned} \tag{10.18}$$

where $\widetilde{\omega}$ is the misorientation angle between $\boldsymbol{P}$ and $\boldsymbol{Q}$, and we have appealed to (1.127) and the bi-invariance of the Riemannian metric.

Case (ii): $\widetilde{\omega} = \pi$. There are two shortest geodesics from $\boldsymbol{I}$ to $\boldsymbol{M}$, which are of equal length π. They are: $\boldsymbol{\alpha}$ defined in (10.17) and $\boldsymbol{\beta} : [0, 1] \to \mathrm{SO}(3)$ defined by

$$\boldsymbol{\beta}(t) = \exp(-t\,\widetilde{\omega}\widetilde{\boldsymbol{n}}\times). \tag{10.19}$$

In both cases we have $d_{\mathrm{SO}(3)}(\boldsymbol{P}, \boldsymbol{Q}) = \widetilde{\omega}$. We summarize our finding as a theorem.

Theorem 10.1 *Let $\boldsymbol{P}$ and $\boldsymbol{Q}$ be rotations, and let $d_{SO(3)}(\boldsymbol{P}, \boldsymbol{Q})$ be the Riemannian distance between $\boldsymbol{P}$ and $\boldsymbol{Q}$. Then $d_{SO(3)}(\boldsymbol{P}, \boldsymbol{Q}) = \widetilde{\omega}$, where $\widetilde{\omega}$ is the misorientation angle between $\boldsymbol{P}$ and $\boldsymbol{Q}$.* □

10.3 Riemannian Metric on SO(3) in Euler Angles

In this section we determine the explicit form of the metric tensor on SO(3) at points where the Euler angles (ψ, θ, ϕ) can be used as local coordinates, and we compute the volume of SO(3).

Let U be an open set in SO(3), and let $\varphi : U \to \mathbb{R}^3$, $\boldsymbol{R} \mapsto (\xi_1, \xi_2, \xi_3)$ be a chart on SO(3). Let $\boldsymbol{P} \in U$ and $T_{\boldsymbol{P}}\mathrm{SO}(3)$ be the tangent space to SO(3) at $\boldsymbol{P}$. The vectors

$$\frac{\partial \boldsymbol{R}}{\partial \xi_1}(\boldsymbol{P}), \frac{\partial \boldsymbol{R}}{\partial \xi_2}(\boldsymbol{P}), \frac{\partial \boldsymbol{R}}{\partial \xi_3}(\boldsymbol{P})$$

constitute a basis of the tangent space $T_{\boldsymbol{P}}\mathrm{SO}(3)$. Under local coordinates (ξ_1, ξ_2, ξ_3), the components of the metric tensor at $\boldsymbol{P} \in U \subset \mathrm{SO}(3)$ are given by

$$g_{ij}(\boldsymbol{P}) = \frac{\partial \boldsymbol{R}}{\partial \xi_i}(\boldsymbol{P}) \cdot \frac{\partial \boldsymbol{R}}{\partial \xi_j}(\boldsymbol{P}). \tag{10.20}$$

In what follows $(\xi_1, \xi_2, \xi_3) = (\psi, \theta, \phi)$, the Euler angles which are defined in Sect. 1.7, and $\varphi(U) = \{(\psi, \theta, \phi) : 0 < \psi < 2\pi, 0 < \theta < \pi, 0 < \phi < 2\pi\}$.

For later convenience, we list the chosen basis in Skw in matrix form:

$$\boldsymbol{E}_1 = \begin{pmatrix} 0 & 0 & 0 \\ 0 & 0 & -1 \\ 0 & 1 & 0 \end{pmatrix}, \quad \boldsymbol{E}_2 = \begin{pmatrix} 0 & 0 & 1 \\ 0 & 0 & 0 \\ -1 & 0 & 0 \end{pmatrix}, \quad \boldsymbol{E}_3 = \begin{pmatrix} 0 & -1 & 0 \\ 1 & 0 & 0 \\ 0 & 0 & 0 \end{pmatrix}. \tag{10.21}$$

Note that under the inner product (10.1) we have $\boldsymbol{E}_i \cdot \boldsymbol{E}_j = \delta_{ij}$.

By (1.87) and (1.124), we have

$$\boldsymbol{R}(\psi, \theta, \phi) = \exp(\psi \boldsymbol{E}_3) \exp(\theta \boldsymbol{E}_2) \exp(\phi \boldsymbol{E}_3). \tag{10.22}$$

It follows that

$$\frac{\partial \boldsymbol{R}}{\partial \phi} = \exp(\psi \boldsymbol{E}_3) \exp(\theta \boldsymbol{E}_2) \exp(\phi \boldsymbol{E}_3) \boldsymbol{E}_3, \tag{10.23}$$

$$\frac{\partial \boldsymbol{R}}{\partial \theta} = \exp(\psi \boldsymbol{E}_3) \exp(\theta \boldsymbol{E}_2) \boldsymbol{E}_2 \exp(\phi \boldsymbol{E}_3), \tag{10.24}$$

$$\frac{\partial \boldsymbol{R}}{\partial \psi} = \exp(\psi \boldsymbol{E}_3) \boldsymbol{E}_3 \exp(\theta \boldsymbol{E}_2) \exp(\phi \boldsymbol{E}_3). \tag{10.25}$$

After some algebraic manipulations, we get

$$\boldsymbol{R}^{-1} \frac{\partial \boldsymbol{R}}{\partial \phi} = \boldsymbol{E}_3, \tag{10.26}$$

$$\begin{aligned} \boldsymbol{R}^{-1} \frac{\partial \boldsymbol{R}}{\partial \theta} &= \exp(-\phi \boldsymbol{E}_3) \boldsymbol{E}_2 \exp(\phi \boldsymbol{E}_3) \\ &= \begin{pmatrix} 0 & 0 & \cos\phi \\ 0 & 0 & -\sin\phi \\ -\cos\phi & \sin\phi & 0 \end{pmatrix} = \sin\phi \boldsymbol{E}_1 + \cos\phi \boldsymbol{E}_2. \end{aligned} \tag{10.27}$$

$$\boldsymbol{R}^{-1}\frac{\partial \boldsymbol{R}}{\partial \psi} = \exp(-\phi \boldsymbol{E}_3)\exp(-\theta \boldsymbol{E}_2)\boldsymbol{E}_3 \exp(\theta \boldsymbol{E}_2)\exp(\phi \boldsymbol{E}_3)$$

$$= \begin{pmatrix} \cos\theta\cos\phi & \sin\phi & -\sin\theta\cos\phi \\ -\cos\theta\sin\phi & \cos\phi & \sin\theta\sin\phi \\ \sin\theta & 0 & \cos\theta \end{pmatrix} \begin{pmatrix} 0 & -1 & 0 \\ 1 & 0 & 0 \\ 0 & 0 & 0 \end{pmatrix}$$

$$\times \begin{pmatrix} \cos\theta\cos\phi & -\cos\theta\sin\phi & \sin\theta \\ \sin\phi & \cos\phi & 0 \\ -\sin\theta\cos\phi & \sin\theta\sin\phi & \cos\theta \end{pmatrix}$$

$$= \begin{pmatrix} 0 & -\cos\theta & \sin\theta\sin\phi \\ \cos\theta & 0 & \sin\theta\cos\phi \\ -\sin\theta\sin\phi & -\sin\theta\cos\phi & 0 \end{pmatrix}$$

$$= -\sin\theta\cos\phi \boldsymbol{E}_1 + \sin\theta\sin\phi \boldsymbol{E}_2 + \cos\theta \boldsymbol{E}_3. \tag{10.28}$$

By using the fact that

$$\boldsymbol{R}^{-1}\frac{\partial \boldsymbol{R}}{\partial \xi_i} \cdot \boldsymbol{R}^{-1}\frac{\partial \boldsymbol{R}}{\partial \xi_j} = \frac{\partial \boldsymbol{R}}{\partial \xi_i} \cdot \frac{\partial \boldsymbol{R}}{\partial \xi_j},$$

we obtain

$$(g_{ij}) = \begin{pmatrix} \frac{\partial \boldsymbol{R}}{\partial \psi}\cdot\frac{\partial \boldsymbol{R}}{\partial \psi} & \frac{\partial \boldsymbol{R}}{\partial \psi}\cdot\frac{\partial \boldsymbol{R}}{\partial \theta} & \frac{\partial \boldsymbol{R}}{\partial \psi}\cdot\frac{\partial \boldsymbol{R}}{\partial \phi} \\ \frac{\partial \boldsymbol{R}}{\partial \theta}\cdot\frac{\partial \boldsymbol{R}}{\partial \psi} & \frac{\partial \boldsymbol{R}}{\partial \theta}\cdot\frac{\partial \boldsymbol{R}}{\partial \theta} & \frac{\partial \boldsymbol{R}}{\partial \theta}\cdot\frac{\partial \boldsymbol{R}}{\partial \phi} \\ \frac{\partial \boldsymbol{R}}{\partial \phi}\cdot\frac{\partial \boldsymbol{R}}{\partial \psi} & \frac{\partial \boldsymbol{R}}{\partial \phi}\cdot\frac{\partial \boldsymbol{R}}{\partial \theta} & \frac{\partial \boldsymbol{R}}{\partial \phi}\cdot\frac{\partial \boldsymbol{R}}{\partial \phi} \end{pmatrix} = \begin{pmatrix} 1 & 0 & \cos\theta \\ 0 & 1 & 0 \\ \cos\theta & 0 & 1 \end{pmatrix}. \tag{10.29}$$

In Euler angles, the volume element on SO(3) is then given by

$$\sqrt{\det(g_{ij})} = \sqrt{1-\cos^2\theta} = \sin\theta. \tag{10.30}$$

The set of points $\mathrm{SO}(3) \setminus U$ has zero group volume. Thus the group volume of SO(3) is given by

$$\mathcal{V}(\mathrm{SO}(3)) = \int_0^{2\pi}\int_0^{\pi}\int_0^{2\pi} \sin\theta \, d\psi d\theta d\phi = 8\pi^2. \tag{10.31}$$

For a Borel set A in SO(3), the normalized Haar measure is:

$$\mathfrak{g}(A) = \frac{1}{8\pi^2}\int_A \sin\theta \, d\psi d\theta d\phi. \tag{10.32}$$

10.4 Riemannian Metric on Orientation Space

Let $G_{\rm cr} = \{\boldsymbol{P}_1, \ldots, \boldsymbol{P}_{N_{\rm cr}}\} \neq \{\boldsymbol{I}\}$ be a Type I crystallographic point group, and let $M := \mathrm{SO}(3)/G_{\rm cr} = \{\boldsymbol{R}G_{\rm cr} : \boldsymbol{R} \in \mathrm{SO}(3)\}$ be the orientation space of crystallites with $G_{\rm cr}$ as their group of rotational symmetry (see Sect. 6.1.1). The right action $\mathcal{T}^{(\rm cr)} : \mathrm{SO}(3) \times G_{\rm cr} \to \mathrm{SO}(3)$ of $G_{\rm cr}$ on SO(3) defined by

$$\mathcal{T}^{(\rm cr)}(\boldsymbol{R}, \boldsymbol{P}) = \mathcal{T}^{(\rm cr)}_{\boldsymbol{P}}(\boldsymbol{R}) = \boldsymbol{R}\boldsymbol{P} \qquad \text{for each } \boldsymbol{R} \in \mathrm{SO}(3) \text{ and } \boldsymbol{P} \in G_{\rm cr} \tag{10.33}$$

is properly discontinuous; see Lemma B.17 in Appendix B. Moreover, for each $\boldsymbol{P} \in G_{\rm cr}$ the map $\mathcal{T}^{(\rm cr)}_{\boldsymbol{P}} : \mathrm{SO}(3) \to \mathrm{SO}(3)$ is a diffeomorphism and an isometry.

Let $\pi : \mathrm{SO}(3) \to M$, $\boldsymbol{R} \mapsto \boldsymbol{R}G_{\rm cr}$ be the projection. We give the orientation space M the differentiable structure with respect to which π is a local diffeomorphism (see do Carmo [71, pp. 22–23]), i.e.: For each $\boldsymbol{R}\boldsymbol{P}_i \in \boldsymbol{R}G_{\rm cr}$, there is an open neighborhood U of $\boldsymbol{R}\boldsymbol{P}_i$ in SO(3) and an open neighborhood of $\boldsymbol{R}G_{\rm cr}$ in M such that $\pi|_U : U \to V$ is a diffeomorphism. We make the orientation space M a Riemannian manifold by endowing it with the metric induced by the projection π defined as follows (cf. [71, p. 165]): Let u and v be tangent vectors in the tangent space $T_{\boldsymbol{R}G_{\rm cr}}M$. Pick an element $\boldsymbol{R}\boldsymbol{P}_j \in \boldsymbol{R}G_{\rm cr}$. We define the inner product of u and v by

$$\langle u, v\rangle_{\boldsymbol{R}G_{\rm cr}} := \langle (D\pi(\boldsymbol{R}\boldsymbol{P}_j))^{-1}[u], (D\pi(\boldsymbol{R}\boldsymbol{P}_j))^{-1}[v]\rangle_{\boldsymbol{R}\boldsymbol{P}_j}. \tag{10.34}$$

Since $\mathcal{T}^{(\rm cr)}_{\boldsymbol{P}} : \mathrm{SO}(3) \to \mathrm{SO}(3)$ is an isometry for each $\boldsymbol{P} \in G_{\rm cr}$, we can easily show that (10.34) is well defined, as it is independent of the choice of $\boldsymbol{R}\boldsymbol{P}_j \in \boldsymbol{R}G_{\rm cr}$, and that the projection π is a local isometry. Moreover, the Riemannian distance between two orientations $\boldsymbol{R}_1G_{\rm cr}$ and $\boldsymbol{R}_2G_{\rm cr}$ is given by

$$d_M(\boldsymbol{R}_1G_{\rm cr}, \boldsymbol{R}_2G_{\rm cr}) = \min\{d_{\mathrm{SO}(3)}(\boldsymbol{R}_1\boldsymbol{P}_i, \boldsymbol{R}_2\boldsymbol{P}_j) : \boldsymbol{P}_i, \boldsymbol{P}_j \in G_{\rm cr}\} = \widetilde{\omega}_d, \tag{10.35}$$

where $\widetilde{\omega}_d$ is the disorientation angle between the two orientations in question; see Godefroy [130, pp. 63–67] for a proof.

10.5 Riemannian Metric on O(3)

For brevity we shall sometimes write G for SO(3) in this section. Let $\boldsymbol{\mathcal{I}} = -\boldsymbol{I}$ be the inversion. Clearly we have

$$\boldsymbol{\mathcal{I}} \in \mathrm{O}(3), \quad \det\boldsymbol{\mathcal{I}} = -1, \quad \text{and} \quad \boldsymbol{\mathcal{I}}\boldsymbol{Q} = \boldsymbol{Q}\boldsymbol{\mathcal{I}} \quad \text{for any } \boldsymbol{Q} \in \mathrm{O}(3). \tag{10.36}$$

Each $\boldsymbol{Q} \in \mathrm{O}(3)$ is orthogonal. Thus $\det\boldsymbol{Q}$ satisfies

$$(\det\boldsymbol{Q})^2 = (\det\boldsymbol{Q})(\det\boldsymbol{Q}^T) = \det(\boldsymbol{Q}\boldsymbol{Q}^T) = \det\boldsymbol{I} = 1, \tag{10.37}$$

which implies $\det\boldsymbol{Q} = \pm 1$. If $\det\boldsymbol{Q} = 1$, then $\boldsymbol{Q} \in \mathrm{SO}(3)$. If $\det\boldsymbol{Q} = -1$, then $\det(\boldsymbol{\mathcal{I}}\boldsymbol{Q}) = 1$ and there is an $\boldsymbol{R} \in \mathrm{SO}(3)$ such that $\boldsymbol{\mathcal{I}}\boldsymbol{Q} = \boldsymbol{R}$ or $\boldsymbol{Q} = \boldsymbol{\mathcal{I}}\boldsymbol{R}$. Since the map $\det : \mathrm{O}(3) \to \mathbb{R}$, $\boldsymbol{Q} \mapsto \det\boldsymbol{Q}$, is continuous, O(3) is the disjoint union of $\mathsf{G} := \mathrm{SO}(3)$ and

$$\boldsymbol{\mathcal{I}}\mathsf{G} := \{\boldsymbol{\mathcal{I}}\boldsymbol{R} : \boldsymbol{R} \in \mathrm{SO}(3)\}. \tag{10.38}$$

The orthogonal group O(3) and rotational group SO(3), as embedded submanifolds in M(3), inherit their Riemannian metric from M(3). The inherited Riemannian metric of

SO(3), which we have studied in Sect. 10.2, is the same as that which SO(3) inherits from O(3) as an open submanifold.

In Sect. 10.1.2 we have shown that every left-translation on O(3) is an isometry. In particular, the left-translation $L_{\mathcal{I}} : \mathrm{O}(3) \to \mathrm{O}(3)$ is an isometry. Let $\mathcal{V}_{\mathrm{O}(3)}$ be the bi-invariant volume measure on O(3) defined as follows:

Let $A = A_1 \cup A_2$ be a Borel subset of O(3), where A_1 and A_2 are Borel subsets of SO(3) and $\mathcal{I}\mathrm{SO}(3)$, respectively. Then

$$\mathcal{V}_{\mathrm{O}(3)}(A) = \mathcal{V}(A_1) + \mathcal{V}(A_2), \tag{10.39}$$

where $\mathcal{V}$ is the Riemannian volume on SO(3). Since

$$L_{\mathcal{I}}(\mathsf{G}) = \mathcal{I}\mathsf{G}, \quad \text{and} \quad L_{\mathcal{I}}(\mathcal{I}\mathsf{G}) = \mathsf{G}, \tag{10.40}$$

we see that the two sets G and $\mathcal{I}\mathsf{G}$ have the same group volume. By (10.31) and (10.39), we conclude that the group volume of O(3) is

$$\mathcal{V}_{\mathrm{O}(3)}(\mathrm{O}(3)) = 16\pi^2. \tag{10.41}$$

Let $\mathfrak{g}$ be the normalized Haar measure on O(3). Then we have

$$\mathfrak{g}(A) = \frac{1}{16\pi^2}\mathcal{V}(A), \tag{10.42}$$

for each measurable subset of O(3).

10.5.1 O(3) as Metric Space

Let us see how we can define a distance function $d_{\mathrm{O}(3)} : \mathrm{O}(3) \times \mathrm{O}(3) \to \mathbb{R}$ which agrees with the Riemannian metric $d_{\mathrm{SO}(3)}$ on SO(3), i.e.,

$$d_{\mathrm{O}(3)}(\boldsymbol{P}, \boldsymbol{Q}) = d_{\mathrm{SO}(3)}(\boldsymbol{P}, \boldsymbol{Q}) \qquad \text{for } \boldsymbol{P}, \boldsymbol{Q} \in \mathrm{SO}(3). \tag{10.43}$$

Since the Riemannian metric on O(3) is bi-invariant (see Sect. 10.1.2), what follows should hold:

$$d_{\mathrm{O}(3)}(\mathcal{I}\boldsymbol{P}, \mathcal{I}\boldsymbol{Q}) = d_{\mathrm{SO}(3)}(\boldsymbol{P}, \boldsymbol{Q}) \qquad \text{for } \boldsymbol{P}, \boldsymbol{Q} \in \mathrm{SO}(3). \tag{10.44}$$

On the other hand, for $\boldsymbol{P} \in \mathrm{SO}(3)$ and $\mathcal{I}\boldsymbol{Q} \in \mathcal{I}\mathrm{SO}(3)$, $d_{\mathrm{O}(3)}(\boldsymbol{P}, \boldsymbol{Q})$ is undefined.

A family of distance functions can be defined on O(3) by adding to (10.43) and (10.44) the following assignment:

$$d_{\mathrm{O}(3)}(\boldsymbol{P}, \mathcal{I}\boldsymbol{Q}) = d_{\mathrm{SO}(3)}(\boldsymbol{P}, \boldsymbol{Q}) + K \quad \text{where } K > 0, \qquad \text{for } \boldsymbol{P}, \boldsymbol{Q} \in \mathrm{SO}(3). \tag{10.45}$$

It is easily checked that with (10.43)–(10.45) $d_{\mathrm{O}(3)}$ satisfies all the requirements in Definition 1.18 for distance function. A choice of $K > \pi$ has the added benefit that $d_{\mathrm{O}(3)}(\boldsymbol{P}, \boldsymbol{Q}) > \pi$ indicates that one of the two elements $\boldsymbol{P}$ and $\boldsymbol{Q}$ is in SO(3) and the other in $\mathcal{I}\mathrm{SO}(3)$.

10.6 Invariant Integration

10.6.1 On SO(3)

Let $f \in L^2(\mathrm{SO}(3), \mathbb{C})$. The integral $I(f) := \int_{\mathrm{SO}(3)} f(\boldsymbol{R})\, d\mathcal{V}(\boldsymbol{R})$ is said to be left-invariant if

$$I(f) = \int_{\mathrm{SO}(3)} f(\boldsymbol{P}^{-1}\boldsymbol{R})\, d\mathcal{V}(\boldsymbol{R}) \qquad \text{for each } \boldsymbol{P} \in \mathrm{SO}(3); \tag{10.46}$$

it is right-invariant if

$$I(f) = \int_{\mathrm{SO}(3)} f(\boldsymbol{R}\boldsymbol{P})\, d\mathcal{V}(\boldsymbol{R}) \qquad \text{for each } \boldsymbol{P} \in \mathrm{SO}(3); \tag{10.47}$$

see Sects. 3.2 and 3.6. The integral $I(f)$ is bi-invariant if it is both left-invariant and right-invariant.

Since the Riemannian metric on SO(3) is bi-invariant, it follows easily that $I(f)$ is bi-invariant. Indeed, to show that $I(f)$ is left-invariant, let $\widetilde{\boldsymbol{R}} = \boldsymbol{P}^{-1}\boldsymbol{R}$. Then $\boldsymbol{R} = \boldsymbol{P}\widetilde{\boldsymbol{R}}$, and

$$\int_{\mathrm{SO}(3)} f(\boldsymbol{P}^{-1}\boldsymbol{R})\, d\mathcal{V}(\boldsymbol{R}) = \int_{\mathrm{SO}(3)} f(\widetilde{\boldsymbol{R}})\, d\mathcal{V}(\boldsymbol{P}\widetilde{\boldsymbol{R}}) = \int_{\mathrm{SO}(3)} f(\widetilde{\boldsymbol{R}})\, d\mathcal{V}(\widetilde{\boldsymbol{R}}) = I(f). \tag{10.48}$$

That $I(f)$ is also right-invariant can be shown similarly.

10.6.2 On O(3)

Definition 10.2 For $f \in \mathscr{C}(\mathrm{O}(3), \mathbb{C})$, the normalized Haar integral $I(f)$ on O(3) is given by

$$I(f) := \int_{\mathrm{O}(3)} f(\boldsymbol{Q})\, d\mathfrak{g}(\boldsymbol{Q}), \tag{10.49}$$

where $\mathfrak{g}$ denotes the normalized Haar measure on O(3). □

Since O(3) is a compact topological group, the existence and uniqueness of the normalized Haar integral (or equivalently, the normalized Haar measure) on O(3) is guaranteed by the general theory (cf. Sect. C.3). In what follows, we will derive a formula for $I(f)$, namely (10.53), that we shall use later. Before we proceed further, we need to introduce another definition, which first appears in [109] in the context where f is an ODF.

Definition 10.3 Let $f : \mathrm{O}(3) \to \mathbb{C}$. Define $f^{R/L} : \mathrm{SO}(3) \to \mathbb{C}$ by

$$f^R(\boldsymbol{R}) = f(\boldsymbol{R}), \qquad f^L(\boldsymbol{R}) = f(\mathcal{I}\boldsymbol{R}), \qquad \text{for } \boldsymbol{R} \in \mathrm{SO}(3). \tag{10.50}$$

□

Remark 10.4 Clearly f is specified by the pair (f^R, f^L) and vice versa. Type I crystals are enantiomorphic. They can exist in right- and left-handed forms. Polycrystalline aggregates of right-handed and of left-handed crystallites have their ODFs $w = (w^R, 0)$ and $w = (0, w^L)$, respectively. We will discuss further about left-handed and right-handed crystallites in Chap. 12. □

Since $\mathrm{O}(3) = \mathrm{SO}(3) \cup \boldsymbol{\mathcal{I}}\mathrm{SO}(3)$, by (10.49) we have

$$I(f) = \int_{\mathrm{SO}(3)} f(\boldsymbol{Q})\, d\mathsf{g}(\boldsymbol{Q}) + \int_{\boldsymbol{\mathcal{I}}\mathrm{SO}(3)} f(\boldsymbol{Q})\, d\mathsf{g}(\boldsymbol{Q}). \tag{10.51}$$

Let $\varphi_{\boldsymbol{\mathcal{I}}} : \mathrm{SO}(3) \to \boldsymbol{\mathcal{I}}\mathrm{SO}(3)$ be defined by $\varphi_{\boldsymbol{\mathcal{I}}}(\boldsymbol{R}) = \boldsymbol{\mathcal{I}}\boldsymbol{R}$. The function $\varphi_{\boldsymbol{\mathcal{I}}}$ is a bijective isometry and is measure-preserving, and $f^L = f \circ \varphi_{\boldsymbol{\mathcal{I}}}$. In terms of f^R and f^L, we recast $I(f)$ as

$$I(f) = \int_{\mathrm{SO}(3)} f^R(\boldsymbol{R})\, d\mathsf{g}(\boldsymbol{R}) + \int_{\mathrm{SO}(3)} f^L(\boldsymbol{R})\, d\mathsf{g}(\boldsymbol{R}) \tag{10.52}$$

$$= \frac{1}{16\pi^2}\Big(\int_{\mathrm{SO}(3)} f^R(\boldsymbol{R})\, d\mathcal{V}(\boldsymbol{R}) + \int_{\mathrm{SO}(3)} f^L(\boldsymbol{R})\, d\mathcal{V}(\boldsymbol{R})\Big), \tag{10.53}$$

where $\mathcal{V}$ in (10.53) is the bi-invariant volume measure on SO(3) with $\mathcal{V}(\mathrm{SO}(3)) = 8\pi^2$.

For $f : \mathrm{O}(3) \to \mathbb{C}$ and $\boldsymbol{P} \in \mathrm{O}(3)$, let $\mathscr{L}_{\boldsymbol{P}} f$ and $\mathscr{R}_{\boldsymbol{P}} f$ be the functions resulted from f after O(3) undergoes the left translation $L_{\boldsymbol{P}} : \boldsymbol{Q} \mapsto \boldsymbol{P}\boldsymbol{Q}$ and right translation $R_{\boldsymbol{P}} : \boldsymbol{Q} \mapsto \boldsymbol{Q}\boldsymbol{P}$, respectively, i.e.,

$$(\mathscr{L}_{\boldsymbol{P}} f)(\boldsymbol{Q}) = f(\boldsymbol{P}^{-1}\boldsymbol{Q}), \qquad (\mathscr{R}_{\boldsymbol{P}} f)(\boldsymbol{Q}) = f(\boldsymbol{Q}\boldsymbol{P}). \tag{10.54}$$

The integral $I(f)$ is left-invariant and right-invariant if $I(f) = I(\mathscr{L}_{\boldsymbol{P}} f)$ and $I(f) = I(\mathscr{R}_{\boldsymbol{P}} f)$ for each $\boldsymbol{P} \in \mathrm{O}(3)$, respectively.

By the findings in Sect. 10.6.1 and by (10.53), clearly we have

$$I(f) = I(\mathscr{L}_{\boldsymbol{P}} f) \quad \text{and} \quad I(f) = I(\mathscr{R}_{\boldsymbol{P}} f) \qquad \text{for each } \boldsymbol{P} \in \mathrm{SO}(3). \tag{10.55}$$

To prove that $I(f)$ is bi-invariant, it suffices to prove that $I(f) = I((\mathscr{L}_{\boldsymbol{\mathcal{I}}} f))$.

For $f : \mathrm{O}(3) \to \mathbb{C}$, we have

$$(\mathscr{L}_{\boldsymbol{\mathcal{I}}} f)(\boldsymbol{Q}) = f(\boldsymbol{\mathcal{I}}^{-1}\boldsymbol{Q}) = f(\boldsymbol{\mathcal{I}}\boldsymbol{Q}). \tag{10.56}$$

By (10.50), we observe that for each $\boldsymbol{R} \in \mathrm{SO}(3)$,

$$(\mathscr{L}_{\boldsymbol{\mathcal{I}}} f)^R(\boldsymbol{R}) = f(\boldsymbol{\mathcal{I}}\boldsymbol{R}) = f^L(\boldsymbol{R}), \qquad (\mathscr{L}_{\boldsymbol{\mathcal{I}}} f)^L(\boldsymbol{R}) = f(\boldsymbol{\mathcal{I}}^2\boldsymbol{R}) = f^R(\boldsymbol{R}). \tag{10.57}$$

It follows that

$$I(\mathscr{L}_{\boldsymbol{\mathcal{I}}} f) = \frac{1}{16\pi^2}\Big(\int_{\mathrm{SO}(3)} (\mathscr{L}_{\boldsymbol{\mathcal{I}}} f)^R(\boldsymbol{R})\, d\mathcal{V}(\boldsymbol{R}) + \int_{\mathrm{SO}(3)} (\mathscr{L}_{\boldsymbol{\mathcal{I}}} f)^L(\boldsymbol{R})\, d\mathcal{V}(\boldsymbol{R})\Big)$$

$$= \frac{1}{16\pi^2}\Big(\int_{\mathrm{SO}(3)} f^L(\boldsymbol{R})\, d\mathcal{V}(\boldsymbol{R}) + \int_{\mathrm{SO}(3)} f^R(\boldsymbol{R})\, d\mathcal{V}(\boldsymbol{R})\Big) = I(f), \tag{10.58}$$

where we have appealed to (10.57). Hence the integral $I(f)$ is bi-invariant.

Chapter 11

11 Rotations Revisited

11.1 Euler-Rodrigues Parameters

11.1.1 The Quaternions

A skew-field is a set K equipped with two operations called the addition "+" and the multiplication "$\cdot$", respectively, which satisfies what follows:

1. K is an abelian group under addition, with identity denoted as "0".
2. $K \setminus \{0\}$ is a group under multiplication, with identity denoted as "1".
3. For all a, b, and c in K, the distributive laws hold, i.e.,

$$(a+b)\cdot c = a\cdot c + b\cdot c, \quad \text{and} \quad a\cdot(b+c) = a\cdot c + a\cdot c.$$

A field is a skew-field with commutative multiplication.

Let $\mathbb{R}$ be the set of real numbers. We will introduce a rule of multiplication in $\mathbb{R}^4$ so that under this operation of multiplication and component-wise addition it becomes a skew-field $\mathbb{H}$ whose elements are called the quaternions. We assign special symbols to the following elements of $\mathbb{H}$:

$$0 = (0,0,0,0), \qquad 1 = (1,0,0,0),$$
$$i = (0,1,0,0), \qquad j = (0,0,1,0), \qquad k = (0,0,0,1),$$

and denote its generic elements by roman letters such as

$$x = (x_0, x_1, x_2, x_3), \qquad y = (y_0, y_1, y_2, y_3),$$

etc. In $\mathbb{H}$, the operation of addition "+" is defined component-wise:

$$(x_0, x_1, x_2, x_3) + (y_0, y_1, y_2, y_3) = (x_0 + y_0, x_1 + y_1, x_2 + y_2, x_3 + y_3),$$

while the operation of multiplication "$\cdot$" is defined by the rules

$$1\cdot 1 = 1, \quad 1\cdot i = i\cdot 1 = i, \quad 1\cdot j = j\cdot 1 = j, \quad 1\cdot k = k\cdot 1 = k,$$
$$i\cdot i = j\cdot j = k\cdot k = -1,$$
$$i\cdot j = k, \quad j\cdot k = i, \quad k\cdot i = j,$$
$$j\cdot i = -k, \quad k\cdot j = -i, \quad i\cdot k = -j,$$

and by the distributive laws

$$x\cdot(y+z) = x\cdot y + x\cdot z, \quad (y+z)\cdot x = y\cdot x + z\cdot x.$$

Thus, we have

$$x\cdot y = (x_0y_0 - x_1y_1 - x_2y_2 - x_3y_3, x_0y_1 + x_1y_0 + x_2y_3 - x_3y_2, x_0y_2 + x_2y_0 + x_3y_1 - x_1y_3,$$
$$x_0y_3 + x_3y_0 + x_1y_2 - x_2y_1). \tag{11.1}$$

Henceforth, whenever no confusion should arise, we shall suppress the "$\cdot$" and write xy for $x \cdot y$, x^2 for $x \cdot x$, etc.

Each quaternion x can be written as a sum:

$$x = x_0 + \boldsymbol{x},$$

where

$$x_0 = (x_0, 0, 0, 0) \qquad \text{and} \qquad \boldsymbol{x} = (0, x_1, x_2, x_3)$$

are called the scalar and vector part of x, respectively. The reader may have already noticed that we use the same symbol x_0 to denote (i) the real number defining the scalar part of a quaternion x and (ii) the quaternion with its scalar part defined by x_0 and vector part zero. Following usual practice, we shall also use the same symbol $\boldsymbol{x}$ to denote (i) the 3-vector $\boldsymbol{x} = (x_1, x_2, x_3)$ defining the vector part of a quaternion x and (ii) the quaternion with its vector part defined by $\boldsymbol{x}$ and scalar part zero. Under this notation, the product of two quaternions can be recast as

$$xy = x_0 y_0 - \boldsymbol{x} \cdot \boldsymbol{y} + x_0 \boldsymbol{y} + y_0 \boldsymbol{x} + \boldsymbol{x} \times \boldsymbol{y}, \tag{11.2}$$

where $\boldsymbol{x} \cdot \boldsymbol{y}$ and $\boldsymbol{x} \times \boldsymbol{y}$ are, respectively, the usual scalar product and cross product of vectors in $\mathbb{R}^3$. Quaternions with their scalar part zero, e.g., i, j, k, are sometimes called "pure quaternions". Under our present notation, for pure quaternions we have $x = \boldsymbol{x}$. Thus, $i = \boldsymbol{i}$, $j = \boldsymbol{j}$, and $k = \boldsymbol{k}$.

It follows from (11.2) that

$$xy - yx = 2\boldsymbol{x} \times \boldsymbol{y}. \tag{11.3}$$

Thus the product of two quaternions x and y is not commutative unless $\boldsymbol{x} \times \boldsymbol{y} = \boldsymbol{0}$ (i.e., $\boldsymbol{x} = \boldsymbol{0}$ or $\boldsymbol{y} = \boldsymbol{0}$ or $\boldsymbol{x} \parallel \boldsymbol{y}$).

Given $x = x_0 + x_1 i + x_2 j + x_3 k \in \mathbb{H}$, the quaternion

$$\overline{x} = x_0 - x_1 i - x_2 j - x_3 k \tag{11.4}$$

is called the conjugate of x, and the non-negative real number

$$|x| = \sqrt{x_0^2 + x_1^2 + x_2^2 + x_3^2} \tag{11.5}$$

is called the norm of x. It follows immediately from definitions (11.4) and (11.5) that

$$\overline{(\overline{x})} = x, \qquad |x| = |\overline{x}|. \tag{11.6}$$

Proposition 11.1 *Let $x, y \in \mathbb{H}$. The following identities are valid*:

$$x\overline{x} = \overline{x}x = |x|^2, \qquad \overline{xy} = \overline{y}\,\overline{x}, \qquad |xy| = |x||y|. \tag{11.7}$$

Proof From (11.3) we observe that $x\overline{x} - \overline{x}x = -2\boldsymbol{x} \times \boldsymbol{x} = 0$. That $x\overline{x} = |x|^2$ follows easily by substituting $\overline{x}$ for y in (11.2). By (11.2) and (11.4) we have

$$\begin{aligned} \overline{y}\,\overline{x} &= y_0 x_0 - (-\boldsymbol{y}) \cdot (-\boldsymbol{x}) + y_0(-\boldsymbol{x}) + x_0(-\boldsymbol{y}) + (-\boldsymbol{y}) \times (-\boldsymbol{x}) \\ &= x_0 y_0 - \boldsymbol{x} \cdot \boldsymbol{y} - x_0 \boldsymbol{y} - y_0 \boldsymbol{x} - \boldsymbol{x} \times \boldsymbol{y} = \overline{xy}. \end{aligned}$$

Finally, by appealing to $(11.7)_1$ and $(11.7)_2$, we get

$$|xy|^2 = xy\overline{xy} = xy\overline{y}\,\overline{x} = x|y|^2\overline{x} = |x|^2|y|^2. \qquad \square$$

Note that $\mathbb{H}$ is an abelian group under addition, with 0 being the additive identity, and $\mathbb{H} \setminus \{0\}$ is a (non-commutative) group under multiplication, with 1 being the multiplicative identity and

$$x^{-1} = \frac{\overline{x}}{|x|^2} \tag{11.8}$$

being the multiplicative inverse of $x \neq 0$. Hence $\mathbb{H}$ is a skew-field.

If we identify the reals $\mathbb{R}$ with $\{(x_0, 0, 0, 0) \in \mathbb{H} : x_0 \in \mathbb{R}\}$ and the complex numbers $\mathbb{C}$ with $\{(x_0, x_1, 0, 0)\} \in \mathbb{H} : x_0, x_1 \in \mathbb{R}\}$, then we have

$$\mathbb{R} \subset \mathbb{C} \subset \mathbb{H}.$$

In closing this subsection, we prove a lemma for later use.

Lemma 11.2 *If $q \in \mathbb{H}$ commutes with every pure quaternion $\boldsymbol{x}$, then its vector part $\boldsymbol{q} = \boldsymbol{0}$.*

Proof By hypothesis, $q = q_0 + \boldsymbol{q}$ commutes with $\boldsymbol{i}$, $\boldsymbol{j}$, and $\boldsymbol{k}$, respectively. If follows then from (11.3) that

$$\boldsymbol{q} \times \boldsymbol{i} = \boldsymbol{q} \times \boldsymbol{j} = \boldsymbol{q} \times \boldsymbol{k} = \boldsymbol{0}.$$

Hence $\boldsymbol{q} = \boldsymbol{0}$. $\square$

11.1.2 Rotations and the Symplectic Group Sp(1)

Let $\mathrm{Sp}(1) = \{x \in \mathbb{H} : |x| = 1\}$ be the set of quaternions with unit norm. We identify $\mathbb{R}^4$ with the skew-field of quaternions $\mathbb{H}$ by the mapping $(x_0, x_1, x_2, x_3) \mapsto x_0 + x_1 i + x_2 j + x_3 k$. As a subset of $\mathbb{R}^4$, Sp(1) is nothing but $\mathcal{S}^3$, the 3-dimensional unit sphere. We endow Sp(1) with the topology defined through the identification between Sp(1) and $\mathcal{S}^3$ (as a subspace of $\mathbb{R}^4$). By $(11.7)_3$, we observe that

$$x \in \mathrm{Sp}(1) \text{ and } y \in \mathrm{Sp}(1) \Longrightarrow xy \in \mathrm{Sp}(1).$$

Moreover, by $(11.6)_2$ and (11.8), we have

$$x \in \mathrm{Sp}(1) \Longrightarrow x^{-1} \in \mathrm{Sp}(1).$$

Therefore Sp(1) is a subgroup of the multiplicative group of quaternions. It is called the symplectic group of order 1.

Let $q \in \mathrm{Sp}(1)$ and let $\boldsymbol{x}$ be a pure quaternion. Using (11.2) we deduce by direct computations that

$$\begin{aligned} q\boldsymbol{x}\overline{q} &= (q_0 + \boldsymbol{q})(0 + \boldsymbol{x})(q_0 - \boldsymbol{q}) \\ &= (q_0^2 - |\boldsymbol{q}|^2)\boldsymbol{x} + 2(\boldsymbol{q} \cdot \boldsymbol{x})\boldsymbol{q} + 2q_0(\boldsymbol{q} \times \boldsymbol{x}) \\ &= (2q_0^2 - 1)\boldsymbol{x} + 2(\boldsymbol{q} \cdot \boldsymbol{x})\boldsymbol{q} + 2q_0(\boldsymbol{q} \times \boldsymbol{x}), \end{aligned} \tag{11.9}$$

where we have made use of the vector identity

$$(\boldsymbol{q} \times \boldsymbol{x}) \times \boldsymbol{q} = (\boldsymbol{q} \cdot \boldsymbol{q})\boldsymbol{x} - (\boldsymbol{q} \cdot \boldsymbol{x})\boldsymbol{q}.$$

If we interpret the pure quaternions $\boldsymbol{q}$ and $\boldsymbol{x}$ as 3-vectors and q_0 as a real number, then the right-hand side of (11.9) defines a 3-vector. Under this interpretation of $q\boldsymbol{x}\overline{q}$, the function $\boldsymbol{R}_q : \boldsymbol{x} \mapsto q\boldsymbol{x}\overline{q}$ is a mapping from $\mathbb{R}^3$ to $\mathbb{R}^3$. Moreover, a glance at (11.9) reveals that $\boldsymbol{R}_q$ is a linear transformation. Under the standard basis $\boldsymbol{i}$, $\boldsymbol{j}$ and $\boldsymbol{k}$, $\boldsymbol{R}_q$ is represented by the matrix

$$(2q_0^2 - 1)\begin{pmatrix} 1 & 0 & 0 \\ 0 & 1 & 0 \\ 0 & 0 & 1 \end{pmatrix} + 2\begin{pmatrix} q_1^2 & q_1q_2 & q_1q_3 \\ q_2q_1 & q_2^2 & q_2q_3 \\ q_3q_1 & q_3q_2 & q_3^2 \end{pmatrix} + 2q_0\begin{pmatrix} 0 & -q_3 & q_2 \\ q_3 & 0 & -q_1 \\ -q_2 & q_1 & 0 \end{pmatrix},$$

or

$$\boldsymbol{R}_q = \begin{pmatrix} 2q_0^2 - 1 + 2q_1^2 & 2q_1q_2 - 2q_0q_3 & 2q_1q_3 + 2q_0q_2 \\ 2q_1q_2 + 2q_0q_3 & 2q_0^2 - 1 + 2q_2^2 & 2q_2q_3 - 2q_0q_1 \\ 2q_1q_3 - 2q_0q_2 & 2q_2q_3 + 2q_0q_1 & 2q_0^2 - 1 + 2q_3^2 \end{pmatrix}. \tag{11.10}$$

It is clear from the preceding formula that $\boldsymbol{R}_q = \boldsymbol{R}_{-q}$. Note that for each $q \in \mathrm{Sp}(1)$

$$\boldsymbol{R}_q\boldsymbol{x} = q\boldsymbol{x}\overline{q} \qquad \text{for each } \boldsymbol{x} \in \mathbb{R}^3, \tag{11.11}$$

where we have identified pure quaternions with 3-vectors in $\mathbb{R}^3$.

We claim that $\boldsymbol{R}_q$ is a rotation on $\mathbb{R}^3$ for each $q \in \mathrm{Sp}(1)$. Indeed, for each $\boldsymbol{x} \in \mathbb{R}^3$ we have

$$\|\boldsymbol{R}_q\boldsymbol{x}\| = |q\boldsymbol{x}\overline{q}| = |q||\boldsymbol{x}||\overline{q}| = |\boldsymbol{x}| = \|\boldsymbol{x}\|,$$

where we have appealed to $(11.7)_3$. It follows that for $\boldsymbol{x}, \boldsymbol{y} \in \mathbb{R}^3$,

$$\begin{aligned} \langle \boldsymbol{R}_q\boldsymbol{x}, \boldsymbol{R}_q\boldsymbol{y} \rangle &= \frac{1}{4}(\|\boldsymbol{R}_q\boldsymbol{x} + \boldsymbol{R}_q\boldsymbol{y}\|^2 - \|\boldsymbol{R}_q\boldsymbol{x} - \boldsymbol{R}_q\boldsymbol{y}\|^2) \\ &= \frac{1}{4}(\|\boldsymbol{x} + \boldsymbol{y}\|^2 - \|\boldsymbol{x} - \boldsymbol{y}\|^2) \\ &= \langle \boldsymbol{x}, \boldsymbol{y} \rangle. \end{aligned}$$

Therefore $\boldsymbol{R}_q$ is orthogonal, and $\det \boldsymbol{R}_q = \pm 1$. From formula (11.10) we observe that the mapping $q \mapsto \det \boldsymbol{R}_q$ from $\mathrm{Sp}(1)$ (or $\mathcal{S}^3$) to $\mathbb{R}$ is continuous. For $q = 1$, $\boldsymbol{R}_q = \boldsymbol{I}$ and $\det \boldsymbol{R}_q = 1$. Since $\mathrm{Sp}(1)$ is connected, we have $\det \boldsymbol{R}_q = 1$ for all $q \in \mathrm{Sp}(1)$.

Let $\mathrm{Ad} : \mathrm{Sp}(1) \to \mathrm{SO}(3)$ be defined by

$$\mathrm{Ad}(q) = \boldsymbol{R}_q. \tag{11.12}$$

We claim that the function Ad is a homomorphism. Indeed, for any $\boldsymbol{x} \in \mathbb{R}^3$ and $q^{(1)}, q^{(2)} \in \mathbb{H}$, we have

$$\begin{aligned} \mathrm{Ad}(q^{(1)}q^{(2)})\boldsymbol{x} = \boldsymbol{R}_{q^{(1)}q^{(2)}}\boldsymbol{x} &= q^{(1)}q^{(2)}\boldsymbol{x}\overline{q^{(1)}q^{(2)}} = q^{(1)}\left(q^{(2)}\boldsymbol{x}\overline{q^{(2)}}\right)\overline{q^{(1)}} = q^{(1)}\left(\boldsymbol{R}_{q^{(2)}}\boldsymbol{x}\right)\overline{q^{(1)}} \\ &= \boldsymbol{R}_{q^{(1)}}\boldsymbol{R}_{q^{(2)}}\boldsymbol{x}, \end{aligned}$$

and thence

$$\mathrm{Ad}(q^{(1)}q^{(2)}) = \mathrm{Ad}(q^{(1)})\mathrm{Ad}(q^{(2)}). \tag{11.13}$$

The homomorphism Ad, as defined by (11.12), is called the adjoint action or adjoint representation of the group Sp(1). The following proposition characterizes the kernel of the homomorphism Ad.

Proposition 11.3 $\mathrm{Ker}(\mathrm{Ad}) = \{1, -1\}$.

Proof Let $q \in \mathrm{Ker}(\mathrm{Ad})$, i.e., $\mathrm{Ad}(q) = \boldsymbol{I}$. Then for each pure quaternion $\boldsymbol{x}$, by (11.11) we have

$$\boldsymbol{R}_q\boldsymbol{x} = \boldsymbol{I}\boldsymbol{x} = \boldsymbol{x} = q\boldsymbol{x}\overline{q}.$$

Thus q commutes with every pure quaternion $\boldsymbol{x}$. By Lemma 11.2, we conclude that $\boldsymbol{q}$, the vector part of q, is zero. Since $q_0^2 + \boldsymbol{q}\cdot\boldsymbol{q} = 1$, we conclude that $q = (\pm 1, 0, 0, 0)$. □

For each $q \in \mathrm{Sp}(1)$, $q_0^2 + |\boldsymbol{q}|^2 = 1$. Since $-1 \le q_0 \le 1$, we may, without loss of generality, put $q_0 = \cos\theta$ for some $0 \le \theta \le \pi$. Then $|\boldsymbol{q}| = \sin\theta$. Thus every quaternion $q \neq \pm 1$ in Sp(1) can be put in the form

$$q = \cos\theta + \sin\theta\boldsymbol{n}, \qquad \text{for some} \quad \theta \in (0, \pi) \tag{11.14}$$

where

$$\boldsymbol{n} = \frac{\boldsymbol{q}}{\|\boldsymbol{q}\|}$$

is the direction of $\boldsymbol{q}$. Substituting (11.14) into (11.9) leads to the formula

$$\boldsymbol{R}_q\boldsymbol{x} = (\cos 2\theta)\boldsymbol{x} + (1 - \cos 2\theta)(\boldsymbol{n}\otimes\boldsymbol{n})\boldsymbol{x} + (\sin 2\theta)\boldsymbol{n}\times\boldsymbol{x}. \tag{11.15}$$

A comparison of the preceding equation with the Rodrigues rotation formula (1.107) reveals that for $q \neq \pm 1 \in \mathrm{Sp}(1)$ with $q_0 = \cos\theta$, $\boldsymbol{R}_q$ is the rotation of angle 2θ about the axis defined by $\boldsymbol{n} = \boldsymbol{q}/\|\boldsymbol{q}\|$, i.e., $\boldsymbol{R}_{\cos\theta+\sin\theta\boldsymbol{n}} = \boldsymbol{R}(\boldsymbol{n}, 2\theta)$. Conversely, given $\boldsymbol{R}(\boldsymbol{n}, \omega) \neq \boldsymbol{I}$, define the unit quaternion $q = \cos\frac{\omega}{2} + \sin\frac{\omega}{2}\boldsymbol{n}$; then $\boldsymbol{R}(\boldsymbol{n}, \omega) = \boldsymbol{R}_q$. Earlier we have already mentioned that for $q = 1$, $\boldsymbol{R}_q = \boldsymbol{I}$. Thus we have proved the following proposition.

Proposition 11.4 *The homomorphism* $\mathrm{Ad} : \mathrm{Sp}(1) \to \mathrm{SO}(3)$ *is surjective.* □

Gathering what we have learned about the homomorphism Ad, we conclude from general theorems in group theory that Ker(Ad) is a normal subgroup of Sp(1)—an obvious fact for the present case as $\mathrm{Ker}(\mathrm{Ad}) = \{1, -1\}$, and the quotient group $\mathrm{Sp}(1)/\{\pm 1\}$ is isomorphic to SO(3). Under the adjoint action Ad, two diametrically opposite points in $\mathcal{S}^3$ are mapped to the same rotation in SO(3), a fact which we have alluded to earlier when we mention $\boldsymbol{R}_q = \boldsymbol{R}_{-q}$. We shall say more on this double covering of SO(3) by Sp(1) later in this exposition.

Definition 11.5 We call the pair $(q_0, \boldsymbol{q})$, where

$$q_0 = \cos\frac{\omega}{2}, \qquad \boldsymbol{q} = \sin\frac{\omega}{2}\boldsymbol{n} \qquad (0 \le \omega \le \pi), \tag{11.16}$$

the Euler-Rodrigues parameters of the rotation $\boldsymbol{R}(\boldsymbol{n}, \omega)$. □

Note that formula (11.16) applies also to the identity $\boldsymbol{I}$, which has $\omega = 0$ and Euler-Rodrigues parameters $(q_0, \boldsymbol{q}) = (1, \boldsymbol{0})$. Under the Euler-Rodrigues parameters, rotations are written $\boldsymbol{R}(q_0, \boldsymbol{q})$, where $q_0 \in \mathbb{R}$, $\boldsymbol{q} \in \mathbb{R}^3$, and $q_0^2 + |\boldsymbol{q}|^2 = 1$.

For two quaternions $q^{(1)}, q^{(2)}$ in Sp(1), and $\boldsymbol{x} \in \mathbb{R}^3$, we have

$$\begin{aligned} \boldsymbol{R}(q_0^{(2)}, \boldsymbol{q}^{(2)})\boldsymbol{R}(q_0^{(1)}, \boldsymbol{q}^{(1)})\boldsymbol{x} &= q^{(2)}q^{(1)}\boldsymbol{x}\overline{q^{(1)}}\,\overline{q^{(2)}} \\ &= q^{(2)}q^{(1)}\boldsymbol{x}\overline{q^{(2)}q^{(1)}} \\ &= \boldsymbol{R}(q_0^{(3)}, \boldsymbol{q}^{(3)})\boldsymbol{x}, \end{aligned} \tag{11.17}$$

$$q_0^{(3)} = q_0^{(2)}q_0^{(1)} - \boldsymbol{q}^{(2)} \cdot \boldsymbol{q}^{(1)}, \qquad \boldsymbol{q}^{(3)} = q_0^{(2)}\boldsymbol{q}^{(1)} + q_0^{(1)}\boldsymbol{q}^{(2)} + \boldsymbol{q}^{(2)} \times \boldsymbol{q}^{(1)}. \tag{11.18}$$

The preceding simple formula delivers in closed form the Euler-Rodrigues parameters of the product of two given rotations. In particular, using (11.16), we may recast $(11.18)_1$ as

$$\cos\frac{\omega_3}{2} = \cos\frac{\omega_2}{2}\cos\frac{\omega_1}{2} - \sin\frac{\omega_2}{2}\sin\frac{\omega_1}{2}(\boldsymbol{n}_2 \cdot \boldsymbol{n}_1). \tag{11.19}$$

11.2 More on Sp(1)

11.2.1 Sp(1) as a Differentiable Manifold and a Lie Group

Geometrically we identify $\mathrm{Sp}(1) = \{x \in \mathbb{H} : |x| = 1\}$ with $\mathcal{S}^3$, the unit sphere in $\mathbb{R}^4$. As an embedded submanifold of $\mathbb{R}^4$, the differentiable structure of $\mathcal{S}^3$ is defined by the atlas $\{(U_i^{\pm}, \varphi_i) : i = 0, 1, 2, 3\}$, where

$$U_i^+ = \{(x_0, x_1, x_2, x_3) \in S^3 : x_i > 0\}, \quad U_i^- = \{(x_0, x_1, x_2, x_3) \in \mathcal{S}^3 : x_i < 0\},$$

and $\varphi_i^{\pm}$ is the projection of $U_i^{\pm}$ to the hyperplane $x_i = 0$.

For later use we give $\mathcal{S}^3$ or Sp(1) a differentiable structure with an atlas containing two charts defined through stereographic projections.

Let us call $(1, \boldsymbol{0})$ and $(-1, \boldsymbol{0})$ the "north pole" and the "south pole" of Sp(1) or $\mathcal{S}^3$, respectively. Let $U_N = \mathcal{S}^3 \setminus \{(1, \boldsymbol{0})\}$ and $U_S = \mathcal{S}^3 \setminus \{(-1, \boldsymbol{0})\}$. We define a chart $\varphi_N : U_N \to \mathbb{R}^3$ through stereographic projection from the north pole as follows. For each point $x \in U_N \subset \mathcal{S}^3$, we draw a straight line that passes through the north pole $(1, \boldsymbol{0})$ and x, and we define $\varphi_N(x)$ to be the point where this straight line meets the "equatorial (hyper)plane" $\{(0, \boldsymbol{w}) : \boldsymbol{w} \in \mathbb{R}^3\}$. The mapping φ_N is clearly a bijection. Let $\boldsymbol{y} = \varphi_N(x)$, where $x = (x_0, \boldsymbol{x}) \in U_N$. The straight line connecting $(1, \boldsymbol{0})$ to $(0, \boldsymbol{y})$ is specified parametrically by the equation

$$q(t) = t(0, \boldsymbol{y}) + (1 - t)(1, \boldsymbol{0}) = (1 - t, t\,\boldsymbol{y}), \qquad \text{where} \quad -\infty < t < \infty.$$

This straight line meets the unit sphere $\mathcal{S}^3$ at those t for which $|q(t)| = 1$, i.e., at $t = 0$ and $t = 2/(\|\boldsymbol{y}\|^2 + 1)$. When $t = 0$, $q(0)$ is none other than the north pole. When $t = 2/(\|\boldsymbol{y}\|^2 + 1)$, q is $\varphi_N^{-1}(\boldsymbol{y}) = x$. Some simple calculations lead to the formula

$$x = \varphi_N^{-1}(\boldsymbol{y}) = \frac{(\|\boldsymbol{y}\|^2 - 1, 2y_1, 2y_2, 2y_3)}{\|\boldsymbol{y}\|^2 + 1}. \tag{11.20}$$

Conversely, given x, by solving the preceding equation for $\boldsymbol{y}$, we obtain

$$\boldsymbol{y} = \varphi_N(x) = \frac{\boldsymbol{x}}{1 - x_0}. \tag{11.21}$$

Similarly, we define the chart $\varphi_S : U_S \to \mathbb{R}^3$ through stereographic projection from the south pole. For $x \in U_S$, let $\varphi_S(x) = \boldsymbol{z}$. We have

$$x = \varphi_S^{-1}(\boldsymbol{z}) = \frac{(1 - \|\boldsymbol{z}\|^2, 2z_1, 2z_2, 2z_3)}{\|\boldsymbol{z}\|^2 + 1}, \tag{11.22}$$

$$\boldsymbol{z} = \varphi_S(x) = \frac{\boldsymbol{x}}{1 + x_0}. \tag{11.23}$$

From (11.20)–(11.23), we see that the transition maps $\varphi_S \circ \varphi_N^{-1} : \mathbb{R}^3 \setminus \{\mathbf{0}\} \to \mathbb{R}^3 \setminus \{\mathbf{0}\}$ and $\varphi_N \circ \varphi_S^{-1} : \mathbb{R}^3 \setminus \{\mathbf{0}\} \to \mathbb{R}^3 \setminus \{\mathbf{0}\}$ are given by the formula

$$\boldsymbol{z} = \varphi_S \circ \varphi_N^{-1}(\boldsymbol{y}) = \frac{\boldsymbol{y}}{\|\boldsymbol{y}\|^2}, \tag{11.24}$$

and

$$\boldsymbol{y} = \varphi_N \circ \varphi_S^{-1}(\boldsymbol{z}) = \frac{\boldsymbol{z}}{\|\boldsymbol{z}\|^2}, \tag{11.25}$$

respectively, and they are C^∞ diffeomorphisms. Hence the atlas $\{(U_N, \varphi_N), (U_S, \varphi_S)\}$ defines a C^∞ differentiable structure on Sp(1). It can easily be shown that the differentiable structure defined by this atlas is the same as that of $\mathcal{S}^3$ as an embedded submanifold of $\mathbb{R}^4$.

Now let us introduce "polar coordinates" on $\mathcal{S}^3$. For any $x = (x_0, x_1, x_2, x_3) \in \mathcal{S}^3$, since $x_0^2 + x_1^2 + x_2^2 + x_3^2 = 1$, we have $-1 \le x_0 \le 1$. Hence there exists a unique real number $\theta_1 \in [0, \pi]$ such that $x_0 = \cos\theta_1$. Then (x_1, x_2, x_3) satisfies

$$x_1^2 + x_2^2 + x_3^2 = \sin^2\theta_1.$$

In other words, (x_1, x_2, x_3) is a point on the 2-dimensional sphere of radius $\sin\theta_1$. Introducing the usual "spherical coordinates" on this 2-dimensional sphere, we have

$$\begin{aligned} x_0 &= \cos\theta_1, \\ x_1 &= \sin\theta_1 \cos\theta_2, \\ x_2 &= \sin\theta_1 \sin\theta_2 \cos\theta_3, \\ x_3 &= \sin\theta_1 \sin\theta_2 \sin\theta_3, \end{aligned} \tag{11.26}$$

where $0 \le \theta_2 \le \pi$ and $0 \le \theta_3 < 2\pi$. The polar coordinates $(\theta_1, \theta_2, \theta_3)$ are local coordinates on $\mathcal{S}^3$. They are not defined for all points of $\mathcal{S}^3$. Indeed θ_2 and θ_3 are not defined when $\theta_1 = 0$ or π; θ_3 is not defined when $\theta_2 = 0$ or π. A moment's examination reveals that the polar coordinates $(\theta_1, \theta_2, \theta_3)$ are well defined on the domain $U_p = \mathcal{S}^3 \setminus \{(x_0, x_1, 0, 0) : x_0^2 + x_1^2 = 1\}$. The singular set may also be written as $\{(\cos\theta_1, \pm\sin\theta_1, 0, 0) : 0 \le \theta_1 \le \pi\}$. We use (11.26) to define a chart (U_p, φ_p), where $\varphi_p : U_p \to \mathbb{R}^3$. Let $D_p = \{(\theta_1, \theta_2, \theta_3) : 0 < \theta_1 < \pi, 0 < \theta_2 < \pi, 0 \le \theta_3 < 2\pi\}$ and $X_1 = \{(x_1, 0, 0) : x_1 \in \mathbb{R}\}$. It is easy to see that $U_p \subset U_N$, $U_p \subset U_S$, $\varphi_N(U_p) = \varphi_S(U_p) = \mathbb{R}^3 \setminus X_1$, and $\varphi_N \circ \varphi_p^{-1} : D_p \to \mathbb{R}^3 \setminus X_1$, $\varphi_S \circ \varphi_p^{-1} : D_p \to \mathbb{R}^3 \setminus X_1$ are C^∞ diffeomorphisms. Hence the chart (U_p, φ_p) is compatible with the differentiable structure of $\mathcal{S}^3$ or Sp(1).

By formula (11.1) for the product of two quaternions, we see that the group operation $\mathrm{Sp}(1) \times \mathrm{Sp}(1) \to \mathrm{Sp}(1)$, $(x, y) \mapsto xy$ is of class C^∞ or smooth. For $x = (x_0, \boldsymbol{x})$ in Sp(1), we have $x^{-1} = \overline{x} = (x_0, -\boldsymbol{x})$. Thus the group operation $x \mapsto x^{-1}$ is also smooth. Hence Sp(1) is a Lie group.

For a given $q \in \mathrm{Sp}(1)$, the right translation $\mathcal{T}_q^r$ and left translation $\mathcal{T}_q^l$ on $\mathrm{Sp}(1)$ are defined by $\mathcal{T}_q^r(x) = xq$ and $\mathcal{T}_q^l(x) = qx$ for each $x \in \mathrm{Sp}(1)$, respectively. Clearly $\mathcal{T}_q^r$ and $\mathcal{T}_q^l$ are C^∞ diffeomorphisms on $\mathrm{Sp}(1)$.

11.2.2 Sp(1) as a Riemannian Manifold with a Bi-invariant Metric

The unit sphere $\mathcal{S}^3$ is a submanifold in $\mathbb{R}^4$. For each $x \in \mathcal{S}^3$, the tangent space to $\mathcal{S}^3$ at x, which we denote by $T_x\mathcal{S}^3$, is a linear subspace of $T_x\mathbb{R}^4$, the tangent space to $\mathbb{R}^4$ at x. Now, $\mathbb{R}^4$ is a Euclidean space with the inner product

$$\langle x, y\rangle = x_0y_0 + x_1y_1 + x_2y_2 + x_3y_3. \tag{11.27}$$

For every $x \in \mathbb{R}^4$, we identify $T_x\mathbb{R}^4$ with $\mathbb{R}^4$ and give it the same inner product (11.27). As a linear subspace of $T_x\mathbb{R}^4$, $T_x\mathcal{S}^3$ inherits an inner product from $T_x\mathbb{R}^4$. After we endow the tangent spaces $T_x\mathcal{S}^3$ at $x \in \mathcal{S}^3$ with the corresponding inner product inherited from $T_x\mathbb{R}^4$, we have defined a second-order, symmetric and positive definite, covariant tensor field $\boldsymbol{g}(\cdot)$ on $\mathcal{S}^3$. We call $\boldsymbol{g}$ the metric tensor. Since the embedding of $\mathcal{S}^3$ into $\mathbb{R}^4$ is smooth, $\boldsymbol{g}(\cdot)$ is a smooth tensor function on $\mathcal{S}^3$. The pair $(\mathcal{S}^3, \boldsymbol{g})$ is then a Riemannian manifold.

In what follows we shall use bold-faced roman letters such as $\mathbf{u}, \mathbf{v}, \mathbf{E}$, etc. to denote 4-vectors which lie in some given tangent space $T_x\mathcal{S}^3$ of $\mathcal{S}^3$.

It is straightforward to derive explicit formulas for the components g_{ij} of the metric tensor $\boldsymbol{g}$ under specific coordinate charts. For illustration, let us write down the formulas for g_{ij} under the polar coordinates $(\theta_1, \theta_2, \theta_3)$. For $x \in U_p$, the vectors

$$\mathbf{E}_i = \frac{\partial x}{\partial \theta_i} = \left(\frac{\partial x_0}{\partial \theta_i}, \frac{\partial x_1}{\partial \theta_i}, \frac{\partial x_2}{\partial \theta_i}, \frac{\partial x_3}{\partial \theta_i}\right) \qquad (i = 1, 2, 3) \tag{11.28}$$

are linearly independent in $T_x\mathcal{S}^3$. For two tangent vectors $\mathbf{u}, \mathbf{v} \in T_x\mathcal{S}^3$, we have

$$\mathbf{u} = u_1\mathbf{E}_1 + u_2\mathbf{E}_2 + u_3\mathbf{E}_3,$$
$$\mathbf{v} = v_1\mathbf{E}_1 + v_2\mathbf{E}_2 + v_3\mathbf{E}_3.$$

It follows that

$$\langle \mathbf{u}, \mathbf{v}\rangle = \sum_{i,j=1}^{3} g_{ij}u_iv_j, \tag{11.29}$$

where

$$g_{ij} = \langle \mathbf{E}_i, \mathbf{E}_j\rangle \tag{11.30}$$

are the components of the metric tensor $\boldsymbol{g}$ under the polar coordinates $(\theta_1, \theta_2, \theta_3)$. Explicitly, we have

$$\mathbf{E}_1 = (-\sin\theta_1, \cos\theta_1\cos\theta_2, \cos\theta_1\sin\theta_2\cos\theta_3, \cos\theta_1\sin\theta_2\sin\theta_3),$$
$$\mathbf{E}_2 = (0, -\sin\theta_1\sin\theta_2, \sin\theta_1\cos\theta_2\cos\theta_3, \sin\theta_1\cos\theta_2\sin\theta_3),$$
$$\mathbf{E}_3 = (0, 0, -\sin\theta_1\sin\theta_2\sin\theta_3, \sin\theta_1\sin\theta_2\cos\theta_3),$$

and

$$g_{11} = \mathbf{E}_1 \cdot \mathbf{E}_1 = 1, \quad g_{12} = \mathbf{E}_1 \cdot \mathbf{E}_2 = 0, \quad g_{13} = \mathbf{E}_1 \cdot \mathbf{E}_3 = 0,$$
$$g_{22} = \mathbf{E}_2 \cdot \mathbf{E}_2 = \sin^2\theta_1, \quad g_{23} = \mathbf{E}_2 \cdot \mathbf{E}_3 = 0, \quad g_{33} = \mathbf{E}_3 \cdot \mathbf{E}_3 = \sin^2\theta_1 \sin^2\theta_2.$$

As expected, it is clear from these formulas that the metric tensor $\boldsymbol{g}$ is smooth on the domain U_p of the coordinate chart in question. It is customary to denote

$$g = \det \boldsymbol{g}. \tag{11.31}$$

From the formulas above, we obtain

$$g = \sin^4\theta_1 \sin^2\theta_2 \tag{11.32}$$

under the polar coordinates $(\theta_1, \theta_2, \theta_3)$. Hence the volume element on Sp(1) is

$$\sqrt{\det \boldsymbol{g}} = \sin^2\theta_1 \sin\theta_2, \tag{11.33}$$

and the volume of Sp(1) is

$$V(\mathrm{Sp}(1)) = \int_0^{2\pi}\int_0^{\pi}\int_0^{\pi} \sin^2\theta_1 \sin\theta_2 d\theta_1 d\theta_2 d\theta_3 = 2\pi^2. \tag{11.34}$$

From formula (11.1) for the product of two quaternions, we observe that for a given $q = (q_0, q_1, q_2, q_3) \in \mathbb{H}$, the mapping $x \mapsto qx$ from $\mathbb{H}$ to $\mathbb{H}$ can be looked upon as a linear transformation on $\mathbb{H}$. Indeed, we may write

$$qx = \begin{pmatrix} q_0 & -q_1 & -q_2 & -q_3 \\ q_1 & q_0 & -q_3 & q_2 \\ q_2 & q_3 & q_0 & -q_1 \\ q_3 & -q_2 & q_1 & q_0 \end{pmatrix} \begin{pmatrix} x_0 \\ x_1 \\ x_2 \\ x_3 \end{pmatrix}. \tag{11.35}$$

Let us denote the 4×4 matrix in (11.35) by R_q^l. Note that for $q \in \mathrm{Sp}(1)$, R_q^l is orthogonal and thus $\det R_q^l = \pm 1$. Since the mapping $q \mapsto \det R_q^l$ from Sp(1) to $\mathbb{R}$ is continuous and $\det R_q^l = 1$ when $q = (1, 0, 0, 0)$, we have $\det R_q^l = 1$ for all $q \in \mathrm{Sp}(1)$. Therefore for $q \in \mathrm{Sp}(1)$, R_q^l is a rotation on $\mathbb{R}^4$, i.e., $R_q^l \in \mathrm{SO}(4)$.

Similarly, from the representation

$$xq = R_q^r x = \begin{pmatrix} q_0 & -q_1 & -q_2 & -q_3 \\ q_1 & q_0 & q_3 & -q_2 \\ q_2 & -q_3 & q_0 & q_1 \\ q_3 & q_2 & -q_1 & q_0 \end{pmatrix} \begin{pmatrix} x_0 \\ x_1 \\ x_2 \\ x_3 \end{pmatrix}, \tag{11.36}$$

we see that for a given $q \in \mathrm{Sp}(1)$ the mapping $x \mapsto xq$ can be taken as a rotation $R_q^r \in \mathrm{SO}(4)$ on $\mathbb{R}^4$.

Clearly the left translation $\mathcal{T}_q^l$ and right translation $\mathcal{T}_q^r$ on Sp(1) are simply the restrictions of the rotations R_q^l and R_q^r on $\mathcal{S}^3$, respectively.

A Riemannian metric on a Lie group G is said to be left-invariant if

$$\langle u, v\rangle_x = \langle D\mathcal{T}_q^l u, D\mathcal{T}_q^l v\rangle_{\mathcal{T}_q^l x}$$

for all $q, x \in G$ and $u, v \in T_x G$. Similarly, a Riemannian metric is right-invariant if each right translation $\mathcal{T}_q^r : G \to G$ is an isometry. A metric on G that is both left-invariant and right-invariant is said to be bi-invariant. Clearly the metric on $\mathcal{S}^3$ or Sp(1) is bi-invariant.

11.3 The Sp(1) → SO(3) Double Covering

We have proved earlier that the map $\mathrm{Ad} : \mathrm{Sp}(1) \to \mathrm{SO}(3)$, $x \mapsto \boldsymbol{R}_x$, is a surjective homomorphism with $\mathrm{Ker}(\mathrm{Ad}) = \{1, -1\}$. From formula (11.10) for the double covering in question, it is clear that Ad is a smooth map. In fact, Ad is a local diffeomorphism, i.e., for each $x \in \mathrm{Sp}(1)$ there exists a neighborhood N_x of x in Sp(1) such that N_x is diffeomorphic to $\mathrm{Ad}(N_x)$. To prove the preceding assertion, we begin with a lemma.

Lemma 11.6 *Consider the differential of* Ad *at the identity* $1 \in \mathrm{Sp}(1)$, *i.e.*, $D(\mathrm{Ad})(1) : T_1\mathrm{Sp}(1) \to T_{\boldsymbol{I}}\mathrm{SO}(3)$. *We have*

$$D(\mathrm{Ad})(1)[\boldsymbol{i}] = 2\boldsymbol{E}_1, \quad D(\mathrm{Ad})(1)[\boldsymbol{j}] = 2\boldsymbol{E}_2, \quad D(\mathrm{Ad})(1)[\boldsymbol{k}] = 2\boldsymbol{E}_3, \tag{11.37}$$

where $\boldsymbol{E}_1 = -\boldsymbol{e}_2 \otimes \boldsymbol{e}_3 + \boldsymbol{e}_3 \otimes \boldsymbol{e}_3$, $\boldsymbol{E}_2 = -\boldsymbol{e}_3 \otimes \boldsymbol{e}_1 + \boldsymbol{e}_1 \otimes \boldsymbol{e}_3$, *and* $\boldsymbol{E}_3 = -\boldsymbol{e}_1 \otimes \boldsymbol{e}_2 + \boldsymbol{e}_2 \otimes \boldsymbol{e}_1$ *are the chosen orthonormal basis tensors in* Skw.

Proof For any smooth curve $x(t)$ in Sp(1) with $x(0) = 1$, we have

$$D(\mathrm{Ad})(1)\left[\frac{dx}{dt}(0)\right] = \frac{d}{dt}\boldsymbol{R}_{x(t)}\big|_{t=0}.$$

The map $x(t) = \cos t + \sin t\, \boldsymbol{i}$ defines a smooth curve in Sp(1) that satisfies $x(0) = 1$ and $dx/dt(0) = \boldsymbol{i}$. Substituting $x(t) = \cos t + \sin t\, \boldsymbol{i}$ into (11.10), we get

$$\boldsymbol{R}_{x(t)} = \begin{pmatrix} 1 & 0 & 0 \\ 0 & \cos 2t & -\sin 2t \\ 0 & \sin 2t & \cos 2t \end{pmatrix},$$

which implies

$$\frac{d}{dt}\boldsymbol{R}_{x(t)}\big|_{t=0} = \begin{pmatrix} 0 & 0 & 0 \\ 0 & 0 & -2 \\ 0 & 2 & 0 \end{pmatrix} = 2\boldsymbol{E}_1.$$

Hence it follows that $D(\mathrm{Ad})(1)[\boldsymbol{i}] = 2\boldsymbol{E}_1$. Similarly we obtain the remaining two formulas in (11.37) by considering the smooth curves $y(t) = \cos t + \sin t\, \boldsymbol{j}$ and $z(t) = \cos t + \sin t\, \boldsymbol{k}$. □

Proposition 11.7 *The double covering* $\mathrm{Ad} : \mathrm{Sp}(1) \to \mathrm{SO}(3)$ *is a local diffeomorphism.*

Proof It suffices to prove that the rank of the linear map $D(\mathrm{Ad})(q)$ is 3 for each $q \in \mathrm{Sp}(1)$, as the conclusion will then follow from the inverse function theorem. From the preceding lemma, we see that $\mathrm{rank}(D(\mathrm{Ad}(1))) = 3$. We proceed to show that $\mathrm{rank}(D(\mathrm{Ad}(q))) = 3$ for each $q \in \mathrm{Sp}(1)$.

For convenience, let $\boldsymbol{i}_1 := \boldsymbol{i}$, $\boldsymbol{i}_2 := \boldsymbol{j}$, and $\boldsymbol{i}_3 := \boldsymbol{k}$. Let $x_j(t) = \cos t + \sin t\, \boldsymbol{i}_j$ for $j = 1, 2, 3$. For $q \in \mathrm{Sp}(1)$, consider the smooth curves $qx_j(t)$ $(j = 1, 2, 3)$, which all passes q at $t = 0$. Moreover, for $j = 1, 2, 3$, we have

$$\frac{d}{dt} q x_j(t)\big|_{t=0} = q\boldsymbol{i}_j, \qquad \frac{d}{dt} \boldsymbol{R}_{qx_j(t)}\big|_{t=0} = 2\boldsymbol{R}_q \boldsymbol{E}_j.$$

Note that $\{q\boldsymbol{i}_j : j = 1, 2, 3\}$ constitutes an orthonormal basis in $T_q\mathrm{Sp}(1)$ and $\{2\boldsymbol{R}_q \boldsymbol{E}_j : j = 1, 2, 3\}$ an orthogonal basis in $T_{\boldsymbol{R}_q}\mathrm{SO}(3)$. Hence $\mathrm{rank}(D(\mathrm{Ad}(q))) = 3$. □

Let $U \subset \mathrm{Sp}(1)$ be an open set which satisfies the condition that if $x \in U$, then $-x \notin U$. Let (U, φ), where $\varphi : U \to \mathbb{R}^3$, $x \mapsto (\xi_1(x), \xi_2(x), \xi_3(x))$, be a chart on $\mathrm{Sp}(1)$. Since $\mathrm{Ad}\big|_U : U \to \mathrm{Ad}(U)$ is a diffeomorphism, $(\mathrm{Ad}(U), \varphi \circ (\mathrm{Ad}\big|_U)^{-1})$ is a chart on SO(3). Under this chart, $\boldsymbol{R}_x \in \mathrm{Ad}(U)$ is mapped to $(\xi_1(x), \xi_2(x), \xi_3(x))$. Let us investigate the relationship, under the coordinates (ξ_1, ξ_2, ξ_3), between the metric tensors $\widetilde{\boldsymbol{g}}$ and $\boldsymbol{g}$ on $U \subset \mathrm{Sp}(1)$ and on $\mathrm{Ad}(U) \subset \mathrm{SO}(3)$, respectively. To make the idea underlying the present discussion as clear as possible, let us first assume that $1 \in U$. In the tangent space $T_1\mathrm{Sp}(1)$, each basis vector $\partial x/\partial \xi_k$ can be written as a linear combination of the orthonormal basis vectors $\boldsymbol{i}_j$ $(j = 1, 2, 3)$, say

$$\frac{\partial x}{\partial \xi_k} = \sum_{j=1}^{3} \alpha_{jk} \boldsymbol{i}_j. \tag{11.38}$$

Then we have, in the tangent space $T_{\boldsymbol{I}}\mathrm{SO}(3)$,

$$\begin{aligned} \frac{\partial \boldsymbol{R}_x}{\partial \xi_k} &= D(\mathrm{Ad})(1)\left[\frac{\partial x}{\partial \xi_k}\right] = D(\mathrm{Ad})(1)\left[\sum_{j=1}^{3} \alpha_{jk} \boldsymbol{i}_j\right] \\ &= \sum_{j=1}^{3} \alpha_{jk} D(\mathrm{Ad})(1)\left[\boldsymbol{i}_j\right] = 2\sum_{j=1}^{3} \alpha_{jk} \boldsymbol{E}_j. \end{aligned} \tag{11.39}$$

Thus we obtain

$$\widetilde{g}_{kl}(1) = \langle \frac{\partial x}{\partial \xi_k}, \frac{\partial x}{\partial \xi_l} \rangle_1 = \sum_{i=1}^{3} \alpha_{ik}\alpha_{il}, \tag{11.40}$$

and

$$g_{kl}(\boldsymbol{I}) = \langle \frac{\partial \boldsymbol{R}_x}{\partial \xi_k}, \frac{\partial \boldsymbol{R}_x}{\partial \xi_l} \rangle_{\boldsymbol{I}} = 4\sum_{i=1}^{3} \alpha_{ik}\alpha_{il}. \tag{11.41}$$

Hence we conclude that

$$g_{kl}(\boldsymbol{I}) = 4\,\widetilde{g}_{kl}(1). \tag{11.42}$$

Now consider any $q \in U$. In the tangent space $T_q\mathrm{Sp}(1)$, each basis vector $\partial x/\partial \xi_k$ can be written as a linear combination of the orthonormal basis vectors $q\boldsymbol{i}_j$ $(j = 1, 2, 3)$, say

$$\frac{\partial x}{\partial \xi_k} = \sum_{j=1}^{3} \alpha_{jk} q \boldsymbol{i}_j. \tag{11.43}$$

Then we have, in the tangent space $T_{\boldsymbol{R}_q}\mathrm{SO}(3)$,

$$\begin{aligned} \frac{\partial \boldsymbol{R}_x}{\partial \xi_k} &= D(\mathrm{Ad})(q)\left[\frac{\partial x}{\partial \xi_k}\right] = D(\mathrm{Ad})(q)\left[\sum_{j=1}^{3} \alpha_{jk} q \boldsymbol{i}_j\right] \\ &= \sum_{j=1}^{3} \alpha_{jk} D(\mathrm{Ad})(q)\left[q\boldsymbol{i}_j\right] = 2\sum_{j=1}^{3} \alpha_{jk} \boldsymbol{R}_q \boldsymbol{E}_j. \end{aligned} \tag{11.44}$$

Thus we obtain

$$\widetilde{g}_{kl}(q) = \langle \frac{\partial x}{\partial \xi_k}, \frac{\partial x}{\partial \xi_l} \rangle_q = \sum_{i=1}^{3} \alpha_{ik}\alpha_{il}, \tag{11.45}$$

and

$$g_{kl}(\boldsymbol{I}) = \langle \frac{\partial \boldsymbol{R}_x}{\partial \xi_k}, \frac{\partial \boldsymbol{R}_x}{\partial \xi_l} \rangle_{\boldsymbol{R}_q} = 4\sum_{i=1}^{3} \alpha_{ik}\alpha_{il}. \tag{11.46}$$

Hence we conclude that

$$g_{kl}(\boldsymbol{R}_q) = 4\,\widetilde{g}_{kl}(q), \tag{11.47}$$

which implies

$$\sqrt{\det \boldsymbol{g}(\xi_1, \xi_2, \xi_3)}\, d\xi_1 d\xi_2 d\xi_3 = 8\sqrt{\det \widetilde{\boldsymbol{g}}(\xi_1, \xi_2, \xi_3)}\, d\xi_1 d\xi_2 d\xi_3. \tag{11.48}$$

Note that if $\mathcal{S}^3 \setminus U$ has measure zero in $\mathcal{S}^3$, then $\mathrm{Ad}(S^3 \setminus U)$ has measure zero in SO(3).

11.3.1 Volume Element on SO(3) in Axis-Angle Parameters

As an application of (11.48) we use it to determine the volume element on SO(3) in axis-angle parameters.

Recall that the pair (U_p, φ_p), where $U_p = \mathcal{S}^3 \setminus \{(x_0, x_1, 0, 0) : x_0^2 + x_1^2 = 1\}$ and φ_p maps each $x \in U_p$ to its polar coordinates $(\theta_1, \theta_2, \theta_3)(x)$, is a chart on Sp(1). Let $U_p^+ := U_p \cap \{x \in \mathcal{S}^3 : x_0 > 0\}$. Then $(U_p^+, \varphi_p\big|_{U_p^+})$ is a chart on Sp(1) which satisfies the condition that $-x \notin U_p^+$ if $x \in U_p^+$. Hence $(\mathrm{Ad}(U_p^+), \varphi_p \circ (\mathrm{Ad}\big|_{U_p^+})^{-1})$, $\boldsymbol{R}_x \mapsto (\theta_1, \theta_2, \theta_3)(x)$, is a chart on SO(3).

Note that both the sets $\{(x_0, x_1, 0, 0) : x_0^2 + x_1^2 = 1\}$ and $\{x \in \mathcal{S}^3 : x_0 = 0\}$ have measure zero in $\mathcal{S}^3$. Hence $\mathrm{Ad}(U_p^+)$ has the same group volume as that of SO(3).

Let $(\boldsymbol{n}, \omega)$ be the axis-angle parameters pertaining to $\boldsymbol{R}_x$. We choose "spherical coordinates" (Θ, Ψ) for $\boldsymbol{n}$, which are defined through the formulas

$$n_1 = \cos\Theta, \qquad n_2 = \sin\Theta\cos\Phi, \qquad n_3 = \sin\Theta\sin\Phi.$$

By abuse of language, we refer to $(\omega; \Theta, \Phi)$ also as the axis-angle parameters of the rotation $\boldsymbol{R}(\boldsymbol{n}(\Theta, \Phi), \omega)$. From the formula $x = \cos\frac{\omega}{2} + \sin\frac{\omega}{2}\boldsymbol{n}$ (cf. (11.14)), we obtain:

$$\begin{aligned} x_0 &= \cos\frac{\omega}{2}, & x_1 &= \sin\frac{\omega}{2}\cos\Theta, \\ x_2 &= \sin\frac{\omega}{2}\sin\Theta\cos\Phi, & x_3 &= \sin\frac{\omega}{2}\sin\Theta\sin\Phi. \end{aligned} \tag{11.49}$$

A comparison of (11.49) with formula (11.26), which gives $x = (x_0, x_1, x_2, x_3) \in U_p^+$ in terms of its polar coordinates $(\theta_1, \theta_2, \theta_3)$, reveals that the two formulas become the same if we put

$$\theta_1 = \frac{\omega}{2}, \qquad \theta_2 = \Theta, \qquad \theta_3 = \Phi. \tag{11.50}$$

By (11.14), (11.48), and (11.50), the volume element on SO(3) is given in axis-angle parameters by the formula

$$8\sin^2\theta_1 \sin\theta_2\, d\theta_1 d\theta_2 d\theta_3 = 4\sin^2\frac{\omega}{2}\sin\Theta\, d\omega d\Theta d\Phi, \tag{11.51}$$

the right-hand side of which in none other that $d\mathcal{V}$ in (3.48). Note that

$$\mathrm{Ad}(U_p^+) = \{(\omega; \Theta, \Phi) : 0 < \omega < \pi, 0 < \Theta < \pi, 0 \le \Phi < 2\pi\}, \tag{11.52}$$

and $\mathcal{V}(\mathrm{SO}(3)) = \mathcal{V}(\mathrm{Ad}(U_p^+))$. Hence we have

$$\mathcal{V}(\mathrm{SO}(3)) = 4\int_0^{2\pi}\int_0^{\pi}\int_0^{\pi} \sin^2\frac{\omega}{2}\sin\Theta\, d\omega d\Theta d\Phi = 8\pi^2. \tag{11.53}$$

For $0 \le a < \pi$, let $\mathrm{B}_a = \{\boldsymbol{R}(\boldsymbol{n}, \omega) : 0 \le \omega \le a\}$ be the ball of radius a centered at the identity $\boldsymbol{I}$.[139] The volume of B_a is given by

$$\mathcal{V}(\mathrm{B}_a) = 4\int_0^{2\pi}\int_0^{\pi}\int_0^{a} \sin^2\frac{\omega}{2}\sin\Theta\, d\omega d\Theta d\Phi = 8\pi(a - \sin a). \tag{11.54}$$

For $a = \pi/2$, we have

$$\mathcal{V}(\mathrm{B}_{\pi/2}) = 8\pi^2\left(\frac{1}{2} - \frac{1}{\pi}\right) \approx 0.1817 \times \mathcal{V}(\mathrm{SO}(3)). \tag{11.55}$$

11.4 SU(2)

The special unitary group of degree 2 or SU(2) consists of 2×2 complex matrices A that satisfy

$$A^{-1} = \overline{A^T}, \qquad \text{and} \qquad \det A = 1. \tag{11.56}$$

[139] The rotation group SO(3) is a metric space with the distance $d(\boldsymbol{R}_1, \boldsymbol{R}_2)$ between two rotations $\boldsymbol{R}_1$ and $\boldsymbol{R}_2$ given by the angle $\omega \in [0, \pi]$ of the rotation $\boldsymbol{R}_2\boldsymbol{R}_1^T$ that takes $\boldsymbol{R}_1$ to $\boldsymbol{R}_2$. See Sects. 1.10 and 10.2.

Let $A = \begin{pmatrix} z_1 & z_2 \\ z_3 & z_4 \end{pmatrix}$, where $z_i \in \mathbb{C}$ $(i = 1, 2, 3, 4)$. The requirements given in (11.56) dictate that

$$\begin{pmatrix} z_4 & -z_2 \\ -z_3 & z_1 \end{pmatrix} = \begin{pmatrix} \overline{z_1} & \overline{z_3} \\ \overline{z_2} & \overline{z_4} \end{pmatrix},$$

which implies that

$$z_4 = \overline{z_1}, \qquad z_3 = -\overline{z_2}.$$

Hence we have

$$\mathrm{SU}(2) = \left\{ \begin{pmatrix} z & w \\ -\overline{w} & \overline{z} \end{pmatrix} : z, w \in \mathbb{C}, |z|^2 + |w|^2 = 1 \right\}. \tag{11.57}$$

11.4.1 Identification with Sp(1)

Proposition 11.8 *Let* $\Psi : \mathrm{Sp}(1) \to \mathrm{SU}(2)$ *be defined by*

$$\Psi(x_0 + x_1 i + x_2 j + x_3 k) = \begin{pmatrix} x_0 + x_1 i & x_2 + x_3 i \\ -x_2 + x_3 i & x_0 - x_1 i \end{pmatrix}. \tag{11.58}$$

Then Ψ *is a homeomorphic isomorphism.*

Proof By (11.57), $\Psi(x) \in \mathrm{SU}(2)$ for each $x \in \mathrm{Sp}(1)$. Clearly Ψ is injective and is linear, i.e.,

$$\Psi(x + y) = \Psi(x) + \Psi(y) \qquad \text{for each } x, y \in \mathrm{Sp}(1), \tag{11.59}$$

$$\Psi(\lambda x) = \lambda \Psi(x) \qquad \text{for each } \lambda \in \mathbb{R} \text{ and } x \in \mathrm{Sp}(1). \tag{11.60}$$

To see that Ψ is surjective, let $g \in \mathrm{SU}(2)$. By (11.57),

$$g = \begin{pmatrix} z & w \\ -\overline{w} & \overline{z} \end{pmatrix} \qquad \text{for some } z, w \in \mathbb{C} \text{ such that } |z|^2 + |w|^2 = 1.$$

Let $z = x_0 + x_1 i$ and $w = x_2 + x_3 i$. Then $x_0^2 + x_1^2 + x_2^2 + x_3^2 = 1$, $x := x_0 + x_1 i + x_2 j + x_3 k \in \mathrm{Sp}(1)$, and $\Psi(x) = g$. Moreover, the mapping Ψ is clearly continuous. Since $\mathrm{Sp}(1)$ (i.e., the unit sphere $\mathcal{S}^3$ in $\mathbb{R}^4$) is compact and $\mathrm{SU}(2)$ is a Hausdorff space, the continuous bijection Ψ is a homeomorphism (see, e.g., [242, p. 167]). That Ψ is a homomorphism, i.e.,

$$\Psi(xy) = \Psi(x)\Psi(y), \tag{11.61}$$

can be checked as follows. Notice that

$$\Psi(1) = \begin{pmatrix} 1 & 0 \\ 0 & 1 \end{pmatrix}, \qquad \Psi(i) = \begin{pmatrix} i & 0 \\ 0 & -i \end{pmatrix}, \tag{11.62}$$

$$\Psi(j) = \begin{pmatrix} 0 & 1 \\ -1 & 0 \end{pmatrix}, \qquad \Psi(k) = \begin{pmatrix} 0 & i \\ i & 0 \end{pmatrix}. \tag{11.63}$$

Then (11.61) can be checked easily for $x, y \in \{1, i, j, k\}$, and its validity for any $x, y \in \mathrm{Sp}(1)$ follows from (11.59) and (11.60). Since Ψ is a bijective homomorphism, Sp(1) and SU(2) are isomorphic. □

In what follows, we identify SU(2) with Sp(1).

Let $g \in \mathrm{SU}(2)$. Its eigenvalues satisfy the equation

$$\begin{vmatrix} z-\lambda & w \\ -\overline{w} & \overline{z}-\lambda \end{vmatrix} = \lambda^2 - (z+\overline{z})\lambda + 1 = \lambda^2 - 2\cos\theta_1\,\lambda + 1 = 0, \tag{11.64}$$

where we have used the fact that $z + \overline{z} = 2x_0 = 2\cos\theta_1$. Hence the eigenvalues of g are: $e^{i\theta_1}$, $e^{-i\theta_1}$, where $0 \le \theta_1 \le \pi$.

In fact any $g \in \mathrm{SU}(2)$ is conjugate to a diagonal matrix $h \in \mathrm{SU}(2)$ of the form

$$h(\theta) = \begin{pmatrix} e^{i\theta} & 0 \\ 0 & e^{-i\theta} \end{pmatrix}, \qquad \text{where } 0 \le \theta \le \pi; \tag{11.65}$$

that is,

$$g = uh(\theta)u^{-1} \tag{11.66}$$

for some $u \in \mathrm{SU}(2)$. Indeed, it is well known[140] that there exists $w \in \mathrm{U}(2)$ such that (11.66) is valid. But we may replace such a w by $u = \alpha w$ with a suitable $\alpha \in \mathbb{C}$ such that $\det(\alpha w) = 1$.

11.4.2 Convention in Physics

In the physics literature (see, e.g., Biedenharn and Louck [28, p. 18]), instead of (11.58), the homeomorphic homomorphism $\widetilde{\Psi} : \mathrm{Sp}(1) \to \mathrm{SU}(2)$ is often written as

$$\widetilde{\Psi}(q_0 + q_1 i + q_2 j + q_3 k) = q_0\sigma_0 - i(q_1\sigma_1 + q_2\sigma_2 + q_3\sigma_3), \tag{11.67}$$

where σ_0 is the 2×2 identity matrix and σ_i $(i = 1, 2, 3)$ are the Pauli matrices given by

$$\sigma_1 = \begin{pmatrix} 0 & 1 \\ 1 & 0 \end{pmatrix}, \qquad \sigma_2 = \begin{pmatrix} 0 & -i \\ i & 0 \end{pmatrix}, \qquad \sigma_3 = \begin{pmatrix} 1 & 0 \\ 0 & -1 \end{pmatrix}. \tag{11.68}$$

Hence a generic element of SU(2) is written as

$$g = \begin{pmatrix} q_0 - iq_3 & -q_2 - iq_1 \\ q_2 - iq_1 & q_0 + iq_3 \end{pmatrix}, \tag{11.69}$$

which should be contrasted with (11.58). Also, the polar coordinates (11.26) on $\mathcal{S}^3$ are rearranged such that the coordinates (q_0, q_1, q_2, q_3) of $q \in \mathcal{S}^3$ are given by

$$\begin{aligned} q_0 &= \cos\frac{\omega}{2}, \qquad & q_1 &= \sin\frac{\omega}{2}\sin\Theta\cos\Phi, \\ q_2 &= \sin\frac{\omega}{2}\sin\Theta\sin\Phi, \qquad & q_3 &= \sin\frac{\omega}{2}\cos\Theta, \end{aligned} \tag{11.70}$$

[140] A complex square matrix A is diagonalizable by the transformation $A \mapsto U^{-1}AU$ with a unitary matrix U if and only if A is a normal matrix, i.e., A satisfies $AA^* = A^*A$, where $A^* := \overline{A^T}$ (see, e.g., Satake [282, p. 192]). A unitary matrix is clearly normal.

where $0 \le \omega \le 2\pi$, $0 \le \Theta \le \pi$, $0 \le \Phi < 2\pi$. Note that the correspondence between $q \in \mathcal{S}^3$ and the "axis-angle parameters" $(\omega; \Theta, \Phi)$ is one-to-one except at points in the singular set $\{q \in \mathcal{S}^3 : q_0^2 + q_3^2 = 1\}$ (cf. the discussions in the paragraph that contains (11.26)). We call $(q_0, \boldsymbol{q}) = (\cos\frac{\omega}{2}, \sin\frac{\omega}{2}\boldsymbol{n})$, where $0 \le \omega \le 2\pi$ and $\boldsymbol{n} = (\sin\Theta\cos\Phi, \sin\Theta\sin\Phi, \cos\Theta)$ with $\boldsymbol{n} \cdot \boldsymbol{n} = 1$, the Euler-Rodrigues parameters for SU(2), and call (11.69) with q_0, q_1, q_2, and q_3 given by (11.70) the parametrization of SU(2) by Euler-Rodrigues parameters.

Chapter 12

12 Texture Analysis Based on the Orthogonal Group

With ODFs defined on SO(3), classical texture analysis suffers from the limitation that the groups of texture and crystallite symmetry G_{tex} and G_{cr} are restricted to be rotational. Thus, strictly speaking, all polycrystalline materials that have their G_{cr} being improper, which include most engineering materials (e.g., metals) with important applications, are not covered by the theory of classical texture analysis. That in applications of texture analysis substituting an improper G_{cr} by its proper peer in the same Laue class seems to have often worked does not validate such an *ad hoc* practice. On the contrary, such unexpected "successes" of the classical theory should be explained, and the conditions which render them possible delineated.

Bunge and his coworkers [60, 64, 65, 109] were the first to introduce ODFs that are defined on O(3). However, they stopped pursuing further after giving some basic properties of the ODF that include the restrictions imposed on it by texture and crystal symmetries and some discussions that concern its measurement by X-ray diffraction.

In what follows we will adopt the approach initiated by Roe [270, 271] but will assume that for polycrystalline aggregates of Type II or Type III crystallites orientation probability measures and orientation distribution functions be defined on O(3). The main references for our treatment in this chapter are [94, 95, 206].

12.1 Orientation Distribution Functions Defined on O(3)

The Roe approach in classical texture analysis starts with a treatment for aggregates of Type I triclinic crystallites, i.e., those with $G_{\text{cr}} = C_1 = \{\boldsymbol{I}\}$. While there is another type of triclinic crystallites, i.e., those with $G_{\text{cr}} = C_i = \{\boldsymbol{I}, \boldsymbol{\mathcal{I}}\}$ (Type II; see Table 3), polycrystalline aggregates of such crystallites are treated in classical texture analysis as if the crystallites were of Type I. To introduce ODFs defined on O(3) in the Roe approach, one option would be to begin with aggregates of Type II triclinic crystallites. However, it is more instructive to begin by considering a mixture of "right-handed" and "left-handed" Type I triclinic crystallites of the same substance S, which we will do here.

Let us return to the setting discussed in Sect. 3.1. Consider a manufacturing process $\mathfrak{P}$ which produces macroscopically identical samples $\mathcal{P}_\alpha$ of polycrystal P, which consist of Type I triclinic crystallites of substance S. We choose an ideal single crystal C of S with configuration $\boldsymbol{\kappa}_0(\mathsf{C})$ as reference. The triclinic crystals of S, however, can occur in two forms, namely: crystals whose possible configurations are: (i) rotated versions of $\boldsymbol{\kappa}_0(\mathsf{C})$, which we call right-handed, and (ii) rotated versions of $\boldsymbol{\mathcal{I}} \circ \boldsymbol{\kappa}_0(\mathsf{C})$, which we call left-handed. Suppose each of the macroscopically identical polycrystalline samples $\mathcal{P}_\alpha$ is a mixture of right-handed and left-handed crystallites of substance S. Take an ensemble $\mathcal{E}$ of polycrystalline samples $\mathcal{P}_\alpha$ produced in the process $\mathfrak{P}$. We measure the crystallite orientation at the same point $\mathtt{X}$ of each sample $\mathcal{P}_\alpha$ in the ensemble. From sample $\mathcal{P}_\alpha$ we obtain the orientation $\boldsymbol{Q}_\alpha$ with respect to the reference $\boldsymbol{\kappa}_0(\mathsf{C})$, where $\boldsymbol{Q}_\alpha \in \mathrm{O}(3) = \mathrm{SO}(3) \cup \boldsymbol{\mathcal{I}}\mathrm{SO}(3)$. If $\boldsymbol{Q}_\alpha$ is a rotation (resp. roto-inversion) with respect to $\boldsymbol{\kappa}_0(\mathsf{C})$, then the orientation at $\mathtt{X}$ is taken to that of a right-handed (resp. left-handed) crystal and $\boldsymbol{Q}_\alpha \in \mathrm{SO}(3)$ (resp. $\boldsymbol{Q}_\alpha \in \boldsymbol{\mathcal{I}}\mathrm{SO}(3)$). In texture analysis we assume that the orientations at $\mathtt{X}$ for the ensemble $\mathcal{E}$ is characterized by a probability measure $\wp(\cdot; \mathtt{X})$ on O(3) specific to the process $\mathfrak{P}$. We call $\wp(\cdot; \mathtt{X})$ the orientation (probability) measure at $\mathtt{X}$, which defines the crystallographic texture at $\mathtt{X}$. If the texture is homogeneous, then $\wp$ will be independent of $\mathtt{X}$. Even if the texture is inhomogeneous, it is customary to suppress the explicit dependence of $\wp$ on $\mathtt{X}$ except at places where

such dependence should be emphasized. Whether the texture is homogenous or not should be clear from the context.

For probability measures $\wp$ which are absolutely continuous with respect to the bi-invariant group volume $\mathcal{V}_{\mathrm{O}(3)}$, the ODF, i.e., the Radon-Nikodym derivative of $\wp$ with respect to $\mathcal{V}_{\mathrm{O}(3)}$, is well defined:

$$w(\boldsymbol{Q}) = \frac{d\wp}{d\mathcal{V}_{\mathrm{O}(3)}(\boldsymbol{Q})} \tag{12.1}$$

so that for a measurable subset A of O(3)

$$\wp(A) = \int_A w(\boldsymbol{Q}) d\mathcal{V}_{\mathrm{O}(3)}(\boldsymbol{Q}) \tag{12.2}$$

gives the probability of finding the crystallite orientation at the sampling point in question to be in A, and

$$\int_{\mathrm{O}(3)} w(\boldsymbol{Q}) d\mathcal{V}_{\mathrm{O}(3)}(\boldsymbol{Q}) = 1; \tag{12.3}$$

see Sects. 10.5 and 10.6.2 for the definition of $\mathcal{V}_{\mathrm{O}(3)}$ and of the invariant integral on O(3). We will work with ODFs $w \in L^2(\mathrm{O}(3), \mathbb{R})$. There is no loss of generality in doing so, as such ODFs are dense in the space of orientation measures under the vague topology (see [206] and the references therein).

12.1.1 Series Expansions and Texture Coefficients

Following Esling et al. [109], we introduce w^R and w^L, the orientation distribution functions of the right-handed and left-handed crystallites, respectively.

Definition 12.1 Let $w : \mathrm{O}(3) \to \mathbb{R}$. Define $w^{R/L} : \mathrm{SO}(3) \to \mathbb{R}$ by

$$w^R(\boldsymbol{R}) = w(\boldsymbol{R}), \qquad w^L(\boldsymbol{R}) = w(\mathcal{I}\boldsymbol{R}), \qquad \text{for } \boldsymbol{R} \in \mathrm{SO}(3). \tag{12.4}$$

The functions w^R and w^L are called the right-handed and left-handed parts of w, respectively. □

Regarding w^R and w^L as functions in $L^2(\mathrm{SO}(3), \mathbb{C})$, we write down their expansions in terms of the Wigner D-functions:

$$w(\boldsymbol{Q}) = \begin{cases} w^R(\boldsymbol{R}) = \sum_{l=0}^{\infty} \sum_{m=-l}^{l} \sum_{n=-l}^{l} c_{mn}^{l,R} D_{mn}^{l}(\boldsymbol{R}(\psi,\theta,\phi)) & \text{for } \boldsymbol{Q} = \boldsymbol{R} \in \mathrm{SO}(3) \\ w^L(\boldsymbol{R}) = \sum_{l=0}^{\infty} \sum_{m=-l}^{l} \sum_{n=-l}^{l} c_{mn}^{l,L} D_{mn}^{l}(\boldsymbol{R}(\psi,\theta,\phi)) & \text{for } \mathcal{I}\boldsymbol{Q} = \boldsymbol{R} \in \mathrm{SO}(3). \end{cases} \tag{12.5}$$

Since the functions w^R and w^L are real-valued, their texture coefficients satisfy the constraints (cf. (4.46)) that

$$c_{\bar{m}\bar{n}}^{l,R} = (-1)^{n-m} \overline{c_{mn}^{l,R}}, \qquad c_{\bar{m}\bar{n}}^{l,L} = (-1)^{n-m} \overline{c_{mn}^{l,L}}. \tag{12.6}$$

Let λ and $1-\lambda$ be the volume fractions of right-handed and left-handed crystallites in the mixture, respectively. Then we have

$$c_{00}^{0,R} = \frac{\lambda}{8\pi^2}, \qquad c_{00}^{0,L} = \frac{1-\lambda}{8\pi^2}, \tag{12.7}$$

$$\int_{\mathrm{SO}(3)} w^R(\boldsymbol{R})d\mathcal{V}(\boldsymbol{R}) = \lambda, \qquad \int_{\mathrm{SO}(3)} w^L(\boldsymbol{R})d\mathcal{V}(\boldsymbol{R}) = 1-\lambda. \tag{12.8}$$

By Corollary 15.8 of the Peter-Weyl theorem, each orientation distribution function $w \in L^2(\mathrm{O}(3), \mathbb{C})$ can be expanded as an infinite series in terms of the matrix elements $D_{mn}^{l,\pm}$ of the complete set of irreducible unitary representations $\mathcal{D}_l^{\pm}$ of O(3) (cf. Theorem 14.14):

$$w(\boldsymbol{Q}) = \sum_{l=0}^{\infty}\sum_{m=-l}^{l}\sum_{n=-l}^{l} c_{mn}^{l,+} D_{mn}^{l,+}(\boldsymbol{Q}) + \sum_{l=0}^{\infty}\sum_{m=-l}^{l}\sum_{n=-l}^{l} c_{mn}^{l,-} D_{mn}^{l,-}(\boldsymbol{Q}) \tag{12.9}$$

$$= \begin{cases} \displaystyle\sum_{l=0}^{\infty}\sum_{m=-l}^{l}\sum_{n=-l}^{l} (c_{mn}^{l,+} + c_{mn}^{l,-}) D_{mn}^{l}(\boldsymbol{R}(\psi,\theta,\phi)) & \text{for } \boldsymbol{Q} = \boldsymbol{R} \in \mathrm{SO}(3) \\ \displaystyle\sum_{l=0}^{\infty}\sum_{m=-l}^{l}\sum_{n=-l}^{l} (c_{mn}^{l,+} - c_{mn}^{l,-}) D_{mn}^{l}(\boldsymbol{R}(\psi,\theta,\phi)) & \text{for } \boldsymbol{Q} = \boldsymbol{\mathcal{I}R} \in \boldsymbol{\mathcal{I}}\mathrm{SO}(3). \end{cases} \tag{12.10}$$

A comparison of (12.10) and (12.5) reveals that

$$c_{mn}^{l,R} = c_{mn}^{l,+} + c_{mn}^{l,-}, \qquad c_{mn}^{l,L} = c_{mn}^{l,+} - c_{mn}^{l,-}. \tag{12.11}$$

Thus we have

$$c_{mn}^{l,+} = \frac{1}{2}(c_{mn}^{l,R} + c_{mn}^{l,L}), \qquad c_{mn}^{l,-} = \frac{1}{2}(c_{mn}^{l,R} - c_{mn}^{l,L}). \tag{12.12}$$

From (12.6) and (12.12) we observe that the texture coefficients $c_{mn}^{l,\pm}$ satisfy the conditions

$$c_{\bar{m}\bar{n}}^{l,\pm} = (-1)^{n-m}\overline{c_{mn}^{l,\pm}}, \tag{12.13}$$

which follows from the fact that w is real-valued. From (12.7) and (12.12) we obtain

$$c_{00}^{0,+} = \frac{1}{16\pi^2}, \qquad c_{00}^{0,-} = \frac{2\lambda-1}{16\pi^2}. \tag{12.14}$$

Note that $c_{00}^{0,-} = 0$ if and only if $\lambda = 1/2$.

Remark 12.2 For aggregates of Type II crystallites, we shall see in (12.25) that $\lambda = 1/2$. For aggregates of Type III crystallites, the same conclusion follows from (12.45), the formula for the orientation measure of a singe crystal. □

12.2 Discrete Probability Measures on O(3)

Let us return to the substance S, the Type I triclinic crystallites of which can occur in both the right- and left-handed forms. A single crystal of S whose orientation with respect to the

reference crystal $(\mathsf{C}, \boldsymbol{\kappa}_0)$ is specified by $\boldsymbol{Q} \in \mathrm{O}(3)$ has its orientation measure given by the Dirac measure $\delta_{\boldsymbol{Q}}$, which satisfies

$$\delta_{\boldsymbol{Q}}(A) = \begin{cases} 1 & \text{if } \boldsymbol{Q} \in A \\ 0 & \text{if } \boldsymbol{Q} \notin A, \end{cases} \quad \text{for each measurable } A \subset \mathrm{O}(3). \tag{12.15}$$

In particular, the orientation measures of a right-handed and a left-handed single crystal whose orientation with respect to the reference is defined by a rotation $\boldsymbol{R}$ and roto-inversion $\boldsymbol{\mathcal{I}R}$ are $\delta_{\boldsymbol{R}}$ and $\delta_{\boldsymbol{\mathcal{I}R}}$, respectively.

A probability measure $\wp$ on O(3) is said to be discrete if it is a convex combination of Dirac measures, i.e.,

$$\wp = \sum_{i=1}^{N} a_i \delta_{\boldsymbol{Q}_i}, \qquad \left(\sum_{i=1}^{N} a_i = 1; \;\; a_i > 0, \;\; \boldsymbol{Q}_i \in \mathrm{O}(3) \;\; \text{for each } i \right) \tag{12.16}$$

In general, say, K and $N - K$ of the $\boldsymbol{Q}_i$ are in SO(3) and $\boldsymbol{\mathcal{I}}$SO(3), respectively. Then we may change the indices so that $\boldsymbol{Q}_i = \boldsymbol{R}_i \in \mathrm{SO}(3)$ for $1 \le i \le K$, and $\boldsymbol{Q}_i = \boldsymbol{\mathcal{I}R}_i \in \boldsymbol{\mathcal{I}}\mathrm{SO}(3)$ for $K + 1 \le i \le N$. Thus

$$\wp = \sum_{i=1}^{K} a_i \delta_{\boldsymbol{R}_i} + \sum_{i=K+1}^{N} a_i \delta_{\boldsymbol{\mathcal{I}R}_i} \tag{12.17}$$

can be interpreted as the orientation measure of a polycrystalline aggregate of K right-handed and $N - K$ left-handed crystallites of S, where the one labelled i has volume fraction a_i and orientation specified by rotation $\boldsymbol{R}_i$ or roto-inversion $\boldsymbol{\mathcal{I}R}_i$ with respect to the reference crystal. Associated with the orientation measure $\wp$ in (12.17) are its right-handed and left-handed parts

$$\wp^R = \sum_{i=1}^{K} a_i \delta_{\boldsymbol{R}_i}, \qquad \wp^L = \sum_{i=K+1}^{N} a_i \delta_{\boldsymbol{R}_i}, \tag{12.18}$$

which are Radon measures defined on SO(3) and pertain to the right-handed and left-handed crystallites, respectively, so that (cf. (10.52))

$$\int_{\mathrm{O}(3)} f(\boldsymbol{Q}) d\wp(\boldsymbol{Q}) = \int_{\mathrm{SO}(3)} f^R(\boldsymbol{R}) d\wp^R(\boldsymbol{R}) + \int_{\mathrm{SO}(3)} f^L(\boldsymbol{R}) d\wp^L(\boldsymbol{R}) \tag{12.19}$$

for each $f \in \mathscr{C}(\mathrm{O}(3), \mathbb{R})$.

Let $w : \mathrm{O}(3) \to \mathbb{R}$ be an ODF, and let w^R and w^L be its right- and left-handed parts. Let $\wp$ be the orientation measure on O(3) defined by w, and let $\wp^R$, and $\wp^L$ be the right-handed and left-handed parts of $\wp$. Since discrete probability measures are dense under the vague topology [206] in the metrizable space of orientation measures, there is a sequence of discrete probability measures $\wp_s^d$ $(s = 1, 2, 3, \ldots)$ on O(3) such that $\wp_s^d \to \wp$ as $s \to \infty$. For each s, let $\wp_s^{d,R}$ and $\wp_s^{d,L}$ be the right-handed and left-handed parts of $\wp_s^d$, respectively. Clearly we have $\wp_s^{d,R} \to \wp^R$ and $\wp_s^{d,L} \to \wp^L$ as $s \to \infty$.

12.3 Transformations and Symmetries

12.3.1 Inversion of Reference Placement

Let us continue our discussion on the polycrystal P (see Sect. 12.1), which is a mixture of right-handed and left-handed (Type I) triclinic crystallites of substance S in volume fractions of λ and $1-\lambda$, respectively. Recall that we have chosen a right-handed crystal C in placement $\boldsymbol{\kappa}_0(\mathsf{C})$ as reference. Let $w : \mathrm{O}(3) \to \mathbb{R}$ be the ODF that characterizes the texture at a material point $\mathtt{X}$ of P. Now consider a change of reference to a left-handed crystal, which is exactly in the placement $\boldsymbol{\mathcal{I}} \circ \boldsymbol{\kappa}_0(\mathsf{C})$, where $\boldsymbol{\mathcal{I}} = -\boldsymbol{I}$ is the inversion. Let $\widetilde{\mathcal{T}}_{\boldsymbol{\mathcal{I}}} w$ be the ODF at $\mathtt{X}$ after the change of reference. Similar to the discussions on (5.9), we arrive at the conclusion that the transformed ODF is given by

$$(\widetilde{\mathcal{T}}_{\boldsymbol{\mathcal{I}}} w)(\boldsymbol{P}) = w(\boldsymbol{P}\boldsymbol{\mathcal{I}}) = w(\boldsymbol{\mathcal{I}}\boldsymbol{P}) \qquad \text{for each } \boldsymbol{P} \in \mathrm{O}(3). \tag{12.20}$$

It then follows from Definition 12.1 that

$$(\widetilde{\mathcal{T}}_{\boldsymbol{\mathcal{I}}} w)^R(\boldsymbol{R}) = (\widetilde{\mathcal{T}}_{\boldsymbol{\mathcal{I}}} w)(\boldsymbol{R}) = w(\boldsymbol{\mathcal{I}}\boldsymbol{R}) = w^L(\boldsymbol{R}) \qquad \text{for } \boldsymbol{R} \in \mathrm{SO}(3), \tag{12.21}$$

$$(\widetilde{\mathcal{T}}_{\boldsymbol{\mathcal{I}}} w)^L(\boldsymbol{R}) = (\widetilde{\mathcal{T}}_{\boldsymbol{\mathcal{I}}} w)(\boldsymbol{\mathcal{I}}\boldsymbol{R}) = w(\boldsymbol{R}) = w^R(\boldsymbol{R}) \qquad \text{for } \boldsymbol{R} \in \mathrm{SO}(3). \tag{12.22}$$

Hence, if we put w as $w = (w^R, w^L)$, then

$$\widetilde{\mathcal{T}}_{\boldsymbol{\mathcal{I}}} w = \big((\widetilde{\mathcal{T}}_{\boldsymbol{\mathcal{I}}} w)^R, (\widetilde{\mathcal{T}}_{\boldsymbol{\mathcal{I}}} w)^L\big) = (w^L, w^R). \tag{12.23}$$

12.3.2 Polycrystalline Aggregates of Type II Crystallites

Consider a polycrystal P that consists of Type II crystallites of some substance S. Let $(\mathsf{C}, \boldsymbol{\kappa}_0)$ be an ideal crystal C of S in the placement $\boldsymbol{\kappa}_0$. We choose a coordinates system in $\boldsymbol{\kappa}_0(\mathsf{C})$ so that the origin O is at a center of inversion of the crystal. Then $\boldsymbol{\mathcal{I}}$ is an element of the point group G_2 of the ideal crystal, which implies $\boldsymbol{\mathcal{I}} \circ \boldsymbol{\kappa}_0(\mathsf{C}) = \boldsymbol{\kappa}_0(\mathsf{C})$. Suppose at the sampling point $\mathtt{X}$ of P the ODF is $w : \mathrm{O}(3) \to \mathbb{R}$. Let w^R and w^L be the right-handed and left-handed parts of w, respectively. Under an inversion of the reference crystal $\boldsymbol{\kappa}_0(\mathsf{C})$, as nothing has changed the ODF remains the same, i.e.,

$$\widetilde{\mathcal{T}}_{\boldsymbol{\mathcal{I}}} w = w = (w^R, w^L). \tag{12.24}$$

On the other hand, by (12.23) we have $\widetilde{\mathcal{T}}_{\boldsymbol{\mathcal{I}}} w = (w^L, w^R)$, which together with (12.24) imply that $(w^R, w^L) = (w^L, w^R)$ or $w^R = w^L$. Hence we arrive at the following proposition.

Proposition 12.3 *The right- and left-handed parts w^R and w^L of the ODF w of any polycrystalline aggregate of Type II crystallites are identical.* □

From (12.8) and Proposition 12.3 we immediately obtain for the ODF w of any polycrystalline aggregate of Type II crystallites the relations

$$\int_{\mathrm{SO}(3)} w^R(\boldsymbol{R})\, d\mathcal{V} = \frac{1}{2}, \qquad \int_{\mathrm{SO}(3)} w^L(\boldsymbol{R})\, d\mathcal{V} = \frac{1}{2}. \tag{12.25}$$

In fact (12.25) can also be read off from the consequence of Proposition 12.3 that $c_{mn}^{l,R} = c_{mn}^{l,L}$ for all l, m, and n. For $l = m = n = 0$, we obtain from $(12.12)_1$ and $(12.14)_1$ that

$$c_{00}^{0,R} = c_{00}^{0,L} = c_{00}^{0,+} = \frac{1}{16\pi^2}. \tag{12.26}$$

We can gain a deeper understanding of the rationale behind Proposition 12.3 in another way. Since G_2 is of Type II, we have $G_2 = G_1 \cup \mathcal{I}G_1$, where G_1 is the proper point group in the same Laue class of G_2; see Table 3. Let

$$G_1 = \{\boldsymbol{R}_1, \ldots, \boldsymbol{R}_N\}, \qquad G_2 = \{\boldsymbol{R}_1, \ldots, \boldsymbol{R}_N, \mathcal{I}\boldsymbol{R}_1, \ldots, \mathcal{I}\boldsymbol{R}_N\}. \tag{12.27}$$

The orientation measure of an ideal crystal of S whose orientation with respect to the reference configuration $\boldsymbol{\kappa}_0(\mathsf{C})$ can be specified by a rotation $\boldsymbol{R}_0$ is (cf. [95, 206]; see also (8.12))

$$\wp_2(\boldsymbol{R}_0) = \frac{1}{2N}\left(\sum_{i=1}^{N}(\delta_{\boldsymbol{R}_0\boldsymbol{R}_i} + \delta_{\mathcal{I}\boldsymbol{R}_0\boldsymbol{R}_i})\right). \tag{12.28}$$

Let $\wp_2^R(\boldsymbol{R}_0)$ and $\wp_2^L(\boldsymbol{R}_0)$ be the corresponding right-handed and left-handed parts of $\wp_2(\boldsymbol{R}_0)$, respectively; see Sect. 12.2. We have

$$\wp_2^R(\boldsymbol{R}_0) = \wp_2^L(\boldsymbol{R}_0) = \frac{1}{2N}\sum_{i=1}^{N}\delta_{\boldsymbol{R}_0\boldsymbol{R}_i}. \tag{12.29}$$

It follows from (8.11) and (12.29) that the texture coefficients pertaining to $\wp_2^R(\boldsymbol{R}_0)$ and $\wp_2^L(\boldsymbol{R}_0)$ are:

$$c_{mn}^{l,R} = c_{mn}^{l,L} = \frac{2l+1}{8\pi^2}\cdot\frac{1}{2N}\sum_{i=1}^{N}\overline{D_{mn}^{l}(\boldsymbol{R}_0\boldsymbol{R}_i)}. \tag{12.30}$$

Consider a generic polycrystalline aggregate of a finite number of crystallites of S, which are indexed by $\alpha \in \{1, 2, \ldots, K\}$, have volume fractions a_α, and have orientations with respect to the reference $(\mathsf{C}, \boldsymbol{\kappa}_0)$ specified by the rotations $\boldsymbol{R}_0^{(\alpha)}$. The orientation measure of the polycrystalline aggregate is the discrete measure

$$\wp^d = \sum_{\alpha=1}^{K} a_\alpha \wp_2(\boldsymbol{R}_0^{(\alpha)}), \qquad \left(\sum_{\alpha=1}^{K} a_\alpha = 1; \quad a_\alpha > 0 \ \text{ for each } \alpha\right) \tag{12.31}$$

with corresponding right-handed and left-handed parts

$$\wp^{d,R} := \sum_{\alpha=1}^{K} a_\alpha \wp_2^R(\boldsymbol{R}_0^{(\alpha)}), \qquad \wp^{d,L} := \sum_{\alpha=1}^{K} a_\alpha \wp_2^L(\boldsymbol{R}_0^{(\alpha)}) \tag{12.32}$$

defined on SO(3). We have

$$\wp^{d,R} = \wp^{d,L}, \tag{12.33}$$

because $\wp_2^R(\boldsymbol{R}_0^{(\alpha)}) = \wp_2^L(\boldsymbol{R}_0^{(\alpha)})$ for each α. It follows immediately that the equality $c_{mn}^{l,R} = c_{mn}^{l,L}$ between all corresponding texture coefficients pertaining to $\wp_2^R(\boldsymbol{R}_0^{(\alpha)})$ and $\wp_2^L(\boldsymbol{R}_0^{(\alpha)})$

remains valid. Let a square-integrable ODF $w : \mathrm{O}(3) \to \mathbb{R}$ be given, and let w^R and w^L be its right- and left-handed parts. Let $\wp$ be the probability measure defined by w, and let $\wp^R$ and $\wp^L$ be the right-handed and left-handed parts of $\wp$, respectively. Clearly we have $w^R = d\wp^R/d\mathcal{V}$ and $w^L = d\wp^L/d\mathcal{V}$. Since discrete probability measures are dense under the vague topology in the metrizable space of orientation measures on O(3) [206], there is a sequence of discrete probability measures $\wp_s^d$ $(s = 1, 2, \ldots)$ in O(3) with corresponding right-handed and left-handed parts $\wp_s^{d,R}$ and $\wp_s^{d,L}$ on SO(3), which satisfy $\wp_s^{d,R} = \wp_s^{d,L}$ for each s, such that $\wp_s^d \to \wp$, $\wp_s^{d,R} \to \wp^R$, and $\wp_s^{d,L} \to \wp^L$, as $s \to \infty$. It follows that $\wp^R = \wp^L$ and $w^R = w^L$.

12.3.3 Texture and Crystallite Symmetries

Let $w : \mathrm{O}(3) \to \mathbb{R}$ be the ODF that characterizes the texture at a material point $\mathtt{x}$ of a given polycrystal. Let $\mathcal{T}_{\boldsymbol{Q}} w$ and $\widetilde{\mathcal{T}}_{\boldsymbol{Q}} w$ be the ODF of the polycrystal after it undergoes a rotation or roto-inversion and after the configuration of the reference single crystal undergoes a rotation or roto-inversion $\boldsymbol{Q} \in \mathrm{O}(3)$, respectively. Parallel to (5.3) and (5.9), we have

$$(\mathcal{T}_{\boldsymbol{Q}} w)(\boldsymbol{P}) = w(\boldsymbol{Q}^T \boldsymbol{P}) \qquad \text{for each } \boldsymbol{P} \in \mathrm{O}(3), \tag{12.34}$$

and

$$(\widetilde{\mathcal{T}}_{\boldsymbol{Q}} w)(\boldsymbol{P}) = w(\boldsymbol{P}\boldsymbol{Q}) \qquad \text{for each } \boldsymbol{P} \in \mathrm{O}(3). \tag{12.35}$$

The groups of texture symmetry and crystallite symmetry are defined respectively as follows:

$$G_{\mathrm{tex}} = \{\boldsymbol{Q} \in \mathrm{O}(3) : \mathcal{T}_{\boldsymbol{Q}} w = w\}, \tag{12.36}$$

$$G_{\mathrm{cr}} = \{\boldsymbol{Q} \in \mathrm{O}(3) : \widetilde{\mathcal{T}}_{\boldsymbol{Q}} w = w\}. \tag{12.37}$$

Similar to the findings in Chap. 5, texture and crystallite symmetry will each impose restrictions on texture coefficients. See [65] and [94] for details.

12.4 The Reduced ODF

Let P be a polycrystal of Type II or Type III crystallites, and let $w : \mathrm{O}(3) \to \mathbb{R}$ be the ODF of P as given by (12.5). The crystallites of P have an improper G_{cr}. In the Laue class that contains G_{cr}, however, there is one rotational member G_{cr}^I. In classical texture analysis the crystallites of P are treated as if their point group were G_{cr}^I, not G_{cr}. The crystallographic texture of polycrystal P is then represented by the reduced ODF $w_r : \mathrm{SO}(3) \to \mathbb{R}$ with the expansion

$$w_r(\boldsymbol{R}) = \frac{1}{8\pi^2} + \sum_{l=1}^{\infty} \sum_{m=-l}^{l} \sum_{n=-l}^{l} c_{mn}^l D_{mn}^l(\boldsymbol{R}(\psi, \theta, \phi)), \tag{12.38}$$

which satisfies the normalization condition

$$\int_{\mathrm{SO}(3)} w_r(\psi, \theta, \phi)\, d\mathcal{V} = 1. \tag{12.39}$$

Henceforth we shall call the texture coefficients of P in classical texture analysis, namely c^l_{mn}, the reduced texture coefficients of P.

The question that we want to address in this section is [206]: How are the reduced texture coefficients c^l_{mn} of w_r related to the coefficients $c^{l,R}_{mn}$ and $c^{l,L}_{mn}$ of w?

Our analysis in Sect. 12.3.2 has largely provided an answer to this question for polycrystalline aggregates of Type II crystallites. If we regard the crystallites of P with $G_{\mathrm{cr}} = G_2$ in (12.27) as having $G_{\mathrm{cr}} = G_1$ in the same equation, then the orientation measure given in (12.31) for the single crystal with orientation specified by a rotation $\boldsymbol{R}_0$ with respect to the reference will be replaced by

$$\wp_r(\boldsymbol{R}_0) = \frac{1}{N}\sum_{i=1}^{N} \delta_{\boldsymbol{R}_0 \boldsymbol{R}_i} = 2\wp_2^R(\boldsymbol{R}_0) \qquad \text{on SO(3)}, \tag{12.40}$$

where we have appealed to (12.29). It follows that the discrete measure $\wp^d$ given in (12.31) will be replaced by

$$\wp_r^d = 2\wp^{d,R}, \tag{12.41}$$

where $\wp^{d,R}$ is given by $(12.32)_1$. If we go through the analysis in Sect. 12.3.2, we will get at the end $w_r = 2w^R$ and

$$c^l_{mn} = 2c^{l,R}_{mn} = c^{l,R}_{mn} + c^{l,L}_{mn}. \tag{12.42}$$

12.4.1 Polycrystalline Aggregates of Type III Crystallites

Let P be a polycrystal of Type III crystallites of a substance S. Let $G_{\mathrm{cr}} = G_3$ and $G_1 \subset \mathrm{SO}(3)$ be the proper point group in the same Laue class as G_3. By Theorem 2.35, there is a normal subgroup H of index 2 in G_1 and a rotation $\boldsymbol{P} \in G_1 \setminus H$ such that

$$G_1 = H \cup \boldsymbol{P}H, \qquad G_3 = H \cup \boldsymbol{\mathcal{I}}\boldsymbol{P}H. \tag{12.43}$$

Let H have order N, and let $\boldsymbol{R}_k$ $(k = 1, \ldots, N)$ be the elements of H. Then we have

$$G_1 = \{\boldsymbol{R}_1, \ldots, \boldsymbol{R}_N, \boldsymbol{P}\boldsymbol{R}_1, \ldots, \boldsymbol{P}\boldsymbol{R}_N\}, \qquad G_3 = \{\boldsymbol{R}_1, \ldots \boldsymbol{R}_N, \boldsymbol{\mathcal{I}}\boldsymbol{P}\boldsymbol{R}_1, \ldots, \boldsymbol{\mathcal{I}}\boldsymbol{P}\boldsymbol{R}_N\}. \tag{12.44}$$

To describe the crystallite orientation at a point $\mathtt{x}$ in a sample of P, we choose an ideal crystal C of S in a reference configuration $\boldsymbol{\kappa}_0(\mathsf{C})$. Instead of the polycrystal P, we start by considering a single crystal $(\mathsf{C}, \boldsymbol{\kappa}_{\boldsymbol{R}_0})$ of S whose placement in space is given by $\boldsymbol{\kappa}_{\boldsymbol{R}_0} = \boldsymbol{R}_0 \circ \boldsymbol{\kappa}_0$, where $\boldsymbol{R}_0$ is a rotation. The orientation measure of the single crystal with placement $\boldsymbol{\kappa}_{\boldsymbol{R}_0}$ is given by (cf. [95, 206]; see also (8.12))

$$\wp_3(\boldsymbol{R}_0) = \frac{1}{2N}\left(\sum_{i=1}^{N}(\delta_{\boldsymbol{R}_0\boldsymbol{R}_i} + \delta_{\boldsymbol{\mathcal{I}}\boldsymbol{R}_0\boldsymbol{P}\boldsymbol{R}_i})\right). \tag{12.45}$$

The corresponding right-handed and left-hand parts of $\wp_3(\boldsymbol{R}_0)$, namely

$$\wp_3^R(\boldsymbol{R}_0) = \frac{1}{2N}\sum_{i=1}^{N}\delta_{\boldsymbol{R}_0\boldsymbol{R}_i}, \qquad \wp_3^L(\boldsymbol{R}_0) = \frac{1}{2N}\sum_{i=1}^{N}\delta_{\boldsymbol{R}_0\boldsymbol{P}\boldsymbol{R}_i}, \tag{12.46}$$

respectively, are Radon measures defined on SO(3) such that for $f \in \mathscr{C}(\mathrm{O}(3), \mathbb{C})$ we have (cf. Sect. 10.6.2)

$$\int_{\mathrm{O}(3)} f(\boldsymbol{Q}) d\wp_3(\boldsymbol{Q}) = \int_{\mathrm{SO}(3)} f^R(\boldsymbol{R}) d\wp_3^R(\boldsymbol{R}) + \int_{\mathrm{SO}(3)} f^L(\boldsymbol{R}) d\wp_3^L(\boldsymbol{R}). \tag{12.47}$$

The texture coefficients pertaining to $\wp_3^R(\boldsymbol{R}_0)$ and $\wp_3^L(\boldsymbol{R}_0)$ are

$$c_{mn}^{l,R} = \frac{2l+1}{8\pi^2} \cdot \frac{1}{2N} \sum_{i=1}^{N} \overline{D_{mn}^l(\boldsymbol{R}_0 \boldsymbol{R}_i)}, \qquad c_{mn}^{l,l} = \frac{2l+1}{8\pi^2} \cdot \frac{1}{2N} \sum_{i=1}^{N} \overline{D_{mn}^l(\boldsymbol{R}_0 \boldsymbol{P} \boldsymbol{R}_i)}, \tag{12.48}$$

respectively. If G_{cr} of the single crystal in question is taken to be G_1, then the orientation measure of the crystal is

$$\wp_r(\boldsymbol{R}_0) = \frac{1}{2N} \sum_{i=1}^{2N} \left(\delta_{\boldsymbol{R}_0 \boldsymbol{R}_i} + \delta_{\boldsymbol{R}_0 \boldsymbol{P} \boldsymbol{R}_i} \right), \tag{12.49}$$

and the corresponding reduced texture coefficients are given by

$$c_{mn}^{l} = \frac{2l+1}{8\pi^2} \cdot \frac{1}{2N} \sum_{i=1}^{N} \left(\overline{D_{mn}^l(\boldsymbol{R}_0 \boldsymbol{R}_i)} + \overline{D_{mn}^l(\boldsymbol{R}_0 \boldsymbol{P} \boldsymbol{R}_i)} \right). \tag{12.50}$$

Note that we have

$$\wp_r(\boldsymbol{R}_0) = \wp_3^R(\boldsymbol{R}_0) + \wp_3^L(\boldsymbol{R}_0), \qquad c_{mn}^{l} = c_{mn}^{l,R} + c_{mn}^{l,L}. \tag{12.51}$$

Consider a generic polycrystalline aggregate of a finite number of crystallites of S, which are indexed by $\alpha \in \{1, 2, \ldots, K\}$, have volume fractions a_α, and have orientations with respect to the reference $(\mathsf{C}, \boldsymbol{\kappa}_0)$ specified by the rotations $\boldsymbol{R}_0^{(\alpha)}$. The orientation measure of the polycrystalline aggregate is the discrete measure

$$\wp^d = \sum_{\alpha=1}^{K} a_\alpha \wp_3(\boldsymbol{R}_0^{(\alpha)}), \qquad \left(\sum_{\alpha=1}^{K} a_\alpha = 1; \quad a_\alpha > 0 \ \text{ for each } \alpha \right) \tag{12.52}$$

on O(3), which has corresponding right-handed and left-handed parts

$$\wp^{d,R} := \sum_{\alpha=1}^{K} a_\alpha \wp_3^R(\boldsymbol{R}_0^{(\alpha)}), \qquad \wp^{d,L} := \sum_{\alpha=1}^{K} a_\alpha \wp_3^L(\boldsymbol{R}_0^{(\alpha)}) \tag{12.53}$$

defined on SO(3). In comparison, if we treat the crystallites as if their G_{cr} is G_1, the orientation measure of the polycrystal becomes

$$\wp_r^d = \sum_{\alpha=1}^{K} a_\alpha \wp_r(\boldsymbol{R}_0^{(\alpha)}) = \sum_{\alpha=1}^{K} a_\alpha \left(\wp_3^R(\boldsymbol{R}_0^{(\alpha)}) + \wp_3^L(\boldsymbol{R}_0^{(\alpha)}) \right) = \wp^{d,R} + \wp^{d,L}. \tag{12.54}$$

Let $w : \mathrm{O}(3) \to \mathbb{R}$ be the square-integrable ODF that defines the texture of a polycrystalline aggregate P of Type III crystallites, and let $\wp$ be the orientation measure on O(3)

defined by w. Let $w^R, w^L : \mathrm{SO}(3) \to \mathbb{R}$ be the right-handed and left-handed parts of w, respectively, and let $w_r : \mathrm{SO}(3) \to \mathbb{R}$ be the reduced ODF pertaining to P. Let $\wp^R$, $\wp^L$, and $\wp_r$ be the Radon measures on SO(3) defined by w^R, w^L, and w_r, respectively. Since discrete probability measures are dense under the vague topology in the metrizable space of orientation measures on O(3), there is a sequence of discrete probability measures $\wp_s^d$ $(s = 1, 2, \ldots)$ in O(3) such that $\wp_s^d \to \wp$ as $s \to \infty$. For each s, the discrete Radon measures $\wp_s^{d,R}$, $\wp_s^{d,L}$ and $\wp_{r,s}^d$ are well defined on SO(3) and by (12.54)

$$\wp_{r,s}^d = \wp_s^{d,R} + \wp_s^{d,L}. \tag{12.55}$$

We have $\wp_s^{d,R} \to \wp^R$, $\wp_s^{d,L} \to \wp^L$, and $\wp_{r,s}^d \to \wp_r$, as $s \to \infty$. It follows that $\wp_r = \wp^R + \wp^L$ and

$$c_{mn}^l = c_{mn}^{l,R} + c_{mn}^{l,L}. \tag{12.56}$$

See [206] for more details.

PART III. GROUP REPRESENTATIONS

Chapter 13

13 Group Representations

13.1 Preliminaries: Complex Inner-Product Spaces

Let X be a finite-dimensional vector space over the field $\mathbb{C}$ of complex numbers, which we shall simply call complex vector space. A Hermitian inner product on X is a mapping $\langle \cdot, \cdot \rangle : X \times X \to \mathbb{C}$ that satisfies the following conditions:

1. For all $\boldsymbol{x}_1, \boldsymbol{x}_2$, and $\boldsymbol{y} \in X$, $\langle \boldsymbol{x}_1 + \boldsymbol{x}_2, \boldsymbol{y} \rangle = \langle \boldsymbol{x}_1, \boldsymbol{y} \rangle + \langle \boldsymbol{x}_2, \boldsymbol{y} \rangle$.
2. For all $\boldsymbol{x}, \boldsymbol{y} \in X$ and $\alpha \in \mathbb{C}$, $\langle \alpha \boldsymbol{x}, \boldsymbol{y} \rangle = \alpha \langle \boldsymbol{x}, \boldsymbol{y} \rangle$.
3. For all $\boldsymbol{x}, \boldsymbol{y} \in X$, $\langle \boldsymbol{x}, \boldsymbol{y} \rangle = \overline{\langle \boldsymbol{y}, \boldsymbol{x} \rangle}$.
4. For all $\boldsymbol{x} \in X$, $\langle \boldsymbol{x}, \boldsymbol{x} \rangle \geq 0$, and $\langle \boldsymbol{x}, \boldsymbol{x} \rangle = 0$ if and only if $\boldsymbol{x} = \boldsymbol{0}$.

From conditions 2 and 3 we infer that

$$\langle \boldsymbol{x}, \alpha \boldsymbol{y} \rangle = \overline{\alpha} \langle \boldsymbol{x}, \boldsymbol{y} \rangle \qquad \text{for all } \boldsymbol{x}, \boldsymbol{y} \in X \text{ and } \alpha \in \mathbb{C}. \tag{13.1}$$

A complex vector space equipped with a Hermitian inner product is called a complex inner-product space (or simply inner product space if no confusion should arise).

13.1.1 Adjoint, Hermitian, Unitary, and Normal Transformations

Let X and Y be complex inner-product spaces. Given a linear transformation $\boldsymbol{A} : X \to Y$, there is a unique linear transformation $\boldsymbol{A}^*$, called the adjoint of $\boldsymbol{A}$, such that

$$\langle \boldsymbol{A}\boldsymbol{x}, \boldsymbol{y} \rangle_Y = \langle \boldsymbol{x}, \boldsymbol{A}^* \boldsymbol{y} \rangle_X \qquad \text{for each } \boldsymbol{x} \in X \text{ and } \boldsymbol{y} \in Y; \tag{13.2}$$

see, e.g., [40, 105–108], [273, 227–228]. It is easy to verify that adjoint linear transformations enjoy the following properties: (1) $(\boldsymbol{A} + \boldsymbol{B})^* = \boldsymbol{A}^* + \boldsymbol{B}^*$; (2) $(\alpha \boldsymbol{A})^* = \overline{\alpha} \boldsymbol{A}^*$ for each $\alpha \in \mathbb{C}$; (3) $(\boldsymbol{A}^*)^* = \boldsymbol{A}$; (4) if $\boldsymbol{A}$ is invertible, so is $\boldsymbol{A}^*$, and $(\boldsymbol{A}^*)^{-1} = (\boldsymbol{A}^{-1})^*$; (5) for $\boldsymbol{A} : X \to Y$ and $\boldsymbol{B} : Y \to Z$, $(\boldsymbol{B}\boldsymbol{A})^* = \boldsymbol{A}^* \boldsymbol{B}^*$.

A linear transformation $\boldsymbol{A} : X \to X$ is said to be Hermitian, unitary, and normal if its adjoint satisfies $\boldsymbol{A}^* = \boldsymbol{A}$, $\boldsymbol{A}^* = \boldsymbol{A}^{-1}$, and $\boldsymbol{A}\boldsymbol{A}^* = \boldsymbol{A}^* \boldsymbol{A}$, respectively. Hermitian and unitary transformations are clearly normal.

If $\boldsymbol{A}$ is a unitary linear transformation, we have

$$\langle \boldsymbol{A}\boldsymbol{x}, \boldsymbol{A}\boldsymbol{y} \rangle = \langle \boldsymbol{x}, \boldsymbol{A}^* \boldsymbol{A} \boldsymbol{y} \rangle = \langle \boldsymbol{x}, \boldsymbol{y} \rangle \qquad \text{for all } \boldsymbol{x}, \boldsymbol{y} \in X. \tag{13.3}$$

Let $\dim X = n$, and let $\{\boldsymbol{e}_1, \ \ldots, \boldsymbol{e}_n\}$ be an orthonormal basis in X, i.e., a set of vectors in X which satisfy

$$\langle \boldsymbol{e}_i, \boldsymbol{e}_j \rangle = \delta_{ij}. \tag{13.4}$$

Let $\boldsymbol{A}$ be unitary and let $A = [A_{ij}]$ be the matrix that represents $\boldsymbol{A}$ with respect to the basis $\{\boldsymbol{e}_i\}$. Then we have $\boldsymbol{A}\boldsymbol{e}_k = \sum_j A_{jk} \boldsymbol{e}_j$, and

$$\begin{aligned} \langle \boldsymbol{A}\boldsymbol{e}_i, \boldsymbol{A}\boldsymbol{e}_j \rangle &= \sum_k \sum_l A_{ki} \overline{A_{lj}} \langle \boldsymbol{e}_k, \boldsymbol{e}_l \rangle = \sum_k \sum_l A_{ki} \overline{A_{lj}} \, \delta_{kl} \\ &= \sum_k A_{ki} \overline{A_{kj}} = \sum_k A^T_{ik} \overline{A_{kj}}. \end{aligned} \tag{13.5}$$

On the other hand, there holds

$$\langle \boldsymbol{A}\boldsymbol{e}_i, \boldsymbol{A}\boldsymbol{e}_j \rangle = \langle \boldsymbol{e}_i, \boldsymbol{e}_j \rangle = \delta_{ij}, \tag{13.6}$$

because $\boldsymbol{A}$ is unitary. Comparing (13.5) with (13.6), we conclude that

$$A^{-1} = \overline{A}^T. \tag{13.7}$$

Similarly, a square matrix A that represents a Hermitian linear transformation $\boldsymbol{A} : X \to X$ under an orthonormal basis in X satisfies the equation $A = \overline{A}^T$.

13.2 Basic Definitions and Theorems

As far as group representations are concerned, we are mainly interested in their applications to texture analysis, which serve also as preparations for the study of physics of textured polycrystals. For these purposes we shall restrict attention to finite and compact topological groups and focus on the following topics: (1) irreducible unitary representations of SO(3), O(3), and their subgroups; (2) derivation of the Wigner D-functions as matrix elements of a complete set of irreducible unitary representations of SO(3); (3) an elementary proof of the Peter-Weyl theorem, which when applied to the rotation group shows that any continuous function on SO(3) can be uniformly approximated by linear combinations of the Wigner D-functions; (4) tensor and pseudotensor representations of SO(3) and O(3). To prepare for our discussions on these topics, we shall present in this chapter the basics of finite-dimensional representations of finite and compact groups, as no mention of infinite-dimensional representations of compact groups on Hilbert spaces is necessary.[141] Our main general references for this chapter are Naimark and Štern [245] and Serre [296].

The theory of finite-dimensional representations for finite groups and for compact topological groups are essentially the same. For both, an essential tool is the invariant mean $M(f)$ of a function $f : G \to \mathbb{C}$ on the group G in question, where

$$M(f) = \begin{cases} \frac{1}{|G|} \sum_{h \in G} f(h), & \text{for finite group } G \\ \int_G f(h)\, d\mathfrak{g}(h) & \text{for compact group } G. \end{cases} \tag{13.8}$$

In (13.8) for finite groups, $|G|$ is the order of G. For compact groups, the integral in (13.8) denotes the normalized Haar integral (or equivalently, $\mathfrak{g}$ denotes the normalized Haar measure).[142] For both cases, the invariant mean satisfies

$$M(f) = M_h(f(gh)) = M_h(f(hg)) \quad \text{for each } g \in G, \qquad M_h(f(h^{-1})) = M_h(f(h)). \tag{13.9}$$

[141] On the other hand, note that any irreducible unitary representation of a compact group on a Hilbert space is finite dimensional; see, e.g., [243], [305, pp. 16–18].

[142] In this exposition we have derived the existence, uniqueness, and main properties of the normalized Haar integral only for the groups SO(3) and O(3), and we shall only use those in applications discussed later. For the general theory of the Haar integral on compact groups, we refer the reader to the literature (see the references cited in Sect. C.3 of Appendix C.

13.2.1 Finite-Dimensional Representations of Groups

Definition 13.1 Let G be a group and $X \neq \{\mathbf{0}\}$ a finite-dimensional complex vector space. A (finite-dimensional) linear representation $(\boldsymbol{T}, X)$ of G is a homomorphism of G into the group $\mathrm{GL}(X)$ of invertible linear transformations on X, i.e., $\boldsymbol{T} : G \to \mathrm{GL}(X)$, which satisfies

$$\boldsymbol{T}(g_1)\boldsymbol{T}(g_2) = \boldsymbol{T}(g_1 g_2) \qquad \text{for all } g_1, g_2 \in G. \tag{13.10}$$

The linear space X and $\dim X$ are called the representation space and the dimension of representation $\boldsymbol{T}$, respectively.

When G is a topological group, the representation $(\boldsymbol{T}, X)$ is said to be continuous if it is a continuous map from G to $\mathrm{GL}(X)$. □

Remark 13.2 Let $\dim X = n$. If we choose a basis in X so that each $\boldsymbol{T}(g)$ is represented by an $n \times n$ matrix $[T_{ij}(g)]$, then $\boldsymbol{T}(g)$ can be taken as an operator on $\mathbb{C}^n$ and the correspondence $g \mapsto [T_{ij}(g)]$ satisfies (13.10). Conversely, suppose a matrix function $\boldsymbol{T}$ from G to the space $M_n(\mathbb{C})$ of $n \times n$ matrices is defined so that (13.10) is observed. Then $\boldsymbol{T} : G \to \mathrm{GL}(\mathbb{C}^n)$ is a representation of G. Hence we can view each finite-dimensional representation of G as a matrix representation. If G is a compact topological group, a representation $\boldsymbol{T}$ of G is continuous if and only if for each $g \in G$ the matrix elements $T_{ij}(g)$ are continuous functions of g. □

Henceforth in this chapter we shall only consider finite-dimensional representations of groups and shall omit the adjective "finite-dimensional" except at times for emphasis.

It follows from (13.10) that

$$\boldsymbol{T}(e) = \boldsymbol{I}, \qquad \boldsymbol{T}(g^{-1}) = (\boldsymbol{T}(g))^{-1}, \tag{13.11}$$

where e is the identity element in G, g^{-1} the inverse of g, and $\boldsymbol{I}$ the identity operator on X. In what follows, when there should be no confusion on the space X on which the linear transformations $\boldsymbol{T}(g)$ are defined, we shall often simply refer to $(\boldsymbol{T}, X)$ as representation $\boldsymbol{T}$ of G.

Let $\mathrm{Ker}\,\boldsymbol{T} = \{g \in G : \boldsymbol{T}(g) = \boldsymbol{I}\}$ be the kernel of the homomorphism $\boldsymbol{T}$. The representation $\boldsymbol{T}$ is said to be faithful if $\mathrm{Ker}\,\boldsymbol{T} = \{e\}$. For all matrix groups $G \subset \mathrm{GL}(\mathbb{C}^n)$, the self-representation $\boldsymbol{T}_s : g \mapsto g$ is clearly a faithful representation of G.

A subspace $M \subset X$ is said to be invariant under a representation $\boldsymbol{T}$ or G-invariant if it is invariant under all operators $\boldsymbol{T}(g)$ of this representation.

Definition 13.3 Let $\boldsymbol{T} : G \to \mathrm{GL}(X)$ be a representation, and let M be a G-invariant subspace of X. For each $g \in G$, let $\boldsymbol{T}(g)|_M$ be the restriction of the operator $\boldsymbol{T}(g)$ to M. The map $\boldsymbol{T}|_M : G \to \mathrm{GL}(M)$, $g \mapsto \boldsymbol{T}(g)|_M$ is a homomorphism, and the representation $(\boldsymbol{T}|_M, M)$ is called the restriction of the representation $\boldsymbol{T}$ to M and a subrepresentation of $\boldsymbol{T}$. □

Definition 13.4 A representation $(\boldsymbol{T}, X)$ of group G is said to be irreducible if X contains no G-invariant subspace except $\{\mathbf{0}\}$ and X itself. A representation that is not irreducible is called reducible. □

Proposition 13.5 *Every finite-dimensional representation has an irreducible subrepresentation.*

Proof Let $(\boldsymbol{T}, X)$ be a finite-dimensional representation of group G. If $\boldsymbol{T}$ is irreducible, then the proof is done. If $\boldsymbol{T}$ is reducible, then there is a G-invariant subspace M_1 such that $\{\mathbf{0}\} \subsetneqq M_1 \subsetneqq X$. If the subrepresentation $\boldsymbol{T}\big|_{M_1}$ is irreducible, the proof is done. If $\boldsymbol{T}\big|_{M_1}$ is reducible, then there is a G-invariant subspace M_2 such that $\{\mathbf{0}\} \subsetneqq M_2 \subsetneqq M_1$. By repeating this argument, we obtain G-invariant subspaces $X \supsetneqq M_1 \supsetneqq M_2 \cdots \supsetneqq M_k \supsetneqq \{\mathbf{0}\}$, where $\dim X > \dim M_1 > \dim M_2 > \cdots \geq 1$. Since $\dim X$ is finite, the process must stop at some G-invariant subspace M_k such that the subrepresentation $\boldsymbol{T}\big|_{M_k}$ is irreducible. □

13.2.2 Equivalence of Representations

Definition 13.6 Two representations $(\boldsymbol{T}, X)$ and $(\boldsymbol{S}, Y)$ of a group G are said to be equivalent, where we write $(\boldsymbol{T}, X) \cong (\boldsymbol{S}, Y)$ or simply $\boldsymbol{T} \cong \boldsymbol{S}$, if there is a linear isomorphism $\boldsymbol{A} : X \to Y$ such that

$$\boldsymbol{A}\boldsymbol{T}(g) = \boldsymbol{S}(g)\boldsymbol{A} \qquad \text{for each } g \in G. \tag{13.12}$$

□

Theorem 13.7 *Two finite-dimensional representations $(\boldsymbol{T}, X)$ and $(\boldsymbol{S}, Y)$ of a group G are equivalent if and only if (i) $\dim X = \dim Y$ and (ii) suitable basis can be chosen in X and in Y such that $\boldsymbol{T}(g)$ and $\boldsymbol{S}(g)$ are represented by the same matrix $[T_{ij}(g)]$ for each $g \in G$.*

Proof Suppose the finite-dimensional representations $(\boldsymbol{T}, X)$ and $(\boldsymbol{S}, Y)$ of the group G are equivalent. It is obvious that $\dim X = \dim Y = n$ for some positive integer n. Let $\boldsymbol{e}_1, \ldots, \boldsymbol{e}_n$ be an arbitrary basis in X. Let $\boldsymbol{f}_j = \boldsymbol{A}\boldsymbol{e}_j$ $(j = 1, \ldots, n)$. Since $\boldsymbol{A} : X \to Y$ is a linear isomorphism, $\boldsymbol{f}_1, \ldots, \boldsymbol{f}_n$ constitute a basis in Y. Consider a specific $g \in G$. Let $[T_{jk}(g)]$ be the matrix that represents $\boldsymbol{T}(g)$ under the basis $\{\boldsymbol{e}_j : j = 1, \ldots, n\}$ in X. Then we have

$$\boldsymbol{T}(g)\boldsymbol{e}_k = \sum_j T_{jk}(g)\boldsymbol{e}_j. \tag{13.13}$$

Applying $\boldsymbol{A}$ to both sides of (13.13) and appealing to (13.12), we obtain for each $k = 1, \ldots, n$,

$$\boldsymbol{S}(g)\boldsymbol{f}_k = \boldsymbol{S}(g)\boldsymbol{A}\boldsymbol{e}_k = \boldsymbol{A}\boldsymbol{T}(g)\boldsymbol{e}_k = \sum_j T_{jk}(g)\boldsymbol{A}\boldsymbol{e}_j = \sum_j T_{jk}(g)\boldsymbol{f}_j. \tag{13.14}$$

Hence $\boldsymbol{T}(g)$ and $\boldsymbol{S}(g)$ are represented by the same matrix.

Conversely, let $\dim X = \dim Y = n$ and, under the basis $\{\boldsymbol{e}_j : j = 1, \ldots, n\}$ in X and $\{\boldsymbol{f}_j : j = 1, \ldots, n\}$ in Y, $\boldsymbol{T}(g)$ and $\boldsymbol{S}(g)$ are represented by the same matrix for each $g \in G$. Define a linear mapping $\boldsymbol{A} : X \to Y$ by

$$\boldsymbol{A}\boldsymbol{e}_j = \boldsymbol{f}_j \qquad (j = 1, \ldots, n). \tag{13.15}$$

Then $\boldsymbol{A}$ is a linear isomorphism that satisfies condition (13.12). □

13.2.3 Irreducible Representations, Schur's Lemma

Theorem 13.8 (Schur's lemma) *Let $\boldsymbol{T} : G \to \mathrm{GL}(X)$ and $\boldsymbol{S} : G \to \mathrm{GL}(Y)$ be finite-dimensional irreducible representations of group G. Let $\boldsymbol{A} : X \to Y$ be a linear mapping such that*

$$\boldsymbol{A}\boldsymbol{T}(g) = \boldsymbol{S}(g)\boldsymbol{A} \qquad \textit{for each } g \in G. \tag{13.16}$$

The two following assertions are valid:

(i) *Either* $\boldsymbol{A} = \boldsymbol{0}$ *or* $\boldsymbol{A}$ *is a linear isomorphism of* X *onto* Y (*i.e., the representations* $\boldsymbol{T}$ *and* $\boldsymbol{S}$ *are equivalent*).
(ii) *If* $X = Y$ *and* $\boldsymbol{T} = \boldsymbol{S}$, *then* $\boldsymbol{A} = \lambda \boldsymbol{I}$ *for some* $\lambda \in \mathbb{C}$.

Proof (i) It is obvious that (13.16) is satisfied if $\boldsymbol{A} = \boldsymbol{0}$.

Suppose $\boldsymbol{A} \neq \boldsymbol{0}$. Let $\operatorname{Ker} \boldsymbol{A} := \{\boldsymbol{x} \in X : \boldsymbol{A}\boldsymbol{x} = \boldsymbol{0}\}$ be the kernel of $\boldsymbol{A}$. It is a subspace of X. For each $\boldsymbol{x} \in \operatorname{Ker} \boldsymbol{A}$ and $g \in G$, we have

$$\boldsymbol{A}(\boldsymbol{T}(g)\boldsymbol{x}) = \boldsymbol{S}(g)\boldsymbol{A}\boldsymbol{x} = \boldsymbol{0}, \tag{13.17}$$

which implies $\boldsymbol{T}(g)\boldsymbol{x} \in \operatorname{Ker} \boldsymbol{A}$. Hence $\operatorname{Ker} \boldsymbol{A}$ is an invariant subspace of X under the irreducible representation $\boldsymbol{T}$ of G. It follows that either $\operatorname{Ker} \boldsymbol{A} = \{\boldsymbol{0}\}$ or $\operatorname{Ker} \boldsymbol{A} = X$. Since by hypothesis $\operatorname{Ker} \boldsymbol{A} \neq X$, we conclude that $\operatorname{Ker} \boldsymbol{A} = \{\boldsymbol{0}\}$.

Let $\operatorname{Im} \boldsymbol{A} := \{\boldsymbol{y} \in Y : \boldsymbol{y} = \boldsymbol{A}\boldsymbol{x} \text{ for some } \boldsymbol{x} \in X\}$ be the image of X under $\boldsymbol{A}$. It is a subspace of Y. Let $\boldsymbol{y} = \boldsymbol{A}\boldsymbol{x} \in \operatorname{Im} \boldsymbol{A}$, where $\boldsymbol{x} \in X$, and let $g \in G$. By (13.16) we have

$$\boldsymbol{S}(g)\boldsymbol{y} = \boldsymbol{S}(g)\boldsymbol{A}\boldsymbol{x} = \boldsymbol{A}(\boldsymbol{T}(g)\boldsymbol{x}) \in \operatorname{Im} \boldsymbol{A}, \tag{13.18}$$

because $\boldsymbol{T}(g)\boldsymbol{x} \in X$. Equation (13.18) is valid for each $\boldsymbol{y} \in \operatorname{Im} \boldsymbol{A}$ and each $g \in G$. Hence $\operatorname{Im} \boldsymbol{A}$ is an invariant subspace of Y under the irreducible representation $\boldsymbol{S}$ of G. Thus either $\operatorname{Im} \boldsymbol{A} = \{\boldsymbol{0}\}$ or $\operatorname{Im} \boldsymbol{A} = Y$. As by hypothesis $\boldsymbol{A} \neq \boldsymbol{0}$, we have $\operatorname{Im} \boldsymbol{A} = Y$.

Since $\operatorname{Ker} \boldsymbol{A} = \{\boldsymbol{0}\}$ and $\operatorname{Im} \boldsymbol{A} = Y$, we conclude that $\boldsymbol{A}$ is a linear isomorphism of X onto Y.

(ii) Consider the case $X = Y$ and $\boldsymbol{T} = \boldsymbol{S}$. Let λ be an eigenvalue of $\boldsymbol{A}$; there exists at least one eigenvalue because X is a complex vector space. Let $\boldsymbol{B} = \boldsymbol{A} - \lambda \boldsymbol{I}$. Since $\boldsymbol{A}$ commutes with $\boldsymbol{T}(g)$ for each $g \in G$, it is easy to verify that $\boldsymbol{B}$ commutes with $\boldsymbol{T}(g)$ for each $g \in G$. By assertion (i), either $\boldsymbol{B} = \boldsymbol{0}$ or $\boldsymbol{B}$ is a linear isomorphism on X. Since λ is an eigenvalue of $\boldsymbol{A}$, there is a vector $\boldsymbol{x} \in X$ such that $\boldsymbol{B}\boldsymbol{x} = (\boldsymbol{A} - \lambda \boldsymbol{I})\boldsymbol{x} = \boldsymbol{0}$. Hence $\boldsymbol{B}$ cannot be a linear isomorphism. It follows that $\boldsymbol{B} = \boldsymbol{0}$, i.e., $\boldsymbol{A} = \lambda \boldsymbol{I}$ for some $\lambda \in \mathbb{C}$. □

13.2.4 Unitary Representations, Unitary Equivalence

Definition 13.9 Let X be a finite-dimensional complex inner-product space. A representation $(\boldsymbol{T}, X)$ of group G is said to be unitary if for every $g \in G$ the linear transformation $\boldsymbol{T}(g) : X \to X$ is unitary, i.e., it satisfies

$$\langle \boldsymbol{T}(g)\boldsymbol{x}, \boldsymbol{T}(g)\boldsymbol{y} \rangle = \langle \boldsymbol{x}, \boldsymbol{y} \rangle, \qquad \text{for each } g \in G \text{ and } \boldsymbol{x}, \boldsymbol{y} \in X. \tag{13.19}$$

□

By (13.7), under an orthonormal basis in X, each $\boldsymbol{T}(g)$ is represented by a unitary matrix $[T_{ij}(g)]$ that satisfies $[T_{ij}(g)]^{-1} = [\overline{T_{ij}(g)}]^T$.

Proposition 13.10 *Let* G *be a finite or compact topological group,* X *be a complex vector space, and* $(\boldsymbol{T}, X)$ *be a finite-dimensional linear representation of* G. *A Hermitian inner product can be chosen on* X *such that the representation* $\boldsymbol{T}$ *is unitary.*

Proof We begin by picking an arbitrary Hermitian inner product $\langle \cdot, \cdot \rangle_1$ on X. (For example, let $\dim X = n$ and $\{\boldsymbol{f}_i : 1 \le i \le n\}$ be a basis in X. For $\boldsymbol{x} = \sum_i x_i \boldsymbol{f}_i$, $\boldsymbol{y} = \sum_i y_i \boldsymbol{f}_i \in X$, let $\langle \boldsymbol{x}, \boldsymbol{y} \rangle_1 = \sum_i x_i \overline{y_i}$.) For each $h \in G$ and $\boldsymbol{x}, \boldsymbol{y} \in X$, let

$$f(h; \boldsymbol{x}, \boldsymbol{y}) := \langle \boldsymbol{T}(h)\boldsymbol{x}, \boldsymbol{T}(h)\boldsymbol{y} \rangle_1. \tag{13.20}$$

Define a new Hermitian inner product on X by

$$\langle \boldsymbol{x}, \boldsymbol{y} \rangle = M_h(f(h; \boldsymbol{x}, \boldsymbol{y})) \qquad \text{for } \boldsymbol{x}, \boldsymbol{y} \in X, \tag{13.21}$$

where M_h is the invariant mean of f on the group G as defined in (13.8). Because $\langle \cdot, \cdot \rangle_1$ is a Hermitian inner product on X, and because by definition (13.8) $M(\alpha f) = \alpha M(f)$, it is easily verified that $\langle \cdot, \cdot \rangle$ is a Hermitian inner product on X. Then for each $g \in G$ and $\boldsymbol{x}, \boldsymbol{y} \in X$, we have

$$\begin{aligned} \langle \boldsymbol{T}(g)\boldsymbol{x}, \boldsymbol{T}(g)\boldsymbol{y} \rangle &= M_h(f(h; \boldsymbol{T}(g)\boldsymbol{x}, \boldsymbol{T}(g)\boldsymbol{y})) \\ &= M_h(\langle \boldsymbol{T}(h)\boldsymbol{T}(g)\boldsymbol{x}, \boldsymbol{T}(h)\boldsymbol{T}(g)\boldsymbol{y} \rangle_1) \\ &= M_h(\langle \boldsymbol{T}(hg)\boldsymbol{x}, \boldsymbol{T}(hg)\boldsymbol{y} \rangle_1) \\ &= M_h(f(hg; \boldsymbol{x}, \boldsymbol{y})) = M_h(f(h; \boldsymbol{x}, \boldsymbol{y})) = \langle \boldsymbol{x}, \boldsymbol{y} \rangle, \end{aligned} \tag{13.22}$$

where we have appealed to $(13.9)_2$ at the next-to-last step. Hence under the new Hermitian form on X, the representation $\boldsymbol{T}$ is unitary. □

Let X and Y be complex inner-product spaces. A linear isomorphism $\boldsymbol{U} : X \to Y$ is called an isometric isomorphism if it satisfies

$$\langle \boldsymbol{U}\boldsymbol{x}_1, \boldsymbol{U}\boldsymbol{x}_2 \rangle_Y = \langle \boldsymbol{x}_1, \boldsymbol{x}_2 \rangle_X \qquad \text{for each } \boldsymbol{x}_1, \boldsymbol{x}_2 \in X. \tag{13.23}$$

Note that (13.23) implies that

$$\langle \boldsymbol{x}_1, \boldsymbol{U}^*\boldsymbol{U}\boldsymbol{x}_2 \rangle_X = \langle \boldsymbol{x}_1, \boldsymbol{x}_2 \rangle_X \qquad \text{for each } \boldsymbol{x}_1, \boldsymbol{x}_2 \in X, \tag{13.24}$$

where $\boldsymbol{U}^*$ is the adjoint of $\boldsymbol{U}$. Hence we have

$$\boldsymbol{U}^*\boldsymbol{U} = \boldsymbol{I}_X, \tag{13.25}$$

where $\boldsymbol{I}_X$ denotes the identity operator on X.

Definition 13.11 Let X and Y be complex inner-product spaces. Two finite-dimensional unitary representations $(\boldsymbol{T}, X)$ and $(\boldsymbol{S}, Y)$ of a group G are said to be unitarily equivalent if there is an isometric isomorphism $\boldsymbol{U} : X \to Y$ such that

$$\boldsymbol{U}\boldsymbol{T}(g) = \boldsymbol{S}(g)\boldsymbol{U} \qquad \text{for each } g \in G. \tag{13.26}$$

□

Theorem 13.12 *Let X and Y be complex inner-product spaces. If two finite-dimensional unitary representations $(\boldsymbol{T}, X)$ and $(\boldsymbol{S}, Y)$ of a group G are equivalent, they are also unitarily equivalent.*

Proof Since the two representations $(\boldsymbol{T}, X)$ and $(\boldsymbol{S}, Y)$ are equivalent, there is a linear isomorphism $\boldsymbol{A} : X \to Y$ such that $\boldsymbol{AT}(g) = \boldsymbol{S}(g)\boldsymbol{A}$ for each $g \in G$. By the polar decomposition theorem (see, e.g., [40, pp. 168–169], where the proof presented is for $\boldsymbol{A} : X \to X$, but it applies almost verbatim to our present case), we have $\boldsymbol{A} = \boldsymbol{UB}$, where $\boldsymbol{U} : X \to Y$ is unitary and $\boldsymbol{B} : X \to X$ is Hermitian and positive definite. Substituting $\boldsymbol{A} = \boldsymbol{UB}$ into (13.12), we obtain

$$\boldsymbol{UBT}(g) = \boldsymbol{S}(g)\boldsymbol{UB} \qquad \text{for each } g \in G. \tag{13.27}$$

It follows that $(\boldsymbol{UBT}(g^{-1}))^* = (\boldsymbol{S}(g^{-1})\boldsymbol{UB})^*$ or

$$\boldsymbol{T}(g)\boldsymbol{BU}^* = \boldsymbol{BU}^*\boldsymbol{S}(g), \tag{13.28}$$

where have appealed to the fact that $\boldsymbol{T}(g)$ is unitary and $\boldsymbol{B}$ is Hermitian. From (13.25), (13.27), and (13.28) we obtain

$$\boldsymbol{T}(g)\boldsymbol{B}^2 = \boldsymbol{T}(g)\boldsymbol{BU}^*\boldsymbol{UB} = \boldsymbol{BU}^*\boldsymbol{S}(g)\boldsymbol{UB} = \boldsymbol{BU}^*\boldsymbol{UBT}(g) = \boldsymbol{B}^2\boldsymbol{T}(g) \tag{13.29}$$

for each $g \in G$. Thus $\boldsymbol{B}^2$ commutes with $\boldsymbol{T}(g)$ for each g. Since $\boldsymbol{B} = \sqrt{\boldsymbol{B}^2}$ can be written[143] as a polynomial of $\boldsymbol{B}^2$, $\boldsymbol{B}$ commutes with $\boldsymbol{T}(g)$ for each g. Hence it follows from (13.27) that $\boldsymbol{UT}(g)\boldsymbol{B} = \boldsymbol{S}(g)\boldsymbol{UB}$ or $\boldsymbol{UT}(g) = \boldsymbol{S}(g)\boldsymbol{U}$ for each $g \in G$. □

Theorem 13.13 *Two unitary representations $(\boldsymbol{T}, X)$ and $(\boldsymbol{S}, Y)$ of group G on complex inner-product spaces are equivalent if and only if there are orthonormal bases in X and Y with respect to which $\boldsymbol{T}(g)$ and $\boldsymbol{S}(g)$ are represented by the same unitary matrix $[T_{ij}(g)]$ for each $g \in G$.*

Proof By Theorem 13.12, if the unitary representations $(\boldsymbol{T}, X)$ and $\boldsymbol{S}, Y)$ are equivalent, there is an isometric isomorphism $\boldsymbol{U} : X \to Y$ such that $\boldsymbol{UT}(g) = \boldsymbol{S}(g)\boldsymbol{U}$ for each $g \in G$. Let $\dim X = \dim Y = n$. Arbitrarily pick an orthonormal basis $\{\boldsymbol{e}_i : i = 1, \ldots, n\}$ in X. Then

$$\boldsymbol{T}(g)\boldsymbol{e}_j = \sum_{i=1}^{n} T_{ij}(g)\boldsymbol{e}_i \qquad \text{for } 1 \le j \le n \text{ and for each } g \in G, \tag{13.30}$$

where $[T_{ij}(g)]$ is the unitary matrix that represents $\boldsymbol{T}(g)$ under the basis $\{\boldsymbol{e}_i\}$. Let $\boldsymbol{f}_i = \boldsymbol{U}\boldsymbol{e}_i$ $(i = 1, \ldots, n)$. Since $\boldsymbol{U}$ is an isometric isomorphism, $\{\boldsymbol{f}_i\}$ constitutes an orthonormal basis in Y. Moreover, we have for each $g \in G$

$$\boldsymbol{S}(g)\boldsymbol{f}_j = \boldsymbol{S}(g)\boldsymbol{U}\boldsymbol{e}_j = \boldsymbol{UT}(g)\boldsymbol{e}_j = \boldsymbol{U}\left(\sum_{i=1}^{n} T_{ij}(g)\boldsymbol{e}_i\right) = \sum_{i=1}^{n} T_{ij}(g)\boldsymbol{f}_i. \tag{13.31}$$

Hence under the orthonormal basis $\{\boldsymbol{f}_i\}$, $\boldsymbol{S}(g)$ is represented by the same unitary matrix $[T_{ij}(g)]$. For the converse of this theorem, the same proof for its counterpart in Theorem 13.7 is applicable here also. □

The following rewording of a part of Theorem 13.13 has a more direct appeal in some applications.

[143] See, e.g., [33, p. 299], [66, p. 47]; cf. (2.68) for the special case where $\dim X = 3$.

Corollary 13.14 *Let $\boldsymbol{T} : G \to \mathrm{GL}(\mathbb{C}^n)$, $g \mapsto [T_{ij}(g)]$, be a unitary matrix representation of group G. Let $(\boldsymbol{S}, Y)$ be a unitary representation of G on a complex inner-product space Y, and let $(\boldsymbol{S}, Y) \cong (\boldsymbol{T}, \mathbb{C}^n)$. There is an orthonormal basis $\{\boldsymbol{f}_1, \ldots, \boldsymbol{f}_n\}$ in Y for which $\boldsymbol{S}(g)\boldsymbol{f}_j = \sum_{i=1}^n T_{ij}(g)\boldsymbol{f}_i$ for $1 \le j \le n$ and for each $g \in G$.* □

13.2.5 Complete Reducibility

Let $(\boldsymbol{T}, X)$ be a finite-dimensional representation of group G. Suppose there are G-invariant subspaces M_k $(k = 1, \ldots, r)$ such that $X = M_1 \oplus \cdots \oplus M_r$, where the symbol "$\oplus$" denotes the direct sum. Then each $\boldsymbol{x} \in X$ can be uniquely expressed as

$$\boldsymbol{x} = \boldsymbol{x}_1 + \cdots + \boldsymbol{x}_r, \qquad \text{where } \boldsymbol{x}_k \in M_k \text{ for } k = 1, \ldots r. \tag{13.32}$$

Let $\boldsymbol{T}^k := \boldsymbol{T}\big|_{M_k}$ denote the restriction of $\boldsymbol{T}$ to M_k. Clearly for each $g \in G$, we have

$$\boldsymbol{T}(g)\boldsymbol{x} = \boldsymbol{T}^1(g)\boldsymbol{x}_1 + \cdots + \boldsymbol{T}^r(g)\boldsymbol{x}_r. \tag{13.33}$$

We say that the representation $\boldsymbol{T}$ is a direct sum of the representations $\boldsymbol{T}^k$ $(k = 1, \ldots, r)$ and write $\boldsymbol{T} = \boldsymbol{T}^1 + \cdots + \boldsymbol{T}^r$. If G is a compact topological group and the representation $\boldsymbol{T}$ is continuous, then all $\boldsymbol{T}^k$ are continuous because they are subrepresentations of $\boldsymbol{T}$.

Definition 13.15 A finite dimensional representation is said to be completely reducible if it is the direct sum of a finite number of irreducible subrepresentations. □

If a completely reducible representation $\boldsymbol{T}$ is the direct sum of irreducible subrepresentations, among which there are m_k representations equivalent to an irreducible representation $\boldsymbol{T}^k$ for $k = 1, \ldots, r$, we write

$$\boldsymbol{T} = m_1\boldsymbol{T}^1 + \cdots + m_r\boldsymbol{T}^r, \tag{13.34}$$

where m_k is called the multiplicity of the irreducible representation $\boldsymbol{T}^k$ in $\boldsymbol{T}$. We refer to (13.34) as the formula that decomposes representation $\boldsymbol{T}$ into its irreducible parts.

We proceed to prove that every finite-dimensional representation of a finite or compact group is completely reducible. To this end, we start with unitary representations.

Lemma 13.16 *Let $(\boldsymbol{T}, X)$ be a unitary representation of group G, and let M be a G-invariant subspace of X. Then $M^\perp$, the orthogonal complement of M, is also G-invariant, and $X = M \oplus M^\perp$.*

Proof Let $\langle \cdot, \cdot \rangle$ be the Hermitian inner product on X. By definition, $M^\perp = \{\boldsymbol{y} \in X : \langle \boldsymbol{y}, \boldsymbol{x} \rangle = 0 \text{ for each } \boldsymbol{x} \in M\}$. That $M^\perp$ is a subspace of X and $X = M \oplus M^\perp$ is a well-known fact in linear algebra (see, e.g., [40, pp. 72–73]). It remains to show that $M^\perp$ is G-invariant. Let $\boldsymbol{y} \in M^\perp$ be given. Since M is G-invariant, we have $\langle \boldsymbol{y}, \boldsymbol{T}(g^{-1})\boldsymbol{x} \rangle = 0$ for each $g \in G$ and $\boldsymbol{x} \in M$. On the other hand, since the representation $\boldsymbol{T}$ is unitary, for each $g \in G$ and $\boldsymbol{x} \in M$

$$\langle \boldsymbol{y}, \boldsymbol{T}(g^{-1})\boldsymbol{x} \rangle = \langle \boldsymbol{T}(g)\boldsymbol{y}, \boldsymbol{T}(g)\boldsymbol{T}(g^{-1})\boldsymbol{x} \rangle = \langle \boldsymbol{T}(g)\boldsymbol{y}, \boldsymbol{x} \rangle. \tag{13.35}$$

Thus $\langle \boldsymbol{T}(g)\boldsymbol{y}, \boldsymbol{x} \rangle = 0$ for each $g \in G$ and $\boldsymbol{x} \in M$, which implies $\boldsymbol{T}(g)\boldsymbol{y} \in M^\perp$ for each $g \in G$. Hence $M^\perp$ is G-invariant. □

Theorem 13.17 *Every finite-dimensional unitary representation is completely reducible.*

Proof Let $(\boldsymbol{T}, X)$ be a finite-dimensional unitary representation of group G. By Proposition 13.5, there is a G-invariant subspace $M_1 \neq \{\mathbf{0}\}$ of X such that the subrepresentation $\boldsymbol{T}\big|_{M_1}$ is irreducible. If $M_1 = X$, the proof is done. If $M_1 \neq X$, then by Lemma 13.16 $X = M_1 \oplus M_2$, where $M_2 = M_1^{\perp} \neq \{\mathbf{0}\}$. If $\boldsymbol{T}\big|_{M_2}$ is irreducible, we are through. If M_2 is reducible, by Lemma 13.16 $X = (M_1 \oplus M_2) \oplus M_3$, where $M_3 = (M_1 \oplus M_2)^{\perp}$. If $\boldsymbol{T}\big|_{M_3}$ is irreducible, then X is completely reducible. If $\boldsymbol{T}\big|_{M_3}$ is reducible, continue the process of decomposition as before. Since $\dim X$ is finite and $\dim M_k \geq 1$ for each k, the process of decomposition will stop at some $k = K \leq \dim X$. Then $X = M_1 \oplus \cdots \oplus M_K$ is a decomposition of X into a direct sum of G-invariant subspaces M_k $(k = 1, \ldots, K)$; on each M_k the subrepresentation $\boldsymbol{T}\big|_{M_k}$ is irreducible. □

Corollary 13.18 *Every finite-dimensional representation of a finite or a compact topological group is completely reducible.*

Proof Let $(\boldsymbol{T}, X)$ be a finite-dimensional representation of group G, Since G is finite or compact, by Proposition 13.10 the complex vector space X can be given a Hermitian inner product so that the representation $\boldsymbol{T}$ is unitary with respect to the inner product. The rest follows from Theorem 13.17. □

Remark 13.19 Corollary 13.18 can be proved without the introduction of a Hermitian inner product in the representation space. See Serre [296, pp. 6–7], where the proof is versed in the context of finite groups. The same proof, however, goes through for compact groups if the invariant mean (cf. (13.8)) for finite groups is replaced by its counterpart for compact groups in the proof. □

13.3 The Space $L^2(G)$. The Regular Representations

Let G be a compact topological group with normalized Haar measure $\mathfrak{g}$. One important class of finite-dimensional representations $(\boldsymbol{T}, X)$ of G that we shall consider are those where the representation space X is a subspace of $L^2(G, \mathbb{C})$, the space of complex-valued functions which are square-integrable with respect to the normalized Haar measure $\mathfrak{g}$. Since we consider only representations with representation space X being a complex vector space, subspaces of $L^2(G, \mathbb{R})$ will not be used as representation space. For simplicity we will henceforth write $L^2(G)$ for $L^2(G, \mathbb{C})$. We define a Hermitian inner product on $L^2(G)$ by[144]

$$\langle f_1, f_2 \rangle = \int_G f_1(g)\overline{f_2(g)}\, d\mathfrak{g} \qquad \text{for } f_1, f_2 \in L^2(G). \tag{13.36}$$

For a finite group G, for convenience we denote by $L^2(G)$ the linear space of functions $f : G \to \mathbb{C}$ with vector addition and scalar multiplication defined by

$$(f_1 + f_2)(g) = f_1(g) + f_2(g) \qquad \text{for } f_1, f_2 \in L^2(G), \text{ and } g \in G, \tag{13.37}$$

$$(\alpha f)(g) = \alpha f(g) \qquad \text{for } \alpha \in \mathbb{C},\ f \in L^2(G), \text{ and } g \in G, \tag{13.38}$$

[144] In Parts I and II, we follow Roe [270] and, for SO(3), primarily use $\mathcal{V} = 8\pi^2\mathfrak{g}$, where $\mathfrak{g}$ is the normalized Haar measure, as the volume measure of the group. The number $8\pi^2$ arises haphazardly just as a consequence of Roe's use of Euler angles for parametrization of SO(3). Here, as we study theorems and formulas that apply to all compact groups, the only reasonable uniform choice is to assign each group its normalized Haar measure.

respectively. In parallel to (13.36), we define a Hermitian inner product on $L^2(G)$ for finite G by

$$\langle f_1, f_2\rangle = \frac{1}{N}\sum_{g\in G} f_1(g)\overline{f_2(g)} \qquad \text{for } f_1, f_2 \in L^2(G), \tag{13.39}$$

where $N = |G|$, the number of elements in G.

Let G be a finite or a compact group. For a given $h \in G$, let $\mathcal{T}_r(h) : L^2(G) \to L^2(G)$ be defined by

$$(\mathcal{T}_r(h)f)(g) = f(gh) \qquad \text{for all } g \in G \text{ and } f \in L^2(G). \tag{13.40}$$

For finite G, clearly $\mathcal{T}_r(h)f \in L^2(G)$ for each $f \in L^2(G)$. For compact G, $\mathcal{T}_r(h)f$ is measurable as f is measurable. Moreover, for $f \in L^2(G)$, we have

$$\int_G |(\mathcal{T}_r(h)f)(g)|^2 d\mathfrak{g} = \int_G |f(gh)|^2 d\mathfrak{g} = \int_G |f(g)|^2 d\mathfrak{g} < +\infty.$$

Hence $\mathcal{T}_r(h)f \in L^2(G)$ if $f \in L^2(G)$, and the map $\mathcal{T}_r(h)$ is well defined. It is straightforward to verify that the map $\mathcal{T}_r(h)$ is a linear operator on $L^2(G)$. For $h_1, h_2 \in G$, we have

$$(\mathcal{T}_r(h_1)(\mathcal{T}_r(h_2)f))(g) = (\mathcal{T}_r(h_1)f)(gh_2) = f((gh_1)h_2) = (\mathcal{T}_r(h_1h_2)f)(g) \tag{13.41}$$

for any $g \in G$. Let e be the identity element in G. Then

$$(\mathcal{T}_r(e)f)(g) = f(ge) = f(g) \qquad \text{for all } g \in G \text{ and } f \in L^2(G). \tag{13.42}$$

From (13.41) and (13.42) we observe that the map $h \mapsto \mathcal{T}_r(h)$ defines a representation of G on any finite-dimensional G-invariant subspace of $L^2(G)$.[145] This representation is called the right-regular representation of G.[146]

Let G be compact. For a given $h \in G$ and $f_1, f_2 \in L^2(G)$, we have

$$\langle \mathcal{T}_r(h)f_1, \mathcal{T}_r(h)f_2\rangle = \int_G f_1(gh)\overline{f_2(gh)}d\mathfrak{g}(g) = \int_G f_1(g)\overline{f_2(g)}d\mathfrak{g} = \langle f_1, f_2\rangle. \tag{13.43}$$

Hence the right-regular representation is unitary. That the same assertion is valid for the case where G is finite can be proved in the same way.

Similarly we define the left-regular representations for finite or compact groups G. For a given $h \in G$, let $\mathcal{T}_l(h) : L^2(G) \to L^2(G)$ be defined by

$$(\mathcal{T}_l(h)f)(g) = f(h^{-1}g) \qquad \text{for all } g \in G \text{ and } f \in L^2(G). \tag{13.44}$$

For both finite and compact groups, we can easily show what follows: (i) $\mathcal{T}_l(h)f \in L^2(G)$ for each $f \in L^2(G)$; (ii) the map $\mathcal{T}_l(h)$ is a linear operator on $L^2(G)$; (iii) the map $h \mapsto \mathcal{T}_l(h)$ defines a unitary representation of G on any finite-dimensional G-invariant subspace of $L^2(G)$.

[145] In fact this representation is defined on the infinite-dimensional Hilbert space $L^2(G)$. As mentioned in the introductory remarks at the beginning of Sect. 13.2, for our purposes we need not go into the mathematics of infinite-dimensional representations of compact groups on Hilbert spaces.

[146] See [245, p. 187] for a proof that the right-regular representation $\mathcal{T}_r : h \mapsto \mathcal{T}_r(h)$ of any compact group G, with $L^2(G)$ as the representation space, is continuous. We shall not use this fact in this exposition.

13.4 Orthogonality Relations

Theorem 13.20 *Let $(\boldsymbol{T}, X)$ and $(\boldsymbol{S}, Y)$ be irreducible, finite-dimensional, continuous unitary representations of the compact group G. For $g \in G$, let $(T_{kl}(g))$ and $(S_{ij}(g))$ be unitary matrices that represent $\boldsymbol{T}(g)$ and $\boldsymbol{S}(g)$ under some chosen orthonormal basis in X and in Y, respectively. Then the following orthogonality relations in $L^2(G)$ hold for the matrix elements of the irreducible representations in question*:

$$\langle S_{ij}, T_{kl}\rangle = \int_G S_{ij}(g)\overline{T_{kl}(g)}d\mathfrak{g} = 0 \quad \textit{for all } i, j, k, l \quad \textit{if } \boldsymbol{T} \textit{ and } \boldsymbol{S} \textit{ are inequivalent}, \tag{13.45}$$

and

$$\langle T_{ij}, T_{kl}\rangle = \int_G T_{ij}(g)\overline{T_{kl}(g)}d\mathfrak{g} = \frac{1}{n}\delta_{ik}\delta_{jl}, \tag{13.46}$$

where $n = \dim X$ and the integral on G is defined with respect to the normalized Haar measure.

Proof Let $\boldsymbol{B} \in \mathrm{Lin}(X, Y)$, and let $\boldsymbol{C} := \int_G \boldsymbol{S}(g)\boldsymbol{B}\boldsymbol{T}(g^{-1})d\mathfrak{g}$. Clearly $\boldsymbol{C} \in \mathrm{Lin}(X, Y)$. Moreover, for each $h \in G$ we have

$$\boldsymbol{C}\boldsymbol{T}(h) = \int_G \boldsymbol{S}(g)\boldsymbol{B}\boldsymbol{T}(g^{-1}h)d\mathfrak{g}(g) = \int_G \boldsymbol{S}(hg)\boldsymbol{B}\boldsymbol{T}(g^{-1})d\mathfrak{g}(g) = \boldsymbol{S}(h)\boldsymbol{C}, \tag{13.47}$$

where we have appealed to the left invariance of the Haar measure on G. If the irreducible representations $\boldsymbol{T}$ and $\boldsymbol{S}$ are inequivalent, we conclude from (13.47) and Schur's lemma that $\boldsymbol{C} = \boldsymbol{0}$. Hence for all entries C_{ik} of the matrix that represents $\boldsymbol{C}$ under the chosen orthonormal bases in X and Y, we have

$$C_{ik} = \sum_p \sum_q \int_G S_{ip}(g)B_{pq}T_{qk}(g^{-1})d\mathfrak{g} = 0. \tag{13.48}$$

Note that $\boldsymbol{B} \in \mathrm{Lin}(X, Y)$ is arbitrary and the matrix $[T_{kl}(g)]$ is unitary. Putting

$$B_{pq} = \begin{cases} 1 & \text{if } p = j \text{ and } q = l \\ 0 & \text{otherwise} \end{cases}$$

in (13.48), we obtain

$$\int_G S_{ij}(g)T_{lk}(g^{-1})d\mathfrak{g} = \int_G S_{ij}(g)\overline{T_{kl}(g)}d\mathfrak{g} = 0.$$

Equation (13.47) remains valid when $\boldsymbol{S} = \boldsymbol{T}$ and $Y = X$, which by Schur's lemma dictates that $\boldsymbol{C} = \lambda\boldsymbol{I}$ for some $\lambda \in \mathbb{C}$; here $\boldsymbol{I}$ denotes the identity map in $\mathrm{Lin}(X, X)$. Hence we have

$$n\lambda = \mathrm{tr}\,\boldsymbol{C} = \mathrm{tr}\left(\int_G \boldsymbol{T}(g)\boldsymbol{B}\boldsymbol{T}(g^{-1})\,d\mathfrak{g}\right) = \int_G \mathrm{tr}(\boldsymbol{T}(g)\boldsymbol{B}\boldsymbol{T}(g^{-1}))d\mathfrak{g} = \mathrm{tr}\,\boldsymbol{B}, \tag{13.49}$$

which gives $\lambda = \frac{1}{n}\operatorname{tr} \boldsymbol{B}$ and

$$\boldsymbol{C} = \int_G \boldsymbol{T}(g)\boldsymbol{B}\boldsymbol{T}(g^{-1})\, d\mathfrak{g} = \frac{1}{n}(\operatorname{tr} \boldsymbol{B})\boldsymbol{I}, \tag{13.50}$$

which is valid for any $\boldsymbol{B} \in \operatorname{Lin}(X, X)$. In components, $(13.50)_2$ reads:

$$\sum_p \sum_q \int_G T_{ip}(g) B_{pq} T_{qk}(g^{-1}) d\mathfrak{g} = \frac{1}{n}\left(\sum_{s=1}^{n} B_{ss}\right)\delta_{ik}. \tag{13.51}$$

Putting

$$B_{pq} = \begin{cases} 1 & \text{if } p = j \text{ and } q = l \\ 0 & \text{otherwise} \end{cases}$$

in (13.51), we conclude that

$$\int_G T_{ij}(g)\overline{T_{kl}(g)} d\mathfrak{g} = \frac{1}{n}\delta_{ik}\delta_{jl},$$

where we have used the fact that $T_{lk}(g^{-1}) = \overline{T_{kl}(g)}$. □

After replacement of the inner product (13.36) for compact groups by its counterpart (13.39) for finite groups, the theorem and its proof above carry over almost verbatim for finite groups G. We record this version of the theorem as a corollary.

Corollary 13.21 *Let $(\boldsymbol{T}, X)$ and $(\boldsymbol{S}, Y)$ be irreducible, finite-dimensional, unitary representations of the finite group G. For $g \in G$, let $[T_{kl}(g)]$ and $[S_{ij}(g)]$ be unitary matrices that represent $\boldsymbol{T}(g)$ and $\boldsymbol{S}(g)$ under some fixed chosen basis in X and in Y, respectively. Then the following orthogonality relations in $L^2(G)$ hold for the matrix elements of the irreducible representations in question*:

$$\langle S_{ij}, T_{kl}\rangle = \frac{1}{N}\sum_{g\in G} S_{ij}(g)\overline{T_{kl}(g)} = 0 \quad \textit{for all } i, j, k, l \quad \textit{if } \boldsymbol{T} \textit{ and } \boldsymbol{S} \textit{ are inequivalent}, \tag{13.52}$$

and

$$\langle T_{ij}, T_{kl}\rangle = \frac{1}{N}\sum_{g\in G} T_{ij}(g)\overline{T_{kl}(g)} = \frac{1}{n}\delta_{ik}\delta_{jl}, \tag{13.53}$$

where $n = \dim X$ and $N = |G|$. □

13.5 Completeness Theorem for Finite Groups

Let G be a finite group of order N. Then $L^2(G)$ is a linear space with $\dim L^2(G) = N$. Earlier we have shown that the matrix elements of inequivalent irreducible unitary representations of G are orthogonal in $L^2(G)$. Hence there can be at most N of such orthogonal

elements. It follows immediately that the number of inequivalent irreducible unitary representations of a finite group G is finite and cannot be larger than the order of G.

A family $(\boldsymbol{T}^1, X^1), \ldots, (\boldsymbol{T}^m, X^m)$ of irreducible unitary representations of finite group G is said to be complete if it satisfies the following conditions:

1. The representations $(\boldsymbol{T}^1, X^1), \ldots, (\boldsymbol{T}^m, X^m)$ are pairwise inequivalent.
2. Any irreducible representation of G is equivalent to some representation $(\boldsymbol{T}^l, X^l)$ in the family.

Let a complete family $(\boldsymbol{T}^1, X^1), \ldots, (\boldsymbol{T}^m, X^m)$ of irreducible unitary representations of the finite group G be given. Let $\dim X^k = n_k$ for $k = 1, \ldots, m$. Since the matrix elements of the irreducible unitary representations, say $T^k_{ij}(\cdot)$, constitute an orthogonal set in $L^2(G)$ with $n_1^2 + n_2^2 + \cdots + n_m^2$ members, we know that

$$n_1^2 + n_2^2 + \cdots + n_m^2 \leq N.$$

In fact, it turns out that $n_1^2 + n_2^2 + \cdots + n_m^2 = N$, which follows immediately as a corollary of the following completeness theorem.

Theorem 13.22 *Let $(\boldsymbol{T}^1, X^1), \ldots, (\boldsymbol{T}^m, X^m)$ be a complete family of irreducible unitary representations of the finite group G. For $g \in G$ and $k = 1, \ldots, m$, let $(T^k_{ij}(g))$ be the unitary matrix that represents $\boldsymbol{T}^k(g)$ under some chosen orthonormal basis in X^k. The set of $n_1^2 + n_2^2 + \cdots + n_m^2$ matrix elements $T^k_{ij}(\cdot)$ constitutes an orthogonal basis in $L^2(G)$.*

Proof We have already proved that the matrix elements $T^k_{ij}(\cdot)$ are orthogonal functions in $L^2(G)$. Hence it suffices to show that every function $L^2(G)$ can be expressed as a linear combination of these matrix elements. The right-regular representation $\mathcal{T}_r : G \to \mathrm{GL}(L^2(G))$ is unitary and is thence completely reducible. Let

$$L^2(G) = Y_1 \oplus Y_2 \oplus \cdots \oplus Y_p, \qquad \mathcal{T}_r = \mathcal{T}_r^{(1)} + \mathcal{T}_r^{(2)} + \cdots + \mathcal{T}_r^{(p)}$$

be the decomposition of the right-regular representation of G into its irreducible parts, where each subspace Y_s $(s = 1, \ldots, p)$ of $L^2(G)$ is invariant under $\mathcal{T}_r(h)$ for each $h \in G$ and each subrepresentation $(\mathcal{T}_r^{(s)}, Y_s)$, where $\mathcal{T}_r^{(s)}$ is the restriction of $\mathcal{T}_r$ to Y_s, is irreducible.

Consider a specific irreducible subrepresentation $(\mathcal{T}_r^{(s)}, Y_s)$. It is equivalent to some $(\boldsymbol{T}^l, X^l)$. By Corollary 13.14 there is a basis $\{f_\beta : \beta = 1, \ldots, n_l\}$ in Y_s with respect to which the matrix that represents $(\mathcal{T}_r^{(s)}, Y_s)$ under this basis in none other than $[T^l_{ij}(\cdot)]$, i.e.,

$$\mathcal{T}_r^{(s)}(h) f_\beta = \sum_{\alpha=1}^{n_l} T^l_{\alpha\beta}(h) f_\alpha \qquad \text{for each } h \in G. \tag{13.54}$$

On the other hand, by definition of the right-regular representation we have

$$(\mathcal{T}_r^{(s)}(h) f_\beta)(g) = f_\beta(gh) \qquad \text{for each } g, h \in G. \tag{13.55}$$

Combining (13.54) and (13.55), we obtain

$$f_\beta(gh) = \sum_{\alpha=1}^{n_l} T^l_{\alpha\beta}(h) f_\alpha(g) \qquad \text{for each } g, h \in G. \tag{13.56}$$

Putting $g = e$ and $c_\alpha = f_\alpha(e)$ in (13.56), we conclude that

$$f_\beta(h) = \sum_{\alpha=1}^{n_l} c_\alpha T^l_{\alpha\beta}(h) \qquad \text{for each } h \in G. \tag{13.57}$$

In other words, each basis function $f_\beta(\cdot)$ in Y_s ($\beta = 1, \ldots, n_l$) and thence every function $f^{(s)}$ in Y_s can be expressed as a linear combination of the matrix elements $T^k_{ij}(\cdot)$. Similarly, every function $f^{(q)}$ in Y_q ($q = 1, \ldots, p$) can be expressed as a linear combination of the matrix elements $T^k_{ij}(\cdot)$. Therefore each function in $L^2(G)$ can be written as a linear combination of the matrix elements $T^k_{ij}(\cdot)$. □

This completeness theorem immediately leads to the following corollary, which is known as Burnside's theorem in the literature.

Corollary 13.23 *The order N of a finite group G is equal to the sum of the squares of any complete family of irreducible unitary representations of the group, i.e.,*

$$n_1^2 + n_2^2 + \cdots + n_m^2 = N. \tag{13.58}$$

□

By the completeness theorem and the orthogonality relations (13.45) and (13.46), the functions

$$E^k_{ij}(\cdot) := \sqrt{n_k}\, T^k_{ij}(\cdot) \qquad (k = 1, \ldots, m;\ 1 \le i \le n_k \text{ and } 1 \le j \le n_k \text{ for each } k) \tag{13.59}$$

constitute an orthonormal basis in $L^2(G)$. Every function $f \in L^2(G)$ can be expressed as a linear combination of the orthonormal basis $\{E^k_{ij}\}$ as

$$f = \sum_{k=1}^{m} \sum_{i,j=1}^{n_k} \langle f, E^k_{ij}\rangle E^k_{ij}. \tag{13.60}$$

Hence we have

$$\|f\|^2 = \langle f, f\rangle = \sum_{k=1}^{m} \sum_{i,j=1}^{n_k} |\langle f, E^k_{ij}\rangle|^2. \tag{13.61}$$

In anticipation of the parallel formula for compact groups, we call (13.61) Parceval's equality for the finite group G.

13.6 Characters of Group Representations

Let G be a finite or a compact group. Let $(\boldsymbol{T}, X)$ be a finite-dimensional representation of G. The character of the representation[147] $\boldsymbol{T}$ is the function $\chi_{\boldsymbol{T}} : G \to \mathbb{C}$ defined by

$$\chi_{\boldsymbol{T}}(g) = \mathrm{tr}(\boldsymbol{T}(g)) \qquad \text{for each } g \in G. \tag{13.62}$$

[147] For brevity, we shall henceforth refer to representation $\boldsymbol{T}$ rather than $(\boldsymbol{T}, X)$ whenever no confusion should arise.

Under any chosen basis in X, where $[T_{ij}(g)]$ is the matrix that represents $\boldsymbol{T}(g)$, $\chi_{\boldsymbol{T}}(g)$ is the sum of the diagonal entries of $[T_{ij}(g)]$, i.e., $\chi_{\boldsymbol{T}}(g) = T_{11}(g) + T_{22}(g) + \cdots + T_{nn}(g)$, where $n = \dim X$.

In what follows, for two representations $\boldsymbol{T}$ and $\boldsymbol{S}$ of a group G, $\boldsymbol{T} \cong \boldsymbol{S}$ (resp. $\boldsymbol{T} \ncong \boldsymbol{S}$) means that representations $\boldsymbol{T}$ and $\boldsymbol{S}$ are equivalent (resp. inequivalent).

13.6.1 Basic Properties

Some basic properties of group characters follow immediately from those of the trace.

Proposition 13.24 *Let G be a finite or a compact group. The characters of finite-dimensional representations of G enjoy the following properties*:

(1) *If $\boldsymbol{T} \cong \boldsymbol{S}$, then $\chi_{\boldsymbol{T}} = \chi_{\boldsymbol{S}}$.*
(2) *For all $g, h \in G$, $\chi_{\boldsymbol{T}}(h) = \chi_{\boldsymbol{T}}(ghg^{-1})$.*
(3) *If $\boldsymbol{T}$ is unitary, then $\chi_{\boldsymbol{T}}(g^{-1}) = \overline{\chi_{\boldsymbol{T}}(g)}$.*
(4) *If $\boldsymbol{T} = \boldsymbol{T}^1 + \boldsymbol{T}^2$, then $\chi_{\boldsymbol{T}} = \chi_{\boldsymbol{T}^1} + \chi_{\boldsymbol{T}^2}$.*
(5) *Let e be the identity in G. Then $\chi_{\boldsymbol{T}}(e) = n$, where n is the dimension of the representation $\boldsymbol{T}$.* □

While the theorems and proofs in this subsubsection are phrased in terms of compact groups, they hold almost verbatim for finite groups. Just use the appropriate inner product (13.39) in $L^2(G)$ for finite G, i.e.,

$$\langle \chi_{\boldsymbol{T}}, \chi_{\boldsymbol{S}} \rangle = \frac{1}{|G|} \sum_{g \in G} \chi_{\boldsymbol{T}}(g) \overline{\chi_{\boldsymbol{S}}(g)}, \tag{13.63}$$

and delete the adjective "continuous".

Theorem 13.25 *Let $(\boldsymbol{T}, X)$ and $(\boldsymbol{S}, Y)$ be finite-dimensional, continuous, unitary irreducible representations of compact group G. Then*

$$\langle \chi_{\boldsymbol{T}}, \chi_{\boldsymbol{S}} \rangle = \begin{cases} 0 & \text{if } \boldsymbol{T} \ncong \boldsymbol{S} \\ 1 & \text{if } \boldsymbol{T} \cong \boldsymbol{S}. \end{cases} \tag{13.64}$$

Proof Suppose $\dim X = n$ and $\dim Y = m$. For $g \in G$, let $(T_{ij}(g))$ and $(S_{ij}(g))$ be unitary matrices that represent $\boldsymbol{T}(g)$ and $\boldsymbol{S}(g)$ under chosen orthonormal basis in X and in Y, respectively. If $\boldsymbol{T} \ncong \boldsymbol{S}$, we have

$$\langle \chi_{\boldsymbol{T}}, \chi_{\boldsymbol{S}} \rangle = \int_G \left(\sum_{i=1}^{n} T_{ii}(g) \right) \left(\sum_{k=1}^{m} \overline{S_{kk}(g)} \right) d\mathfrak{g} = 0. \tag{13.65}$$

On the other hand, if $\boldsymbol{T} \cong \boldsymbol{S}$, we obtain

$$\begin{aligned} \langle \chi_{\boldsymbol{T}}, \chi_{\boldsymbol{S}} \rangle = \langle \chi_{\boldsymbol{T}}, \chi_{\boldsymbol{T}} \rangle &= \int_G \left(\sum_{i=1}^{n} T_{ii}(g) \right) \left(\sum_{k=1}^{n} \overline{T_{kk}(g)} \right) d\mathfrak{g} \\ &= \sum_{i,k=1}^{n} \int_G T_{ii}(g) \overline{T_{kk}(g)} d\mathfrak{g} = \sum_{i=1}^{n} \frac{1}{n} = 1. \end{aligned} \tag{13.66}$$

□

Theorem 13.26 *A finite-dimensional continuous unitary representation* $(\boldsymbol{T}, X)$ *of a compact group* G *is irreducible if and only if* $\langle \chi_{\boldsymbol{T}}, \chi_{\boldsymbol{T}} \rangle = 1$.

Proof Sufficiency. Suppose $\langle \chi_{\boldsymbol{T}}, \chi_{\boldsymbol{T}} \rangle = 1$. Since the representation $\boldsymbol{T}$ is unitary, it is completely reducible. Let

$$\boldsymbol{T} = m_1 \boldsymbol{T}^1 + m_2 \boldsymbol{T}^2 + \cdots + m_l \boldsymbol{T}^l \tag{13.67}$$

be the decomposition of $\boldsymbol{T}$ into its irreducible parts, where m_j $(j = 1, \ldots, l)$ is the multiplicity that the irreducible subrepresentation $\boldsymbol{T}^j$ appears in the decomposition. Without loss of generality, we may assume that $m_j \geq 1$ for all j. It follows immediately from decomposition (13.67) that

$$\chi_{\boldsymbol{T}} = m_1 \chi_{\boldsymbol{T}^1} + m_2 \chi_{\boldsymbol{T}^2} + \cdots + m_l \chi_{\boldsymbol{T}^l} \tag{13.68}$$

Since the characters $\chi_{\boldsymbol{T}^j}$ $(j = 1, \ldots, l)$ are orthonormal, we have

$$\langle \chi_{\boldsymbol{T}}, \chi_{\boldsymbol{T}} \rangle = \sum_{j=1}^{l} m_j^2 = 1, \tag{13.69}$$

which is impossible unless $l = 1$. Then $\boldsymbol{T} = \boldsymbol{T}^1$, which is irreducible.

The necessity part of the theorem is already proved in (13.66). □

Since (13.67) implies (13.68) and the characters $\chi_{\boldsymbol{T}^j}$ $(j = 1, \ldots, l)$ are orthonormal, we immediately arrive at the following assertion.

Theorem 13.27 *Let* $\boldsymbol{T} = m_1 \boldsymbol{T}^1 + m_2 \boldsymbol{T}^2 + \cdots + m_l \boldsymbol{T}^l$ *be the decomposition of* $\boldsymbol{T}$ *into its irreducible parts. The multiplicities* m_j *can be determined by the formula*

$$m_j = \langle \chi_{\boldsymbol{T}}, \chi_{\boldsymbol{T}^j} \rangle = \int_G \chi_{\boldsymbol{T}}(g) \overline{\chi_{\boldsymbol{T}^j}}(g) \, d\mathfrak{g}. \tag{13.70}$$

□

Theorem 13.28 *Two finite-dimensional continuous unitary representations* $(\boldsymbol{T}, X)$ *and* $(\boldsymbol{S}, Y)$ *of a compact group* G *are equivalent if and only if* $\chi_{\boldsymbol{T}} = \chi_{\boldsymbol{S}}$.

Proof Sufficiency. Let (13.67) give the decomposition of $\boldsymbol{T}$ into its irreducible parts. Then we have

$$\langle \chi_{\boldsymbol{S}}, \chi_{\boldsymbol{T}^j} \rangle = \langle \chi_{\boldsymbol{T}}, \chi_{\boldsymbol{T}^j} \rangle = m_j. \tag{13.71}$$

It follows that

$$\boldsymbol{S} \cong m_1 \boldsymbol{T}^1 + m_2 \boldsymbol{T}^2 + \cdots + m_l \boldsymbol{T}^l = \boldsymbol{T}. \tag{13.72}$$

The necessity part is already proved earlier. □

13.6.2 Completeness Theorem on Characters of Finite Groups

Let G be a finite group. Let $M = \{f \in L^2(G) : f(h) = f(ghg^{-1})$ for all $g, h \in G\}$; in other words M consists of those functions which are constant on each conjugacy class of G. It is clear that M is a linear subspace of $L^2(G)$ and $\dim M = p$, where p is the number of conjugacy classes of G.

Let $(\boldsymbol{T}^1, X^1), (\boldsymbol{T}^2, X^2), \ldots, (\boldsymbol{T}^m, X^m)$ be a complete set of irreducible unitary representations of G, where $\dim X^k = n_k$ $(k = 1, 2, \ldots, m)$. Clearly $\chi_{\boldsymbol{T}^k} \in M$ for each k. Since $\langle \chi_{\boldsymbol{T}^j}, \chi_{\boldsymbol{T}^k} \rangle = 0$ for $j \neq k$, the functions $\chi_{\boldsymbol{T}^k}$ are linearly independent in M. It follows that $m \leq p$. In fact, we have $m = p$, which follows from the following completeness theorem.

Theorem 13.29 *Let $(\boldsymbol{T}^1, X^1), (\boldsymbol{T}^2, X^2), \ldots, (\boldsymbol{T}^m, X^m)$ be a complete set of irreducible unitary representations of G. The characters $\chi_{\boldsymbol{T}^1}, \chi_{\boldsymbol{T}^2}, \ldots, \chi_{\boldsymbol{T}^m}$ constitute an orthonormal basis in M.*

Proof We already know that the characters $\chi_{\boldsymbol{T}^k}$ are orthonormal. It suffices to show that every function in M can be written as a linear combination of these characters. Let $f \in M$ be given. By the completeness theorem on the matrix elements $T^k_{i,j}(\cdot)$ of the given complete set of irreducible unitary representations, we have for each $g, h \in G$

$$\begin{aligned} f(h) = f(ghg^{-1}) &= \sum_{k=1}^{m} \sum_{i,j=1}^{n_k} c^k_{ij} T^k_{ij}(ghg^{-1}) \\ &= \sum_{k=1}^{m} \sum_{i,j=1}^{n_k} c^k_{ij} \sum_{r,s=1}^{n_k} T^k_{ir}(g) T^k_{rs}(h) T^k_{sj}(g^{-1}) \end{aligned} \tag{13.73}$$

for some coefficients c^k_{ij}. Let $N = |G|$. Averaging both sides of the preceding equation with respect to g over G, we obtain

$$\begin{aligned} f(h) = \frac{1}{N} \sum_{g \in G} f(h) &= \frac{1}{N} \sum_{g \in G} \left(\sum_{k=1}^{m} \sum_{i,j=1}^{n_k} c^k_{ij} \sum_{r,s=1}^{n_k} T^k_{ir}(g) T^k_{rs}(h) T^k_{sj}(g^{-1}) \right) \\ &= \sum_{k=1}^{m} \sum_{i,j=1}^{n_k} \sum_{r,s=1}^{n_k} c^k_{ij} T^k_{rs}(h) \left(\frac{1}{N} \sum_{g \in G} T^k_{ir}(g) \overline{T^k_{js}(g)} \right) \\ &= \sum_{k=1}^{m} \sum_{i,j=1}^{n_k} \sum_{r,s=1}^{n_k} c^k_{ij} T^k_{rs}(h) \frac{1}{n_k} \delta_{ij} \delta_{rs} \\ &= \sum_{k=1}^{m} \left(\sum_{i=1}^{n_k} c^k_{ii} \frac{1}{n_k} \right) \chi_{\boldsymbol{T}^k}(h) \end{aligned} \tag{13.74}$$

for each $h \in G$. □

Corollary 13.30 *The number of members in a complete set of irreducible unitary representations of a finite group is equal to the number of conjugacy classes of the group.* □

13.6.3 Example

As illustration we will determine a complete set of irreducible unitary representations for the dihedral group

$$D_3 = \{e, r, r^2, s, sr, sr^2\},$$

where $e = \boldsymbol{I}$, $r = \boldsymbol{R}(\boldsymbol{e}_3, 2\pi/3)$, and $s = \boldsymbol{R}(\boldsymbol{e}_1, \pi)$. The group D_3 has three conjugacy classes, namely (see Example A.8 in Appendix A)

$$[e] = \{e\}, \qquad [r] = \{r, r^2\}, \qquad [s] = \{s, sr, sr^2\}. \tag{13.75}$$

By Corollary 13.30 there are three members in any complete set of irreducible unitary representations of D_3. Let $\boldsymbol{T}^1$, $\boldsymbol{T}^2$, $\boldsymbol{T}^3$ be one such complete set with dimensions $n_1 \le n_2 \le n_3$. By Burnside's theorem, we have

$$n_1^2 + n_2^2 + n_3^2 = 6.$$

The only solution is: $n_1 = 1, n_2 = 1, n_3 = 2$. We take $\boldsymbol{T}^1$ to be the trivial representation defined by $\boldsymbol{T}^1(g) = 1$ for all $g \in D_3$. Since $\boldsymbol{T}^2$ is a 1-dimensional representation, we know that $\boldsymbol{T}^2(e) = 1$. Let $\boldsymbol{T}^2(r) = \chi_{\boldsymbol{T}^2}(r) = x$, $\boldsymbol{T}^2(s) = \chi_{\boldsymbol{T}^2}(s) = y$. Then $\boldsymbol{T}^2(r^2) = \chi_{\boldsymbol{T}^2}(r^2) = x^2$, $\boldsymbol{T}^2(sr) = \chi_{\boldsymbol{T}^2}(sr) = yx$. On the other hand, since the character of any finite-dimensional representation is a class function, we have $\chi_{\boldsymbol{T}^2}(r) = \chi_{\boldsymbol{T}^2}(r^2)$, $\chi_{\boldsymbol{T}^2}(s) = \chi_{\boldsymbol{T}^2}(sr)$. Hence we obtain

$$x = x^2, \qquad y = yx,$$

which imply either (i) $x = 0$ and $y = 0$ or (ii) $x = 1$. The solution $x = 0$ and $y = 0$ must be rejected because it implies $\langle \chi_{\boldsymbol{T}^2}, \chi_{\boldsymbol{T}^2} \rangle = 1/6 \neq 1$. Therefore $x = 1$. The remaining unknown y can then be evaluated by the orthogonality of the characters $\chi_{\boldsymbol{T}^1}$ and $\chi_{\boldsymbol{T}^2}$. By (13.63) we have

$$\langle \chi_{\boldsymbol{T}^1}, \chi_{\boldsymbol{T}^2} \rangle = \frac{1}{6} \sum_{g \in D_3} \chi_{\boldsymbol{T}^1}(g) \overline{\chi_{\boldsymbol{T}^2}(g)} = \frac{1}{6}(1 + 2 \times 1 + 3\overline{y}) = 0,$$

which gives $y = -1$.

Representation $\boldsymbol{T}^3$ is two-dimensional. Hence $\chi_{\boldsymbol{T}^3}(e) = 2$. Let $\chi_{\boldsymbol{T}^3}(r) = z$, $\chi_{\boldsymbol{T}^3}(s) = w$. By the orthogonality of $\chi_{\boldsymbol{T}^3}$ to both $\chi_{\boldsymbol{T}^1}$ and $\chi_{\boldsymbol{T}^2}$, we have

$$\langle \chi_{\boldsymbol{T}^3}, \chi_{\boldsymbol{T}^1} \rangle = \frac{1}{6}(2 + 2z + 3w) = 0,$$
$$\langle \chi_{\boldsymbol{T}^3}, \chi_{\boldsymbol{T}^2} \rangle = \frac{1}{6}(2 + 2z - 3w) = 0,$$

from which we get $z = -1$ and $w = 0$. We summarize our findings in Table 10.

A realization of the two-dimensional irreducible unitary representation of D_3 is furnished by taking $\mathbb{R}^2$ as the representation space, and by taking

$$\boldsymbol{T}^3(r) = \begin{pmatrix} -1/2 & -\sqrt{3}/2 \\ \sqrt{3}/2 & -1/2 \end{pmatrix}, \qquad \boldsymbol{T}^3(s) = \begin{pmatrix} 1 & 0 \\ 0 & -1 \end{pmatrix}. \tag{13.76}$$

Table 10 Character table of group D_3

D_3	$[e]$	$2[r]$	$3[s]$
$\chi_{\boldsymbol{T}^1}$	1	1	1
$\chi_{\boldsymbol{T}^2}$	1	1	-1
$\chi_{\boldsymbol{T}^3}$	2	-1	0

Remark 13.31 By Theorem 2.35 each point group G of Type III is isomorphic to the proper point group G^+ in the Laue class that contains G. For example, the group C_{3v} is isomorphic to D_3 (see Tables 3 and 4 in Sect. 2.6). Thus C_{3v} and D_3 have the same abstract group structure, and they can be taken as different realizations of the same abstract group. Indeed, if we interpret the letter s in Table 1 of Sect. 2.1 and in (13.75) as $\mathcal{I}\boldsymbol{R}(\boldsymbol{e}_1, \pi)$ rather than $\boldsymbol{R}(\boldsymbol{e}_1, \pi)$, then Table 1 becomes the multiplication table and (13.75) the list of conjugacy classes for C_{3v}. Moreover, the derivation above for the characters for a complete set of irreducible representations $\boldsymbol{T}^1$, $\boldsymbol{T}^2$, and $\boldsymbol{T}^3$ of D_3 becomes a derivation of the same for the group C_{3v}. This example of C_{3v} and D_3 illustrates the common assertion that isomorphic groups have the same character table. In particular a point group of Type III has the same character table as that of the proper point group in the same Laue class. □

13.7 Tensor Product of Representations

Let X^1 and X^2 be two complex vector spaces, and let $X^1 \otimes X^2$ be their tensor product.[148] Let $(\boldsymbol{T}^1, X^1)$ and $(\boldsymbol{T}^2, X^2)$ be two finite-dimensional representations of group G. Let $\boldsymbol{T} : G \to \mathrm{GL}(X^1 \otimes X^2)$ be the mapping defined by

$$\boldsymbol{T}(g)(\boldsymbol{x}^1 \otimes \boldsymbol{x}^2) = \boldsymbol{T}^1(g)\boldsymbol{x}^1 \otimes \boldsymbol{T}^2(g)\boldsymbol{x}^2 \tag{13.77}$$

for all $\boldsymbol{x}^1 \in X^1$ and $\boldsymbol{x}^2 \in X^2$. It is easily checked that $\boldsymbol{T}$ is well defined and is a homomorphism. Hence $\boldsymbol{T}$ is a representation of G on the tensor product $X^1 \otimes X^2$. We write $\boldsymbol{T} = \boldsymbol{T}^1 \otimes \boldsymbol{T}^2$ and call it the tensor product of the representations $\boldsymbol{T}^1$ and $\boldsymbol{T}^2$.

For $k = 1, 2$, let $\dim X^k = n_k$, and let $\boldsymbol{f}^k_1, \ldots, \boldsymbol{f}^k_{n_k}$ be a basis in X^k. Then $\{\boldsymbol{f}^1_i \otimes \boldsymbol{f}^2_j : 1 \le i \le n_1, 1 \le j \le n_2\}$ constitutes a basis in $X^1 \otimes X^2$. For each $g \in G$, let $[T^k_{\mu\nu}(g)]$ be the matrix that represents $\boldsymbol{T}^k(g)$ under the given basis in X^k. Note that

$$\begin{aligned}\boldsymbol{T}(g)(\boldsymbol{f}^1_i \otimes \boldsymbol{f}^2_j) &= \boldsymbol{T}^1(g)\boldsymbol{f}^1_i \otimes \boldsymbol{T}^2(g)\boldsymbol{f}^2_j \\ &= \sum_{p=1}^{n_1}\sum_{q=i}^{n_2} T^1_{pi}(g)T^2_{qj}(g)\boldsymbol{f}^1_p \otimes \boldsymbol{f}^2_q.\end{aligned}$$

We denote the matrix elements of the representation $\boldsymbol{T} = \boldsymbol{T}^1 \otimes \boldsymbol{T}^2$ under the basis $\{\boldsymbol{f}^1_i \otimes \boldsymbol{f}^2_j\}$, which are complex-valued functions defined on G, by

$$T_{pqij}(g) = T^1_{pi}(g)T^2_{qj}(g). \tag{13.78}$$

The character of the representation $\boldsymbol{T}$ is given by

$$\chi_{\boldsymbol{T}}(g) = \chi_{\boldsymbol{T}^1 \otimes \boldsymbol{T}^2} = \sum_{p=1}^{n_1}\sum_{q=1}^{n_2} T^1_{pp}(g)T^2_{qq}(g) = \chi_{\boldsymbol{T}^1}(g)\chi_{\boldsymbol{T}^2}(g) \tag{13.79}$$

for each $g \in G$.

[148] See, e.g., [273, Chap. 14], for the definition and basic properties of tensor products of vector spaces.

The discussion above can be generalized immediately to the tensor product of r representations for $r > 2$. Let $(\boldsymbol{T}^1, X^1), (\boldsymbol{T}^2, X^2), \ldots, (\boldsymbol{T}^r, X^r)$ be finite-dimensional representations of group G, where $\dim X^k = n_k$ $(k = 1, 2, \ldots, r)$. The tensor product $\boldsymbol{T} = \boldsymbol{T}^1 \otimes \boldsymbol{T}^2 \otimes \cdots \otimes \boldsymbol{T}^r$ of the representations $\boldsymbol{T}^1, \boldsymbol{T}^2, \ldots \boldsymbol{T}^r$ is the homomorphism $\boldsymbol{T} : G \to \mathrm{GL}(X^1 \otimes X^2 \otimes \cdots \otimes X^r)$ defined by

$$\boldsymbol{T}(g)(\boldsymbol{x}^1 \otimes \boldsymbol{x}^2 \otimes \cdots \otimes \boldsymbol{x}^r) = \boldsymbol{T}^1(g)\boldsymbol{x}^1 \otimes \boldsymbol{T}^2(g)\boldsymbol{x}^2 \otimes \cdots \otimes \boldsymbol{T}^r(g)\boldsymbol{x}^r \tag{13.80}$$

for all $\boldsymbol{x}^k \in X^k$ $(k = 1, 2, \ldots, r)$. Let $\boldsymbol{f}^k_1, \ldots, \boldsymbol{f}^k_{n_k}$ be a basis in X^k. Then $\{\boldsymbol{f}^1_{i_1} \otimes \boldsymbol{f}^2_{i_2} \otimes \cdots \boldsymbol{f}^r_{i_r} : 1 \le i_1 \le n_1, 1 \le i_2 \le n_2, \ldots, 1 \le i_r \le n_r\}$ constitutes a basis in $X^1 \otimes X^2 \otimes \cdots \otimes X^r$. For each $g \in G$, let $[T^k_{\mu\nu}(g)]$ be the matrix that represents $\boldsymbol{T}^k(g)$ under the given basis in X^k. Then the matrix elements of the representation $\boldsymbol{T} = \boldsymbol{T}^1 \otimes \boldsymbol{T}^2 \otimes \cdots \otimes \boldsymbol{T}^r$ under the basis $\{\boldsymbol{f}^1_{i_1} \otimes \boldsymbol{f}^2_{i_2} \otimes \cdots \otimes \boldsymbol{f}^r_{i_r}\}$ are given by

$$T_{p_1 p_2 \cdots p_r i_1 i_2 \cdots i_r}(g) = T^1_{p_1 i_1}(g) T^2_{p_2 i_2} \cdots T^r_{p_r i_r}(g). \tag{13.81}$$

The character of the representation $\boldsymbol{T}$ is given by

$$\chi_{\boldsymbol{T}}(g) = \chi_{\boldsymbol{T}^1}(g)\chi_{\boldsymbol{T}^2}(g) \cdots \chi_{\boldsymbol{T}^r}(g) \tag{13.82}$$

for each $g \in G$.

13.8 Unitary Representations on Spaces of Symmetric Tensors

13.8.1 Symmetric Tensors

Let S_r $(r \ge 2)$ be the symmetric group of permutations on $\{1, \ldots, r\}$, and let X be a complex vector space with $\dim X = n$. For each $\sigma \in S_r$, let $\mathcal{L}_\sigma : X^{\otimes r} \to X^{\otimes r}$ be the linear mapping defined by

$$\mathcal{L}_\sigma(\boldsymbol{x}_{i_1} \otimes \cdots \otimes \boldsymbol{x}_{i_r}) = \boldsymbol{x}_{i_{\sigma(1)}} \otimes \cdots \otimes \boldsymbol{x}_{i_{\sigma(r)}} \tag{13.83}$$

for all $\boldsymbol{x}_{i_k}$ $(i_k = 1, 2, 3; k = 1, \ldots, r)$ in X. An rth-order tensor $\boldsymbol{A}$ in $X^{\otimes r}$ is said to be symmetric if $\mathcal{L}_\sigma(\boldsymbol{A}) = \boldsymbol{A}$ for all $\sigma \in S_r$.[149] We denote the set of all rth-order symmetric tensors in $X^{\otimes r}$ by $[X^{\otimes r}]$.

Let $\mathcal{S} : X^{\otimes r} \to X^{\otimes r}$ be the linear mapping defined by

$$\mathcal{S} = \frac{1}{r!} \sum_{\sigma \in S_r} \mathcal{L}_\sigma. \tag{13.84}$$

Clearly for any $\sigma \in S_r$ we have

$$\mathcal{L}_\sigma \circ \mathcal{S} = \mathcal{S} \circ \mathcal{L}_\sigma = \mathcal{S}, \tag{13.85}$$

where $\circ$ denotes the composition of the linear mappings in question.

Proposition 13.32 *An rth-order tensor $\boldsymbol{A} \in X^{\otimes r}$ is symmetric if and only if*

$$\mathcal{S}(\boldsymbol{A}) = \frac{1}{r!} \sum_{\sigma \in S_r} \mathcal{L}_\sigma(\boldsymbol{A}) = \boldsymbol{A}. \tag{13.86}$$

[149] Backus [15] calls such a tensor $\boldsymbol{A}$ "totally symmetric".

Proof If $\boldsymbol{A}$ is symmetric, then

$$\mathcal{S}(\boldsymbol{A}) = \frac{1}{r!}\sum_{\sigma\in S_r}\mathcal{L}_\sigma(\boldsymbol{A}) = \frac{1}{r!}\sum_{\sigma\in S_r}\boldsymbol{A} = \boldsymbol{A}.$$

Conversely, if $\mathcal{S}(\boldsymbol{A}) = \boldsymbol{A}$, then for each $\sigma \in S_r$,

$$\mathcal{L}_\sigma(\boldsymbol{A}) = \mathcal{L}_\sigma(\mathcal{S}(\boldsymbol{A})) = (\mathcal{L}_\sigma \circ \mathcal{S})(\boldsymbol{A}) = \mathcal{S}(\boldsymbol{A}) = \boldsymbol{A}.$$

Hence $\boldsymbol{A}$ is symmetric. □

Note that $\mathcal{S}\circ\mathcal{S} = \mathcal{S}$, i.e., $\mathcal{S}$ is a projection. Moreover, $\mathcal{S}(X^{\otimes r}) = [X^{\otimes r}]$, i.e., $\mathcal{S}$ projects the space of rth-order tensors onto the space of rth-order symmetric tensors.

For $\boldsymbol{x}_1, \ldots, \boldsymbol{x}_n \in X$ and $\sigma \in S_r$, since $\mathcal{S}\circ\mathcal{L}_\sigma = \mathcal{S}$, the rth-order symmetric tensor

$$\mathcal{S}(\boldsymbol{x}_{i_1}\otimes\cdots\otimes\boldsymbol{x}_{i_r}) = \frac{1}{r!}\sum_{\sigma\in S_r}\boldsymbol{x}_{i_{\sigma(1)}}\otimes\cdots\otimes\boldsymbol{x}_{i_{\sigma(r)}},$$

where $i_k \in \{1, \ldots, n\}$ for each k, depends only on the number of times $p_j \geq 0$ that each $\boldsymbol{x}_j$ appears in the tensor product $\boldsymbol{x}_{i_1}\otimes\cdots\otimes\boldsymbol{x}_{i_r}$. Hence we can denote the symmetric tensor $\mathcal{S}(\boldsymbol{x}_{i_1}\otimes\cdots\otimes\boldsymbol{x}_{i_r})$, without ambiguity, by the symbol

$$\boldsymbol{x}_{i_1}\cdots\boldsymbol{x}_{i_r}, \quad \text{where } 1 \leq i_1 \leq \cdots \leq i_r \leq n,$$

or by

$$\boldsymbol{x}_1^{p_1}\cdots\boldsymbol{x}_n^{p_n}, \quad \text{where } p_k\ (k = 1, \ldots, n) \text{ is a non-negative integer and } p_1 + \cdots + p_n = r.$$

Proposition 13.33 *Let $\{\boldsymbol{f}_1, \ldots, \boldsymbol{f}_n\}$ be a basis of X. Then*

$$\left\{\frac{1}{r!}\sum_{\sigma\in S_r}\boldsymbol{f}_{i_{\sigma(1)}}\otimes\cdots\otimes\boldsymbol{f}_{i_{\sigma(r)}} : 1 \leq i_1 \leq \cdots \leq i_r \leq n\right\}$$

is a basis of $[X^{\otimes r}]$. Moreover,

$$dim\,[X^{\otimes r}] = C_r^{n+r-1} = \frac{(n+r-1)!}{r!(n-1)!}. \tag{13.87}$$

Proof Let $B = \{\boldsymbol{f}_{i_1}\otimes\cdots\otimes\boldsymbol{f}_{i_r} : 1 \leq i_1 \leq n, \ldots, 1 \leq i_r \leq n\}$, which constitutes a basis of $X^{\otimes r}$. Then, since $\mathcal{S}(X^{\otimes r}) = [X^{\otimes r}]$,

$$\begin{aligned}\mathcal{S}(B) &= \{\mathcal{S}(\boldsymbol{f}_{i_1}\otimes\cdots\otimes\boldsymbol{f}_{i_r}) : 1 \leq i_1 \leq \cdots \leq i_r \leq n\}\\ &= \{\boldsymbol{f}_1^{p_1}\cdots\boldsymbol{f}_n^{p_n} : p_k\ (k = 1, \ldots, n) \text{ is a non-negative integer, and } p_1 + \cdots + p_n = r\}\end{aligned}$$

spans $[X^{\otimes r}]$. The tensors in $\mathcal{S}(B)$ are linearly independent. Indeed, if $(p_1, \ldots, p_n) \neq (q_1, \ldots, q_n)$, then the tensors $\boldsymbol{f}_1^{p_1}\cdots\boldsymbol{f}_n^{p_n}$ and $\boldsymbol{f}_1^{q_1}\cdots\boldsymbol{f}_n^{q_n}$ are linear combinations of two non-intersecting sets of basis elements in $X^{\otimes r}$, respectively. The number of elements in

$\mathcal{S}(B)$ is none other than the number of partitions of r into a sum of n non-negative integers or the number of multisets[150] of r elements chosen from $\{1, \ldots, n\}$. This number is[151] C_r^{n+r-1}. □

13.8.2 Characters of Representations on Symmetric Tensors

Let $(\boldsymbol{T}, X)$ be an n-dimensional unitary representation of group G. For each $g \in G$, let $\boldsymbol{e}_i(g)$ $(i = 1, \ldots, n)$ be orthonormal eigenvectors of $\boldsymbol{T}(g)$ with corresponding eigenvalues λ_i, i.e., $\boldsymbol{T}(g)\boldsymbol{e}_i(g) = \lambda_i(g)\boldsymbol{e}_i(g)$ for each i, where we have appealed to the spectral theorem for normal operators [273, p. 236]. The subspace $[X^{\otimes 2}]$ of symmetric tensors in $X^{\otimes 2} = X \otimes X$ is generated by the basis

$$\{\frac{1}{2}\left(\boldsymbol{e}_i(g) \otimes \boldsymbol{e}_j(g) + \boldsymbol{e}_j(g) \otimes \boldsymbol{e}_i(g)\right) : 1 \le i \le j \le n\}.$$

Note that $[X^{\otimes 2}]$ is invariant under the tensor-product representation $\boldsymbol{T}^{\otimes 2} = \boldsymbol{T} \otimes \boldsymbol{T}$, and

$$\dim[X^{\otimes 2}] = C_2^{n+2-1} = \frac{(n+1)!}{2!\,(n-1)!} = \frac{n(n+1)}{2}.$$

Let $\boldsymbol{S}^{(2)}$ be the subrepresentation of $\boldsymbol{T}^{\otimes 2}$ on $[X^{\otimes 2}]$. Since

$$\begin{aligned}
&\boldsymbol{S}^{(2)}(g)\left(\frac{1}{2}(\boldsymbol{e}_i(g) \otimes \boldsymbol{e}_j(g) + \boldsymbol{e}_j(g) \otimes \boldsymbol{e}_i(g))\right) \\
&= \boldsymbol{T}^{\otimes 2}(g)\left(\frac{1}{2}(\boldsymbol{e}_i(g) \otimes \boldsymbol{e}_j(g) + \boldsymbol{e}_j(g) \otimes \boldsymbol{e}_i(g))\right) \\
&= \lambda_i(g)\lambda_j(g)\left(\frac{1}{2}(\boldsymbol{e}_i(g) \otimes \boldsymbol{e}_j(g) + \boldsymbol{e}_j(g) \otimes \boldsymbol{e}_i(g))\right),
\end{aligned} \tag{13.88}$$

the character of the representation $\boldsymbol{S}^{(2)} = \boldsymbol{T}^{\otimes 2}\big|_{[X^{\otimes 2}]}$ is given by the formula

$$\chi_{\boldsymbol{S}^{(2)}}(g) = \sum_{i \le j} \lambda_i(g)\lambda_j(g). \tag{13.89}$$

The discussion above can be immediately generalized to the subrepresentation $\boldsymbol{S}^{(r)}$ of $\boldsymbol{T}^{\otimes r}$ on $[X^{\otimes r}]$ for $r > 2$. For each $(i_1, i_2, \ldots, i_r)$ that satisfies $1 \le i_1 \le i_2 \le \cdots \le i_r \le n$, let

$$(\boldsymbol{e}_{i_1} \cdots \boldsymbol{e}_{i_r})(g) := \frac{1}{r!} \sum_{\sigma \in \mathcal{S}_r} \boldsymbol{e}_{i_{\sigma(1)}}(g) \otimes \cdots \otimes \boldsymbol{e}_{i_{\sigma(r)}}(g).$$

[150] Multisets are sets with possible repetition of elements. Some examples of multisets of 3 elements chosen from $\{1, 2, 3, 4\}$ are $\{1, 1, 2\}, \{2, 2, 2\}, \{1, 3, 4\}$.

[151] To see how to arrive at this number, consider the example of $n = 3$ and $r = 3$. Write in a line a pattern of $r = 3$ crosses and $n - 1 = 2$ bars, e.g., $\times||\times\times$, which pertains to $(p_1, p_2, p_3) = (1, 0, 2)$, a partition of 3 into the sum of 3 non-negative integers that corresponds to $\boldsymbol{f}_1^1\boldsymbol{f}_2^0\boldsymbol{f}_3^2$, or to the multiset $\{1, 3, 3\}$ that corresponds to $\boldsymbol{f}_1\boldsymbol{f}_3\boldsymbol{f}_3$. Another example is the pattern $|\times\times|\times$, which corresponds to $(p_1, p_2, p_3) = (0, 2, 1)$, i.e., $\boldsymbol{f}_1^0\boldsymbol{f}_2^2\boldsymbol{f}_3^1$, or to the multiset $\{2, 2, 3\}$, i.e., $\boldsymbol{f}_2\boldsymbol{f}_2\boldsymbol{f}_3$. In total there are $5!/(3!2!) = 10$ such patterns. In general the number we want to determine is the number of linear patterns of r crosses and $n - 1$ bars, or $(r + n - 1)!/(r!\,(n-1)!)$.

As shown in the preceding subsection, the tensors $(\boldsymbol{e}_{i_1}\cdots\boldsymbol{e}_{i_r})(g)$ form a basis in $[X^{\otimes r}]$, which is invariant under $\boldsymbol{T}^{\otimes r}=\boldsymbol{T}\otimes\cdots\otimes\boldsymbol{T}$ (r factors) and is of dimension C_r^{n+r-1}. Since

$$\boldsymbol{S}^{(r)}(g)\big((\boldsymbol{e}_{i_1}\cdots\boldsymbol{e}_{i_r})(g)\big)=\boldsymbol{T}^{\otimes r}(g)\big((\boldsymbol{e}_{i_1}\cdots\boldsymbol{e}_{i_r})(g)\big)=\lambda_{i_1}(g)\cdots\lambda_{i_r}(g)(\boldsymbol{e}_{i_1}\cdots\boldsymbol{e}_{i_r})(g), \tag{13.90}$$

the character of the representation $\boldsymbol{S}^{(r)}=\boldsymbol{T}^{\otimes r}\big|_{[X^{\otimes r}]}$ is given by the formula

$$\chi_{\boldsymbol{S}^{(r)}}(g)=\sum_{i_1\le i_2\le\cdots\le i_r}\lambda_{i_1}(g)\lambda_{i_2}(g)\cdots\lambda_{i_r}(g). \tag{13.91}$$

13.9 Irreducible Representations of Direct Product of Groups

Let G_1 and G_2 be two groups and $G_1\times G_2$ be their direct product (see Definition A.26 in Appendix A). Let $(\boldsymbol{T}_{G_1},X_1)$ and $(\boldsymbol{T}_{G_2},X_2)$ be finite-dimensional representations of G_1 and G_2, respectively, where $\dim\boldsymbol{T}_{G_1}=n_1$ and $\dim\boldsymbol{T}_{G_2}=n_2$. Let $\boldsymbol{T}:G_1\times G_2\to\mathrm{GL}(X_1\otimes X_2)$ be defined by

$$\boldsymbol{T}(g_1,g_2)(\boldsymbol{x}_1\otimes\boldsymbol{x}_2)=\boldsymbol{T}_{G_1}(g_1)\boldsymbol{x}_1\otimes\boldsymbol{T}_{G_2}(g_2)\boldsymbol{x}_2 \tag{13.92}$$

for all $g_1\in G_1$, $g_2\in G_2$, $\boldsymbol{x}_1\in X_1$, and $\boldsymbol{x}_2\in X_2$. It is easily verified that $(\boldsymbol{T},X_1\otimes X_2)$ is an n_1n_2-dimensional representation of $G_1\times G_2$ and

$$\chi_{\boldsymbol{T}}(g_1,g_2)=\chi_{\boldsymbol{T}_{G_1}}(g_1)\chi_{\boldsymbol{T}_{G_2}}(g_2)\qquad\text{for all }(g_1,g_2)\in G_1\times G_2. \tag{13.93}$$

We shall denote representation $\boldsymbol{T}$ of $G_1\times G_2$ in (13.92) also by $\boldsymbol{T}=\boldsymbol{T}_{G_1}\otimes\boldsymbol{T}_{G_2}$. If $\boldsymbol{T}_{G_1}$ and $\boldsymbol{T}_{G_2}$ are unitary representations of G_1 and G_2, respectively, it is clear that $\boldsymbol{T}_{G_1}\otimes\boldsymbol{T}_{G_2}$ is a unitary representation of $G_1\times G_2$.

Proposition 13.34 *Let G_1 and G_2 be compact groups, and let $\boldsymbol{T}_{G_1}$, $\boldsymbol{T}_{G_2}$ be finite dimensional continuous irreducible unitary representations of G_1 and G_2, respectively. Then $\boldsymbol{T}_{G_1}\otimes\boldsymbol{T}_{G_2}$ is a continuous unitary irreducible representation of $G_1\times G_2$.*

Proof It suffices to show that $\boldsymbol{T}_{G_1}\otimes\boldsymbol{T}_{G_2}$ is irreducible, because its other attributes are obvious. We will prove that $\langle\chi_{\boldsymbol{T}_{G_1}\otimes\boldsymbol{T}_{G_2}},\chi_{\boldsymbol{T}_{G_1}\otimes\boldsymbol{T}_{G_2}}\rangle_{G_1\times G_2}=1$. Indeed, we have

$$\begin{aligned}
&\langle\chi_{\boldsymbol{T}_{G_1}\otimes\boldsymbol{T}_{G_2}},\chi_{\boldsymbol{T}_{G_1}\otimes\boldsymbol{T}_{G_2}}\rangle_{G_1\times G_2}\\
&=\int_{G_1\times G_2}\chi_{\boldsymbol{T}_{G_1}\otimes\boldsymbol{T}_{G_2}}(g_1,g_2)\overline{\chi_{\boldsymbol{T}_{G_1}\otimes\boldsymbol{T}_{G_2}}(g_1,g_2)}\,d(g_1\times g_2)\\
&=\int_{G_1}\left(\int_{G_2}\chi_{\boldsymbol{T}_{G_1}}(g_1)\chi_{\boldsymbol{T}_{G_2}}(g_2)\overline{\chi_{\boldsymbol{T}_{G_1}}(g_1)\chi_{\boldsymbol{T}_{G_2}}(g_2)}\,d\mathfrak{g}_2\right)d\mathfrak{g}_1\\
&=\left(\int_{G_1}\chi_{\boldsymbol{T}_{G_1}}(g_1)\overline{\chi_{\boldsymbol{T}_{G_1}}(g_1)}\,d\mathfrak{g}_1\right)\left(\int_{G_2}\chi_{\boldsymbol{T}_{G_2}}(g_2)\overline{\chi_{\boldsymbol{T}_{G_2}}(g_2)}\,d\mathfrak{g}_2\right)\\
&=\langle\chi_{\boldsymbol{T}_{G_1}},\chi_{\boldsymbol{T}_{G_1}}\rangle_{G_1}\,\langle\chi_{\boldsymbol{T}_{G_2}},\chi_{\boldsymbol{T}_{G_2}}\rangle_{G_2}=1.
\end{aligned}$$

□

Remark 13.35 The proposition and its proof, with obvious modifications, remain valid if one or both of the groups G_1 and G_2 are finite. For instance, if G_1 is compact and G_2 is finite, then

$$\begin{aligned}&\langle \chi_{\boldsymbol{T}_{G_1}\otimes\boldsymbol{T}_{G_2}}, \chi_{\boldsymbol{T}_{G_1}\otimes\boldsymbol{T}_{G_2}}\rangle_{G_1\times G_2}\\ &= \int_{G_1}\left(\frac{1}{|G_2|}\sum_{g_2\in G_2}\chi_{\boldsymbol{T}_{G_1}}(g_1)\chi_{\boldsymbol{T}_{G_2}}(g_2)\overline{\chi_{\boldsymbol{T}_{G_1}}(g_1)\chi_{\boldsymbol{T}_{G_2}}(g_2)}\right) d\mathfrak{g}_1.\end{aligned}$$

□

Theorem 13.36 *Let $\{\boldsymbol{T}^1_{G_1},\ldots,\boldsymbol{T}^{m_1}_{G_1}\}$ and $\{\boldsymbol{T}^1_{G_2},\ldots,\boldsymbol{T}^{m_2}_{G_2}\}$ be complete sets of irreducible unitary representations of the finite groups G_1 and G_2, respectively. Then $\{\boldsymbol{T}^i_{G_1}\otimes\boldsymbol{T}^j_{G_2}: 1\le i\le m_1, 1\le j\le m_2\}$ is a complete set of irreducible unitary representations of $G_1\times G_2$.*

Proof Let $\mathsf{A}=\{\boldsymbol{T}^i_{G_1}\otimes\boldsymbol{T}^j_{G_2}: 1\le i\le m_1, 1\le j\le m_2\}$. Since

$$\langle \chi_{\boldsymbol{T}^i_{G_1}\otimes\boldsymbol{T}^j_{G_2}},\ \chi_{\boldsymbol{T}^p_{G_1}\otimes\boldsymbol{T}^q_{G_2}}\rangle_{G_1\times G_2}=\delta_{ip}\delta_{pq},$$

the representations $\boldsymbol{T}^i_{G_1}\otimes\boldsymbol{T}^j_{G_2}\in\mathsf{A}$ are pairwise inequivalent. To prove completeness of the set A, we will show that any irreducible unitary representation $\boldsymbol{T}$ of $G_1\times G_2$ is equivalent to some member of A. We shall prove by contradiction.

Let $\boldsymbol{T}$ be an irreducible unitary representation of $G_1\times G_2$ that is inequivalent to any $\boldsymbol{T}^i_{G_1}\otimes\boldsymbol{T}^j_{G_2}$ in A. Then we have

$$\begin{aligned}&\langle \chi_{\boldsymbol{T}}, \chi_{\boldsymbol{T}^i_{G_1}}\otimes\chi_{\boldsymbol{T}^j_{G_2}}\rangle_{G_1\times G_2}\\ &=\frac{1}{|G_1||G_2|}\sum_{g_1\in G_1}\sum_{g_2\in G_2}\chi_{\boldsymbol{T}}(g_1,g_2)\overline{\chi_{\boldsymbol{T}^i_{G_1}}(g_1)\chi_{\boldsymbol{T}^j_{G_2}}(g_2)}\\ &=\frac{1}{|G_1|}\sum_{g_1\in G_1}\left(\frac{1}{|G_2|}\sum_{g_2\in G_2}\chi_{\boldsymbol{T}}(g_1,g_2)\overline{\chi_{\boldsymbol{T}^j_{G_2}}(g_2)}\right)\overline{\chi_{\boldsymbol{T}^i_{G_1}}(g_1)}=0\end{aligned}\tag{13.94}$$

for all $1\le i\le m_1$, $1\le j\le m_2$. Let

$$f(g_1)=\frac{1}{|G_2|}\sum_{g_2\in G_2}\chi_{\boldsymbol{T}}(g_1,g_2)\overline{\chi_{\boldsymbol{T}^j_{G_2}}(g_2)}.\tag{13.95}$$

Since f is a class function and $\{\chi_{\boldsymbol{T}^i_{G_1}}: 1\le i\le m_1\}$ is a basis in the subspace of class functions defined on G_1, we infer from (13.94) that $f(g_1)=0$ for all $g_1\in G_1$. Hence we have

$$\frac{1}{|G_2|}\sum_{g_2\in G_2}\chi_{\boldsymbol{T}}(g_1,g_2)\overline{\chi_{\boldsymbol{T}^j_{G_2}}(g_2)}=0$$

for all $g_1\in G_1$, which, when combined with the fact that $\{\chi_{\boldsymbol{T}^j_{G_2}}: 1\le j\le m_2\}$ is a basis in the subspace of class functions defined on G_2, implies that $\chi_{\boldsymbol{T}}(g_1,g_2)=0$ for all $g_1\in G_1$ and $g_2\in G_2$. Then

$$\langle\chi_{\boldsymbol{T}},\chi_{\boldsymbol{T}}\rangle_{G_1\times G_2}=0,$$

contradicting the hypothesis that the representation $\boldsymbol{T}$ is irreducible. □

Table 11 Characters of group C_i

C_i	$[\boldsymbol{I}]$	$[\mathcal{I}]$
χ_{ρ^+}	1	1
χ_{ρ^-}	1	-1

Remark 13.37 By Corollary 13.30, since the number of basis elements in the complete set A is $m_1 m_2$, the number of conjugacy classes of $G_1 \times G_2$ is likewise $m_1 m_2$. □

13.10 Irreducible Representations of Improper Crystallographic Point Groups

As discussed in Sect. 2.6.1, the 32 crystallographic point groups can be classified into three types. Type I consists of 11 proper groups, i.e., they are subgroups of SO(3). The rest are improper (i.e., they are subgroups of O(3) but not of SO(3)) and are divided into two types. As we shall show in this section, once the problem of finding the character table and a complete set of irreducible unitary representations of each proper point group is solved, the parallel problem for all improper point groups can be handled easily.

13.10.1 Crystallographic Point Groups of Type II

There are 11 improper point groups of Type II, each of which is of the form $H \times C_i$, where H is a proper point group and $C_i = \{\boldsymbol{I}, \mathcal{I}\}$. Let us now examine the irreducible representations of improper point groups of Type II.

Since C_i has two elements, by Burnside's theorem it has only two inequivalent irreducible representations of dimension 1. Let us call these ρ^+ and ρ^-, with characters given by Table 11. Without loss of generality, we may take a one-dimensional space X as representation space for both ρ^+ and ρ^-. Let $\{\boldsymbol{e}\}$ be a unit vector in X. Then we have

$$\rho^+(\boldsymbol{I})\boldsymbol{e} = \boldsymbol{e}, \quad \rho^+(\mathcal{I})\boldsymbol{e} = \boldsymbol{e}; \qquad \rho^-(\boldsymbol{I})\boldsymbol{e} = \boldsymbol{e}, \quad \rho^-(\mathcal{I})\boldsymbol{e} = -\boldsymbol{e}. \tag{13.96}$$

Let $H \subset \mathrm{SO}(3)$ be a proper crystallographic point group, and let $(\boldsymbol{T}^1, X^1), \ldots, (\boldsymbol{T}^m, X^m)$ be a complete set of irreducible unitary representations of H. For $l = 1, \ldots, m$, let $\dim \boldsymbol{T}^l = n_l$ and $\{\boldsymbol{f}^l_1, \ldots, \boldsymbol{f}^l_{n_l}\}$ be an orthonormal basis in X^l. From what we have learned in Sect. 13.9, a complete set of irreducible unitary representations of $H \times C_i$ is given by

$$\{\boldsymbol{T}^l \otimes \rho^+ : 1 \le l \le m\} \cup \{\boldsymbol{T}^l \otimes \rho^- : 1 \le l \le m\}. \tag{13.97}$$

Let $T^l_{ij}(\boldsymbol{R})$ be the matrix elements of $\boldsymbol{T}^l(\boldsymbol{R})$ for $\boldsymbol{R} \in H$. Then we have

$$(\boldsymbol{T}^l \otimes \rho^+)(\boldsymbol{R}, \boldsymbol{I})(\boldsymbol{f}^l_i \otimes \boldsymbol{e}) = (\boldsymbol{T}^l(\boldsymbol{R}) \otimes \rho^+(\boldsymbol{I}))(\boldsymbol{f}^l_i \otimes \boldsymbol{e}) = \sum_{p=1}^{n_l} T^l_{pi}(\boldsymbol{R})(\boldsymbol{f}^l_p \otimes \boldsymbol{e}), \tag{13.98}$$

$$(\boldsymbol{T}^l \otimes \rho^+)(\boldsymbol{R}, \mathcal{I})(\boldsymbol{f}^l_i \otimes \boldsymbol{e}) = (\boldsymbol{T}^l(\boldsymbol{R}) \otimes \rho^+(\mathcal{I}))(\boldsymbol{f}^l_i \otimes \boldsymbol{e}) = \sum_{p=1}^{n_l} T^l_{pi}(\boldsymbol{R})(\boldsymbol{f}^l_p \otimes \boldsymbol{e}), \tag{13.99}$$

and

$$(\boldsymbol{T}^l \otimes \rho^-)(\boldsymbol{R}, \boldsymbol{I})(\boldsymbol{f}^l_i \otimes \boldsymbol{e}) = (\boldsymbol{T}^l(\boldsymbol{R}) \otimes \rho^-(\boldsymbol{I}))(\boldsymbol{f}^l_i \otimes \boldsymbol{e}) = \sum_{p=1}^{n_l} T^l_{pi}(\boldsymbol{R})(\boldsymbol{f}^l_p \otimes \boldsymbol{e}), \tag{13.100}$$

Table 12 Characters of irreducible representations of group $H \times C_i$ as given in terms of those of H

$H \times C_i$	$\boldsymbol{R}$	$\boldsymbol{R\mathcal{I}}$
$\chi_{\boldsymbol{T}^l \otimes \rho^+}$	$\chi_{\boldsymbol{T}^l}(\boldsymbol{R})$	$\chi_{\boldsymbol{T}^l}(\boldsymbol{R})$
$\chi_{\boldsymbol{T}^l \otimes \rho^-}$	$\chi_{\boldsymbol{T}^l}(\boldsymbol{R})$	$-\chi_{\boldsymbol{T}^l}(\boldsymbol{R})$

Table 13 Character table of group $D_{3h} = D_3 \times C_i$

D_{3h}	$[e]$	$2[r]$	$3[s]$	$[i]$	$2[ri]$	$3[si]$
$\chi_{\boldsymbol{T}^1 \otimes \rho^+}$	1	1	1	1	1	1
$\chi_{\boldsymbol{T}^1 \otimes \rho^-}$	1	1	1	−1	−1	−1
$\chi_{\boldsymbol{T}^2 \otimes \rho^+}$	1	1	−1	1	1	−1
$\chi_{\boldsymbol{T}^2 \otimes \rho^-}$	1	1	−1	−1	−1	1
$\chi_{\boldsymbol{T}^3 \otimes \rho^+}$	2	−1	0	2	−1	0
$\chi_{\boldsymbol{T}^3 \otimes \rho^-}$	2	−1	0	−2	1	0

Table 14 Crystallographic point groups of Type III and their corresponding isomorphic rotational point groups

Type III	C_s	S_4	C_{3h}	C_{2v}	C_{3v}	C_{4v}	D_{2d}	C_{6v}	D_{3h}	T_d
Type I	C_2	C_4	C_6	D_2	D_3	D_4	D_4	D_6	D_6	O

$$(\boldsymbol{T}^l \otimes \rho^-)(\boldsymbol{R}, \boldsymbol{\mathcal{I}})(\boldsymbol{f}_i^l \otimes \boldsymbol{e}) = (\boldsymbol{T}^l(\boldsymbol{R}) \otimes \rho^-(\boldsymbol{\mathcal{I}}))(\boldsymbol{f}_i^l \otimes \boldsymbol{e}) = \sum_{p=1}^{n_l} (-T_{pi}^l(\boldsymbol{R}))(\boldsymbol{f}_p^l \otimes \boldsymbol{e}). \tag{13.101}$$

Equations (13.98)–(13.101) give the matrix elements of the complete set (13.97) of irreducible unitary representations of $H \times C_i$. Hence once the matrix elements of a complete set of irreducible unitary representations of H have been ascertained, so are the matrix elements of a complete set of irreducible unitary representations of $H \times C_i$. Likewise, the characters of the irreducible representations of $H \times C_i$ are related to those of H as shown in Table 12. Using this table, we can immediately write down the character table of $H \times C_i$ if we already have that of H in hand. In other words, we can easily write down the character tables of all 11 improper point groups of Type II if we know the character tables of the 11 rotational point groups. As example, we give in Table 13 the character table of $D_{3h} = D_3 \times C_i$. To be consistent with our notation for group elements of D_3, we write e for $\boldsymbol{I}$ and i for $\boldsymbol{\mathcal{I}}$ in the table.

13.10.2 Crystallographic Point Groups of Type III

Two groups that are isomorphic have the same complete set of irreducible unitary representations and the same character table. Each crystallographic point group of Type III is isomorphic to the rotational point group in its Laue class (see Table 14). Hence, the problem to find the character table and a complete set of irreducible unitary representations for a Type III point group reduces to the parallel problem for its isomorphic rotational point group.

Chapter 14

14 Irreducible Representations of SU(2), SO(3), and O(3)

We will obtain a complete set of finite-dimensional, continuous, irreducible unitary representations of SO(3) by seeking a complete set of such representations for SU(2) and then applying the SU(2) (or Sp(1)) $\to$ SO(3) double covering. Once a complete set of irreducible representations has been determined for SO(3), getting such a set for O(3) will be straightforward.

14.1 Irreducible Representations of SU(2)

Our derivation of the irreducible representations of SU(2) and SO(3) largely follows the presentation of Weyl's method[152] by Sugiura [305, Chapter II]. Recall that

$$\mathrm{SU}(2) = \left\{ \begin{pmatrix} z & w \\ -\overline{w} & \overline{z} \end{pmatrix} : z, w \in \mathbb{C}, |z|^2 + |w|^2 = 1 \right\} \tag{14.1}$$

is the special unitary group of degree 2; see Sect. 11.4.

14.1.1 Construction of a Set of Continuous Unitary Representations

Let V_n be the space of homogeneous polynomials of degree n in two complex variables z_1 and z_2. Then V_n is a linear space of dimension $n+1$, which has a basis given by $z_1^{n-r} z_2^r$ $(0 \le r \le n)$. For each $g \in \mathrm{SU}(2)$, let $\mathsf{T}_g^n : V_n \to V_n$ be defined by

$$\mathsf{T}_g^n \varphi(\boldsymbol{z}) = \varphi(\boldsymbol{z} g) \qquad \text{for each } \varphi \in V_n \text{ and } \boldsymbol{z} \in \mathbb{C}_2, \tag{14.2}$$

where $\boldsymbol{z} = (z_1, z_2) \in \mathbb{C}_2$ are *row* vectors and g acts on $\boldsymbol{z}$ from the right. In what follows we shall also write $\mathsf{T}^n(g)$ for T_g^n.

Example 14.1 Consider the case $n = 2$. Let $\varphi_{2,0} = z_1^2$, $\varphi_{1,1} = z_1 z_2$, and $\varphi_{0,2} = z_2^2$, which together constitute a basis in V_2. Let

$$g = \begin{pmatrix} a & b \\ -\overline{b} & \overline{a} \end{pmatrix}$$

be in SU(2). Note that for each $\varphi \in V_2$,

$$(\mathsf{T}_g^2 \varphi)(z_1, z_2) = \varphi(\boldsymbol{z} g) = \varphi(a z_1 - \overline{b} z_2, b z_1 + \overline{a} z_2).$$

By direct computations we obtain

$$\begin{aligned} \mathsf{T}_g^2 \varphi_{2,0} &= a^2 \varphi_{2,0} - 2a\overline{b}\varphi_{1,1} + \overline{b}^2 \varphi_{0,2} \\ \mathsf{T}_g^2 \varphi_{1,1} &= ab\varphi_{2,0} + (a\overline{a} - b\overline{b})\varphi_{1,1} - \overline{a}\overline{b}\varphi_{0,2} \\ \mathsf{T}_g^2 \varphi_{0,2} &= b^2 \varphi_{2,0} + 2\overline{a}b\varphi_{1,1} + \overline{a}^2 \varphi_{0,2}. \end{aligned}$$

[152] The name was coined by Wigner ([340, p. 168], [341, p. 157]).

Under the given basis, T^2_g is represented by the matrix

$$\begin{pmatrix} a^2 & ab & b^2 \\ -2a\overline{b} & a\overline{a} - b\overline{b} & 2\overline{a}b \\ \overline{b}^2 & -\overline{a}\overline{b} & \overline{a}^2 \end{pmatrix},$$

which is not unitary. However, if we use the basis

$$\psi_{2,0} = \frac{1}{\sqrt{2}}\varphi_{2,0}, \quad \psi_{1,1} = \varphi_{1,1}, \quad \psi_{0,2} = \frac{1}{\sqrt{2}}\varphi_{0,2},$$

the matrix that represent T^2_g under the new basis is

$$\begin{pmatrix} a^2 & \sqrt{2}ab & b^2 \\ -\sqrt{2}a\overline{b} & a\overline{a} - b\overline{b} & \sqrt{2}\overline{a}b \\ \overline{b}^2 & -\sqrt{2}\overline{a}\overline{b} & \overline{a}^2 \end{pmatrix},$$

which is unitary. □

Proposition 14.2 *For each non-negative integer n, the map $\mathsf{T}^n : \mathrm{SU}(2) \to \mathrm{GL}(V_n)$, $g \mapsto \mathsf{T}^n_g$ is a continuous representation of* SU(2) *on V_n.*

Proof Note that for any $g_1, g_2 \in \mathrm{SU}(2)$ and $\varphi \in V_n$,

$$(\mathsf{T}^n_{g_1}(\mathsf{T}^n_{g_2}\varphi))(z) = (\mathsf{T}^n_{g_2}\varphi)(zg_1)) = \varphi(zg_1g_2) = (\mathsf{T}^n_{g_1g_2}\varphi)(z).$$

Hence the map $g \mapsto \mathsf{T}^n_g$ is a representation of SU(2) on V_n.

Under the basis given by $\varphi_{n,0} = z_1^n, \varphi_{n-1,1} = z_1^{n-1}z_2, \ldots, \varphi_{0,n} = z_2^n$, the linear transformation T^n_g is represented by the matrix whose entries are polynomial functions of the matrix elements of g. Hence the given map is continuous. □

Proposition 14.3 *For each non-negative integer n, let $\langle \cdot, \cdot \rangle$ be the inner product on V_n defined by*

$$\langle \sum_{r=0}^{n} \alpha_r z_1^{n-r} z_2^r, \sum_{r=0}^{n} \beta_r z_1^{n-r} z_2^r \rangle = \sum_{r=0}^{n} (n-r)!r!\alpha_r\overline{\beta_r}. \tag{14.3}$$

Then the representation T^n defined in Proposition 14.2 is unitary.

Proof Let $\mathbb{C}^2$ be the space of two-dimensional *column* vectors with complex components. For $\boldsymbol{z} \in \mathbb{C}_2$ and $\boldsymbol{a} \in \mathbb{C}^2$, let

$$<\boldsymbol{z}, \boldsymbol{a}> = z_1a_1 + z_2a_2. \tag{14.4}$$

Let $\varphi_{\boldsymbol{a}}(\boldsymbol{z}) = (<\boldsymbol{z}, \boldsymbol{a}>)^n = (z_1 a_1 + z_2 a_2)^n$. Then by definition of the inner product on V_n, we have

$$\begin{aligned}\langle \varphi_{\boldsymbol{a}}, \varphi_{\boldsymbol{b}} \rangle &= \langle \sum_{r=0}^{n} C_r^n a_1^{n-r} a_2^r z_1^{n-r} z_2^r, \sum_{r=0}^{n} C_r^n b_1^{n-r} b_2^r z_1^{n-r} z_2^r \rangle \\ &= \sum_{r=0}^{n} r!(n-r)! \left(C_r^n\right)^2 a_1^{n-r} a_2^r \overline{b_1}^{n-r} \overline{b_2}^r \\ &= n! \sum_{r=0}^{n} C_r^n (a_1 \overline{b_1})^{n-r} (a_2 \overline{b_2})^r \\ &= n! (a_1 \overline{b_1} + a_2 \overline{b_2})^n = n! (\boldsymbol{a}, \boldsymbol{b})^n, \end{aligned} \tag{14.5}$$

where $(\boldsymbol{a}, \boldsymbol{b}) = a_1 \overline{b_1} + a_2 \overline{b_2}$ is the Hermitian inner product on $\mathbb{C}^2$.

We claim that

$$\langle \mathsf{T}_g^n \varphi_{\boldsymbol{a}}, \mathsf{T}_g^n \varphi_{\boldsymbol{b}} \rangle = \langle \varphi_{\boldsymbol{a}}, \varphi_{\boldsymbol{b}} \rangle \tag{14.6}$$

for all $g \in \mathrm{SU}(2)$ and $\boldsymbol{a}, \boldsymbol{b} \in \mathbb{C}^2$. To see the validity of this claim, first note that

$$(\mathsf{T}_g^n \varphi_{\boldsymbol{a}})(\boldsymbol{z}) = \varphi_{\boldsymbol{a}}(\boldsymbol{z}g) = (<\boldsymbol{z}g, \boldsymbol{a}>)^n = (<\boldsymbol{z}, g\boldsymbol{a}>)^n = \varphi_{g\boldsymbol{a}}(\boldsymbol{z}). \tag{14.7}$$

Hence it follows from (14.5) and (14.7) that

$$\langle \mathsf{T}_g^n \varphi_{\boldsymbol{a}}, \mathsf{T}_g^n \varphi_{\boldsymbol{b}} \rangle = \langle \varphi_{g\boldsymbol{a}}(\boldsymbol{z}), \varphi_{g\boldsymbol{b}}(\boldsymbol{z}) \rangle = n! (g\boldsymbol{a}, g\boldsymbol{b})^n = n! (\boldsymbol{a}, \boldsymbol{b})^n = \langle \varphi_{\boldsymbol{a}}, \varphi_{\boldsymbol{b}} \rangle,$$

where we have appealed to the identity

$$(g\boldsymbol{a}, g\boldsymbol{b}) = (\boldsymbol{a}, \boldsymbol{b}) \qquad \text{for all } \boldsymbol{a}, \boldsymbol{b} \in \mathbb{C}^2$$

because $g \in \mathrm{SU}(2)$ is unitary.

By (14.6), T_g^n is unitary on V_n for each $g \in \mathrm{SU}(2)$ if the set $\{\varphi_{\boldsymbol{a}} : \boldsymbol{a} \in \mathbb{C}^2\}$ contains a basis of V_n. One such basis is furnished by the following $n+1$ polynomials:

$$\varphi_{(1,\omega^k)} = (z_1 + \omega^k z_2)^n \quad (1 \le k \le n), \qquad \text{and} \quad \varphi_{(0,1)} = z_2^n,$$

where $\omega = e^{i2\pi/n}$ is a primitive root of unity. Since

$$(z_1 + \omega^k z_2)^n = z_1^n + C_1^n \omega^k z_1^{n-1} z_2 + \cdots + C_{n-1}^n (\omega^k)^{n-1} z_1 z_2^{n-1} + (\omega^k)^n z_2^n,$$

to prove that the aforementioned $n+1$ polynomials constitute a basis of V_n it suffices to show that the determinant

$$D = \begin{vmatrix} 1 & C_1^n \omega & \cdots & C_l^n \omega^l & \cdots & C_{n-1}^n \omega^{n-1} & \omega^n \\ & & \cdots & & \cdots & & \\ 1 & C_1^n \omega^k & \cdots & C_l^n (\omega^k)^l & \cdots & C_{n-1}^n (\omega^k)^{n-1} & (\omega^k)^n \\ & & \cdots & & \cdots & & \\ 1 & C_1^n \omega^n & \cdots & C_l^n (\omega^n)^l & \cdots & C_{n-1}^n (\omega^n)^{n-1} & (\omega^n)^n \\ 0 & 0 & \cdots & 0 & \cdots & 0 & 1 \end{vmatrix}$$

is not zero. But, after expanding D by the last row, we observe that

$$D = \left(\prod_{l=1}^{n-1} C_l^n\right) \cdot \begin{vmatrix} 1 & \omega & \cdots & \omega^l & \cdots & \omega^{n-1} \\ & & \cdots & & \cdots & \\ 1 & \omega^k & \cdots & (\omega^k)^l & \cdots & (\omega^k)^{n-1} \\ & & \cdots & & \cdots & \\ 1 & \omega^n & \cdots & (\omega^n)^l & \cdots & (\omega^n)^{n-1} \end{vmatrix} \tag{14.8}$$

$$= \left(\prod_{l=1}^{n-1} C_l^n\right) \cdot \prod_{1 \le k < l \le n} (\omega^l - \omega^k) \neq 0,$$

where we have used the fact that the determinant on the right-hand side of (14.8) is the Vandermonde determinant in $\omega^1, \ldots, \omega^l, \ldots, \omega^n$, which are all distinct. Hence T_g^n is unitary for all $g \in \mathrm{SU}(2)$. □

Remark 14.4 If $m \neq n$, the representations T^m and T^n have different dimensions and thence are clearly inequivalent. □

Remark 14.5 Under the inner product defined on V_n by (14.3), the set

$$\left\{ \frac{z_1^{n-r} z_2^r}{\sqrt{(n-r)!r!}} : 0 \le r \le n \right\} \tag{14.9}$$

clearly constitutes an orthonormal basis in V_n. □

14.1.2 Characters and Irreducibility

By (11.66), each $g \in \mathrm{SU}(2)$ with $\mathrm{tr}\, g = 2\cos\theta$ $(0 \le \theta \le \pi)$ is conjugate to

$$h(\theta) = \begin{pmatrix} e^{i\theta} & 0 \\ 0 & e^{-i\theta} \end{pmatrix}. \tag{14.10}$$

Hence, to find the character $\chi_n(g) := \mathrm{tr}(\mathsf{T}_g^n) = \mathrm{tr}(\mathsf{T}_{h(\theta)}^n)$, we may find the trace of the matrix that represents $\mathsf{T}_{h(\theta)}^n$ under the basis

$$\varphi_{n,0} = z_1^n, \quad \ldots, \quad \varphi_{n-r,r} = z_1^{n-r} z_2^r, \quad \ldots, \quad \varphi_{0,n} = z_2^n$$

of V_n. Since $(z_1, z_2)h(\theta) = (z_1 e^{i\theta}, z_2 e^{-i\theta})$, by (14.2) we have

$$\mathsf{T}_{h(\theta)}^n \varphi_{n-r,r} = (e^{i\theta})^{n-2r} \varphi_{n-r,r} \qquad \text{for } 0 \le k \le n. \tag{14.11}$$

Hence, if $\theta \neq 0, \pi$ (i.e., $\mathrm{tr}\, g \neq 2, -2$), then

$$\chi_n(g) = \chi_n(h(\theta)) = \sum_{r=0}^{n} (e^{i\theta})^{n-2r} = \frac{1}{e^{in\theta}} \cdot \frac{1 - e^{i(2n+2)\theta}}{1 - e^{i2\theta}}$$

$$= \frac{e^{i(n+1)\theta} - e^{-i(n+1)\theta}}{e^{i\theta} - e^{-i\theta}} = \frac{\sin(n+1)\theta}{\sin\theta}. \tag{14.12}$$

Moreover, we have

$$\chi_n(g) = \chi_n(h(\theta)) = \begin{cases} n+1 & \text{if } \theta = 0 \text{ (i.e., } \operatorname{tr} g = 2) \\ (-1)^n(n+1) & \text{if } \theta = \pi \text{ (i.e., } \operatorname{tr} g = -2). \end{cases} \tag{14.13}$$

Since

$$\lim_{\theta\to 0} \frac{\sin(n+1)\theta}{\sin\theta} = n+1, \qquad \lim_{\theta\to\pi} \frac{\sin(n+1)\theta}{\sin\theta} = (-1)^n(n+1), \tag{14.14}$$

$\chi_n(h(\theta))$ is continuous on $[0, \pi]$.

Let G be a group. A function $f : G \to \mathbb{C}$ is called a class function if

$$f(ghg^{-1}) = f(h) \qquad \text{for any } g, h \in G. \tag{14.15}$$

Proposition 14.6 *Let $f : \mathrm{SU}(2) \to \mathbb{C}$ be an integrable class function. Then the integral of f with respect to the normalized Haar measure on* SU(2) *is given by*

$$\int_{SU(2)} f(g)\, dg = \frac{2}{\pi} \int_0^\pi f(\theta) \sin^2\theta\, d\theta, \tag{14.16}$$

where $f(\theta) = f(h(\theta))$ and $h(\theta)$ is given by (14.10).

Proof Since f is a class function, we have $f(g(\theta_1, \theta_2, \theta_3)) = f(h(\theta_1)) = f(\theta_1)$, where $(\theta_1, \theta_2, \theta_3)$ denotes the polar coordinates on $\mathcal{S}^3$; cf. (11.26) and Sect. 11.4. It follows then from (11.33) and (11.34) that

$$\begin{aligned} \int_{\mathrm{SU}(2)} f(g)\, dg &= \frac{1}{2\pi^2} \int_0^{2\pi} \int_0^\pi \int_0^\pi f(\theta_1) \sin^2\theta_1 \sin\theta_2\, d\theta_1 d\theta_2 d\theta_3 \\ &= \frac{1}{2\pi^2} \cdot 4\pi \int_0^\pi f(\theta_1) \sin^2\theta_1\, d\theta_1 = \frac{2}{\pi} \int_0^\pi f(\theta) \sin^2\theta\, d\theta, \end{aligned}$$

where we have written the dummy variable in the integral as θ. □

Proposition 14.7 *The representations $\mathrm{T}^n : \mathrm{SU}(2) \to \mathrm{GL}(V_n)$ $(n = 0, 1, 2, \ldots)$ are irreducible.*

Proof The characters χ_n of the representations T^n (see (14.12)–(14.14)) are continuous class functions. By appealing to (14.16), we obtain

$$\begin{aligned} \langle \chi_n, \chi_n \rangle &= \frac{2}{\pi} \int_0^\pi \frac{\sin^2(n+1)\theta}{\sin^2\theta} \sin^2\theta\, d\theta \\ &= \frac{2}{\pi} \int_0^\pi \sin^2(n+1)\theta\, d\theta = \frac{2}{\pi} \int_0^\pi \frac{1}{2} \left(1 - \cos 2(n+1)\theta\right) d\theta = 1. \end{aligned} \tag{14.17}$$

Therefore the representations T^n $(n = 0, 1, 2, \ldots)$ are irreducible. □

14.1.3 Completeness

Definition 14.8 Let G be a compact topological group and J be an index set. A set $\{\boldsymbol{T}^\alpha : \alpha \in J\}$ of pairwise inequivalent, finite-dimensional, continuous, irreducible unitary representations of G is said to be complete if every finite-dimensional continuous irreducible representation of G is equivalent to one of the representations $\boldsymbol{T}^\alpha$. □

In this section we shall prove that $\{\mathsf{T}^n : n = 0, 1, 2, \ldots\}$ constitutes a complete set of pairwise-inequivalent, finite-dimensional, continuous, irreducible unitary representations of SU(2).

By (14.12)–(14.14), the characters χ_n are even functions of θ. This fact can also be seen from the identity

$$\begin{pmatrix} 0 & -1 \\ 1 & 0 \end{pmatrix} \begin{pmatrix} e^{i\theta} & 0 \\ 0 & e^{-i\theta} \end{pmatrix} \begin{pmatrix} 0 & -1 \\ 1 & 0 \end{pmatrix}^{-1} = \begin{pmatrix} e^{-i\theta} & 0 \\ 0 & e^{i\theta} \end{pmatrix},$$

which indicates that $h(\theta)$ is conjugate to $h(-\theta)$.

In what follows, we consider the characters χ_n both as functions defined on SU(2) and as even functions in $L^2[-\pi, \pi]$. For brevity we shall use the symbol X to denote $L^2[-\pi, \pi]$, particularly in subscripts. We shall write $\langle \cdot, \cdot \rangle$ and $\| \cdot \|$ for the inner product and norm on $L^2(\mathrm{SU}(2), \mathbb{C})$, and write $\langle \cdot, \cdot \rangle_X$ and $\| \cdot \|_X$ for the inner product and norm on $L^2[-\pi, \pi]$. Recall from the theory of Fourier series that the functions

$$e_n(\theta) = \frac{1}{\sqrt{2\pi}} e^{in\theta} \qquad (n = 0, \pm 1, \pm 2, \ldots)$$

form an orthonormal basis in $L^2[-\pi, \pi]$, and that for $f \in L^2[-\pi, \pi]$, there holds the Parseval equality

$$\|f\|_X^2 = \sum_{n=-\infty}^{\infty} |\langle f, e_n \rangle|_X^2. \tag{14.18}$$

Theorem 14.9 *Any irreducible finite-dimensional continuous representation of* SU(2) *is equivalent to one of the representations* T^n *constructed in Sect.* 14.1.1.

Proof Let ρ be an irreducible finite-dimensional continuous representation of SU(2), and let χ_ρ be its character. From the discussions above, we know that $\chi_\rho(\theta)$, as a function in $L^2[-\pi, \pi]$, is even. Let $\xi \in L^2[-\pi, \pi]$ be defined by $\xi(\theta) = \chi_\rho(\theta) \sin\theta$. Clearly ξ is odd.

For $n = 1, 2, \ldots$, we have

$$\begin{aligned} \langle \xi, e_{\pm n} \rangle_X &= \frac{1}{\sqrt{2\pi}} \int_{-\pi}^{\pi} \xi(\theta) e^{\mp in\theta} \, d\theta \\ &= \frac{1}{\sqrt{2\pi}} \int_{-\pi}^{\pi} \xi(\theta)(\cos n\theta \mp i \sin n\theta) \, d\theta \\ &= \mp i \sqrt{\frac{2}{\pi}} \int_0^{\pi} \xi(\theta) \sin n\theta \, d\theta = \mp i \sqrt{\frac{2}{\pi}} \int_0^{\pi} \chi_\rho(\theta) \sin n\theta \sin\theta \, d\theta \end{aligned}$$

$$= \mp i\sqrt{\frac{2}{\pi}} \int_0^\pi \chi_\rho(\theta)\chi_{n-1}(\theta)\sin^2\theta\, d\theta = \mp i\sqrt{\frac{2}{\pi}} \cdot \frac{\pi}{2} \langle \chi_\rho, \chi_{n-1}\rangle$$

$$= \mp i\sqrt{\frac{\pi}{2}} \langle \chi_\rho, \chi_{n-1}\rangle. \tag{14.19}$$

By (14.18), (14.19), and the fact that $\langle \xi, e_0\rangle_X = 0$, we obtain

$$\|\xi\|_X^2 = \pi \sum_{n=1}^{\infty} |\langle \chi_\rho, \chi_{n-1}\rangle|^2. \tag{14.20}$$

On the other hand,

$$\|\xi\|_X^2 = \int_{-\pi}^{\pi} (\chi_\rho(\theta))^2 \sin^2\theta\, d\theta = \pi \cdot \frac{2}{\pi} \int_0^\pi (\chi_\rho(\theta))^2 \sin^2\theta\, d\theta = \pi \|\chi_\rho\|^2. \tag{14.21}$$

Comparing (14.20) and (14.21), we conclude that

$$\|\chi_\rho\|^2 = \sum_{n=0}^{\infty} |\langle \chi_\rho, \chi_n\rangle|^2. \tag{14.22}$$

Suppose the irreducible representation ρ is inequivalent to any of the T^n. Then

$$\langle \chi_\rho, \chi_n\rangle = 0 \qquad \text{for any } n = 0, 1, 2, \ldots,$$

which by (14.22) implies $\|\chi_\rho\| = 0$, contradicting the hypothesis that χ_ρ is irreducible, which implies $\langle \chi_\rho, \chi_\rho\rangle = 1$. Hence ρ must be equivalent to one of the T^n. □

Gathering Propositions 14.2, 14.3, and 14.7, Theorem 14.9, and Remark 14.4, we have proved the following theorem.

Theorem 14.10 *The representations* $\mathsf{T}^n : \mathrm{SU}(2) \to \mathrm{GL}(V_n)$ $(n = 0, 1, 2, \ldots)$ *form a complete set of pairwise-inequivalent, finite-dimensional, continuous, irreducible unitary representations of* $SU(2)$. □

14.1.4 A Simple Criterion for Irreducibility

For later use in Chap. 17 we present in this subsection a simple criterion for a finite-dimensional unitary representation of SU(2) to be irreducible.

Proposition 14.11 *Let* $(\boldsymbol{T}, X)$ *be a finite-dimensional unitary representation of* SU(2), *where* $\dim X = n + 1$. *A necessary and sufficient condition for* $(\boldsymbol{T}, X)$ *to be equivalent to* (T^n, V_n) *is that* $\exp(in\theta)$ *is an eigenvalue of* $\boldsymbol{T}(h(\theta))$, *where* $h(\theta) \in \mathrm{SU}(2)$ *is given by* (14.10).

Proof Necessity of the given condition is obvious from (14.11). To prove sufficiency, let

$$\boldsymbol{T} = n_1 \mathsf{T}^{\alpha_1} + \cdots + n_p \mathsf{T}^{\alpha_p} \tag{14.23}$$

be a decomposition of $\boldsymbol{T}$ as a direct sum of multiples of irreducible unitary representations $\mathsf{T}^{\alpha_1}, \ldots, \mathsf{T}^{\alpha_p}$ of SU(2). Clearly $\alpha_i \leq n$ for each $i = 1, \ldots, p$; otherwise there must hold $\dim X > n+1$, contradicting the hypothesis that $\dim X = n+1$. If $\alpha_i < n$ for all $i = 1, \ldots, p$, then all the eigenvalues of $\boldsymbol{T}(h(\theta))$ are of the form $\exp(im\theta)$ with $|m| < n$, which contradicts the hypothesis that $\exp(in\theta)$ is an eigenvalue of $\boldsymbol{T}(h(\theta))$. Therefore at least one of the α_i's must be equal to n. Since $\dim X = n+1 = \dim V_n$, we conclude that the representation $(\boldsymbol{T}, X)$ is equivalent to the irreducible representation (T^n, V_n). □

14.2 The Wigner D-Functions

The Wigner D-functions are matrix elements of the representations T^n $(n = 0, 1, 2, \ldots)$ under a chosen basis in V_n (to be specified below) orthonormal with respect to the inner product (14.3). In what follows we will modify our notation to conform with that commonly used in the physics literature.

For each ordered pair of non-negative integers (n, r), where $0 \leq r \leq n$, we define (j, m) by $n = 2j$ and $r = j - m$. Then we have

$$j = n/2, \quad j \geq m \geq -j, \quad j + m = n - r, \quad j - m = r. \tag{14.24}$$

We rename T^n as $\mathcal{D}^j$ and T^n_g as $\mathcal{D}^j(g)$, where $j = 0, \frac{1}{2}, 1, \frac{3}{2}, 2, \ldots$, and $g \in \mathrm{SU}(2)$ is given by

$$g = \begin{pmatrix} a & b \\ -\overline{b} & \overline{a} \end{pmatrix}. \tag{14.25}$$

For each $V_{2j} = V_n$, consider the orthonormal basis—with inner product defined by (14.3)—given in (14.9), which after a change of labeling from (n, r) to (j, m) reads (cf. [274, Appendix II], [336, Sect. 8.1]):

$$e^j_m(z_1, z_2) = \frac{z_1^{j+m} z_2^{j-m}}{\sqrt{(j+m)!(j-m)!}}. \qquad (j \geq m \geq -j) \tag{14.26}$$

By (14.2), we have

$$\begin{aligned}
\mathcal{D}^j(g) e^j_m(z_1, z_2) &= e^j_m(z_1 a - z_2 \overline{b}, z_1 b + z_2 \overline{a}) \\
&= \frac{(z_1 a - z_2 \overline{b})^{j+m} (z_1 b + z_2 \overline{a})^{j-m}}{\sqrt{(j+m)!(j-m)!}} \\
&= \sum_{k=0}^{j+m} \sum_{k'=0}^{j-m} \frac{C_k^{j+m} C_{k'}^{j-m}}{\sqrt{(j+m)!(j-m)!}} (z_1 a)^{j+m-k} (-z_2 \overline{b})^k (z_1 b)^{j-m-k'} (z_2 \overline{a})^{k'} \\
&= \sum_{k=0}^{j+m} \sum_{k'=0}^{j-m} (-1)^k \frac{\sqrt{(j+m)!(j-m)!}}{k!(j+m-k)!k'!(j-m-k')!} \\
&\qquad \times a^{j+m-k} b^{j-m-k'} \overline{a}^{k'} \overline{b}^k z_1^{2j-k-k'} z_2^{k+k'}.
\end{aligned} \tag{14.27}$$

Note that in (14.27) the double summation extends over all integer values of the indices k and k' under which the factorial arguments in the denominator are non-negative.[153] Let $m' = j - k - k'$. Then $2j - k - k' = j + m'$, $k + k' = j - m'$, and we recast (14.27) as

$$\mathcal{D}^j(g)e^j_m(z_1, z_2) = \sum_{m'=-j}^{j} \sum_k (-1)^k \frac{\sqrt{(j+m)!(j-m)!(j+m')!(j-m')!}}{k!(j+m-k)!(j-m'-k)!(m'-m+k)!} \times a^{j+m-k} b^{m'-m+k} \overline{a}^{j-m'-k} \overline{b}^k e^j_{m'}(z_1, z_2), \tag{14.28}$$

where the summation index k runs over all integer values such that the factorial arguments in the denominator are non-negative. It follows from (14.28) that the elements of the matrix which represents $\mathcal{D}^j(g)$ under the orthonormal basis $\{e^j_m : j \geq m \geq -j\}$ are given by[154]

$$D^j_{m'm}(g) = \sum_k (-1)^k \frac{\sqrt{(j+m)!(j-m)!(j+m')!(j-m')!}}{k!(j+m-k)!(j-m'-k)!(m'-m+k)!} \times a^{j+m-k} b^{m'-m+k} \overline{a}^{j-m'-k} \overline{b}^k, \tag{14.29}$$

where the summation is over integer values of k that satisfy

$$k \geq 0, \quad k \leq j + m, \quad k \leq j - m', \quad k \geq m - m'. \tag{14.30}$$

Expressions of the Wigner D-functions appear in many equivalent forms. For example, if $(14.27)_3$ is written in the form

$$\begin{aligned} \mathcal{D}^j(g)e^j_m(z_1, z_2) &= \sum_{k'=0}^{j+m} \sum_{k=0}^{j-m} \frac{C^{j+m}_{k'} C^{j-m}_k}{\sqrt{(j+m)!(j-m)!}} (z_1 a)^{j+m-k'} (-z_2 \overline{b})^{k'} (z_1 b)^k (z_2 \overline{a})^{j-m-k} \\ &= \sum_{k=0}^{j-m} \sum_{k'=0}^{j+m} (-1)^{k'} \frac{\sqrt{(j+m)!(j-m)!}}{k'!(j+m-k')!k!(j-m-k)!} \\ &\quad \times a^{j+m-k'} b^k \overline{a}^{j-m-k} \overline{b}^{k'} z_1^{j+m+k-k'} z_2^{j-m-k+k'}, \end{aligned} \tag{14.31}$$

then by putting $m' = m - k' + k$ in (14.31) we obtain, instead of (14.28), the following expression:

$$\mathcal{D}^j(g)e^j_m = \sum_{m'=-j}^{j} \sum_k (-1)^{m-m'+k} \frac{\sqrt{(j+m)!(j-m)!(j+m')!(j-m')!}}{k!(j-m-k)!(j+m'-k)!(m-m'+k)!} \times a^{j+m'-k} b^k \overline{a}^{j-m-k} \overline{b}^{m-m'+k} e^j_{m'}, \tag{14.32}$$

where the summation index k extends over all integer values such that the factorial arguments in the denominator are non-negative. We then read off from (14.32) the following

[153] As pointed out by Rose [274, p. 232], another option is to define $1/n! = 0$ for $n < 0$. Then the summation indices k and k' can go from $-\infty$ to ∞.

[154] Cf. Biedenharn and Louck [28, p. 217, Eq. (5.44)], where $u_{11} = a$, $u_{12} = b$, $u_{21} = -\overline{b}$, and $u_{22} = \overline{a}$.

expression for the Wigner D-functions:

$$D^j_{m'm}(g) = \sum_k (-1)^{m-m'+k} \frac{\sqrt{(j+m)!(j-m)!(j+m')!(j-m')!}}{k!(j-m-k)!(j+m'-k)!(m-m'+k)!} \times a^{j+m'-k} b^k \overline{a}^{j-m-k} \overline{b}^{m-m'+k}, \tag{14.33}$$

where the summation extends over integer values of k that satisfy

$$k \geq 0, \quad k \leq j-m, \quad k \leq j+m', \quad k \geq m'-m. \tag{14.34}$$

Obviously there are still other expressions of the Wigner D-functions that are equivalent to (14.29) and (14.33). Let us give one more example. Equation $(14.27)_2$ can also be expanded as

$$\begin{aligned} \mathcal{D}^j(g) e^j_m(z_1, z_2) &= \sum_{k=0}^{j+m} \sum_{k'=0}^{j-m} \frac{C^{j+m}_k C^{j-m}_{k'}}{\sqrt{(j+m)!(j-m)!}} (z_1 a)^k (-z_2 \overline{b})^{j+m-k} (z_1 b)^{j-m-k'} (z_2 \overline{a})^{k'} \\ &= \sum_{k=0}^{j+m} \sum_{k'=0}^{j-m} (-1)^{j+m-k} \frac{\sqrt{(j+m)!(j-m)!}}{k!(j+m-k)!k'!(j-m-k')!} \\ &\quad \times a^k b^{j-m-k'} \overline{a}^{k'} \overline{b}^{j+m-k} z_1^{j-m+k-k'} z_2^{j+m-k+k'}. \end{aligned} \tag{14.35}$$

Then by putting $m' = -m + k - k'$ in (14.35) so that

$$z_1^{j-m+k-k'} z_2^{j+m-k+k'} = \sqrt{(j+m')!(j-m')!}\, e^j_{m'},$$

we obtain, for the matrix elements of $\mathcal{D}^j(g)$ under the basis $\{e^j_m\}$, the expression

$$D^j_{m'm}(g) = \sum_k (-1)^{j+m-k} \frac{\sqrt{(j+m)!(j-m)!(j+m')!(j-m')!}}{k!(j+m-k)!(j+m'-k)!(k-m-m')!} \times a^k b^{j+m'-k} \overline{a}^{k-m-m'} \overline{b}^{j+m-k}, \tag{14.36}$$

where the summation index k extends over all integer values such that the factorial arguments in the denominator are non-negative.

In this section we have followed Weyl's method and derived three general formulas that express the Wigner D-functions in terms of the entries of a generic SU(2) matrix (14.25). Various explicit expressions of the Wigner D-functions are obtained when formulas for various parametrizations of SU(2) are substituted into (14.29), (14.33), (14.36), and other expressions equivalent to them. In the next section we will write down some explicit expressions of Wigner D-functions in Euler Angles.

14.2.1 Wigner D-Functions in Euler Angles

We begin by expressing the Euler-Rodrigues parameters (q_0, q_1, q_2, q_3) of a rotation $\boldsymbol{R}$ in terms of its Euler angles (ψ, θ, ϕ). Since $\boldsymbol{R}(\psi, \theta, \phi) = \boldsymbol{R}(\boldsymbol{e}_3, \psi)\boldsymbol{R}(\boldsymbol{e}_2, \theta)\boldsymbol{R}(\boldsymbol{e}_3, \phi)$, the

quaternion pertaining to $\boldsymbol{R}(\psi,\theta,\phi)$ can be expressed as

$$\begin{aligned} q &= \left(\cos\frac{\psi}{2}+\sin\frac{\psi}{2}\boldsymbol{k}\right)\left(\cos\frac{\theta}{2}+\sin\frac{\theta}{2}\boldsymbol{j}\right)\left(\cos\frac{\phi}{2}+\sin\frac{\phi}{2}\boldsymbol{k}\right) \\ &= \left(\cos\frac{\psi}{2}\cos\frac{\theta}{2}+\cos\frac{\psi}{2}\sin\frac{\theta}{2}\boldsymbol{j}+\cos\frac{\theta}{2}\sin\frac{\psi}{2}\boldsymbol{k}-\sin\frac{\psi}{2}\sin\frac{\phi}{2}\boldsymbol{i}\right)\left(\cos\frac{\phi}{2}+\sin\frac{\phi}{2}\boldsymbol{k}\right) \\ &= q_0+q_1\boldsymbol{i}+q_2\boldsymbol{j}+q_3\boldsymbol{k}, \end{aligned} \tag{14.37}$$

where

$$\begin{aligned} q_0 &= \cos\frac{\theta}{2}\cos\frac{\psi+\phi}{2}, \qquad & q_1 &= \sin\frac{\theta}{2}\sin\frac{\phi-\psi}{2}, \\ q_2 &= \sin\frac{\theta}{2}\cos\frac{\psi-\phi}{2}, \qquad & q_3 &= \cos\frac{\theta}{2}\sin\frac{\psi+\phi}{2}. \end{aligned} \tag{14.38}$$

For SO(3), the domain of the Euler angles is defined by $\psi\in[0,2\pi)$, $\theta\in[0,\pi]$, $\phi\in[0,2\pi)$. From (14.38), we observe that if (ψ,θ,ϕ) pertains to the quaternion x, then $(\psi,\theta+2\pi,\phi)$ delivers $-x$. Hence a domain of the Euler angles that will cover $\mathcal{S}^3$ is given by:

$$0\le\psi<2\pi, \qquad 0\le\theta\le\pi \quad \text{or} \quad 2\pi\le\theta\le3\pi, \qquad 0\le\phi<2\pi. \tag{14.39}$$

The correspondence between the Euler angles (ψ,θ,ϕ) and $q\in\mathcal{S}^3$ is not one-to-one when $\theta=0,\pi,2\pi,3\pi$, which correspond to the sets $V_1=\{(q_0,q_1,q_2,q_3)\in\mathcal{S}^3: q_0^2+q_3^2=1\}$ and $V_2=\{(q_0,q_1,q_2,q_3)\in\mathcal{S}^3: q_1^2+q_2^2=1\}$. It is one-to-one on $U=\mathcal{S}^3\setminus(V_1\cup V_2)$.

Substituting (14.38) into (11.69), we have

$$g=\begin{pmatrix} e^{-i\psi/2}\cos\frac{\theta}{2}e^{-i\phi/2} & -e^{-i\psi/2}\sin\frac{\theta}{2}e^{i\phi/2} \\ e^{i\psi/2}\sin\frac{\theta}{2}e^{-i\phi/2} & e^{i\psi/2}\cos\frac{\theta}{2}e^{i\phi/2} \end{pmatrix}, \tag{14.40}$$

where the domain of the Euler angles is given by (14.39).

Substituting $a=e^{-i\psi/2}\cos\frac{\theta}{2}e^{-i\phi/2}$ and $b=-e^{-i\psi/2}\sin\frac{\theta}{2}e^{i\phi/2}$ into (14.29), we obtain the following formula for the Wigner D-functions in Euler angles:

$$D^j_{m'm}(\psi,\theta,\phi)=e^{-im'\psi}d^j_{m'm}(\theta)e^{-im\phi}; \tag{14.41}$$

here $\psi\in[0,2\pi)$, $\theta\in[0,\pi]\cup[2\pi,3\pi]$, $\phi\in[0,2\pi)$, and

$$\begin{aligned} d^j_{m'm}(\theta)=\sum_k(-1)^{m'-m+k}\frac{\sqrt{(j+m)!(j-m)!(j+m')!(j-m')!}}{k!(j+m-k)!(j-m'-k)!(m'-m+k)!} \\ \times\left(\cos\frac{\theta}{2}\right)^{2j+m-m'-2k}\left(\sin\frac{\theta}{2}\right)^{m'-m+2k}, \end{aligned} \tag{14.42}$$

where the summation runs over all integer values of index k that satisfy (14.30). Note that the function $d^j_{m'm}$ is real-valued. When (14.42) is substituted in (14.41), we obtain the formula for $D^j_{m'm}(\psi,\theta,\phi)$ given in the book by Rose [274, p. 234]; see also [325, p. 77, equation (5)].

Similarly, if $a = e^{-i\psi/2}\cos\frac{\theta}{2}e^{-i\phi/2}$ and $b = -e^{-i\psi/2}\sin\frac{\theta}{2}e^{i\phi/2}$ are substituted into (14.33) and (14.36), respectively, we obtain (14.41) but, instead of (14.42), we get the expressions[155]

$$d^j_{m'm}(\theta) = \sum_k (-1)^k \frac{\sqrt{(j+m)!(j-m)!(j+m')!(j-m')!}}{k!(j-m-k)!(j+m'-k)!(m-m'+k)!} \times \left(\cos\frac{\theta}{2}\right)^{2j+m'-m-2k} \left(\sin\frac{\theta}{2}\right)^{m-m'+2k}, \tag{14.43}$$

and

$$d^j_{m'm}(\theta) = \sum_k (-1)^{j+m'-k} \frac{\sqrt{(j+m)!(j-m)!(j+m')!(j-m')!}}{k!(j+m-k)!(j+m'-k)!(k-m'-m)!} \times \left(\cos\frac{\theta}{2}\right)^{2k-m'-m} \left(\sin\frac{\theta}{2}\right)^{2j+m'+m-2k}, \tag{14.44}$$

respectively, where the summation index k extends over all integer values such that the factorial arguments in the denominator are non-negative. A collection of explicit expressions of the Wigner D-functions in terms of Euler angles has been compiled by Varshalovich et al. [325, Sect. 4.3]. In particular, formulas (14.42), (14.43), and (14.44) are listed as equations (5), (4), and (3), respectively, in [325, pp. 76–77].

14.2.2 Wigner D-Functions in Euler-Rodrigues Parameters

Formulas (14.29), (14.33), and (14.36) are valid for any parametrizations of SU(2). As illustration, let us put (14.29) in Euler-Rodrigues parameters (see Sect. 11.4.2). Substituting (11.70) into (11.69), we observe that a generic element g of SU(2) is given by the formula

$$g = \begin{pmatrix} \cos\frac{\omega}{2} - i\sin\frac{\omega}{2}\cos\Theta & -i\sin\frac{\omega}{2}\sin\Theta\, e^{-i\Phi} \\ -i\sin\frac{\omega}{2}\sin\Theta\, e^{i\Phi} & \cos\frac{\omega}{2} + i\sin\frac{\omega}{2}\cos\Theta \end{pmatrix}. \tag{14.45}$$

Substituting $a = \cos\frac{\omega}{2} - i\sin\frac{\omega}{2}\cos\Theta$, $b = -i\sin\frac{\omega}{2}\sin\Theta\, e^{-i\Phi}$ into the general formula (14.29) for $D^j_{m'm}(g)$, we obtain[156]

$$\begin{aligned} &D^j_{m'm}(\omega;\Theta,\Phi) \\ &= \sum_k \frac{\sqrt{(j+m)!(j-m)!(j+m')!(j-m')!}}{k!(j+m-k)!(j-m'-k)!(m'-m+k)!} a^{j+m-k} b^{m'-m+k} (-\overline{b})^k \overline{a}^{j-m'-k} \\ &= (-iv)^{m'-m}(1-v^2)^{j+m}\overline{a}^{-(m'+m)} e^{-i(m'-m)\Phi} \\ &\quad \times \sum_k \frac{\sqrt{(j+m)!(j-m)!(j+m')!(j-m')!}}{k!(j+m-k)!(j-m'-k)!(m'-m+k)!} \left(\frac{v^2}{1-v^2}\right)^k, \end{aligned} \tag{14.46}$$

[155] Messiah [230, p. 1072] calls (14.43) "the Wigner formula".

[156] Cf. Biedenharn and Louck [28, p. 54, Eq. (3.89)].

where $v := \sin\frac{\omega}{2}\sin\Theta$ and the summation index k extends over all integer values such that the factorial arguments in the denominator are non-negative. Note that all the exponents of each summand in $(14.46)_1$ are non-negative integers. Hence $D^j_{m'm} : \mathcal{S}^3 \to \mathbb{C}$ is continuous.

It should be emphasized that there are many expressions for $D^j_{m'm}(\omega;\Theta,\Phi)$, not only because there are different equivalent general expressions for $D^j_{m'm}(g)$, but also because there are different ways to parametrize SU(2) with axis-angle parameters. For example, Carmeli ([69]; see also [70, pp. 25–39]) also uses Weyl's method to derive an expression for $D^j_{m'm}(\omega;\Theta,\Phi)$. But the general expression for $D^j_{m'm}(g)$ that he adopts is different than those we have derived, and his (a,b) is, in our notation, $(\overline{a},\overline{b})$. Varshalovich et al. [325, p. 81] briefly outline several methods to derive expressions for $D^j_{m'm}(\omega;\Theta,\Phi)$, one of which is the method we have presented above. They write down two explicit expressions under this method, one of which is clearly related to the general formula (14.36). But their (a,b) is, in our notation, $(a,-\overline{b})$. In our presentation we have followed the convention adopted in the treatise of Biedenharn and Louck [28].

Remark 14.12 In 2008–2009 Mason and Schuh [212, 213] and Mason [211] promoted using series expansion of the ODF in hyperspherical harmonics[157] in texture analysis so that "the analysis of crystallographic information may be performed entirely in the axis-angle parametrization" [211]. The benefits of using axis-angle parameters over using Euler angles as arguments of the ODF, particularly for texture data from single-orientation measurements, are amply supported by references cited in their papers. The hyperspherical harmonics are defined on $\mathcal{S}^3$, the polar coordinates of which are the (re-ordered) Euler-Rodrigues parameters, and they constitute an orthogonal basis in $L^2(\mathcal{S}^3,\mathbb{C})$. These properties of the hyperspherical harmonics might have drawn the attention of Mason and Schuh, who, however, seem to have overlooked the fact that the Wigner D-functions enjoy the same properties. In his famous 1931 book, Wigner ([340]; see also the 1959 English edition [341]) follows the method suggested by Weyl and derives a complete set of irreducible representations of SU(2) as the first step to do the same for the rotation group. Thus he starts by obtaining a general explicit formula (see [340, p. 176, Eq. (21)] or [341, p. 164, eq. (15.21)]) for what we now call the Wigner D-functions $D^j_{m'm} : \mathrm{SU}(2) \to \mathbb{C}$, expressed in terms of the entries a, b, $-\overline{b}$, and $\overline{a}$ of a generic element g in $\mathrm{SU}(2) \cong \mathrm{Sp}(1)$ or $\mathcal{S}^3$; cf. our (14.29), (14.33), and (14.36). Such general formulas are valid for all parametrizations of $\mathcal{S}^3$. Putting a and b in Euler-Rodrigues parameters here will, in the next step, lead to Wigner D-functions D^l_{mn} for SO(3) with the axis-angle parameters $(\omega;\Theta,\Phi)$ as independent variables.

Commenting on two other derivations of an explicit formula for $D^l_{mn}(\omega;\Theta,\Phi)$ by Moses [239, 240], Carmeli [69], who obtains the same formula derived by Moses by using Weyl's method, points out that "the present method is much easier for the interested physicist to follow than the previous works [i.e., the derivations by Moses] since it is most closely related to the usual derivation of the representation, such as Wigner's, when the Euler angles are used". By the same token practitioners of texture analysis are familiar with the Wigner D-functions or the generalized spherical harmonics as functions of the Euler angles. It will be easier for them to use these same functions with the axis-angles parameters as independent variables than to learn about hyperspherical harmonics anew. □

[157] Here hyperspherical harmonics mean polynomial solutions of the Laplace equation in $\mathbb{R}^4$ which are matrix elements of a complete set of irreducible representations of SO(4). Cf. e.g., Talman [309, Chap. 10].

14.3 Irreducible Unitary Representations of SO(3)

Recall that $\mathrm{Ad} : \mathrm{SU}(2) \to \mathrm{SO}(3)$ is a smooth homomorphism and local diffeomorphism with $\mathrm{Ker}(\mathrm{Ad}) = \{\pm \boldsymbol{I}\}$. It follows that we can obtain a complete set of irreducible unitary representations of SO(3) from the irreducible unitary representations T^n of SU(2) constructed in Sect. 14.1, as shown in the following theorem.

Theorem 14.13 *For each non-negative integer l, there is an irreducible unitary representation $\mathcal{D}^l$ of* SO(3) *defined by*

$$\mathcal{D}^l \circ \mathrm{Ad} = \mathsf{T}^{2l}, \tag{14.47}$$

where T^{2l} is the irreducible representation T^n of SU(2) *(see Sect. 14.1) with $n = 2l$. Any irreducible unitary representation $\mathcal{D}$ of* SO(3) *is equivalent to $\mathcal{D}^l$ for some non-negative integer l, and $\{\mathcal{D}^l : l = 0, 1, 2, \ldots\}$ provides a complete set of finite-dimensional, continuous, irreducible unitary representations of* SO(3).

Proof Let $\boldsymbol{I}$ be the identity matrix in SU(2). For the basis $\varphi_{n-r,r} = z_1^{n-r} z_2^r$ $(0 \le r \le n)$ in V_n, we have

$$(\mathsf{T}^n(-\boldsymbol{I})\varphi_{n-r,r})(z_1, z_2) = \varphi_{n-r,r}(-z_1, -z_2) = (-1)^n \varphi_{n-r,r}(z_1, z_2) \tag{14.48}$$

for each $0 \le k \le n$. It follows that

$$\mathsf{T}^n(-\boldsymbol{I}) = (-1)^n \boldsymbol{I}_{V_n}, \tag{14.49}$$

where $\boldsymbol{I}_{V_n}$ is the identity on V_n. Hence, if $n = 2l$ $(l = 0, 1, 2, \ldots)$, then $\mathrm{Ker}(\mathrm{Ad}) \subset \mathrm{Ker}(\mathsf{T}^{2l})$. In fact, it can be seen from (14.10)–(14.13) that $\mathrm{Ker}(\mathsf{T}^{2l}) = \mathrm{Ker}(\mathrm{Ad}) = \{\boldsymbol{I}, -\boldsymbol{I}\}$. Clearly there exists a homomorphism $\mathcal{D}^l : \mathrm{SO}(3) \to \mathrm{GL}(V_{2l})$ such that equation (14.47) is valid. Indeed the matrix that represents $\mathcal{D}^l$ under the orthonormal basis e^l_m (see (14.26)) in V_{2l}, where $-l \le m \le l$, is exactly that which represents T^{2l}. Hence $\mathcal{D}^l$ is a $(2l+1)$-dimensional, continuous, irreducible unitary representation of SO(3) on V_{2l}.

Let $\mathcal{D}$ be an irreducible representation of SO(3). Then $\mathsf{T} := \mathcal{D} \circ \mathrm{Ad}$ is an irreducible representation of SU(2) and is thence equivalent to T^n for some non-negative integer n. Since

$$\mathsf{T}^n(-\boldsymbol{I}) = \mathcal{D}(\mathrm{Ad}(-\boldsymbol{I})) = \mathcal{D}(\boldsymbol{I}_{\mathrm{SO}(3)}) = \boldsymbol{I}_{V_n}, \tag{14.50}$$

we conclude by a comparison of (14.49) and (14.50) that $n = 2l$ for some non-negative integer l. Hence $\mathcal{D}$ is equivalent to $\mathcal{D}^l$ for some non-negative integer l. For $l \ne l'$, we clearly have $\mathcal{D}^l \ncong \mathcal{D}^{l'}$ because they are of different dimensions.

Gathering what we have proved, we conclude that $\{\mathcal{D}^l : l = 0, 1, 2, \ldots\}$ provides a complete set of finite-dimensional, continuous, irreducible unitary representations of SO(3). □

The matrix elements $D^l_{mn}(\boldsymbol{R})$ $(l = 0, 1, 2, \ldots; -l \le m \le l, -l \le n \le l)$ of the irreducible unitary representations $\mathcal{D}^l$ play a central role in texture analysis. From (14.41), (14.42), and (14.47), we obtain

$$D^l_{mn}(\psi, \theta, \phi) = e^{-im\psi} d^l_{mn}(\theta) e^{-in\phi}, \tag{4.18}$$

where $\psi \in [0, 2\pi)$, $\theta \in [0, \pi]$, $\phi \in [0, 2\pi)$,

$$d^l_{mn}(\theta) = \sum_k (-1)^{m-n+k} \frac{\sqrt{(l+m)!(l-m)!(l+n)!(l-n)!}}{k!(l+n-k)!(l-m-k)!(m-n+k)!} \times \left(\cos\frac{\theta}{2}\right)^{2l+n-m-2k} \left(\sin\frac{\theta}{2}\right)^{2k+m-n}, \tag{4.19}$$

and the summation in (4.19) extends over integer values of k that satisfy

$$k \geq 0, \quad k \leq l+n, \quad k \leq l-m, \quad k \geq n-m. \tag{14.51}$$

We call (4.19) our first explicit formula for the reduced matrix element $d^l_{mn}(\theta)$; cf. Footnote 62 in Sect. 4.2. Note that the function d^l_{mn} is real-valued and the inequalities (14.51) guarantee that the power of $\cos(\theta/2)$ and of $\sin(\theta/2)$ in (4.19) are non-negative. If we use (14.41), (14.43), and (14.47), we obtain (4.18) but, instead of (4.19), we get our second explicit formula for $d^l_{mn}(\theta)$:

$$d^l_{mn}(\theta) = \sum_k (-1)^{k} \frac{\sqrt{(l+m)!(l-m)!(l+n)!(l-n)!}}{k!(l-n-k)!(l+m-k)!(n-m+k)!} \times \left(\cos\frac{\theta}{2}\right)^{2l-n+m-2k} \left(\sin\frac{\theta}{2}\right)^{2k+n-m}, \tag{14.52}$$

where the summation extends over integer values of k that satisfy

$$k \geq 0, \quad k \leq l-n, \quad k \leq l+m, \quad k \geq m-n. \tag{14.53}$$

Comparing (4.19) with (14.52), we obtain the identity

$$d^l_{mn}(\theta) = (-1)^{m-n} d^l_{nm}(\theta). \tag{14.54}$$

Let (ψ, θ, ϕ) be the Euler angles of a rotation $\boldsymbol{R}$. By (1.94), (4.18), and (14.54), we have

$$\begin{aligned} D^l_{mn}(\boldsymbol{R}^{-1}) &= D^l_{mn}(\pi-\phi, \theta, \pi-\psi) = e^{-im(\pi-\phi)} d^l_{mn}(\theta) e^{-in(\pi-\phi)} \\ &= e^{in\psi} \left((-1)^{m-n} d^l_{mn}(\theta)\right) e^{im\phi} = \overline{e^{-in\psi} d^l_{nm}(\theta) e^{-im\phi}} = \overline{D^l_{nm}(\boldsymbol{R})}, \end{aligned} \tag{14.55}$$

which verifies that the matrix $[D^l_{mn}]$ is unitary.

Likewise, if we put in (14.46) $j = l = 0, 1, 2, \ldots$ and write (m, n) for (m', m), where $-l \leq m \leq l$ and $-l \leq n \leq l$, and if we restrict the range of ω to $[0, \pi]$, then (14.46) reduces to an explicit formula for $D^l_{mn}(\boldsymbol{n}(\Theta, \Phi), \omega)$, i.e., the Wigner D-functions of SO(3) in axis-angle parameters. Other equivalent formulas for $D^l_{mn}(\boldsymbol{n}(\Theta, \Phi), \omega)$ can be derived in a similar way.

14.4 Irreducible Representations of O(3)

Theorem 14.14 ([95, Theorem 2], [232, p. 248]) *A complete set of finite-dimensional, continuous, irreducible unitary representations of* O(3) *is given by* $\mathcal{D}^{l,\pm}$ *of dimension* $2l+1$

($l = 0, 1, 2, \ldots$), *which are defined by* $\mathcal{D}^{l,\pm} : \boldsymbol{Q} \mapsto [D^{l,\pm}_{mn}(\boldsymbol{Q})]$ ($-l \le m \le l, -l \le n \le l$), *where* $\boldsymbol{Q} \in \mathrm{O}(3)$, *and*

$$D^{l,+}_{mn}(\boldsymbol{Q}) = \begin{cases} D^{l}_{mn}(\boldsymbol{R}), \text{ if } \boldsymbol{Q} = \boldsymbol{R} \in \mathrm{SO}(3); \\ D^{l}_{mn}(\boldsymbol{R}), \text{ if } \boldsymbol{Q} = \boldsymbol{\mathcal{I}}\boldsymbol{R} \in \boldsymbol{\mathcal{I}}\mathrm{SO}(3). \end{cases} \tag{14.56}$$

$$D^{l,-}_{mn}(\boldsymbol{Q}) = \begin{cases} D^{l}_{mn}(\boldsymbol{R}), \text{ if } \boldsymbol{Q} = \boldsymbol{R} \in \mathrm{SO}(3); \\ -D^{l}_{mn}(\boldsymbol{R}), \text{ if } \boldsymbol{Q} = \boldsymbol{\mathcal{I}}\boldsymbol{R} \in \boldsymbol{\mathcal{I}}\mathrm{SO}(3). \end{cases} \tag{14.57}$$

Proof Let $\boldsymbol{I}$ be the identity in O(3) and $\boldsymbol{\mathcal{I}} = -\boldsymbol{I}$. Let $\widetilde{\mathcal{D}} : \mathrm{O}(3) \to \mathrm{GL}(X)$ be a finite-dimensional irreducible unitary representation of O(3). Since $\widetilde{\mathcal{D}}(\boldsymbol{\mathcal{I}})\widetilde{\mathcal{D}}(\boldsymbol{Q}) = \widetilde{\mathcal{D}}(\boldsymbol{Q})\widetilde{\mathcal{D}}(\boldsymbol{\mathcal{I}})$ for each $\boldsymbol{Q} \in \mathrm{O}(3)$, by Schur's lemma (see Theorem 13.8) we conclude that

$$\widetilde{\mathcal{D}}(\boldsymbol{\mathcal{I}}) = \lambda \boldsymbol{I}_X \qquad \text{for some } \lambda \in \mathbb{C}, \tag{14.58}$$

where $\boldsymbol{I}_X$ is the identity on X. On the other hand, we have

$$(\widetilde{\mathcal{D}}(\boldsymbol{\mathcal{I}}))^2 = (\widetilde{\mathcal{D}}(\boldsymbol{\mathcal{I}}))(\widetilde{\mathcal{D}}(\boldsymbol{\mathcal{I}})) = \widetilde{\mathcal{D}}(\boldsymbol{\mathcal{I}}^2) = \widetilde{\mathcal{D}}(\boldsymbol{I}) = \boldsymbol{I}_X. \tag{14.59}$$

From (14.58) and (14.59) we obtain $\lambda^2 = 1$, which implies $\lambda = \pm 1$.

We claim that $\widetilde{\mathcal{D}}\big|_{\mathrm{SO}(3)}$ is irreducible. Indeed, suppose there is a non-trivial proper subspace $W \subset X$ such that $\widetilde{\mathcal{D}}(\boldsymbol{R})W \subset W$ for each $\boldsymbol{R} \in \mathrm{SO}(3)$. Then for each $\boldsymbol{w} \in W$, $\widetilde{\mathcal{D}}(\boldsymbol{\mathcal{I}}\boldsymbol{R})\boldsymbol{w} = \pm\widetilde{\mathcal{D}}(\boldsymbol{\mathcal{I}}\boldsymbol{R})\boldsymbol{w} \in W$ for each $\boldsymbol{R} \in \mathrm{SO}(3)$. Thus W is invariant under $\widetilde{\mathcal{D}}(\boldsymbol{Q})$ for each $\boldsymbol{Q} \in \mathrm{O}(3)$, contradicting the hypothesis that the representation $(\widetilde{\mathcal{D}}, X)$ is irreducible.

Hence $\widetilde{\mathcal{D}}|_{\mathrm{SO}(3)} \cong \mathcal{D}^l$ for some $l = 0, 1, 2, \ldots$, because $\{\mathcal{D}^l : l = 0, 1, 2, \ldots\}$ is a complete set of finite-dimensional, continuous, irreducible unitary representation of SO(3). With the fact that $\widetilde{\mathcal{D}}(\boldsymbol{\mathcal{I}}) = \pm\boldsymbol{I}_X$, we have $\widetilde{\mathcal{D}}(\boldsymbol{R}) = \mathcal{D}^l(\boldsymbol{R})$ and $\widetilde{\mathcal{D}}(\boldsymbol{\mathcal{I}}\boldsymbol{R}) = \pm\mathcal{D}^l(\boldsymbol{R})$ for any $\boldsymbol{R} \in \mathrm{SO}(3)$. It follows that for each $l = 0, 1, 2, \ldots$, there are two irreducible representations of O(3), namely $\mathcal{D}^{l,+}$ and $\mathcal{D}^{l,-}$, which are defined by (14.56) and (14.57), respectively.

The argument above shows also that any finite-dimensional, continuous, irreducible representation of O(3) must be equivalent to one of the representations in the set $\mathcal{D}^{l,+}$, $\mathcal{D}^{l,-}$ ($l = 0, 1, 2, \ldots$). That the representations $\mathcal{D}^{l,\pm}$ are also pairwise-inequivalent follows immediately from (14.56), (14.57), and the fact that the representations $\mathcal{D}^l$ are pairwise-inequivalent. □

Definition 14.15 We call $D^{l,\pm}_{mn} : \mathrm{O}(3) \to \mathbb{C}$ ($l = 0, 1, 2, \ldots; -l \le m \le l, -l \le n \le l$) the Wigner D-functions of O(3). □

Chapter 15

15 The Peter-Weyl Theorem

In this chapter we present an elementary proof (cf. Talman [309, pp. 92–102]) of the Peter-Weyl theorem for the special case where the compact group has a faithful representation. Recall that a representation $\rho : G \to \mathrm{GL}(X)$ of G on complex vector space X is faithful if it is injective. Every matrix group $G \subset \mathrm{GL}(\mathbb{C}^n)$ has a faithful representation as the self-representation $g \mapsto g$ is faithful. In this exposition we are concerned only with matrix groups such as SO(3), O(3), etc., so the elementary proof suffices for our purpose here.[158]

In the rest of this chapter G always denotes a compact group with normalized Haar measure $\mathfrak{g}$, and $L^2(G) := L^2(G, \mathbb{C})$.

15.1 Preliminaries

Lemma 15.1 *Let $(\boldsymbol{T}, X)$ be a finite-dimensional unitary representation of compact group G and χ be its character. For each $g \in G$, let $T_{ij}(g)$ be elements of the unitary matrix that represents $\boldsymbol{T}$ under some orthonormal basis in X. The following assertions are valid*:

(a) *For any $g, h \in G$,*

$$\chi(h^{-1}g) = \sum_{i,j} \overline{T_{ij}(h)} T_{ij}(g). \tag{15.1}$$

(b) *Let e be the identity in G. Then*

$$|\chi(g)| \le \chi(e) \qquad \text{for each } g \in G. \tag{15.2}$$

(c) *For each $g \in G$, let $\boldsymbol{T}'(g) \in \mathrm{GL}(X)$ be defined by $\boldsymbol{T}'(g) = \overline{\boldsymbol{T}(g)}$ for each $g \in G$. Then $\boldsymbol{T}' : G \to \mathrm{GL}(X)$ is a representation of G on X and its character χ' satisfies $\chi'(g) = \overline{\chi(g)}$ for each $g \in G$. Moreover, $\boldsymbol{T}'$ is irreducible if and only if $\boldsymbol{T}$ is irreducible.*

Proof (a) Because the matrix $[T_{ij}(g)]$ is unitary for each $g \in G$, we have

$$\sum_{i,j} \overline{T_{ij}(h)} T_{ij}(g) = \sum_{i,j} T_{ji}(h^{-1}) T_{ij}(g) = \sum_{j} T_{jj}(h^{-1}g) = \chi(h^{-1}g)$$

for each $g, h \in G$.

(b) Substituting $h = g$ in (15.1), we obtain

$$\chi(e) = \sum_{i,j} |T_{ij}(g)|^2 \qquad \text{for each } g \in G.$$

Appealing to the Cauchy-Schwarz inequality, we observe that

$$\begin{aligned} |\chi(h^{-1}g)|^2 &= |\sum_{i,j} \overline{T_{ij}(h)} T_{ij}(g)|^2 \\ &\le \left(\sum_{i,j} |T_{ij}(h)|^2 \right) \left(\sum_{i,j} |T_{ij}(g)|^2 \right) = (\chi(e))^2 \end{aligned}$$

[158] For proofs without invoking the additional assumption that the compact group in question has a faithful representation, see, e.g., [55, Chap. 4], [245, pp. 186–194].

for each $g, h \in G$. Putting $h = e$ in the preceding inequality, we obtain

$$|\chi(g)| \leq \chi(e) \qquad \text{for each } g \in G.$$

(c) It is easy to verify that $\boldsymbol{T}'$ is a representation of G and that $\chi'(g) = \chi(g)$ for each $g \in G$. The last assertion of the lemma follows from the fact that $\int_G |\chi'(g)|^2 d\mathfrak{g} = \int_G |\chi(g)|^2 d\mathfrak{g}$. □

We call $\boldsymbol{T}'$ in Lemma 15.1(c) the representation contragredient to $\boldsymbol{T}$.

Henceforth we adopt the following notation. Let G be a compact topological group, and let $\{\boldsymbol{T}^\alpha : \alpha \in J\}$, be a complete set (cf. Definition 14.8) of pairwise inequivalent, finite-dimensional, continuous, irreducible unitary representations of G. Let $\dim \boldsymbol{T}^\alpha = n_\alpha$, and let $T^\alpha_{ij}(\cdot)$ $(1 \leq i, j \leq n_\alpha)$ be the matrix elements of the representation $\boldsymbol{T}^\alpha$ under some orthonormal basis in the representation space of $\boldsymbol{T}^\alpha$. For each $\alpha \in J$, the character of $\boldsymbol{T}^\alpha$ will be denoted by χ^α.

Next we show that if G has a faithful representation, then a set of real-valued non-negative functions on G, which are finite linear combinations of the characters χ^α, can be constructed so that these functions are the densities of probability measures which approximate the Dirac measure at e arbitrarily closely in the sense specified in the following proposition.

Proposition 15.2 *Let G be a compact topological group with a faithful finite-dimensional continuous representation $\boldsymbol{T}^f$, and let $\{\boldsymbol{T}^\alpha : \alpha \in J\}$, where J is an index set, be a complete set of finite-dimensional, continuous, irreducible unitary representations of G. Then there is a sequence of functions $\psi_N : G \to \mathbb{R}$ which satisfies the following conditions*:

(a) *Each ψ_N is a finite linear combination of characters χ^l, i.e.,*

$$\psi_N(g) = \sum_{\alpha \in J_N} c_N^\alpha \chi^\alpha(g), \tag{15.3}$$

where the index set J_N is finite.

(b) *Each ψ_N satisfies*

$$\psi_N(g) \geq 0 \quad \text{for each } g \in G, \quad \text{and} \quad \int_G \psi_N(g)\, d\mathfrak{g} = 1. \tag{15.4}$$

(c) *For any $\varepsilon > 0$, and any open neighborhood U of e, there is an N such that*

$$\psi_N(g) < \varepsilon \qquad \text{for each } g \in G \setminus U. \tag{15.5}$$

Proof Since $\boldsymbol{T}^f$ is a finite-dimensional faithful representation of G, for $g \neq h \in G$ we have

$$\sum_{i,j} (T^f_{ij}(g) - T^f_{ij}(h))\overline{(T^f_{ij}(g) - T^f_{ij}(h))} = \sum_{i,j} |T^f_{ij}(g) - T^f_{ij}(h)|^2 > 0. \tag{15.6}$$

By (15.1), we can recast inequality (15.6) as

$$2\chi^f(e) - \chi^f(h^{-1}g) - \overline{\chi^f(h^{-1}g)} > 0 \qquad \text{for any } g \neq h \in G. \tag{15.7}$$

Let $\boldsymbol{T}^{f'}$ be the representation contragredient to the faithful representation $\boldsymbol{T}^f$. Then $\chi^{f'}(g) = \overline{\chi^f(g)}$ for each $g \in G$. Let $\boldsymbol{T}^r$ be the direct sum of $\boldsymbol{T}^f$ and $\boldsymbol{T}^{f'}$, i.e., $\boldsymbol{T}^r =$

$\boldsymbol{T}^f + \boldsymbol{T}^{f'}$. Then $\chi^r(g) = \chi^f(g) + \overline{\chi^f(g)}$ for each $g \in G$. Note that $\chi^r(g)$ is real for each g. By (15.2) and (15.7), we see that

$$-\chi^r(e) \le \chi^r(g) < \chi^r(e) \tag{15.8}$$

for any $g \neq e \in G$. Let $m = \dim \boldsymbol{T}^r$, and let $\boldsymbol{T}^0$ be the 1-dimensional identity representation (i.e., $\boldsymbol{T}^0(g) = 1$ for each $g \in G$). Let $\boldsymbol{T} = m\boldsymbol{T}^0 + \boldsymbol{T}^r$, which is a finite-dimensional representation of G with character χ given by $\chi(g) = m + \chi^r(g)$ for each $g \in G$. Clearly the character χ satisfies

$$0 \le \chi(g) < \chi(e) \qquad \text{for each } g \neq e \in G. \tag{15.9}$$

Let

$$\psi_N(g) = c_N(\chi(g))^N, \tag{15.10}$$

where $c_N > 0$ is to be determined by the condition $\int_G \psi_N(g)d\mathfrak{g} = 1$. Let $\boldsymbol{T}^{\otimes N}$ be the N-fold tensor product of representation $\boldsymbol{T}$. Since the set $\{\boldsymbol{T}^\alpha\}$ of finite-dimensional irreducible unitary representations of G is complete, by decomposing $\boldsymbol{T}^{\otimes N}$ into its irreducible parts (cf. (13.34)), we observe that $(\chi(\cdot))^N$, the character of $\boldsymbol{T}^{\otimes N}$, can be written as a finite linear combination of the characters χ^α, i.e.

$$(\chi(g))^N = \sum_{\alpha \in J_N} b_N^\alpha \chi^\alpha(g), \tag{15.11}$$

where J_N is a finite index set and b_N^α are positive integers; cf. (13.68). Let $\varepsilon > 0$, and let an open neighborhood U of e be given. Since χ is continuous on G, there is an $a \in G \setminus U$ such that

$$\chi(a) \ge \chi(g) \qquad \text{for each } g \in G \setminus U.$$

Since $a \neq e$, by (15.9) we have

$$\chi(e) > \chi(a) \ge \chi(g) \qquad \text{for each } g \in G \setminus U. \tag{15.12}$$

It follows from the continuity of χ that there is a neighborhood V of e such that

$$\chi(g) > \frac{\chi(e) + \chi(a)}{2} \qquad \text{for each } g \in V. \tag{15.13}$$

By (15.13) clearly we have

$$\int_G (\chi(g))^N d\mathfrak{g} \ge \int_V (\chi(g))^N d\mathfrak{g} > \mathfrak{g}(V) \left(\frac{\chi(e) + \chi(a)}{2}\right)^N,$$

which implies

$$c_N := \frac{1}{\int_G (\chi(g))^N d\mathfrak{g}} < \frac{1}{\mathfrak{g}(V)} \left(\frac{2}{\chi(e) + \chi(a)}\right)^N. \tag{15.14}$$

Hence for $g \in G \setminus U$ and a sufficiently large N, we have

$$\psi_N(g) = c_N(\chi(g))^N < \frac{1}{\mathfrak{g}(V)} \left(\frac{2\chi(g)}{\chi(e) + \chi(a)} \right)^N < \frac{1}{\mathfrak{g}(V)} \left(\frac{2\chi(a)}{\chi(e) + \chi(a)} \right)^N < \varepsilon. \quad (15.15)$$

By (15.10) and (15.11), $\psi_N(g) = \sum_{\alpha \in J_N} c_N^\alpha \chi^\alpha(g)$, where $c_N^\alpha = c_N b_N^\alpha$. □

Remark 15.3 Both in the statement and the proof of Proposition 15.2 we have closely followed Talman [309, Theorem 7-1, pp. 96–98], who also asserts that "[t]he proof of Theorem 7-1 is essentially that given by Wigner [342] in his notes on this subject". The mimeographed notes (by Talman) of Wigner's 1955 lectures at Princeton, while unpublished, are included in the holdings of many university libraries in the United States. □

Definition 15.4 Let G be a topological group. A function $f : G \to \mathbb{C}$ is continuous at $a \in G$ if for any $\varepsilon > 0$ there is a neighborhood V_a of a such that for each $g \in V_a$, $|f(g) - f(a)| < \varepsilon$; f is continuous on G if it is continuous at each $a \in G$.

A function $f : G \to \mathbb{C}$ is left (reps. right) uniformly continuous on G if for any $\varepsilon > 0$ there is an open neighborhood V of e such that for all $g, h \in G$ which satisfy $h^{-1}g \in V$ (resp. $gh^{-1} \in V$), there holds $|f(g) - f(h)| < \varepsilon$. A function f is uniformly continuous on G if it is both left and right uniformly continuous on G. □

Proposition 15.5 *Let G be a compact group. If $f : G \to \mathbb{C}$ is continuous on G, it is uniformly continuous on G.*

Proof Let $\varepsilon > 0$ be given. Since f is continuous on G, for each $a \in G$ there is an open neighborhood U_a of a such that if $g \in U_a$, then $|f(g) - f(a)| < \varepsilon/2$. Since $ae = a$ and the operation of group multiplication from $G \times G$ to G is continuous, there is an open neighborhood W_a of a and an open neighborhood V_a of e such that $W_a V_a \subset U_a$. Note that $W_a \subset U_a$. Since G is compact and $\bigcup_{a \in G} W_a$ is an open covering of G, there is a finite subcovering $\bigcup_{i=1}^n W_{a_i} = G$ for some $a_i \in G$ $(i = 1, 2, \ldots, n)$.

Let $V = \bigcap_{i=1}^n V_{a_i}$. Let $g, h \in G$ with $h^{-1}g \in V$. Then $h \in W_{a_i}$ for some i, and $g \in hV$, which implies $g \in W_{a_i} V_{a_i}$ because $V \subset V_{a_i}$. Since $g \in W_{a_i} V_{a_i} \subset U_{a_i}$ and $h \in W_{a_i} \subset U_{a_i}$, we have

$$|f(g) - f(h)| \le |f(g) - f(a_i)| + |f(a_i) - f(h)| < \varepsilon/2 + \varepsilon/2 = \varepsilon.$$

Hence f is left uniformly continuous on G. That f is also right uniformly continuous on G can be proved similarly. □

15.2 Proof of the Peter-Weyl Theorem

Theorem 15.6 (The Peter-Weyl theorem [258]) *Let G be a compact topological group with a faithful finite-dimensional representation, and let $\{\boldsymbol{T}^\alpha : \alpha \in J\}$, where J is an index set, be a complete set of finite-dimensional, continuous, irreducible unitary representations of G. A function continuous on G can be uniformly approximated by finite linear combinations of matrix elements $T_{ij}^\alpha(\cdot)$ of the irreducible unitary representations $\boldsymbol{T}^\alpha$ $(\alpha \in J)$.*

Proof Let $\varepsilon > 0$ be given. First we shall show there is an N such that

$$\left| \int_G \psi_N(h^{-1}g) f(h) \, d\mathfrak{g}(h) - f(g) \right| < \varepsilon \qquad \text{for each } g \in G. \quad (15.16)$$

Indeed by (15.4) and the bi-invariance of the Haar measure, we have

$$\left|\int_G \psi_N(h^{-1}g)f(h)\,d\mathfrak{g}(h) - f(g)\right| = \left|\int_G \psi_N(h^{-1}g)(f(h)-f(g))\,d\mathfrak{g}(h)\right|$$
$$\leq \int_G \psi_N(h^{-1}g)\,|f(h)-f(g)|\,d\mathfrak{g}(h). \tag{15.17}$$

Since f is uniformly continuous on G, there is an open neighborhood V of e such that for all $g, h \in G$ which satisfy $h^{-1}g \in V$, we have $|f(h)-f(g)| < \varepsilon/2$. Consider a specific $g \in G$. Let $\Omega = \{h \in G : h^{-1}g \in V\}$. The integral on the right-hand side of (15.17) can be written as a sum of two term as follows:

$$\int_G \psi_N(h^{-1}g)\,|f(h)-f(g)|\,d\mathfrak{g}(h) = \int_\Omega \psi_N(h^{-1}g)\,|f(h)-f(g)|\,d\mathfrak{g}(h)$$
$$+ \int_{G\setminus\Omega} \psi_N(h^{-1}g)\,|f(h)-f(g)|\,d\mathfrak{g}(h). \tag{15.18}$$

On Ω, we have $h^{-1}g \in V$ and thence $|f(h)-f(g)| < \varepsilon/2$. Thus

$$\int_\Omega \psi_N(h^{-1}g)\,|f(h)-f(g)|\,d\mathfrak{g}(h) < \frac{\varepsilon}{2}\int_\Omega \psi_N(h^{-1}g)\,d\mathfrak{g}(h) \leq \frac{\varepsilon}{2}. \tag{15.19}$$

Since f is continuous on G, which is compact, there is an $A > 0$ such that $|f(h)-f(g)| < A$ for all $g, h \in G$. By part (c) of Proposition 15.2, given an open neighborhood V of e, there is an N such that

$$\psi_N(h^{-1}g) < \frac{\varepsilon}{2A} \qquad \text{if } h^{-1}g \notin V. \tag{15.20}$$

For this N, we have

$$\int_{G\setminus\Omega} \psi_N(h^{-1}g)\,|f(h)-f(g)|\,d\mathfrak{g}(h) < A\int_{G\setminus\Omega} \psi_N(h^{-1}g)\,d\mathfrak{g}(h) < A\cdot\frac{\varepsilon}{2A} = \frac{\varepsilon}{2}. \tag{15.21}$$

Substituting (15.19) and (15.21) into (15.18), we have proved (15.16).

By (15.10), (15.11), and (15.1), we have

$$\psi_N(h^{-1}g) = \sum_{\alpha\in J_N} c_N b_N^\alpha \chi^\alpha(h^{-1}g) = \sum_{\alpha\in J_N} c_N b_N^\alpha \sum_{i,j} \overline{T_{ij}^\alpha(h)}\,T_{ij}^\alpha(g). \tag{15.22}$$

It follows that

$$\int_G \psi_N(h^{-1}g)f(h)\,d\mathfrak{g}(h) = \sum_{\alpha\in J_N} c_N b_N^\alpha \sum_{i,j}\left(\int_G \overline{T_{ij}^\alpha(h)}\,f(h)\,d\mathfrak{g}(h)\right) T_{ij}^\alpha(g)$$
$$= \sum_{\alpha\in J_N}\sum_{i,j} c_{ij}^{\alpha,N} T_{ij}^\alpha(g), \tag{15.23}$$

where

$$c_{ij}^{\alpha,N} = c_N b_N^{\alpha} \int_G \overline{T_{ij}^{\alpha}(h)} f(h)\, d\mathfrak{g}(h). \tag{15.24}$$

We observe from (15.16) and (15.23) that $f(\cdot)$ is uniformly approximated by finite linear combinations of the matrix elements $T_{ij}^{\alpha}(\cdot)$. □

Corollary 15.7 *The set* $\{\sqrt{n_\alpha}\, T_{ij}^{\alpha}(\cdot) : \alpha \in J,\ 1 \le i, j \le n_\alpha\}$ *constitutes a complete orthonormal basis in* $L^2(G)$.

Proof That $\{\sqrt{n_\alpha}\, T_{ij}^{\alpha}(\cdot) : \alpha \in J,\ 1 \le i, j \le n_\alpha\}$ is an orthonormal set in $L^2(G)$ follows from the orthogonality relations pertaining to matrix elements of irreducible unitary representations. To prove completeness, it suffices to show that the set of finite linear combinations of $\sqrt{n_\alpha}\, T_{ij}^{\alpha}$ is dense in $L^2(G)$. Let $f \in L^2(G)$ be given. Since the set of continuous functions is dense in $L^2(G)$, there is a continuous function $\widetilde{f}$ such that $\|f - \widetilde{f}\|_{L^2} < \varepsilon/2$. By Theorem 15.6, there is a finite linear combination s_N of $\sqrt{n_\alpha}\, T_{ij}^{\alpha}$ such that $\|\widetilde{f} - s_N\|_{L^2} < \varepsilon/2$ and $\|f - s_N\|_{L^2} \le \|f - \widetilde{f}\|_{L^2} + \|\widetilde{f} - s_N\|_{L^2} < \varepsilon$. □

Corollary 15.8 *Every function* $f \in L^2(G)$ *can be written in the form*

$$f(g) = \sum_{\alpha \in J} \sum_{i,j=1}^{n_\alpha} c_{ij}^{\alpha} T_{ij}^{\alpha}(g), \tag{15.25}$$

where the series converges in $L^2(G)$ *and the expansion coefficients are given by*

$$c_{ij}^{\alpha} = n_\alpha \langle f, T_{ij}^{\alpha} \rangle. \tag{15.26}$$

□

If the compact group G has a countable base, then the set of orthonormal functions $\{\sqrt{n_\alpha}\, T_{ij}^{\alpha}(\cdot)\} \subset L^2(G)$ is countable [261, p. 213]. Hence we infer that the complete set $\{\boldsymbol{T}^{\alpha}\}$ of finite-dimensional, continuous, irreducible unitary representations of G is also countable.

Remark 15.9 In Theorem 14.13, we have proved that $\{\mathcal{D}^l : l = 0, 1, 2, \ldots\}$ provides a complete set of finite-dimensional, continuous, irreducible unitary representations of SO(3) and that the elements of the $(2l+1) \times (2l+1)$ matrix which represents $\mathcal{D}^l$ can be selected to be the Wigner D-functions $D_{mn}^{l}(\cdot)$ $(-l \le m \le l, -l \le n \le l)$. Since the ODF $w \in L^2(\mathrm{SO}(3))$, by (15.25) we can expand it as an infinite series as follows:

$$w(\boldsymbol{R}) = \sum_{l=0}^{\infty} \sum_{m=-l}^{l} \sum_{n=-l}^{l} c_{mn}^{l} D_{mn}^{l}(\boldsymbol{R}) \qquad \text{for each } \boldsymbol{R} \in \mathrm{SO}(3), \tag{15.27}$$

which justifies (4.45) in Chap. 4. That w is real-valued results in constraint (4.46) on the texture coefficients c_{mn}^{l}. □

15.3 The Right-Regular Representation

We consider the case[159] where the compact topological group G has a countable base so that the index set J can be written as $J = \{0\} \cup \mathbb{N}$, where $\mathbb{N}$ denotes the set of natural numbers. Then by (15.25) each $f \in L^2(G)$ can be expanded as an infinite series as

$$f(g) = \sum_{\alpha=0}^{\infty} \sum_{i,j=1}^{n_\alpha} c_{ij}^{\alpha} T_{ij}^{\alpha}(g). \tag{15.28}$$

Let X^α be the finite-dimensional subspace of $L^2(G)$ spanned by the basis functions T_{ij}^α $(i, j = 1, \ldots, n_\alpha)$. Consider the restriction of the right-regular representation (cf. Sect. 13.3) to X^α, namely $\mathcal{T}_r\,|_{X^\alpha}$. For each $h \in G$, we have

$$(\mathcal{T}_r(h))T_{ij}^{\alpha}(g) = T_{ij}^{\alpha}(gh) = \sum_{k=1}^{n_\alpha} T_{ik}^{\alpha}(g)T_{kj}^{\alpha}(h) = \sum_{k=1}^{n_\alpha} T_{kj}^{\alpha}(h)T_{ik}^{\alpha}(g). \tag{15.29}$$

Hence X^α is a G-invariant subspace of $L^2(G)$ under the right-regular representation. Looking at (15.29) more carefully, we observe that

$$(\mathcal{T}_r(h))T_{ij}^{\alpha}(\cdot) = \sum_{k=1}^{n_\alpha} T_{kj}^{\alpha}(h)T_{ik}^{\alpha}(\cdot) \qquad \text{for each fixed } i. \tag{15.30}$$

Thus if we denote by X_i^α the subspace generated by the basis functions $T_{i1}^\alpha, \ldots, T_{in_\alpha}^\alpha$, then X_i^α is a G-invariant subspace of $L^2(G)$ under the right-regular representation and dim $X_i^\alpha = n_\alpha$. Moreover, the $n_\alpha \times n_\alpha$ matrix that represents $\mathcal{T}_r(h)\Big|_{X_i^\alpha}$ under the basis $T_{i1}^\alpha, \ldots, T_{in_\alpha}^\alpha$ is $[T_{kj}^\alpha(h)]$. Therefore the representation $\mathcal{T}_r(h)\Big|_{X_i^\alpha}$ is equivalent to $\boldsymbol{T}^\alpha$. Because of the orthogonality relations between the matrix elements $T_{ij}^\alpha(\cdot)$, the subspaces X^α are orthogonal to each other. Likewise the subspaces X_p^α and X_q^α are orthogonal if $p \neq q$.

Let the Hilbert-space direct sum (see, e.g., [75, p. 24]) of the finite-dimensional subspaces $X^\alpha \subset L^2(G)$ $(\alpha = 0, 1, 2, \ldots)$ be denoted by

$$\bigoplus_{\alpha=0}^{\infty} X^\alpha = \left\{ \sum_{\alpha=0}^{\infty} f^\alpha : f^\alpha \in X^\alpha, \sum_{\alpha=0}^{\infty} \|f^\alpha\|^2 < \infty \right\}. \tag{15.31}$$

Clearly we have

$$L^2(G) = \bigoplus_{\alpha=0}^{\infty} X^\alpha. \tag{15.32}$$

[159] This includes the instances that $G = \mathrm{SO}(3)$ and $G = \mathrm{O}(3)$, which are compact metric spaces. Every compact metric space has a countable base [242, p. 194].

Chapter 16

16 Tensor and Pseudotensor Representations of SO(3), O(3), and Their Finite Subgroups

16.1 Mathematical Preliminaries

16.1.1 Tensor Algebra

Let V be the translation space of the three-dimensional physical space E^3, and let $V^r = V \times \cdots \times V$ (r copies). A mapping $\boldsymbol{H} : V^r \to \mathbb{R}$ is multilinear if it is linear with respect to each of its vector arguments, i.e.,

$$\boldsymbol{H}[\boldsymbol{v}_1, \ldots, \boldsymbol{v}_i + \alpha \boldsymbol{v}_i', \ldots, \boldsymbol{v}_r] = \boldsymbol{H}[\boldsymbol{v}_1, \ldots, \boldsymbol{v}_i, \ldots, \boldsymbol{v}_r] + \alpha \boldsymbol{H}[\boldsymbol{v}_1, \ldots, \boldsymbol{v}_i', \ldots, \boldsymbol{v}_r] \quad (16.1)$$

for each $\boldsymbol{v}_i$ ($1 \le i \le r$), $\boldsymbol{v}_i' \in V$ and $\alpha \in \mathbb{R}$. In mathematics such multilinear mappings are called rth-order tensors. Let $\boldsymbol{u}_1, \ldots, \boldsymbol{u}_r$ be in V. The tensor product of $\boldsymbol{u}_1, \ldots, \boldsymbol{u}_r$ is the rth-order tensor $\boldsymbol{u}_1 \otimes \cdots \otimes \boldsymbol{u}_r : V^r \to \mathbb{R}$ defined by

$$\boldsymbol{u}_1 \otimes \cdots \otimes \boldsymbol{u}_r[\boldsymbol{v}_1, \ldots, \boldsymbol{v}_r] = (\boldsymbol{u}_1 \cdot \boldsymbol{v}_1) \cdots (\boldsymbol{u}_r \cdot \boldsymbol{v}_r) \quad \text{for each } (\boldsymbol{v}_1, \ldots, \boldsymbol{v}_r) \in V^r. \quad (16.2)$$

We call tensor products of vectors simple tensors. Under the usual definition of addition and of scalar multiplication of mappings, the set of rth-order tensors clearly forms a linear space over $\mathbb{R}$, which we denote by $V^{\otimes r}$ and call the space of rth-order tensors.

Let $\boldsymbol{e}_1$, $\boldsymbol{e}_2$, and $\boldsymbol{e}_3$ constitute a right-handed orthonormal basis in V, and let $\boldsymbol{H} \in V^{\otimes r}$. For any vectors $\boldsymbol{u}^{(1)}, \ldots, \boldsymbol{u}^{(r)} \in V$, we have

$$\begin{aligned}
\boldsymbol{H}[\boldsymbol{u}^{(1)}, \ldots, \boldsymbol{u}^{(r)}] &= \boldsymbol{H}[u_{i_1}^{(1)} \boldsymbol{e}_{i_1}, \ldots, u_{i_r}^{(r)} \boldsymbol{e}_{i_r}] \\
&= \boldsymbol{H}[\boldsymbol{e}_{i_1}, \ldots, \boldsymbol{e}_{i_r}] u_{i_1}^{(1)} \cdots u_{i_r}^{(r)} \\
&= \boldsymbol{H}[\boldsymbol{e}_{i_1}, \ldots, \boldsymbol{e}_{i_r}] (\boldsymbol{u}^{(1)} \cdot \boldsymbol{e}_{i_1}) \cdots (\boldsymbol{u}^{(r)} \cdot \boldsymbol{e}_{i_r}) \\
&= H_{i_1 \cdots i_r} (\boldsymbol{u}^{(1)} \cdot \boldsymbol{e}_{i_1}) \cdots (\boldsymbol{u}^{(r)} \cdot \boldsymbol{e}_{i_r}) \\
&= (H_{i_1 \cdots i_r} \boldsymbol{e}_{i_1} \otimes \cdots \otimes \boldsymbol{e}_{i_r})[\boldsymbol{u}^{(1)}, \ldots, \boldsymbol{u}^{(r)}], \qquad (16.3)
\end{aligned}$$

where the Einstein summation convention is in force, and

$$H_{i_1 i_2 \cdots i_r} = \boldsymbol{H}[\boldsymbol{e}_{i_1}, \boldsymbol{e}_{i_2}, \ldots, \boldsymbol{e}_{i_r}]. \quad (16.4)$$

Thus every $\boldsymbol{H} \in V^{\otimes r}$ can be written in the form

$$\boldsymbol{H} = H_{i_1 i_2 \cdots i_r} \boldsymbol{e}_{i_1} \otimes \boldsymbol{e}_{i_2} \otimes \cdots \otimes \boldsymbol{e}_{i_r}. \quad (16.5)$$

We define an inner product $\langle \cdot, \cdot \rangle$ on $V^{\otimes r}$ by requiring that

$$\langle \boldsymbol{u}_1 \otimes \cdots \otimes \boldsymbol{u}_r, \boldsymbol{w}_1 \otimes \cdots \otimes \boldsymbol{w}_r \rangle = (\boldsymbol{u}_1 \cdot \boldsymbol{w}_1) \cdots (\boldsymbol{u}_r \cdot \boldsymbol{w}_r). \quad (16.6)$$

Clearly simple tensors of the form $\boldsymbol{e}_{i_1} \otimes \boldsymbol{e}_{i_2} \otimes \cdots \otimes \boldsymbol{e}_{i_r}$, where each suffix runs over the indices 1, 2, and 3, constitute an orthonormal basis in $V^{\otimes r}$. Hence $\dim V^{\otimes r} = 3^r$. For

$$\boldsymbol{H} = H_{i_1 i_2 \cdots i_r} \boldsymbol{e}_{i_1} \otimes \boldsymbol{e}_{i_2} \otimes \cdots \otimes \boldsymbol{e}_{i_r} \quad \text{and} \quad \boldsymbol{K} = K_{j_1 j_2 \cdots j_r} \boldsymbol{e}_{j_1} \otimes \boldsymbol{e}_{j_2} \otimes \cdots \otimes \boldsymbol{e}_{j_r}, \quad (16.7)$$

we have

$$\langle \boldsymbol{H}, \boldsymbol{K} \rangle = H_{i_1 i_2 \cdots i_r} K_{i_1 i_2 \cdots i_r}. \tag{16.8}$$

Each orthogonal linear transformation $\boldsymbol{Q}$ on V induces an orthogonal linear transformation $\boldsymbol{Q}^{\otimes r} : V^{\otimes r} \to V^{\otimes r}$ defined by

$$\boldsymbol{Q}\boldsymbol{u}_1 \otimes \cdots \otimes \boldsymbol{Q}\boldsymbol{u}_r = \boldsymbol{Q}^{\otimes r} \boldsymbol{u}_1 \otimes \cdots \otimes \boldsymbol{Q}^{\otimes r} \boldsymbol{u}_r, \tag{16.9}$$

for all $\boldsymbol{u}_1, \ldots, \boldsymbol{u}_r \in V$. Let $Q_{ij} = \boldsymbol{e}_i \cdot \boldsymbol{Q}\boldsymbol{e}_j$. Then $\boldsymbol{Q}\boldsymbol{e}_j = (\boldsymbol{e}_i \cdot \boldsymbol{Q}\boldsymbol{e}_j)\boldsymbol{e}_i = Q_{ij}\boldsymbol{e}_i$. For each $\boldsymbol{H} \in V^{\otimes r}$, we have

$$\begin{aligned} \boldsymbol{Q}^{\otimes r} \boldsymbol{H} &= H_{j_1 \cdots j_r} \boldsymbol{Q}\boldsymbol{e}_{j_1} \otimes \cdots \otimes \boldsymbol{Q}\boldsymbol{e}_{j_r} \\ &= H_{j_1 \cdots j_r} (Q_{k_1 j_1} \boldsymbol{e}_{k_1}) \otimes \cdots \otimes (Q_{k_r j_r} \boldsymbol{e}_{k_r}) \\ &= H_{j_1 \cdots j_r} Q_{k_1 j_1} \cdots Q_{k_r j_r} \boldsymbol{e}_{k_1} \otimes \cdots \otimes \boldsymbol{e}_{k_r}, \end{aligned} \tag{16.10}$$

and

$$\begin{aligned} (\boldsymbol{Q}^{\otimes r} \boldsymbol{H})[\boldsymbol{e}_{i_1}, \ldots, \boldsymbol{e}_{i_r}] &= H_{j_1 \cdots j_r} Q_{k_1 j_1} \cdots Q_{k_r j_r} \delta_{i_1 k_1} \cdots \delta_{i_r k_r} \\ &= Q_{i_1 j_1} \cdots Q_{i_r j_r} H_{j_1 \cdots j_r} \end{aligned} \tag{16.11}$$

16.1.2 Complexification of Vector and Tensor Spaces

Let V be the translation space of the three-dimensional Euclidean space, and let $\{\boldsymbol{e}_1, \boldsymbol{e}_2, \boldsymbol{e}_3\}$ be a right-handed orthonormal basis in V. Let

$$V_c = \left\{ \sum_i a_i \boldsymbol{e}_i : a_i \in \mathbb{C} \right\} = \left\{ \boldsymbol{u} + \sqrt{-1}\boldsymbol{v} : \boldsymbol{u} \in V, \boldsymbol{v} \in V \right\} \tag{16.12}$$

be the complexification[160] of V, with vector addition and scalar multiplication defined respectively by

$$(\boldsymbol{u} + \sqrt{-1}\boldsymbol{v}) + (\boldsymbol{u}' + \sqrt{-1}\boldsymbol{v}') = (\boldsymbol{u} + \boldsymbol{u}') + \sqrt{-1}(\boldsymbol{v} + \boldsymbol{v}'), \tag{16.13}$$

$$(\alpha_1 + \sqrt{-1}\alpha_2)(\boldsymbol{u} + \sqrt{-1}\boldsymbol{v}) = (\alpha_1 \boldsymbol{u} - \alpha_2 \boldsymbol{v}) + \sqrt{-1}(\alpha_2 \boldsymbol{u} + \alpha_1 \boldsymbol{v}) \tag{16.14}$$

for $\boldsymbol{u}, \boldsymbol{v}, \boldsymbol{u}', \boldsymbol{v}' \in V$ and $\alpha_1, \alpha_2 \in \mathbb{R}$. We equip V_c with the (Hermitian) inner product induced by the dot product in V for real vectors as follows: Let $\boldsymbol{w} = \boldsymbol{u} + \sqrt{-1}\boldsymbol{v}$, $\boldsymbol{z} = \boldsymbol{x} + \sqrt{-1}\boldsymbol{y}$, where $\boldsymbol{u}, \boldsymbol{v}, \boldsymbol{x}, \boldsymbol{y} \in V$. Then the inner product of $\boldsymbol{w}$ and $\boldsymbol{z}$ is defined by

$$\begin{aligned} \langle \boldsymbol{w}, \boldsymbol{z} \rangle &= \langle \boldsymbol{u} + \sqrt{-1}\boldsymbol{v}, \boldsymbol{x} + \sqrt{-1}\boldsymbol{y} \rangle \\ &:= \boldsymbol{u} \cdot \boldsymbol{x} + \boldsymbol{v} \cdot \boldsymbol{y} + \sqrt{-1}(\boldsymbol{v} \cdot \boldsymbol{x} - \boldsymbol{u} \cdot \boldsymbol{y}). \end{aligned} \tag{16.15}$$

Under the chosen orthonormal basis $\boldsymbol{e}_1, \boldsymbol{e}_2, \boldsymbol{e}_3$ in V (and thence also in V_c), we have $\boldsymbol{w} = (w_1, w_2, w_3)$ and $\boldsymbol{z} = (z_1, z_2, z_3)$ in V_c, where $w_i = u_i + \sqrt{-1}v_i$, $z_i = x_i + \sqrt{-1}y_i$ for $i =$

[160] Cf. e.g., Roman [273, pp. 53–55].

1, 2, 3. It is easily checked by direct computation that, in terms of components, the inner product (16.15) of $\boldsymbol{w}$ and $\boldsymbol{z}$ is given by the formula

$$\langle \boldsymbol{w}, \boldsymbol{z} \rangle = w_1 \overline{z_1} + w_2 \overline{z_2} + w_3 \overline{z_3}. \tag{16.16}$$

An orthogonal transformation $\boldsymbol{Q}$ on V has a natural extension to a linear transformation on V_c (called the complexification of $\boldsymbol{Q}$ [273, pp. 82–83]), which we still denote by $\boldsymbol{Q}$, defined as follows:

$$\boldsymbol{Q}(\boldsymbol{u} + \sqrt{-1}\boldsymbol{v}) := \boldsymbol{Q}\boldsymbol{u} + \sqrt{-1}\,\boldsymbol{Q}\boldsymbol{v} \tag{16.17}$$

for each $\boldsymbol{u}$, $\boldsymbol{v}$ in V. In what follows whether $\boldsymbol{Q}$ really denotes an orthogonal transformation on V or its extension on V_c should be clear from the context. By (16.15) we have, for any two vectors $\boldsymbol{w} = \boldsymbol{u} + \sqrt{-1}\boldsymbol{v}$, $\boldsymbol{z} = \boldsymbol{x} + \sqrt{-1}\boldsymbol{y} \in V_c$,

$$\begin{aligned} \langle \boldsymbol{Q}\boldsymbol{w}, \boldsymbol{Q}\boldsymbol{z} \rangle &= \boldsymbol{Q}\boldsymbol{u} \cdot \boldsymbol{Q}\boldsymbol{x} + \boldsymbol{Q}\boldsymbol{v} \cdot \boldsymbol{Q}\boldsymbol{y} + \sqrt{-1}(\boldsymbol{Q}\boldsymbol{v} \cdot \boldsymbol{Q}\boldsymbol{x} - \boldsymbol{Q}\boldsymbol{u} \cdot \boldsymbol{Q}\boldsymbol{y}) \\ &= \boldsymbol{u} \cdot \boldsymbol{x} + \boldsymbol{v} \cdot \boldsymbol{y} + \sqrt{-1}(\boldsymbol{v} \cdot \boldsymbol{x} - \boldsymbol{u} \cdot \boldsymbol{y}) = \langle \boldsymbol{w}, \boldsymbol{z} \rangle. \end{aligned} \tag{16.18}$$

Hence $\boldsymbol{Q} : V_c \to V_c$ is unitary.

Let $(V^{\otimes r})_c$ be the complexification of $V^{\otimes r}$, and let $V_c^{\otimes r} := V_c \otimes \cdots \otimes V_c$ (r factors) be the r-fold tensor product of V_c with itself. Since both $(V^{\otimes r})_c$ and $V_c^{\otimes r}$ are linear spaces over the field $\mathbb{C}$ and both have $\{\boldsymbol{e}_{i_1} \otimes \cdots \otimes \boldsymbol{e}_{i_r} : 1 \le i_k \le 3, 1 \le k \le r\}$ as basis, we see that $(V^{\otimes r})_c = V_c^{\otimes r}$. Henceforth we denote the complexification of $V^{\otimes r}$ by $V_c^{\otimes r}$ and still call its elements r-th order tensors. We equip $V_c^{\otimes r}$ with the (Hermitian) inner product induced by that on V_c (see (16.15)), which satisfies

$$\langle \boldsymbol{w}_1 \otimes \cdots \otimes \boldsymbol{w}_r, \boldsymbol{z}_1 \otimes \cdots \otimes \boldsymbol{z}_r \rangle = \prod_{j=1}^{r} \langle \boldsymbol{w}_j, \boldsymbol{z}_j \rangle \tag{16.19}$$

for all $\boldsymbol{w}_1, \ldots, \boldsymbol{w}_r$ and $\boldsymbol{z}_1, \ldots, \boldsymbol{z}_r$ in V_c; in (16.19), as no confusion should arise, we have used the same symbol to denote the inner product on $V_c^{\otimes r}$ and that on V_c. Under this inner product, for two rth-order tensors $\boldsymbol{A} = A_{i_1 \ldots i_r} \boldsymbol{e}_{i_1} \otimes \cdots \otimes \boldsymbol{e}_{i_r}$ and $\boldsymbol{B} = B_{j_1 \ldots j_r} \boldsymbol{e}_{j_1} \otimes \cdots \otimes \boldsymbol{e}_{j_r}$, where the Einstein summation convention is in force, we have

$$\langle \boldsymbol{A}, \boldsymbol{B} \rangle = A_{i_1 \cdots i_r} \overline{B_{i_1 \cdots i_r}}, \tag{16.20}$$

and $\|\boldsymbol{A}\| := \sqrt{\langle \boldsymbol{A}, \boldsymbol{A} \rangle}$ defines the norm of $\boldsymbol{A}$. The inner product on $V_c^{\otimes r}$ reduces to an inner product on $V^{\otimes r}$ when it is restricted to $V^{\otimes r} \times V^{\otimes r}$.

Each orthogonal transformation $\boldsymbol{Q}$ on V induces a linear transformation $\boldsymbol{Q}^{\otimes r}$ on $V^{\otimes r}$ and its namesake on $V_c^{\otimes r}$ defined by

$$\boldsymbol{Q}^{\otimes r}(\boldsymbol{w}_1 \otimes \cdots \otimes \boldsymbol{w}_r) = \boldsymbol{Q}\boldsymbol{w}_1 \otimes \cdots \otimes \boldsymbol{Q}\boldsymbol{w}_r \tag{16.21}$$

for all $\boldsymbol{w}_1, \ldots, \boldsymbol{w}_r$ in V and in V_c, respectively. It is easily seen that $\boldsymbol{Q}^{\otimes r} : V_c^{\otimes r} \to V_c^{\otimes r}$ is a unitary transformation on $V_c^{\otimes r}$. Indeed, by (16.18), (16.19) and (16.21), we have

$$\begin{aligned} \langle \boldsymbol{Q}^{\otimes r}(\boldsymbol{w}_1 \otimes \cdots \otimes \boldsymbol{w}_r), \boldsymbol{Q}^{\otimes r}(\boldsymbol{z}_1 \otimes \cdots \otimes \boldsymbol{z}_r) \rangle &= \langle \boldsymbol{Q}\boldsymbol{w}_1 \otimes \cdots \otimes \boldsymbol{Q}\boldsymbol{w}_r, \boldsymbol{Q}\boldsymbol{z}_1 \otimes \cdots \otimes \boldsymbol{Q}\boldsymbol{z}_r \rangle \\ &= \prod_{j=1}^{r} \langle \boldsymbol{Q}\boldsymbol{w}_j, \boldsymbol{Q}\boldsymbol{z}_j \rangle = \prod_{j=1}^{r} \langle \boldsymbol{w}_j, \boldsymbol{z}_j \rangle \end{aligned}$$

$$= \langle \boldsymbol{w}_1 \otimes \cdots \otimes \boldsymbol{w}_r, \boldsymbol{z}_1 \otimes \cdots \otimes \boldsymbol{z}_r \rangle \tag{16.22}$$

for all $\boldsymbol{w}_1, \ldots, \boldsymbol{w}_r$ and $\boldsymbol{z}_1, \ldots \boldsymbol{z}_r$ in V_c.

16.2 Material Tensors and Pseudotensors

In continuum physics, many attributes of material points are characterized by multilinear mappings. Let a physical attribute Π of a given material point P be described by an rth-order tensor $\boldsymbol{H}$. When the material point P undergoes a rotation or a roto-inversion defined by $\boldsymbol{Q} \in \mathrm{O}(3)$, the multilinear mapping that characterizes its attribute Π changes from $\boldsymbol{H}$ to $\mathcal{T}_{\boldsymbol{Q}}\boldsymbol{H}$. We say that Π is characterized by a material tensor $\boldsymbol{H}$ if

$$\mathcal{T}_{\boldsymbol{Q}}\boldsymbol{H} = \boldsymbol{Q}^{\otimes r}\boldsymbol{H}, \tag{16.23}$$

and by a material pseudotensor $\boldsymbol{H}$ if

$$\mathcal{T}_{\boldsymbol{Q}}\boldsymbol{H} = (\det \boldsymbol{Q})\,\boldsymbol{Q}^{\otimes r}\boldsymbol{H}. \tag{16.24}$$

When we restrict $\boldsymbol{Q}$ in $\mathcal{T}_{\boldsymbol{Q}}$ to rotations, we will write $\mathcal{T}_{\boldsymbol{R}}$, where $\boldsymbol{R}$ denotes a rotation.

The following simple observation will play a crucial role in our proofs of the decomposition theorem in Sect. 16.5.2 and Proposition 16.17 in Sect. 16.6.2.

Remark 16.1 Both material tensors and pseudotensors are "tensors" in the sense of multilinear mappings as defined by (16.1). An r-th order material tensor (resp. pseudotensor) is an "r-th order tensor" that obeys transformation law (16.23) (resp. (16.24)) under $\mathcal{T}_{\boldsymbol{Q}}$. □

Lemma 16.2 *For an rth-order material tensor (resp. pseudotensor) $\boldsymbol{H}$, $\mathcal{T}_{\mathcal{I}}\boldsymbol{H} = (-1)^r\boldsymbol{H}$ (resp. $\mathcal{T}_{\mathcal{I}}\boldsymbol{H} = (-1)^{r+1}\boldsymbol{H}$).*

Proof For an rth-order material tensor $\boldsymbol{H}$,

$$\begin{aligned}\mathcal{T}_{\mathcal{I}}\boldsymbol{H} &= \mathcal{I}^{\otimes r}\boldsymbol{H} = \mathcal{I}^{\otimes r}(H_{i_1\cdots i_r}\boldsymbol{e}_{i_1} \otimes \cdots \otimes \boldsymbol{e}_{i_r}) \\ &= H_{i_1\cdots i_r}\mathcal{I}\boldsymbol{e}_{i_1} \otimes \cdots \otimes \mathcal{I}\boldsymbol{e}_{i_r} \\ &= H_{i_1\cdots i_r}(-\boldsymbol{e}_{i_1}) \otimes \cdots \otimes (-\boldsymbol{e}_{i_r}) = (-1)^r\boldsymbol{H}.\end{aligned} \tag{16.25}$$

For an rth-order pseudotensor $\boldsymbol{H}$,

$$\begin{aligned}\mathcal{T}_{\mathcal{I}}\boldsymbol{H} &= (\det\mathcal{I})\mathcal{I}^{\otimes r}\boldsymbol{H} = -\mathcal{I}^{\otimes r}(H_{i_1\cdots i_r}\boldsymbol{e}_{i_1} \otimes \cdots \otimes \boldsymbol{e}_{i_r}) \\ &= (-1)^{r+1}\boldsymbol{H}.\end{aligned} \tag{16.26}$$

□

The mappings $\boldsymbol{\Phi}^{(r)} : \mathrm{SO}(3) \to \mathrm{GL}(V_c^{\otimes r})$, $\boldsymbol{R} \mapsto \boldsymbol{R}^{\otimes r}$, and $\boldsymbol{\Psi}^{(r)} : \mathrm{O}(3) \to \mathrm{GL}(V_c^{\otimes r})$, $\boldsymbol{Q} \mapsto \boldsymbol{Q}^{\otimes r}$, are clearly representations of SO(3) and O(3), respectively, on representation space $V_c^{\otimes r}$. Likewise, $\boldsymbol{\Theta}^{(r)} : \mathrm{O}(3) \to \mathrm{GL}(V_c^{\otimes r})$, $\boldsymbol{Q} \mapsto (\det \boldsymbol{Q})\boldsymbol{Q}^{\otimes r}$, is a representation of O(3) on $V_c^{\otimes r}$. To see this, let $\boldsymbol{Q}_1, \boldsymbol{Q}_2 \in \mathrm{O}(3)$. Then we have $\det(\boldsymbol{Q}_1\boldsymbol{Q}_2)(\boldsymbol{Q}_1\boldsymbol{Q}_2)^{\otimes r} = (\det \boldsymbol{Q}_1)(\det \boldsymbol{Q}_2)\boldsymbol{Q}_1^{\otimes r}\boldsymbol{Q}_2^{\otimes r} = (\det \boldsymbol{Q}_1)\boldsymbol{Q}_1^{\otimes r}(\det \boldsymbol{Q}_2)\boldsymbol{Q}_2^{\otimes r}$. Moreover, the representations $\boldsymbol{\Phi}^{(r)}$, $\boldsymbol{\Psi}^{(r)}$ and $\boldsymbol{\Theta}^{(r)}$ are clearly unitary and continuous. The representations $\boldsymbol{\Phi}^{(r)}$, $\boldsymbol{\Psi}^{(r)}$ are examples of (material) tensor representations, and $\boldsymbol{\Theta}^{(r)}$ of (material) pseudotensor representations.

Definition 16.3 Let G be a subgroup of O(3) and X an O(3)-invariant subspace of $V_c^{\otimes r}$. If $G \nsubseteq \mathrm{SO}(3)$, a representation $\boldsymbol{T} : G \to \mathrm{GL}(X)$, $\boldsymbol{Q} \mapsto \mathcal{T}_{\boldsymbol{Q}}$ is called an r-th order (material) tensor and pseudotensor representation of G, respectively, if $\mathcal{T}_{\boldsymbol{Q}}$ obeys transformation law (16.23) and (16.24), respectively. If $G \subset \mathrm{SO}(3)$, the map $\boldsymbol{R} \mapsto \mathcal{T}_{\boldsymbol{R}}$ is called a tensor representation of G. □

To specify the various types of tensorial representation spaces, we adopt a system of notation slightly modified from that advocated by Jahn [164] and Sirotin [299]. In this notation, $V^{\otimes 2}$ stands for the tensor product $V \otimes V$, $[V^{\otimes 2}]$ the space of symmetric second-order tensors, $V \otimes [V^{\otimes 2}]$ the tensor product of V and $[V^{\otimes 2}]$, $[[V^{\otimes 2}]^{\otimes 2}]$ the symmetric square of $[V^{\otimes 2}]$ (i.e., the symmetrized tensor product of $[V^{\otimes 2}]$ and $[V^{\otimes 2}]$), $[[V^{\otimes 2}]^3]$ the symmetric cube of $[V^{\otimes 2}]$, $[V^{\otimes 2}] \otimes [[V^{\otimes 2}]^{\otimes 2}]$ the tensor product of $[V^{\otimes 2}]$ and $[[V^{\otimes 2}]^{\otimes 2}]$, ..., etc. In the same spirit, we denote by $[V^{\otimes 2}]_0$ the space of traceless, symmetric second-order tensors, $[[V^{\otimes 2}]_0^{\otimes 2}]$ the symmetric square of $[V^{\otimes 2}]_0$ (i.e., the symmetrized tensor product of $[V^{\otimes 2}]_0$ and $[V^{\otimes 2}]_0$), $[[V^{\otimes 2}]_0^3]$ the symmetric cube of $[V^{\otimes 2}]_0$, ..., etc. In this notation, for instance, the fourth-order elasticity tensor is of type $[[V^{\otimes 2}]^{\otimes 2}]$, the sixth-order acoustoelastic tensor [200, 205, 255] of type $[[V^{\otimes 2}]^{\otimes 2}] \otimes [V^{\otimes 2}]$, and if we write [201] the plastic potential of an orthorhombic sheet metal as a Taylor expansion in the deviatoric stress $\boldsymbol{\sigma}$, the cubic term is of type $[[V^{\otimes 2}]_0^3]$.

When V is replaced by its complexification V_c, the same procedure to construct tensor space Z will result in its complexification Z_c. Thus $V_c^{\otimes 2}$ is the complexification of $V^{\otimes 2}$, $[[V_c^{\otimes 2}]^{\otimes 2}]$ is the complexification of $[[V^{\otimes 2}]^{\otimes 2}]$, etc.

16.3 Decomposition of Representations on Tensor and Pseudotensor Spaces into Irreducible Parts

In continuum mechanics it is well known that $V \otimes V$, the space of second-order tensors, can be written as a direct sum of three subspaces, namely: the 1-dimensional subspace of spherical tensors $\mathrm{Sph} = \{\alpha \boldsymbol{I} : \alpha \in \mathbb{R}\}$, the 3-dimensional subspace Skw of skew tensors, and the 5-dimensional subspace Sym_0 of traceless symmetric tensors:

$$V^{\otimes 2} = \mathrm{Sph} \oplus \mathrm{Skw} \oplus \mathrm{Sym}_0. \tag{16.27}$$

All the spaces in the preceding equation are invariant under the action of the rotation group.[161] Moreover, none of the subspaces in the decomposition formula (16.27) contains any non-trivial proper invariant subspace of $\boldsymbol{R}^{\otimes 2}$. In other words, the restrictions of the representation $\boldsymbol{\Phi}^{(r)} : \mathrm{SO}(3) \to \mathrm{GL}(V^{\otimes 2})$, $\boldsymbol{R} \mapsto \boldsymbol{R}^{\otimes 2}$, to Sph, Skw, and Sym_0 are irreducible subrepresentations, which are equivalent to the irreducible representations $\mathcal{D}^0$, $\mathcal{D}^1$, and $\mathcal{D}^2$, respectively. In what follows, we shall focus only on the problem of writing tensor and pseudotensor representations as direct sums of their irreducible subrepresentations. Thus instead of (16.27), we will present algorithms by which we can derive the formula

$$V_c^{\otimes 2} = \mathcal{D}^0 + \mathcal{D}^1 + \mathcal{D}^2. \tag{16.28}$$

Strictly speaking, the symbol $\boldsymbol{\Phi}^{(2)}$ (i.e., the name of the representation in question) should appear on the left-hand side of (16.28) instead of the name of the representation space, because mathematically it is the decomposition of representation ρ into its irreducible parts. However, we elect to use the name of the representation space for the following reasons:

[161] A space Z of rth-order tensor is said to be invariant under the action of the rotation group (or rotationally invariant) if $\boldsymbol{R}^{\otimes r} Z \subset Z$ for all $\boldsymbol{R} \in \mathrm{SO}(3)$.

– In what follows we shall only consider, for some $r \geq 0$, representations $\boldsymbol{R} \mapsto \boldsymbol{R}^{\otimes r}$ of SO(3), and $\boldsymbol{Q} \mapsto \boldsymbol{Q}^{\otimes r}$ or $\boldsymbol{Q} \mapsto (\det \boldsymbol{Q})\, \boldsymbol{Q}^{\otimes r}$ of O(3), on complexified spaces of rth-order tensors or pseudotensors. The irreducible representations in each decomposition formula will reveal whether the formula pertains to representations of SO(3) or of O(3). Moreover, for representations of O(3), whether material tensors or pseudotensors are in question will be spelled out at the outset. Hence, specifying the tensor or pseudotensor space of the representation is sufficient for providing all the information on the representation. For example, from the irreducible subrepresentations on the right-hand side of (16.28) we learn that the formula pertains to representations of SO(3), which together with the representation space given on the left-hand side let us know that the formula concerns the representation which maps SO(3) into $\mathrm{GL}(V_c^{\otimes 2})$.
– Formula (16.28), as it stands, can be interpreted as saying that the space $V_c^{\otimes 2}$ is a direct sum of three SO(3)-invariant subspaces, the subrepresentations on which are equivalent to the irreducible representations $\mathcal{D}^0$, $\mathcal{D}^1$, and $\mathcal{D}^2$, respectively.

In applications, the goal is often formulas for decomposition of tensor and pseudotensor spaces such as (16.27), not those such as (16.28) on decomposition of group representations into irreducible parts. Nevertheless, obtaining the group-theoretic decomposition formulas could be the first step in arriving at corresponding formulas for decomposition of tensor and pseudotensor spaces. See for example [95, 203], where group-theoretic decomposition formulas such as (16.28) are used in the derivation of representation theorems that delineate the effects of weak crystallographic texture on the material tensors and pseudotensors of polycrystals.

We have already learned in Theorem 13.27 how group characters can be used for decomposition of finite-dimensional representations into irreducible parts. Here we will detail the specifics of applying the method of characters to decompose tensor and pseudotensor representations of SO(3) and O(3).

16.3.1 Method of Characters

As a glance at the complete set of finite-dimensional unitary representations of O(3) given in Theorem 14.14 may suggest, formulas for decompositions of representations of O(3) would just be slight modifications of the corresponding decomposition formulas for representations of SO(3). That hunch turns out to be correct. In describing the method of characters in this section, we will simply restrict attention to decomposition of representations of SO(3) as prime example.[162]

Let $\mathrm{GL}(V_c^{\otimes r})$ be the set of non-singular linear transformations on $V_c^{\otimes r}$. It is easily checked that the mappings $\boldsymbol{\Phi}^{(r)} : \mathrm{SO}(3) \to \mathrm{GL}(V_c^{\otimes r})$, $\boldsymbol{R} \mapsto \boldsymbol{R}^{\otimes r}$ are representations of SO(3) on $V_c^{\otimes r}$. Moreover, the representations $\boldsymbol{\Phi}^{(r)}$ are unitary and continuous. Indeed, by (16.22) the functions $\boldsymbol{R}^{\otimes r} : V_c^{\otimes r} \to V_c^{\otimes r}$ are unitary. As for continuity of the representations ρ_r, note that the matrix elements of $\boldsymbol{R}^{\otimes r}$ under the basis $\{\boldsymbol{e}_{i_1} \otimes \boldsymbol{e}_{i_2} \otimes \cdots \otimes \boldsymbol{e}_{i_r} : 1 \leq i_k \leq 3 \text{ for } k = 1, \ldots r\}$ are polynomial functions of R_{ij}, the matrix elements of $\boldsymbol{R}$ under the basis $\boldsymbol{e}_1, \boldsymbol{e}_2, \boldsymbol{e}_3$.

A subspace $Z \subset V^{\otimes r}$ is said to be invariant under the action of the rotation group SO(3) if it remains invariant under $\boldsymbol{R}^{\otimes r}$ for each $\boldsymbol{R} \in \mathrm{SO}(3)$. If Z is an invariant subspace of $V^{\otimes r}$ under the action of SO(3), then its complexification Z_c is an invariant subspace of $V_c^{\otimes r}$. Since

[162] Decomposition of representations of SO(3) into irreducible parts has been well documented in the physics and mechanics literature. See, e.g., [164, 317, 356] and [299, 357] for decomposition by the method of characters and by other methods, respectively.

every finite-dimensional continuous unitary representation of a compact group is completely reducible, each tensor representation of the rotation group $\boldsymbol{\Phi}^{(r)}|_{Z_c} : \boldsymbol{R} \mapsto \boldsymbol{R}^{\otimes r}|_{Z_c}$ can be decomposed as a direct sum of irreducible subrepresentations, each of which is equivalent to some $\mathcal{D}^k$ ($k := 0, 1, 2, \ldots, r$):[163]

$$Z_c = m_0\mathcal{D}^0 + m_1\mathcal{D}^1 + \cdots + m_k\mathcal{D}^k + \cdots + m_r\mathcal{D}^r, \tag{16.29}$$

where m_k is the multiplicity of $\mathcal{D}^k$ in the decomposition. Note that here and henceforth we denote the tensor representation $\boldsymbol{R} \mapsto \boldsymbol{R}^{\otimes r}|_{Z_c}$ also by the notation Z_c of the tensor space in question. Whether we really mean the tensor space or the corresponding tensor representation should be clear from the context; cf. the comments at the beginning of Sect. 16.3.

Let χ be the character of the representation $\boldsymbol{R} \mapsto \boldsymbol{R}^{\otimes r}$ on Z_c, and let χ_k be the character of the irreducible representation $\mathcal{D}^k$. It follows immediately from decomposition formula (16.29) that

$$\chi = m_0\chi_0 + m_1\chi_1 + \cdots + m_k\chi_k + \cdots + m_r\chi_r. \tag{16.30}$$

By Theorem 13.27, the multiplicity m_k can be determined by the formula

$$m_k = \langle \chi, \chi_k \rangle = \int_{\mathrm{SO}(3)} \chi(\boldsymbol{R})\overline{\chi_k(\boldsymbol{R})}\, d\mathfrak{g}(\boldsymbol{R}). \tag{16.31}$$

To proceed further, we need: (i) formulas for $\chi_l(\boldsymbol{R})$ for $\boldsymbol{R} \in \mathrm{SO}(3)$ and $l = 0, 1, 2, \ldots$; (ii) for the tensor space Z_c in question, at least one method to determine the character χ of representation $\boldsymbol{R} \mapsto \boldsymbol{R}^{\otimes r}$ on Z_c.

16.4 Decomposition of Tensor Representations of SO(3)

16.4.1 Characters of Irreducible Representations of SO(3)

By definition, $\chi_l(\boldsymbol{R}) = \mathrm{tr}\,[D^l_{mn}(\boldsymbol{R}(\boldsymbol{n}, \omega)]$. For $\omega = 0$, $\boldsymbol{R} = \boldsymbol{I}$ and $[D^l_{mn}(\boldsymbol{I})]$ is the $(2l+1) \times (2l+1)$ identity matrix. Hence $\chi_l(\boldsymbol{I}) = 2l + 1$. For $0 < \omega \leq \pi$, under a Cartesian coordinate system where $\boldsymbol{n} = \boldsymbol{e}_3$, the Euler angles of $\boldsymbol{R}$ is $(\omega, 0, 0)$, $D^l_{mm}(\omega, 0, 0) = e^{-im\omega}$ (no sum), and

$$\chi_l(\boldsymbol{R}) = \mathrm{tr}[D^l_{mn}(\boldsymbol{R}(\boldsymbol{n}, \omega))] = \sum_{m=-l}^{l} e^{im\omega} = 1 + 2\sum_{m=1}^{l} \cos m\omega. \tag{16.32}$$

The sum in $(16.32)_2$ is a geometric progression with first term $e^{-il\omega}$, common factor $e^{i\omega}$, and a total of $(2l+1)$ terms. Hence the sum is

$$\sum_{m=-l}^{l} e^{im\omega} = \frac{e^{i(l+1)\omega} - e^{-il\omega}}{e^{i\omega} - 1} = \frac{e^{i(l+\frac{1}{2})\omega} - e^{-i(l+\frac{1}{2})\omega}}{e^{i\omega/2} - e^{-i\omega/2}} = \frac{\sin(l + \frac{1}{2})\omega}{\sin\frac{1}{2}\omega} \tag{16.33}$$

In summary, we have

$$\chi_l(\boldsymbol{R}) = \begin{cases} \dfrac{\sin(l+\frac{1}{2})\omega}{\sin\frac{1}{2}\omega} & \text{for } \omega \neq 0 \\ 2l+1 & \text{for } \omega = 0 \end{cases} \tag{16.34}$$

[163] It suffices to consider $k \leq r$; see Proposition 16.4 below.

From the orthogonality relation (4.21) of the Wigner D-functions, we obtain

$$\begin{aligned}\langle \chi_l, \chi_{l'} \rangle &= \int_{\mathrm{SO}(3)} \left(\sum_{m=-l}^{l} D^l_{mm}(\boldsymbol{R}) \right) \overline{\left(\sum_{n=-l'}^{l'} D^{l'}_{nn}(\boldsymbol{R}) \right)} d\mathrm{g}(\boldsymbol{R}) \\ &= \sum_{m=-l}^{l} \sum_{n=-l'}^{l'} \int_{\mathrm{SO}(3)} D^l_{mm}(\boldsymbol{R}) \overline{D^{l'}_{nn}(\boldsymbol{R})}\, d\mathrm{g}(\boldsymbol{R}) \\ &= \sum_{m=-l}^{l} \sum_{n=-l'}^{l'} \frac{1}{2l+1} \delta_{ll'} \delta_{mn} = \delta_{ll'}. \end{aligned} \tag{16.35}$$

That the characters of the representations $\mathcal{D}^l$ $(l = 0, 1, 2, \ldots)$ are orthonormal verifies that the representations $\mathcal{D}^l$ of SO(3) are irreducible and are pairwise inequivalent.

Consider the self-representation $\boldsymbol{\Phi}^{(1)} : \mathrm{SO}(3) \to \mathrm{GL}(V_c)$, $\boldsymbol{R} \mapsto \boldsymbol{R}$. As a linear transformation on V_c, $\boldsymbol{R}(\boldsymbol{n}, \omega)$ has three eigenvalues

$$\lambda_1 = e^{-i\omega}, \quad \lambda_2 = 1, \quad \lambda_3 = e^{i\omega}. \tag{16.36}$$

It follows immediately that

$$\chi_{\boldsymbol{\Phi}^{(1)}} = e^{-i\omega} + 1 + e^{i\omega} = 1 + 2\cos\omega. \tag{16.37}$$

Consider the tensor representation $\boldsymbol{\Phi}^{(r)} : \mathrm{SO}(3) \to \mathrm{GL}(V_c^{\otimes r})$, $\boldsymbol{R} \mapsto \boldsymbol{R}^{\otimes r}$. By (13.82), the character of $\boldsymbol{\Phi}^{(r)}$ is given by the formula

$$\chi_{\boldsymbol{\Phi}^{(r)}} = (e^{-i\omega} + 1 + e^{i\omega})^r. \tag{16.38}$$

Note that the highest power of $e^{i\omega}$ in $\chi_{V_c^{\otimes r}}$ and in $\chi_l = \sum_{m=-l}^{l} e^{i\omega}$ are r and l, respectively, and the coefficient of $e^{ir\omega}$ in (16.38) is 1. Hence $\boldsymbol{\Phi}^{(r)}$ does not have a subrepresentation equivalent to $\mathcal{D}^l$ with $l > r$. Moreover, when the tensor-product representation $\boldsymbol{\Phi}^{(r)}$ is decomposed into its irreducible parts, the multiplicity of $\mathcal{D}^r$ in the decomposition formula is 1. We record this simple observation as the following proposition.

Proposition 16.4 *Let Z_c be a subspace of $V_c^{\otimes r}$ invariant under the action of* SO(3)*, and let $\boldsymbol{\Phi}^{(r)}|_{Z_c}$ be the restriction of the tensor representation $\boldsymbol{\Phi}^{(r)} : \mathrm{SO}(3) \to \mathrm{GL}(V_c^{\otimes r})$, $\boldsymbol{R} \mapsto \boldsymbol{R}^{\otimes r}$, to Z_c. When $\boldsymbol{\Phi}^{(r)}|_{Z_c}$ is decomposed into its irreducible parts, the decomposition formula is of the form*

$$Z_c = m_0 \mathcal{D}^0 + m_1 \mathcal{D}^1 + \cdots + m_r \mathcal{D}^r, \tag{16.39}$$

where some of the multiplicities m_j in (16.39) may be equal to zero and m_r is either 0 *or* 1*. Moreover, when $Z_c = V_c^{\otimes r}$, $m_r = 1$.* □

There is a formula, known as the Clebsch-Gordan series, for the decomposition of the tensor product of irreducible representations $\mathcal{D}^l$ and $\mathcal{D}^k$.

Proposition 16.5 *For $k \geq 0$ and $l \geq 0$,*

$$\mathcal{D}^l \otimes \mathcal{D}^k = \mathcal{D}^{|l-k|} + \mathcal{D}^{|l-k|+1} + \cdots + \mathcal{D}^{l+k-1} + \mathcal{D}^{l+k}. \tag{16.40}$$

Proof Without loss of generality, say $k \le l$. For $r \ge 0$ and $\boldsymbol{R} \in \mathrm{SO}(3)$, by $(16.32)_2$ and $(16.33)_1$ we have

$$\chi_r(\boldsymbol{R}) = \sum_{m=-r}^{r} e^{ir\omega} = \begin{cases} \dfrac{e^{i(r+1)\omega} - e^{-ir\omega}}{e^{i\omega} - 1}, & \text{for } \omega \neq 0; \\ 2r+1, & \text{for } \omega = 0. \end{cases} \tag{16.41}$$

Using (16.41), we obtain for $\omega \neq 0$

$$\begin{aligned} \chi_l \cdot \chi_k &= \frac{e^{i(l+1)\omega} - e^{-il\omega}}{e^{i\omega} - 1} \cdot \left(1 + \sum_{m=1}^{k} \left(e^{im\omega} + e^{-im\omega}\right)\right) \\ &= \chi_l + \sum_{m=1}^{k} \frac{e^{i(l+m+1)\omega} - e^{-i(l-m)\omega} + e^{i(l-m+1)\omega} - e^{-i(l+m)\omega}}{e^{i\omega} - 1} \\ &= \chi_l + \sum_{m=1}^{k} \frac{e^{i(l+m+1)\omega} - e^{-i(l+m)\omega}}{e^{i\omega} - 1} + \sum_{m=1}^{k} \frac{e^{i(l-m+1)\omega} - e^{-i(l-m)\omega}}{e^{i\omega} - 1} \\ &= \chi_l + \sum_{m=1}^{k} \chi_{l+m} + \sum_{m=1}^{k} \chi_{l-m} \\ &= \chi_{l-k} + \chi_{l-k+1} + \cdots + \chi_{l-1} + \chi_l + \chi_{l+1} + \cdots + \chi_{l+k-1} + \chi_{l+k}; \end{aligned} \tag{16.42}$$

for $\omega = 0$, $\chi_l \cdot \chi_k = (2l+1)(2k+1)$, which is equal to $\sum_{m=|l-k|}^{l+k}(2m+1)$, the sum of characters on the right-hand side of (16.42). □

As a simple application of (16.40), we have

$$V_c^{\otimes 2} = V_c \otimes V_c = \mathcal{D}^1 \otimes \mathcal{D}^1 = \mathcal{D}^0 + \mathcal{D}^1 + \mathcal{D}^2, \tag{16.43}$$

which is none other than (16.28). We shall present another example later.

16.4.2 Examples

In what follows we shall present several examples where unitary representations which are restrictions of $\boldsymbol{\Phi}^{(r)} : \boldsymbol{R} \mapsto \boldsymbol{R}^{\otimes r}$ (for some $r \ge 2$) to various subspaces Z_c of $V_c^{\otimes r}$ are decomposed in their irreducible parts. In all the examples the main tool will be formula (13.91).

As discussed at the beginning of Sect. 16.3, since all the representations in question will be restrictions of $\boldsymbol{\Phi}^{(r)}$, we shall, for convenience, write Z_c for $\boldsymbol{\Phi}^{(r)}|_{Z_c}$ whenever no confusion should arise. For example, we shall write χ_{Z_c} for the character of the representation $\boldsymbol{\Phi}^{(r)}|_{Z_c}$.

Example 16.6 Let $\chi_{[V_c^{\otimes 2}]}$ be the character of the representation $\boldsymbol{R} \mapsto \boldsymbol{R}^{\otimes 2}|_{[V_c^{\otimes 2}]}$. Since the tensor space $[V_c^{\otimes 2}]$ is the symmetric square of V_c, we can use formula (13.89), a special case of (13.91); see also [296, 317]. Note that X and $\boldsymbol{T}$ in (13.89) are here V_c and $\boldsymbol{\Phi}^{(1)} : \mathrm{SO}(3) \to \mathrm{GL}(V_c)$, $\boldsymbol{R} \mapsto \boldsymbol{R}$, respectively. Hence we have

$$\chi_{[V_c^{\otimes 2}]} = \sum_{1 \le i \le j \le 3} \lambda_i \lambda_j, \tag{16.44}$$

where λ_i $(i = 1, 2, 3)$ are given in (16.36). Substituting the values of λ_i into (16.44), we obtain

$$\begin{aligned}\chi_{[V_c^{\otimes 2}]} &= \lambda_1\lambda_1 + \lambda_1\lambda_2 + \lambda_1\lambda_3 + \lambda_2\lambda_2 + \lambda_2\lambda_3 + \lambda_3\lambda_3 \\ &= e^{-i2\omega} + e^{-i\omega} + 1 + 1 + e^{i\omega} + e^{i2\omega} = \chi_0 + \chi_2. \end{aligned} \tag{16.45}$$

Hence we have the following decomposition of the representation $\boldsymbol{R} \mapsto \boldsymbol{R}^{\otimes 2}|_{[V_c^{\otimes 2}]}$:

$$[V_c^{\otimes 2}] = \mathcal{D}^0 + \mathcal{D}^2. \tag{16.46}$$

□

Example 16.7 The fourth-order elasticity tensor in linear elasticity is of type $[[V_c^{\otimes 2}]^{\otimes 2}]$. The inner $[\cdot]$ in $[[V_c^{\otimes 2}]^{\otimes 2}]$ accounts for the minor symmetry, i.e., the fact that we are building fourth-order tensors with second-order *symmetric* tensors, and the outer $[\cdot]$ the major symmetry, which refers to the *symmetric square* of the 6-dimensional vector space $[V_c^{\otimes 2}]$. It is easy to check that $[[V_c^{\otimes 2}]^{\otimes 2}]$ is invariant under $\boldsymbol{R}^{\otimes 4}$ for each $\boldsymbol{R} \in \mathrm{SO}(3)$. As shown in (16.46), the representation $\boldsymbol{R} \mapsto \boldsymbol{R}^{\otimes 2}|_{[V_c^{\otimes 2}]}$ is equivalent to the direct sum of the irreducible unitary representations $\mathcal{D}^2$ and $\mathcal{D}^0$. Hence it is equivalent to a 6×6 matrix representation which, for each rotation $\boldsymbol{Q}$, has a diagonal 5×5 block given by the matrix $[D^2_{mn}(\boldsymbol{Q}(\boldsymbol{n}, \omega))]$, the remaining diagonal element equal to 1, and the other entries equal to zero. In fact under the Kelvin notation (see, e.g., [202, 228]), $[V^{\otimes 2}]$ is treated as a 6-dimensional vector space X. An orthonormal basis is chosen in $[V^{\otimes 2}]$, or equivalently in X, so that each element in X is a 6×1 column vector. Let $\hat{\boldsymbol{A}}$ and $\hat{\boldsymbol{B}}$ in X correspond to $\boldsymbol{A}$ and $\boldsymbol{B}$ in $[V^{\otimes 2}]$, respectively. For each $\boldsymbol{R}(\boldsymbol{n}, \omega) \in \mathrm{SO}(3)$, $\boldsymbol{R}^{\otimes 2}|_{[V^{\otimes 2}]}$ corresponds to an orthogonal transformation R on X. Let X_c be the complexification of X. Under a suitable Cartesian coordinate system. $\mathsf{R} : X_c \to X_c$ is given by the 6×6 diagonal matrix with elements $\lambda_1, \ldots, \lambda_6$ as follows:

$$\lambda_1 = e^{-i2\omega}, \quad \lambda_2 = e^{-i\omega}, \quad \lambda_3 = 1, \quad \lambda_4 = e^{i\omega}, \quad \lambda_5 = e^{i2\omega}, \quad \lambda_6 = 1. \tag{16.47}$$

Let $\chi_{[[V_c^{\otimes 2}]^{\otimes 2}]}$ be the character of the representation $\boldsymbol{R} \mapsto \boldsymbol{R}^{\otimes 4}|_{[[V_c^{\otimes 2}]^{\otimes 2}]}$ or $\boldsymbol{R} \mapsto \mathsf{R}^{\otimes 2}$. Then we have

$$\begin{aligned}\chi_{[[V_c^{\otimes 2}]^{\otimes 2}]} &= \sum_{1 \le i \le j \le 6} \lambda_i\lambda_j = 5 + 6\cos\omega + 6\cos 2\omega + 2\cos 3\omega + 2\cos 4\omega \\ &= 2\chi_0 + 2\chi_2 + \chi_4. \end{aligned} \tag{16.48}$$

The multiplicities $m_0 = 2$, $m_1 = 0$, $m_2 = 2$, $m_3 = 0$, and $m_4 = 1$ can be obtained by integration, or by inspection, or by using a counting formula [356]. The decomposition formula for $[[V_c^{\otimes 2}]^{\otimes 2}]$ then follows easily:

$$[[V_c^{\otimes 2}]^{\otimes 2}] = 2\mathcal{D}^0 + 2\mathcal{D}^2 + \mathcal{D}^4. \tag{16.49}$$

By formula (13.87), as here $n = 6$ and $r = 2$, we have

$$\dim\left([[V_c^{\otimes 2}]^{\otimes 2}]\right) = C_2^{6+2-1} = \frac{7!}{2!\,5!} = 21.$$

The sum of the dimensions of the invariant subspaces in the decomposition (16.49) is $2 \times 1 + 2 \times 5 + 1 \times 9 = 21$. □

Example 16.8 In classical acoustoelastic theory (see [321] and the references therein), where the initial stress is caused by a deformation of an elastic material from a stress-free natural configuration, the acoustoelastic constants are determined by tensor of type $[[V_c^{\otimes 2}]^{\otimes 3}]$. With reference to the discussions in Example 16.7, the representation $\boldsymbol{R} \mapsto \boldsymbol{R}^{\otimes 6}|_{[[V_c^{\otimes 2}]^{\otimes 3}]}$ can be taken as the representation $\boldsymbol{R} \mapsto \mathsf{R}^{\otimes 3}$. By formula (13.91), the character of the representation is given by

$$\begin{aligned}\chi_{[[V_c^{\otimes 2}]^{\otimes 3}]} &= \sum_{1\le i\le j\le k\le 6} \lambda_i\lambda_j\lambda_k \\ &= 10 + 14\cos\omega + 14\cos 2\omega + 8\cos 3\omega + 6\cos 4\omega + 2\cos 5\omega + 2\cos 6\omega \\ &= 3\chi_0 + 3\chi_2 + \chi_3 + 2\chi_4 + \chi_6. \end{aligned} \tag{16.50}$$

Hence we obtain the decomposition formula

$$[[V_c^{\otimes 2}]^{\otimes 3}] = 3\mathcal{D}^0 + 3\mathcal{D}^2 + \mathcal{D}^3 + 2\mathcal{D}^4 + \mathcal{D}^6. \tag{16.51}$$

By formula (13.87), as here $n = 6$ and $r = 3$, we have

$$\dim\left([[V_c^{\otimes 2}]^{\otimes 3}]\right) = C_3^{6+3-1} = \frac{8!}{3!\,5!} = 56.$$

The sum of the dimensions of the invariant subspaces in the decomposition (16.51) is $3 \times 1 + 3 \times 5 + 1 \times 7 + 2 \times 9 + 1 \times 13 = 56$. □

Example 16.9 The third-order term of the Taylor expansion of the plastic potential is determined by a tensor of the type $[X^{\otimes 3}]$, where $X = [V_c^{\otimes 2}]_0$ is a 5-dimensional vector space [201]. A rotation $\boldsymbol{R}$ induces a linear transformation $\boldsymbol{R}^{\otimes 2}|_X$ on X, and the map $\boldsymbol{\Phi}_X^{(2)} : \boldsymbol{R} \mapsto \boldsymbol{R}^{\otimes 2}|_X$ is a representation of SO(3). For each rotation $\boldsymbol{R}(\boldsymbol{n}, \omega)$, $\boldsymbol{R}^{\otimes 2}|_X$ has five eigenvalues, namely:

$$\lambda_1 = e^{-i2\omega}, \quad \lambda_2 = e^{-i\omega}, \quad \lambda_3 = 1, \quad \lambda_4 = e^{i\omega}, \quad \lambda_5 = e^{i2\omega}. \tag{16.52}$$

The character of representation $\boldsymbol{\Phi}^{(6)}_{[[V_c^{\otimes 2}]_0^{\otimes 3}]}$ is given by

$$\begin{aligned}\chi_{[[V_c^{\otimes 2}]_0^{\otimes 3}]} &= \sum_{1\le i\le j\le k\le 5} \lambda_i\lambda_j\lambda_k \\ &= 5 + 8\cos\omega + 8\cos 2\omega + 6\cos 3\omega + 4\cos 4\omega + 2\cos 5\omega + 2\cos 6\omega \\ &= \chi_0 + \chi_2 + \chi_3 + \chi_4 + \chi_6. \end{aligned} \tag{16.53}$$

Hence we have the decomposition formula

$$[[V_c^{\otimes 2}]_0^{\otimes 3}] = \mathcal{D}^0 + \mathcal{D}^2 + \mathcal{D}^3 + \mathcal{D}^4 + \mathcal{D}^6. \tag{16.54}$$

By formula (13.87), as here $n = 5$ and $r = 3$, we obtain

$$\dim\left([[V_c^{\otimes 2}]_0^{\otimes 3}]\right) = C_3^{5+3-1} = \frac{7!}{3!\,4!} = 35.$$

The sum of the dimensions of the invariant subspaces in the decomposition (16.51) is $1 + 5 + 7 + 9 + 13 = 35$. □

Example 16.10 We use formula (16.40) to decompose $[[V_c]^{\otimes 2}]^{\otimes 2}] \otimes [V_c^{\otimes 2}]$ as a direct sum of its irreducible parts. In the theory of acoustoelasticity proposed by Man and Paroni [200, 205, 255], the acoustoelastic tensor is of this type. Since $[[V_c]^{\otimes 2}]^{\otimes 2}] = 2\mathcal{D}^0 + 2\mathcal{D}^2 + \mathcal{D}^4$ and $[V_c^{\otimes 2}] = \mathcal{D}^0 + \mathcal{D}^2$, by assertion 4 of Proposition 13.24, formulas (13.79) and (16.40) we obtain

$$\begin{aligned}[[V_c^{\otimes 2}]^{\otimes 2}] \otimes [V_c^{\otimes 2}] &= (2\mathcal{D}^0 + 2\mathcal{D}^2 + \mathcal{D}^4) \otimes (\mathcal{D}^0 + \mathcal{D}^2) \\ &= (2\mathcal{D}^0 + 2\mathcal{D}^2 + \mathcal{D}^4) + 2\mathcal{D}^2 + 2(\mathcal{D}^0 + \mathcal{D}^1 + \mathcal{D}^2 + \mathcal{D}^3 + \mathcal{D}^4) \\ &\quad + (\mathcal{D}^2 + \mathcal{D}^3 + \mathcal{D}^4 + \mathcal{D}^5 + \mathcal{D}^6) \\ &= 4\mathcal{D}^0 + 2\mathcal{D}^1 + 7\mathcal{D}^2 + 3\mathcal{D}^3 + 4\mathcal{D}^4 + \mathcal{D}^5 + \mathcal{D}^6. \end{aligned} \tag{16.55}$$

□

16.5 Decomposition of Tensor and Pseudotensor Representations of O(3)

16.5.1 Characters of Irreducible Representations of O(3)

In Theorem 14.14, we have derived a complete set of finite-dimensional, continuous, irreducible unitary representations of O(3), namely: $\mathcal{D}^{l,+}$, $\mathcal{D}^{l,-}$ for $l = 0, 1, 2, \ldots$. For each l and $\boldsymbol{Q} \in \mathrm{O}(3)$, $\mathcal{D}^{l,\pm} : \boldsymbol{Q} \mapsto [D^{l,\pm}_{mn}(\boldsymbol{Q})]$ $(-l \le m \le l, -l \le n \le l)$, where the entries of the two $(2l+1) \times (2l+1)$ matrices are given in terms of the Wigner D-functions by (14.56) and (14.57), respectively. It follows that the character of representation $\mathcal{D}^{l,+}$ is given by

$$\chi_l^+(\boldsymbol{Q}) = \mathrm{tr}[D^{l,+}_{mn}(\boldsymbol{Q})] = \mathrm{tr}[D^l_{mn}(\boldsymbol{R})] = \chi_l(\boldsymbol{R}) \qquad \text{for } \boldsymbol{Q} = \boldsymbol{R} \text{ or } \boldsymbol{Q} = \boldsymbol{\mathcal{I}R}, \tag{16.56}$$

and that of representation $\mathcal{D}^{l,-}$ by

$$\chi_l^-(\boldsymbol{Q}) = \mathrm{tr}[D^{l,-}_{mn}(\boldsymbol{Q})] = \begin{cases} \mathrm{tr}[D^l_{mn}(\boldsymbol{R})] = \chi_l(\boldsymbol{R}) & \text{for } \boldsymbol{Q} = \boldsymbol{R} \\ -\mathrm{tr}[D^l_{mn}(\boldsymbol{R})] = -\chi_l(\boldsymbol{R}) & \text{for } \boldsymbol{Q} = \boldsymbol{\mathcal{I}R}, \end{cases} \tag{16.57}$$

where $\chi_l(\boldsymbol{R}(\boldsymbol{n}, \omega))$ is given by (16.34).

By Definition 10.3 and (16.56) we have

$$(\chi_l^+ \overline{\chi_{l'}^+})^R(\boldsymbol{R}) = \chi_l^+(\boldsymbol{R})\overline{\chi_{l'}^+(\boldsymbol{R})} = \chi_l(\boldsymbol{R})\chi_{l'}(\boldsymbol{R}), \tag{16.58}$$

$$(\chi_l^+ \overline{\chi_{l'}^+})^L(\boldsymbol{R}) = \chi_l^+(\boldsymbol{\mathcal{I}R})\overline{\chi_{l'}^+(\boldsymbol{\mathcal{I}R})} = \chi_l(\boldsymbol{R})\chi_{l'}(\boldsymbol{R}). \tag{16.59}$$

It follows from (10.53) that

$$\begin{aligned}\langle \chi_l^+, \chi_{l'}^+ \rangle &= \int_{\mathrm{O}(3)} \chi_l^+(\boldsymbol{Q})\overline{\chi_{l'}^+(\boldsymbol{Q})}\, d\mathrm{g}(\boldsymbol{Q}) \\ &= \frac{1}{16\pi^2}\Big(\int_{\mathrm{SO}(3)} (\chi_l^+ \overline{\chi_{l'}^+})^R(\boldsymbol{R})\, d\mathcal{V}(\boldsymbol{R}) + \int_{\mathrm{SO}(3)} (\chi_l^+ \overline{\chi_{l'}^+})^L(\boldsymbol{R})\, d\mathcal{V}(\boldsymbol{R}) \Big) \\ &= \frac{1}{16\pi^2} \cdot 2 \int_{\mathrm{SO}(3)} \chi_l(\boldsymbol{R})\chi_{l'}(\boldsymbol{R})\, d\mathcal{V}(\boldsymbol{R}) = \delta_{ll'}. \end{aligned} \tag{16.60}$$

By the same token, we observe that

$$(\chi_l^+\overline{\chi_{l'}^-})^R(\boldsymbol{R}) = \chi_l^+(\boldsymbol{R})\overline{\chi_{l'}^-(\boldsymbol{R})} = \chi_l(\boldsymbol{R})\chi_{l'}(\boldsymbol{R}), \tag{16.61}$$

$$(\chi_l^+\overline{\chi_{l'}^-})^L(\boldsymbol{R}) = \chi_l^+(\mathcal{I}\boldsymbol{R})\overline{\chi_{l'}^-(\mathcal{I}\boldsymbol{R})} = \chi_l(\boldsymbol{R})\,(-\chi_{l'}(\boldsymbol{R})) \tag{16.62}$$

which imply

$$\begin{aligned}\langle \chi_l^+, \chi_{l'}^-\rangle &= \int_{\mathrm{O}(3)} \chi_l^+(\boldsymbol{Q})\overline{\chi_{l'}^-(\boldsymbol{Q})}\,d\mathrm{g}(\boldsymbol{Q})\\ &= \frac{1}{16\pi^2}\Big(\int_{\mathrm{SO}(3)} (\chi_l^+\overline{\chi_{l'}^-})^R(\boldsymbol{R})\,d\mathcal{V}(\boldsymbol{R}) + \int_{\mathrm{SO}(3)} (\chi_l^+\overline{\chi_{l'}^-})^L(\boldsymbol{R})\,d\mathcal{V}(\boldsymbol{R})\Big)\\ &= \frac{1}{16\pi^2}\Big(\int_{\mathrm{SO}(3)} \big(\chi_l(\boldsymbol{R})\chi_{l'}(\boldsymbol{R}) - \chi_l(\boldsymbol{R})\chi_{l'}(\boldsymbol{R})\big)\,d\mathcal{V}(\boldsymbol{R})\Big) = 0.\end{aligned} \tag{16.63}$$

Similarly, we find $\langle \chi_l^-, \chi_{l'}^-\rangle = \delta_{ll'}$.

The orthonormality relations $\langle \chi_l^+, \chi_{l'}^+\rangle = \delta_{ll'}$, $\langle \chi_l^-, \chi_{l'}^-\rangle = \delta_{ll'}$, and $\langle \chi_l^+, \chi_{l'}^-\rangle = 0$ verify that the representations $\mathcal{D}^{l,+}$ and $\mathcal{D}^{l,-}$ $(l = 0, 1, 2, \ldots)$ are each irreducible and are pairwise inequivalent.

16.5.2 Decomposition Theorem

A subspace $Z \subset V^{\otimes r}$ is said to be invariant under the action of the orthogonal group O(3) if it remains invariant under $\boldsymbol{Q}^{\otimes r}$ for each $\boldsymbol{Q} \in \mathrm{O}(3)$. If Z is an invariant subspace of $V^{\otimes r}$ under the action of the orthogonal group, then its complexification Z_c is an invariant subspace of $V_c^{\otimes r}$. Since every finite-dimensional continuous unitary representation of a compact group is completely reducible, each tensor representation of the orthogonal group $\boldsymbol{\Psi}^{(r)}|_{Z_c} : \boldsymbol{Q} \mapsto \boldsymbol{Q}^{\otimes r}|_{Z_c}$ can be decomposed as a direct sum of irreducible subrepresentations, each of which is equivalent to some $\mathcal{D}^{k,\pm}$ $(k := 1, 2, \ldots, r)$:[164]

$$Z_c = m_0^+\mathcal{D}^{0,+} + m_1^+\mathcal{D}^{1,+} + \cdots + m_r^+\mathcal{D}^{r,+} + m_0^-\mathcal{D}^{0,-} + m_1^-\mathcal{D}^{1,-} + \cdots + m_r^-\mathcal{D}^{r,-}, \tag{16.64}$$

where $m_k^\pm$ is the multiplicity of $\mathcal{D}^{k,\pm}$ in the decomposition. Let χ_{Z_c} be the character of the representation $\boldsymbol{\Psi}^{(r)}|_{Z_c}$, which decomposes into the direct sum given in (16.64). This decomposition dictates that we have

$$\chi_{Z_c} = m_0^+\chi_0^+ + m_1^+\chi_1^+ + \cdots + m_r^+\chi_r^+ + m_0^-\chi_0^- + m_1^-\chi_1^- + \cdots + m_r^-\chi_r^-. \tag{16.65}$$

By the orthonormality of the characters $\chi_l^\pm$, we obtain the following formula for the multiplicities $m_k^\pm$ $(k = 0, 1, \ldots, r)$ in the decomposition (16.64): for brevity, we shall write

$$m_k^\pm = \langle \chi_\rho, \chi_k^\pm\rangle = \int_{\mathrm{O}(3)} \chi_\rho(\boldsymbol{Q})\overline{\chi_k^\pm(\boldsymbol{Q})}d\mathrm{g}(\boldsymbol{Q}). \tag{16.66}$$

Hence, once the character χ_{Z_c} of a representation $\boldsymbol{\Psi}^{(r)}|_{Z_c} : \boldsymbol{Q} \mapsto \boldsymbol{Q}^{\otimes r}|_{Z_c}$ is obtained, the decomposition formula for the representation follows immediately.

[164] It suffices to consider $k \le r$; see Proposition 16.4.

In what follows we will sharpen the decomposition formula (16.64) for tensor representations and its counterpart for pseudotensor representations of the orthogonal group through the following lemma and theorem.

Lemma 16.11 *For $k \geq 1$, let Z be a $(2k+1)$-dimensional subspace of the tensor space $V^{\otimes r}$ invariant under $\boldsymbol{R}^{\otimes r}$ for each $\boldsymbol{R} \in \mathrm{SO}(3)$, and let Z_c be its complexification. Suppose the representation $\boldsymbol{R} \mapsto \boldsymbol{R}^{\otimes r}|_{Z_c}$ is equivalent to the irreducible unitary representation $\mathcal{D}^k$. Then Z_c is invariant under $\mathcal{T}_{\boldsymbol{Q}} : V_c^{\otimes r} \to V_c^{\otimes r}$ for each $\boldsymbol{Q} \in \mathrm{O}(3)$, where $\mathcal{T}_{\boldsymbol{Q}} = \boldsymbol{Q}^{\otimes r}$ for material tensors and $\mathcal{T}_{\boldsymbol{Q}} = (\det \boldsymbol{Q})\boldsymbol{Q}^{\otimes r}$ for material pseudotensors, respectively. For material tensors, the representation $\boldsymbol{Q} \mapsto \mathcal{T}_{\boldsymbol{Q}}|_{Z_c}$ is equivalent to $\mathcal{D}^{k,+}$ if r is even and to $\mathcal{D}^{k,-}$ if r is odd. For material pseudotensors, the representation $\boldsymbol{Q} \mapsto \mathcal{T}_{\boldsymbol{Q}}|_{Z_c}$ is equivalent to $\mathcal{D}^{k,+}$ if r is odd and to $\mathcal{D}^{k,-}$ if r is even.*

Proof Under both transformation laws (16.23) and (16.24), by Lemma 16.2 we have $\mathcal{T}_{\boldsymbol{\mathcal{I}}}\boldsymbol{H} = \pm\boldsymbol{H}$ for any $\boldsymbol{H} \in Z_c$, irrespective of whether $\boldsymbol{H}$ is a material tensor or pseudotensor. Since Z_c is invariant under $\boldsymbol{R}^{\otimes r}$, it is also invariant under $(\boldsymbol{\mathcal{I}}\boldsymbol{R})^{\otimes r} = \boldsymbol{\mathcal{I}}^{\otimes r}\boldsymbol{R}^{\otimes r}$ and $(\det(\boldsymbol{\mathcal{I}}\boldsymbol{R}))(\boldsymbol{\mathcal{I}}\boldsymbol{R})^{\otimes r} = -\boldsymbol{\mathcal{I}}^{\otimes r}\boldsymbol{R}^{\otimes r}$. It follows that Z_c is invariant under $\mathcal{T}_{\boldsymbol{Q}}$ for each $\boldsymbol{Q} \in \mathrm{O}(3)$ for both transformation laws (16.23) and (16.24).

Consider first the case of material tensors, which obey the transformation law $\mathcal{T}_{\boldsymbol{Q}} = \boldsymbol{Q}^{\otimes r}$. Let $\boldsymbol{\Psi}^{(r)}|_{Z_c} : \mathrm{O}(3) \to \mathrm{GL}(Z_c)$ be the representation $\boldsymbol{Q} \mapsto \boldsymbol{Q}^{\otimes r}|_{Z_c}$. By the hypothesis that the representation $\boldsymbol{R} \mapsto \boldsymbol{R}^{\otimes r}|_{Z_c}$ is equivalent to the irreducible unitary representation $\mathcal{D}^k$ of SO(3), there exists in Z_c an orthonormal basis $\boldsymbol{A}_j$ $(-k \leq j \leq k)$ under which $\boldsymbol{R}^{\otimes r}$ is represented by the $(2k+1) \times (2k+1)$ matrix $[D^k_{mn}]$. By Lemma 16.2, we obtain for each $\boldsymbol{R} \in \mathrm{SO}(3)$,

$$\boldsymbol{\mathcal{I}}^{\otimes r}(\boldsymbol{R}^{\otimes r}\boldsymbol{A}_j) = (-1)^r\boldsymbol{R}^{\otimes r}\boldsymbol{A}_j \qquad \text{for each } -k \leq j \leq k, \tag{16.67}$$

which implies that $(\boldsymbol{\mathcal{I}}\boldsymbol{R})^{\otimes r}$ is represented by the matrix $(-1)^r[D^k_{mn}]$. Thus we have

$$\chi_\rho(\boldsymbol{Q}) = \begin{cases} \chi_k(\boldsymbol{R}) & \text{for } \boldsymbol{Q} = \boldsymbol{R} \\ (-1)^r\chi_k(\boldsymbol{R}) & \text{for } \boldsymbol{Q} = \boldsymbol{\mathcal{I}}\boldsymbol{R} \end{cases} = \begin{cases} \chi_k^+(\boldsymbol{Q}) & \text{if } r \text{ is even} \\ \chi_k^-(\boldsymbol{Q}) & \text{if } r \text{ is odd.} \end{cases} \tag{16.68}$$

Thus we conclude that for material tensors the representation $\boldsymbol{Q} \mapsto \mathcal{T}_{\boldsymbol{Q}}|_{Z_c}$ is equivalent to $\mathcal{D}^{k,+}$ if r is even and to $\mathcal{D}^{k,-}$ if r is odd.

For pseudotensors, which observe the transformation law $\mathcal{T}_{\boldsymbol{Q}} = (\det \boldsymbol{Q})\boldsymbol{Q}^{\otimes r}$, instead of (16.67) we derive from Lemma 16.2 the formula that for each $\boldsymbol{R} \in \mathrm{SO}(3)$,

$$(\det(\boldsymbol{\mathcal{I}}\boldsymbol{R}))(\boldsymbol{\mathcal{I}}\boldsymbol{R})^{\otimes r}\boldsymbol{A}_j = (-1)^{r+1}\boldsymbol{R}^{\otimes r}\boldsymbol{A}_j \qquad \text{for each } -k \leq j \leq k, \tag{16.69}$$

from which it follows that the representation $\mathcal{T}_{\boldsymbol{Q}}|_{Z_c}$ is equivalent to $\mathcal{D}^{k,+}$ if r is odd and to $\mathcal{D}^{k,-}$ if r is even. □

The following theorem is an immediate consequence of (16.64), (16.65), and Lemma 16.11.

Theorem 16.12 ([95]) *Let $Z \subset V^{\otimes r}$ be a subspace invariant under the action of the orthogonal group* O(3)*, and let Z_c be its complexification. For material tensors (resp. pseudotensors), which obey transformation law* (16.23) (*resp.* (16.24))*, Z_c is decomposed into its irreducible parts under* O(3) *as*

$$Z_c = \begin{cases} m_0\mathcal{D}^{0,+} + m_1\mathcal{D}^{1,+} + \cdots + m_r\mathcal{D}^{r,+} & \text{if } r \text{ is even (resp. odd)} \\ m_0\mathcal{D}^{0,-} + m_1\mathcal{D}^{1,-} + \cdots + m_r\mathcal{D}^{r,-} & \text{if } r \text{ is odd (resp. even),} \end{cases} \tag{16.70}$$

where the multiplicities m_k $(k = 0, 1, \ldots, r)$ *are exactly those that appear in the decomposition*

$$Z_c = m_0\mathcal{D}^0 + m_1\mathcal{D}^1 + \cdots + m_r\mathcal{D}^r \tag{16.71}$$

under the rotation group SO(3); *here some of the* m_k*'s may be zero but* $\sum_{k=0}^{r} m_k(2k+1) = \dim Z_c$. *In the decomposition formula* (16.70), $m_r \leq 1$; *when* $Z_c = V_c^{\otimes r}$, $m_r = 1$.

Proof Since $\mathrm{SO}(3) \subset \mathrm{O}(3)$, Z_c is invariant under SO(3). Under SO(3), the decomposition of Z_c into its irreducible parts is of the form (16.71) (cf. Proposition 16.4), where the multiplicity m_k $(k = 0, 1, \ldots, r)$ is the number of times that the irreducible representation $\mathcal{D}^k$ appears in the representation $\boldsymbol{R} \mapsto \boldsymbol{R}^{\otimes r}|_{Z_c}$. By applying Lemma 16.11 to each irreducible invariant subspace of Z_c under SO(3), we obtain decomposition (16.70) of Z_c under O(3) for material tensors (resp. pseudotensors). The last assertion follows from Proposition 16.4. □

In summary, a subspace Z_c of $V^{\otimes r}$ is invariant under the action of SO(3) if and only if it is invariant under the action of O(3). By Theorem 16.12, once we have in hand the decomposition formula for the tensor representation of SO(3) with representation space Z_c (i.e., the representation $\boldsymbol{R} \mapsto \boldsymbol{R}^{\otimes r}|_{Z_c}$), we can immediately write down the parallel decomposition formulas for the tensor representation ($\boldsymbol{Q} \mapsto \boldsymbol{Q}^{\otimes r}|_{Z_c}$) and pseudotensor representation ($\boldsymbol{Q} \mapsto (\det \boldsymbol{Q})\,\boldsymbol{Q}^{\otimes r}\big|_{Z_c}$) of O(3) with the same representation space. For example, consider the space $Z_c = [[V_c^{\otimes 2}]^{\otimes 3}]$ of sixth-order tensors. The decomposition formula (16.51) for the representation $\boldsymbol{R} \mapsto \boldsymbol{R}^{\otimes 6}|_{Z_c}$ of SO(3) reads (cf. Example 16.8):

$$[[V_c^{\otimes 2}]^{\otimes 3}] = 3\mathcal{D}^0 + 3\mathcal{D}^2 + \mathcal{D}^3 + 2\mathcal{D}^4 + \mathcal{D}^6.$$

Then the decomposition formula for the tensor representation $\boldsymbol{Q} \mapsto \boldsymbol{Q}^{\otimes 6}|_{Z_c}$ of O(3) is:

$$[[V_c^{\otimes 2}]^{\otimes 3}] = 3\mathcal{D}^{0,+} + 3\mathcal{D}^{2,+} + \mathcal{D}^{3,+} + 2\mathcal{D}^{4,+} + \mathcal{D}^{6,+}. \tag{16.72}$$

The decomposition formula for the pseudotensor tensor representation $\boldsymbol{Q} \mapsto (\det \boldsymbol{Q})\,\boldsymbol{Q}^{\otimes 6}|_{Z_c}$ of O(3) is:

$$[[V_c^{\otimes 2}]^{\otimes 3}] = 3\mathcal{D}^{0,-} + 3\mathcal{D}^{2,-} + \mathcal{D}^{3,-} + 2\mathcal{D}^{4,-} + \mathcal{D}^{6,-}. \tag{16.73}$$

16.6 Point-Group Symmetry of Tensors and Pseudotensors

16.6.1 Proper Point Groups (Type I)

Consider a crystal C which belongs to the crystal class defined by some proper point group G_{cr}. Some physical property of C is characterized by an rth-order tensor $\boldsymbol{A}$ in some SO(3)-invariant (and thence also O(3)-invariant) subspace Z of $V^{\otimes r}$. (For example, the elastic response is defined by the fourth-order elasticity tensor in $[[V^{\otimes 2}]^{\otimes 2}]$.) How many independent material constants will be required to specify the material tensor $\boldsymbol{A}$? Here we will present a general group-theoretical method ([26]; see also [27, Chapter XIII]) to obtain (at least) an upper bound on the number of independent material constants required for the specification of $\boldsymbol{A}$.

A fundamental postulate in crystal physics is Neumann's principle,[165] which may be stated as follows [252, p. 20]:

[165] Given the history [173, 184] of this postulate, it should more properly be called the Neumann–Minnigerode–Curie principle; see [47], [297, p. 334].

The symmetry elements of any physical property of a crystal must include the symmetry elements of the point group of the crystal.

Given $\boldsymbol{A} \in Z$, let $G(\boldsymbol{A}) = \{\boldsymbol{Q} \in \mathrm{O}(3) : \boldsymbol{Q}^{\otimes r}\boldsymbol{A} = \boldsymbol{A}\}$ be the symmetry group of $\boldsymbol{A}$.[166] In our present context, Neumann's principle can be succinctly expressed as (cf. [47], [297, p. 334])

$$G_{\mathrm{cr}} \subset G(\boldsymbol{A}). \tag{16.74}$$

Let $\mathscr{M} = \{\boldsymbol{B} \in Z : \boldsymbol{Q}^{\otimes r}\boldsymbol{B} = \boldsymbol{B} \text{ for each } \boldsymbol{Q} \in G(\boldsymbol{A})\}$. Each $\boldsymbol{B} \in \mathscr{M}$ is said to be a fixed point of Z under the action of the group $G(\boldsymbol{A})$. Clearly the set of fixed points $\mathscr{M}$ is a subspace of Z, and $\boldsymbol{A} \in \mathscr{M}$. Let $N(\boldsymbol{A})$ be the number of independent material constants required to specify a material tensor $\boldsymbol{A} \in \mathscr{M}$. Clearly $N(\boldsymbol{A}) = \dim \mathscr{M}$. To determine $N(\boldsymbol{A})$, the group $G(\boldsymbol{A})$ must be ascertained first, which does not seem to be amenable to a general procedure that easily delivers solutions for various types of material tensors $\boldsymbol{A}$.

On the other hand, let $M = \{\boldsymbol{B} \in Z : \boldsymbol{Q}^{\otimes r}\boldsymbol{B} = \boldsymbol{B} \text{ for each } \boldsymbol{Q} \in G_{\mathrm{cr}}\}$. Then M is determined by the equation

$$\boldsymbol{Q}^{\otimes r}\boldsymbol{A} = \boldsymbol{A} \qquad \text{for each } \boldsymbol{Q} \in G_{\mathrm{cr}}, \tag{16.75}$$

where $\boldsymbol{A} \in Z$. There is, however, a group-theoretical method by which $\dim M$ can be determined easily for any G_{cr} and any material tensor $\boldsymbol{A}$. By Neumann's principle (16.74), $\mathscr{M}$ is a subspace of M, which implies[167]

$$\dim M \geq \dim \mathscr{M} = N(\boldsymbol{A}). \tag{16.76}$$

In the rest of this chapter we shall present the general group-theoretical method [26] mentioned earlier to determine $\dim M$ for various groups G_{cr} and material tensors $\boldsymbol{A}$. The same method will deliver $\dim \mathscr{M} = N(\boldsymbol{A})$ if we have ascertained $G(\boldsymbol{A})$ and use it in place of G_{cr}.

Since $\dim M = \dim M_c$, where $M_c = \{\boldsymbol{A} \in Z_c : \boldsymbol{Q}^{\otimes r}\boldsymbol{A} = \boldsymbol{A} \text{ for each } \boldsymbol{Q} \in G_{\mathrm{cr}}\}$, we can work with the complexified spaces M_c and Z_c and rephrase the problem at hand as that of determination of $\dim M_c$.

The general group-theoretical method in question is well illustrated by the following simple example.

Example 16.13 Let $G_{\mathrm{cr}} = D_3$, $Z_c = V_c^{\otimes 2}$, and $\boldsymbol{\Phi}^{(2)} : \mathrm{SO}(3) \to \mathrm{GL}(V_c^{\otimes 2})$. By (16.38), we have

$$\chi_{\boldsymbol{\Phi}^{(2)}}(\boldsymbol{R}(\boldsymbol{n}, \omega)) = (1 + 2\cos\omega)^2. \tag{16.77}$$

Let $\boldsymbol{T} : D_3 \to \mathrm{GL}(V^{\otimes 2})$ be the restriction of $\boldsymbol{\Phi}^{(2)}$ to D_3, i.e.,

$$\boldsymbol{T}(\boldsymbol{R}) = \boldsymbol{R} \otimes \boldsymbol{R} \qquad \text{for each } \boldsymbol{R} \in D_3. \tag{16.78}$$

The representation $\boldsymbol{T}$ is unitary because $\boldsymbol{\Phi}^{(2)}$ is unitary. Hence $\boldsymbol{T}$ is completely reducible. Let us decompose $\boldsymbol{T}$ into its irreducible parts under D_3, as doing so will lead to the answer

[166] Or, let $G(\boldsymbol{A}) = \{\boldsymbol{R} \in \mathrm{SO}(3) : \boldsymbol{R}^{\otimes r}\boldsymbol{A} = \boldsymbol{A}\}$ in contexts (e.g., in classical texture analysis) where attention is restricted to rotations.

[167] In the literature the tacit assumption that $N(\boldsymbol{A})$ can be inferred from (16.75) is often made. That this assumption is not generally valid can be seen from a counter-example. Let $\boldsymbol{A} \in [[V^{\otimes 2}]^{\otimes 2}]$ be the elasticity tensor of a tetragonal crystal $\subset$ with $G_{\mathrm{cr}} = C_4$. Equation (16.75) leads to the finding that $\dim M = 7$ (see, e.g., [252, p. 139]). On the other hand, it can be shown that $G(\boldsymbol{A}) = D_{4h}$ and $N(\boldsymbol{A}) = 6$; see [77, 118, 175].

Table 15 Characters of representation $\boldsymbol{T} : \boldsymbol{R} \mapsto \boldsymbol{R}^{\otimes 2}$ for $\boldsymbol{R} \in D_3$ and those of the irreducible representations of D_3

D_3	$[e]$	$2[r]$	$3[s]$
$\chi_{\boldsymbol{T}^1}$	1	1	1
$\chi_{\boldsymbol{T}^2}$	1	1	-1
$\chi_{\boldsymbol{T}^3}$	2	-1	0
$\chi_{\boldsymbol{T}}$	9	0	1

Table 16 Characters for computing the number of material constants required to specify a material tensor in $V_c^{\otimes r}$ that has D_3 symmetry

D_3	$[e]$	$2[r]$	$3[s]$
$\chi_{\boldsymbol{T}^1}$	1	1	1
$\chi_{\boldsymbol{\Phi}^{(r)}\vert D_3}$	3^r	0	$(-1)^r$

we seek. To this end, we compute the characters of $\boldsymbol{T}$. See Table 15, where we have, for convenience of computations below, also reproduced from Table 10 of Sect. 13.6.3 the characters of the complete set of irreducible unitary representations $\boldsymbol{T}^1$, $\boldsymbol{T}^2$ and $\boldsymbol{T}^3$ of D_3. Using (13.63), Theorem 13.27, and Table 15, we obtain

$$\begin{aligned}\boldsymbol{T} &= \langle \chi_{\boldsymbol{T}}, \chi_{\boldsymbol{T}^1} \rangle \boldsymbol{T}^1 + \langle \chi_{\boldsymbol{T}}, \chi_{\boldsymbol{T}^2} \rangle \boldsymbol{T}^2 + \langle \chi_{\boldsymbol{T}}, \chi_{\boldsymbol{T}^3} \rangle \boldsymbol{T}^3 \\ &= 2\boldsymbol{T}^1 + \boldsymbol{T}^2 + 3\boldsymbol{T}^3. \end{aligned} \tag{16.79}$$

For our purpose the crucial information carried by the decomposition (16.79) is as follows: As $\boldsymbol{T}^1$ is the one-dimensional identity representation, the first term $2\boldsymbol{T}^1$ means that there are two non-zero tensors $\boldsymbol{A}_i \in V_c^{\otimes 2}$ $(i = 1, 2)$ such that $\boldsymbol{R}^{\otimes 2}\boldsymbol{A}_i = \boldsymbol{A}_i$ for each $\boldsymbol{R} \in D_3$ and $\boldsymbol{A}_1 \perp \boldsymbol{A}_2$. Moreover, let W_1 and W_2 be the one-dimensional spaces spanned by $\boldsymbol{A}_1$ and $\boldsymbol{A}_2$, respectively. Then for each $\boldsymbol{A} \in (W_1 \oplus W_2)^{\perp}$, $\boldsymbol{R}^{\otimes 2}\boldsymbol{A} \neq \boldsymbol{A}$ for some $\boldsymbol{R} \in D_3$. Hence the dimension of the subspace $M_c = \{\boldsymbol{A} \in V_c^{\otimes 2} : \boldsymbol{R}^{\otimes 2}\boldsymbol{A} = \boldsymbol{A} \text{ for each } \boldsymbol{R} \in D_3\}$ is 2. □

It should now be clear that in the case where the material tensor $\boldsymbol{A}$ in question is of rth-order and $Z_c = V_c^{\otimes r}$, the number of independent material constants required to specify $\boldsymbol{A}$ with D_3 symmetry is given by $\langle \chi_{\boldsymbol{\Phi}^{(r)}\vert D_3}, \chi_{\boldsymbol{T}^1} \rangle$; recall that the symbol $\boldsymbol{\Phi}^{(r)}\vert D_3$ means the representation which is the restriction of $\boldsymbol{\Phi}^{(r)}$ to D_3. The values of $\chi_{\boldsymbol{\Phi}^{(r)}}(\boldsymbol{R})$ for $\boldsymbol{R} \in D_3$ can be determined by using (16.38), i.e.,

$$\chi_{\boldsymbol{\Phi}^{(r)}} = (1 + 2\cos\omega)^r.$$

They are listed with the character $\chi_{\boldsymbol{T}^1}$ in Table 16. Using this table, we obtain

$$\langle \chi_{\boldsymbol{\Phi}^{(r)}\vert D_3}, \chi_{\boldsymbol{T}^1} \rangle = \frac{1}{6}\left(3^r + 3(-1)^r\right) = \frac{1}{2}\left(3^{r-1} + (-1)^r\right),$$

which is precisely the number of independent parameters required to specify, for any finite r, a material tensor $\boldsymbol{A} \in V^{\otimes r}$ that has D_3 symmetry.

In practice, many material tensors are characterized by special classes of tensors which enjoy some intrinsic symmetries. For instance, dielectric tensors are second-order symmetric tensors, and elasticity tensors are fourth-order tensors which carry the major and minor symmetries. We will consider these two classes of tensors in the next example.

Table 17 Characters for computing the number of material constants required to specify a material tensor in $[V_c^{\otimes 2}]$ with D_3 symmetry

D_3	$[e]$	$2[r]$	$3[s]$
$\chi_{\boldsymbol{T}^1}$	1	1	1
$\chi_{[V_c^{\otimes 2}]}$	6	0	2

Table 18 Characters for computing the number of elastic constants required to specify an elasticity tensor with D_3 symmetry

D_3	$[e]$	$2[r]$	$3[s]$
$\chi_{\boldsymbol{T}^1}$	1	1	1
$\chi_{[[V_c^{\otimes 2}]^{\otimes 2}]}$	21	0	5

Example 16.14 Let $\boldsymbol{A} \in [V_c^{\otimes 2}]$. To use the method above to determine the number of material constants required to specify $\boldsymbol{A}$ with D_3 symmetry, we need information on the character of the representation $\boldsymbol{\Phi}^{\otimes 2}|D_3 : D_3 \to \mathrm{GL}([V_c^{\otimes 2}])$. In other words, we have to determine the values of $\chi_{[V_c^{\otimes 2}]}(\boldsymbol{R})$ for $\boldsymbol{R} \in D_3$. In formula (16.45), i.e.,

$$\chi_{[V_c^{\otimes 2}]} = \sum_{1 \le i \le j \le 3} \lambda_i \lambda_j = 2 + 2\cos\omega + 2\cos 2\omega,$$

we have already had the formula for any $\boldsymbol{R}$ in SO(3). In Table 17 we list the values of $\chi_{[V_c^{\otimes 2}]}(\boldsymbol{R})$ for $\boldsymbol{R} \in D_3$ together with the character $\chi_{\boldsymbol{T}^1}$. Using the table, we get

$$\langle \chi_{[V_c^{\otimes 2}]}, \chi_{\boldsymbol{T}^1} \rangle = \frac{1}{6}(6 + 3 \times 2) = 2.$$

Hence the number of material constants required to specify $\boldsymbol{A} \in [V_c^{\otimes 2}]$ is 2.

Elasticity tensors belong to the tensor space $[[V_c^{\otimes 2}] \otimes [V_c^{\otimes 2}]] = [[V_c^{\otimes 2}]^{\otimes 2}]$, i.e., the symmetric square of second-order symmetric tensors. In (16.48) we have already obtained a formula for $\chi_{[[V_c^{\otimes 2}]^{\otimes 2}]}$, i.e., the character of the representation $\boldsymbol{\Phi}^{(4)}|_{[[V_c^{\otimes 2}]^{\otimes 2}]}$:

$$\chi_{[[V_c^{\otimes 2}]^{\otimes 2}]} = 5 + 6\cos\omega + 6\cos 2\omega + 2\cos 3\omega + 2\cos 4\omega.$$

To answer the question of how many elastic constants are required to specify an elasticity tensor with D_3 symmetry, we determine the values of $\chi_{[[V_c^{\otimes 2}]^{\otimes 2}]}(\boldsymbol{R})$ for $\boldsymbol{R} \in D_3$, which are listed with $\chi_{\boldsymbol{T}^1}$ of D_3 in Table 18. Using this table, we get

$$\langle \chi_{[[V_c^{\otimes 2}]^{\otimes 2}]}, \chi_{\boldsymbol{T}^1} \rangle = \frac{1}{6}(21 + 3 \times 5) = 6.$$

Hence an elasticity tensor with D_3 symmetry has 6 undetermined elastic constants. □

In general, let G be a rotational point group, and let $Z \subset V^{\otimes r}$ be a subspace invariant under $\boldsymbol{R}^{\otimes r}$ for all rotations $\boldsymbol{R}$. Suppose that a physical property Π of a crystal is characterized by tensors $\boldsymbol{A} \in Z$, and that $\boldsymbol{A}$ is symmetric under rotations $\boldsymbol{R} \in G$ (i.e., $\boldsymbol{R}^{\otimes r}\boldsymbol{A} = \boldsymbol{A}$ for each $\boldsymbol{R} \in G$). To determine $N(A)$, the minimum number of material parameters to specify $\boldsymbol{A} \in Z$, the group in question should be $G = G(\boldsymbol{A})$. In the absence of information on $G(\boldsymbol{A})$, however, we take $G = G_{\mathrm{cr}}$, which is generally a subgroup of $G(\boldsymbol{A})$. Then the method described

Table 19 Characters for computing the number of elastic constants required to specify an elasticity tensor with D_2 symmetry

D_2	$[e]$	$[r]$	$[s]$	$[sr]$
$\chi_{\boldsymbol{T}^1}$	1	1	1	1
$\chi_{[[V_c^{\otimes 2}]^{\otimes 2}]}$	21	5	5	5

in this section can be used to determine[168] the number of independent material parameters required to specify $\boldsymbol{A}$ under symmetry group G if:

(1) We have ascertained the conjugacy classes of G.
(2) We know the values of the character $\chi_{Z_c}(\boldsymbol{R})$ of the subrepresentation $(\boldsymbol{\Phi}^{(r)}, Z_c)$ for $\boldsymbol{R} \in G$.

For example, because we know [118] that for elasticity tensors $\boldsymbol{A}$ of orthorhombic crystals $G(\boldsymbol{A}) = G_{\mathrm{cr}} = D_2$, and because we have already determined in (16.48) $\chi_{[[V_c^{\otimes 2}]^{\otimes 2}]}(\boldsymbol{R})$ for all rotations $\boldsymbol{R}$, we need only to find out the structure of the conjugacy classes of D_2 to determine the number of elastic constants for an orthorhombic elastic material. It is easy to see that D_2 has 4 conjugacy classes, each of which is a singleton, namely: $\{e\}$, $\{r\}$, $\{s\}$, and $\{rs\}$, where $e = \boldsymbol{I}$, $r = \boldsymbol{R}(\boldsymbol{e}_3, \pi)$, and $s = \boldsymbol{R}(\boldsymbol{e}_2, \pi)$. All the information needed for finding the number in question is given in Table 19, where $\chi_{\boldsymbol{T}^1}$ denotes the character of the one-dimensional identity representation. The answer is:

$$\langle \chi_{[[V_c^{\otimes 2}]^{\otimes 2}]}, \chi_{\boldsymbol{T}^1} \rangle = \frac{1}{4}(21 + 5 + 5 + 5) = 9.$$

We will work out one more example, to which we shall refer when we study tensorial texture coefficients in Chap. 17.

Example 16.15 Let $Z \subset V^{\otimes l}$ be a subspace of dimension $2l + 1$ such that $\boldsymbol{\Phi}^{(l)}|_{Z_c} \cong \mathcal{D}^l$. It turns out that there is a unique subspace of $V_c^{\otimes l}$, called the space $\mathscr{H}^l$ of harmonic tensors of order l (see Remark 17.12), which enjoys the specified property. In what follows, we shall refer to the elements of Z_c harmonic tensors, and we shall write $\boldsymbol{\tau}^{(l)} := \boldsymbol{\Phi}^{(l)}|_{\mathscr{H}^l}$. Let $M_c = \{\boldsymbol{A} \in Z_c : \boldsymbol{R}^{\otimes l}\boldsymbol{A} = \boldsymbol{A} \text{ for each } \boldsymbol{R} \in G\}$. Here we will determine $\dim M_c$ for the orthorhombic and the cubic symmetry, i.e., $G = D_2$ and $G = O$, respectively. Recall that the character of the irreducible unitary representation $\mathcal{D}^l$ is given by formula (16.34):

$$\chi_l(\boldsymbol{R}(\boldsymbol{n}, \omega)) = \begin{cases} \dfrac{\sin(l + \frac{1}{2})\omega}{\sin \frac{1}{2}\omega} & \text{for } \omega \neq 0 \\ 2l + 1 & \text{for } \omega = 0. \end{cases}$$

The point group D_2 has four conjugacy classes, namely $[e]$, $[r]$, $[s]$, and $[sr]$, each of which contains only one element, i.e., the identity e, $r = \boldsymbol{R}(\boldsymbol{e}_3, \pi)$, $s = \boldsymbol{R}(\boldsymbol{e}_2, \pi)$, and $sr = \boldsymbol{R}(\boldsymbol{e}_1, \pi)$. It is straightforward to compute from the displayed formula of χ_l the values of $\chi_{\boldsymbol{\tau}^{(l)}|_{D_2}}$ for the four conjugacy classes of D_2, which are given in Table 20. Hence we obtain

$$\dim M_c(l) = \frac{1}{4}\left((2l + 1) + 3(-1)^l\right) = \begin{cases} \frac{l}{2} + 1 & \text{if } l \text{ is even (i.e., } l = 0, 2, 4, \ldots) \\ \frac{l-1}{2} & \text{if } l \text{ is odd (i.e., } l = 1, 3, 5, \ldots). \end{cases} \tag{16.80}$$

[168] The mathematical procedure is the same while the physical meaning of the resulting number for $G = G(\boldsymbol{A})$ is different from that for $G = G_{\mathrm{cr}}$. If $G = G(\boldsymbol{A})$, the number delivered by the computations will be $N(\boldsymbol{A})$; if $G = G_{\mathrm{cr}}$, it will generally be an upper bound of $N(\boldsymbol{A})$.

Table 20 Characters for computation of $\dim M_c$ for l-th order harmonic tensors with orthorhombic (D_2) symmetry

D_2	$[e]$	$[r]$	$[s]$	$[sr]$
$\chi_{\boldsymbol{T}^1}$	1	1	1	1
$\chi_{\boldsymbol{\tau}^{(l)}\|D_2}$	$2l+1$	$(-1)^l$	$(-1)^l$	$(-1)^l$

Table 21 Characters for computation of $\dim M_c(l)$ for l-th order harmonic tensors with cubic (O) symmetry

O	$[e]$	$6\mathfrak{C}_2$	$8\mathfrak{C}_3$	$6\mathfrak{C}_4$	$3\mathfrak{C}_4^2$
$\chi_{\boldsymbol{T}^1}$	1	1	1	1	1
$\chi_{\boldsymbol{\tau}^l\|O}$	$2l+1$	$(-1)^l$	$\frac{\sin((2l+1)\pi/3)}{\sin(\pi/3)}$	$\sin(l\pi/2)+\cos(l\pi/2)$	$(-1)^l$

By the preceding formula, $\dim M_c$ clearly satisfies the recursion formula $\dim M_c(l+2) = \dim M_c(l) + 1$.

The point group O has five conjugacy classes, namely $[e]$, $\mathfrak{C}_2$, $\mathfrak{C}_3$, $\mathfrak{C}_4$, and $\mathfrak{C}_4^2$. The class $[e]$ has the identity as the only element. The class $\mathfrak{C}_2$ contains 6 rotations of angle π about six 2-fold axes, $\mathfrak{C}_3$ 8 rotations of angle $\pm 2\pi/3$ about four 3-fold axes, $\mathfrak{C}_4$ 6 rotations of angle $\pm\pi/2$ about three 4-fold axes, and $\mathfrak{C}_4^2$ 6 rotations of angle π about three 4-fold axes. The values of $\chi_{\boldsymbol{\tau}^{(l)}|O}$ for these five classes are displayed in Table 21. It follows that

$$\dim M_c(l) = \frac{1}{24}\left((2l+1) + 9(-1)^l + 8\cdot\frac{\sin((2l+1)\pi/3)}{\sin(\pi/3)} + 6\big(\sin(l\pi/2)+\cos(l\pi/2)\big)\right). \tag{16.81}$$

In Table 22 we display the values of $\dim M_c$ for $l = 0, 1, 2, \ldots, 15$. In fact it is easily shown that $\dim M_c(l+12) = \dim M_c(l) + 1$, which together with Table 22 delivers the value of $\dim M_c(l)$ for each $l \geq 0$. □

Remark 16.16 A comparison of Table 22 with Table 7 of Section 5.4.3 reveals that for a given l in the two tables the value of $\dim M_c$ is the same as the number of independent texture coefficients c_{mn}^l for a fixed m. This finding, however, is expected. Equation (5.20), which describes the restrictions on texture coefficients c_{mn}^l imposed by the group of crystallite symmetry G_{cr}, can be interpreted as follows: For a fixed l and m, let $[e_l] = (1, 0, \ldots, 0)^T$, $[e_{l-1}] = (0, 1, \ldots, 0)^T, \ldots, [e_{\bar{l}}] = (0, 0, \ldots, 1)^T$ be column vectors which form the standard orthonormal basis in $\mathbb{C}^{2l+1}$, and let $[x] = \sum_{p=-l}^{l} c_{mp}^l [e_p]$. Then (5.20) is none other than the equation $[x] = [D^l(\boldsymbol{R})][x]$ for each $\boldsymbol{R} \in G_{\mathrm{cr}}$; here $[D^l(\boldsymbol{R})]$ is the $(2l+1)\times(2l+1)$ matrix with the Wigner D-functions $D_{mn}^l(\boldsymbol{R})$ as matrix elements (cf. Sect. 4.2). Since $\boldsymbol{\tau}^{(l)} \cong \mathcal{D}^l$, we can choose an orthonormal basis in $\mathscr{H}^l$ such that $\boldsymbol{\tau}^{(l)}(\boldsymbol{R})$ is represented by the matrix $[D^l(\boldsymbol{R})]$ for each $\boldsymbol{R} \in G = G_{\mathrm{cr}}$. Under the chosen orthonormal basis, the equation $\boldsymbol{R}^{\otimes l}\boldsymbol{A} = \boldsymbol{A}$ for $\boldsymbol{R} \in G$ and $\boldsymbol{A} \in \mathscr{H}^l$ becomes $[D^l(\boldsymbol{R})][A] = [A]$ for $\boldsymbol{R} \in G$, where $[A]$ is the column vector in $\mathbb{C}^{2l+1}$ that represents $\boldsymbol{A}$ under the chosen orthonormal basis in $\mathscr{H}^l$. Hence $\dim M_c$ is equal to the number of independent texture coefficients in $\{c_{mn}^l : -l \leq n \leq l\}$ for a fixed l and m. □

16.6.2 Improper Point Groups (Type II)

Let G be a point group of Type II. Then $G = H \cup \mathcal{I}H$, where H is a proper subgroup of G; see Theorem 2.35 and Table 3 in Sects. 2.5.3 and 2.6.1, respectively. For $r \geq 1$, let Z_c be a subspace of $V_c^{\otimes r}$ invariant under the action of O(3). Let each $\boldsymbol{A} \in Z_c$ be a material

Table 22 Values of $\dim M_c(l)$ for various l for restrictions imposed by cubic (O) symmetry on harmonic tensors of order l

l	0	1	2	3	4	5	6	7	8	9	10	11	12	13	14	15
$\dim M_c(l)$	1	0	0	0	1	0	1	0	1	1	1	0	2	1	1	1

tensor (resp. pseudotensor) that characterizes the physical property Π of a crystal in the geometric class defined by point group G. Here our objective is to determine $\dim M_c$, where for $\mathcal{T}_{\boldsymbol{Q}} = \boldsymbol{Q}^{\otimes r}$ for material tensors (resp. $\mathcal{T}_{\boldsymbol{Q}} = (\det \boldsymbol{Q})\,\boldsymbol{Q}^{\otimes r}$ for material pseudotensors)

$$M_c = \{\boldsymbol{A} \in Z_c : \boldsymbol{A} = \mathcal{T}_{\boldsymbol{Q}}\boldsymbol{A} \text{ for each } \boldsymbol{Q} \in G\}.$$

Let $M_c^H = \{\boldsymbol{A} \in Z_c : \boldsymbol{R}^{\otimes r}\boldsymbol{A} = \boldsymbol{A} \text{ for each } \boldsymbol{R} \in H\}$. Since $H \subset G$, clearly we have

$$\dim M_c \le \dim M_c^H. \tag{16.82}$$

Let $\boldsymbol{A} \in M_c^H$. Then $\boldsymbol{R}^{\otimes r}\boldsymbol{A} = \boldsymbol{A}$ for each $\boldsymbol{R} \in H$. For $\boldsymbol{Q} \in G \setminus H$, we have $\boldsymbol{Q} = \boldsymbol{\mathcal{I}}\boldsymbol{R}$ for some $\boldsymbol{R} \in H$, and for material tensors

$$\mathcal{T}_{\boldsymbol{Q}}\boldsymbol{A} = \boldsymbol{Q}^{\otimes r}\boldsymbol{A} = (\boldsymbol{\mathcal{I}}\boldsymbol{R})^{\otimes r}\boldsymbol{A} = \boldsymbol{\mathcal{I}}^{\otimes r}\boldsymbol{R}^{\otimes r}\boldsymbol{A} = \boldsymbol{\mathcal{I}}^{\otimes r}\boldsymbol{A} = (-1)^r\boldsymbol{A}, \tag{16.83}$$

where we have appealed to Lemma 16.2 at the last step. For material pseudotensors, (16.83) is replaced by

$$\mathcal{T}_{\boldsymbol{Q}}\boldsymbol{A} = (\det \boldsymbol{Q})\,\boldsymbol{Q}^{\otimes r}\boldsymbol{A} = (-1)^{r+1}\boldsymbol{A}. \tag{16.84}$$

For material tensors (resp. pseudotensors), if r is even (resp. odd), then $\mathcal{T}_{\boldsymbol{Q}}\boldsymbol{A} = \boldsymbol{A}$ for each $\boldsymbol{Q} \in G$ and each $\boldsymbol{A} \in M_c^H$, which implies $M_c^H \subset M_c$ and $\dim M_c^H \le \dim M_c$. Combining the preceding inequality with (16.82), we conclude that $\dim M_c = \dim M_c^H$ for material tensors (resp. pseudotensors) if r is even (resp. odd),.

On the other hand for material tensors (resp. pseudotensors), if r is odd (resp. even) and $\mathcal{T}_{\boldsymbol{Q}}\boldsymbol{A} = \boldsymbol{A}$ for $\boldsymbol{Q} \in G \setminus H$ and $\boldsymbol{A} \in M_c^H$, by (16.83) (resp. (16.84)) we have $\boldsymbol{A} = \boldsymbol{0}$, i.e., $\dim M_c = 0$.

We summarize our findings in the following proposition.

Proposition 16.17 *Let $G = H \cup \boldsymbol{\mathcal{I}}H$, where H is proper, be a crystallographic point group of Type II. For $r \ge 1$, let Z_c be a subspace of $V_c^{\otimes r}$ invariant under the action of* O(3). *Suppose that the property Π of a material is characterized by an rth-order material tensor (resp. pseudotensor) $\boldsymbol{A} \in Z_c$. Let $M_c = \{\boldsymbol{A} \in Z_c : \mathcal{T}_{\boldsymbol{Q}}\boldsymbol{A} = \boldsymbol{A}$ for each $\boldsymbol{Q} \in G\}$, where $\mathcal{T}_{\boldsymbol{Q}} = \boldsymbol{Q}^{\otimes r}$ (resp. $\mathcal{T}_{\boldsymbol{Q}} = (\det \boldsymbol{Q})\,\boldsymbol{Q}^{\otimes r}$) for material tensors (resp. pseudotensors), and $M_c^H = \{\boldsymbol{A} \in Z_c : \boldsymbol{R}^{\otimes}\boldsymbol{A} = \boldsymbol{A}$ for each $\boldsymbol{R} \in H\}$. For material tensors (resp. pseudotensors) we have*

$$\dim M_c = \begin{cases} \dim M_c^H & \text{if } r \text{ is even (resp. odd)} \\ 0 & \text{if } r \text{ is odd (resp. even)} \end{cases}. \tag{16.85}$$

The number $\dim M_c^H$ can be determined by the method presented in Sect. 16.6.1.

Table 23 Characters for computation of dim M_c for lth-order harmonic tensors with C_{3v} symmetry

C_{3v}	$[e]$	$2[r]$	$3[\imath s]$
$\chi_{\boldsymbol{T}^1}$	1	1	1
$\chi(\cdot;\boldsymbol{\Psi}^{(l)}\vert_{\mathscr{H}^l})$, even l	$2l+1$	$\frac{\sin((2l+1)\pi/3)}{\sin(\pi/3)}$	$(-1)^l$
$\chi(\cdot;\boldsymbol{\Psi}^{(l)}\vert_{\mathscr{H}^l})$, odd l	$2l+1$	$\frac{\sin((2l+1)\pi/3)}{\sin(\pi/3)}$	$(-1)^{l+1}$

16.6.3 Improper Point Groups (Type III)

By Theorem 2.35 each point group G of Type III is isomorphic to the proper point group G^+ in the Laue class that contains G; e.g., the group C_{3v} is isomorphic to D_3 (see Tables 3 and 4 in Sect. 2.6). Then G and G^+ have the same abstract group structure. Those of their properties which depend only on abstract group structure are the same. If the same symbol is used to represent the two corresponding elements under the isomorphism, then they have the same multiplication table, the same conjugacy classes, and the same character table (cf. Remark 13.31). For example, if the symbol s in Table 1 of Sect. 2.1 and in (13.75) stands for $\mathcal{I}\boldsymbol{R}(\boldsymbol{e}_1,\pi)$ rather than $\boldsymbol{R}(\boldsymbol{e}_1,\pi)$, then Table 1 and (13.75) become the multiplication table and the list of conjugacy classes for C_{3v}. Under this interpretation, Table 10 of Sect. 13.6.3 becomes the character table of C_{3v}. On the other hand, D_3 and C_{3v} are different as transformation groups. In particular, $\dim M_c = \dim\{\boldsymbol{A}\in Z_c : \boldsymbol{Q}^{\otimes r}\boldsymbol{A}=\boldsymbol{A} \text{ for } \boldsymbol{Q}\in G\}$, where Z_c is some SO(3)- and O(3)-invariant subspace of $V_c^{\otimes r}$, need not be the same for $G=D_3$ and $G=C_{3v}$.

Example 16.18 As illustration, let us compute $\dim M_c$ for the tensor representations $\boldsymbol{\Psi}^{(l)}|C_{3v}$ on the spaces of lth-order harmonic tensors $\mathscr{H}^l$ $(l=0,1,2,\ldots)$ and compare them with the $\dim M_c$ of the representations $\boldsymbol{\tau}^{(l)}|D_3 : D_3\to \mathrm{GL}(\mathscr{H}^l)$. To this end, the first step is to write down the conjugacy classes of group C_{3v}. They are (cf. Remark 13.31):

$$[e]=\{e\},\qquad [r]=\{r,r^2\},\qquad [\imath s]=\{\imath s,\imath sr,\imath sr^2\},\tag{16.86}$$

where $e=\boldsymbol{I}$, $r=\boldsymbol{R}(\boldsymbol{e}_3,2\pi/3)$, $\imath=\mathcal{I}$, and $s=\boldsymbol{R}(\boldsymbol{e}_1,\pi)$. Next we need to determine the characters of the subrepresentations $\boldsymbol{\Psi}^{(l)}|_{\mathscr{H}^l}$ as restricted to the subgroup C_{3v} of O(3). By Lemma 16.11, we should distinguish two cases:

(i) l is even. We have $\boldsymbol{\Psi}^{(l)}|_{\mathscr{H}^l}\cong\mathcal{D}^{l,+}$, with character[169] $\chi(\cdot;\boldsymbol{\Psi}^{(l)}|_{\mathscr{H}^l})(\cdot)=\chi_l^+(\cdot)$, where $\chi_l^+(\boldsymbol{Q})=\chi_l(\boldsymbol{R})$ for $\boldsymbol{Q}=\boldsymbol{R}$ or $\boldsymbol{Q}=\mathcal{I}\boldsymbol{R}$.

(ii) l is odd. Then $\boldsymbol{\Psi}^{(l)}|_{\mathscr{H}^l}\cong\mathcal{D}^{l,-}$, with character $\chi(\cdot;\boldsymbol{\Psi}^{(l)}|_{\mathscr{H}^l})(\cdot)=\chi_l^-(\cdot)$, where $\chi_l^-(\boldsymbol{Q})=\chi_l(\boldsymbol{R})$ for $\boldsymbol{Q}=\boldsymbol{R}$ and $\chi_l^-(\boldsymbol{Q})=-\chi_l(\boldsymbol{R})$ for $\boldsymbol{Q}=\mathcal{I}\boldsymbol{R}$.

The information required for the computation of $\dim M_c$ for l-th order harmonic tensors with C_{3v} symmetry, where

$$M_c=\{\boldsymbol{A}\in\mathscr{H}^l : \boldsymbol{Q}^{\otimes l}\boldsymbol{A}=\boldsymbol{A} \text{ for } \boldsymbol{Q}\in C_{3v}\},$$

[169] To avoid the staggering of subscripts, here we use $\chi(\cdot;\boldsymbol{\Psi}^{(l)}|_{\mathscr{H}^l})$ to denote the character of the representation $\boldsymbol{\Psi}^{(l)}|_{\mathscr{H}^l}$.

Table 24 Values of $\dim M_c$ for various l for restrictions imposed by D_3 and C_{3v} symmetry on harmonic tensors of order l

	l	0	1	2	3	4	5	6	7	8	9	10	11
D_3	$\dim M_c$	1	0	1	1	2	1	3	2	3	3	4	3
C_{3v}	$\dim M_c$	1	1	1	2	2	2	3	3	3	4	4	4

Table 25 Characters for computing the number of elastic constants required to specify an elasticity tensor with C_{3v} symmetry

C_{3v}	$[e]$	$2[r]$	$3[\imath s]$
$\chi_{\boldsymbol{T}^1}$	1	1	1
$\chi(\cdot;\boldsymbol{\Theta}^{(2)}\vert_{[[V_c^{\otimes 2}]^{\otimes 2}]})$	21	0	−5

is given in Table 23. Hence we obtain for harmonic tensors that enjoy C_{3v} symmetry:

$$\dim M_c = \begin{cases} \frac{1}{6}\left((2l+1)+2\cdot\frac{\sin((2l+1)\pi/3)}{\sin(\pi/3)}+3(-1)^l\right) & \text{for even } l \\ \frac{1}{6}\left((2l+1)+2\cdot\frac{\sin((2l+1)\pi/3)}{\sin(\pi/3)}+3(-1)^{l+1}\right) & \text{for odd } l. \end{cases} \tag{16.87}$$

On the other hand, for harmonic tensors that observes D_3 symmetry, and for $M_c = \{\boldsymbol{A} \in \mathscr{H}^l : \boldsymbol{R}^{\otimes l}\boldsymbol{A} = \boldsymbol{A} \text{ for each } \boldsymbol{R} \in D_3\}$, we get for all l the formula in (16.87) for even l. The values of $\dim M_c$ for $l = 0, 1, \ldots, 11$ that pertain to harmonic tensors with D_3 and C_{3v} symmetry, respectively, are listed in Table 24. The values for D_3 symmetry satisfy the recursion relation $\dim M_c(l+6) = \dim M_c(l) + 2$, whereas those for C_{3v} symmetry observe the recursion relation $\dim M_c(l+3) = \dim M_c(l) + 1$. □

Before we end this section, we give one example on pseudotensors.

Example 16.19 Consider the pseudotensor representation $\boldsymbol{\Theta}^{(4)} : \mathrm{O}(3) \to \mathrm{GL}(V_c^{\otimes 4})$ and its restriction to the subgroup C_{3v} and to the subspace $[[V_c^{\otimes 2}]^{\otimes 2}]$, i.e., the representation $(\boldsymbol{\Theta}^{(4)}|C_{3v})|_{[[V_c^{\otimes 2}]^{\otimes 2}]}$. Let

$$M_c = \{\boldsymbol{A} \in [[V_c^{\otimes 2}]^{\otimes 2}] : (\det \boldsymbol{Q})\,\boldsymbol{Q}^{\otimes 4}\boldsymbol{A} = \boldsymbol{A} \text{ for each } \boldsymbol{A} \in C_{3v}\}.$$

By (16.48) and Theorem 16.12, we see that the representation $\boldsymbol{\Theta}^{(4)}|_{[[V_c^{\otimes 2}]^{\otimes 2}]}$ decomposes into its irreducible parts as follows:

$$\boldsymbol{\Theta}^{(4)}|_{[[V_c^{\otimes 2}]^{\otimes 2}]} = 2\mathcal{D}^{0,-} + 2\mathcal{D}^{2,-} + \mathcal{D}^{4,-}.$$

Since $\chi_l^-(\boldsymbol{Q}) = \chi_l(\boldsymbol{R})$ for $\boldsymbol{Q} = \boldsymbol{R}$ and $\chi_l^-(\boldsymbol{Q}) = -\chi_l(\boldsymbol{R})$ for $\boldsymbol{Q} = \mathcal{I}\boldsymbol{R}$, a glance at Table 18 allows us to write down immediately the entries in Table 25. It follows that

$$\dim M_c = \frac{1}{6}(21 - 3\times 5) = 1.$$

□

Chapter 17

17 Harmonic Tensors and Tensorial Texture Coefficients

The purpose of this chapter is to introduce the tensorial Fourier expansion of the ODF and the tensorial texture coefficients [1, 34, 132, 190, 355] in Sect. 17.6. As preparations we will go over some preliminaries on harmonic tensors in Sects. 17.1–17.3. In Sect. 17.4 we derive formulas for the harmonic decomposition of (totally) symmetric tensors. In Sect. 17.5 we show that in each space of harmonic tensors there is a special orthonormal basis, which, as we shall show in Sect. 17.6.2, plays a crucial role in expressing the classical ODF expansion as a tensorial Fourier series. Our main references for the preliminaries and Sect. 17.4 are: Backus [15] and Sternberg [304, pp. 185–188].

17.1 Symmetric Tensors and Homogeneous Polynomials

In what follows we shall write the Cartesian coordinates of the position vector $\boldsymbol{x}$ interchangeably as (x, y, z) or (x_1, x_2, x_3).

Definition 17.1 A complex-valued polynomial $f(x, y, z)$ on $\mathbb{R}^3$ is homogeneous of degree $r \geq 0$ if it is a linear combination of monomials $x^p y^q z^k$ with $p + q + k = r$ $(p, q, k \geq 0)$, i.e.,

$$f(x, y, z) = \sum_{p+q+k=r} c_{pqk} x^p y^q z^k, \qquad \text{where the coefficients } c_{pqk} \in \mathbb{C}. \tag{17.1}$$

□

Let $\mathcal{P}^r$ be the set of all homogeneous polynomials of degree r. It is a linear space over the complex numbers, with the monomials $x^p y^q z^k$ $(p + q + k = r)$ serving as a basis. The dimension of $\mathcal{P}^r$ is equal to the number of such monomials. By the same argument as that which we use to determine the dimension of the space $[V^{\otimes r}]$ of symmetric tensors (see Proposition 13.33), we obtain

$$\dim \mathcal{P}^r = C_r^{r+2} = \frac{(r+2)(r+1)}{2}, \tag{17.2}$$

which is equal to $\dim [V^{\otimes r}]$. In fact there is an even more intimate relationship between $\mathcal{P}^r$ and the complexification of $[V^{\otimes r}]$, which is the same as $[V_c^{\otimes r}]$.

Given a symmetric tensor $\boldsymbol{A}$ in $[V_c^{\otimes r}]$, we can write it as

$$\boldsymbol{A} = A_{i_1 i_2 \cdots i_r} \boldsymbol{e}_{i_1} \otimes \boldsymbol{e}_{i_2} \otimes \cdots \otimes \boldsymbol{e}_{i_r}, \qquad \text{where } A_{i_1 i_2 \cdots i_r} \in \mathbb{C}. \tag{17.3}$$

Then we have

$$\begin{aligned} \boldsymbol{A}(\boldsymbol{x}, \boldsymbol{x}, \ldots, \boldsymbol{x}) &= A_{i_1 i_2 \cdots i_r} (\boldsymbol{e}_{i_1} \cdot \boldsymbol{x})(\boldsymbol{e}_{i_2} \cdot \boldsymbol{x}) \cdots (\boldsymbol{e}_{i_r} \cdot \boldsymbol{x}) \\ &= A_{i_1 i_2 \cdots i_r} x_{i_1} x_{i_2} \cdots x_{i_r}, \end{aligned} \tag{17.4}$$

which is a homogeneous polynomial in $\mathcal{P}^r$. Moreover, the map $\mathscr{L}_r : [V_c^{\otimes r}] \to \mathcal{P}^r$, $\boldsymbol{A} \mapsto \boldsymbol{A}(\boldsymbol{x}, \boldsymbol{x}, \ldots, \boldsymbol{x})$ is linear and is injective, because it maps each basis tensor of $[V_c^{\otimes r}]$ in the

set

$$\left\{ \frac{1}{r!} \sum_{\sigma \in S_r} \boldsymbol{e}_{i_{\sigma(1)}} \otimes \cdots \otimes \boldsymbol{e}_{i_{\sigma(r)}} : 1 \le i_1 \le \cdots \le i_r \le n \right\}$$

to the corresponding monomial in $\mathcal{P}^r$. It is surjective, because $\dim[V_c^{\otimes r}] = \dim \mathcal{P}^r$. Hence $\mathscr{L}_r$ is a linear isomorphism. For brevity, henceforth we will write $p_{\boldsymbol{A}}(\boldsymbol{x}) := \mathscr{L}_r(\boldsymbol{A}) = \boldsymbol{A}(\boldsymbol{x}, \boldsymbol{x}, \ldots, \boldsymbol{x})$.

A rotation $\boldsymbol{R}$ on V induces the linear transformation $\boldsymbol{R}^{\otimes r}$ on $[V_c^{\otimes r}]$ and a linear transformation $\mathscr{T}_{\boldsymbol{R}}^{(r)}$ on $\mathcal{P}^r$ defined by

$$(\mathscr{T}_{\boldsymbol{R}}^{(r)} f)(\boldsymbol{x}) = f(\boldsymbol{R}^{-1}\boldsymbol{x}). \tag{17.5}$$

It is easy to verify that $\mathscr{L}_r \circ \boldsymbol{R}^{\otimes r} = \mathscr{T}_{\boldsymbol{R}}^{(r)} \circ \mathscr{L}_r$. Indeed we have

$$\begin{aligned} \mathscr{T}_{\boldsymbol{R}}^{(r)} \circ \mathscr{L}_r(\boldsymbol{A}) &= \mathscr{T}_{\boldsymbol{R}}^{(r)}\, p_{\boldsymbol{A}}(\boldsymbol{x}) = p_{\boldsymbol{A}}(\boldsymbol{R}^T\boldsymbol{x}) \\ &= \boldsymbol{A}(\boldsymbol{R}^T\boldsymbol{x}, \ldots, \boldsymbol{R}^T\boldsymbol{x}) = A_{i_1 i_2 \cdots i_r}(\boldsymbol{e}_{i_1} \cdot \boldsymbol{R}^T\boldsymbol{x}) \cdots (\boldsymbol{e}_{i_r} \cdot \boldsymbol{R}^T\boldsymbol{x}) \\ &= A_{i_1 i_2 \cdots i_r}(\boldsymbol{R}\boldsymbol{e}_{i_1} \cdot \boldsymbol{x}) \cdots (\boldsymbol{R}\boldsymbol{e}_{i_r} \cdot \boldsymbol{x}) = (\boldsymbol{R}^{\otimes r}\boldsymbol{A})(\boldsymbol{x}, \ldots, \boldsymbol{x}) \\ &= \mathscr{L}_r \circ \boldsymbol{R}^{\otimes r}(\boldsymbol{A}) \end{aligned} \tag{17.6}$$

for each $\boldsymbol{A}$ in $[V_c^{\otimes r}]$.

17.2 Homogeneous Harmonic Polynomials

17.2.1 Trace of a Symmetric Tensor

Let $r \ge 2$. For an r-th order tensor $\boldsymbol{A}$ in $V_c^{\otimes r}$, the $(r-1, r)$ trace of $\boldsymbol{A}$ is the $(r-2)$-th order tensor $\mathrm{tr}_{(r-1,r)}\boldsymbol{A}$ defined by the condition

$$(\mathrm{tr}_{(r-1,r)}\boldsymbol{A})(\boldsymbol{u}_1, \ldots, \boldsymbol{u}_{r-2}) = \boldsymbol{A}(\boldsymbol{u}_1, \ldots, \boldsymbol{u}_{r-2}, \boldsymbol{e}_j, \boldsymbol{e}_j) \quad \text{for any } \boldsymbol{u}_1, \ldots, \boldsymbol{u}_{r-2} \in V, \tag{17.7}$$

where the summation convention on repeated indices is in force. Let $\boldsymbol{A} = A_{i_1 \ldots i_r} \boldsymbol{e}_{i_1} \otimes \cdots \otimes \boldsymbol{e}_{i_r}$. Then for any $\boldsymbol{u}_1, \ldots, \boldsymbol{u}_{r-2} \in V$,

$$\begin{aligned} (\mathrm{tr}_{(r-1,r)}\boldsymbol{A})(\boldsymbol{u}_1, \ldots, \boldsymbol{u}_{r-2}) &= A_{i_1 \cdots i_r} \boldsymbol{e}_{i_1} \otimes \cdots \otimes \boldsymbol{e}_{i_r}(\boldsymbol{u}_1, \ldots, \boldsymbol{u}_{r-2}, \boldsymbol{e}_j, \boldsymbol{e}_j) \\ &= A_{i_1 \cdots i_r}(\boldsymbol{e}_{i_1} \cdot \boldsymbol{u}_1) \cdots (\boldsymbol{e}_{i_{r-2}} \cdot \boldsymbol{u}_{r-2})(\boldsymbol{e}_{i_{r-1}} \cdot \boldsymbol{e}_j)(\boldsymbol{e}_{i_r} \cdot \boldsymbol{e}_j) \\ &= A_{i_1 \cdots i_r}(\boldsymbol{e}_{i_1} \cdot \boldsymbol{u}_1) \cdots (\boldsymbol{e}_{i_{r-2}} \cdot \boldsymbol{u}_{r-2}) \delta_{i_{r-1} j} \delta_{i_r j} \\ &= A_{i_1 \cdots i_{r-2} jj}(\boldsymbol{e}_{i_1} \cdot \boldsymbol{u}_1) \cdots (\boldsymbol{e}_{i_{r-2}} \cdot \boldsymbol{u}_{r-2}). \end{aligned} \tag{17.8}$$

Hence we have

$$\mathrm{tr}_{(r-1,r)}\boldsymbol{A} = A_{i_1 \cdots i_{r-2} jj} \boldsymbol{e}_{i_1} \otimes \cdots \otimes \boldsymbol{e}_{i_{r-2}}. \tag{17.9}$$

For $1 \le p < q \le r$, the (p, q) trace of the r-th order tensor $\boldsymbol{A}$ is defined similarly. In particular for $1 < p < q < r$ we have

$$\mathrm{tr}_{(p,q)}\boldsymbol{A} = A_{i_1 \cdots i_{p-1} j i_{p+1} \cdots i_{q-1} j i_{q+1} \cdots i_r} \boldsymbol{e}_{i_1} \otimes \cdots \otimes \boldsymbol{e}_{i_{p-1}} \otimes \boldsymbol{e}_{i_{p+1}} \cdots \otimes \boldsymbol{e}_{i_{q-1}} \otimes \boldsymbol{e}_{i_{q+1}} \cdots \otimes \boldsymbol{e}_{i_r}. \tag{17.10}$$

When the r-th order tensor A is symmetric, all its (p,q) traces are the same, which we denote by $\mathrm{tr}\boldsymbol{A}$ without subscript. In particular, from (17.9) we observe that for an r-th order symmetric tensor $\boldsymbol{A} = A_{i_1 i_2 \cdots i_r} \boldsymbol{e}_{i_1} \otimes \boldsymbol{e}_{i_2} \otimes \cdots \otimes \boldsymbol{e}_{i_r}$, we may express $\mathscr{L}_{r-2}(\mathrm{tr}\boldsymbol{A}) \in \mathcal{P}^{r-2}$ as

$$\mathscr{L}_{r-2}(\mathrm{tr}\boldsymbol{A}) = (\mathrm{tr}\boldsymbol{A})(\boldsymbol{x}, \ldots, \boldsymbol{x}) = A_{i_1 i_2 \cdots i_{r-2} jj} x_{i_1} x_{i_2} \cdots x_{i_{r-2}}. \tag{17.11}$$

17.2.2 Laplace Equation and Homogeneous Harmonic Polynomials

The differential operator

$$\Delta := \frac{\partial^2}{\partial x^2} + \frac{\partial^2}{\partial y^2} + \frac{\partial^2}{\partial z^2} \tag{17.12}$$

and the differential equation

$$\Delta f = 0 \tag{17.13}$$

are called the Laplace operator and the Laplace equation, respectively. The function Δf is called the Laplacian of f.

Definition 17.2 A homogeneous polynomial f is said to be harmonic if it satisfies the Laplace equation $\Delta f = 0$. □

Homogeneous polynomials in $\mathcal{P}^0$ and $\mathcal{P}^1$ clearly satisfy the Laplace equation and are harmonic. We shall derive a formula for $\Delta p_{\boldsymbol{A}}$ for the homogeneous polynomial $p_{\boldsymbol{A}} = \mathscr{L}_r(\boldsymbol{A})$ that corresponds to a symmetric r-th order tensor $\boldsymbol{A}$. The logic behind the computations for the general formula is laid bare in the special case of $r = 3$.

Example 17.3 Let $\boldsymbol{A} = A_{ijk} \boldsymbol{e}_i \otimes \boldsymbol{e}_j \otimes \boldsymbol{e}_k \in [V_c^{\otimes 3}]$. Then $p_{\boldsymbol{A}} = A_{ijk} x_i x_j x_k$. We have

$$\begin{aligned} \frac{\partial p_{\boldsymbol{A}}}{\partial x_m} &= A_{ijk}\delta_{mi} x_j x_k + A_{ijk} x_i \delta_{mj} x_k + A_{ijk} x_i x_j \delta_{mk} \\ &= A_{mjk} x_j x_k + A_{imk} x_i x_k + A_{ijm} x_i x_j \\ &= 3 A_{ijm} x_i x_j, \end{aligned} \tag{17.14}$$

where at the last step we have renamed dummy indices and appealed to the fact that $\boldsymbol{A}$ is (totally) symmetric. Thus the Laplacian of $p_{\boldsymbol{A}}$ is given by the formula

$$\begin{aligned} \Delta p_{\boldsymbol{A}} = \frac{\partial}{\partial x_m}\left(\frac{\partial p_{\boldsymbol{A}}}{\partial x_m}\right) &= \frac{\partial}{\partial x_m}\left(3 A_{ijm} x_i x_j\right) \\ &= 3\left(A_{ijm}\delta_{mi} x_j + A_{ijm} x_i \delta_{mj}\right) \\ &= 6 A_{imm} x_i = 6\mathscr{L}_1(\mathrm{tr}\boldsymbol{A}). \end{aligned} \tag{17.15}$$

□

Proposition 17.4 *For $r \geq 2$, let $\boldsymbol{A} = A_{i_1 i_2 \cdots i_r} \boldsymbol{e}_{i_1} \otimes \boldsymbol{e}_{i_2} \otimes \cdots \otimes \boldsymbol{e}_{i_r} \in [V_c^{\otimes r}]$ and $p_{\boldsymbol{A}} = \mathscr{L}_r(\boldsymbol{A}) \in \mathcal{P}^r$. There holds the formula*

$$\Delta p_{\boldsymbol{A}} = r(r-1)\mathscr{L}_{r-2}(\mathrm{tr}\boldsymbol{A}). \tag{17.16}$$

Proof The following derivation of the formula is entirely analogous to that of the special case for $r = 3$. By the definition of $p_{\boldsymbol{A}}$, we have

$$\begin{aligned}\frac{\partial p_{\boldsymbol{A}}}{\partial x_m} &= \frac{\partial}{\partial x_m}\left(A_{i_1 i_2 \cdots i_r} x_{i_1} x_{i_2} \cdots x_{i_r}\right)\\ &= A_{i_1 i_2 \cdots i_r}\delta_{m i_1} x_{i_2} \cdots x_{i_r} + A_{i_1 i_2 \cdots i_r} x_{i_1}\delta_{m i_2} \cdots x_{i_r} + \cdots + A_{i_1 i_2 \cdots i_r} x_{i_1} x_{i_2} \cdots \delta_{m i_r}\\ &= A_{m i_2 \cdots i_r} x_{i_2} \cdots x_{i_r} + A_{i_1 m \cdots i_r} x_{i_1} x_{i_3} \cdots x_{i_r} + \cdots + A_{i_1 i_2 \cdots i_{r-1} m} x_{i_1} x_{i_2} \cdots x_{i_{r-1}}\\ &= r\, A_{i_1 i_2 \cdots i_{r-1} m} x_{i_1} x_{i_2} \cdots x_{i_{r-1}}, \end{aligned} \tag{17.17}$$

where at the last step we have renamed dummy indices and appealed to the fact that $\boldsymbol{A}$ is (totally) symmetric. Thus the Laplacian of $p_{\boldsymbol{A}}$ is given by the formula

$$\begin{aligned}\Delta p_{\boldsymbol{A}} = \frac{\partial}{\partial x_m}\left(\frac{\partial p_{\boldsymbol{A}}}{\partial x_m}\right) &= \frac{\partial}{\partial x_m}\left(r\, A_{i_1 i_2 \cdots i_{r-1} m} x_{i_1} x_{i_2} \cdots x_{i_{r-1}}\right)\\ &= r\left(A_{i_1 i_2 \cdots i_{r-1} m}\delta_{m i_1} x_{i_2} \cdots x_{i_{r-1}} + A_{i_1 i_2 \cdots i_{r-1} m} x_{i_1}\delta_{m i_2} \cdots x_{i_{r-1}}\right.\\ &\qquad \left. + \cdots + A_{i_1 i_2 \cdots i_{r-1} m} x_{i_1} x_{i_2} \cdots \delta_{m i_{r-1}}\right)\\ &= r\left(A_{m i_2 \cdots i_{r-1} m} x_{i_2} \cdots x_{i_{r-1}} + A_{i_1 m \cdots i_{r-1} m} x_{i_1} x_{i_3} \cdots x_{i_{r-1}}\right.\\ &\qquad \left. + \cdots + A_{i_1 i_2 \cdots i_{r-2} m m} x_{i_1} x_{i_2} \cdots x_{r-2}\right)\\ &= r(r-1) A_{i_1 i_2 \cdots i_{r-2} m m} x_{i_1} x_{i_2} \cdots x_{r-2}, \end{aligned} \tag{17.18}$$

where we have again used the total symmetry of $\boldsymbol{A}$ and renamed some dummy indices. A comparison of (17.9) with the right-hand side at the end of the preceding equation delivers the required formula. □

From formula (17.16) we can immediately write down the following corollary.

Corollary 17.5 *Let $\boldsymbol{A}$ be a symmetric tensor of order $r \geq 2$. A homogeneous polynomial $p_{\boldsymbol{A}}$ is harmonic if and only if the symmetric tensor $\boldsymbol{A}$ is traceless, i.e.*, $\mathrm{tr}\boldsymbol{A} = \boldsymbol{0}$.[170] □

17.3 Spaces of Harmonic Tensors

Definition 17.6 An r-th order tensor (with $r \geq 2$) is said to be harmonic if it is symmetric and traceless. □

For $r \geq 0$, let $\mathcal{H}^r := \{f \in \mathcal{P}^r : \Delta f = 0\}$ be the set of homogeneous harmonic polynomials of degree r. It clearly constitutes a linear subspace of $\mathcal{P}^r$. In particular, $\mathcal{H}^0 = \mathcal{P}^0 = \mathbb{C}$; $\mathcal{H}^1 = \mathcal{P}^1 = \sum_i c_i x_i$. For $r \geq 2$, the inverse image $\mathscr{L}_r^{-1}(\mathcal{H}^r) := \mathscr{H}^r \subset [V_c^{\otimes r}]$ of $\mathcal{H}^r$ under the linear isomorphism $\mathscr{L}_r : [V_c^{\otimes r}] \to \mathcal{P}^r$ is the space of harmonic tensors. The restriction of $\mathscr{L}_r$ on $\mathscr{H}^r$, which for simplicity we still denote by $\mathscr{L}_r$, is a linear isomorphism from $\mathscr{H}^r$ onto $\mathcal{H}^r$. In particular, they have the same dimension, which is given in the next proposition.

Proposition 17.7 *For $r \geq 2$, $\dim \mathscr{H}^r = \dim \mathcal{H}^r = 2r + 1$.*

[170] Backus [15] calls such a symmetric tensor $\boldsymbol{A}$ "totally traceless".

Proof A glance at (17.18) reveals that the linear map $\Delta : \mathcal{P}^r \to \mathcal{P}^{r-2}$, $f \mapsto \Delta f$, is surjective. Since

$$\dim(\mathrm{Ker}\Delta) + \dim(\mathrm{Im}\Delta) = \dim \mathcal{P}^r, \tag{17.19}$$

we have

$$\dim \mathcal{H}^r = \dim \mathcal{P}^r - \dim \mathcal{P}^{r-2} = \frac{(r+2)(r+1)}{2} - \frac{r(r-1)}{2} = 2r+1. \tag{17.20}$$

□

For each rotation $\boldsymbol{R}$ and $r \geq 2$, the space of harmonic tensors $\mathscr{H}^r = \{\boldsymbol{A} \in [V_c^{\otimes r}] : \mathrm{tr}\,\boldsymbol{A} = \boldsymbol{0}\}$ is clearly invariant under $\boldsymbol{R}^{\otimes r}$. By (17.6) we see that $\mathcal{H}^r$ is invariant under $\mathscr{T}^{(r)}_{\boldsymbol{R}}$, a fact which can alternatively be demonstrated through the invariance of the Laplace equation under rotations. At any rate we can legitimately ask whether the representation $\boldsymbol{R} \mapsto \boldsymbol{R}^{\otimes r}$ of SO(3) on $\mathscr{H}^r$ is irreducible. We will give an affirmative answer by examining the representation $\boldsymbol{R} \mapsto \mathscr{T}^{(r)}_{\boldsymbol{R}}$ of SO(3) on $\mathcal{H}^r$.

Theorem 17.8 *The representation* $\boldsymbol{\sigma}^{(r)} : \mathrm{SO}(3) \to \mathrm{GL}(\mathcal{H}^r)$, $\boldsymbol{R} \mapsto \mathscr{T}^{(r)}_{\boldsymbol{R}}$, *is irreducible.*

Proof Since $\dim \mathcal{H}^r = 2r+1$, by Proposition 14.11 and Theorem 14.13 it suffices to show that $\exp(i2r\theta)$ is an eigenvalue of $\boldsymbol{\sigma}^{(r)} \circ \mathrm{Ad}(h(\theta))$, where $h(\theta) \in \mathrm{SU}(2)$ is defined in (14.10). Note that

$$\mathrm{Ad}(h(\theta)) = \begin{pmatrix} \cos 2\theta & -\sin 2\theta & 0 \\ \sin 2\theta & \cos 2\theta & 0 \\ 0 & 0 & 1 \end{pmatrix} = \boldsymbol{R}(\boldsymbol{e}_3, 2\theta). \tag{17.21}$$

Let $f(\boldsymbol{x}) = f(x,y,z) = (x-iy)^r$. Clearly f is a homogeneous polynomial of degree r, and it is easy to check by direct computations that $\triangle f = 0$. Hence we have $f \in \mathcal{H}^r$. Since

$$\boldsymbol{R}(\boldsymbol{e}_3, 2\theta)^{-1}\boldsymbol{x} = (x\cos 2\theta + y\sin 2\theta, -x\sin 2\theta + y\cos 2\theta, z), \tag{17.22}$$

the homogeneous polynomial $f \in \mathcal{H}^r$ transforms under the rotation $\boldsymbol{Q} := \boldsymbol{R}(\boldsymbol{e}_3, 2\theta)$ as

$$\begin{aligned} \mathscr{T}^{(r)}_{\boldsymbol{Q}} f(\boldsymbol{x}) &= f(\boldsymbol{R}(\boldsymbol{e}_3, 2\theta)^{-1}\boldsymbol{x}) \\ &= (x\cos 2\theta + y\sin 2\theta - i(-x\sin 2\theta + y\cos 2\theta))^r \\ &= (x(\cos 2\theta + i\sin 2\theta) - iy(\cos 2\theta + i\sin 2\theta))^r \\ &= \exp(i2r\theta) f(\boldsymbol{x}). \end{aligned} \tag{17.23}$$

Hence $f(\boldsymbol{x}) = (x - iy)^r \in \mathcal{H}^r$ is an eigenvector of $\boldsymbol{\sigma}^{(r)} \circ \mathrm{Ad}(h(\theta))$ with eigenvalue $\exp(i2r\theta)$. □

Corollary 17.9 *The representations* $\boldsymbol{\tau}^{(r)} : \mathrm{SO}(3) \to \mathrm{GL}(\mathscr{H}^r)$, $\boldsymbol{R} \mapsto \boldsymbol{R}^{\otimes r}$, *is irreducible and is equivalent to the representation* $\mathcal{D}^r$.

Proof By (17.6) the representations $\boldsymbol{\tau}^{(r)}$ and $\boldsymbol{\sigma}^{(r)}$ are equivalent. Hence $\boldsymbol{\tau}^{(r)}$ is an irreducible representation of SO(3). By Proposition 17.7 both $\boldsymbol{\tau}^{(r)}$ and $\boldsymbol{\sigma}^{(r)}$ are equivalent to the irreducible representation $\mathcal{D}^r$. □

17.4 Harmonic Decomposition of Symmetric Tensors

Let $r \geq 2$ and $\rho^2 = x^2 + y^2 + z^2$. The mapping

$$\vartheta : \mathcal{P}^{r-2} \to \mathcal{P}^r, \quad p_{\boldsymbol{A}} \mapsto \rho^2 p_{\boldsymbol{A}}, \qquad \text{for } \boldsymbol{A} \in [V_c^{\otimes r-2}]$$

is clearly linear and injective. Moreover, $\dim(\mathrm{Im}\,\vartheta) = \dim \mathcal{P}^{r-2} = r(r-1)/2$. When $[V_c^{\otimes r}]$ (i.e., the space of r-th order symmetric-tensors) is decomposed into its irreducible parts under SO(3):

$$[V_c^{\otimes r}] = n_0\mathcal{D}^0 + n_1\mathcal{D}^1 + \cdots + n_{r-1}\mathcal{D}^{r-1} + n_r\mathcal{D}^r, \tag{17.24}$$

where $n_k \geq 0$ $(k = 0, 1, \ldots r)$ and $\sum_{k=0}^{r} n_k(2k+1) = (r+2)(r+1)/2$, we know that $n_r = 1$. Indeed, since $[V_c^{\otimes r}]$ is a subspace of $V_c^{\otimes r}$, there holds $n_r \leq 1$. On the other hand, the harmonic tensors $\mathscr{H}^r$ constitute an invariant subspace of $[V_c^{\otimes r}]$ and the representation $\boldsymbol{\tau}^{(r)}$ of SO(3) on $\mathscr{H}^r$ is equivalent to $\mathcal{D}^r$. Therefore the only possibility is $n_r = 1$.

If we write the decomposition of $[V_c^{\otimes r}]$ as

$$[V_c^{\otimes r}] = \mathscr{H}^r \oplus (\mathscr{H}^r)^{\perp}, \tag{17.25}$$

then $(\mathscr{H}^r)^{\perp}$ contains invariant subspaces, on each of which the subrepresentation of $\boldsymbol{\tau}^{(r)}$ is equivalent to some $\mathcal{D}^k$ with $k < r$. We can choose an inner product in $\mathcal{P}^r$ such that the decomposition of $\mathcal{P}^r$ parallel to (17.25) takes the form

$$\mathcal{P}^r = \mathcal{H}^r \oplus (\mathcal{H}^r)^{\perp}. \tag{17.26}$$

It follows from the definition of the mapping ϑ that

$$\mathrm{Im}\,\vartheta = \{\rho^2 p_{\boldsymbol{A}} : \boldsymbol{A} \in [V_c^{\otimes r-2}]\} := \rho^2\mathcal{P}^{r-2}. \tag{17.27}$$

Since $\mathscr{L}_r^{-1}(\rho^2\mathcal{P}^{r-2}) = [\{\boldsymbol{I}\} \otimes [V_c^{\otimes r-2}]]$, which cannot contain $\mathscr{H}^r$ as an invariant subspace, because the irreducible representations pertaining to $[\{\boldsymbol{I}\} \otimes [V_c^{\otimes r-2}]]$ can be equivalent only to $\mathcal{D}^k$ with $k \leq r-2$. Thus we infer that $\rho^2\mathcal{P}^{r-2} \subset (\mathcal{H}^r)^{\perp}$. But $\dim(\rho^2\mathcal{P}^{r-2}) = r(r-1)/2 = \dim(\mathcal{H}^r)^{\perp}$. Hence we conclude that $(\mathcal{H}^r)^{\perp} = \rho^2\mathcal{P}^{r-2}$. Hence we obtain a decomposition of $\mathcal{P}^r$ into the following direct sum:

$$\mathcal{P}^r = \mathcal{H}^r \oplus \rho^2\mathcal{P}^{r-2}. \tag{17.28}$$

Repeating the same decomposition for $\mathcal{P}^{r-2}$, we have

$$\mathcal{P}^r = \mathcal{H}^r \oplus \rho^2(\mathcal{H}^{r-2} \oplus \rho^2\mathcal{P}^{r-4}) = \mathcal{H}^r \oplus \rho^2\mathcal{H}^{r-2} \oplus \rho^4\mathcal{P}^{r-4}. \tag{17.29}$$

Repeating the decomposition procedure iteratively until it stops, we arrive at the theorem on harmonic decomposition of homogeneous polynomials.

Theorem 17.10 *The space $\mathcal{P}^r$ $(r \geq 0)$ of homogeneous polynomials can be written as a direct sum of subspaces in terms of harmonic polynomials as follows*:

– *for* $r = 2p$, $\mathcal{P}^{2p} = \mathcal{H}^{2p} \oplus \rho^2\mathcal{H}^{2p-2} \oplus \cdots \oplus \rho^{2p-2}\mathcal{H}^2 \oplus \rho^{2p}\mathcal{H}^0$;
– *for* $r = 2p+1$, $\mathcal{P}^{2p+1} = \mathcal{H}^{2p+1} \oplus \rho^2\mathcal{H}^{2p-1} \oplus \cdots \oplus \rho^{2p-2}\mathcal{H}^3 \oplus \rho^{2p}\mathcal{H}^1$. □

Rewriting the preceding theorem for symmetric and harmonic tensors, we obtain the following corollary[171] on harmonic decomposition of symmetric tensors. In what follows, $\mathscr{H}^0 := \mathbb{C}$, and $\mathscr{H}^1 := V_c$.

Corollary 17.11 *The space* $[V_c^{\otimes r}]$ $(r \geq 0)$ *of (totally) symmetric tensors can be written as a direct sum of subspaces in terms of harmonic tensors as follows*:

- *for* $r = 2p$, $[V_c^{\otimes 2p}] = \mathscr{H}^{2p} \oplus [\boldsymbol{I} \otimes \mathscr{H}^{2p-2}] \oplus \cdots \oplus [\boldsymbol{I}^{\otimes p-1} \otimes \mathscr{H}^2] \oplus [\boldsymbol{I}^{\otimes p}]$;
- *for* $r = 2p+1$, $[V_c^{\otimes 2p+1}] = \mathscr{H}^{2p+1} \oplus [\boldsymbol{I} \otimes \mathscr{H}^{2p-1}] \oplus \cdots \oplus [\boldsymbol{I}^{\otimes p-1} \otimes \mathscr{H}^3] \oplus [\boldsymbol{I}^{\otimes p} \otimes \mathscr{H}^1]$. □

It follows from Corollary 17.11 that $[V_c^{\otimes r}]$ decompose into its irreducible parts as follows:

$$[V_c^{\otimes 2p}] = \mathcal{D}^0 + \mathcal{D}^2 + \cdots + \mathcal{D}^{2p-2} + \mathcal{D}^{2p}, \quad \text{for } r = 2p; \tag{17.30}$$

$$[V_c^{\otimes 2p+1}] = \mathcal{D}^1 + \mathcal{D}^3 + \cdots + \mathcal{D}^{2p-1} + \mathcal{D}^{2p+1}, \quad \text{for } r = 2p+1. \tag{17.31}$$

Remark 17.12 By Proposition 16.4, when the tensor representation $\boldsymbol{\Phi}^{(l)} : \mathrm{SO}(3) \to \mathrm{GL}(V^{\otimes l})$ is decomposed into its irreducible parts, there is a unique subrepresentation of dimension $2l+1$, say $\boldsymbol{\Phi}^{(l)}|_W$, such that $\boldsymbol{\Phi}^{(l)}|_W \cong \mathcal{D}^l$. Since $[V_c^{\otimes l}]$ is a subspace of $V_c^{\otimes l}$ and $\boldsymbol{\Phi}^{(l)}|_{[V_c^{\otimes l}]}$ contains also one irreducible subrepresentation of dimension $2l+1$, namely $\boldsymbol{\Phi}^{(l)}|_{\mathscr{H}^l}$, such that $\boldsymbol{\Phi}^{(l)}|_{\mathscr{H}^l} \cong \mathcal{D}^l$, the equality $W = \mathscr{H}^l$ necessarily holds. Hence the space $\mathscr{H}^l$ of harmonic tensors of order l may be defined as the subspace of $V_c^{\otimes l}$ such that $\boldsymbol{\Phi}^{(l)}|_{\mathscr{H}^l} \cong \mathcal{D}^l$. □

Remark 17.13 Any tensor in $V_c^{\otimes r}$ can be expressed [302] in terms of symmetric tensors of orders not higher than r, the second-order identity tensor $\boldsymbol{I}$, and the third-order alternating tensor $\boldsymbol{\varepsilon} = \varepsilon_{ijk}\boldsymbol{e}_i \otimes \boldsymbol{e}_j \otimes \boldsymbol{e}_k$, where

$$\varepsilon_{ijk} = \begin{cases} 1 & \text{if } (i,j,k) \text{ is a cyclic permutation of } (1,2,3) \\ -1 & \text{if } (i,j,k) \text{ is a non-cyclic permutation of } (1,2,3) \\ 0 & \text{if } i,j,k \text{ are not distinct.} \end{cases} \tag{17.32}$$

Combining this assertion with Corollary 17.11, we see that any tensor $\boldsymbol{A}$ in $V^{\otimes r}$ can be expressed in terms of harmonic tensors of orders not higher than r, the second-order identity tensor $\boldsymbol{I}$, and the third-order alternating tensor $\boldsymbol{\varepsilon}$. Such an expression is called a harmonic decomposition of tensor $\boldsymbol{A}$. While the harmonic decomposition of a symmetric tensor by Corollary 17.11 is unique, expressing a tensor in terms of symmetric tensors and isotropic tensors $\boldsymbol{I}$, $\boldsymbol{\varepsilon}$ is generally not. Moreover, harmonic decomposition of a tensor which is not totally symmetric need not go through Corollary 17.11 as an immediate step; this fact is well illustrated by the example of harmonic decompositions of the elasticity tensor [16, 76, 233]. As far as decomposing a tensor into its irreducible parts for some specific application is concerned, some harmonic decomposition may be more convenient than another; cf. [233]. □

[171] Cf. [356] for an alternate derivation.

17.5 Irreducible Tensor Basis in Space of Harmonic Tensors

Consider the space $\mathscr{H}^l$ $(l = 1, 2, 3, \ldots)$. Since the representation $\boldsymbol{\tau}^{(l)} : \mathrm{SO}(3) \to \mathrm{GL}(\mathscr{H}^l)$, $\boldsymbol{R} \mapsto \boldsymbol{R}^{\otimes l}$, is equivalent to $\mathcal{D}^l : \boldsymbol{R} \mapsto [D^l_{mn}(\boldsymbol{R})]$, by Corollary 13.14 there is an orthonormal basis $\boldsymbol{A}^l_m$ $(-l \le m \le l)$ such that $\boldsymbol{R}^{\otimes l}\boldsymbol{A}^l_m = \sum_p D^l_{pm}(\boldsymbol{R})\boldsymbol{A}^l_p$. Let $\boldsymbol{B}^l_m = \overline{\boldsymbol{A}^l_m}$ $(-l \le m \le l)$. Thus there is an orthonormal basis $\boldsymbol{B}^l_m$ $(-l \le m \le l)$ in $\mathscr{H}^l$ such that

$$\boldsymbol{R}^{\otimes l}\boldsymbol{B}^l_m = \sum_{p=-l}^{l} \overline{D^l_{pm}(\boldsymbol{R})}\boldsymbol{B}^l_p = \sum_{p=-l}^{l} D^l_{mp}(\boldsymbol{R}^T)\boldsymbol{B}^l_p. \tag{17.33}$$

By Schur's Lemma and Theorem 13.12, any orthonormal basis $\widetilde{\boldsymbol{B}}^l_m$ $(-l \le m \le l)$ in $\mathscr{H}^l$ that satisfies (17.33) can differ from $\boldsymbol{B}^l_m$ only by a common multiplicative factor $\lambda \in \mathbb{C}$ with $|\lambda| = 1$, i.e., $\widetilde{\boldsymbol{B}}^l_m = \lambda \boldsymbol{B}^l_m$ for each m. In what follows, we present a procedure (cf. [203, Sect. 5.1]) by which an explicit orthonormal basis in $\mathscr{H}^l$ that satisfies (17.33) and the further condition

$$\boldsymbol{B}^l_m = (-1)^m \overline{\boldsymbol{B}^l_{\bar{m}}} \qquad (-l \le m \le l) \tag{17.34}$$

can be generated. Since condition (17.34) requires that $\boldsymbol{B}^l_0$ be real, an orthonormal basis in $\mathscr{H}^l$ that satisfies (17.33) and (17.34) is uniquely determined up to a common multiplicative factor $\lambda = \pm 1$.

For $\boldsymbol{A} \in \mathscr{H}^l$ and $-l \le m \le l$, let $\mathscr{F}^l_m : \mathscr{H}^l \to \mathscr{H}^l$ be defined by

$$\mathscr{F}^l_m(\boldsymbol{A}) = \int_{\mathrm{SO}(3)} \boldsymbol{R}^{\otimes l}\boldsymbol{A}\, D^l_{m0}(\boldsymbol{R}) d\mathfrak{g}(\boldsymbol{R}), \tag{17.35}$$

where $\mathfrak{g}$ denotes the normalized Haar measure on SO(3); cf. (3.42). We determine an explicit orthonormal basis $\boldsymbol{B}^l_m$ in $\mathscr{H}^l$ that satisfies (17.33) and (17.34) as follows:

Step 1: Determination of $\boldsymbol{B}^l_0$. Note that the existence of an orthonormal basis $\boldsymbol{B}^l_m$ which satisfies (17.33) is already guaranteed by the general theory. When we write $\boldsymbol{B}^l_m$ $(-l \le m \le l)$ without specification, we mean members of one such basis. By (17.33) and (17.35) we observe that

$$\begin{aligned}\mathscr{F}^l_0(\boldsymbol{B}^l_m) &= \int_{\mathrm{SO}(3)} \boldsymbol{R}^{\otimes l}\boldsymbol{B}^l_m\, D^l_{00}(\boldsymbol{R}) d\mathfrak{g}(\boldsymbol{R}) = \int_{\mathrm{SO}(3)} \Big(\sum_p D^l_{mp}(\boldsymbol{R}^T)\boldsymbol{B}^l_p\Big) D^l_{00}(\boldsymbol{R}) d\mathfrak{g}(\boldsymbol{R}) \\ &= \sum_p \Big(\int_{\mathrm{SO}(3)} \overline{D^l_{pm}(\boldsymbol{R})} D^l_{00}(\boldsymbol{R})\, d\mathfrak{g}(\boldsymbol{R})\Big)\boldsymbol{B}^l_p = \sum_p \frac{1}{2l+1}\delta_{p0}\delta_{m0}\boldsymbol{B}^l_p = \frac{1}{2l+1}\delta_{m0}\boldsymbol{B}^l_0.\end{aligned} \tag{17.36}$$

Equation (17.36) indicates that $\mathscr{F}^l_0(\boldsymbol{B}^l_m) = \boldsymbol{0}$ if $m \neq 0$, and $(2l+1)\mathscr{F}^l_0(\boldsymbol{B}^l_0) = \boldsymbol{B}^l_0$.

In what follows a tensor is said to be real if its imaginary part is zero. Let $\boldsymbol{A} \in \mathscr{H}^l$ be non-zero and real. Since $D^l_{00}(\boldsymbol{R})$ is real for each rotation $\boldsymbol{R}$, by (17.35) $\mathscr{F}^l_0(\boldsymbol{A})$ is real. By (17.36) we observe that $\mathscr{F}^l_0(\boldsymbol{A})$ is non-zero if $\boldsymbol{A}$ has a non-zero $\boldsymbol{B}^l_0$-component. Take an arbitrary real basis in $\mathscr{H}^l$. If we let $\mathscr{F}^l_0(\cdot)$ runs over, one-by-one, the members of this real basis, we will certainly hit upon one member, which we now call $\widetilde{\boldsymbol{A}}$ such that $\mathscr{F}^l_0(\widetilde{\boldsymbol{A}}) \neq \boldsymbol{0}$. We take

$$\boldsymbol{B}^l_0 = \mathscr{F}^l_0(\widetilde{\boldsymbol{A}})/\|\mathscr{F}^l_0(\widetilde{\boldsymbol{A}})\|; \tag{17.37}$$

Clearly $\boldsymbol{B}_0^l$ is real and $\|\boldsymbol{B}_0^l\| = 1$.

Step 2: Computation of $\boldsymbol{B}_m^l$ for $m \neq 0$. The other members of the basis we seek are computed from the formula

$$\boldsymbol{B}_m^l = \mathscr{F}_m^l((2l+1)\boldsymbol{B}_0^l), \qquad \text{where } -l \le m \le l. \tag{17.38}$$

Note that the preceding formula remains valid for $m = 0$.

Step 3: Verifications. We claim that for each $\boldsymbol{Q} \in \mathrm{SO}(3)$ and $\boldsymbol{A} \in \mathscr{H}^l$ there holds

$$\boldsymbol{Q}^{\otimes l}\mathscr{F}_m^l(\boldsymbol{A}) = \sum_{p=-l}^{l} D_{mp}^l(\boldsymbol{Q}^T)\mathscr{F}_p^l(\boldsymbol{A}). \tag{17.39}$$

Indeed we have

$$\begin{aligned}
\boldsymbol{Q}^{\otimes l}\mathscr{F}_m^l(\boldsymbol{A}) &= \boldsymbol{Q}^{\otimes l}\int_{\mathrm{SO}(3)} \boldsymbol{R}^{\otimes l}\boldsymbol{A}\, D_{m0}^l(\boldsymbol{R})d\mathfrak{g}(\boldsymbol{R}) = \int_{\mathrm{SO}(3)} (\boldsymbol{Q}\boldsymbol{R})^{\otimes l}\boldsymbol{A}\, D_{m0}^l(\boldsymbol{R})d\mathfrak{g}(\boldsymbol{R}) \\
&= \int_{\mathrm{SO}(3)} \widetilde{\boldsymbol{Q}}^{\otimes l}\boldsymbol{A}\, D_{m0}^l(\boldsymbol{Q}^T\widetilde{\boldsymbol{Q}})d\mathfrak{g}(\boldsymbol{Q}^T\widetilde{\boldsymbol{Q}}), \qquad \text{where } \widetilde{\boldsymbol{Q}} := \boldsymbol{Q}\boldsymbol{R} \\
&= \int_{\mathrm{SO}(3)} \widetilde{\boldsymbol{Q}}^{\otimes l}\boldsymbol{A}\left(\sum_p D_{mp}^l(\boldsymbol{Q}^T)D_{p0}^l(\widetilde{\boldsymbol{Q}})\right)d\mathfrak{g}(\widetilde{\boldsymbol{Q}}) = \sum_p D_{mp}^l(\boldsymbol{Q}^T)\mathscr{F}_p^l(\boldsymbol{A}).
\end{aligned} \tag{17.40}$$

By putting $\boldsymbol{A} = (2l+1)\boldsymbol{B}_0^l$ in the preceding formula, we see that the tensors $\boldsymbol{B}_m^l$ $(-l \le m \le l)$, as defined by (17.38) satisfy the requirement (17.33).

Next we show that the tensors $\boldsymbol{B}_m^l$ $(-l \le m \le l)$ as defined by (17.38) are orthonormal. Since $\boldsymbol{R}^{\otimes l}$ is unitary for each rotation $\boldsymbol{R}$, we have for $m \neq p$

$$\begin{aligned}
\langle \boldsymbol{B}_m^l, \boldsymbol{B}_p^l\rangle &= \int_{\mathrm{SO}(3)} \langle \boldsymbol{R}^{\otimes l}\boldsymbol{B}_m^l, \boldsymbol{R}^{\otimes l}\boldsymbol{B}_p^l\rangle d\mathfrak{g}(\boldsymbol{R}) \\
&= \int_{\mathrm{SO}(3)} \Big\langle \sum_s D_{ms}^l(\boldsymbol{R}^T)\boldsymbol{B}_s^l, \sum_q D_{pq}^l(\boldsymbol{R}^T)\boldsymbol{B}_q^l\Big\rangle d\mathfrak{g}(\boldsymbol{R}) \\
&= \sum_{s,q}\Big(\int_{\mathrm{SO}(3)} D_{ms}^l(\boldsymbol{R}^T)\overline{D_{pq}^l(\boldsymbol{R}^T)}d\mathfrak{g}(\boldsymbol{R})\Big)\langle \boldsymbol{B}_s^l, \boldsymbol{B}_q^l\rangle \\
&= \frac{1}{2l+1}\sum_{s,q}\delta_{sq}\delta_{mp}\langle \boldsymbol{B}_s^l, \boldsymbol{B}_q^l\rangle = 0.
\end{aligned} \tag{17.41}$$

By construction, $\|\boldsymbol{B}_0^l\| = 1$. We proceed to prove that $\|\boldsymbol{B}_m^l\| = 1$ for each m. By (17.41) we observe that

$$\langle \boldsymbol{R}^{\otimes l}\boldsymbol{B}_m^l, \boldsymbol{B}_0^l\rangle = \Big\langle \sum_{q=-l}^{l} D_{mq}^l(\boldsymbol{R}^T)\boldsymbol{B}_q^l, \boldsymbol{B}_0^l\Big\rangle = D_{m0}^l(\boldsymbol{R}^T)\|\boldsymbol{B}_0^l\|^2 \tag{17.42}$$

for each m and for each rotation $\boldsymbol{R}$. On the other hand, we have

$$\langle \boldsymbol{R}^{\otimes l}\boldsymbol{B}^l_m, \boldsymbol{B}^l_0\rangle = \langle \boldsymbol{B}^l_m, (\boldsymbol{R}^T)^{\otimes r}\boldsymbol{B}^l_0\rangle = \Big\langle \boldsymbol{B}^l_m, \sum_{q=-l}^{l} D^l_{0q}(\boldsymbol{R})\boldsymbol{B}^l_q\Big\rangle$$

$$= \overline{D^l_{0m}(\boldsymbol{R})}\|\boldsymbol{B}^l_m\|^2 = D^l_{m0}(\boldsymbol{R}^T)\|\boldsymbol{B}^l_m\|^2. \tag{17.43}$$

It follows from (17.42) and (17.43) that

$$\|\boldsymbol{B}^l_m\| = \|\boldsymbol{B}^l_0\| = 1 \qquad \text{for each } -l \le m \le l. \tag{17.44}$$

Hence the $2l+1$ tensors $\boldsymbol{B}^l_m$ $(-l \le m \le l)$ constitute an orthonormal basis in $\mathscr{H}^l$.

Finally we prove that the basis tensors $\boldsymbol{B}^l_m$ satisfy the condition (17.34). Indeed we have

$$\boldsymbol{B}^l_{\bar m} = (2l+1)\mathscr{F}^l_{\bar m}(\boldsymbol{B}^l_0) = (2l+1)\int_{\mathrm{SO}(3)} \boldsymbol{R}^{\otimes l}\boldsymbol{B}^l_0 D^l_{\bar m 0}(\boldsymbol{R})d\mathfrak{g}(\boldsymbol{R})$$

$$= (2l+1)\int_{\mathrm{SO}(3)} \boldsymbol{R}^{\otimes l}\boldsymbol{B}^l_0\Big((-1)^m\overline{D^l_{m0}(\boldsymbol{R})}\Big)d\mathfrak{g}(\boldsymbol{R})$$

$$= (-1)^m(2l+1)\overline{\int_{\mathrm{SO}(3)} \boldsymbol{R}^{\otimes l}\boldsymbol{B}^l_0 D^l_{m0}(\boldsymbol{R})d\mathfrak{g}(\boldsymbol{R})} = (-1)^m\overline{\boldsymbol{B}^l_m}, \tag{17.45}$$

where we have appealed to $(4.40)_2$ and the fact that $\boldsymbol{B}^l_0$ is real.

The preceding findings about a special orthonormal basis in $\mathscr{H}^l$ remain valid in a slightly more general context, which we record as the following theorem (cf. [203, Theorem 1]).

Theorem 17.14 *For $k \ge 0$, let Z be a $(2k+1)$-dimensional subspace of the tensor space $V^{\otimes r}$ invariant under $\boldsymbol{Q}^{\otimes r}$ for each rotation $\boldsymbol{Q}$, and let Z_c be the complexification of Z. Suppose the restriction of the representation $\boldsymbol{Q} \mapsto \boldsymbol{Q}^{\otimes r}$ on Z_c is equivalent to the irreducible unitary representation $\mathcal{D}^k$. There exists an orthonormal basis $\boldsymbol{B}_m$ $(-k \le m \le k)$ in Z_c, unique up to a common multiplicative factor $\lambda = \pm 1$, which satisfies the conditions that*

$$\boldsymbol{Q}^{\otimes r}\boldsymbol{B}_m = \sum_{p=-k}^{k} D^k_{mp}(\boldsymbol{Q}^T)\boldsymbol{B}_p, \qquad \textit{for each } \boldsymbol{Q} \in \mathrm{SO}(3), \tag{17.46}$$

$$\boldsymbol{B}_m = (-1)^m\overline{\boldsymbol{B}_{\bar m}}, \tag{17.47}$$

for each $-k \le m \le k$. □

The case $r = 0$ is trivial for Theorem 17.14. For $r \ge 1$ and $Z_c = \mathscr{H}^l$, we have already proved the theorem and presented a procedure by which a set of explicit orthonormal basis tensors $\boldsymbol{B}_m$ that satisfy conditions (17.46) and (17.47) can be determined. The proof and the procedure, after obvious changes in notation (e.g., with k and Z_c replacing l and $\mathscr{H}^l$, respectively) remain applicable to the setting described in the theorem; cf. [203, Theorem 1 and Sects. 5.1–5.2].

Definition 17.15 A set of tensors $\boldsymbol{B}_m$ $(-k \le m \le k)$ in a complexified $(2k+1)$-dimensional subspace Z_c of $V_c^{\otimes r}$ is said to constitute an irreducible tensor basis of Z_c if it satisfies (17.46) and (17.47). □

In general, let the subspace $Z_c \subset V_c^{\otimes r}$ be decomposed into its irreducible parts (see Proposition 16.4) as $Z_c = \sum_{k=0}^{r} n_k \mathcal{D}^k = X_0 \oplus X_1 \oplus \cdots \oplus X_r$, where $X_k = n_k \mathcal{D}^k$ and terms with $n_k = 0$ are dropped in the summation. A procedure is given in [203] to determine an orthonormal basis $\boldsymbol{H}_m^{k,s}$ ($0 \le k \le r$ and $n_k \ne 0$; $-k \le m \le k$, $1 \le s \le n_k$) in Z_c such that for each k and s the set of orthonormal tensors $\boldsymbol{H}_m^{k,s}$ ($-k \le m \le k$) constitutes an irreducible tensor basis in $X_k^{(s)}$ and $X_k = X_k^{(1)} \oplus \cdots \oplus X_k^{(n_k)}$.

17.5.1 Cartan Decomposition

Under the setting of Theorem 17.14, there is a useful decomposition of Z_c. Since the tensors $\boldsymbol{B}_m$ ($-k \le m \le k$) constitute an orthonormal basis in Z_c, every $\boldsymbol{A} \in Z_c$ can be written as

$$\boldsymbol{A} = \sum_{m=-k}^{k} \alpha_m \boldsymbol{B}_m = \alpha_0 \boldsymbol{B}_0 + \sum_{m=1}^{k} (\alpha_m \boldsymbol{B}_m + \alpha_{\bar{m}} \boldsymbol{B}_{\bar{m}}), \tag{17.48}$$

where $\alpha_m \in \mathbb{C}$ for each $-k \le m \le k$. For $\boldsymbol{A} \in Z$, $\boldsymbol{A}$ is real; the condition $\boldsymbol{A} = \overline{\boldsymbol{A}}$ implies that the coefficients α_k satisfies the restriction

$$\alpha_m = (-1)^m \overline{\alpha_{\bar{m}}} \qquad \text{for } -k \le m \le k. \tag{17.49}$$

Let the subspaces $\mathcal{W}_m$ ($0 \le m \le k$) of Z_c be defined by

$$\mathcal{W}_0 := \operatorname{span}\{\boldsymbol{B}_0\}, \qquad \mathcal{W}_m := \operatorname{span}\{\boldsymbol{B}_m, \boldsymbol{B}_{\bar{m}}\} \quad \text{for } 1 \le m \le k. \tag{17.50}$$

Then the space Z_c can be written as the direct sum

$$Z_c = \mathcal{W}_0 \oplus \mathcal{W}_1 \oplus \cdots \oplus \mathcal{W}_k, \tag{17.51}$$

where $\mathcal{W}_0$ is 1-dimensional and each $\mathcal{W}_m$ ($1 \le m \le k$) is 2-dimensional. Following Golubitsky et al. [131, p. 110], who examine the case $Z_c = \mathscr{H}^k$, we call (17.51) the Cartan decomposition of Z_c.[172] Unlike [118, 131], where decomposition (17.51) is derived for harmonic tensors through the properties of homogeneous harmonic polynomials, here its validity is based on the premise that the representation $\mathrm{SO}(3) \to \mathrm{GL}(Z_c)$, $\boldsymbol{Q} \mapsto \boldsymbol{Q}^{\otimes r}|_{Z_c}$, is equivalent to the irreducible unitary representation $\mathcal{D}^k$ (see Theorem (17.14)).

Since $[D_{mp}^k(\boldsymbol{R}(\boldsymbol{e}_3, -\Theta))] = \operatorname{diag}(e^{ik\Theta}, \ldots, e^{i\Theta}, 1, e^{-i\Theta}, \ldots, e^{-ik\Theta})$, by (17.46) we have

$$(\boldsymbol{R}(\boldsymbol{e}_3, \Theta))^{\otimes r} \boldsymbol{B}_m = e^{im\Theta} \boldsymbol{B}_m \qquad \text{for } -k \le m \le k. \tag{17.52}$$

For $m = 0$, (17.52) indicates that $(\boldsymbol{R}(\boldsymbol{e}_3, \Theta))^{\otimes r}$ keeps every tensor in $\mathcal{W}_0$ unchanged. For $1 \le m \le k$, let $\boldsymbol{s}_m := \mathfrak{Im}\, \boldsymbol{B}_m$ and $\boldsymbol{t}_m := \mathfrak{Re}\, \boldsymbol{B}_m$. The real tensors $\boldsymbol{s}_m$ and $\boldsymbol{t}_m$ constitute a basis in the subspace $\mathcal{W}_m$. By direct computations, we obtain from (17.52) the following equations:

$$(\boldsymbol{R}(\boldsymbol{e}_3, \Theta))^{\otimes r} \boldsymbol{s}_m = (\cos m\Theta) \boldsymbol{s}_m + (\sin m\Theta) \boldsymbol{t}_m, \tag{17.53}$$

$$(\boldsymbol{R}(\boldsymbol{e}_3, \Theta))^{\otimes r} \boldsymbol{t}_m = (-\sin m\Theta) \boldsymbol{s}_m + (\cos m\Theta) \boldsymbol{t}_m. \tag{17.54}$$

[172] See also Forte and Vianello [118], where the Cartan decomposition of $\mathscr{H}^4$, which appears in the harmonic decomposition of the elasticity tensor, is discussed in detail.

Hence the restriction of $(\boldsymbol{R}(\boldsymbol{e}_3, \Theta))^{\otimes r}$ on $\mathcal{W}_m$ is a rotation of angle $m\Theta$.

Another two useful formulas are as follows:

$$(\boldsymbol{R}(\boldsymbol{e}_2, \pi))^{\otimes r} \boldsymbol{B}_m = (-1)^k \overline{\boldsymbol{B}_m}, \tag{17.55}$$

$$(\boldsymbol{R}(\boldsymbol{e}_1, \pi))^{\otimes r} \boldsymbol{B}_m = (-1)^{k+m} \overline{\boldsymbol{B}_m}. \tag{17.56}$$

To prove (17.55), note that by $(4.33)_1$ we have $D^k_{mp}(\boldsymbol{R}(\boldsymbol{e}_2, \pi)) = (-1)^{k+m}\delta_{m\bar{p}}$. Hence, by (17.46), we see that

$$(\boldsymbol{R}(\boldsymbol{e}_2, \pi))^{\otimes r} \boldsymbol{B}_m = \sum_p (-1)^{k+m}\delta_{m\bar{p}} \boldsymbol{B}_p = (-1)^{k+m} \boldsymbol{B}_{\bar{m}} = (-1)^k \overline{\boldsymbol{B}_m}. \tag{17.57}$$

Formula (17.56) follows from (17.52), (17.55), and the fact that $\boldsymbol{R}(\boldsymbol{e}_1, \pi) = \boldsymbol{R}(\boldsymbol{e}_3, \pi)\boldsymbol{R}(\boldsymbol{e}_2, \pi)$.

17.6 Tensorial Fourier Expansion of the ODF

17.6.1 Harmonic Tensor Basis and Tensorial Fourier Expansion

Let $L^2(\mathrm{SO}(3)) := L^2(\mathrm{SO}(3), \mathbb{C})$ be the space of square-integrable complex-valued functions defined on SO(3); cf. Sects. 3.6, 4.2, and 13.3.[173] Applying the discussion in Sect. 15.3 to $L^2(\mathrm{SO}(3))$, we see that $L^2(\mathrm{SO}(3))$ is a Hilbert-space direct sum of pairwise-orthogonal subspaces X^l $(l = 0, 1, 2, \ldots)$, each of which is spanned by the $(2l+1)^2$ Wigner D-functions $D^l_{mn}(\cdot)$ as basis. Moreover, each X^l is a direct sum of $2l+1$ subspaces X^l_m $(-l \le m \le l)$ with basis D^l_{mn} $(-l \le n \le l)$, on each of which the restriction of the right-regular representation $\mathcal{T}_r$ to X^l_m, namely $\mathcal{T}_r\big|_{X^l_m}$, satisfies (cf. (15.30)

$$(\mathcal{T}_r(\boldsymbol{P})D^l_{mn})(\cdot) = \sum_{k=-l}^{l} D^l_{kn}(\boldsymbol{P})D^l_{mk}(\cdot) \qquad \text{for each fixed } m \text{ and for each } \boldsymbol{P} \in \mathrm{SO}(3). \tag{17.58}$$

Hence the representation $\mathcal{T}_r\big|_{X^l_m}$ is equivalent to the irreducible representation $\mathcal{D}^l$. For a given l, a function $f^{(l)} \in X^l \subset L^2(\mathrm{SO}(3))$ can be written as

$$f^{(l)}(\boldsymbol{R}) = \sum_{m=-l}^{l} \sum_{n=-l}^{l} c^l_{mn} D^l_{mn}(\boldsymbol{R}), \tag{17.59}$$

where the expansion coefficients are given by

$$c^l_{mn} = \frac{2l+1}{8\pi^2} \int_{\mathrm{SO}(3)} f^{(l)}(\boldsymbol{R})\overline{D^l_{mn}(\boldsymbol{R})}d\mathcal{V}(\boldsymbol{R}).$$

In what follows we will show that we can recast the decomposition of $L^2(\mathrm{SO}(3))$ described above in terms of harmonic tensors in $\mathscr{H}^l$ $(l = 0, 1, 2, \ldots)$.

[173] In Sect. 17.6 we shall use $\langle \cdot, \cdot \rangle$ to denote only the Hermitian product on $V_c^{\otimes r}$. The Hermitian product on $L^2(\mathrm{SO}(3))$, as defined by (4.13), will be written out explicitly.

For each $l = 0, 1, 2, \ldots$, choose an orthonormal basis $\hat{\boldsymbol{H}}^l_1, \ldots, \hat{\boldsymbol{H}}^l_{2l+1}$ in $\mathscr{H}^l$.[174] By Corollary 17.9, for each l the mapping $\boldsymbol{\tau}^{(l)} : \mathrm{SO}(3) \to \mathrm{GL}(\mathscr{H}^l)$, $\boldsymbol{R} \mapsto \boldsymbol{R}^{\otimes l}$, is an irreducible representation equivalent to $\mathcal{D}^l$. By Theorem 13.20 the elements of the matrices that represent $\boldsymbol{\tau}^{(l)}(\boldsymbol{R})$ $(l = 0, 1, 2, \ldots)$ under the orthonormal basis $\hat{\boldsymbol{H}}^l_\beta$ $(\beta = 1, \ldots, 2l+1)$, namely

$$\tau^l_{\alpha\beta}(\boldsymbol{R}) = \langle \hat{\boldsymbol{H}}^l_\alpha, \boldsymbol{R}^{\otimes l} \hat{\boldsymbol{H}}^l_\beta \rangle, \qquad (1 \le \alpha, \beta \le 2l+1) \tag{17.60}$$

satisfy the orthogonality relations

$$\int_{\mathrm{SO}(3)} \tau^l_{\alpha\beta}(\boldsymbol{R}) \overline{\tau^{l'}_{\alpha'\beta'}(\boldsymbol{R})}\, d\mathcal{V}(\boldsymbol{R}) = \frac{8\pi^2}{2l+1} \delta_{ll'} \delta_{\alpha\alpha'} \delta_{\beta\beta'}. \tag{17.61}$$

Moreover by the Peter-Weyl theorem and its corollaries (see Sects. 15.2 and 15.3), $L^2(\mathrm{SO}(3)) = \bigoplus_{l=0}^{\infty} X^l$ and the matrix elements $\tau^l_{\alpha\beta}(\cdot)$ constitute a basis in X^l. Thus each $f^{(l)} \in X^l$ can be expressed as

$$\begin{aligned} f^{(l)}(\boldsymbol{R}) &= \sum_{\alpha,\beta} V^l_{\alpha\beta} \tau^l_{\alpha\beta}(\boldsymbol{R}) = \sum_{\alpha,\beta} V^l_{\alpha\beta} \langle \hat{\boldsymbol{H}}^l_\alpha, \boldsymbol{R}^{\otimes l} \hat{\boldsymbol{H}}^l_\beta \rangle \\ &= \sum_\beta \Big\langle \sum_\alpha V^l_{\alpha\beta} \hat{\boldsymbol{H}}^l_\alpha, \boldsymbol{R}^{\otimes l} \hat{\boldsymbol{H}}^l_\beta \Big\rangle = \sum_\beta \langle \boldsymbol{V}^l_\beta, \boldsymbol{R}^{\otimes l} \hat{\boldsymbol{H}}^l_\beta \rangle, \end{aligned} \tag{17.62}$$

where the expansion coefficients $V^l_{\alpha\beta}$ are given by the formula

$$V^l_{\alpha\beta} = \frac{2l+1}{8\pi^2} \int_{\mathrm{SO}(3)} f^{(l)}(\boldsymbol{R}) \overline{\tau^l_{\alpha\beta}(\boldsymbol{R})} d\mathcal{V}(\boldsymbol{R}), \tag{17.63}$$

and for each β

$$\boldsymbol{V}^l_\beta := \sum_{\alpha=1}^{2l+1} V^l_{\alpha\beta} \hat{\boldsymbol{H}}^l_\alpha \tag{17.64}$$

is a harmonic tensor.

Thus for a function $f \in L^2(\mathrm{SO}(3))$, we obtain the following tensorial Fourier series of f [1, 34, 132, 190, 355]:

$$f(\boldsymbol{R}) = \sum_{l=0}^{\infty} f^{(l)}(\boldsymbol{R}) = \sum_{l=0}^{\infty} \sum_{\beta=1}^{2l+1} \langle \boldsymbol{V}^l_\beta, \boldsymbol{R}^{\otimes l} \hat{\boldsymbol{H}}^l_\beta \rangle. \tag{17.65}$$

The harmonic tensors $\boldsymbol{V}^l_\beta$, which are written out explicitly in (17.64), are called the tensorial Fourier coefficients of the expansion.

17.6.2 Classical ODF Expansion as Tensorial Fourier Series

Consider an ODF $w \in L^2(\mathrm{SO}(3))$ that pertains to a triclinic aggregate of triclinic crystallites. Comparing the tensorial Fourier series of w (cf. (17.65)) and its classical expansion (4.45)

[174] In what follows, $\hat{\mathcal{H}}^0_1 := 1$; $\boldsymbol{R}^{\otimes 0} := 1$, and $\tau^0_{00}(\boldsymbol{R}) = 1$ for all $\boldsymbol{R} \in \mathrm{SO}(3)$.

in Wigner D-functions, i.e.,

$$w(\boldsymbol{R}) = \sum_{l=0}^{\infty} w^{(l)}(\boldsymbol{R}) = \sum_{l=0}^{\infty} \sum_{\beta=1}^{2l+1} \langle \boldsymbol{V}^l_\beta, \boldsymbol{R}^{\otimes l} \hat{\boldsymbol{H}}^l_\beta \rangle = \sum_{l=0}^{\infty} \sum_{m=-l}^{l} \sum_{n=-l}^{l} c^l_{mn} D^l_{mn}(\boldsymbol{R}), \tag{17.66}$$

we see that

$$\sum_{\beta=1}^{2l+1} \langle \boldsymbol{V}^l_\beta, \boldsymbol{R}^{\otimes l} \hat{\boldsymbol{H}}^l_\beta \rangle = \sum_{m=-l}^{l} \sum_{n=-l}^{l} c^l_{mn} D^l_{mn}(\boldsymbol{R}). \tag{17.67}$$

The harmonic tensors $\boldsymbol{V}^l_\beta$ in $(17.66)_2$ or (17.67) are called the tensorial texture coefficients of the ODF w, a name that we shall justify in the next section. Starting from (17.67), Lobos Fernández and Böhlke [190, equation (44)] write down two general equations involving the classical and tensorial texture coefficients, which, after a specific set of harmonic tensor basis $\{\hat{\boldsymbol{H}}^l_\beta\}$ is chosen in $\mathscr{H}^l$, express c^l_{mn} in terms of $\boldsymbol{V}^l_\beta$ and vice versa, respectively.[175] In what follows we choose a special orthonormal basis in $\mathscr{H}^l$ under which the classical ODF expansion directly becomes a tensorial Fourier series.

Since the representation $\boldsymbol{\tau}^{(l)} : \mathrm{SO}(3) \to \mathrm{GL}(\mathscr{H}^l)$, $\boldsymbol{R} \mapsto \boldsymbol{R}^{\otimes l}$, is equivalent to $\mathcal{D}^l : \boldsymbol{R} \mapsto [D^l_{mn}(\boldsymbol{R})]$, an orthonormal basis $\boldsymbol{B}^l_n$ $(-l \le n \le l)$, unique up to a common multiplicative factor $\lambda = \pm 1$, can be determined in $\mathscr{H}^l$ (see Sect. 17.5) such that

$$\boldsymbol{R}^{\otimes l} \boldsymbol{B}^l_n = \sum_{p=-l}^{l} \overline{D^l_{pn}(\boldsymbol{R})} \boldsymbol{B}^l_p = \sum_{p=-l}^{l} D^l_{np}(\boldsymbol{R}^T) \boldsymbol{B}^l_p, \qquad \text{for each } \boldsymbol{R} \in \mathrm{SO}(3), \tag{17.68}$$

$$\boldsymbol{B}^l_n = (-1)^n \overline{\boldsymbol{B}^l_{\bar{n}}}. \tag{17.69}$$

Note that $(17.68)_1$ implies that

$$\langle \boldsymbol{B}^l_m, \boldsymbol{R}^{\otimes l} \boldsymbol{B}^l_n \rangle = D^l_{mn}(\boldsymbol{R}). \tag{17.70}$$

For an ODF w, we have

$$\begin{aligned} w^{(l)}(\boldsymbol{R}) &= \sum_{n=-l}^{l} \sum_{m=-l}^{l} c^l_{mn} D^l_{mn}(\boldsymbol{R}) = \sum_{n=-l}^{l} \sum_{m=-l}^{l} c^l_{mn} \langle \boldsymbol{B}^l_m, \boldsymbol{R}^{\otimes l} \boldsymbol{B}^l_n \rangle \\ &= \sum_{n=-l}^{l} \Big\langle \sum_{m=-l}^{l} c^l_{mn} \boldsymbol{B}^l_m, \boldsymbol{R}^{\otimes l} \boldsymbol{B}^l_n \Big\rangle. \end{aligned} \tag{17.71}$$

Comparing $(17.71)_3$ with (17.67), we observe that under the basis $\{\boldsymbol{B}^l_n : -l \le n \le l\}$, the tensorial texture coefficients are given by

$$\boldsymbol{V}^l_n = \sum_{m=-l}^{l} c^l_{mn} \boldsymbol{B}^l_m, \qquad \text{which implies } c^l_{mn} = \langle \boldsymbol{V}^l_n, \boldsymbol{B}^l_m \rangle. \tag{17.72}$$

[175] Lobos Fernández and Böhlke adopt a convention and notation different than ours. Here we have rewritten theirs in our notation and convention. In their paper the authors also provide, for orthorhombic aggregates of cubic crystallites and $l = 4$, a formula to convert between the independent classical coefficients c^4_{00}, c^4_{20}, c^4_{40} and their counterparts in the corresponding tensorial Fourier expansion.

Thus under the orthonormal basis $\{\boldsymbol{B}_n^l\}$ in $\mathscr{H}^l$ $(l = 0, 1, 2, \ldots)$, the classical ODF expansion assumes the form

$$w(\boldsymbol{R}) = \sum_{l=0}^{\infty} \sum_{n=-l}^{l} \sum_{m=-l}^{l} c_{mn}^l \langle \boldsymbol{B}_m^l, \boldsymbol{R}^{\otimes l} \boldsymbol{B}_n^l \rangle = \sum_{l=0}^{\infty} \sum_{n=-l}^{l} \langle \boldsymbol{V}_n^l, \boldsymbol{R}^{\otimes l} \boldsymbol{B}_n^l \rangle, \tag{17.73}$$

where we have appealed to (17.70), $(17.71)_3$, and $(17.72)_1$.

17.6.3 Texture and Crystallite Symmetries

Consider an ODF w which observes texture symmetry defined by the proper point group G_{tex}. Then for each $\boldsymbol{Q} \in G_{\text{tex}}$, we have

$$w^{(l)}(\boldsymbol{R}) = w^{(l)}(\boldsymbol{Q}^T \boldsymbol{R}) = \sum_n \langle \boldsymbol{V}_n^l, (\boldsymbol{Q}^T \boldsymbol{R})^{\otimes l} \boldsymbol{B}_n^l \rangle = \sum_n \langle \boldsymbol{Q}^{\otimes l} \boldsymbol{V}_n^l, \boldsymbol{R}^{\otimes l} \boldsymbol{B}_n^l \rangle. \tag{17.74}$$

We claim that the condition[176]

$$\boldsymbol{Q}^{\otimes l} \boldsymbol{V}_n^l = \boldsymbol{V}_n^l \qquad \text{for each } \boldsymbol{Q} \in G_{\text{tex}} \text{ and } -l \le n \le l \tag{17.75}$$

is equivalent to the restriction (5.19) imposed by G_{tex} on c_{mn}^l. Indeed, since

$$\boldsymbol{Q}^{\otimes l} \boldsymbol{V}_n^l = \sum_m c_{mn}^l \boldsymbol{Q}^{\otimes l} \boldsymbol{B}_m^l = \sum_m c_{mn}^l \Big(\sum_p D_{mp}^l(\boldsymbol{Q}^T) \boldsymbol{B}_p^l \Big), \tag{17.76}$$

the equation $\boldsymbol{V}_n^l = \boldsymbol{Q}^{\otimes l} \boldsymbol{V}_n^l$ is equivalent to

$$\sum_m c_{mn}^l \boldsymbol{B}_m^l = \sum_m c_{mn}^l \Big(\sum_p D_{mp}^l(\boldsymbol{Q}^T) \boldsymbol{B}_p^l \Big) = \sum_m \Big(\sum_p c_{pn}^l D_{pm}^l(\boldsymbol{Q}^T) \Big) \boldsymbol{B}_m^l, \tag{17.77}$$

where we have renamed indices on the right-hand side of $(17.77)_2$. It is obvious that $(17.77)_2$ is equivalent to (5.19). Hence the condition $\boldsymbol{Q}^{\otimes l} \boldsymbol{V}_n^l = \boldsymbol{V}_n^l$ for each $\boldsymbol{Q} \in G_{\text{tex}}$ and $-l \le n \le l$ describes texture symmetry, which justifies calling the harmonic tensors $\boldsymbol{V}_n^l$ tensorial texture coefficients. Each tensorial texture coefficient $\boldsymbol{V}_n^l$ lies in a subspace $\mathfrak{V}^l$ of $\mathscr{H}^l$ defined by

$$\mathfrak{V}^l = \{\boldsymbol{V}^l \in \mathscr{H}^l : \boldsymbol{Q}^{\otimes l} \boldsymbol{V}^l = \boldsymbol{V}^l \text{ for each } \boldsymbol{Q} \in G_{\text{tex}}\}. \tag{17.78}$$

Henceforth we write $\mathfrak{n}_{\boldsymbol{V}}^l = \dim \mathfrak{V}^l$.

On the other hand, since the index "n" in $\boldsymbol{V}_n^l$ is restricted by crystallite symmetry, the number of independent $\boldsymbol{V}_n^l$ is given by $\mathfrak{n}_{\boldsymbol{H}}^l = \dim \mathfrak{H}^l$, where

$$\mathfrak{H}^l = \{\boldsymbol{H}^l \in \mathscr{H}^l : \boldsymbol{P}^{\otimes l} \boldsymbol{H}^l = \boldsymbol{H}^l \text{ for each } \boldsymbol{P} \in G_{\text{cr}}\}. \tag{17.79}$$

The problem to determine $\mathfrak{n}_{\boldsymbol{V}}^l$ and $\mathfrak{n}_{\boldsymbol{H}}^l$, respectively, is of the same type. In fact, we have already studied this problem in Examples 16.15 and 16.18, where we pose the problem as follows:

[176] Note that in the presence of crystallite symmetry some of the $\boldsymbol{V}_n^l$ may be $\boldsymbol{0}$ or may be equal to a linear combination of a selected set of independent ones. Nevertheless (17.75) remains valid.

– Let G be a crystallographic point group, and let

$$M_c(l) = \{\boldsymbol{A} \in \mathscr{H}^l : \boldsymbol{Q}^{\otimes l}\boldsymbol{A} = \boldsymbol{A} \text{ for each } \boldsymbol{Q} \in G\},$$

Determine $\dim M_c(l)$, the dimension of the subspace M_c of $\mathscr{H}^l$.

As illustrated in Examples 16.15 and 16.18, by using group-theoretic methods we can find $M_c(l)$ for any of the 32 point groups G and any $l = 0, 1, 2, \ldots$.

For instance, for sixth-order harmonic tensors that observe cubic symmetry (i.e., $G = O$), from Table 22 we see that $\dim M_c(6) = 1$. That means: we can choose an orthonormal basis $\boldsymbol{A}_\beta$ $(\beta = 1, 2, \ldots, 13)$ in $\mathscr{H}^6$ such that only $\boldsymbol{A}_1$ is invariant under the action of the point group O. For sixth-order harmonic tensors that enjoy orthorhombic symmetry (i.e., $G = D_2$), from formula (16.80) we obtain $\dim M_c(6) = 4$. Thus we can choose an orthonormal basis $\boldsymbol{A}_\beta$ $(\beta = 1, 2, \ldots, 13)$ in $\mathscr{H}^6$ such that only $\boldsymbol{A}_1, \boldsymbol{A}_2, \boldsymbol{A}_3$, and $\boldsymbol{A}_4$ are invariant under the action of the point group D_2.

In the presence of texture and/or crystallite symmetry, we can recast the classical expansion of the ODF as a tensorial Fourier series, i.e.,

$$w(\boldsymbol{R}) = \sum_{l=0}^{\infty}\sum_{n=-l}^{l}\sum_{m=-l}^{l} c_{mn}^l D_{mn}^l(\boldsymbol{R}) = \sum_{l=0}^{\infty}\sum_{\beta=1}^{\mathfrak{n}_{\boldsymbol{H}}} \langle \boldsymbol{V}_\beta^l, \boldsymbol{R}^{\otimes l}\boldsymbol{H}_\beta^l\rangle, \tag{17.80}$$

where $\boldsymbol{V}_\beta^l \in \mathfrak{V}^l$ and $\boldsymbol{H}_\beta^l \in \mathfrak{H}^l$ are harmonic tensors that satisfy

$$\boldsymbol{Q}^{\otimes l}\boldsymbol{V}_\beta^l = \boldsymbol{V}_\beta^l \quad \text{for each } \boldsymbol{Q} \in G_{\text{tex}}, \qquad \text{and} \qquad \boldsymbol{P}^{\otimes l}\boldsymbol{H}_\beta^l = \boldsymbol{H}_\beta^l \quad \text{for each } \boldsymbol{P} \in G_{\text{cr}}, \tag{17.81}$$

respectively. For each l, we can determine $\boldsymbol{V}_\beta^l$ and $\boldsymbol{H}_\beta^l$ in terms of c_{mn}^l and the special orthonormal basis $\{\boldsymbol{B}_n^l\}$ in $\mathscr{H}^l$ by the following steps: (1) Determine the special orthonormal basis $\{\boldsymbol{B}_n^l\}$ described in (17.68) by the method [203, Sect. 5] presented in Sect. 17.5. (2) Replace $D_{mn}^l(\boldsymbol{R})$ by $\langle \boldsymbol{B}_m^l, \boldsymbol{R}^{\otimes l}\boldsymbol{B}_n^l\rangle$, and impose the restrictions imposed by texture symmetry and crystallite symmetry on c_{mn}^l as given in Chap. 5. (3) Gather terms according to the independent texture coefficients c_{mn}^l, and identify the harmonic tensors $\boldsymbol{V}_\beta^l$ and $\boldsymbol{H}_\beta^l$. A more detailed discussion with examples on these procedures will be presented elsewhere.[177]

See [1, 34, 132, 190, 275, 355] for further details and applications of tensorial Fourier expansions under various crystallite and sample symmetries.

[177] [Note added in proof] See Man C.-S., Du, W.: Recasting classical expansion of orientation distribution function as tensorial Fourier expansion. J. Elast., submitted.

APPENDICES

Appendix A

A Basics of Abstract Group Theory

Readers of Part I are presumed to be acquainted with matrix algebra and advanced multivariate calculus. In Sect. A.1 we go over the fundamental concepts of sets, relations, and functions, the main purpose of which is to specify terminology and notation. In the rest of this appendix, we briefly present some basics of abstract group theory. Our main references are: Armstrong [6] and Miller [232, Chap. 1], where the reader will find more details and examples.

A.1 Sets, Relations, and Functions

A set is a collection of objects, which are its members or elements. Let X be a set. We write $x \in X$ for the assertion that x is an element in X. If x is not a member of X, we write $x \notin X$. To specify a set, we may either list its elements or put a defining statement of its elements within braces. For example, $X = \{1, -1\}$ is a set with the numbers 1 and -1 as elements; $S = \{\theta \in \mathbb{R} : \cos\theta = 0\}$ is the set of real solutions of the equation $\cos\theta = 0$. Two sets X and Y are equal, i.e., $X = Y$, if they have the same elements.

A set X is a subset of set Y, written $X \subset Y$, if every element of X is an element of Y; Y is then a superset of X, written $Y \supset X$. If $X \subset Y$ and $X \neq Y$, X is said to be a proper subset of Y, written $X \subsetneqq Y$. Clearly $X = Y$ if and only if $X \subset Y$ and $Y \subset X$.

Let X and Y be sets. The union $X \cup Y$ (resp. intersection $X \cap Y$) of sets X and Y is defined by the statement: $s \in X \cup Y$ (resp. $z \in X \cap Y$) if and only if $s \in X$ or (resp. and) $s \in Y$. If X and Y have no element in common, we write $X \cap Y = \emptyset$, where $\emptyset$ denotes the empty set or the set with no element. Let J (e.g., the natural numbers $\mathbb{N}$) be an index set and $\{X_j : j \in J\}$ be a family of sets. The union $\bigcup_{j\in J} X_j$ (resp. intersection $\bigcap_{j\in J} X_j$) is the set specified by the statement: $x \in \bigcup_{j\in J} X_j$ (resp. $x \in \bigcap_{j\in J} X_j$) if and only if $x \in X_j$ for some (resp. for all) $j \in J$. We define the set difference $X \setminus Y := \{x \in X : x \notin Y\}$.

Given two sets X and Y, we define their Cartesian product $X \times Y$ as the set of all ordered pairs (x, y), where $x \in X$ and $y \in Y$, i.e., $X \times Y := \{(x, y) : x \in X \text{ and } y \in Y\}$. A relation $\mathtt{R}$ between X and Y is a subset of $X \times Y$. To say that x is $\mathtt{R}$-related to y, it is more convenient to write $x\,\mathtt{R}\,y$ for $(x, y) \in \mathtt{R}$.

A relation $\mathtt{R}$ between X and itself (i.e., $\mathtt{R} \subset X \times X$) is said to be a relation on X. A relation $\mathtt{R}$ on set X is an equivalence relation if (i) it is reflexive: $x\,\mathtt{R}\,x$ for all $x \in X$; (ii) it is symmetric: $x\,\mathtt{R}\,y$ implies $y\,\mathtt{R}\,x$; (iii) it is transitive: $x\,\mathtt{R}\,y$ and $y\,\mathtt{R}\,z$ imply $x\,\mathtt{R}\,z$. Given an equivalence relation $\mathtt{R}$ on X, for each $x \in X$ the set $\mathtt{R}[x] = \{y \in X : y\,\mathtt{R}\,x\}$ is the collection of points in X which are $\mathtt{R}$-related to x; it is called the equivalence class of x. Note that for each $x \in X$, $\mathtt{R}[x] \neq \emptyset$, because $x \in \mathtt{R}[x]$. It is easy to show (see, e.g., [6, pp. 61–63]) that $X = \bigcup_{x\in X} \mathtt{R}[x]$ and, for $x, y \in X$, either $\mathtt{R}[x] = \mathtt{R}[y]$ or $\mathtt{R}[x] \cap \mathtt{R}[y] = \emptyset$. We say that the set X is partitioned into a disjoint union of the equivalence classes $\mathtt{R}[x]$, called the equivalence class determined by x, which we will simply write $[x]$ when no confusion should arise on the equivalence relation at issue. The set of all these equivalence classes is denoted by $X/\mathtt{R} = \{[x] : x \in X\}$ and is called the quotient set of X by $\mathtt{R}$.

A function (or mapping, map) f from X to Y, written as $f : X \to Y$, is a relation $f \subset X \times Y$ which satisfies the following requirement: For each $x \in X$, there is a unique $y \in Y$, denoted by $y = f(x)$, such that $(x, y) \in f$. The sets X and Y are called the domain and

range (or codomain) of the function f, respectively. The equation $y = f(x)$ is also written as $f : x \mapsto y$, or simply as $x \mapsto y$ if the name of the function is already specified or not important.

Let $f : X \to Y$ be a function, and let $A \subset X$. The restriction of f to A, written as $f|_A$ or $f|A$, is the function $f|_A : A \to Y$ defined by $f|_A(x) = f(x)$ for $x \in A$. The image of A under f is the set $f(A) = \{y \in Y : y = f(x) \text{ for some } x \in A\}$. In particular, $f(A)$ is called the image of f. The function f is said to be surjective or to map X onto Y if $f(X) = Y$. The function f is said to be injective or one-to-one if any two distinct points in X are mapped onto distinct points in Y, i.e., $f(x) = f(x')$ implies $x = x'$. The function f is said to be bijective if f is injective and surjective.

Let $B \subset Y$. The set $f^{-1}(B) = \{x \in X : f(x) \in B\}$ is called the inverse image of B under f. When B is a singleton, say $B = \{b\}$, it is customary to write the inverse image as $f^{-1}(b)$ instead of $f^{-1}(\{b\})$.

Given two functions $f : X \to Y$ and $g : Y \to Z$, their composition $g \circ f$ is the function $g \circ f : X \to Z$ defined by $(g \circ f)(x) = g(f(x))$ for each $x \in X$. When $f : X \to Y$ is bijective, the inverse function $f^{-1} : Y \to X$ of f is well defined, which satisfies $(f^{-1} \circ f)(x) = x$ for each $x \in X$ and $(f \circ f^{-1})(y) = y$ for each $y \in Y$.

A.2 Groups and Subgroups

Definition A.1 A group G is a set of objects together with a binary operation called multiplication which associates any ordered pair (g, h) of elements in G a third element gh and satisfies the following requirements:

- Associative law. For all $g, h, k \in G$, $(gh)k = g(hk)$.
- Existence of identity. There is an element $e \in G$ such that $eg = ge = g$ for each element $g \in G$.
- Existence of inverses. For each element $g \in G$, there is an element $h \in G$ such that $gh = hg = e$. □

It is easy to prove that the inverse of any element in a group G is unique. Indeed let $g \in G$ have two inverses, say h_1 and h_2. Then $gh_1 = e$. Multiplying both sides of the preceding equation on the left by h_2. By the associative law, we obtain $h_2(gh_1) = (h_2g)h_1 = h_2$ or $h_1 = h_2$, because $h_2g = e$. Henceforth we denote the inverse of $g \in G$ by g^{-1}. Also, it is straightforward to show that $(gh)^{-1} = h^{-1}g^{-1}$. Similarly, the identity is unique: suppose there is another identity $e' \in G$. Then $e'g = g$ for $g \in G$, which implies $e'gg^{-1} = gg^{-1}$, i.e., $e'e = e$ or $e' = e$, because e is an identity element.

A group G is said to be finite or of finite order if it has a finite number of elements. The number of elements in a finite group G is denoted by $|G|$ and called the order of G.

A subset X of a finite group G is said to generate G if each element of G can be expressed as a product of the form $g_1^{m_1}g_2^{m_2}\cdots g_k^{m_k}$, where $g_1, \ldots, g_k \in X$ (they need not be distinct) and $m_1, \ldots, m_k$ are integers. Such an $X \subset G$ is said to be a set of generators for G, and the elements of X are called generators for G.

If the set of generators for the finite group G is a singleton $\{g\}$, we say that G is a cyclic group. As G is finite, there is a smallest positive integer n such that $g^n = e$ and $G = \{e, g, g^2, \ldots, g^{n-1}\}$.

Definition A.2 A subset H of a group G is said to be a subgroup of G if it is a group under the group multiplication defined in G. □

Proposition A.3 *A non-empty $H \subset G$ is a subgroup of G if it satisfies the following two conditions*:

(1) *If $h, k \in H$, then $hk \in H$.*
(2) *If $h \in H$, then $h^{-1} \in H$.*

Proof Suppose H satisfies the two given conditions. The elements of H are elements of G, which observe the associative law under the group multiplication defined in G. Since H is non-empty, there is some $h \in H$. By (1) and (2), $hh^{-1} = e \in H$, where e is the identity in G, but it serves also as the identity in H. Conversely, if $H \neq \emptyset$ is a group, its elements obviously satisfy conditions (1) and (2). □

Let G be a finite group and $g \in G$. The order of the element g is the order of the cyclic subgroup generated by $\{g\}$.

A.3 Cosets, Conjugacy Classes, and Normal Subgroups

A.3.1 Coset Decomposition

Definition A.4 Let H be a subgroup of the group G and let $g \in G$. The set $gH = \{gh : h \in H\}$ (resp. $Hg = \{hg : h \in H\}$) is called a left coset (resp. right coset) of H. □

Since each element of gH is an element of G, $\bigcup_{g\in G} gH \subset G$. Conversely, as the identity $e \in H$, $g = ge \in gH$ for each $g \in G$. Hence we have $G = \bigcup_{g\in G} gH$. We claim that two left cosets g_1H and g_2H of H are either disjoint or equal. Indeed, suppose $g_1H \cap g_2H \neq \emptyset$. Let $k = g_1h_1 = g_2h_2 \in G$. Then $g_1 = g_2(h_2h_1^{-1}) \in g_2H$, which implies $g_1H \subset g_2H$. Similarly, we can prove that $g_2H \subset g_1H$. Hence we have $g_1H = g_2H$. Therefore $G = \bigcup_{g\in G} gH$ is the decomposition of G into a disjoint union of left cosets of H. Similarly, we can show that $G = \bigcup_{g\in G} Hg$ is the decomposition of G into a disjoint union of right cosets of H.

Let G be a finite group and let H be a subgroup of G. It is easy to verify that the mapping $h \mapsto gh$ is a bijection of H onto gH. Hence all the left cosets of H have the same number of elements as H. Let $(G : H)$ be the number of left cosets of H in G. By the properties of left cosets listed above, we observe that

$$|G| = (G : H)|H|, \tag{A.1}$$

where $(G : H)$ is called the index of H in G. With (A.1) we have proved Lagrange's theorem:

Theorem A.5 *The order of a subgroup of a finite group divides the order of the group.* □

A.3.2 Conjugacy

Definition A.6 Let G be a group. An element $h \in G$ is said to be conjugate to $k \in G$ if there is some $g \in G$ such that $ghg^{-1} = k$. Let $\subset \subset G \times G$ be the conjugacy relation defined as follows: $h \subset k$ if and only if h is conjugate to k. □

It is straightforward to verify that the conjugacy relation $\subset$ is reflexive, symmetric, and transitive; hence $\subset$ is an equivalence relation. The equivalence classes under $\subset$ are called conjugacy classes. The conjugacy class determined by $h \in G$ is $[h] = \{ghg^{-1} : g \in G\}$. Note that the conjugacy class determined by the identity e is the singleton $\{e\}$, and that the set G is a disjoint union of the conjugacy classes.

Example A.7 Let us consider the conjugacy class in the rotation group SO(3) that contains the rotation $\boldsymbol{R}(\boldsymbol{n}, \omega)$, where $\boldsymbol{n}$ is a unit vector and $\omega \in [0, \pi)$; see Sect. 1.6 for explanation of the notation. By Euler's theorem (1.82), we have $\boldsymbol{Q}\boldsymbol{R}(\boldsymbol{n}, \omega)\boldsymbol{Q}^{-1} = \boldsymbol{R}(\boldsymbol{Q}\boldsymbol{n}, \omega)$ for each $\boldsymbol{Q} \in \mathrm{SO}(3)$. Hence the conjugacy class $[\boldsymbol{R}(\boldsymbol{n}, \omega)]$ consists of all rotations with rotation angle ω. □

Example A.8 Consider the group $D_3 = \{e, r, r^2, s, sr, sr^2\}$, where $e = \boldsymbol{I}$, $r = \boldsymbol{R}(\boldsymbol{e}_3, 2\pi/3)$, and $s = \boldsymbol{R}(\boldsymbol{e}_1, \pi)$, which is the symmetry group of an equilateral triangle in the 1-2 plane with centroid at the origin; see Examples 2.1, 2.31, and Table 3 of Sect. 2.6.1. By the discussion in Example A.7, all the rotations in the same conjugacy class necessarily have the same rotation angle $\omega \in [0, \pi)$. Hence there are at least three conjugacy classes, namely $[e]$, $[r]$ $(\omega = 2\pi/3)$, and $[s]$ $(\omega = \pi)$. Indeed, because $s^{-1} = s$, $r^{-1} = r^2$, from the multiplication table of group D_3 (see Table 1 of Sect. 2.1) we observe that $srs^{-1} = srs = r^2$, $sr^2s^{-1} = r$, $rsr^{-1} = rsr^2 = sr$, $r(sr)r^{-1} = rs = sr^2$, and $r(sr^2)r^{-1} = rsr = s$. Thus the group D_3 has three conjugacy classes:

$$[e] = \{e\}, \qquad [r] = \{r, r^2\}, \qquad [s] = \{s, sr, sr^2\}. \tag{A.2}$$

Note that $r^2 = \boldsymbol{R}(-\boldsymbol{e}_3, 2\pi/3)$. □

The conjugacy relation can be similarly defined on the set of all subgroups of G.

Definition A.9 A subgroup H of the group G is said to be conjugate to a subgroup K of G if there is some $g \in G$ such that $gHg^{-1} = K$ as sets (i.e., $gH = Kg$). □

It is easy to verify that the conjugacy relation as specified in Definition A.9 is an equivalence relation on the set of all subgroups of G. Hence we can talk about conjugacy classes of subgroups of G. In particular, the conjugacy class determined by the subgroup H is $[H] = \{gHg^{-1} : g \in G\}$.

Remark A.10 Each conjugacy class $[\mathcal{G}]$ of space groups as subgroups of the Euclidean group E(3) can be taken as describing one type of crystal symmetry. Two space groups $\mathcal{G}$ and $\mathcal{G}'$ in the same conjugacy class can be interpreted as pertaining to the same ideal crystal under two right-handed affine coordinate systems. Likewise, the crystallographic point groups $\mathcal{K}$ and $\mathcal{K}'$ of two conjugate space groups $\mathcal{G}$ and $\mathcal{G}'$, respectively, are in the same conjugacy class of subgroups of O(3). They can be taken as describing the point-group symmetry of the same ideal crystal under two Cartesian coordinate systems and are of the same point-group type. Cf. Sects. 2.3.5 and 2.3.7. □

A.3.3 Normal Subgroups

Let G be a group, and let $X, Y \subset G$. We define the product of the subsets X and Y of G by

$$XY = \{hk : h \in X \text{ and } k \in Y\}. \tag{A.3}$$

Definition A.11 A subgroup H of the group G is said to be a normal subgroup of G if $gHg^{-1} = H$ or equivalently $gH = Hg$ for each $g \in G$. □

Proposition A.12 *Let H be a normal subgroup of the group G. The left cosets of H form a group under the multiplication defined by* (A.3).

Proof Let g_1H and g_2H be left cosets of H, where g_1 and g_2 are any two elements of G. Since H is a normal subgroup of G, we have $gH = Hg$ for each $g \in G$. By (A.3), we obtain for multiplication of left cosets:

$$(g_1H)(g_2H) = g_1(Hg_2)H = g_1g_2HH = g_1g_2H, \tag{A.4}$$

as $HH = H$. Under (A.4), associative law follows from its counterpart in G; the coset $eH = H$ serves as the identity, and $g^{-1}H$ is the inverse of gH. □

The group of left cosets with multiplication defined by (A.4) is called the quotient group of G by H and is denoted by G/H.

Proposition A.13 *Let G be a finite group and H be a subgroup of index 2 in G. Then H is a normal subgroup of G and the quotient group G/H is cyclic of order 2.*

Proof To prove that H is a normal subgroup of G, it suffices to show that $gH = Hg$ for each $g \in G$. We distinguish two cases: (i) $g \in H$; (ii) $g \in G \setminus H$. For (i) $g \in H$, clearly we have $gH = Hg$. For (ii) $g \in G \setminus H$, since H is a subgroup of index 2 in G, there are only two left cosets, namely H and gH. Then $G = H \cup gH$, where $H \cap gH = \emptyset$. Similarly, $G = H \cup Hg$, where $H \cap Hg = \emptyset$. Hence we have $gH = Hg$ for $g \in G \setminus H$.

As the quotient group has only two elements, it is cyclic of order 2. □

A.4 Homomorphisms, Isomorphisms, and Automorphisms

Definition A.14 Let G and G' be groups. A mapping $\varphi : G \to G'$ is called a homomorphism if it preserves multiplication, i.e., $\varphi(gh) = \varphi(g)\varphi(h)$ for any $g, h \in G$. A bijective homomorphism is called an isomorphism. □

Let e and e' be the identity in G and in G', respectively, and $\varphi : G \to G'$ be a homomorphism. Since $\varphi(e) = \varphi(ee) = \varphi(e)\varphi(e)$, multiplying both sides of the equation on the left by $(\varphi(e))^{-1}$ yields $\varphi(e) = e'$.

Similarly, for any $g \in G$, we have $\varphi(g)\varphi(g^{-1}) = \varphi(gg^{-1}) = \varphi(e) = e'$, which implies $\varphi(g^{-1}) = (\varphi(g))^{-1}$.

Definition A.15 Let $\varphi : G \to G'$ be a homomorphism. The kernel and image of φ are defined as

$$\operatorname{Ker}\varphi := \varphi^{-1}(e') = \{g \in G : \varphi(g) = e'\}, \tag{A.5}$$

$$\operatorname{Im}\varphi := \varphi(G) = \{g' \in G' : g' = \varphi(g) \text{ for some } g \in G\}, \tag{A.6}$$

respectively. □

Lemma A.16 *Let $\varphi : G \to G'$ be a homomorphism. Then $\operatorname{Ker}\varphi$ is a normal subgroup of G, and $\operatorname{Im}\varphi$ a subgroup of G'.*

Proof Since $\varphi(e) = e'$, by definition $\operatorname{Ker}\varphi$ and $\operatorname{Im}\varphi$ are non-empty subsets of G and G', respectively. If $g, h \in \operatorname{Ker}\varphi$, then $\varphi(g) = \varphi(h) = e'$. Hence $\varphi(gh) = \varphi(g)\varphi(h) = e'e' = e'$. Also, we have $\varphi(g^{-1}) = (\varphi(g))^{-1} = (e')^{-1} = e'$. By Proposition A.3, $\operatorname{Ker}\varphi$ is a subgroup of G.

Similarly, if $g', h' \in \operatorname{Im}\varphi$, then $g' = \varphi(g)$ and $h' = \varphi(h)$ for some $g, h \in G$. Since $gh \in G$ and $\varphi(gh) = \varphi(g)\varphi(h) = g'h'$, $g'h' \in \operatorname{Im}\varphi$. Moreover, if $g' \in \operatorname{Im}\varphi$ and $g' = \varphi(g)$ for some $g \in G$, then $g'^{-1} = (\varphi(g))^{-1} = \varphi(g^{-1}) \in \operatorname{Im}\varphi$, because $g^{-1} \in G$.

To prove that $\operatorname{Ker}\varphi$ is a normal subgroup of G, it suffices to show that $gkg^{-1} \in \operatorname{Ker}\varphi$ for all $k \in \operatorname{Ker}\varphi$. Since $\varphi(gkg^{-1}) = \varphi(g)\varphi(k)\varphi(g^{-1}) = \varphi(g)e'\varphi(g)^{-1} = e'$, the conclusion follows. □

Theorem A.17 *Let $\varphi : G \to G'$ be a homomorphism. Then the quotient group $G/\operatorname{Ker}\varphi$ is isomorphic to $\operatorname{Im}\varphi$.*

Proof For brevity, write $K := \operatorname{Ker}\varphi$. Let $g, h \in G$. First we prove the following assertion:

$$gK = hK \qquad \text{if and only if} \qquad \varphi(g) = \varphi(h).$$

Suppose $gK = hK$. Then $gk_1 = hk_2$ for some $k_1, k_2 \in K$. Hence $\varphi(gk_1) = \varphi(gk_2)$, which implies $\varphi(g)\varphi(k_1) = \varphi(h)\varphi(k_2)$ or $\varphi(g) = \varphi(h)$, as $\varphi(k_1) = \varphi(k_2) = e'$. Conversely, suppose $\varphi(g) = \varphi(h)$. Then $\varphi(h^{-1}g) = \varphi(h^{-1})\varphi(g) = (\varphi(h))^{-1}\varphi(g) = e'$, which implies $h^{-1}g \in K$ or $g \in hK$. Since $g \in gK$ and different left cosets are disjoint, we have $gK = hK$.

Let $\widetilde{\varphi} : G/K \to G'$ be defined by $\widetilde{\varphi}(gK) = \varphi(g)$. By the assertion proved above, the map $\widetilde{\varphi}$ is well defined. We claim that it is one-to-one. Indeed, suppose $\widetilde{\varphi}(gK) = \widetilde{\varphi}(hK)$. Then $\varphi(g) = \varphi(h)$, which implies $gK = hK$. Thus $\widetilde{\varphi}$ is one-to-one. It follows that $\widetilde{\varphi}$ is a bijective mapping from the quotient group G/K to the subgroup $\operatorname{Im}\varphi$ of G'. Moreover, $\widetilde{\varphi}$ is a homomorphism, because

$$\widetilde{\varphi}((gK)(hK)) = \widetilde{\varphi}(ghK) = \varphi(gh) = \varphi(g)\varphi(h) = \widetilde{\varphi}(gK)\widetilde{\varphi}(hK).$$

Hence $\widetilde{\varphi}$ is an isomorphism from $G/\operatorname{Ker}\varphi$ to $\operatorname{Im}\varphi$. □

Definition A.18 An automorphism of a group G is an isomorphism from G to G. The set of all automorphisms on G, with multiplication defined by the composition of mappings, forms a group called the automorphism group of G and denoted by $\operatorname{Aut}(G)$. □

A.5 Permutations, Transformation Groups, and Orbits

Definition A.19 Let X be a non-empty set. The bijective mappings $f : X \to X$ are called permutations on X. The set of all permutations on X is denoted by S_X. □

Proposition A.20 *The set S_X of permutations on X, with multiplication defined by the composition of mappings, forms a group called the full symmetric group on X.*

Proof The composition of mappings clearly observes both the closure requirement and the associative law. The identity map $i_X : X \to X$ defined by $i_X(x) = x$, which is clearly a bijection, serves as the identity of the group. For each permutation f, its inverse in the group is the inverse function f^{-1}. □

Definition A.21 A transformation group on X is a subgroup of S_X. □

Let G be a transformation group on X and $g \in G$. Henceforth, for simplicity, we shall write gx for $g(x)$ when no confusion should arise. We define a relation G on X as follows.

Definition A.22 An element $x \in X$ is said to be $\mathbb{G}$-equivalent to y (i.e., $x \,\mathbb{G}\, y$) if there is a $g \in G$ such that $gx = y$. □

It is easy to verify that $\mathbb{G}$ is an equivalence relation on X. Indeed, we have (i) $x \,\mathbb{G}\, x$ for each $x \in X$, because i_X is the identity in G. (ii) If $x \,\mathbb{G}\, y$, then there is a $g \in G$ such that $gx = y$, which implies $g^{-1}y = x$, i.e., $y \,\mathbb{G}\, x$, as $g^{-1} \in G$. (iii) If $x \,\mathbb{G}\, y$ and $y \,\mathbb{G}\, z$, then $g_1 x = y$ and $g_2 y = z$ for some $g_1, g_2 \in G$. Then $(g_2 g_1)x = z$ and $g_2 g_1 \in G$, which implies $x \,\mathbb{G}\, z$.

We denote the $\mathbb{G}$-equivalence class by

$$G(x) = \{gx \in X : g \in G\}$$

and call it the G-orbit of x in X. By the property of equivalence relations, we can immediately write down the following lemma.

Lemma A.23 *X is a disjoint union of G-orbits.* □

Let $G_x = \{g \in G : gx = x\}$. Clearly G_x constitutes a subgroup of G, which we call the isotropy subgroup of G at x or the stabilizer of x.

Lemma A.24 *Let the transformation group G on X be finite. If x and y lie in the same G-orbit, then $|G_x| = |G_y|$.*

Proof Since x and y lie in the same G-orbit, there is some $g \in G$ such that $gx = y$. Let $h \in G_x$. Then $ghg^{-1} \in G_y$, because $ghg^{-1}(y) = ghg^{-1}(gx) = gh(x) = gx = y$. We claim that the mapping $f : G_x \longrightarrow G_y$ defined by $f(h) = ghg^{-1}$ is a bijection. In fact, that f is injective is obvious. To show that f is surjective, consider $s \in G_y$. Since $g^{-1}sg(x) = g^{-1}s(y) = g^{-1}(y) = x$, we see that $g^{-1}sg \in G_x$. Since $f(g^{-1}sg) = g(g^{-1}sg)g^{-1} = s$, we finish our proof. □

Proposition A.25 *Let the transformation group G on X be finite, and let $|G(x)|$ be the number of elements in the G-orbit of x in X. We have $|G(x)| = |G|/|G_x|$.*

Proof Consider the mapping $f : gx \mapsto gG_x$ from $G(x)$ to the set of left cosets of G_x in G. First we show that f is well defined. Indeed, if $g_1 x = g_2 x$, then $g_2^{-1} g_1 \in G_x$. Hence $g_2 G_x = g_2(g_2^{-1} g_1)G_x = g_1 G_x$. The mapping f is clearly surjective. Let us now proceed to show that f is injective. If $f(g_1 x) = f(g_2 x)$, then $g_1 G_x = g_2 G_x$, which implies $g_1 = g_2 h$ for some $h \in G_x$. Therefore $g_2^{-1} g_1 \in G_x$. It follow that $g_2^{-1} g_1 x = x$ or $g_1 x = g_2 x$. Since f is bijective, we conclude that $|G(x)|$ = number of left cosets of G_x in $G = (G : G_x) = |G|/|G_x|$, where we have appealed to (A.1). □

A.6 Direct Products and Semidirect Products

Definition A.26 Let G_1 and G_2 be groups. The direct product $G_1 \times G_2$ of G_1 and G_2 is the set of ordered pairs (g_1, g_2) endowed with group structure as follows. Multiplication is defined by

$$(g_1, g_2)(h_1, h_2) = (g_1 h_1, g_2 h_2) \qquad \text{for } g_1, h_1 \in G_1 \text{ and } g_2, h_2 \in G_2. \tag{A.7}$$

Associativity of multiplication in $G_1 \times G_2$ follows from that in G_1 and G_2. The identity in $G_1 \times G_2$ is (e_1, e_2), where e_1 and e_2 are the identity in G_1 and G_2, respectively. For each $(g_1, g_2) \in G_1 \times G_2$, its inverse is (g_1^{-1}, g_2^{-1}). □

The groups G_1 and G_2 can be identified with the subgroups of $G_1 \times G_2$ that consist of pairs of the form (g_1, e_2) and (e_1, g_2), respectively. Under this identification, the elements of G_1 commute with those of G_2.

Conversely, suppose G_1 and G_2 are subgroups of group G that satisfy what follows: (i) $G_1 G_2 = G$; (ii) $G_1 \cap G_2 = \{e\}$, where e is the identity of G; (iii) for each $g_1 \in G_1$ and $g_2 \in G_2$, $g_1 g_2 = g_2 g_1$. Then the map

$$\varphi : G_1 \times G_2 \to G, \qquad (g_1, g_2) \mapsto g_1 g_2$$

is an isomorphism. Indeed, for all $(g_1, g_2), (h_1, h_2) \in G_1 \times G_2$,

$$\varphi((g_1, g_2)(h_1, h_2)) = \varphi(g_1 h_1, g_2 h_2) = g_1 h_1 g_2 h_2 = g_1 g_2 h_1 h_2 = \varphi(g_1, g_2)\varphi(h_1, h_2);$$

hence φ is a homomorphism. If $\varphi(g_1, g_2) = e$, then $g_1 g_2 = e$, which implies $g_1 = g_2^{-1}$. But $g_1 \in G_1$ and $g_2^{-1} \in G_2$. It follows then from (ii) that $g_1 = g_2 = e$. Hence φ is injective. By (i), it is clear that φ is surjective. Therefore φ is an isomorphism. Thus we can identify G with $G_1 \times G_2$ and say that G is the direct product of its subgroups G_1, G_2.

Example A.27 Consider the orthogonal group O(3) and its subgroups SO(3) and $C_i = \{\boldsymbol{I}, \boldsymbol{\mathcal{I}}\}$, where $\boldsymbol{\mathcal{I}} = -\boldsymbol{I}$. Clearly $\mathrm{O}(3) = \mathrm{SO}(3) \times C_i$. □

When we discuss the Euclidean group in Sect. 2.2 and the symmorphic space groups in Sect. 2.10.3, we mention the notion of semidirect product of two groups. Here we give a formal definition.

Definition A.28 Let G be a group with subgroups H and K that satisfies the following requirements:

(i) All $g \in G$ can be written as $g = hk$ for some $h \in H$ and $k \in K$.
(ii) For each $k \in K$, $kHk^{-1} = H$.
(iii) $H \cap K = \{e\}$, where e is the identity in G.

Then G is said to be the semidirect product of H and K, and we write $G = H \wedge K$. □

Remark A.29 We adopt Definition A.28 for semidirect product from Bradley and Cracknell [42, p. 14]. There is another definition for semidirect product of two groups in the literature, where the semidirect product G of two groups H and K is constructed from the given groups and a homomorphism from K to the automorphism group Aut(H). See, e.g., [6, p. 133–134], [232, 14–15], where the reader will also find discussions on how one can arrive at Definition A.28 from the constructive approach. □

Appendix B

B Topology, Group Actions, and Strict Fundamental Domains

B.1 Basic Definitions in Topology

Definition B.1 A topology $\mathscr{T}$ on a set X is a collection of subsets of X which has the following three properties:

(i) $\emptyset \in \mathscr{T}$ and $X \in \mathscr{T}$.
(ii) If $\{U_\alpha\}$ is an arbitrary collections of members of $\mathscr{T}$, then $\bigcup_\alpha U_\alpha \in \mathscr{T}$.
(iii) If $U_i \in \mathscr{T}$ for $i = 1, \ldots, n$, then $U_i \cap \cdots \cap U_n \in \mathscr{T}$.

A set X for which a topology $\mathscr{T}$ has been specified is called a topological space. The members of $\mathscr{T}$ are called the open sets in X. □

Let $x \in X$. A neighborhood U of x is an open set that contains x. A subset E of X is said to be closed if $X \setminus E$ is open.

Definition B.2 A family $\mathscr{B} \subset \mathscr{T}$ is called a base of the topological space $(X, \mathscr{T})$ if every non-empty open set in X can be written as a union of a subfamily of sets in $\mathscr{B}$. □

It is easily verified that $\mathscr{B}$ is a base for $(X, \mathscr{T})$ if and only if for any $x \in X$ and any neighborhood U of x there is a $V \in \mathscr{B}$ such that $x \in V \subset U$.

Definition B.3 Let X and Y be topological spaces. A function $f : X \to Y$ is said to be continuous if $f^{-1}(V)$ is an open set in X for each open set V in Y. If the function f is bijective, and if both f and $f^{-1} : Y \to X$ are continuous, then f is said to be a homeomorphism. □

Remark B.4 Let $p : X \to Y$, where X is a topological space and Y a set, be surjective. Consider the collection $\mathfrak{Q} := \{V \subset Y : p^{-1}(V) \text{ is open in } X\}$ of subsets of Y. Since $p^{-1}(\emptyset) = \emptyset$, $p^{-1}(Y) = X$, and

$$p^{-1}\left(\bigcup_\alpha V_\alpha\right) = \bigcup_\alpha p^{-1}(V_\alpha), \qquad p^{-1}\left(\bigcap_{i=1}^n V_i\right) = \bigcap_{i=1}^n p^{-1}(V_i),$$

$\mathfrak{Q}$ is a topology on Y, which is called the quotient topology induced by p. When Y is endowed with the quotient topology, the map p is continuous and is called the quotient map. □

Definition B.5 A topological space X is called a Hausdorff space if for each pair x_1 and x_2 of distinct points in X, there are neighborhoods U_1 of x_1 and U_2 of x_2 such that $U_1 \cap U_2 = \emptyset$. □

A collection $\mathfrak{U} = \{U_\alpha\}$ of open subsets of a topological space X is said to cover X, or to be an open covering of X, if $\bigcup_\alpha U_\alpha = X$.

Definition B.6 A topological space X is said to be compact if every open covering $\mathfrak{U}$ of X contains a finite subcollection that also covers X. □

Remark B.7 There are two definitions of "compact topological space", which are extensively used in the mathematics literature. Definition B.6 is one, and the other requires the additional condition that the space in question satisfies the Hausdorff condition, i.e., X is compact if and only if it satisfies both Definitions B.5 and B.6. For the references cited in this exposition, e.g., Definition B.6 for compactness is adopted in [96, 116, 186, 242, 278], whereas Definition B.6 and the Hausdorff condition are required for compactness in [24, 25, 97, 102, 318]. □

B.1.1 Metric and Metrizable Spaces

Let X be a set. In Sect. 1.10 we have presented the definition of a distance function $d(\cdot, \cdot)$ on X. For $x, y \in X$, $d(x, y)$ gives the distance between x and y. Given $x \in X$ and a real number $\varepsilon > 0$, the set

$$B_d(x, \varepsilon) = \{y \in X : d(x, y) < \varepsilon\} \tag{B.1}$$

is called the ball centered at x with radius ε.

Definition B.8 Let X be a set endowed with a distance function d. The metric topology $\mathscr{T}_d$ induced by the distance function d on X is defined as follows: A set $U \subset X$ is open if and only if for each $x \in U$ there is an $\varepsilon > 0$ such that the $B_d(x, \varepsilon) \subset U$. □

By the triangle inequality for d, it is easily verified that each ball $B_d(x, \varepsilon)$, as defined in (B.1), is an open set in X. It follows then from the comment that follows Definition B.2 that the collection $\mathscr{B}_d$ of balls $B_d(x, \varepsilon)$, where $x \in X$ and $\varepsilon > 0$, constitutes a base for the metric topology $\mathscr{T}_d$ on X.

Definition B.9 A topological space X is said to be metrizable if a distance function d can be defined on X such that the metric topology induced by d is the same as the initial topology on X. A metric space is a metrizable space X with a specified distance function d that gives the topology of X. □

The next assertion is essentially the Urysohn metrization theorem (see, e.g., [97, p. 195], [242, p. 217]), as every compact Hausdorff space is regular (see, e.g., [97, p. 223], [242, p. 198]).

Theorem B.10 *Every compact Hausdorff space with a countable base is metrizable.* □

B.2 Action of a Finite Group on a Topological Space

In what follows we assume that G_{tex} is a finite rotation group and G_{cr} is a Type I crystallographic point group.

Definition B.11 Let X be a topological space and $K = \{k_1, \ldots, k_N\}$, where N is the order of K, be a finite group. A mapping $T : X \times K \to X$ (resp. $T : K \times X \to X$) is said to be a right (resp. left) action of the finite group K on X if the mapping T satisfies what follows:

(i) If e is the identity element of K, then

$$T(x, e) = x \quad (\text{resp. } T(e, x) = x) \qquad \text{for all } x \in X.$$

(ii) For each $k \in K$, the function $T_k : X \to X$ defined by $T_k(x) := T(x, k)$ (resp. $T_k(x) = T(k, x)$) is continuous.
(iii) If $k_i, k_j \in K$, then

$$T_{k_j} \circ T_{k_i} = T_{k_i k_j} \quad (\text{resp. } T_{k_j} \circ T_{k_i} = T_{k_j k_i}) \qquad \text{for all } x \in X. \qquad \square$$

By condition (iii), we observe for any right-action that $T_{k_j} \circ T_{k_i} = T_{k_i k_j}$, which implies $T_k \circ T_{k^{-1}} = T_{k^{-1}} \circ T_k = T_e$, i.e., the identity map on X by (i). Hence we have

$$T_{k^{-1}} = (T_k)^{-1} \qquad \text{for each } k \in K. \tag{B.2}$$

Clearly (B.2) can be shown to be valid for any left-action by a similar argument. It follows that for both right and left actions the map T_k is a bijection on X for each $k \in K$. Moreover, by condition (ii) and (B.2), $(T_k)^{-1}$ is continuous for each $k \in K$, and thence each T_k is a homeomorphism (i.e., T_k is bijective, and both T_k and $(T_k)^{-1}$ are continuous).

For $x \in X$, let $x/K = \{T_k(x) : k \in K\}$ be the orbit of x under the (right or left) action of K. Let $X/K = \{x/K : x \in X\}$ be the quotient set (i.e., the set of orbits), and let $\pi : X \to X/K$, $x \mapsto x/K$, be the natural surjection (or projection). We give X/K the quotient topology (see Remark B.4) that $U \subset X/K$ is open if and only if $\pi^{-1}(U)$ is open in X. Then the projection π is continuous, and we call X/K the quotient space.

Proposition B.12 *The projection $\pi : X \to X/K$ is an open mapping (i.e., $\pi(U)$ is open in X/K for each open $U \subset X$).*

Proof Let $U \subset X$ be open. Note that $\pi^{-1}(\pi(U)) = \bigcup_{k \in K} T_k(U)$. Since T_k is a homeomorphism, $T_k(U)$ is open in X and so is $\pi^{-1}(\pi(U))$. Therefore $\pi(U)$ is open in X/K. $\square$

In this exposition we are primarily interested in one right action and one left action:

1. $X = \mathrm{SO}(3)$, $K = G_{\mathrm{cr}} = \{\boldsymbol{P}_1, \ldots, \boldsymbol{P}_{N_{cr}}\}$, and the right action in question is $\mathcal{T}^{(\mathrm{cr})} : \mathrm{SO}(3) \times G_{\mathrm{cr}} \to \mathrm{SO}(3)$ defined by

$$\mathcal{T}^{(\mathrm{cr})}(\boldsymbol{R}, \boldsymbol{P}) = \mathcal{T}^{(\mathrm{cr})}_{\boldsymbol{P}}(\boldsymbol{R}) = \boldsymbol{R}\boldsymbol{P} \qquad \text{for each } \boldsymbol{R} \in \mathrm{SO}(3) \text{ and } \boldsymbol{P} \in G_{\mathrm{cr}}. \tag{B.3}$$

   In this case the orbit of $\boldsymbol{R}$ under the action $\mathcal{T}^{(\mathrm{cr})}$ is the left coset $\boldsymbol{R}G_{\mathrm{cr}} = \{\boldsymbol{R}\boldsymbol{P}_1, \ldots, \boldsymbol{R}\boldsymbol{P}_{N_{\mathrm{cr}}}\}$. Hence we will simply denote the orbits by $\boldsymbol{R}G_{\mathrm{cr}}$ instead of the generic notation $\boldsymbol{R}/G_{\mathrm{cr}}$. The quotient space is the orientation space $\mathrm{SO}(3)/G_{\mathrm{cr}}$. Note (see Sect. 1.10) that $\mathrm{SO}(3)$ is a metric space with distance function $d_{\mathrm{SO}(3)}(\cdot, \cdot)$ which satisfies $d_{\mathrm{SO}(3)}(\boldsymbol{R}\boldsymbol{P}, \boldsymbol{Q}\boldsymbol{P}) = d_{\mathrm{SO}(3)}(\boldsymbol{R}, \boldsymbol{Q})$ for all $\boldsymbol{R}, \boldsymbol{P}, \boldsymbol{Q} \in \mathrm{SO}(3)$. Hence for each $\boldsymbol{P}_i \in G_{\mathrm{cr}}$ the map $\mathcal{T}^{(\mathrm{cr})}_{\boldsymbol{P}_i} : \mathrm{SO}(3) \to \mathrm{SO}(3)$ is an isometry and an homeomorphism.
2. $X = \mathrm{SO}(3)/G_{\mathrm{cr}}$, $K = G_{\mathrm{tex}} = \{\boldsymbol{Q}_1, \ldots, \boldsymbol{Q}_{N_{\mathrm{tex}}}\}$, and we are concerned with the left action $\mathcal{T}^{(\mathrm{tex})} : G_{\mathrm{tex}} \times M \to M$, where $M := \mathrm{SO}(3)/G_{\mathrm{cr}}$, defined by

$$\mathcal{T}^{(\mathrm{tex})}(\boldsymbol{Q}, \boldsymbol{R}G_{\mathrm{cr}}) = \mathcal{T}^{(\mathrm{tex})}_{\boldsymbol{Q}}(\boldsymbol{R}G_{\mathrm{cr}}) = \boldsymbol{Q}\boldsymbol{R}G_{\mathrm{cr}} \qquad \text{for each } \boldsymbol{R}G_{\mathrm{cr}} \in M \text{ and } \boldsymbol{Q} \in G_{\mathrm{tex}}. \tag{B.4}$$

   We denote by $[\boldsymbol{R}G_{\mathrm{cr}}]$ and by M/G_{tex} the G_{tex}-orbit of $\boldsymbol{R}G_{\mathrm{cr}}$ and the space of G_{tex}-orbits in M, respectively. The orientation space M is a metric space with distance function d_M defined in (6.35). It follows easily from this definition of d_M that for each $\boldsymbol{Q}_i \in G_{\mathrm{tex}}$ the map $\mathcal{T}^{(\mathrm{tex})}_{\boldsymbol{Q}_i} : M \to M$ is an isometry and an homeomorphism.

B.3 Existence of Strict Fundamental Domain

Let X be a topological space, K a finite group, and T a right or left action of K on X. Let X/K be the space of K-orbits, and $\pi : X \to X/K$ the natural surjection.

Definition B.13 A right or left action T of K on X is said to be properly discontinuous[178] if it satisfies the following condition:

– Each element $x \in X$ has a neighborhood U_x of x such that $T_k(U_x) \cap U_x = \emptyset$ for each $k \in K$ except $k = e$, the identity in K. □

Lemma B.14 *If the action T of finite group K on X is properly discontinuous, then the natural surjection π is a local homeomorphism.*

Proof Let $x \in X$. By hypothesis and Definition B.13, there is a neighborhood U_x of x such that $T_k(U_x) \cap U_x = \emptyset$ for $k \neq e \in K$. We claim that the restriction $\pi|_{U_x} : U_x \to X/K$ be injective. To see this, let $x_1, x_2 \in U_x$ and $\pi(x_1) = \pi(x_2)$. Then $x_2 \in \pi^{-1}(\pi(x_1))$, which implies $x_2 \in T_k(x_1)$ for some $k \in K$. Since $x_2 \in U_x$, we conclude that $x_2 \in T_e(x_1)$ and $x_2 = x_1$.

By abuse of language, let us still denote by $\pi|_{U_x}$ the map that results when the range of $\pi|_{U_x}$ is restricted to its image $\pi(U_x)$. Then the map $\pi|_{U_x}$ is bijective. Since π is continuous, $\pi|_{U_x}$ is continuous. That $(\pi|_{U_x})^{-1}$ is continuous is a consequence of Proposition B.12. □

The following definition is adapted from [179, p. 96].

Definition B.15 A subset $\mathcal{F} \subset X$ is said to be a strict fundamental domain in X for X/K if

(i) the restriction $\pi|_{\mathcal{F}} : \mathcal{F} \to X/K$ is bijective;
(ii) $\mathcal{F}$ is a Borel set in X. □

The proof of the following theorem is adapted from that of a similar theorem in [179, pp. 96–97].

Theorem B.16 *Let the topological space X be compact. If the action T of finite group K on X is properly discontinuous, there exists a strict fundamental domain $\mathcal{F}$ in X for the orbit space X/K.*

Proof By Lemma B.14, each $x \in X$ has a neighborhood U_x such that $\pi|_{U_x} : U_x \to \pi(U_x)$ is bijective. The family $\{U_x : x \in X\}$ provides an open covering of X. Since G is compact, there is a finite subfamily, which we denote by $\{U_i : i = 1, \ldots, N\}$ such that $\bigcup_{i=1}^{N} U_i = G$. For $i = 1, \ldots, N$, let

$$F_i = U_i \setminus U_i \cap \pi^{-1}(\pi(U_1 \cup \cdots \cup U_{i-1})). \tag{B.5}$$

Writing out (B.5) for $i = 1, 2, \ldots$, and N, we have

$$F_1 = U_1, \quad F_2 = U_2 \setminus U_2 \cap \pi^{-1}(\pi(U_1)), \quad \ldots, \quad F_N = U_N \setminus U_N \cap \pi^{-1}(\pi(U_1 \cup \cdots \cup U_{N-1})). \tag{B.6}$$

[178] Cf. [50, p. 98], [71, p. 22].

We claim that $\mathcal{F} := F_1 \cup \cdots \cup F_N$ is a strict fundamental domain in G for G/K. To prove this claim, we have to show that (i) the restriction $\pi|_{\mathcal{F}} : \mathcal{F} \to G/K$ is bijective and (ii) $\mathcal{F}$ is a Borel set (see Definition C.2). Let us start with (ii), as proving it is straightforward. Note that each F_i is the set difference of two open sets; hence it is a Borel set. It follows that $\mathcal{F}$, which is the union of a finite number of Borel sets, is itself a Borel set.

Let us proceed to prove (i). Since $\pi|_{U_i}$ is injective and $F_i \subset U_i$, from (B.5) we have

$$\pi(F_i) = \pi(U_i) \setminus \pi(U_i) \cap \pi(U_1 \cup \cdots \cup U_{i-1}) = \pi(U_i) \setminus \pi(U_i) \cap (\pi(U_1) \cup \cdots \cup \pi(U_{i-1})). \tag{B.7}$$

Given two sets A and B, there holds the identity $A \cup B = A \cup (B \setminus (B \cap A))$. Applying the preceding set identity repeatedly and using (B.7) for various i, we obtain

$$\begin{aligned}
\pi(F_1) \cup \pi(F_2) &= \pi(U_1) \cup (\pi(U_2) \setminus (\pi(U_2) \cap \pi(U_1)) \\
&= \pi(U_1) \cup \pi(U_2), \\
(\pi(F_1) \cup \pi(F_2)) \cup \pi(F_3) &= (\pi(U_1) \cup \pi(U_2)) \cup (\pi(U_3) \\
&\qquad \setminus (\pi(U_3) \cap (\pi(U_1) \cup \pi(U_2))) \\
&= (\pi(U_1) \cup \pi(U_2)) \cup \pi(U_3),
\end{aligned}$$

etc., which can be written as

$$\pi(F_1) \cup \pi(F_2) \cup \cdots \cup \pi(F_i) = \pi(U_1) \cup \pi(U_2) \cup \cdots \cup \pi(U_i) \tag{B.8}$$

for $i = 1, 2, \ldots, N$. In particular, equation (B.8) for $i = N$ implies

$$\pi(\mathcal{F}) = \pi(F_1 \cup F_2 \cup \cdots \cup F_N) = \pi(U_1 \cup U_2 \cup \cdots \cup U_N) = \pi(G) = G/K. \tag{B.9}$$

Hence the function $\pi|_{\mathcal{F}} : \mathcal{F} \to G/K$ is surjective.

Substituting (B.8) into (B.7), we see that for $i = 2, \ldots, N$,

$$\pi(F_i) = \pi(U_i) \setminus \pi(U_i) \cap (\pi(F_1) \cup \cdots \cup \pi(F_{i-1})). \tag{B.10}$$

Hence $\pi(F_i) \cap (\pi(F_1) \cup \cdots \cup \pi(F_{i-1})) = \emptyset$ for $i = 2, \ldots, N$, which implies that the sets $\pi(F_i)$ are pairwise disjoint. Since $\pi|_{F_i}$ is injective for all i, the map $\pi|_{\mathcal{F}}$ is injective. Thus $\pi|_{\mathcal{F}}$ is bijective, and $\mathcal{F}$ is a strict fundamental domain. □

In what follows we assume that G_{tex} is a finite rotation group and G_{cr} a Type I crystallographic point group. Let $G_{\text{tex}} = \{\boldsymbol{Q}_1, \boldsymbol{Q}_2, \ldots, \boldsymbol{Q}_{N_{\text{tex}}}\}$ and $G_{\text{cr}} = \{\boldsymbol{P}_1, \boldsymbol{P}_2, \ldots, \boldsymbol{P}_{N_{\text{cr}}}\}$, where $\boldsymbol{Q}_1 = \boldsymbol{I}$, $\boldsymbol{P}_1 = \boldsymbol{I}$, $N_{\text{tex}} = |G_{\text{tex}}|$, and $N_{\text{cr}} = |G_{\text{cr}}|$.

Lemma B.17 *The actions $\mathcal{T}^{(\text{cr})}$ and $\mathcal{T}^{(\text{tex})}$, as defined by (B.3) and (B.4), respectively, are properly discontinuous.*

Proof Consider first the right action $\mathcal{T}^{(\text{cr})} : \text{SO}(3) \times G_{\text{cr}} \to \text{SO}(3)$. The rotation group SO(3) is a metric space with distance function $d_{\text{SO}(3)}$ defined by (1.137), and the map $\mathcal{T}^{(\text{cr})}_{\boldsymbol{P}_i} : \boldsymbol{R} \mapsto \boldsymbol{R}\boldsymbol{P}_i$ is an isometry of SO(3) for each $\boldsymbol{P}_i \in G_{\text{cr}}$.

Let $\boldsymbol{R} \in \text{SO}(3)$. Consider the set $A := \{\boldsymbol{R}\boldsymbol{P}_i : i = 1, \ldots, N_{\text{cr}}\}$ of points in SO(3). Choose $\varepsilon > 0$ such that 2ε is smaller than the shortest of the distances between $\boldsymbol{R}$ and $\boldsymbol{R}\boldsymbol{P}_i$ for $\boldsymbol{P}_i \neq \boldsymbol{I}$. Let $U_{\boldsymbol{R}} \subset \text{SO}(3)$ be the open ball of radius ε centered at $\boldsymbol{R}$. Then $U_{\boldsymbol{R}}\boldsymbol{P}_i$ is a ball of

radius ε centered at $\boldsymbol{P}_i$. Hence $U_{\boldsymbol{R}}\boldsymbol{P}_i \cap U_{\boldsymbol{R}} = \emptyset$ for all $\boldsymbol{P}_i \neq \boldsymbol{I}$. Therefore the right action $\mathcal{T}^{(\mathrm{cr})}$ is properly discontinuous.

The orientation space $M := \mathrm{SO}(3)/G_{\mathrm{tex}}$ is a metric space with distance function d_M defined by (6.35), and the map $\mathcal{T}^{(\mathrm{tex})}_{\boldsymbol{Q}_i} : \boldsymbol{R}G_{\mathrm{cr}} \mapsto \boldsymbol{Q}_i\boldsymbol{R}G_{\mathrm{cr}}$ is an isometry on M for each $\boldsymbol{Q}_i \in G_{\mathrm{tex}}$. Hence we can similarly prove that the left action $\mathcal{T}^{(\mathrm{tex})}$ is properly discontinuous. □

Gathering Theorem B.16 and Lemma B.17, we immediately obtain the following proposition.

Proposition B.18 *There exists a strict fundamental domain in* $\mathrm{SO}(3)$ *for the orientation space* $M := \mathrm{SO}(3)/G_{\mathrm{cr}}$ *and in* M *for the space of* G_{tex}*-orbits* M/G_{tex}*, respectively.* □

A slight modification of the argument given in the proof of Lemma B.17 leads to a proof of the following proposition.

Proposition B.19 *Let* $M = \mathrm{SO}(3)/G_{\mathrm{cr}}$ *be the orientation space. The space* M/G_{tex} *of* G_{tex}*-orbits of orientations is a Hausdorff space.*

Proof Let $\boldsymbol{R}G_{\mathrm{cr}}$ and $\boldsymbol{R}'G_{\mathrm{cr}}$ be two orientations in M such that $\boldsymbol{R}'G_{\mathrm{cr}} \notin [\boldsymbol{R}G_{\mathrm{cr}}]$. We claim that there are neighborhoods $U_{\boldsymbol{R}G_{\mathrm{cr}}}$ and $U_{\boldsymbol{R}'G_{\mathrm{cr}}}$ of $\boldsymbol{R}G_{\mathrm{cr}}$ and $\boldsymbol{R}'G_{\mathrm{cr}}$, respectively, such that $U_{\boldsymbol{R}G_{\mathrm{cr}}} \cap \boldsymbol{Q}U_{\boldsymbol{R}'G_{\mathrm{cr}}} = \emptyset$ for all $\boldsymbol{Q} \in G_{\mathrm{tex}}$. To prove the claim, choose $\varepsilon > 0$ such that $2\varepsilon < \min_{\boldsymbol{Q}\in G_{\mathrm{tex}}}\{d_M(\boldsymbol{R}G_{\mathrm{cr}}, \boldsymbol{Q}\boldsymbol{R}'G_{\mathrm{cr}})\}$. Let $U_{\boldsymbol{R}G_{\mathrm{cr}}}$ (resp. $U_{\boldsymbol{R}'G_{\mathrm{cr}}}$) be the open ball with center $\boldsymbol{R}G_{\mathrm{cr}}$ (resp. $\boldsymbol{R}'G_{\mathrm{cr}}$) and radius ε. Then $U_{\boldsymbol{R}G_{\mathrm{cr}}} \cap \boldsymbol{Q}U_{\boldsymbol{R}'G_{\mathrm{cr}}} = \emptyset$ for all $\boldsymbol{Q} \in G_{\mathrm{tex}}$.

Note that $\hat{\pi} : M \to M/G_{\mathrm{tex}}$, $\boldsymbol{R}G_{\mathrm{cr}} \mapsto [\boldsymbol{R}G_{\mathrm{cr}}]$, is a continuous open surjection. Hence $\hat{\pi}(U_{\boldsymbol{R}G_{\mathrm{cr}}})$ and $\hat{\pi}(U_{\boldsymbol{R}'G_{\mathrm{cr}}})$ are neighborhoods of $[\boldsymbol{R}G_{\mathrm{cr}}]$ and $[\boldsymbol{R}'G_{\mathrm{cr}}]$, respectively. Moreover, we have $\hat{\pi}(U_{\boldsymbol{R}G_{\mathrm{cr}}}) \cap \hat{\pi}(U_{\boldsymbol{R}'G_{\mathrm{cr}}}) = \emptyset$. □

Appendix C

C Measures and Quotient Measures

C.1 Basic Definitions in Measure Theory and Probability

Definition C.1 A collection $\mathfrak{M}$ of subsets of a set X is called a σ-algebra in X if it has the following three properties:

(i) $X \in \mathfrak{M}$.
(ii) If $A \in \mathfrak{M}$, then $A^c := X \setminus A \in \mathfrak{M}$.
(iii) If $A = \bigcup_{n=1}^{\infty} A_n$ and if $A_n \in \mathfrak{M}$ for $n = 1, 2, 3, \ldots$, then $A \in \mathfrak{M}$.

If a σ-algebra $\mathfrak{M}$ in X has been specified, then X (or the ordered pair $(X, \mathfrak{M})$) is called a measurable space, and the members of $\mathfrak{M}$ are the measurable sets in X. □

What follows are immediate consequences of properties (i) through (iii) of $\mathfrak{M}$:

(a) $\emptyset = X \setminus X \in \mathfrak{M}$.
(b) Putting $A_m = \emptyset$ for $m \geq n + 1$ in (iii), we see that $A_1 \cup \cdots \cup A_n \in \mathfrak{M}$ if $A_i \in \mathfrak{M}$ for $1 \leq i \leq n$.
(c) Since $\bigcap_{n=1}^{\infty} A_n = \left(\bigcup_{n=1}^{\infty} A_n^c\right)^c$, by (ii), (iii) and (b) we see that the σ-algebra $\mathfrak{M}$ is closed under countable and finite intersections.
(d) If $A \in \mathfrak{M}$ and $B \in \mathfrak{M}$, then $A \setminus B = A \cap B^c \in \mathfrak{M}$.

Let $\mathfrak{H}$ be any collection of subsets of X. There exists (see, e.g., [278, p. 12]) a smallest σ-algebra $\mathfrak{M}$ in X such that $\mathfrak{H} \subset \mathfrak{M}$. The adjective "smallest" here means that if $\mathfrak{M}^*$ is any σ-algebra in X which satisfies $\mathfrak{H} \subset \mathfrak{M}^*$, then $\mathfrak{M} \subset \mathfrak{M}^*$.

Definition C.2 Let X be a topological space. We denote by $\mathfrak{B}$ the smallest σ-algebra in X that contains all the open sets in X. The members of $\mathfrak{B}$ are called the Borel sets of X. □

In Part I we are mainly interested in the orientation spaces SO(3) ($G_{\text{tex}} = \{\boldsymbol{I}\}$, $G_{\text{cr}} = \{\boldsymbol{I}\}$), SO(3)/$G_{\text{cr}}$ ($G_{\text{tex}} = \{\boldsymbol{I}\}$, $G_{\text{cr}} \neq \{\boldsymbol{I}\}$), and the space of G_{tex}-orbits of orientations (SO(3)/(G_{cr})/G_{tex} ($G_{\text{tex}} \neq \{\boldsymbol{I}\}$), which are all topological spaces. For each of these spaces, we take its Borel sets as the measurable sets.

Definition C.3 Let X be a measurable space and $\mathfrak{M}$ the σ-algebra of its measurable sets. A finite positive measure on X is a map $\mu : \mathfrak{M} \to [0, \infty)$ which is countably additive: if $\{A_i\}$ is a disjoint countable collection of members of $\mathfrak{M}$, then

$$\mu\left(\bigcup_{i=1}^{\infty} A_i\right) = \sum_{i=1}^{\infty} \mu(A_i). \tag{C.1}$$

The ordered triple $(X, \mathfrak{M}, \mu)$ (or simply X when the σ-algebra and measure in question is understood) is called a measure space. □

Note that according to Definition C.3 a map $\mu : \mathfrak{M} \to [0, \infty)$ defined by $\mu(A) = 0$ for each $A \in \mathfrak{M}$ is a finite positive measure.

The following properties of measure μ follow easily from its definition:

(*a*) In (C.1), put $A_1 = A$ and $A_i = \emptyset$ for $i \geq 2$. It follows that $\mu(\emptyset) = 0$.

(*b*) In (C.1), put $A_i = \emptyset$ for $i > n$. Then (C.1) reduces to the form

$$\mu(A_1 \cup \cdots \cup A_n) = \mu(A_1) + \cdots + \mu(A_n) \qquad \text{if } A_1, \ldots, A_n \in \mathfrak{M} \text{ are pairwise disjoint.} \tag{C.2}$$

(*c*) Let $A \in \mathfrak{M}$, $B \in \mathfrak{M}$, and $A \subset B$. Then $B = A \cup (B \setminus A)$ and $A \cap (B \setminus A) = \emptyset$. It follows from (*b*) that $\mu(B) = \mu(A) + \mu(B \setminus A) \geq \mu(A)$.

(*d*) It follows from (*c*) that $\mu(A) \leq \mu(X)$ for each $A \in \mathfrak{M}$.

In this exposition we are mainly interested in the special case where X is a compact Hausdorff space.

Definition C.4 A finite positive measure defined on the Borel σ-algebra $\mathfrak{B}$ in a compact Hausdorff space X is called a Borel measure on X. □

Definition C.5 Let λ and μ be two positive finite measures on a measurable space X with σ-algebra $\mathfrak{M}$. The measure λ is said to be absolutely continuous with respect to the measure μ if $\lambda(A) = 0$ for each $A \in \mathfrak{M}$ for which $\mu(A) = 0$. □

Definition C.6 A finite positive measure μ on a set X is said to be a probability measure if $\mu(X) = 1$. □

Definition C.7 A measure space $(\Omega, \mathfrak{M}, P)$ is called a probability space if P is a probability measure. The set Ω is called a sample space, and each measurable set in $\mathfrak{M}$ is called an event. □

C.2 Radon Measures and the Riesz Representation Theorem

Let X be a compact metric or metrizable space, and let $\mathscr{C}(X) := \mathscr{C}(X, \mathbb{R})$ be the space of real-valued continuous functions defined on X. A function $\mu : \mathscr{C}(X) \to \mathbb{R}$ is called a positive linear functional on $\mathscr{C}(X)$ if it satisfies the following conditions: (i) $\mu(f) \geq 0$ if $f \geq 0$; (ii) $\mu(c_1 f_1 + c_2 f_2) = c_1 \mu(f_1) + c_2 \mu(f_2)$ for any $c_1, c_2 \in \mathbb{R}$ and $f_1, f_2 \in \mathscr{C}(X)$. While we are working in a much simpler context, we follow the French school (cf. [38, 89, 318]) and call positive linear functionals on $\mathscr{C}(X)$ Radon measures.

The name "Radon measure", however, has also been used in another sense in the literature. These two usages are related through the Riesz representation theorem.

Theorem C.8 (Riesz representation theorem I) *Let X be a compact metric or metrizable space. For each positive linear functional μ on $\mathscr{C}(X)$, there is a unique finite, positive Borel measure $\breve{\mu}$ on X such that*

$$\mu(f) = \int_X f \, d\breve{\mu} \qquad \textit{for each } f \in \mathscr{C}(X). \tag{C.3}$$

Proof See Taylor [311, p. 183] and Remark C.10. This version of the Riesz representation theorem was first derived by Banach [17]. Saks [281] gave an elementary proof of this theorem in 1938. See Diestel and Spasbury [88, Chap. 4] for an exposition of Banach's approach to the Lebesgue integral in abstract spaces, which includes also a presentation of Saks's proof. □

Remark C.9 In (C.3) we call μ on the left-hand side the Radon measure and $\breve{\mu}$ on the right-hand side the representing Borel measure. But it is also common to call Borel measures which satisfy various regularity conditions[179] "Radon measures" (see, e.g., [25, p. 155], [116, p. 212]) or "regular Borel measures" (see, e.g., [278, p. 47], [311, p. 183]). On a compact metrizable space, every finite Borel measure is regular and is a Radon measure in this sense [25, p. 158]. Hence, according to this nomenclature, the representing Borel measure $\breve{\mu}$ on the right-hand side of (C.3) is the Radon measure that represents the positive linear functional μ on the left-hand side. □

Theorem C.8 indicates that the map $\mu \mapsto \breve{\mu}$ from Radon measures (or positive linear functionals on $\mathscr{C}(X)$) to the representing Borel measures is a bijection. But more can be said about the relationship. Since X is compact, the linear space $\mathscr{C}(X)$ is a Banach space under the supremum norm $\|f\| = \sup\{|f(x)| : x \in X\}$. Moreover, by C.3 we have $|\mu(f)| \leq \breve{\mu}(X)\|f\|$ for $f \in \mathscr{C}(X)$. Hence each positive linear functional μ on $\mathscr{C}(X)$ is bounded, i.e., $\mu \in \mathscr{C}(X)^*$, the dual space of $\mathscr{C}(X)$.

Theorem C.8 can be extended so that for each $\rho \in \mathscr{C}(X)^*$ there is a unique finite, signed Borel measure $\breve{\rho}$ on X such that (C.3) holds with ρ and $\breve{\rho}$ replacing μ and $\breve{\mu}$, respectively; see Taylor [311, p. 185]. Moreover, $\mathscr{C}(X)^*$ is a Banach space with the operator norm $\|\rho\| := \sup\{|\rho(f)| : \|f\| = 1, f \in \mathscr{C}(X)\}$. The linear space $\mathscr{M}(X)$ of finite signed Borel measures is a Banach space with the norm $\|\breve{\rho}\| := |\breve{\rho}|(X)$, where $|\breve{\rho}|$ is the total variation of $\breve{\rho}$. The map $\rho \mapsto \breve{\rho}$ from $\mathscr{C}(X)^*$ to $\mathscr{M}(X)$ is an isometric isomorphism.

When X is a metric or metrizable space, we shall generally identify each positive linear functional $\mu \in \mathscr{C}(X)^*$ with its representing Borel measure $\breve{\mu} \in \mathscr{M}(X)$, rewrite (C.3) as

$$\langle \mu, f \rangle = \int_X f \, d\mu \qquad \text{for each } f \in \mathscr{C}(X), \tag{C.4}$$

and call μ on both sides of (C.4) a Radon measure. For example, the Dirac measure δ_x, where $x \in X$, stands both for the element in $\mathscr{C}(X)^*$ such that $\langle \delta_x, f \rangle = f(x)$ for each $f \in \mathscr{C}(X)$ and for the Borel measure defined by $\delta_x(A) = 1$ if $x \in A$ and $\delta_x(A) = 0$ if $x \notin A$ for each Borel set $A \subset X$. Whether a Radon measure μ stands for an element of $\mathscr{C}(X)^*$ or its representing Borel measure on X should be clear from the context. On occasions, however, for historical reasons or for clarity (e.g., when we talk about Haar functionals) we shall use different symbols to denote a positive linear functional and its representing (regular) Borel measure.

Remark C.10 The restrictive context of Riesz representation theorem I, which covers the specific cases that concern us (i.e., $X = \mathrm{SO}(3)$, $\mathrm{O}(3)$, $\mathrm{SO}(3)/G_{\mathrm{cr}}$, or $(\mathrm{SO}(3)/G_{\mathrm{cr}})/G_{\mathrm{tex}}$), makes the theorem much simpler both in its statement and in its proof than the more general version commonly presented in graduate texts (see, e.g., [25, 116, 278]), where X is a locally compact Hausdorff space and the space $\mathscr{C}(X)$ is replaced by $\mathscr{C}_c(X)$, the space of continuous functions with compact support. Bauer [25, pp. 184–185], however, presents a theorem which shows that the representing Borel measure is unique if the locally compact Hausdorff space X has a countable base. That theorem clearly covers Theorem C.8 as a special case, as every compact Hausdorff space with a countable base is metrizable (cf. Theorem B.10). □

[179] The regularity conditions required for a Borel measure to be called "Radon measure" could differ from one author to another. For definiteness, in our present contexts (where X is a compact metric space in Theorem C.8 and a compact Hausdorff space in Theorem C.11) we equate "Radon measure" in this sense to "regular Borel measure", where "regular" means "inner regular" and "outer regular"; see Bauer [25, pp. 153–154] or Rudin [278, p. 47] for definitions of "inner regular" and "outer regular".

When we discuss Haar measure on compact groups in Sect. C.3, we shall appeal to a version of Riesz representation theorem as follows.

Theorem C.11 (Riesz representation theorem II) *Let X be a compact Hausdorff space. For each positive linear functional μ on $\mathscr{C}(X)$, there is a unique finite positive, regular Borel measure $\breve{\mu}$ on X such that*

$$\mu(f) = \int_X f \, d\breve{\mu} \qquad \text{for each } f \in \mathscr{C}(X). \tag{C.5}$$

Proof See Bauer [25, Theorem 29.1, 29.3, and Corollary 29.7]. While Bauer focuses on a more general setting (cf. Remark C.10), the cited theorems and corollary together cover what we call Riesz Representation Theorem II. □

When X is a compact Hausdorff space, there is at least one but may be more than one finite positive Borel measure on X that represents a positive linear functional μ on X in the sense of (C.5). The set of representing finite positive Borel measures, however, always contains one and only member that is regular.

C.3 Topological Groups, Compact Groups, and Haar Measure

Definition C.12 Let G be a set that is both a group and a topological space. We call G a topological group if it satisfies the following requirements:

(i) the mapping $(g, h) \mapsto gh$ of $G \times G$ (with the product topology) onto G is continuous;
(ii) the mapping $g \mapsto g^{-1}$ of G onto G is continuous;
(iii) G is a Hausdorff space. □

Condition (iii) is often replaced by some other requirement which is weaker than (iii) for general topological spaces but is equivalent to it for topological groups (see, e.g. [227, p. 111], [261, pp. 52, 96]). Some authors (e.g., [149], [279, p. 128]) keep only conditions (i) and (ii) in their definition of topological groups but add a general requirement equivalent to (iii) for the classes of topological groups they consider.

It follows immediately from (i) that for $a \in G$ the left and right translations by a, i.e., the maps $g \mapsto ag$ and $g \mapsto ga$, are homeomorphisms on G. Likewise by (ii) the inversion $g \mapsto g^{-1}$ is a homeomorphism on G.

Definition C.13 A topological group G which is compact as a topological space is called a compact topological group or, simply, a compact group. □

Let G be a compact group, and let $\mathscr{C}(G)$ be the space of real-valued continuous functions defined on G. Let $\mathscr{L}_s : \mathscr{C}(G) \to \mathscr{C}(G)$ (resp. $\mathscr{R}_s : \mathscr{C}(G) \to \mathscr{C}(G)$) be defined for each $s \in G$ by

$$\mathscr{L}_s f(g) = f(s^{-1}g) \qquad (\text{resp. } \mathscr{R}_s f(g) = f(gs)) \qquad \text{for each } f \in \mathscr{C}(G) \text{ and } g \in G. \tag{C.6}$$

Let $\mathscr{J} : G \to G$ be defined by $\mathscr{J}(g) = g^{-1}$.

Theorem C.14 *Let G be a compact group. There is a unique positive linear functional $I : \mathscr{C}(G) \to \mathbb{R}$ which satisfies the normalization condition $I(1) = 1$ and is*:

(1) *left-invariant, i.e.*, $I(\mathscr{L}_s f) = I(f)$, *for each* $s \in G$ *and* $f \in \mathscr{C}(G)$;
(2) *right-invariant, i.e.*, $I(\mathscr{R}_s f) = I(f)$, *for each* $s \in G$ *and* $f \in \mathscr{C}(G)$;
(3) *inverse-invariant, i.e.*, $I(f \circ \mathscr{J}) = I(f)$, *for each* $f \in \mathscr{C}(G)$.

The positive linear functional I *is called the normalized Haar functional on* $\mathscr{C}(G)$. □

In 1935 von Neumann [328] published an elementary proof of Theorem C.14. See [88, Chap. 5] and [261, pp. 192–199] for expositions. The proof presented by Rudin [279, pp. 130–132] is "essentially that of von Neumann" [279, p. 403] but is shorter because more advanced tools are used.

Let $A \subset G$. We define $A^{-1} := \{g^{-1} \in G : g \in A\}$. For $s \in G$, let $sA := \{sg \in G : g \in A\}$, and $As := \{gs : g \in A\}$. The following corollary follows immediately from Theorem C.11 (i.e., Riesz representation theorem II) and Theorem C.14.

Corollary C.15 *On each compact group* G *there is a unique finite positive regular Borel probability measure* g *which satisfies the normalization condition* $\mathsf{g}(G) = 1$ *and is*:

(i) *left-invariant, i.e.*, $\mathsf{g}(sA) = \mathsf{g}(A)$ *for each* $s \in G$ *and each Borel set* $A \subset G$;
(ii) *right-invariant, i.e.*, $\mathsf{g}(As) = \mathsf{g}(A)$ *for each* $s \in G$ *and each Borel set* $A \subset G$;
(iii) *inverse-invariant, i.e.*, $\mathsf{g}(A^{-1}) = \mathsf{g}(A)$ *for each Borel set* $A \subset G$.

This measure g *is called the normalized Haar measure of* G. □

C.4 Quotient Measure

The definition of quotient measure is based on the following proposition.

Proposition C.16 *Let* X *and* Y *be topological spaces with Borel* σ*-algebras* $\mathfrak{B}_X$ *and* $\mathfrak{B}_Y$, *respectively. Let* μ *be a finite positive measure on* X, *and let* $p : X \to Y$ *be a continuous surjective map.*

(i) *Let* E *be a Borel set in* Y. *Then* $p^{-1}(E)$ *is a Borel set in* X.
(ii) *Let* $\nu : \mathfrak{B}_Y \to [0, \infty)$ *be defined by* $\nu(E) = \mu(p^{-1}(E))$ *for each Borel set* E *in* $\mathfrak{B}_Y$. *Then* ν *is a finite positive measure on* Y.

Proof (i) Let $\Omega = \{A \subset Y : p^{-1}(A) \in \mathfrak{B}_X\}$. We claim that Ω is a σ-algebra in Y. Indeed we have $p^{-1}(Y) = X \in \mathfrak{B}_X$, which implies $Y \in \Omega$. Let $A \in \Omega$. Then $p^{-1}(Y \setminus A) = X \setminus p^{-1}(A) \in \mathfrak{B}_X$. Hence $Y \setminus A \in \Omega$. Finally, let $\{A_\alpha\}$ be a family of subsets of Y such that each $A_\alpha \in \Omega$. Then $p^{-1}(\bigcup_\alpha A_\alpha) = \bigcup_\alpha p^{-1}(A_\alpha) \in \mathfrak{B}_X$. Therefore $\bigcup_\alpha A_\alpha \in \Omega$.

For each open set V in Y, $p^{-1}(V)$ is open in X as p is continuous, so $p^{-1}(V) \in \mathfrak{B}_X$ and thence $V \in \Omega$. Therefore Ω is a σ-algebra in Y that contains all the open sets in Y, which implies $\mathfrak{B}_Y \subset \Omega$. Let $E \in \mathfrak{B}_Y$. Then $E \in \Omega$ and, by definition of Ω, $p^{-1}(E) \in \mathfrak{B}_X$.

(ii) It suffices to show that ν is countably additive. Let $\{E_n\}$ be a family of disjoint Borel sets in Y. Then $\{p^{-1}(E_n)\}$ is a family of disjoint Borel sets in X. Since

$$\nu\left(\bigcup_{n=1}^{\infty} E_n\right) = \mu\left(p^{-1}\left(\bigcup_{n=1}^{\infty} E_n\right)\right) = \mu\left(\bigcup_{n=1}^{\infty} p^{-1}(E_n)\right) = \sum_{n=1}^{\infty} \mu\left(p^{-1}(E_n)\right) = \sum_{n=1}^{\infty} \nu(E_n),$$

ν is countably additive. □

Let G be a Type I crystallographic point group and G_{tex} a finite rotation group. We are primarily interested in two specific cases covered by Proposition C.16 as follows:

1. $X = \mathrm{SO}(3)$, Y is the orientation space $\mathrm{SO}(3)/G_{\mathrm{cr}}$, and p is the natural surjection $\pi : \mathrm{SO}(3) \to \mathrm{SO}(3)/G_{\mathrm{cr}}$, $\boldsymbol{R} \mapsto \boldsymbol{R}G_{\mathrm{cr}}$. The measure on $\mathrm{SO}(3)$ (denoted by μ in Proposition C.16) is the bi-invariant volume measure $\mathcal{V}$. We denote by $\hat{\mathcal{V}}$ (in place of ν) the measure on the quotient space $\mathrm{SO}(3)/G_{\mathrm{cr}}$ delivered by Proposition C.16, and we call it the quotient measure. Note that

$$\hat{\mathcal{V}}(\hat{A}) = \mathcal{V}(\pi^{-1}(\hat{A})) \qquad \text{for each Borel set } \hat{A} \subset \mathrm{SO}(3)/G_{\mathrm{cr}}. \tag{C.7}$$

   For each continuous function $\hat{f} : \mathrm{SO}(3)/G_{\mathrm{cr}} \to \mathbb{R}$ and $f = \hat{f} \circ \pi$, we have

$$\int_{\hat{A}} \hat{f}(\boldsymbol{R}G_{\mathrm{cr}})\, d\hat{\mathcal{V}}(\boldsymbol{R}G_{\mathrm{cr}}) = \int_{\pi^{-1}(\hat{A})} f(\boldsymbol{R})\, d\mathcal{V}(\boldsymbol{R}). \tag{C.8}$$

2. $X = \mathrm{SO}(3)/G_{\mathrm{cr}}$, Y is the texture-symmetrized orientation space $(\mathrm{SO}(3)/G_{\mathrm{cr}})/G_{\mathrm{tex}}$, and p is the natural surjection $\hat{\pi} : \mathrm{SO}(3)/G_{\mathrm{cr}} \to (\mathrm{SO}(3)/G_{\mathrm{cr}})/G_{\mathrm{tex}}$, $\boldsymbol{R}G_{\mathrm{cr}} \mapsto [\boldsymbol{R}G_{\mathrm{cr}}]$, where $[\boldsymbol{R}G_{\mathrm{cr}}] = \{\boldsymbol{Q}\boldsymbol{R}G_{\mathrm{cr}} : \boldsymbol{Q} \in G_{\mathrm{tex}}\}$. The measure on $\mathrm{SO}(3)/G_{\mathrm{cr}}$ is $\hat{\mathcal{V}}$. We denote by $\widetilde{\mathcal{V}}$ the quotient measure on the quotient space $(\mathrm{SO}(3)/G_{\mathrm{cr}})/G_{\mathrm{tex}}$.

Similar to (C.7) and (C.8), we have

$$\widetilde{\mathcal{V}}(\widetilde{A}) = \hat{\mathcal{V}}(\hat{\pi}^{-1}(\widetilde{A})) \qquad \text{for each Borel set } \widetilde{A} \subset (\mathrm{SO}(3)/G_{\mathrm{cr}})/G_{\mathrm{tex}}, \tag{C.9}$$

and for a continuous function $\widetilde{f} : (\mathrm{SO}(3)/G_{\mathrm{cr}})/G_{\mathrm{tex}} \to \mathbb{R}$ and $\hat{f} = \widetilde{f} \circ \hat{\pi}$,

$$\int_{\widetilde{A}} \widetilde{f}([\boldsymbol{R}G_{\mathrm{cr}}])\, d\widetilde{\mathcal{V}}([\boldsymbol{R}G_{\mathrm{cr}}]) = \int_{\hat{\pi}^{-1}(\widetilde{A})} \hat{f}(\boldsymbol{R}G_{\mathrm{cr}})\, d\hat{\mathcal{V}}(\boldsymbol{R}G_{\mathrm{cr}}). \tag{C.10}$$

Moreover, by (C.8) and (C.10) we obtain in particular

$$\begin{aligned}\int_{(\mathrm{SO}(3)/G_{\mathrm{cr}})/G_{\mathrm{tex}}} \widetilde{f}([\boldsymbol{R}G_{\mathrm{cr}}])\, d\widetilde{\mathcal{V}}([\boldsymbol{R}G_{\mathrm{cr}}]) &= \int_{\mathrm{SO}(3)/G_{\mathrm{cr}}} \hat{f}(\boldsymbol{R}G_{\mathrm{cr}})\, d\hat{\mathcal{V}}(\boldsymbol{R}G_{\mathrm{cr}}) \\ &= \int_{\mathrm{SO}(3)} f(\boldsymbol{R})\, d\mathcal{V}(\boldsymbol{R}).\end{aligned} \tag{C.11}$$

Since G_{cr} is a subgroup of $\mathrm{SO}(3)$, more can be said of the quotient measure $\hat{\mathcal{V}}$ on the orientation space $\mathrm{SO}(3)/G_{\mathrm{cr}}$.

Consider a polycrystal P with $G_{\mathrm{cr}} = \{\boldsymbol{P}_1, \ldots, \boldsymbol{P}_{N_{\mathrm{cr}}}\}$, where $\boldsymbol{P}_i \in \mathrm{SO}(3)$ for each i. Let $\boldsymbol{R} \in \mathrm{SO}(3)$. Suppose at a sampling point $\mathtt{x}$ in a sample $\mathcal{P}$ of P, the crystallite orientation is $\boldsymbol{R}G_{\mathrm{cr}} = \{\boldsymbol{R}\boldsymbol{P}_1, \ldots, \boldsymbol{R}\boldsymbol{P}_{N_{\mathrm{cr}}}\}$. After the sample $\mathcal{P}$ undergoes a rotation $\boldsymbol{Q}$, the crystallite orientation at $\mathtt{x}$ becomes $\boldsymbol{Q}\boldsymbol{R}G_{\mathrm{cr}} = \{\boldsymbol{Q}\boldsymbol{R}\boldsymbol{P}_1, \ldots, \boldsymbol{Q}\boldsymbol{R}\boldsymbol{P}_{N_{\mathrm{cr}}}\}$. In other words, the rotation operation $\boldsymbol{Q}$ induces a mapping $L_{\boldsymbol{Q}} : \mathrm{SO}(3)/G_{\mathrm{cr}} \to \mathrm{SO}(3)/G_{\mathrm{cr}}$ such that $L_{\boldsymbol{Q}}(\boldsymbol{R}G_{\mathrm{cr}}) = \boldsymbol{Q}\boldsymbol{R}G_{\mathrm{cr}}$. Under $L_{\boldsymbol{Q}}$, we have $L_{\boldsymbol{Q}}(\hat{A}) = \boldsymbol{Q}\hat{A}$ for each $\hat{A} \subset \mathrm{SO}(3)/G_{\mathrm{cr}}$.

Definition C.17 A finite positive measure $\hat{\nu}$ on $\mathrm{SO}(3)/G_{\mathrm{cr}}$ is said to be left $\mathrm{SO}(3)$-invariant if it satisfies

$$\hat{\nu}(\boldsymbol{Q}\hat{A}) = \hat{\nu}(\hat{A}) \tag{C.12}$$

for each $\boldsymbol{Q} \in \mathrm{SO}(3)$ and for each Borel set $\hat{A} \subset \mathrm{SO}(3)/G_{\mathrm{cr}}$. □

Proposition C.18 *The quotient measure $\hat{\mathcal{V}}$ on $\mathrm{SO}(3)/G_{\mathrm{cr}}$ is left $\mathrm{SO}(3)$-invariant.*

Proof For brevity, let us denote $\mathrm{SO}(3)$ and G_{cr} by G and K, respectively. We claim that for each $h \in G$ and Borel set $\hat{A} \subset G/K$

$$\pi^{-1}(h\hat{A}) = h\pi^{-1}(\hat{A}). \tag{C.13}$$

Indeed we have for each $g \in G$,

$$\begin{aligned} g \in \pi^{-1}(h\hat{A}) &\Longleftrightarrow \pi(g) \in h\hat{A} \Longleftrightarrow gK \in h\hat{A} \\ &\Longleftrightarrow h^{-1}gK \in \hat{A} \Longleftrightarrow \pi(h^{-1}g) \in \hat{A} \\ &\Longleftrightarrow h^{-1}g \in \pi^{-1}(\hat{A}) \Longleftrightarrow g \in h\pi^{-1}(\hat{A}). \end{aligned}$$

It follows from (C.13) and the left invariance of $\mathcal{V}$ that

$$\begin{aligned} \hat{\mathcal{V}}(h\hat{A}) &= \mathcal{V}(\pi^{-1}(h\hat{A})) = \mathcal{V}(h\pi^{-1}(\hat{A})) \\ &= \mathcal{V}(\pi^{-1}(\hat{A})) = \hat{\mathcal{V}}(\hat{A}) \qquad \text{for each } h \in G, \end{aligned} \tag{C.14}$$

i.e., $\hat{\mathcal{V}}$ is left G-invariant. □

Proposition C.19 *The left $\mathrm{SO}(3)$-invariant measure on $\mathrm{SO}(3)/G_{\mathrm{cr}}$ is unique up to a multiplicative positive constant.*

Proof Let $G_{\mathrm{cr}} = \{\boldsymbol{P}_1, \ldots, \boldsymbol{P}_{N_{\mathrm{cr}}}\}$. For each $f \in \mathscr{C}(\mathrm{SO}(3))$, let $f^\sharp \in \mathscr{C}(\mathrm{SO}(3)/G_{\mathrm{cr}})$ be given by

$$f^\sharp(\boldsymbol{R}G_{\mathrm{cr}}) = \frac{1}{N_{\mathrm{cr}}} \sum_{i=1}^{N_{\mathrm{cr}}} f(\boldsymbol{R}\boldsymbol{P}_i), \tag{C.15}$$

which is clearly well defined. We claim that the map $f \mapsto f^\sharp$ from $\mathscr{C}(\mathrm{SO}(3))$ to $\mathscr{C}(\mathrm{SO}(3)/G_{\mathrm{cr}})$ is surjective. Indeed, let $\hat{h} \in \mathscr{C}(\mathrm{SO}(3)/G_{\mathrm{cr}})$. Then $h := \hat{h} \circ \pi$, where $\pi : \mathrm{SO}(3) \to \mathrm{SO}(3)/G_{\mathrm{cr}}$ is the natural surjection, is in $\mathscr{C}(\mathrm{SO}(3))$ and

$$\frac{1}{N_{\mathrm{cr}}} \sum_{i=1}^{N_{\mathrm{cr}}} h(\boldsymbol{R}\boldsymbol{P}_i) = \frac{1}{N_{\mathrm{cr}}} \sum_{i=1}^{N_{\mathrm{cr}}} \hat{h} \circ \pi(\boldsymbol{R}\boldsymbol{P}_i) = \hat{h}(\boldsymbol{R}G_{\mathrm{cr}}). \tag{C.16}$$

Let $\hat{\nu}$ be a left $\mathrm{SO}(3)$-invariant measure on $\mathrm{SO}(3)/G_{\mathrm{cr}}$. We proceed to show that $\hat{\nu}$ determines a Haar measure on $\mathrm{SO}(3)$. Let $I : \mathscr{C}(\mathrm{SO}(3)) \to \mathbb{R}$ be defined by

$$I(f) = \int_{\mathrm{SO}(3)/G_{\mathrm{cr}}} f^\sharp(\boldsymbol{R}G_{\mathrm{cr}})\, d\hat{\nu}(\boldsymbol{R}G_{\mathrm{cr}}), \tag{C.17}$$

which is a positive linear functional on $\mathscr{C}(\mathrm{SO}(3))$. By the Riesz representation theorem C.8, there is a unique finite, positive Borel measure μ on $\mathrm{SO}(3)$ such that

$$I(f) = \int_{\mathrm{SO}(3)} f(\boldsymbol{R})\, d\mu(\boldsymbol{R}). \tag{C.18}$$

By (C.17), (C.18), and the hypothesis that $\hat{\nu}$ is left SO(3)-invariant on $\mathrm{SO}(3)/G_{\mathrm{cr}}$, it follows immediately that μ is a left-invariant measure on SO(3) and thence a bi-invariant Haar measure there (see Footnote 53 in Chap. 3). Thus each left SO(3)-invariant measure on $\mathrm{SO}(3)/G_{\mathrm{cr}}$ determines a Haar measure on SO(3).

Let $\hat{\nu}_1$ and $\hat{\nu}_2$ be two left SO(3)-invariant measures on $\mathrm{SO}(3)/G_{\mathrm{cr}}$, which determine Haar measures μ_1 and μ_2 on SO(3), respectively. By Corollary 3.6, there is a real number $c > 0$ such that $\mu_1 = c\mu_2$. Since the map $f \mapsto f^\sharp$ from $\mathscr{C}(\mathrm{SO}(3))$ to $\mathscr{C}(\mathrm{SO}(3)/G_{\mathrm{cr}})$ is surjective, we conclude that $\hat{\nu}_1 = c\,\hat{\nu}_2$, where $c > 0$. □

Appendix D

D X-Ray Diffraction by Crystals

X-rays are electromagnetic waves with wavelengths in the range from 0.1 Å to 100 Å, while those with wavelengths within the interval from 0.4 Å to 2 Å are most useful in crystallography.[180] For measurement of crystallographic texture, the X-ray beams that are used as probe should be monochromatic.

Conventional X-ray tubes generate unpolarized waves with a line spectrum superimposed on a continuous spectrum. Crystal monochromators can be applied ([234, pp. 309–311], [277, pp. 182–184]) to obtain an effectively monochromatic beam, which also becomes partially polarized. In what follows we shall always assume that the X-ray beam which we use as probe be monochromatic.

When X-rays fall on a substance, in general they are partly scattered elastically, partly scattered inelastically, and partly absorbed by the atoms of the target. In elastic (or coherent, unmodified) scattering, the scattered radiation has the same wavelength as that of the incident radiation. In inelastic (or incoherent, modified) scattering, which results from the Compton effect, the scattered radiation has a longer wavelength than the incident one. Absorption results in rise of temperature, ionization, and may lead to emission of fluorescent X-rays. Structure determination of materials by X-ray diffraction is mainly based on the interaction process of elastic scattering.[181]

As background for our discussions on X-ray measurements of texture, we summarize in this Appendix several main ingredients of the kinematical (or geometrical) theory[182] of X-ray diffraction by crystals [4, 114, 127, 165, 334]. Much of this theory was developed in the early days of X-ray crystallography (1912–1917) before the creation of quantum mechanics.[183] Within the context of the phenomena it is meant to describe, however, the kinematical theory with improvements at places where the use of quantum mechanics is necessary (e.g., in the evaluation of the atomic scattering factor; see Sect. D.3) has stood the test of time as a first approximation.

D.1 Thomson Scattering

Radiation from air through which X-ray was passing was first noticed by Röntgen. When X-rays fall on a solid or liquid surface, there is a diffuse radiation from the surface. Such diffuse radiations induced by primary X-rays are called secondary (Röntgen) radiations or secondary X-rays. Depending on the wavelength of the primary X-ray, the mass density of the target, and the atomic number of the target atoms, the secondary radiation can be predominantly resulting from coherent and/or incoherent scattering. For example, in his experimental study on secondary radiation from gases subject to X-rays, Barkla [18, p. 697]

[180] As W.L. Bragg remarked [45, p. 374] in an expository article in 1913, "The atoms of a crystal are regularly arranged and on the whole the intervals between them bear about the same relation to the wave length [of X-rays] as does the 'constant' of a diffraction grating to the wave length of visible light. To these waves a crystal is really a most perfectly ruled grating."

[181] "In X-ray crystallography, Compton scattering is a parasitic phenomenon which increases the background noise." [277, p. 140]

[182] The kinematical theory, in contrast to the dynamical theory, ignores multiple scattering of X-rays.

[183] See Authier [10] for a definitive account of the birth and early developments of X-ray crystallography. With an exhaustive bibliography it serves also as a valuable guide for readers interested in the original literature.

found that "the primary and secondary radiations only differ appreciably in intensity", and he concluded that "the radiation proceeding from gases subject to X-rays is due to scattering of the primary radiation."

Thomson proposed ([314, pp. 268–273], [315, pp. 321–327]) a theory of the secondary X-rays that arise from elastic scattering. He summarized the physics behind his theory as follows:

> The secondary radiation is readily explained if we take the view ... that the Röntgen rays consist of exceedingly thin pulses of very intense electric and magnetic force. [314, p. 268]
>
> Let us suppose that such a pulse is travelling through a medium containing corpuscles [i.e., electrons]—it is not necessary that the corpuscles should be free: when the pulse reaches a charged corpuscle the corpuscle will be acted on by a very intense force and its motion accelerated. Now when the velocity of a charged body is changing pulses of electric and magnetic force proceed from the body, the magnitude of these forces being proportional to the acceleration of the body: thus while the primary Röntgen pulse is passing over the corpuscle and accelerating its motion, the corpuscle gives out a pulse of electric and magnetic force—the second Röntgen pulse—the second pulse ceasing as soon as the acceleration of the primary pulse has passed over. [315, p. 323]

He wrote down the formulas on "the distribution of the electric and magnetic forces in the pulse" when "the velocity of the particle is small compared with that of light".

Remark D.1 The two quotations above are taken from the first (1903) and second edition (1906) of Thomson's book. There, in the sections in question, he uses classical electromagnetic theory to treat the elastic scattering of X-rays by a free electron. Two questions naturally arise, namely: (i) Should quantum mechanics be used for the problem at hand? (ii) In reality atomic electrons are bounded. Would formulas pertaining to scattering by a free electron be of any use? For the first question, it turns out that the full quantum mechanical treatment yields ([115, §12], [208, pp. 18–20], [230, pp. 1045–1049]) the same intensity formula for scattering as that of the classical Thomson scattering. We shall address the second question in Sect. D.3. □

We now proceed to go over the theory of Thomson scattering. For later use, instead of an electron we consider scattering by a particle with arbitrary charge q.

Let a particle with charge q be moving (e.g., oscillating) within a bounded region Ω in space E^3. Pick a point $O \in \Omega$ as the origin to define position vectors for locations in E^3. Let $\boldsymbol{r}(t)$ be the position vector of the charged particle at time t. Let $P \in E^3$, $R = \|\mathbf{OP}\|$, and $\boldsymbol{n} = \mathbf{OP}/R$. We are interested in the electric field $\boldsymbol{E}(R\boldsymbol{n}, t)$ and magnetic field $\boldsymbol{B}(R\boldsymbol{n}, t)$ of the charged particle at location P and time t. Let $\boldsymbol{x}(t) = R\boldsymbol{n} - \boldsymbol{r}(t)$; clearly $\|\boldsymbol{x}(t)\|$ is the distance between P and the charged particle at time t. Let $\boldsymbol{v}(t)$ and $\dot{\boldsymbol{v}}(t)$ be the velocity and acceleration of the particle at time t. We assume the motion of the charged particle be non-relativistic so that terms with factor $\|\boldsymbol{v}\|/c$, where c here denotes the speed of light, can be dropped. Moreover, we adopt the dipole approximation and consider locations P in the far field so that (i) $\|\boldsymbol{r}(t)\| \ll R$ and $\|\boldsymbol{x}(t)\| \approx R$ for all t; (ii) terms with factors of $1/R$ of order higher than 1 are dropped. Then by classical electromagnetic theory (see, e.g.,

[4, Appendix B], [181, pp. 173–175]) we have

$$\boldsymbol{E}(R\boldsymbol{n},t)=\frac{q}{4\pi\epsilon_0 c^2 R}\big(\boldsymbol{n}\times(\boldsymbol{n}\times\dot{\boldsymbol{v}}(t-R/c))\big), \tag{D.1}$$

$$\boldsymbol{B}(R\boldsymbol{n},t)=\frac{q}{4\pi\epsilon_0 c^3 R}\big(\dot{\boldsymbol{v}}(t-R/c)\times\boldsymbol{n}\big), \tag{D.2}$$

$$\boldsymbol{B}=\frac{1}{c}\boldsymbol{n}\times\boldsymbol{E},\qquad \boldsymbol{E}=c\boldsymbol{B}\times\boldsymbol{n}, \tag{D.3}$$

where ϵ_0 is the permittivity of free space. The Poynting vector (i.e., the electromagnetic energy-flux vector) is given by

$$\boldsymbol{S}=\frac{1}{\mu_0}\boldsymbol{E}\times\boldsymbol{B}=c\epsilon_0(\boldsymbol{E}\cdot\boldsymbol{E})\boldsymbol{n}, \tag{D.4}$$

where μ_0 is the permeability of free space and we have appealed to the formula $\epsilon_0\mu_0=1/c^2$.

Consider a monochromatic, linearly polarized, electromagnetic plane wave with wave vector $\boldsymbol{k}_0$:[184]

$$\boldsymbol{E}_0=E_0e^{i(\boldsymbol{k}_0\cdot\boldsymbol{x}-\omega t)}\hat{\boldsymbol{\epsilon}}_0,\qquad \boldsymbol{B}_0=\frac{1}{c}\boldsymbol{s}_0\times\boldsymbol{E}_0, \tag{D.5}$$

$$\boldsymbol{k}_0\cdot\boldsymbol{E}_0=0,\qquad \boldsymbol{k}_0\cdot\boldsymbol{B}_0=0,\qquad \boldsymbol{E}_0\cdot\boldsymbol{B}_0=0; \tag{D.6}$$

here E_0 is the amplitude of $\boldsymbol{E}_0$, $\hat{\boldsymbol{\epsilon}}_0$ is a unit vector that defines the polarization of $\boldsymbol{E}_0$, ω is the angular frequency, $\boldsymbol{s}_0=\boldsymbol{k}_0/\|\boldsymbol{k}_0\|$, and $\|\boldsymbol{k}_0\|=2\pi/\lambda$, where λ is the wavelength. The electromagnetic wave falls on a particle with charge q, which is at rest at $\boldsymbol{x}=\boldsymbol{0}$ at $t=0$, and sets it in motion. The equation of motion of the charged particle is:

$$m\dot{\boldsymbol{v}}=q(\boldsymbol{E}_0+\boldsymbol{v}\times\boldsymbol{B}_0)=q\left(\boldsymbol{E}_0+\boldsymbol{v}\times\frac{1}{c}(\boldsymbol{s}_0\times\boldsymbol{E}_0)\right)\approx qE_0e^{-i\omega t}\hat{\boldsymbol{\epsilon}}_0, \tag{D.7}$$

where we have dropped the magnetic force whose magnitude is of order $\|\boldsymbol{v}\|/c$ times the magnitude of the electric force. Note that after dropping the magnetic term, the particle moves in the plane $\boldsymbol{k}_0\cdot\boldsymbol{x}=0$. Thus we obtain the acceleration of the particle

$$\dot{\boldsymbol{v}}(t)=\frac{q}{m}E_0e^{-i\omega t}\hat{\boldsymbol{\epsilon}}_0. \tag{D.8}$$

Substituting (D.8) into (D.1), we obtain for the secondary radiation

$$\begin{aligned}\boldsymbol{E}(R\boldsymbol{n},t)&=\frac{q^2}{4\pi\epsilon_0 mc^2}\cdot\frac{E_0e^{-i\omega(t-R/c)}}{R}\big(\boldsymbol{n}\times\big(\boldsymbol{n}\times\hat{\boldsymbol{\epsilon}}_0\big)\big)\\&=\frac{q^2}{4\pi\epsilon_0 mc^2}\cdot\frac{E_0e^{-i\omega(t-R/c)}}{R}\big(-(\hat{\boldsymbol{\epsilon}}_0-(\hat{\boldsymbol{\epsilon}}_0\cdot\boldsymbol{n})\boldsymbol{n})\big)\\&=\frac{q^2}{4\pi\epsilon_0 mc^2}\cdot\frac{E_0e^{-i\omega(t-R/c)}}{R}\sin\varphi\,\hat{\boldsymbol{\epsilon}},\end{aligned} \tag{D.9}$$

[184] We follow the real-part convention in physics. Physical quantities are sometimes complexified to facilitate computations. Only the real part of the complexified quantity has physical significance. For example, (D.5) may be written as $\boldsymbol{E}_0=E_0\cos(\boldsymbol{k}_0\cdot\boldsymbol{x}-\omega t)\hat{\boldsymbol{\epsilon}}_0$.

where $\varphi \in [0, \pi]$ is the angle between the two unit vectors $\hat{\boldsymbol{\epsilon}}_0$ and $\boldsymbol{n}$, and $\hat{\boldsymbol{\epsilon}}$ is the unit vector in the direction of $\boldsymbol{n} \times (\boldsymbol{n} \times \hat{\boldsymbol{\epsilon}}_0)$. Let us derive $(D.9)_3$ from $(D.9)_1$. For $\varphi \in (0, \pi)$, $\boldsymbol{n} \times \hat{\boldsymbol{\epsilon}}_0$ is a vector normal to the plane Π subtended by $\boldsymbol{n}$ and $\hat{\boldsymbol{\epsilon}}_0$ and has its magnitude $\|\boldsymbol{n} \times \hat{\boldsymbol{\epsilon}}_0\| = \sin\varphi$. It follows that $\boldsymbol{n} \times (\boldsymbol{n} \times \hat{\boldsymbol{\epsilon}}_0)$ is a vector in Π and is orthogonal to $\boldsymbol{n}$; moreover, $\|\boldsymbol{n} \times (\boldsymbol{n} \times \hat{\boldsymbol{\epsilon}}_0)\| = \sin\varphi$. Thus we have $\boldsymbol{n} \times (\boldsymbol{n} \times \hat{\boldsymbol{\epsilon}}_0) = (\sin\varphi)\hat{\boldsymbol{\epsilon}}$.

For $\varphi = 0$ or $\varphi = \pi$, both $(D.9)_3$ and $(D.9)_1$ give $\boldsymbol{E} = \boldsymbol{0}$. For $\varphi = \pi/2$, a comparison of $(D.9)_2$ and $(D.9)_3$ clearly yields $\hat{\boldsymbol{\epsilon}} = -\hat{\boldsymbol{\epsilon}}_0$. For a general φ, since

$$\begin{aligned} \hat{\boldsymbol{\epsilon}}_0 \cdot (\sin\varphi)\hat{\boldsymbol{\epsilon}} &= \hat{\boldsymbol{\epsilon}}_0 \cdot (\boldsymbol{n} \times (\boldsymbol{n} \times \hat{\boldsymbol{\epsilon}}_0)) \\ &= (\hat{\boldsymbol{\epsilon}}_0 \times \boldsymbol{n}) \cdot (\boldsymbol{n} \times \hat{\boldsymbol{\epsilon}}_0) = -\|\boldsymbol{n} \times \hat{\boldsymbol{\epsilon}}_0\|^2 = -\sin^2\varphi, \end{aligned} \tag{D.10}$$

we obtain

$$\hat{\boldsymbol{\epsilon}}_0 \cdot \hat{\boldsymbol{\epsilon}} = -\sin\varphi. \tag{D.11}$$

Note that by (D.9) the scattered wave observed at P, which is in the far field, can be taken as a plane wave with wave vector $\boldsymbol{k} = \frac{2\pi}{\lambda}\boldsymbol{n}$. In the physics literature of X-ray diffraction, it is common to write (see, e.g., [4, 127, 128, 334]) the unit vector parallel to $\boldsymbol{k}$ as $\boldsymbol{s}$. Henceforth we shall also write $\boldsymbol{k} = \frac{2\pi}{\lambda}\boldsymbol{s}$ and use $\boldsymbol{n}$ and $\boldsymbol{s}$ interchangeably.

For the case of scattering by an electron, $q = -e$. Henceforth in this Appendix, we shall often encounter the quantity

$$r_0 = \frac{e^2}{4\pi\epsilon_0 m c^2} \approx 2.82 \times 10^{-5}\ \text{Å}, \tag{D.12}$$

which is called the Thomson scattering length, or classical radius, of the electron.

We adopt the definition that the (average) intensity of X-rays as electromagnetic waves is the time-average of the Poynting flux $\boldsymbol{S} \cdot \boldsymbol{n}$. For the incident electromagnetic wave (D.5), by (D.4) the intensity is

$$I_0 = \frac{1}{T}\int_0^T c\,\epsilon_0 E_0^2 \cos^2(\boldsymbol{k}_0 \cdot \boldsymbol{x} - \omega t)dt = \frac{1}{2}c\,\epsilon_0 E_0^2, \tag{D.13}$$

where $T = 2\pi/\omega$ is the period. For the scattering by an electron, the intensity of the scattered wave is given by

$$I_{\text{e}} = \frac{r_0^2 c\,\epsilon_0 E_0^2 \sin^2\varphi}{2R^2}. \tag{D.14}$$

Comparing (D.14) with (D.13), we obtain

$$I_{\text{e}} = \frac{r_0^2 \sin^2\varphi}{R^2} I_0. \tag{D.15}$$

Equation (D.15) is often called the Thomson scattering equation. The expression $\sin^2\varphi$ is called the polarization factor of the intensity.

In quantum mechanical treatments of scattering, one works with transition probabilities and differential cross sections. In our present context, the differential cross section $d\sigma/d\Omega$

is the power scattered into the solid angle $d\Omega$ normalized by the incident flux. In terms of the differential cross section, the Thomson scattering equation (D.15) reads:

$$\frac{d\sigma}{d\Omega} = \frac{I_e R^2}{I_0} = r_0^2 \sin^2\varphi = r_0^2 \, |\hat{\boldsymbol{\varepsilon}}_0 \cdot \hat{\boldsymbol{\varepsilon}}|^2, \tag{D.16}$$

where we have used (D.11) to put $\sin\varphi = |\hat{\boldsymbol{\varepsilon}}_0 \cdot \hat{\boldsymbol{\varepsilon}}|$. See [208, pp. 18–19] or [230, pp. 1045–1049] for a quantum mechanical derivation of $(D.16)_3$.

D.2 Classical Scattering by a Finite Number of Electrons

To prepare for our discussion of X-ray scattering by atoms, we consider classical scattering by a finite number N electrons. The setting is basically the same as that of the preceding section, except that instead of one electron oscillating about the origin under the action of a monochromatic linearly-polarized electromagnetic plane wave there are N free electrons, which oscillate about the locations $\boldsymbol{r}_n = \boldsymbol{r}_n(0)$ $(n = 1, \ldots, N)$ they occupy at $t = 0$. We shall express the electric field $\boldsymbol{E}_n$ of the secondary radiation from the n-th electron in relation to that of an imaginary electron oscillating about the origin, which is given by equation (D.9). We assume that for each n the distance $\|\boldsymbol{r}_n\|$ of the n-th electron from the origin is sufficiently small as compared with R that the approximations used below be valid.

Let us choose a Cartesian coordinate system such that the wave vector of the incident plane electromagnetic wave is $\boldsymbol{k}_0 = \frac{2\pi}{\lambda}\boldsymbol{s}_0 = \frac{2\pi}{\lambda}\boldsymbol{e}_1$. Suppose $\boldsymbol{r}_n \cdot \boldsymbol{e}_1 > 0$. Consider a wavefront that hits the first electron at the origin O at $t = 0$. It reaches the n-th electron after a further path length of $\boldsymbol{r}_n \cdot \boldsymbol{e}_1 = \boldsymbol{r}_n \cdot \boldsymbol{s}_0$. The path length of the scattered wave from the n-th electron is

$$\begin{aligned} \|R\boldsymbol{n} - \boldsymbol{r}_n\| &= \big((R\boldsymbol{n} - \boldsymbol{r}_n) \cdot (R\boldsymbol{n} - \boldsymbol{r}_n)\big)^{1/2} = (R^2 - 2R\boldsymbol{n} \cdot \boldsymbol{r}_n + \boldsymbol{r}_n \cdot \boldsymbol{r}_n)^{1/2} \\ &= R\left(1 - 2\frac{\boldsymbol{n} \cdot \boldsymbol{r}_n}{R} + \frac{\boldsymbol{r}_n \cdot \boldsymbol{r}_n}{R^2}\right)^{1/2} \approx R - \boldsymbol{n} \cdot \boldsymbol{r}_n. \end{aligned} \tag{D.17}$$

Hence when the wave front in question arrives at the point of observation P, its path length is $\boldsymbol{r}_n \cdot \boldsymbol{s}_0 + R - \boldsymbol{s} \cdot \boldsymbol{r}_n$, where we have put $\boldsymbol{n}$ as $\boldsymbol{s}$. It is easily checked that this expression remains valid for $\boldsymbol{r}_n \cdot \boldsymbol{e}_1 \le 0$. Clearly the expression for path length is independent of the Cartesian coordinate system chosen. Note that the path difference between the scattered waves from the n-th and the imaginery electron oscillating about the origin is $(\boldsymbol{s}_0 - \boldsymbol{s}) \cdot \boldsymbol{e}_1$, which is equivalent to a phase difference of

$$\frac{\omega}{c}(\boldsymbol{s} - \boldsymbol{s}_0) \cdot \boldsymbol{r}_n = \frac{2\pi}{\lambda}(\boldsymbol{s} - \boldsymbol{s}_0) \cdot \boldsymbol{r}_n = (\boldsymbol{k} - \boldsymbol{k}_0) \cdot \boldsymbol{r}_n. \tag{D.18}$$

It is now easy to write down, in parallel to $(D.9)_2$ the electric field of the scattered radiation from the n-th electron:

$$\boldsymbol{E}_n(R\boldsymbol{n}, t) = r_0 \cdot \frac{E_0 e^{-i\omega(t - R/c)}}{\|R\boldsymbol{n} - \boldsymbol{r}_n\|} e^{i(\boldsymbol{k} - \boldsymbol{k}_0) \cdot \boldsymbol{r}_n}\big(-(\hat{\boldsymbol{\varepsilon}}_0 - (\hat{\boldsymbol{\varepsilon}}_0 \cdot \boldsymbol{m})\boldsymbol{m})\big), \tag{D.19}$$

where r_0 is the Thomson scattering length and $\boldsymbol{m} = (R\boldsymbol{n} - \boldsymbol{r}_n)/\|R\boldsymbol{n} - \boldsymbol{r}_n\|$. We now apply the following approximations, the rationale of which is that for each factor we keep only

terms of the lowest order in $1/R$. For the factor $1/\|R\boldsymbol{n}-\boldsymbol{r}_n\|$, we have

$$\begin{aligned}\|R\boldsymbol{n}-\boldsymbol{r}_n\|^{-1} &= (R^2-2R\boldsymbol{n}\cdot\boldsymbol{r}_n+\boldsymbol{r}_n\cdot\boldsymbol{r}_n)^{-1/2}\\ &= \frac{1}{R}\cdot\left(1-\frac{2\boldsymbol{n}\cdot\boldsymbol{r}_n}{R}+\frac{\boldsymbol{r}_n\cdot\boldsymbol{r}_n}{R^2}\right)^{-1/2}\\ &\approx \frac{1}{R}\left(1+\frac{\boldsymbol{n}\cdot\boldsymbol{e}_1}{R}+\cdots\right)\approx\frac{1}{R}.\end{aligned}\tag{D.20}$$

For the unit vector $\boldsymbol{m}$, we get

$$\boldsymbol{m}=\frac{R\boldsymbol{n}-\boldsymbol{r}_n}{\|R\boldsymbol{n}-\boldsymbol{r}_n\|}\approx\frac{R\boldsymbol{n}-\boldsymbol{r}_n}{R}\approx\boldsymbol{n}-\frac{\boldsymbol{r}_n}{R}.\tag{D.21}$$

It follows that $(\hat{\boldsymbol{\varepsilon}}_0\cdot\boldsymbol{m})\boldsymbol{m}\approx(\hat{\boldsymbol{\varepsilon}}_0\cdot\boldsymbol{n})\boldsymbol{n}$. After these approximations, the electric field of the scattered radiation from the n-th electron is

$$\begin{aligned}\boldsymbol{E}_n(R\boldsymbol{n},t) &= r_0\cdot\frac{E_0e^{-i\omega(t-R/c)}}{R}e^{i(\boldsymbol{k}-\boldsymbol{k}_0)\cdot\boldsymbol{r}_n}\big(-(\hat{\boldsymbol{\varepsilon}}_0-(\hat{\boldsymbol{\varepsilon}}_0\cdot\boldsymbol{n})\boldsymbol{n})\big),\\ &= r_0\cdot\frac{E_0e^{-i\omega(t-R/c)}}{R}e^{i(\boldsymbol{k}-\boldsymbol{k}_0)\cdot\boldsymbol{r}_n}\sin\varphi\,\hat{\boldsymbol{\varepsilon}},\end{aligned}\tag{D.22}$$

which differs from (D.9) only in the presence of the factor $e^{i(\boldsymbol{k}-\boldsymbol{k}_0)\cdot\boldsymbol{r}_n}$. The resultant electric field of secondary radiations from all N electrons is the linear superposition of all $\boldsymbol{E}_n$, i.e.,

$$\boldsymbol{E}(R\boldsymbol{n},t)=r_0\cdot\frac{E_0e^{-i\omega(t-R/c)}}{R}\left(\sum_{n=1}^{N}e^{i(\boldsymbol{k}-\boldsymbol{k}_0)\cdot\boldsymbol{r}_n}\right)\sin\varphi\,\hat{\boldsymbol{\varepsilon}}.\tag{D.23}$$

It follows that the intensity of the secondary radiation is given by

$$I=I_{\mathrm{e}}\left|\sum_{n=1}^{N}e^{i(\boldsymbol{k}-\boldsymbol{k}_0)\cdot\boldsymbol{r}_n}\right|^2.\tag{D.24}$$

D.3 Scattering by an Atom

Let us compare the Thomson scattering intensity of a free proton with that of a free electron under the same setting described in Sect. D.1. Let m_{p} and m_{e} be the mass of a proton and of an electron, respectively, and let I_{p} and I_{e} be the corresponding scattering intensity. By the Thomson scattering equation (D.15) for the electron and its analog for the proton, we have

$$\frac{I_{\mathrm{p}}}{I_{\mathrm{e}}}=\frac{m_{\mathrm{e}}^2}{m_{\mathrm{p}}^2}\approx\frac{1}{(1836)^2}.\tag{D.25}$$

Hence in the scattering of X-rays by a hydrogen atom, the contribution of the proton to the secondary radiation can be ignored if the Thomson scattering equation is applicable. By the same token, the same can be said of the scattering of X-rays by the atoms of other elements. Indeed a motto since the early days of X-ray crystallography is that "it is the electrons in atoms which scatter X-rays." [74] Henceforth we shall consider only scattering of X-rays by atomic electrons.

One assumption in the derivation of the Thomson scattering equation is that the electron in question be subject to no forces other than the Lorentz force of the incident electromagnetic wave. How does this assumption fare with atomic electrons? The answer is long and complicated, which for our present purpose we need not bother with. Here are some rough guidelines [277, p. 141] in lieu of a reply:

> Electrons of light atoms and external electrons of heavy atoms behave towards X-rays as free electrons, since their binding energy with the nucleus corresponds to natural frequencies very much lower than those of the incident radiation. For inner shell electrons of heavy atoms, the binding energy is comparable to that of the radiation, and coupling, giving rise to [anomalous] scattering, may result.

We will proceed to treat atomic electrons as free electrons as far as X-ray scattering is concerned and add some comments on corrections of this treatment in Remark D.4 at the end of this section.

In his 1915 Bakerian Lecture to the Royal Society, W.H. Bragg [46] discussed "the rapid diminution of intensities" with increasing order of X-ray reflection.[185] To give an ample explanation of the phenomenon, he proposed "the highly probable hypothesis that the scattering power of the atom is not localized at one central point in each, but is distributed through the volume of the atom." Moreover, "[w]e should expect the scattering centres of the atom to be not only diffused through its volume, but also to be less dense at the edges than at the centre". After the advent of quantum mechanics, Bragg's picture of atomic electrons as a diffuse distribution of charge around the nucleus had its first precise expression in Schrödinger's use of the wave function to describe charge distribution or charge density [285, 287]. While Schrödinger's interpretation of charge distribution was not widely accepted (cf. e.g., Born's critical remarks [14, p. 426] at the 1927 Solvay Conference), it did lead to a correct formula for the atomic scattering factor (see [165, Chap. 3] and the references therein), Hartree's computations [141] of the charge distributions in the He atom and the Rb^+, Na^+, Cl^- ions by the method of self-consistent fields that he developed, and other interesting findings (see, e.g., [166]). Over the years the Schrödinger distribution of charge has been superseded by electron density, a refined version of the Schrödinger charge density divided by the charge of the electron $-e$, which has become a basic concept in various subfields of physics and chemistry. In particular, electron density plays a central role in the definition of the atomic scattering factor.

D.3.1 Electron Density

Consider two distinguishable particles in space. Suppose the probability density $\Theta : \mathbb{R}^3 \times \mathbb{R}^3 \longrightarrow [0, \infty)$ is given such that

$$\Theta(\boldsymbol{r}, \boldsymbol{r}')\, d\mathrm{V}(\boldsymbol{r}) d\mathrm{V}(\boldsymbol{r}') \tag{D.26}$$

is the probability of finding particle 1 at $\boldsymbol{r}$ and particle 2 at $\boldsymbol{r}'$. Let Ω be a region in space. Then

$$\int_{\Omega}\int_{\mathbb{R}^3} \Theta(\boldsymbol{r}, \boldsymbol{r}')\, d\mathrm{V}(\boldsymbol{r}') d\mathrm{V}(\boldsymbol{r}) \qquad \text{and} \qquad \int_{\Omega}\int_{\mathbb{R}^3} \Theta(\boldsymbol{r}, \boldsymbol{r}')\, d\mathrm{V}(\boldsymbol{r}) d\mathrm{V}(\boldsymbol{r}') \tag{D.27}$$

[185] See Sect. D.4.2 for definition of the term "order of X-ray reflection". There we shall also explain the physical basis behind the rapid diminution of intensities with increasing order of X-ray reflection.

are the probabilities of finding particle 1 and particle 2 in Ω, respectively. If the probability density Θ is symmetric, i.e., $\Theta(\boldsymbol{r}, \boldsymbol{r}') = \Theta(\boldsymbol{r}', \boldsymbol{r})$ for all $\boldsymbol{r}, \boldsymbol{r}' \in \mathbb{R}^3$, then the two expressions given in (D.27) are equal. If the two particles are indistinguishable, then the probability density Θ is symmetric and the function

$$\rho(\boldsymbol{r}) = 2 \int_{\mathbb{R}^3} \Theta(\boldsymbol{r}, \boldsymbol{r}')\, d\mathrm{V}(\boldsymbol{r}') \tag{D.28}$$

is called the particle density of the two-particle system.

The electron is a particle with spin $1/2$. In non-relativistic quantum mechanics, the state space of an electron can be described (see, e.g., [232, p. 267], [323, p. 125]) as follows. Let $\mathscr{K}$ be the Hilbert space of vector-valued wave functions

$$\boldsymbol{\Psi}(\boldsymbol{r}) = \begin{pmatrix} \psi_1(\boldsymbol{r}) \\ \psi_2(\boldsymbol{r}) \end{pmatrix} = \psi_1 \begin{pmatrix} 1 \\ 0 \end{pmatrix} + \psi_2 \begin{pmatrix} 0 \\ 1 \end{pmatrix} = \psi_1 \boldsymbol{e}_1 + \psi_2 \boldsymbol{e}_2, \tag{D.29}$$

where the components functions ψ_i $(i = 1, 2)$ are square integrable (i.e., $\int_{\mathbb{R}^3} \psi_i \overline{\psi_i} d\mathrm{V} = \int_{\mathbb{R}^3} |\psi_i|^2 d\mathrm{V} < \infty$), and the inner product of two wave functions $\boldsymbol{\Phi}$ and $\boldsymbol{\Psi}$ is defined by

$$\int_{\mathbb{R}^3} \big\langle \boldsymbol{\Phi}(\boldsymbol{r}), \boldsymbol{\Psi}(\boldsymbol{r}) \big\rangle d\mathrm{V}(\boldsymbol{r}) = \int_{\mathbb{R}^3} \Big(\phi_1(\boldsymbol{r}) \overline{\psi_1(\boldsymbol{r})} + \phi_2(\boldsymbol{r}) \overline{\psi_2(\boldsymbol{r})} \Big) d\mathrm{V}(\boldsymbol{r}). \tag{D.30}$$

Each state of the electron is defined by a wave function $\boldsymbol{\Psi}$ that satisfies the normalization condition

$$\int_{\mathbb{R}^3} \big\langle \boldsymbol{\Psi}(\boldsymbol{r}), \boldsymbol{\Psi}(\boldsymbol{r}) \big\rangle d\mathrm{V}(\boldsymbol{r}) = \int_{\mathbb{R}^3} (|\psi_1|^2 + |\psi_2|^2)\, d\mathrm{V} = 1. \tag{D.31}$$

Physically for a region $\Omega \subset \mathbb{R}^3$, the components ψ_1 and ψ_2 of $\boldsymbol{\Psi}$ are wave functions such that

$$\int_{\Omega} |\psi_1(\boldsymbol{r})|^2\, d\mathrm{V}(\boldsymbol{r}) \qquad \text{and} \qquad \int_{\Omega} |\psi_2(\boldsymbol{r})|^2\, d\mathrm{V}(\boldsymbol{r}) \tag{D.32}$$

are the probabilities of finding the electron in Ω with "spin up" and "spin down", respectively, and

$$\int_{\Omega} \big\langle \boldsymbol{\Psi}(\boldsymbol{r}), \boldsymbol{\Psi}(\boldsymbol{r}) \big\rangle d\mathrm{V}(\boldsymbol{r}) \tag{D.33}$$

is the probability of finding the electron in Ω irrespective of spin. For the one-electron system the function

$$\rho(\boldsymbol{r}) = |\psi_1(\boldsymbol{r})|^2 + |\psi_2(\boldsymbol{r})|^2 \tag{D.34}$$

is called the electron density.

Let $\mathscr{K} \otimes \mathscr{K}$ be the Hilbert space of tensor-valued wave functions of the form

$$\boldsymbol{\Psi}(\boldsymbol{r}_1, \boldsymbol{r}_2) = \sum_{i,j=1}^{2} \psi_{ij}(\boldsymbol{r}_1, \boldsymbol{r}_2) \boldsymbol{e}_i \otimes \boldsymbol{e}_j, \tag{D.35}$$

where the component wave functions ψ_{ij} are square integrable, and the inner product of two wave functions $\boldsymbol{\Phi}$ and $\boldsymbol{\Psi}$ is defined by

$$\begin{aligned} &\int_{\mathbb{R}^3} \int_{\mathbb{R}^3} \big\langle \boldsymbol{\Phi}(\boldsymbol{r}_1, \boldsymbol{r}_2), \boldsymbol{\Psi}(\boldsymbol{r}_1, \boldsymbol{r}_2) \big\rangle d\mathrm{V}(\boldsymbol{r}_1) d\mathrm{V}(\boldsymbol{r}_2) \\ &= \int_{\mathbb{R}^3} \int_{\mathbb{R}^3} \Big(\sum_{i,j=1}^{2} \phi_{ij}(\boldsymbol{r}_1, \boldsymbol{r}_2) \overline{\psi_{ij}(\boldsymbol{r}_1, \boldsymbol{r}_2)} \Big) d\mathrm{V}(\boldsymbol{r}_1) d\mathrm{V}(\boldsymbol{r}_2). \end{aligned} \tag{D.36}$$

For a two-electron system, the state space is a proper closed subspace of $\mathscr{K} \otimes \mathscr{K}$, the elements of which satisfy two further conditions:

$$\begin{aligned} \int_{\mathbb{R}^3} \int_{\mathbb{R}^3} \|\boldsymbol{\Psi}(\boldsymbol{r}_1, \boldsymbol{r}_2)\|^2 d\mathrm{V}(\boldsymbol{r}_1) d\mathrm{V}(\boldsymbol{r}_2) &= \int_{\mathbb{R}^3} \int_{\mathbb{R}^3} \big\langle \boldsymbol{\Psi}(\boldsymbol{r}_1, \boldsymbol{r}_2), \boldsymbol{\Psi}(\boldsymbol{r}_1, \boldsymbol{r}_2) \big\rangle d\mathrm{V}(\boldsymbol{r}_1) d\mathrm{V}(\boldsymbol{r}_2) \\ &= \int_{\mathbb{R}^3} \int_{\mathbb{R}^3} \Big(\sum_{i,j=1}^{2} |\psi_{ij}(\boldsymbol{r}_1, \boldsymbol{r}_2)|^2 \Big) d\mathrm{V}(\boldsymbol{r}_1) d\mathrm{V}(\boldsymbol{r}_2) \\ &= 1, \end{aligned} \tag{D.37}$$

and, as required by the Pauli exclusion principle,

$$\psi_{ij}(\boldsymbol{r}_1, \boldsymbol{r}_2) = -\psi_{ji}(\boldsymbol{r}_2, \boldsymbol{r}_1) \qquad \text{for all } i, j \in \{1, 2\}. \tag{D.38}$$

Note that by (D.38) the function $\sum_{i,j=1}^{2} |\psi_{ij}(\boldsymbol{r}_1, \boldsymbol{r}_2)|^2$ is symmetric, and it is the probability density of finding one electron at $\boldsymbol{r}_1$ and one electron at $\boldsymbol{r}_2$ irrespective of spin. Hence it is a special case of the function Θ discussed in the paragraph containing (D.26) for two indistinguishable particles (with no internal degree of freedom). It follows from (D.28) that the electron density is given by

$$\rho(\boldsymbol{r}) = 2 \int_{\mathbb{R}^3} \Big(\sum_{i,j=1}^{2} |\psi_{ij}(\boldsymbol{r}, \boldsymbol{r}_2)|^2 \Big) d\mathrm{V}(\boldsymbol{r}_2). \tag{D.39}$$

The preceding discussion on systems of two electrons can be easily extended to systems of $N > 2$ electrons. Let $\mathscr{K}^{\otimes N}$ be the Hilbert space of tensor-valued wave functions of the form

$$\boldsymbol{\Psi}(\boldsymbol{r}_1, \ldots \boldsymbol{r}_N) = \sum_{i_1, \ldots, i_N = 1}^{2} \psi_{i_1 \cdots i_N}(\boldsymbol{r}_1, \ldots, \boldsymbol{r}_N) \boldsymbol{e}_{i_1} \otimes \cdots \boldsymbol{e}_{i_N}, \tag{D.40}$$

where the component wave functions $\psi_{i_1\cdots i_N}$ are square integrable, and the inner product of two wave functions $\boldsymbol{\Phi}$ and $\boldsymbol{\Psi}$ is defined by

$$\int_{\mathbb{R}^3}\cdots\int_{\mathbb{R}^3}\big\langle\boldsymbol{\Phi}(\boldsymbol{r}_1,\ldots,\boldsymbol{r}_N),\boldsymbol{\Psi}(\boldsymbol{r}_1,\ldots,\boldsymbol{r}_N)\big\rangle d\mathrm{V}(\boldsymbol{r}_1)\cdots d\mathrm{V}(\boldsymbol{r}_N)$$

$$=\int_{\mathbb{R}^3}\cdots\int_{\mathbb{R}^3}\Big(\sum_{i_1,\ldots,i_N=1}^{2}\phi_{i_1\cdots i_N}(\boldsymbol{r}_1,\ldots,\boldsymbol{r}_N)\overline{\psi_{i_1\cdots i_N}(\boldsymbol{r}_1,\ldots,\boldsymbol{r}_N)}\Big)d\mathrm{V}(\boldsymbol{r}_1)\cdots d\mathrm{V}(\boldsymbol{r}_N). \quad \text{(D.41)}$$

For an N-electron system, the state space is a proper closed subspace of $\mathscr{K}^{\otimes N}$, the elements of which satisfy the normality condition

$$\int_{\mathbb{R}^3}\cdots\int_{\mathbb{R}^3}\|\boldsymbol{\Psi}(\boldsymbol{r}_1,\ldots,\boldsymbol{r}_N)\|^2 d\mathrm{V}(\boldsymbol{r}_1)\cdots d\mathrm{V}(\boldsymbol{r}_N)$$

$$=\int_{\mathbb{R}^3}\cdots\int_{\mathbb{R}^3}\Big(\sum_{i_1,\ldots,i_N=1}^{2}|\psi_{i_1\cdots i_N}(\boldsymbol{r}_1,\ldots,\boldsymbol{r}_N)|^2\Big)d\mathrm{V}(\boldsymbol{r}_1)\cdots d\mathrm{V}(\boldsymbol{r}_N)=1, \quad \text{(D.42)}$$

and the condition imposed by the Pauli exclusion principle. Let S_n be the group of permutations of the set $\{1,2,\ldots,n\}$. The Pauli exclusion principle requires that for each permutation $\tau\in S_n$, the component wave functions of $\boldsymbol{\Psi}$ satisfy

$$\psi_{i_{\tau(1)}\cdots i_{\tau(N)}}(\boldsymbol{r}_{\tau(1)},\ldots,\boldsymbol{r}_{\tau(N)})=\mathrm{sgn}(\tau)\psi_{i_1\cdots i_N}(\boldsymbol{r}_1,\ldots,\boldsymbol{r}_N), \quad \text{(D.43)}$$

where $\mathrm{sgn}(\tau)$ is the sign of permutation τ.[186] By (D.43) the function $\|\boldsymbol{\Psi}(\boldsymbol{r}_1,\boldsymbol{r}_2,\ldots,\boldsymbol{r}_N)\|^2$ is symmetric, and physically it gives the probability density of finding one electron at $\boldsymbol{r}_1$, one electron at $\boldsymbol{r}_2,\ldots$, and one electron at $\boldsymbol{r}_N$ irrespective of their states of spin. It follows that the function

$$\rho(\boldsymbol{r})=N\int_{\mathbb{R}^3}\cdots\int_{\mathbb{R}^3}\|\boldsymbol{\Psi}(\boldsymbol{r},\boldsymbol{r}_2,\ldots,\boldsymbol{r}_N)\|^2 d\mathrm{V}(\boldsymbol{r}_2)\cdots d\mathrm{V}(\boldsymbol{r}_N)$$

$$=N\int_{\mathbb{R}^3}\cdots\int_{\mathbb{R}^3}\Big(\sum_{i_1,\ldots,i_N=1}^{2}|\psi_{i_1\cdots i_N}(\boldsymbol{r},\boldsymbol{r}_2,\ldots,\boldsymbol{r}_N)|^2\Big)d\mathrm{V}(\boldsymbol{r}_2)\cdots d\mathrm{V}(\boldsymbol{r}_N) \quad \text{(D.44)}$$

is the electron density of the N-electron system.

D.3.2 Atomic Scattering Factor

Consider an atom with atomic number Z, which has its nucleus "clamped" [306] at the origin. The electrons in the atom are governed by quantum mechanics. Let $\rho(\cdot)$ be the density

[186] There are many ways to write a permutation $\tau\in S_n$ as a product of transpositions, i.e., two-cycles of the form (ij) which sends i to j and j to i. However, no matter how one writes τ as such a product, the number of transpositions is either always odd or always even. We define the sign of τ as 1 (resp. -1), i.e., $\mathrm{sgn}(\tau)=1$ (resp. $\mathrm{sgn}(\tau)=-1$) if τ can be represented as the product of an even (resp. odd) number of transpositions.

of the atomic electrons. The value $\rho(\boldsymbol{r})$ gives the number density of electrons at the location specified by the position vector $\boldsymbol{r}$. By (D.42) and (D.44), clearly we have

$$\int_{\mathbb{R}^3} \rho(\boldsymbol{r})\, d\mathrm{V}(\boldsymbol{r}) = Z. \tag{D.45}$$

We are interested in the elastic scattering of X-rays by the electrons of the atom in question under the setting specified in Sect. D.1. A semi-classical treatment of the problem (without the quantization of the electromagnetic field) was developed independently by Wentzel and Waller in 1927 (see [165, Chap. 3] and the references therein), while the foundations of a full quantum mechanical analysis was laid down in the same year by Dirac [92, 93] (see also [115]). Going into the quantum mechanical analysis, however, is beyond the scope of this Appendix. We are content just to reproduce the formula for the differential cross section, which is of utmost interest to us.

Suppose the atomic electrons are in the ground state defined by the wave function $\boldsymbol{\Psi}_0$. A parallel beam of X-ray photons with wave vector $\boldsymbol{k}_0$ and polarization $\hat{\boldsymbol{\varepsilon}}_0$ falls upon the atom. Elastic scattering in the direction $\boldsymbol{k}$ involves the annihilation of incident photons and the simultaneous creation, one for one, of photons with wave number $\boldsymbol{k}$ and polarization $\hat{\boldsymbol{\varepsilon}}$, while there is no change in the state of the atomic electrons. The transition probability from the state of the system (i.e., atomic electrons plus electromagnetic field) before scattering and the state after scattering can be computed, and the differential cross section of the scattering determined (see [114, equation (49)]):

$$\frac{d\sigma}{d\Omega} = r_0^2\, |\hat{\boldsymbol{\varepsilon}}_0 \cdot \hat{\boldsymbol{\varepsilon}}|^2 \Big| \int_{\mathbb{R}^3} \rho(\boldsymbol{r}) e^{i(\boldsymbol{k}-\boldsymbol{k}_0)\cdot \boldsymbol{r}}\, d\mathrm{V}(\boldsymbol{r}) \Big|^2. \tag{D.46}$$

It follows that the intensity of the scattered beam is

$$I = I_{\mathrm{e}} \Big| \int_{\mathbb{R}^3} \rho(\boldsymbol{r}) e^{i(\boldsymbol{k}-\boldsymbol{k}_0)\cdot \boldsymbol{r}}\, d\mathrm{V}(\boldsymbol{r}) \Big|^2. \tag{D.47}$$

In the semi-classical treatment [165, Chap. 3], the electric field of the secondary radiation at the point of observation $R\boldsymbol{n}$ is:

$$\boldsymbol{E}(R\boldsymbol{n}, t) = r_0 \cdot \frac{E_0 e^{-i\omega(t-R/c)}}{R} \Big(\int_{\mathbb{R}^3} \rho(\boldsymbol{r}) e^{i(\boldsymbol{k}-\boldsymbol{k}_0)\cdot \boldsymbol{r}}\, d\mathrm{V}(\boldsymbol{r}) \Big) \sin\varphi\, \hat{\boldsymbol{\varepsilon}}, \tag{D.48}$$

which also delivers the intensity formula (D.47). The expression

$$f(\boldsymbol{q}) = \int_{\mathbb{R}^3} \rho(\boldsymbol{r}) e^{i\boldsymbol{q}\cdot \boldsymbol{r}}\, d\mathrm{V}(\boldsymbol{r}), \qquad \text{where } \boldsymbol{q} := \boldsymbol{k} - \boldsymbol{k}_0, \tag{D.49}$$

is called the atomic scattering factor and $\boldsymbol{q}$ the scattering vector. As indicated by (D.49), the atomic scattering factor f is mathematically the Fourier transform of the electron density ρ. Indeed much of what we shall present in the rest of this Appendix can be couched more generally and more elegantly in the language of Fourier transforms. We will, however, follow an approach which makes use of Laue's argument in his theoretical part of the 1912

joint paper [120] with Friedrich and Knipping, a paper that marks the beginning of X-ray crystallography.[187]

We end this section by presenting two mathematical properties of the atomic scattering factor f.

Lemma D.2 *Let the electron density $\rho(\cdot)$ be centrally symmetric, i.e., $\rho(\boldsymbol{r}) = \rho(-\boldsymbol{r})$ for each $\boldsymbol{r} \in \mathbb{R}^3$. Then $f(\cdot)$ is real-valued.*

Proof Let $\boldsymbol{r}' = -\boldsymbol{r}$. Then by hypothesis $\rho(\boldsymbol{r}') = \rho(\boldsymbol{r})$. Since

$$\overline{f(\boldsymbol{q})} = \int_{\mathbb{R}^3} \rho(\boldsymbol{r}) e^{-i\boldsymbol{q}\cdot\boldsymbol{r}} d\mathrm{V}(\boldsymbol{r}) = \int_{\mathbb{R}^3} \rho(\boldsymbol{r}') e^{i\boldsymbol{q}\cdot\boldsymbol{r}'} d\mathrm{V}(\boldsymbol{r}') = f(\boldsymbol{q}), \tag{D.50}$$

the conclusion follows immediately. □

Lemma D.3 *Let the electron density $\rho(\cdot)$ be isotropic, i.e., $\rho(\boldsymbol{R}\boldsymbol{r}) = \rho(\boldsymbol{r})$ for each rotation $\boldsymbol{R}$ and each $\boldsymbol{r} \in \mathbb{R}^3$. Then $f(\cdot)$ is isotropic and real-valued.*

Proof Let $\boldsymbol{r}' = \boldsymbol{R}^{-1}\boldsymbol{r}$. Then $\boldsymbol{r} = \boldsymbol{R}\boldsymbol{r}'$. For each rotation $\boldsymbol{R}$ and each $\boldsymbol{q} \in \mathbb{R}^3$, we have

$$f(\boldsymbol{R}\boldsymbol{q}) = \int_{\mathbb{R}^3} \rho(\boldsymbol{R}\boldsymbol{r}') e^{i\boldsymbol{R}\boldsymbol{q}\cdot\boldsymbol{r}} d\mathrm{V}(\boldsymbol{R}\boldsymbol{r}') = \int_{\mathbb{R}^3} \rho(\boldsymbol{r}') e^{i\boldsymbol{q}\cdot\boldsymbol{r}'} d\mathrm{V}(\boldsymbol{r}') = f(\boldsymbol{q}). \tag{D.51}$$

Hence the function $f(\cdot)$ is isotropic and $f(\boldsymbol{q}) = f(\|\boldsymbol{q}\|)$ for each $\boldsymbol{q}$.

If ρ is isotropic, then $f(\boldsymbol{r}) = f(\|\boldsymbol{r}\|) = f(-\boldsymbol{r})$. Hence it is also centrally symmetric. By Lemma D.2, $f(\cdot)$ is real-valued. □

Remark D.4 Under the assumption that atomic electrons can be treated as free electrons, the atomic scattering factor f is given by formula (D.49). For some atoms (e.g., the helium atom), the electron density ρ in (D.49) is found to be isotropic (or spherically symmetric). For many other atoms, the isotropy of ρ can be taken as a good first approximation. Under this fact or approximation on ρ, f as given by (D.49) is isotropic and real-valued. Indeed tables that list numerical values of f versus $\|\boldsymbol{q}\|/4\pi$ (cf. Remark D.5) for free atoms of 98 elements and for many chemically significant ions, as computed from *ab initio* methods, are available [210].

When the frequency ω of the incident radiation is much higher than the natural absorption frequencies of the scattering atom (e.g., for lighter atoms), the assumption that atomic electrons be treated as free electrons is a good approximation. But, when ω is of the same order of the absorption frequencies, dispersion corrections should be made. Then the atomic scattering factor is given by

$$f = f^0 + f' + if''; \tag{D.52}$$

here f^0 is the part defined by (D.49) and is given in the tables; f' and f'' are the real and imaginary parts of the dispersion correction, respectively. An atom is said to undergo anomalous scattering if its atomic scattering factor becomes complex because dispersion correction

[187] Cf. Ewald [112, Chaps. 4–5] for his vivid descriptions of Laue's discovery of X-ray diffraction by crystals and the contributions of W.L. Bragg and W.H. Bragg in the origin of crystal structure analysis.

is necessary. We shall refrain from making dispersion corrections and shall henceforth set them aside, except to note that Friedel's rule (see Sect. D.6) breaks down when the unit cell contains more than one type of atoms and at least one atom in the cell undergoes anomalous scattering. □

D.4 Diffraction by a Crystallite

We consider polycrystalline materials, the crystallites of which have an average grain size[188] which is small as compared with the length of the wave path of the reflected X-ray beam from the sample to the detector (in the range of 150–450 mm for most laboratory $\theta/2\theta$ diffractometers[189]), but is huge as compared with the size of the unit cell of the crystalline sample. For example, for commercial O-temper aluminum alloys, the average grain size is typically in the range of 5 to 20 microns (10^{-6} m), whereas the fcc unit cell of aluminum has cell parameter $a \approx 4 \times 10^{-10}$ m.

Let us return to the setting discussed in Sect. D.2, except that the electrons are replaced by atoms with their nuclei located at $\boldsymbol{r}_1, \ldots, \boldsymbol{r}_N$ and electron densities $\rho_1, \ldots, \rho_N$, respectively. By (D.48), at the point $R\boldsymbol{n}$ in the far field the electric field of the secondary radiation due to the atom with nucleus located at $\boldsymbol{r}_n$ is given by

$$\boldsymbol{E}(R\boldsymbol{n}, t) = r_0 \cdot \frac{E_0 e^{-i\omega(t-R/c)}}{\|R\boldsymbol{n} - \boldsymbol{r}_n\|} \Big(\int_{\mathbb{R}^3} \rho_n(\boldsymbol{r} - \boldsymbol{r}_n) e^{i(\boldsymbol{k}-\boldsymbol{k}_0)\cdot \boldsymbol{r}} d\mathrm{V}(\boldsymbol{r}) \Big) \sin\varphi\, \hat{\boldsymbol{\varepsilon}}, \tag{D.53}$$

Let $\boldsymbol{r}' = \boldsymbol{r} - \boldsymbol{r}_n$. By a change of variables, the integral in (D.53) can be written as

$$\int_{\mathbb{R}^3} \rho_n(\boldsymbol{r} - \boldsymbol{r}_n) e^{i(\boldsymbol{k}-\boldsymbol{k}_0)\cdot \boldsymbol{r}} d\mathrm{V}(\boldsymbol{r}) = e^{i(\boldsymbol{k}-\boldsymbol{k}_0)\cdot \boldsymbol{r}_n} \int_{\mathbb{R}^3} \rho_n(\boldsymbol{r}') e^{i(\boldsymbol{k}-\boldsymbol{k}_0)\cdot \boldsymbol{r}'} d\mathrm{V}(\boldsymbol{r}') = e^{i(\boldsymbol{k}-\boldsymbol{k}_0)\cdot \boldsymbol{r}_n} f_n, \tag{D.54}$$

where f_n is the atomic scattering factor of the atom with nucleus located at $\boldsymbol{r}_n$. Under the approximation that $\|R\boldsymbol{n} - \boldsymbol{r}_n\| \approx \|R\boldsymbol{n}\| = R$, the electric field at $R\boldsymbol{n}$ is

$$\boldsymbol{E}(R\boldsymbol{n}, t) = r_0 \cdot \frac{E_0 e^{-i\omega(t-R/c)}}{R} \Big(\sum_{n=1}^{N} f_n e^{i(\boldsymbol{k}-\boldsymbol{k}_0)\cdot \boldsymbol{r}_n} \Big) \sin\varphi\, \hat{\boldsymbol{\varepsilon}}. \tag{D.55}$$

Note that (D.55) reduces to (D.23) if $f_n = 1$ or $\rho_n(\boldsymbol{r}) = \delta(\boldsymbol{r} - \boldsymbol{r}_n)$, where $\delta(\cdot)$ denotes the delta function, for each n.

Let $(\mathsf{C}, \boldsymbol{\kappa}_0)$ be an ideal crystal with lattice L, primitive sublattice $\mathcal{L}^{(p)}(\boldsymbol{0}) = \{m_1\boldsymbol{a}_1 + m_2\boldsymbol{a}_2 + m_3\boldsymbol{a}_3 : m_i \in \mathbb{Z} \text{ for } i = 1, 2, 3\}$ (see (2.118)), and conventional unit cell $\Pi[\boldsymbol{a}_1, \boldsymbol{a}_2, \boldsymbol{a}_3]$, where the lattice vectors $\boldsymbol{a}_i$ $(i = 1, 2, 3)$ constitute a conventional basis of lattice L that serves also as the chosen primitive basis of the sublattice $\mathcal{L}^{(p)}(\boldsymbol{0})$. Let M_1, M_2, and M_3 be positive integers, all of which are of the order of 10^4. Let $\mathcal{L}_\mathrm{c}$ be the set of translations defined

[188] "Grain size" is a technical term. For our present purpose, however, a rough idea will suffice. For simplicity and definiteness, consider statistically equiaxed grains, for which "grain size" can be taken as the diameter.

[189] See [30, pp. 15–16] for a brief description of such diffractometers.

by[190]

$$\mathcal{L}_{\rm c} = \{(\boldsymbol{u}, \boldsymbol{I}) \in \mathcal{G} : \boldsymbol{u} \in \mathcal{L}^{(p)}, -M_i \le m_i \le M_i - 1 \text{ for } i = 1, 2, 3\}. \tag{D.56}$$

In what follows we consider a thought-experiment of X-ray diffraction that has as target a small crystallite

$$\mathcal{C} = \bigcup_{h \in \mathcal{L}_{\rm c}} h\, \Pi[\boldsymbol{a}_1, \boldsymbol{a}_2, \boldsymbol{a}_3], \tag{D.57}$$

which is in the shape of a parallelepiped of sides $2M_i\|\boldsymbol{a}_i\|$ $(i = 1, 2, 3)$ that consists of $8M_1M_2M_3$ translates of the unit cell.

The setting of the thought-experiment is similar to that described in Sect. D.1, now with the crystallite $\mathcal{C}$ placed so that the corner $(0, 0, 0)$ of the unit cell $\Pi[\boldsymbol{a}_1, \boldsymbol{a}_2, \boldsymbol{a}_3]$ is at the origin which defines the starting point of all position vectors in the diffraction experiment. Let there be N basis atoms in the unit cell, which have electron densities $\rho_1, \ldots, \rho_N$ and their nuclei located at $\boldsymbol{r}_1, \ldots, \boldsymbol{r}_N$, respectively. In the crystallite $\mathcal{C}$, the atoms with electron density ρ_n have their nuclei located at

$$\boldsymbol{r}_n + m_1\boldsymbol{a}_1 + m_2\boldsymbol{a}_2 + m_3\boldsymbol{a}_3, \tag{D.58}$$

where the integers m_i runs from $-M_i$ to $M_i - 1$ for $i = 1, 2, 3$. We assume that the crystallite $\mathcal{C}$ is sufficiently small that $\|R\boldsymbol{n} - (\boldsymbol{r}_n + m_1\boldsymbol{a}_1 + m_2\boldsymbol{a}_2 + m_3\boldsymbol{a}_3)\| \approx R$ for all n and m_i. Replacing $\boldsymbol{r}_n$ in (D.54) by the expression given in (D.58) and summing the contributions from all atoms in $\mathcal{C}$, we observe that the electric field of the secondary radiation at $R\boldsymbol{n}$ in the far field is:

$$\boldsymbol{E}(R\boldsymbol{n}, t) = r_0 \cdot \frac{E_0 e^{-i\omega(t-R/c)}}{R} \Big(\sum_{n=1}^{N} f_n e^{i(\boldsymbol{k}-\boldsymbol{k}_0)\cdot\boldsymbol{r}_n} \Big) \Big(\prod_{i=1}^{3} \sum_{m_i=-M_i}^{M_i-1} e^{i(\boldsymbol{k}-\boldsymbol{k}_0)\cdot m_i\boldsymbol{a}_i} \Big) \sin\varphi\, \hat{\boldsymbol{\varepsilon}}. \tag{D.59}$$

Let $\eta_i = (\boldsymbol{k} - \boldsymbol{k}_0)\cdot\boldsymbol{a}_i$. The sum $\sum_{m_i=-M_i}^{M_i-1} e^{i(\boldsymbol{k}-\boldsymbol{k}_0)\cdot m_i\boldsymbol{a}_i} = \sum_{m_i=-M_i}^{M_i-1} e^{im_i\eta_i}$ is a finite geometric series. Its sum is

$$\sum_{m_i=-M_i}^{M_i-1} e^{im_i\eta_i} = \frac{\sin(M_i\eta_i)}{\frac{1}{2}i(1 - e^{i\eta_i})}. \tag{D.60}$$

Hence the intensity of the secondary radiation at $R\boldsymbol{n}$ is given by the formula

$$\begin{aligned} I &= I_{\rm e} \Big| \sum_{n=1}^{N} f_n e^{i(\boldsymbol{k}-\boldsymbol{k}_0)\cdot\boldsymbol{r}_n} \Big|^2 \cdot \prod_{i=1}^{3} \Big| \frac{\sin(M_i\eta_i)}{\frac{1}{2}i(1 - e^{i\eta_i})} \Big|^2 \\ &= I_{\rm e} \Big| \sum_{n=1}^{N} f_n e^{i(\boldsymbol{k}-\boldsymbol{k}_0)\cdot\boldsymbol{r}_n} \Big|^2 \cdot \frac{\sin^2 M_1\eta_1}{\sin^2 \frac{1}{2}\eta_1} \cdot \frac{\sin^2 M_2\eta_2}{\sin^2 \frac{1}{2}\eta_2} \cdot \frac{\sin^2 M_3\eta_3}{\sin^2 \frac{1}{2}\eta_3}. \end{aligned} \tag{D.61}$$

[190] Cf. [120], where Laue let m_i run from $-M_i$ to M_i. That Laue made a trivial error is clear when one sums the finite geometric series in (D.60). Ewald [112, p. 49] repeated Laue's error when he asserted that "Laue assumes the (finite) crystal to form a block of $[(2M_1 + 1)(2M_2 + 1)(2M_3 + 1)]$ cells". Here we have used our notation to write M_1, M_2, and M_3 for Laue's M, N, and P, respectively.

The equation on intensity in [120] that shows

$$I \propto \frac{\sin^2 M_1\eta_1}{\sin^2 \frac{1}{2}\eta_1} \cdot \frac{\sin^2 M_2\eta_2}{\sin^2 \frac{1}{2}\eta_2} \cdot \frac{\sin^2 M_3\eta_3}{\sin^2 \frac{1}{2}\eta_3}, \tag{D.62}$$

in the words of Authier [10, p. 110], "is the basis of the geometrical, or kinematical, theory of diffraction."

Intensity formula (D.61) can be taken as the product of two factors: one gives the scattering intensity due to the atoms in the unit cell, and the other is the function

$$\mathfrak{I}(\eta_1, \eta_2, \eta_3) = \frac{\sin^2 M_1\eta_1}{\sin^2 \frac{1}{2}\eta_1} \cdot \frac{\sin^2 M_2\eta_2}{\sin^2 \frac{1}{2}\eta_2} \cdot \frac{\sin^2 M_3\eta_3}{\sin^2 \frac{1}{2}\eta_3}, \tag{D.63}$$

which gives the multiplicative effect of interference among contributions from $8M_1M_2M_3$ translates of the unit cell that are arranged orderly according to the pattern of the crystal sublattice $\mathcal{L}^{(p)}(\mathbf{0})$ to form a parallelepiped of the given dimensions. We call $\mathfrak{I}$ the Laue interference function.

D.4.1 The Laue Equations

For $i = 1, 2, 3$, let $\xi_i = \frac{1}{\lambda}(\boldsymbol{s} - \boldsymbol{s}_0) \cdot \boldsymbol{a}_i$ and $N_i = 2M_i$. For later convenience, we recast Laue's interference function as follows:

$$\mathfrak{I}(\xi_1, \xi_2, \xi_3) = \frac{\sin^2 N_1\pi\xi_1}{\sin^2 \pi\xi_1} \cdot \frac{\sin^2 N_2\pi\xi_2}{\sin^2 \pi\eta_2} \cdot \frac{\sin^2 N_3\pi\xi_3}{\sin^2 \pi\xi_3}. \tag{D.64}$$

For $i = 1, 2, 3$, let $A_i(\xi_i) = \sin^2 N_i\pi\xi_i / \sin^2 \pi\xi_i$, and let N_i be all of order 10^4. Each A_i assume their maximum value of N_i^2 at $\xi_i = h_i$, for each $h_i \in \mathbb{Z}$. In the vicinity of each maximum, the value of A_i drops precipitously to zero at $\xi_i = h_i \pm 1/N_i$, rises to a secondary maximum of magnitude about 5% (resp. 2%, 1%, 0.5%) of N_i^2 in the intervals $(h_i + 1/N_i, h_i + 2/N_i)$ and $(h_i - 2/N_i, h_i - 1/N_i)$ (resp. $(h_i + r/N_i, h_i + (r+1)/N_i)$ and $(h_i - (r+1)/N_i, h_i - r/N_i)$ for $r = 2, 3, 4$), respectively, drops to zero again at $\xi_i = h_i \pm 2/N_i$ (resp. $\xi_i = h_i \pm (r+1)/N_i$ for $r = 2, 3, 4$), and is negligibly small as compared with N_i^2 everywhere else away from another maximum. Hence each A_i may be taken as zero outside the immediate vicinity of the sharp maxima at $\xi_i = h_i$, where $h_i \in \mathbb{Z}$. Thus the Laue interference function will attain its maximum value of $N_1^2N_2^2N_3^2$ when the three equations $\xi_i = h_i$ for some integer h_i are satisfied for all $i = 1, 2, 3$. As $\xi_i = \frac{1}{\lambda}(\boldsymbol{s} - \boldsymbol{s}_0) \cdot \boldsymbol{a}_i$, these three equations can be recast as

$$\frac{\boldsymbol{s} - \boldsymbol{s}_0}{\lambda} \cdot \boldsymbol{a}_1 = h, \quad \frac{\boldsymbol{s} - \boldsymbol{s}_0}{\lambda} \cdot \boldsymbol{a}_2 = k, \quad \frac{\boldsymbol{s} - \boldsymbol{s}_0}{\lambda} \cdot \boldsymbol{a}_3 = l \qquad \text{for some } h, k, l \in \mathbb{Z}, \tag{D.65}$$

which are called the Laue equations. In (D.65) we have silently written h, k, and l for h_1, h_2, and h_3, respectively, to conform with the usual notation in the literature of X-ray crystallography. In what follows we shall use (h, k, l) and (h_1, h_2, h_3) interchangeably.

We can put the Laue equations in a more compact form. Let $\boldsymbol{a}_1^*$, $\boldsymbol{a}_2^*$, and $\boldsymbol{a}_3^*$ be the triad of reciprocal basis vectors corresponding to the primitive basis $\{\boldsymbol{a}_i : i = 1, 2, 3\}$ of the primitive

sublattice $\mathcal{L}^{(p)}(\mathbf{0})$. Then by $(1.40)_2$ we have

$$\begin{aligned}\frac{\boldsymbol{s}-\boldsymbol{s}_0}{\lambda} &= \Big(\frac{\boldsymbol{s}-\boldsymbol{s}_0}{\lambda}\cdot\boldsymbol{a}_1\Big)\boldsymbol{a}_1^* + \Big(\frac{\boldsymbol{s}-\boldsymbol{s}_0}{\lambda}\cdot\boldsymbol{a}_2\Big)\boldsymbol{a}_2^* + \Big(\frac{\boldsymbol{s}-\boldsymbol{s}_0}{\lambda}\cdot\boldsymbol{a}_3\Big)\boldsymbol{a}_3^* \\ &= h\boldsymbol{a}_1^* + k\boldsymbol{a}_2^* + l\boldsymbol{a}_3^* \\ &= \mathbf{H}_{hkl}, \qquad (h,k,l\in\mathbb{Z})\end{aligned} \tag{D.66}$$

where $\mathbf{H}_{hkl} = h\boldsymbol{a}_1^* + k\boldsymbol{a}_2^* + l\boldsymbol{a}_3^* \in \mathsf{L}^*$ is a reciprocal lattice vector with coordinates (h,k,l). Hence the three Laue equations are equivalent to the requirement that $\frac{1}{\lambda}(\boldsymbol{s}-\boldsymbol{s}_0)$ be a reciprocal lattice vector.

Since (ξ_1,ξ_2,ξ_3) simply gives the coordinates of the vector $\frac{1}{\lambda}(\boldsymbol{s}-\boldsymbol{s}_0)$ with respect to the reciprocal basis $\{\boldsymbol{a}_i^*\}$, the Laue interference function $\mathfrak{I}$ and its three factors A_i can be taken as functions of $\frac{1}{\lambda}(\boldsymbol{s}-\boldsymbol{s}_0)$. Let

$$\Pi_{hkl} = \left\{(\xi_1,\xi_2,\xi_3) : h_i - \frac{5}{N_i} \le \xi_i \le h_i + \frac{5}{N_i} \text{ for } i=1,2,3\right\} \tag{D.67}$$

be the parallelepiped centered at (h,k,l) and sides of length $10\|\boldsymbol{a}_i^*\|/N_i$ parallel to the reciprocal basis vectors $\boldsymbol{a}_i^*$ for $i=1,2,3$, respectively. From our discussions on the properties of the functions A_i at the beginning of this subsection, we observe that not only does the Laue interference function assume sharp maxima at $(h,k,l)\in\mathsf{L}^*$, but there also holds

$$\mathfrak{I}\Big(\frac{\boldsymbol{s}-\boldsymbol{s}_0}{\lambda}\Big) \approx 0 \qquad \text{for } \frac{\boldsymbol{s}-\boldsymbol{s}_0}{\lambda} \notin \bigcup_{h,k,l} \Pi_{hkl}. \tag{D.68}$$

D.4.2 Bragg's Law

W.L. Bragg first heard [139, p. 410] about the news of Laue's discovery [120] from his father W.H. Bragg, who learned of it himself through a letter dated 26 June 1912 from the Norwegian physicist Lars Vegard; see [312]. "Walking along the Backs in Cambridge one day in the autumn" [259] W.L. Bragg, then a 22-year old graduate student, had an idea that led to the publication of two seminal papers [43, 44] by December 2012. While Laue saw in the crystal a three-dimensional diffraction grating, Bragg realized [44] that "Laue's crystallographs can be shown to be due to partial reflection of the incident beam in sets of parallel planes in the crystal on which the atom centres may be arranged, the simplest of which are the actual cleavage planes of the crystal." In an experiment, "[a] narrow pencil of X-rays ... was allowed to fall at an angle of incidence of 80° on a slip of mica ... Variation of the angle of incidence and of the distance of plate from mica left no doubt that the laws of reflection were obeyed." But Bragg also knew well that what he called partial reflection "is merely another way of looking at the diffraction." In fact Bragg reflections, where the angle of incidence is equal to the angle of reflection (cf. Fig. 2), will not occur unless the equation

$$2d\sin\theta = n\lambda \qquad (n=1,2,3,\ldots) \tag{D.69}$$

is observed; here d is the distance between the parallel lattice planes that serve as sheets of atomic mirrors; θ is the glancing angle of the incident X-ray beam; λ is the X-ray wavelength; the natural number n is called the order of the reflection. Equation (D.69), now

called Bragg's law or the Bragg equation, first appeared in [43], where the angle of incidence $\pi/2 - \theta$ was used instead of the glancing angle or Bragg angle θ.[191]

The Bragg equation can be derived from the Laue equations. Indeed, taking the norm on both sides of (D.66), we obtain

$$\|\boldsymbol{s} - \boldsymbol{s}_0\| = \lambda \|\mathbf{H}_{hkl}\|, \qquad \text{or} \qquad 2\sin\theta = \frac{\lambda}{d_{hkl}}. \tag{D.70}$$

If the integers h, k, and l have no common factor larger than 1, then $d = d_{hkl}$ and (D.70$_2$) reduces to the Bragg equation for a first-order reflection. If the highest common factor of h, k, and l is $n > 1$, i.e., $h = nh'$, $k = nk'$, and $l = nl'$, then $d_{hkl} = d_{h'k'l'}/n$ and $d = d_{h'k'l'}$, under which (D.70$_2$) gives the Bragg equation for an n-th order reflection.

Remark D.5 As a first approximation the electron density ρ in the integrand of the atomic scattering factor f is often taken as isotropic or spherical symmetric. It follows then from (D.49), the definition of the atomic scattering factor, that f is isotropic, i.e.,

$$f(\boldsymbol{k} - \boldsymbol{k}_0) = f(\|\boldsymbol{k} - \boldsymbol{k}_0\|), \tag{D.71}$$

and is real-valued. Since $\|\boldsymbol{k} - \boldsymbol{k}_0\| = \frac{2\pi}{\lambda}\|\boldsymbol{s} - \boldsymbol{s}_0\| = 4\pi \sin\theta/\lambda$, the atomic scattering factor is a function of $\sin\theta/\lambda$. For the elements, tables of the values of f as a function of $\sin\theta/\lambda$, as computed by *ab initio* methods, are available. For further discussion on the Bragg reflections, let us present some general observations and copy a few numbers from the table reprinted in [334, pp. 369–371]. The table lists the values of atomic scattering factor f at some values of $\sin\theta/\lambda$ (in units of Å^{-1}) for the elements with atomic numbers Z from 1 to 92. For each element, $f(0) = Z$, which is the maximum value of f, and the function f is monotonic decreasing as $\sin\theta/\lambda$ increases. For example, for Al, $f(0) = 13.000$, $f(0.2) = 9.158$, $f(0.4) = 6.766$, $f(0.6) = 4.713$; for Ti, $f(0) = 22.000$, $f(0.2) = 16.044$, $f(0.4) = 10.852$, $f(0.6) = 8.007$.

Consider an X-ray diffraction experiment (cf. Fig. 2) in which both the target, say an aluminum sample, and the X-ray wavelength λ are fixed, but we can vary θ to get different orders of Bragg reflections. Suppose we get first-order reflection at $\sin\theta/\lambda = 0.2$. By Bragg's law, we shall obtain second-order and third-order reflections at $\sin\theta/\lambda = 0.4$ and 0.6, respectively. However, from the values of the atomic scattering factor given in the preceding paragraph, for Al the intensity of the second-order and third-order reflections are $(6.766/9.158)^2 \approx 0.55$ and $(4.713/9.158)^2 \approx 0.26$ times the intensity of the first-order reflection. For Ti the drops in intensity of the higher-order reflections are similar. In fact the decline of intensity with increasing order of reflection is a general phenomenon already noted independently by W.H. Bragg [46] and by Compton [74] in 1915. Hence as far as (hkl) X-ray pole figures for measurement of texture are concerned, those (hkl) that pertain to first-order reflections may enjoy an advantage of higher intensity over those of higher-order reflections. □

[191] We shall write the Bragg angle as θ_B when we want to emphasize that θ_B satisfies the Bragg equation (D.69) for specific measurements.

D.4.3 Integrated Intensity from a Crystallite

As explained in Sect. D.4.1, the Laue interference function $\mathfrak{I}$ in the intensity formula (cf. (D.61))

$$I = I_{\mathrm{e}} \Big| \sum_{n=1}^{N} f_n e^{i(\boldsymbol{k}-\boldsymbol{k}_0)\cdot \boldsymbol{r}_n} \Big|^2 \mathfrak{I}\Big(\frac{\boldsymbol{s}-\boldsymbol{s}_0}{\lambda}\Big) \tag{D.72}$$

attains its sharp peak value when the incident and diffracted beams are such that $\frac{1}{\lambda}(\boldsymbol{s}-\boldsymbol{s}_0)$ is exactly equal to a reciprocal lattice vector. In practice, however, the incident beam cannot be made perfectly parallel and, as real crystals have imperfections, the set of reflecting planes are not exactly parallel throughout the entire crystallite. In an experiment where a roughly collimated beam falls on a crystallite oriented such that the incident beam makes roughly the correct Bragg angle θ_{B} for the set of (hkl) planes, the tip of $\frac{1}{\lambda}(\boldsymbol{s}-\boldsymbol{s}_0)$ will cover a range of values around $\mathbf{H}_{hkl}$. As discussed in Sect. D.4.1, there will still be appreciable intensity in a diffracted beam with $\frac{1}{\lambda}(\boldsymbol{s}-\boldsymbol{s}_0) \in \Pi_{hkl}$ even if condition (D.66) is not satisfied. To overcome these difficulties, methods are designed to scan the entire region Π_{hkl}, where $\mathfrak{I}$ is not negligible, to measure a method-dependent quantity called "integrated intensity".

In what follows we will describe one of the simplest of such methods, namely the rotating crystal method.[192] In a $\theta/2\theta$ scan, where the incident beam is effectively monochromatic and the crystallite set so that the incident beam is at the correct Bragg angle θ_{B} to the chosen (hkl) planes,

> [t]he crystal is then slowly rotated with a uniform angular velocity $[\dot{\theta}]$ about a line that is parallel to the reflecting planes and perpendicular to the plane containing the incident and diffracted beams. This rotation is normally begun, say 1° before the ideal Bragg-angle value and terminated 2° later, so that every irradiated part of the crystal has an equal opportunity to reflect every nonparallel ray incident on it. During the rotation of the crystal the intensity of the diffracted beam is continuously recorded by a detector large enough to intercept every diffracted ray. [11, p. 194].

Let us start with a Cartesian coordinate system usually adopted in $\theta/2\theta$ scans, under which the following specifications hold: the top reflecting plane of the crystallite is in the 1-2 plane; the center of the incident beam hits at the origin of the coordinate system; the vector $(0, 0, 1)$ is normal to the reflecting planes; the incident and diffracted rays with the correct Bragg angle have $\boldsymbol{s}_0 = (\cos\theta_{\mathrm{B}}, 0, -\sin\theta_{\mathrm{B}})$ and $\boldsymbol{s} = (\cos\theta_{\mathrm{B}}, 0, \sin\theta_{\mathrm{B}})$; the crystallite is rotating with uniform angular velocity $\dot{\theta}$ about the $(0, 1, 0)$ axis. For our discussion, however, it is more convenient to use the coordinate system obtained by rotating the original system by the Bragg angle θ_{B} about the $(0, 1, 0)$ axis. Let $\hat{\boldsymbol{i}}$, $\hat{\boldsymbol{j}}$, and $\hat{\boldsymbol{k}}$ be the orthonormal basis of the new Cartesian coordinate system. Then $\boldsymbol{s}_0 = \hat{\boldsymbol{i}}$, $\boldsymbol{s} = \cos 2\theta_{\mathrm{B}}\, \hat{\boldsymbol{i}} + \sin 2\theta_{\mathrm{B}}\, \hat{\boldsymbol{k}}$, and the axis defined by $\hat{\boldsymbol{j}}$ remains the axis of rotation of the crystallite.

Instead of having the X-ray source fixed and letting the sample rotate, let us consider the equivalent arrangement where the sample is fixed and at time t the direction of the incident beam is $\boldsymbol{s}_0'(t) = \cos\Delta\theta(t)\,\hat{\boldsymbol{i}} - \sin\Delta\theta(t)\,\hat{\boldsymbol{k}}$, with $\Delta\theta(t)$ running from $-|\Delta\theta|_{\max}$ to $|\Delta\theta|_{\max}$ (e.g., $|\Delta\theta|_{\max} = 1°$ as stated in the quoted description above). Because of the slight deviations from parallelism in the incident beam and of the imperfections in the crystallite, the rays of the diffracted beam have directions $\boldsymbol{s}'$ that cover some narrow solid angle Ω.

[192] See Zachariasen [351, pp. 86–89] for a classification and general discussion of "all conceivable methods" in this regard.

Let dS be a surface area element of the detector which is reached by the diffracted ray with propagation direction $\boldsymbol{s}'$, and let R be the distance of dS from the origin. Let $d\mathcal{E}$ be the radiant energy received by dS from the instant t to $t+dt$. Then by (D.72) we have

$$d\mathcal{E} = I\,dS\,dt = \frac{I_e R^2}{\dot{\theta}}\Big|\sum_{n=1}^{N} f_n e^{i(\boldsymbol{k}'-\boldsymbol{k}'_0)\cdot\boldsymbol{r}_n}\Big|^2 \mathfrak{I}\Big(\frac{\boldsymbol{s}'-\boldsymbol{s}'_0}{\lambda}\Big)\,d\Omega\,d\theta, \tag{D.73}$$

where $\boldsymbol{k}' = 2\pi\boldsymbol{s}'/\lambda$ and $\boldsymbol{k}'_0 = 2\pi\boldsymbol{s}'_0/\lambda$.

In the reciprocal space, draw the vector $\boldsymbol{s}_0/\lambda$ such that its tip is at O, the origin of the reciprocal lattice. Let C be the starting point of $\boldsymbol{s}_0/\lambda$. With C as starting point, draw the vector $\boldsymbol{s}/\lambda$, the tip of which by (D.66) must end at the tip (h,k,l) of the reciprocal vector $\mathbf{H}_{hkl}$. Let $D=(h,k,l)$. With C as center, draw a sphere $\mathcal{S}_E$ with $1/\lambda$ as radius. This sphere is called the Ewald sphere. Clearly the points C, D, and O lie in the same circular cross-section of the Ewald sphere $\mathcal{S}_E$. Let $T_D\mathcal{S}_E$ be the tangent plane to the Ewald sphere at the point D. Note that D is also the center of the small parallelepiped Π_{hkl}.

The argument $\frac{1}{\lambda}(\boldsymbol{s}'-\boldsymbol{s}'_0)$ of the Laue interference function $\mathfrak{I}$ can be written as

$$\begin{aligned}\frac{\boldsymbol{s}'-\boldsymbol{s}'_0}{\lambda} &= \frac{\boldsymbol{s}-\boldsymbol{s}_0}{\lambda} + \frac{(\boldsymbol{s}'-\boldsymbol{s})+(\boldsymbol{s}_0-\boldsymbol{s}'_0)}{\lambda}\\ &= \mathbf{H}_{hkl} + \frac{\Delta\boldsymbol{S}}{\lambda}, \qquad \text{where } \Delta\boldsymbol{S} = (\boldsymbol{s}'-\boldsymbol{s})+(\boldsymbol{s}_0-\boldsymbol{s}'_0).\end{aligned} \tag{D.74}$$

Let us consider the difference $\frac{1}{\lambda}(\boldsymbol{s}'-\boldsymbol{s})$ first. The direction $\boldsymbol{s}'$ is within the narrow cone Ω of directions of diffracted rays that are slightly different from $\boldsymbol{s}$ because of various imperfections. The vector $\boldsymbol{s}'/\lambda$ is within Ω and, as a position vector, $\boldsymbol{s}'/\lambda \in \mathcal{S}_E$ is close to D. On the other hand, $\boldsymbol{s}/\lambda = \mathbf{CD}$. Hence, as an approximation, we may replace $\frac{1}{\lambda}(\boldsymbol{s}'-\boldsymbol{s})$ by its orthogonal projection onto the tangent plane $T_D\mathcal{S}_E$. Likewise, we approximate the cap $\Omega\cap\mathcal{S}_E$ by its orthogonal projection, say $\mathcal{D}$, onto $T_D\mathcal{S}_E$.

We choose a Cartesian coordinate system in the reciprocal space with D as the origin and orthonormal basis

$$\hat{\boldsymbol{i}}' = -\sin 2\theta_B\,\hat{\boldsymbol{i}} + \cos 2\theta_B\,\hat{\boldsymbol{k}}, \qquad \hat{\boldsymbol{j}}' = \hat{\boldsymbol{j}}, \qquad \hat{\boldsymbol{k}}' = -\cos 2\theta_B\,\hat{\boldsymbol{i}} - \sin 2\theta_B\,\hat{\boldsymbol{k}}, \tag{D.75}$$

where $\hat{\boldsymbol{i}}'$ and $\hat{\boldsymbol{j}}'$ lie in the tangent plane $T_D\mathcal{S}_E$ and $\hat{\boldsymbol{k}}'$ is normal to the tangent plane. The Cartesian coordinates of a point under this system will be written as (x',y',z'). With this preparation we turn to examine the term $\frac{1}{\lambda}(\boldsymbol{s}_0-\boldsymbol{s}'_0)$. We have

$$\frac{\boldsymbol{s}_0-\boldsymbol{s}'_0}{\lambda} = \frac{(1-\cos\Delta\theta)\,\hat{\boldsymbol{i}} - \sin\Delta\theta\,\hat{\boldsymbol{k}}}{\lambda} \approx -\frac{\Delta\theta}{\lambda}\hat{\boldsymbol{k}}, \tag{D.76}$$

where the approximation is based on the fact that $|\Delta\theta| \le 1^\circ \approx 0.0175$ radian. The component of $\frac{1}{\lambda}(\boldsymbol{s}_0-\boldsymbol{s}'_0)$ in the direction of $\hat{\boldsymbol{k}}'$ is

$$\Delta z' = -\frac{d\theta}{\lambda}\hat{\boldsymbol{k}}\cdot\hat{\boldsymbol{k}}' = -\frac{\Delta\theta}{\lambda}\hat{\boldsymbol{k}}\cdot(-\cos 2\theta_B\,\hat{\boldsymbol{i}} - \sin 2\theta_B\,\hat{\boldsymbol{k}}) = \frac{\sin 2\theta_B}{\lambda}\Delta\theta. \tag{D.77}$$

Let $d = \frac{1}{\lambda}\sin 2\theta_B|\Delta\theta|_{\max}$. We assume that the cylinder $\mathcal{D}\times[-d,d]$ is large enough that it covers Π_{hkl}. Clearly this assumption will become invalid when θ_B is too close to 0 or $\pi/2$.

We claim that $d\Omega d\theta$ in (D.73) can be written as

$$d\Omega d\theta = \frac{\lambda^3}{\mathrm{V_{uc}} \sin 2\theta_{\mathrm{B}}} d\xi_1 d\xi_2 d\xi_3, \tag{D.78}$$

where $\mathrm{V_{uc}} = \boldsymbol{a}_1 \cdot (\boldsymbol{a}_2 \times \boldsymbol{a}_3)$ is the volume of the unit cell of the primitive sublattice in direct space. Indeed, as $d\Omega$ is an element of solid angle within the narrow cone Ω, we have

$$\frac{d\Omega}{\lambda^2} = dx'dy' \tag{D.79}$$

as an approximation. By (D.77), we observe that

$$dz' = \frac{\sin 2\theta_{\mathrm{B}}}{\lambda} d\theta. \tag{D.80}$$

Combining (D.79) and (D.80), we obtain

$$d\Omega d\theta = \frac{\lambda^3}{\sin 2\theta_{\mathrm{B}}} dx'dy'dz'. \tag{D.81}$$

The volume elements $dx'dy'dz'$ (of the Cartesian coordinate system with basis $\hat{\boldsymbol{i}}', \hat{\boldsymbol{j}}', \hat{\boldsymbol{k}}'$) and $d\xi_1 d\xi_2 d\xi_3$ (of the affine coordinate system with basis $\boldsymbol{a}_1^*, \boldsymbol{a}_2^*, \boldsymbol{a}_3^*$) are related by

$$dx'dy'dz' = \left| \frac{\partial(x', y', z')}{\partial(\xi_1, \xi_2, \xi_3)} \right| d\xi_1 d\xi_2 d\xi_3 = \mathrm{V_{uc}^*} d\xi_1 d\xi_2 d\xi_3 = \frac{1}{\mathrm{V_{uc}}} d\xi_1 d\xi_2 d\xi_3, \tag{D.82}$$

where $\mathrm{V_{uc}^*} = \boldsymbol{a}_1^* \cdot (\boldsymbol{a}_2^* \times \boldsymbol{a}_3^*) = 1/\mathrm{V_{uc}}$ is the volume of the unit cell in reciprocal space. Substituting (D.82) into (D.81) leads to (D.78).

We write the Laue interference function $\mathfrak{I}$ as a function of the coordinates of $\frac{1}{\lambda}(\boldsymbol{s}' - \boldsymbol{s}_0')$ under the reciprocal basis $\{\boldsymbol{a}_i^*\}$, i.e., (cf. (D.74))

$$\xi_i = \frac{\boldsymbol{s}' - \boldsymbol{s}_0'}{\lambda} \cdot \boldsymbol{a}_i = \mathbf{H}_{hkl} \cdot \boldsymbol{a}_i + \frac{\Delta \boldsymbol{S}}{\lambda} \cdot \boldsymbol{a}_i, \qquad \text{for } (i = 1, 2, 3). \tag{D.83}$$

For convenience, let us put $(h, k, l) = (h_1, h_2, h_3)$ and

$$\frac{\Delta \boldsymbol{S}}{\lambda} = \boldsymbol{p} = p_1 \boldsymbol{a}_1^* + p_2 \boldsymbol{a}_2^* + p_3 \boldsymbol{a}_3^*, \qquad \frac{\Delta \boldsymbol{S}}{\lambda} \cdot \boldsymbol{a}_i = p_i. \tag{D.84}$$

Since $h_i \in \mathbb{Z}$, we have

$$\begin{aligned} \sin^2(N_i \pi \xi_i) &= \sin^2(N_i \pi (h_i + p_i)) = \sin^2(N_i \pi p_i), \\ \sin^2(\pi \xi_i) &= \sin^2(\pi (h_i + p_i)) = \sin^2(\pi p_i). \end{aligned} \tag{D.85}$$

It follows that the Laue interference function is given by

$$\mathfrak{I}(\xi_1, \xi_2, \xi_3) = \mathfrak{I}(h_1 + p_1, h_2 + p_2, h_3 + p_3) = \prod_{i=1}^{3} \frac{\sin^2(N_i \pi p_i)}{\sin^2(\pi p_i)}. \tag{D.86}$$

Since $\xi_i = h_i + p_i$, we have $d\xi_i = dp_i$ and $d\xi_1 d\xi_2 d\xi_3 = dp_1 dp_2 dp_3$. By (D.78), we may recast (D.73) as

$$d\mathcal{E} = \frac{I_e R^2}{\dot{\theta}} \Big| \sum_{n=1}^{N} f_n e^{i(\boldsymbol{k}' - \boldsymbol{k}'_0)\cdot \boldsymbol{r}_n} \Big|^2 \Big(\prod_{i=1}^{3} \frac{\sin^2(N_i \pi p_i)}{\sin^2(\pi p_i)} \Big) \frac{\lambda^3}{\mathrm{V_{uc}} \sin 2\theta_{\mathrm{B}}} \, dp_1 dp_2 dp_3. \tag{D.87}$$

Under the assumption that the region scanned in the reciprocal space $\Omega \times [-d, d] \supset \Pi_{hkl}$, the total energy received by the detector in one scan is

$$\mathcal{E} = \frac{I_e R^2}{\dot{\theta}} \cdot \frac{\lambda^3}{\mathrm{V_{uc}} \sin 2\theta_{\mathrm{B}}} \cdot \iiint_{\Pi_{hkl}} \Big| \sum_{n=1}^{N} f_n e^{i(\boldsymbol{k}' - \boldsymbol{k}'_0)\cdot \boldsymbol{r}_n} \Big|^2 \Big(\prod_{i=1}^{3} \frac{\sin^2(N_i \pi p_i)}{\sin^2(\pi p_i)} \Big) dp_1 dp_2 dp_3. \tag{D.88}$$

Since $\boldsymbol{k}' - \boldsymbol{k}'_0 = \frac{2\pi}{\lambda}(\boldsymbol{s}' - \boldsymbol{s}_0)$, we use (D.84) to recast the expression that involves $\boldsymbol{k}' - \boldsymbol{k}'_0$ in the integrand of (D.88) as

$$F := \sum_{n=1}^{N} f_n e^{i(\boldsymbol{k}' - \boldsymbol{k}'_0)\cdot \boldsymbol{r}_n} = \sum_{n=1}^{N} f_n e^{i2\pi(\mathbf{H}_{hkl} + \boldsymbol{p})\cdot \boldsymbol{r}_n}. \tag{D.89}$$

Over the domain of integration Π_{hkl}, the slow-varying function F can be replaced by its value at $\boldsymbol{p} = \mathbf{0}$, i.e.,

$$F_{hkl} := \sum_{n=1}^{N} f_n e^{i2\pi \mathbf{H}_{hkl}\cdot \boldsymbol{r}_n}. \tag{D.90}$$

The energy received by the detector in one scan is then given by

$$\mathcal{E} = \frac{I_e R^2}{\dot{\theta}} \cdot \frac{\lambda^3}{\mathrm{V_{uc}} \sin 2\theta_{\mathrm{B}}} \cdot |F_{hkl}|^2 \iiint_{\Pi_{hkl}} \Big(\prod_{i=1}^{3} \frac{\sin^2(N_i \pi p_i)}{\sin^2(\pi p_i)} \Big) dp_1 dp_2 dp_3. \tag{D.91}$$

By (D.67), in terms of the variables p_i $(i = 1, 2, 3)$,

$$\Pi_{hkl} = \{(p_1, p_2, p_3) : -5/N_i \le p_i \le 5/N_i, \text{ for } i = 1, 2, 3\}. \tag{D.92}$$

Hence the triple integral in (D.91) is a product of three single integrals:

$$\iiint_{\Pi_{hkl}} \Big(\prod_{i=1}^{3} \frac{\sin^2(N_i \pi p_i)}{\sin^2(\pi p_i)} \Big) dp_1 dp_2 dp_3 = \prod_{i=1}^{3} \int_{-5/N_i}^{5/N_i} \frac{\sin^2(N_i \pi p_i)}{\sin^2(\pi p_i)} \, dp_i. \tag{D.93}$$

As N_i is of order 10^4, we observe that on the interval $[-5/N_i, 5/N_i]$, $\sin^2(\pi p_i) \approx \pi^2 p_i^2$. Therefore we have

$$\int_{-5/N_i}^{5/N_i} \frac{\sin^2(N_i \pi p_i)}{\sin^2(\pi p_i)} \, dp_i \approx \int_{-5/N_i}^{5/N_i} \frac{\sin^2(N_i \pi p_i)}{\pi^2 p_i^2} \, dp_i \approx \int_{-\infty}^{\infty} \frac{\sin^2(N_i \pi p_i)}{\pi^2 p_i^2} \, dp_i = N_i, \tag{D.94}$$

where we have extended the domain of integration of the third integral to the entire real line.[193] Let $\mathcal{N} = N_1 N_2 N_3$, which is the number of translates of the unit cell contained in the crystallite. As the triple integral in (D.91) is equal to $\mathcal{N}$, we obtain the formula

$$\mathcal{E} = \frac{I_0 r_0^2 |\hat{\boldsymbol{\varepsilon}}_0 \cdot \hat{\boldsymbol{\varepsilon}}|^2}{\dot{\theta}} \cdot \frac{\mathcal{N}\lambda^3}{\mathrm{V_{uc}} \sin 2\theta_\mathrm{B}} \cdot |F_{hkl}|^2 . \tag{D.95}$$

We define the integrated intensity pertaining to the rotating crystal method as[194]

$$\mathcal{I}_{hkl} = \mathcal{E}\dot{\theta} = I_0 r_0^2 |\hat{\boldsymbol{\varepsilon}}_0 \cdot \hat{\boldsymbol{\varepsilon}}|^2 \cdot \frac{\mathrm{V_{cr}}\lambda^3}{\mathrm{V_{uc}^2}} \cdot \frac{1}{\sin 2\theta_\mathrm{B}} \cdot |F_{hkl}|^2 ; \tag{D.96}$$

here we have put $\mathcal{N} = \mathrm{V_{cr}}/\mathrm{V_{uc}}$, where $\mathrm{V_{cr}}$ is the volume of the crystallite in question. For each method of measurement, the integrated intensity has a specific factor called the Lorentz factor. The expression $1/\sin 2\theta_\mathrm{B}$ in (D.96) is the Lorentz factor for the rotating crystal method. So far we have restricted our discussion on incident beams which are linearly polarized. The expression $|\hat{\boldsymbol{\varepsilon}}_0 \cdot \hat{\boldsymbol{\varepsilon}}|^2$ in (D.96), called the polarization factor, has its present form because the incident beam is assumed to be linearly polarized. If the incident beam is unpolarized, the polarization factor is $\frac{1}{2}(1 + \cos^2 2\theta_\mathrm{B})$.

Remark D.6 Formula (D.96) is meant to describe the integrated intensity of coherent X-ray scattering from a small single crystal as measured by the rotating crystal method. Even within this specific context, the formula is still incomplete as it stands. There should be a few more multiplicative correction factors (cf. [85, Sect. 12.3.1], [127, pp. 178–179], [277, pp. 158–159]), which include: (i) the temperature factor that accounts for the effect of thermal motion of the atoms on the intensity (see, e.g., Warren [334, Sect. 3.4]); (ii) the multiplicity factor, which depends on crystallite symmetry $\mathcal{F}_{hkl}$ of (hkl) planes in question; (iii) the absorption correction. For our present purpose all the important ingredients for the integrated intensity, namely $\mathrm{V_{cr}}$ and $|F_{hkl}|^2$, are already included in (D.96); see Remark D.8 for further discussion. □

[193] It is standard practice (see, e.g., [11, p. 198], [334, p. 44], [351, p. 106]) to make this extension to get the final formula (D.95). Doing so adds an extraneous number $M := 2\int_{5/N_i}^{\infty} \sin^2(N_i \pi p_i)/(\pi^2 p_i^2) dp_i$ to the original integral. Let us estimate M. On each interval $[m/N_i, (m+1)/N_i]$ of p_i, there holds $N_i^2/((m+1)^2\pi^2) \le 1/(\pi^2 p_i^2) \le N_i^2/(\pi^2 m^2)$. Hence we have

$$M < 2\sum_{m=5}^{\infty} \frac{N_i^2}{\pi^2 m^2} \int_{m/N_i}^{(m+1)/N_i} \sin^2(N_i \pi p_i) dp_i = \frac{N_i}{\pi^2} \sum_{m=5}^{\infty} \frac{1}{m^2}$$

$$= \frac{N_i}{\pi^2} \left(\frac{\pi^2}{6} - \left(1 + \frac{1}{2^2} + \frac{1}{3^2} + \frac{1}{4^2} \right) \right) \approx 0.0224\, N_i .$$

Similarly we obtain the estimate $M > (N_i/\pi^2) \sum_{m=6}^{\infty} 1/m^2 \approx 0.0184 N_i$. Thus the error introduced in extending the domain of integration is about 2%.

[194] There are three different definitions of "integrated intensity" in the literature. Here we follow Zachariasen [351, p. 108] and Als-Nielsen & Morrow [4, p. 182]. Note that $\mathcal{I}_{hkl}$ in (D.96) has the dimensions of energy (received by the detector) per unit time. Some authors (e.g., Azároff [11, p. 198], Warren [334, p. 44]) take the energy received $\mathcal{E}$ as the "integrated intensity". Others define $E\dot{\theta}/I_0 = \mathcal{I}_{hkl}$, which has the dimensions of area, as "integrated intensity" (Authier [9, p. 65]) or "integrated reflection" as an alternate name (James [165, pp. 41–43 and p. 657 of Index]).

Remark D.7 The expression F_{hkl} in (D.96) is called the structure factor, a term coined by Ewald [111]. Even if we include in (D.96) the factor that accounts for thermal motion, the structure factor is the only place in the integrated-intensity formula where the locations of the atoms appear—see (D.90)—and thence is the only factor in the formula that carries structural information on the crystal in question. Under the kinematical theory of X-ray diffraction, $|F_{hkl}|^2$ appears as a multiplicative factor in integrated-intensity formulas of all measurement methods [351, pp. 86–89 and 103–110]. □

Remark D.8 As far as XRD is concerned, we are primarily interested in the role of X-ray pole figures as records of quantitative texture information on polycrystalline materials. In this regard, $\mathrm{V_{cr}}$ and $|F_{hkl}|^2$ are the two most significant factors in the intensity formula (D.96) and its fully-corrected version:

1. Each pole figure P_{hkl} is defined by a chosen family of real or fictitious[195] (hkl) planes for Bragg reflection. In the XRD experiment to obtain a P_{hkl} pole figure by Bragg reflection, while all the parameters of the diffractometer are fixed, the sample (e.g., a small piece of sheet metal) is measured at a number of its orientations, each of which is specified by a pair of angles (α_i, β_i) $(i = 1, \ldots, n)$, and the angles are chosen so that they are the nodes of an (almost) *equal-area* grid[196] which partitions the (α, β) space; cf. Sect. 9.2. At each orientation of the sample, the (hkl) planes of a different set $\mathfrak{C}(\alpha_i, \beta_i)$ of crystallites in the sampling volume serve as Bragg mirrors. The corrected[197] integrated intensity $I(\alpha_i, \beta_i)$ of the reflected beam received by the detector is proportional to $\mathrm{V}(\mathfrak{C}(\alpha_i, \beta_i))$,[198] the total volume of crystallites in the sampling volume which contribute to $I(\alpha_i, \beta_i)$. Hence the normalized (integrated) intensity

$$p(\alpha_i, \beta_i) = \frac{I(\alpha_i, \beta_i)}{\sum_{i=1}^{n} I(\alpha_i, \beta_i)} \tag{D.97}$$

   gives an estimate of the volume fraction of the crystallites in $\mathfrak{C}(\alpha_i, \beta_i)$ in the sampling volume.
2. As determined by the crystal structure, the value of $|F_{hkl}|$ generally depends on (h, k, l) and may be zero for some (h, k, l). For example, $F_{100} = 0$ for the fcc structure. Hence aluminum, the single crystal of which is of fcc structure, does not have a (100) pole figure. This phenomenon, which is called the systematic absence of the pole figure in question, will be discussed in more detail in the next section. Also, Friedel's rule, which has important implications on determination of texture by XRD, is versed in terms of the structure factor. We will examine Friedel's rule and its implications in Sect. D.6. □

[195] Cf. Sect. 7.4 for definition of real and of fictitious (hkl) planes.

[196] See Engler and Randle [104, Sect. 4.3.3] and the references therein.

[197] The integrated intensity received by the detector in pole figure measurements requires corrections. See Remark 9.5 for more details. There we write the corrected intensity as $I(\alpha, \beta; \Theta, \Phi)$, where Θ and Φ are the spherical coordinates of the unit normal $\boldsymbol{h}$ of the (hkl) planes. Both here and there we are listing only the independent variables that affect the problem being studied. Here for example, as we are concerned with one specific pole figure, the dependence of I on $\mathbf{H}_{hkl}$, the reciprocal lattice vector that defines the (hkl) planes, is suppressed.

[198] Note that $\mathrm{V}(\mathfrak{C}(\alpha_i, \beta_i))$ for the polycrystal replaces $\mathrm{V_{cr}}$ for a single crystallite in (D.96).

D.5 Structure Factor and Systematic Absences

Because of possible destructive interference between secondary radiations from different atoms in the unit cell, it may occur that the structure factor $F_{hkl} = 0$ for some (h, k, l). When that happens, the intensity of the reflected beam in question is zero. Such extinctions are called systematic absences or systematic extinctions.

Remark D.9 In his first published paper W.L. Bragg [43] began by describing Laue's explanation of the diffraction pattern in the crystallograph of zinc blende (ZnS) [120, Fig. 5], which he deemed "unsatisfactory". Laue was not able to provide a satisfactory explanation for the absence of some spots in the aforementioned crystallograph which should have appeared if the lattice of zinc blende were simple cubic as he assumed. Bragg showed that he could account for the "absences" in the spot pattern should the atoms of zinc blende occupy the lattice nodes of a face-centered cubic structure. Bragg was the first to apply the concept of systematic absences in explaining diffraction patterns. □

In the rest of this section, we shall examine systematic absences in three common metal structures: bcc, fcc, and hcp.

D.5.1 Systematic Absences in Body-Centered and Face-Centered Cubic Structures

For both the body-centered and face-centered cubic structures, we may choose a Cartesian coordinate system such that the primitive lattice vectors for the sublattice $\mathcal{L}^{(p)}$ are $\boldsymbol{a}_i = a\boldsymbol{e}_i$ for $i = 1, 2, 3$, where $a > 0$ is the length of an edge of the cubic unit cell. Then the corresponding reciprocal basis vectors are $\boldsymbol{a}_i^* = \boldsymbol{e}_i/a$.

Body-centered cubic structure

There are two atoms in the unit cell of the body-centered cubic structure, the nuclei of which are located at $\boldsymbol{r}_1 = (0, 0, 0)$ and $\boldsymbol{r}_2 = a(\frac{1}{2}, \frac{1}{2}, \frac{1}{2})$, respectively. By (D.90) the structure factor is given by

$$F_{hkl} = f \sum_{n=1}^{2} e^{i2\pi \mathbf{H}_{hkl}\cdot \boldsymbol{r}_n} = f\left(1 + e^{i(h+k+l)\pi}\right) = f\left(1 + (-1)^{h+k+l}\right)$$
$$= \begin{cases} 2f, & \text{if } h+k+l \text{ is even,} \\ 0, & \text{if } h+k+l \text{ is odd,} \end{cases} \tag{D.98}$$

where we have made use of the fact that the two atoms are of the same type and we put $f_1 = f_2 = f$. Since the atomic structure factor f is real, we have

$$|F_{hkl}|^2 = \begin{cases} 4f^2, & \text{if } h+k+l \text{ is even,} \\ 0, & \text{if } h+k+l \text{ is odd.} \end{cases} \tag{D.99}$$

If pole figures are to be prepared for measurement of texture in a polycrystalline material of bcc crystallites, we should use (hkl) pole figures with $h + k + l$ even, e.g., (110), (211), (310), etc.

Face-centered cubic structure

There are four atoms in the unit cell of the face-centered cubic structure, the nuclei of which are located at $\boldsymbol{r}_1 = (0,0,0)$, $\boldsymbol{r}_2 = a(0, \frac{1}{2}, \frac{1}{2})$, $\boldsymbol{r}_3 = a(\frac{1}{2}, 0, \frac{1}{2})$, and $\boldsymbol{r}_4 = a(\frac{1}{2}, \frac{1}{2}, 0)$ respectively. By (D.90) the structure factor is given by

$$\begin{aligned} F_{hkl} &= f \sum_{n=1}^{4} e^{i2\pi \mathbf{H}_{hkl}\cdot \boldsymbol{r}_n} \\ &= f\left(1 + e^{i(k+l)\pi} + e^{i(l+h)\pi} + e^{i(h+k)\pi}\right) \\ &= f(1 + (-1)^{k+l} + (-1)^{l+h} + (-1)^{h+k}). \end{aligned} \tag{D.100}$$

The integers h, k, and l are said to be unmixed if they are all odd or all even, otherwise they are said to be mixed. It can be easily checked from (D.100) directly that

$$F_{hkl} = \begin{cases} 4f, & \text{for unmixed } h,k,l, \\ 0, & \text{for mixed } h,k,l. \end{cases} \tag{D.101}$$

For X-ray measurement of texture in polycrystalline materials of fcc crystallites, (hkl) pole figures with unmixed h,k,l, e.g., (111), (200), (220), (311), etc. should be used.

D.5.2 Systematic Absences in Hexagonal Close-Packed Structure

There are two atoms in the unit cell. For convenience in the present calculations, we choose the primitive hexagonal lattice such that the nuclei of the atoms are located at $\boldsymbol{r}_1 = (0,0,0)$ and $\boldsymbol{r}_2 = \frac{2}{3}\boldsymbol{a}_1 + \frac{1}{3}\boldsymbol{a}_2 + \frac{1}{2}\boldsymbol{a}_3 = (\frac{2}{3}, \frac{1}{3}, \frac{1}{2})$, respectively; cf. Sect. 2.10.2, where $\boldsymbol{r}_1$ and $\boldsymbol{r}_2$ are called A and B, respectively. By (D.90) the structure factor is given by

$$F_{hkl} = \sum_{n=1}^{2} f_n e^{i2\pi \mathbf{H}_{hkl}\cdot \boldsymbol{r}_n} = f\left(1 + e^{i2\pi\left(\frac{2h+k}{3} + \frac{l}{2}\right)}\right), \tag{D.102}$$

where we have put $f_1 = f_2 = f$ as the atomic scattering factors of the two atoms are the same.

Let $q = \left(\frac{2h+k}{3} + \frac{l}{2}\right)$. Then we have $F_{hkl} = f(1 + e^{i2\pi q})$, and

$$\begin{aligned} |F_{hkl}|^2 &= f^2(1 + e^{i2\pi q})(1 + e^{-i2\pi q}) = f^2(2 + 2\cos(2\pi q)) \\ &= 4f^2 \cos^2\left[\left(\frac{2h+k}{3} + \frac{l}{2}\right)\pi\right]. \end{aligned} \tag{D.103}$$

It is easily checked from (D.103) that $|F_{hkl}|^2$ can have four different values as follows:

$$|F_{hkl}|^2 = \begin{cases} 0, & \text{if } 2h+k = 3m \text{ and } l \text{ is odd}, \\ 4f^2, & \text{if } 2h+k = 3m \text{ and } l \text{ is even}, \\ 3f^2, & \text{if } 2h+k = 3m \pm 1 \text{ and } l \text{ is odd}, \\ f^2, & \text{if } 2h+k = 3m \pm 1 \text{ and } l \text{ is even}, \end{cases} \tag{D.104}$$

where m is an arbitrary integer. Note that a different choice of the unit cell and the basis vectors $\boldsymbol{a}_1$ and $\boldsymbol{a}_2$ yields $\boldsymbol{r}_1 = (0,0,0)$ and $\boldsymbol{r}_2 = (\frac{1}{3}, \frac{2}{3}, \frac{1}{2})$ (see, e.g., [35, p. 25], [334, p. 34],

[335, pp. 99–101]). Then in (D.103) we have

$$|F_{hkl}|^2 = 4f^2 \cos^2\Big[\Big(\frac{h+2k}{3} + \frac{l}{2}\Big)\pi\Big], \tag{D.105}$$

which leads to the replacement of $2h+k$ by $h+2k$ in (D.104). However, if $2h+k = 3m$, then $h+2k = 3(2m-h) = 3m'$, where $m' \in \mathbb{Z}$. If $2h+k = 3m+1$, then $h+2k = 3(2m-h+1)-1 = 3m'-1$, where $m' \in \mathbb{Z}$; if $2h+k = 3m-1$, then $h+2k = 3(2m-h-1)+1 = 3m'+1$, where $m' \in \mathbb{Z}$. Hence $2h+k$ and $h+2k$ can be used interchangeably in (D.103).

D.6 Friedel's Rule

Friedel [119], in a short 1913 paper, presented verbal arguments to refute Laue's belief then that a difference between right and left quartz could be discovered in X-ray radiograms of quartz. He concluded from his arguments that "in no case can [X-ray] radiograms reveal the absence of a center", and "whatever the structure, the radiograms can only reveal eleven symmetries", namely those of what we now call the eleven Laue classes. We shall show in this section that these conclusions of Friedel can be derived mathematically provided that the equality[199]

$$|F_{hkl}| = |F_{\bar{h}\bar{k}\bar{l}}| \qquad \text{for each } (h,k,l) \in \mathbb{Z}^3, \tag{D.106}$$

where F_{hkl} is the structural factor given by (D.90), is valid. Assertion (D.106) is commonly called "Friedel's law" or "Friedel's rule". Ewald and Hermann [113] were the first to question the general validity of Friedel's rule, albeit in the context of the dynamical theory of X-ray diffraction. Before we examine how Friedel's conclusions can be derived from assertion (D.106), we present some common conditions under which Friedel's rule will be valid in the kinematical theory.

Let $(\mathsf{C}, \boldsymbol{\kappa}_0)$ be an ideal crystal and $\mathcal{G}$ be its space group. Let a Cartesian coordinate system be chosen in the Euclidean space E^3 such that each symmetry operation in $\mathcal{G}$ is an ordered pair $(\boldsymbol{v}, \boldsymbol{Q}) = (\boldsymbol{v}, \boldsymbol{I})(\boldsymbol{0}, \boldsymbol{Q})$, where $(\boldsymbol{v}, \boldsymbol{I})$ is a translation of $\boldsymbol{\kappa}_0(\mathsf{C})$ and $(\boldsymbol{0}, \boldsymbol{Q})$ a rotation, inversion, or roto-inversion of $\boldsymbol{\kappa}_0(\mathsf{C})$ about the origin of the coordinate system. Let $\mathcal{L}$ and $\mathcal{K}$ be the lattice group and crystallographic point group of $\mathcal{G}$, respectively, and let $\mathsf{L} = \mathcal{L}(\boldsymbol{0})$ be the lattice chosen to represent $\mathcal{L}$. Let $\{\boldsymbol{a}_i : i = 1, 2, 3\}$ be a right-handed triad of conventional lattice vectors; they also constitute the primitive basis of the primitive sublattice $\mathcal{L}^{(p)}(\boldsymbol{0})$. Cf. Sects. 2.2, 2.3.1, 2.3.3, and 2.8.

Let $\boldsymbol{a}_1^*$, $\boldsymbol{a}_2^*$, and $\boldsymbol{a}_3^*$ be the right-handed triad of basis vectors reciprocal to the direct lattice basis $\{\boldsymbol{a}_i : i = 1, 2, 3\}$ (of the primitive sublattice $\mathcal{L}^{(p)}(\boldsymbol{0})$). Let $\mathsf{L}^* = \{\mathbf{H}_{hkl} \in \tau(V^*) : \mathbf{H}_{hkl} = h\boldsymbol{a}_1^* + k\boldsymbol{a}_2^* + l\boldsymbol{a}_3^* : h, k, l \in \mathbb{Z}\}$ be the reciprocal lattice; cf. Sect. 7.2 for definition of $\tau(V^*)$. Note that for each $\boldsymbol{Q} \in \mathcal{K}$, $\boldsymbol{Q}\mathsf{L} = \mathsf{L}$ (see Sect. 2.3.3), which implies $\boldsymbol{Q}\mathsf{L}^* = \mathsf{L}^*$ (see, e.g., [277, pp. 87–90]).

In what follows we shall write $\mathbf{H}$ for a generic reciprocal lattice vector when it serves no purpose to spell out its components.

Proposition D.10 *Let $(\mathsf{C}, \boldsymbol{\kappa}_0)$ be an ideal crystal, $\mathcal{G}$ be its space group, and $\mathcal{K}$ be the point group of $\mathcal{G}$. Then $|F_{\mathbf{H}}| = |F_{\boldsymbol{Q}\mathbf{H}}|$ for each $\boldsymbol{Q} \in \mathcal{K}$.*

[199] See, e.g., [127, p. 170]. In the words of Zachariasen [351, p. 137], "[t]his is the theoretical explanation of the empirical rule due to G. Friedel."

Proof Let $(\boldsymbol{v}, \boldsymbol{Q}) \in \mathcal{G}$. The configuration $\boldsymbol{\kappa}_0(\mathrm{C})$ remains invariant under the rigid tansplacement $\boldsymbol{x} \mapsto \boldsymbol{Q}\boldsymbol{x} + \boldsymbol{v}$. Hence we have

$$F_{\mathbf{H}} = \sum_{n=1}^{N} f_n e^{i2\pi \mathbf{H}\cdot \boldsymbol{r}_n} = \sum_{n=1}^{N} f_n e^{i2\pi \mathbf{H}\cdot(\boldsymbol{Q}\boldsymbol{r}_n + \boldsymbol{v})}$$

$$= e^{i2\pi \mathbf{H}\cdot \boldsymbol{v}} \sum_{n=1}^{N} f_n e^{i2\pi\, \boldsymbol{Q}^T \mathbf{H}\cdot \boldsymbol{r}_n} = e^{i2\pi \mathbf{H}\cdot \boldsymbol{v}} F_{\boldsymbol{Q}^T \mathbf{H}}. \tag{D.107}$$

Hence we obtain $|F_{\mathbf{H}}| = |F_{\boldsymbol{Q}^T \mathbf{H}}|$. As $(\boldsymbol{v}, \boldsymbol{Q})$ runs over $\mathcal{G}$, $\boldsymbol{Q}^T$ runs over $\mathcal{K}$. □

From Proposition D.10, we immediately obtain the following corollary.

Corollary D.11 *If* $(\mathbf{0}, \mathcal{I}) \in \mathcal{G}$, *then* $|F_{\mathbf{H}}| = |F_{-\mathbf{H}}|$. □

Corollary D.11 asserts that $|F_{hkl}| = |F_{\bar{h}\bar{k}\bar{l}}|$ if the ideal crystal in question has an inversion center. In the next proposition we give some conditions under which Friedel's rule is valid even if $(\mathbf{0}, \mathcal{I}) \notin \mathcal{G}$.

Proposition D.12 *Let* F_{hkl} *be the structure factor given by* (D.90). *Then* $|F_{hkl}| = |F_{\bar{h}\bar{k}\bar{l}}|$ *if at least one of the following conditions holds*: (*i*) *all* f_n $(n = 1, \ldots, N)$ *are real-valued*; (*ii*) *all* f_n *are equal*.

Proof (i) Let all f_n be real-valued, and let $\boldsymbol{a}_1^*$, $\boldsymbol{a}_2^*$, and $\boldsymbol{a}_3^*$ be the chosen triad of reciprocal basis vectors. Since $\mathbf{H}_{hkl} = h\boldsymbol{a}_1^* + k\boldsymbol{a}_2^* + l\boldsymbol{a}_3^*$, we have $\mathbf{H}_{\bar{h}\bar{k}\bar{l}} = -\mathbf{H}_{hkl}$ and thence

$$F_{\bar{h}\bar{k}\bar{l}} = \sum_{n=1}^{N} f_n e^{i2\pi \mathbf{H}_{\bar{h}\bar{k}\bar{l}}\cdot \boldsymbol{r}_n} = \sum_{n=1}^{N} f_n e^{-i2\pi \mathbf{H}_{hkl}\cdot \boldsymbol{r}_n} = \overline{F_{hkl}}. \tag{D.108}$$

Hence we conclude that

$$|F_{\bar{h}\bar{k}\bar{l}}|^2 = F_{\bar{h}\bar{k}\bar{l}}\overline{F_{\bar{h}\bar{k}\bar{l}}} = \overline{F_{hkl}} F_{hkl} = |F_{hkl}|^2. \tag{D.109}$$

(ii) Let $f_n = f$ for all n. Then we have

$$F_{hkl} = f \sum_{n=1}^{N} e^{i2\pi \mathbf{H}_{hkl}\cdot \boldsymbol{r}_n}, \qquad F_{\bar{h}\bar{k}\bar{l}} = f \sum_{n=1}^{N} e^{-i2\pi \mathbf{H}_{hkl}\cdot \boldsymbol{r}_n}, \tag{D.110}$$

which imply

$$F_{hkl}\overline{F_{hkl}} = \Big(f \sum_{n=1}^{N} e^{i2\pi \mathbf{H}_{hkl}\cdot \boldsymbol{r}_n}\Big)\Big(\overline{f} \sum_{n=1}^{N} e^{-i2\pi \mathbf{H}_{hkl}\cdot \boldsymbol{r}_n}\Big), \tag{D.111}$$

$$F_{\bar{h}\bar{k}\bar{l}}\overline{F_{\bar{h}\bar{k}\bar{l}}} = \Big(f \sum_{n=1}^{N} e^{-i2\pi \mathbf{H}_{hkl}\cdot \boldsymbol{r}_n}\Big)\Big(\overline{f} \sum_{n=1}^{N} e^{i2\pi \mathbf{H}_{hkl}\cdot \boldsymbol{r}_n}\Big). \tag{D.112}$$

A comparison of (D.111) and (D.112) leads to the conclusion that $|F_{hkl}|^2 = |F_{\bar{h}\bar{k}\bar{l}}|^2$. □

Remark D.13 By Corollary D.11, Friedel's rule is valid when the ideal crystal in question has an inversion center (i.e., $(\mathbf{0}, \mathcal{I}) \in \mathcal{G}$), which includes the cases where the crystal has face-centered cubic, body-centered cubic, or hexagonal close-packed structure. Even if the crystal does not have an inversion center, by Proposition D.12 Friedel's rule is observed when (i) all the atoms in the unit cell have their scattering factors f_n real-valued or (ii) when the atoms are of the same species (irrespective of whether their atomic scattering factor f is real or complex). Condition (i) is a good approximation when X-ray scattering is predominantly elastic. Friedel's rule breaks down when absorption and anomalous scattering cannot be ignored; see Remark D.4 of Sect. D.3.2.[200] □

To see how "Friedel's rule" leads to the conclusions in Friedel's 1913 paper, let us consider a simple example.

Example D.14 Consider the point groups $C_2 = \{\boldsymbol{I}, \boldsymbol{R}(\boldsymbol{e}_3, \pi)\}$, $C_s = \{\boldsymbol{I}, \mathcal{I}\boldsymbol{R}(\boldsymbol{e}_3, \pi)\}$, and $C_{2h} = \{\boldsymbol{I}, \boldsymbol{R}(\boldsymbol{e}_3, \pi), \mathcal{I}, \mathcal{I}\boldsymbol{R}(\boldsymbol{e}_3, \pi)\}$, which are in the same Laue class. The C_2, C_s, and C_{2h} crystal classes are all in the monoclinic system. Let the reciprocal basis vectors $\boldsymbol{a}_1^*$ and $\boldsymbol{a}_2^*$ be in the 1-2 plane, and $\boldsymbol{a}_3^* = \|\boldsymbol{a}_3^*\|\boldsymbol{e}_3$. It is easy to verify that $\boldsymbol{R}(\boldsymbol{e}_3, \pi)\mathbf{H}_{hkl} = \mathbf{H}_{\bar{h}\bar{k}l}$, $\mathcal{I}\mathbf{H}_{hkl} = \mathbf{H}_{\bar{h}\bar{k}\bar{l}}$, and $\mathcal{I}\boldsymbol{R}(\boldsymbol{e}_3, \pi)\mathbf{H}_{hkl} = \mathbf{H}_{hk\bar{l}}$.

For a crystal whose space group has C_{2h} as its point group, by Proposition D.10 its structure factor satisfies $|F_{\mathbf{H}}| = |F_{\boldsymbol{Q}\mathbf{H}}|$ for each $\boldsymbol{Q} \in \mathcal{K}$, i.e.,

$$|F_{hkl}| = |F_{\bar{h}\bar{k}l}| = |F_{\bar{h}\bar{k}\bar{l}}| = |F_{hk\bar{l}}| \qquad \text{for all } h, k, l \in \mathbb{Z}. \tag{D.113}$$

For a crystal whose space group has C_2 (resp. C_s) as its point group, by Proposition D.10 its structure factor satisfies $|F_{hkl}| = |F_{\bar{h}\bar{k}l}|$ (resp. $|F_{hkl}| = |F_{hk\bar{l}}|$). Addition of Friedel's rule that $|F_{hkl}| = |F_{\bar{h}\bar{k}\bar{l}}|$ for all $h, k, l \in \mathbb{Z}$ leads to (D.113) as the equation satisfied by the structure factor of both the Type I and Type III crystals. Thus, as far as the structure factor is concerned, Friedel rule in effect adds an inversion center to the point group in question. □

For point groups in other Laue classes, similar analyses lead to the conclusion that if Friedel's rule is valid, the structure factor of a Type I or Type III crystal in a Laue class satisfies all the relations observed by a Type II crystal in the same Laue class. Since the structure factor contains all information on crystal structure delivered by X-ray diffraction, we arrive at the conclusions of Friedel cited at the beginning of this section if "Friedel's rule" is valid.

[200] Note also that electron diffraction is exempt from Friedel's rule. Hence in principle electron backscatter diffraction could be used for identification of the point groups of crystals that goes beyond their Laue classes. Indeed Baba-Kishi and Dingley [12] report that "[s]tudies carried out on bulk specimens selected from the 32-point groups indicate that 27 of the 32-point groups can be determined unambiguously using BKPs [i.e., EBSD patterns]". But using this technique to determine the point group of a crystal "becomes increasingly difficult and complex as the symmetry of the crystal decreases" [231, p. 83]. See also [90, 91].

Bibliography

1. Adams, B.L., Boehler, J.P., Guidi, M., Onat, E.T.: Group theory and representation of microstructure and mechanical behavior of polycrystals. J. Mech. Phys. Solids **40**, 723–737 (1992)
2. Adams, B.L., Wright, S.I., Kunze, K.: Orientation imaging: the emergence of a new microscopy. Metall. Trans. A **24A**, 819–831 (1993)
3. Adams, B.L., Kalidindi, S.R., Fullwood, D.T.: Microstructure-Sensitive Design for Performance Optimization. Butterworth-Heinemann, Amsterdam (2013)
4. Als-Nielsen, J., McMorrow, D.: Elements of Modern X-Ray Physics, 2nd edn. Wiley, Chichester (2011)
5. Andreescu, T., Andrica, D., Cucurezeanu, I.: An Introduction to Diophantine Equations: A Problem-Based Approach. Birkhäuser, Boston (2010)
6. Armstrong, M.A.: Groups and Symmetry. Springer, New York (1988)
7. Aroyo, M.I. (ed.): International Tables for Crystallography. Volume A: Space-Group Symmetry, 6th edn. Wiley, West Sussex (2016)
8. ASTM Standards: E2627-13 Practice for determining average grain size using electron backscatter diffraction (EBSD) in fully recrystallized polycrystalline materials. ASTM International, West Conshohocken, Pennsylvania (2013)
9. Authier, A.: Dynamical Theory of X-Ray Diffraction. Oxford University Press, Oxford (2001)
10. Authier, A.: Early Days of X-Ray Crystallography. Oxford University Press, Oxford (2013)
11. Azároff, L.V.: Elements of X-Ray Crystallography. McGraw-Hill, New York (1968)
12. Baba-Kishi, K.Z., Dingley, D.J.: Backscatter Kikuchi diffraction in the SEM for identification of crystallographic point groups. Scanning **11**, 305–312 (1989)
13. Bäbler, F.: Über einen Satz aus der Theorie der Kristallklassen. Comment. Math. Helv. **20**, 65–67 (1947)
14. Bacciagaluppi, G., Valentini, A.: Quantum Theory at the Crossroads: Reconsidering the 1927 Solvay Conference. Cambridge University Press, Cambridge (2009)
15. Backus, G.: A geometrical picture of anisotropic elastic tensors. Reviews of Geophysics and Space Physics **8**, 633–671 (1970)
16. Baerheim, R.: Harmonic decomposition of the anisotropic elasticity tensor. Q. J. Mech. Appl. Math. **46**, 391–418 (1993)
17. Banach, S.: The Lebesgue integral in abstract spaces. Note II in [280], pp. 320–330 (1937)
18. Barkla, C.G.: Secondary radiation from gases subject to X-rays. Philos. Mag. Ser. **6**(5), 685–698 (1903)
19. Barlow, W.: Probable nature of the internal symmetry of crystals. Nature **29**, 186–188 (1883). 205–207
20. Barlow, W., Pope, W.J.: The relation between the crystalline form and the chemical constitution of simple inorganic substances. J. Chem. Soc. **91**, 1150–1214 (1907)
21. Barlow, W., Miers, H.A., Smith, H.: The structure of crystals. Part I: report on the development of the geometrical theories of crystal structure, 1666–1901. In: Report of the Seventy-First Meeting of the British Association for the Advancement of Science held at Glasgow in September 1901, pp. 297–337. John Murray, London (1901)
22. Baudin, T., Penelle, R.: Determination of the total texture function from individual orientation measurements by electron backscattering pattern. Metall. Trans. A **24A**, 2299–2311 (1993)
23. Baudin, T., Jura, J., Penelle, R., Pospiech, J.: Estimation of the minimum grain number for the orientation distribution function calculation from individual orientation measurements on Fe-3%Si and Ti-4Al-6V alloys. J. Appl. Crystallogr. **28**, 582–589 (1995)
24. Bauer, H.: Probability Theory and Elements of Measure Theory. Academic, London (1981)
25. Bauer, H.: Measure and Integration Theory. de Gruyter, Berlin (2001)
26. Bhagavantam, S., Suryanarayana, D.: Crystal symmetry and physical properties: application of group theory. Acta Crystallogr. **2**, 21–26 (1949)
27. Bhagavantam, S., Venkatarayudu, T.: Theory of Groups and Its Application to Physical Problems. Academic Press, New York (1969)
28. Biedenharn, L.C., Louck, J.D.: Angular Momentum in Quantum Physics: Theory and Application. Addison-Wesley, Reading (1981)
29. Bijvoet, J.M., Burgers, W.G., Hägg, G. (eds.): Early Papers on Diffraction of X-Rays by Crystals Oosthoek, Utrecht (1969)
30. Birkholz, M., Fewster, P.F., Genzel, C.: Thin Film Analysis by X-Ray Scattering. Wiley-VCH, Weinheim (2006)
31. Biswas, A., Vajragupta, N., Hielscher, R., Hartmaier, A.: Optimized reconstruction of the crystallographic orientation density function based on a reduced set of orientations. J. Appl. Crystallogr. **53**, 178–187 (2020)
32. Bitter, F.: Introduction to Ferromagnetism. McGraw-Hill, New York (1937)

33. Bôcher, M.: Introduction to Higher Algebra. MacMillan, New York (1915). Reprinted, Forgotten Books, London (2018)
34. Böhlke, T.: Texture simulation based on tensorial Fourier coefficients. Comput. Struct. **84**, 1086–1094 (2006)
35. Bollmann, W.: Crystal Defects and Crystalline Interfaces. Springer, New York (1970)
36. Boothby, W.M.: An Introduction to Differentiable Manifolds and Riemannian Geometry, 2nd edn. Academic, Orlando (1986)
37. Borchardt-Ott, W.: Crystallography: An Introduction, 3rd edn. Springer, Heidelberg (2011)
38. Bourbaki, N.: Intégration. Chapter 1–4. Hermann, Paris (1965). Translated into English by S.K. Berberian: Integration I. Chapter 1–6. Springer, Berlin (2004)
39. Bouten, M.: On the rotation operators in quantum mechanics. Physica **42**, 572–580 (1969)
40. Bowen, R.M., Wang, C.-C.: Introduction to Vectors and Tensors, 2nd edn. Dover, Mineola (2008)
41. Bozzolo, N., Gerspach, F., Sawina, G., Wagner, F.: Accuracy of orientation distribution function determination based on EBSD data – a case study of a recrystallized low alloyed Zr sheet. J. Microsc. **227**, 275–283 (2007)
42. Bradley, C.J., Cracknell, A.P.: The Mathematical Theory of Symmetry in Solids: Representation Theory for Point Groups and Space Groups. Clarendon Press, Oxford (2010)
43. Bragg, W.L.: The diffraction of short electromagnetic waves by a crystal. Proc. Camb. Philos. Soc. **17**, 43–57 (1912)
44. Bragg, W.L.: The specular reflection of X-rays. Nature **90**, 410 (1912)
45. Bragg, W.L.: X-rays and crystals. Sci. Prog. Twent. Century **7**, 372–389 (1913)
46. Bragg, W.H.: Bakerian lecture: X-rays and crystal structure. Philos. Trans. R. Soc. A **215**, 253–274 (1915)
47. Brandmüller, J.: An extension of the Neumann–Minnigerode–Curie Principle. Comput. Math. Appl. **12B**, 97–100 (1986)
48. Bravais, A.: Mémoire sur les polyèdres de forme symétriques. J. Math. Pures Appl. **14**, 141–180 (1849). = pp. XIX–LXII of Études Cristallographiques. Gauthier-Villars, Paris (1866)
49. Bravais, A.: Mémoire sur les systèmes formés par des points distribués regulièrement sur un plan ou dans l'espace. J. Éc. Polytech. **19**, 1–128 (1850). Translated into English by A.J. Shaler: On the Systems Formed by Points Regularly Distributed on a Plane or in Space. Crystallographic Society of America (1949); reprinted, Dover, Mineola, New York (2005)
50. Brickell, F., Clark, R.S.: Differentiable Manifolds. Van Nostrand, London (1970)
51. Brink, D.M., Satchler, G.R.: Angular Momentum, 3rd edn. Clarendon Press, Oxford (1993)
52. Britton, T.B., Jiang, J., Guob, Y., Vilalta-Clemente, A., Wallis, D., Hansenc, L.N., Winkelmann, A., Wilkinson, A.J.: Tutorial: crystal orientations and EBSD – or which way is up? Mater. Charact. **117**, 113–126 (2016)
53. Brough, I., Bate, P.S., Humphreys, F.J.: Optimising the angular resolution of EBSD. Mater. Sci. Technol. **22**, 1279–1286 (2006)
54. Buerger, M.J.: The crystallographic symmetries determinable by X-ray diffraction. Proc. Natl. Acad. Sci. USA **36**, 324–329 (1950)
55. Bump, D.: Lie Groups, 2nd edn. Springer, New York (2013)
56. Bunge, H.-J.: Zur Darstellung allgemeiner Texturen. Z. Metallkde. **56**, 872–874 (1965)
57. Bunge, H.-J.: Mathematische Methoden der Texturen. Akademie-Verlag, Berlin (1969)
58. Bunge, H.J.: Determination of the orientation distribution function from isolated axis density values. Textures Cryst. Solids **2**, 169–174 (1977)
59. Bunge, H.-J.: Texture analysis by orientation distribution functions (ODF analysis). Z. Metallkde. **68**, 571–581 (1977)
60. Bunge, H.-J.: Texture Analysis in Materials Science: Mathematical Methods. Butterworths, London (1982)
61. Bunge, H.J. (ed.): Experimental Techniques of Texture Analysis. DGM Inf. Ges, Oberursel (1986)
62. Bunge, H.J.: Physical versus mathematical aspects in texture analysis. Textures Microstruct. **25**, 71–108 (1996)
63. Bunge, H.-J., Haessner, F.: Three-dimensional orientation distribution function of crystals in cold-rolled copper. J. Appl. Phys. **39**, 5503–5514 (1968)
64. Bunge, H.J., Esling, C., Muller, J.: The role of the inversion centre in texture analysis. J. Appl. Crystallogr. **13**, 544–554 (1980)
65. Bunge, H.J., Esling, C., Muller, J.: The influence of crystal and sample symmetries on the orientation distribution function of the crystallites in polycrystalline materials. Acta Crystallogr. A **37**, 889–899 (1981)
66. Burckhardt, J.J.: Die Bewegungsgruppen der Kristallographie. Birkhäuser, Basel (1947). Second edition, Birkhäuser, Basel (1966)

67. Burckhardt, J.J.: Zur Geschichte der Entdeckung der 230 Raumgruppen. Arch. Hist. Exact Sci. **4**, 235–246 (1967)
68. Burns, G., Glazer, A.M.: Space Groups for Solid State Scientists, 2nd edn. Academic, Boston (1990)
69. Carmeli, M.: Representations of the three-dimensional rotation group in terms of direction and angle of rotation. J. Math. Phys. **9**, 1987–1992 (1968)
70. Carmeli, M., Malin, S.: Representations of the Rotation and Lorentz Groups: An Introduction. Dekker, New York (1976)
71. Carmo, M.P.d.: Riemannian Geometry. Birkhäuser, Boston (1992)
72. Casselman, W.: Packing pennies in the plane: an illustrated proof of Kepler's conjecture in 2D. AMS Feature Column Archive (2000). http://www.ams.org/publicoutreach/feature-column/fcarc-cass1
73. Coddington, E.A.: An Introduction to Ordinary Differential Equations. Dover, New York (1961)
74. Compton, A.H.: The distribution of the electrons in atoms. Nature **95**, 343–344 (1915)
75. Conway, J.B.: A Course in Functional Analysis, 2nd edn. Springer, New York (2000)
76. Cowin, S.C.: Properties of the anisotropic elasticity tensor. Q. J. Mech. Appl. Math. **42**, 249–266 (1989). Corrigendum **46**, 541–542 (1993)
77. Cowin, S.C.: On the number of distinct elastic constants associated with certain anisotropic elastic symmetries. Z. Angew. Math. Phys. **46**, S210–S224 (1995). Special Issue
78. Coxeter, H.S.M.: Introduction to Geometry, 2nd edn. Wiley, New York (1969)
79. Coxeter, H.S.M.: Regular Polytopes, 3rd edn. Dover, New York (1973)
80. Cushing, J.T.: Applied Analytical Mathematics for Physical Scientists. Wiley, New York (1975)
81. Dahms, M.: The iterative series-expansion method for quantitative texture analysis. II. Applications. J. Appl. Crystallogr. **25**, 258–267 (1992)
82. Dahms, M.: Introduction of the phone-concept into pole figure inversion using the iterative series expansion method. Textures Microstruct. **19**, 169–174 (1992)
83. Dahms, M., Bunge, H.J.: A positivity method for the determination of complete orientation distribution functions. Textures Microstruct. **10**, 21–35 (1988)
84. Dahms, M., Bunge, H.J.: The iterative series-expansion method for quantitative texture analysis. I. General outline. J. Appl. Crystallogr. **22**, 439–447 (1989)
85. De Graef, M., McHenry, M.E.: Structure of Materials: An Introduction to Crystallography, Diffraction, and Symmetry. Cambridge University Press, Cambridge (2007)
86. Demirel, M.C., El-Dasher, B.S., Adams, B.L., Rollett, A.D.: Studies on the accuracy of electron backscatter diffraction measurements. In: [288], pp. 65–74 (2000)
87. Dempster, A.P.: The minimum of a definite ternary quadratic form. Can. J. Math. **9**, 232–234 (1957)
88. Diestel, J., Spalsbury, A.: The Joys of Haar Measure. Am. Math. Soc., Providence (2014)
89. Dieudonné, J.: Treatise on Analysis. Volume II (Enlarged and Corrected Printing). Academic, New York (1976)
90. Dingley, D.J., Wright, S.I.: Phase identification through symmetry determination in EBSD patterns. In: [289], pp. 97–107 (2009)
91. Dingley, D.J., Baba-Kishi, K.Z., Randle, V.: Atlas of Backscattering Kikuchi Diffraction Patterns. Institute of Physics Publishing, Bristol (1995)
92. Dirac, P.A.M.: The quantum theory of the emission and absorption of radiation. Proc. R. Soc. A **114**, 243–265 (1927)
93. Dirac, P.A.M.: The quantum theory of dispersion. Proc. R. Soc. A **114**, 710–728 (1927)
94. Du, W.: Material tensors and pseudotensors of weakly-textured polycrystals with orientation measure defined on the orthogonal group. Doctoral dissertation, University of Kentucky, Lexington (2015)
95. Du, W., Man, C.-S.: Material tensors and pseudotensors of weakly-textured polycrystals with orientation distribution function defined on the orthogonal group. J. Elast. **127**, 197–233 (2017)
96. Dudley, R.M.: Real Analysis and Probability. Cambridge University Press, Cambridge (2002)
97. Dugundji, J.: Topology. Allyn and Bacon, Boston (1966)
98. Edmonds, A.R.: Angular Momentum in Quantum Mechanics. Princeton University Press, Princeton (1957)
99. Edmonds, A.R.: Angular Momentum in Quantum Mechanics. Princeton University Press, Princeton (1974). Third printing of the second edition, with corrections
100. Eghtesad, A., Barrett, T.J., Knezevic, M.: Compact reconstruction of orientation distributions using generalized spherical harmonics to advance large-scale crystal plasticity modeling: verification using cubic, hexagonal, and orthorhombic polycrystals. Acta Mater. **155**, 418–432 (2018)
101. Engel, P.: Geometric Crystallography: An Axiomatic Introduction to Crystallography. D. Reidel, Dordrecht (1986)
102. Engelking, R.: Outline of General Topology. North-Holland, Amsterdam (1968). Translated from the Polish by K. Sieklucki

103. Engler, O.: Comparison of X-ray and electron backscatter diffraction textures for back-annealed Al–Mg alloys. J. Appl. Crystallogr. **42**, 1147–1157 (2009)
104. Engler, O., Randle, V.: Introduction to Texture Analysis: Macrotexture, Microtexture and Orientation Mapping, 2nd edn. CRC Press, Boca Raton (2010)
105. Engler, O., Yang, P., Gottstein, G., Jura, J., Pospiech, J.: Behaviour of statistical texture parameters applied to single grain orientation measurements in recrystallized Al-Mn. Mater. Sci. Forum **157**(162), 933–938 (1994)
106. Engler, O., Jura, J., Matthies, S.: Influence of number and arrangement of single orientation measurements on their statistical relevance. In: [307], pp. 68–73 (1999)
107. Ericksen, J.L.: On the symmetry of deformable crystals. Arch. Ration. Mech. Anal. **72**, 1–13 (1979)
108. Eschner, Th.: Texture analysis by means of model functions. Textures Microstruct. **21**, 139–146 (1993)
109. Esling, C., Bunge, H.J., Muller, J.: Description of the texture by distribution functions on the space of orthogonal transformations. Implications on the inversion centre. J. Phys. Lett. **41**, 543–545 (1980)
110. Esling, C., Bechler-Ferry, E., Bunge, H.J.: Three-dimensional texture analysis after Bunge and Roe: correspondence between the respective mathematical techniques. Textures Microstruct. **5**, 92–125 (1982)
111. Ewald, P.P.: Die Berechnung der Kristallstruktur aus Interferenzenaufnahmen mit X-Strahlen. Phys. Z. **15**, 339–401 (1914). Text of paper reproduced in full in [29, pp. 82–86], but the Abstract is not included
112. Ewald, P.P.: Fifty Years of X-Ray Diffraction: Dedicated to the International Union of Crystallography on the Occasion of the Commemoration Meeting in Munich July 1962. Utrecht, Oosthoek (1962)
113. Ewald, P.P., Hermann, C.: Gilt der Friedelsche Satz über die Symmetrie der Röntgeninterferenzen? Z. Kristallogr. **65**, 251–259 (1927)
114. Feil, D.: Diffraction physics. Isr. J. Chem. **16**, 103–110 (1977)
115. Fermi, E.: Quantum theory of radiation. Rev. Mod. Phys. **4**, 87–132 (1932)
116. Folland, G.B.: Real Analysis: Modern Techniques and Their Applications, 2nd edn. Wiley, New York (1999)
117. Ford, L.R.: Automorphic Functions, 2nd edn. Chelsea, New York (1951)
118. Forte, S., Vianello, M.: Symmetry classes for elasticity tensors. J. Elast. **43**, 81–108 (1996)
119. Friedel, G.: Sur les symétries cristallines que peut révéler la diffraction des rayons Röntgen. C. R. Hebd. Séances Acad. Sci. **157**, 1533–1536 (1913)
120. Friedrich, W., Knipping, P., Laue, M.: Interferenz-Erscheinungen bei Röntgenstrahlen. Sitzungsber. Math.-Phys. Kl. K.B. Akad. Wiss. München **Jahrg. 1912**, 303–332 (1912). Text of paper reproduced in full in [29, pp. 7–22], but Figs. 2, 8–10, and 12 of the plates are not included.
121. Fulks, W.: Advanced Calculus: An Introduction to Analysis. Wiley, New York (1961)
122. Fullwood, D.T., Niezgoda, S.R., Adams, B.L., Kalidindi, S.R.: Microstructure sensitive design for performance optimization. Prog. Mater. Sci. **55**, 477–562 (2010)
123. Gauss, C.F.: Untersuchungen über die Eigenschaften der positiven ternären quadratischen Formen von Ludwig August Seeber. Göttingische gelehrte. Anzeigen, 1831 Juli 9. J. Reine Angew. Math. **20**, 312–320 (1840). = pp. 188–196 of Werke, Zweiter Band, Königlichen Gesellschaft der Wissenschaften, Göttingen (1863)
124. Gel'fand, I.M., Šapiro, Z.Ya.: Representations of the group of rotations in three-dimensional space and their applications [in Russian]. Usp. Mat. Nauk (N.S.) **7**(47), 3–117 (1952). [English translation] American Mathematical Society Translations, Series 2 **2**, 207–316 (1956)
125. Gel'fand, I.M., Minlos, R.A., Shapiro, Z.Ya.: Representations of the Rotation and Lorentz Groups and Their Applications. MacMillan, New York (1963)
126. Giacovazzo, C. (ed.): Fundamentals of Crystallography, 2nd edn. Oxford University Press, Oxford (2002)
127. Giacovazzo, C.: The diffraction of X-rays by crystals. In: [126], pp. 153–225 (2002)
128. Glazer, A.M.: A Journey Into Reciprocal Space: A Crystallographer's Perspective. Morgan & Claypool, San Rafae (2017)
129. Glazer, A.M., Burns, G.: Space Group for Solid State Scientists, 3rd edn. Academic, Waltham (2013)
130. Godefroy, H.A.P.: A study of orientation maps: crystallographic symmetry, mean orientation, and applications. Doctoral dissertation, University of Kentucky, Lexington (2008)
131. Golubitsky, M., Stewart, I., Schaeffer, D.G.: Singularities and Groups in Bifurcation Theory. Volume II. Springer, New York (1988)
132. Guidi, M., Adams, B.L., Onat, E.T.: Tensorial representation of the orientation distribution function in cubic polycrystals. Textures Microstruct. **19**, 147–167 (1992)
133. Hahn, Th. (ed.): International Tables for Crystallography. Volume A: Space-Group Symmetry Springer, Dordrecht (2005). Fifth, revised edition; reprinted with corrections
134. Hales, T.C.: A proof of the Kepler conjecture. Ann. Math. **162**, 1063–1183 (2005)
135. Hales, T.C.: Historical overview of the Kepler conjecture. Discrete Comput. Geom. **36**, 5–20 (2006)

136. Hales, T.: Dense Sphere Packings: A Blueprint for Formal Proofs. Cambridege University Press, Cambridge (2012)
137. Hales, T., Adams, M., Bauer, G., Dang, T., Harrison, J., Hoang, L., Zumkeller, R.: A formal proof of the Kepler conjecture. Forum Math. Pi **5**, E2 (2017). https://doi.org/10.1017/fmp.2017.1
138. Hall, B.C.: Lie Groups, Lie Algebras, and Representations: An Elementary Introduction, 2nd edn. Springer, New York (2015)
139. Hammond, C.: The Basics of Crystallography and Diffraction, 4th edn. Oxford University Press, Oxford (2016). Reprinted with corrections
140. Hansen, J., Pospiech, J., Lücke, K.: Tables for Texture Analysis of Cubic Crystals. Springer, Berlin (1978)
141. Hartree, D.R.: The wave mechanics of an atom with a non-Coulomb central field. Part II. Some results and discussion. Proc. Camb. Philos. Soc. **24**, 111–132 (1928)
142. Helming, K.: Some applications of the texture component model. Mater. Sci. Forum **157**(162), 363–368 (1994)
143. Helming, K.: Texturapproximation durch Modellkomponenten. Habilitation Thesis, TU Clausthal, Clausthal-Zellerfeld (1995). Curvillier Verlag, Göttingen (1998)
144. Helming, K.: A nearly equal distant grid of orientations for quantitative texture analysis. Textures Microstruct. **28**, 219–230 (1997)
145. Helming, K.: Texture approximations by model components. In: [290], pp. 125–132 (1998)
146. Helming, K., Eschner, Th.: A new approach to texture analysis of multiphase materials using a texture component model. Cryst. Res. Technol. **25**, K203–K208 (1990)
147. Helming, K., Kruse, R., Siegesmund, S.: Texture analysis of an amphibolite using the component method. Mater. Sci. Forum **157**(162), 529–534 (1994)
148. Helming, K., Schwarzer, R.A., Rauschenbach, B., Geier, S., Leiss, B., Wenk, H.-R., Ullemeyer, K., Heinitz, J.: Texture estimates by means of components. Z. Metallkde. **85**, 545–553 (1994)
149. Hewitt, E., Ross, K.A.: Abstract Harmonic Analysis. Volume 1: Structure of Topological Groups, Integration Theory, Group Representations. Springer, Berlin (1963)
150. Hielscher, R.: Kernel density estimation on the rotation group and its application to crystallographic texture analysis. J. Multivar. Anal. **119**, 119–143 (2013)
151. Hielscher, R., Schaeben, H.: A novel pole figure inversion method: specification of the MTEX algorithm. J. Appl. Crystallogr. **41**, 1024–1037 (2008)
152. Hilbert, D., Cohn-Vossen, S.: Geometry and the Imagination. Chelsea, New York (1952)
153. Hilton, H.: Mathematical Crystallography and the Theory of Groups of Movements. Clarendon Press, Oxford (1903). Reprinted, Dover, New York (1963)
154. Hilton, H.: An Introduction to the Theory of Groups of Finite Order. Clarendon Press, Oxford (1908)
155. Hirsch, M.W., Smale, S.: Differential Equations, Dynamical Systems, and Linear Algebra. Academic, New York (1974)
156. Hsiang, W.-Y.: Least Action Principle of Crystal Formation of Dense Packing Type and Kepler's Conjecture. World Scientific, Singapore (2001)
157. Huang, M., Man, C.-S.: Constitutive relation of elastic polycrystal with quadratic texture dependence. J. Elast. **72**, 183–212 (2003)
158. Humbert, M.: Intensity corrections, resolving power and statistical relevance in pole figure measurements. In: [61], pp. 29–50 (1986)
159. Humphreys, F.J.: Quantitative metallography by electron backscattered diffraction. J. Microsc. **195**, 170–185 (1999)
160. Hutchinson, W.B., Lindh, E., Bate, P.: On the determination of textures from discrete orientation measurements. In: [307], pp. 34–51 (1999)
161. Huynh, D.Q.: Metrics for 3D rotations: comparison and analysis. J. Math. Imaging Vis. **35**, 155–164 (2009)
162. Iserles, A., Munthe-Kaas, H.Z., Nørsett, S.P., Zanna, A.: Lie-group methods. Acta Numer. **9**, 215–365 (2000)
163. Iyanaga, S., Sugiura, M.: Algebra [in Japanese]. In: Yamanouchi, T., et al. (eds.) Iwanami Course in Modern Applied Mathematics, vol. A.1.1–A.1.3. Iwanami, Tokyo (1957). Translated into Chinese by Q. Xiong, Shanghai Science and Technology Press, Shanghai (1962)
164. Jahn, H.A.: Note on the Bhagavantam-Suryanarayana method of enumerating the physical constants of crystals. Acta Crystallogr. **2**, 30–33 (1949)
165. James, R.W.: The Optical Principles of the Diffraction of X-Rays. Cornell University Press, Ithaca (1965)
166. James, R.W., Waller, I., Hartree, D.R.: An investigation into the existence of zero-point energy in the rock-salt lattice by an X-ray diffraction method. Proc. R. Soc. A **118**, 334–350 (1928)

167. Jöchen, K., Böhlke, T.: Representative reduction of crystallographic orientation data. J. Appl. Crystallogr. **46**, 960–971 (2013)
168. Jordan, C.: Essai sur géométrie à n dimensions. Bull. Soc. Math. Fr. **3**, 103–174 (1875). = Œuvres de Camille Jordan, Tome III, pp. 79–149. Gauthier-Villars, Paris (1962)
169. Jura, J., Pospiech, J., Gottstein, G.: Estimation of the minimum number of single grain orientation measurements for ODF determination. Z. Met.kd. **87**, 476–480 (1996)
170. Kallend, J.S.: Determination of the orientation distribution from pole figure data. In: [180], Chap. 3, pp. 102–124 (1998)
171. Kallend, J.S., Kocks, U.F., Rollett, A.D., Wenk, H.-R.: Operational texture analysis. Mater. Sci. Eng. A **132**, 1–11 (1991)
172. Kallend, J.S., Kocks, U.F., Rollett, A.D., Wenk, H.-R.: popLA – an integrated software system for texture analysis. Textures Microstruct. **14–18**, 1203–1208 (1991)
173. Katzir, S.: The emergence of the principle of symmetry in physics. Hist. Stud. Phys. Biol. Sci. **35**, 35–65 (2004)
174. Kepler, J.: Strena seu De Nive Sexangula. Gottfried Tampach, Frankfurt am Main (1611). Translated into English by J. Bromberg: The Six-Cornered Snowflake: A New Year's Gift. Paul Dry Books, Philadelphia (2010)
175. Khatkevich, A.G.: The elastic constants of crystals [in Russian]. Kristallografiya **6**, 700–703 (1961). [English translation] Soviet Physics – Crystallgraphy **6**, 561–563 (1962)
176. Kim, S.K.: The 32 general generator sets of 230 double space groups. J. Math. Phys. **27**, 1471–1483 (1986)
177. Kim, S.K.: Group Theoretical Methods and Applications to Molecules and Crystals. Cambridge University Press, Cambridge (1999)
178. Klein, F.: Vorlesungen über das Ikosaeder und die Auflösung der Gleichungen vom fünften Grade. Teubner, Leipzig (1884). Translated into English by G.G. Morrice: Lectures on the Ikosahedron, and the Solution of Equations of the Fifth Degree. Trübner, London (1888)
179. Knightly, A., Li, C.: Traces of Hecke Operators. Am. Math. Soc., Providence (2006)
180. Kocks, U.F., Tomé, C.N., Wenk, H.-R. (eds.): Texture and Anisotropy: Preferred Orientations in Polycrystals and Their Effect on Materials Properties Cambridge University Press, Cambridge (1998)
181. Kovetz, A.: Electromagnetic Theory. Oxford University Press, Oxford (2000)
182. Kronig, R.d.L., Rabi, I.I.: The symmetrical top in the undulatory mechanics. Phys. Rev. **29**, 262–269 (1927)
183. Ladd, M.F.C., Palmer, R.A.: Structure Determination by X-Ray Crystallography, 3rd edn. Plenum, New York (1993)
184. Lalena, J.N.: From quartz to quasicrystals: probing nature's geometric patterns in crystalline substances. Crystallogr. Rev. **12**, 125–180 (2006)
185. Lang, S.: Real Analysis. Addison-Wesley, Reading (1969)
186. Lee, J.M.: Introduction to Smooth Manifolds. Springer, New York (2006)
187. Liang, Z., Zuo, L., Chu, Y. (eds.): Proceedings of the Eleventh International Conference on Textures of Materials, ICOTOM 11, September 16–20, 1996, Xi'an, China. International Academic Publishers, Beijing (1996)
188. Liu, Y.S., Penelle, R., Wang, F.H., Xu, J.Z., Liang, Z.D.: Estimate the grain number for true ODF determination by individual orientation detection method. Mater. Sci. Forum **157**(162), 375–380 (1994)
189. Lobos, M., Böhlke, T.: Materials design for the anisotropic linear elastic properties of textured cubic crystal aggregates using zeroth-, first- and second-order bounds. Int. J. Mech. Mater. Des. **11**, 59–78 (2015)
190. Lobos Fernández, M., Böhlke, T.: Representations of Hashin-Shtrikman bounds in terms of texture coefficients for arbitrarily anisotropic polycrystalline materials. J. Elast. **134**, 1–38 (2019)
191. Lobos Fernández, M., Yuzbasioglu, T., Böhlke, T.: Homogenization and materials design of anisotropic multiphase linear elastic materials using central model functions. J. Elast. **128**, 17–60 (2017)
192. Lu, J.: Finite rotation groups [in Chinese], pp. 282–294. Shanghai Science and Technology Press, Shanghai (1962). Appendix in Chinese Translation of [163]
193. Lücke, K., Pospiech, J., Virnich, K.H., Jura, J.: On the problem of the reproduction of the true orientation distribution from pole figures. Acta Metall. **29**, 167–185 (1981)
194. Lücke, K., Pospiech, J., Jura, J., Hirsch, J.: On the presentation of orientation distribution functions by model functions. Z. Metallkde. **77**, 312–321 (1986)
195. Lyubarskii, G.Ya.: The Application of Group Theory in Physics. Pergamon, New York (1960)
196. Mackenzie, J.K.: Second paper on statistics associated with the random disorientation of cubes. Biometrika **45**, 229–240 (1958)
197. Mackenzie, J.K., Thomson, M.J.: Some statistics associated with the random disorientation of cubes. Biometrika **44**, 205–210 (1957)

198. Malgrange, C., Ricolleau, C., Schlenker, M.: Symmetry and Physical Properties of Crystals. Springer, Dordrecht (2014)
199. Man, C.-S.: On the constitutive equations of some weakly-textured materials. Arch. Ration. Mech. Anal. **143**, 77–103 (1998)
200. Man, C.-S.: Effects of crystallographic texture on the acoustoelastic coefficients of polycrystals. Nondestruct. Test. Eval. **15**, 191–214 (1999)
201. Man, C.-S., Huang, M.: Identification of material parameters in yield functions and flow rules for weakly-textured sheets of cubic metals. Int. J. Non-Linear Mech. **36**, 501–514 (2001)
202. Man, C.-S., Huang, M.: A simple explicit formula for the Voigt-Reuss-Hill average of elastic polycrystals with arbitrary crystal and texture symmetries. J. Elast. **105**, 29–48 (2011)
203. Man, C.-S., Huang, M.: A representation theorem for material tensors of weakly-textured polycrystals and its applications in elasticity. J. Elast. **106**, 1–42 (2012)
204. Man, C.-S., Noble, L.: Designing textured polycrystals with specific isotropic material tensors: the ODF method. Rend. Semin. Mat. Univ. Pol. Torino **58**, 155–170 (2000)
205. Man, C.-S., Paroni, R.: On the separation of stress-induced and texture-induced birefringence in acoustoelasticity. J. Elast. **45**, 91–116 (1996)
206. Man, C.-S., Zhao, D.: Remarks on texture coefficients of polycrystals with improper crystallite symmetry. J. Elast. **138**, 111–124 (2020)
207. Man, P.P.: Wigner active and passive rotation matrices applied to NMR tensor. Concepts Magn. Reson., Part A **45A**, e21385 (2017)
208. Mandl, F., Shaw, G.: Quantum Field Theory, 2nd edn. Wiley, Hoboken (2010)
209. Margenau, H., Murphy, G.M.: The Mathematics of Physics and Chemistry, 2nd edn. Van Nostrand, Princeton (1956)
210. Maslen, E.N., Fox, A.G., O'keefe, M.A.: Sect. 6.1.1. X-ray scattering. In: [265], pp. 554–590 (2004)
211. Mason, J.K.: The relationship of the hyperspherical harmonics to SO(3), SO(4) and orientation distribution functions. Acta Crystallogr. A **65**, 259–266 (2009)
212. Mason, J.K., Schuh, C.A.: Hyperspherical harmonics for the representation of crystallographic texture. Acta Mater. **56**, 6141–6155 (2008)
213. Mason, J.K., Schuh, C.A.: Expressing crystallographic textures through the orientation distribution function: conversion between generalized spherical harmonic and hyperspherical harmonic expansions. Metall. Mater. Trans. A **40A**, 2590–2602 (2009)
214. Matthies, S.: On the reproducibility of the orientation distribution function of texture samples from pole figures (ghost phenomena). Phys. Status Solidi (b) **92**, K135–K138 (1979)
215. Matthies, S.: On the reproducibility of the orientation distribution function of texture samples from pole figures (I): relationship between the ODF and pole figures. Kristall und Technik **15**, 431–444 (1980)
216. Matthies, S.: Standard functions in the texture analysis. Phys. Status Solidi (b) **101**, K111–K115 (1980)
217. Matthies, S.: Form effects in the description of the orientation distribution function (ODF) of texturized materials by model components. Phys. Status Solidi (b) **112**, 705–716 (1982)
218. Matthies, S.: Some remarks on theoretical developments in quantitative texture analysis and on the optimal calculation of harmonic quantities with high precision. Textures Microstruct. **8–9**, 115–129 (1988)
219. Matthies, M., Vinel, G.W.: On the reproduction of the orientation distribution function of textured samples from reduced pole figures using the conception of a conditional ghost correction. Phys. Status Solidi (b) **112**, K111–K114 (1982)
220. Matthies, S., Wagner, F.: Study of the ghost phenomena in mathematical texture analysis by means of standard functions. Phys. Status Solidi (b) **107**, 591–601 (1981)
221. Matthies, S., Wagner, F.: On a 1/n law on texture related single orientation analysis. Phys. Status Solidi (b) **196**, K11–K15 (1996)
222. Matthies, S., Wagner, F.: Using sets of individual orientations for ODF determination. In: [307], pp. 40–45 (1999)
223. Matthies, S., Wenk, H.-R.: ODF reproduction with conditional ghost correction. In: [337], pp. 139–147 (1985)
224. Matthies, S., Vinel, G.W., Helming, K.: Standard Distributions in Texture Analysis: Maps for the Case of Cubic-Orthorhombic Symmetry. Akademie-Verlag, Berlin (1987)
225. Matthies, S., Muller, J., Vinel, G.W.: On the normal distribution in the orientation space. Textures Microstruct. **10**, 77–96 (1988)
226. Matthies, S., Wenk, H.-R., Vinel, G.W.: Some basic concepts of texture analysis and comparison of three methods to calculate orientation distributions from pole figures. J. Appl. Crystallogr. **21**, 285–304 (1988)
227. McCarty, G.: Topology: An Introduction with Application to Topological Groups. McGraw-Hill, New York (1967)

228. Mehrabadi, M.M., Cowin, S.C.: Eigentensors of linear anisotropic elastic materials. Q. J. Mech. Appl. Math. **43**, 15–41 (1990)
229. Meng, D., Zhu, P.: Representation Theory of Finite Groups [in Chinese]. Science Press, Beijing (2006)
230. Messiah, A.: Quantum Mechanics. Volume 2. North-Holland, Amsterdam (1962). Translated from the French by J. Potter
231. Michael, J.R.: Phase identification using electron backscattered diffraction in the scanning electron microscope. In: [288], pp. 75–89 (2000)
232. Miller, W.: Symmetry Groups and Their Applications. Academic Press, New York (1972)
233. Mochizuki, E.: Spherical harmonic decomposition of an elastic tensor. Geophys. J. **93**, 521–526 (1988)
234. Monaco, H.L., Artioli, G.: Experimental methods in X-ray and neutron crystallography. In: [126], pp. 295–411 (2002)
235. Morawiec, A.: Orientations and Rotations: Computations in Crystallographic Textures. Springer, Berlin (2004)
236. Morris, P.R.: Program for calculation of augmented Jacobi polynomials. Texture **2**, 57–66 (1975)
237. Morris, P.R.: Symmetry requirements of W_{lmn} with odd l for cubic crystal symmetry. Textures Microstruct. **4**, 241–242 (1982)
238. Morrison, M.A., Parker, G.A.: A guide to rotations in quantum mechanics. Aust. J. Phys. **40**, 465–497 (1987)
239. Moses, H.E.: Irreducible representations of the rotation group in terms of Euler's theorem. Nuovo Cimento **40A**, 1120–1138 (1965)
240. Moses, H.E.: Irreducible representations of the rotation group in terms of the axis and angle of rotation. Ann. Phys. **37**, 224–226 (1966)
241. Müller, U.: Symmetry Relationships Between Crystal Structures: Applications of Crystallographic Group Theory in Crystal Chemistry. Oxford University Press, Oxford (2013)
242. Munkres, J.R.: Topology: A First Course. Prentice-Hall, Englewood Cliffs (1975)
243. Nachbin, L.: On the finite dimensionality of every irreducible unitary representation of a compact group. Proc. Am. Math. Soc. **12**, 11–12 (1961)
244. Naimark, M.A.: Linear Representations of the Lorentz Group. Pergamon, Oxford (1964). Distributed by MacMillan, New York
245. Naimark, M.A., Štern, A.I.: Theory of Group Representations. Springer, New York (1982). Translated into English by Elizabeth Hewitt; translation editor Edwin Hewitt
246. Nespolo, M., Aroyo, M.I., Souvignier, B.: Crystallographic shelves: space-group hierarchy explained. J. Appl. Crystallogr. **51**, 1481–1491 (2018)
247. Nesse, W.D.: Introduction to Mineralogy. Oxford University Press, New York (2000)
248. Newnham, R.E.: Properties of Materials: Anisotropy, Symmetry, Structure. Oxford University Press, Oxford (2005)
249. Nielsen, H.H.: The vibration-rotation energies of molecules. Rev. Mod. Phys. **23**, 90–136 (1951)
250. Niezgoda, S.R., Glover, J.: Unsupervised learning for effective texture estimation from limited discrete orientation data. Metall. Mater. Trans. A **44A**, 4891–4905 (2013)
251. Nowell, M.M., Chui-Sabourin, M., Carpenter, J.O.: Recent advances in high-speed orientation mapping. Microsc. Today **14**(6), 6–9 (2006)
252. Nye, J.F.: Physical Properties of Crystals: Their Representation by Tensors and Matrices. Oxford University Press, Oxford (1985)
253. Paroni, R.: Homogenization of polycrystalline aggregates. Arch. Ration. Mech. Anal. **151**, 311–337 (2000)
254. Paroni, R.: Optimal bounds on texture coefficients. J. Elast. **60**, 19–34 (2000)
255. Paroni, R., Man, C.-S.: Constitutive equations of elastic polycrystalline materials. Arch. Ration. Mech. Anal. **150**, 153–177 (1999)
256. Pauling, L., Wilson, E.B. Jr.: Introduction to Quantum Mechanics: With Applications to Chemistry. McGraw-Hill, New York (1935)
257. Perlwitz, H.-J., Lücke, K., Pitsch, W.: Determination of the orientation distribution of the crystallites in rolled copper and brass by electron microscopy. Acta Metall. **17**, 1183–1195 (1969)
258. Peter, F., Weyl, H.: Die Vollständigkeit der primitiven Darstellungen einer geschlossenen kontinuierlichen Gruppe. Math. Ann. **97**, 737–755 (1927)
259. Phillips, D.C.: William Lawrence Bragg, 31 March 1890–1 July 1971. Biogr. Mem. Fellows R. Soc. **25**, 74–143 (1979)
260. Pitteri, M., Zanzotto, G.: Continuum Models for Phase Transitions and Twinning in Crystals. Chapman & Hall/CRC, Boca Raton (2003)
261. Pontryagin, L.S.: Topological Groups, 2nd edn. Gordon and Breach, New York (1966)
262. Pospiech, J., Jura, J.: Determination of the orientation distribution function from incomplete pole figures. Z. Metallkde. **65**, 324–330 (1974)

263. Pospiech, J., Lücke, K.: The rolling textures of copper and α-brass discussed in terms of the orientation distribution function. Acta Metall. **23**, 997–1007 (1975)
264. Pospiech, J., Jura, J., Gottstein, G.: Statistical-analysis of single grain-orientation data generated from model textures. Mater. Sci. Forum **157**(162), 407–412 (1994)
265. Prince, E. (ed.): International Tables for Crystallography. Volume C: Mathematical, Physical and Chemical Tables Kluwer, Dordrecht (2004)
266. Rainville, E.D.: Special Functions. Macmillan, New York (1960)
267. Ram, F., Zaefferer, S., Jäpel, T., Raabe, D.: Error analysis of the crystal orientations and disorientations obtained by the classical electron backscatter diffraction technique. J. Appl. Crystallogr. **48**, 797–813 (2015)
268. Ramírez Galarza, A.I., Seade, J.: Introduction to Classical Geometries. Birkhäuser, Basel (2007)
269. Reiche, R., Rademacher, H.: Die Quantelung des symmetrischen Kreisels nach Schrödingers Undulationsmechanik. Z. Phys. **39**, 444–464 (1926)
270. Roe, R.-J.: Description of crystallite orientation in polycrystalline materials. III. General solution to pole figures. J. Appl. Phys. **36**, 2024–2031 (1965)
271. Roe, R.-J.: Inversion of pole figures for materials having cubic crystal symmetry. J. Appl. Phys. **37**, 2069–2072 (1966)
272. Roe, R.-J.: Methods of X-Ray and Neutron Scattering in Polymer Science. Oxford University Press, New York (2000)
273. Roman, S.: Advanced Linear Algebra, 3rd edn. Springer, New York (2008)
274. Rose, M.E.: Elementary Theory of Angular Momentum. Wiley, New York (1957)
275. Rossin, J., Leser, P., Pusch, K., Frey, C., Murray, S., Torbet, C., Smith, S., Daly, S., Pollock, T.M.: Bayesian inference of elastic constants and texture coefficients in additively manufactured cobalt-nickel superalloys using resonant ultrasound spectroscopy. Acta Mater. **220**, 117287 (2021).
276. Rossmann, W.: Lie Groups: An Introduction Through Linear Groups. Oxford, New York (2002)
277. Rousseau, J.-J.: Basic Crystallography. J. Wiley, Chichester (1998)
278. Rudin, W.: Real and Complex Analysis, 3rd edn. McGraw-Hill, New York (1987)
279. Rudin, W.: Functional Analysis, 2nd edn. McGraw-Hill, New York (1991)
280. Saks, S.: Theory of the Integral. Hafner, New York (1937). Second revised edition. Translated into English by L.C. Young
281. Saks, S.: Integration in abstract metric spaces. Duke Math. J. **4**, 408–411 (1938)
282. Satake, I.: Linear Algebra. Dekker, New York (1975)
283. Schaeben, H.: A unified view of methods to resolve the inverse problem of texture goniometry. Textures Microstruct. **25**, 171–181 (1996)
284. Schaeben, H., van den Boogaart, K.G.: Spherical harmonics in texture analysis. Tectonophysics **370**, 253–268 (2003)
285. Schrödinger, E.: Quantisierung als Eigenwertproblem (Vierte Mitteilung). Ann. Phys. **81**, 109–139 (1926). [English translation] Quantisation as a problem of proper values. Part IV. In: [286], pp. 102–123
286. Schrödinger, E.: Collected Papers on Wave Mechanics. Chelsea, New York (1982)
287. Schrödinger, E.: Wave mechanics. In: [14], pp. 406–424 (2009)
288. Schwartz, A.J., Kumar, K., Adams, B.L. (eds.): Electron Backscatter Diffraction in Materials Science Kluwer/Plenum, New York (2000)
289. Schwartz, A.J., Kumar, K., Adams, B.L., Fields, D.P. (eds.): Electron Backscatter Diffraction in Materials Science 2nd edn. Springer, New York (2009)
290. Schwarzer, R.A. (ed.) Texture and Anisotropy of Polycrystals: Proceedings of the International Conference on Texture and Anisotropy of Polycrystals, ITAP, Clausthal, Germany, September 1997. Materials Science Forum, vol. 273–275. Trans Tech Publications, Uetikon-Zürich (1998)
291. Schwarzer, R.A.: Measurement of macrotexture by automated crystal orientation mapping: an alternative to X-ray diffraction. Mater. Sci. Technol. **16**, 1384–1388 (2000)
292. Schwarzer, R.A.: A fast ACOM/EBSD system. Arch. Metall. Mater. **53**, 5–10 (2008)
293. Schwarzer, R.A., Fields, D.P., Adams, B.L., Kumar, K., Schwartz, A.J.: Present state of electron backscatter diffraction and prospective developments. In: [289], pp. 1–20 (2009)
294. Senechal, M.: Finding the finite groups of symmetries of the sphere. Am. Math. Mon. **97**, 329–335 (1990)
295. Senechal, M.: Crystalline Symmetries: An Informal Mathematical Introduction. Adam Hilger, Bristol (2000)
296. Serre, J.-P.: Linear Representations of Finite Groups. Springer, New York (1977)
297. Shubnikov, A.V., Koptsik, V.A.: Symmetry in Science and Art. Plenum, New York (1974)
298. Shurman, J.: Geometry of the Quintic. Wiley, New York (1997)
299. Sirotin, Yu.I.: Decomposition of material tensors into irreducible parts. Sov. Phys. Crystallogr. **19**, 565–568 (1975)

300. Sneddon, I.N.: Special Functions of Mathematical Physics and Chemistry. Oliver and Boyd, Edinburgh (1961)
301. Souvignier, B.: 1.3. A general introduction to space groups. In: [7], pp. 22–41 (2016)
302. Spencer, A.J.M.: A note on the decomposition of tensors into traceless symmetric tensors. Int. J. Eng. Sci. **8**, 475–481 (1970)
303. Stephenson, R.A.: On the uniqueness of the square-root of a symmetric, positive-definite tensor. J. Elast. **10**, 214–215 (1980)
304. Sternberg, S.: Group Theory and Physics. Cambridge University Press, Cambridge (1994)
305. Sugiura, M.: Unitary Representations and Harmonic Analysis: An Introduction, 2nd edn. North-Holland, Amsterdam (1990)
306. Sutcliffe, B., Woolley, R.G.: The position of the clamped nuclei electronic Hamiltonian in quantum mechanics. Leszczynski, J. (ed.): Handbook of Computational Chemistry, pp. 13–54. Springer, Dordrecht (2012)
307. Szpunar, J.A. (ed.): Proceedings of the Twelfth International Conference on Textures of Materials, ICOTOM-12, McGill University, Montreal, Canada, August 9–13, 1999, vol. 1. NRC Research Press, Ottawa (1999)
308. Szwacki, N.G., Szwacka, T.: Basic Elements of Crystallography. Pan Stanford, Singapore (2010)
309. Talman, J.D.: Special Functions: A Group Theoretic Approach. Benjamin, New York (1968). Based on Lectures by Eugene P. Wigner
310. Tapp, K.: Matrix Groups for Undergraduates. Am. Math. Soc., Providence (2005)
311. Taylor, M.E.: Measure Theory and Integration. Am. Math. Soc., Providence (2006)
312. Thomas, J.M.: William Lawrence Bragg: The pioneer of X-ray crystallography and his pervasive influence. Angew. Chem., Int. Ed. **51**, 12946–12958 (2012)
313. Thompson, W.J.: Angular Momentum: An illustrated Guide to Rotational Symmetries for Physical Systems. Wiley, New York (1994)
314. Thomson, J.J.: Conduction of Electricity through Gases. Cambridge University Press, Cambridge (1903)
315. Thomson, J.J.: Conduction of Electricity Through Gases, 2nd edn. Cambridge University Press, Cambridge (1906)
316. Ting, T.C.T.: Determination of $C^{1/2}$, $C^{-1/2}$ and more general isotropic tensor functions of C. J. Elast. **15**, 319–323 (1985)
317. Tisza, L.: Zur Deutung der Spektren mehratomiger Moleküle. Z. Phys. **82**, 48–72 (1933)
318. Tjur, T.: Probability Based on Radon Measures. Wiley, Chichester (1980)
319. Torquato, S.: Random Heterogeneous Materials: Microstructure and Macroscopic Properties. Springer, New York (2002)
320. Toth, G.: Finite Möbius Groups, Minimal Immersions of Spheres, and Moduli. Springer, New York (2002)
321. Toupin, R.A., Bernstein, B.: Sound waves in deformed perfectly elastic materials. Acoustoelastic effect. J. Acoust. Soc. Am. **33**, 216–225 (1961)
322. Truesdell, C.: A First Course in Continuum Mechanics, vol. 1, 2nd edn. Academic, Boston (1991)
323. van der Waerden, B.L.: Group Theory and Quantum Mechanics. Springer, New York (1974)
324. Van Houtte, P., Wagner, F.: Development of textures by slip and twinning. In: [337], pp. 233–258 (1985)
325. Varshalovich, D.A., Moskalev, A.N., Khersonskii, V.K.: Quantum Theory of Angular Momentum. World Scientific, Singapore (1988)
326. Viglin, A.S.: A quantitative measure of the texture of a polycrystalline material: texture function [in Russian]. Fiz. Tverd. Tela **2**, 2463–2476 (1960). [English translation] Soviet Physics – Solid State **2**, 2195–2207 (1961)
327. Vilenkin, N.Ja.: Special Functions and the Theory of Group Representations. Am. Math. Soc., Providence (1968)
328. von Neumann, J.: Zum Haarschen Mass in topologischen Gruppen. Compos. Math. **1**, 106–114 (1935)
329. Wagner, F.: Texture determination by individual orientation measurements. In: [61], pp. 115–123 (1986)
330. Wagner, F., Wenk, H.R., Esling, C., Bunge, H.J.: Importance of odd coefficients in texture calculations for trigonal-triclinic symmetries. Phys. Status Solidi (a) **67**, 269–285 (1981)
331. Wagner, F., Humbert, M., Muller, J., Esling, C.: Optimization of the positivity method in quantitative texture analysis. Europhys. Lett. **11**, 479–483 (1990)
332. Wagner, F., Matthies, S., Van Landuyt, O.: Processing individual orientations data to calculate ODFs. In: [290], pp. 89–98 (1998)
333. Wang, Y., Yu, C., Xing, L., Li, K., Chen, J., Liu, W., Ma, J., Shen, Z.: A data-driven scheme for quantitative analysis of texture. Metall. Mater. Trans. A **51A**, 940–950 (2020)
334. Warren, B.E.: X-Ray Diffraction. Addison-Wesley, Reading (1969)

335. Waseda, Y., Matsubara, E., Shinoda, K.: X-Ray Diffraction Crystallography: Introduction, Examples and Solved Problems. Springer, Berlin (2011)
336. Wawrzyńczyk, A.: Group Representations and Special Functions. D. Reidel, Dordrecht (1984)
337. Wenk, H.-R. (ed.): Preferred Orientation in Deformed Metals and Rocks: An Introduction to Modern Texture Analysis Academic, Orlando (1985)
338. Wenk, H.-R., Van Houtte, P.: Texture and anisotropy. Rep. Prog. Phys. **67**, 1367–1428 (2004)
339. Weyl, H.: Symmetry. Princeton University Press, Princeton (1952)
340. Wigner, E.P.: Gruppentheorie und ihre Anwendung auf die Quantenmechanik der Atomspektren. Vieweg, Braunschweig (1931)
341. Wigner, E.P.: Group Theory and Its Applications to the Quantum Mechanics of Atomic Spectra. Academic, New York (1959). Translated from the German by J.J. Griffin. Expanded and improved edition
342. Wigner, E.P.: The application of group theory to the special functions of mathematical physics. Lectures during the Spring Term of 1955. Notes by J.D. Talman. Princeton University, Princeton (unpublished)
343. Wolf, A.A.: Rotation operators. Am. J. Phys. **37**, 53–536 (1969)
344. Wondratschek, H.: Part 8. Introduction to space-group symmetry. In: [133], pp. 719–740 (2005)
345. Wright, S.I.: Random thoughts on non-random misorientation distributions. Mater. Sci. Technol. **22**, 1287–1296 (2006)
346. Wright, A.I., Adams, B.L.: An evaluation of the single orientation method for texture determination in materials of moderate texture strength. Textures Microstruct. **12**, 65–76 (1990)
347. Wright, A.I., Kocks, U.F.: A comparison of different texture analysis techniques. In: [187], pp. 53–62 (1996)
348. Wright, S.I., Nowell, M.M., Bingert, J.F.: A comparison of textures measured using X-ray and electron backscatter diffraction. Metall. Mater. Trans. A **38A**, 1845–1855 (2007)
349. Yale, P.: Geometry and Symmetry. Holden-Day, San Francisco (1968)
350. Yamanouchi, T., Sugiura, M.: Introduction to the Theory of Continuous Groups [in Japanese]. Baifukan, Tokyo (1960)
351. Zachariasen, W.H.: Theory of X-Ray Diffraction in Crystals. Wiley, New York (1945)
352. Zare, R.N.: Angular Momentum: Understanding Spatial Aspects in Chemistry and Physics. Wiley, New York (1988)
353. Zassenhaus, H.: Lehrbuch der Gruppentheorie. Erster Band. Teubner, Leipzig (1937). Translated into English by S. Kravetz: The Theory of Groups. Chelsea, New York (1949). Second English edition, Chelsea, New York (1958)
354. Zassenhaus, H.: Über einen Algorithmus zur Bestimmung der Raumgruppen. Comment. Math. Helv. **21**, 117–141 (1948)
355. Zheng, Q-s., Fu, Y-b.: Orientation distribution functions for microstructures of heterogeneous materials (II) – crystal distribution functions and irreducible tensors restricted by various material symmetries. Appl. Math. Mech. **22**, 885–903 (2001)
356. Zheng, Q.-S., Zou, W.-N.: Irreducible decompositions of physical tensors of high orders. J. Eng. Math. **37**, 273–288 (2000)
357. Zou, W.-N., Zheng, Q.-S., Du, D.-X., Rychlewski, J.: Orthogonal irreducible decompositions of tensors of higher orders. Math. Mech. Solids **6**, 249–267 (2001)

Index